

# Advanced Multimedia Information Processing Technologies for Wireless Communication Networks

Lead Guest Editor: Hangjun Che

Guest Editors: Yuchuan Luo, Xinqi Li, and Wenming Cao





---

# **Advanced Multimedia Information Processing Technologies for Wireless Communication Networks**



Security and Communication Networks

---

# **Advanced Multimedia Information Processing Technologies for Wireless Communication Networks**

Lead Guest Editor: Hangjun Che





Guest Editors: Yuchuan Luo, Xinqi Li, and  
Wenming Cao



# Chief Editor

Roberto Di Pietro, Saudi Arabia

## Associate Editors

Jiankun Hu , Australia  
Emanuele Maiorana , Italy  
David Megias , Spain  
Zheng Yan , China

## Academic Editors

Saed Saleh Al Rabae , United Arab Emirates  
Shadab Alam, Saudi Arabia  
Goutham Reddy Alavalapati , USA  
Jehad Ali , Republic of Korea  
Jehad Ali, Saint Vincent and the Grenadines  
Benjamin Aziz , United Kingdom  
Taimur Bakhshi , United Kingdom  
Spiridon Bakiras , Qatar  
Musa Balta, Turkey  
Jin Wook Byun , Republic of Korea  
Bruno Carpentieri , Italy  
Luigi Catuogno , Italy  
Ricardo Chaves , Portugal  
Chien-Ming Chen , China  
Tom Chen , United Kingdom  
Stelvio Cimato , Italy  
Vincenzo Conti , Italy  
Luigi Coppolino , Italy  
Salvatore D'Antonio , Italy  
Juhriyansyah Dalle, Indonesia  
Alfredo De Santis, Italy  
Angel M. Del Rey , Spain  
Roberto Di Pietro , France  
Wenxiu Ding , China  
Nicola Dragoni , Denmark  
Wei Feng , China  
Carmen Fernandez-Gago, Spain  
AnMin Fu , China  
Clemente Galdi , Italy  
Dimitrios Geneiatakis , Italy  
Muhammad A. Gondal , Oman  
Francesco Gringoli , Italy  
Biao Han , China  
Jinguang Han , China  
Khizar Hayat, Oman  
Azeem Irshad, Pakistan

M.A. Jabbar , India  
Minho Jo , Republic of Korea  
Arijit Karati , Taiwan  
ASM Kayes , Australia  
Farrukh Aslam Khan , Saudi Arabia  
Fazlullah Khan , Pakistan  
Kiseon Kim , Republic of Korea  
Mehmet Zeki Konyar, Turkey  
Sanjeev Kumar, USA  
Hyun Kwon, Republic of Korea  
Maryline Laurent , France  
Jegatha Deborah Lazarus , India  
Huaizhi Li , USA  
Jiguo Li , China  
Xueqin Liang, Finland  
Zhe Liu, Canada  
Guangchi Liu , USA  
Flavio Lombardi , Italy  
Yang Lu, China  
Vincente Martin, Spain  
Weizhi Meng , Denmark  
Andrea Michienzi , Italy  
Laura Mongioi , Italy  
Raul Monroy , Mexico  
Naghme Moradpoor , United Kingdom  
Leonardo Mostarda , Italy  
Mohamed Nassar , Lebanon  
Qiang Ni, United Kingdom  
Mahmood Niazi , Saudi Arabia  
Vincent O. Nyangaresi, Kenya  
Lu Ou , China  
Hyun-A Park, Republic of Korea  
A. Peinado , Spain  
Gerardo Pelosi , Italy  
Gregorio Martinez Perez , Spain  
Pedro Peris-Lopez , Spain  
Carla Ràfols, Germany  
Francesco Regazzoni, Switzerland  
Abdalhossein Rezai , Iran  
Helena Rifà-Pous , Spain  
Arun Kumar Sangaiah, India  
Nadeem Sarwar, Pakistan  
Neetesh Saxena, United Kingdom  
Savio Sciancalepore , The Netherlands



De Rosal Ignatius Moses Setiadi ,  
Indonesia  
Wenbo Shi, China  
Ghanshyam Singh , South Africa  
Vasco Soares, Portugal  
Salvatore Sorce , Italy  
Abdulhamit Subasi, Saudi Arabia  
Zhiyuan Tan , United Kingdom  
Keke Tang , China  
Je Sen Teh , Australia  
Bohui Wang, China  
Guojun Wang, China  
Jinwei Wang , China  
Qichun Wang , China  
Hu Xiong , China  
Chang Xu , China  
Xuehu Yan , China  
Anjia Yang , China  
Jiachen Yang , China  
Yu Yao , China  
Yinghui Ye, China  
Kuo-Hui Yeh , Taiwan  
Yong Yu , China  
Xiaohui Yuan , USA  
Sherali Zeadally, USA  
Leo Y. Zhang, Australia  
Tao Zhang, China  
Youwen Zhu , China  
Zhengyu Zhu , China

# Contents

**Retracted: A Review of Motion Vector-Based Video Steganography**

Security and Communication Networks

Retraction (1 page), Article ID 9824673, Volume 2024 (2024)

**Retracted: Enterprise Credit Security Prediction and Evaluation Based on Multimodel Fusion**

Security and Communication Networks

Retraction (1 page), Article ID 9842580, Volume 2024 (2024)

**Retracted: Analysis and Construction of Software Engineering OBE Talent Training System Structure Based on Big Data**

Security and Communication Networks

Retraction (1 page), Article ID 9896387, Volume 2023 (2023)

**Retracted: Based on Fuzzy Comprehensive Evaluation, the Online and Offline Hybrid Teaching Mode of Physical Education Courses is Constructed**

Security and Communication Networks

Retraction (1 page), Article ID 9894050, Volume 2023 (2023)

**Retracted: Design of the Intelligent Recognition Model for English Translation Based on the BP Neural Algorithm**

Security and Communication Networks

Retraction (1 page), Article ID 9876197, Volume 2023 (2023)

**Retracted: A Hybrid Model for Commercial Brand Marketing Prediction Based on Multiple Features with Image Processing**

Security and Communication Networks

Retraction (1 page), Article ID 9876134, Volume 2023 (2023)

**Retracted: Application of Fuzzy Analytic Hierarchy Process in the Quality Monitoring and Evaluation of College Teachers and the Construction of Index System**

Security and Communication Networks

Retraction (1 page), Article ID 9870958, Volume 2023 (2023)

**Retracted: Component-Based Software Testing Method Based on Deep Adversarial Network**

Security and Communication Networks

Retraction (1 page), Article ID 9864593, Volume 2023 (2023)

**Retracted: Fault Diagnosis Method of Rotor Magnetic Field Local Demagnetization in Permanent Magnet Synchronous Motor Model Predictive Current Control System**

Security and Communication Networks

Retraction (1 page), Article ID 9856936, Volume 2023 (2023)

**Retracted: Implementation of Efficient Teaching Scheme of Human Anatomy and Physiology Based on Multimedia Information Processing Technologies**

Security and Communication Networks

Retraction (1 page), Article ID 9856192, Volume 2023 (2023)

**Retracted: Modeling and Optimization Analysis of Ancient Building Construction Rule Components Based on Deep Learning**

Security and Communication Networks

Retraction (1 page), Article ID 9849074, Volume 2023 (2023)

**Retracted: Action Recognition and Application of Table Tennis Training Based on IOT Perception**

Security and Communication Networks

Retraction (1 page), Article ID 9845741, Volume 2023 (2023)

**Retracted: Application and Analysis of Artificial Intelligence in College Students' Career Planning and Employment and Entrepreneurship Information Recommendation**

Security and Communication Networks

Retraction (1 page), Article ID 9842350, Volume 2023 (2023)

**Retracted: Optimization and Evaluation of Oral English CAF Based on Artificial Intelligence and Corpus**

Security and Communication Networks

Retraction (1 page), Article ID 9830320, Volume 2023 (2023)

**Retracted: Design of Network Intrusion Detection Model Based on TCA**

Security and Communication Networks

Retraction (1 page), Article ID 9827541, Volume 2023 (2023)

**Retracted: Research on the Cultivation of College English Listening, Speaking, Reading, and Writing Ability by VR Technology**

Security and Communication Networks

Retraction (1 page), Article ID 9826390, Volume 2023 (2023)

**Retracted: The Application of Modern Computer-Aided Technology in Fine Art Education**

Security and Communication Networks

Retraction (1 page), Article ID 9825819, Volume 2023 (2023)

**Retracted: Evaluation and Analysis of the Informatization Degree of College English Education Based on Big Data Technology**

Security and Communication Networks

Retraction (1 page), Article ID 9824397, Volume 2023 (2023)

**Retracted: Data-Driven Winter Landscape Design and Pleasant Factor Analysis of Elderly Friendly Parks in Severe Cold Cities in Northeast China under the Background of Artificial Intelligence**

Security and Communication Networks

Retraction (1 page), Article ID 9821850, Volume 2023 (2023)

**Retracted: Influence Analysis of Hotel and Tourism Economic Development Based on Computational Intelligence**

Security and Communication Networks

Retraction (1 page), Article ID 9817941, Volume 2023 (2023)



# Contents

**Retracted: Image Analysis Method of Substation Equipment Based on Convolutional Neural Network**

Security and Communication Networks

Retraction (1 page), Article ID 9816085, Volume 2023 (2023)

**Retracted: Design and Application of Intelligent Management Platform Based on Big Data**

Security and Communication Networks

Retraction (1 page), Article ID 9808274, Volume 2023 (2023)

**Retracted: An Improved Machine Translation Model and its Application in Japanese Multi-Context Translation**

Security and Communication Networks

Retraction (1 page), Article ID 9806835, Volume 2023 (2023)

**Retracted: Research on Segmentation Method of Greening Landscape of Urban Community Based on Improved U-Net Network**

Security and Communication Networks

Retraction (1 page), Article ID 9806760, Volume 2023 (2023)

**Retracted: Analysis of Artistic Creation and Design Methods in Universities Based on Augmented Reality and 5G Communication Technology**

Security and Communication Networks

Retraction (1 page), Article ID 9798715, Volume 2023 (2023)

**Retracted: Data Collection and Analysis of Physical Education Teaching Practice Based on Multisensor Perception**

Security and Communication Networks

Retraction (1 page), Article ID 9784542, Volume 2023 (2023)

**Retracted: Traffic Equilibrium Problems with Cross-Boundary Traffic: A Tradable Credit Approach**

Security and Communication Networks

Retraction (1 page), Article ID 9783713, Volume 2023 (2023)

**Retracted: Big Data Analysis and Modeling of Higher Education Reform Based on Cloud Computing Technology**

Security and Communication Networks

Retraction (1 page), Article ID 9782536, Volume 2023 (2023)

**Retracted: Construction of Student Mental Health Education Expert Platform Based on Cloud Native Model**

Security and Communication Networks

Retraction (1 page), Article ID 9782486, Volume 2023 (2023)

**Retracted: Quality Evaluation and Informatization Analysis of Physical Education Teaching Reform Based on Artificial Intelligence**

Security and Communication Networks

Retraction (1 page), Article ID 9768586, Volume 2023 (2023)

**Retracted: Application Exploration of Scenario Logistics Ecosystem Based on beyond 5G and IoT Architecture**

Security and Communication Networks

Retraction (1 page), Article ID 9756796, Volume 2023 (2023)

**Retracted: Research on Location of Logistics Distribution Center Based on K-Means Clustering Algorithm**

Security and Communication Networks

Retraction (1 page), Article ID 9754017, Volume 2023 (2023)

**Retracted: Correlation Analysis between Early Reading Amount and Expressive Ability of Young Children Aided by Multiple Information Processing Techniques under the Heuristic Pattern**

Security and Communication Networks

Retraction (1 page), Article ID 9874153, Volume 2023 (2023)

**Retracted: Cultivation of Students' Independent Learning Ability in Teaching Chinese as a Foreign Language Based on the CDIO Model of Guiding Data Structures and Hidden Markov Algorithms**

Security and Communication Networks

Retraction (1 page), Article ID 9831438, Volume 2023 (2023)

**Retracted: Dance Movement Recognition Based on Modified GMM-Based Motion Target Detection Algorithm**

Security and Communication Networks

Retraction (1 page), Article ID 9871714, Volume 2023 (2023)

**Retracted: Research on the Effective Fusion of Traditional Art and Old Street Culture Construction Based on Fuzzy Algorithm**

Security and Communication Networks

Retraction (1 page), Article ID 9830213, Volume 2023 (2023)

**Retracted: Value Assessment for a Theory-Oriented Flipped Classroom of Physical Education Based on Multi-Source Data Analysis**

Security and Communication Networks

Retraction (1 page), Article ID 9834736, Volume 2023 (2023)

**Retracted: Analysis of Practical Training Characteristics and Teaching System Reform Path of College Physical Education Curriculum Based on Deep Learning**

Security and Communication Networks

Retraction (1 page), Article ID 9810281, Volume 2023 (2023)

**Retracted: Visual Feature Evaluation of Shenyang Greenway Landscape Based on Deep Learning**

Security and Communication Networks

Retraction (1 page), Article ID 9793153, Volume 2023 (2023)

# Contents

**Retracted: Material Analysis and Application Based on Intelligent Computing in the Context of Contemporary Watercolor Painting**

Security and Communication Networks

Retraction (1 page), Article ID 9793059, Volume 2023 (2023)

**Retracted: Improving and Evaluating Business Management in the Digital Economy Based on Data Analysis**

Security and Communication Networks

Retraction (1 page), Article ID 9780532, Volume 2023 (2023)

**Retracted: Research on Optimal Route Planning for Self-Driving Tour Based on Road Network Structure**

Security and Communication Networks

Retraction (1 page), Article ID 9761316, Volume 2023 (2023)

**Retracted: Security Research in Personnel Electronic File Management Based on Blockchain Technology**

Security and Communication Networks

Retraction (1 page), Article ID 9856127, Volume 2023 (2023)

**Retracted: Evaluation and Application of College English Mixed Flipping Classroom Teaching Quality Based on the Fuzzy Judgment Model**

Security and Communication Networks

Retraction (1 page), Article ID 9853202, Volume 2023 (2023)

**Retracted: Evaluation of Political Classroom Teaching Quality in Universities Based on DA-BP Algorithm**

Security and Communication Networks

Retraction (1 page), Article ID 9878924, Volume 2023 (2023)

**Retracted: Analysis of Management Innovation of State-Owned Enterprises in the Context of Artificial Intelligence and Market-Oriented Economic Fluctuations**

Security and Communication Networks

Retraction (1 page), Article ID 9834879, Volume 2023 (2023)

**Retracted: A Novel Maximum Flow Algorithm with Neural Network for Time-Varying Wastage Networks**

Security and Communication Networks

Retraction (1 page), Article ID 9834319, Volume 2023 (2023)



**Retracted: Modeling and Analysis Method of National Fitness Big Data for Basketball Projects Based on a Multivariate Statistical Model**

Security and Communication Networks

Retraction (1 page), Article ID 9827126, Volume 2023 (2023)



**[Retracted] Component-Based Software Testing Method Based on Deep Adversarial Network**

Weiyu Fu  and Lixia Wang 


Research Article (11 pages), Article ID 4231083, Volume 2022 (2022)

**[Retracted] Design and Application of Intelligent Management Platform Based on Big Data**

Yunuo Su, Minhui Dai , and Haoyu Zhou


Research Article (14 pages), Article ID 1790678, Volume 2022 (2022)

**[Retracted] The Application of Modern Computer-Aided Technology in Fine Art Education**

Baoqi Wang 



Research Article (10 pages), Article ID 8038178, Volume 2022 (2022)

**[Retracted] Design of the Intelligent Recognition Model for English Translation Based on the BP Neural Algorithm**

Zhan Wang 


Research Article (12 pages), Article ID 3799061, Volume 2022 (2022)

**Research Overview on Edge Detection Algorithms Based on Deep Learning and Image Fusion**

Bin Tian  and Wei Wei 


Research Article (11 pages), Article ID 1155814, Volume 2022 (2022)

**[Retracted] A Novel Maximum Flow Algorithm with Neural Network for Time-Varying Wastage Networks**

Baowen Zhang, Kaiwen Jiang , and Wei Huang


Research Article (9 pages), Article ID 3782761, Volume 2022 (2022)

**[Retracted] Research on Optimal Route Planning for Self-Driving Tour Based on Road Network Structure**

Ping Zong, Yao Han, and Chenbo Xu 


Research Article (11 pages), Article ID 6588288, Volume 2022 (2022)

**[Retracted] Based on Fuzzy Comprehensive Evaluation, the Online and Offline Hybrid Teaching Mode of Physical Education Courses is Constructed**

Xiaodong Qian and Xinhua Li 





Research Article (18 pages), Article ID 8571077, Volume 2022 (2022)

**[Retracted] Correlation Analysis between Early Reading Amount and Expressive Ability of Young Children Aided by Multiple Information Processing Techniques under the Heuristic Pattern**

Fude Duan, Jianhua Zhou , and Peng Li

Research Article (11 pages), Article ID 8139963, Volume 2022 (2022)


**[Retracted] A Review of Motion Vector-Based Video Steganography**

Jun Li , Mingqing Zhang , Ke Niu , and Xiaoyuan Yang 

Review Article (19 pages), Article ID 2946812, Volume 2022 (2022)

# Contents

**[Retracted] Analysis of Practical Training Characteristics and Teaching System Reform Path of College Physical Education Curriculum Based on Deep Learning**

Ping Fang 

Research Article (13 pages), Article ID 9614356, Volume 2022 (2022)

**[Retracted] Evaluation of Political Classroom Teaching Quality in Universities Based on DA-BP Algorithm**

Hui Guan and Dongxiang Zhu 


Research Article (10 pages), Article ID 3391881, Volume 2022 (2022)

**[Retracted] Modeling and Optimization Analysis of Ancient Building Construction Rule Components Based on Deep Learning**

Hao Ni 


Research Article (13 pages), Article ID 1119059, Volume 2022 (2022)

**[Retracted] Modeling and Analysis Method of National Fitness Big Data for Basketball Projects Based on a Multivariate Statistical Model**

Qi Zhao 


Research Article (11 pages), Article ID 2591633, Volume 2022 (2022)

**[Retracted] Data Collection and Analysis of Physical Education Teaching Practice Based on Multisensor Perception**

JinFeng Tong and Liu Ge 


Research Article (12 pages), Article ID 5758292, Volume 2022 (2022)

**[Retracted] Influence Analysis of Hotel and Tourism Economic Development Based on Computational Intelligence**

Canhui Wei , Jiayu Li, and Xiya Guo


Research Article (9 pages), Article ID 7549628, Volume 2022 (2022)

**[Retracted] Research on the Effective Fusion of Traditional Art and Old Street Culture Construction Based on Fuzzy Algorithm**

Miao Gong 


Research Article (9 pages), Article ID 9616634, Volume 2022 (2022)

**[Retracted] Material Analysis and Application Based on Intelligent Computing in the Context of Contemporary Watercolor Painting**

Jianyu Feng and Yifei Zhang 


Research Article (10 pages), Article ID 9517615, Volume 2022 (2022)

**[Retracted] A Hybrid Model for Commercial Brand Marketing Prediction Based on Multiple Features with Image Processing**

Furong Wang and Li Zhao 


Research Article (10 pages), Article ID 5455745, Volume 2022 (2022)

**[Retracted] Research on Segmentation Method of Greening Landscape of Urban Community Based on Improved U-Net Network**

Jing Sui 



Research Article (9 pages), Article ID 4834952, Volume 2022 (2022)

**[Retracted] Application and Analysis of Artificial Intelligence in College Students' Career Planning and Employment and Entrepreneurship Information Recommendation**

Hui Zhang  and Zhuonan Zheng


Research Article (8 pages), Article ID 8073232, Volume 2022 (2022)

**[Retracted] Fault Diagnosis Method of Rotor Magnetic Field Local Demagnetization in Permanent Magnet Synchronous Motor Model Predictive Current Control System**

Tao Chen  and Bing Chen 


Research Article (13 pages), Article ID 9344484, Volume 2022 (2022)

**[Retracted] Analysis of Management Innovation of State-Owned Enterprises in the Context of Artificial Intelligence and Market-Oriented Economic Fluctuations**

Yanwen Wang and Lu Sun 


Research Article (10 pages), Article ID 1518447, Volume 2022 (2022)

**[Retracted] Cultivation of Students' Independent Learning Ability in Teaching Chinese as a Foreign Language Based on the CDIO Model of Guiding Data Structures and Hidden Markov Algorithms**

Ye Wen  and Shuang Peng



Research Article (7 pages), Article ID 7114217, Volume 2022 (2022)

**[Retracted] Action Recognition and Application of Table Tennis Training Based on IOT Perception**

Zhijian Zhang 


Research Article (11 pages), Article ID 8911564, Volume 2022 (2022)

**[Retracted] Quality Evaluation and Informatization Analysis of Physical Education Teaching Reform Based on Artificial Intelligence**

Yixiong Xu , Shuai Huang , and Lei Li

Research Article (13 pages), Article ID 5473153, Volume 2022 (2022)

**[Retracted] Optimization and Evaluation of Oral English CAF Based on Artificial Intelligence and Corpus**

Zhan Wang 

Research Article (10 pages), Article ID 4649643, Volume 2022 (2022)

**[Retracted] Enterprise Credit Security Prediction and Evaluation Based on Multimodel Fusion**


Lei Zhang , Jie He , and Zihao Zhao 

Research Article (12 pages), Article ID 2754302, Volume 2022 (2022)




# Contents

**[Retracted] Image Analysis Method of Substation Equipment Based on Convolutional Neural Network**

Jingjing Zhang , Yuxin Liu, Lin Yuan, and Haowei Jia


Research Article (10 pages), Article ID 1718514, Volume 2022 (2022)

**[Retracted] Construction of Student Mental Health Education Expert Platform Based on Cloud Native Model**

Song Jin 



Research Article (15 pages), Article ID 5301723, Volume 2022 (2022)

**[Retracted] Analysis of Artistic Creation and Design Methods in Universities Based on Augmented Reality and 5G Communication Technology**

Ying Li 


Research Article (10 pages), Article ID 4005210, Volume 2022 (2022)

**[Retracted] Improving and Evaluating Business Management in the Digital Economy Based on Data Analysis**

Lu Sun  and Yanwen Wang 


Research Article (7 pages), Article ID 5908877, Volume 2022 (2022)

**[Retracted] Dance Movement Recognition Based on Modified GMM-Based Motion Target Detection Algorithm**

Jing Tian and Xiaoqiang Yang 


Research Article (12 pages), Article ID 6023784, Volume 2022 (2022)

**[Retracted] Evaluation and Analysis of the Informatization Degree of College English Education Based on Big Data Technology**

Zongying Wang 


Research Article (11 pages), Article ID 2420071, Volume 2022 (2022)

**[Retracted] Big Data Analysis and Modeling of Higher Education Reform Based on Cloud Computing Technology**

Ziye Tang 

Research Article (11 pages), Article ID 4926636, Volume 2022 (2022)

**[Retracted] Application Exploration of Scenario Logistics Ecosystem Based on beyond 5G and IoT Architecture**

Wei Yao  and Yudong Li


Research Article (11 pages), Article ID 5797503, Volume 2022 (2022)

**[Retracted] Visual Feature Evaluation of Shenyang Greenway Landscape Based on Deep Learning**

Tianyang Pan  and Min Jiang 

Research Article (11 pages), Article ID 8730399, Volume 2022 (2022)

**[Retracted] Application of Fuzzy Analytic Hierarchy Process in the Quality Monitoring and Evaluation of College Teachers and the Construction of Index System**

Xiaoyan Shi 


Research Article (11 pages), Article ID 5124433, Volume 2022 (2022)

**[Retracted] Data-Driven Winter Landscape Design and Pleasant Factor Analysis of Elderly Friendly Parks in Severe Cold Cities in Northeast China under the Background of Artificial Intelligence**

Pengyu Shan  and Wan Sun

Research Article (11 pages), Article ID 8218468, Volume 2022 (2022)

**[Retracted] Research on the Cultivation of College English Listening, Speaking, Reading, and Writing Ability by VR Technology**

Zhen Zeng 


Research Article (9 pages), Article ID 4241870, Volume 2022 (2022)

**[Retracted] Value Assessment for a Theory-Oriented Flipped Classroom of Physical Education Based on Multi-Source Data Analysis**

Na Li 


Research Article (9 pages), Article ID 6540710, Volume 2022 (2022)

**[Retracted] Evaluation and Application of College English Mixed Flipping Classroom Teaching Quality Based on the Fuzzy Judgment Model**

Xiaoyan Gao 


Research Article (9 pages), Article ID 9611611, Volume 2022 (2022)

**[Retracted] An Improved Machine Translation Model and its Application in Japanese Multi-Context Translation**

Huichao Wen 

Research Article (10 pages), Article ID 8364278, Volume 2022 (2022)

**[Retracted] Analysis and Construction of Software Engineering OBE Talent Training System Structure Based on Big Data**

Zhang Jie 

Research Article (10 pages), Article ID 3208318, Volume 2022 (2022)

**[Retracted] Security Research in Personnel Electronic File Management Based on Blockchain Technology**

Hongbing Wang  and Jian Zhang 

Research Article (8 pages), Article ID 7875825, Volume 2022 (2022)

**[Retracted] Research on Location of Logistics Distribution Center Based on K-Means Clustering Algorithm**


Ping Wang, Xianjun Chen , and Xuebin Zhang

Research Article (9 pages), Article ID 2546429, Volume 2022 (2022)

# Contents


---

**[Retracted] Design of Network Intrusion Detection Model Based on TCA**

Quan Wen 



Research Article (6 pages), Article ID 9248853, Volume 2022 (2022)

**[Retracted] Implementation of Efficient Teaching Scheme of Human Anatomy and Physiology Based on Multimedia Information Processing Technologies**

Yue Ma and Zhuangzhi Zhi 

Research Article (7 pages), Article ID 4134864, Volume 2022 (2022)

**[Retracted] Traffic Equilibrium Problems with Cross-Boundary Traffic: A Tradable Credit Approach**

Qingnan Liang , Agachai Sumalee, and Renxin Zhong 

Research Article (12 pages), Article ID 2431019, Volume 2022 (2022)

## Retraction

# Retracted: A Review of Motion Vector-Based Video Steganography

### Security and Communication Networks

Received 23 January 2024; Accepted 23 January 2024; Published 24 January 2024

Copyright © 2024 Security and Communication Networks. This is an open access article distributed under the Creative Commons Attribution License, which permits unrestricted use, distribution, and reproduction in any medium, provided the original work is properly cited.

This article has been retracted by Hindawi following an investigation undertaken by the publisher [1]. This investigation has uncovered evidence of one or more of the following indicators of systematic manipulation of the publication process:

- (1) Discrepancies in scope
- (2) Discrepancies in the description of the research reported
- (3) Discrepancies between the availability of data and the research described
- (4) Inappropriate citations
- (5) Incoherent, meaningless and/or irrelevant content included in the article
- (6) Manipulated or compromised peer review

The presence of these indicators undermines our confidence in the integrity of the article's content and we cannot, therefore, vouch for its reliability. Please note that this notice is intended solely to alert readers that the content of this article is unreliable. We have not investigated whether authors were aware of or involved in the systematic manipulation of the publication process.

Wiley and Hindawi regrets that the usual quality checks did not identify these issues before publication and have since put additional measures in place to safeguard research integrity.

We wish to credit our own Research Integrity and Research Publishing teams and anonymous and named external researchers and research integrity experts for contributing to this investigation.

The corresponding author, as the representative of all authors, has been given the opportunity to register their agreement or disagreement to this retraction. We have kept a record of any response received.

### References

- [1] J. Li, M. Zhang, K. Niu, and X. Yang, "A Review of Motion Vector-Based Video Steganography," *Security and Communication Networks*, vol. 2022, Article ID 2946812, 19 pages, 2022.

## Retraction

# Retracted: Enterprise Credit Security Prediction and Evaluation Based on Multimodel Fusion

### Security and Communication Networks

Received 8 January 2024; Accepted 8 January 2024; Published 9 January 2024

Copyright © 2024 Security and Communication Networks. This is an open access article distributed under the Creative Commons Attribution License, which permits unrestricted use, distribution, and reproduction in any medium, provided the original work is properly cited.

This article has been retracted by Hindawi following an investigation undertaken by the publisher [1]. This investigation has uncovered evidence of one or more of the following indicators of systematic manipulation of the publication process:

- (1) Discrepancies in scope
- (2) Discrepancies in the description of the research reported
- (3) Discrepancies between the availability of data and the research described
- (4) Inappropriate citations
- (5) Incoherent, meaningless and/or irrelevant content included in the article
- (6) Manipulated or compromised peer review

The presence of these indicators undermines our confidence in the integrity of the article's content and we cannot, therefore, vouch for its reliability. Please note that this notice is intended solely to alert readers that the content of this article is unreliable. We have not investigated whether authors were aware of or involved in the systematic manipulation of the publication process.

Wiley and Hindawi regrets that the usual quality checks did not identify these issues before publication and have since put additional measures in place to safeguard research integrity.

We wish to credit our own Research Integrity and Research Publishing teams and anonymous and named external researchers and research integrity experts for contributing to this investigation.

The corresponding author, as the representative of all authors, has been given the opportunity to register their agreement or disagreement to this retraction. We have kept a record of any response received.

### References

- [1] L. Zhang, J. He, and Z. Zhao, "Enterprise Credit Security Prediction and Evaluation Based on Multimodel Fusion," *Security and Communication Networks*, vol. 2022, Article ID 2754302, 12 pages, 2022.

## *Retraction*

# **Retracted: Analysis and Construction of Software Engineering OBE Talent Training System Structure Based on Big Data**

### **Security and Communication Networks**

Received 26 December 2023; Accepted 26 December 2023; Published 29 December 2023

Copyright © 2023 Security and Communication Networks. This is an open access article distributed under the Creative Commons Attribution License, which permits unrestricted use, distribution, and reproduction in any medium, provided the original work is properly cited.

This article has been retracted by Hindawi, as publisher, following an investigation undertaken by the publisher [1]. This investigation has uncovered evidence of systematic manipulation of the publication and peer-review process. We cannot, therefore, vouch for the reliability or integrity of this article.

Please note that this notice is intended solely to alert readers that the peer-review process of this article has been compromised.

Wiley and Hindawi regret that the usual quality checks did not identify these issues before publication and have since put additional measures in place to safeguard research integrity.

We wish to credit our Research Integrity and Research Publishing teams and anonymous and named external researchers and research integrity experts for contributing to this investigation.

The corresponding author, as the representative of all authors, has been given the opportunity to register their agreement or disagreement to this retraction. We have kept a record of any response received.

### **References**

- [1] Z. Jie, "Analysis and Construction of Software Engineering OBE Talent Training System Structure Based on Big Data," *Security and Communication Networks*, vol. 2022, Article ID 3208318, 10 pages, 2022.

## *Retraction*

# **Retracted: Based on Fuzzy Comprehensive Evaluation, the Online and Offline Hybrid Teaching Mode of Physical Education Courses is Constructed**

### **Security and Communication Networks**

Received 26 December 2023; Accepted 26 December 2023; Published 29 December 2023

Copyright © 2023 Security and Communication Networks. This is an open access article distributed under the Creative Commons Attribution License, which permits unrestricted use, distribution, and reproduction in any medium, provided the original work is properly cited.

This article has been retracted by Hindawi, as publisher, following an investigation undertaken by the publisher [1]. This investigation has uncovered evidence of systematic manipulation of the publication and peer-review process. We cannot, therefore, vouch for the reliability or integrity of this article.

Please note that this notice is intended solely to alert readers that the peer-review process of this article has been compromised.

Wiley and Hindawi regret that the usual quality checks did not identify these issues before publication and have since put additional measures in place to safeguard research integrity.

We wish to credit our Research Integrity and Research Publishing teams and anonymous and named external researchers and research integrity experts for contributing to this investigation.

The corresponding author, as the representative of all authors, has been given the opportunity to register their agreement or disagreement to this retraction. We have kept a record of any response received.

## **References**

- [1] X. Qian and X. Li, “Based on Fuzzy Comprehensive Evaluation, the Online and Offline Hybrid Teaching Mode of Physical Education Courses is Constructed,” *Security and Communication Networks*, vol. 2022, Article ID 8571077, 18 pages, 2022.

## *Retraction*

# **Retracted: Design of the Intelligent Recognition Model for English Translation Based on the BP Neural Algorithm**

### **Security and Communication Networks**

Received 26 December 2023; Accepted 26 December 2023; Published 29 December 2023

Copyright © 2023 Security and Communication Networks. This is an open access article distributed under the Creative Commons Attribution License, which permits unrestricted use, distribution, and reproduction in any medium, provided the original work is properly cited.

This article has been retracted by Hindawi, as publisher, following an investigation undertaken by the publisher [1]. This investigation has uncovered evidence of systematic manipulation of the publication and peer-review process. We cannot, therefore, vouch for the reliability or integrity of this article.

Please note that this notice is intended solely to alert readers that the peer-review process of this article has been compromised.

Wiley and Hindawi regret that the usual quality checks did not identify these issues before publication and have since put additional measures in place to safeguard research integrity.

We wish to credit our Research Integrity and Research Publishing teams and anonymous and named external researchers and research integrity experts for contributing to this investigation.

The corresponding author, as the representative of all authors, has been given the opportunity to register their agreement or disagreement to this retraction. We have kept a record of any response received.

### **References**

- [1] Z. Wang, "Design of the Intelligent Recognition Model for English Translation Based on the BP Neural Algorithm," *Security and Communication Networks*, vol. 2022, Article ID 3799061, 12 pages, 2022.



## *Retraction*

# **Retracted: A Hybrid Model for Commercial Brand Marketing Prediction Based on Multiple Features with Image Processing**

### **Security and Communication Networks**

Received 26 December 2023; Accepted 26 December 2023; Published 29 December 2023

Copyright © 2023 Security and Communication Networks. This is an open access article distributed under the Creative Commons Attribution License, which permits unrestricted use, distribution, and reproduction in any medium, provided the original work is properly cited.

This article has been retracted by Hindawi, as publisher, following an investigation undertaken by the publisher [1]. This investigation has uncovered evidence of systematic manipulation of the publication and peer-review process. We cannot, therefore, vouch for the reliability or integrity of this article.

Please note that this notice is intended solely to alert readers that the peer-review process of this article has been compromised.

Wiley and Hindawi regret that the usual quality checks did not identify these issues before publication and have since put additional measures in place to safeguard research integrity.

We wish to credit our Research Integrity and Research Publishing teams and anonymous and named external researchers and research integrity experts for contributing to this investigation.

The corresponding author, as the representative of all authors, has been given the opportunity to register their agreement or disagreement to this retraction. We have kept a record of any response received.

### **References**

- [1] F. Wang and L. Zhao, "A Hybrid Model for Commercial Brand Marketing Prediction Based on Multiple Features with Image Processing," *Security and Communication Networks*, vol. 2022, Article ID 5455745, 10 pages, 2022.

## *Retraction*

# **Retracted: Application of Fuzzy Analytic Hierarchy Process in the Quality Monitoring and Evaluation of College Teachers and the Construction of Index System**

### **Security and Communication Networks**

Received 26 December 2023; Accepted 26 December 2023; Published 29 December 2023

Copyright © 2023 Security and Communication Networks. This is an open access article distributed under the Creative Commons Attribution License, which permits unrestricted use, distribution, and reproduction in any medium, provided the original work is properly cited.

This article has been retracted by Hindawi, as publisher, following an investigation undertaken by the publisher [1]. This investigation has uncovered evidence of systematic manipulation of the publication and peer-review process. We cannot, therefore, vouch for the reliability or integrity of this article.

Please note that this notice is intended solely to alert readers that the peer-review process of this article has been compromised.

Wiley and Hindawi regret that the usual quality checks did not identify these issues before publication and have since put additional measures in place to safeguard research integrity.

We wish to credit our Research Integrity and Research Publishing teams and anonymous and named external researchers and research integrity experts for contributing to this investigation.

The corresponding author, as the representative of all authors, has been given the opportunity to register their agreement or disagreement to this retraction. We have kept a record of any response received.

## **References**

- [1] X. Shi, "Application of Fuzzy Analytic Hierarchy Process in the Quality Monitoring and Evaluation of College Teachers and the Construction of Index System," *Security and Communication Networks*, vol. 2022, Article ID 5124433, 11 pages, 2022.

## *Retraction*

# **Retracted: Component-Based Software Testing Method Based on Deep Adversarial Network**

### **Security and Communication Networks**

Received 26 December 2023; Accepted 26 December 2023; Published 29 December 2023

Copyright © 2023 Security and Communication Networks. This is an open access article distributed under the Creative Commons Attribution License, which permits unrestricted use, distribution, and reproduction in any medium, provided the original work is properly cited.

This article has been retracted by Hindawi, as publisher, following an investigation undertaken by the publisher [1]. This investigation has uncovered evidence of systematic manipulation of the publication and peer-review process. We cannot, therefore, vouch for the reliability or integrity of this article.

Please note that this notice is intended solely to alert readers that the peer-review process of this article has been compromised.

Wiley and Hindawi regret that the usual quality checks did not identify these issues before publication and have since put additional measures in place to safeguard research integrity.

We wish to credit our Research Integrity and Research Publishing teams and anonymous and named external researchers and research integrity experts for contributing to this investigation.

The corresponding author, as the representative of all authors, has been given the opportunity to register their agreement or disagreement to this retraction. We have kept a record of any response received.

### **References**

- [1] W. Fu and L. Wang, "Component-Based Software Testing Method Based on Deep Adversarial Network," *Security and Communication Networks*, vol. 2022, Article ID 4231083, 11 pages, 2022.

## *Retraction*

# **Retracted: Fault Diagnosis Method of Rotor Magnetic Field Local Demagnetization in Permanent Magnet Synchronous Motor Model Predictive Current Control System**

### **Security and Communication Networks**

Received 26 December 2023; Accepted 26 December 2023; Published 29 December 2023

Copyright © 2023 Security and Communication Networks. This is an open access article distributed under the Creative Commons Attribution License, which permits unrestricted use, distribution, and reproduction in any medium, provided the original work is properly cited.

This article has been retracted by Hindawi, as publisher, following an investigation undertaken by the publisher [1]. This investigation has uncovered evidence of systematic manipulation of the publication and peer-review process. We cannot, therefore, vouch for the reliability or integrity of this article.

Please note that this notice is intended solely to alert readers that the peer-review process of this article has been compromised.

Wiley and Hindawi regret that the usual quality checks did not identify these issues before publication and have since put additional measures in place to safeguard research integrity.

We wish to credit our Research Integrity and Research Publishing teams and anonymous and named external researchers and research integrity experts for contributing to this investigation.

The corresponding author, as the representative of all authors, has been given the opportunity to register their agreement or disagreement to this retraction. We have kept a record of any response received.

## **References**

- [1] T. Chen and B. Chen, "Fault Diagnosis Method of Rotor Magnetic Field Local Demagnetization in Permanent Magnet Synchronous Motor Model Predictive Current Control System," *Security and Communication Networks*, vol. 2022, Article ID 9344484, 13 pages, 2022.

## *Retraction*

# **Retracted: Implementation of Efficient Teaching Scheme of Human Anatomy and Physiology Based on Multimedia Information Processing Technologies**

### **Security and Communication Networks**

Received 26 December 2023; Accepted 26 December 2023; Published 29 December 2023

Copyright © 2023 Security and Communication Networks. This is an open access article distributed under the Creative Commons Attribution License, which permits unrestricted use, distribution, and reproduction in any medium, provided the original work is properly cited.

This article has been retracted by Hindawi, as publisher, following an investigation undertaken by the publisher [1]. This investigation has uncovered evidence of systematic manipulation of the publication and peer-review process. We cannot, therefore, vouch for the reliability or integrity of this article.

Please note that this notice is intended solely to alert readers that the peer-review process of this article has been compromised.

Wiley and Hindawi regret that the usual quality checks did not identify these issues before publication and have since put additional measures in place to safeguard research integrity.

We wish to credit our Research Integrity and Research Publishing teams and anonymous and named external researchers and research integrity experts for contributing to this investigation.

The corresponding author, as the representative of all authors, has been given the opportunity to register their agreement or disagreement to this retraction. We have kept a record of any response received.

## **References**

- [1] Y. Ma and Z. Zhi, "Implementation of Efficient Teaching Scheme of Human Anatomy and Physiology Based on Multimedia Information Processing Technologies," *Security and Communication Networks*, vol. 2022, Article ID 4134864, 7 pages, 2022.

## *Retraction*

# **Retracted: Modeling and Optimization Analysis of Ancient Building Construction Rule Components Based on Deep Learning**

## **Security and Communication Networks**

Received 26 December 2023; Accepted 26 December 2023; Published 29 December 2023

Copyright © 2023 Security and Communication Networks. This is an open access article distributed under the Creative Commons Attribution License, which permits unrestricted use, distribution, and reproduction in any medium, provided the original work is properly cited.

This article has been retracted by Hindawi, as publisher, following an investigation undertaken by the publisher [1]. This investigation has uncovered evidence of systematic manipulation of the publication and peer-review process. We cannot, therefore, vouch for the reliability or integrity of this article.

Please note that this notice is intended solely to alert readers that the peer-review process of this article has been compromised.

Wiley and Hindawi regret that the usual quality checks did not identify these issues before publication and have since put additional measures in place to safeguard research integrity.

We wish to credit our Research Integrity and Research Publishing teams and anonymous and named external researchers and research integrity experts for contributing to this investigation.

The corresponding author, as the representative of all authors, has been given the opportunity to register their agreement or disagreement to this retraction. We have kept a record of any response received.

## **References**

- [1] H. Ni, "Modeling and Optimization Analysis of Ancient Building Construction Rule Components Based on Deep Learning," *Security and Communication Networks*, vol. 2022, Article ID 1119059, 13 pages, 2022.

## *Retraction*

# **Retracted: Action Recognition and Application of Table Tennis Training Based on IOT Perception**

### **Security and Communication Networks**

Received 26 December 2023; Accepted 26 December 2023; Published 29 December 2023

Copyright © 2023 Security and Communication Networks. This is an open access article distributed under the Creative Commons Attribution License, which permits unrestricted use, distribution, and reproduction in any medium, provided the original work is properly cited.

This article has been retracted by Hindawi, as publisher, following an investigation undertaken by the publisher [1]. This investigation has uncovered evidence of systematic manipulation of the publication and peer-review process. We cannot, therefore, vouch for the reliability or integrity of this article.

Please note that this notice is intended solely to alert readers that the peer-review process of this article has been compromised.

Wiley and Hindawi regret that the usual quality checks did not identify these issues before publication and have since put additional measures in place to safeguard research integrity.

We wish to credit our Research Integrity and Research Publishing teams and anonymous and named external researchers and research integrity experts for contributing to this investigation.

The corresponding author, as the representative of all authors, has been given the opportunity to register their agreement or disagreement to this retraction. We have kept a record of any response received.

### **References**

- [1] Z. Zhang, "Action Recognition and Application of Table Tennis Training Based on IOT Perception," *Security and Communication Networks*, vol. 2022, Article ID 8911564, 11 pages, 2022.

## *Retraction*

# **Retracted: Application and Analysis of Artificial Intelligence in College Students' Career Planning and Employment and Entrepreneurship Information Recommendation**

### **Security and Communication Networks**

Received 26 December 2023; Accepted 26 December 2023; Published 29 December 2023

Copyright © 2023 Security and Communication Networks. This is an open access article distributed under the Creative Commons Attribution License, which permits unrestricted use, distribution, and reproduction in any medium, provided the original work is properly cited.

This article has been retracted by Hindawi, as publisher, following an investigation undertaken by the publisher [1]. This investigation has uncovered evidence of systematic manipulation of the publication and peer-review process. We cannot, therefore, vouch for the reliability or integrity of this article.

Please note that this notice is intended solely to alert readers that the peer-review process of this article has been compromised.

Wiley and Hindawi regret that the usual quality checks did not identify these issues before publication and have since put additional measures in place to safeguard research integrity.

We wish to credit our Research Integrity and Research Publishing teams and anonymous and named external researchers and research integrity experts for contributing to this investigation.

The corresponding author, as the representative of all authors, has been given the opportunity to register their agreement or disagreement to this retraction. We have kept a record of any response received.

## **References**

- [1] H. Zhang and Z. Zheng, "Application and Analysis of Artificial Intelligence in College Students' Career Planning and Employment and Entrepreneurship Information Recommendation," *Security and Communication Networks*, vol. 2022, Article ID 8073232, 8 pages, 2022.



## *Retraction*

# **Retracted: Optimization and Evaluation of Oral English CAF Based on Artificial Intelligence and Corpus**

### **Security and Communication Networks**

Received 26 December 2023; Accepted 26 December 2023; Published 29 December 2023

Copyright © 2023 Security and Communication Networks. This is an open access article distributed under the Creative Commons Attribution License, which permits unrestricted use, distribution, and reproduction in any medium, provided the original work is properly cited.

This article has been retracted by Hindawi, as publisher, following an investigation undertaken by the publisher [1]. This investigation has uncovered evidence of systematic manipulation of the publication and peer-review process. We cannot, therefore, vouch for the reliability or integrity of this article.

Please note that this notice is intended solely to alert readers that the peer-review process of this article has been compromised.

Wiley and Hindawi regret that the usual quality checks did not identify these issues before publication and have since put additional measures in place to safeguard research integrity.

We wish to credit our Research Integrity and Research Publishing teams and anonymous and named external researchers and research integrity experts for contributing to this investigation.

The corresponding author, as the representative of all authors, has been given the opportunity to register their agreement or disagreement to this retraction. We have kept a record of any response received.

### **References**

- [1] Z. Wang, "Optimization and Evaluation of Oral English CAF Based on Artificial Intelligence and Corpus," *Security and Communication Networks*, vol. 2022, Article ID 4649643, 10 pages, 2022.

## *Retraction*

# **Retracted: Design of Network Intrusion Detection Model Based on TCA**

### **Security and Communication Networks**

Received 26 December 2023; Accepted 26 December 2023; Published 29 December 2023

Copyright © 2023 Security and Communication Networks. This is an open access article distributed under the Creative Commons Attribution License, which permits unrestricted use, distribution, and reproduction in any medium, provided the original work is properly cited.

This article has been retracted by Hindawi, as publisher, following an investigation undertaken by the publisher [1]. This investigation has uncovered evidence of systematic manipulation of the publication and peer-review process. We cannot, therefore, vouch for the reliability or integrity of this article.

Please note that this notice is intended solely to alert readers that the peer-review process of this article has been compromised.

Wiley and Hindawi regret that the usual quality checks did not identify these issues before publication and have since put additional measures in place to safeguard research integrity.

We wish to credit our Research Integrity and Research Publishing teams and anonymous and named external researchers and research integrity experts for contributing to this investigation.

The corresponding author, as the representative of all authors, has been given the opportunity to register their agreement or disagreement to this retraction. We have kept a record of any response received.

### **References**

- [1] Q. Wen, "Design of Network Intrusion Detection Model Based on TCA," *Security and Communication Networks*, vol. 2022, Article ID 9248853, 6 pages, 2022.

## *Retraction*

# **Retracted: Research on the Cultivation of College English Listening, Speaking, Reading, and Writing Ability by VR Technology**

### **Security and Communication Networks**

Received 26 December 2023; Accepted 26 December 2023; Published 29 December 2023

Copyright © 2023 Security and Communication Networks. This is an open access article distributed under the Creative Commons Attribution License, which permits unrestricted use, distribution, and reproduction in any medium, provided the original work is properly cited.

This article has been retracted by Hindawi, as publisher, following an investigation undertaken by the publisher [1]. This investigation has uncovered evidence of systematic manipulation of the publication and peer-review process. We cannot, therefore, vouch for the reliability or integrity of this article.

Please note that this notice is intended solely to alert readers that the peer-review process of this article has been compromised.

Wiley and Hindawi regret that the usual quality checks did not identify these issues before publication and have since put additional measures in place to safeguard research integrity.

We wish to credit our Research Integrity and Research Publishing teams and anonymous and named external researchers and research integrity experts for contributing to this investigation.

The corresponding author, as the representative of all authors, has been given the opportunity to register their agreement or disagreement to this retraction. We have kept a record of any response received.

## **References**

- [1] Z. Zeng, "Research on the Cultivation of College English Listening, Speaking, Reading, and Writing Ability by VR Technology," *Security and Communication Networks*, vol. 2022, Article ID 4241870, 9 pages, 2022.

## *Retraction*

# **Retracted: The Application of Modern Computer-Aided Technology in Fine Art Education**

### **Security and Communication Networks**

Received 26 December 2023; Accepted 26 December 2023; Published 29 December 2023

Copyright © 2023 Security and Communication Networks. This is an open access article distributed under the Creative Commons Attribution License, which permits unrestricted use, distribution, and reproduction in any medium, provided the original work is properly cited.

This article has been retracted by Hindawi, as publisher, following an investigation undertaken by the publisher [1]. This investigation has uncovered evidence of systematic manipulation of the publication and peer-review process. We cannot, therefore, vouch for the reliability or integrity of this article.

Please note that this notice is intended solely to alert readers that the peer-review process of this article has been compromised.

Wiley and Hindawi regret that the usual quality checks did not identify these issues before publication and have since put additional measures in place to safeguard research integrity.

We wish to credit our Research Integrity and Research Publishing teams and anonymous and named external researchers and research integrity experts for contributing to this investigation.

The corresponding author, as the representative of all authors, has been given the opportunity to register their agreement or disagreement to this retraction. We have kept a record of any response received.

### **References**

- [1] B. Wang, "The Application of Modern Computer-Aided Technology in Fine Art Education," *Security and Communication Networks*, vol. 2022, Article ID 8038178, 10 pages, 2022.

## *Retraction*

# **Retracted: Evaluation and Analysis of the Informatization Degree of College English Education Based on Big Data Technology**

### **Security and Communication Networks**

Received 26 December 2023; Accepted 26 December 2023; Published 29 December 2023

Copyright © 2023 Security and Communication Networks. This is an open access article distributed under the Creative Commons Attribution License, which permits unrestricted use, distribution, and reproduction in any medium, provided the original work is properly cited.

This article has been retracted by Hindawi, as publisher, following an investigation undertaken by the publisher [1]. This investigation has uncovered evidence of systematic manipulation of the publication and peer-review process. We cannot, therefore, vouch for the reliability or integrity of this article.

Please note that this notice is intended solely to alert readers that the peer-review process of this article has been compromised.

Wiley and Hindawi regret that the usual quality checks did not identify these issues before publication and have since put additional measures in place to safeguard research integrity.

We wish to credit our Research Integrity and Research Publishing teams and anonymous and named external researchers and research integrity experts for contributing to this investigation.

The corresponding author, as the representative of all authors, has been given the opportunity to register their agreement or disagreement to this retraction. We have kept a record of any response received.

## **References**

- [1] Z. Wang, "Evaluation and Analysis of the Informatization Degree of College English Education Based on Big Data Technology," *Security and Communication Networks*, vol. 2022, Article ID 2420071, 11 pages, 2022.

## *Retraction*

# **Retracted: Data-Driven Winter Landscape Design and Pleasant Factor Analysis of Elderly Friendly Parks in Severe Cold Cities in Northeast China under the Background of Artificial Intelligence**

### **Security and Communication Networks**

Received 26 December 2023; Accepted 26 December 2023; Published 29 December 2023

Copyright © 2023 Security and Communication Networks. This is an open access article distributed under the Creative Commons Attribution License, which permits unrestricted use, distribution, and reproduction in any medium, provided the original work is properly cited.

This article has been retracted by Hindawi, as publisher, following an investigation undertaken by the publisher [1]. This investigation has uncovered evidence of systematic manipulation of the publication and peer-review process. We cannot, therefore, vouch for the reliability or integrity of this article.

Please note that this notice is intended solely to alert readers that the peer-review process of this article has been compromised.

Wiley and Hindawi regret that the usual quality checks did not identify these issues before publication and have since put additional measures in place to safeguard research integrity.

We wish to credit our Research Integrity and Research Publishing teams and anonymous and named external researchers and research integrity experts for contributing to this investigation.

The corresponding author, as the representative of all authors, has been given the opportunity to register their agreement or disagreement to this retraction. We have kept a record of any response received.

## **References**

- [1] P. Shan and W. Sun, "Data-Driven Winter Landscape Design and Pleasant Factor Analysis of Elderly Friendly Parks in Severe Cold Cities in Northeast China under the Background of Artificial Intelligence," *Security and Communication Networks*, vol. 2022, Article ID 8218468, 11 pages, 2022.

## *Retraction*

# **Retracted: Influence Analysis of Hotel and Tourism Economic Development Based on Computational Intelligence**

### **Security and Communication Networks**

Received 26 December 2023; Accepted 26 December 2023; Published 29 December 2023

Copyright © 2023 Security and Communication Networks. This is an open access article distributed under the Creative Commons Attribution License, which permits unrestricted use, distribution, and reproduction in any medium, provided the original work is properly cited.

This article has been retracted by Hindawi, as publisher, following an investigation undertaken by the publisher [1]. This investigation has uncovered evidence of systematic manipulation of the publication and peer-review process. We cannot, therefore, vouch for the reliability or integrity of this article.

Please note that this notice is intended solely to alert readers that the peer-review process of this article has been compromised.

Wiley and Hindawi regret that the usual quality checks did not identify these issues before publication and have since put additional measures in place to safeguard research integrity.

We wish to credit our Research Integrity and Research Publishing teams and anonymous and named external researchers and research integrity experts for contributing to this investigation.

The corresponding author, as the representative of all authors, has been given the opportunity to register their agreement or disagreement to this retraction. We have kept a record of any response received.

### **References**

- [1] C. Wei, J. Li, and X. Guo, "Influence Analysis of Hotel and Tourism Economic Development Based on Computational Intelligence," *Security and Communication Networks*, vol. 2022, Article ID 7549628, 9 pages, 2022.

## *Retraction*

# **Retracted: Image Analysis Method of Substation Equipment Based on Convolutional Neural Network**

### **Security and Communication Networks**

Received 26 December 2023; Accepted 26 December 2023; Published 29 December 2023

Copyright © 2023 Security and Communication Networks. This is an open access article distributed under the Creative Commons Attribution License, which permits unrestricted use, distribution, and reproduction in any medium, provided the original work is properly cited.

This article has been retracted by Hindawi, as publisher, following an investigation undertaken by the publisher [1]. This investigation has uncovered evidence of systematic manipulation of the publication and peer-review process. We cannot, therefore, vouch for the reliability or integrity of this article.

Please note that this notice is intended solely to alert readers that the peer-review process of this article has been compromised.

Wiley and Hindawi regret that the usual quality checks did not identify these issues before publication and have since put additional measures in place to safeguard research integrity.

We wish to credit our Research Integrity and Research Publishing teams and anonymous and named external researchers and research integrity experts for contributing to this investigation.

The corresponding author, as the representative of all authors, has been given the opportunity to register their agreement or disagreement to this retraction. We have kept a record of any response received.

### **References**

- [1] J. Zhang, Y. Liu, L. Yuan, and H. Jia, "Image Analysis Method of Substation Equipment Based on Convolutional Neural Network," *Security and Communication Networks*, vol. 2022, Article ID 1718514, 10 pages, 2022.



## *Retraction*

# **Retracted: Design and Application of Intelligent Management Platform Based on Big Data**

### **Security and Communication Networks**

Received 26 December 2023; Accepted 26 December 2023; Published 29 December 2023

Copyright © 2023 Security and Communication Networks. This is an open access article distributed under the Creative Commons Attribution License, which permits unrestricted use, distribution, and reproduction in any medium, provided the original work is properly cited.

This article has been retracted by Hindawi, as publisher, following an investigation undertaken by the publisher [1]. This investigation has uncovered evidence of systematic manipulation of the publication and peer-review process. We cannot, therefore, vouch for the reliability or integrity of this article.

Please note that this notice is intended solely to alert readers that the peer-review process of this article has been compromised.

Wiley and Hindawi regret that the usual quality checks did not identify these issues before publication and have since put additional measures in place to safeguard research integrity.

We wish to credit our Research Integrity and Research Publishing teams and anonymous and named external researchers and research integrity experts for contributing to this investigation.

The corresponding author, as the representative of all authors, has been given the opportunity to register their agreement or disagreement to this retraction. We have kept a record of any response received.

### **References**

- [1] Y. Su, M. Dai, and H. Zhou, "Design and Application of Intelligent Management Platform Based on Big Data," *Security and Communication Networks*, vol. 2022, Article ID 1790678, 14 pages, 2022.

## *Retraction*

# **Retracted: An Improved Machine Translation Model and its Application in Japanese Multi-Context Translation**

### **Security and Communication Networks**

Received 26 December 2023; Accepted 26 December 2023; Published 29 December 2023

Copyright © 2023 Security and Communication Networks. This is an open access article distributed under the Creative Commons Attribution License, which permits unrestricted use, distribution, and reproduction in any medium, provided the original work is properly cited.

This article has been retracted by Hindawi, as publisher, following an investigation undertaken by the publisher [1]. This investigation has uncovered evidence of systematic manipulation of the publication and peer-review process. We cannot, therefore, vouch for the reliability or integrity of this article.

Please note that this notice is intended solely to alert readers that the peer-review process of this article has been compromised.

Wiley and Hindawi regret that the usual quality checks did not identify these issues before publication and have since put additional measures in place to safeguard research integrity.

We wish to credit our Research Integrity and Research Publishing teams and anonymous and named external researchers and research integrity experts for contributing to this investigation.

The corresponding author, as the representative of all authors, has been given the opportunity to register their agreement or disagreement to this retraction. We have kept a record of any response received.

### **References**

- [1] H. Wen, "An Improved Machine Translation Model and its Application in Japanese Multi-Context Translation," *Security and Communication Networks*, vol. 2022, Article ID 8364278, 10 pages, 2022.

## *Retraction*

# **Retracted: Research on Segmentation Method of Greening Landscape of Urban Community Based on Improved U-Net Network**

### **Security and Communication Networks**

Received 26 December 2023; Accepted 26 December 2023; Published 29 December 2023

Copyright © 2023 Security and Communication Networks. This is an open access article distributed under the Creative Commons Attribution License, which permits unrestricted use, distribution, and reproduction in any medium, provided the original work is properly cited.

This article has been retracted by Hindawi, as publisher, following an investigation undertaken by the publisher [1]. This investigation has uncovered evidence of systematic manipulation of the publication and peer-review process. We cannot, therefore, vouch for the reliability or integrity of this article.

Please note that this notice is intended solely to alert readers that the peer-review process of this article has been compromised.

Wiley and Hindawi regret that the usual quality checks did not identify these issues before publication and have since put additional measures in place to safeguard research integrity.

We wish to credit our Research Integrity and Research Publishing teams and anonymous and named external researchers and research integrity experts for contributing to this investigation.

The corresponding author, as the representative of all authors, has been given the opportunity to register their agreement or disagreement to this retraction. We have kept a record of any response received.

## **References**

- [1] J. Sui, "Research on Segmentation Method of Greening Landscape of Urban Community Based on Improved U-Net Network," *Security and Communication Networks*, vol. 2022, Article ID 4834952, 9 pages, 2022.

## *Retraction*

# **Retracted: Analysis of Artistic Creation and Design Methods in Universities Based on Augmented Reality and 5G Communication Technology**

### **Security and Communication Networks**

Received 26 December 2023; Accepted 26 December 2023; Published 29 December 2023

Copyright © 2023 Security and Communication Networks. This is an open access article distributed under the Creative Commons Attribution License, which permits unrestricted use, distribution, and reproduction in any medium, provided the original work is properly cited.

This article has been retracted by Hindawi, as publisher, following an investigation undertaken by the publisher [1]. This investigation has uncovered evidence of systematic manipulation of the publication and peer-review process. We cannot, therefore, vouch for the reliability or integrity of this article.

Please note that this notice is intended solely to alert readers that the peer-review process of this article has been compromised.

Wiley and Hindawi regret that the usual quality checks did not identify these issues before publication and have since put additional measures in place to safeguard research integrity.

We wish to credit our Research Integrity and Research Publishing teams and anonymous and named external researchers and research integrity experts for contributing to this investigation.

The corresponding author, as the representative of all authors, has been given the opportunity to register their agreement or disagreement to this retraction. We have kept a record of any response received.

## **References**

- [1] Y. Li, "Analysis of Artistic Creation and Design Methods in Universities Based on Augmented Reality and 5G Communication Technology," *Security and Communication Networks*, vol. 2022, Article ID 4005210, 10 pages, 2022.

## *Retraction*

# **Retracted: Data Collection and Analysis of Physical Education Teaching Practice Based on Multisensor Perception**

### **Security and Communication Networks**

Received 26 December 2023; Accepted 26 December 2023; Published 29 December 2023

Copyright © 2023 Security and Communication Networks. This is an open access article distributed under the Creative Commons Attribution License, which permits unrestricted use, distribution, and reproduction in any medium, provided the original work is properly cited.

This article has been retracted by Hindawi, as publisher, following an investigation undertaken by the publisher [1]. This investigation has uncovered evidence of systematic manipulation of the publication and peer-review process. We cannot, therefore, vouch for the reliability or integrity of this article.

Please note that this notice is intended solely to alert readers that the peer-review process of this article has been compromised.

Wiley and Hindawi regret that the usual quality checks did not identify these issues before publication and have since put additional measures in place to safeguard research integrity.

We wish to credit our Research Integrity and Research Publishing teams and anonymous and named external researchers and research integrity experts for contributing to this investigation.

The corresponding author, as the representative of all authors, has been given the opportunity to register their agreement or disagreement to this retraction. We have kept a record of any response received.

### **References**

- [1] J. Tong and L. Ge, "Data Collection and Analysis of Physical Education Teaching Practice Based on Multisensor Perception," *Security and Communication Networks*, vol. 2022, Article ID 5758292, 12 pages, 2022.

## *Retraction*

# **Retracted: Traffic Equilibrium Problems with Cross-Boundary Traffic: A Tradable Credit Approach**

### **Security and Communication Networks**

Received 26 December 2023; Accepted 26 December 2023; Published 29 December 2023

Copyright © 2023 Security and Communication Networks. This is an open access article distributed under the Creative Commons Attribution License, which permits unrestricted use, distribution, and reproduction in any medium, provided the original work is properly cited.

This article has been retracted by Hindawi, as publisher, following an investigation undertaken by the publisher [1]. This investigation has uncovered evidence of systematic manipulation of the publication and peer-review process. We cannot, therefore, vouch for the reliability or integrity of this article.

Please note that this notice is intended solely to alert readers that the peer-review process of this article has been compromised.

Wiley and Hindawi regret that the usual quality checks did not identify these issues before publication and have since put additional measures in place to safeguard research integrity.

We wish to credit our Research Integrity and Research Publishing teams and anonymous and named external researchers and research integrity experts for contributing to this investigation.

The corresponding author, as the representative of all authors, has been given the opportunity to register their agreement or disagreement to this retraction. We have kept a record of any response received.

### **References**

- [1] Q. Liang, A. Sumalee, and R. Zhong, "Traffic Equilibrium Problems with Cross-Boundary Traffic: A Tradable Credit Approach," *Security and Communication Networks*, vol. 2022, Article ID 2431019, 12 pages, 2022.

## *Retraction*

# **Retracted: Big Data Analysis and Modeling of Higher Education Reform Based on Cloud Computing Technology**

### **Security and Communication Networks**

Received 26 December 2023; Accepted 26 December 2023; Published 29 December 2023

Copyright © 2023 Security and Communication Networks. This is an open access article distributed under the Creative Commons Attribution License, which permits unrestricted use, distribution, and reproduction in any medium, provided the original work is properly cited.

This article has been retracted by Hindawi, as publisher, following an investigation undertaken by the publisher [1]. This investigation has uncovered evidence of systematic manipulation of the publication and peer-review process. We cannot, therefore, vouch for the reliability or integrity of this article.

Please note that this notice is intended solely to alert readers that the peer-review process of this article has been compromised.

Wiley and Hindawi regret that the usual quality checks did not identify these issues before publication and have since put additional measures in place to safeguard research integrity.

We wish to credit our Research Integrity and Research Publishing teams and anonymous and named external researchers and research integrity experts for contributing to this investigation.

The corresponding author, as the representative of all authors, has been given the opportunity to register their agreement or disagreement to this retraction. We have kept a record of any response received.

### **References**

- [1] Z. Tang, "Big Data Analysis and Modeling of Higher Education Reform Based on Cloud Computing Technology," *Security and Communication Networks*, vol. 2022, Article ID 4926636, 11 pages, 2022.

## *Retraction*

# **Retracted: Construction of Student Mental Health Education Expert Platform Based on Cloud Native Model**

### **Security and Communication Networks**

Received 26 December 2023; Accepted 26 December 2023; Published 29 December 2023

Copyright © 2023 Security and Communication Networks. This is an open access article distributed under the Creative Commons Attribution License, which permits unrestricted use, distribution, and reproduction in any medium, provided the original work is properly cited.

This article has been retracted by Hindawi, as publisher, following an investigation undertaken by the publisher [1]. This investigation has uncovered evidence of systematic manipulation of the publication and peer-review process. We cannot, therefore, vouch for the reliability or integrity of this article.

Please note that this notice is intended solely to alert readers that the peer-review process of this article has been compromised.

Wiley and Hindawi regret that the usual quality checks did not identify these issues before publication and have since put additional measures in place to safeguard research integrity.

We wish to credit our Research Integrity and Research Publishing teams and anonymous and named external researchers and research integrity experts for contributing to this investigation.

The corresponding author, as the representative of all authors, has been given the opportunity to register their agreement or disagreement to this retraction. We have kept a record of any response received.

### **References**

- [1] S. Jin, "Construction of Student Mental Health Education Expert Platform Based on Cloud Native Model," *Security and Communication Networks*, vol. 2022, Article ID 5301723, 15 pages, 2022.



## *Retraction*

# **Retracted: Quality Evaluation and Informatization Analysis of Physical Education Teaching Reform Based on Artificial Intelligence**

### **Security and Communication Networks**

Received 26 December 2023; Accepted 26 December 2023; Published 29 December 2023

Copyright © 2023 Security and Communication Networks. This is an open access article distributed under the Creative Commons Attribution License, which permits unrestricted use, distribution, and reproduction in any medium, provided the original work is properly cited.

This article has been retracted by Hindawi, as publisher, following an investigation undertaken by the publisher [1]. This investigation has uncovered evidence of systematic manipulation of the publication and peer-review process. We cannot, therefore, vouch for the reliability or integrity of this article.

Please note that this notice is intended solely to alert readers that the peer-review process of this article has been compromised.

Wiley and Hindawi regret that the usual quality checks did not identify these issues before publication and have since put additional measures in place to safeguard research integrity.

We wish to credit our Research Integrity and Research Publishing teams and anonymous and named external researchers and research integrity experts for contributing to this investigation.

The corresponding author, as the representative of all authors, has been given the opportunity to register their agreement or disagreement to this retraction. We have kept a record of any response received.

## **References**

- [1] Y. Xu, S. Huang, and L. Li, "Quality Evaluation and Informatization Analysis of Physical Education Teaching Reform Based on Artificial Intelligence," *Security and Communication Networks*, vol. 2022, Article ID 5473153, 13 pages, 2022.

## *Retraction*

# **Retracted: Application Exploration of Scenario Logistics Ecosystem Based on beyond 5G and IoT Architecture**

### **Security and Communication Networks**

Received 26 December 2023; Accepted 26 December 2023; Published 29 December 2023

Copyright © 2023 Security and Communication Networks. This is an open access article distributed under the Creative Commons Attribution License, which permits unrestricted use, distribution, and reproduction in any medium, provided the original work is properly cited.

This article has been retracted by Hindawi, as publisher, following an investigation undertaken by the publisher [1]. This investigation has uncovered evidence of systematic manipulation of the publication and peer-review process. We cannot, therefore, vouch for the reliability or integrity of this article.

Please note that this notice is intended solely to alert readers that the peer-review process of this article has been compromised.

Wiley and Hindawi regret that the usual quality checks did not identify these issues before publication and have since put additional measures in place to safeguard research integrity.

We wish to credit our Research Integrity and Research Publishing teams and anonymous and named external researchers and research integrity experts for contributing to this investigation.

The corresponding author, as the representative of all authors, has been given the opportunity to register their agreement or disagreement to this retraction. We have kept a record of any response received.

### **References**

- [1] W. Yao and Y. Li, "Application Exploration of Scenario Logistics Ecosystem Based on beyond 5G and IoT Architecture," *Security and Communication Networks*, vol. 2022, Article ID 5797503, 11 pages, 2022.

## *Retraction*

# **Retracted: Research on Location of Logistics Distribution Center Based on K-Means Clustering Algorithm**

### **Security and Communication Networks**

Received 26 December 2023; Accepted 26 December 2023; Published 29 December 2023

Copyright © 2023 Security and Communication Networks. This is an open access article distributed under the Creative Commons Attribution License, which permits unrestricted use, distribution, and reproduction in any medium, provided the original work is properly cited.

This article has been retracted by Hindawi, as publisher, following an investigation undertaken by the publisher [1]. This investigation has uncovered evidence of systematic manipulation of the publication and peer-review process. We cannot, therefore, vouch for the reliability or integrity of this article.

Please note that this notice is intended solely to alert readers that the peer-review process of this article has been compromised.

Wiley and Hindawi regret that the usual quality checks did not identify these issues before publication and have since put additional measures in place to safeguard research integrity.

We wish to credit our Research Integrity and Research Publishing teams and anonymous and named external researchers and research integrity experts for contributing to this investigation.

The corresponding author, as the representative of all authors, has been given the opportunity to register their agreement or disagreement to this retraction. We have kept a record of any response received.

### **References**

- [1] P. Wang, X. Chen, and X. Zhang, "Research on Location of Logistics Distribution Center Based on K-Means Clustering Algorithm," *Security and Communication Networks*, vol. 2022, Article ID 2546429, 9 pages, 2022.

## Retraction

# Retracted: Correlation Analysis between Early Reading Amount and Expressive Ability of Young Children Aided by Multiple Information Processing Techniques under the Heuristic Pattern

### Security and Communication Networks

Received 17 October 2023; Accepted 17 October 2023; Published 18 October 2023

Copyright © 2023 Security and Communication Networks. This is an open access article distributed under the Creative Commons Attribution License, which permits unrestricted use, distribution, and reproduction in any medium, provided the original work is properly cited.

This article has been retracted by Hindawi following an investigation undertaken by the publisher [1]. This investigation has uncovered evidence of one or more of the following indicators of systematic manipulation of the publication process:

- (1) Discrepancies in scope
- (2) Discrepancies in the description of the research reported
- (3) Discrepancies between the availability of data and the research described
- (4) Inappropriate citations
- (5) Incoherent, meaningless and/or irrelevant content included in the article
- (6) Peer-review manipulation

The presence of these indicators undermines our confidence in the integrity of the article's content and we cannot, therefore, vouch for its reliability. Please note that this notice is intended solely to alert readers that the content of this article is unreliable. We have not investigated whether authors were aware of or involved in the systematic manipulation of the publication process.

In addition, our investigation has also shown that one or more of the following human-subject reporting requirements has not been met in this article: ethical approval by an Institutional Review Board (IRB) committee or equivalent, patient/participant consent to participate, and/or agreement to publish patient/participant details (where relevant).

Wiley and Hindawi regrets that the usual quality checks did not identify these issues before publication and have since put additional measures in place to safeguard research integrity.

We wish to credit our own Research Integrity and Research Publishing teams and anonymous and named external researchers and research integrity experts for contributing to this investigation.

The corresponding author, as the representative of all authors, has been given the opportunity to register their agreement or disagreement to this retraction. We have kept a record of any response received.

### References

- [1] F. Duan, J. Zhou, and P. Li, "Correlation Analysis between Early Reading Amount and Expressive Ability of Young Children Aided by Multiple Information Processing Techniques under the Heuristic Pattern," *Security and Communication Networks*, vol. 2022, Article ID 8139963, 11 pages, 2022.

## Retraction

# Retracted: Cultivation of Students' Independent Learning Ability in Teaching Chinese as a Foreign Language Based on the CDIO Model of Guiding Data Structures and Hidden Markov Algorithms

### Security and Communication Networks

Received 17 October 2023; Accepted 17 October 2023; Published 18 October 2023

Copyright © 2023 Security and Communication Networks. This is an open access article distributed under the Creative Commons Attribution License, which permits unrestricted use, distribution, and reproduction in any medium, provided the original work is properly cited.

This article has been retracted by Hindawi following an investigation undertaken by the publisher [1]. This investigation has uncovered evidence of one or more of the following indicators of systematic manipulation of the publication process:

- (1) Discrepancies in scope
- (2) Discrepancies in the description of the research reported
- (3) Discrepancies between the availability of data and the research described
- (4) Inappropriate citations
- (5) Incoherent, meaningless and/or irrelevant content included in the article
- (6) Peer-review manipulation

The presence of these indicators undermines our confidence in the integrity of the article's content and we cannot, therefore, vouch for its reliability. Please note that this notice is intended solely to alert readers that the content of this article is unreliable. We have not investigated whether authors were aware of or involved in the systematic manipulation of the publication process.

In addition, our investigation has also shown that one or more of the following human-subject reporting requirements has not been met in this article: ethical approval by an Institutional Review Board (IRB) committee or equivalent, patient/participant consent to participate, and/or agreement to publish patient/participant details (where relevant).

Wiley and Hindawi regrets that the usual quality checks did not identify these issues before publication and have since put additional measures in place to safeguard research integrity.

We wish to credit our own Research Integrity and Research Publishing teams and anonymous and named external researchers and research integrity experts for contributing to this investigation.

The corresponding author, as the representative of all authors, has been given the opportunity to register their agreement or disagreement to this retraction. We have kept a record of any response received.

## References

- [1] Y. Wen and S. Peng, "Cultivation of Students' Independent Learning Ability in Teaching Chinese as a Foreign Language Based on the CDIO Model of Guiding Data Structures and Hidden Markov Algorithms," *Security and Communication Networks*, vol. 2022, Article ID 7114217, 7 pages, 2022.

## Retraction

# Retracted: Dance Movement Recognition Based on Modified GMM-Based Motion Target Detection Algorithm

### Security and Communication Networks

Received 10 October 2023; Accepted 10 October 2023; Published 11 October 2023

Copyright © 2023 Security and Communication Networks. This is an open access article distributed under the Creative Commons Attribution License, which permits unrestricted use, distribution, and reproduction in any medium, provided the original work is properly cited.

This article has been retracted by Hindawi following an investigation undertaken by the publisher [1]. This investigation has uncovered evidence of one or more of the following indicators of systematic manipulation of the publication process:

- (1) Discrepancies in scope
- (2) Discrepancies in the description of the research reported
- (3) Discrepancies between the availability of data and the research described
- (4) Inappropriate citations
- (5) Incoherent, meaningless and/or irrelevant content included in the article
- (6) Peer-review manipulation

The presence of these indicators undermines our confidence in the integrity of the article's content and we cannot, therefore, vouch for its reliability. Please note that this notice is intended solely to alert readers that the content of this article is unreliable. We have not investigated whether authors were aware of or involved in the systematic manipulation of the publication process.

In addition, our investigation has also shown that one or more of the following human-subject reporting requirements has not been met in this article: ethical approval by an Institutional Review Board (IRB) committee or equivalent, patient/participant consent to participate, and/or agreement to publish patient/participant details (where relevant).

Wiley and Hindawi regrets that the usual quality checks did not identify these issues before publication and have since put additional measures in place to safeguard research integrity.

We wish to credit our own Research Integrity and Research Publishing teams and anonymous and named external researchers and research integrity experts for contributing to this investigation.

The corresponding author, as the representative of all authors, has been given the opportunity to register their agreement or disagreement to this retraction. We have kept a record of any response received.

### References

- [1] J. Tian and X. Yang, "Dance Movement Recognition Based on Modified GMM-Based Motion Target Detection Algorithm," *Security and Communication Networks*, vol. 2022, Article ID 6023784, 12 pages, 2022.

## Retraction

# Retracted: Research on the Effective Fusion of Traditional Art and Old Street Culture Construction Based on Fuzzy Algorithm

### Security and Communication Networks

Received 3 October 2023; Accepted 3 October 2023; Published 4 October 2023

Copyright © 2023 Security and Communication Networks. This is an open access article distributed under the Creative Commons Attribution License, which permits unrestricted use, distribution, and reproduction in any medium, provided the original work is properly cited.

This article has been retracted by Hindawi following an investigation undertaken by the publisher [1]. This investigation has uncovered evidence of one or more of the following indicators of systematic manipulation of the publication process:

- (1) Discrepancies in scope
- (2) Discrepancies in the description of the research reported
- (3) Discrepancies between the availability of data and the research described
- (4) Inappropriate citations
- (5) Incoherent, meaningless and/or irrelevant content included in the article
- (6) Peer-review manipulation

The presence of these indicators undermines our confidence in the integrity of the article's content and we cannot, therefore, vouch for its reliability. Please note that this notice is intended solely to alert readers that the content of this article is unreliable. We have not investigated whether authors were aware of or involved in the systematic manipulation of the publication process.

Wiley and Hindawi regrets that the usual quality checks did not identify these issues before publication and have since put additional measures in place to safeguard research integrity.

We wish to credit our own Research Integrity and Research Publishing teams and anonymous and named external researchers and research integrity experts for contributing to this investigation.

The corresponding author, as the representative of all authors, has been given the opportunity to register their agreement or disagreement to this retraction. We have kept a record of any response received.

### References

- [1] M. Gong, "Research on the Effective Fusion of Traditional Art and Old Street Culture Construction Based on Fuzzy Algorithm," *Security and Communication Networks*, vol. 2022, Article ID 9616634, 9 pages, 2022.

## Retraction

# Retracted: Value Assessment for a Theory-Oriented Flipped Classroom of Physical Education Based on Multi-Source Data Analysis

### Security and Communication Networks

Received 8 August 2023; Accepted 8 August 2023; Published 9 August 2023

Copyright © 2023 Security and Communication Networks. This is an open access article distributed under the Creative Commons Attribution License, which permits unrestricted use, distribution, and reproduction in any medium, provided the original work is properly cited.

This article has been retracted by Hindawi following an investigation undertaken by the publisher [1]. This investigation has uncovered evidence of one or more of the following indicators of systematic manipulation of the publication process:

- (1) Discrepancies in scope
- (2) Discrepancies in the description of the research reported
- (3) Discrepancies between the availability of data and the research described
- (4) Inappropriate citations
- (5) Incoherent, meaningless and/or irrelevant content included in the article
- (6) Peer-review manipulation

The presence of these indicators undermines our confidence in the integrity of the article's content and we cannot, therefore, vouch for its reliability. Please note that this notice is intended solely to alert readers that the content of this article is unreliable. We have not investigated whether authors were aware of or involved in the systematic manipulation of the publication process.

Wiley and Hindawi regrets that the usual quality checks did not identify these issues before publication and have since put additional measures in place to safeguard research integrity.

We wish to credit our own Research Integrity and Research Publishing teams and anonymous and named external researchers and research integrity experts for contributing to this investigation.

The corresponding author, as the representative of all authors, has been given the opportunity to register their agreement or disagreement to this retraction. We have kept a record of any response received.

### References

- [1] N. Li, "Value Assessment for a Theory-Oriented Flipped Classroom of Physical Education Based on Multi-Source Data Analysis," *Security and Communication Networks*, vol. 2022, Article ID 6540710, 9 pages, 2022.



## Retraction

# Retracted: Analysis of Practical Training Characteristics and Teaching System Reform Path of College Physical Education Curriculum Based on Deep Learning

### Security and Communication Networks

Received 8 August 2023; Accepted 8 August 2023; Published 9 August 2023

Copyright © 2023 Security and Communication Networks. This is an open access article distributed under the Creative Commons Attribution License, which permits unrestricted use, distribution, and reproduction in any medium, provided the original work is properly cited.

This article has been retracted by Hindawi following an investigation undertaken by the publisher [1]. This investigation has uncovered evidence of one or more of the following indicators of systematic manipulation of the publication process:

- (1) Discrepancies in scope
- (2) Discrepancies in the description of the research reported
- (3) Discrepancies between the availability of data and the research described
- (4) Inappropriate citations
- (5) Incoherent, meaningless and/or irrelevant content included in the article
- (6) Peer-review manipulation

The presence of these indicators undermines our confidence in the integrity of the article's content and we cannot, therefore, vouch for its reliability. Please note that this notice is intended solely to alert readers that the content of this article is unreliable. We have not investigated whether authors were aware of or involved in the systematic manipulation of the publication process.

In addition, our investigation has also shown that one or more of the following human-subject reporting requirements has not been met in this article: ethical approval by an Institutional Review Board (IRB) committee or equivalent, patient/participant consent to participate, and/or agreement to publish patient/participant details (where relevant).

Wiley and Hindawi regrets that the usual quality checks did not identify these issues before publication and have since put additional measures in place to safeguard research integrity.

We wish to credit our own Research Integrity and Research Publishing teams and anonymous and named external researchers and research integrity experts for contributing to this investigation.

The corresponding author, as the representative of all authors, has been given the opportunity to register their agreement or disagreement to this retraction. We have kept a record of any response received.

### References

- [1] P. Fang, "Analysis of Practical Training Characteristics and Teaching System Reform Path of College Physical Education Curriculum Based on Deep Learning," *Security and Communication Networks*, vol. 2022, Article ID 9614356, 13 pages, 2022.

## Retraction

# Retracted: Visual Feature Evaluation of Shenyang Greenway Landscape Based on Deep Learning

### Security and Communication Networks

Received 8 August 2023; Accepted 8 August 2023; Published 9 August 2023

Copyright © 2023 Security and Communication Networks. This is an open access article distributed under the Creative Commons Attribution License, which permits unrestricted use, distribution, and reproduction in any medium, provided the original work is properly cited.

This article has been retracted by Hindawi following an investigation undertaken by the publisher [1]. This investigation has uncovered evidence of one or more of the following indicators of systematic manipulation of the publication process:

- (1) Discrepancies in scope
- (2) Discrepancies in the description of the research reported
- (3) Discrepancies between the availability of data and the research described
- (4) Inappropriate citations
- (5) Incoherent, meaningless and/or irrelevant content included in the article
- (6) Peer-review manipulation

The presence of these indicators undermines our confidence in the integrity of the article's content and we cannot, therefore, vouch for its reliability. Please note that this notice is intended solely to alert readers that the content of this article is unreliable. We have not investigated whether authors were aware of or involved in the systematic manipulation of the publication process.

Wiley and Hindawi regrets that the usual quality checks did not identify these issues before publication and have since put additional measures in place to safeguard research integrity.

We wish to credit our own Research Integrity and Research Publishing teams and anonymous and named external researchers and research integrity experts for contributing to this investigation.

The corresponding author, as the representative of all authors, has been given the opportunity to register their agreement or disagreement to this retraction. We have kept a record of any response received.

### References

- [1] T. Pan and M. Jiang, "Visual Feature Evaluation of Shenyang Greenway Landscape Based on Deep Learning," *Security and Communication Networks*, vol. 2022, Article ID 8730399, 11 pages, 2022.

## Retraction

# Retracted: Material Analysis and Application Based on Intelligent Computing in the Context of Contemporary Watercolor Painting

### Security and Communication Networks

Received 8 August 2023; Accepted 8 August 2023; Published 9 August 2023

Copyright © 2023 Security and Communication Networks. This is an open access article distributed under the Creative Commons Attribution License, which permits unrestricted use, distribution, and reproduction in any medium, provided the original work is properly cited.

This article has been retracted by Hindawi following an investigation undertaken by the publisher [1]. This investigation has uncovered evidence of one or more of the following indicators of systematic manipulation of the publication process:

- (1) Discrepancies in scope
- (2) Discrepancies in the description of the research reported
- (3) Discrepancies between the availability of data and the research described
- (4) Inappropriate citations
- (5) Incoherent, meaningless and/or irrelevant content included in the article
- (6) Peer-review manipulation

The presence of these indicators undermines our confidence in the integrity of the article's content and we cannot, therefore, vouch for its reliability. Please note that this notice is intended solely to alert readers that the content of this article is unreliable. We have not investigated whether authors were aware of or involved in the systematic manipulation of the publication process.

Wiley and Hindawi regrets that the usual quality checks did not identify these issues before publication and have since put additional measures in place to safeguard research integrity.

We wish to credit our own Research Integrity and Research Publishing teams and anonymous and named external researchers and research integrity experts for contributing to this investigation.

The corresponding author, as the representative of all authors, has been given the opportunity to register their agreement or disagreement to this retraction. We have kept a record of any response received.

### References

- [1] J. Feng and Y. Zhang, "Material Analysis and Application Based on Intelligent Computing in the Context of Contemporary Watercolor Painting," *Security and Communication Networks*, vol. 2022, Article ID 9517615, 10 pages, 2022.

## Retraction

# Retracted: Improving and Evaluating Business Management in the Digital Economy Based on Data Analysis

### Security and Communication Networks

Received 8 August 2023; Accepted 8 August 2023; Published 9 August 2023

Copyright © 2023 Security and Communication Networks. This is an open access article distributed under the Creative Commons Attribution License, which permits unrestricted use, distribution, and reproduction in any medium, provided the original work is properly cited.

This article has been retracted by Hindawi following an investigation undertaken by the publisher [1]. This investigation has uncovered evidence of one or more of the following indicators of systematic manipulation of the publication process:

- (1) Discrepancies in scope
- (2) Discrepancies in the description of the research reported
- (3) Discrepancies between the availability of data and the research described
- (4) Inappropriate citations
- (5) Incoherent, meaningless and/or irrelevant content included in the article
- (6) Peer-review manipulation

The presence of these indicators undermines our confidence in the integrity of the article's content and we cannot, therefore, vouch for its reliability. Please note that this notice is intended solely to alert readers that the content of this article is unreliable. We have not investigated whether authors were aware of or involved in the systematic manipulation of the publication process.

Wiley and Hindawi regrets that the usual quality checks did not identify these issues before publication and have since put additional measures in place to safeguard research integrity.

We wish to credit our own Research Integrity and Research Publishing teams and anonymous and named external researchers and research integrity experts for contributing to this investigation.

The corresponding author, as the representative of all authors, has been given the opportunity to register their agreement or disagreement to this retraction. We have kept a record of any response received.

### References

- [1] L. Sun and Y. Wang, "Improving and Evaluating Business Management in the Digital Economy Based on Data Analysis," *Security and Communication Networks*, vol. 2022, Article ID 5908877, 7 pages, 2022.

## Retraction

# Retracted: Research on Optimal Route Planning for Self-Driving Tour Based on Road Network Structure

### Security and Communication Networks

Received 8 August 2023; Accepted 8 August 2023; Published 9 August 2023

Copyright © 2023 Security and Communication Networks. This is an open access article distributed under the Creative Commons Attribution License, which permits unrestricted use, distribution, and reproduction in any medium, provided the original work is properly cited.

This article has been retracted by Hindawi following an investigation undertaken by the publisher [1]. This investigation has uncovered evidence of one or more of the following indicators of systematic manipulation of the publication process:

- (1) Discrepancies in scope
- (2) Discrepancies in the description of the research reported
- (3) Discrepancies between the availability of data and the research described
- (4) Inappropriate citations
- (5) Incoherent, meaningless and/or irrelevant content included in the article
- (6) Peer-review manipulation

The presence of these indicators undermines our confidence in the integrity of the article's content and we cannot, therefore, vouch for its reliability. Please note that this notice is intended solely to alert readers that the content of this article is unreliable. We have not investigated whether authors were aware of or involved in the systematic manipulation of the publication process.

Wiley and Hindawi regrets that the usual quality checks did not identify these issues before publication and have since put additional measures in place to safeguard research integrity.

We wish to credit our own Research Integrity and Research Publishing teams and anonymous and named external researchers and research integrity experts for contributing to this investigation.

The corresponding author, as the representative of all authors, has been given the opportunity to register their agreement or disagreement to this retraction. We have kept a record of any response received.

### References

- [1] P. Zong, Y. Han, and C. Xu, "Research on Optimal Route Planning for Self-Driving Tour Based on Road Network Structure," *Security and Communication Networks*, vol. 2022, Article ID 6588288, 11 pages, 2022.

## Retraction

# Retracted: Security Research in Personnel Electronic File Management Based on Blockchain Technology

### Security and Communication Networks

Received 8 August 2023; Accepted 8 August 2023; Published 9 August 2023

Copyright © 2023 Security and Communication Networks. This is an open access article distributed under the Creative Commons Attribution License, which permits unrestricted use, distribution, and reproduction in any medium, provided the original work is properly cited.

This article has been retracted by Hindawi following an investigation undertaken by the publisher [1]. This investigation has uncovered evidence of one or more of the following indicators of systematic manipulation of the publication process:

- (1) Discrepancies in scope
- (2) Discrepancies in the description of the research reported
- (3) Discrepancies between the availability of data and the research described
- (4) Inappropriate citations
- (5) Incoherent, meaningless and/or irrelevant content included in the article
- (6) Peer-review manipulation

The presence of these indicators undermines our confidence in the integrity of the article's content and we cannot, therefore, vouch for its reliability. Please note that this notice is intended solely to alert readers that the content of this article is unreliable. We have not investigated whether authors were aware of or involved in the systematic manipulation of the publication process.

Wiley and Hindawi regrets that the usual quality checks did not identify these issues before publication and have since put additional measures in place to safeguard research integrity.

We wish to credit our own Research Integrity and Research Publishing teams and anonymous and named external researchers and research integrity experts for contributing to this investigation.

The corresponding author, as the representative of all authors, has been given the opportunity to register their agreement or disagreement to this retraction. We have kept a record of any response received.

### References

- [1] H. Wang and J. Zhang, "Security Research in Personnel Electronic File Management Based on Blockchain Technology," *Security and Communication Networks*, vol. 2022, Article ID 7875825, 8 pages, 2022.

## Retraction

# Retracted: Evaluation and Application of College English Mixed Flipping Classroom Teaching Quality Based on the Fuzzy Judgment Model

### Security and Communication Networks

Received 8 August 2023; Accepted 8 August 2023; Published 9 August 2023

Copyright © 2023 Security and Communication Networks. This is an open access article distributed under the Creative Commons Attribution License, which permits unrestricted use, distribution, and reproduction in any medium, provided the original work is properly cited.

This article has been retracted by Hindawi following an investigation undertaken by the publisher [1]. This investigation has uncovered evidence of one or more of the following indicators of systematic manipulation of the publication process:

- (1) Discrepancies in scope
- (2) Discrepancies in the description of the research reported
- (3) Discrepancies between the availability of data and the research described
- (4) Inappropriate citations
- (5) Incoherent, meaningless and/or irrelevant content included in the article
- (6) Peer-review manipulation

The presence of these indicators undermines our confidence in the integrity of the article's content and we cannot, therefore, vouch for its reliability. Please note that this notice is intended solely to alert readers that the content of this article is unreliable. We have not investigated whether authors were aware of or involved in the systematic manipulation of the publication process.

In addition, our investigation has also shown that one or more of the following human-subject reporting requirements has not been met in this article: ethical approval by an Institutional Review Board (IRB) committee or equivalent, patient/participant consent to participate, and/or agreement to publish patient/participant details (where relevant).

Wiley and Hindawi regrets that the usual quality checks did not identify these issues before publication and have since put additional measures in place to safeguard research integrity.

We wish to credit our own Research Integrity and Research Publishing teams and anonymous and named external researchers and research integrity experts for contributing to this investigation.

The corresponding author, as the representative of all authors, has been given the opportunity to register their agreement or disagreement to this retraction. We have kept a record of any response received.

### References

- [1] X. Gao, "Evaluation and Application of College English Mixed Flipping Classroom Teaching Quality Based on the Fuzzy Judgment Model," *Security and Communication Networks*, vol. 2022, Article ID 9611611, 9 pages, 2022.

## Retraction

# Retracted: Evaluation of Political Classroom Teaching Quality in Universities Based on DA-BP Algorithm

### Security and Communication Networks

Received 1 August 2023; Accepted 1 August 2023; Published 2 August 2023

Copyright © 2023 Security and Communication Networks. This is an open access article distributed under the Creative Commons Attribution License, which permits unrestricted use, distribution, and reproduction in any medium, provided the original work is properly cited.

This article has been retracted by Hindawi following an investigation undertaken by the publisher [1]. This investigation has uncovered evidence of one or more of the following indicators of systematic manipulation of the publication process:

- (1) Discrepancies in scope
- (2) Discrepancies in the description of the research reported
- (3) Discrepancies between the availability of data and the research described
- (4) Inappropriate citations
- (5) Incoherent, meaningless and/or irrelevant content included in the article
- (6) Peer-review manipulation

The presence of these indicators undermines our confidence in the integrity of the article's content and we cannot, therefore, vouch for its reliability. Please note that this notice is intended solely to alert readers that the content of this article is unreliable. We have not investigated whether authors were aware of or involved in the systematic manipulation of the publication process.

Wiley and Hindawi regrets that the usual quality checks did not identify these issues before publication and have since put additional measures in place to safeguard research integrity.

We wish to credit our own Research Integrity and Research Publishing teams and anonymous and named external researchers and research integrity experts for contributing to this investigation.

The corresponding author, as the representative of all authors, has been given the opportunity to register their agreement or disagreement to this retraction. We have kept a record of any response received.

### References

- [1] H. Guan and D. Zhu, "Evaluation of Political Classroom Teaching Quality in Universities Based on DA-BP Algorithm," *Security and Communication Networks*, vol. 2022, Article ID 3391881, 10 pages, 2022.



## *Retraction*

# **Retracted: Analysis of Management Innovation of State-Owned Enterprises in the Context of Artificial Intelligence and Market-Oriented Economic Fluctuations**

### **Security and Communication Networks**

Received 1 August 2023; Accepted 1 August 2023; Published 2 August 2023

Copyright © 2023 Security and Communication Networks. This is an open access article distributed under the Creative Commons Attribution License, which permits unrestricted use, distribution, and reproduction in any medium, provided the original work is properly cited.

This article has been retracted by Hindawi following an investigation undertaken by the publisher [1]. This investigation has uncovered evidence of one or more of the following indicators of systematic manipulation of the publication process:

- (1) Discrepancies in scope
- (2) Discrepancies in the description of the research reported
- (3) Discrepancies between the availability of data and the research described
- (4) Inappropriate citations
- (5) Incoherent, meaningless and/or irrelevant content included in the article
- (6) Peer-review manipulation

The presence of these indicators undermines our confidence in the integrity of the article's content and we cannot, therefore, vouch for its reliability. Please note that this notice is intended solely to alert readers that the content of this article is unreliable. We have not investigated whether authors were aware of or involved in the systematic manipulation of the publication process.

Wiley and Hindawi regrets that the usual quality checks did not identify these issues before publication and have since put additional measures in place to safeguard research integrity.

We wish to credit our own Research Integrity and Research Publishing teams and anonymous and named external researchers and research integrity experts for contributing to this investigation.

The corresponding author, as the representative of all authors, has been given the opportunity to register their agreement or disagreement to this retraction. We have kept a record of any response received.

### **References**

- [1] Y. Wang and L. Sun, "Analysis of Management Innovation of State-Owned Enterprises in the Context of Artificial Intelligence and Market-Oriented Economic Fluctuations," *Security and Communication Networks*, vol. 2022, Article ID 1518447, 10 pages, 2022.

## Retraction

# Retracted: A Novel Maximum Flow Algorithm with Neural Network for Time-Varying Wastage Networks

### Security and Communication Networks

Received 1 August 2023; Accepted 1 August 2023; Published 2 August 2023

Copyright © 2023 Security and Communication Networks. This is an open access article distributed under the Creative Commons Attribution License, which permits unrestricted use, distribution, and reproduction in any medium, provided the original work is properly cited.

This article has been retracted by Hindawi following an investigation undertaken by the publisher [1]. This investigation has uncovered evidence of one or more of the following indicators of systematic manipulation of the publication process:

- (1) Discrepancies in scope
- (2) Discrepancies in the description of the research reported
- (3) Discrepancies between the availability of data and the research described
- (4) Inappropriate citations
- (5) Incoherent, meaningless and/or irrelevant content included in the article
- (6) Peer-review manipulation

The presence of these indicators undermines our confidence in the integrity of the article's content and we cannot, therefore, vouch for its reliability. Please note that this notice is intended solely to alert readers that the content of this article is unreliable. We have not investigated whether authors were aware of or involved in the systematic manipulation of the publication process.

Wiley and Hindawi regrets that the usual quality checks did not identify these issues before publication and have since put additional measures in place to safeguard research integrity.

We wish to credit our own Research Integrity and Research Publishing teams and anonymous and named external researchers and research integrity experts for contributing to this investigation.

The corresponding author, as the representative of all authors, has been given the opportunity to register their agreement or disagreement to this retraction. We have kept a record of any response received.

### References

- [1] B. Zhang, K. Jiang, and W. Huang, "A Novel Maximum Flow Algorithm with Neural Network for Time-Varying Wastage Networks," *Security and Communication Networks*, vol. 2022, Article ID 3782761, 9 pages, 2022.

## Retraction

# Retracted: Modeling and Analysis Method of National Fitness Big Data for Basketball Projects Based on a Multivariate Statistical Model

### Security and Communication Networks

Received 1 August 2023; Accepted 1 August 2023; Published 2 August 2023

Copyright © 2023 Security and Communication Networks. This is an open access article distributed under the Creative Commons Attribution License, which permits unrestricted use, distribution, and reproduction in any medium, provided the original work is properly cited.

This article has been retracted by Hindawi following an investigation undertaken by the publisher [1].

This investigation has uncovered evidence of one or more of the following indicators of systematic manipulation of the publication process:

- (1) Discrepancies in scope
- (2) Discrepancies in the description of the research reported
- (3) Discrepancies between the availability of data and the research described
- (4) Inappropriate citations
- (5) Incoherent, meaningless and/or irrelevant content included in the article
- (6) Peer-review manipulation

The presence of these indicators undermines our confidence in the integrity of the article's content and we cannot, therefore, vouch for its reliability. Please note that this notice is intended solely to alert readers that the content of this article is unreliable. We have not investigated whether authors were aware of or involved in the systematic manipulation of the publication process.

Wiley and Hindawi regrets that the usual quality checks did not identify these issues before publication and have since put additional measures in place to safeguard research integrity.

We wish to credit our own Research Integrity and Research Publishing teams and anonymous and named external researchers and research integrity experts for contributing to this investigation.

The corresponding author, as the representative of all authors, has been given the opportunity to register their agreement or disagreement to this retraction. We have kept a record of any response received.

### References

- [1] Q. Zhao, "Modeling and Analysis Method of National Fitness Big Data for Basketball Projects Based on a Multivariate Statistical Model," *Security and Communication Networks*, vol. 2022, Article ID 2591633, 11 pages, 2022.

## *Retraction*

# **Retracted: Component-Based Software Testing Method Based on Deep Adversarial Network**

### **Security and Communication Networks**

Received 26 December 2023; Accepted 26 December 2023; Published 29 December 2023

Copyright © 2023 Security and Communication Networks. This is an open access article distributed under the Creative Commons Attribution License, which permits unrestricted use, distribution, and reproduction in any medium, provided the original work is properly cited.

This article has been retracted by Hindawi, as publisher, following an investigation undertaken by the publisher [1]. This investigation has uncovered evidence of systematic manipulation of the publication and peer-review process. We cannot, therefore, vouch for the reliability or integrity of this article.

Please note that this notice is intended solely to alert readers that the peer-review process of this article has been compromised.

Wiley and Hindawi regret that the usual quality checks did not identify these issues before publication and have since put additional measures in place to safeguard research integrity.

We wish to credit our Research Integrity and Research Publishing teams and anonymous and named external researchers and research integrity experts for contributing to this investigation.

The corresponding author, as the representative of all authors, has been given the opportunity to register their agreement or disagreement to this retraction. We have kept a record of any response received.

### **References**

- [1] W. Fu and L. Wang, "Component-Based Software Testing Method Based on Deep Adversarial Network," *Security and Communication Networks*, vol. 2022, Article ID 4231083, 11 pages, 2022.

## Research Article

# Component-Based Software Testing Method Based on Deep Adversarial Network

Weiyu Fu <sup>1,2</sup> and Lixia Wang <sup>3,4</sup>

<sup>1</sup>School of Computer Science & Technology, China University of Mining and Technology, Xuzhou 221116, Jiangsu, China

<sup>2</sup>Jiangsu Vocational College of Finance and Economics, Huai'an 223003, Jiangsu, China

<sup>3</sup>School of Business Administration, Henan Polytechnic University, Jiaozuo 454003, Henan, China

<sup>4</sup>School of Management, China University of Mining and Technology, Xuzhou 221116, Jiangsu, China

Correspondence should be addressed to Weiyu Fu; 19800341@jscj.edu.cn

Received 18 July 2022; Revised 5 September 2022; Accepted 16 September 2022; Published 12 October 2022

Academic Editor: Hangjun Che

Copyright © 2022 Weiyu Fu and Lixia Wang. This is an open access article distributed under the Creative Commons Attribution License, which permits unrestricted use, distribution, and reproduction in any medium, provided the original work is properly cited.

With the continuous updating and application of software, the current problems in software are becoming more and more serious. Aiming at this phenomenon, the application and testing methods of componentized software based on deep adversarial networks are discussed. The experiments show that: (1) some of the software has a high fusion rate, reaching an astonishing 95% adaptability. The instability and greater potential of component-based software are solved through GAN and gray evaluation. With the evaluation system, people are dispelled. Trust degree. (2) According to the data in the graph and table, the deep learning adversarial network solves the vulnerability and closedness of the general network, and the built-in test method with experimental data reaching an average accuracy rate of 90% is the best test method for this system. With the deep learning adversarial network, the average test level of component-based software reaches level 7, which makes the new software industry of component-based software have a long way to go.

## 1. Introduction

We present an in-depth study of reconstruction strategies based on CS-MRI and bridge the gap between untrained traditional methods for processing single image data and prior knowledge of large training datasets. We also propose a new conditional generative deep adversarial network model used in appeal research, and we join forces to sacrifice enemies and sacrifice creative materials to better preserve reconstructed textures and contours. Furthermore, we incorporate frequency band information to improve image and frequency range similarity. We conducted a comprehensive comparative study of traditional CSMRI reconstruction methods and recently explored in-depth research methods. Compared to these methods, our DAGAN method provides excellent reproduction and preservation of identifiable details in images [1]. Deep adversarial networks have been quite new in recent years, and we demonstrate our

recent improvements to the deep adversarial network learning event analysis workflow that improve the continuity and density of estimated fault levels in fault regions. Historically, predictions from traditional deep learning methods and algorithms have been characterized by a “fuzzy” cloud of average probability that is well beyond the margin of error. To address this ambiguity and improve resolution reliability, we demonstrate image preprocessing using a general adversarial network (GAN) that refines seismic images for training and prediction, a honed solution [2]. The deep adversarial network provides a different learning method for (AD), which mainly cures the life problems of the elderly, mainly from their images, but we do not know whether this new learning method can be effective. Many research data are public databases, and the lack of physician participation in quantitative and comparative trials in these studies may affect the generational impact and generalizability of GAN model results. Retrospective studies demonstrate the value

of using adversarial networks in classifying AD conditions and processing AD-related images. Ultimately, this study demonstrates the improved diagnostic ability and clinical utility of deep adversarial networks for AD [3]. Virtual tissue staining using deep adversarial networks provides a realistic approach to these problems, but the use of deep learning methods remains challenging due to the very limited amount of data available for training. Based on the deep adversarial networks concept, a low-processing training method was used to generate self-luminous images of rough areas of ovarian tissue corresponding to hematoxylin-stained areas of ovarian tissue. With the above approach, we establish a controlled state for virtual color correction, which will fine-tune the quality of the finished image in the next virtual grading step [4]. We introduce a new end-to-end multiscale temporal edge aggregation (MTPA) network, which belongs to a class of deep adversarial networks and which proposes MTPA to reduce the temporal and current properties of the reference frame. These MTPA functions are used to drive individual decoders to overcome lost connections. To achieve realistic and consistent foreground components, properly scaling the above frame outputs will give the correct MTPA performance for each decoder input. The performance analysis of the proposed method is validated using CDnet 2014 and the lowest video database [5]. Constructed software is an important part of software development. It can provide considerable benefits in the long run. A high degree of research into it can greatly improve software functions and reduce human costs. The reorganization system is described, the model of the constructed software is investigated and analyzed, and its characteristics are evaluated [6]. The advantages of built-in software are reusability and interoperability, which raises questions about its competitiveness and operation. Reforming and adjusting it through various professional development tools make the built-in software more convenient. These incompatible standards have different object models, repository models, and application protocols that are defined. This incompatibility confuses the market, as ISVs, system integrators, in-house developers, and end users all struggle to understand the relative strengths and weaknesses of standards and the opportunities to be successful in the business. We then examined the recommended OpenDoc, OLE 2, COM, and CORBA standards for both technologies [7]. Constructed software development is recognized as an effective method to improve the efficiency and quality of software development and is widely used to build software systems. However, current software component technologies mainly focus on component implementation patterns and runtime interoperability because they lack a systematic approach to control the entire development process. In recent years, software architecture (SA) research has made great progress. It takes the component as the basic unit and provides a top-down approach for component-driven development by describing the general structure and characteristics of the software system [8]. The role of component-based software in creating an intelligent environment is discussed. A systematic description of the future knowledge environment of the campus. This scenario shows how software components

affect the different stages of development, distribution, and use in a cognitive environment. The main research areas are identified as component architecture, component interface standards, input systems, and protocol development [9]. Component-based software is the embodiment of assembling software. It integrates their advantages to meet the heights they could not reach before, including CBD and related materials to improve software reusability. In addition to improving software reusability, a component view also provides a better understanding of architecture, search, usage, and listing. It is mainly about the correct presentation of components, which ultimately helps programmers to reuse software, which is highly desirable when developing component-based software [10]. Stereotaxic impression anomalies were examined using different tests with two stimuli: (1) a random strong display of stereoscopic contours consisting of a random factor template, and (2) residual images of different physical contours on the retina. The results of these three experiments showed that most individuals classified as the standard imaging variant functioned normally under short exposure conditions, which allowed longer studies to exclude eye movements. These results suggest that the previously reported abnormality in stereo vision is related to the experimental approach rather than to the underlying neurological deficit [11]. The rodent touchscreen test is an automated, computer-assisted behavioral test that allows rodents to graphically display computer-generated stimuli, and the rodents respond to the stimuli directly through the nose. The benefits of this approach are numerous and well-tested, and the mouse can make this distinction well with optimized parameters. Taken together, these experiments optimize the touchscreen method and demonstrate its utility as a high-throughput cognitive test in rodents [12]. A time-based transient test method was developed to rapidly measure array variables and other frequency-dependent properties of centrifugal and noncentrifugal loudspeakers. This method is suitable for systems with random or intermittent high flow rates. Flow and flow experiments were performed on laboratory models of exhaust mufflers, variable channels, and complex channel systems. There is good agreement between theoretical and experimental results. These results not only demonstrate the feasibility of this experimental technique in various practical disciplines but also confirm some unverified theoretical hypotheses through comparison with experimental results [13]. Two in vitro systems were compared to evaluate the pharmacological effects of several plants on (AA) transformation; the first system involved the addition of serum from mice given the herbal medicine, and the second system involved the direct addition of plant extracts to the fermenter middle. Indomethacin, used as a controlled drug, inhibited AA metabolism in a dose-dependent manner in both experimental systems. Direct mixing of rhubarb and ginger extracts in hot water also inhibited AA conversion, while Huanglian and Baishao granule extracts had no effect [14].

Symbolic execution is a powerful software testing method that can catch many types of bugs. However, it has the problem of destroying the traces, and when using only

statements, it still lacks the actual legitimacy of thoroughly testing the traces according to the correct formula. After experimentation, this method carefully handles the relationship between routing and script requests to limit the unification route discovery [15].

## 2. Component Software Analysis

*2.1. Basic Steps of Component Software Development.* In component-based software development, problem analysis and modeling are the first steps. The purpose of software development is to serve and communicate applications, so the problem the software is designed to solve must be clearly assessed. Once the key functions of the software are predicted, the problem is analyzed in detail and then shaped to make the domain and model of each software component more accurate. Better interpretability is manifested by UML models with higher problem areas and model accuracy. Solution domain model design: designing a solution website model is another step in software-based software development. After the analysis has determined the problem area, the problem of the problem area must be solved, which requires the improvement of a solution area. The local problem is accurately modeled and analyzed, and the residential model is obtained. The so-called real neighborhood model refers to the necessary components and architecture of the system. When developing the domain model of the solution, the visual interface is checked for recycled material so that we can determine which components to incorporate and whether new components can be calculated. Finally, the rational and scientific design of the decision point model can guarantee the use of the largest component that matches the basic parameters of the perfect decision point. Component development and assembly: in the component-based software development process, the third important step is to create and assemble components. Based on the problem area and solution area analysis, components are selected from the component library, and then their interface is extended to fit the current project. Use newly developed software components to store them in a component library to make it easier to use the software later. For the component to work, you must also apply it to the current project. After assembly, the entire system is used for quality control. After the test results are qualified, the running software can be released.

*2.2. The Structure of Componentized Software Architecture.* The basic idea of traditional software architecture is vertical layering, and the concept of rules and their destruction is also very useful in component systems. Different from traditional software architectures, component systems not only have a vertical structure but also have a multilayered horizontal structure. This is mainly due to the uniqueness of the component system. Unlike classes and units in traditional software, the smallest unit considered in a componentized system is a component. A specific entry has no meaning. It can only be loaded, activated, and communicated in a specific context and must reside in a framework or ingredient container; the component framework can provide

the necessary protocols for component connectivity while performing site-specific rules. Smaller systems can often be implemented using a component structure; large complex systems require multiple frameworks, and integrating many components requires a higher-level implementation. A component is the basic unit that performs system functions, similar to the actual unit of traditional software, and performs all phases of system operation by combining instances. The components that make up the main vertical structure of the system. System components and frameworks are responsible for management components and collaboration components, respectively, and some software architectures are two-layer structures, including three-layer horizontal structures and multilayer vertical structures. The horizontal structure is fixed and includes components, component frames, and system frames. Each horizontal layer consists of its own vertical structure, the high layer integrates the lower layer by sharing multiple vertical layers, the component framework integrates the component layer by sharing the component communication script layer, and the system framework integrates the infrastructure by sharing the platform media.

*2.3. Analyze Component Library in Componentized Software.* For efficient management of a large number of component collections, as well as fast and convenient component storage and retrieval, there are currently about four types of component catalogs: project-oriented, domain-specific, shared-oriented, and market-driven. They are getting bigger, the target range is getting clearer, and their reuse time is getting bigger and bigger. Because of the different orientations of the objects, the component library handles objects differently. However, a general component library must meet the following requirements: (1) Ease of use: support component management, including adding, deleting, modifying components, unregistering, and unpacking components; (2) Integrity: including domain integrity and component integrity. Incorporating a component list into a specific domain must cover the entire domain, and the corresponding information about the component must be complete to facilitate the search, understanding, and reuse of the component; (3) Rationality: the compositional logical organization of the component list and the classification method for storing components, reasonably storing ingredients to facilitate the expansion, maintenance, and restoration of ingredient lists; (4) Compatibility: components must share components with other components to a certain extent. This requires common and standardized component storage and management; (5) Availability: both library administrators and ordinary users can easily use the component library.

*2.4. Comparison of Component Software Development and Traditional Software Development.* Traditional software development technology is a unique development method. For example, a company always wants to build a huge system to cover all companies and all subsidiaries that need to use it. Is this setting the same as the 4G base station setting? In this model, services “closer” to the central office are harder to use

than services that are further away from the central office. Even for some very specific companies, the system may not meet the requirements at all, causing many companies to spend a lot of money on ERP systems with low efficiency. In fact, their development ideas are centralized, unified, and fragmented, which inevitably leads to rigidity and fragility and cannot meet the local needs of individuals.

The same is true for component-based software development. We revolutionized software development and adopted a downgrade, standardize, and share model. We decompose functional units into small, indivisible units, and then expand each unit into practical components. This development is based on standard communication and then assembling these small unit components. They are connected into an organic whole by machines like neural networks. This method is easier to design, more efficient to design, and can ensure that each part adopts a separate method, thereby ensuring the efficiency of the system. At the same time, each organization transmits data in a shared way, which not only ensures the independence of each organization but also ensures the interaction between data and realizes the connection of all data systems. Constantly expanding information so that software development itself becomes possible. As we all know, each component is actually a component of its processor. These microprocessor components have deepened the understanding of the industry, and the artificial intelligence that shapes big data over time. Processing items will be developed and reworked. In the near future, software development will no longer require humans, but the software itself can develop the corresponding components as needed. It is then collected in the body. We know that in the biological world, it is easier for single-celled organisms to grow and mutate, and the more complex the organism, the more difficult it is to reproduce. When we break software down into small components, we lay the groundwork for our own replication and development. And our main engine, like a neural network, organizes these simple elements into giant creatures that develop complex scenarios on their own. The concept of building software development using component technology will drive future software engineering to transform traditional enterprise-style development into standard development and ultimately automate development.

### 3. Research on the Model of Componentized Software under Deep Adversarial Networks

The GAN model, constraint algorithm, and gray model are used for the component-based software testing method based on the deep adversarial network. This model has a complete system that records the information of the new, crown-infected person into the database, including model optimization technology, even if it is normal to have a little error. After all, there are too many factors to be considered in the system. The psychological characteristics and cognitive characteristics generated by the continuous development of international Chinese education in foreign countries will also be constantly changing and updated. The system effectively saves this data in each area.

**3.1. Generative Adversarial Networks.** GAN uses the idea of the game duo. The Internet is full of creators and discriminators trained by dissidents. The generator “tricks” the discriminator by generating virtual images similar to the training data from the input images. The difference is to distinguish the real data from the generated and returned virtual data and use its evaluation results for the generator. The generator is recycled according to the results to create more realistic images, such that the generator and the differentiator are balanced, and the target action GAN can be described as follows:

$$\min \max V(D, G) = E_{x \sim p_{\text{data}}(x)} [\lg D(x)] + E_{Z \sim P(Z)} [\lg (1 - D(G(Z)))]. \quad (1)$$

Formula (1) represents GAN, where the whole formula represents the relationship between the discriminator and the generator,  $X$  represents some data generated by the generator, and  $p_{\text{data}}(x)$  indicates the existence of these data. The first part of the formula is the discriminator, and the second part is the expression of the generator. Only when they reach a stable state, we can use the deep adversarial network normally. So, we have to strengthen this aspect of construction to avoid system instability.

Among them,  $X$  represents the input data,  $p_{\text{data}}(x)$  represents the location of the data,  $Z$  represents noise, and  $P(Z)$  is the location of the adversarial network. This entire formula indicates that the decider  $D$  can accurately capture the generated image, when  $D(G(Z))$ . The closer it is to 0, the smaller its result is; when  $D(G(Z))$ . When it is closer to 1, its result is the largest, and finally, when  $D(G(Z))$  it is equal to 0.5, the network reaches an equilibrium state. When balanced, it will automatically generate two deep adversarial network models for componentized software, which are expressed as follows:

$$3.2 \text{ Probabili} P(x) = \varepsilon \left( 1 + \frac{1}{1 - \beta} \right) + \lg D(x), \quad (2)$$

$$P(y) = \varepsilon \left( 1 + \frac{1}{1 - \eta} \right) + \lg D(y). \quad (3)$$

Equations (2) and (3), respectively, represent the deep adversarial network model of componentized software. They are not in a relationship of peaceful coexistence but are engaged in constant confrontation and friction in the system so that they can continue to evolve. Generate new images and constantly judge to improve the functions between them, so that the system can be continuously improved and the security and smooth running of the system can be continuously strengthened.

Generative recurrent adversarial network, the goal of CGAN is to cross-modify  $X$ -domain image data and  $Y$ -domain image data, which includes two mapping functions:

$$G = \{x \subseteq y | f(x_i) = \max f(y_i)\}, \quad (4)$$

$$F = \{y \subseteq x | f(y_i) = \max f(x_i)\}.$$

It also includes two discriminators:



$$\begin{aligned} H &= \{D_H \subseteq K | f(h_i) = \min \max V(H, K)\}, \\ J &= \{D_J \subseteq L | f(j_i) = \min \max V(D, L)\}. \end{aligned} \quad (5)$$

The discriminator output causes the  $H$  generator to transform  $h$  into the  $K$  domain. Similarly, the output  $J$  generator is transformed to  $L$  in the  $j$  domain. In the whole system, CGAN also introduces two loop attenuators:

$$\begin{aligned} F_x &= \{x \subseteq y | f(x_i) = \min f(y_i)\}, \\ F_y &= \{y \subseteq x | f(y_i) = \min f(x_i)\}. \end{aligned} \quad (6)$$

The so-called cycle means that after the image moves from the source domain to the destination domain, it can also return from the destination domain to the source domain. This formula determines the instability in the previous cycle; that is, if the image passes through the  $G$  generator from the  $X$  area and then generates  $F$ , it can still be converted into the root domain after the controller. Finally, these formulas are classified and summarized to summarize the recurrent deep adversarial network model of component software in the big data environment as follows:

$$\begin{aligned} P(M) &= \eta \left( 1 + \frac{1}{1 + \beta} \right) + \log D(M) \sum_{M \rightarrow \infty} \ln M, \\ P(N) &= \eta \left( 1 + \frac{1}{1 + \eta} \right) + \log D(N) \sum_{N \rightarrow \infty} \ln N. \end{aligned} \quad (7)$$

**3.2. The Amount of Loss during the Cycle.** In the comparison of componentized software deep adversarial networks, only using adversarial loss will lead to the problem that the network cannot retain its content and data during transformation. At this time, we solve this problem by introducing the principle of unity. For all images in the  $X$  region in the deep adversarial network, the conversion cycle is made into the original image, which is achieved by the following formula:

$$x \longrightarrow G(X) \longrightarrow F(G(X)) \approx x. \quad (8)$$

At the same time, the conversion cycle of all images in the  $y$  area into the original images  $G$  and  $F$  should also satisfy this following principle:

$$y \longrightarrow F(Y) \longrightarrow G(F(Y)) \approx y. \quad (9)$$

Summarizing the above principles yields the following general formula:

$$\begin{aligned} \kappa_{cyc}(G, F) &= \phi_{x-P_{data}(x)} [\|F(G(x)) - x\|_1] \\ &+ \phi_{y-P_{data}(y)} [\|G(F(y)) - y\|_1], \end{aligned} \quad (10)$$

where  $G(x)$  and  $G(y)$  represent the tool that acts on the pregenerated image and the tool that acts on the post-generated image,  $x$  is the image in the  $X$  area,  $y$  is the image in the  $Y$  area,  $\|F(G(x))$  and  $G(F(y))$  both are new and improved image displays. The image displayed by the deep

adversarial network system has brightness and color, and all have color and brightness loss representation. The color loss function has been implemented. By allowing the unit to generate an image with the same color distribution as the blurred color image, it minimizes the error between the blurred image and the reproduced blurred image. The corresponding function is expressed as follows:

$$\ell_{color} = \sum_p \angle(G(F(y))_p, y_p). \quad (11)$$

Where  $p$  is a pixel,  $\angle(\cdot)$  indicates that the angle between the two colors is calculated,  $y$  is the colorless image in the area  $Y$ ,  $G(F(y))$  is the reconstructed image without color, by adjusting the reconstructed image and the colorless image. The sum of the errors of each pixel in the image can solve the problem of color distortion during image editing. In the same way, the brightness of the image displayed by the deep adversarial network system can be expressed as follows:

$$\ell_{brightness} = \sum_t \angle(G(F(y))_t, y_t). \quad (12)$$

We refer to the mapping loss between adversarial networks as feature loss. After adding the feature loss, the  $G$  generator adds  $Y$ -domain image input to the original input to improve the image quality of the componentized software in the adversarial network. The feature loss formula is expressed as follows:

$$\begin{aligned} \kappa_{idt}(G, F) &= \phi_{x-P_{data}(x)} [\|F(x) - x\|_1] \\ &+ \phi_{y-P_{data}(y)} [\|G(y) - y\|_1], \end{aligned} \quad (13)$$

where  $x$  is the image in the  $X$  area and  $y$  is the image in the  $Y$  area,  $G(y)$  and  $F(x)$  represent the generators of the  $Y$  area image input and the  $X$  area image input, respectively. All losses from the improved adversarial network. The formula is expressed as follows:

$$\begin{aligned} L(G, F, D_X, D_Y) &= L_{GAN}(G, D_Y, X, Y), \\ &+ L_{GAN}(F, D_X, Y, X), \\ &+ L_{color} + \lambda L_{cycle}(G, F) + u L_{idt}(G, F). \end{aligned} \quad (14)$$

Equation (14) is the summation of all losses in the componentized software deep adversarial network system, including adversarial loss, color loss in images, uniformity loss across multiple cycles, and each of their characteristic losses. These are not all loss statistics; these are the obvious and representative losses we proposed. We mainly focus on these few to roughly solve the confrontation loss generated in the system, and other inconspicuous losses also occur, so it does not have a big impact. After solving these problems, the system will be smoother and easier to use.

In,  $L_{GAN}$  is against loss,  $L_{color}$  is the color loss,  $L_{cycle}$  is the cyclic uniformity loss,  $L_{idt}$  is the feature loss, and  $\lambda$  and  $u$  are two kinds of parameters.  $\lambda$  The value of  $u$  will not change, but its value will affect the stability of the entire system, so we need to discuss the value of  $u$  differently in the future.

**3.3. Deep Adversarial Network Model Optimization.** In order to deal with the various problems that appear above, we will solve them one by one. These problems can be roughly divided into five categories, and we use two methods to optimize them.

- ① Introduce the constraint algorithm, which is specially adjusted by professionals for color, brightness, and confrontation loss. The formula of the algorithm is expressed as follows:

$$s(u, v, z) = e^{-q \frac{|t_{ui} - t_{vi}|}{t_{\max} - t_{\min}}} + \log z(i). \quad (15)$$

Formula (15) represents the mathematical expression after optimization of color, brightness, and adversarial loss, in which the definition of max and min and the expression of the log function are introduced. This formula is a constraint condition as a whole, and  $u$ ,  $v$ , and  $z$  are the subject objects that need to be optimized. After debugging by professionals, these three problems occur in the component software systems of the deep adversarial network. Although it cannot completely solve the problem, it is not a problem to relieve and release the pressure of the system. In the future, continuous improvement and tuning are required.

Among them,  $u$ ,  $v$ , and  $z$  represent the overall object of color, brightness, and adversarial loss, respectively;  $|t_{ui} - t_{vi}|$  and  $t_{\max} - t_{\min}$  represents the constraints, and with these constraints, the problems arising from these points can be clearly solved.

- ② Introduce the precalculation recommendation function, and you will know it when you hear the name of this function. We plan to erase these two problems before they appear. Will the data be obtained through repeated deductions in the system in advance? Will it have a bad impact? If a problem is found, it will be discarded in advance. The data flows into the next step.

$$CAIC = -\ln L(a) + c \times (1 + \ln K). \quad (16)$$

**3.4. Evaluate the System.** The evaluation of the deep adversarial network model is based on the gray system theory model, which identifies the evaluation of the deep adversarial network model by combining testing, the fuzzy evaluation method, and gray system theory, and adopts consistency monitoring. The weight formula of the analysis index is

$$Ce = \frac{CE_n}{RE_n}, \quad (17)$$

where  $CE_n$  represents the  $n$ th order matrix evaluation consistency index,  $CE_n/RE_n$  represents the  $n$ -order reciprocal matrix consistency evaluation, if  $CE_n \leq 1$ . The final result is generally correct. Otherwise, the result is not credible. Create a separate factor evaluation matrix, given as follows:

$$T = \begin{bmatrix} t_{11} & t_{12} & \cdots & t_{1n} \\ t_{21} & t_{22} & \cdots & t_{2n} \\ \vdots & \vdots & \ddots & \vdots \\ t_{m1} & t_{m2} & \cdots & t_{mn} \end{bmatrix}. \quad (18)$$

Where  $T_i = (t_{i1}, t_{i2}, \dots, t_{in})$  indicates the result obtained from the evaluation of the  $i$ -th factor. Calculate the gray connection, and determine the order between the connection points, the formula is

$$p_{ij}(e) = \frac{\min_i \min_k \Delta_i(e) + p \max_i \max_k \Delta_i(e)}{\Delta_i(e) + p \max_i \max_k \Delta_i(e)}, \quad (19)$$

$$\Omega_i(k) = |A'_j(p) - A'_i(p)|. \quad (20)$$

Equation (19) is a systematic evaluation of deep adversarial networks, and (20) is a systematic evaluation of componentized software, where (19) is a systematic evaluation of deep adversarial networks, and (20) is a systematic evaluation of componentized software, where indicates various data in the deep adversarial network,  $i$  indicates that the introduced data can be replaced by a lot of data, that they can obtain the connection order of the input data through a series of changes and calculations, and finally, according to the size of the connection order calculated by them. It can be known that based on the evaluation results of these deep adversarial network models and the systematic evaluation results of the piecemeal software, the higher the relational sequence shows, the better the evaluation of the deep adversarial network model, and vice versa, the worse the evaluation of the deep adversarial network model.

Where  $p$  represents the coefficient of the resolution,  $A'_j$  represents the initial value of  $A$  like,  $p_{ij}$  indicates the order of connections between them. According to the size of the connection order, the evaluation conclusion of these deep adversarial network models can be known. The higher the connection order shows, the better the evaluation of the deep adversarial network model is. On the contrary, the worse the evaluation of the deep adversarial network model.

## 4. Analysis of Component-Based Software Testing Methods in Deep Adversarial Networks

**4.1. Deep Adversarial Network Technology.** Deep adversarial networks are a brand-new concept. It may be called by other names, such as the generation system for higher-level opponents. At the heart of the web is conflict. Two networks compete with each other, one for sample generation and the other for pattern analysis. These models are trained using other optimization methods, and both models can be improved to the point of being "indistinguishable between real and fake." Now that we understand the concept of adversarial networks, we need to know how to use it in deep learning. In most cases, adversarial networks represent unsupervised learning. In order to develop better deep adversarial networks, we need to do the following: (1)

integrate actual data deeper and evaluate different data expansion patterns as positive modes; (2) consider all kinds of error information and turn more error information into errors; and (3) according to the error settings in the previous step, improve the accuracy of bad data. Figure 1 provides a corresponding explanation for why the deep adversarial network has many benefits.

Although the general learning method cannot solve very advanced problems, it is currently the most suitable social method. Many of our technologies are still very general, and we are far from reaching their advanced level. Shallow learning is better than general learning. To be a little more advanced, it can simply calculate and optimize itself. It is suitable for some software companies that need to calculate. It is widely used in today's world and technology, and deep learning is very deep. The general formula or solution problems should not apply to it; its cost is high, and its future is of high value.

According to the data results in Figure 1, it can be concluded that the deep learning network is very strong except for the low application rate. The reason for the low application rate may be that many industries in the current society have not developed enough to require advanced confrontation. The network is used to solve the problems encountered. At present, the most basic network system is still on the market.

According to Table 1, it can be seen that these three models have their own strengths and are used in different scenarios. The discriminant model gives a picture, determines what the picture is, and generates the model to give many pictures of dogs so as to generate a new dog picture (not in the original picture). The GAN model will combine their two models to generate a confrontation network.

**4.2. Component Software Analysis.** Due to the increasing sophistication and complexity of software systems, software development regulations are becoming more and more stringent. At the same time, software development organizations have higher and higher requirements for software development costs and development cycles. After the object-oriented analysis method and software development, the componentized form of software development has become a new development trend. Integrating third-party components into specific practical applications, and then properly building a fixed application software system, has a huge impact on software integration and reuse and has become a very popular technology in today's software field. Research. Furthermore, before using these components, corresponding tests are carried out and their accuracy is confirmed in practice. The development steps of component-based software are uniformly expressed in the form of Table 2, which is more clear.

According to Table 2, we can see all the processes of componentized software development at a glance. For componentized software, it means that when developing a software system, the process is regarded as a software development method based on architectural principles and the correct use of assembly forms. Assemble components to

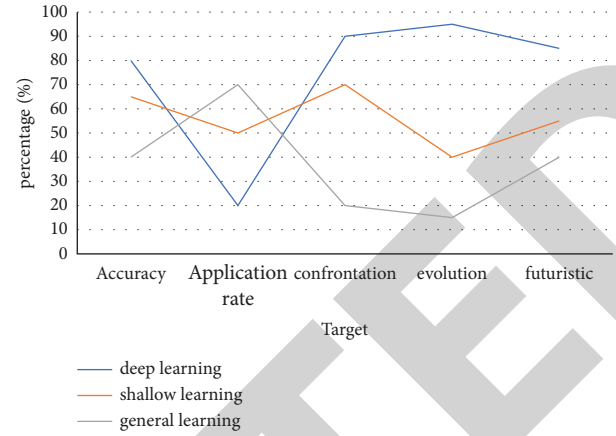


FIGURE 1: Three comparisons.

develop software systems. Also, even their approximate time spent is listed, which can be said to be very detailed. When compared to traditional software, constructed software follows the current trend. From Internet performance to the ability to support server operation, it can meet the needs of human life and work and has made great contributions to the development of software engineering. Because the new structural system of the software cannot replace the functions of traditional software, the traditional software industry must be reformed so that software development stakeholders can quickly analyze software performance, make coordinated changes to the overall software performance at runtime, and perform adjustments cycles of the software system. As for software development, since the development procedures are not uniform, the application programs can be integrated and the component software used by the design. Once released, software developers can separate software components from real life. In a sense, the way of thinking about software components can be transferred to software development, and the content of the appeal can be summarized as a bar chart in Figure 2 to illustrate.

As can be seen from Figure 2, component-based software has many advantages, which are incomparable with traditional software, laying the foundation for innovation in the computer software industry and driving industry innovation. However, componentized software also has security problems. For example, component-based software is still mainly in research and development, and component technology in the computer software industry still has a long way to go. Table 3 establishes the interface tests of the components.

According to the data analysis in Table 3, in the experimental component model, the preconditions determine what is true to ensure that the corresponding interface operations can be executed. Postconditions describe the result of the correct execution of the action. Calling an interface operation when the preceding conditions are not met will cause the following conditions to fail, and if the result matches, the current result is correct. If they do not match, there is an error in the current check step, and it needs to be redefined until it is correct.

TABLE 1: Analysis of deep adversarial network models.

Deep adversarial networks	Advantage	Shortcoming	Application
GAN model	The director of the two sets	It is easy to make mistakes in the game and cause the system to crash	Data augmentation
Discriminative model	Easy to learn, average performance	Just calculate the interface and solve the problem roughly	Creative arts, stylized
Generative model	Fast convergence, learning distributions, estimating variables	Learning complex	Image generation

TABLE 2: Component-based software development process.

Component software development steps	Content	Time (%)	Characteristic
The first stage	Problem domain analysis and building related models	25	Modeling analysis, cornerstone
Second stage	Answer and analyze the domain	15	Building model systems, reusability
The third phase	Building and combining components	35	Test effect
Fourth stage	Evolve the entire system	25	Stages of evolution, applicability

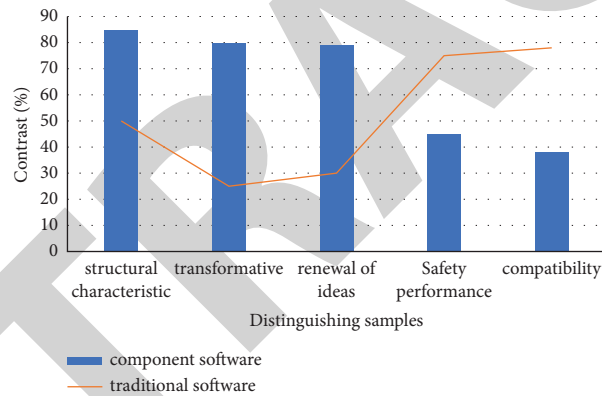


FIGURE 2: The difference between the two.

TABLE 3: Test component interface.

Statute content	Illustrate
Name	Interface name
Constraint	Constraint component interface properties
Enter	Enter the information required by the system
Output	Information returned to the caller
Send	The party to be tested issues a request description
Read	Read the external public information of the system
Change	Change external public information
Rule	System algorithm rules
Assumed	Assume states and conditions that guarantee the result of the system to be true
Result	The interface operation is correct only if the condition is true

4.3. *Application of Deep Adversarial Networks in Componentized Software.* At present, there are not many tests in the market, let alone software-related test methods. After adding the deep adversarial network, the new thing of component software can be developed qualitatively; although it is a new thing that has only appeared in recent years, people saw its

potential and made several corresponding testing methods for it.

In the research on testing methods of componentized software, the deep learning method is the best, and the average of five test results can reach 7 grades, which is far too many grades for several of the methods. The worst normative

test result is the worst. This test method is to simply check the basic parts or functions in the componentized software, so its index data will not be very high.

According to Figure 3, the result can be drawn. The protagonist is the component software because its various tests occupy high scores, which just show the correctness of the application of the deep adversarial network in the component software, which greatly improves the software. The function of the system and the ability to not be afraid of any test, the whole system was tested and divided into five categories for discussion, so that it does not take too much time and there is no need to discuss too much. For these five test methods, we also analyzed and made tabular data results in order to better select the best test method (SSIM is structural consistency, and PSNR is noise ratio).

According to the data results in Table 4, it can be concluded that the best way to test the data results is the built-in test, which mainly tests the components and component sets in the componentized software in the deep adversarial network. The difference between a software system and a traditional software system lies in the definition and assembly of this component.

According to Figures 4–6 after a series of tests (different data ranges), as you can see in Figure 5, integration tests are much less tested on different data ranges than traditional tests, and that's what the built-in testing method does. Figure 6 shows built-in tests have shorter execution times than traditional test builders to test different ranges of data because built-in tests provide parallelism and customizability. All in all, the built-in tests can provide 100% coverage of interface method calls in less time and use a smaller number of test cases than we would like to see. The operation of the deep adversarial network in the system allows the system to generate new adversarial network data, and these new data are drawn through some special monitoring and statistical methods. These uncertain factors may be of great use in the future, and now it is necessary to save statistics on these data.

In Figure 7, five new data have been generated. We can see their complexity. Their generation time is not regular. We currently have no tracking method to know how these new data are generated and their after generation. What is the role? This problem has always existed. We must constantly reform the system to solve this problem and avoid system problems.

According to the data in Figure 7, the laws of this new data cannot be found, because it is generated by the friction between the confrontation networks. We cannot fix how often they collide or what effect will be produced after the collision. Faced with this new data, it is not possible to carry out systematic analysis on him now, and we only store them in a specific domain to prevent their random loss from causing system disorder. Finally, the test method in the system needs to be tested again to ensure the stability of the system.

According to the data in Figure 8, it can be concluded that the built-in test method is the most stable in the running state, with an average of 90%, which reflects the excellence of its test method in this system. This is incomparable to several

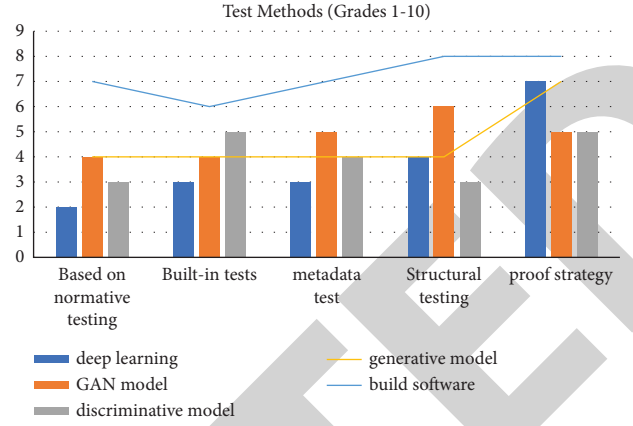


FIGURE 3: Data of several test methods.

TABLE 4: Results of performance indicators of different test methods.

Testing method	SSIM	PSNR
Based on normative testing	0.629	9.52
Built-in tests	0.748	16.81
Metadata test	0.725	14.75
Structural testing	0.651	15.25
Proof strategy	0.695	16.05

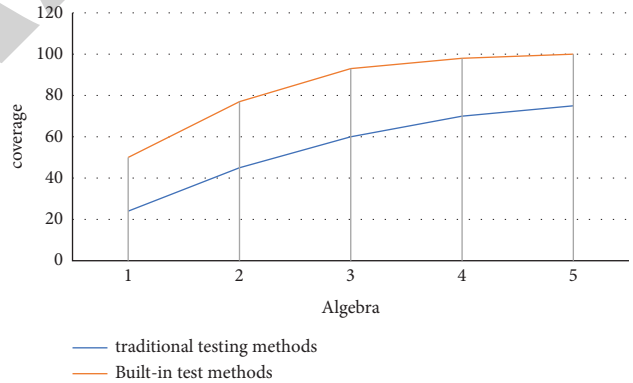


FIGURE 4: Change curve of coverage rate of two test methods.

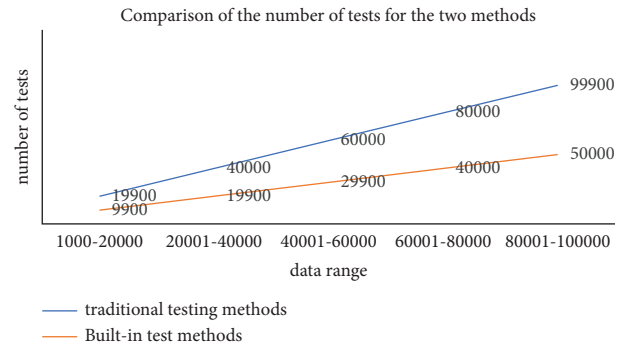


FIGURE 5: Quantity curves of two test methods.

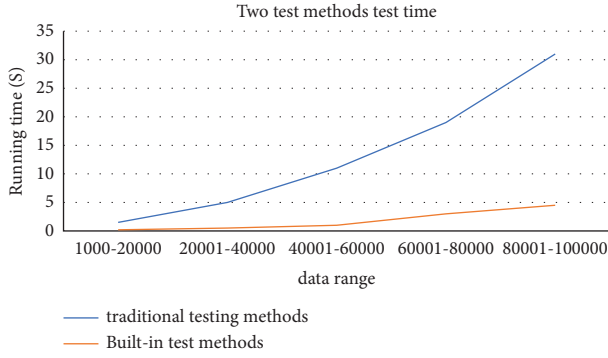


FIGURE 6: Operation times of two test methods.

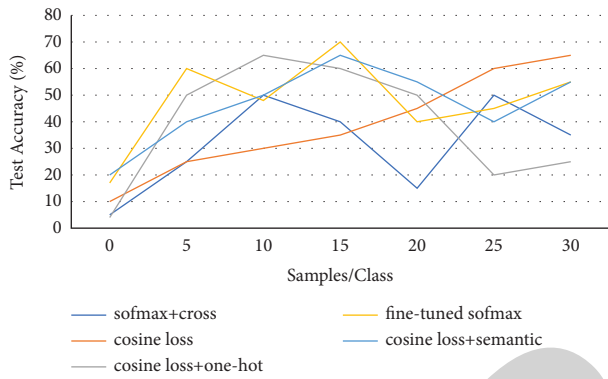


FIGURE 7: Changes in the generation of new data.

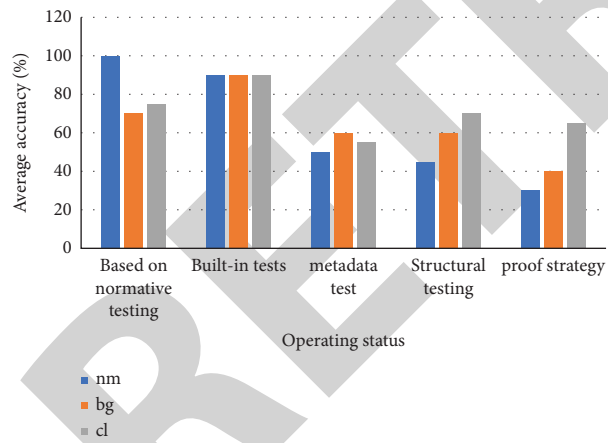


FIGURE 8: Average accuracy.

other methods, but one thing we need to pay attention to is 100% accuracy in nm based on normative tests. Other test results were within expectations.

## 5. Conclusion

The subject is the component-based software testing method based on deep adversarial networks, in which the steps of component-based software development, the analysis of component-based libraries, and the difference between component-based software and traditional software are

discussed, and the software experiments are conducted under deep adversarial networks. Model research mainly studies the growth of component software and the establishment of its overall system with the help of an adversarial network, and it uses several different testing methods to analyze it in all aspects for this new type of software. The highest test method is the built-in test, which is excellent in all aspects and can fully cope with today's various tests. However, it is not certain in the future, so we must always maintain an attitude of continuous improvement to face it. This is the long-term plan.

With the continuous updating and application of software, the current software problems are becoming more and more serious. In response to this phenomenon, we have integrated deep adversarial networks and component-based software to find solutions. Under the vigorous research of enterprises and people, a better way to test software will definitely be devised, and component-based software with a deep adversarial network will be more complicated, but if it is successfully experimented with, it will open up a whole new industry. But before that, it is just an imaginary state, so we have to identify whether this new technology has the ability to be used normally through a large number of test methods. At this time, we need to conduct experiments to explore this problem.

## Data Availability

The experimental data used to support the findings of this study are available from the corresponding author upon request.

## Conflicts of Interest

The authors declared that they have no conflicts of interest.

## References

- [1] G. Yang, S. Yu, H. Dong et al., "DAGAN: deep de-aliasing generative adversarial networks for fast compressed sensing MRI reconstruction," *IEEE Transactions on Medical Imaging*, vol. 37, no. 6, pp. 1310–1321, 2018.
- [2] P. Lu, M. Matt, and B. Seth, "Using generative adversarial networks to improve deep-learning fault interpretation networks[J]," *The Leading Edge*, vol. 37, no. 8, pp. 578–583, 2018.
- [3] C. Qu, Y. Zou, Q. Dai et al., "Advancing diagnostic performance and clinical applicability of deep learning-driven generative adversarial networks for Alzheimer's disease," *Psychoradiology*, vol. 1, no. 4, pp. 225–248, 2021.
- [4] X. Meng, X. Li, and X. Wang, "A computationally virtual histological staining method to ovarian cancer tissue by deep generative adversarial networks," *Computational and Mathematical Methods in Medicine*, vol. 2021, pp. 1–12, Article ID 4244157, 2021.
- [5] P. W. Patil, A. A. Dudhane, and S. Murala, "Deep adversarial network for scene independent moving object segmentation [J]," *IEEE Signal Processing Letters*, vol. 28, no. 99, 2021.
- [6] K. K. Lau and Z. Wang, "Software component models," *IEEE Transactions on Software Engineering*, vol. 33, no. 10, pp. 709–724, 2007.



## *Retraction*

# **Retracted: Design and Application of Intelligent Management Platform Based on Big Data**

### **Security and Communication Networks**

Received 26 December 2023; Accepted 26 December 2023; Published 29 December 2023

Copyright © 2023 Security and Communication Networks. This is an open access article distributed under the Creative Commons Attribution License, which permits unrestricted use, distribution, and reproduction in any medium, provided the original work is properly cited.

This article has been retracted by Hindawi, as publisher, following an investigation undertaken by the publisher [1]. This investigation has uncovered evidence of systematic manipulation of the publication and peer-review process. We cannot, therefore, vouch for the reliability or integrity of this article.

Please note that this notice is intended solely to alert readers that the peer-review process of this article has been compromised.

Wiley and Hindawi regret that the usual quality checks did not identify these issues before publication and have since put additional measures in place to safeguard research integrity.

We wish to credit our Research Integrity and Research Publishing teams and anonymous and named external researchers and research integrity experts for contributing to this investigation.

The corresponding author, as the representative of all authors, has been given the opportunity to register their agreement or disagreement to this retraction. We have kept a record of any response received.

### **References**

- [1] Y. Su, M. Dai, and H. Zhou, "Design and Application of Intelligent Management Platform Based on Big Data," *Security and Communication Networks*, vol. 2022, Article ID 1790678, 14 pages, 2022.

## Research Article

# Design and Application of Intelligent Management Platform Based on Big Data

Yunuo Su,<sup>1</sup> Minhui Dai<sup>2,3</sup> , and Haoyu Zhou<sup>1</sup>

<sup>1</sup>College of Public Administration and Law, Hunan Agricultural University, Changsha 410125, China

<sup>2</sup>Teaching and Research Section of Clinical Nursing, Xiangya Hospital of Central South University, Changsha 410008, China

<sup>3</sup>Department of Ophthalmology, Xiangya Hospital of Central South University, Changsha, China

Correspondence should be addressed to Minhui Dai; [daiminhui@csu.edu.cn](mailto:daiminhui@csu.edu.cn)

Received 17 June 2022; Revised 15 July 2022; Accepted 10 August 2022; Published 11 October 2022

Academic Editor: Hangjun Che

Copyright © 2022 Yunuo Su et al. This is an open access article distributed under the Creative Commons Attribution License, which permits unrestricted use, distribution, and reproduction in any medium, provided the original work is properly cited.

Big data technology has greatly promoted the construction of intelligent administrative management and improved the decision-making ability continuously. Data mining also lays a solid foundation for the construction of administrative management platform and reflects the potential value of data. In this study, an intelligent management platform based on big data is designed and implemented. First, the problems of the intellectualization of administrative management are discussed, and the big data platform and functional framework of administrative management are introduced. Second, in order to apply data mining to administrative management, the object of data mining in administrative management is defined, and a data mining system is designed. Finally, the application of machine learning methods such as cluster analysis in administrative management is analyzed in detail. The research results show that the application of intelligent management platform based on big data can promote the construction of intelligent administration and lay a good foundation for the development of more perfect intelligent administrative management.

## 1. Introduction

With the rise of Internet and big data technology, human society is gradually developing into an interconnected and highly integrated society [1]. Big data makes the development of social, economic, and political life full of new vitality and has become a powerful engine to promote the intellectualization of administrative management [2]. Big data can provide strong technical support for the intellectualization of administrative management. Due to the fragmentation of traditional administration and other reasons, it is impossible to comprehensively and effectively grasp social problems such as social risks [3, 4]. Therefore, applying big data platform and its information processing system to administrative management and realizing multiagent collaborative governance is one of the ways to realize low-cost, fast, and effective management [5]. In intelligent administration, information technology promotes a more reasonable organizational structure of departments through self-

iterative upgrading. It will make the governance behavior more efficient and optimized [6]. Accordingly, with the help of the information technology platform, relevant departments have realized the efficient combination of work organization and work process. It also provides transparent and high-quality services for the whole society, so as to achieve integrated governance [7]. Big data can easily and quickly collect and analyze a wide range of data information and apply it to administrative management. Thus, the administrative department can accurately grasp the goal of social public opinion and realize social risk prediction and real-time optimization of events. In addition, due to the rapid and accurate prediction of risks, the ability of the government or enterprises to control risks is greatly enhanced. This helps to formulate the corresponding treatment plan at the first time, complete the decision more efficiently according to the latest information and development trends, and improve the timeliness, pertinence, and foresight of its response [8]. How to fully explore and realize the value of big



data in administrative management has gradually become a topic of common concern to scholars. It is very necessary to build a reasonable and scientific intelligent management platform based on big data.

In general, domestic and foreign countries have done a lot of research on the definition of the concept, business processes, and mechanism guarantee of big data administrative management platform [9]. However, there is still much room for improvement if we put the development of the management platform into the context of social development and government innovation. It is mainly reflected in the following aspects. First of all, the research on the development of big data administrative platform and the promotion of overall government construction is relatively weak [10]. At present, the construction of the platform is more aimed at the optimization of its own internal business processes, while the research on how to break the shackles of the traditional management system and departmentalism for the platform and realize the integration and optimization of governance resources of various departments is relatively scarce and vague. Second, as a product of the application of big data technology in the field of public management, the government management big data platform is lack of sensitivity and responsiveness to the arrival of the big data era [11]. The powerful data collection, collation, and analysis capabilities of big data will, to a considerable extent, break through the ministry pattern and information island phenomenon and directly promote the transformation of government decision-making mode and business process reengineering. Therefore, the research and application of related aspects are still in the ascendant [12].

The specific contributions of this study are as follows:

- (1) This paper analyzes the problems existing in the intellectualization of administrative management and constructs the big data platform of administrative management.
- (2) Process the data of big data platform, build the functional framework of the platform, and establish the administrative management system structure.
- (3) Applying data mining technology to administrative management, this paper constructs the administrative data warehouse system, explains the objects of data mining, and focuses on the data preprocessing module and data mining module.
- (4) Cluster analysis is applied to administrative management, and the application of clustering algorithm in text analysis is analyzed.

The rest of the paper is organized as follows. Section 2 discusses related studies, and Section 3 introduces the construction of administrative big data platform. Section 4 describes application of data mining in administration chiefly. Application of cluster analysis in administration is discussed in Section 5, and Section 6 serves as a conclusion, providing the summary and future directions of research.

## 2. Related Work

With the practical application of big data and the development of social diversity, the exploration and research on the intellectualization of administrative management have attracted extensive attention of scholars. Especially in developed countries, through the introduction of big data and artificial intelligence technology, the government and academia have effectively improved the efficiency of administrative management in dealing with complex social issues such as public safety, social security, medical, and health care. Some experts and scholars believe that big data will shape the political phenomenon in the new information age and transform the behavior patterns and relationships of political actors such as government, citizens, and political parties. Koren et al. [13] applied the classical *K*-means algorithm to both numeric and categorical attributes in big data platforms. They first presented an algorithm that handled the problem of mixed data. Then they used big data platforms to implement the algorithm. In terms of administration, the wide application of big data in the field of administration makes it more convenient, intelligent, and efficient. Zhao et al. [14] suggested that big data has great potential in improving policy description and strengthening policy prediction ability. Pintye et al. [15] studied the relevant policy framework of big data and proposed that the whole social governance, policies, and aspects closely related to big data should be considered as a complete system, involving user privacy, data accuracy, data collection methods, and social equity.

Zhang [16] employed the future development of intelligent administrative management, believed that the current development of modern social governance is driven by the integration of social Internet and big data, and emphasized how to establish a modern social governance working mechanism by using big data technology to effectively promote and promote administrative management. Seop and Lee [17] pointed out that at present, the application and embedding of big data in promoting administrative management has built a certain material and technical foundation for the government information system and formed an integrated development mechanism combining government public service information disclosure and policy public service supply. Zhou et al. [18] suggested that appropriate governance technology is an effective medium for the modernization of governance system and the modernization of governance ability. Big data can optimize the ecological environment of governance process and expand the elastic space of system design. It is a good opportunity to induce institutional innovation and governance transformation [19]. Big data technology has broad application prospects in the intellectualization of administrative management. Dong [20] pointed out that the sharing and interworking of data is the key in the intellectualization of administrative management and put forward the innovative development strategy of system and mechanism, so as to promote the interworking and cooperation of information and data. On the basis of in-depth study of the historical background,

characteristics, and relevant theoretical data sources of “Internet + Administration,” Wang et al. [21] focused on the deep-seated problems faced in the current construction process and put forward solutions. The application of big data is conducive to promoting the transformation of administrative management mode and improving public satisfaction, providing a theoretical basis for scientific decision-making, and promoting the improvement of government management efficiency and the transparency of supervision [22, 23]. However, big data may also cause some problems in administrative management, such as information security. Therefore, we should objectively, rationally, and comprehensively understand the two sides of big data. In the process of administrative management, we should not only carefully deal with the impact of big data and actively explore effective measures to avoid big data risks but also make full use of the opportunities brought by big data in the process of management to improve the level of administrative management [24, 25].

### 3. Construction of Administrative Big Data Platform

The unified big data platform can effectively solve the problems of information island and information fragmentation and promote the unified integration, sharing, and utilization of departmental data and information. The establishment of administrative big data platform can effectively ensure the orderly flow and sharing of data among departments, realize the connection between information resources and management platform, reduce human interference to data information, and solve the important problem of data separation [26]. Therefore, it is particularly important to build an administrative big data platform. The construction of administrative big data platform should obey the following principles [27, 28]: (1) The unification and standardization of data to ensure the quality of data; (2) to achieve comprehensive integration, the platform should cover all kinds of data information of each department and integrate multisource heterogeneous data across levels, regions, systems, departments, and businesses; (3) the system has objective feasibility and conforms to the current social environment, technical conditions, and economic foundation and has strong operability.

**3.1. Administration Platform.** The realization of intelligent administrative management depends on the big data platform with excellent design and perfect functions. The two ends of the platform are connected with data business and data application, respectively. The general big data platform is composed of data layer, application layer, and cloud platform. The cloud platform includes Software Defined Data Center (SDDC) and intelligent computer room. The data engine is mainly composed of data acquisition layer, data storage layer, data management layer, data subject layer, and data service layer. It is mainly responsible for data collection, data storage, the establishment of data warehouse and data packaging, operation, and maintenance. The

platform has analysis and display functions, such as the analysis of big data by terminal and application layer, which is realized by application layer and application layer. In addition, data engine management can also be divided into operation and maintenance management, data quality management, metadata management, and security management to complete core services such as data storage, processing, and protection. Users can obtain, store, and analyze data on the platform through client software, so as to apply it to specific businesses. The overall structure of the big data platform is shown in Figure 1.

**3.2. Technology Architecture.** Big data involves the process of data collection, management, storage, analysis, and visualization. According to the processing stage of big data, big data technology can be divided into data collection, and structured, semi-structured, and unstructured data can be collected through crawler or other system interfaces; data cleaning, processing repeated data and noise data, standardizing data, storing data, storing data in data warehouse, distributed database, etc. Data analysis: analyze the collected and processed data, such as basic analysis, multidimensional analysis, or use data mining technology for analysis; data application and visualization: the platform can be used for marketing, report making, operation, and index application by analyzing the data [29, 30]. Based on this, this paper proposes a process based big data technology architecture, as shown in Figure 2.

**3.3. Administrative Big Data Integration Technology.** Data integration is mainly the ETL work of data, which transforms heterogeneous data into isomorphic data under data warehouse through data extraction, data transformation, and data loading [31–35]. The main function of data extraction is to collect data from the data source and provide it to the subsequent data warehouse environment. After the data are successfully extracted, it can be transformed and loaded into the data warehouse. The extraction-transformation-loading (ETL) architecture is shown in Figure 3.

For the collection of government data, it is necessary to first clarify the data to be collected and then use big data-related technologies to collect and store the data scattered in departments at all levels. It includes actual data acquisition, batch data acquisition, and data filling, as described below:

- (1) Real time data acquisition: for the business generated in real time such as personnel travel and requiring high timeliness, the real-time data acquisition mechanism is selected and then the changed data resources are collected and published through Kafka component. Finally, the front-end database stores the data in the form of subscription to complete the real-time data acquisition.
- (2) Batch data acquisition: for the business data generated by the daily business of each department with low requirements for data timeliness, select the data batch acquisition mechanism, use ETL tools such as kettle to configure the data collection task regularly,

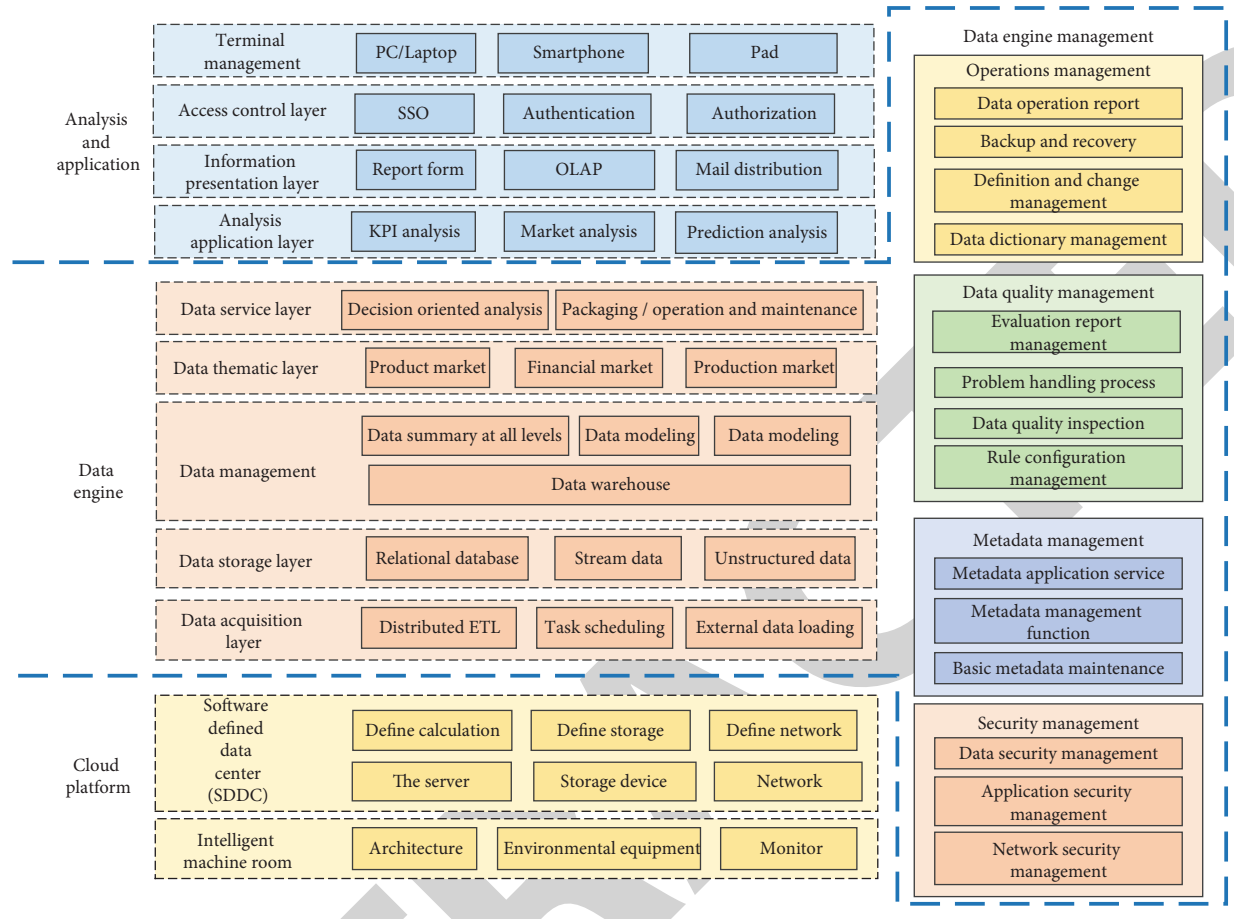


FIGURE 1: Big data platform structure.

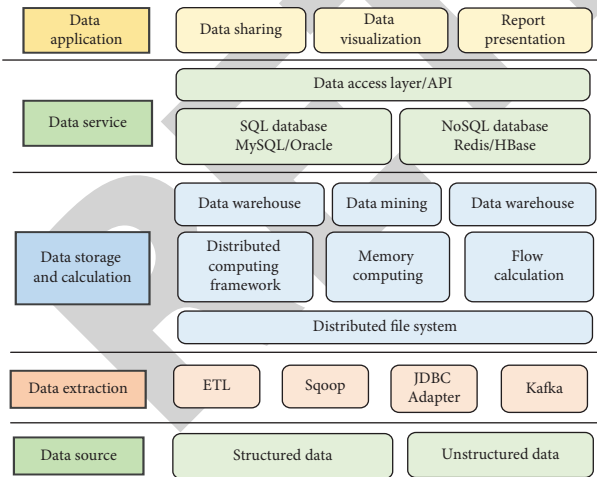


FIGURE 2: Big data technology architecture.

and periodically push the business data to the front database.

- (3) Data reporting: for departments with low development of data intelligence and no independent business system, select the data reporting mechanism to directly report the data stored in the form of

electronic documents and paper documents to the front-end database through the data reporting system.

By integrating administrative data resources, we can accurately record the data resource structure of each department and business system and better realize the integration and sharing of administrative data resources. In addition, the data resource directory is the centralized embodiment of data resource integration, and its specific structure is as follows:

- (1) Department directory. According to the department to which the data belongs, the data of departments and departments at all levels are divided. Different departments connect different front-end databases. In order to facilitate the maintenance and management of data, the department data directory is directly oriented to governments or enterprise departments at all levels.
- (2) Business system directory. According to the business system to which the data belongs, divide the data and classify the different business data in the directory, which helps to improve the business collaboration efficiency between different departments and improve the convenience of data use.

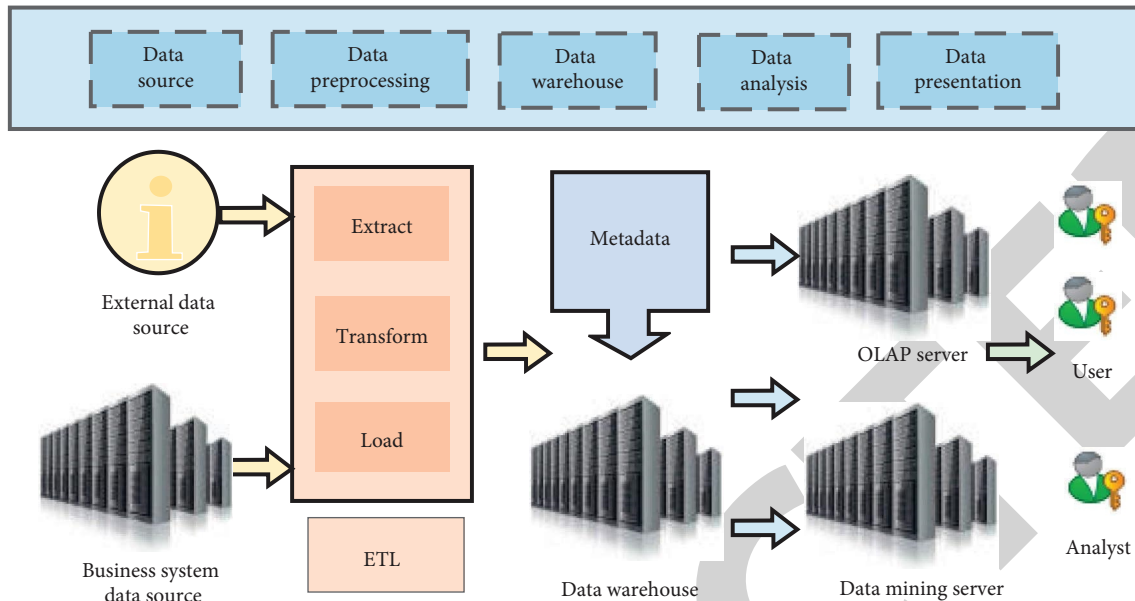


FIGURE 3: ETL architecture.

- (3) Thematic data directory. According to the thematic indicators corresponding to different data, the fused data are removed from the departments and business systems for directory division. The division of the thematic data directory is conducive to the in-depth integration of administrative data.

**3.4. Functional Framework of Administrative Big Data Platform.** The application function framework of administrative big data platform mainly includes infrastructure, data standards and specifications, directory management platform, data sharing demand management subsystem, shared exchange platform, government big data resource pool, data governance subsystem, data service platform, big data analysis and application platform, visual implementation, and application support platform. Relying on the above functional framework, the platform can provide data governance services, data sharing services, etc. As the main body of data resources of the administrative big data platform, the government big data resource pool provides unified and standardized storage support and update management for the data resources of the platform. The government information resource sharing and exchange platform implements data exchange within the response time of business needs to data definition, so as to ensure the data timeliness of the resource pool of the administrative big data platform. The data management subsystem is used to comprehensively improve the data quality and ensure the availability of data in the resource pool. The data service platform encapsulates the data service interface based on the timely government data in the government big data resource pool and provides data services for various business management systems and application support platforms. The data service itself belongs to one of the three ways of sharing and exchanging government information resources. By

using the government information resource sharing and exchange platform, the data will be decrypted and shared to the big data analysis and application platform on the premise of ensuring data security. Subsequently, these data can be used for various thematic and thematic data analysis and support various business applications, auxiliary decision-making, and macro analysis. The functional architecture of the administrative big data platform is shown in Figure 4.

**3.5. Administrative Management System Structure.** The functional modules of the administrative management architecture mainly include several modules as follows: data collection, data aggregation, data storage, data governance, data directory, data standard, data service, and data visualization.

The data acquisition system is the unified data entry of the whole big data platform, which realizes the management of heterogeneous data sources, the configuration and management of data acquisition services and so on.

The data aggregation system realizes the data collection and aggregation under the complete transaction from the source data to the target through data collection and outputs the calculation results to the target of data service.

The data directory system is the organization and description of all the data of the platform. The data entering the platform first need to be registered and catalogued in the directory system. In addition, combined with the scientific simulation model, it can realize the three-dimensional presentation of the description object and relationship model, realize the whole domain digitization, and at the same time, it can be goal oriented and provide various detection, evaluation, and reports based on the template.

With the increasing number of data resources and the change of business form, it is necessary to establish a complete data governance system from the perspective of

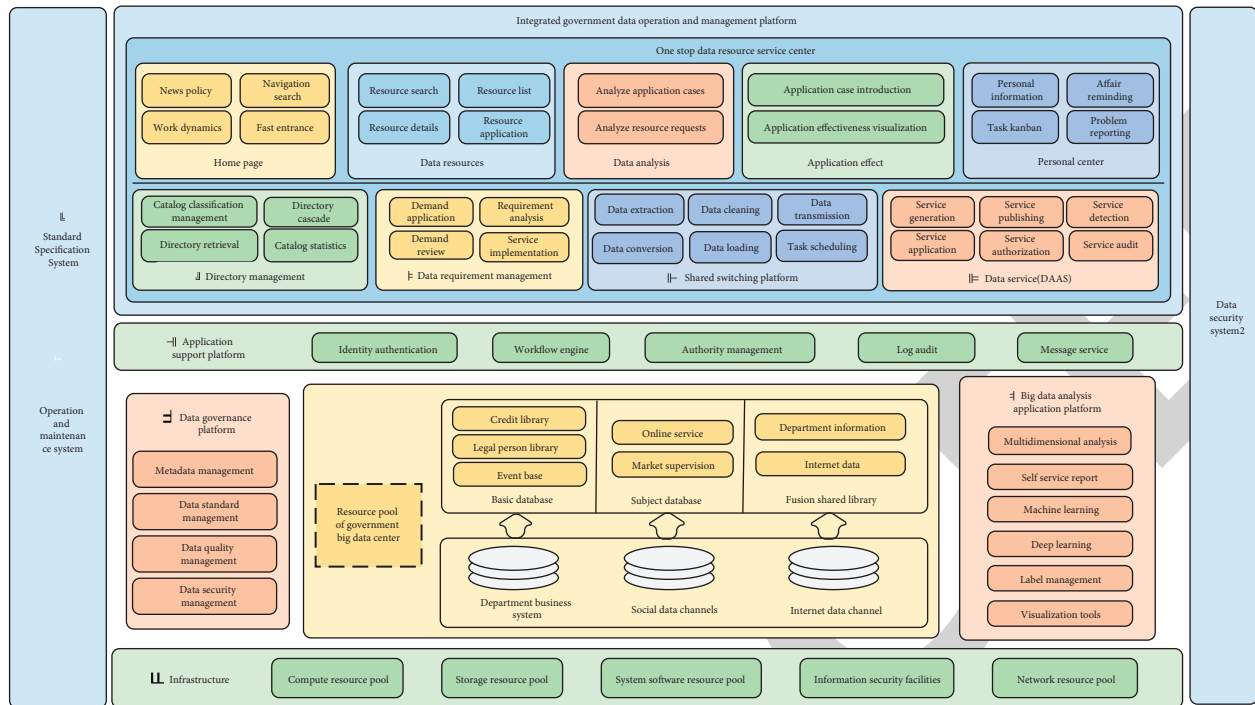


FIGURE 4: Functional framework of administrative big data platform.

data quality improvement and data governance, ensure the quality of data content, improve the platform's ability of data management and governance, and effectively mine data value. The data storage system builds an accurate, complete, consistent, and logically unified data storage system around the process of planning, construction, warehousing, storage, update, and management of information resources, focusing on the construction and use of databases, and realizing the unified storage planning management and external services of the platform.

The data service system is to provide data services for all kinds of data and applications of the data center internally and externally through different service methods, such as industry departments or the public, and open it to the society and industrial chain. Through data services, it can drive the overall development of the upstream and downstream of the data industrial chain, promote information consumption, and drive the development of big data industry.

The data visualization system realizes the visual display of data and the release of applications and other related functions. Through data modeling and visualization tools, it shows the application of each system and monitors the business collaboration, support relationship, and operation status between each system, as shown in Figure 5.

The long-term and stable operation of the data center is inseparable from efficient and scientific management mechanism and management measures. From the perspective of management, it is necessary to realize all-round integrated management control, so as to improve the management level and ability of the big data platform. At present, the business of data management has problems such as unknown resources, uncontrollable data, and lack of

supervision of data. It is necessary to establish a data control system, fully realize the control intervention and scheduling of each component system by the platform, improve the control level and data control efficiency of the administrative big data platform, and realize the long-term and stable operation of the data center.

## 4. Application of Data Mining in Administration

**4.1. Data Mining and Knowledge Discovery.** Data mining (DM) is a process of extracting hidden, unknown but potentially useful information and knowledge from a large number of incomplete, noisy, fuzzy, and random data. Knowledge discovery (KDD) is the process of transforming information into knowledge. Data mining is an important part of knowledge discovery. It can extract useful information and knowledge from a large number of incomplete and fuzzy data by using some specific algorithms. KDD flow chart is shown in Figure 6.

The process of knowledge discovery is to connect multiple stages and conduct human-computer interaction for many times. The specific process is as follows:

- (1) Identify the areas to learn: knowledge and objectives;
- (2) Establishment of target data set: focus on one data set or subsets of multiple data sets;
- (3) Data cleaning and preprocessing: use specific algorithms to remove noisy, irrelevant data and blank data space;
- (4) Data conversion: convert or merge data to form a description form suitable for data processing;





FIGURE 5: System interface of data visualization.

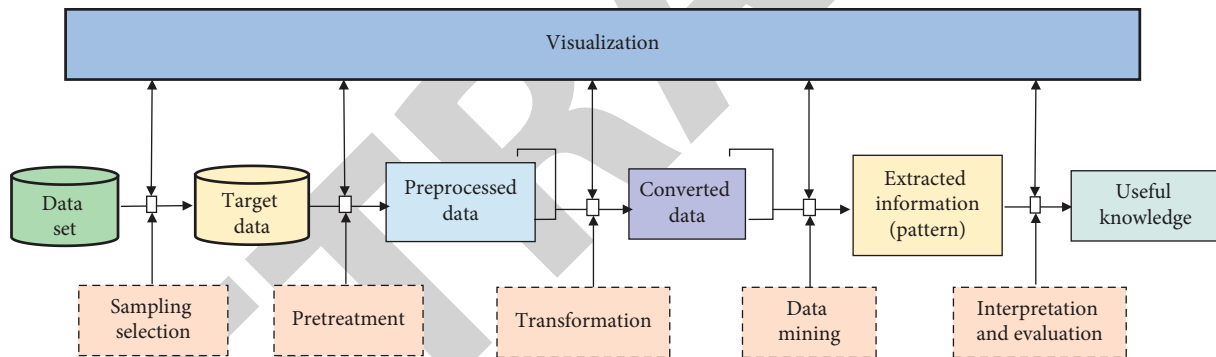


FIGURE 6: Flow chart of knowledge discovery.

- (5) Select data mining algorithms according to features such as summary, clustering, classification, and regression;
- (6) Implementing data mining: mining out potentially useful information;
- (7) Using interpretation mode to extract the information people need and then transform it into knowledge;
- (8) Conduct knowledge evaluation and study and demonstrate the extracted knowledge in practice.

**4.2. Government Data Warehouse.** Data mining is completed in data warehouse. For data mining, database is a data source with rich data. Generally, intelligent decision-making is implemented under the following steps:

- (1) Multidimensional analysis of administrative data warehouse;

- (2) Carry out administrative data mining on the extracted data. The technology of data mining breaks through the traditional data query and finds the value of data at a deeper level.

The data warehouse architecture in administrative management is shown in Figure 7.

The detailed data processed by ETL are stored in the data warehouse and classified according to the subject. Operational data store (ODS) is an optional part of data warehouse structure. ODS has some characteristics of data warehouse and OLTP (on line transaction processing) online transaction processing system. It is "subject oriented, integrated, current, or close to current and changing" data.

**4.3. Objects of Administrative Management Mining.** Data mining is widely used in administrative system. Different businesses have different data structures, such as hierarchical

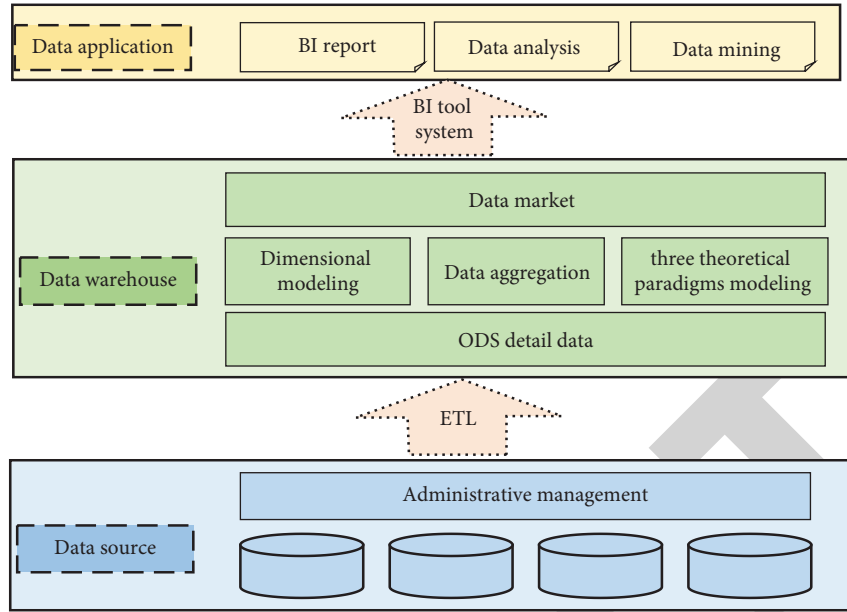


FIGURE 7: Data warehouse architecture in administrative management.

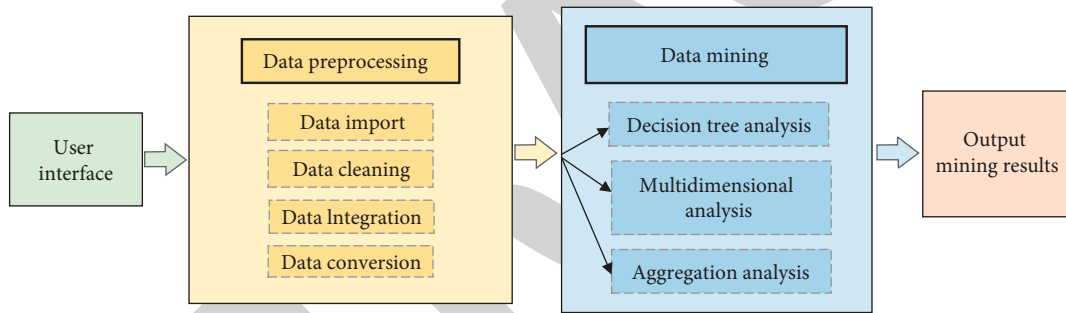


FIGURE 8: Overall framework of data mining.

data, network data, relational data, and object-oriented data. The mining object of administrative management should be determined according to the knowledge content and form required to process data in the administrative business process. Its processing objects mainly face the following aspects:

- (1) Relational database. Relational database is the most complete and abundant database system in administrative management, from which a large amount of relevant knowledge can be mined. Therefore, it is the main data form of administrative data mining.
- (2) Transaction database. Transaction databases usually consist of files, and records represent transactions. Transactions usually contain only the transaction flag and the list of items that make up the transaction. Therefore, transaction database is the largest part of data mining.
- (3) Data warehouse. Data warehouse is the main object of data mining. It is a collection of multiple data elements collected and sorted in the same topic. Thus, data mining from data warehouse can reduce a lot of data preparation time and workload.

**4.4. Design of Data Mining System.** The overall design of data mining is mainly divided into two parts: data preprocessing module and data mining module. First, preprocess the data input into the system, including data cleaning, data integration, data conversion, etc., and then analyze and process the data through data mining algorithms such as decision tree analysis, multidimensional analysis, and aggregation analysis. The overall framework of data mining is shown in Figure 8.

**4.4.1. Data Preprocessing Module.** Data preprocessing is the basis of data mining. In this module, first collect various data according to the needs and then find out the relationship between data through data mining. Data preprocessing mainly includes data cleaning, data integration, and data conversion. The processed high-quality data are a good foundation for data mining.

**Data cleaning:** data cleaning mainly solves incomplete, wrong, and repeated data by filling in missing values, smoothing noise data, identifying or deleting outliers, so as to make the data consistent.

**Data integration:** data integration is the logical or physical integration of data from different sources, formats, and characteristics. It can provide comprehensive data sharing, including periodic integration, real-time integrations, batch integration, and change data capture integration.

**Data conversion:** data conversion operations convert or merge data to obtain a form suitable for data processing. Data conversion includes smoothing processing, total processing, data generalization processing, formatting, and attribute construction.

**4.4.2. Data Mining Module.** Data mining refers to the process of revealing hidden, previously unknown and potentially valuable information from a large number of data in the database. Through data mining, governments, or enterprises can automatically analyze data and conduct inductive reasoning to mine potential patterns. Thus, it can help them adjust management strategies, reduce risks, and make correct decisions. The specific steps are as follows:

- (1) Clarify the purpose of excavation. Before starting to mine knowledge, understand the characteristics of data, use these professional background knowledge, clarify the problems to be solved, and determine the objectives to be mined, so as to select the data to be mined from the massive administrative information data.
- (2) Data preparation. Data preparation must focus on the variables defined in a certain target stage to prepare data, remove redundant, invalid and irrelevant data in the data, and provide high-quality data.
- (3) Data conversion. Convert the obtained data into a format acceptable to data mining software and a form of computer data storage.
- (4) Build the model. According to the actual situation of the data, select the appropriate mining technology and establish the corresponding model. Modeling is an iterative process. We need to carefully examine different models to determine which model is the most suitable.
- (5) Result analysis. Confirm and analyze the mining results and evaluate their value.

There is a large amount of data in the administrative database, which contains a wealth of knowledge. However, it is difficult to find the value of the data and extract useful information from a large amount of data for predicting the development trend or making decisions. Therefore, data mining technology is used to extract these relationships from a large amount of data. It is of great significance to apply it to administration.

## 5. Application of Cluster Analysis in Administration

The traditional classified catalogue system of administrative information resources is no longer suitable for the

management and application needs of government big data. Information mining, dynamic resource analysis, and personalized directory generation of cluster analysis can better meet this development demand.

**5.1. Comparison of Clustering Analysis Algorithms.** Cluster analysis is a process of dividing data objects into different classes or clusters according to their characteristic attributes according to the principle of “similarity compatibility,” so that data objects in the same cluster have greater similarity and objects in different clusters have greater dissimilarity. The process of cluster analysis is to find out some statistical values that can measure the similarity between objects or variables according to multiple observation indexes of data objects, take them as the classification basis, aggregate some objects with high similarity of features into one class, and aggregate other objects with high similarity of features into another class until all objects are aggregated to form a classification system.

Cluster analysis is a method of collecting objects through data modeling. The traditional statistical cluster analysis methods include systematic clustering or hierarchical clustering, decomposition, addition, dynamic clustering, ordered sample clustering, overlapping clustering, and fuzzy clustering. The following is the performance of different clustering algorithms on the toy data set, as shown in Figure 9. The last data set shows a special case of null, and the data are isomorphic. According to the intuition in the figure, the clustering algorithm with better effect is DBSCAN and average linkage algorithm, which can better cluster 2D data, but this intuitive method is not suitable for high-dimensional data. At the same time, the application of clustering algorithm also needs to be selected according to specific conditions.

There is plenty of unstructured text information in administrative management. Cluster analysis divides a large number of detected core or subject words into several groups by tracking the information of each information source and then counts their feature series for calculation and processing. Several main clustering methods are partition method, hierarchy method, density method, grid method, and model-based method.

**5.2. The Value of Cluster Analysis in Administration.** In the field of administrative management, cluster analysis can be used for big data analysis and auxiliary decision making. At present, the amount of data shows an exponential growth trend with the development of social information and business. If there is no good method to analyze the data, it will cause a phenomenon of “data explosion and information scarcity.” In view of this situation, scholars have proposed many clustering algorithms to solve the problem of big data feature collection. Cluster analysis can be used for hot spot clustering of all contents collected by the resource engine, or hot spots in a field, a vertical system, a comprehensive department, etc. In many people’s livelihood decisions, hot events and hot issues are usually direct driving factors.



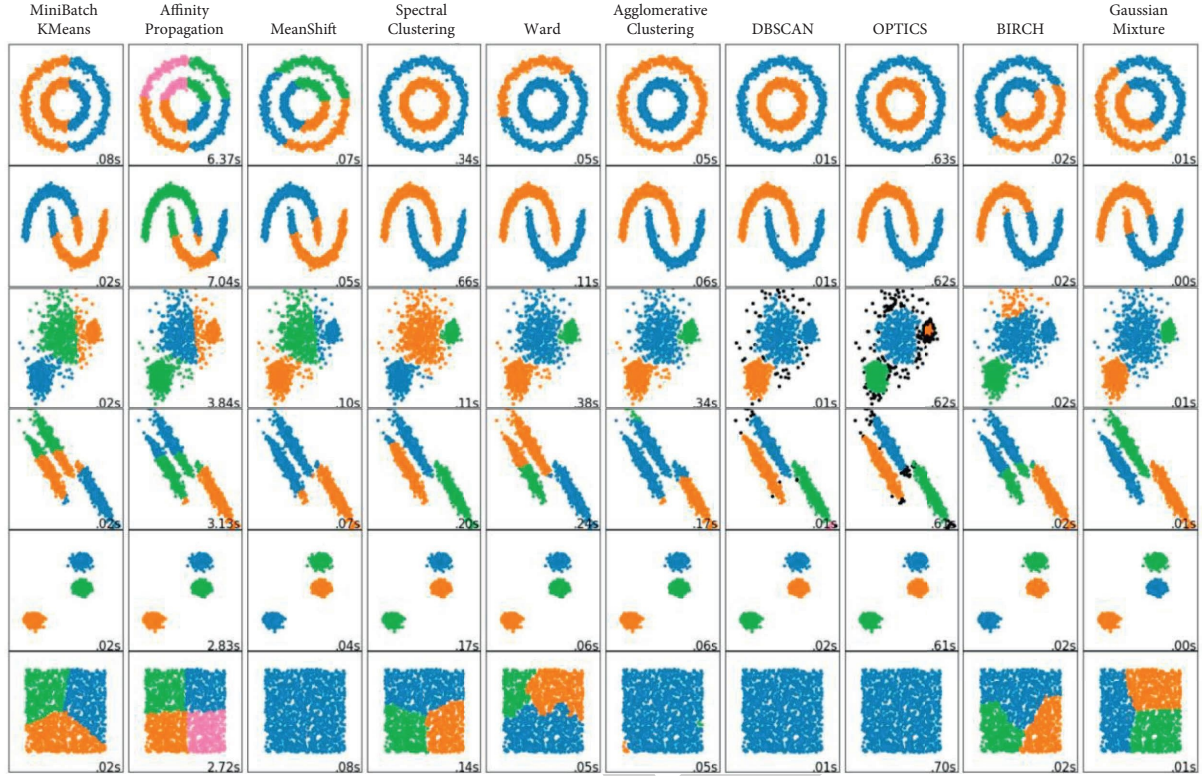


FIGURE 9: Visual display of different clustering algorithms on toy data sets.

From the perspective of time series, the initiation, initiation, development, growth, and extinction of many social events, industrial and economic phenomena have a complete life cycle, which not only conforms to the general cycle law but also has its unique characteristics. The occurrence, evolution, and extinction of some important events will be reflected in various public media and will enter the administrative big data platform through the resource engine. Through information clustering, decision makers can judge the development trend of hot information according to the trend of hot information and take appropriate measures at the appropriate time. At the same time, decision-makers often have to review and refer to the handling of similar events in history and the correctness and suitability of response measures, so as to summarize experience and lessons and make the current decision making more scientific, timely, and reasonable. For example, the course and measures taken by various countries to deal with major epidemics such as SARS, mad cow disease, highly pathogenic avian influenza, and COVID-19 can be used for reference. Therefore, when making decisions, it is often necessary to cluster the information flow of similar events in history, find out its evolution context, and evaluate various coping strategies, measures, and performance at that time, so as to reduce the current decision-making risk. Therefore, finding and analyzing the causes of hot spots and tracking their development are of great significance for scientific decision making, formulating policies, and taking measures.

In the field of administrative management, the advantage of clustering analysis is that it can simply and intuitively

obtain useful information from massive data and transform it into knowledge resources. Then, the knowledge resources of decision analysis are established to help decision makers have an overall insight into the overall situation and form an overall view and depth view. Then, it automatically identifies and tracks the beginning, development, and trend of various events, as well as the evolution process of various themes or the integration with other factors. Finally, help decision-makers establish links between seemingly isolated events and eliminate the knowledge gap. It can find and count some key signal words and subject words in time and respond to the changes of various macro resource gathering.

### 5.3. Application of Clustering Algorithm in Text Analysis.

There are a large number of types of rich data in administrative management, such as text data, and multimedia data, different algorithms should be selected for different types of data. Because there are a lot of unstructured text information in administrative management, clustering text information can find hot events and hot issues, judge their development trend according to the trend, and take corresponding measures. Therefore, this paper gives an example of the application of clustering algorithm in text information.

**5.3.1. Text Similarity Calculation.** The similarity measurement of text is generally divided into two steps: text vectorization representation and similarity calculation [36]. Text vectorization representation is to transform the text

into points in high-dimensional vector space and use high-dimensional vectors to represent the text; similarity calculation is based on the representation form of high-dimensional vectors to calculate the distance between vectors.

The text space vector model is as follows:

- (1) Document: generally refers to general text or fragments in text. Generally refers to an article, represented by  $D$ .
- (2) Item: the content features of a text are often represented by the basic language units, such as words and phrases. These basic language units are collectively referred to as the item of the text, which is represented as  $D(t_1, t_2, \dots, t_n)$ , where  $t_k$  is the item and  $1 \leq k \leq n$ .
- (3) Item weight: for text  $D(t_1, t_2, \dots, t_n)$  with  $n$  items,  $t_k$  is often given a certain weight.  $w_k$  represents their importance in the text, which is recorded as  $D = D(t_1 w_1, t_2 w_2, \dots, t_n w_n)$  and abbreviated as  $D = D(w_1, w_2, \dots, w_n)$ . At this time, the weight of item  $t_k$  is  $w_k$ ,  $1 \leq k \leq n$ , and  $D = D(w_1, w_2, \dots, w_n)$  is the vector representation of text  $D$ .
- (4) Similarity: the content correlation between two texts  $D_1$  and  $D_2$  is usually measured by similarity  $\text{Sim}(D_1, D_2)$ , and the inner product between common vectors represents the text similarity:

$$\text{Sim}(D_1, D_2) = \sum_{k=1}^n W_{1k} W_{2k}. \quad (1)$$

Also, it can be expressed by cosine value of included angle:

$$\text{Sim}(D_1, D_2) = \cos \theta = \frac{\sum_{k=1}^n W_{1k} W_{2k}}{\sqrt{\sum_{k=1}^n W_{1k}^2} \sqrt{\sum_{k=1}^n W_{2k}^2}}. \quad (2)$$

The more representative the items selected in the text are, the higher the language level is, the richer the information they contain. Because vocabulary is the most basic representation item of the text, its occurrence frequency is high in the text and presents a certain statistical law, so words or phrases are selected as feature items, and the more important items account for more weight. For specific government affairs, dealing with similar texts often requires high interpretability of clustering results.

Therefore, the method based on word bag should be selected for text vector representation, and the TF-IDF weight calculation can be defined as  $W_{ik} = tf_{ik} * idf_k$ . The common calculation method is given by

$$W_{ik} = tf_{ik} \cdot \log\left(\frac{N}{N_k} + 0.01\right), \quad (3)$$

where  $tf_{ik}$  represents the number of occurrences of item  $t_k$  in text  $D_i$  and  $idf_k$  is an indicator of the frequency of  $t_k$  in a document set according to document statistics. Besides,  $N$  represents the number of texts in all training sets, and  $N_k$  represents the frequency of  $t_k$  in training texts.

Considering the influence of text length on the weight, it should also be normalized to between  $[0, 1]$ . Thus, the TF-IDF weight can be obtained by

$$W_{ik} = \frac{tf_{ik} \cdot \log(N/N_k + 0.01)}{\sqrt{\sum_{k=1}^n (tf_{ik})^2 \cdot \log^2(N/N_k + 0.01)}}. \quad (4)$$

**5.3.2. K-Means Clustering Algorithm.** K-means clustering is a typical clustering algorithm based on partition. It calculates the distance between the sample points and the cluster centroid and the sample points close to the cluster centroid are divided into the same cluster. K-means measures the similarity between samples by the distance between them. The farther the distance between two samples, the lower the similarity, otherwise the higher the similarity.

In the K-means algorithm,  $k$  clustering centroids  $\mu_1, \mu_2, \dots, \mu_k \in R^{(n)}$  are randomly selected for each  $x^{(i)} \in R^{(n)}$  of the training sample  $\{x^{(1)}, \dots, x^{(m)}\}$ . Then, for each sample, calculate the class it should belong to:  $c^{(i)} = \arg \min_i \|x^{(i)} - \mu_j\|^2$ . For each class  $j$ , recalculate the centroid  $\mu_j = \sum_{i=1}^m 1\{c^{(i)} = j\} x^{(i)} / \sum_{i=1}^m 1\{c^{(i)} = j\}$  of the class and repeat the above process until convergence. When  $k = 3$ , the K-means clustering effect is shown in Figure 10.

**5.3.3. Canopy Clustering Algorithm.** However, K-means algorithm has the problem that the initial clustering center point is sensitive, so it often uses the mixed form of canopy+K-means algorithm for model construction: first use canopy algorithm for rough clustering to get clustering center points and then use K-means algorithm to take  $k$  clustering center points as the initial center points for fine clustering [37].

Canopy algorithm has fast execution speed, does not need a given value, and has many application scenarios. It can alleviate the sensitivity of K-means algorithm to the initial clustering center point. Therefore, it is often selected as the acceleration scheme of K-means algorithm. The application flow of canopy algorithm in text clustering is shown in Figure 11. After receiving a new text, the system first converts the text into TF-IDF vector in high-dimensional space. Next, we need to search the data close to the vector from the historical data, use canopy algorithm for rough clustering, and screen out a few candidate data from the massive historical data. Then calculate the cosine similarity of TF-IDF vector with the new text, respectively. If the similarity of candidate data is greater than the threshold, the new text will be classified into the category to which the data belongs. Otherwise, a new category will be created, and the new text will be used as the initial member of the new category.

Canopy algorithm is a coarse clustering algorithm with fast execution speed but low accuracy. The execution steps of the algorithm are as follows:

- (1) Given sample list  $L = x_1, x_2, \dots, x_m$  and a priori value  $T_1, T_2$  ( $T_1 > T_2$ );

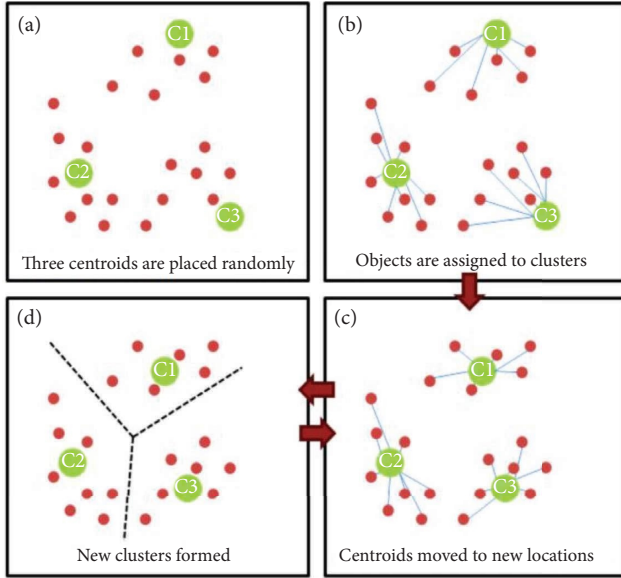
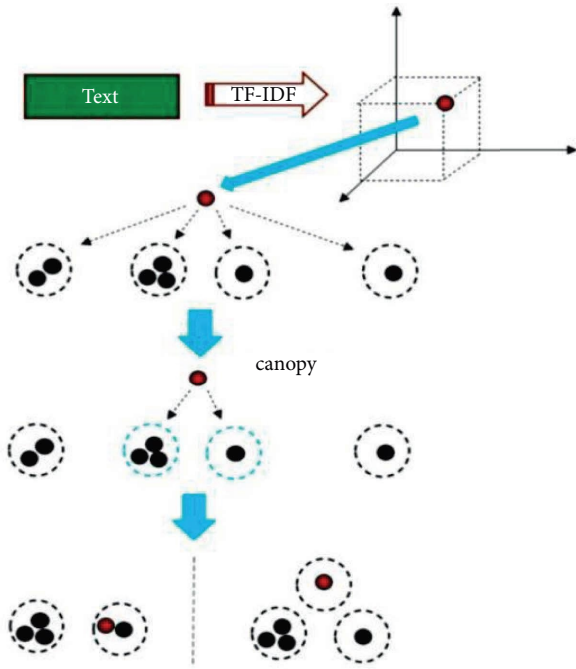
FIGURE 10: K-means clustering effect with  $k = 3$ .

FIGURE 11: Application flow of canopy algorithm in text clustering.

- (2) Obtain a node  $P$  from the list  $L$ , calculate the distance from  $P$  to all cluster centers and select the minimum distance  $D(P, a_j)$ ;
- (3) If the distance  $D$  is less than  $T_1$ , it means that the node belongs to the cluster and is added to the cluster list;
- (4) If the distance  $D$  is less than  $T_2$ , update the center point of the cluster to the center point of all samples of the cluster and delete  $P$  from the list  $L$ ;
- (5) If the distance  $D$  is greater than  $T_1$ , node  $P$  forms a new cluster and deletes  $P$  from list  $L$ ;

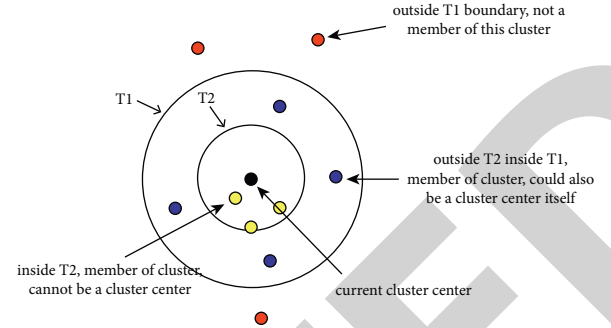


FIGURE 12: Diagram of clustering process of canopy algorithm.

- (6) Execute the loop operation until the element data in list  $L$  are no longer changed or the number of elements is 0.

The clustering process of canopy algorithm is shown in Figure 12:

Administrative management involves a large number of complex problems in different forms, such as science and technology and production. Cluster analysis has broad application space for this. But at the same time, because the problem types of government design are complex, cluster analysis should have good scalability to ensure the clustering effect; the field of administration needs to deal with various types of data and should also have the ability to deal with different types of data; minimize the domain knowledge that determines the input parameters and reduce the burden and time cost of users; and it has the ability to process noise data and reduce the sensitivity of the algorithm to noise data. At the same time, users often hope that the cluster analysis results are interpretable, understandable, and useable. Therefore, the visual display of cluster analysis results in intuitive, dynamic, multifactor, plane, and three-dimensional forms that will achieve better results.

## 6. Conclusion and Future Work

In this study, an intelligent management platform based on big data is designed and implemented. The platform can effectively solve the problem of information's island and fragmentation, promote data sharing, realize the connection between information resources and management platform, and reduce the interference of human factors on data information. We analyzed the application of data mining technology in administration, analyzed the objects of data mining, and designed a data mining system to analyze and process data. In the interim, it mainly includes data pre-processing module and data mining module. Effectively integrate structured, semi-structured, and unstructured data, analyze, and tap its potential value, so as to effectively improve administrative efficiency and competitiveness. Finally, this paper also introduces the application of cluster analysis in administrative management and expounds the value of cluster analysis. Because government data contain a lot of text information, this paper applies clustering algorithm to the text analysis of big data platform. In terms of demand analysis and big data platform construction, some

details need to be further studied. In the future work, we will further improve and optimize the system, carry out clustering analysis for specific businesses, and continue to explore other efficient clustering algorithms.

## Data Availability

The simulation experiment data used to support the findings of this study can be obtained from the corresponding author upon request.

## Conflicts of Interest

The authors declare that there are no conflicts of interest regarding the publication of this paper.

## Authors' Contributions

All authors participated in the design, interpretation of the studies, and analysis of the data and review of the manuscript. Yunuo Su designed the study. Minhui Dai wrote the original draft. Haoyu Zhou implemented the system. Minhui Dai supervised the study.

## Acknowledgments

This work was supported in part by the National Science Foundation of China (Grant no. 61972147).

## References

- [1] M. Qi and J. Wang, "Using the internet of things E-government platform to optimize the administrative management mode," *Wireless Communications and Mobile Computing*, vol. 2021, Article ID 2224957, 11 pages, 2021.
- [2] Y. Xu, "Design system construction of intelligent enterprise management system based on big data technology," in *Proceedings of the 5th International Conference on Smart Grid and Electrical Automation (ICSGEA)*, pp. 363–366, Zhangjiajie, China, June 2020.
- [3] X. He and P. Liu, "Empirical study on the construction of A unified information system with big data analysis A case of social work organizations and civil affairs departments," in *Proceedings of the 20th IEEE International Conference on Computational Science and Engineering (CSE)/15th IEEE/IFIP International Conference on Embedded and Ubiquitous Computing (EUC)*, pp. 228–233, Guangzhou, China, July 2017.
- [4] M. Li, C. Wang, L. Yan, and S. Wei, "Research on the application of medical big data," in *Proceedings of the 14th International Conference on Computer Science and Education (ICCSE)*, pp. 478–482, Toronto, ON, Canada, August 2019.
- [5] W. Chen, "Analysis and application: sports education information management under the background of big data," in *Proceedings of the 13th International Conference on Measuring Technology and Mechatronics Automation (ICMTMA)*, pp. 543–546, Beihai, China, January 2021.
- [6] L. Zhao, "Business intelligence implementation in the framework of enhanced learning application," in *Proceedings of the 2nd International Conference on Advanced Electronic Materials, Computers and Materials Engineering (AEMCME)*, pp. 563–571, Changsha, China, April 2019.
- [7] C. S. Wang, S. L. Lin, T. H. Chou, and B. Y. Li, "An integrated data analytics process to optimize data governance of non-profit organization," *Computers in Human Behavior*, vol. 101, pp. 495–505, 2019.
- [8] L. H. Zhou, G. Du, R. Wang et al., "A tensor framework for geosensor data forecasting of significant societal events," *Pattern Recognition*, vol. 88, pp. 27–37, 2019.
- [9] M. K. Y. Hong, A. R. Skandarajah, and I. P. Hayes, "Administrative data: what surgeons should know about big data," *Anz Journal of Surgery*, vol. 87, no. 9, pp. 650–651, 2017.
- [10] G. H. Park and D. H. Son, "The determinants for the usage of big data in administrative service: perspectives of the quality control of data," *The Journal of Internet Electronic Commerce Research*, vol. 17, pp. 331–339, 2017.
- [11] H. Li and J. Zhai, "Constructing investment open data of Chinese listed companies based on read-write linked data," *International Journal of Electronic Government Research*, vol. 13, no. 4, pp. 15–33, 2017.
- [12] Z. Li, S. Pei, and G. Feng, "The model design of medical data life cycle based on big data platform," *Journal of Physics: Conference Series*, vol. 1865, no. 4, pp. 042088–042093, 2021.
- [13] O. Koren, C. A. Hallin, N. Perel, and D. Bendet, "Decision-making enhancement in a big data environment: application of the K-means algorithm to mixed data," *Journal of Artificial Intelligence and Soft Computing Research*, vol. 9, no. 4, pp. 293–302, 2019.
- [14] D. Zhao, B. Ning, C. Yang, and I. C. Soc, "Application research on application performance management system in big data of power grid," in *Proceedings of the 40th IEEE International Conference on Distributed Computing Systems (ICDCS)*, pp. 1358–1363, Singapore, July 2020.
- [15] I. Pintye, E. Kail, P. Kacsuk, and R. Lovas, "Big data and machine learning framework for clouds and its usage for text classification," *Concurrency and Computation: Practice and Experience*, vol. 33, no. 19, pp. 2311–2318, 2021.
- [16] D. Zhang, "Analyze the current direction of administrative management reform from the big data perspective," in *Proceedings of the 2nd International Conference on Forthcoming Networks and Sustainability in the IoT Era (FoNeS-IoT) Electr Network*, pp. 281–287, Nicosia, Cyprus, January 2022.
- [17] P. J. Seop and S. M. Lee, "Big data analysis of busan civil affairs using the LDA topic modeling technique," *Informatization Policy*, vol. 27, no. 2, pp. 66–83, 2020.
- [18] G. Zhou, K. Chen, and J. Tu, "Research on big data open intelligent platform of guizhou province E-government service," in *Proceedings of the 3rd International Conference on Computer Science and Application Engineering (CSAE)*, pp. 333–339, Sanya, China, October 2019.
- [19] Y. Liu, "Research on the construction of school education management decision system based on Data Mining Framework," in *Proceedings of the 5th International Conference on Mechanical, Control and Computer Engineering (ICMCCE)*, pp. 2215–2218, Harbin, China, December 2020.
- [20] Y. Dong, "On the evaluation of propagation force of new media for government affairs based on the theory of information acceptance technology," *13th International Conference on Multimedia and Ubiquitous Engineering (MUE)/14th International Conference On Future Information Technology (Future Tech)*, vol. 590, pp. 140–146, Springer, Singapore, 2020.
- [21] Y. Wang, H. Liu, and Q. Liu, "Application research of web log mining in the E-commerce," in *Proceedings of the 32nd Chinese Control And Decision Conference (CCDC)*, pp. 349–352, Hefei China, August 2020.

## *Retraction*

# **Retracted: The Application of Modern Computer-Aided Technology in Fine Art Education**

### **Security and Communication Networks**

Received 26 December 2023; Accepted 26 December 2023; Published 29 December 2023

Copyright © 2023 Security and Communication Networks. This is an open access article distributed under the Creative Commons Attribution License, which permits unrestricted use, distribution, and reproduction in any medium, provided the original work is properly cited.

This article has been retracted by Hindawi, as publisher, following an investigation undertaken by the publisher [1]. This investigation has uncovered evidence of systematic manipulation of the publication and peer-review process. We cannot, therefore, vouch for the reliability or integrity of this article.

Please note that this notice is intended solely to alert readers that the peer-review process of this article has been compromised.

Wiley and Hindawi regret that the usual quality checks did not identify these issues before publication and have since put additional measures in place to safeguard research integrity.

We wish to credit our Research Integrity and Research Publishing teams and anonymous and named external researchers and research integrity experts for contributing to this investigation.

The corresponding author, as the representative of all authors, has been given the opportunity to register their agreement or disagreement to this retraction. We have kept a record of any response received.

### **References**

- [1] B. Wang, "The Application of Modern Computer-Aided Technology in Fine Art Education," *Security and Communication Networks*, vol. 2022, Article ID 8038178, 10 pages, 2022.



## Research Article

# The Application of Modern Computer-Aided Technology in Fine Art Education

**Baoqi Wang** 

*Shangqiu Institute of Technology, Department of Education and Modern Art, Shangqiu, Henan 476000, China*

Correspondence should be addressed to Baoqi Wang; 1350002001@sqgxy.edu.cn

Received 20 June 2022; Revised 1 August 2022; Accepted 20 August 2022; Published 10 October 2022

Academic Editor: Hangjun Che

Copyright © 2022 Baoqi Wang. This is an open access article distributed under the Creative Commons Attribution License, which permits unrestricted use, distribution, and reproduction in any medium, provided the original work is properly cited.

With the popularization of modern computer technology, human society has stepped into the information age. Modern computer technology will have an all-round and deep impact on fine art education in China. In fine art education, various information devices play an important role in broadening the resources of fine art education and effectively improving the quality of fine art education. This study analyzes fine art education in the digital era and studies how the quality of fine art education can be improved through computer-aided technology.

## 1. Introduction

At the beginning of the new century, human society has stepped into the information age [1]. With the development and popularity of computer technology and network technology and the rapid extension of modern information technology in the field of education, traditional fine art education is facing an all-round and deep-seated challenge [2, 3]. In the face of such challenges, how fine art education can conform to the trend, change the ideology of educators, and how it can comprehensively and rationally use modern information technology to optimize the teaching process, develop educational teaching resources, promote educational teaching reform, and thus improve the quality of education and teaching, is the main task facing fine art education in China at present [4].

Professor Schlomann [5] of the Massachusetts Institute of Technology pointed out that in order to understand a society, we must study the information and communication facilities belonging to that society. As we can see from the history of human civilization, each revolution in media technology has changed the way humans live, work, and think. Education, as an important aspect of society's activities, is naturally affected. When writing was used as a medium, schools were created, and the creation and development of printing technology led to the birth of the

modern school. Today, in the face of modern computer technology, our education is facing such an inevitable change. Modern information technology, represented by multimedia technology, network technology, and virtual simulation technology, is characterized by multiple sensory stimulations, high information transmission volume, fast transmission speed, a wide range of applications, intuitive images, strong interactivity, and ease of use [6, 7]. Its combination with fine art education will certainly have a great impact on all aspects of fine art education, making fine art teaching develop in a direction more suitable for the content and characteristics of fine art subjects, making fine art teaching individualized, personalized and independent, thus improving the efficiency and level of fine art teaching as a whole. Of course, this is a test for fine art education. The old concept of education, the form of teaching organization, and the ways and means of education and teaching are bound to be impacted in the new period, causing contradictions and conflicts. At the same time, it is an opportunity to develop and improve our fine art education in the midst of change. As a Canadian scholar, Hawlina [8] says that "Conflict and diversity are our friends, and conflict in complex and turbulent conditions is likely to be associated with creative breakthroughs." We look forward to the new vitality of fine art education driven by modern information technology.'

In the 21st century, the shift from visual culture to fine art education has brought about new educational trends, providing unlimited creativity and possibilities for fine art creation, which continue to permeate in the field of fine art, bringing about marked changes in the goals, fields, methods, and evaluation of education [9, 10]. Facing the future social life, students in colleges and universities are required to continuously improve their own literacy, as well as their creative thinking, critical visual literacy, etc. In 2010, the United Nations Educational, Scientific, and Cultural Organization in Seoul, Korea, held the second annual World Conference on Arts Education in Seoul, Korea, where the Seoul Agenda for the development of fine arts education aimed to play an important role in digital media. In 2011, at the 33rd International Art Club World Congress in Budapest, Hungary, the participating experts and scholars pointed out that in teaching, fine art teachers should help students appreciate and create images and other works of fine art in the digital age and in the innovation of teaching methods with the help of digital networks. In 2014, the 34th InSEA International Academy of Fine Arts of the World Congress elaborated on the fine art education diversity and raised important issues such as the teaching of new media fine art and contemporary fine art [11, 12]. Modern fine art education is a multifaceted field covering a wide range of knowledge systems, such as humanities, society, ecology, and technology. It should be identified in a way that includes integration. In the General College Fine Art Curriculum Standards (experimental), "modern media fine art" refers to the fine art of students learning to use video equipment, devices and technology, computer technology, and Internet resources to read and analyze images, pictures, and symbols to complete new media and creative works. Public images and symbols are employed in the teaching of fine art in science, technology, and the media to give students an understanding of the visual culture, the connection between society and culture, and the variety of meanings associated with human existence.

The Chinese educational system has gradually advanced and improved, but for a while in the past, research studies into the advancement of fine art education were rather neglected, leaving the previous educational philosophies and teaching techniques to still have an impact on the field today. The emergence of modern computer technology has provided a new direction for the development of fine art education, and China's fine art education has entered a stage of change. With the continuous development of the times, digital technology has brought great changes to people's daily lives and work. In the background of the digital era, the combination of teaching and information technology is also an inevitable trend in the development of education [13, 14].

## 2. A Brief Analysis of the Background of the Digital Era

*2.1. Analysis of the Definition of the Digital Era.* The digital era uses computers to transform information in life into digital information, the essence of which is the process of digital technology in the field of information advancing to

different areas of human life, which can be reflected in all corners of life, most notably within the field of mass communication. The comprehensive promotion of digital technology has provided great convenience to people's lives and work.

*2.2. Analysis of the Essence of the Digital Era.* The essence of the digital era is development, compatibility, and sharing. Openness is its most basic characteristic and it is the key to its development; and the characteristics of compatibility and sharing are the important foundation for the gradual development and improvement of the digital era (in Figure 1).

## 3. Analysis of the Characteristics of Contemporary Fine Art Education

*3.1. Subjectivity.* The most important feature of contemporary fine art education is students' participation, which is also the core content of contemporary fine art education [15, 16]. It mainly refers to the process of education based on the equal relationship between teachers and students, giving full play to students' subjective initiative and guiding them to form relevant abilities, qualities, and value orientations. In order to effectively engage students in experiential learning and to support their overall development, instructors must not only possess professional knowledge and skills but also be sensitive to the emotional needs of their charges.

*3.2. Systematic.* Contemporary fine art education no longer stays at the visual level, but puts forward more systematic requirements, requiring students to form their own knowledge structure system based on their own ability to discern, analyze, reflect, think, and judge on the basis of visual reception and then apply it to multiple fields, so as to effectively promote their own comprehensive development.

*3.3. Diversity.* With the development of the times, contemporary fine art education not only requires students to have certain knowledge but also requires them to have a pluralistic view of culture and the times. Specifically, teachers should dig deeper into the humanistic factors contained therein, on the basis of static pictures and moving images, and thus effectively broaden students' art horizons.

*3.4. Criticism.* The requirements of contemporary fine art education for students tend to be comprehensive, requiring not only good aesthetic and cognitive analysis skills but also critical visual reading skills. By cultivating students' visual reading skills, students are guided to explore the style and techniques of works and thus gain a deeper understanding of the aesthetic value and the meaning behind them.

### 3.5. Current Problems

*3.5.1. Influence of Inherent Concepts.* Some people do not attach much importance to fine art education, and thus fine art education has a low status in contemporary subject

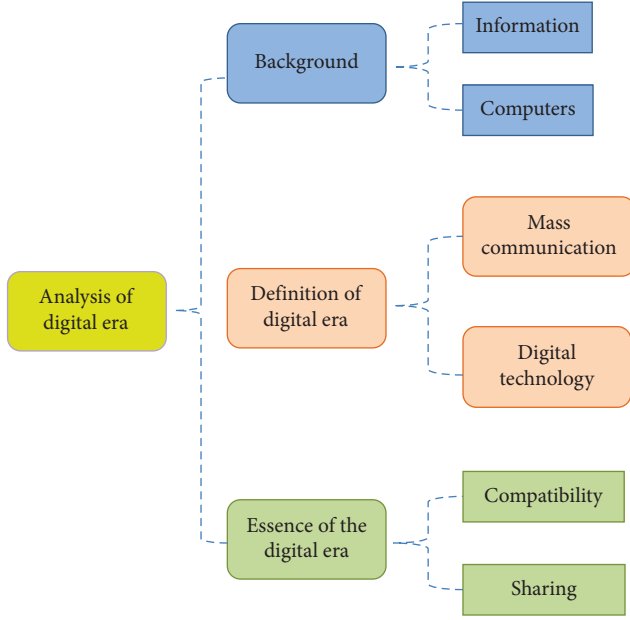


FIGURE 1: The technology roadmap analysis of the digital age.

education, which is very unfavorable to the development of fine art education. In addition, some teachers have an overly strong concept of further education and fail to cultivate students comprehensively, resulting in some students' low core fine art literacy, which limits the development of students' core fine art literacy.

**3.5.2. Teaching Methods Are Too Single.** Some teachers do not know enough about contemporary fine art education, and when they carry out teaching, they adopt the indoctrination teaching mode, which is not only ineffective but also frustrates students' learning enthusiasm, which in turn affects the development of later teaching.

**3.5.3. Teacher Team Construction Is Not Perfect.** In the process of fine art education, the construction of the teacher team is particularly important. As the initiator and guide of teaching activities, teachers directly affect the subsequent teaching efficiency and teaching effect. However, there is an aging phenomenon in the teaching team of some schools, and some teachers are not strong in adapting to the digital era, which is an important factor limiting the development of contemporary fine art education.

**3.5.4. Lack of Effective Teaching Evaluation and Reflection.** Teaching evaluation and reflection are the links to checking and filling in the gaps in teaching, and they are also the keys to the development of teaching. However, in the actual teaching process, the lack of teaching evaluation and reflection is caused by some teachers' insufficient cognition, which affects the efficiency and effectiveness of contemporary fine art education. The relationship curve between teaching evaluation and reflection and the efficiency and

effectiveness of contemporary art education is shown in Figure 2.

## 4. Change of Fine Art Education

**4.1. From the Transmission of Knowledge to the Cultivation of Ability.** Modern information technology is changing people's lives and work. In the field of fine art education, the society in which students live today and the society in which they will live and work in the future are very different from those in the past [17, 18]. The old concept that the function of education is to impart knowledge and skills is no longer suitable for the development of society and must be updated. From the perspective of discipline development, the new knowledge and technology related to fine art in the new society can be said to be rapidly developing and renewing as compared to before, as illustrated in Figure 3. It is almost a luxury to recognize and master all the new knowledge and technology. On the other hand, from the viewpoint of the channels of acquiring knowledge, in the information society, the channels for students to acquire new knowledge and skills are extremely diversified [19]. It is undoubtedly a great waste to use precious school education for such a purpose. Schooling should be an effective education that enables the educated to understand the process of development of knowledge structures so that they can master the ability to construct knowledge themselves. Educators must understand that knowledge is constructed by the learners themselves and not acquired by receiving it from teachers. School education should also equip the educated with the ability to live and work in the information society through effective education. Information overload will be the environment in which students must survive in the future, and being able to search for, pick out, and use information will be a survival skill. Nowadays, learning to search, classify, produce, communicate, and use knowledge creatively is the fundamental goal of education rather than simply teaching people how to record information.

Given the perspective of discipline development, the new knowledge and technology related to art are defined as a set  $\chi = \{X_j\}_{j=1, \dots, J}$ , where  $J$  is the information joints, and the position access to knowledge ( $u$  and  $v$ ) of the  $j$ th a-joint in the fine art is denoted by the vector  $X_j \in x$ . Effective education consists of a process of the development of knowledge structures with the ability to live and work.  $\varphi_t(\mathbf{X})$  in the information society through effective education providing confidence  $S_{jt} \in R^{w \times h}$  for each joint  $j$ , where  $w$  and  $h$  are the ability to search, select, and use information, respectively, and  $t$  denotes the  $t$ th stage. In the first stage, the following equations can provide confidence scores to search, classify, create, communicate, and use the information.

$$\begin{aligned} \varphi_t &= 1(\mathbf{X} | \mathbf{I}), \\ \varphi_t &\longrightarrow \{s_1^j(\mathbf{X}_j = \mathbf{X})\}_{j=1, \dots, J+1}, \\ \varphi_t &= 1(\mathbf{X} | \mathbf{I}) \longrightarrow \{s_1^j(\mathbf{X}_j = \mathbf{X})\}_{j=1, \dots, J+1}. \end{aligned} \quad (1)$$

All subsequent stages generate new confidence scores using the contextual information from the previous stage:



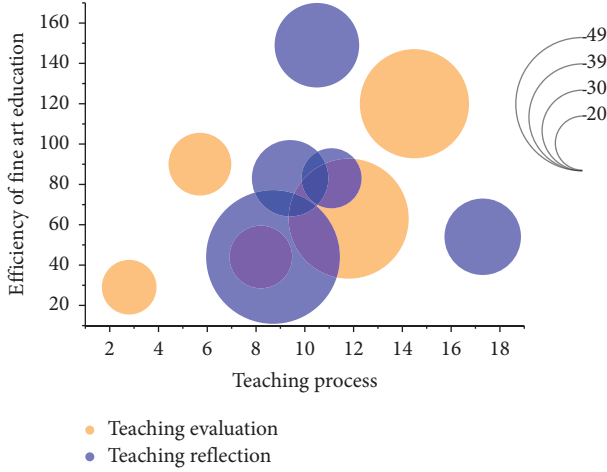


FIGURE 2: The relationship curve between teaching evaluation and reflection and the efficiency and effectiveness of contemporary art education.

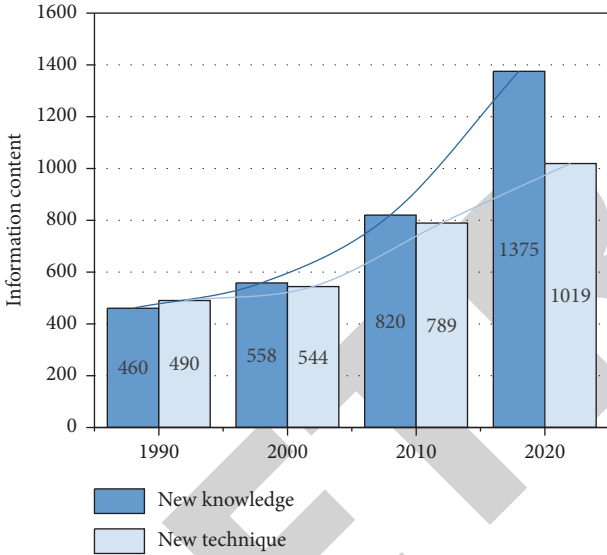


FIGURE 3: Comparison of the growth of new knowledge and new technology over time.

$$\begin{aligned} \varphi_t > 1 [\mathbf{X} | \mathbf{I}, \psi(\mathbf{X}, \mathbf{S}_{t-1})], \\ 1 [\mathbf{X} | \mathbf{I}, \psi(\mathbf{X}, \mathbf{S}_{t-1})] \longrightarrow \{s_t^j(\mathbf{X}_j = \mathbf{X})\}_{j=1, \dots, J+1}, \\ \varphi_t > 1 [\mathbf{X} | \mathbf{I}, \psi(\mathbf{X}, \mathbf{S}_{t-1})] \longrightarrow \{s_t^j(\mathbf{X}_j = \mathbf{X})\}_{j=1, \dots, J+1}. \end{aligned} \quad (2)$$

**4.2. From Closed and Single Passive Learning to Open and Diversified Active Learning.** With the development and popularity of network technology, the restrictions of time and space on learning have been completely lifted, and learning has becoming more free [20]. The network connects schools, families, libraries, museums, fine art galleries, and fine art research institutions. Anyone can get the information they need from the network without any limitation of time and space. From the perspective of fine art teaching,

fine art as a visual art, the “viewing” of artworks is an important part of the fine art learning process. Only through the “viewing” of a large number of artworks can we understand the universal laws of art in all their aspects and can we thoroughly understand and master the techniques and skills of each art discipline. The Internet, with its unique advantages of a large amount of information, fast retrieval, ease of use, and portability, meets the need for such “viewing” in fine art teaching. In the network, students can easily and quickly “watch” any artwork of each historical period that they need to “watch” at any time. A CD-ROM entitled “Encyclopedia of the World’s Best Sketches” contains the sketches of almost all the influential painters of the five centuries from the 15th-century Italian painter Pisanello to the late 20th-century French painter Marsal. Each painter’s masterpieces are included in a comprehensive manner. Taking German sketch master Menzel as an example, the CD-ROM contains 85 of his works, while the book “Menzel Sketch Collection” only contains 52 of his sketches. Thus, we believe that modern information technology has provided us with unprecedented convenience in fine art learning that transcends time and space. This convenience will undoubtedly greatly improve the efficiency of fine art learning. The traditional one-way indoctrination teaching method of teachers explaining and students taking notes, or teachers demonstrating and students copying, cannot adapt to the needs of the new situation as computer and network technology continue to develop, mature, and permeate into the field of education.

Network teaching, distance learning, virtual reality simulation teaching, and other new teaching methods have become possible. The information sources for art students have expanded from traditional teachers, textbooks, and picture books to art museums and museums worldwide, as well as the many professional art websites and forums on the Internet. Students can learn independently through human-computer dialogue using computer-assisted software. Students can also access professional art websites through the Internet to browse the latest art information and artworks, to learn about professional developments, and to gain visual experience [21, 22]. They can also log on to professional art forums for academic discussions or ask experts via e-mail to solve their problems, from which they can learn and consolidate their knowledge. In short, with the involvement of information technology, the ways of learning have become more diversified. In the presence of new learning styles, students’ transition from being passive recipients of knowledge to becoming active learners is observed. The learning initiative of the students is completely developed, which obviously increases the motivation of the students to learn and raises the level of learning quality.

Information sources for art students have originated from many professional art websites and forums on the Internet (each professional art website corresponds to a channel, which represents the  $x$  and  $y$  coordinates of the node, respectively), and then the introduction of multimedia digital technology is induced to produce more diversified learning methods. The involvement of information technology is performed as follows:

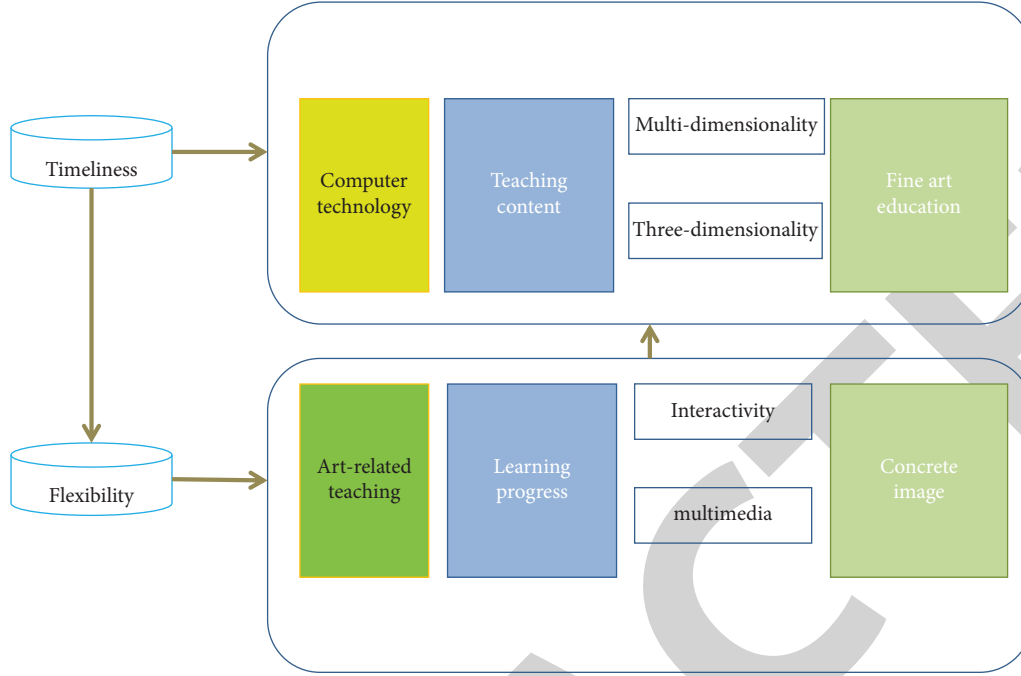


FIGURE 4: The advantages of computer technology in fine art education.

$$\begin{aligned}
 U_j &= G[x_j + F_k(x_j) - x_i]h_k(x_j) + \sqrt{h_k(x_j)}, \\
 f_k(x_k) &= \sum_j \frac{1}{\pi R^2} W_j, \\
 f_k(x_k) &= \sum_j \frac{1}{\pi R^2} G[x_j + F_k(x_j) - x_i]h_k(x_j).
 \end{aligned} \tag{3}$$

## 5. The Advantages of Computer Technology in Fine Art Education

**5.1. Timeliness.** Computer technology can better meet the needs of fine art education by virtue of its own time-sensitive nature [23]. With the assistance of computer technology, teachers can show students the historical changes and evolution of art-related genres through the display of a large amount of information, which is different from the previous summary of a small amount of information but can deepen students' knowledge of art through the comparison and systematic introduction of a large amount of information. In addition, because computer technology can facilitate the collection of contemporary teaching content, the usefulness of fine art teaching will be greatly enhanced, and the distance between students and artworks can be eliminated (Figure 4).

**5.2. Multidimensionality.** The application of this multidimensional feature to fine art education will free fine art education from the confines of a small teacher, and the tutor in a foreign country will be able to teach students through computer technology, which naturally makes fine art

education much more flexible, and the better development of fine art education will also be strongly supported.

**5.3. Flexibility.** If computer technology is used in fine art education, students will be able to learn art at any time and any place through the Internet, and lifelong education will become a reality. Under the influence of computer technology, students can be free from the shackles of family origin, status and wealth, and can participate in fine art education on an equal footing, which naturally increases the effectiveness of fine art education.

**5.4. Three-Dimensionality.** Under the role of computer technology, images, colors, and other factors can form a multimedia three-dimensional information system through the collection, and this is the best expression of the multimedia nature of computer technology [24]. Under the influence of the multimedia of computer technology, fine art education can make many abstract and complicated art-related teaching contents become concrete images through multimedia, so students' interest in art-related learning will be greatly enhanced, which can also change students' passive fine art learning in the past into active learning.

**5.5. Interactivity.** Under the influence of interactivity, students can freely grasp the learning progress and can choose the learning content in the computer technology-assisted fine art education, and the better human-computer interaction achieved in this process will also make the effectiveness of fine art education to be greatly improved.

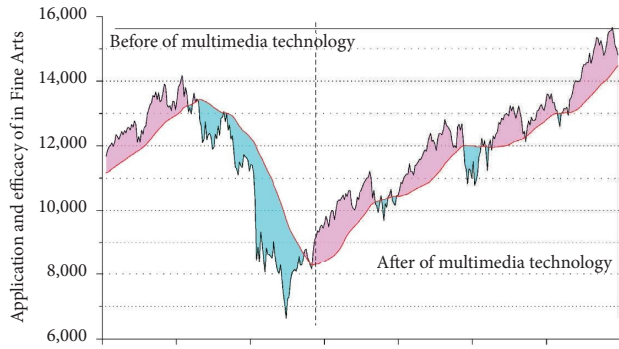


FIGURE 5: Relationship curve between multimedia technology and the art education effect.

## 6. Strategies to Realize the Application of Computer Technology in Fine Art Education

**6.1. The Application of Multimedia Technology.** For the application of multimedia technology in fine art education, the composition of this computer technology can achieve better application in a variety of teaching applications such as drawing, color, composition, art appreciation, and decorative patterns [25]. Take the application of multimedia technology in art appreciation as an example. In traditional fine art education, this education itself tends to be more of a rational knowledge transfer, but the application of multimedia technology makes fine art education to have comprehensive content of sound, text, pictures, and images, which makes the teaching related to art appreciation better developed, as illustrated in Figure 5. In the specific “European Renaissance” painting appreciation, without multimedia equipment, this part of teaching is usually done through textbooks and materials prepared by teachers, but with the support of multimedia equipment, teachers can apply multimedia equipment to play scenic film clips of Florence, Italy, and the works of the great masters of Renaissance painting, and these in turn can show the Renaissance. In this process, if the teacher can supplement the explanation with short stories about Renaissance painters, the rigorous, grand and solemn artistic style of Renaissance painting can be conveyed to students in a more intuitive way. In the teaching of appreciation of Chinese sculptures such as “Terracotta Warriors and Horses” and “Terracotta Warriors and Horses of the First Qin Emperor,” students do not have access to the actual objects and imitations, so this teaching cannot be done only through pictures in books, but with the support of multimedia technology, the multimedia screen can show the relevant sculptures in front of students in 360 degrees without any dead angle, and if this process is supplemented with ethnic music, students will become more attentive to participate in the appreciation teaching, and this process will greatly stimulate students’ interest in fine art learning, and the effectiveness of college fine art education will be greatly enhanced.

**6.2. Application of Digital Interactive Technology.** In addition to multimedia technology, digital interactive technology can also be applied in fine art education. In many large

museums, we can often see digital books that can recognize people’s movements, which is a typical digital interactive technology and combined with the characteristics of digital interactive technology, we can easily find that fine art education can better improve its effectiveness with the support of digital interactive technology. For fine art education, the teaching of art knowledge related to abstract space is often the difficult part of teaching. Students do not have the ability to enter this kind of abstract space to embody it, and the teaching of abstract space naturally cannot be better developed. With the support of digital interactive technology, students will participate in the learning of art knowledge as if they were in the real world, and they will unconsciously integrate it into the learning of art knowledge so that the effectiveness of fine art education can naturally be improved. We anticipate that digital interactive technology will play a bigger role in the future of fine art education because many scientific research organizations in China have already begun to investigate art-related teaching equipment mixed with digital interactive technology.

**6.3. Application of Three-Dimensional Virtual Interactive Technology.** There are two application modes of 3D virtual interactive technology: traditional and innovative.

**6.3.1. Traditional Application Mode.** In the traditional three-dimensional virtual interactive technology application of fine art education, students wear three-dimensional light gate glasses, and teachers apply three-dimensional virtual interactive technology to carry out the relevant fine art knowledge which is the main content of this traditional mode, and in this content of fine art education, students can, in the three-dimensional light gate glasses and three-dimensional virtual interactive technology support, watch three-dimensional artworks and the artist’s growth experience also. The growth experience of the artist can also be shown to students more vividly, which naturally makes fine art education better. It is worth noting that the traditional fine art education mode of 3D virtual interactive technology is more suitable for the theoretical teaching of fine art introduction, sculpture theory class, sketching, color, and drawing.

**6.3.2. Innovative Application Mode.** In addition to the traditional application mode, three-dimensional virtual interactive technology in fine art education is also an innovative application mode. This innovative application mode needs to be supported by VR equipment to be able to be successfully carried out. Specifically, teachers need to prepare VR equipment and open rooms for students, so that they can really feel the real virtual scenes of ancient clothing, Western palace interior scenes, Dunhuang cave murals, etc., through VR equipment, and if teachers can provide students with wireless Bluetooth data gloves, the virtual reality fine art teaching that students participate in can be further improved under the pressure and weight provided by the gloves. Fine art teaching will also be better developed as a result. It is

worth noting that this innovative application of three-dimensional virtual interactive technology is more suitable for fine art teaching and appreciation teaching. 3D virtual interaction technology ( $V_p$ ) is chosen to measure the comparability between the art education mode and the innovative application mode, and the formula is

$$R_i = \sum_i \exp\{-d_{pi}^2/2S_p^2\sigma_i^2\}\delta(v_{pi} = 1),$$

$$OKS_p = \frac{R_i}{\sum \delta(v_{pi} = 1)}, \quad (4)$$

$$V_p = \frac{\sum_i \exp\{-d_{pi}^2/2S_p^2\sigma_i^2\}\delta(v_{pi} = 1)}{\sum \delta(v_{pi} = 1)},$$

where  $p$  is the ID of the 3D virtual interaction technology;  $i$  is the ID of the VR device;  $d_{pi}$  denotes the wireless Bluetooth data between the  $i$ -th key point predicted by the  $p$ -th VR device and the real labeled key point;  $S_2$  denotes the pixel area occupied by the  $p$ -th virtual technology; and  $\sigma$  denotes the innovative application mode factor of the  $i$ -th key point.

## 7. The Significance of Modern Computer Technology Applied in Fine Art Education

**7.1. Pay Attention to the Advantages of Digital Technology in Fine Art Teaching, and Improve Students' Art Literacy with the Clever Use of Digital Technology.** Among the tools used in painting, paints and brushes are still indispensable elements in painting. The accumulation of paints according to painting techniques and sequences will produce paintings that are undoubtedly limited by the lighting environment, the size of the work, the type of work, and other factors. In addition to the external factors that can affect the painting process, the finished painting is not easily preserved, a situation that is sometimes very serious in fine art teaching. A beautiful painting may be destroyed by accidentally staining it with other paints, which is a loss of the work and interrupts the teaching process even more. It would take longer time and labor to redraw a picture, and the fine art teaching schedule does not allow for such remedial measures. Compared with traditional painting, computer painting can show one's design and creativity with digital graphics. Using computers to draw pictures means one does not have to worry about the work being damaged by paints, and it can also be displayed outside the classroom and can be reproduced and widely disseminated according to the designer's needs, which greatly improves the effect of art promotion. It can be said that modern information and digital technology has improved the efficiency of fine art education.

Students are expected to grasp the fundamentals of traditional painting throughout their studies, including painting and modeling techniques as well as picture coordination abilities. Traditional painting is a finished product that has been consistently improved and summarized by past generations. Fine art education has to impart painting skills

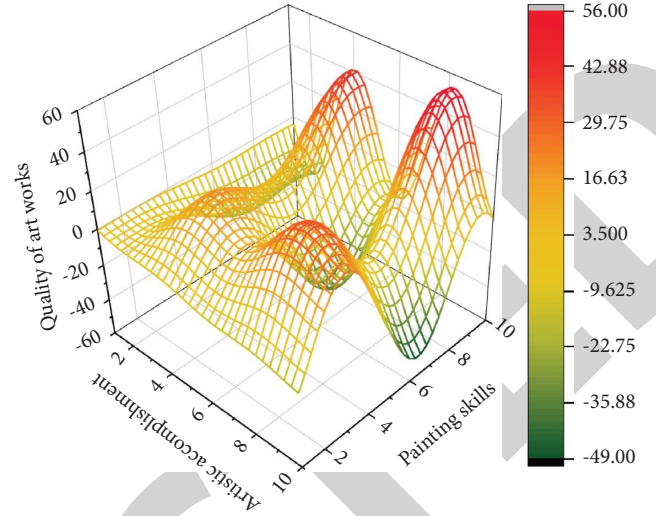


FIGURE 6: The relationship between the quality of students' creative works related to drawing technology and artistic literacy.

to students in a limited time and, more importantly, improve students' art literacy, while the results are often unsatisfactory, with problems such as students' poor mastery of painting skills and difficulties in improving quality education. The constantly improving digital painting technology and software functions can change the drawbacks of the previous teaching. As long as teachers guide students to put more energy into modeling skills exercises and picture construction, no matter how complex the colors are rendered, they can obtain the expected effect, and students will create paintings like the works of painting masters, which will certainly increase their interest in learning. Through the sample statistics, it is found that the quality of students' creative works is closely related to drawing technology and artistic literacy. The relationship between the three is shown in Figure 6.

**7.2. Combine Traditional Painting and Digital Technology to Give Full Play to the Comprehensive Role of Fine Art Education.** The application of digital technology is not to change traditional fine art teaching, but to effectively make up for the deficiencies existing in traditional painting and, to a certain extent, save financial, material, and human resources for fine art education, prompting teachers to spend more educational time on inspiring students' art inspiration, enhancing students' comprehension of paintings, and improving students' artistic quality. The combination of traditional painting and digital painting will undoubtedly improve the efficiency of college fine art teaching and students' art literacy. Modern computer art provides students with a new perspective in terms of line, color, composition, space, etc. Students can complete their learning tasks more easily and quickly through computer painting, and more importantly, they can master art concepts and art skills from it and can develop to a higher level. The teaching of fine art is not a study of painting skills alone but also involves the ability to recognize, shape, aesthetics, and other aspects. In



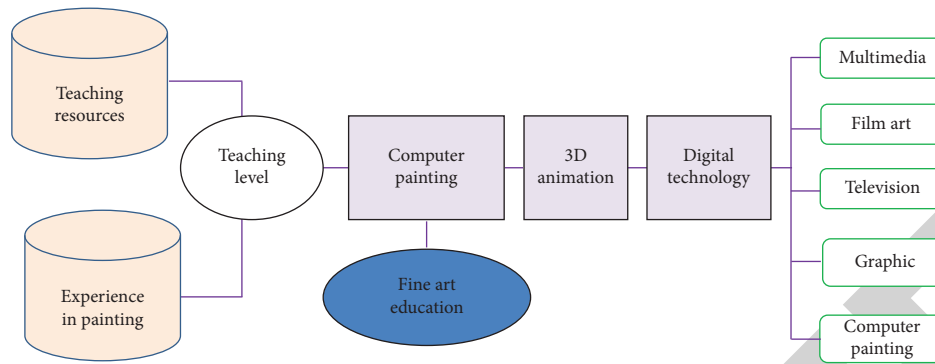


FIGURE 7: Method roadmap to improve the teaching level of fine art teachers.

order to completely realize the overall role of fine art education and to holistically purify the mind, students should not simply give up conventional painting before adopting computer painting software. Instead, they should blend the two skillfully.

### 7.3. Improve the Teaching Level of Fine Art Teachers.

There is no doubt that teachers are an important carrier to play the role of teaching resources and in imparting knowledge, especially in the digital era. Teachers need to have rich experience in painting so as to effectively improve the quality of fine art education in colleges and universities. It can be said that with multimedia teaching, computer painting and digital technology gradually became the social development trend and irreversible trend. Furthermore, it also became the teaching goal to be achieved in contemporary fine art education. Some fine art teachers are not strong in accepting new things and are relatively backward in both educational concepts and teaching methods. Therefore, changing the concept of fine art teachers is a prerequisite for realizing digital fine art education. Teachers should be made fully aware of the advantages of high efficiency and accuracy brought about by computer painting, and more importantly, they should realize that digital technology has been commonly applied to many fields such as 3D animation, film and television advertising design, and graphic design, so that teachers can take the initiative to enrich their teaching experience, change their teaching methods, and improve the effect of fine art education. At the same time, teachers' ability to use modern computer teaching should be continuously improved. The method roadmap to improve the teaching level of fine art teachers is shown in Figure 7. At present, many fine art teachers have rich experience in painting creation and advanced theories but often lack the ability to use computer technology. Teachers can be regularly organized to attend training in digital painting technology, and those who master new knowledge can lead students into the magical digital art world in teaching, exert their talents, and can continuously improve their artistic cultivation and artistic creativity. It can be said that digital technology has become one of the important means of modern fine art education. Compared with

other subjects, art has a closer connection with multimedia information technology. Teachers may easily produce paintings, edit them, and collage them at will using the editing, storage, and switching features of a computer with the use of digital technology, which significantly alters the way that fine art is taught while also enhancing the learning environment in the classroom.

### 7.4. Effectively Improve Art Literacy.

In the digital era, art is able to be taught repeatedly through information technology, making multiple connections to works of art, thus improving the quality of fine art education. In traditional fine art education, most drawing skills are summarized on the basis of previous experiences, which is the core of fine art education. It includes not only the skills of coordinating the picture as well as modeling involved in painting, but also the familiarity with the experimentation of painting tools and materials, as well as the reasonable way of operation. It is only through this all-round teaching that students can really learn how to appreciate and paint a piece of art. But this whole educational process is quite difficult and takes a long time. In education, it is a very difficult task to make students learn a lot of drawing skills in just a few years and at the same time improve their artistic skills. Through practical investigation, it is found that the quality of teaching is hardly satisfactory; many students have average skills in drawing and there is no obvious improvement in artistic quality; they often only get a diploma after several years of study, which is not in line with the purpose of our education and is not conducive to the future development of students. With digital technology, it is possible to get rid of the limitations in traditional teaching by transferring tedious tasks such as mixing paints to the computer and modulating complex colors with only simple instructions. Not only is accuracy guaranteed, but there is no need to invest more time and effort in the time-consuming and labor-intensive aspects of the process. Digital painting skills are growing as science and technology advance, and the advancement of software has made it possible to teach techniques that, in the past, could only be executed by masters. By seeing the works of masters, pupils can mature and develop their artistic qualities, and this will significantly raise their enthusiasm for learning.

## 8. Conclusion

In addition to being a recent invention in the field of fine art education, the utilization of contemporary computer-aided technology is also a sign of the times. The use of contemporary computer-aided technology in fine art education is covered in detail in this article, along with its benefits. Three methods are suggested for implementing computer technology in fine art education: multimedia technology, digital interactive technology, and three-dimensional virtual interactive technology. Thus, we can find that if we want computer technology to better support fine art education, relevant teachers must also master the way of fine art education combined with computer technology, and at the same time they must pay full attention to the advantages of modern computer technology in fine art education. They must skillfully improve art literacy with the help of digital technology, combine traditional teaching with digital technology, and give full play to the comprehensive role of fine art education, so that we can really achieve the better improvement of fine art education.

## Data Availability

The experimental data supporting the current study are available from the author upon request.

## Conflicts of Interest

The author declares that they have no conflicts of interest.

## Acknowledgments

This work was sponsored in part by Henan Province Higher Education Teaching Reform Research and Practice Project, under Grant no. 2021SJGLX311.

## References

- [1] M. Castells, "Space of flows, space of places: materials for a theory of urbanism in the information age[M]," *The City Reader*, pp. 240–251, Routledge, Oxfordshire, England, UK, 2020.
- [2] S. K. Kakhkhorov and Z. D. Rasulova, "Methodology of improving the professional activity of the future teacher of technology on the basis of modern educational technologies," *Universal Journal of Educational Research*, vol. 8, no. 12, pp. 7006–7014, 2020.
- [3] L. N. Mikhailovna and S. E. Anatol'Evna, "Art education as a way of preserving the traditional ethnocultural identity of indigenous minority peoples from the North, Siberia and the Far East[J]," *Science for Education Today*, vol. 8, no. 4, pp. 233–247, 2018.
- [4] N. Sayfullaev, "Current issues on fine ARTS education: continuity and prospects for development[J]," *J. Religación: Revista de Ciencias Sociales y Humanidades*, vol. 4, no. 20, pp. 192–194, 2019.
- [5] A. Schlomann, A. Seifert, S. Zank, C. Woopen, and C. Rietz, "Use of information and communication technology (ICT) devices among the oldest-old: loneliness, anomie, and autonomy," *Innovation in Aging*, vol. 4, no. 2, 2020.
- [6] J. Lines, E. D. Martin, P. Kofuji, and J. Aguilar, "Astrocytes modulate sensory-evoked neuronal network activity," *Nature Communications*, vol. 11, no. 1, pp. 1–12, 2020.
- [7] J. Demas, J. Manley, F. Tejera et al., "High-speed, cortex-wide volumetric recording of neuroactivity at cellular resolution using light beads microscopy," *Nature Methods*, vol. 18, no. 9, pp. 1103–1111, 2021.
- [8] H. Hawlina, A. Gillespie, and T. Zittoun, "Difficult differences: a socio cultural analysis of how diversity can enable and inhibit creativity," *Journal of Creative Behavior*, vol. 53, no. 2, pp. 133–144, 2019.
- [9] R. Wang, "Computer-aided interaction of visual communication technology and art in new media scenes," *Computer-Aided Design and Applications*, vol. 19, no. S3, pp. 75–84, 2021.
- [10] J. Peters and H. Roose, "From starving artist to entrepreneur. Justificatory pluralism in visual artists' grant proposals," *British Journal of Sociology*, vol. 71, no. 5, pp. 952–969, 2020.
- [11] K. S. Kupaysinovna, "Advanced experiences in the use of digital technologies in teaching fine arts (on the example of Finland and South Korea)[J]," *Turkish Journal of Computer and Mathematics Education (TURCOMAT)*, vol. 12, no. 7, pp. 939–946, 2021.
- [12] T. Portnova, "Information technologies in art monuments educational management and the new cultural environment for art historian[J]," *TEM Journal*, vol. 8, no. 1, pp. 189–194, 2019.
- [13] M. Ally, "Competency profile of the digital and online teacher in future education," *International Review of Research in Open and Distance Learning*, vol. 20, no. 2, 2019.
- [14] M. Huda and K. S. M. Teh, "Empowering professional and ethical competence on reflective teaching practice in digital era[M]//Mentorship Strategies in Teacher Education," *IGI Global*, pp. 136–152, 2018.
- [15] D. Kenning, "Art world strategies: neoliberalism and the politics of professional practice in fine art education," *Journal of Visual Art Practice*, vol. 18, no. 2, pp. 115–131, 2019.
- [16] Y. Yang, "Teaching research on higher vocational pre-school education of professional art course based on innovation and entrepreneurship education," *Creative Education*, vol. 09, no. 05, pp. 713–718, 2018.
- [17] T. N. Nozimovich, Y. N. Ibrahimovna, and J. R. Ravshanovich, "Development of student's creative abilities in the fine arts in the higher education system," *The American Journal of Social Science and Education Innovations*, vol. 02, no. 07, pp. 232–238, 2020.
- [18] M. Yeniasir and B. Gökbulut, "Opinions of fine arts students about their profession and their expectations from the future," *Education Sciences*, vol. 8, no. 3, p. 100, 2018.
- [19] J. Wu, Z. Ma, and Z. Liu, "The moderated mediating effect of international diversification, technological capability, and market orientation on emerging market firms' new product performance," *Journal of Business Research*, vol. 99, pp. 524–533, 2019.
- [20] S. Ren, Y. Hao, L. Xu, H. Wu, and N. Ba, "Digitalization and energy: how does internet development affect China's energy consumption?" *Energy Economics*, vol. 98, Article ID 105220, 2021.
- [21] E. M. Schoevers, P. P. M. Leseman, and E. H. Kroesbergen, "Enriching mathematics education with visual arts: effects on elementary school students' ability in geometry and visual arts," *International Journal of Science and Mathematics Education*, vol. 18, no. 8, pp. 1613–1634, 2020.
- [22] E. Villaespesa, "Museum collections and online users: development of a segmentation model for the metropolitan

## *Retraction*

# **Retracted: Design of the Intelligent Recognition Model for English Translation Based on the BP Neural Algorithm**

### **Security and Communication Networks**

Received 26 December 2023; Accepted 26 December 2023; Published 29 December 2023

Copyright © 2023 Security and Communication Networks. This is an open access article distributed under the Creative Commons Attribution License, which permits unrestricted use, distribution, and reproduction in any medium, provided the original work is properly cited.

This article has been retracted by Hindawi, as publisher, following an investigation undertaken by the publisher [1]. This investigation has uncovered evidence of systematic manipulation of the publication and peer-review process. We cannot, therefore, vouch for the reliability or integrity of this article.

Please note that this notice is intended solely to alert readers that the peer-review process of this article has been compromised.

Wiley and Hindawi regret that the usual quality checks did not identify these issues before publication and have since put additional measures in place to safeguard research integrity.

We wish to credit our Research Integrity and Research Publishing teams and anonymous and named external researchers and research integrity experts for contributing to this investigation.

The corresponding author, as the representative of all authors, has been given the opportunity to register their agreement or disagreement to this retraction. We have kept a record of any response received.

### **References**

- [1] Z. Wang, "Design of the Intelligent Recognition Model for English Translation Based on the BP Neural Algorithm," *Security and Communication Networks*, vol. 2022, Article ID 3799061, 12 pages, 2022.

## Research Article

# Design of the Intelligent Recognition Model for English Translation Based on the BP Neural Algorithm

Zhan Wang 

Foreign Language Department, Qinhuangdao Vocational and Technical College, Qinhuangdao 066100, China

Correspondence should be addressed to Zhan Wang; wangz@qvc.edu.cn

Received 4 July 2022; Revised 31 August 2022; Accepted 7 September 2022; Published 6 October 2022

Academic Editor: Hangjun Che

Copyright © 2022 Zhan Wang. This is an open access article distributed under the Creative Commons Attribution License, which permits unrestricted use, distribution, and reproduction in any medium, provided the original work is properly cited.

With the development of modern intelligent recognition, many intelligent recognition translation tools have emerged. These translation tools mainly include machine learning, neural network, KNN, and other artificial intelligence technologies. These technologies have been applied to many fields. Among them, machine translation is the most important and widely used one. A large number of English translation technologies have appeared in this development era. However, the translation accuracy of intelligent recognition technology cannot be guaranteed. Under the background of this English translation environment, we design an intelligent recognition algorithm of English translation based on the BP neural algorithm to improve the rationality of English translation and analyze the intelligent recognition model of English translation. The following conclusions are drawn from the experimental comparison Four Methods of Translation. (1) Compared with some similar algorithms, machine translation based on the BP neural algorithm has many characteristics, such as convenience, which are very suitable for English translation. (2) The intelligent recognition model of English translation using the BP neural network makes the sentence flow higher, which can solve some problems in translation and achieve coherent translation in context. (3) The intelligent recognition model with the BP neural network as the core realizes a variety of permutations and combinations of different characteristics of complex English sentences, solves many poor English sentences, and significantly improves the accuracy of English translation.

## 1. Introduction

In my country, many experts put forward some measures to optimize the network structure. Among them, it has very powerful self-learning and fault tolerance and has been applied in many fields. However, there is no unified and effective scheme for the design of network model structure [1]. English CAI has made great achievements in teaching, but traditional English CAI fails to pay full attention to students' differences in teaching and cannot provide a more perfect service system. To solve this problem, an ICAI Moore system is designed, which can automatically push students' characteristic learning plans according to their different learning effects. Based on students' foreign language knowledge and their own specialties, the system formulates one-to-one learning methods, which is conducive to improving English learning efficiency. The web-based teaching mode can effectively solve the existing problems in

traditional teaching so that both teachers and learners can participate in teaching activities [2]. Syntactic analysis-based English machine translation cannot solve the problem of intelligent recognition in processing a large number of ambiguous parts of English language structure, resulting in low accuracy of machine translation. For the analysis of English translation by perfecting intelligent machine translation tools, an English machine translation model construction method combined with modern intelligent recognition technology is proposed [3]. It can learn to get a new sample and use it to train for another unknown model. Because of the development of neural network technology, in recent 10 years, more and more research studies have been made on neural networks, and some achievements have been made, most of which are focused on financial decision-making. A real estate-listed company is taken as an example for empirical analysis. The results show that the model can accurately reflect the financial distress of enterprises and has



good stability and generalization ability. It shows that the back propagation algorithm is an effective financial risk early warning system [4]. On this basis, a new control strategy, the BP Smith predictor control algorithm, is proposed. Its structure and working principle are also discussed. The relevant results are given. The BP neural network is trained by the classical BP algorithm and the error backpropagation algorithm. Firstly, on this basis, it focuses on how to select the appropriate learning rate to achieve the optimal weight and threshold selection. By comparing the relative deviation between the output of the BP network and the set value under different parameters, the optimal learning rate is determined. Secondly, momentum term and variable step size are introduced to improve the convergence progress of algorithm [5]. This method first converts English sentences into corresponding Chinese sentences and then aligns the Chinese sentences. After training the direct maximum entropy model and obtaining the relevant parameters, the optimal combination mode between different English language features is obtained, which resolved a lot of structural ambiguity in English language and improved the accuracy of English machine translation. After studying and improving the traditional rule-based machine learning algorithm, a new multifeature fusion neural network structure is proposed and applied to word matching in English dictionaries [6]. For the network, the key problem is how to overcome staying at the local minimum point and how to improve the training speed on this basis. An improved scheme is proposed for the selection of learning rate and momentum. When this scheme is applied to digital recognition, it achieves satisfactory results [7]. The constraint response of the BP algorithm is low, and the solution obtained is local optimal. A new power load forecasting model is established by combining the two methods. This model overcomes the characteristics of previous algorithms that are premature. As a global optimization algorithm, the genetic algorithm has strong global search ability, but it is easy to cause premature convergence in practice, and the efficiency of later evolutionary search is not high. A new hybrid genetic operator, simulated annealing, is proposed to solve multiobjective optimization problems. The results of numerical experiments show that this method can be used. The simulated annealing algorithm has the advantages of avoiding falling into local optimal solution and solving premature convergence [8]. The neural network has a wide range of applications in the fields of pattern recognition, image processing, system control, and so on. On this basis, several problems worthy of attention in the future research of artificial neural networks are pointed out. However, the traditional neural network algorithm also has its shortcomings. Network training, for example, is slow and precocious. The artificial neural network optimized by this algorithm is fast and accurate, which can overcome its inherent shortcomings. Therefore, it becomes a very important intelligent information processing technology. Among many artificial neural network models, this algorithm is one of the most important and widely used neural network learning algorithms at present. Because of its easy implementation, it has been recognized and adopted by computer workers. At present,

the BP neural network method has been widely used in various fields. The BP neural network has been widely used, but there are some problems such as slow convergence, easy to fall into local minimum, and difficult to build. In this study, an improved algorithm based on gradient descent is proposed, which adds a new parameter (i.e., weight) to the traditional learning rate formula to accelerate the convergence speed of the network. At the same time, the initial weights are modified to make them close to the optimal solution. The hidden layer structure is determined by experience, but the complex network structure cannot be accurately judged. The artificial neural network can overcome this shortcoming because of its own characteristics. Aiming at the deficiency of the traditional BP neural network, an improved BP neural network algorithm for tobacco industry production data is put forward [9]. English translation plays an important role in our work and life. Our country's economic level is getting higher and higher, science and technology are getting more and more developed, and some algorithms have emerged. We have designed to add the BP neural algorithm to English translation to improve the use effect of English translation; therefore, it is necessary to apply the BP neural network to English teaching [10]. Based on the traditional BP algorithm, this study puts forward a dynamic full-parameter self-adjusting learning algorithm for the BP neural network and then compiles a computer program to make the selection of hidden layer nodes and the learning rate completely dynamic, reduce the influence of human factors on the learning rate, and improve the adaptability of the network. Based on the traditional BP algorithm, this study puts forward a dynamic full-parameter self-adjusting learning algorithm for the BP neural network and then compiles a computer program to make the selection of hidden layer nodes and the learning rate completely dynamic, reduce the influence of human factors on the learning rate, and improve the adaptability of the network. Compared with other commonly used time-series analysis methods, the method proposed in this study has higher calculation results, higher calculation accuracy, and better generalization ability. Finally, based on the above research results, application software is developed to study the short-term fluctuation law of China's stock market. The software consists of the following three parts: system design, data acquisition, and data processing module and output module. Experimental results show that the time-series analysis model based on the artificial neural network has high accuracy and is regressive to the general support vector machine (SVM). The results show that the dynamic full-parameter self-adjustment algorithm based on the BP neural network has better effects than the traditional method. The trained neural network model can not only accurately fit the training values but can also accurately predict the future development trend [11]. Machine translation mainly includes rule-based translation and template-based translation, but they are all based on complex language rules. We introduce the BP neural network to study the problem of sentence transformation in Chinese-English machine translation. In addition to the integrated BP network model, the network architecture, parameter processing, learning

algorithm, and learning samples are discussed in depth [12]. Reasonable English translation teaching activities can promote students' English translation ability and the English cross-cultural communication level. We should actively carry out teaching reform and properly introduce advanced computer technology to promote the quality of college English translation teaching, promote the development of students' comprehensive English ability, and lay a solid foundation for their future study and growth. With the development of science and technology and the progress of social economy, artificial intelligence technology has been widely used. Among them, artificial intelligence translation is a new high-tech means, which has high practicability and convenience, and can effectively improve the shortcomings of the traditional teaching mode. At present, all colleges and universities in China have begun to attach importance to the development of this work and have achieved initial results. Combining with college teaching is also an important direction of teaching reform at present. In view of this situation, this study makes a detailed analysis of college English teaching in the context of artificial intelligence translation, hoping to provide some help for relevant personnel [13]. Translation can be divided into the following categories: rule-based machine translation and template-based machine translation. The former theory is mature and widely used; the latter lacks deep research on Chinese characteristics and no general technology to implement it. So, there are pros and cons to both. However, both language rules are based on complex language rules and are difficult to generalize in nature. A new type of Chinese-English machine translation is based on process language after combining other methods. The integrated BP network model is given and the network structure, parameter processing, learning algorithm, and learning samples are discussed. This work will help improve the intelligence of machine translation [14]. There are many methods for English character recognition methods. As a classical machine learning algorithm, the BP neural network algorithm has achieved great success. The main reason is its strong nonlinear mapping ability, self-organization, and fault tolerance. It has high practical value. However, the traditional BP neural network algorithm also has some problems in practice. Especially, for some small samples, this phenomenon is more serious. Because the BP neural network has the problems of slow learning rate, easy to produce local minimum points, and easy to diverge, its practical application is limited. This will affect the recognition rate of the whole system [15].

## 2. Research on the BP Neural Network Algorithm

It has a complete theoretical system and a perfect learning mechanism. It is widely used in fault diagnosis and detection in practical engineering field. Aiming at the topology optimization problem of the adaptive neural network, a new adaptive neural network optimization method is proposed. It uses the learning mechanism of

signal forward propagation and error reverse regulation to simulate the response of human neurons to external excitation signals by multiple iterative learning and constructs a multilayer perceptron, which successfully establishes an intelligent network model to process nonlinear information.

**2.1. The BP Neural Network Model.** The backpropagation (BP) neural network is a multilayer network for training the weights of nonlinear differentiable functions, which belongs to the field of the forward neural network, which is mainly used for the following:

- (1) Function approximation and prediction analysis: using input vector and corresponding output vector to train network approximations or predictive unknowns
- (2) Pattern recognition: identification of output vector input of input networks and classification of input vector
- (3) Division: clear and appropriate division of input vector
- (4) Data compression reduces the dimension of the output vector and facilitates transmission and storage

In the specific application of the artificial neural network, the BP network or its changed form is used to build the forward neural network model. This forward network is also the heart of the forward network (BP-ANN), which reflects the most essential aspect of the artificial neural network (ANN). The model structure of the BP neural network is shown in Figure 1.

The activation function in the BP network is inevitably differentiable everywhere, so it is impossible to use binary threshold function ( $\{0, 1\}$ ) and symbolic function ( $\{1, 1\}$ ). These activation functions have their own characteristics, so it is necessary to select appropriate activation functions for training according to specific problems in practical application. However, there is no general and effective method to determine the optimal activation function. This study discusses how to use three common activation functions of neural networks, namely, negative tangent activation function, sigmoid activation function, and linear activator, and to solve nonlinear problems. Sigmoid activation function plays a role in the nonlinear amplification system. It can change the input from negative infinity to positive infinity and convert it into 0–1 or –1–1 output. For larger input signals, the amplification coefficient is small, while for smaller signals, the amplification coefficient is large. Therefore, using sigmoid activation function, we can process and approximately describe the nonlinear input-output relationship. However, since the sigmoid activation function is a linear activation function, it cannot be directly applied to practical problems. Therefore, only when the network output is constrained, for example, when the constraint is 0 to 1, the output layer should contain sigmoid type activation function.

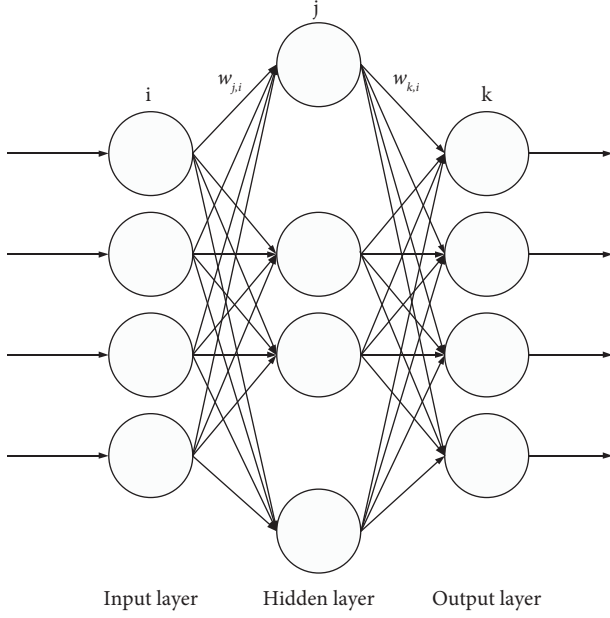


FIGURE 1: The BP neural network model with the hidden layer and the output layer.

**2.2. BP Neural Algorithm Rules.** The BP network refers to a network with three or more layers, where the upper and lower layers are completely connected and the neurons of each layer are not connected. This network structure is called the connectionless neural network topology network model. Because of its simple structure, fast training speed, and strong generalization ability, it has been widely used in many aspects. This study mainly introduces some specific applications of artificial neural network (ANN) technology in fault diagnosis. The neural network technology is summarized and analyzed, and the existing problems and future development direction are pointed out. Finally, I put forward my own views. The BP network is used in pattern recognition, signal processing and other fields, which has become one of the focuses of attention. This study presents an improved BP model. The model consists of three steps.

This algorithm is a supervised learning algorithm. It is proposed according to the “black box” phenomenon in the process of human brain processing information and has been widely used in pattern recognition and other fields. Its main points are as follows: for learning samples with  $N$  inputs:  $X^1, X^2, \dots, X^n$ . It is known that the corresponding output samples are  $T^1, T^2, \dots, T^m$ . The purpose of learning is to use the actual output of the network  $Y^1, Y^2, \dots, Y^m$  and target vector  $T^1, T^2, \dots, T^m$  to correct the weight of the target vector so that the actual output is as close as possible to the target vector. That is, the sum of squares of errors in the network output layer is minimized. The algorithm adopts an improved iterative learning control method, which is called the adaptive iterative learning control algorithm.

In the front, the training neural network is used to predict the predicted value, and then, the gradient descent method is used to solve the nonlinear mapping relationship between the number of hidden layer nodes and the learning rate. The model is applied to transient stability assessment of power

system. If the output layer does not obtain the expected output, the error change value for the output layer is calculated, and the error signal is propagated backwards. Error signals are transmitted through the network along the original connection path to each layer of neurons, and the weight of each layer is calibrated until the desired output is achieved.

### 3. The Intelligent Recognition Model of Translation and the BP Neural Network Algorithm

**3.1. Application of Intelligent Translation Tools in English Translation.** Intelligent machine translation tools came into being. We solve this problem by using modern intelligent recognition technology to assist English translation.

**3.2. An Intelligent Translation Tool-Aided English Translation Model.** If a sentence contains two or more words, its translation should be consistent with the original; otherwise, this condition is not met. This means that each word must be preprocessed. This is especially true for English sentences. If the strings are  $m$  and  $l$ , respectively, it is  $f = f_1^m = f_1 f_2 \dots f_m$  and  $a = a_1^m = a_1 a_2 \dots a_m$ ; there is a point as follows:

$$P(f, A|e) = p(m|e) \prod_{j=1}^m p(\alpha_j | \alpha_1^{j-1}, f_1^{j-1}, m, e) \bullet p(f_j | \alpha_1^j, f_1^{j-1}, m, e). \quad (1)$$

In formula (1), Chinese sentences are generated and aligned according to English sentences. According to English sentences, the sentence length after translation and the position of string of Chinese words can be calculated. Then, according to English sentences, the length of Chinese sentences is obtained. According to the first-place string of the Chinese associated with the English sentence, the first string of the Chinese sentence is obtained. This process can be repeated to get the whole Chinese sentence.

The IBM machine translation model not only simplifies (1) but also sets preconditions:

- (1) If  $P(m|e)$ , there is no correlation use for the length of the target language  $E$  and the length of the source language  $M$ .
- (2) If  $p(\alpha_j | \alpha_1^{j-1}, f_1^{j-1}, m, e)$  is related to the length  $L$  of the target language  $E$ , then

$$p(\alpha_j | \alpha_1^{j-1}, f_1^{j-1}, m, e) = \frac{1}{l+1}. \quad (2)$$

- (3) If  $p(\alpha_j | \alpha_1^{j-1}, f_1^{j-1}, m, e)$  with  $f_j$  and  $f_{al}$  is relevant, the following exists:

$$\varepsilon = P(m|e), \quad (3)$$

$$t(f_j | e_{al}) = p(f_j | \alpha_1^j, f_1^{j-1}, m, e).$$

Equation 4 is the probability  $f_j$  that occurs given  $e_{al}$ . The English machine translation model is defined as follows:

$$h(p, \lambda) = \frac{s}{(l+1)^m} \sum_{a_l=0}^l L \sum_{a_m=0}^l \prod_{j=1}^m t(f_j | \alpha_\theta) - \sum_{\theta} \lambda_\theta \left( \sum_l t(f|e) - 1 \right). \quad (4)$$

The experimental results show that, under the same conditions, the statistical machine based on reverse motion has higher accuracy and recall than the traditional statistical machine. At the same time, the accuracy of Chinese recognition has been greatly improved. The conversion within the statistical machine source channel model is as follows:

$$\hat{\theta} = \arg \max_{\theta} \prod_{s=1}^s p_{\theta}(f_s | e_s). \quad (5)$$

Formula (5) in this study is a process of converting the acquisition process of maximum probability of English translation into Lagrange coefficient and finding the maximum value of the auxiliary function factor of random state  $\lambda_1$ :

$$\hat{\gamma} = \arg \max_{\gamma} \prod_{s=1}^s p_{\gamma}(e_s). \quad (6)$$

The formula obtained is as follows:

$$\hat{e}_1^l = \arg \max_{e_1^l} \left\{ p_{\gamma}(e_1^l) \cdot P_{\theta}(f_1^l | e_1^l) \right\}. \quad (7)$$

After that,  $P_{\theta}(e_j | f_l | 1)$  replaces  $P_{\theta}(f_1^l | e_1^l)$ . The resulting framework is as follows:

$$\hat{e}_1^l = \arg \max_{e_1^l} \left\{ p_{\gamma}(e_1^l) \cdot P_{\theta}(e_1^l | f_1^l) \right\}. \quad (8)$$

### 3.3. The Intelligent Recognition Model for English Translation.

On this basis, the relationship between the spectrum peak and the corresponding fundamental frequency under different parameters is compared to determine whether there is no accent. When there is no stress, it is considered that the speaker has begun to speak so as to improve the quality of processing. A high-frequency signals' enhancement filter with 6 dB SNR is used for technical processing of in-band speech signals above 800 Hz. Weighting factor  $\alpha$  is at 0.9 ~ 1.0; calculation formulas after weight processing signal calculation formula of  $y(n)$  are as follows:

$$y(n) = T[x(n)] = ax(n) + b(a, b \neq 0). \quad (9)$$

- (1) In the study,  $y(n)$  in formula (10) represents the emphasis processing signal.
- (2) In formula (11),  $x(n)$  represents enter the voice signal. After signal processing, the second step of

speech signal processing, the half frame overlap method is selected to realize the intraframe method.

There  $x(n)$  is import voice signal. After the signal processing in step 2, the frame division operation is carried out in the way of half frame overlap. Based on the above research results and algorithms, an intelligent speech recognition terminal based on stm32f103zet6 is designed and tested in the laboratory environment. This study presents an intelligent speech acquisition and recognition system based on DSP and FPGA. To understand the speech signal, the speech signal into  $t$  frames is divided and its formula is given as follows:

$$z(n) = \frac{1}{t} y(n), \quad (10)$$

where  $x(n)$  is the input voice signal. After the signal processing in step 2, the frame division operation is carried out in the way of half frame overlap. The formula is as follows:

$$w(n) = w(n) \times z(n). \quad (11)$$

On this basis, an adaptive detection method based on short-time energy, instantaneous zero crossing rate, and Hilbert envelope spectrum peak position is proposed to judge whether there are discontinuities in speech. Fast Fourier transform (FFT) makes use of the odd, even, imaginary, and real properties of discrete Fourier transform (DFT), improves the DFT algorithm, and improves a DFT speech signal with limited length. The following formula is obtained as follows:

$$X[K] = \sum_{n=0}^{N-1} x[n] e^{-j \frac{2\pi}{N} nk}, k = 0, 1, 2, \dots, N. \quad (12)$$

Of these, an audio denoising method based on short-time Fourier transform and wavelet packet decomposition is proposed. Firstly, the wavelet denoising method is used to remove noise. Then, the short-time Fourier algorithm is used to further analyze the original signal. Transform discrete speech sequences to MFCC scale as follows:

$$\text{Mel}(f) = 2579 \lg \left( 1 + \frac{f}{700} \right). \quad (13)$$

DTC is applied to filter output to obtain the speech signal  $w(n)$  feature parameter extraction effect:

$$P = \overline{Z}_{n=1}^N F(l) w(n) \cos(\pi n(M + 0.5)). \quad (14)$$

A segment of speech signal needs to be weighted, windowed, and framed after generating the spectrum. Fast FFT is performed on each short-time analysis window to obtain spectrum information, and then, Mel filtering is performed to obtain two-dimensional MFCC map.

- (1) Video images are simpler in the transformation domain than in the spatial domain.
- (2) The correlation of video images has obviously decreased, and the signal energy is mainly focused on several transformation coefficients. Quantification and entropy coding can compress data effectively.

- (3) It has strong anti-interference ability, and the impact of the error code on image quality during transmission is far less than that of predictive coding. In general, for high quality images, DMCP requires channel bit error rate, while transform coding requires channel bit error rate too.

**3.4. BP Neural Network Calculation.** The detailed steps of the algorithm are as follows:

- (1) Sampling (randomness): take  $J$  input samples randomly from sufficient training sample database, and the corresponding value is expected to be output.
- (2) Calculate the input and output values of population individuals (including hidden layers)  $h_{ih}(j), h_{oh}(j), y_{ih}(j), y_{oh}(j)$ , as shown in formulas (15)–(18):

$$h_{ih}(j) = \sum_{i=1}^n W_{ih} x_i(j) b_h, h = 1, 2, \dots, p, \quad (15)$$

$$h_{oh}(j) = f(h_{ih}(j)), h = 1, 2, \dots, p, \quad (16)$$

$$y_{io}(j) = \sum_{h=1}^p W_{oh} h_{oh}(j), o = 1, 2, \dots, p, \quad (17)$$

$$y_{io}(j) = f(y_{io}(j)), o = 1, 2, \dots, p. \quad (18)$$

- (3) Partial derivatives of output layer neurons and hidden layer neurons to error function are shown in equations (19) and (20):

$$\delta_0(k) = (d_0(k) - y_0(k)(1 - y_0(k))), \quad (19)$$

$$\delta_h(k) = \left[ \sum_{o=1}^q \delta_o(k) W_{ho} \right] v_h(k)(1 - v_h(k)). \quad (20)$$

- (4) Adopt  $\delta_o(k)$  and  $v_h(k)$  pair connection weight values  $W_{ho}$  and threshold  $\gamma$  of amendment, as shown in equations (21) and (22):

$$W_{ho}^{N+1}(k) = W_{ho}^N(k) + \eta \delta_0(k) v_h k, \quad (21)$$

$$\gamma^{N+1}(k) = \gamma^N(k) + \eta \delta_0(k), \quad (22)$$

where  $\eta$  is between 0 and 1.

- (5) Adopt  $\delta_h(k)$  and  $x_i(k)$  pair connection weight values  $W_{ih}$  and threshold  $\theta$  of amendment, as shown in equations (23) and (24):

$$W_{ih}^{N+1}(k) = W_{ih}^N(k) + \eta \delta_h(k) x_i(k), \quad (23)$$

$$\theta^{N+1}(k) = \theta^N(k) + \eta \delta_h(k). \quad (24)$$

- (6) Calculate the global error  $E$ , as shown in equation (25):

$$E = \frac{1}{2m} \sum_{k=1}^m \sum_{o=1}^q (d_o(k) - y_o(k))^2. \quad (25)$$

- (7) According to the calculation result of  $E$ , the end algorithm can be determined. If  $E < \varepsilon$ , or if the detector executes this content more than the set maximum number of times, the algorithm will automatically end; otherwise, you need to re-enter the program (1) and take samples again to start learning.

## 4. Experimental Analysis of the Translation Model

**4.1. Validation.** In order to verify the accuracy of the English translation intelligent recognition model, an English translation proofreading test is carried out and the experimental data are recorded and analyzes the system performance. The results show that the system automatically classifies words and sentences and calculates the correct rate. The algorithm is used to automatically identify part of speech, collocation, and other information, which can accurately determine the position of words or phrases in the sentence. Additionally, the accuracy is high. The experimental results show that, in terms of speed, the proposed method can achieve a vocabulary recognition speed of about 25 kb/s between 400 and 500 articles. The accuracy of English translation results after proofreading and before proofreading is compared, as shown in Table 1.

From Table 1, it can be seen that the highest accuracy of the change calibration is 75%, and the accuracy of the intelligent recognition by using the module in the text is 99%. There is a significant difference between the two; this proves that the system's English translation intelligent recognition model is correct, as shown in Figure 2.

In order to test the effect of the improved BP neural network algorithm in translation, it is necessary to test and evaluate the BP neural network algorithm to show the performance of the BP neural network algorithm in translation. Key indicators of achievement assessed for English-Chinese translation tasks included translation accuracy, speed of translation, and ability to update. Finally, the experimental results are analyzed and the corresponding conclusions are given. Finally, the above evaluation methods are applied to practical engineering and good results are obtained.

Evaluation process: three English-Chinese machine translators translated 50 assigned phrases and 50 random network sentences. English-Chinese translation professionals translated the same designated phrases and 50 random sentences. After comparing machine translation with manual translation, the grader will score the three English-Chinese machine algorithms. The rules for scoring are shown in Table 2.

As shown in Table 3, the experimental corpus uses 586538 sentences from the Chinese-English Parallel Corpus of Zhongjun company. One thousand sentences are

TABLE 1: Accuracy of translation before and after change.

Experiment no.	The accuracy	
	Before change (%)	After change (%)
A	58.21	99.11
B	72.42	98.62
C	67.53	98.41
D	72.14	99.15
E	75.11	98.56
Precision mean	69.02	98.72

randomly collected from the experimental corpus as the test corpus, 2000 sentences as the development corpus, and the rest as the training corpus. In order to ensure that the test results have high reliability and accuracy, this study also designed the corresponding evaluation indicators and verified that the evaluation indicators have achieved the expected results through experiments. Finally, after the completion of the above work, a summary and an outlook are made. According to the different length of sentences, the test corpus is divided. It is divided into three following test sets: single sentence, common sentence, and difficult sentence.

As shown in Figure 3, the test corpus is divided into three following test sets according to sentence length: single sentence, common sentence, and difficult sentence. The translation accuracy of single sentence is relatively good, while the translation accuracy of common sentences and difficult sentences is more reasonable than that of traditional translation methods.

The Bleu value of the test set in Table 3 is calculated by using the calculation results that are shown in Table 4. Analysis of Table 4 shows that, in the process of machine translation, the larger the Bleu value is, the larger the Bleu is, which indicates that this method is more effective than other commonly used parsing machine reading method. The smaller the Bleu, the more effective this method is than other commonly used parsing methods. This shows that, on the basis of the BP neural algorithm, the optimal combination mode between various English language features in complex sentences can be obtained, some structural ambiguities can be eliminated, and the accuracy of English machine translation can be improved, as shown in Figure 4.

A machine translation system based on machine learning is designed and implemented. The system improves the traditional machine translation methods and uses statistical features and neural network models to assist machine translation. Lastly, the experiment proves that the system is feasible. Experimental results show that the improved algorithm can effectively improve the recall rate and time efficiency, while ensuring the accuracy.

The probability results obtained by different methods are mapped with the real machine translation results, so as to compare the retrieval range of different methods. Aiming at the disadvantages of complex and time-consuming construction of large-scale corpus, this method uses tree model to model and classify natural language sentences. The calculation of Chinese sentence similarity in tree structure is

studied, and an improved algorithm combined with the FCM clustering algorithm is proposed. On this basis, a prototype of Chinese text semantic extraction and analysis, which is the core part of Chinese text information retrieval system, is implemented. Experiments show that this method is more efficient than the traditional syntactic mechanism translation method. In this algorithm, the left circle represents the accurate translation probability results of different methods, while the right circle represents the probability distribution of the actual machine translation results, as shown in Figure 5.

As can be seen from Figure 5, the final probability retrieved by the traditional parsing machine translation method is in the lower left corner, while the probability of the real machine translation result is in the upper right corner, and this method cannot be mapped to the real result, which verifies the poor translation accuracy of the traditional method. To solve this problem, an improved algorithm is proposed: the part of speech information and context features are weighted to improve the quality of translation. This weight is added to the traditional machine learning model to improve the system performance.

The points obtained from the internal syntax analysis of the tree-based machine translation method are not the most likely points in the real machine translation results, as shown in Figure 6. Therefore, the probability distribution needs to be expanded and optimized to achieve better results. Tree structure is proposed and the corresponding algorithm implementation process is given. Although the result probability obtained by the tree-based machine translation method cannot correspond to the actual machine translation results, it can be mapped on these results, but the mapping range is very small.

The points obtained from the internal syntax analysis of the forest-based machine translation method are not the most likely points in the real machine translation results, as shown in Figure 7. Therefore, the probability distribution needs to be expanded and optimized to achieve better results. Tree structure is proposed and the corresponding algorithm implementation process is given. Although the result probability obtained by the tree-based machine translation method cannot correspond to the actual machine translation results, it can be mapped on these results, but the mapping range is very small.

The comparison between the machine translation method in this paper and the retrieval range of the actual machine translation results is shown in Figure 8. The maximum entropy value retrieved by the direct maximum entropy method is the maximum entropy value of the actual machine translation, which can be basically mapped to the actual machine translation. Compared with other traditional syntactic parsing machine versions, the proposed algorithm has certain advantages and comparative significance. To solve this problem, after studying various improved machine translation algorithms, a new machine translation scheme based on tree structure is proposed. The tree-based machine translation method is used, and the decoding performance of the forest-based machine translation method and the

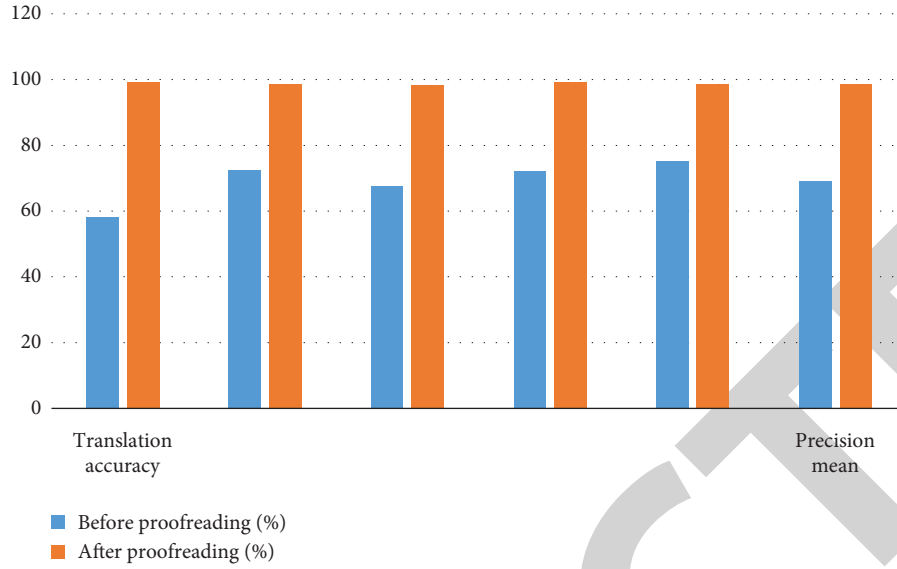


FIGURE 2: Accuracy of translation before and after change.

TABLE 2: Scoring rule table.

Project	Scoring requirements
Accuracy of identification	Score the content according to its rigor and rationality, and the perfect score is 100 points
Calculate the recognition speed formula	The calculation formula is recognition time multiplied by percentage divided by times
Renewal capability	The calculation formula is update time multiplied by percentage divided by number of times

TABLE 3: Test set classification results.

Sentence type	M numbers	Targets' numbers
Single sentences	$M < 9$	432
Common sentences	$9 \leq M < 20$	325
Difficult sentences	$M \geq 20$	168

method in the text is gradually enhanced, as shown in Figure 9.

Figures 5–8 in this study show the probability distribution of the traditional parsing machine translation method, the tree-based translation method, and the translation method based on forest and the BP neural algorithm between the accurate translation probability calculation result and the real machine translation calculation result. The calculation result is as follows:

- (1) It is proved that the translation accuracy of traditional methods is poor.
- (2) Although the result probability obtained by the tree-based machine translation method cannot correspond to the actual machine translation results, it can be mapped to them, but the mapping range is small.
- (3) The mapping range of forest-based machine translation method is large, but its mapping accuracy is low.
- (4) The best advantage of the translation method based on the BP neural algorithm for syntactic analysis

and retrieval is the best advantage of the actual machine translation results, which can be completely mapped to the actual machine translation results.

It can be seen from Figure 9 that the retrieval range of these three methods is increasing. The method Bleu in this study has the largest number of rules, and the number of rules obtained is more than the traditional tree-based machine translation method and the forest-based machine translation method, and the decoding and retrieval performance is higher.

**4.2. Test Results.** Figure 10 shows that the speech recognition machine translation based on the BP neural network is one of the best in terms of recognition accuracy, recognition speed, and updating ability. As shown in Figure 10, the average score of the BP algorithm is 92.3, which is higher than the average score of the statistical algorithm and the dynamic memory algorithm, indicating that the BP algorithm has strong updating ability. Therefore, as an important method and tool for automatic text classification system, the neural network has a broad application prospect. At the same time, the BP algorithm provides a good example for future research. This can be seen in Figures 10 and 11 that the BP algorithm has obvious advantages over other algorithms in performance.

As can be seen from Figure 11, by comparing statistical algorithm, dynamic memory algorithm, BP neural network

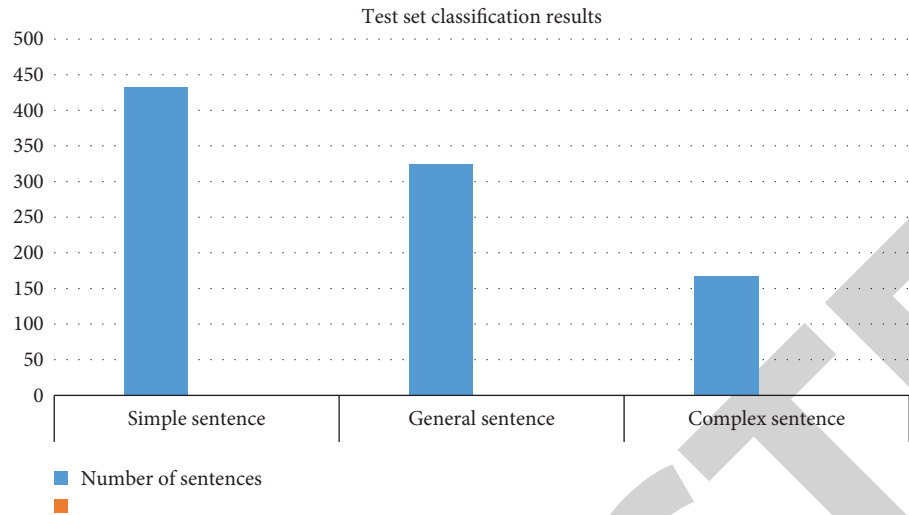


FIGURE 3: Test set classification results.

TABLE 4: Comparison of machine translation performance based on test set classification.

Machine translation methods	Simple sentence	General sentence	Complex sentence
Traditional parsing machine translation methods	33.58	32.85	27.24
Modern intelligent recognition, analysis, and translation methods	33.60	33.32	30.12
The translation method based on the BP neural algorithm	33.62	33.64	32.18

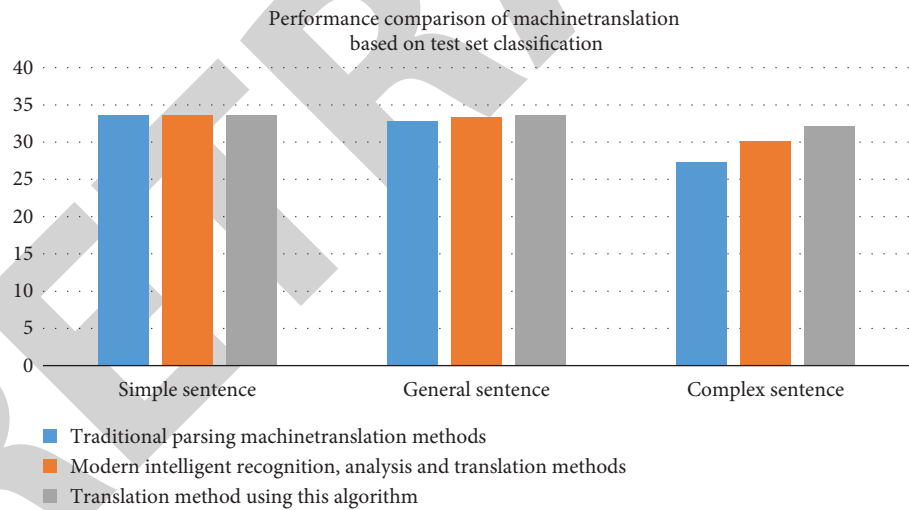


FIGURE 4: Comparison of machine translation performance based on test set classification.

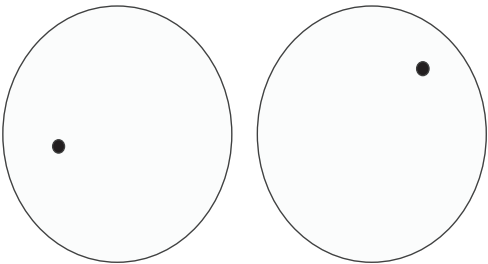


FIGURE 5: Comparison of retrieval range based on traditional parsing machine translation methods.



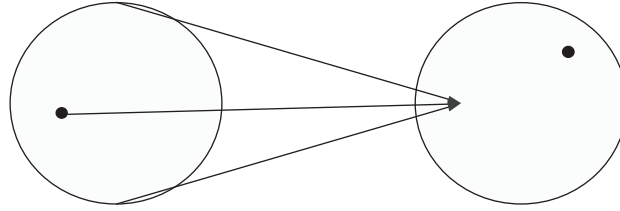


FIGURE 6: Comparison of retrieval range of tree-based machine translation methods.

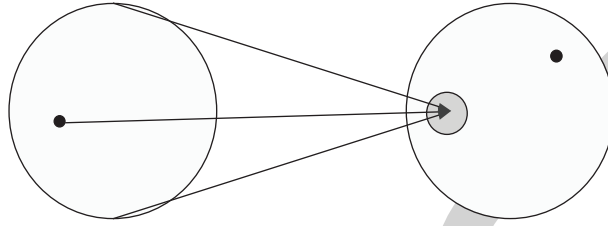


FIGURE 7: Difference in probability distribution based on the forest translation method.

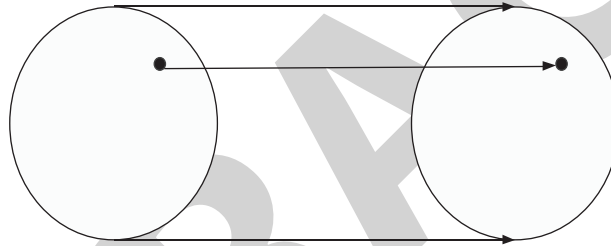


FIGURE 8: Comparison of search scope based on this method.

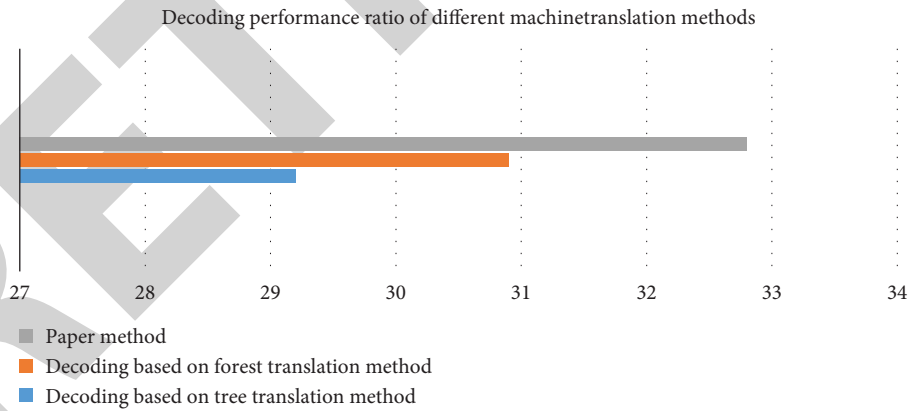


FIGURE 9: Decoding the performance ratio of different machine translation methods.

algorithm, machine translation, and manual translation, the score of the BP neural network algorithm is better than the other three algorithms. This shows that the ability of the BP neural network algorithm is the best among similar algorithms in recognition accuracy, recognition speed, and updating ability.

The comparison experiment also uses a real translation case and selects the sentence “the price limit of beef noodles

by Xi’an Price Bureau” as the translation. Finally, the comparison results of machine translation list the statistical algorithm, dynamic memory algorithm, BP neural algorithm, and manual translation in Table 5.

It can be seen from Table 5, that the word “Price Bureau” is not translated by machine translation according to the statistical algorithm and the dynamic memory algorithm, but by machine translation according

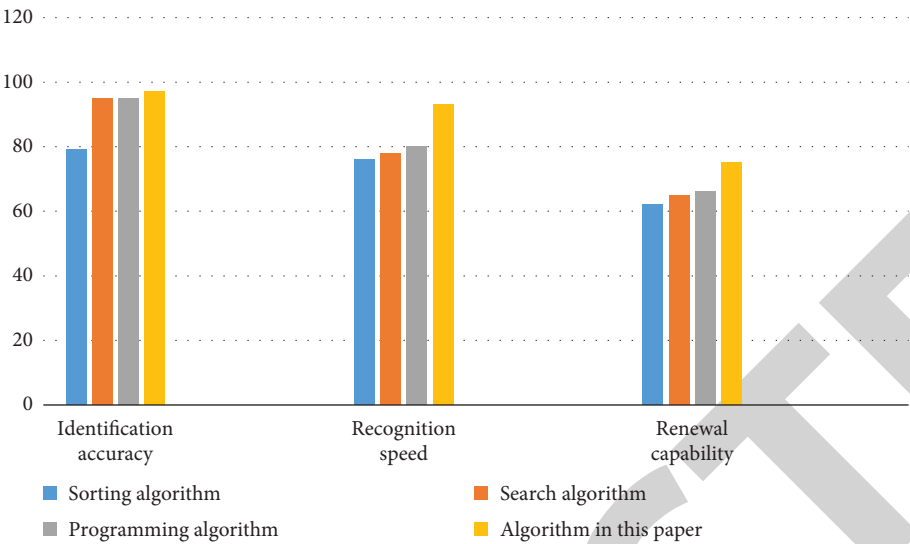


FIGURE 10: Test chart of four English-Chinese translation algorithms.

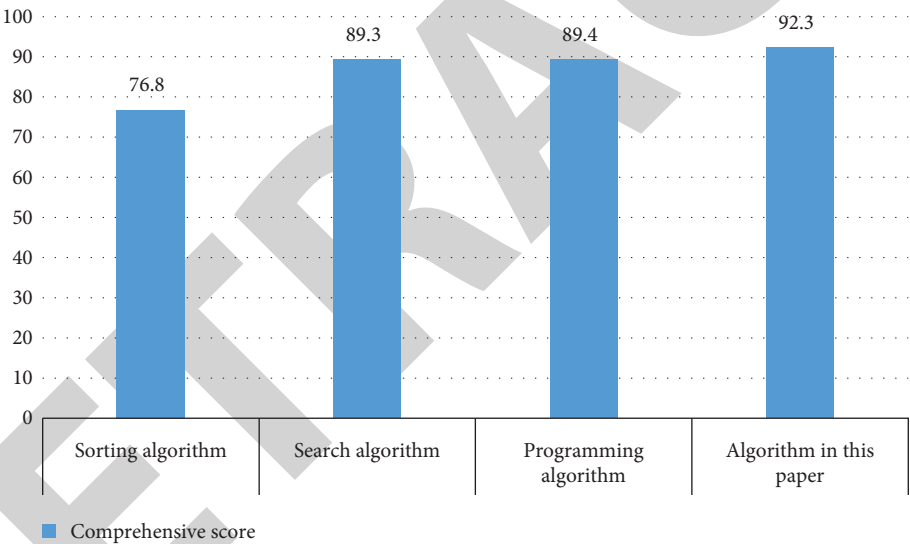


FIGURE 11: Comprehensive test chart of four algorithms.

TABLE 5: Comparison of translation example results.

Translation methods	Translation content
Statistical method	There are so many people in this world, it's fate for everyone. Cherish the time you spend with those around you.
Dynamic memory algorithm	There are so many people in this world, everyone is fate, cherish the time with those around you.
GLR algorithm	There are so many people in this world, it's fate for everyone. Cherish the time you spend with those around you.
BP neural algorithm	There are so many people in this world, and it is fate for everyone to meet. Cherish the time with people around you.
Human translation	There are so many people in this world, it's fate for everyone. Cherish the time you spend with those around you.

## Research Article

# Research Overview on Edge Detection Algorithms Based on Deep Learning and Image Fusion

Bin Tian <sup>1</sup> and Wei Wei <sup>2</sup>

<sup>1</sup>School of Electronic and Information Engineering, Lanzhou Jiaotong University, Lanzhou 730070, China

<sup>2</sup>Xi'an University of Technology, School of Computer Science and Engineering, Xi'an 710048, China

Correspondence should be addressed to Bin Tian; [tianbin@lztu.edu.cn](mailto:tianbin@lztu.edu.cn)

Received 28 June 2022; Revised 1 September 2022; Accepted 8 September 2022; Published 30 September 2022

Academic Editor: Yuchuan Luo

Copyright © 2022 Bin Tian and Wei Wei. This is an open access article distributed under the Creative Commons Attribution License, which permits unrestricted use, distribution, and reproduction in any medium, provided the original work is properly cited.

Edge detection is a boundary-based segmentation method to extract important information from an image, and it is a research hotspot in the fields of computer vision and image analysis. Especially feature extraction is also the basis of image segmentation, target detection, and recognition. In recent years, in order to solve the problems of edge detection refinement and low detection accuracy, the industry has proposed multiscale fusion wavelet edge, spectral clustering, network reconstruction, and other edge detection algorithms based on deep learning. In order to enable researchers to understand the current research status of edge detection, this paper first introduces the classic algorithm of traditional edge detection, compare with advantages and disadvantages of different edge detection algorithms. Then, it summarizes the main edge detection methods based on deep learning in recent years and classifies and compares them according to the implementation technology. Finally, it shows the development direction of edge detection algorithm research.

## 1. Introduction

The image edge refers to the step change in the gray level of surrounding pixels in the image, which is the most basic feature of the image [1] and often carries the most important information in the image. Based on boundaries, edge detection is a segmentation method which plays an important role in computer vision, image analysis, and other applications and provides a valuable feature parameter for people to describe or recognize targets and interpret images. How to quickly and accurately extract the edge information of an image has always been a research hotspot at home and abroad. At present, edge detection is a problem in image processing. Many existing researches studies have shown that edge detection is of great significance in many fields such as image high-level feature extraction, feature description, target recognition, and image segmentation. How to locate and extract image edge feature information quickly and accurately has become one of the research hotspots [2].

Aiming at the two main problems such as positioning and extraction, researchers have put forward a variety of edge detection methods through continuous experiments. According to the time sequence of research progress, the methods can be divided into two categories: classic traditional algorithms and algorithms based on deep learning. Figure 1 lists some classic traditional algorithms (above the arrow) and algorithms based on deep learning (below the arrow) in the research of image edge detection. In recent years, with the continuous rise of neural networks and image fusion technology, some people have also proposed an edge detection algorithm for image fusion [3].

Because the edge of an image contains a lot of background information and important structural information, traditional edge detection methods often use hand-made low-level features (such as color, brightness, texture, and gradient) as the priority of edge detection, for example, (1) traditional edge detection algorithms, such as the gradient operator Roberts [4], Prewitt [5], Sobel [6], and the widely

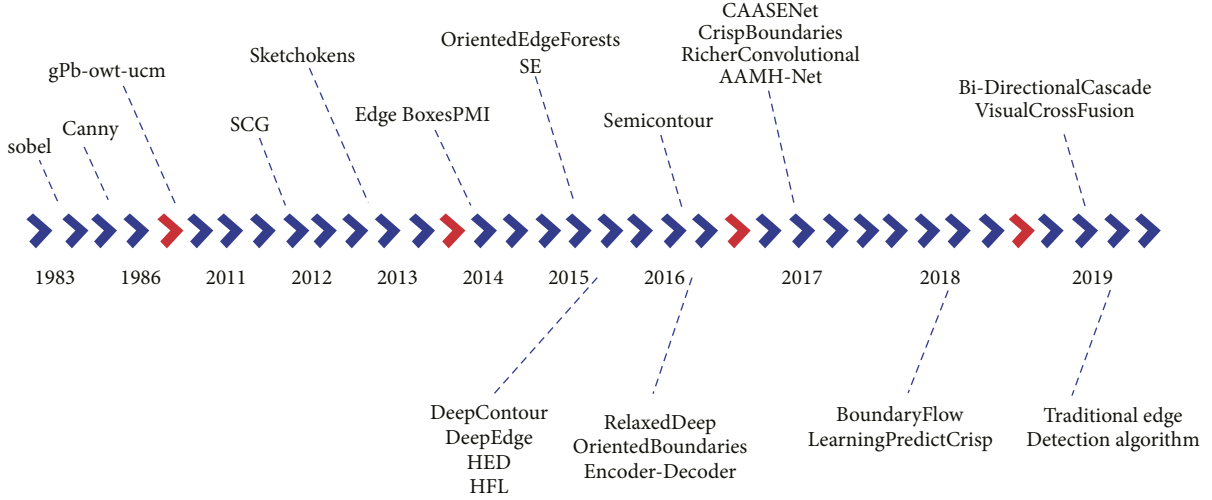


FIGURE 1: Classic traditional algorithms and algorithms based on deep learning.

used Canny operator [7], (2) feature generation methods based on information theory artificial design, such as gPbowl-ucm algorithm [8] and SCG (Sparse Code Gradients) algorithm [9], and (3) structured edge detection algorithm such as SE (structured forests edge detection) algorithm [10]. Although the edge detection methods using low-level features have made great progress, its limitations are also obvious. With the development of deep learning technology [11], especially the emergence of convolutional neural networks (CNN), which has the advantages of having a strong ability to automatically learn high-level representations of natural images, using CNN for edge detection has become a new trend. In 2015, Xie and Tu [12] proposed holistically nested edge detection (HED) to detect and extract the edges of natural images in a nested manner; in 2015, Ou et al. [13] proposed to apply full convolution to semantic segmentation, which lays the foundation for full convolution application in contour detection; in 2016, Ma et al. [4] proposed an end-to-end convolution architecture Deep-Edge; in 2016, Lu et al. [14] proposed a depth condition random domain stereo matching method based on convolutional neural network; in 2017, Zhang et al. [15] proposed the edge detection technology of multiscale moving targets; in 2017, Zhong et al. [16] proposed the use of VLAD (vector of locally aggregated descriptor) and descriptors based on deep learning for efficient retrieval of interest regions; in 2018, Liu et al. [17] proposed a richer convolution feature image edge detection extraction algorithm based on five-layer feature diversity; in 2018, Han et al. [18] proposed an end-to-end edge-preserving neural network (called regional network) based on the fast R-CNN (Region-CNN) framework for prominent target detection; in 2019, Zhao et al. [19] proposed a subdivided network for prominent target detection; and in 2022, Zheng proposed anisotropic multiscale edge detection algorithm.

The above algorithms require considerable professional knowledge, sophisticated processing algorithms, and network architecture design to convert the original image data

into appropriate feature vectors to construct edge detection models and classifiers.

## 2. Overview of Classic Algorithms for Edge Detection

**2.1. First-Order and Second-Order Edge Detection Operators.** First-order and second-order edge detection operators mainly identify and locate the mutation position in the image, which is usually between target and background, target and target, region and region, primitive and primitive. According to the different principles, it can be roughly divided into two categories: the first-order edge detection operator is to find the derivative of the image gray change curve, which can highlight the edge of the object in the image, and the second-order edge detection operator is to find the derivative of the image gray change derivative and is very sensitive to the strong changes of the gray in the image, which can highlight the texture structure of the image (Table 1).

Among them, the Canny algorithm is relatively typical and suitable for various edge detection fields. The method is not susceptible to noise interference and is able to detect true weak edges. The advantage is that the strong and weak edges are detected separately using two different thresholds and that the weak edges are included in the output image only when the weak and strong edges are connected.

**2.2. Traditional Edge Detection.** Edge detection is a part of the process called image segmentation, and the main purpose of image segmentation is to identify areas in the image. Technically speaking, edge detection is the process of locating edge pixels, while edge enhancement is the process of increasing the contrast between the edge and the background so that the edge can be seen more clearly. In addition, edge tracing is a process of tracing along the edge, which usually collects edge pixels into a list. There are many possible definitions of edge, and each definition is

TABLE 1: Comparison of first-order and second-order edge detection operators.

Classification	Operator name	Performance advantages and disadvantages
First-order edge detection operators	Robert operator [20]	Since the smooth part is not included, it is more sensitive to noise, but the extracted edge is relatively coarse, and the positioning is not very accurate
	Sobel operator [6]	It is a weighted average filtering and detection, which has a better detection effect on images with gradual gray scale and low noise, and a more accurate edge positioning
	Prewitt operator [5]	It is an average filter, which has a better detection effect on images with gradual gray scale and low noise. It is not as good as the Roberts operator for the positioning of the edges of the image with multiple complex noises
	Isotropic Sobel operator [21]	Its position weighting coefficient is more accurate, and the amplitude of the gradient is the same when detecting edges in different directions
Second-order edge detection operators	Canny operator [7]	It is not easy to be disturbed by noise and can detect real weak edges. The algorithm is not easily “filled” by noise, but the programming is more complicated and the operation is relatively slow
	Marri-Hildreth operator [22]	It can give a closed edge boundary, which is helpful for the recursive calculation of threshold
	LOG (Laplacian of Gaussian) operator [23]	It is usually used to determine whether the edge pixels are located in the bright or dark areas of the image
	DOG (difference of Gaussian) operator [24]	It enhances the difference of Gaussian function, thereby increasing the denoising ability

applicable to certain specific situations. One of the most commonly used and generally defined one is the ideal step edge.

Edge detection describes the process of grayscale changes in an image based on the physical process that causes the grayscale changes of the image. The physical process that causes the grayscale discontinuity of the image may be geometric (deep discontinuities, surface orientation, and color and texture differences), or optical (surface reflections, shadows generated by nontarget objects, and internal reflections, etc.). The mixing of these features will make subsequent extraction very difficult, and the image data is often contaminated by noise in actual situations. The ill-conditioned problem of signal numerical differentiation: a small change in the input signal will cause a large change in the output signal. Noise elimination and edge location are two contradictory parts, which are the two difficulties in edge detection.

**2.3. Structured Edge Detection Algorithm.** In 2017, Wang et al. [25] proposed an image crack detection method based on multiscale down-sampling normalized cuts in view of the low accuracy of multiscale normalized cuts in edge detection and the long time required to solve feature vectors. The method first uses the semireconstruction characteristics of the antisymmetric biorthogonal wavelet transform to extract edge features at multiple scales of the image to be tested; secondly, it combines the strength and location characteristics of each scale to construct a multiscale similarity matrix and a multiscale normalized similarity matrix, then the multiscale similarity matrix is down-sampled and the spectral segmentation method is used to achieve the down-sampling eigenvector solution; finally, the multiscale normalized similarity matrix is used to up-sample the down-sampled eigenvectors and discretized to obtain the final result. The experimental results of the proposed method and

the multiscale normalization cut on a single target image of three datasets show that it not only improves the detection accuracy but also reduces the computing time. In view of the problem that existing deep learning methods cannot guarantee the effective transmission and fusion of crack feature mapping under complex backgrounds, and structured forests cannot accurately distinguish similar and random crack features, Wang et al. [26] proposed a crack segmentation method for structure based on full convolutional neural network and structured forest in 2020 [27]. First, based on the full convolutional neural network framework, five ablation neural networks are constructed to expand the global characteristics of microcracks; secondly, a crack segmentation parameter competition strategy based on multiscale structured forest is proposed to effectively improve the ability to distinguish microcracks; finally, a coupled segmentation method based on ablation neural network and structured forest is used for joint prediction of crack images. The experimental verification of the proposed method on the two types of structural crack datasets shows that the proposed method can improve the accuracy of crack detection under complex and similar backgrounds and can realize effective structural health monitoring.

### 3. Overview of Edge Detection Algorithms for Deep Learning

With the rise of artificial intelligence in the world, deep learning has also become a research hotspot as one of the realization means. Traditional edge detection technology has made great progress, but there are also many limitations [28]. As the edge extraction scene becomes more and more complex, the texture or background of the image has a great impact on these classic edge detection methods that use low-level edge features. The biggest difference between deep learning and traditional edge detection methods is that the features it use are automatically learned from big data

instead of manual design. The deep learning model has powerful learning capabilities and efficient feature expression capabilities. A more important advantage is that it extracts information layer by layer from pixel-level raw data to abstract semantic concepts, which makes it outstanding in extracting image global features and contextual information and brings new ideas for solving traditional computer vision problems (such as image recognition and image edge detection). Many scholars at home and abroad have tried to add deep learning high-level semantics to the field of image edge detection to deal with complex scenes. The classification and typical algorithms of edge detection algorithms based on deep learning are shown in Figure 2, which will be introduced separately below. Deep learning edge detection algorithms are also divided into fully supervised learning edge detection algorithms and weakly supervised learning edge detection algorithms.

### 3.1. Fully Supervised Learning Edge Detection Algorithm.

Fully supervised learning is to use samples of known categories (that is, labeled samples), adjust the parameters of the classifier, and train to obtain an optimal model to achieve the required performance. Then use this trained model to map all inputs to corresponding outputs and judge the outputs simply to achieve the purpose of edge detection. At present, most edge detection algorithms are implemented based on full supervision. According to the overall design ideas and key technologies used in the algorithm implementation process, this paper divides them into five categories: edge detection algorithms based on spectral clustering, multiscale fusion edge detection algorithm, network reconstruction edge detection algorithm, codec-based edge detection algorithm, and subpixel convolution edge detection algorithm. Methods based on spectral clustering and subpixel have high detection accuracy, but poor antinoise performance, methods based on neural network, and codec solves the problem of poor antinoise performance, but the detection accuracy is insufficient [29].

#### 3.1.1. Multiscale Fusion Wavelet Edge Detection Algorithm.

In order to further improve the edge detection performance of image processing, a fusion-based edge detection algorithm with good noise resistance is proposed [30], combining the highlights of wavelet transform and multiscale morphology [31]. The main idea is to preprocess the image, use multiscale morphological filtering and wavelet transform technology to detect the edge of the image from both the horizontal and vertical directions, and then merge the two based on image fusion to get complete image edges. Through experimental analysis and comparison, it is found that the proposed algorithm has good antinoise performance [32], retains more detailed information, and has a certain timeliness, which make it satisfy the needs of different types of image edge detection.

#### 3.1.2. Edge Detection Algorithm Based on Spectral Clustering.

The spectral clustering algorithm is based on the spectrogram theory and clustering by using the eigenvectors of the

similarity matrix of the data. The advantage is simple thinking, easy to implement, and capable of identifying non-Gaussian distributions, which enables it to be used in edge detection algorithms [33].

In 2018, Jianmin and Jing [34] found that distinguishing high-frequency noise points and edge points is one of the difficult points in extracting the edges of noise images. In order to obtain clear edges of noise images, an edge detection algorithm based on spectral curvature clustering (SCC) was proposed [35]. This method transforms the edge detection problem into a classification problem and uses the property of image edge points, smooth points, and noise points located in different subspaces. While effectively clustering smooth points and edge points, SCC can suppress noise points. In addition, the algorithm edits the clustering label and converts it into a binary image, on which simple processing is performed to get the edge of the image [36], thus avoiding the threshold selection problem in traditional algorithms successfully. Compared with traditional edge detection methods, the experimental results prove the effectiveness of the proposed algorithm.

#### 3.1.3. Edge Detection Algorithm Based on Codec.

The encoder and decoder structure is a mechanism for image semantic parsing by using the symmetric network structure. Its essence is to encode the captured pixel position information and image features by using the encoder constituted by convolutional and pooling operations in deep learning technology. The decoder composed of deconvolution or unpooling operations is used to analyze the image and restore the spatial dimension and pixel location information of the image.

The function of the encoder is to transform an indefinite input sequence into a fixed background variable and encode the sequence information in the background variable [37]. The commonly used encoder is the RNN [38] model, which converts the entire source sequence which is read as a fixed-length code. The decoder is also a RNN model, which decodes the encoded input sequence to output the target sequence. The encoder is used to analyze the input sequence, and the decoder is used to generate the output sequence [39]. The spatial dimension and pixel location information of the image are restored through operations such as convolution and pooling through two cyclic neural networks [40].

#### 3.1.4. Network Reconstruction Edge Detection Algorithm.

CNN is a feed forward neural network. Its artificial neurons can respond to the surrounding units of a partial coverage and perform well for large image processing and seek speed and accuracy by reconstructing network architectures such as AlexNet [41], VGGnet, Inception, and ResNet [42].

In 2017, Wang [43] et al. proposed that edge detection is a core step of image processing, and its detection effect directly determines the quality of image processing, but there has been a lack of quantitative standard evaluation methods for image edge detection. They suggested using an algorithm which reconstructs the source image by the edge image, searching the source set in horizontal and vertical

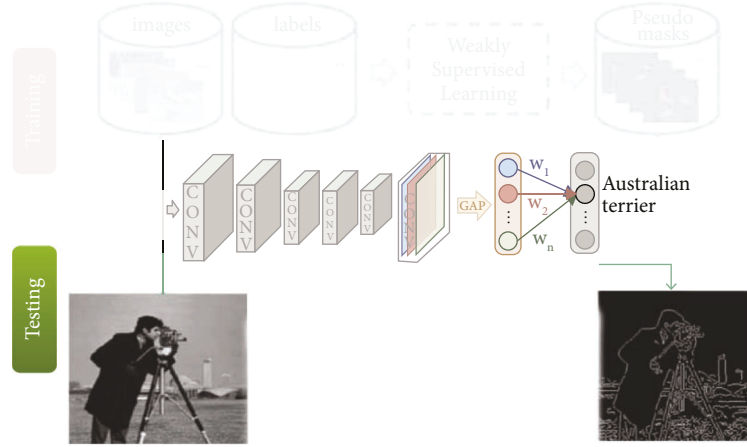


FIGURE 2: Fully convolutional neural network model.

directions, reconstructing new pixels by a mixture of linear interpolation and gradual interpolation, and reconstructing the similarity of the image and the source image to evaluate the edge detection effect. Through a variety of experiments, the performance and effect of the reconstruction algorithm are verified. Experimental results show that the algorithm can reconstruct the source image from the edge image quickly and effectively and can evaluate the edge detection effect effectively. Its reconstruction and evaluation results are in line with human visual perception, which means it has good application value for high-level image processing and automatic image processing.

**3.1.5. Subpixel Convolution Edge Detection Algorithm.** Subpixel is the subdivision of the basic unit of pixel, which is a unit smaller than the pixel, thereby improving the image resolution. Under normal circumstances, subpixel edge points exist in the areas of the image that gradually undergo excessive changes. We can use polynomial fitting and other methods to obtain the subpixel positions of the edge points. Subpixel positioning can be understood as a method of using software algorithms to improve the accuracy of edge detection when the hardware conditions of the camera system remain unchanged, or an image processing technology which can make the resolution less than one pixel.

In 2021, Liu and Zhu [44] adopted a subpixel edge detection algorithm based on improved Zernike moments in order to meet the high-precision positioning requirements for spot edges in beam quality detection. First, perform rough positioning of the light spot by the Sobel operator and then relocate the acquired pixel-level edge by the edge model of Zernike moments. Finally, according to the improved edge judgment conditions, the actual subpixel edge points in the image are determined to complete the subpixel edge extraction of the light spot image. By analyzing the results of subpixel edge extraction of emulational images, it is found that the improved Zernike moment algorithm has a maximum error of 0.338 pixels and a minimum error of 0.088

pixels, and the average running time of the algorithm is 319 ms, which is reduced 35.294% compared to those of the traditional ones.

**3.2. Weakly Supervised and Unsupervised Learning Edge Detection Algorithms.** The local optimal solution of weakly supervised target detection refers to the phenomenon that the detection results usually only cover a small part of the target object and the target detection task can be achieved through the class label of the sample. Unsupervised learning means that the data learned by the model has no labels, so the goal of unsupervised learning is to reveal the inherent characteristics and laws of the data through the learning of these unlabeled samples, and its representative is clustering.

Aiming at the problems of low adaptability, increased parameters, large calculations, and discontinuous detection edges in multiscale edge detection based on deep learning, Zhang and Ren [45] put forward a multiscale edge detection method based on improved overall nesting in 2020. This method combines multiscale detection and weak supervision model to solve the problem of multiple parameters and large amount of calculation [46]. In order to make full use of the powerful feature expression ability of convolution, a multiscale deep learning structure is proposed based on the overall nested edge detection, i.e., a mutually independent multinet network multiscale structure composed of multiple networks with different depths and outputs. At the same time, introduce the overall nested weight mixing layer which combines all the weakly supervised prediction results together and learn the blended weights during the training process. The performance of the proposed method is evaluated on the dataset BSDS500 through evaluation indicators. The experimental results show that the proposed method can achieve good performance on the dataset BSDS500.

In 2016, Zhang and Zhao [47] proposed an unsupervised boundary detection algorithm based on orientation contrast for large-scale image collections on the Internet without real demarcated boundaries or with high acquisition costs, and in the calculation of orientation contrast, differences of

TABLE 2: Comparison of edge detection algorithms based on fully supervised learning.

Classification	Representative algorithm	Advantages and disadvantages	Basic network	Key technology	Test dataset
Multiscale fusion edge detection algorithm	Deep edge [48] HED [49] RDS [50] HFL [51]	Advantages: Increases the receptive field of the feature map and alleviate the problem of low resolution of the feature map Disadvantages: The increase in parameters requires a lot of calculation	Knet VGG16 VGG16 VGG16	Canny detector Transfer learning and loss function Canny and SE detector Edge semantic segmentation technology	BSDS500 (0.753) BSDS500 (0.788) NYUD (0.746) BSDS500 (0.792) NYUD (0.674) BSDS500 (0.767)
Edge detection algorithm based on spectral clustering	Deep contour [52]	Advantages: Simple, easy to implement, and capable of identifying non-Gaussian distributions Disadvantages: The selection of scale parameters for spectral clustering lacks self-adaptability. They are set all based on experience	CNN	Spectral clustering and divide-and-conquer strategies	BSDS500 (0.757)
Edge detection algorithm based on the codec	CEDN [53]	Advantages: Avoid the problem of reduced resolution of feature maps after pooling Disadvantages: Too many parameters and large amount of calculation.	VGG16	Encoder-decoder	NYUD (0.79) BSDS500 (0.753)
Network reconstruction edge detection algorithm	N-4fields [54] COB [55] AMH-Net [56]	Advantages: Improves accuracy and speed Disadvantages: Pixel local information is not connected	AlexNet VGG16 ResNet AlexNet, VGG16 ResNet	The nearest search technology Sparse boundary representation method Use of attention gating to control the conditional random domain	BSDS500 (0.793) BSDS500 (0.798) NYUD (0.771)
Subpixel convolution edge detection algorithm	Deep crisp boundaries [57]	Advantages: it can save costs and improve recognition rate Disadvantages: The application has certain prerequisites such as the ready-to-detect target is not composed of isolated single pixels, but composed of multiple pixels, and these pixels should have certain distribution characteristics, such as grayscale distribution and geometric shape distribution features	ConvNet	Subpixel convolution	BSDS500 (0.803)



TABLE 3: Comparison of classic convolutional neural network architectures.

Name	Features
LeNet5	LeNet5 was one of the earliest convolutional neural networks in 1994, which is divided into two parts: convolutional layer block and fully connected layer block. It consists of seven layers of CNN (not including the input layer). Through convolution, parameter sharing, pooling, and other operations to extract features, it avoids a lot of computational costs. Then it uses a fully connected neural network for classification and recognition. This network is also the starting point of a large number of neural network architectures recently
AlexNet	AlexNet is the first convolutional neural network structure with eight layers in 2012, which proves that the learned features can surpass the features of manual design, thus breaking the previous state of computer vision research
VGGNet	VGGNet introduces ReLU, dropout, data enhancement, and pooling to cover each other, with three convolutions and one maximum pooling plus three fully connected layers. To prevent overfitting and improve generalization ability, VGGNet uses $1 \times 1$ and $3 \times 3$ convolution kernels and $2 \times 2$ maximum pooling to make the number of layers deeper. VGG16 and VGG19 are commonly used. The generalization performance of the VGGNet network is very good, and it is easy to migrate to other image recognition projects, and the trained parameters of VGGNet can also be downloaded to perform good initialization weight operations. Therefore, in recent years, the edge detection algorithms based on deep learning take this network as the basis
Google, Inception net	Google and inception net control the amount of calculation and the amount of parameters to obtain better classification performance. Advantages are as follows: (1) remove the last fully connected layer and replace it with a global average pooling and (2) introduce the inception module which is a combination of four branches. The $1 \times 1$ convolution kernel is used in all branches to reduce the amount of parameters, (3) $5 \times 5$ in inception V2 becomes two $3 \times 3$ , and the famous batch normalization is proposed. (4) inception V3 convolves two-dimensional convolution into two one-dimensional convolutions to speed up calculations and reduce overfitting. At the same time, the inception module structure is changed
ResNet	(1) introduce the highway structure to make the neural network very deep, (2) ResNet V2 turns the ReLU activation function into a linear function of $y=x$

multiple directions were considered. In particular, this model is particularly suitable for detecting the boundaries of objects surrounded by natural textures. The test results on the Rug standard database show that the proposed algorithm is better than the current best unsupervised boundary detection algorithm, which verifies the effectiveness of the model (Table 2).

#### 4. Overview of Edge Detection Algorithms for Image Fusion

Using multiscale morphology for edge detection can reduce the impact of image noise to a certain extent [58] and can improve the accuracy of edge detection performed by wavelet transform [59], and the image is subjected to wavelet transform to complete the separation of low-frequency information and high-frequency information, realize the multiresolution representation of the image and the fusion of the sequential image multiazimuth angle information, and complete the image preprocessing operation. Combining multiscale morphological filtering and wavelet transform technology to fuse these two methods, the proposed algorithm synthesizes the advantages of the two methods to improve the resolution of target detection and suppress the detection noise of different sensors [60]. The specific method is as follows [61]: (1) Add Gaussian white noise to the original image, and use mathematical morphology to denoise the image; (2) apply a method based on multiscale structure morphology to the image edge detection; (3) use the wavelet transform method to detect the edge of the image by firstly selecting sym4 as the wavelet function to perform wavelet transform on the image, and secondly, through transforming coefficients, obtain the

wavelet transform coefficients in the horizontal and vertical directions of the image and the modulus and argument of the dyadic wavelet transform, and then, the edge points of the image are obtained according to the magnitude of the modulus and the argument, and finally, the edge points are connected and selected rationally; and (4) apply image fusion function to the two edge images for image fusion, that is, firstly, use sym4 wavelet to perform 3-layer wavelet decomposition on two images, then take the average of the low-frequency and high-frequency components of the two images for fusion, and then the reconstructed image obtained by the inverse wavelet transform is the final edge image.

#### 5. The Key Technology of Edge Detection

*5.1. The Main Model of Edge Detection.* The basic idea used in edge detection is to simplify image information and use edge lines to represent the information carried by the image. Edge detection mainly includes the following four steps: filtering, enhancement, detection, and positioning. Fully convolutional neural network is widely used in image detection. It is a new type of deep convolution structure, which can accept images of any format and size and can use one convolution to obtain multiple image area features [62]. As shown in Figure 2, it can be seen that the fully convolutional neural network model includes two parts: a fully convolutional network and a loss layer. The fully convolutional network is used to represent image features. The loss layer is mainly responsible for processing the image with completed feature representation, in which the loss function is used to calculate the loss of image, obtain model parameters, and optimize the fully convolutional neural network model.

CNN has three key operations, namely, local receptive field, weight sharing, and the pooling layer, which effectively reduces the number of network parameters and alleviates the overfitting problem of the model. Typical convolutional neural network architectures (Table 3) include LeNet5 [63], AlexNet [64], VGGNet [65], Google InceptionNet [66], ResNet [67], and DenseNet [68].

The mostly used convolutional neural network structure for edge detection algorithms is VGGNet, which is an improvement made by the Visual Geometry Group of Oxford University on the basis of AlexNet. The entire network uses the same size of  $3 \times 3$  convolution kernel and  $2 \times 2$  maximum pooling. The network results are simple with fewer parameters, and the  $3 \times 3$  convolution kernel can better maintain image features.

**5.2. Dataset.** At present, the most commonly used edge detection dataset is the Berkeley segmentation dataset (BSDS500), which is the dataset provided by the computer vision group of the University of Berkeley that can be used for image segmentation and object edge detection. The dataset contains 200 training images, 100 verification images, and 200 test images, and all truth values are saved in .mat files, including segmentation and boundaries. Each image corresponds to five truth values, which are the truth values marked by five individuals. When training, the true value can be averaged or used to expand the data. The evaluation code will compare these five true values in turn. Recently, many edge detection algorithms, such as BDCN [69], CRF [70], HED [71], and VCF [72] expand data on the BSDS500 training set and validation set in order to improve the detection accuracy, including rotation, flip, and scale scaling.

In addition to the above-mentioned classic image edge detection algorithms and emerging deep learning image edge detection algorithms, there are also simulated annealing algorithms, ant colony algorithms, genetic algorithms, wavelet transform algorithms, and mathematical morphology algorithms. There are a large number of application research studies in the image edge detection, so it will not be covered again here [73].

## 6. Conclusions

Edge detection is still a very challenging technical problem because of the following reasons [74]. For weakly supervised and unsupervised edge detection, the training of deep learning-based edge detectors usually relies on a large number of well-annotated images. The annotation process is time-consuming, expensive, and inefficient. In weakly supervised detection technology, only image-level annotations or part of bounding box annotations are used to train the detector, which is of great significance for reducing labor costs and improving detection flexibility [75]. For edge detection of small targets, detecting small targets in large scenes has always been a challenge. Some potential applications of this research direction include the use of remote sensing images to count wild animal populations and to

detect the status of some important military targets. For dynamic video edge detection, real-time target tracking edge detection in high-definition video is of great significance for video surveillance and autonomous driving [76]. General edge detection is usually designed for images, while ignoring the correlation between video frames. Using spatio-temporal correlation to improve detection is an important research direction [77].

With the rapid development of graphics processing and automated detection, improved classic edge detection algorithms and deep learning edge detection algorithms will become research hotspots [78]. Especially in complex scenes, algorithms with accurate image edge positioning, short algorithm response time, and strong antinoise ability will be an important research direction in the future [79].

## Data Availability

The simulation experiment data used to support the findings of this study are available from the corresponding author upon request.

## Conflicts of Interest

The authors declare that there are no conflicts of interest regarding the publication of this paper.

## Acknowledgments

This work was supported by the Natural Science Fund Project of Gansu Province (No. 21JR7RA300), the Open Project of Gansu Provincial Research Center for Conservation of Dunhuang Cultural Heritage (No. GDW2021YB15), the Science Foundation of Shanxi Province of China (2021JM-344), and Shanxi Key Laboratory of Intelligent Processing for Big Energy Data (No. IPBED7).

## References

- [1] A. Dumka, A. Ashok, and P. Verma, *Advanced Digital Image Processing and its Applications in Big Data*, CRC Press, Uttarakhand, India, 2020.
- [2] C. Zhong, "Review of image edge detection algorithms based on deep learning," *Journal of Computer Applications*, vol. 40, no. 11, pp. 3280–3288, 2020.
- [3] Y. Xu, Y. Qian, and J. Wang, "Image fusion method of the K-svd algorithm and Canny edge detection in the DTCWT domain," *Journal of Jiamusi University (Natural Science Edition)*, vol. 38, no. 05, pp. 48–51, 2020.
- [4] K. Ma, Q. Xu, and B. Wang, "Roberts' Adaptive edge detection method," *Journal of Xi'an Jiaotong University*, vol. 42, no. 10, pp. 1240–1244, 2008.
- [5] V. Torre and T. Poggio, "On edge detection," *IEEE Transactions on Pattern Analysis and Machine Intelligence*, vol. 8, no. 2, pp. 147–163, 2008.
- [6] J. Kittler, "On the accuracy of the Sobel edge detector," *Image and Vision Computing*, vol. 1, no. 1, pp. 37–42, 1983.
- [7] J. Canny, "A computational approach to edge detection," *IEEE Transactions on Pattern Analysis and Machine Intelligence*, vol. 8, no. 6, pp. 679–698, 1986.
- [8] P. Arbeláez, M. Maire, C. Fowlkes, and J. Malik, "Contour detection and hierarchical image segmentation," *IEEE*

- Transactions on Pattern Analysis and Machine Intelligence*, vol. 33, no. 5, pp. 898–916, 2011.
- [9] X. Ren and B. Li, “Discriminatively trained sparse code gradients for contour detection,” *Advances in Neural Information Processing Systems*, vol. 15, no. 1, pp. 584–592, 2012.
  - [10] P. Dollar and C. L. Zitnick, “Fast edge detection using structured forests,” *IEEE Transactions on Pattern Analysis and Machine Intelligence*, vol. 37, no. 8, pp. 1558–1570, 2015.
  - [11] Y. Shi, W. Yang, H. Du, L. Wang, T. Wang, and S. Li, “Overview of image captions based on deep learning,” *Acta Electronica Sinica*, vol. 49, no. 10, pp. 2048–2060, 2021.
  - [12] S. Xie and Z. Tu, “Holistically-nested edge detection,” in *Proceedings of the 2015 IEEE international conference on computer vision (ICCV)*, vol. 02, no. 12, p. 15, December 2016.
  - [13] Y. Ou, X. He, and S. Qu, “Fully convolutional neural network with attention module for semantic segmentation,” *Journal of Frontiers of Computer Science and Technology*, vol. 16, no. 5, pp. 1136–1145, 2022.
  - [14] X. Lu, J. Lu, and T. Tu, “Stereo matching method based on multi-scale CNN,” *Computer Engineering and Design*, vol. 39, no. 09, pp. 2918–2922, 2018.
  - [15] L. Zhang, Y. Liang, and D. Wu, “Strip steel surface defects imaging edge inspection based on improved multi-scale morphology,” *Laser & Infrared*, vol. 44, no. 03, pp. 330–334, 2014.
  - [16] X. Zhong, J. Li, and W. Huang, “Deep multi-label hashing for image retrieval,” in *Proceedings of the 2019 IEEE 31st international conference on tools with artificial intelligence (ICTAI)*, vol. 31, no. 10, pp. 00–94, IEEE, Portland, OR, USA, November 2019.
  - [17] Y. Liu, M. M. Cheng, X. Hu et al., “Richer convolutional features for edge detection,” *IEEE Transactions on Pattern Analysis and Machine Intelligence*, vol. 41, no. 8, pp. 1939–1946, 2019.
  - [18] K. Han, H. Zhang, and Y. Wang, “A vehicle detection method based on faster R-CNN,” *Journal of Southwest University of Science and Technology*, vol. 32, no. 04, pp. 65–70, 2017.
  - [19] F. Zhao, W. Zhang, and Z. Yan, “Multi-feature map pyramid fusion deep network for semantic segmentation on remote sensing data,” *Journal of Electronics and Information Technology*, vol. 41, no. 10, pp. 2525–2531, 2019.
  - [20] D. Marr and E. Hildreth, “Theory of edge detection,” *Proceedings of the Royal Society of London*, vol. 207, no. 1167, pp. 187–217, 1980.
  - [21] C. G. Harris and M. J. Stephens, *A Combined Corner and Edge detector*, 1988.
  - [22] Miroslav and Trajkovi, “Fast corner detection,” *Image and Vision Computing*, vol. 16, no. 2, pp. 75–87, 1998.
  - [23] D. G. Lowe, “Distinctive image features from scale-invariant keypoints,” *International Journal of Computer Vision*, vol. 60, no. 2, pp. 91–110, 2004.
  - [24] X. Che, L. Wang, and X. Guo, “Improved boundary detection based on multi-scale cues fusion,” *Journal of Jilin University (Engineering and Technology Edition)*, vol. 48, no. 05, pp. 1621–1628, 2018.
  - [25] S. Wang, X. Wu, Y. Zhang, and Q. Chen, “Image crack detection with multi – scale down-sampled normalized cut,” *Chinese Journal of Scientific Instrument*, vol. 38, no. 11, pp. 2788–2796, 2017.
  - [26] S. Wang, X. Wu, Y. Zhang, and X. Liu, “Structure crack segmentation using fully convolutional neural network and structured forest,” *Chinese Journal of Scientific Instrument*, vol. 41, no. 08, pp. 170–179, 2020.
  - [27] W. Wei, H. Song, H. Wang, and X. Fan, “Research and simulation of queue management algorithms in ad hoc networks under DDoS attack,” *IEEE Access*, vol. 5, pp. 27810–27817, 2017.
  - [28] W. Wei, S. Liu, W. Li, and D. Du, “Fractal intelligent privacy protection in online social network using attribute-based encryption schemes,” *IEEE Transactions on Computational Social Systems*, vol. 5, no. 3, pp. 736–747, 2018.
  - [29] W. Wang, F. Xia, and H. Nie, “Vehicle trajectory clustering based on dynamic representation learning of Internet of vehicles,” *IEEE Transactions on Intelligent Transportation Systems*, vol. 22, no. 6, pp. 1–10, 2020.
  - [30] Q. Shi, J. Li, and W. Yang, “Multi-aspect SAR image fusion method based on wavelet transform,” *Beijing Hangkong Hangtian Daxue Xuebao/Journal of Beijing University of Aeronautics and Astronautics*, vol. 43, no. 10, pp. 2135–2142, 2017.
  - [31] L. Wei, S. Zhang, and Z. Xie, “Application of SAR image fusion based on wavelet and directional template,” *Application Research of Computers*, vol. 24, no. 03, pp. 280–282, 2007.
  - [32] Y. Liu, X. Sun, and W. Wei, “Enhancing energy-efficient and QoS dynamic virtual machine consolidation method in cloud environment,” *IEEE Access*, vol. 6, pp. 31224–31235, 2018.
  - [33] J. Yang, H. Wang, Z. Lv et al., “Multimedia recommendation and transmission system based on cloud platform,” *Future Generation Computer Systems*, vol. 70, pp. 94–103, 2017.
  - [34] M. Jianmin and Y. Jing, “Optimistic multi-granulation interval-set rough sets,” *Journal of Zhengzhou University*, vol. 50, no. 3, pp. 87–93, 2018.
  - [35] J. Chen, C. Du, Y. Zhang, P. Han, and W. Wei, “A clustering-based coverage path planning method for autonomous heterogeneous UAVs,” *IEEE Transactions on Intelligent Transportation Systems*, vol. 99, pp. 1–11, 2021.
  - [36] W. Wei, H. Srivastava, and Y. Zhang, “A local fractional integral inequality on fractal space analogous to Anderson’s inequality,” *Abstract and Applied Analysis*, vol. 2014, pp. 1–7, Article ID 797561, 2014.
  - [37] D. Połap, M. Woźniak, W. Wei, and R. Damasevicius, “Multi-threaded learning control mechanism for neural networks,” *Future Generation Computer Systems*, vol. 87, pp. 16–34, 2018.
  - [38] P. Siva Raja and A. V. Rani, “Brain tumor classification using a hybrid deep autoencoder with Bayesian fuzzy clustering-based segmentation approach,” *Biocybernetics and Biomedical Engineering*, vol. 40, no. 1, pp. 440–453, 2020.
  - [39] G. Chen, C. Li, W. Wei et al., “Fully convolutional neural network with augmented atrous spatial pyramid pool and fully connected fusion path for high resolution remote sensing image segmentation,” *Applied Sciences*, vol. 9, no. 9, p. 1816, 2019.
  - [40] D. Guo, J. Xie, and X. Zhou, “Exploiting efficient and scalable shuffle transfers in future data center networks[J],” *Parallel & Distributed Systems IEEE Transactions on*, vol. 26, no. 4, pp. 997–1009, 2014.
  - [41] A. Krizhevsky, I. Sutskever, and G. E. Hinton, “ImageNet classification with deep convolutional neural networks,” *Communications of the ACM*, vol. 60, no. 6, pp. 84–90, 2017.
  - [42] X. Li, L. Ding, and W. Li, “FPGA accelerates deep residual learning for image recognition,” in *Proceedings of the 2017 IEEE 2nd Information Technology, Networking, Electronic and Automation Control Conference (ITNEC)*, pp. 837–840, IEEE, September 2017.
  - [43] H. Wang, X. Zhang, and Y. Dou, “An image edge detection effects evaluation algorithm based on image reconstruction,”

- Journal of Northwestern Polytechnical University*, vol. 35, no. 6, pp. 1112–1118, 2017.
- [44] Y. Liu and J. Zhu, “Sub-pixel edge detection algorithm of spot image based on improved Zernike moment,” *Laser Journal*, vol. 42, no. 05, pp. 32–35, 2021.
  - [45] X. Zhang and Y. Ren, “Improved multi-scale edge detection method based on HED,” *Microelectronics & Computer*, vol. 38, no. 6, pp. 1–6, 2021.
  - [46] S. Xia, D. Peng, and D. Meng, “A fast adaptive k-means with No bounds,” *IEEE Transactions on Pattern Analysis and Machine Intelligence*, vol. 44, no. 1, pp. 87–99, 2020.
  - [47] H. Zhang and J. Zhao, “An unsupervised boundary detection algorithm based on orientation contrast model,” *Journal of University of Science and Technology of China*, vol. 47, no. 1, pp. 26–31, 2017.
  - [48] G. Bertasius, J. Shi, and L. Torresani, “DeepEdge: a multi-scale bifurcated deep network for top-down contour detection,” in *Proceedings of the 2015 IEEE Conference on Computer Vision and Pattern Recognition (CVPR)*, pp. 4380–4389, Boston, MA, USA, October 2015.
  - [49] N. Yu, Z. Zhang, and Q. Xu, “An Improved Method for Cloth Pattern Cutting Based on Holistically-Nested Edge Detection,” in *Proceedings of the 2021 IEEE 10th Data Driven Control and Learning Systems Conference (DDCLS)*, pp. 1246–1251, Suzhou, China, May 2021.
  - [50] Y. Liu and M. S. Lew, “Learning relaxed deep supervision for better edge detection,” in *Proceedings of the 2016 IEEE Conference on Computer Vision and Pattern Recognition (CVPR)*, pp. 231–240, IEEE, Las Vegas, NV, USA, June 2016.
  - [51] G. Bertasius, J. Shi, and L. Torresani, *High-for-Low and Low-For-High: Efficient Boundary Detection from Deep, Object Features and its Applications to High-Level Vision*, pp. 504–512, 2015.
  - [52] S. Wei, X. Wang, and W. Yan, “DeepContour: a deep convolutional feature learned by positive-sharing loss for contour detection,” in *Proceedings of the Computer Vision & Pattern Recognition*, pp. 3982–3991, IEEE, June 2015.
  - [53] J. Yang, B. Price, and S. Cohen, “Object Contour Detection with a Fully Convolutional Encoder-Decoder Network,” in *Proceedings of the IEEE Computer Society*, pp. 193–202, Las Vegas, NV, USA, December 2016.
  - [54] Y. Ganin and V. Lempitsky, “\$N\_4\$-Fields: Neural Network Nearest Neighbor Fields for Image Transforms,” in *Proceedings of the Asian Conference on Computer Vision*, pp. 536–551, Springer, Cham, June 2014.
  - [55] K. Maninis, J. Pont-Tuset, and P. Arbelaez, “Convolutional oriented boundaries: from image segmentation to high-level tasks,” *IEEE Transactions on Pattern Analysis and Machine Intelligence*, vol. 40, no. 4, pp. 819–833, 2018.
  - [56] X. Dan, W. Ouyang, X. Alameda-Pineda, E. Ricci, X. Wang, and N. Sebe, “Learning Deep Structured Multi-Scale Features Using Attention-Gated CRFs for Contour Prediction,” pp. 3964–3973, 2017, <https://arxiv.org/abs/1801.00524>.
  - [57] P. Yu and X. Wang, “Deep crisp boundaries: from boundaries to higher-level tasks,” *IEEE Transactions on Image Processing: A Publication of the IEEE Signal Processing Society*, vol. 28, no. 3, pp. 1285–1298, 2018.
  - [58] Y. L. Hu, Y. F. Sun, and B. C. Yin, “Information sensing and interaction technology in Internet of things,” *Chinese Journal of Computers*, vol. 35, no. 6, p. 1147, 2012.
  - [59] W. Guo, X. Li, and T. Wen, “Watershed Algorithm Combining Multi-Structure Filter and Multi-Scale reconstruction,” *Computer Engineering & Applications*, vol. 51, no. 14, pp. 151–157, 2015.
  - [60] Z. Ji, H. Pi, and W. Wei, “Recommendation Based on Review Texts and Social Communities: A Hybrid Model,” *IEEE Access*, vol. 2019, pp. 40416–40427, 2019.
  - [61] G. He, C. Hao, and Y. Tian, “Image Fusion Algorithm Based on Stationary Wavelet Transform,” *Journal of Data Acquisition & Processing*, vol. 39, no. 5, pp. 325–333, 2007.
  - [62] L. Bondi, L. Baroffio, D. Güera, P. Bestagini, E. J. Delp, and S. Tubaro, “First steps toward camera model identification with convolutional neural networks,” *IEEE Signal Processing Letters*, vol. 24, no. 3, pp. 259–263, 2017.
  - [63] Y. Lecun, L. Bottou, Y. Bengio, and P. Haffner, “Gradient-based learning applied to document recognition,” *Proceedings of the IEEE*, vol. 86, no. 11, pp. 2278–2324, 1998.
  - [64] M. Alom, T. Taha, C. Yakopcic et al., “The History Began from AlexNet: A Comprehensive Survey on Deep Learning Approaches,” 2018, <https://arxiv.org/abs/1803.01164>.
  - [65] K. Simonyan and A. Zisserman, *Very Deep Convolutional Networks for Large-Scale Image Recognition*, pp. 1–14, 2014, <https://arxiv.org/abs/1409.1556>.
  - [66] C. Szegedy, L. Wei, Y. Jia et al., “Going Deeper with convolutions,” in *Proceedings of the 2015 IEEE Conference on Computer Vision and Pattern Recognition (CVPR)*, pp. 1–9, IEEE, Boston, MA, USA, June 2015.
  - [67] C. Szegedy, S. Ioffe, V. Vanhoucke, and A. Alemi, “Inception-v4, inception-ResNet and the impact of residual connections on learning,” pp. 4278–4284, 2016, <https://arxiv.org/abs/1602.07261>.
  - [68] L. Wang, Y. Shen, H. Liu, and Z. Guo, “An accurate and efficient multi-category edge detection method,” *Cognitive Systems Research*, vol. 58, pp. 160–172, 2019.
  - [69] J. He, S. Zhang, M. Yang et al., “Bi-Directional Cascade Network for Perceptual Edge Detection,” in *Proceedings of the 2019 IEEE/CVF Conference on Computer Vision and Pattern Recognition (CVPR)*, pp. 100–113, IEEE, June 2020.
  - [70] Y. Liu, M. Cheng, and X. Hu, “Richer Convolutional Features for Edge Detection,” *IEEE Computer Society*, vol. 41, no. 8, pp. 1939–1946, 2016.
  - [71] X. Soria, E. Riba, and A. Sappa, “Dense extreme inception network: towards a robust CNN model for edge detection,” pp. 1912–1921, 2020, <https://arxiv.org/abs/1909.01955>.
  - [72] R. Du, Q. Li, and Y. Liu, “Summary of image edge detection,” *Optical Technique*, vol. 3, pp. 415–419, 2005.
  - [73] S. Qi, Y. Lu, W. Wei, and X. Chen, “Efficient Data Access Control with Fine-Grained Data Protection in Cloud-Assisted IIoT,” *IEEE Internet of Things Journal*, vol. 8, no. 99, pp. 2886–2899, 2020.
  - [74] W. Wang, X. Zhao, Z. Gong, Z. Chen, N. Zhang, and W. Wei, “An attention-based deep learning framework for trip destination prediction of sharing bike,” *IEEE Transactions on Intelligent Transportation Systems*, vol. 22, no. 7, pp. 4601–4610, 2021.
  - [75] A. Rampun, K. López-Linares, P. J. Morrow et al., “Breast pectoral muscle segmentation in mammograms using a modified holistically-nested edge detection network,” *Medical Image Analysis*, vol. 57, pp. 1–17, 2019.
  - [76] A. Jafar and L. Myungho, “Hyperparameter optimization for deep residual learning in image classification,” in *Proceedings of the 2020 IEEE International Conference on Autonomic Computing and Self-Organizing Systems Companion (ACSOS-C)*, pp. 24–29, IEEE, Washington, DC, USA, August 2020.

- [77] C. Cai, J. Wang, F. Zhang, X. Liu, P. Zhang, and Y. G. Zhou, "A multichannel wireless UAV charging system with compact receivers for improving transmission stability and capacity," *IEEE Systems Journal*, vol. 16, no. 1, pp. 997–1008, 2022.
- [78] R. Jiang, Y. Xin, Z. Chen, and Y. Zhang, "A medical big data access control model based on fuzzy trust prediction and regression analysis," *Applied Soft Computing*, vol. 117, pp. 108423–108520, 2022.
- [79] Y. Yu, M. Rashidi, B. Samali, M. Mohammadi, T. N. Nguyen, and X. Zhou, "Crack detection of concrete structures using deep convolutional neural networks optimized by enhanced chicken swarm algorithm," *Structural Health Monitoring*, vol. 21, no. 5, pp. 2244–2263, 2022.

## Retraction

# Retracted: A Novel Maximum Flow Algorithm with Neural Network for Time-Varying Wastage Networks

### Security and Communication Networks

Received 1 August 2023; Accepted 1 August 2023; Published 2 August 2023

Copyright © 2023 Security and Communication Networks. This is an open access article distributed under the Creative Commons Attribution License, which permits unrestricted use, distribution, and reproduction in any medium, provided the original work is properly cited.

This article has been retracted by Hindawi following an investigation undertaken by the publisher [1]. This investigation has uncovered evidence of one or more of the following indicators of systematic manipulation of the publication process:

- (1) Discrepancies in scope
- (2) Discrepancies in the description of the research reported
- (3) Discrepancies between the availability of data and the research described
- (4) Inappropriate citations
- (5) Incoherent, meaningless and/or irrelevant content included in the article
- (6) Peer-review manipulation

The presence of these indicators undermines our confidence in the integrity of the article's content and we cannot, therefore, vouch for its reliability. Please note that this notice is intended solely to alert readers that the content of this article is unreliable. We have not investigated whether authors were aware of or involved in the systematic manipulation of the publication process.

Wiley and Hindawi regrets that the usual quality checks did not identify these issues before publication and have since put additional measures in place to safeguard research integrity.

We wish to credit our own Research Integrity and Research Publishing teams and anonymous and named external researchers and research integrity experts for contributing to this investigation.

The corresponding author, as the representative of all authors, has been given the opportunity to register their agreement or disagreement to this retraction. We have kept a record of any response received.

### References

- [1] B. Zhang, K. Jiang, and W. Huang, "A Novel Maximum Flow Algorithm with Neural Network for Time-Varying Wastage Networks," *Security and Communication Networks*, vol. 2022, Article ID 3782761, 9 pages, 2022.

## Research Article

# A Novel Maximum Flow Algorithm with Neural Network for Time-Varying Wastage Networks

Baowen Zhang, Kaiwen Jiang , and Wei Huang

*School of Computer Science and Engineering, Tianjin University of Technology, Tianjin, China*

Correspondence should be addressed to Kaiwen Jiang; [jiang512@email.tjut.edu.cn](mailto:jiang512@email.tjut.edu.cn)

Received 16 May 2022; Revised 10 June 2022; Accepted 15 June 2022; Published 30 September 2022

Academic Editor: Hangjun Che

Copyright © 2022 Baowen Zhang et al. This is an open access article distributed under the Creative Commons Attribution License, which permits unrestricted use, distribution, and reproduction in any medium, provided the original work is properly cited.

This paper introduces a time-varying wastage maximum flow problem (TWMFP) and proposes a time-flow neural network (TFNN) for solving the TWMFPs. The time-varying wastage maximum flow problem is concerned with finding the maximum flow in a network with time-varying arc capacities and additive flow losses on the arcs. This problem has multiple applications in transportation, communication, and financial network. For example, solving the maximum traffic flow of the transportation network and the maximum profit of the financial network. Unlike traditional neural network algorithms, the proposed TFNN does not require any training by means of its time-flow mechanism. The time-flow mechanism is realized by each active neuron sending pulses to its successor neurons. In order to maximize the network flow, the proposed TFNN can be divided into two parts: path-pulse neural networks (PPNNs) and subnet-flow neural networks (SFNN). PPNN is to generate two subnet sets (viz. with wastage arcs and without), and SFNN is to find the maximum flow value of each subnet. The subnet computing strategy of the proposed algorithm greatly improves the solution accuracy of TWMFPs. Theoretical analysis and experiments have proved the effectiveness of TFNN. The experiment results of the transportation network (viz. New York Road) show that the proposed TFNN has better performance (viz. error rate and computational time) compared to classical algorithms.

## 1. Introduction

The maximum flow problem (MFP) is a classical network optimization problem [1, 2], and it is also a general problem in vehicular networks [3], network optimization [4], social network [5, 6], and other fields. Ford and Fulkerson first solved the maximum flow problem using the labeling algorithm (viz. Ford-Fulkerson (FF) algorithm) [7]. Then, many improved labeling algorithms have been proposed for solving the maximum flow problems [8], such as Edmonds-Karp algorithm [9], and the Cai-Sha algorithm [10]. With the increasing complexity of networks, some intelligent algorithms have been used for solving the MFP, such as the genetic algorithm (GA) [11].

The time-varying wastage maximum flow problem is the maximum flow problem with time-varying arc capacities and additive flow losses on the arcs, which can be applied to intelligent transportation [12, 13], communication network [14], financial analysis [15, 16], and other fields. In financial networks, Eboli [17] has described the balance-sheet as a loss

flow on the arc. The time-varying maximum flow problem (TMFP) [18, 19] and wastage maximum flow problem (WMFP) [20] have been investigated extensively. Li and Buzdalov et al. [21, 22] proposed their algorithms for solving the TMFPs. Cai [23] and Song [24] have researched different WMFPs. These existing algorithms were improved labeling algorithms [25]. While to the best of our knowledge, a question with regard to find the maximum flow value of time-varying wastage maximum flow problem remains open.

In this paper, we propose a novel neural network framework for solving the time-varying wastage maximum flow problem (TWMFP). The TWMFP is the maximum flow problem with time-varying arc capacities and additive flow losses on the arcs. The advantages of the proposed time-flow neural network (TFNN) are summarized as follows: first, different with general neural networks, the proposed TFNN does not require any training based on its time-flow mechanism. Second, compared with classical labeling algorithms, the proposed TFNN greatly improves



the calculation speed based on its parallel computing feature. Third, unlike existing maximum flow algorithms, the unique group calculation idea of the proposed TFNN improves the accuracy for solving TWMFPs. In addition, the proposed TFNN can find an accurate solution to the general network maximum flow problems, such as MFP and TMFP.

The remainder of this paper is organized as follows: in Section 2, some basic concepts of TWMFP are introduced. In Section 3, the TFNN algorithm is developed and an example of a TWMFP is given. In Section 4, the experimental results are reported. And, Section 5 gives a conclusion to this paper.

## 2. Mathematical Formulation

The goal of the time-varying wastage maximum flow problem is to find the maximum flow from the departure node to the destination node within a predetermined period, where arc capacities change over time and flow on the arc may be consumed. Such problems introduced in this paper can be applied to fields such as intelligent transportation and financial analysis. For example, in a transportation network, road congestion during peak periods represents time-varying arc capacities and car accident emergency represents consumption/wastage on the arc.

**Definition 1** [Wastage Network (WN)]. Let  $V$  be a set of network nodes,  $A = \{(v_i, v_j)/v_i, v_j \in V\}$  be a set of network arcs,  $C = \{c_{ij}/(v_i, v_j) \in A\}$  be a set of arc capacities, and  $W = \{w_{ij}/(v_i, v_j) \in A\}$  be a set of arc wastage, then the network  $G = (V, A, C, W)$  is defined as a wastage network.

**Definition 2** [Time-Varying Wastage Network (TWN)]. Assume there is a wastage network  $G = (V, A, C, W)$ , given a piecewise function  $C(\xi) = \{C_{ij}(\xi_i)/v_i, v_j \in A, \xi_i \in T_{ij}\}$  stands for a set of arc capacities, where  $\xi = (\xi_j/\xi_j = \xi_i + b_{ij}, (v_i, v_j) \in A)$ ,  $\xi_i$  denotes the depart time of node  $v_i$ ,  $b_{ij}$  represents the length of arc  $(v_i, v_j)$ ,  $T_{ij} = \{[t_s^z, t_d^z]/(v_i, v_j) \in A, z = 1, \dots, Z\}$  means a set of time windows,  $t_s^z$  and  $t_d^z$  represent the earliest and latest depart times,  $z$  and  $Z$  denotes the index and number of time windows. Then, network  $G = (V, A, C(\xi), W)$  is a time-varying wastage network.

The arc lengths of time-varying wastage networks are set as a predetermined number  $\delta t$ . The arrival time of the destination node is calculated as follows:

$$\xi_d = \max\{\xi_i + b_{id}\}. \quad (1)$$

**Definition 3** [Feasible Flow]. Given a TWN  $G = (V, A, C(\xi), W)$ , then the feasible flow  $F_{ij}(\xi)$  of the arc  $(v_i, v_j)$  can be expressed as follows:

$$F_{ij}(\xi) = f_{ij}(\xi) - f_{ij}(\xi) * w_{ij}, \quad (2)$$

where

$$f_{ij}(\xi) = \min\left(\sum_{(v_g, v_i) \in A} F_{gi}(\xi_g), C_{ij}(\xi_i)\right). \quad (3)$$

Considering the particularity of the departure node  $v_s$ , then the feasible flow  $F_{sy}(\xi)$  can be calculated by the following equation:

$$F_{sy}(\xi) = C_{sy}(\xi_s) - C_{sy}(\xi_s) * w_{sy}. \quad (4)$$

**Definition 4** [Model of the TWMFP]. Given a time limitation  $T_0$ . Follows from (1)–(4), the model of the TWMFP is formulated by the following equation:

$$\left\{ \begin{array}{l} \max \quad \sum_{(v_r, v_d) \in A} F_{rd}(\xi), \\ \xi_d \leq T_0, \\ F_{ij}(\xi_i) \leq C_{ij}(\xi_i), \\ \text{s.t.} \quad \sum_{(v_s, v_y) \in A} F_{sy}(\xi) - \sum_{(v_r, v_d) \in A} F_{rd}(\xi) \geq 0, \\ \sum_{(v_j, v_i) \in A} F_{ji}(\xi) - \sum_{(v_i, v_j) \in A} F_{ij}(\xi) = 0, \end{array} \right. \quad (5)$$

where

$$\left\{ \begin{array}{l} F_{sy}(\xi) = C_{sy}(\xi_s) - C_{sy}(\xi_s) * w_{sy}, \\ \dots \\ F_{ij}(\xi) = f_{ij}(\xi) - f_{ij}(\xi) * w_{ij}, \\ \dots \\ F_{rd}(\xi) = f_{rd}(\xi) - f_{rd}(\xi) * w_{rd}. \end{array} \right. \quad (6)$$

$$f_{rd}(\xi) = \min\left(\sum_{(v_x, v_r) \in A} F_{xr}(\xi), C_{rd}(\xi)\right). \quad (7)$$

## 3. Time-Flow Neural Network Algorithm Description

Generally, the labeling algorithms are used to find the solution of maximum flow problems. A disadvantage of these approaches is that they usually obtain large error rate solutions due to the time-varying and wastage in TWMFPs. This paper provides a better way to solve the time-varying wastage maximum flow problem.

In this section, the proposed TFNN algorithm will be described at first. And, then the construction of path-pulse neural networks (PPNNs) and subnet-flow neural networks (SFNNs) are depicted. To show the structure and algorithm of TFNN, the description of symbols are shown in Table 1.

**3.1. Description of TFNN.** The underlying idea of using TFNN to solve TWMFP is that a neuron sends “preflows” (viz. pulses) to its successor neurons when the current neuron received pulses. With this new viewpoint, the proposed TFNN can reach a better solution of TWMFPs. There are two main parts in the design of TFNN, the first part is to find two subnet sets (viz. with wastage arcs and without) by path-pulse neural networks (PPNN), while the second part is to calculate the maximum flow of the subnets based on subnet-flow neural networks (SFNNs). The detailed steps of TFNN are shown in Algorithm 1.

**3.2. Description of PPNN.** PPNN is used to generate two subnet sets (viz. with and without wastage arcs) through the following parts: first, initialize neurons by Step 1. Second, generate pulses from the departure neuron  $s$  at every time by Step 3. Third, update all nodes but  $s$  at every time by Step 4. Fourth, update subnet sets at every time by Steps 5–10. Finally, output subnet sets. The detailed steps of PPNN are shown in Algorithm 2.

All neurons in the PPNN will no longer generate pulses when the time limitation is reached. A general structure of a neuron in PPNN is shown in Figure 1.

**3.2.1. Input.** The input part is used to receive pulses from its predecessor neurons.

**3.2.2. Pulse Receiver.** The pulse receiver part is used to filter the received pulses and consists of  $P_{ni}^{t1}$ ,  $y$  and time window  $T_i$ . Time window  $T_i$  is initialized by Algorithm 2 (PPNN).  $P_{ni}^{t1}$  is explained as follows:

$$P_{ni}^{t1} = \begin{cases} U_{ni}, & \text{if the input has received pulse,} \\ \emptyset, & \text{if the input does not received pulse,} \end{cases} \quad (8)$$

where

$$U_{ni} = \begin{cases} w_{si}^t, & \text{if } n = s, \\ w_{sa}^{t0}, \dots, w_{ni}^t, & \text{if } n \neq s. \end{cases} \quad (9)$$

$y$  is explained as follows:

$$y = g1(P_{ni}^{t1}) = \begin{cases} 1, & \text{if } P_{ni}^{t1} \neq \emptyset, \\ 0, & \text{if } P_{ni}^{t1} = \emptyset. \end{cases} \quad (10)$$

where  $P_{ni}^{t1} \neq \emptyset$  means at least one pulse has reached at  $t1$ .

If the current neuron is the destination neuron  $d$ , the neuron no longer generates pulses and output the path  $R(P_{nd}^{t1})$  and the wastage  $O(P_{nd}^{t1})$ . Their expressions are shown as follows:

TABLE 1: Description of the symbols used in TFNN.

Symbols	Explanation
$P_{ni}^{t1}$	A pulse from neuron $n$ to neuron $i$ at time $t1$
$w_{xi}$	Wastage of arc $(v_x, v_i)$
$U_{ni}$	Wastage list of the path from neuron $s$ to $i$ , where $n$ on the path
$T_{ij}^z$	The $z$ th time window of arc $(v_i, v_j)$
$c_{ij}^z$	Capacity from neuron $i$ to neuron $j$ at time window $T_{ij}^z$
$B_i$	The relation neuron of neuron $i$
$f_{zi}$	The flow of arc $(v_z, v_i)$
$G_o$	The set of subnets without wastage arcs
$G_w$	The set of subnets with wastage arcs
$U_{ix}$	Pulse information of arc $(v_i, v_x)$

$$R(P_{nd}^{t1}) = \begin{cases} \langle \emptyset \rangle, & \text{if } P_{nd}^{t1} = \emptyset; \\ \langle (s, t), \dots, (d, t1) \rangle, & \text{if } P_{nd}^{t1} = w_{si}^t, \dots, w_{nd}^{t1}, \end{cases} \quad (11)$$

$$O(P_{nd}^{t1}) = \begin{cases} -1, & \text{if } P_{ni}^{t1} = \emptyset, \\ \sum_{w_{ij} \in P_{nd}^{t1}} w_{ij}^t, & \text{if } P_{ni}^{t1} \neq \emptyset. \end{cases} \quad (12)$$

**3.2.3. Neuron State.** The neuron state part is used to select the time window and consists of  $w_{ix}^{t1}$ ,  $x = f, \dots, h$ .  $w_{ix}^{t1}$  is explained in the following equation:

$$w_{ix}^{t1} = g2(W_i) = \begin{cases} w_{ix}, & \text{if } t1 \in T_{ix}^z, \\ -1, & \text{if } t1 \notin T_{ix}^z. \end{cases} \quad (13)$$

**3.2.4. Pulse Sender.** The pulse sender part is used to calculate the parameter and generates pulses and consists of  $t2$  and  $P_{ix}^{t2}$ ,  $x = f, \dots, h$ . The expression of them are shown as follows:

$$t2 = t1 + \Delta t, \quad (14)$$

$$P_{ix}^{t2} = g3(P_{ni}^{t1}, w_{ix}^{t1}, t2) = \begin{cases} U_{ix}, & \text{if the output has sent pulse;} \\ \emptyset, & \text{if the output does not send pulse,} \end{cases} \quad (15)$$

where

$$U_{ix} = \begin{cases} w_{sx}, & \text{if } i = s, \quad t1 \in T_{ix}^z; \\ w_{sa}^{t0}, \dots, w_{ni}^t, w_{ix}^{t1}, & \text{if } i \neq s, \quad t1 \in T_{ix}^z. \end{cases} \quad (16)$$

**3.2.5. Output.** The output part is used to send the pulse to its successor neurons.

**3.3. Description of SFNN.** SFNN is used to find the maximum flow of subnets through the following parts: first, initialize neurons by Step 1. Second, update all nodes,

**Input:**  $\Delta t, T_0, G$ .  
**Output:**  $f^*$  /\* The maximum flow. \*/  
(1) Set  $t = 0, f^* = 0, G_o = \emptyset, G_w = \emptyset$ .  
(2) Do  
(3)       Generate subnet sets  $G_o$  and  $G_w$  from  $G$  by **PPNN**.  
(4)       Set  $t = t + \Delta t$ .  
(5) Until  $t > T_0$  /\* End step2 \*/  
(6) Update  $f^*$  of all subnets in  $G_o$  by **SFNN**.  
(7) Update  $f^*$  of all subnets in  $G_w$  by **SFNN**.  
(8) Report the maximum flow  $f^*$ .

ALGORITHM 1: Time-flow Neural Network (TFNN).

**Input:**  $\Delta t, G, t, G_o, G_w$ .  
**Output:**  $G_o, G_w$  /\* Subnet sets of  $G$ . \*/  
(1) Set  $t1 = 0, P_{ni}^t = \emptyset, T_i = TW(i), y = 0, w_{ix}^t = -1$   
(2) Do  
(3)   Update  $w_{sx}^{t1}, t2$ , and  $P_{sx}^{t2}$  of  $s$  using (13)–(16).  
(4)   Update all nodes  $i \in V/\{s\}$  using (8)–(16).  
(5)   If  $O(P_{nd}^{t1}) = 0$   
(6)     Set  $G_o = G_o \cup R(P_{nd})$ .  
(7)   End If /\* End step5 \*/  
(8)   If  $O(P_{nd}^{t1}) > 0$   
(9)     Set  $G_w = G_w \cup R(P_{nd})$ .  
(10)   End If /\* End step8 \*/  
(11)   Set  $t1 = t1 + \Delta t$   
(12) Until  $t1 > t$  /\* End step2 \*/  
(13) Report two subnet sets  $G_o$  and  $G_w$ .

ALGORITHM 2: Path-pulse Neural Networks (PPNN).

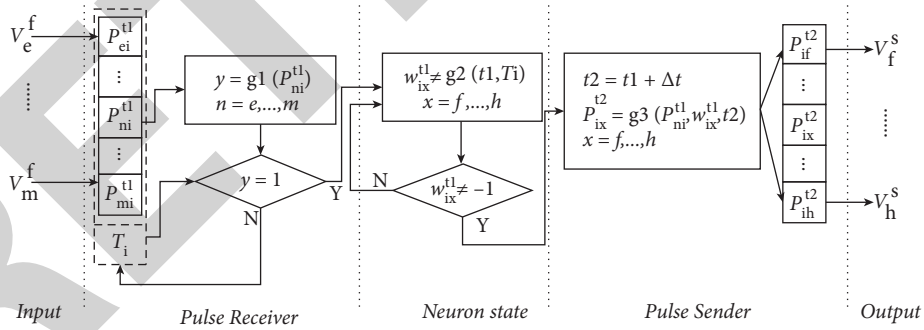


FIGURE 1: A general structure of PPNN.

$f(p), c_{ij}, f_{ij}^t, B_i$ , and  $f^*$  by Steps 2–7. Third, update  $D$  by Steps 8–10. Final, output the maximum flow. The detailed steps of SFNN are shown in Algorithm 3.

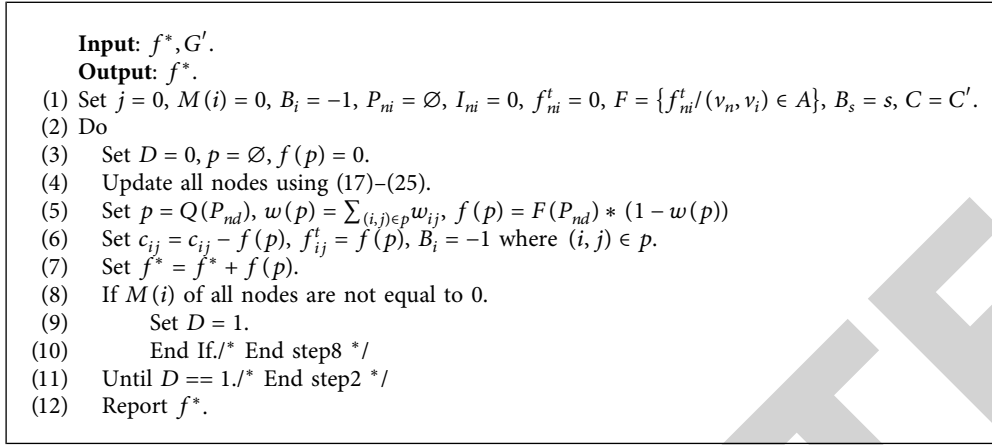
Each neuron in SFNN will reserve the first pulse received in an iteration. A general structure of a neuron in subnet-flow neural networks is shown in Figure 2.

**3.3.1. Input.** The input part is used to receive pulses coming from its relational neurons.

**3.3.2. Pulse Receiver.** The pulse receiver part is used to filter the received pulses and consists of  $P_{ni}$ ,  $j$ ,  $B$ ,  $F$ , and  $C$ . The value of  $B$ ,  $F$ , and  $C$  are calculated by the SFNN Algorithm.  $P_{ni}$  is shown as follows:

$$P_{ni} = \begin{cases} U_{ni}, & \text{if the input has received pulse;} \\ \emptyset, & \text{if the input does not received pulse,} \end{cases} \quad (17)$$

where



ALGORITHM 3: Subnet-flow Neural Networks (SFNNs).

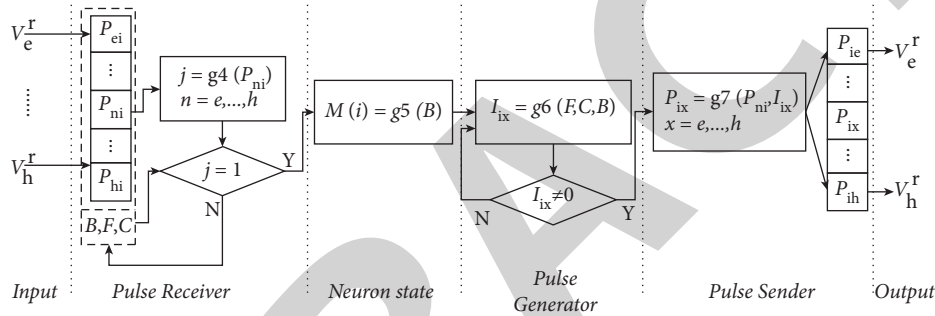


FIGURE 2: A general structure of SFNN.

$$U_{ni} = \begin{cases} I_{si}, & \text{if } n = s; \\ I_{sa}, \dots, I_{ni}, & \text{if } n \neq s. \end{cases} \quad (18)$$

$j$  is explained as follows:

$$j = g4(P_{ni}) = \begin{cases} 1, & \text{if } P_{ni} \neq \emptyset; \\ 0, & \text{otherwise.} \end{cases} \quad (19)$$

The value of  $P_{ni}$  not equals  $\emptyset$  means at least one pulse has reached at current neuron  $i$  at  $t$ .

If current neuron  $i$  is the destination neuron  $d$ , the neuron no longer generates pulses and output the path  $Q(P_{nd})$  and the path flow  $F(P_{nd})$ . Their expressions are shown as follows:

$$Q(P_{nd}) = \begin{cases} \langle \emptyset \rangle, & \text{if } P_{nd} = \emptyset; \\ \langle s, \dots, d \rangle, & \text{if } P_{nd} = I_{sa}, \dots, I_{nd}, \end{cases} \quad (20)$$

$$F(P_{nd}) = \begin{cases} 0, & \text{if } P_{nd} = \emptyset; \\ \min\{I_{ij} | I_{ij} \in P_{nd}\}, & \text{if } P_{nd} \neq \emptyset. \end{cases} \quad (21)$$

**3.3.3. Neuron State.** The neuron state part is used to record whether the current neuron has received a pulse and consists of  $M(i)$ . It is explained as follows:

$$M(i) = g5(B) = \begin{cases} M(i) + 1, & \text{if } B_x = -1; \\ M(i), & \text{otherwise.} \end{cases} \quad (22)$$

where  $x \in V_R(i)$ . The value of  $M(i)$  is initialized as 0.

**3.3.4. Pulse Generator.** The pulse generator part is used to calculate the parameter for sending pulses. This part consists of  $I_{ix}$ ,  $x = e, \dots, h$ .  $I_{ix}$  is shown as follows:

$$I_{ix} = g6(F, C, B) = \begin{cases} c_{ix}^z - f_{ix}^t, & \text{if } f_{ix}^t < c_{ix}^z, \quad B_x = -1; \\ f_{zi}^t, & \text{if } f_{zi}^t > 0, \quad B_z = -1; \\ 0, & \text{otherwise.} \end{cases} \quad (23)$$

**3.3.5. Pulse Sender.** The pulse sender part is used to generate pulses and consists of  $P_{ix}$ ,  $x = e, \dots, h$ .  $P_{ix}$  is explained as follows:

$$P_{ix} = g7(P_{ni}, I_{ix}) = \begin{cases} U_{ix}, & \text{if the output has sent pulse;} \\ \emptyset, & \text{if the output does not send pulse,} \end{cases} \quad (24)$$

where

$$U_{ix} = \begin{cases} I_{ix}, & \text{if } i = s; \\ I_{sa}, \dots, I_{ni}, I_{ix}, & \text{if } i \neq s. \end{cases} \quad (25)$$

3.3.6. *Output.* The output part is used to send pulses to its relational neurons.

3.4. *An Example.* The detailed steps of TFNN for solving the TWMFPs are illustrated by an example. The topology and description of a time-varying wastage network are described as shown in Figure 3 and Table 2. The time limitation is  $T_0 = 3$ .

The proposed TFNN can solve this problem by the following steps:

First, find two subnet sets (viz. with wastage arcs  $G_w$  and without  $G_o$ ).

$G_o = \{\text{Path1}, t = 0\}$ , where  $V_o = \{s, i, j, d\}$ ,  $W_o = \{0, 0, 0\}$ ,  $C_o = \{10, 10, 10\}$ .

$G_w = \{\text{Path2}, t = 0, \text{ and } 1\}$ , where  $V_w = \{s, i, d\}$ ,  $W_w = \{0, 0.5\}$ ,  $C_w = \{10, 10\}$  at  $t = 0$ ,  $C_w = \{5, 10\}$  at  $t = 1$ .

Second, calculate the maximum flow of the subnet.

The flow of  $G_o$  is equal to  $f1 = 10 - 10 * 0 = 10$ . Then, the capacity of arc  $(s, i)$  with depart time  $t = 0$  is adjusted to 0. The flow of Path2 with depart time  $t = 0$  is equal to 0. Therefore, the flow of  $G_w$  is equal to  $f2 = 5 - 5 * 0.5 = 2.5$ .

To sum up, the maximum flow is  $f^* = f1 + f2 = 12.5$ .

### 3.5. Time Complexity

**Theorem 1** [Time Complexity of TFNN]. *Given a TWN  $G$ ,  $n$  represents the nodes number in  $G$ ,  $m$  denotes the arcs number in  $G$ ,  $T_0$  represents the time limitation,  $\Delta t$  means a unit time. Then, TFNN solves the time-varying wastage maximum flow problem in  $o(43mn^2(\text{int})(T_0/\Delta t)^2)$  time, where  $\text{int}$  denotes the top of the integral function.*

*Proof.* The overall PPNN consists of two parts. The time complexity of the first part (viz. Steps 1–5) depends on the PPNN algorithm and the second part (viz. Steps 6–8) depends on the SFNN algorithm.

For the PPNN algorithm, there is one loop and the worst time complexity is equal to  $o(5 + T_0/\Delta t(3 + 12n + 2)) = o(5T_0/\Delta t(12n + 5))$ . Based on the time complexity of PPNN, the time complexity of the first part of TFNN is equal to  $o(4 + T_0/\Delta t(5 + T_0/\Delta t(12n + 5) + 1))$ .

For the SFNN algorithm, there is one loop and the worst time complexity is equal to  $o(7 + T_0/\Delta t(3 + 9n + 2 + m + 2)) = o(7 + T_0/\Delta t(9n + m + 7))$ . According to the number of subnetworks is less than  $n$ , the time complexity of the second part of TFNN is equal to  $o(2n(7 + T_0/\Delta t(9n + m + 7)))$ .

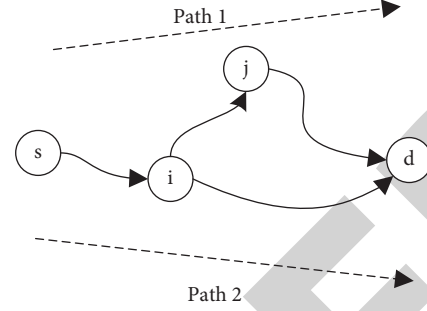


FIGURE 3: An example of TFNN.

TABLE 2: Description of a time-varying wastage network.

Node	Arc	Time window	Capacity	Wastage
s	$s \rightarrow i$	$[0, 1]$	10	0
		$[1, 3]$	5	0
i	$i \rightarrow j$	$[0, 3]$	10	0
		$[0, 3]$	10	0.5
j	$j \rightarrow d$	$[0, 3]$	10	0

To sum up, the time complexity of TFNN is equal to  $o(4 + T_0/\Delta t(5 + T_0/\Delta t(12n + 5) + 1) + 2n(7 + T_0/\Delta t(9n + m + 7))) = o(4 + 14n + (18n^2 + 2mn + 14n)T_0/\Delta t + (12n + 5)T_0/\Delta t^2)$ . Because there are at least two nodes (viz.  $n \geq 2$ ) and one arc (viz.  $m \geq 1$ ) in a network, we have.  $o(4 + 14n + (18n^2 + 2mn + 14n)T_0/\Delta t + (12n + 5)T_0/\Delta t^2) \leq o((18n^2 + 40n + 2mn + 9)(T_0/\Delta t^2)) \leq o((43mn^2)(T_0/\Delta t^2))$ .

According to  $\Delta t \geq 1$ , the time complexity of TFNN can be simplified as follows:  $o((43mn^2)(T_0/\Delta t^2)) < = o(kmn^2T_0^2)$ , here  $k$  denotes a constant.

Theorem 1 is proven.  $\square$

## 4. Experiments

A large transportation network (viz. New York Road) is used to test the performance of the proposed TFNN algorithm. Time-varying and wastage components are added to some arcs in the network. The Ford–Fulkerson (FF) [26], genetic algorithm (GA) [22], Edmonds–Karp (EK) [10], and the Cai–Sha (CS) algorithm [11] will be used for experimental comparison with the proposed TFNN. There are 100 generations and 50 populations preset in the genetic algorithm [27].

The error rate and computational time of these algorithms are compared as follows: the percentage deviation of the mean value (PDM) and the percentage deviation of the best value (PDB) are used as performance indexes (PI) to illustrate the error rate (ER) of different algorithms. PDM and PDB, respectively, are the mean and best value of ER for a set of networks. ER can be calculated as  $ER = (F_m - F_a)/F_m * 100\%$ , where  $F_m$  is the maximum flow among these algorithms and  $F_a$  is the flow value of each algorithm. We used 1000-node, 3000-node, and 5000-node networks for experiments and analyzed the error rate and computational time of the results. Table 3 reports the experimental results of TFNN, FF, GA, EK, and CS algorithms. Compared with other algorithms, the proposed TFNN

TABLE 3: Comparative results of the TFNN and other algorithms.

Dataset	Nodes	Arcs	PI	FF	GA	EK	CS	TFNN
Data1	1000	2067	PDM (%)	9.911	7.159	8.491	5.067	0.00
			PDB (%)	7.261	5.590	7.013	3.960	0.00
			Time (ms)	49.13	1776	52.03	57.41	60.25
Data2	3000	6106	PDM (%)	16.40	13.26	17.52	10.05	0.00
			PDB (%)	13.51	10.94	13.19	8.108	0.00
			Time (ms)	304.85	3574	317.49	436.53	240.93
Data3	5000	10095	PDM (%)	27.45	25.88	31.61	17.48	0.00
			PDB (%)	23.08	23.57	28.19	15.38	0.00
			Time (ms)	955.64	6346	915.96	1213.96	582.21

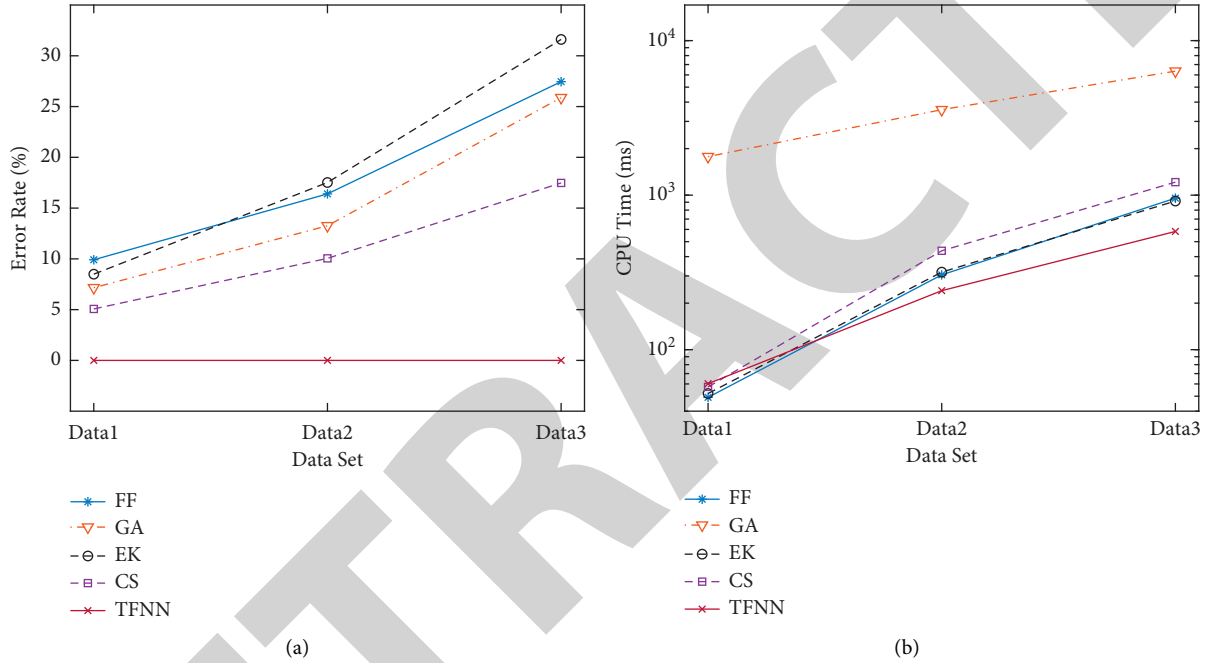


FIGURE 4: Experimental results of FF, GA, EK, CS, and TFNN with different datasets. (a) PDM. (b) Computational time.

always can find the best solutions in all cases. The error rate of other algorithms increases with the increase of nodes number. The PDM of other algorithms on Data3 all exceed 17.48% and the PDM of FF and EK are 27.45% and 31.61%, while TFNN is 0.00%. This is because both of FF and EK fail to take into time-varying components. GA adopts a random search mechanism. CS algorithm always finds the shortest path first, it reduces the solution accuracy. These results show that the proposed TFNN has better performance than existing algorithms (including FF, GA, EK, and CS). The tendency of the error rate of FF, GA, EK, CS, and the proposed TFNN algorithms are shown in Figure 4(a).

The calculation times of TFNN, FF, GA, EK, and CS algorithms are shown in Table 3. The computational time of the proposed TFNN is relatively short than other algorithms. First, GA requires more time to find a solution due to its pure random search mechanism. Second, as the number of nodes increases, the calculation time of TFNN is gradually better than the other three algorithms. The reason is that the complexity of the CS algorithm largely depends on the

number of nodes, while the FF and EK algorithm will take more time to iterate as the number of nodes increases. The tendency of computational time of FF, GA, EK, CS, and the proposed TFNN algorithms are described in Figure 4(b).

## 5. Conclusions

In this research, we introduce the time-varying wastage maximum flow problem and propose the Time-flow Neural Network to solve the TWMFPs. The proposed TFNN does not require any training by means of a time-flow mechanism. Experimental results show that the proposed TFNN has better performance than traditional algorithms (including FF, EK, and CS) and intelligent algorithm (such as GA). The main advantages of TFNN are shown as follows.

First, compared with existing maximum flow algorithms, TFNN has higher accuracy when solving the TWMFPs. The proposed TFNN can obtain a larger flow due to its group calculation idea. The experiment results show that the error rate of TFNN is lower (17.48% lower than CS and 31.61%

lower than EK) on a large network (5000 nodes and 10095 arcs).

Second, TFNN has a higher calculation speed based on its parallel computing feature. The experiment results show that the computational time of TFNN is 52% shorter than CS on a large network (5000 nodes and 10095 arcs).

In future research, more constraints can be considered when solving the time-varying wastage maximum flow problems. And, the neural network framework should be improved for the maximum flow problems under uncertain environments.

## Data Availability

The simulation experiment data used to support the findings of this study are available from the corresponding author upon request.

## Conflicts of Interest

The authors declare that they have no conflicts of interest.

## Acknowledgments

This work was supported in part by the National Science Foundation of China (Grant no. 61673295).

## References

- [1] S. Zhao, X. Sun, J. Chen, Z. Duan, Y. Z. Yanping, and Y. Z. Yiwen, "Relational granulation method based on Quotient Space Theory for maximum flow problem," *Information Sciences*, vol. 507, pp. 472–484, 2020.
- [2] D. P. Khanal, U. Pyakurel, and T. N. Dhamala, "Maximum multicommodity flow with intermediate storage," *Mathematical Problems in Engineering*, vol. 2021, Article ID 5063207, 11 pages, 2021.
- [3] K. F. Goodchild and A. Goodchild, "The isolated community evacuation problem with mixed integer programming," *Transportation Research Part E: Logistics and Transportation Review*, vol. 161, Article ID 102710, 2022.
- [4] L. Fan, H. Su, W. Wang et al., "A systematic method for the optimization of gas supply reliability in natural gas pipeline network based on Bayesian networks and deep reinforcement learning," *Reliability Engineering & System Safety*, vol. 225, Article ID 108613, 2022.
- [5] L. Jiang, J. Liu, D. Zhou, Q. Zhou, X. Yang, and G. Yu, "Predicting the evolution of hot topics: a solution based on the online opinion dynamics model in social network," *IEEE Transactions on Systems Man Cybernetics Systems*, vol. 50, no. 10, pp. 3828–3840, 2010.
- [6] P. Yuan, L. Jiang, J. Liu, D. Zhou, P. Li, and Y. Gao, "Dual-level attention based on heterogeneous graph convolution network for aspect-based sentiment classification," *Wireless Communications and Mobile Computing*, vol. 2021, Article ID 6625899, 13 pages, 2021.
- [7] G. Borradaile, P. N. Klein, S. Mozes, Y. Nussbaum, and C. Wulff-Nilsen, "Multiple-source multiple-sink maximum flow in directed planar graphs in near-linear time," *SIAM Journal on Computing*, vol. 46, no. 4, pp. 1280–1303, 2017.
- [8] A. Aalipour, H. Kebriaei, and M. Ramezani, "Analytical optimal solution of perimeter traffic flow control based on mfd dynamics: a pontryagin's maximum principle approach," *IEEE Transactions on Intelligent Transportation Systems*, vol. 20, no. 9, pp. 3224–3234, 2019.
- [9] H. S. Hosseini and S. A. Hosseini, "Maximum flow problem on dynamic generative network flows with time-varying bounds," *Applied Mathematical Modelling*, vol. 34, no. 8, pp. 2136–2147, 2010.
- [10] J. Marquez, I. Gutierrez, and E. Sanchez, "Approach of multicasting routing with solution for network coding applying edmonds-karp," in *Proceedings of the 2018 IEEE international Conference on Automation/XXIII Congress of the Chilean Association of Automatic Control (ICA-ACCA)*, pp. 1–8, Concepcion, Chile, October 2018.
- [11] X. Cai, D. Sha, and C. Wong, "Time-varying universal maximum flow problems," *Mathematical and Computer Modelling*, vol. 33, no. 4–5, pp. 407–430, 2001.
- [12] D. Bauer, G. Richter, J. Asamer, B. Heilmann, G. Lenz, and R. Kolbl, "Quasi-Dynamic estimation of OD flows from traffic counts without prior OD matrix," *IEEE Transactions on Intelligent Transportation Systems*, vol. 19, no. 6, pp. 2025–2034, 2018.
- [13] J. D. Weir, "Average longest path and maximum cost network flows with multiple-criteria weights," *Electronic Notes in Discrete Mathematics*, vol. 69, pp. 181–188, 2018.
- [14] N. Ahmed, S. Das, and S. Purusotham, "The problem of maximum flow with minimum attainable cost in a network," *Opsearch*, vol. 50, no. 2, pp. 197–214, 2012.
- [15] T. H. Szymanski, "Max-flow min-cost routing in a future-internet with improved QoS guarantees," *IEEE Transactions on Communications*, vol. 61, no. 4, pp. 1485–1497, 2013.
- [16] G. Park and M. Song, "Prediction-based resource allocation using LSTM and minimum cost and maximum flow algorithm," in *Proceedings of the International Conference on Process Mining (ICPM)*, pp. 1–9, Aachen, Germany, June 2019.
- [17] M. Eboli, "A flow network analysis of direct balance-sheet contagion in financial networks," *Journal of Economic Dynamics and Control*, vol. 103, pp. 205–233, 2019.
- [18] I. O. Tartibu, L. K. Okwu, and M. O. Okwu, "Prediction and modeling of traffic flow of human-driven vehicles at a signalized road intersection using artificial neural network model: a South African road transportation system scenario," *Transport Engineer*, vol. 6, Article ID 100095, 2021.
- [19] C. Peng and J. Peng, "Models and algorithm of maximum flow problem in uncertain network," in *Proceedings of the International Conference on Artificial Intelligence & Computational Intelligence (AICI)*, pp. 101–109, Taiyuan, China, September 2011.
- [20] H. H. Gharehbolagh, A. Hafezalkotob, A. Makui, and S. Raissi, "Cooperative strategies for maximum-flow problem in uncertain decentralized systems using reliability analysis," *Security and Communication Networks*, vol. 2016, Article ID 2349712, 9 pages, 2016.
- [21] H. Li, T. Zhang, Y. Zhang, K. Wang, and J. Li, "A maximum flow algorithm based on storage time aggregated graph for delay-tolerant networks," *Ad Hoc Networks*, vol. 59, no. 1, pp. 63–70, 2017.
- [22] M. Buzdalov and A. Shalyto, "Hard test generation for augmenting path maximum flow algorithms using genetic algorithms: Revisited," in *Proceedings of the 2015 IEEE Congress on Evolutionary Computation (CEC)*, pp. 2121–2128, Sendai, Japan, May 2015.
- [23] F. J. Cai and M. C. Cai, "Shortest path and maximum flow problems in networks with additive losses and gains," *Theoretical Computer Science*, vol. 412, no. 4–5, pp. 391–401, 2011.



## Retraction

# Retracted: Research on Optimal Route Planning for Self-Driving Tour Based on Road Network Structure

### Security and Communication Networks

Received 8 August 2023; Accepted 8 August 2023; Published 9 August 2023

Copyright © 2023 Security and Communication Networks. This is an open access article distributed under the Creative Commons Attribution License, which permits unrestricted use, distribution, and reproduction in any medium, provided the original work is properly cited.

This article has been retracted by Hindawi following an investigation undertaken by the publisher [1]. This investigation has uncovered evidence of one or more of the following indicators of systematic manipulation of the publication process:

- (1) Discrepancies in scope
- (2) Discrepancies in the description of the research reported
- (3) Discrepancies between the availability of data and the research described
- (4) Inappropriate citations
- (5) Incoherent, meaningless and/or irrelevant content included in the article
- (6) Peer-review manipulation

The presence of these indicators undermines our confidence in the integrity of the article's content and we cannot, therefore, vouch for its reliability. Please note that this notice is intended solely to alert readers that the content of this article is unreliable. We have not investigated whether authors were aware of or involved in the systematic manipulation of the publication process.

Wiley and Hindawi regrets that the usual quality checks did not identify these issues before publication and have since put additional measures in place to safeguard research integrity.

We wish to credit our own Research Integrity and Research Publishing teams and anonymous and named external researchers and research integrity experts for contributing to this investigation.


The corresponding author, as the representative of all authors, has been given the opportunity to register their agreement or disagreement to this retraction. We have kept a record of any response received.

### References

- [1] P. Zong, Y. Han, and C. Xu, "Research on Optimal Route Planning for Self-Driving Tour Based on Road Network Structure," *Security and Communication Networks*, vol. 2022, Article ID 6588288, 11 pages, 2022.

## Research Article

# Research on Optimal Route Planning for Self-Driving Tour Based on Road Network Structure

Ping Zong,<sup>1</sup> Yao Han,<sup>1</sup> and Chenbo Xu<sup>2</sup> 

<sup>1</sup>Hilton School of Hospitality Management Sichuan Tourism University, Chengdu 610100, China

<sup>2</sup>Sichuan Normal University, Chengdu 610000, China

Correspondence should be addressed to Chenbo Xu; 20210083@sicnu.edu.cn

Received 5 July 2022; Revised 8 August 2022; Accepted 18 August 2022; Published 29 September 2022

Academic Editor: Hangjun Che

Copyright © 2022 Ping Zong et al. This is an open access article distributed under the Creative Commons Attribution License, which permits unrestricted use, distribution, and reproduction in any medium, provided the original work is properly cited.

Today's social and economic development continues to improve people's quality of life, and private cars are widely popularized, and self-driving tours have developed. The rapid development of self-driving travel has played an important role in the development of the national economy, and self-driving travel has become popular. Because the development of self-driving tours has caused some problems, the road network structure has become more and more complex, and the roads have become very congested. Especially during the holidays, there are more private cars in tourist attractions and the roads are more congested. How to use the information of roads and attractions and then choose the optimal travel route becomes particularly important. In response to this problem, we first analyze the topology of the road network, then analyze the accessibility of scenic spots and related factors that affect self-driving travel, and use the A\* algorithm, Dijkstra algorithm, and other calculation methods to calculate the optimal path. The experiment found that there are many influencing factors of self-driving travel, and the road network structure has the greatest influence on it. The A\* algorithm has obvious advantages over the Dijkstra algorithm.

## 1. Introduction

With the continuous development of the global economy, people's demand for tourism is increasing [1], and the tourism destination focuses on the scenic spots in surrounding cities, expanding to neighboring provinces, cities, countries, and even the world. However, there is no more complete and systematic tourism route planning scheme. Therefore, this study hopes to give relevant recommendations according to the needs of tourists and plan the optimal route according to the departure and destination given by tourists [2].

Up to now, a large number of scholars have studied the related issues of tourism routes. Some scholars use the correlation function of travel time and travel cost to represent the tourist utility, because they find that the degree of crowding has an important impact on the tourist experience [3]; some scholars use A\* algorithm [4], Dijkstra algorithm and other calculation methods [5], Floyd algorithm [6], "breadcrumb" fitting [7], and other research methods to plan travel routes [8].

## 2. Materials and Methods

We first analyze the road network structure and then calculate whether it is reachable or not. Combined with the relevant factors that affect the self-driving tour, a variety of algorithms are used to find the shortest path.

**2.1. Results and Discussion.** The experiment found that there are many influencing factors of self-driving travel. The road network structure has the greatest influence on it. The A\* algorithm has obvious advantages over Dijkstra's algorithm.

**2.2. Topological Structure Quantitative Index.** This study aims to help the self-driving tourists to find a suitable travel route and to avoid spending a lot of time on the road. It also aims to effectively reduce traffic problems and reduce traffic congestion caused by holidays. Every holiday, the travel experience of tourists is often affected by traffic congestion, and it is not convenient for local residents to travel.

There are several common road network structures. A-side format: there are vertical or horizontal near-parallel roads at regular intervals. B circular radial: it consists of several circular roads connected to each other. C freestyle: the terrain is complex and has no fixed geometry. D mixed type: it is a combination of the above forms.

There are two methods for road network topology: path structure analysis and space syntax. Considering various spatial factors, this research mainly analyzes road network topology from the perspective of space syntax. In order to be applicable to various road networks, this study selects two indicators: comprehensibility and integration.

Comprehensibility: it refers to the coordination degree of the local and the whole of the road network [9].

Integration degree: the degree of scattered or dense distribution between road sections is an indicator of whether the road is congested or not. The greater the degree of integration, the more concentrated the roads, which means the more the center can be deviated and the more traffic can be attracted. The integration degree can be divided into global and local integration degrees: the global integration degree represents all road relationships of a complete road segment, and the local integration degree represents the road segment relationship of a partial area of a complete road segment, which are calculated as follows:

$$\begin{aligned} RA(x) &= \frac{DM(x) - 1}{n/2 - 1}, \\ AR &= \frac{n|\log_2(n/3) - 1| + 1}{(n-1)(n-2)/2}, \\ \text{Intergration}(x) &= \frac{AR}{RA(x)}. \end{aligned} \quad (1)$$

In the formula,  $n$  is the number of axes;  $DM$  is the average depth;  $RA$  is the relative asymmetry;  $AR$  is the relative asymmetry value of the diamond-shaped topology; Intergration is the degree of integration.

Modern transportation is becoming more and more developed, and the road network structure is very complex. People who travel to other places are not familiar with the road network structure, and it is easy to make mistakes. Some tourists drive to Chongqing to travel, but they are not familiar with the road. They choose to follow the navigation and cannot find the place they want to go. In order to effectively avoid such situations, we analyze the road network structure and then avoid areas with complex road network structures, so that self-driving tourists can find suitable roads and scenic roads.

**2.3. Accessibility Calculation.** The different scenic spots to be visited by the self-driving tourist will have corresponding impacts on different groups of people and different vehicles. For example, if the road you are going to is uneven, there is deep water, and there are many mountain roads, it will be difficult for ordinary vehicles to travel, and off-road vehicles

are required to pass normally. People who do not have an off-road vehicle will have a lot of problems driving to it, and even the car will break down halfway down the road. Computational reachability is designed to avoid such problems.

By calculating the distance traveled on the GIS grid to deduce the accessibility [10] and fully considering various factors such as mountains and waters that hinder the movement, the accessibility to a certain location in the region can be better simulated. The weighted distance from one place on the GIS grid to another on the grid is calculated. This algorithm is a cumulative cost distance algorithm. The calculation formula is as follows:

$$Ki = \begin{cases} \frac{1}{2} \sum_{i=1}^n (Ci + Ci + 1), \\ \frac{\sqrt{2}}{2} \sum_{i=1}^n (Ci + Ci + 1). \end{cases} \quad (2)$$

In the formula, the time cost of the  $i$ -th pixel is  $Ci$ ; the time cost of the  $i+1$ -th element along the movement direction is denoted by  $Ci+1$ ;  $n$  represents the total number of pixels; the scenic spot accessibility of the  $i$ -th grid is denoted by  $Ki$ . The above formula is used to calculate the time cost in the horizontal or vertical direction of the grid surface, and the following formula is used to calculate the time cost in the diagonal direction of the grid surface.

**2.4. Relevant Factors Affecting the Destination of Self-Driving Tours.** The cost factors affecting the self-driving tour are as follows: ① gasoline cost: for ordinary private cars, highways are more than 1 yuan/km, and ordinary kilometers are 0.6 yuan/km (excluding ordinary toll roads). ② accommodation fee: the level is suitable for each person, and the standard room is 100–150 yuan per day. ③ meal fee: the amount varies from one person to another, generally speaking, about 60 yuan per person. ④ tickets: the price varies, so it is not easy to calculate; in many places, the elderly are free or half price, but tickets are still required for sightseeing cars and ropeways.

**2.4.1. Tourist Factor.** The scoring indicators of each scenic spot are mainly the data on major tourism websites and the data of travel notes learned by tourists [11]. The formula is as follows:

$$ti = \sum_{j=1}^s \frac{ni \cdot xij}{ni}. \quad (3)$$

where the evaluation of the  $j$ -th tourist of the tourist attraction  $i$  is represented by  $xij$ , the number of useful comments of the  $j$ -th tourist of the  $i$ -th tourist attraction is represented by  $ni$ , the sum of the useful numbers of the  $i$ -th tourist attraction is represented by  $ni$ , and the weighted score of the tourists of the  $i$ -th tourist attraction is expressed by  $ti$ .

**2.4.2. Environmental Factor.** It is the score data of tourists on the scenic spot environment, which is divided into very poor, poor, average, good, and very good. It is set to 1, 2, 3, 4, and 5 points [12]. The formula is as follows:

$$y_i = \frac{1}{4} \sum_{j=1}^4 X_j, \quad i = 1, 2, \dots, n, \quad (4)$$

where the three factors of scenic spot environment, traffic, and infrastructure are denoted by  $X_j$ , the comprehensive score of the  $i$  scenic spot environment is denoted by  $y_i$ , and  $n$  is the number of  $n$  scenic spots.

**2.4.3. Road Factor.** Relevant studies have shown that tourists prefer to travel to areas where the spatial distribution of attractions is more concentrated, which is convenient for travel. The accessibility of measuring the spatial distance is expressed by the spatial distance formula, and the formula [13] is as follows:

$$A_i = \sum_{j=1}^n l_{ij}. \quad (5)$$

Among them, the minimum distance between two scenic spots ( $i, j$ ) is represented by  $l_{ij}$ , and the sum of the distances from the  $i$  scenic spot to the rest of the scenic spots is represented by  $A_i$ , and the number of scenic spots is  $n$ .

**2.5. Reverse Order Recursion Model.** The travel process is divided into six stages, each stage is represented by  $k$ , and  $S$  is used to represent the  $k$ -stage bit; that is,  $s$  is a dynamic variable [14], and the  $k$ -stage route is selected as  $Xk$ . The state transition equation is as follows:

$$Sk + 1 = Sk - Xk. \quad (6)$$

$f_x$  indicates  $Sk$  the cost of the  $k$ -stage to the end point, and  $vk$  represents the  $k$ -stage distance. The recursion formula is as follows:

$$f_x = \min\{vk + fk + 1\}, \quad k = 6, 5, 4, 3, 2, 1, \quad (7)$$

where  $x_k^*$  represents the optimal decision; when the boundary condition  $k=7$ ,  $f_7=0$ . The reverse order recursion equation is as follows:

$$f_k(S_k) = \min\{d(S_k, u_k) + f_{k+1}(S_{k+1})\}, \quad (8)$$

$$k = 6, 5, 4, 3, 2, 1; f_7(S_7) = 0.$$

Matlab is used to find the shortest path from the first to the sixth stage, and the following is obtained:

$$f_1(A) = \min\{d(A, C) + f_2(C), d(A, D) + f_2(D)\}. \quad (9)$$

**2.6. Dijkstra Algorithm to Solve the Optimal Path.** Dijkstra's algorithm is an efficient algorithm for solving the shortest path [15], and this study expresses its algorithm in the form of a flow chart. Dijkstra's algorithm will create two node sets during the search process, open, and closed sets.

The closed set represents the shortest node set to the target point, and the open represents other nodes. The starting value of the source node is 0, and the weight of other nodes is  $\infty$ . When the target point reaches the closed set, the search is completed. The flow chart is shown in Figure 1.

**2.7. DV Algorithm to Find the Optimal Path.** DV algorithm, also known as Bellman-Fords routing algorithm [16], can also be used for shortest path solution. The Bellman-Ford equation is as follows:

$$dx(y) = \min_v \{c(x, v) + dv(y)\}. \quad (10)$$

In the above formula, the weight from node  $x$  to node  $v$  is denoted by  $c(x, v)$ , the weight of the shortest path from node  $x$  to node  $y$  is denoted by  $dx(y)$ , and the weight of the shortest path from node  $v$  to node  $y$  is denoted by  $dv(y)$ .

A, B, C, D, and E represent nodes, and  $c$  and  $d$  represent paths. Figure 2 is a schematic diagram of the Bellman-Ford algorithm.

The pseudocode of the Bellman-Ford algorithm is an intuitive embodiment of the algorithm, from which the optimal path can be directly obtained. The code calculates the optimal solution step by step [17]. The code is shown in Algorithm 1:

**2.8. DI\_END\_CITY\_DIS\_and\_NATURE Method.** The following formula is used to evaluate the relevant cities:

$$\text{city\_score} = \frac{(\sum_{i=1}^n X_i)}{n}. \quad (11)$$

In the above formula,  $X_i$  represents the popularity of the  $i$  scenic spot.

The following formula is used to find the shortest path:

$$\text{result} = \sqrt{D^2 + (1000H)^2}. \quad (12)$$

The following formula is used to derive the approximate number of kilometers traveled:

$$\text{KM} = 3 * \text{Days} * V. \quad (13)$$

Days means the number of days tourists travel, and  $V$  means the driving speed.

### 3. Shortest Path Optimization Algorithm

The above various algorithms are not calculated in combination with the topology structure of the road network, and the optimal path algorithm combined with the analysis of the topology structure of the road network will be used below.

**3.1. A\* Algorithm.** Dijkstra's algorithm calculates the length of the shortest path from the source point to all other points, and A\* focuses on the shortest path from point to point (including specific paths). The Dijkstra algorithm is based on a more abstract graph theory level, and the A\* algorithm can be more easily used in things such as game map pathfinding.

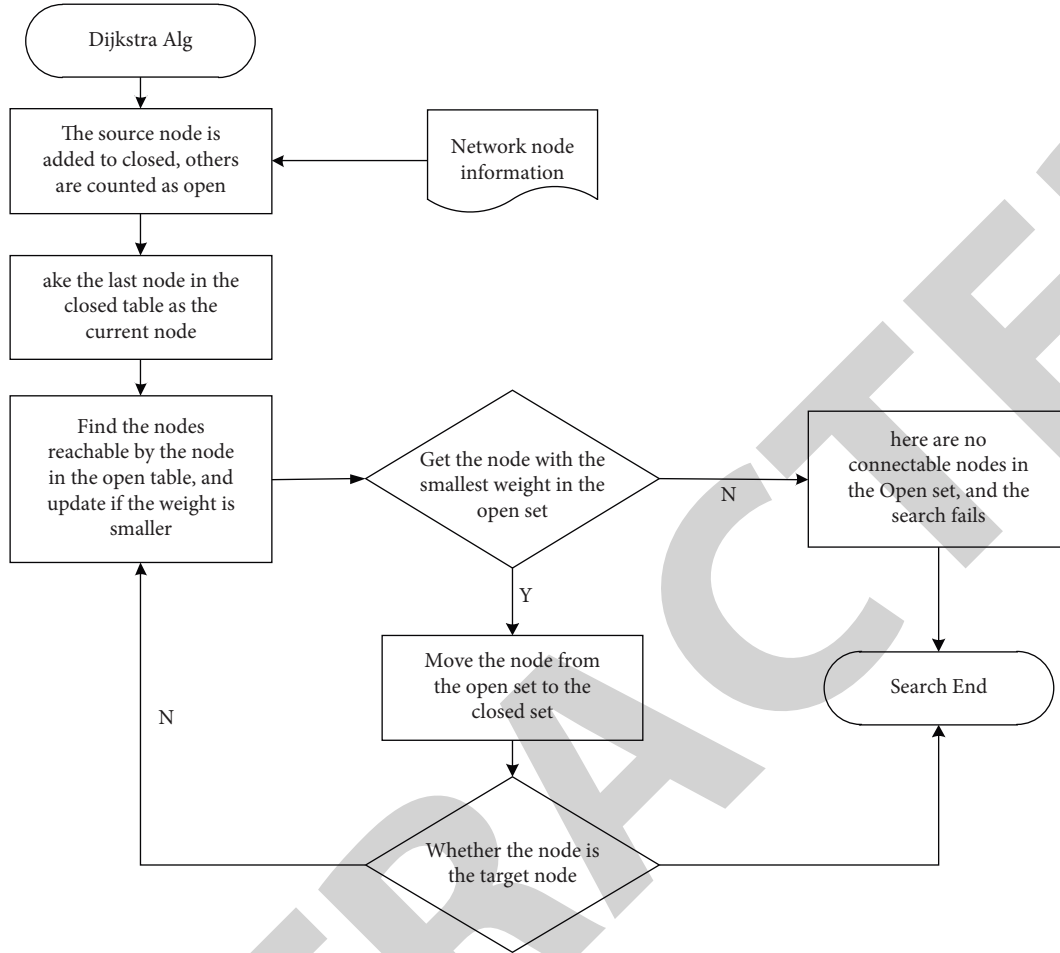


FIGURE 1: Flow chart of Dijkstra algorithm.

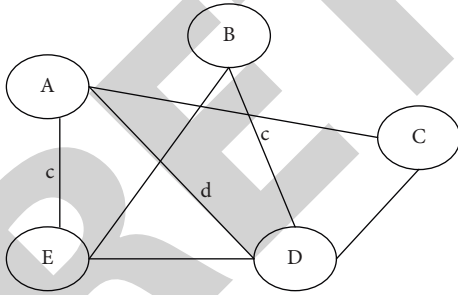


FIGURE 2: Schematic diagram of Bellman-Ford algorithm.

The essence of Dijkstra's algorithm is breadth-first search, which is a divergent search, so the space complexity and time complexity are relatively high. For the current point on the path, the A\* algorithm not only records the cost to the source point, but also calculates the expected cost from the current point to the target point. It is a heuristic algorithm and can also be considered as a depth-first algorithm.

Dijkstra's algorithm is the most traditional routing algorithm [18], and there is a problem that the retrieval is blind and does not consider the target point, but only the source point. This problem can cause the search space to be too large, which is not conducive to computation.

A\* algorithm is one of the optimal algorithms in static network, and A\* algorithm is an improved algorithm based on Dijkstra algorithm. The A\* algorithm introduces a weight function:

$$F(i) = G(i) + H(i). \quad (14)$$

The node depth is represented by  $b$ , and the performance evaluation index is represented by  $b * \text{branching factor}$ . The relationship can be represented by the following formula:

$$N + 1 = 1 + b * + (b *)^2 + \dots + (b *)^d. \quad (15)$$

There is a single node state, and the evaluation function  $h(x)$  satisfies the formula:

$$|h(x) - h * (x)| = 0(\log h * (x)). \quad (16)$$

The A\* algorithm is calculated as follows:

$$h = \frac{(n_i - n_r) \cos t_N}{\delta n_E}. \quad (17)$$

The A\* process is divided into 4 steps. Step 1: set the source node  $\{n_s, 0, 0, \text{null}\}$ , the node enters the closed set, and the adjacent node enters the open set. The initial value of  $w$  is the current node and the source node of  $n_s$  the link

```

Bellman-Ford Algorithm
Input  $k$ : information of network topology
Output: shortest path between nodes ( $x$  for start node,  $y$  for end node)
Initialization
(1) for all  $y$  in network
(2)    $dx(y) = c(x, y)$ /*if  $y$  is not a neighbor, then  $c(x, y) = \infty$ 
(3) for each neighbor  $w$ :
(4)    $dw(y) = \infty$  for  $dw(y) = \infty$ 
(5) for each neighbor  $w$ :
(6)   Send distance vector  $dx = [dx(y): y \text{ in } N]$  to  $w$ 
Loop:
(7) wait until a link cost change or receive a distance vector from neighbor
(8) for each  $y$  in network:
(9)    $dx(y) = \min_v \{c(x, y) + dv(y)\}$ 
(10) if  $dx(y)$  changed for any  $y$ :
(11)   Send distance vector  $dx = [dx(y): y \text{ in } N]$  to all neighbors
Forever

```

ALGORITHM 1: Pseudo code of Bellman-Ford algorithm

length. Step 2: find a node in the open set whose  $w + h$  value is the smallest, and the node enters the closed set from the open set. Step 3: if  $S_n = n_d$ , the target node has been found and the algorithm ends. Step 4: no: go back to Step 2 to perform another calculation, so that the target node appears in the closed set, the search is completed, and the shortest path is obtained [19]. The flow chart is shown in Figure 3.

If  $h(n)$  is always lower than the shortest distance value of  $n$  nodes to the target point,  $A^*$  can find the shortest path. Otherwise, the optimal path cannot be found.

This is proved by the backward method [20], taking the second-to-last node  $n$  as an example. Let the starting point be  $s$ , the target point be  $t$ , the next node selection of node  $n$  is  $j$ ,  $q$ , the next node of node  $j$ ,  $q$  is  $t$ , and the  $q$  node is in the optimal path. Among them, the optimal value of the link length of  $a$  and  $b$  from  $a$  to  $b$  is denoted by  $p_{ad}$ , and the evaluation value of  $a$  to  $b$  is denoted by  $hab$ . Node  $q$  is in the optimal path, so we have

$$g_{sn} + p_{nj} + p_{jt} > g_{sn} + p_{nq} + p_{qt}. \quad (18)$$

At  $n$  node selection,  $h_{qt} > h_{jt}$  results in

$$g_{sn} + p_{nj} + p_{jt} < g_{sn} + p_{nq} + p_{qt}. \quad (19)$$

The current node selects the next search node  $j$  and  $h_{qt} \leq p_{qt}$ :

$$g_{sn} + p_{nj} + p_{jt} + 0 > g_{sn} + p_{nq} + p_{qt} \geq g_{sn} + p_{nq} + h_{qt}. \quad (20)$$

Therefore, the  $q$  node will be found again. By analogy, it can be proved that the path that can be finally found must be the shortest path. After finding the shortest path, the distance can be calculated in three ways [21].

(i) Harmanton distance:

$$h(x) = abs(x_2 - x_1) + abs(y_2 - y_1). \quad (21)$$

(ii) Chebyshev distance:

$$h(x) = \max\{abs(x_2 - x_1), abs(y_2 - y_1)\}. \quad (22)$$

(iii) Euclidean distance:

$$h(x) = \sqrt{(x_2 - x_1)^2 + (y_2 - y_1)^2}. \quad (23)$$

(iv) Cosine distance:

$$\cos \theta = \frac{x_1 x_2 + y_1 y_2}{\sqrt{x_1^2 + x_2^2} \sqrt{y_1^2 + y_2^2}}. \quad (24)$$

#### 4. Analysis and Experiment of Road Network Topology

To find the shortest path, we must first analyze the road network structure. Table 1 takes the historical old city as an example and takes Prada [22], Gulou District, and the old city as samples to analyze the integration degree of the road network topology.

The analysis of these cities allows us to avoid cities with complicated road conditions and choose the optimal route when choosing a destination city for a self-driving tour. Prada, Gulou District, and the old city have different degrees of integration and understanding, but the difference is not big. When choosing a purpose, you can choose whatever you want.

It can be seen intuitively from Figure 4 that Prada, Gulou District, and the old city have different degrees of integration and understanding. The overall gap is not very big, and these cities can be used as destinations.

Table 2 shows the analysis of the peripheral area and the expansion area. Taking Jianye District, Glasgow, Bayswater, and the Outer Qinhua River as samples [23], these areas are integrated and analyzed.

The road network analysis of the expansion area of the peripheral area is also to avoid the scenic spots with complicated road conditions and to help self-driving tourists to

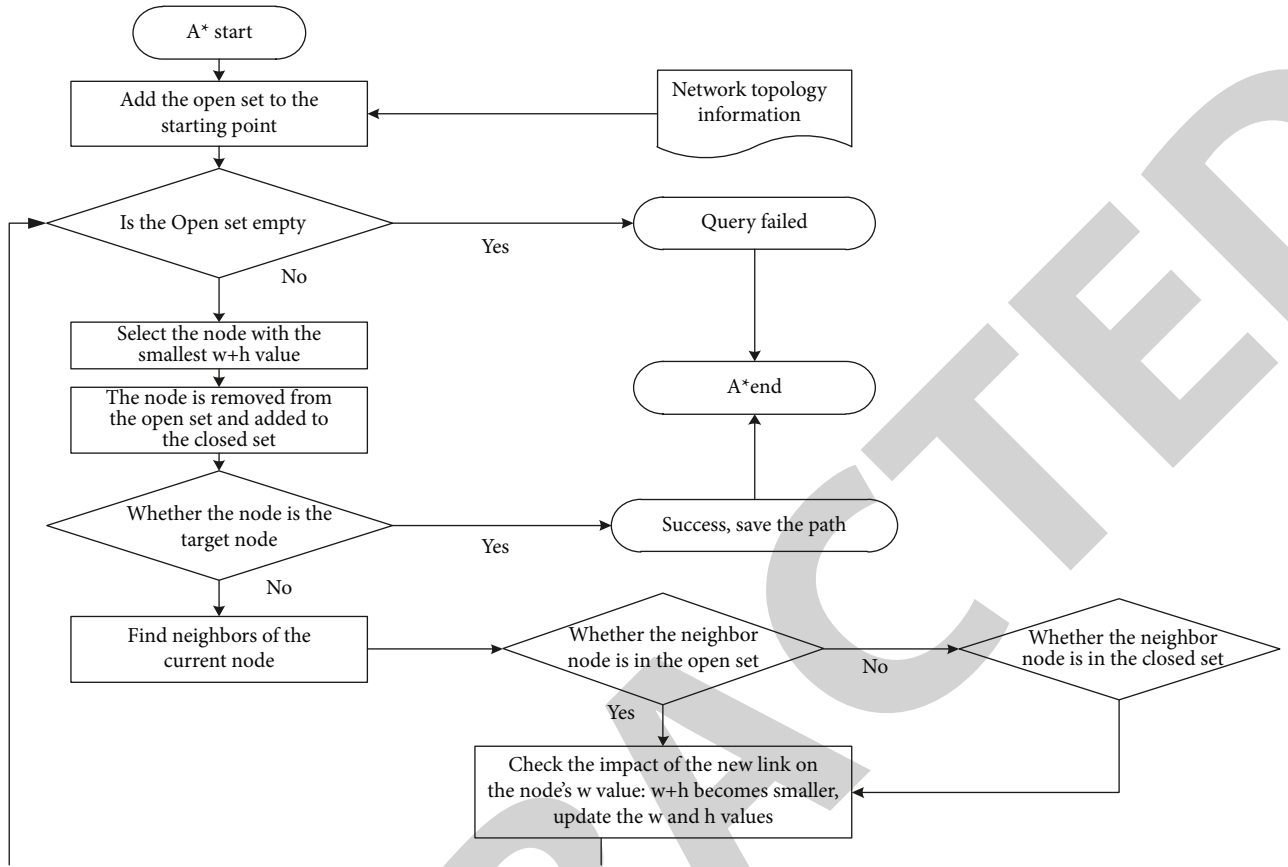


FIGURE 3: A\* algorithm flow chart.

TABLE 1: Analysis of the road network structure in the historic old city.

Road network area	Road network sample	Global integration	Local integration	Intelligibility
Historic old town	Prada (Athens)	1.34	1.37	0.81
	Gulou District (Kaifeng)	1.68	1.91	0.94
	Old town (Suzhou)	1.78	2.03	0.95

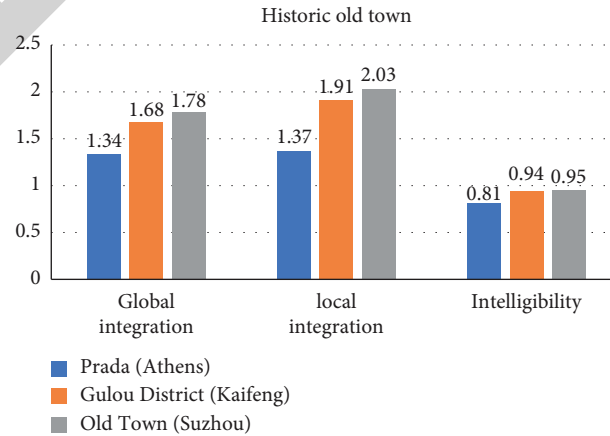


FIGURE 4: Analysis of the road network structure in the historic old city.

TABLE 2: Road network analysis of the expansion area and the peripheral area.

Road network area	Road network sample	Global integration	Local integration	Intelligibility
Expansion and outer zones	Jianye District (Nanjing)	2.51	2.55	0.99
	Glasgow (Scotland)	2.28	2.04	0.96
	Bayswater (London)	1.299	1.64	0.87
	Outer Qinhuai River (Nanjing)	0.73	1.29	0.64

choose. From the above table, it can be seen that the integration degree of Jianye District, Glasgow, Bayswater, and Outer Qinhuai River is quite different. Careful analysis is required when choosing a travel destination.

Figure 5 is an intuitive representation of the road network analysis of the expansion area of the peripheral area. The integration degree of Jianye District and Glasgow is much more understandable than that of Bayswater and the Outer Qinhuai River. Tourists choose the destination is best to choose the first two cities. The latter two are prone to traffic jams.

Table 3 is a comparison table of the historical old city and the expansion area and the outer area.

The comparison shows that the peripheral area and the expansion area are generally more integrated than the old city, which shows that the old city often has complex road conditions, while the peripheral area and the expansion area are relatively better and more suitable for self-driving tourists.

It can be seen intuitively from the statistical chart in Figure 6 that Jianye District has the greatest degree of integration and intelligibility, and the integration degree of several cities in the expansion area and peripheral area is higher than that of several cities in the historic old city. If the degree is larger, there will be intuitive reference data for the selection of tourist destinations for tourists.

**4.1. Comparing the Performance of Different Algorithms.** The following table is a comparison of the running time of different algorithms.

As can be seen from Table 4, with the increase of traffic volume, the running time of A\* algorithm is shorter than that of Dijkstra algorithm and Bellman-Ford algorithm [24], which indicates that the more traffic volume, the better performance of A\* algorithm. The Dijkstra algorithm and the Bellman-Ford algorithm take more time as the traffic increases.

From the broken line above in Figure 7, it can be intuitively shown that the running time of the A\* algorithm has no obvious upward trend with the increase of the business volume, while the Dijkstra algorithm and the Bellman-Ford algorithm have an obvious upward trend. The shorter the search time, the better the search efficiency. The efficiency of the A\* algorithm is better than that of the Dijkstra algorithm and the Bellman-Ford algorithm.

The following table is a comparison of the search space of different algorithms.

It can be seen from Table 5 that the search space of Dijkstra algorithm is generally larger than that of Bellman-Ford algorithm, and the search space of Bellman-Ford

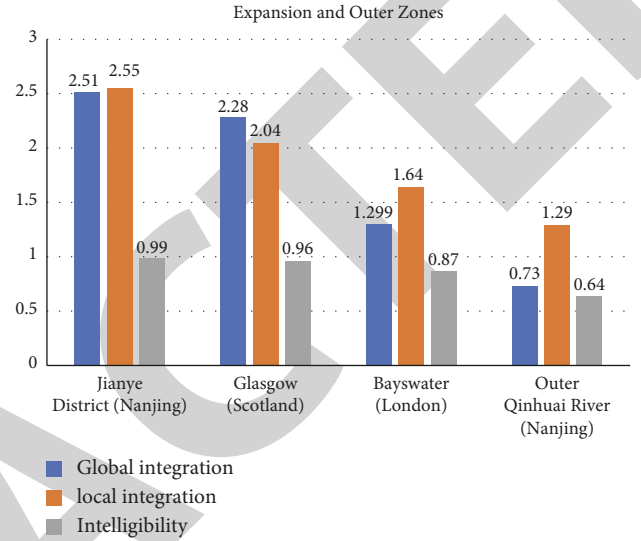


FIGURE 5: Road network analysis of the expansion area and the peripheral area.

algorithm is much larger than that of A\* algorithm. The search space of Dijkstra algorithm and Bellman-Ford algorithm is too large, which will lead to inaccurate finding of the optimal path. The search space of A\* algorithm is small, so the shortest path is more accurate.

Figure 8 more intuitively shows the search space size of Dijkstra algorithm, Bellman-Ford algorithm, and A\* algorithm. It can be seen at a glance that A\* algorithm is better than Dijkstra algorithm and Bellman-Ford algorithm. Because the search space of the A\* algorithm is small, the search results are accurate, while other search spaces are too broad, and the results are not accurate enough.

**4.2. Finding the Shortest Path.** Because the A\* algorithm is better than the Dijkstra algorithm and the Bellman-Ford algorithm, the A\* algorithm is used to find the shortest path between the starting point A and the target point B [25]. The statistics are shown in Table 6.

The weight is the analysis of the road network structure, and the distance is the intuitive expression of finding the shortest path. The weight of path 6 is larger and the distance is the smallest. The other paths are either too small in weight or too far away, which are obviously not suitable for self-driving travel.

From Figure 9, it can be concluded that path 6 is the optimal path, which occupies a high weight and has the shortest distance. Other paths have different problems: either the path is long or the weight is small.



TABLE 3: Comparison table.

Road network area	Road network sample	Global integration	Local integration	Intelligibility
Historic old town	Prada (Athens)	1.34	1.37	0.81
	Gulou District (Kaifeng)	1.68	1.91	0.94
	Old Town (Suzhou)	1.78	2.03	0.95
Expansion and outer zones	Jianye District (Nanjing)	2.51	2.55	0.99
	Glasgow (Scotland)	2.28	2.04	0.96
	Bayswater (London)	1.29	1.64	0.87
	Outer Qinhuai River (Nanjing)	0.73	1.29	0.64

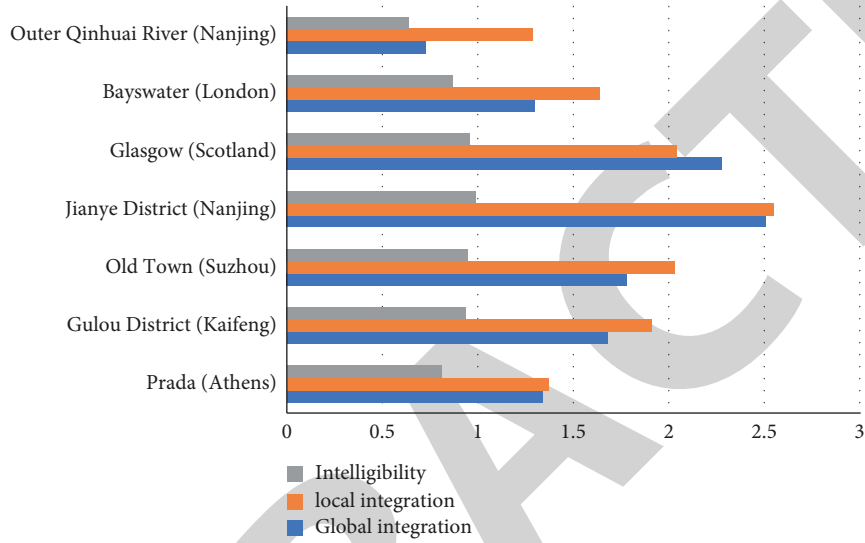


FIGURE 6: Comparison chart.

TABLE 4: Running time of different algorithms.

	Dijkstra's algorithm	Bellman-Ford algorithm	A* algorithm
Business volume	Running time (ms)	Running time (ms)	Running time (ms)
100	129	82	1741
300	342	265	1803
600	545	408	1769
900	1032	603	1796
1200	1360	1206	1864
1500	1707	1532	1872
1800	2013	1857	1900
2100	2365	2043	1934
2400	2681	2465	1989
2700	2964	2689	2041
3000	3335	3013	2103

Comparison data graph

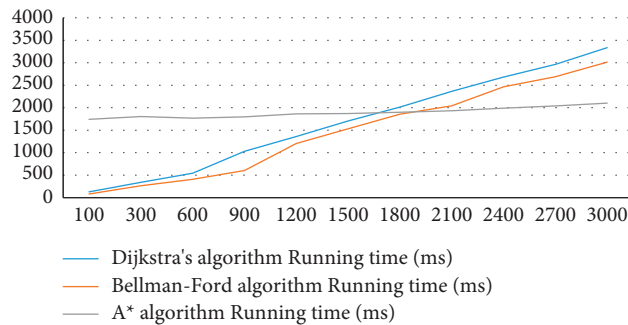


FIGURE 7: Running time of different algorithms.

TABLE 5: Search spaces of different algorithms.

	Dijkstra's algorithm	Bellman-Ford algorithm	A* algorithm
Business volume	Search space	Search space	Search space
100	13.84	11.21	5.43
300	12.75	10.32	5.68
600	13.21	11.32	6.96
900	13.95	10.35	4.83
1200	12.62	11.33	5.32
1500	13.78	11.47	5.23
1800	13.85	11.43	4.84
2100	12.96	11.68	6.32
2400	13.54	10.96	5.67
2700	13.47	11.54	6.23
3000	13.78	11.67	5.93

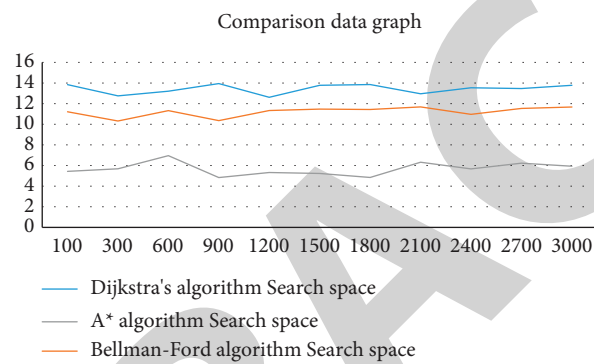


FIGURE 8: Search space comparison of different algorithms.

TABLE 6: Distance and weight of different paths.

	Attraction weight	Journey
Path one	4	6.5
Path two	3	5.5
Path three	4	4.3
Path four	3	5.7
Path five	6	6.2
Path six	6	4.1

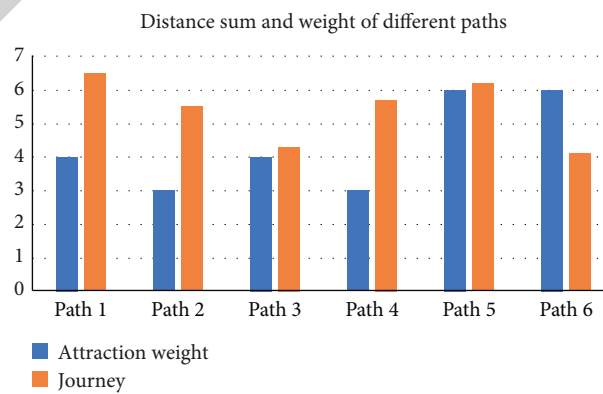


FIGURE 9: Distance and weight of different paths.

## 5. Conclusion

Recalling the preface, this study selects two indicators, comprehensibility and integration, to analyze the structure of the road network, then analyzes the accessibility to the destination, and calculates the relevant factors that affect self-driving travel. For the calculation of the optimal path, methods such as A\* algorithm, Dijkstra algorithm, Bellman-Ford algorithm, and reverse order recursion model are introduced. The A\* algorithm is an optimization of Dijkstra algorithm, Bellman-Ford algorithm, and other methods. The degree of integration and intelligibility of some road network topology structures are obtained through experiments. In the comparative experiments, the A\* algorithm shows obvious advantages in calculating the shortest path. Finally, the A\* method is used to find the shortest path from the starting point A to the target point B. It is hoped that research can become more rational and make people's travel life more convenient. With the in-depth research to develop good software, visitors only need to enter their destination, origin, vehicle model, budget, and travel time. You can quickly plan the best travel itinerary. If the information entered by the passenger is unreasonable, or the passenger's destination conflicts with various problems in the route, the software will remind the passenger to change the destination and will also give the passenger relevant recommendations.

## Data Availability

The experimental data used to support the findings of this study are available from the corresponding author upon request.

## Conflicts of Interest

The authors declared that they have no conflicts of interest regarding this work.

## Acknowledgments

This study was supported by the grant from The Sichuan-Tibet Synergism and Innovation Center of Tourism Industry Competitiveness (no. 21CZZX06) and fund project: Soft Science Research Project of Science and Technology Department in Sichuan Province "Study on the Income Effect of Tourism Poverty Alleviation and Prevention Mechanism of "Returning To Poverty" in Tibetan Areas of Sichuan" (Item no. 2021JDR0178).

## References

- [1] C. Liu, R. Yu, and J. Zeng, "Complexity of spatial structure on the urban-rural road network in Wuhan Metropolitan Area," *Scientia Geographica Sinica*, vol. 32, no. 4, pp. 426–433, 2012.
- [2] M. Wei, Y. Huang, D. Wan, and L. K. Deng, "Emergency road network structure and planning optimization in mountainous regions in Southwest China under earthquake scenarios," *Journal of Mountain Science*, vol. 19, no. 3, pp. 771–780, 2022.
- [3] Kocur-Bera and Katarzyna, "Scale-free network theory in studying the structure of the road network in Poland," *Promet-traffic & transportation: Scientific journal on traffic and transportation research*, vol. 26, no. 3, pp. 235–242, 2014.
- [4] C. Araujo, E. Kowler, and M. Pavel, "Eye movements during visual search: the costs of choosing the optimal path," *Vision Research*, vol. 41, no. 25–26, pp. 3613–3625, 2001.
- [5] M. Sharifzadeh, M. Kolahdouzan, and C. Shahabi, "The optimal sequenced route query," *The VLDB Journal*, vol. 17, no. 4, pp. 765–787, 2008.
- [6] I. B. Schwartz, E. Forgoston, S. Bianco, and L. B. Shaw, "Converging towards the optimal path to extinction," *Journal of The Royal Society Interface*, vol. 8, no. 65, pp. 1699–1707, 2011.
- [7] A. Monokrousos, A. Bottaro, L. Brandt, A. Di Vita, and D. S. Henningson, "Nonequilibrium thermodynamics and the optimal path to turbulence in shear flows," *Physical Review Letters*, vol. 106, no. 13, Article ID 134502, 2011.
- [8] S. J. Weber, A. Chantasri, J. Dressel, A. N. Jordan, K. W. Murch, and I. Siddiqi, "Mapping the optimal route between two quantum states," *Nature*, vol. 511, no. 7511, pp. 570–573, 2014.
- [9] W. Tanaka, N. Yamanaka, M. Onishi, M. Ko, J. Yamanaka, and E. Okamoto, "Optimal route of administration of mixed endothelin receptor antagonist (TAK-044) in liver transplantation," *Journal of Gastroenterology*, vol. 35, no. 2, pp. 120–126, 2000.
- [10] Q. Xu, K. Yang, S. Peng, and L. Hong, "A distance-adaptive refueling recommendation algorithm for self-driving travel," *ISPRS International Journal of Geo-Information*, vol. 7, no. 3, p. 94, 2018.
- [11] K. Wang and G. Akar, "Effects of neighborhood environments on perceived risk of self-driving: evidence from the 2015 and 2017 Puget Sound Travel Surveys," *Transportation*, vol. 46, no. 6, pp. 2117–2136, 2019.
- [12] Q. C. Pham, "A general, fast, and robust implementation of the time-optimal path parameterization algorithm," *IEEE Transactions on Robotics*, vol. 30, no. 6, pp. 1533–1540, 2014.
- [13] C. Hallam, K. J. Harrison, and J. A. Ward, "A multiobjective optimal path algorithm," *Digital Signal Processing*, vol. 11, no. 2, pp. 133–143, 2001.
- [14] H. Zhang and Z. Li, "Weighted ego network for forming hierarchical structure of road networks," *International Journal of Geographical Information Science*, vol. 25, no. 2, pp. 255–272, 2011.
- [15] A. D. Barbour and G. Reinert, "The shortest distance in random multi-type intersection graphs," *Random Structures and Algorithms*, vol. 39, no. 2, pp. 179–209, 2011.
- [16] Y. Liu, "Research on optimal path planning for self-driving tour based on improved Dijkstra algorithm," *Heilongjiang Science and Technology Information*, vol. 000, no. 017, pp. 75–77, 2020.
- [17] H. Yan and Y. Liu, "Discussion on the shortest path algorithm of urban road network based on GIS," *Journal of Computers*, vol. 23, no. 2, p. 6, 2000.
- [18] F. Lu, "The shortest path algorithm: classification system and research progress," *Journal of Surveying and Mapping*, vol. 30, no. 3, p. 7, 2001.
- [19] Z. Jia, H. Jing, and W. Li, "Design of self-driving tour route based on GIS and traveling salesman problem," *Surveying and Mapping and Spatial Geographic Information*, vol. 37, no. 9, p. 4, 2014.
- [20] L. ianxiong and Y. Wang, "Innovation of the tourism industry in the Greater Bay Area based on the "double innovation" system of teacher-student collaboration--Taking the construction of the optimization platform for self-driving tour

## *Retraction*

# **Retracted: Based on Fuzzy Comprehensive Evaluation, the Online and Offline Hybrid Teaching Mode of Physical Education Courses is Constructed**

### **Security and Communication Networks**

Received 26 December 2023; Accepted 26 December 2023; Published 29 December 2023

Copyright © 2023 Security and Communication Networks. This is an open access article distributed under the Creative Commons Attribution License, which permits unrestricted use, distribution, and reproduction in any medium, provided the original work is properly cited.

This article has been retracted by Hindawi, as publisher, following an investigation undertaken by the publisher [1]. This investigation has uncovered evidence of systematic manipulation of the publication and peer-review process. We cannot, therefore, vouch for the reliability or integrity of this article.

Please note that this notice is intended solely to alert readers that the peer-review process of this article has been compromised.

Wiley and Hindawi regret that the usual quality checks did not identify these issues before publication and have since put additional measures in place to safeguard research integrity.

We wish to credit our Research Integrity and Research Publishing teams and anonymous and named external researchers and research integrity experts for contributing to this investigation.


The corresponding author, as the representative of all authors, has been given the opportunity to register their agreement or disagreement to this retraction. We have kept a record of any response received.

## **References**

- [1] X. Qian and X. Li, “Based on Fuzzy Comprehensive Evaluation, the Online and Offline Hybrid Teaching Mode of Physical Education Courses is Constructed,” *Security and Communication Networks*, vol. 2022, Article ID 8571077, 18 pages, 2022.

## Research Article

# Based on Fuzzy Comprehensive Evaluation, the Online and Offline Hybrid Teaching Mode of Physical Education Courses is Constructed

Xiaodong Qian<sup>1</sup> and Xinhua Li<sup>2</sup> 

<sup>1</sup>Hubei University of Education, Wuhan 430205, China

<sup>2</sup>Hainan College of Economics and Business, Haikou 455000, China

Correspondence should be addressed to Xinhua Li; [lixinhua0716@hceb.edu.cn](mailto:lixinhua0716@hceb.edu.cn)

Received 5 July 2022; Revised 15 August 2022; Accepted 20 August 2022; Published 29 September 2022

Academic Editor: Hangjun Che

Copyright © 2022 Xiaodong Qian and Xinhua Li. This is an open access article distributed under the Creative Commons Attribution License, which permits unrestricted use, distribution, and reproduction in any medium, provided the original work is properly cited.

With the continuous development of the times, the educational concept in the information age continues to advance, in order to meet the needs of the society, each school in China has reformed and piloted according to its own situation to improve the quality of teaching. The research of conventional mixed physical education teaching, from the perspective of research methods, can be divided into two orientations: qualitative and quantitative. On the other hand, from the perspective of sample size, traditional research is a small sample study, and these objective behavioral data have opened up a new perspective for the research of blended physical education teaching from the research methods and research content. In this context, this paper combines the fuzzy comprehensive evaluation method to propose fuzzy comprehensive evaluation methods for mixed physical education teaching, such as preclass preparation, in-class links, teaching content, and teaching methods and designs an online and offline hybrid teaching mode for physical education courses based on a fuzzy comprehensive evaluation to construct an evaluation system, determine its fuzzy operators, determine indicators, and evaluate them comprehensively, reasonably and accurately through experiments. The fuzzy comprehensive evaluation method is based on the fuzzy mathematics comprehensive evaluation method, which can evaluate the evaluation object from all aspects, can objectively reflect the essential characteristics of things, and the evaluation process of the mixed mode construction of physical education courses is more scientific and reasonable. The application of the fuzzy comprehensive evaluation method has effectively promoted the reform and improvement of education and provided a foundation for the continuous improvement and innovation of students' learning and teachers' teaching effects.

## 1. Introduction

In this paper, the construction of online and offline hybrid teaching mode of physical education courses based on fuzzy comprehensive evaluation is carried out, and the construction of online and offline mixed teaching modes of physical education courses is studied and analyzed by using the fuzzy comprehensive evaluation method. The fuzzy comprehensive evaluation method is a comprehensive assessment method and is an evaluation method based on fuzzy mathematics [1]. From the mathematical affiliation of the fuzzy comprehensive evaluation, the fuzzy comprehensive evaluation method transforms the quality

assessment into a quantitative assessment; that is, the fuzzy comprehensive evaluation method will be used to make a comprehensive assessment of something or things that are limited by multiple factors. It has clear results, powerful systematicness, and it can better solve the problem that is difficult to quantify blurry problems; can also be used to resolve any uncertain issues. Hesse Biber first proposed the concept of fuzzy sets, on which it developed into fuzzy mathematics [2]. The essence of a fuzzy set is to use a membership function to turn uncertainty into a quantified form because it quantifies uncertainty and then provides a mathematical tool to solve the uncertainty. Over the past 40 years, the fuzzy theory has been widely used in the fields of

integrated assessment and decision-making, data processors, data collection methods, and data collection control [3]. Factors of objects are assessed based on the results of the assessment, and a comprehensive assessment of the objects resulting from a large number of assessments is made [4]. In actual calculations, objects are often uncertain, and uncertainties are the most important, so a vague and comprehensive assessment can be obtained. A comprehensive assessment (FCE) of objects with multiple ambiguity factors is good [5]. In a complex system containing many factors considering the following factors, can be divided into many layers to construct judgment at each level. Factors should be divided into assessments. The number of assessments at each level is the same. The number of evaluations between the grades should have a unique connection with each other, thus facilitating mathematical processing and operation, determining the correspondence of each level, and preserving its vague matrix [6]. The order of evaluation is: the lowest level is first fully assessed, then the lowest level evaluation conclusion constitutes a fuzzy matrix for comprehensive assessment, and the first level will be a fuzzy matrix from bottom to top for a comprehensive evaluation, and the overall comprehensive evaluation conclusion of the system can be received [7]. During 1989, Japan used robotics, process control, iron, traffic management, error diagnosis, medical diagnosis, image processing, market forecasting, and many other fields in fuzzy technology [8]. The use of fuzzy theory and fuzzy algorithms in Japan and its huge market prospects shocked the Western business community and became widely accepted in academia. The steps of the fuzzy composite rating method are usually divided into four steps: constructing a composite rating index, statistical values, and a combination of weights and weight vectors. The construction of a comprehensive assessment index means that a comprehensive evaluation system is the basis for a comprehensive assessment. The appropriateness of the selection of the assessment index directly affects the accuracy of the comprehensive assessment [9]. The establishment of evaluation indexes should incorporate, to a large extent, commercial data on evaluation systems or relevant laws and regulations [10]. Constructing a good weight vector means establishing a good weight vector by a professional empirical method or an AHP analysis method [11]. Creating a fuzzy synthesis evaluation matrix is to establish the appropriate membership function and then start running it. The synthesis of evaluation matrices and weights is synthesized using appropriate synthesis factors and the result vectors are interpreted. Physical education should be a targeted and organized learning process based on the student's participation plan [12]. Physical education classes are co-organized by teachers and students. His mission was to teach students sports knowledge, techniques, and skills, improve physical fitness, and develop ethics, perseverance, and quality [13]. This is the basic form of physical education in schools, one of which includes the possibility of sports development. Physical education, which refers to education through physical activity, is literally translated as physical education in English, abbreviation: physical education. With the strengthening of international exchanges, the degree and

level of development of sports have become an important symbol of the development and progress of the country and society, and an important means of diplomatic and cultural exchanges between countries [14]. Sports can be divided into a wide range of sports, competitive sports, school sports, traditional national sports, etc. Including sports culture, physical education, sports competitions, sports installations, sports organization, sports science and technology, sports economics, and other factors [15]. The philosophy of physical education is aimed at teaching students physical education knowledge, techniques, and skills, effectively developing the student's body, improving the student's body, and cultivating their moral will [16]. The idea of physical education should attach great importance to teaching and the education of the people, attach importance to morality, sincerity, encouragement, and friendship; in terms of teaching methods, we should pay attention to individualization and diversity, pay attention to the interaction between teachers and students, and fully consider the creativity of students. It emphasizes patience, diligence, and adapting measures to individual needs. Strengthen students' ability and enthusiasm for participation and give full play to students' creativity. Promote the good psychological quality of students, promote their physical and mental health and coordinate their development. Improving students' ability to adapt to modern society can improve physical health. Through the course, students can improve their understanding of body and health, master physical health knowledge and scientific fitness methods, and improve their awareness of self-care; exercise to improve physical health and promote physical health; develop a healthy lifestyle [17]. By studying this course and improving mental health, students will feel the warmth of the collective and the joy of emotion in a harmonious, equal, and friendly sports environment; in the process of experiencing setbacks and overcoming difficulties, improve the ability to encounter setbacks, adjust emotions, and develop strong willpower; in the process of continuous progress and success, these three concepts enhance self-worth and self-confidence, cultivate innovation and ability, and form a positive, optimistic and happy outlook on life. Blended teaching is an "online" + "offline" model that combines the advantages of online learning with traditional learning. Thanks to the implementation of a new organizational format, students can learn from a deep depth. Online hybrid teaching is a new teaching model that combines information technology with traditional classroom teaching. It means that teachers use modern information technologies such as the internet, mobile devices, and cloud computing to build online education platforms, while students use online web platforms to complete self-directed learning [18]. There are online resources, and those resource structures specified can explain the knowledge. Online resources are the premise of hybrid teaching, because the hybrid teaching we endorse lies in the traditional classroom, through the video promotion to give students enough relearning and each student can have a better knowledge base as possible, to ensure the quality of classes in the classroom. In the classroom, our classes only discuss the key points and difficulties, which are common

problems that students learn online. There are physical activities that test, integrate, and convert online knowledge. As mentioned above, students can basically master these most basic knowledge through online learning. Offline and online, and after the teacher filled in the gaps, we made a key breakthrough. It is through carefully designed classroom teaching activities to organize students to grasp the basics of online learning and use it flexibly. Interaction between teachers and students is leveraged to achieve more progressive curriculum goals, giving students more opportunities to engage in cognitive learning rather than focusing on students in the classroom as they have in the past. The teacher's teaching process must be tested and evaluated. Online or offline testing based on online learning platforms or other small courses is an important way to measure students' learning perspectives. Getting feedback can help us improve the relevance of our teaching activities, so that students can get clear learning, and teachers can get clear teaching. If we use the results of these quizzes as an important basis for process evaluation, it is true that people should pay attention to both results and results in the learning process. Even we should pay more attention to this process evaluation when the solid process is the most reliable foundation. The exploration of the online and offline hybrid teaching mode of physical education curriculum using fuzzy comprehensive evaluation provides a new research direction for the teaching method in the context of education in the new era.

## 2. Perception of the Content of the Study

**2.1. Traditional Physical Education Teaching Model.** Since the reform and opening up, colleges and universities have continuously deepened and promoted educational reform, strengthened the concept of teaching, improved the teaching content, and improved the teaching methods and means, which is a method of retaining traditional education and learning on the basis of other curriculum reform experience to develop modern physical education [19]. Through the investigation, it was found that for a long time, China's reform status has been constantly innovating and changing, and China's education has not changed much in essence, or the practice of teachers lecturing and students doing problems. On the one hand, this teaching mode is conducive to teachers to organize and manage the classroom in a timely manner, to understand and monitor the learning and learning of students in a timely manner, and to make timely adjustments to classroom teaching. On the other hand, it assists in the comprehensive and systematic learning of teachers' knowledge and the development of active skills in the language. However, with the rapid development of information technology, the shortcomings of traditional teaching methods are becoming more and more prominent. In the learning process, middle school students are too dependent on teachers, lack the spirit of learning and exploration, resulting in their gradual loss of self-control, autonomy, and innovation. Continuous improvement of students' learning methods and the rapid development of new media technologies have uncovered various problems in

the classroom: low amount of traditional teaching knowledge, single teaching methods, teachers and students can not communicate well, and so on. The interaction between teachers and students and the lack of interest in learning and the development of modern teaching are seriously hindered. Its teaching process is shown in Figure 1.

**2.2. Online Online Teaching.** The advent of education informatization 2.0, the strengthening of the development of the digital education system, and the cultivation of talents in the modern information society have become an inevitable trends in the development of higher education. In the work of "informatization teaching" carried out in 2017, education stressed that we should vigorously promote the research done by higher education and university networks, and actively support "online and offline" research. It is the promotion of mixed teaching methods in national policies and the continuous development and education of "in the process of education," new modes of teaching, including the extensive provision of "general education," "small education," and "SPOC" in colleges and universities. This new model of teaching will reshape the dynamism of physical education reform [20]. First of all, online teaching uses multimedia technology to make classroom teaching more vivid and intuitive, completely destroying the traditional classroom personal and fixed teaching mode. Second, students can share learning resources over the Internet to get the information they need. The knowledge acquired is no longer limited to textbook knowledge and teacher education, it expands the opportunities for students to acquire knowledge. Ultimately, the online classroom achieves the goal of "one-on-one" learning between teachers and students. Students choose what to learn according to their own abilities and abilities, solve the problem of personal differences, and teach according to the appropriate situation. Online teaching can effectively offset the shortcomings of traditional education and improve teaching efficiency.

**2.3. Online and Offline Mixed Teaching.** With the continuous advancement of information-based education reform, China's education gap in the new era has transformed into a contradiction between the diverse and individualized needs of individuals and the needs of a unified, highly educated person. Therefore, under the guidance of new teaching objections, strengthening teaching facilities, building high-quality teaching tools, innovating teaching methods and resources, and improving teaching evaluation systems have become the main challenges of the current education reform [21].

With the rapid development of science and technology in China, China officially introduced the "universal space" in 2012. New online education models, such as "silent lessons" and smart courses, have used new blood to teach Chinese learning methods. However, due to the deepening of research on online teaching models, several shortcomings of the new teaching models have been found: for example, online teachers are unable to accurately grasp the learning status and progress of students, nor can they systematically

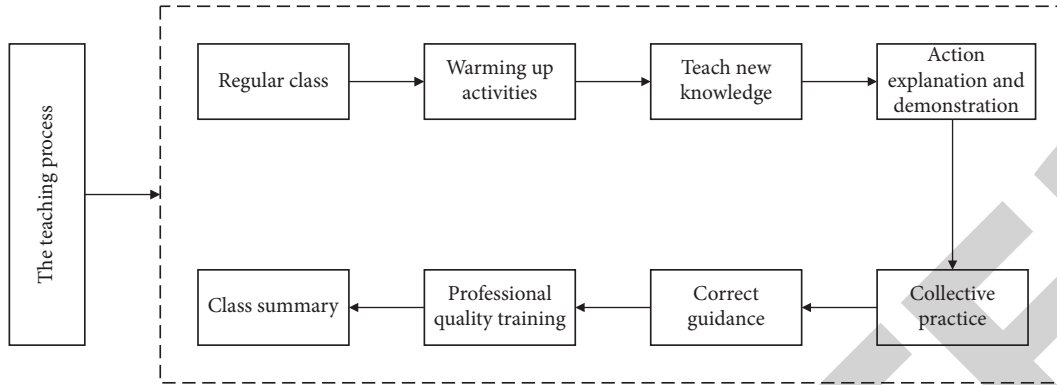


FIGURE 1: The flow of the traditional physical education teaching model.

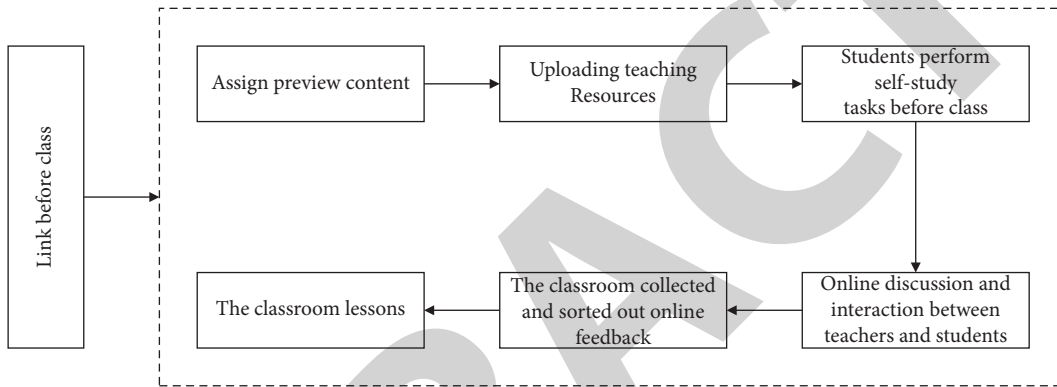


FIGURE 2: Online and offline mixed teaching preclass process.

and comprehensively evaluate students' learning experiences; The Internet has a rich reserve of information, which is easy to distract students' attention and is not conducive to the concentration of their thinking [22]. Given the challenges of online teaching, researchers began to combine online teaching with traditional teaching and suggested a "hybrid" approach to teaching. On the one hand, to make up for this traditional teaching content, the benefits of online teaching do not belong to the traditional classroom participation method at all, using its advantages to teach students after class, such as video, pictures, and audio introductions, to enhance students' interest in learning; online teaching can stimulate students' enthusiasm for learning, strengthen communication and interaction between teachers and students and create a positive learning atmosphere in the classroom through online response, online debate, class testing, communication, and sharing. On the other hand, students can also organize detailed information on course content by holding hands-on practical courses and collating them to strengthen and improve students' control over course content. Based on the existing research, the mixed teaching explores the improvement of the basic and online and offline mixed teaching suitable for teaching. The reform provides new ideas in the context of creating education in the new era. Its preclass teaching process is shown in Figure 2.

As can be seen in Figure 2, the preparation for online teaching before class is mainly based on the use of documents

and sports videos. The teaching materials mainly include five parts of action demonstration and action demonstration; The main elements of the action technique, teaching steps, protective measures, and scoring criteria. The time point of the video is about 3 minutes per episode: the introduction and transmission of the file is mainly to illustrate the theoretical knowledge of motion. The middle of the lesson is shown in Figure 3.

From Figure 3, it can be seen that another major purpose of the course is to explain and correct the problems and doubts of online automatic learning, and to guide students to master and integrate knowledge. Through offline teaching, they can improve the accuracy, consistency, and coordination of technical movements and can also improve the understanding and control of technical movements. The after-school session is shown in Figure 4.

As shown in Figure 4, the after-class link is mainly after class, the teacher provides feedback on the actual learning of the students, and tests the students' theoretical knowledge. Among these students, theoretical knowledge comes mainly in the form of practice questions, which can be asked 5–10 questions at a time, mainly for technical aspects, key points and difficulties, and evaluation criteria for actions.

**2.4. Fuzzy Comprehensive Evaluation Method.** Fuzzy synthesis evaluation is a comprehensive investigation method based on fuzzy mathematics [23]. According to fuzzy



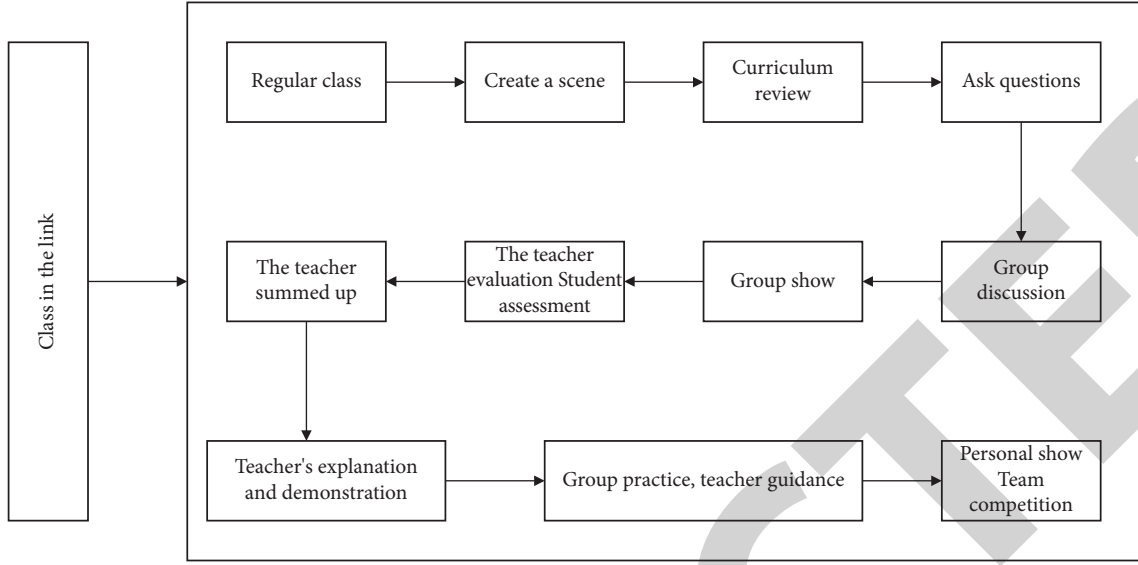


FIGURE 3: The process of online and offline mixed teaching courses.

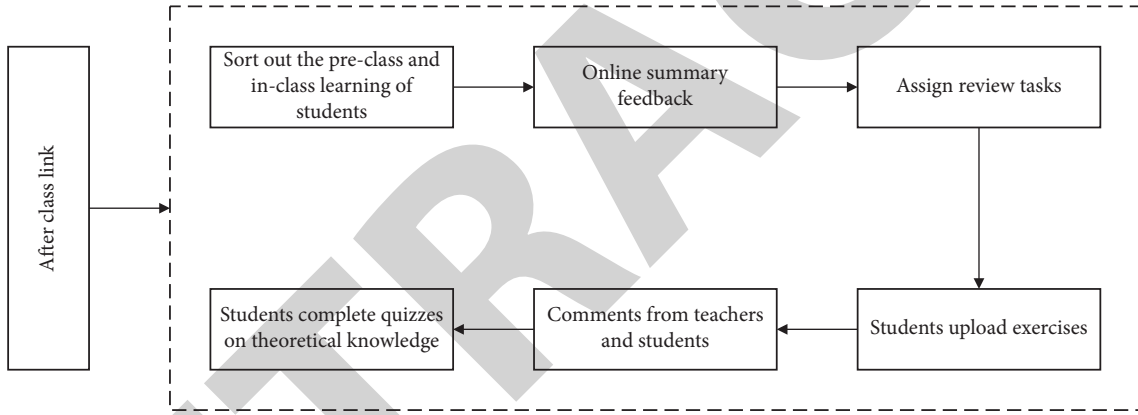


FIGURE 4: Learning process in the after-school period.

mathematical theory, this method translates into qualitative evaluation, that is, through a comprehensive assessment, fuzzy mathematics makes a comprehensive assessment of something or object that is limited by multiple factors. This approach quantifies certain problems that are uncertain and cannot be quantified. The characteristics of the Fuzzy Comprehensive Evaluation Specification are as follows:

- (1) When considering the optimal benchmark rating factor, the evaluation value is 1: the rating value of other suboptimal rating factors is determined according to the benchmark number.
- (2) According to the nature of several rating factors, the relationship between the rating value and the rating factor can be determined.

The steps are as follows:

Determine the object factor domain

$P$  evaluation indicators,  $u = \{u_1, u_2, LL, u_p\}$

Determine the evaluation hierarchy domain

$$v = \{v_1, v_2, LL, v_p\}, \quad (1)$$

$v$ -hierarchical collection;

Indicates that each level corresponds to a fuzzy subset.

Establish its relationship matrix  $R$

In summary,  $u_i (i = 1, 2, LL, p)$  quantify the valuation object of each term to get the member rank of the corresponding fuzzy sub- $|u_i|$ , and then wait until the fuzzy subrelationship matrix:

$$R = \begin{bmatrix} R|u_1 \\ R|u_2 \\ \wedge \\ R|u_p \end{bmatrix} = \begin{bmatrix} r_{11} & r_{12} & \wedge & r_{1m} \\ r_{21} & r_{22} & \wedge & r_{2m} \\ \wedge & \wedge & \wedge & \wedge \\ r_{p1} & r_{p2} & \wedge & r_{pm} \end{bmatrix}_{p \times m}, \quad (2)$$

where  $r_{ij}$  represents the element of column  $j$  in row  $i$ ;  $r_{ij}$  Matrix  $Ru_i$  indicates that there are weaker member ranks in terms of hierarchy factors. In a given factor, the

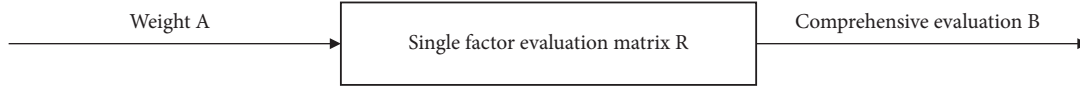


FIGURE 5: Unipolar fuzzy comprehensive evaluation model.

performance of a computed object itself is analyzed by a fuzzy  $u_i$  vector  $(R|u_i) = (r_{i1}, r_{i2}, LL, r_{im})$ , whereas other calculus methods are shown exponentially. A comprehensive assessment, therefore, requires more information in this regard and can be assessed in many ways.

Determining the right vector

Comprehensive fuzzy analysis yields a weight vector for evaluation factors: the  $A$ -value analysis  $A = (a_1, a_2, LL, a_p)$  membership is used to determine the order between the evaluation indices, and to determine whether the weight coefficients are unified before synthesis. The formula is as follows:

$$\sum_{i=1}^p a_i = 1, \quad a_i \geq 0, \quad i = 1, 2, LL, n. \quad (3)$$

Its result vectors

The synthesis of  $A$  and  $R$  obtains the fuzzy comprehensive evaluation result  $B$ , and  $A$  must be calculated using a suitable operator, and its formula is as follows:

$$AnR = (a_1, a_2, LL, a_p) \begin{bmatrix} r_{11} & r_{12} \wedge r_{1m} \\ r_{21} & r_{22} \wedge r_{2m} \\ \wedge & \wedge \wedge \wedge \\ r_{p1} & r_{p2} \wedge r_{pm} \end{bmatrix} = (b_1, b_2, \wedge b_m) = B, \quad (4)$$

where  $b_1$ -It is obtained by the operation of the weight vector ( $A$ ) and the fuzzy relationship matrix ( $R$ ) on the  $j$  case, indicating the degree of membership of an evaluation object of the whole on the fuzzy subset  $v_j$ .

The algorithm in the evaluation process basically contains the evaluation of all the attributes of each object, many evaluation objects reflect various characteristics from all aspects, these characteristics have a certain degree of ambiguity, which means that the fuzzy comprehensive evaluation method of comprehensive evaluation method is scientific and reasonable, and its results are closer to the actual situation, the algorithm basically realizes the fairness and justice of the evaluation.

### 3. Establishment of a Fuzzy Comprehensive Evaluation Model for Online and Offline Physical Education Courses

**3.1. Establishment of Fuzzy Comprehensive Evaluation Model.** Let, for the finite domain of theory,  $U = \{x_1, x_2, x_3, \wedge, x_n\}$   $V = \{y_1, y_2, K, y_m\}$   $A$  is a fuzzy vector over  $U$ , and  $R$  is a Fuzzy matrix on  $U * V$ , which is a composite of two Fuzzy matrices. That is, Fuzzy can be seen as a fuzzy machine for dumpsters, which is the Fuzzy dumpster is the fuzzy dumpster

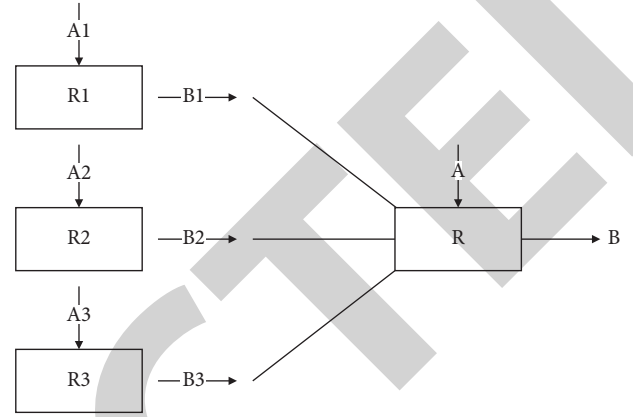


FIGURE 6: Secondary fuzzy comprehensive judgment model.

concept of  $A$  to  $U$ , and transforms the Fuzzy dumper to  $B$  to the discourse field  $V$ . It is precisely through the fuzzy matrix  $R$  between  $U$  and  $V$  that  $B = AnR$  the transformation is made. The specific evaluation model is shown in Figure 5.

In the figure:

$B$ -Fuzzy comprehensive evaluation results;

$A$ -Fuzzy evaluation factor weight set;

$R$ -Represents a fuzzy relationship from  $U$  to  $V$ .

The secondary fuzzy comprehensive evaluation formula is as follows:

$$B = AnR = An \begin{bmatrix} B_1 \\ B_2 \\ M \\ B_i \end{bmatrix} = An \begin{bmatrix} A_1 n R_1 \\ A_2 n R_2 \\ M \\ A_i n R_i \end{bmatrix} = (b_1, b_2, L, b_m). \quad (5)$$

The model diagram is shown in Figure 6.

**3.2. Fuzzy Operators.** Earlier in the article, there is a fuzzy relation  $R$  from  $U$  to  $V$ , and a fuzzy map is obtained: it is to assemble the fuzzy comprehensive valuation decision model, where  $TR(U, V, R)B = AnR$  is the fuzzy subset of  $V$ :

$$b_j = \vee (a_k \wedge k_j), \quad k = 1, 2, L, n \quad j = 1, 2, L, m. \quad (6)$$

The result is a normalized treatment of the result, and the result is, that is, the result is a decision on the case  $\sum_{i=1}^m b_i \neq 1$   $b_j = \max\{b_1, b_2, \wedge, b_m\} b_j$ . Different decisions are made according to different operational definitions, and the decision model is as follows.

#### 3.2.1. $A(\wedge, \vee)$ Model

$$b_j = \max\{(a_i \wedge r_{ij}), 1 \leq i \leq n\}, \quad j = 1, 2, \wedge, m. \quad (7)$$

Due to the large number of factors in this model, the weighted value of each factor is very small, which will eventually reduce the reliability of the result, that is, the weight coefficient is modified.  $a_i$ . The process is as follows:

$$a_i = \frac{na_i}{m \sum_{i=1}^n a_i}, i = 1, 2, \wedge, n. \quad (8)$$

Then, the weight coefficients are uniformized. Here,  $a'_i = (n/m)a_i$ ,  $a'_i$ -Correction weight coefficient;  $n$ -the number of evaluation factors;  $m$ -The number of factors in the evaluation set.

**3.2.2. Model  $M(n, \vee)$ .** There are two modes for operations: one is expressed by the regular multiplication “ $n$ ,” and the other is just the large operation  $V$  expression:

$$b_j = \max\{(a_i n r_{ij}), 1 \leq i \leq n\}, j = 1, 2, \wedge, m. \quad (9)$$

Multiplication in the above equation does not lose information, and vice versa. If  $a_i n r_{ij}$ , less than 1, i.e., if multiple factors are considered, the corrected value correlates with the primary factor  $a_i r_{ij}$  ( $a_i$ ) and ignores the secondary factor, which better reflects the importance of univariate assessment.

**3.2.3. Model  $M(n, +)$ .** At this time,

$$b_j = \sum_{i=1}^n a_i n r_{ij}, j = 1, 2, \wedge, m, \sum_{i=1}^n a_i = 1. \quad (10)$$

Model III applies to the effect of multiple factors on the evaluation object, fully considers the impact of the factors involved, and retains all information about the individual factors, and there is no upper limit for the calculation of neutrality, but it must be equal to 1.  $a_i r_{ij}$  ( $i = 1, 2, \wedge, n$   $j = 1, 2, \wedge, m$ )  $a_i$ .

**3.2.4. Model  $M(n, n)$ .** The calculations under this model are  $b_j$

$$b_j = \sum_{i=1}^n a_i n r_{ij}, j = 1, 2, \wedge, m \text{ or } b_j = \min 1, \left[ \sum_{i=1}^n a_i n r_{ij} \right], \quad (11)$$

$$j = 1, 2, \wedge, m.$$

**3.2.5.  $M(\wedge, n)$  Model.** Model five represents a summation operation with an upper limit of 1, using small operations and cyclic operations  $n$ , and its expression is, then,  $xny = \min\{1, x + y\}$   $b_j = \sum_{i=1}^n a_i \wedge r_{ij}$  obtain:

$$b_j = \min \left[ 1, \sum_{i=1}^n a_i \wedge r_{ij} \right], j = 1, 2, \wedge, m. \quad (12)$$

**3.2.6.  $M(\wedge, n)$  Model.** At this time,

$$b_j = n_{i=1}^{i=1} (r_{ij}^{a_i}), j = 1, 2, L, m. \quad (13)$$

Because each operator has a different operating principle, different evaluation results are produced. According to the relevant data, there are many operators in model three, and a variety of factors can be considered. All this operator is used.  $M(n, +)$ .

**3.3. Indicator Processing.** After obtaining the indicators from the previous analysis, the target specific results of the rating can be carried out using the maximum membership method, the weighting method, and the fuzzy distribution method.  $b_j(1, 2, \dots, m)$ .

**3.3.1. Maximum Membership Method.** Take the (optional element) corresponding to the (maximum evaluation index) as the evaluation result, that is,  $\max b_j V_L$

$$V = (V_L | V_L \longrightarrow \max b_j). \quad (14)$$

The disadvantage of the maximum membership method is that it only takes into account the role of the largest evaluation index and excludes other directory information [24]. If there are more maximum rating indices, it is difficult to judge the evaluation results using the maximum degree of membership method. To solve this problem, we can consider changing the grey association theory. The theory is as follows:

$$\eta_{ij}(k) = \frac{\min \Delta_i(k) + \rho_{\max} \Delta_i(k)}{\Delta_i(k) + \rho_{\max} \Delta_i(k)} \quad \rho \in (0, 1),$$

$$\Delta_{ij}(k) = |A'_j(k) - A'_i(k)|, \quad (15)$$

$$\eta_{ij} = \frac{1}{k} \sum_{i=1}^k \eta_{ij}(k).$$

where  $A'_j$ - the initial value of  $A$ ;  $A'_i$ ,  $\rho$ -is the resolution coefficient;  $\eta_{ij}$ -Relevance.

**3.3.2. Weighted Average Method.** For weights, the weighted average of each (alternative element) is the evaluation result. Rule:  $b_j v_j$

$$V = \frac{\sum_{j=1}^n b_j v_j}{\sum_{j=1}^n b_j}. \quad (16)$$

$$\text{If so, } b_j = 1V = \sum_{j=1}^n b_j v_j$$

If the object of evaluation is a quantitative quantity, the values calculated according to the above two methods are the results of the comprehensive assessment of the fuzzy comprehensive evaluation. If the rating object is a non-quantitative quantity, the maximum subordinate method is used instead of the weighted average method.

**3.3.3. Fuzzy Distribution Method.** The method directly takes the evaluation index as the evaluation result or 1 and then uses the standard evaluation index as the evaluation result. The specific method of attribution to 1 is as follows.

Sum of the evaluation indicators:

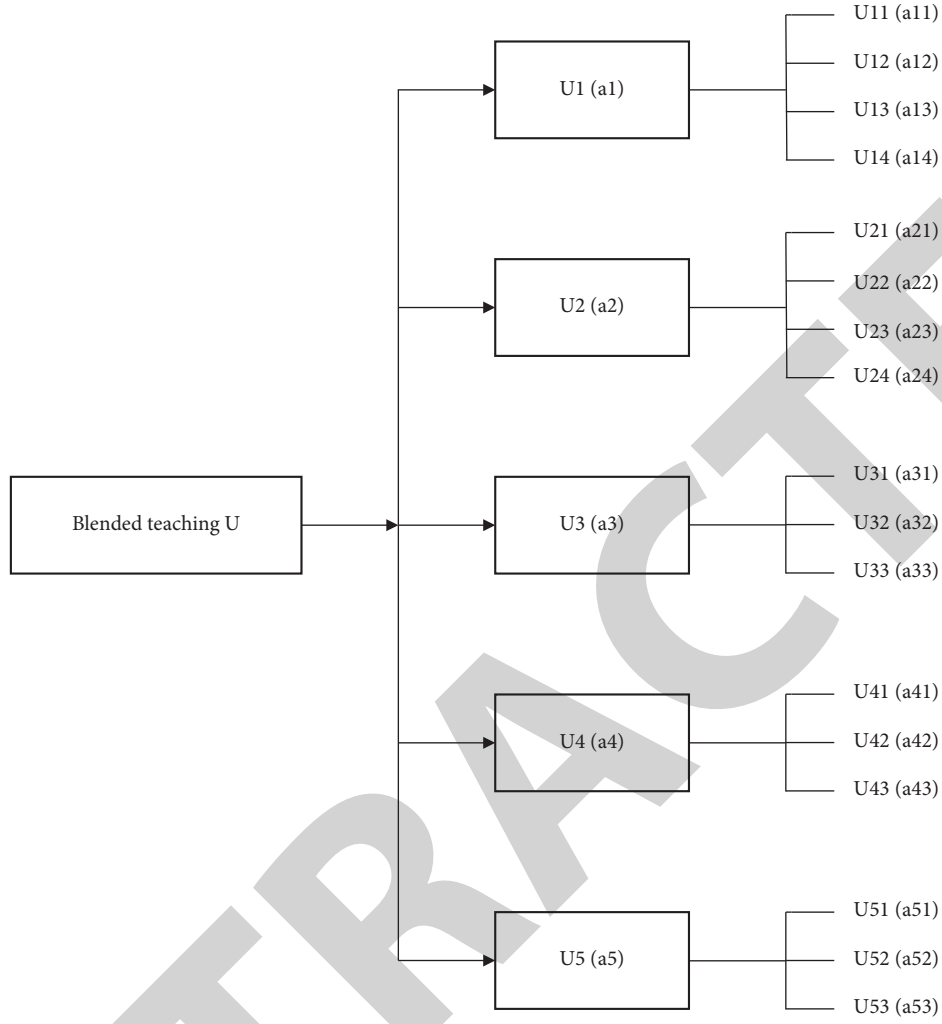


FIGURE 7: Simplifies the structure of the mixed teaching evaluation index system.

$$b = b_1 + b_2 + \wedge + b_m = \sum_{j=1}^m b_j. \quad (17)$$

Divide the original evaluation indicators by the sum of the evaluation indicators:

$$B' = \left( \frac{b_1}{b}, \frac{b_2}{b}, \wedge, \frac{b_m}{b} \right) = (b'_1, b'_2, \wedge, b'_m), \quad (18)$$

where  $B'$  - Normalized fuzzy comprehensive evaluation set;  $b'_j (1, 2, \wedge, m)$  - Indicates a standardized fuzzy comprehensive evaluation index.

To sum up.  $\sum_{j=1}^m b'_j = 1$

### 3.4. Establishment of an Online and Offline Hybrid Teaching Model for Physical Education Courses with Fuzzy Comprehensive Evaluation

**3.4.1. Establishment of a Factor Set.** The set of factors consisting of the individual factors of the evaluation object is called the factor set ( $U$ ), i.e., It represents the various factors.

They have a certain ambiguity.  $U = \{U_1, U_2, U_3, \wedge, U_n\} (U_1, U_2, \dots, U_n)$

There are five first-level evaluation indexes in Figure 7, which are represented by  $U = \{U_1, U_2, U_3, U_4, U_5\}$ . Among them, mixed teaching preparation, teaching, explaining knowledge, teaching methods, and students' acceptance of knowledge are represented by  $U_1, U_2, U_3, U_4$ , and  $U_5$ , respectively. There are multiple secondary indicators for each first-level indicator, such as "sports demonstration and action demonstration;" "main points of sports dynamic technology;" "teaching steps;" "protective measures" under the (mixed teaching preparation) as the second-level evaluation indicators, which are expressed. The same can be obtained  $U_2, U_3, U_4, U_5$  as shown in Figure There are a total of 17 evaluation points, which are weighted  $U = \{U_1, U_2, U_3, U_4, U_5\}$   $U_1 U_2 U_3 U_4 U_5 U_1 U_1 = \{U_{11}, U_{12}, U_{13}, U_{14}\} U_2 U_3 U_4 U_5 (a_i)$ .

**3.4.2. Establishment of a Set of Weights.** Since the evaluation results are affected by each evaluation factor, in order to optimize this problem, each influencing factor is given a

corresponding appropriate weight value according to its degree of influence  $u_i$  ( $i = 1, 2, \wedge, n$ )  $a_i$  ( $i = 1, 2, \wedge, n$ ). That is, the set it consists of is called a set of weights. In general, the individual weights satisfy normalization and non-negativity, as follows:  $A = \{a_1, a_2, \wedge, a_m\}$

$$\sum_{i=1}^n a_i = 1, \quad a \geq 0 \quad (i = 1, 2, 3, \wedge, n). \quad (19)$$

It can be seen as the degree to which the results of the membership evaluation correspond to the factors  $u_i$  ( $i = 1, 2, \wedge, n$ ), and the weight set can also be attributed to the fuzzy subparts within the factor set. Weights are usually determined by the rating staff as the actual situation requires. For the same influencing factors, different weights will obviously lead to different evaluation results, and for indicators that use more education, require more, and directly affect the quality, a higher value should be allocated when determining weight; instead, a lower value should be allocated. Thus, it represents the holistic orientation of blended teaching.

**3.4.3. Establishment of Evaluation Sets.** The evaluation set refers to the collection of various evaluation results made by the evaluator to the evaluation object. Each element conveys a different possible outcome fuzzy synthesis evaluation whose primary purpose is to select the best outcome based on all influencing factors [25].

**3.4.4. Determining the Fuzzy Judgment Matrix.** A fuzzy comprehensive evaluation is the final result of the most scientific and rational assessment of the influencing factors of the evaluation object, which is thoughtful, meticulous, and the result is close to reality. It is based on a factor to set up a rating object, which can ( $U_i$ ) evaluate the first item, the degree of affiliation ( $\wedge$ ) and the item element in the factor on the number of factors; It is easy to get a chapter count according to the rules of operation  $ir_{ij}j(V_j)$  of the first factor  $R_i$  ( $R_i = r_{i1}, r_{i2}, \wedge, r_{im}$ ).

Similarly, the influencing factors corresponding to each factor in the fuzzy comprehensive evaluation are as follows:

$$\begin{aligned} R_1 &= (r_{11}, r_{12}, \wedge, r_{1m}), \\ R_2 &= (r_{21}, r_{22}, \wedge, r_{2m}), \\ &\quad \wedge, \\ R_n &= (r_{n1}, r_{n2}, \wedge, r_{nm}). \end{aligned} \quad (20)$$

The rate of rating by each factor represents the first single-factor rating matrix  $R$ :

$$R_i = \begin{bmatrix} r_{i11} & r_{i12} & \wedge & r_{i1m} \\ r_{i21} & r_{i22} & \wedge & r_{i2m} \\ M & M & M & M \\ r_{in1} & r_{in2} & \wedge & r_{inm} \end{bmatrix}. \quad (21)$$

A more comprehensive assessment can only be achieved through a comprehensive assessment of all influencing

factors. The weight set  $a$  can be  $n$  columns in the fuzzy matrix, and the fuzzy comprehensive evaluation is obtained by combining the weight set with the one-factor fuzzy evaluation matrix  $B_i$ .

$$B_i = A_i n R_i = (a_1, a_2, \wedge, a_m) n \begin{bmatrix} r_{i11} & r_{i12} & \wedge & r_{i1m} \\ r_{i21} & r_{i22} & \wedge & r_{i2m} \\ M & M & M & M \\ r_{in1} & r_{in2} & \wedge & r_{inm} \end{bmatrix}, \quad (22)$$

$b_j$  ( $j = 1, 2, \wedge, m$ ) is the fuzzy index. This is the fuzzy evaluation membership of the two-step assessment corresponding to the level of the substitution index that fully meets the influence of all factors, and the first-level evaluation matrix of the fuzzy comprehensive evaluation can be obtained.

$$R = \begin{bmatrix} B_1 \\ B_2 \\ M \\ B_m \end{bmatrix}. \quad (23)$$

Obtained (first-level fuzzy comprehensive evaluation set)  $B = A n R_s$ .

**3.4.5. Overall Evaluation Score**

$$M = B n V^T = (b_1, b_2, \wedge, b_m) n \begin{bmatrix} V_1 \\ V_2 \\ M \\ V_m \end{bmatrix}, \quad (24)$$

where  $M$ -Quantitative score of the comprehensive evaluation;  $B$ -Fuzzy comprehensive evaluation results;  $V$ -The specific score of the evaluation level.

## 4. Case Studies

**4.1. Study Design.** The experiment set up a fuzzy comprehensive evaluation of the physical education course online and offline mixed mode teaching as the experimental group (30 people), on the contrary, in the conventional group (30 people), a total of 120 questionnaires were collected, a total of 60 pre-experimental groups and conventional groups, and a total of 60 experimental groups and conventional groups after the experiment. Their sports theoretical knowledge, sports technical ability, physical education teaching effect, and feedback results were tested and analyzed. In order to ensure that the basic conditions of the experimental group and the conventional group are equal, the basic conditions are shown in Tables 1 and 2.

Through the analysis of Tables 1 and 2, it can be concluded that the experimental group and the conventional group conducting the experiment are greater than 0.05 in terms of a physical fitness test and exercise attitude, and all selected students provide reliability for the experiment and ensure the continuation of the experiment.

TABLE 1: Comparative analysis table of physical fitness level premeasurement in the experimental group and conventional group.

Test	Constituencies	Number	mean $\pm s$	<i>P</i>
Physical test scores	Experimental group	30	60.55 $\pm$ 6.14	0.83
	General groups	30	60.85 $\pm$ 4.85	
BMI	Experimental group	30	21.68 $\pm$ 2.99	0.50
	General groups	30	21.66 $\pm$ 1.68	
Vital capacity	Experimental group	30	3875.00 $\pm$ 499.06	0.55
	General groups	30	3796.12 $\pm$ 614.53	
Stand up for the long jump	Experimental group	30	2.05 $\pm$ 0.30	0.35
	General groups	30	1.98 $\pm$ 0.12	
Seated body flexed forward	Experimental group	30	12.76 $\pm$ 7.89	0.72
	General groups	30	13.54 $\pm$ 6.23	
50 m run	Experimental group	30	8.31 $\pm$ 0.79	0.45
	General groups	30	8.21 $\pm$ 0.86	
1000 m run	Experimental group	30	3.67 $\pm$ 0.22	0.56
	General groups	30	3.79 $\pm$ 0.33	
800 m (female) run	Experimental group	10	4.25 $\pm$ 0.20	0.22
	General groups	10	4.12 $\pm$ 0.10	
Pull-up	Experimental group	30	7.60 $\pm$ 2.30	0.51
	General groups	30	7.12 $\pm$ 3.05	
Sit-up	Experimental group	10	43.00 $\pm$ 3.99	0.19
	General groups	10	42.54 $\pm$ 3.10	

TABLE 2: Comparative analysis of exercise attitudes in the experimental group and the regular group.

Test	Constituencies	Number	( )mean $\pm s$	<i>P</i>
Behavioral attitudes	Experimental group	30	30.555.65 $\pm$	0.61
	General groups	30	27.576.99 $\pm$	
Goal attitude	Experimental group	30	46.557.26 $\pm$	0.17
	General groups	30	44.667.32 $\pm$	
Behavioral cognition	Experimental group	30	28.408.10 $\pm$	0.68
	General groups	30	29.664.60 $\pm$	
Behavioral habits	Experimental group	30	37.2611.20 $\pm$	0.31
	General groups	30	39.517.82 $\pm$	
Behavioral intent	Experimental group	30	28.958.47 $\pm$	0.67
	General groups	30	30.716.50 $\pm$	
Emotional experience	Experimental group	30	38.0111.22 $\pm$	0.60
	General groups	30	40.517.25 $\pm$	
Sense of behavioral control	Experimental group	30	24.113.33 $\pm$	0.62
	General groups	30	24.544.08 $\pm$	
Subjective criteria	Experimental group	30	21.127.85 $\pm$	0.22
	General groups	30	22.566.90 $\pm$	
Exercise attitude overall score	Experimental group	30	254.9849.11 $\pm$	0.12
	General groups	30	260.1033.14 $\pm$	

#### 4.2. Data Processing and Analysis

**4.2.1. Knowledge of Sports Theory.** In order to understand the mastery of the basic theoretical knowledge of the students learned by the conventional teaching mode and the mixed teaching mode, the conventional teaching mode is set as the conventional group and the mixed teaching mode is the experimental group. The basic theoretical knowledge of these two groups is tested uniformly, and the test results are shown in Figure 8.

From Figure 8, it can be seen that the number of people in the experimental group with excellent test scores is more

than the number of people in the regular group, with 13 people with scores distributed between 90 and 100 points, and 7 people with scores between 80 and 89, and the number of people in the regular group is more in the low segment. There are only 7 people with a score of 80 to 100.

As can be seen from Table 3, the average score of the experimental group was 84.21, fluctuating between the values of 10.38, while the average score of the regular group was 71.48. In the fluctuation between the 8.30 values, the experimental group, and the conventional group were tested independently in the sample (*T*), the result (*P*), the average score of the experimental group was obviously higher than

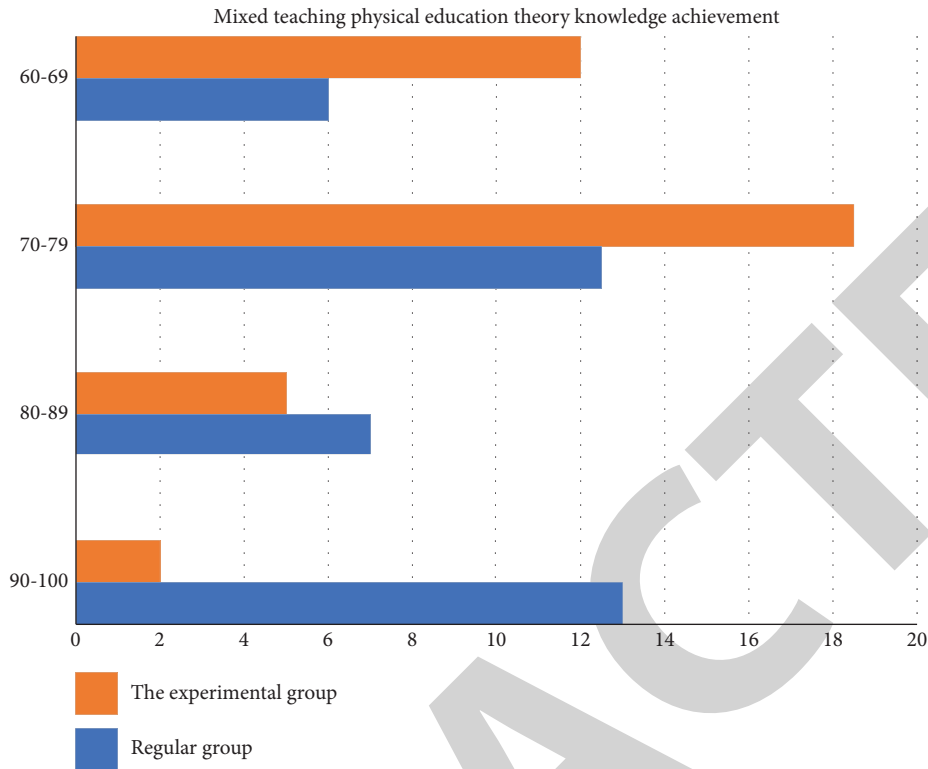


FIGURE 8: Comparison of sports theory knowledge scores in the experimental group and the conventional group.

TABLE 3: Comparison of theoretical knowledge scores between experimental groups and regular groups.

Test the content	Experimental group	General groups	<i>T</i>	<i>P</i>
Athletic theory achievements	84.21 ± 10.38	71.48 ± 8.30	4.87	<0.01

that of the conventional group, and there was a large difference between the two groups, that is, the fuzzy comprehensive average of the online and offline mixed teaching of physical education courses had a greater role in promoting students' mastery of sports theory knowledge  $P < 0.01$ .

**4.2.2. Sports Technical Ability.** The regular and experimental groups of students were tested with standing jumps and skills, and the number of students in different score segments was sorted as shown in Figure 9.

It can be seen that the experimental group and the regular group had a majority of sports skills tests between 70–89, and the experimental group had as many as 27 people, accounting for 72.8% of the total number, while the regular group had 25 people in this range. The experimental and regular groups improved their performance in the physical skills test compared with before, with 8 people in the experimental group and 7 people accounting for 21.5% of the total number of people and 7 people accounting for 19.4% of the total number of people, respectively.

As can be obtained from Table 4, the average scores of the two sports skills tests of the experimental group, the standing long jump, and skill were 79.82 and 82.32 points, respectively, and the standard deviation was 0.23 and 0.31.

The two scores in the regular group were 77.93 points, 80.81 points, 0.31 points, and 0.15 points, respectively. Their independent sample *T* tested the *P*-values of 0.504 and 0.355, respectively, that is, whether it was the long jump or skill, the performance of the students in the two groups was significantly different ( $P > 0.05$ ).

**4.2.3. Effect of Physical Education Teaching.** In the process of teaching, student interest has become an important indicator of testing the effectiveness of teaching. After the experiment, a questionnaire was submitted to the experimental and regular groups to study learning interest, self-directed learning ability, and investigation cooperation ability. The questionnaire was distributed and collected in the form of an electronic questionnaire that collected the results of the survey in real time, and the results of the questionnaire were compared with the changes in the interest of physical education students after the experiment ended. The result is as follows.

After sorting out the questionnaire, the data in Table 5 can be seen that the experimental group is very different from the regular group, and the reason is that the teacher will send the courseware to the online learning platform for students to learn before the class, and the students will prepare according to the requirements. In this regard,

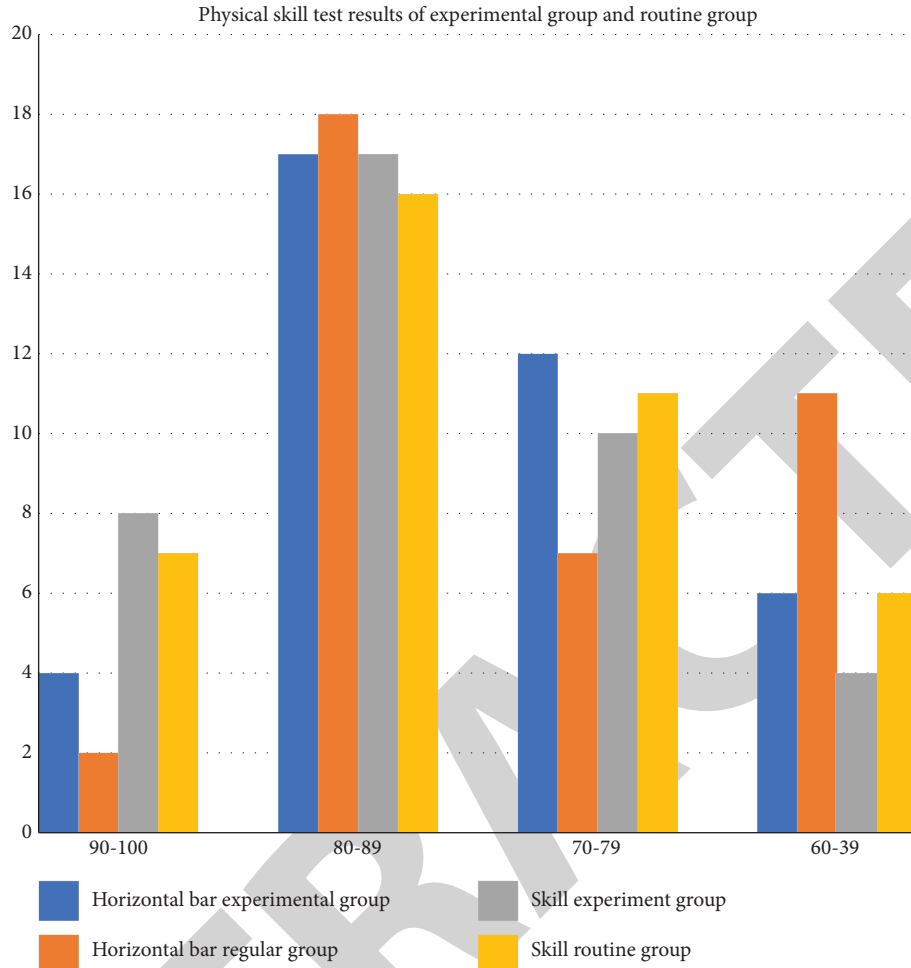


FIGURE 9: Comparison of athletic skills test scores in experimental and regular groups.

TABLE 4: Comparative analysis of sports skills results in experimental and regular groups.

Project	Constituencies	Test scores	Highest score	Lowest score	<i>T</i>	<i>P</i>
Stand up for the long jump	Experimental group	$79.82 \pm 0.23$	100	60	0.848	0.504
	General groups	$77.93 \pm 0.22$	90	60		
Skill	Experimental group	$82.32 \pm 0.31$	100	65	0.959	0.355
	General groups	$80.81 \pm 0.15$	96	60		

students can not only complete the homework requirements assigned by the teacher but also improve their independent learning ability. The learning effect of the experimental group and the conventional group was sorted out and analyzed to obtain Table 6, and Figure 10 was obtained according to Table 6, and the results showed that the experimental group had a higher teaching effect than the conventional group.

As can be seen from Table 6, the results of the *T* test for the independent sample can be concluded, and the test results of the experimental group in all aspects are higher than those of the conventional group. This shows that there are significant differences between the two sets of experiments  $P < 0.05$ .

Combined with Table 6 and Figure 10, it can be seen that through the results of the mixed teaching of online and

offline mixed teaching of physical education courses with fuzzy comprehensive evaluation, students have been improved in all aspects and are more likely to absorb teaching knowledge.

**4.2.4. Mixed Physical Education Feedback Results.** Through experiments, the effect of mixed-mode physical education in the teaching process was investigated, and the feedback on the effect of mixed-mode physical education was investigated by a questionnaire method to investigate the satisfaction with mixed-mode physical education, and the specific survey results are shown in Figure 11.

As shown in Figure 11, 52% are very satisfied with the mixed teaching model; 42.42% are satisfied, while only six percent of the students show a general attitude, which shows



TABLE 5: Questionnaire on the effect of physical education after experiments in experimental groups and conventional groups.

		Exactly (%)	Basically compliant (%)	Generally compliant (%)	Essential not compliant (%)	Completely not compliant (%)
Question 1	Experimental group	37.5	40.8	22.2	0	0
	General groups	26.2	20.4	50.1	2.8	0
Question 2	Experimental group	48.9	37.8	13.1	0	0
	General groups	26.5	36.6	31.8	2.7	0
Question 3	Experimental group	55.6	38.9	6.2	0	0
	General groups	40.5	36.3	17.5	1.3	0
Question 4	Experimental group	54.0	37.8	4.6	0	0
	General groups	30.0	39.3	17.5	2.8	0
Question 5	Experimental group	29.4	41.2	6.2	0	0
	General groups	23.6	49.5	23.3	0	0
Question 6	Experimental group	56.5	38.1	7.8	0	0
	General groups	44.8	31.8	20.5	1.4	0
Question 7	Experimental group	69.1	39.7	7.5	0	0
	General groups	59.2	32.4	28.2	1.4	0

TABLE 6: Comparative analysis of learning effects between experimental groups and regular groups.

	Question 1	Question 2	Question 3	Question 4	Question 5	Question 6	Question 7
Experimental group $\bar{x} \pm s$	4.25 $\pm$ 0.74	4.37 $\pm$ 0.70	4.52 $\pm$ 0.58	4.48 $\pm$ 0.61	4.48 $\pm$ 0.63	4.52 $\pm$ 0.65	4.36 $\pm$ 0.63
General groups $\bar{x} \pm s$	3.82 $\pm$ 0.87	4.06 $\pm$ 0.83	4.27 $\pm$ 0.76	4.26 $\pm$ 0.67	4.18 $\pm$ 0.83	4.32 $\pm$ 0.79	4.01 $\pm$ 0.424
<i>T</i>	2.412	2.337	2.078	2.195	2.359	1.605	2.130
<i>P</i>	0.016	0.022	0.030	0.028	0.017	0.108	0.034

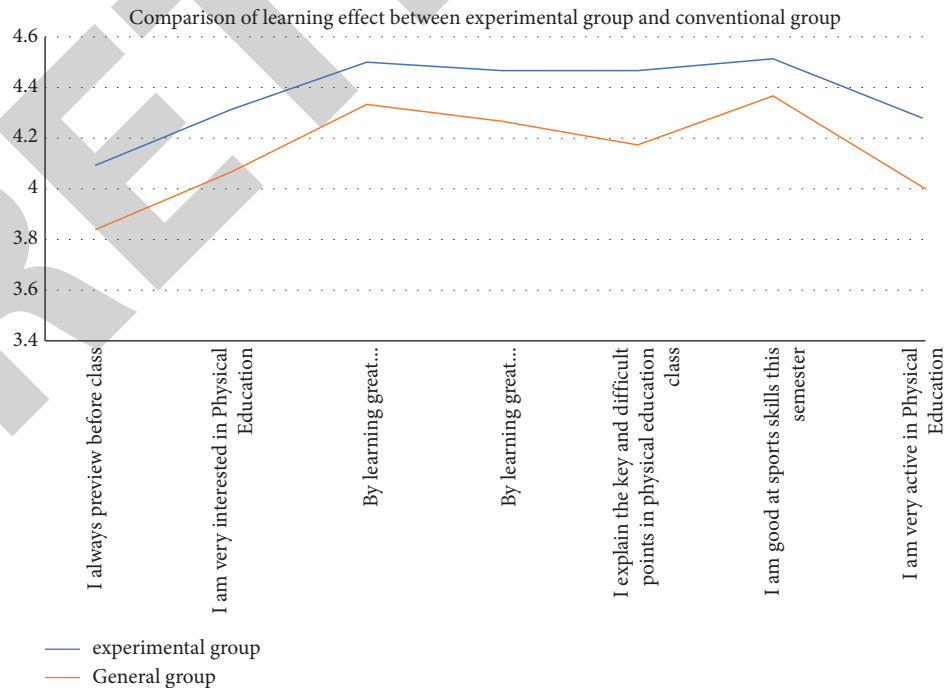


FIGURE 10: Comparison of learning effects between experimental group and regular group.

Survey on satisfaction of mixed physical education teaching mode

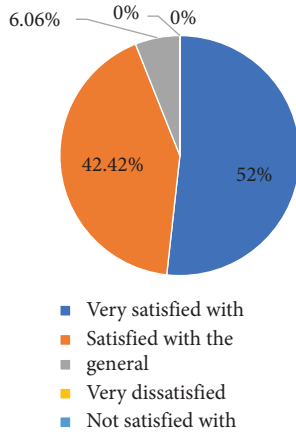


FIGURE 11: Satisfaction survey of mixed physical education teaching models.

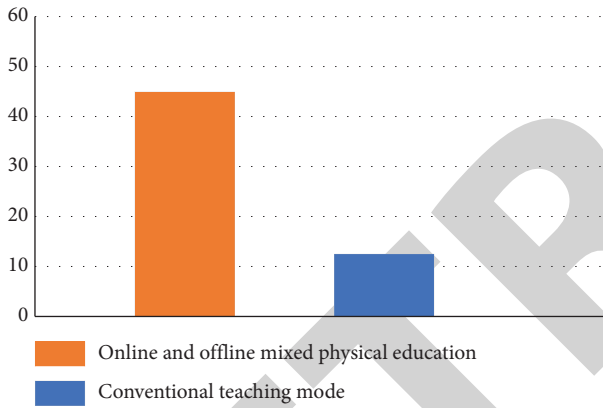


FIGURE 12: Comparison of students' attitudes towards mixed physical education and regular physical education.

that the mixed mode of physical education is deeply loved and approved by students, and this mode of teaching breaks the problem that conventional teaching is subject to the venue and cannot be guided in time. It can help students better learn relevant knowledge and skills so that students' grades can be improved. In this way, it will improve students' interest in learning and promote the development of mixed-mode physical education. A questionnaire survey was conducted on the question "Mixed-mode physical education and conventional teaching, which kind of teaching is preferred" and a total of 60 people were selected, of which 80% of the students chose mixed mode teaching, and only 20% chose conventional teaching as shown in Figure 12.

It can be seen that mixed teaching is more helpful for students' learning, enabling students to better learn knowledge and skills, break the conventional teaching thinking, and site restrictions, no longer let students be forced to learn, but to guide students, thereby improving students' learning effect and improving the quality of teachers' teaching.

#### 4.3. Calculation of Data Results

- (1) Using the evaluation index system represented in the figure in Section 3.4, the weight of each evaluation index is determined according to the needs, and the online and offline mixed teaching of physical education based on fuzzy comprehensive evaluation is set as  $E$ , and vice versa as  $H$ .

The weights are shown in Table 7.

##### 4.3.1. Comprehensive Evaluation of First-Level Indicators.

If  $R_{11} = \{0.4, 0.5, 0.1, 0, 0\}$ , the  $R_{11} = \{0.4, 0.5, 0.1, 0, 0\}$   $R_{12} = \{0.3, 0.3, 0.3, 0.1, 0\}$   $R_{13} = \{0.4, 0.2, 0.3, 0.1, 0\}$   $R_{14} = \{0.4, 0.4, 0.2, 0, 0\}$  fuzzy matrix between the first-level evaluation index and the evaluation level  $V$  is

$$R_1 = \begin{bmatrix} 0.4 & 0.5 & 0.1 & 0 & 0 \\ 0.3 & 0.3 & 0.3 & 0.1 & 0 \\ 0.4 & 0.2 & 0.3 & 0.1 & 0 \\ 0.4 & 0.4 & 0.2 & 0 & 0 \end{bmatrix}. \quad (25)$$

##### 4.3.2. Comprehensive Evaluation of Secondary Indicators.

According to Table 7, the secondary fuzzy evaluation matrix of the two teaching models  $A$  and  $B$  is obtained.

Prepare before class

$$R_1(E) = \begin{bmatrix} 0.3 & 0.6 & 0.1 & 0 & 0 \\ 0.2 & 0.5 & 0.3 & 0 & 0 \\ 0.6 & 0.2 & 0.2 & 0 & 0 \\ 0.4 & 0.5 & 0.1 & 0 & 0 \end{bmatrix}, \quad (26)$$

$$R_1(H) = \begin{bmatrix} 0.3 & 0.6 & 0.1 & 0 & 0 \\ 0.2 & 0.5 & 0.3 & 0 & 0 \\ 0.6 & 0.1 & 0.2 & 0.1 & 0 \\ 0.4 & 0.4 & 0.1 & 0 & 0 \end{bmatrix}.$$

In-class sessions,

$$R_2(E) = \begin{bmatrix} 0.2 & 0.7 & 0.1 & 0 & 0 \\ 0.3 & 0.6 & 0.1 & 0 & 0 \\ 0.4 & 0.4 & 0.2 & 0 & 0 \\ 0.3 & 0.5 & 0.2 & 0 & 0 \end{bmatrix}, \quad (27)$$

$$R_2(H) = \begin{bmatrix} 0.3 & 0.5 & 0.1 & 0.1 & 0 \\ 0.2 & 0.5 & 0.2 & 0.1 & 0 \\ 0.2 & 0.6 & 0.2 & 0 & 0 \\ 0.3 & 0.6 & 0.1 & 0 & 0 \end{bmatrix}.$$

Lecture content

$$R_3(E) = \begin{bmatrix} 0.4 & 0.6 & 0 & 0 & 0 \\ 0.5 & 0.4 & 0.1 & 0 & 0 \\ 0.5 & 0.3 & 0.2 & 0 & 0 \end{bmatrix}, \quad (28)$$

$$R_3(H) = \begin{bmatrix} 0.4 & 0.5 & 0.1 & 0 & 0 \\ 0.4 & 0.4 & 0.1 & 0.1 & 0 \\ 0.6 & 0.2 & 0.2 & 0 & 0 \end{bmatrix}.$$

TABLE 7: Statistical table of comprehensive evaluation results of mixed teaching mode.

First-level indicator (weight)	Secondary indicators (weights)	Rating (E)					Rating (H)				
		Excellent	Good	Middle	And	Difference	Excellent	Good	Middle	And	Difference
Preclass preparation (0.1800)	$U_{11}$ (0.2334)	0.3	0.6	0.1	0	0	0.3	0.6	0.1	0	0
	$U_{12}$ (0.2334)	0.2	0.5	0.3	0	0	0.3	0.4	0.3	0	0
	$U_{13}$ (0.3000)	0.6	0.2	0.2	0	0	0.6	0.1	0.2	0.1	0
	$U_{14}$ (0.1322)	0.4	0.5	0.1	0	0	0.4	0.4	0.1	0.1	0
Session during the lesson (0.1400)	$U_{21}$ (0.4111)	0.2	0.7	0.1	0	0	0.3	0.5	0.1	0.1	0
	$U_{22}$ (0.1823)	0.3	0.6	0.1	0	0	0.2	0.5	0.2	0.1	0
	$U_{23}$ (0.2822)	0.4	0.4	0.2	0	0	0.2	0.6	0.2	0	0
	$U_{24}$ (0.1332)	0.3	0.5	0.2	0	0	0.3	0.6	0.1	0	0
Lecture content (0.2400)	$U_{31}$ (0.5222)	0.4	0.6	0	0	0	0.4	0.5	0.1	0	0
	$U_{32}$ (0.2444)	0.5	0.4	0.1	0	0	0.4	0.5	0.1	0	0
	$U_{33}$ (0.2444)	0.5	0.3	0.2	0	0	0.6	0.2	0.2	0	0
Teaching method (0.1500)	$U_{41}$ (0.3111)	0.3	0.3	0.3	0.1	0	0.4	0.3	0.2	0.1	0
	$U_{42}$ (0.5000)	0.5	0.3	0.2	0	0	0.4	0.2	0.2	0	0
	$U_{43}$ (0.2222)	0.2	0.3	0.3	0.2	0	0.5	0.3	0.2	0	0
Teaching effect (0.2900)	$U_{51}$ (0.5333)	0.3	0.7	0	0	0	0.2	0.6	0.2	0	0
	$U_{52}$ (0.1322)	0.4	0.4	0.1	0.1	0	0.5	0.3	0.2	0	0
	$U_{53}$ (0.3776)	0.5	0.4	0.1	0	0	0.4	0.4	0.1	0.1	0

Teaching style

$$R_4(E) = \begin{bmatrix} 0.4 & 0.6 & 0 & 0 & 0 \\ 0.5 & 0.4 & 0.1 & 0 & 0 \\ 0.5 & 0.3 & 0.2 & 0 & 0 \end{bmatrix},$$

$$R_4(H) = \begin{bmatrix} 0.4 & 0.3 & 0.2 & 0.1 & 0 \\ 0.4 & 0.2 & 0.2 & 0 & 0 \\ 0.5 & 0.3 & 0.2 & 0 & 0 \end{bmatrix}.$$

(29)

In-class sessions,

$$B_2(E) = A_2 \cdot R_2(E)$$

$$= (0.23340.23340.30000.1222). \begin{bmatrix} 0.20.70.100 \\ 0.30.60.100 \\ 0.40.40.200 \\ 0.30.50.200 \end{bmatrix}$$

$$= (0.28840.56880.141600)$$

Teaching effectiveness

$$R_5(E) = \begin{bmatrix} 0.3 & 0.7 & 0 & 0 & 0 \\ 0.4 & 0.4 & 0.1 & 0.1 & 0 \\ 0.5 & 0.4 & 0.1 & 0 & 0 \end{bmatrix},$$

$$R_5(H) = \begin{bmatrix} 0.2 & 0.6 & 0.2 & 0 & 0 \\ 0.5 & 0.3 & 0.2 & 0 & 0 \\ 0.4 & 0.4 & 0.1 & 0.1 & 0 \end{bmatrix}.$$

(30)

$$B_2(H) = A_2 \cdot R_2(H)$$

$$= (0.23340.23340.50000.1332). \begin{bmatrix} 0.30.50.10.10 \\ 0.20.50.20.10 \\ 0.20.60.2 & 0 & 0 \\ 0.30.60.1 & 0 & 0 \end{bmatrix}$$

$$= (0.25440.54170.14650.05820).$$

(32)

Calculate the comprehensive fuzzy evaluation set of secondary indicators.

Prepare before class

$$B_1(E) = A_1 \cdot R_1(E)$$

$$= (0.23340.23340.50000.1222). \begin{bmatrix} 0.30.60.1 & 0 & 0 \\ 0.20.50.30.10 \\ 0.60.20.2 & 0 & 0 \\ 0.40.50.1 & 0 & 0 \end{bmatrix}$$

$$= (0.42000.420220.187600),$$

$$B_1(H) = A_1 \cdot R_1(H)$$

$$= (0.23340.23340.50000.1332). \begin{bmatrix} 0.30.60.1 & 0 & 0 \\ 0.30.40.3 & 0 & 0 \\ 0.60.10.20.10 \\ 0.40.40.10.10 \end{bmatrix}$$

$$= (0.43320.32670.18650.05220).$$

(31)

Lecture content

$$B_3(E) = A_3 \cdot R_3(E)$$

$$= (0.52220.23340.2334). \begin{bmatrix} 0.40.6 & 0 & 0 & 0 \\ 0.50.40.1 & 0 & 0 \\ 0.40.40.1 & 0 & 0 \end{bmatrix}$$

$$= (0.55770.47330.060000)$$

$$B_3(H) = A_3 \cdot R_3(H)$$

$$= (0.53340.23340.2334). \begin{bmatrix} 0.50.60.1 & 0 & 0 \\ 0.40.30.20.20 \\ 0.70.10.1 & 0 & 0 \end{bmatrix}$$

$$= (0.55770.407770.12440.03220).$$

(33)

Teaching style

$$\begin{aligned}
B_4(E) &= A_4 \cdot R_4(E) \\
&= (0.2000 \ 0.4000 \ 0.3000) \cdot \begin{bmatrix} 0.2 & 0.2 & 0.2 & 0.3 & 0 \\ 0.4 & 0.5 & 0.2 & 0 & 0 \\ 0.1 & 0.4 & 0.4 & 0.1 & 0 \end{bmatrix} \\
&= (0.3700 \ 0.020000 \ 0.26000 \ 0.06000), \\
B_4(H) &= A_4 \cdot R_4(H) \\
&= (0.2000 \ 0.6000 \ 0.3000) \cdot \begin{bmatrix} 0.3 & 0.4 & 0.3 & 0.2 & 0 \\ 0.3 & 0.1 & 0.3 & 0 & 0 \\ 0.5 & 0.3 & 0.2 & 0 & 0 \end{bmatrix} \\
&= (0.43000 \ 0.26000 \ 0.10000 \ 0.02000).
\end{aligned} \tag{34}$$

Teaching effectiveness

$$\begin{aligned}
B_5(E) &= A_5 \cdot R_5(E) \\
&= (0.6000 \ 0.1444 \ 0.3668) \cdot \begin{bmatrix} 0.4 & 0.6 & 0 & 0 & 0 \\ 0.5 & 0.5 & 0.2 & 0.2 & 0 \\ 0.4 & 0.5 & 0.3 & 0 & 0 \end{bmatrix} \\
&= (0.38760 \ 0.66000 \ 0.0600 \ 0.01220) \\
B_5(H) &= A_5 \cdot R_5(H) \\
&= (0.6000 \ 0.1444 \ 0.3668) \cdot \begin{bmatrix} 0.1 & 0.5 & 0.3 & 0 & 0 \\ 0.6 & 0.2 & 0.3 & 0 & 0 \\ 0.5 & 0.5 & 0.1 & 0.1 & 0 \end{bmatrix} \\
&= (0.31440 \ 0.48760 \ 0.16220 \ 0.03760).
\end{aligned} \tag{35}$$

**4.3.3. First-Level Fuzzy Evaluation Method.** The first step is to obtain a first-level fuzzy evaluation matrix based on the second-level fuzzy evaluation set, as follows:

$$\begin{aligned}
R(E) &= \begin{bmatrix} B_1 \\ B_2 \\ B_3 \\ B_4 \\ B_5 \end{bmatrix} = \begin{bmatrix} 0.4200 & 0.4022 & 0.1876 & 0 & 0 \\ 0.2884 & 0.5688 & 0.1416 & 0 & 0 \\ 0.5577 & 0.4733 & 0.0600 & 0 & 0 \\ 0.3700 & 0.2000 & 0.2600 & 0.0600 & 0 \\ 0.3876 & 0.6600 & 0.0600 & 0.0122 & 0 \end{bmatrix}, \\
R(M) &= \begin{bmatrix} B_1 \\ B_2 \\ B_3 \\ B_4 \\ B_5 \end{bmatrix} = \begin{bmatrix} 0.4332 & 0.3267 & 0.1865 & 0.0522 & 0 \\ 0.2544 & 0.5417 & 0.1465 & 0.0582 & 0 \\ 0.5577 & 0.4077 & 0.1244 & 0.0322 & 0 \\ 0.4300 & 0.2600 & 0.1000 & 0.0200 & 0 \\ 0.3144 & 0.4876 & 0.1622 & 0.0376 & 0 \end{bmatrix}.
\end{aligned} \tag{36}$$

The second step is to calculate the first-level fuzzy comprehensive evaluation set

$$\begin{aligned}
B(E) &= A \cdot (E) \\
&= (0.1700 \ 0.1300 \ 0.2500 \ 0.1600 \ 0.2910) \cdot \begin{bmatrix} 0.4200 & 0.4022 & 0.1876 & 0 & 0 \\ 0.2838 & 0.5799 & 0.1714 & 0 & 0 \\ 0.6644 & 0.4822 & 0.0600 & 0 & 0 \\ 0.3811 & 0.4000 & 0.2600 & 0.0600 & 0 \\ 0.3768 & 0.6600 & 0.0600 & 0.0143 & 0 \end{bmatrix} \\
&= (0.3805 \ 0.47920 \ 0.22910 \ 0.01500), \\
B(H) &= A \cdot (H) \\
&= (0.1700 \ 0.1500 \ 0.2300 \ 0.1600 \ 0.2800) \cdot \begin{bmatrix} 0.4222 & 0.3366 & 0.1876 & 0.0355 & 0 \\ 0.2533 & 0.5164 & 0.1535 & 0.0538 & 0 \\ 0.5577 & 0.5044 & 0.1322 & 0.0400 & 0 \\ 0.4300 & 0.2600 & 0.1000 & 0.0200 & 0 \\ 0.4133 & 0.4786 & 0.1733 & 0.0371 & 0 \end{bmatrix} \\
&= (0.37540 \ 0.48010 \ 0.14610 \ 0.02990).
\end{aligned} \tag{37}$$

Finally, the comprehensive evaluation is calculated.

If  $V$  (evaluation set) is assigned to  $V = \{95, 80, 70, 60, 50\}$ , the comprehensive evaluation result of mixed teaching is

$$M(E) = B(E).V^T$$

$$= (0.3905 \ 0.4728 \ 0.1180 \ 0.0144 \ 0) \cdot \begin{bmatrix} 95 \\ 80 \\ 70 \\ 60 \\ 50 \end{bmatrix} = 85.1. \quad (38)$$

The results of the comprehensive evaluation of routine teaching are as follows:

$$M(H) = B(H).V^T$$

$$= (0.3655 \ 0.4207 \ 0.1611 \ 0.0258 \ 0) \cdot \begin{bmatrix} 95 \\ 80 \\ 70 \\ 60 \\ 50 \end{bmatrix} = 83.0. \quad (39)$$

After calculating the results of both teaching methods, the results are between 80 and 95, and the evaluation results of mixed teaching are better than those of conventional teaching. That is, mixed teaching is better than regular teaching.

**4.4. Analysis of Results.** The fuzzy comprehensive evaluation is used to construct the online and offline hybrid teaching model of physical education courses, and the mixed teaching is evaluated, which solves the shortcomings of qualitative evaluation, combines qualitative and nonqualitative, and reduces the impact of human factors on its results, so as to make the fuzzy comprehensive evaluation more comprehensive, reasonable and accurate expression. In the calculation of data results, the preclass preparation, the middle of the class, the teaching content, the teaching method, the teaching effect are calculated, and the results obtained are that its mixed teaching is higher than that of conventional teaching, from which it can be obtained that mixed teaching provides a strong help for students to learn knowledge and teachers to teach knowledge.

## 5. Conclusion

Based on the construction of the online and offline hybrid teaching mode of physical education courses with fuzzy comprehensive evaluation, through the establishment of the fuzzy comprehensive evaluation model, the processing of fuzzy operators and indicators is determined, and the online and offline hybrid teaching model of physical education with fuzzy comprehensive evaluation is obtained, and the experiments are designed and the experiments are grouped into experimental groups (online and offline mixed teaching mode) and conventional groups (traditional teaching mode), and the two groups are prepared before class, in the middle

of class, teaching content, teaching methods, The teaching effect is calculated in these aspects, and the online and offline hybrid teaching model is analyzed and compared to obtain the online and offline hybrid teaching model, which not only improves the students' independent learning ability but also enables students to grasp the knowledge and skills taught in physical education faster and better, so that the teaching effect is greatly improved and the student's performance is also improved. Although this paper has achieved some results on this basis, we can also optimize and improve this problem, such as:

- (1) In the calculation of data results in this paper, the calculation process is too complicated to calculate the results in combination with programming
- (2) Fuzzy comprehensive evaluation is applied to the online and offline mixed mode structure study of physical education courses to show its advantages; in this regard, fuzzy comprehensive evaluation can be further optimized, which is also a direction for future research

## Data Availability

The experimental data used to support the findings of this study are available from the corresponding author upon request.

## Conflicts of Interest

The authors declared that they have no conflicts of interest regarding this work.

## Acknowledgments

The study was supported by Teaching reform project of Hubei Provincial Department of Education, China-Research on the practice of integrating "online and offline" mixed teaching mode into physical education curriculum under the background of normal professional certification (Grant no. 2021456).

## References

- [1] Tawakoni, "Teachers' conceptions of effective teaching and their teaching practices: a mixed-method approach," *Teachers and Teaching*, vol. 6, no. 23, pp. 674–688, 2017.
- [2] S. Hesse-Biber, "The problems and prospects in the teaching of mixed methods research," *International Journal of Social Research Methodology*, vol. 18, no. 5, pp. 463–477, 2015.
- [3] K. O. Remeasurement, "Point prediction of flatness geometric tolerance by using grey theory," *Precision Engineering*, vol. 25, pp. 33–37, 2011.
- [4] B. Baesens, R. Setiono, C. Mues, and J. Vanthienen, "Using neural network rule extraction and decision tables for credit-risk evaluation," *Management Science*, vol. 49, no. 3, pp. 312–329, 2003.
- [5] A. Nieto-Morote, "A fuzzy approach to construction project risk assessment," *International Journal of Project Management*, vol. 2, pp. 105–107, 2010.

## Retraction

# Retracted: Correlation Analysis between Early Reading Amount and Expressive Ability of Young Children Aided by Multiple Information Processing Techniques under the Heuristic Pattern

### Security and Communication Networks

Received 17 October 2023; Accepted 17 October 2023; Published 18 October 2023

Copyright © 2023 Security and Communication Networks. This is an open access article distributed under the Creative Commons Attribution License, which permits unrestricted use, distribution, and reproduction in any medium, provided the original work is properly cited.

This article has been retracted by Hindawi following an investigation undertaken by the publisher [1]. This investigation has uncovered evidence of one or more of the following indicators of systematic manipulation of the publication process:

- (1) Discrepancies in scope
- (2) Discrepancies in the description of the research reported
- (3) Discrepancies between the availability of data and the research described
- (4) Inappropriate citations
- (5) Incoherent, meaningless and/or irrelevant content included in the article
- (6) Peer-review manipulation

The presence of these indicators undermines our confidence in the integrity of the article's content and we cannot, therefore, vouch for its reliability. Please note that this notice is intended solely to alert readers that the content of this article is unreliable. We have not investigated whether authors were aware of or involved in the systematic manipulation of the publication process.

In addition, our investigation has also shown that one or more of the following human-subject reporting requirements has not been met in this article: ethical approval by an Institutional Review Board (IRB) committee or equivalent, patient/participant consent to participate, and/or agreement to publish patient/participant details (where relevant).

Wiley and Hindawi regrets that the usual quality checks did not identify these issues before publication and have since put additional measures in place to safeguard research integrity.

We wish to credit our own Research Integrity and Research Publishing teams and anonymous and named external researchers and research integrity experts for contributing to this investigation.

The corresponding author, as the representative of all authors, has been given the opportunity to register their agreement or disagreement to this retraction. We have kept a record of any response received.

### References

- [1] F. Duan, J. Zhou, and P. Li, "Correlation Analysis between Early Reading Amount and Expressive Ability of Young Children Aided by Multiple Information Processing Techniques under the Heuristic Pattern," *Security and Communication Networks*, vol. 2022, Article ID 8139963, 11 pages, 2022.

## Research Article

# Correlation Analysis between Early Reading Amount and Expressive Ability of Young Children Aided by Multiple Information Processing Techniques under the Heuristic Pattern

Fude Duan,<sup>1</sup> Jianhua Zhou<sup>2</sup>,<sup>3</sup> and Peng Li<sup>3</sup>

<sup>1</sup>Department of Chinese Literature, Ganzhou Teachers College, Ganzhou 341000, China

<sup>2</sup>Institute of Education, Xiamen University, Xiamen, Fujian 361005, China

<sup>3</sup>Department of Chinese Literature, Ganzhou Teachers College, Ganzhou, Jiangxi 341000, China

Correspondence should be addressed to Jianhua Zhou; [zhoujh@stu.xmu.edu.cn](mailto:zhoujh@stu.xmu.edu.cn)

Received 1 July 2022; Revised 9 August 2022; Accepted 20 August 2022; Published 27 September 2022

Academic Editor: Hangjun Che

Copyright © 2022 Fude Duan et al. This is an open access article distributed under the Creative Commons Attribution License, which permits unrestricted use, distribution, and reproduction in any medium, provided the original work is properly cited.

The cultivation of reading ability runs through a child's life. Children are in a critical period of early reading ability formation. Only based on the actual development characteristics of children and adopting effective training methods, can early childhood educators better meet the needs of children's long-term development. Based on the data of 22 classes in 7 public kindergartens in X City in Mainland of China, this study first compared the effects of two different teaching modes and then analyzed the relationship between early reading amount and expressive ability of children. Independent sample *T* test, OLS regression, and Lasso regression were used to demonstrate the correlation between early reading amount and expressive ability, and the possible mechanisms of family background are also explored. The results show the following: firstly, heuristic teaching mode has positive teaching effect. The effect quantities of heuristic teaching mode on transmission ability, communication ability, transfer ability, and generalization ability are 0.21, 0.25, 0.31, 0.30, and 0.32, respectively, which belong to medium intensity, indicating that heuristic teaching mode has a good intervention effect on improving students' expression ability. Secondly, there is a high correlation between early reading and children's expressive ability. Thirdly, there are two aspects of the influence of early reading amount on children's expressive ability: explicit influence and implicit influence. Fourthly, the association between early reading and different presentation skills is not the same. To sum up, we should actively encourage the use of heuristic teaching mode, realize the heterogeneity of early reading amount, and promote the improvement of children's expressive ability through both explicit and implicit paths.

## 1. Introduction

Expressive ability is one of the common ability young children rely on to communicate with others. It is the ability to express one's thoughts, feelings, ideas, and intentions clearly and unambiguously in words, characters, graphics, expressions, gestures, etc. The better the ability to express oneself, the better others can understand and appreciate what one wants to express. Previous research has explored the influencing factors of children's expression ability from multiple angles. For preschool children, expression ability is closely related with their family environment, which is very important to the children's development in the future. The

focus on expressive ability has rich education significance and great research value. Existing research shows that different education methods and educational ideas will have different effects on the development of children's expression ability. Therefore, for kindergartens and parents, it is worth pondering how to take effective educational measures to promote the complete and all-round development of children's expression ability. Unfortunately, no researchers have explored children's expressive ability based on longitudinal follow-up data, and the existing correlation evidence has failed to control the influence of some interfering factors [1].

Based on previous theory and practice, this research will adopt three-phase tracking data, perform in-depth analysis

of the influence factors of children's expressive ability, and at the same time, based on the perspective of early reading, analyze the key influencing factors and correlation coefficient in mechanism, and provide valuable advice for the practical level of education workers.

In addition, the data of this study are mainly from front-line practical classes. After teaching, teachers use the remaining 10 to 15 minutes of class to measure children's expressive ability and store the statistic in the data system for data analysis. Students' family background and demographic data are collected from the information platform of the school and matched based on students' IDs.

Teaching models have a significant impact on young children's representational skills. Therefore, this paper takes the teaching model as one of the core concepts of the study. Teaching mode refers to the following: "it systematically explores the interaction between educational objectives, teaching strategies, curriculum design, and teaching materials, as well as social and psychological theories to model teachers' behavior in various alternative types of teaching." The teaching mode is divided into traditional teaching and heuristic teaching in this study. The traditional teaching mode is a teacher-centered, book-centered, and classroom-centered teaching mode. Heuristic teaching is conducted according to the purpose of teaching, content, students' knowledge level, and the law of knowledge. Using a variety of teaching tools, the inspirational and inducement approach is used to impart knowledge and develop abilities so that students can learn actively to promote physical and mental development.

Early reading refers to "providing infants and toddlers with materials related to visual stimulation and allowing them to receive information about the materials. Based on observation, thinking, and imagination, infants and toddlers can make initial comprehension and verbal expression of the material, express their own opinions, and listen to adult narratives. From 1997 to 2000, the American Council on Early Reading pointed out in its research report, "Preventing Dyslexia in Children at an Early age," that there were about 2.56 million school-age children with dyslexia in the United States, accounting for 4.43% of the total school-age population from 6 to 21 [2, 3]. About 80 percent of children with learning difficulties in the United States are dyslexic, and forty percent of U.S. citizens cannot read effectively or even cannot read, which has affected their daily life and the functioning of the social work system. The research report once again put forward the importance of early reading from the perspective of preventing reading difficulties, which has aroused strong response in major educational developed countries in the world. In China, research on early reading education mainly includes the exploration of activities, such as reading materials, reading instruction, and activity evaluation, involved in early reading education in kindergartens and families, and there is still a vague understanding of the basic issues of early reading. Early reading helps children to contact written language, develop their behavior of learning written language, and lay a good foundation for formal written language learning in school age. It is an important way to improve children's language ability. Early

reading can enrich children's vocabulary, broaden their knowledge, expand the scope of life and learning, form good listening and speaking habits, and help children communicate in appropriate languages. In this study, early reading mainly refers to the general vocabulary mastered by students before entering school.

## 2. Research Design

**2.1. Experiment Groups.** The grouping of teaching model is as follows: a total of 22 classes from 7 kindergartens received instructor training. Among them, 11 class is set as the experimental group. The teacher has carried on the experimental training for 2 months. The system theory of heuristic teaching mode, teaching the key core, was carried on during the study and practice.

The control group was composed of the remaining 11 classes. The teachers also participated in the training without learning heuristic teaching, however, they carried out communication and discussion according to the conventional teaching plan to ensure that the teachers in the experimental group would not get experimental intervention, except for the heuristic teaching mode, because of the training. In the middle of the experiment, 1 experimental group and 2 control groups quit the training because of insufficient training time and failed to pass the assessment.

**2.2. Survey Subjects.** The subject data were selected by the convenience sampling method from 22 classes in 7 public kindergartens in X City from March 1, 2019, to June 1, 2019. Inclusion criteria are as follows: (1) children aged 3 to 5 years, (2) normal IQ, and (3) parents and teachers were informed, and they agreed to the study. Exclusion criteria are as follows: (1) class teacher training fails to reach the standard, and (2) students could not understand the content of the scale. According to the previous analysis, the sample size was 10 times the number of scale items, and the 20% loss to follow-up rate (elimination, shedding, etc.) was considered. Therefore, at least 144 questionnaires should be issued in this study. Finally, 240 questionnaires were sent out and 221 valid questionnaires were collected, with a sample recovery rate of 92.08%. There were 115 males (52.0%) and 106 females (48.0%).

**2.3. Scale Design.** The hybrid research method, including qualitative research with quantitative research, was used in this study. Firstly, the researcher analyzes and summarizes the concept and dimensions of expressive ability in pre-school education using a large number of literatures, reading, and interviews with all teachers involved in training, which are subdivided into four dimensions, namely transmission ability, communication ability, migration ability, and generalization ability. The transmission ability is based on the students' improvisation, while the generalization ability is based on the teacher's evaluation of the simplification of students' retelling stories. Communication ability is to investigate young children involved in communication with teachers' story elements of the



comprehensive migration ability, which refers to the communication of ideas about the story by involving the children [4].

SPSS25.0 software was used for statistical analysis. Qualitative data were described by frequency and percentage (%). The scale validity was evaluated by content validity and structure validity, which is evaluated by Cronbach's  $\alpha$  coefficient and retest reliability. The critical ratio method and correlation analysis method were used to judge the differentiation and suitability of scale items. The content validity of the scale was evaluated by the expert consultation method, and the structure validity was evaluated by the confirmatory factor analysis. Cronbach's  $\alpha$  coefficient and split-and-half reliability were used to evaluate the reliability of the scale.

The quality of the teacher's scoring from student data collected in the teacher's class is assessed to test the reliability and validity of the data obtained using Cronbach's  $\alpha$  coefficient for reliability evaluation. Among them, the total  $K$  is for measurement subject,  $S_i^2$  is the variation situation of the subject, and  $S_x^2$  is all questions of total variance, and they are extracted with the use of the average variance combination reliability to evaluate the questionnaire topic structure validity, where  $\lambda$  is the factor load,  $N$  is the sample size, and  $\epsilon$  is the error term. The specific formulas are as follows:

$$\begin{aligned}\alpha &= \frac{K}{K-1} \left( 1 - \frac{\sum S_i^2}{S_x^2} \right), \\ \text{AVE} &= \frac{(\sum \lambda^2)}{N}, \\ l_{CR} &= \frac{(\sum \lambda)^2}{(\sum \lambda)^2 + \sum \epsilon}.\end{aligned}\quad (1)$$

The transmission ability evaluated by teachers is on the basis of children's retelling of the story of the "little white rabbit." Teachers need to assess three small paragraphs that involve repeat key words and key elements of scores. In this situation, students communicate with the students in the back row and share the story information they just got from the teacher. Communication ability is composed of students' expressions observed by teachers in the process of communicating with teachers and other students. Teachers focus on whether students have inappropriate details or unclear themes. The four stories are randomly distributed to students. Students' transfer ability is based on their situational response. Teachers randomly check whether they can retell a story similar to the one they read. Teachers score students according to their expression of grammar and vocabulary. Considering that different evaluation criteria may lead to unclear distribution of scoring data, the scale and scoring were revised for several rounds to ensure that students' presentation ability could be measured more accurately. RMSEA and CFI are used to describe the matching degree of the model.

After several rounds of testing of the reliability and validity of items in questionnaire and teacher evaluation

criteria, scale and dimensions all passed the standard of reliability and validity. RMSEA and CFI, which represent model fitting, also reach the standard. The concrete numerical value is shown in Figure 1.

**2.4. Data Collection.** In addition to the children's expressive ability collected through measurement, this study also collected information on gender, age, family background, and early reading amount of students through a questionnaire survey of parents. The family background based on Bourdieu's theory of capital is subdivided into three types: economy, culture, and society. Economic capital is composed of parents' annual income standardized scores. Cultural capital is transformed by parents' years of schooling. Social capital is classified according to the occupation of parents and occupational standards, and scored by the expert method. Bourdieu believes that children's family cultural background is long-term. Hence, we should pay attention to the possibility of cultural atmosphere and provide more choices for children. For example, family culture will affect children's visual cognitive ability and computing ability [5, 6].

A further fitting of family background variables was carried out by AHP hierarchy. It is a system engineering method that regards a complex multiobjective decision-making problem as a whole, decomposes the overall objective into multiple subobjectives or criteria, and then further decomposes into several levels of multiple indicators or criteria and constraints to decompose into an orderly hierarchical structure. Through the method of fuzzy quantification of qualitative indicators to calculate the single ranking (weight number) and total ranking of each level are calculated based on fuzzy quantification for qualitative indicators to optimize the decision-making of multi-objective, multi index and multi scheme.

The weight vector was fitted by the least square method to minimize the sum of the squares of residuals. The expression is as follows:

$$\begin{aligned}\min Z &= \sum_{i=1}^n \sum_{j=1}^n (a_{ij}w_j - w_i)^2 \sqrt{b^2 - 4ac} \\ \text{s.t. } \sum_{i=1}^n w_i &= 1 \\ w_i &> 0, \quad i = 1, 2, \dots, n.\end{aligned}\quad (2)$$

$W_i$  is the regression coefficient of economic capital, cultural capital, and social capital in the calculation formula of family background, and family background is further expressed as follows:

$$\text{ESCS}_i = \beta_0 + W_1 \text{Economic}_i + W_2 \text{Culture}_i + W_3 \text{Social}_i + \epsilon_i. \quad (3)$$

In addition, since parents cannot have an objective and unified evaluation of students' early reading amount, the estimation of early reading amount needs to be realized based on certain algorithms. The C4.5 algorithm is adopted

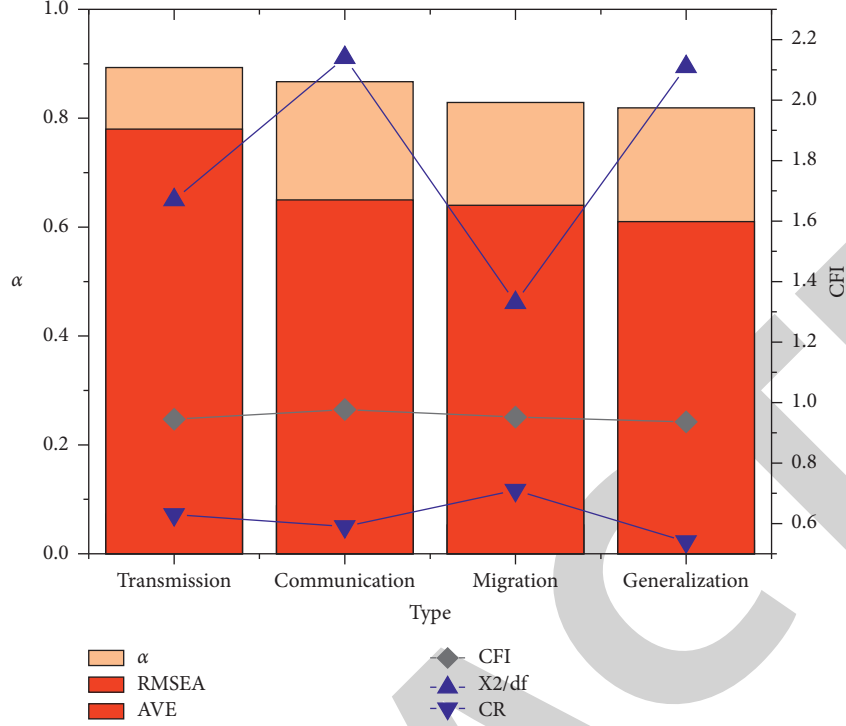


FIGURE 1: Scale quality.

in the decision tree model to do the estimation. The algorithm uses the maximum information gain rate as a measure of node splitting. The use of information gain rate to select attributes can handle incomplete data while avoiding the disadvantage of selecting attributes with too many offset values.

A series of questions on students' reading behavior were set for parents, and the final reading amount was fitted based on these decision attributes. The decision tree adopts the top-down recursion method, which is a data mining method that classified data through a series of rules. It has a variety of algorithms [7], among which the CHAID algorithm is the chi-squared automatic interaction detector [8]. According to the type of variables, the data was segmented optimally using the chi-square test or variance analysis principle, and the multivariate contingency table was automatically divided according to the  $P$ -value to generate a multifork tree, which supported discrete target variables and continuous target variables, and the main influencing factor 0 can be efficiently mined. When a variable is a continuous variable, the CHAID algorithm will determine its grouping according to the analysis of variance from the root node. Each step in the selection and target variable has the strongest effect of input variables. If the category of each input variable has no statistically significant differences between the target variable, it will be merged. When the node data and  $P$  value (the significance level, common standard is 0.05) cannot meet the set requirements, the algorithm will stop segmentation.

The attribute values are compared in the internal nodes of the decision tree, and the branch down from this

node is judged according to different attribute values. A path in the leaf node of the decision tree corresponds to a joining rule, and the whole decision tree corresponds to a set of disjunctive expression rules. One of the biggest advantages of the learning algorithm based on the decision tree is that it does not require users to know a lot of background knowledge in the learning process (which is also its biggest disadvantage). As long as training examples can be expressed in the way of attribute-conclusion, the algorithm can be used to learn. This algorithm is briefly described as follows:

$$\text{SplitInfomation}_A(s) = - \sum_{j=1}^m \frac{|S_j|}{|S|} \log_2 \frac{|S_j|}{|S|}. \quad (4)$$

The formula above is the calculation of the splitting of decision attributes. In the formula, training set  $S$  is divided into  $m$  subsets by training math  $A$ .  $|S_j|$  denotes the size of the sample in the  $j$  subdata set, and  $|S|$  represents the total sample size. Whether the value of attribute  $A$  is the best splitting attribute can be judged by calculating the gain information of attribute  $A$  after sample splitting [9]. The calculation formula of gain information is shown in the following formula:

$$\text{InfoGain}(S, A) = E(S) - E_A(S). \quad (5)$$

Finally, on the basis of these equations, information entropy is further calculated.  $E(S)$  is the entropy of training data set  $S$ , and  $E_A(S)$  is the information entropy of attribute  $A$  after splitting. The calculation formulas of  $E(S)$  and  $E_A(S)$  are as follows:

$$\begin{cases} E(S) = -\sum_{i=1}^N p(x_i) \log_2 p(x_i), \\ E_A(S) = -\sum_{j=1}^m \frac{|S_j|}{|S|} E(S_j). \end{cases} \quad (6)$$

**2.5. Evaluation Methods.** This study mainly tests the correlation between early reading amount and children's expressive ability, and it will use independent sample *T* test, multiple linear regression, and LASSO regression model to explore the relationship between the two. Lasso regression is a least square problem with limited regression coefficients, which can better deal with the "over learning" problem in model learning and realize variable selection while estimating model parameters

In the evaluation, firstly, the independent sample *T*-test was used to demonstrate the positive effect of the heuristic teaching model. Then, multiple linear regression was used to calculate the regression coefficient of the early reading amount. Finally, a lasso model was established to further test the correlation between the two.

**2.6. Research Procedures.** To sum up, in the first round of data sampling, this study first conducted a questionnaire survey among parents, interviewed teachers, generated scales, and conducted reliability and validity tests. It then generated students' early reading amount in the second round of data sampling and finally generated the final ability variables in the third round of data sampling. The flow chart is shown in Figure 2.

### 3. Research Results

**3.1. Preliminary Difference Analysis.** The differences between the groups in early reading, transmission ability, communication ability, migration ability, and generalization ability are shown in Figure 3. Preliminarily, the score of the experimental group in expression ability is significantly better than the control group, and the early reading amount is also higher than the control group.

The independent sample *T* test was further used to analyze the differences between the two groups and prove the positive significance of the heuristic teaching mode from the data level [10]. The score of the experimental group using the heuristic teaching mode is significantly higher than that of the experimental group using the traditional teaching mode. The difference analysis data are shown in Figure 4. According to the data in the figure, there are significant differences in the four abilities and early reading amount between the two groups of data, among which the difference in transmission is the most obvious.

The difference value is converted into effect value, and the calculation formula is as follows:

$$s = \sqrt{\frac{(n_1 - 1)s_1^2 + (n_2 - 1)s_2^2}{n_1 + n_2 - 2}}, \quad (7)$$

$n_1$  and  $n_2$  are the sample sizes of the two groups of data,  $s_1$  and  $s_2$  are the standard deviations of the two groups of samples, and the standard deviations of the samples are obtained after dimensionalization. In the case of mean comparison between the two groups, it is most intuitive to use the mean difference between the two groups as the effect size. However, in psychological studies, when the mean difference of original data is used as the effect size, there will be problems of unit inconsistency, and the effect size cannot be compared between studies. Cohen [11] proposed to replace the original mean difference with the standardized value of the mean difference, which is the basis of the differential effect size. Based on the sample number  $n$  of the experimental group and the control group, the combined standard deviation  $s$  was calculated, and the mean score of the experimental group and the control group was calculated at the same time. The effect size value was calculated using the following formula:

$$d = \frac{\bar{x}_1 - \bar{x}_2}{s}. \quad (8)$$

There are two interpretations of effect size. One is the relative position (percentile grade) of the experimental group's mean value in the control group, and the other is the degree of nonoverlap between the distributions of the two groups. Cohen proposed that  $d=0.2$ ,  $d=0.5$ , and  $d=0.8$  correspond to small, medium, and large effect sizes, respectively. The "percentage grade of the experimental group mean in the control group" corresponding to these three effect sizes are 58%, 69%, and 79%, respectively, and the "proportion of nonoverlapping distribution between the two groups" are 14.7%, 33.0%, and 47.4%, respectively. However, Cohen cautioned against blindly using this standard. The effect size of heuristic teaching mode on transmission ability, communication ability, transfer ability, and generalization ability were 0.21, 0.25, 0.31, 0.30, and 0.32, respectively, which were of moderate intensity, indicating that heuristic teaching mode had a good intervention effect on improving students' expressive ability.

**3.2. Regression Prediction under Heuristic Teaching Model.** In spite of the positive effects of heuristic teaching model, researchers still hope to establish the relationship between early reading amount and students' expressive ability. Based on this, the regression model is constructed. Firstly, model (11) is constructed, and only demographic variables and family background variables are included. Ability<sub>*i*</sub> is student *i*'s expressive ability score, and Family<sub>*i*</sub> is the final fitting family background score. Background is the background variable of the student.

$$\text{Ability}_i = \beta_0 + \beta_1 \text{Background} + \beta_2 \text{Family}_i + \varepsilon_i. \quad (9)$$

Then, the variables of early reading volume were included to build model (12), represented as Reading<sub>*i*</sub>, and it

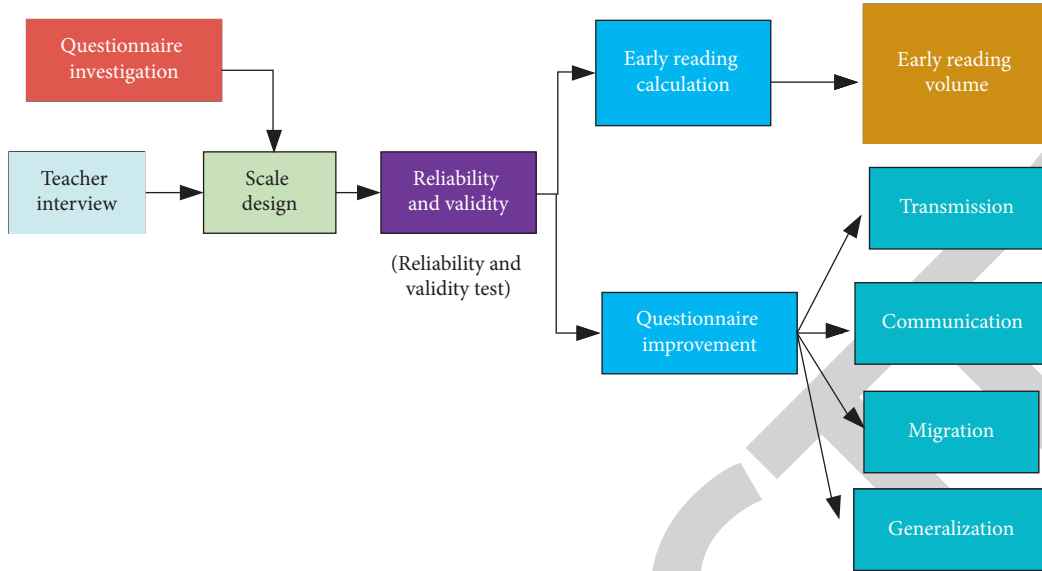


FIGURE 2: Research process.

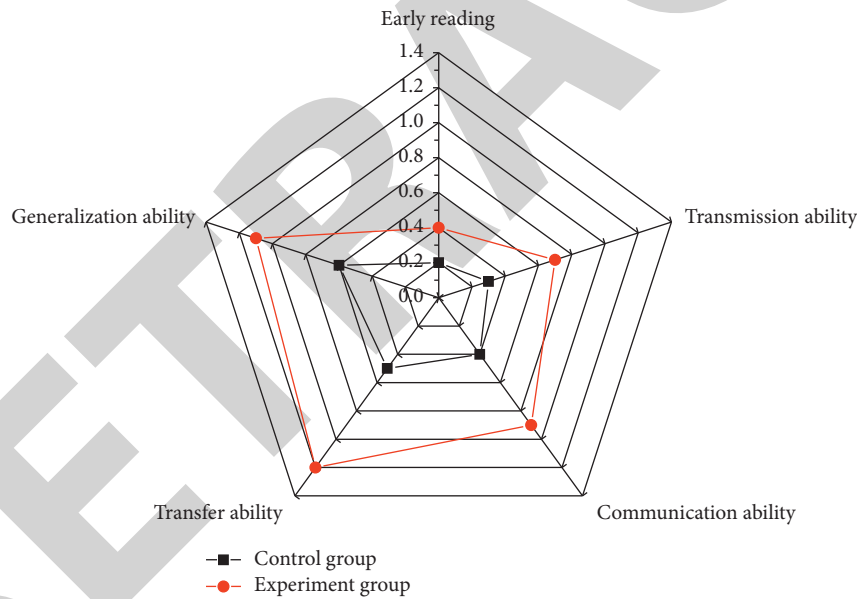


FIGURE 3: Experimental group and control group radar diagram.

was determined whether early reading volume had a good explanatory power by observing changes in  $R^2$ .

$$\text{Ability}_i = \beta_0 + \beta_1 \text{Background} + \beta_2 \text{Family}_i + \beta_3 \text{Reading}_i + \varepsilon_i. \quad (10)$$

Based on this, multiple linear regression was constructed to calculate the regression coefficients of demographic variables and family background variables, respectively, with transmission ability, communication ability, migration ability, and generalization ability as dependent variables, and then, they included the early reading amount. The specific regression coefficients are shown in Figure 5. The bars in the

figure show the effect of each variable on the four abilities. Gender has a significant impact on students' ability of expression. Girls' ability of expression is 0.12–0.24 standard points higher than boys' ability of expression. Family background also has a significant impact on students' ability of expression. The regression coefficients ranged from 0.13 to 0.19.

After the variables of early reading amount were added, the goodness of fit of the model was significantly improved, indicating that early reading amount had a good explanatory power to students' expressive ability. As can be seen in Figure 6, for each unit increase in early reading, students' transmission ability, communication ability, migration

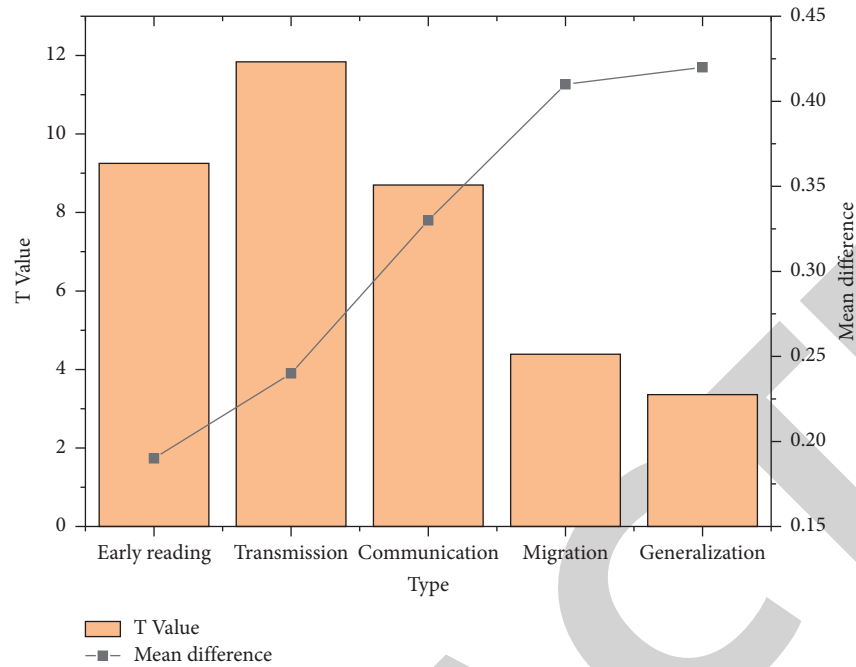


FIGURE 4: Difference analysis.

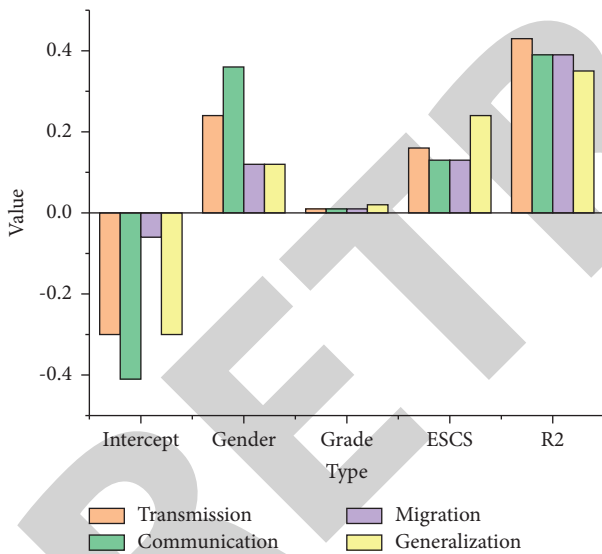


FIGURE 5: OLS statistic.

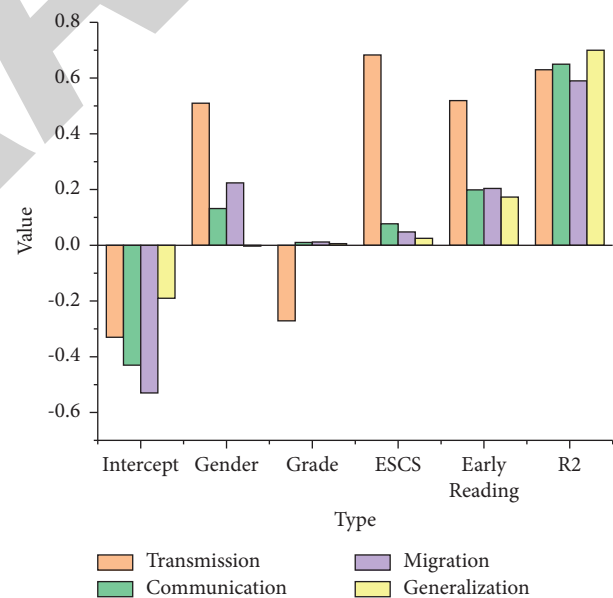


FIGURE 6: OLS2.

ability, and generalization ability will increase by 0.519 points, 0.199 points, 0.204 points, and 0.173 points, all at the level of 0.01, indicating that children's early reading amount does improve their later expression ability.

**3.3. Correlation Test Based on Ridge Regression and Lasso Regression.** Considering that the economic, cultural, and social capital of the subordinate dimensions of the family background variable may have different relationships with the early reading amount, it should be differentiated and further controlled. To ensure that the inclusion of such

multivariable will not bring collinearity interference, the prediction was carried out using the range regression and lasso regression.

Ridge regression is a linear model commonly used in regression analysis. It can effectively prevent the overfitting of the model. In ridge regression, the model will retain all the characteristic variables but will reduce the weight value of the characteristic variables, and the unified influence of the characteristic variables on the prediction results becomes smaller. This method, which avoids overfitting by retaining all eigenvectors and reducing only the coefficient values of

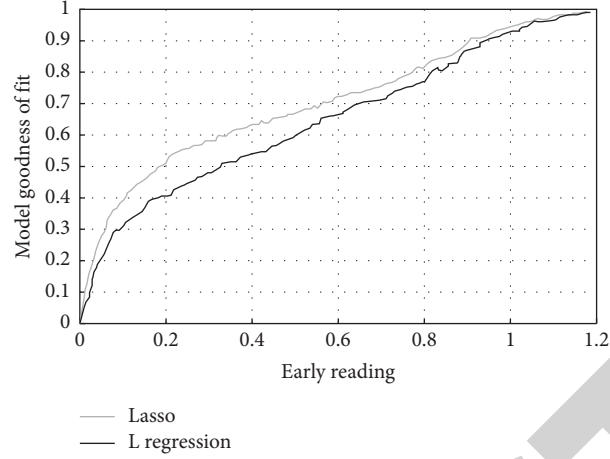


FIGURE 7: ROC curve.

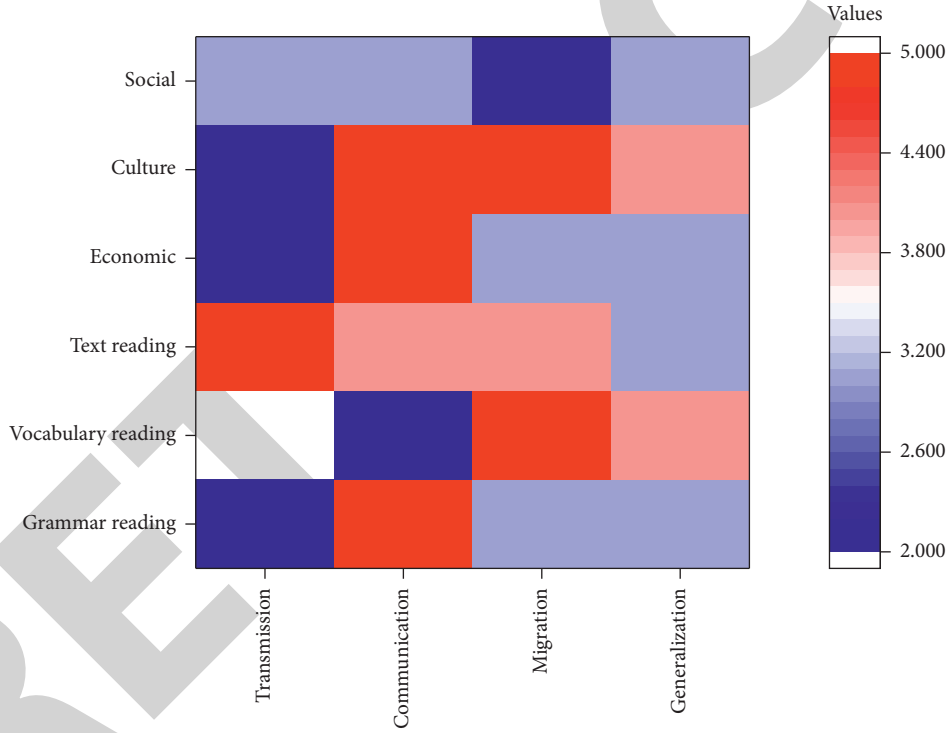


FIGURE 8: Correlation coefficient heat map.

eigenvectors, is called *L2* regularization. *L2* regularization formula is very simple, directly adding the sum of the squares of weight parameters, which is represented as  $w_j$  in the subsequent formula, on the basis of the original loss function, and  $E_{in}$  is the penalty parameter in the model.

$$L = E_{in} + \lambda \sum_j w_j^2. \quad (11)$$

Lasso regression is a regularization model for linear regression in addition to ridge regression. Like ridge regression, it also limits the coefficient of feature vector to a range very close to 0, however, it limits the coefficient in a

different way. It directly adds the absolute value of weight parameters on the basis of the original loss function. Different from the previous formula, this time, the weight is an absolute value, avoiding excessive fitting, and the specific formula is as follows:

$$L = E_{in} + \lambda \sum_j |w_j|. \quad (12)$$

In this study, the two methods were used for model fitting, and ROC curves were drawn to compare the goodness of fit of the two models, which can be seen in Figure 7. The comparison showed that the goodness of fit of

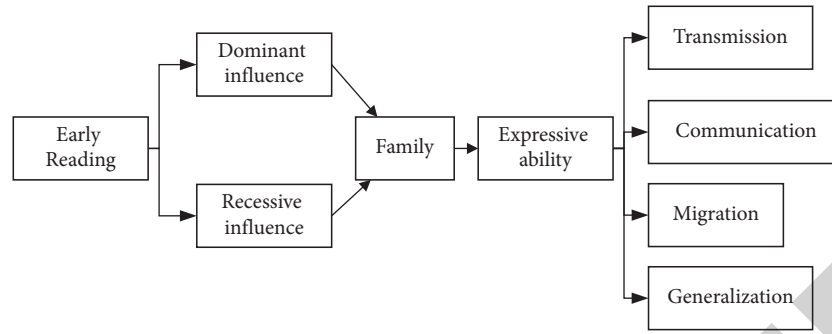


FIGURE 9: Mechanism analysis.

Lasso regression was higher than that of ridge regression, and lasso regression kept higher explanatory power in early reading.

Therefore, this paper further analyzes the relationship between economic capital, cultural capital, social capital, early reading, and the four expressive abilities, and it presents them in the way of heat map.

According to the heat map (as shown in Figure 8), different amount of early reading has different influence on expressive ability. Specifically, grammar reading has the greatest correlation with communication ability, vocabulary reading has the greatest correlation with transfer ability, and text vocabulary has the greatest correlation with transmission and communication ability. At the level of family background, the correlation of cultural capital is greater than that of other capital, which indicates that cultural capital is one of the variables with profound influence on students' cognitive ability.

**3.4. Mechanism Analysis of Early Reading and Expressive Ability.** Finally, the researchers analyzed the possible influence mechanism of early reading quantity from two aspects of dominant influence and recessive influence. The mechanism diagram is shown in Figure 9. First of all, the dominant effects mainly refer to reading and expression ability, and both belong to the category of cognitive dimension. The individual's early reading can also be regarded as a kind of capital accumulation for the future cognitive behavior [12]. To master certain cognitive ability, the individual makes cognitive investment. The more cognitive capital accumulation in the early stage, the faster the individual can master the cognitive ability of the next stage [13, 14]. In terms of recessive influence, the accumulation of individual reading may not directly promote the improvement of their cognitive ability but will affect the generation of their noncognitive ability. For example, students with more early reading experience may have better learning attitude, confidence, and motivation, which will also obviously improve their expression ability [15, 16].

It should be noted that family plays a "black box" role between these two kinds of influence and expressional ability, and the two kinds of influence are not doomed to promote the improvement of expressional ability. Family may play a role in promoting and improving the positive

influence of early reading, however, it may also play a role in eliminating and offsetting a part of the positive influence.

## 4. Research Conclusions

**4.1. Heuristic Teaching Mode Has High Application Value.** This study found that compared with other teaching modes, students in the heuristic teaching mode performed significantly better than those in the control group in all aspects, which demonstrated the teaching value of this mode. Heuristic teaching is a dynamic, open, and orderly system. It is the main direction of modern education and teaching reform to constantly emphasize students' subjectivity. The traditional teaching mode is mostly one-way communication with teachers as the main body, which greatly ignores the enthusiasm and initiative of students in learning. This study demonstrates the precious value of heuristic teaching mode based on the experimental data, which is a more robust piece of evidence.

**4.2. There Is a High Correlation between Early Reading Amount and Children's Expressive Ability.** The baby is still in the stage of language development [17], and children's early reading amount was positively correlated with an expressive ability according to the basic data statistics on all the expressive ability [18]. That is to say, as a general cognitive ability, high reading amount in early stage will account for high expression ability. In contrast, if the amount of early reading is insufficient, children will not be able to achieve the accumulation and precipitation of knowledge, and it will affect the control and play of the language environment and language use. This finding suggests that some early book reading is very important. Teachers or parents should focus on developing children's interest in reading and helping them to develop some basic reading skills. The only way for children to develop good reading habits is to learn how to read properly.

**4.3. The Correlation between Early Reading Amount and Children's Different Expressive Ability Is Different.** For student, the sufficient early reading amount means specific prerequisites for further learning. As a prerequisite, sufficient vocabulary provides efficiency for children to establish

association with novel knowledge. However, this study also found that the facilitating value of early reading amount for four dimensions of expressive ability are not the same. According to Piaget's theory of cognition [19], language and thought are interdependent, and reading and expression may be the same. However, for each smaller dimension, the mechanism can be complex and entirely different. It means that the impact of early reading on students' overall ability may be a process of dramatic change.

**4.4. Family Background Plays an Important Role.** In general, there are two ways that family background influences children's expressive ability: firstly, families influence children's expressive ability using their social and economic resources to compete and purchase high-quality educational resources. Secondly, parents cultivate children's learning interest and habits through educational participation and behavioral support, thus affecting children's ability to express. In both paths, early reading amount is a potential mediator variable [20, 21].

However, it should be noted that young children's development is influenced by local sociocultural and family backgrounds. Because of the constraints of the study, the sample selected in this paper did not take into account the influence of geographical factors. Therefore, the findings do not represent the developmental patterns and characteristics of young children across the country. Therefore, the data from other regions should be analyzed in the follow-up study to consider the influence of geographical factors.

## Data Availability

The experimental data used to support the findings of this study are available from the corresponding author upon request.

## Conflicts of Interest

The authors declare that they have no conflicts of interest regarding this work.

## Acknowledgments

This study was supported by Research project of basic Education in Jiangxi Province in 2020: Research on reading assistance for rural preschool children under the guidance of "reading with adults" (No. SZUGGYW2020-965).

## References

- [1] I. E. Boerma, S. E. Mol, and J. Jolles, "The role of home literacy environment, mentalizing, expressive verbal ability, and print exposure in third and fourth graders' reading comprehension," *Scientific Studies of Reading*, vol. 21, no. 3, pp. 179–193, 2017.
- [2] I. L. V. D. Spek, M. C. J. P. Franken, R. M. Swarte, and N. W. Kuperus, "Validity of an early parent-report questionnaire for language disorder in very preterm children from 2 to 10 years of age," *European Journal of Paediatric Neurology*, vol. 34, pp. 1–6, 2021.
- [3] T. V. Phan, D. M. Sima, C. Beelen, J. Vanderauwera, D. Smeets, and M. Vandermosten, "Evaluation of methods for volumetric analysis of pediatric brain data: the child metrix pipeline versus adult-based approaches," *Neuroimage Clinical*, vol. 19, pp. 734–744, 2018.
- [4] R. W. Cheung, C. Hartley, and P. Monaghan, "Receptive and expressive language ability differentially support symbolic understanding over time: p," *Journal of Experimental Child Psychology*, vol. 214, Article ID 105305, 2022.
- [5] N. Notten and B. Becker, "Early home literacy and adolescents' online reading behavior in comparative perspective," *International Journal of Comparative Sociology*, vol. 58, no. 6, pp. 475–493, 2017.
- [6] A. Breinholt and M. M. Jger, "How does cultural capital affect educational performance: signals or skills?" *British Journal of Sociology*, vol. 71, 2020.
- [7] B. Talekar, "A detailed review on decision tree and random forest," *Bioscience Biotechnology Research Communications*, vol. 13, no. 14, pp. 245–248, 2020.
- [8] Y. Xia, C. Liu, Y. Y. Li, and N. Liu, "A boosted decision tree approach using Bayesian hyper-parameter optimization for credit scoring," *Expert Systems with Applications*, vol. 78, pp. 225–241, 2017.
- [9] G. Ke, M. Qi, F. Thomas et al., "LightGBM: a highly efficient gradient boosting decision tree," in *Proceedings of the Neural Information Processing Systems*, Curran Associates Inc, Long Beach, CA, U.S.A, December 2017.
- [10] R. A. Cooper, "Making decisions with data: comparing sun leaves to shade leaves with a t-test," *The American Biology Teacher*, vol. 83, no. 4, pp. 229–234, 2021.
- [11] J. Cohen, *The Effect Size Index: D. Statistical Power Analysis for the Behavioral Sciences*, Routledge, New York, NY, U.S.A, 1988.
- [12] A. Strobel, G. Wieder, P. C. Paulus et al., "Dispositional cognitive effort investment and behavioral demand avoidance: are they related?" *PLoS One*, vol. 15, no. 10, 2020.
- [13] B. S. Nayak and P. K. Sahu, "Socio-demographic and educational factors associated with depression, anxiety and stress among health professions students," *Psychology Health & Medicine*, vol. 27, no. 4, pp. 848–853, 2021.
- [14] M. P. Ferra, R. L. Quijano, and I. G. Martínez, "Impact of educational habits on the learning of 3–6 Year old children from the perspective of early childhood education teachers," *Sustainability*, vol. 12, no. 11, p. 4388, 2020.
- [15] Y. Wang, Z. Yang, Y. Zhang, F. Wang, T. Liu, and T. Xin, "The effect of social-emotional competency on child development in western China," *Frontiers in Psychology*, vol. 10, p. 1282, 2019.
- [16] G. M. Pion and M. W. Lipsey, "Impact of the Tennessee voluntary prekindergarten program on children's literacy, language, and mathematics skills: results from a regression-discontinuity design," *AERA Open*, vol. 7, no. 2, pp. 233285842110413–233285842110497, 2021.
- [17] I. Saitadze, "Mediating effects of early childhood programs and high quality home environments on the cognitive development of poor children involved in the child welfare system," *Children and Youth Services Review*, vol. 120, Article ID 105736, 2021.
- [18] Z. Xu and D. Liu, "A comparison of embodied methods to improve Chinese children's reading comprehension: observed and participant performed manipulations," *Journal of Research in Reading*, vol. 43, no. 4, pp. 556–576, 2020.
- [19] L. Boonk, H. J. Gijssels, H. Ritzen, and S. B. Gruwel, "A review of the relationship between parental involvement



## Retraction

# Retracted: A Review of Motion Vector-Based Video Steganography

### Security and Communication Networks

Received 23 January 2024; Accepted 23 January 2024; Published 24 January 2024

Copyright © 2024 Security and Communication Networks. This is an open access article distributed under the Creative Commons Attribution License, which permits unrestricted use, distribution, and reproduction in any medium, provided the original work is properly cited.

This article has been retracted by Hindawi following an investigation undertaken by the publisher [1]. This investigation has uncovered evidence of one or more of the following indicators of systematic manipulation of the publication process:

- (1) Discrepancies in scope
- (2) Discrepancies in the description of the research reported
- (3) Discrepancies between the availability of data and the research described
- (4) Inappropriate citations
- (5) Incoherent, meaningless and/or irrelevant content included in the article
- (6) Manipulated or compromised peer review

The presence of these indicators undermines our confidence in the integrity of the article's content and we cannot, therefore, vouch for its reliability. Please note that this notice is intended solely to alert readers that the content of this article is unreliable. We have not investigated whether authors were aware of or involved in the systematic manipulation of the publication process.

Wiley and Hindawi regrets that the usual quality checks did not identify these issues before publication and have since put additional measures in place to safeguard research integrity.

We wish to credit our own Research Integrity and Research Publishing teams and anonymous and named external researchers and research integrity experts for contributing to this investigation.

The corresponding author, as the representative of all authors, has been given the opportunity to register their agreement or disagreement to this retraction. We have kept a record of any response received.

### References

- [1] J. Li, M. Zhang, K. Niu, and X. Yang, "A Review of Motion Vector-Based Video Steganography," *Security and Communication Networks*, vol. 2022, Article ID 2946812, 19 pages, 2022.

## Review Article

# A Review of Motion Vector-Based Video Steganography

Jun Li <sup>1,2</sup>, Mingqing Zhang <sup>1,2</sup>, Ke Niu <sup>1,2</sup> and Xiaoyuan Yang <sup>1,2</sup>

<sup>1</sup>Key Laboratory of Network and Information Security Under the Chinese People's Armed Police Force (PAP), Xi'an 710086, China

<sup>2</sup>College of Cryptography Engineering in Engineering University of PAP, Xi'an 710086, China

Correspondence should be addressed to Mingqing Zhang; [api\\_zmq@126.com](mailto:api_zmq@126.com)

Received 11 June 2022; Accepted 16 August 2022; Published 26 September 2022

Academic Editor: Yuchuan Luo

Copyright © 2022 Jun Li et al. This is an open access article distributed under the Creative Commons Attribution License, which permits unrestricted use, distribution, and reproduction in any medium, provided the original work is properly cited.

Steganography is a popular research direction in the field of information security. Due to the widespread use of video media, video steganography has received much attention from the research community. Among video steganography, motion vector (MV)-based video steganography has become one of the critical concerns of researchers due to its large embedding capacity and high visual quality. In this article, we focus on the research of MV-based video steganography. Firstly, the basic principles and evaluation criteria for MV-based steganography are discussed. Secondly, according to the different technical characteristics, the MV-based steganography is divided into three categories: the traditional MV domain steganography, the code-based MV domain steganography, and the adaptive MV domain steganography based on the framework of minimizing embedding distortion. The advantages and possible improvement directions of the above representative methods are illustrated. And then, the MV-based video steganalysis is outlined according to different perspectives of feature extraction, which is conducive to the design of better steganography algorithms. Finally, five future research directions are presented, such as designing distortion functions based on multiple factors, embedding methods based on new video coding standards, deep learning-based MV steganography, multi-domain embedding strategies, and moving the MV-based steganography from the laboratory into the real world.

## 1. Introduction

The development of modern information technology has dramatically changed how people obtain and transmit information. People protect information security by encrypting secret information into unintelligible ciphertext through cryptography. However, cryptography cannot conceal the existence of communication behavior, and information hiding technology can make up for this defect. The generalized information hiding technology achieves the purpose of information security by hiding the secret message into common carriers, which has two main branches: digital watermarking and digital steganography [1]. Digital watermarking is to embed authentication information into multimedia to achieve the purpose of copyright protection, and it is mainly concerned with embedding capacity and robustness. On the other hand, digital steganography embeds secret information in a common carrier to conceal the fact that communication is taking place without attracting

the attention of third parties, thus achieving the purpose of covert communication, which is mainly concerned with embedding capacity and security. However, steganography also has the possibility of being misused by terrorists [2, 3], so the corresponding steganalysis technique was born. The main goal of steganalysis is to determine whether the detected object has steganographic traces or not. It achieves the purpose of discriminative classification with the help of knowledge from fields such as pattern recognition and machine learning. Steganography and steganalysis are two sides of a game, which confront and promote each other, and have made significant progress in the last two decades.

The typical carriers used for steganographic are text, image, audio, video, etc. Since images are very widely used, the research on image steganography is the earliest and most profound. Hence, the development of image steganography has some guidance to the development of audio, video, and text steganography. The development of image steganography has gone through four main stages: the first stage is

traditional steganography, typically the LSB (least significant bit) replacement algorithm [4], the PVD (pixel value differencing) algorithm [5], and the quantization index modulation algorithm [6]. Their primary purpose is to embed the information into the image without causing noticeable visual distortion. The second stage is based on steganography code [7–9], and the primary goal of this class of methods is to improve the embedding efficiency and to be able to resist the attacks of steganalysis with low-order statistical features. The third stage is adaptive steganography based on the framework of minimizing embedding distortion [10]. The core task of these methods is to assign a reasonable cost value to each carrier element in the image and then encode it using STCs (syndrome trellis codes) [10], polar codes [11], etc. These methods are convenient and have high statistical security, and the typical algorithms are HUGO (Highly Undetectable steGO) [12], UNIWARD (UNiversal Wavelet Relative Distortion) [13], etc. The fourth stage is the implementation of embedding by drawing on the research results in the field of deep learning, which has a promising future. There are two main research works in this stage. On the one hand, deep learning is used to learn the distortion function [14] automatically. On the other hand, the method is called generative-based steganography [15, 16], in which the stego images are usually generated automatically by neural networks without the modification process.

With the improvement of network bandwidth and the development of video coding standards, video-on-demand and live streaming services have rapidly gained popularity, and video has gradually replaced images as the most popular and adopted information transmission medium. Globally, the amount of time people spend viewing short videos per week is climbing [17], with data showing that 14.9% of millennials aged 26 to 35 watch 10 to 20 hours of online video per week as of August 2020. Moreover, according to the 48th China Internet Development Report [18], the size of Chinese online video users reached 944 million by June 2021, accounting for 93.4% of Internet users as a whole. Therefore, video media is considered an ideal vehicle for steganography compared to images and text. However, compared with image steganography, video steganography started late and developed slowly, and there are still many urgent scientific problems to be solved. The basic component unit of video is the image, so video steganography has many similarities with image steganography. However, due to its complex coding rules, video has more embedding domains suitable for steganography than images, so video steganography has many features that distinguish it from image steganography.

Video steganography can be classified into the spatial domain and the compressed domain according to whether it is compressed by an encoder or not. Uncompressed spatial domain video is similar to the image spatial domain, so the relevant algorithms are mainly based on image steganography. The application of spatial video steganography is limited because it is difficult to preserve the embedded information after compression, while compression domain video steganography mainly refers to the combination of the embedding process and the video compression process,

which can be classified according to the video coding standards they use, mainly MPEG series [19], H.264/AVC [20], and H.265/HEVC [21]. In the past ten years, H.264/AVC has been the most widely used standard, while H.265 is expected to be promoted in the future. Although different video coding standards have different performances, they all use a hybrid coding framework, which usually contains techniques such as prediction, variation, quantization, entropy coding, intraframe prediction, interframe prediction, and loop filtering. Therefore, video steganography can be classified into intraframe prediction modes [22, 23], interframe prediction modes [24, 25], MVs [26, 27], transform coefficients [28, 29], quantization parameters [30], and entropy coding coefficients [31]. Table 1 lists the advantages and disadvantages of various embedding domain steganography in the video. Among these classifications, MV-based steganography has a larger embedding capacity because the compressed domain video has a large amount of MVs. Moreover, MV-based steganography is usually closely related to the encoding process. The embedding perturbation to the MV is handled automatically by the subsequent encoding process so that the MV-based steganography method can obtain better visual quality and coding efficiency. In short, the MV-based steganography has long received wide attention from researchers, so we focus on the MV-based steganography in this article.

Some literature has been reviewed on video steganography or steganalysis in recent years. Sadek et al. [32] summarized the early video steganography techniques. Zhang et al. [33] mainly summarized video steganalysis's research status and development direction for different embedding domains. Dalal et al. [34] reviewed the video steganography based on the spatial domain. Liu et al. [35] classified video steganography into intra-embedding, pre-embedding, and postembedding. They also summarized the reversible steganography and robust steganography. Dalal et al. [36] conducted a qualitative and quantitative analysis of video steganography and steganalysis. The experimental analysis of some prominent techniques using different quality metrics has also been performed. Patel et al. [37] provide a systematic overview of video steganography in the compressed and uncompressed domains. However, there is no published literature specifically summarizing MV-based video steganography techniques to the best of our knowledge. Moreover, the above review articles on MV-based steganography are not comprehensive enough. Therefore, to promote the development of MV-based video steganography, it is necessary to summarize and sort out the current status of research on MV-based steganography and steganalysis in recent years and discuss the possible future research directions, which would provide a reference for researchers in related fields. The remainder of this article is organized as follows: Section 2 presents the process of interframe predictive coding and the basic principles of MV-based steganography. Section 3 analyzes the development stages of MV-based video steganography and various types of steganographic embedding methods. Section 4 reviews the current research status of MV-based video steganalysis. The existing problems and possible future research

TABLE 1: Advantages and disadvantages of video steganography with different embedding domains.

Embedding domain	Cover	Embedding technology	Advantages	Disadvantages
Spatial domain	Pixels, transform domain coefficients	Modifies pixel or transform domain coefficients.	Independent of coding, can use research results from image steganography.	Distortion exists after compression.
Compressed domain	MV	Modify the horizontal or vertical component of the MV.	High embedding capacity, high visual quality, and no distortion drift.	Higher complexity.
	Intraframe prediction modes	Establishing the mapping relationship between intraframe prediction modes and secret message.	Lower complexity.	Usually used only in I-frames, lower embedding capacity, distortion drift.
	Interframe prediction modes	Establishing the mapping relationship between interframe prediction modes and secret message.	Embedding message in P-frames or B-frames.	Distortion drift.
	Transform domain coefficients	Modify the quantized DCT (discrete cosine transform) coefficients.	Can use research results from JPEG image steganography.	Low embedding capacity, distortion drift.
	Entropy coding coefficients	Modify the entropy coding coefficients.	Lower complexity, lower bit rate increment.	Low embedding capacity.

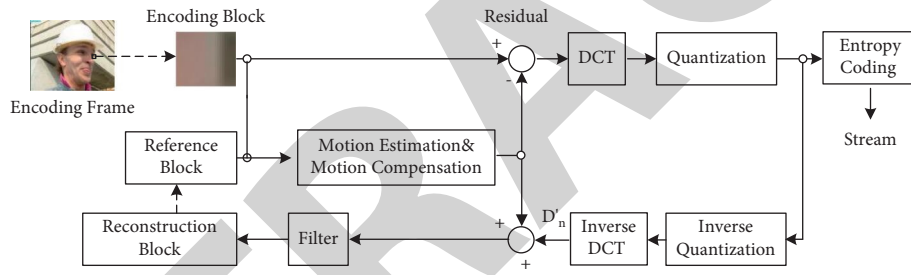


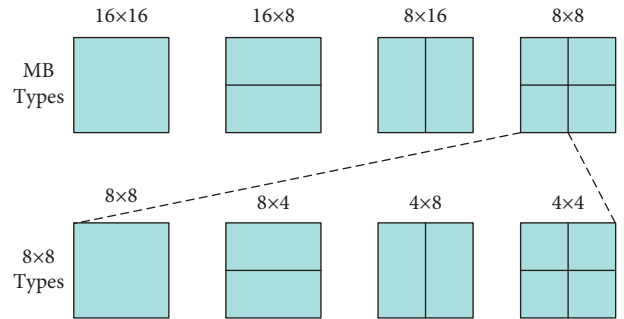
FIGURE 1: Interframe prediction for video coding.

directions are discussed in Section 5. Section 6 concludes the article.

## 2. Relevant Knowledge

Since MVs are generated in video interframe coding, this section first introduces the basic process of video interframe prediction coding, then describes the general principle of MV-based video steganography, and finally composes the common evaluation metrics of MV-based steganography.

**2.1. Interframe Prediction for Video Coding.** Most of the current video coding standards adopt a hybrid video coding framework, mainly consisting of intraframe prediction, interframe prediction, and entropy coding processes for compressing spatial redundancy, temporal redundancy, and statistical redundancy. Among them, temporal redundancy is the most extensive redundancy in the video because natural video consists of consecutive frames, and adjacent frames usually contain the same content between them, especially in scenarios such as surveillance and conferences. Interframe prediction coding can reduce these temporal redundancies, whose framework is shown in Figure 1. Since H.264 and HEVC videos are mainly used for steganography,

FIGURE 2: Segmentations of the macroblock for motion compensation (MC) in H.264/AVC. Top: segmentation of MB, bottom: segmentation of  $8 \times 8$  partitions.

this section focuses on these two standards' interframe prediction coding process.

In the H.264 coding standard, the currently encoding frame is divided into  $16 \times 16$  pixel-sized nonoverlapping MBs (MacroBlocks), and the luminance MBs are divided into various sizes such as  $16 \times 16$ ,  $16 \times 8$ ,  $8 \times 16$ , and  $8 \times 8$ , and the  $8 \times 8$  MBs can continue to be divided into  $8 \times 8$ ,  $8 \times 4$ ,  $4 \times 8$ , or  $4 \times 4$  sub-blocks, as shown in Figure 2. For encoding block  $B$ , the interframe prediction algorithm finds the most suitable

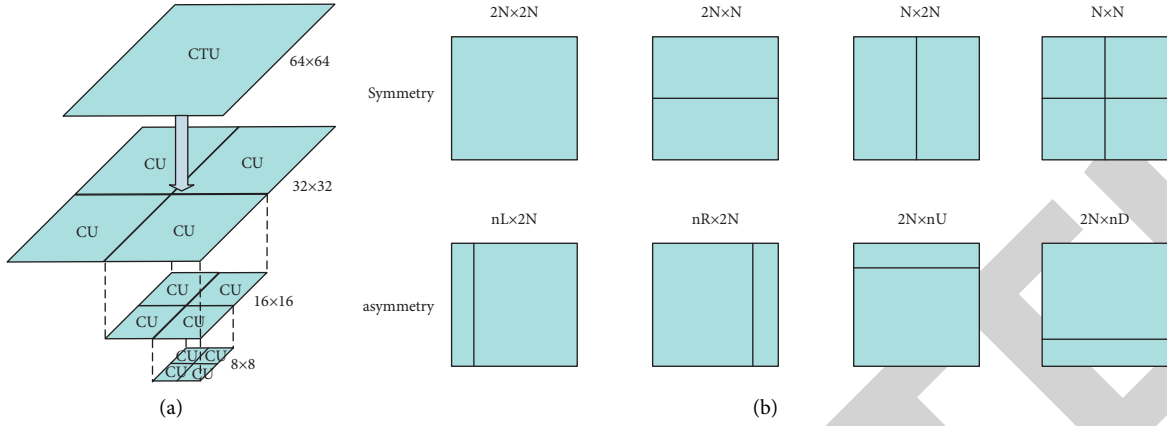


FIGURE 3: Partition modes of blocks in H.265/HEVC. (a) Subdivision of a CTU into CUs. (b) Modes for splitting a CU into PUs.

reference block  $T$  in the reference frame based on the Lagrangian rate distortion optimization model using motion estimation (ME):

$$J_{\text{motion}}(B, mv(h, v)) = D(B, T) + \lambda R(mv(h, v)), \quad (1)$$

where  $J_{\text{motion}}$  is the Lagrangian distortion of the interframe prediction and  $D(B, T)$  is the pixel distortion between the encoding block  $B$  and the corresponding prediction block  $T$ .  $\lambda$  is the Lagrangian parameter to control the balance between the code rate and distortion. The relative distance of  $B$  and  $T$  is the MV, which contains the horizontal and the vertical component.  $R(mv(h, v))$  is the number of bits needed to transmit the MV. On the one hand, the residual block outputs a video compressed stream after DCT transformation, quantization, and entropy coding. On the other hand, the quantified coefficients should be carried out by reverse quantified, and inverse DCT transformed to reconstruct the residual. Finally, the reconstructed residual was added with the prediction block to obtain the reconstructed block as the reference block for the subsequent encoded block.

Compared with H.264's macroblock model that fixed size, the HEVC coding standard adopts a more flexible way of dividing coding blocks. For each encoding frame, HEVC divides it into nonoverlapping coding tree units (CTUs), which are similar in concept to the MBs in H.264, and the size is specified by the encoder (usually  $64 \times 64$ ). According to the quadratic tree division principle, each CTU can be further divided into smaller coding units (CUs) of  $64 \times 64$ ,  $32 \times 32$ ,  $16 \times 16$ , or  $8 \times 8$ , which are shown in Figure 3(a). In the interframe prediction mode, a CU with the size of  $2N \times 2N$  can be divided into eight different sizes of prediction unit (PU) for MV prediction according to the symmetric and asymmetric approaches, as shown in Figure 3(b). It can be seen that HEVC has a more flexible interframe prediction mode than H.264. In addition, HEVC adopts new technologies such as AMVP (advanced MV prediction) to predict MVs, so there are richer ways to perform steganographic embedding on MVs.

**2.2. The MV-Based Steganography.** The process of MV-based video steganography is closely combined with the process of video compression coding, and its basic block diagram is

shown in Figure 4. First, motion estimation and motion compensation are carried out according to the normal coding process to obtain the original MV, coding parameters, quantized DCT coefficients, and other information. Then, the original MV is modified according to the embedding algorithm to get the stego MV. Since the modified MV will affect the corresponding reference and reconstruction blocks, it is necessary to update the QDCT coefficients, coding parameters, and other information. Finally, the updated information is encoded to obtain the video code stream.

Specifically, MV-based video steganography takes the  $mv(h, v)$  obtained according to motion estimation as the original cover, and then, the cover is modified by the embedding algorithm  $E$ :

$$\begin{aligned} mv(h', v') &= E(mv(h, v)) \\ &= mv(h \pm \Delta h, v \pm \Delta v), \end{aligned} \quad (2)$$

where  $\Delta h$  and  $\Delta v$  are 0 or positive integers, indicating the magnitude of modification, which usually should not be too large. Figure 5 shows the case after the MV is modified from  $mv(h, v)$  to  $mv(h', v')$ . Obviously, the reference block  $T$  will change to  $T'$ . At the same time, the reconstruction block used for the subsequent reference will also be changed, thus affecting the whole subsequent encoding process. Therefore, the steganography embedding will inevitably affect the various original statistical properties of the MVs, etc., leaving space for possible attacks. The main goal of the MV-based steganographic algorithm is to ensure that the stego video is as close as possible to the original video in terms of visual quality, bit rate, and various statistical features. Steganalysis aims at destroying the covert communication by mining the statistical differences between the cover video and the stego video.

**2.3. Performance Assessment Metrics for MV-Based Steganography.** The core purpose of steganography is covert communication, so the most important metric to evaluate a video steganographic algorithm is statistical security, represented by the ability to resist steganalysis. The performance assessment metrics for MV-based steganography should also



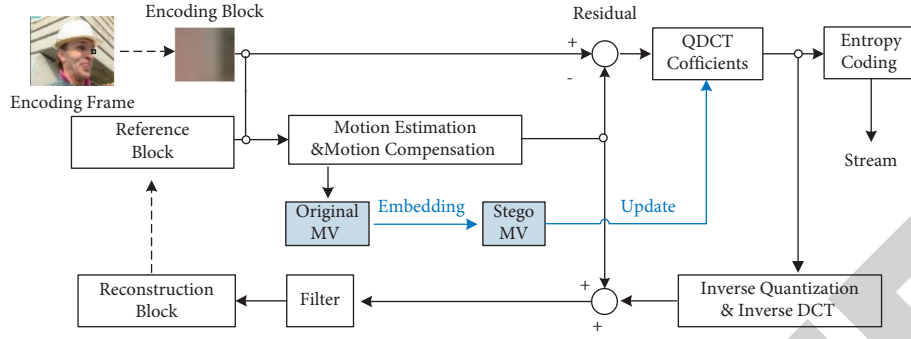


FIGURE 4: The block diagram of the MV-based steganography.

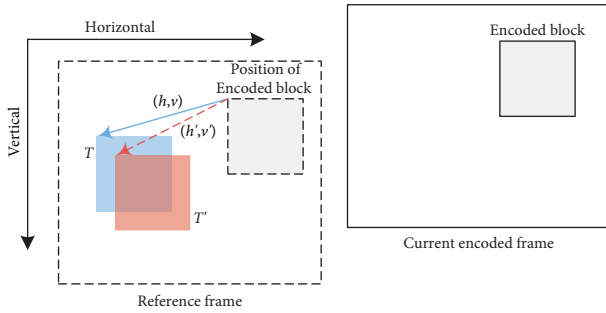


FIGURE 5: Modifying the MV in interframe prediction.

include embedding capacity, visual quality, coding efficiency, and computational complexity.

**2.3.1. Embedding Capacity.** The embedding capacity can be classified into absolute embedding capacity and relative embedding capacity. The primary absolute embedding capacity metric is bpf (bits per frame); that is, the number of bits that can be embedded into one frame. The relative embedding capacity is commonly used as cmvr (corrupted MV ration), representing the ratio of corrupted MVs' number to the total number of MVs in each frame. It is also possible to use bpmv (bits per MV), the average number of bits that can be embedded per MV. In addition, there is no MV in the situation when the macroblock is in skip mode, so the bpnsmv (bits per non-skip MV) is used as an evaluation metric. Since adaptive steganographic algorithms based on minimizing embedding distortion usually extract the lowest bit of the MV as the cover first and then combine it with STC coding for embedding, the relative capacity in STC coding can also be used to describe the overall embedding capacity.

Different MV-based steganography methods usually embed messages with different types of MVs as covers. For example, some methods select MVs with values larger than a certain threshold as covers, while some select only MVs with macroblocks divided into  $16 \times 16$  or  $8 \times 8$  as covers, and some embed for all MVs. The number of MVs varies widely for different encoding parameters, so in this case, we believe that it is unfair to conduct a cross-sectional comparison of different methods with relative embedding capacity. Therefore, an absolute embedding capacity (e.g., bpf) should be used for comparison.

**2.3.2. Visual Quality.** The visual quality of the compressed video is an important metric to judge an encoder, and the most widely used evaluation criteria are peak signal-to-noise ratio (PSNR) and structural similarity (SSIM). Embedding operation inevitably impacts the visual quality, so MV-based steganography also uses these metrics to evaluate the algorithm. The PSNR represents the difference between the original video and the compressed reconstructed video in the pixel domain, which is defined as

$$\text{PSNR} = 10 \cdot \log \frac{\text{MAX}^2}{\text{MSE}}, \quad (3)$$

$$\text{MSE} = \frac{1}{WH} \sum_{i=1}^W \sum_{j=1}^H (f(i, j) - d(i, j))^2,$$

where  $f$  and  $d$  are the encoded frame and the reconstructed decoded frame, respectively, with dimensions of  $W \times H$ . MSE is the mean square error of the encoded and decoded frames, and MAX is the maximum number of colors. Larger PSNR values indicate better visual quality, and this metric is simple to implement but does not reflect the visual properties of the human eye.

The other metric, SSIM, models distortion as three different factors: luminance, contrast, and structure. It is defined as

$$\text{SSIM} = \frac{(2\mu_f\mu_d + c_f)(2\sigma_{fd} + c_d)}{(\mu_f^2 + \mu_d^2 + c_f)(\sigma_f^2 + \sigma_d^2 + c_d)}, \quad (4)$$

where  $\mu_f$  and  $\mu_d$  are the mean values of the original and decoded frames,  $\sigma_f^2$ ,  $\sigma_d^2$ ,  $\sigma_{fd}$  are the variances of the original and decoded frames and their covariances.  $c_f = (0.01 * \text{MAX})^2$  and  $c_d = (0.03 * \text{MAX})^2$  are hyper-parameters, and MAX is defined as above. The value range of SSIM is  $[-1, 1]$ , and the larger value means the better visual quality, which can reflect the visual characteristics of human eyes.

**2.3.3. Video Bit Rate and Computational Complexity.** The bit rate after video compression is a very important metric, and the core task of every new coding standard is to reduce the bit rate while maintaining the visual quality. Steganographic algorithms usually lead to an increase in the

video bit rate. To not attract the attention of attackers, steganographic algorithms should minimize the variation of bit rate. The impact of steganography on coding efficiency can be measured by bit rate increment (BRI), which is defined as follows:

$$\text{BRI} = \frac{\text{BR}_s - \text{BR}_c}{\text{BR}_c} \times 100, \quad (5)$$

where  $\text{BR}_c$  is the bit rate for normal encoding and  $\text{BR}_s$  is the bit rate for encoding with the steganographic embedding. The computational complexity of the steganographic algorithm is another important metric. Since video compression coding is a process of finding the optimal parameters among a large number of coding parameters, the encoder usually possesses a high complexity. For the steganographic algorithm to be applied to practical scenarios, the computational complexity of the steganographic algorithm should not be too high. And the computational complexity of steganography is usually described using the embedding speed.

### 3. Review of MV-Based Video Steganography

Referring to the development history of image steganography, we divide the development process of MV-based steganography into three stages. The first stage is traditional steganography, which is mainly implemented by modifying the magnitude of MV, MVD (MV difference), and phase of MV. The second stage is based on matrix coding [7], wet paper coding [8], and other steganographic codes to achieve the primary goal of improving embedding efficiency. The third stage is adaptive steganography based on minimizing embedding distortion [10], and these steganography methods have high embedding capacity and high security, which are still the current research hotspots.

**3.1. Traditional MV-Based Steganography.** Before the emergence of steganography code, the primary goal of MV-based steganography was to find suitable MVs for message embedding by setting up certain rules, which examined objects such as the magnitude of the MV, the magnitude of the prediction error of the encoding block, and the phase of the MV.

Xu et al. [38] designed a steganography method based on the magnitude of MVs in P-frames and B-frames with the MPEG coding standard. They concluded that the larger the magnitude value of the modified MVs, the less impact it brings to the cover in the coding process. First, the MVs whose magnitude values (the sum of the squares of the horizontal and vertical components) are greater than a certain threshold are selected as the embedding cover. Then, the decision of which component to modify is based on the magnitude of phase between horizontal and vertical components. Finally, the corresponding MVs' component is modified using LSB replacement. However, Aly et al. [39] argue that the magnitude of the MVs does not accurately reflect the effect of the steganographic perturbation, but the magnitude of the corresponding prediction residuals of the coding block reflects the steganographic perturbation. Those

coding blocks with prediction residuals larger than a threshold are first selected. The MVs in these blocks are used as embedding covers, and steganographic embedding is performed using LSB substitution on both the horizontal and vertical components of the MVs. This method is equivalent to selecting those MVs corresponding to texturally complex regions as embedding covers, which can effectively improve the visual quality of stego videos.

Fang et al. [40] embed secret information by establishing the correspondence between the magnitude of the phase between two MVs' components and the secret messages. First, the MV with an amplitude greater than a threshold value is selected as the candidate. Then, the phase between the horizontal and vertical components in each MV is calculated. Finally, judging whether the phase angle difference between two adjacent sets of MVs satisfies the preset message mapping rule. If the mapping rule is satisfied, the corresponding two sets of MVs remain unchanged; otherwise, a new search for a new MV is required to realize the message embedding. This method does not use the LSBs of the MV as the embedding covers but adjusts the MV corresponding to the encoded block with the preset message mapping rule. Rana et al. [41] embed the secret message mainly in homogeneous regions. Since homogeneous or smooth regions contain macroblocks with similar prediction errors, it helps to reduce the detected by masking the embedding noise in adjacent macroblocks with similar prediction errors possibility. Van et al. [42] embed secret information in QDCT coefficients and MVs based on the HEVC standard, and the reduction in the PSNR is controlled within 1 db with better visual quality.

From the above literature, it can be seen that the early traditional MV-based steganography methods mainly focus on the improvement of embedding capacity and visual quality and pay less attention to statistical security. Although these algorithms cannot resist steganalysis attacks based on statistical properties, these MV candidate rules provide a good basis for the development of later steganography techniques.

**3.2. Embedding Methods Based on Steganographic Codes.** With the emergence of matrix codes [7], wet paper codes [8], and ZZW coding construction [9] in image steganography, MV-based video steganography has been developed rapidly. The primary goal of algorithms at this stage is to reduce the modification of covers by combining steganographic codes, thus improving the embedding efficiency and achieving the goal of higher security and visual quality.

In order to improve the embedding efficiency, Pan et al. [43] constructed  $(n, k)$  linear block codes based on the LSBs of MVs to embed secret messages. Hao et al. [44] proposed a low modification rate steganography method using matrix codes. Firstly, the candidate MVs were selected as embedding covers by the MVs' magnitude and phase, and the LSBs of  $2^k - 1$  MVs are as a set of covers named  $A$ . After calculating  $X = A \cdot H$ , where  $H$  is the matrix with  $(2^k - 1) \times k$ , they take  $k$  secret messages  $C = \{c_1 \dots c_k\}$  and then calculated  $R = C \oplus X$ . Finally, they modified 1 bit in  $A$  by judging the

value of  $R$ . This algorithm can achieve the purpose of embedding  $k$  bits of secret information with only modifying 1 bit in  $A$ , which effectively improves the embedding efficiency.

Cao et al. [45] aim at improving the algorithm's security by constructing MVs' suboptimal alternatives with wet paper codes. In the first step, they consider the motion estimation as a process of outputting the optimal prediction block for the current coding block. In order to achieve information embedding, a suboptimal prediction block can be filtered out according to the prediction residuals less than a certain threshold value. Then, the MVs corresponding to these coding blocks with suboptimal prediction blocks are "dry" covers, which can be used to embed secret messages, while the MVs corresponding to other blocks are "wet" covers, which cannot be used to embed messages. In the second step, the sender and the receiver share a key used to construct the random matrix. In the third step, the sender determines whether the MVs corresponding to the encoded blocks needs to be modified by computing a linear system of equations. If they need to be modified, the MVs are replaced by the MVs corresponding to the suboptimal prediction blocks. The advantage of this algorithm is that it achieves adaptive embedding, which allows secret embedding information in "dry" covers that result in better statistical security and visual quality. Based on the literature [45], Cao et al. [46] proposed a steganographic algorithm with better performance by obtaining more suitable suboptimal alternative MVs through multipath motion estimation and ZZW construction to achieve higher embedding efficiency.

Duan et al. [47] argued that steganographic algorithms that maintain the statistical features of MV residuals can maintain the spatiotemporal correlation of MVs. They combined variable-length matrix codes to embed secret messages in MVD, which is more secure in resisting attacks on spatiotemporal correlation features, but the limited embedding capacity. Yang et al. [48] proposed a space coding steganography method based on the HEVC standard. They gave the construction and encoding method of MV space. They defined the mapping relationship between the set of MVs and the points in this space, which can achieve the effect of embedding a  $2N + 1$  binary number by changing at most one component among  $N$  MV components, with high embedding capacity.

The performance comparison of the above typical code-based steganographic algorithms is shown in Table 2. From these papers, it can be seen that these steganographic algorithms usually first select certain candidate MVs from all MVs as the covers to be embedded. And then, they combine with one of the codes to improve the embedding efficiency, achieving a certain degree of adaptive steganography embedding. Overall, these methods' visual quality and security are better than the traditional MV steganography.

**3.3. MV-Based Adaptive Steganography Using Framework of Minimizing Embedding Distortion.** Also inspired by the framework of minimizing embedding distortion in image steganography, the third stage of MV-based steganography is mainly based on the adaptive steganography method of

this framework, which is the mainstream framework of the whole multimedia steganography direction at present. The basic idea is to minimize the overall distortion by assigning a cost value to each MV cover and then encoding it with STC. This class of methods dramatically improves the security of steganographic algorithms, and it facilitates the steganographic algorithms to move from the laboratory to the practical application scenarios. According to the design perspective of the distortion function, it can be divided into methods based on complexity, methods based on the MV's local optimality, and methods based on multiple factors.

#### 3.3.1. Designing of Distortion Function Based on Complexity.

In image steganography, it is a fundamental principle to prioritize embedding messages in those texture complexity regions. There is more high-frequency redundant information in texture regions than smooth regions, and steganalysis features are challenging to model in these regions. Therefore most adaptive image steganographic algorithms aim at embedding secret messages in texture complexity regions, such as HUGO [12], WOW [52], and S-UNIWARD [13] in the spatial domain, and J-UNIWARD [13] and UERD [53] in the compressed domain. From the perspective of information hiding, any steganographic algorithm adds a certain amount of noise to a specific digital cover, so that the higher the texture complexity (statistical complexity) of the original cover, the more complex the added noise will be detected and the less impact it will have on the statistical properties of the original cover. Similarly, in MV-based video steganography, treating MVs as ordinary digital covers, they have their unique statistical properties, both spatial and temporal. Thus, secret messages should be embedded in those statistical complexity regions.

Yao [54] et al. considered that modifying MVs would bring perturbations to their temporal and spatial correlations and leave spaces for steganalysis. They designed a distortion function based on the covariance matrix of MV residuals and interframe prediction errors and combined it with STC coding to achieve message embedding. In the first step, for the  $t$ -th video frame containing  $H \times W$  inter-frame coding blocks, the horizontal and vertical components of the MV are constructed into matrices  $MVX_t$  and  $MVY_t$  with the dimension of  $H \times W$ , respectively. In the second step, for any element in  $MVX_t$  and  $MVY_t$ , the second-order difference arrays in four directions (horizontal, vertical, diagonal, and antidiagonal) are calculated to obtain the spatial statistics distortion. Similarly, the second-order difference arrays of horizontal and vertical components are computed in the time direction of adjacent frames to obtain the temporal statistical distortion. The MV's statistical distribution change (SDC) before and after modification is obtained based on the temporal and spatial distortions. The third step is to calculate the prediction error change (PEC) of the corresponding coding block before and after the MV's modification. In the fourth step, the final embedding distortion of the MV is calculated based on SDC and PEC, and the message embedding is performed with STCs. This scheme introduces the framework of minimizing embedding distortion to MV-



TABLE 2: The performance comparison of typical code-based steganographic algorithms.

Literature	Codes	Security	Visual quality (PSNR)	Embedding capacity
Pan et al. [43]	Linear block codes	Without test	Minimum 39.38 db for foreman sequence	Maximum 0.67 bpmv when using (6, 4) linear block codes
Hao et al. [44]	Matrix codes	Without test	Minimum 36.08 db for foreman sequence	Depends on $k$
Cao et al. [45]	Wet paper codes	High (resist [49, 50])	Average increase 0.49 db for foreman sequence	Average 33.2 bpf for foreman sequence
Cao et al. [46]	ZZW construction	High (resist [50, 51])	Average increase 0.61 db	Average 40 bpf
Yang et al. [48]	Space codes	High (resist [51])	High	Embedding a $2N + 1$ binary number in $N$ MV components

based steganography for the first time, which changes the traditional embedding model and improves the statistical safety and visual quality of stego videos. However, when calculating the statistical complexity of MVs, only the fixed size mode of macroblocks in the H.264 standard is considered, and the variable block size mode is not considered, which has a limited application. In addition, the algorithm has high computational complexity.

Wang et al. [55] gave a formal description related to MVs in the process of video coding and analyzed two factors of MVs, including local optimality and adjacency correlations. They pointed out that modifying the MV corresponding to a simple macroblock of texture does not easily cause significant local optimality anomalies. They also discussed the distribution law of the MV components, arguing that modifications that make the components closer to the mean of the distribution can better maintain correlation. They proposed a distortion function designing method (adaptive macroblock complex, AMC) based on the coding block's complexity. In addition, this scheme can also directly use the complexity of the coding block as the threshold value for whether to embed or not, without using coding methods such as STC, and thus has the characteristics of flexible usage and large embedding capacity. It is worth noting that the concept of complexity in this algorithm contains two aspects: one refers to the complexity of the pixel content, that is, the image texture complexity; and the other refers to the correlation of the MV itself. However, taking MVs that correspond to smooth coding blocks for embedding, which does not apply to the case of variable size macroblock partition. Because regions with complex textures will have a finer division of coding blocks in H.264 and HEVC standards mean that there are more different MVs available for embedding in that coding block, thus having higher security under the same conditions. In addition, this algorithm chooses smooth regions for embedding to ensure that the local optimality of the MVs is not subject to large perturbations. However, with the appearance of other different types of steganalysis features [56, 57], the security of this algorithm will be reduced.

**3.3.2. Designing of Distortion Function Based on Local Optimality.** Macroscopically, video coding is an output process of optimal coding parameters. In a normal

interframe coding process, from the coding side, the rate distortion  $J_{\text{motion}}(B, mv(h, v))$  should be minimal after the motion estimation process determines the  $mv(h, v)$ ; that is, the MV at the coding side is locally optimal. But after the steganography operation, this local optimality is likely to be disturbed. Therefore, some scholars have designed steganalysis features, such as AoSO (adding or subtracting one) feature sets [58], NPELO (near-perfect estimation for local optimality) feature sets [59], and generalized local optimality (GLO) feature sets [60]. These features are still effective for detecting steganography in the MV domain. Therefore, it is essential to consider whether the modified MVs can maintain local optimality when embedding messages from the perspective of designing steganographic algorithms. Table 3 lists the primary comparisons of typical algorithms.

Cao et al. [61] explored the possibility that the stego MV is still determined to be locally optimal based on the uncertainty of the surrounding SAD (Sum of Absolute Differences) matrix caused by video compression. They first defined a number of MVs with a "1-distance optimal neighbor" to measure the magnitude of distortion. And then proposed an adaptive video steganography method based on motion estimation perturbation optimization. This method tries to modify only those MVs that are still judged to be locally optimal after modification and constructs a double-layer embedding channel by combining wet paper codes (WPCs) [8] and STC [10], thus improving the security under AoSO's attacks. However, this method considers local optimality only from the perspective of SAD, not from the perspective of rate distortion, and thus cannot resist attacks with rate distortion local optimality features such as NPELO. In addition, the method may not have enough alternative MVs as carriers for embedding under high bit rate compression and has limited application in practical scenarios [64].

Cao et al. [62] argued that the output MVs conform to the local optimality of the surrounding SAD matrix from the encoder side but not necessarily from the decoder side. This is because different motion estimation algorithms may lead to searching for different MVs. Generally speaking, the information of the motion estimation algorithm used on the encoder side is not available on the decoder side, so there is uncertainty in the local optimality of the MVs. Therefore, they proposed that the embedding behavior of the secret

TABLE 3: Comparisons of typical algorithms based on local optimality.

Algorithms	Motivation	Distortion calculation	Codes	Against features
Cao et al. [61]	Uncertainty of the surrounding SAD matrix at the decoder	1-distance optimal neighbor	STC + WPC	AoSO
Cao et al. [62]	ME's uncertainty	The degree of ME's uncertainty	STC	AoSO
Zhang et al. [26]	Uncertainty of the surrounding SAD matrix at the decoder	The difference of Lagrangian rate distortion between original and modified MVs	STC	AoSO, SPOM [63], MVRB [51]

information should be confused with the different motion estimation behaviors. In this case, the steganalysis detector cannot distinguish whether the local optimality perturbation is caused by motion estimation or steganographic embedding.

Zhang et al. [26] proposed an MV-based steganography method called MVMPLO (Motion vector Modification with Preserved Local Optimality), which can guarantee the local optimality of modified MVs. This algorithm uses the difference Lagrangian rate distortion between the original MV and the alternative MV as the embedding cost value, which is more reasonable and effective. However, this method needs to search for candidate optimal MVs in a large range, which may lead to excessive modifications and thus bring about large perturbations in the spatiotemporal correlation of MVs. That is to say, although local optimality is guaranteed, it leads to the risk of being attacked by other statistical features.

**3.3.3. Designing of Distortion Function considering Multiple Factors.** Due to the complexity of interframe prediction coding, it is difficult to resist different types of steganalysis attacks when designing distortion functions using only complexity features or local optimality features. More and more MV-based steganographic algorithms consider multiple factors, such as complexity, local optimality, consistency within block groups, coding block prediction errors, etc., to obtain higher statistical security.

Wang et al. [64] designed a distortion function considering three factors, such as motion characteristics of video content, local optimality of MVs, and statistical distribution of MVs, to resist attacks from different steganalysis features. First, they claimed that embedding information in regions with rich motion characteristics is more beneficial to maintaining concealment. They measure motion characteristics based on the magnitude of MVs and the QP difference of neighboring macroblocks. Second, by combining the advantages in the literature [26, 61], they design a strategy to select candidate MVs adaptively, thus being able to resist the attack of AoSO features. Then, the second-order residuals of the MVs are constructed in the spatial and temporal domains, and the cost value representing the statistical distribution properties of the MVs was proposed. Finally, an adaptive integrated distortion function is designed by considering the three aspects. Experiments show that the security can be effectively improved against AoSO and MVRBR (MV reversion-based steganalysis revisited) [65]. However, the algorithm does not consider the case of variable macroblock size and thus has limited application in the real world.

Zhu et al. [66] considered the steganography system as a multiobjective optimization problem and designed the distortion function by considering the MV distribution correlation, local optimality, and reconstructed frame distortion. They used the CV (Coefficient of Variance) of the MV residuals to measure the statistical distribution properties of the MVs. The number of 0 values in the QDCT coefficients and the SATD (Sum of Absolute Transformed Difference) values of the coding block are used for calculating the distortion of local optimality. The SAD difference before and after the MV modification is used to calculate the reconstruction frame distortion. In addition, the algorithm treats the horizontal and vertical components of the MV as separate covers. They calculated the cost value of the horizontal component and performed steganography embedding first, then calculated the distortion of the vertical component and performed steganography embedding, which can effectively improve the security. However, this algorithm only aims to maintain Gaussian distribution when calculating the distortion of the statistical distribution of MVs. It does not give the calculation method of distortion when macroblock using the model of variable block size. Ghamsarian et al. [67], investigated the effect of the modified MVs and the cover order on the statistical properties of intraframe and interframe coding. The algorithm first finds the optimal alternative MV from all candidate MVs based on the principle of minimal change in Lagrangian rate distortion. It then calculates its spatial and temporal statistical distortion as steganographic coding distortion. The algorithm considers the case of variable size in macroblocks, which is beneficial for application in practical scenarios.

The MVC (motion vector consistency) feature sets proposed in the literature [57] point out that the MVs within the same block group are weakly correlated. And the MV values are often different, indicating that these MVs have weak consistency. However, the common  $\oplus$  operation in the embedding process will significantly change this MV consistency. In order to resist the attacks of MVC, Liu et al. [27] proposed the first algorithm that can resist MVC attacks. They considered MV consistency within a block group, statistical complexity, and local optimality. First, the degree of consistency of MV is described based on the number of identical MVs in the block group. Then, the complexity is measured using the difference between the MV and other MVs in the same block group. The local optimality of the MV before and after embedding is kept constant. Finally, a comprehensive distortion function is designed based on these three factors. The embedding is combined with a two-stage embedding strategy, i.e., the embedding of the horizontal and vertical components of the MVs is performed

TABLE 4: Comparison of distortion function considering multiple factors.

Algorithms	Factors to consider	Whether to consider variable size macroblock partition	Against features
Wang et al. [64]	Motion characteristics of video content, local optimality, statistical distribution	No	AoSO, MVRBR
Zhu et al. [66]	MV distribution correlation, local optimality, reconstructed frame distortion	No	NPELO
Ghamsarian et al. [67]	Statistical properties of intraframe, statistical properties of interframe, cover order, local optimality	Yes	AoSO, MVRB, NPELO
Liu et al. [27]	Consistency, statistical complexity, local optimality	Yes	NPELO, MVC
Li et al. [68]	Statistical complexity, local optimality, consistency	Yes	NPELO, MVC, CCF [56]

separately. The experimental results show that the algorithm significantly improves both security and coding efficiency.

From the above literature, it can be seen that the design of the distortion function must consider various factors due to the emergence of different types of steganalysis features. It can be summarized that the main factors that should consider are the statistical complexity, the local optimality, and the consistency. Based on the above observations, in our previous work [68], we proposed a method based on distortion design principles, which summarized three principles of distortion assignment: local optimality, consistency, and complexity priority. We designed three new distortion function assignment methods, respectively, and finally defined them as a joint distortion. The experimental results show that not only the three independent distortion assignment methods can effectively resist the corresponding steganalysis attacks, but also the final joint distortion can resist the attacks of the three steganalysis features simultaneously, in addition to obtaining good visual quality and coding efficiency.

Table 4 lists the comparison of distortion functions considering multiple factors. Although different algorithms consider roughly the same factors, the specific design details differ greatly, which indicates that different algorithms have some disagreement in defining distortion, and there is still space for research.

### 3.3.4. Other Methods for Designing Distortion Function.

In addition to the above methods, scholars have also proposed different distortion function design methods from other perspectives. There are mainly methods based on multi-embedded domain strategy, methods based on HEVC coding characteristics, methods based on capacity allocation, and methods based on nonadditive distortion.

To make full use of the multiple embedding domain covers provided in video coding, Zhai et al. [69] proposed a video steganography method based on MVs and interframe prediction modes. They presented two embedding strategies: sequential embedding and simultaneous embedding. The multiple domain steganography methods can effectively improve capacity and security through reasonable capacity allocation and distortion function definition. However, there is a correlation between each embedding domain, and their mutual influence needs to be further studied and explored.

Guo et al. [70], for the HEVC coding standard, first counted the motion trend of each frame and established an MTB (motion trend-based) mapping strategy between the MV and the secret message. Then, they used the SATD difference before and after the MV modification as the embedding distortion. This algorithm only uses the SATD value without considering the overall rate distortion has some limitations. In the base of SAMVP (steganography by advanced MV prediction) [71], Liu et al. [72] proposed the Adaptive-SAMVP algorithm based on the HEVC standard by defining the distortion function and combining it with STC coding. Since AMVP encodes MVs by index numbers and MV residuals, they embed the information in the index values of the candidate list and use the bite rate difference between two candidate MVs to define the distortion function. Unlike the general information embedding based on the interframe motion estimation and compensation process, this algorithm's embedding and extraction process is only implemented in the entropy decoding process of the video stream of HEVC. Thus, the complexity is lower, and the MV is not directly modified, so there is no degradation in visual quality. However, this algorithm theoretically implements information embedding by selecting different candidate MVs, and thus it will destroy the local optimality of the candidate MVs, and there is a security risk.

Yao et al. [73] asserted that when the MVs are modified, it causes residual offset propagation for subsequent frames. Based on the residual offset propagation analysis results, they designed a capacity allocation strategy to try to allocate capacity to frames that cause less offset propagation, which helps to maintain the overall safety. It is worth noting that the algorithm does not design a new distortion function but improves security through a capacity adjustment strategy, which is theoretically applicable to all distortion functions. However, the algorithm essentially concentrates the embedding capacity on specific frames, which will have security crises if the attacker adopts an adaptive steganalysis strategy [74, 75].

Usually, embedding distortion is nonadditive since the impact of embedding in individual cover elements on the overall distortion is not independent. However, the optimal solution under nonadditive conditions is difficult to solve, and the optimal problem under additive conditions is well solved by codes such as STC. Therefore, in the initial research stage on steganographic algorithms, most scholars

design steganographic algorithms by assuming that distortion is additive, which is obviously out of touch with the actual situation. Many nonadditive steganographic algorithms appeared in the spatial domain [76–78] and JPEG domain [79, 80] in image steganography, which greatly promoted the development of steganography in a more efficient and practical direction. However, in video steganography, nonadditive research is still in its infancy [28, 81]. In the MV domain, Li et al. [82] designed a joint distortion function reflecting the influence of embedding for MVs based on the joint distortion in the image spatial domain [78]. The algorithm first transforms the joint distortion into a joint modification probability. It decomposes the joint modification probability into an edge modification probability for the horizontal component and a conditional modification probability for the vertical component. Then the two modification probabilities are transformed into the corresponding distortion values, and finally, the secret message is embedded into the two components of the MV using STCs. However, the algorithm only considers the interaction between MVs' horizontal and vertical components, but not the interaction between the elements in each component.

#### 4. Review of MV-Based Video Steganalysis

As a rival of steganography, steganalysis aims at detecting whether the multimedia contains secret messages. The block diagram of MV-based steganalysis is shown in Figure 6. The basic process of MV-based video steganalysis is first to decode the video compressed stream and extract the statistical features related to MV modification from the decoding parameters. Then, train using a classifier and finally classify the detected objects and obtain the discriminative results.

In image steganalysis, since the steganography operation mainly destroys the correlation between pixels or DCT coefficients, the designed steganalysis features are mainly used to reflect the correlation anomalies before and after steganography. And due to the complexity of video coding, the MV-based video steganography leads to the perturbation of different types of coding parameters, and the angles of extracting steganalysis features are more diverse and complex. Therefore, according to the starting point of feature extraction, MV-based video steganalysis can be divided into five categories: the first category is based on the spatiotemporal statistical properties of MVs [83, 84], and the motivation of this category is the existence of a correlation between MVs. The second category is based on MV calibration methods [56] because the MVs tend to recover to the original MVs after recompression of the stego video. The third category is based on the local optimality of the MV [58, 59]. Since the MV is a locally optimal output process in the sense of rate distortion, the steganography operation is likely to destroy it. The fourth category is steganalysis algorithms [57] designed based on the fact that MVs of subblocks in a macroblock are usually different. In addition, there are also steganalysis methods based on convolutional neural networks [85, 86], which is the fifth category.

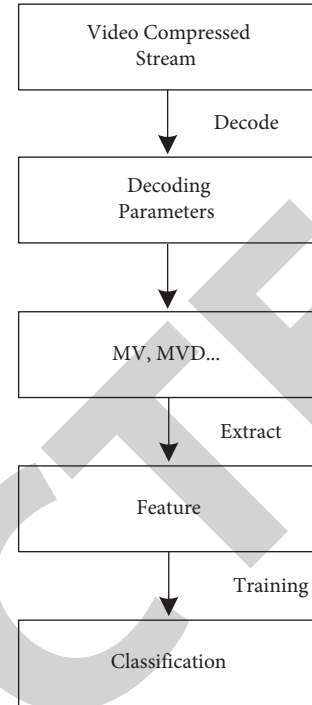


FIGURE 6: The block diagram of MV-based steganalysis.

**4.1. Steganalysis Based on the SpatioTemporal Statistical Properties of MVs.** Because of the strong correlation between adjacent coding blocks within a frame and between coding blocks at the same position between adjacent frames, the MVs have strong spatial and temporal correlations. Steganography will inevitably destroy this spatiotemporal correlation, so constructing statistical features of the difference in spatiotemporal correlation before and after steganography will effectively distinguish the cover video from the stego video.

For the fixed macroblock division, such as the MPEG-2 standard, Zhang et al. [50] and Su et al. [83] considered that the steganography operation is equivalent to adding additive noise to the horizontal and vertical components of the MV, respectively, and designed steganalysis feature sets based on the aliasing effect. The method extracts 3-dimensional features (including probability mass function and center of mass) from the temporal and spatial domains of the horizontal and vertical components, respectively. It can detect earlier conventional video watermarking algorithms that mainly modify the amplitude of MVs [87]. Based on the literature [83], Deng et al. [88] extended the MV first-order difference to second-order difference with improved performance.

Inspired by the rich model feature sets in image steganalysis [89] and combined with preprocessing techniques such as high-pass filtering, quantization, stage, and dimensionality reduction, Tasdemir et al. [84] proposed a 44785-dimensional video spatiotemporal rich model (STRM) feature sets, with higher correct detection accuracy. The literature [83, 84, 88] and others consider the temporal and spatial statistical properties of MVs for fixed macroblock

sizes. They cannot extract features for variable size macroblock divisions with limited applications. Li et al. [90] averaged all MVs within a macroblock to obtain an MV and then combined with the correlation network model to design steganalysis features, which could not consider the actual situation of variable sizes. In contrast, Wang et al. [91] proposed a four-way scanning method applicable to variable block size and designed 392-dimensional features based on the correlation anomaly of MVs, which can effectively detect methods such as those in the literature [39, 45]. In addition, Ghamsarian et al. [92] designed a method by considering intraframe statistical features, interframe statistical features, and local optimality of MVs, which further improved the performance of steganalysis.

From the above literature, it can be seen that steganalysis algorithms based on spatiotemporal statistical properties of MVs are mainly designed for early traditional MV-based steganography and fixed macroblock size division. Although high-dimensional features based on rich models have been widely used in image steganalysis, the current mainstream video coding standards usually use variable block size division, leading to difficulties for feature extraction. In addition, since video coding and decoding have high complexity, it is difficult to promote steganalysis algorithms with too high feature dimensions in practical applications. Therefore, how to design features with low dimensionality that can fully reflect spatiotemporal statistical features for variable block size division is a problem worthy of study.

**4.2. Steganalysis Based on Calibration.** The idea of calibration [93] is derived from JPEG image steganalysis, which refers to the fact that the coding parameters of JPEG images can be returned to the original state to some extent after recompression. For videos after MV-based embedding, it is possible to recover the original MVs by calibration techniques, which provides a basis for determining whether they have secret messages or not.

Cao et al. [51] found that after the calibration of the stego video with the same parameters as the first time, the MVs will show the nature of returning to the original values. Therefore, they designed the 15-dimensional feature sets of MVRB (MV reversion-based) based on the difference between the MV and prediction error before and after calibration. However, its performance is greatly affected by the encoding parameters. The second coding cannot achieve the detection purpose when it uses a different motion estimation algorithm and macroblock partition mode. Deng et al. [94] proposed calibration-based steganalysis features from the perspective of adjacent MV prediction, but there is still the problem of poor applicability. Therefore, Wang et al. [65], in order to solve the problem of encoding parameter mismatch, first collected various types of invariant encoding parameters (e.g., size and bit rate) and then obtained the best motion estimation algorithm by a search method, which has a certain performance improvement, but has high computational complexity.

To construct steganalysis features with rich statistical properties and applicable to various types of coding

standards from multiple perspectives, Zhai et al. [56] constructed a joint calibration feature with a dimension of 124 from three aspects: neighborhood optimality of MVs, MVs' residual distribution, and MV calibration. The features contain optimality probability features based on segmentation neighborhood, inter- and intra-co-occurrence features based on the MV residuals, and window optimal MV calibration features. Since the algorithm considers several factors and macroblock's variable size, its steganalysis performance and applicability are strong and can be applied to mainstream coding standards. However, this algorithm did not consider the interaction between the locally optimal features and the statistical features of the residual distribution.

**4.3. Steganalysis Based on Local Optimality.** Video coding maintains visual quality and reduces the bit rate through a search process of optimal parameters, and is an output process of optimal coding parameters. The mainstream compression standards, such as H.264/AVC and H.265/HEVC, use a rate distortion optimization model based on the Lagrangian optimization algorithm to achieve interframe coding control. The goal of the encoder is to find the MV that minimizes  $J_{\text{motion}} = D + R$ , where  $D$  is the coding block distortion, and  $R$  is the bit rate required to transmit the coded information. Therefore, in the normal interframe coding process, from the encoder side, the rate distortion  $J_{\text{motion}}$  should be locally minimal after the motion estimation process determines the MV. However, this local optimality is likely to be disturbed after the embedding operation, so the attacker can design the steganalysis features based on this.

Wang et al. [58] performed the adding or subtracting one operation on the decoded MVs to obtain the candidate MVs. They proposed the 18-dimensional AoSO (adding or subtracting one) features based on the MV matrix and the reconstructed SAD matrix. AoSO can effectively detect the traditional MV-based and code-based algorithms. However, AoSO only uses the surrounding SAD matrix of the reconstructed block to determine whether the MV is locally optimal without considering other factors such as rate distortion. Therefore, in the literature [59], the local optimality of the MV is considered in the sense of rate distortion. Both SAD and SATD distortion measures are used to evaluate the value of distortion, and the 36-dimensional feature NPELO (near-perfect estimation for local optimality) is proposed. This feature can describe local optimality more accurately and effectively detect earlier steganographic algorithms designed based on local optimality [26, 62]. Ren et al. [63] used calibration technique to counting the variation of the local optimality of MVs, but the application is limited due to the mismatch of encoding parameters in the calibration technique itself.

Zhai et al. [60] proposed a steganalysis feature for generalized local optimality of H.264/AVC. The so-called generalized local optimality has two aspects. First, the local optimality measured in a rate distortion sense is jointly determined by MV and predicted motion vector (PMV). The variability of PMV will affect the estimation for local

optimality. Hence, they generalize the local optimality from a static estimation to a dynamic one. Second, they generalize the local optimality from the MV domain to the PMV domain. The proposed features effectively improve the MV-based steganographic algorithm's detection performance for H.264/AVC coding and is one of the best algorithms at present.

For the HEVC coding standard, MV-based steganography can only modify the MV index but not the MV itself [72] to embed messages. Therefore, the traditional MV-based steganalysis features are ineffective for this steganographic algorithm. However, if the MV index value is modified, the local optimality of the MVs in the index list will also be destroyed. Based on this observation, Liu et al. [95] constructed their steganalysis features based on local optimality on both the MVs and the MV candidate list, which effectively improved the detection performance in HEVC videos.

The above literature review shows that MV local optimality-based features are effective and can be applied to all coding standards. However, the starting point of such features is the assumption of an optimal parameter output process at the encoder side. However, in practical applications, due to lossy compression, the attacker at the decoder side cannot obtain accurate information at the encoder side. Therefore, the steganalysis features based on local optimality may have inevitable errors. It is a worthwhile direction to explore how to predict the original unknown information from the decoder side.

**4.4. Steganalysis Based on MVs' Consistency.** The current mainstream video coding standards usually adopt a variable block size for dividing macroblocks or coding tree units. In order to examine the relationship between individual MVs within a macroblock, Zhai et al. [57] defined the concepts of "big-block" and "small-block": if a coding block can be divided into multiple smaller blocks, the block is called a big-block; and if the sub-block that makes up a big-block is not further divided, such a block is called a small-block. All the small-blocks corresponding to the same big-block compose a small-block group. In addition, a block is said to have MV consistency if at least two horizontally or vertically adjacent small-blocks within the same group have identical values. They pointed out that in the cover H.264 video, the MVs within the same group are weakly correlated, and the MV values are often different, indicating that the MVs in the same group in the cover video have low MV consistency. The common  $\hat{s}_1$  operation in the embedding process will cause a significant change in this MV consistency. They proposed a 12-dimensional universal steganalysis features MVC (MV consistency) based on this phenomenon, which can detect video steganography in both the interframe prediction mode domain and the MV domain, achieving the best current detection accuracy.

Shanableh et al. [96] extended the MV consistency feature from the H.264 to HEVC standard. They redefined the concept of block group based on the coding depth according to the characteristics of the HEVC standard. They

proposed steganalysis features based on MV consistency and coding unit residuals, which can effectively detect MV-based steganography in the HEVC standard.

**4.5. Steganalysis Based on Convolutional Neural Network.** Deep learning-based steganalysis has made significant progress in image steganalysis. Huang et al. [85] introduced convolutional neural networks to the quantitative steganalysis of MV video based on the HEVC standard. They proposed the VSRNet (Video Steganalysis Residual Network) network structure, whose input data contain the MV matrix and the prediction residual matrix. Independent VSRNet subnetworks are constructed for different embedding rates, and finally, all subnetworks are connected to form a quantitative steganalysis convolutional neural network capable of capacity estimation. They performed experimental validation for the traditional MV steganographic algorithm [38, 39] in the HEVC standard and obtained better results. Based on this, Huang et al. [86] further introduced the selection-channel-aware mechanism to improve the performance of steganalysis. The literature [85, 86] has made useful explorations in deep learning-based steganalysis of MV domains. However, it is still a challenge to propose more effective convolutional neural networks for minimizing embedding distortion in adaptive MV-based steganography.

## 5. Future Research Directions and Recommendations

According to the above literature review, the research on MV-based video steganography has made significant progress despite the late start. However, video steganography still has many issues that deserve further exploration due to the complexity of video coding and the emergence of new coding standards, which are shown in Figure 7.

**5.1. Designing of Distortion Function considering Multiple Factors.** Section 4 summarizes that the current mainstream MV-based steganalysis features are based on spatiotemporal statistical complexity, calibration differences, local optimality, consistency, etc. Therefore, the distortion functions summarized in Section 3.3 are also designed based on one or more of these factors. Since there are big differences in these steganalysis features, the design of distortion functions must consider all existing factors. The current main approach is to view the design of the distortion function as a multiobjective optimization problem. However, the interplay between factors has not been fully studied: how to optimize the distortion function, whether there is a conflict between factors, and how to deal with it if there is a conflict? For example, from the perspective of image content texture complexity, the more complex the texture, the finer the partition of macroblocks or coding tree units. It means that there are more MVs available as embedding covers, and the difference in MV magnitude/phase is also larger, so it is more favorable to maintain the spatiotemporal statistical properties of MVs. However, existing studies have shown



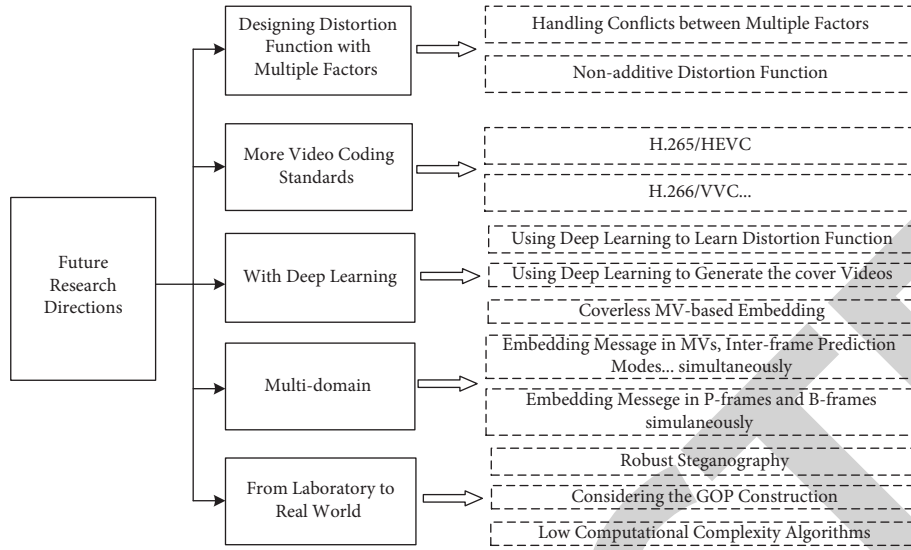


FIGURE 7: Future research directions.

that embedding in complex texture regions tends to lead to the destruction of local optimality of MVs [55], and steganography in smooth regions should be chosen, meaning that there exists conflict between the statistical properties of MVs and local optimality. We believe that similar conflicts exist between other factors as well. Therefore, it is an important research topic to propose algorithms that can maintain all kinds of statistical features simultaneously by fully considering the interplay between factors.

Secondly, most of the current distortion functions are based on additive assumptions, obviously out of touch with the actual situation. Compared with image nonadditive steganography, video MV-based nonadditive steganography has more challenges. Since the video coding adopts sequential coding, when the MV of a block in a frame is modified, the corresponding reconstruction block will be changed. This reconstruction block will provide a reference for the subsequent blocks, thus affecting the motion estimation and motion compensation of the subsequent blocks. Thus, it can be seen that the interplay between MVs is more significant, and how to fully exploit their interplay to design a nonadditive distortion function is a crucial issue worth exploring.

In addition, the design of all current distortion functions is based on the MVs of one frame; that is, STC coding can only achieve the overall optimum in one frame's range and cannot operate for the whole video sequence. That is to say, the current adaptive embedding only targets frames and does not consider the differences between different frames in the same video sequence. There are differences in complexity and motion speed between frames, so how to design a uniform distortion function for all MVs in all frames and use once STC coding for embedding is another crucial issue.

**5.2. MV-Based Steganography Using Other Video Coding Standards.** MV-based video steganography is still mainly focused on MPEG-2, H.264/AVC, while algorithms using

H.265/HEVC and H.266/VVC [97] are less studied. At present, it is not easy to be replaced in a short time because of the broad application of H.264/AVC standards, but the promotion and application of new standards is an inevitable trend. In addition, the current research based on the new standard algorithm mainly focuses on DCT coefficients, intraframe prediction mode and interframe prediction mode [98], while the research based on MV is still rare.

New coding standards always require a huge improvement in compression efficiency over the previous standard; for example, both VVC and HEVC aim at doubling the coding efficiency over the previous generation, and thus, information redundancy will become less and less under the new standards. Essentially, information hiding is the embedding of secret information in data redundancy. On the one hand, as compression standards iterate, data redundancy becomes less and less, so theoretically, there will be fewer and harder "covers" for steganographic algorithms to embed information. Therefore, algorithms under the old standard may not be directly portable to the new standard. On the other hand, new coding standards are bound to introduce more coding techniques and more complex coding details, providing new entry points for steganographic algorithms. For example, the HEVC adopts advanced MV prediction (AMVP), so MV-based steganography can modify the MV and the index value of the corresponding MV candidate list. The interframe prediction in VVC is more elaborate, thus providing new opportunities and challenges for the design of steganographic algorithms.

**5.3. MV-Based Steganography Using Deep Learning.** Deep learning techniques have made breakthroughs in image steganography and steganalysis, and their performance has caught up with or even surpassed that of traditional algorithms. However, the application of deep learning technology in MV-based video steganography is still in its initial stage. We believe that the main reasons may be the

following: firstly, the complexity of video coding itself is high, and adding deep learning technology to the video coding process for message embedding will greatly improve the overall complexity of the algorithm. Secondly, steganography based on deep learning usually requires a large number of samples for model training. Currently, MV-based steganography usually takes the MVs in a frame as the basic embedded cover, and the number of MVs is limited.

Deep learning-based MV domain video steganography can be studied from the following aspects. One is the design of distortion functions based on deep learning. The current manual design of the distortion function usually needs to consider various factors. This way is subject to human experience interference, and it is difficult to achieve optimally. The use of deep neural networks (such as generative adversarial networks) to automatically learn distortion can effectively reduce the interference of human factors. Secondly, the deep learning technology directly generates the cover video sequence, based on which the existing adaptive steganography technology is used to embed, which can enrich the application scope of the existing MV domain steganography technology. Thirdly, using deep learning techniques to carry out coverless MV-based embedding (generative steganography). We can establish the mapping relationship between MVs and secret information without modifying original MVs, which can resist the current steganalysis attacks based on the statistical differences between the cover video and the stego video.

**5.4. Multi-domain Video Steganography.** Various coding elements in video coding can all be used as embedding covers. However, most current algorithms are usually based on single-domain embedding and do not fully utilize all embedding covers. More importantly, single-domain-based embedding algorithms ignore the fact that embedding in one domain also causes anomalies in the statistical properties of other domains. For example, the literature [57] demonstrated that embedding in the interframe prediction model leads to statistical anomalies in the MV domain. Therefore, it is important to make comprehensive use of the different characteristics of each embedding domain, to spread the steganographic capacity over different embedding covers.

Specifically, the MV domain is closely related to the interframe prediction mode domain. The division of interframe prediction patterns directly determines the number and distribution of MVs in macroblocks or coding tree cells. Their mutual constraint relationship can be fully utilized to design algorithms conducive to masking steganographic perturbation signals. In addition, except for interframe prediction coding blocks, there can also exist intraframe prediction coding blocks in P-frames or B-frames. The coding parameters of these intraframe prediction coding blocks can be fully utilized to effectively improve the steganographic capacity and security.

**5.5. Moving Video Steganography from Laboratory Environment to Practical Application.** In digital steganography and steganalysis, it has been an important concern for

researchers to be able to apply the research results in the laboratory environment to the real-world environment [99]. Similarly, in MV-based steganography, there are still many “laboratory conditions” in the current research, and it is necessary to investigate algorithms that can be applied to real-world scenarios under more complex conditions.

The first one is about robust steganography. The videos that people upload to various platforms are usually compressed twice. Ensuring that the secret information can still be extracted normally after the secondary compression is a crucial issue. Although the research of video robust watermarking has been developed relatively mature, most of the current steganographic algorithms based on the MV domain do not consider robustness, limiting its application in practical scenarios. Therefore, how guaranteeing the embedding capacity, security, and robustness of MV-based steganographic algorithms is an important research direction.

The second one is about the GOP (group of pictures) structure in the video. Most current MV-based steganographic algorithms are usually studied in terms of GOP structure as IPPP... and the size of GOP is usually within 15. In practice, there are usually tens or even hundreds of frames between two I-frames, which means that the residual perturbation generated by the MV modification in the previous frames of the GOP will propagate to the subsequent frames in the GOP. This perturbation propagation becomes more severe as the number of frames in the GOP increases. In addition, there are usually many B-frames in a GOP, and since the MVs in B-frames are obtained from the MVs of the two reference frames before and after, modifying the MVs in B-frames will affect more coding blocks. Therefore, it is also essential to fully consider the real-world GOP structure in the design of the steganographic algorithm.

The third one is about the computational complexity of the steganographic algorithm. Video coding, especially in real-time communication, is a technology with very high requirements for real-time performance. With the iteration of new video coding standards, the complexity is getting higher. The computational complexity of steganographic algorithms is also increasing due to the constant pursuit of security and its consideration of more and more factors. Suppose the complexity of the steganographic algorithm is too high and affects the normal video coding. In that case, it will not only be detrimental to the normal video coding process but also cause suspicion of attackers. Therefore, designing a lightweight MV-based video steganographic algorithm is also an important issue.

## 6. Conclusion

Although video steganography has received less attention than image steganography, the increasing proportion of video media on the Internet has contributed significantly to the development of video steganography, and many significant results have been achieved in recent years. This article presents a comprehensive overview of the basic principles and development process of MV-based video steganography, focusing on the research status and problems



of adaptive MV domain steganography based on minimizing embedding distortion. The typical MV-based steganalysis techniques were also reviewed from the perspective of feature extraction. Finally, because of the development status of video coding and the problems of existing algorithms, possible future research directions are elaborated, hoping to provide some reference for readers.

## Data Availability

The data supporting this review are from previously reported studies and datasets, which have been cited.

## Conflicts of Interest

The authors declare that there are no conflicts of interest regarding the publication of this article.

## Acknowledgments

This work was supported by the National Natural Science Foundation of China under Grant no. 61872384 and Basic Research Foundation of Engineering University of PAP under Grant no. WJY202140.

## References

- [1] K. T. Cox I, M. Miller, J. Bloom, and J. Fridrich, *Digital Watermarking and Steganography*, Morgan Kaufmann Publishers Inc, San Francisco, 2nd ed edition, 2008.
- [2] B. Schneier, *Terrorists and Steganography*, ZDNet, San Francisco, CA, USA, 2001, <http://www.zdnet.com/article/terrorists-and-steganography>.
- [3] The State of Security, "Hackers Exfiltrating Data with Video Steganography via Cloud Video Services," 2014, <https://www.tripwire.com/state-of-security/incident-detection/hackers-exfiltrating-data-with-video-steganography-via-cloud-video-services>.
- [4] F. A. P. Petitcolas, R. J. Anderson, and M. G. Kuhn, "Information hiding—a survey," in *Proceedings of the IEEE*, vol. 87, no. 7, pp. 1062–1078, 1999.
- [5] D.-C. Wu and W.-H. Tsai, "A steganographic method for images by pixel-value differencing," *Pattern Recognition Letters*, vol. 24, no. 9–10, pp. 1613–1626, 2003.
- [6] B. Chen and G. W. Wornell, "Quantization index modulation: a class of provably good methods for digital watermarking and information embedding," *IEEE Transactions on Information Theory*, vol. 47, no. 4, pp. 1423–1443, May 2001.
- [7] J. Fridrich and D. Soukal, "Matrix embedding for large payloads," *IEEE Transactions on Information Forensics and Security*, vol. 1, no. 3, pp. 390–395, 2006.
- [8] J. Fridrich, M. Goljan, P. Lisoněk, and D. Soukal, "Writing on wet paper," *IEEE Transactions on Signal Processing*, vol. 53, no. 10, pp. 3923–3935, 2005.
- [9] W. Zhang, J. Liu, X. Wang, and N. Yu, "Generalization and analysis of the paper folding method for steganography," *IEEE Transactions on Information Forensics and Security*, vol. 5, no. 4, pp. 694–704, Dec. 2010.
- [10] T. Filler, J. Judas, and J. Fridrich, "Minimizing additive distortion in steganography using syndrome-trellis codes," *IEEE Transactions on Information Forensics and Security*, vol. 6, no. 3, pp. 920–935, 2011.
- [11] W. Li, W. Zhang, L. Li, H. Zhou, and N. Yu, "Designing near-optimal steganographic codes in practice based on polar codes," *IEEE Transactions on Communications*, vol. 68, no. 7, pp. 3948–3962, 2020.
- [12] T. Pevný, T. Filler, and P. Bas, "Using high-dimensional image models to perform highly undetectable steganography," in *Proceedings of the 2010 International Workshop on Information Hiding*, pp. 161–177, Calgary, Canada, June 2010.
- [13] V. Holub, J. Fridrich, and T. Denemark, "Universal distortion function for steganography in an arbitrary domain," *EURASIP Journal on Information Security*, vol. 2014, no. 1, pp. 1–24, 2014.
- [14] W. Tang, S. Tan, B. Li, and J. Huang, "Automatic steganographic distortion learning using a generative adversarial network," *IEEE Signal Processing Letters*, vol. 24, no. 10, pp. 1547–1551, 2017.
- [15] D. Volkhonskiy, I. Nazarov, and E. Burnaev, "Steganographic generative adversarial networks," in *Proceedings of the 12th International Conference on Machine Vision (ICMV 2019)*, p. 97, Amsterdam, The Netherlands, January 2020.
- [16] D. Hu, L. Wang, W. Jiang, S. Zheng, and B. Li, "A novel image steganography method via deep convolutional generative adversarial networks," *IEEE Access*, vol. 6, pp. 38303–38314, 2018.
- [17] Statista, "Weekly Time Spent with Online Video According to Internet Users Worldwide as of August 2020, by Age Group," 2020, <https://www.statista.com/statistics/611750/millennial-time-spent-with-online-video/>.
- [18] China Internet Network Information Center, "The 48th Statistical Report on China's Internet Development," 2021, <http://www.cnnic.net.cn/hlwfzyj/hlwzxbg/hlwjtjbg/202108/P020210827326243065642.pdf>.
- [19] T. Sikora, "MPEG digital video-coding standards," *IEEE Signal Processing Magazine*, vol. 14, no. 5, pp. 82–100, 1997.
- [20] T. Wiegand, G. J. Sullivan, G. Bjøntegaard, and A. Luthra, "Overview of the H.264/AVC video coding standard," *IEEE Transactions on Circuits and Systems for Video Technology*, vol. 13, no. 7, pp. 560–576, 2003.
- [21] G. J. Sullivan, J.-R. Ohm, W.-J. Han, and T. Wiegand, "Overview of the high efficiency video coding (HEVC) standard," *IEEE Transactions on Circuits and Systems for Video Technology*, vol. 22, no. 12, pp. 1649–1668, 2012.
- [22] Y. Hu, C. Zhang, and Y. Su, "Information hiding based on intra prediction modes for H.264/AVC," in *Proceedings of the Multimedia and Expo, 2007 IEEE International Conference on*, pp. 1231–1234, Beijing, China, July 2007.
- [23] Y. Wang, Y. Cao, X. Zhao, Z. Xu, and M. Zhu, "Maintaining rate-distortion optimization for IPM-based video steganography by constructing isolated channels in HEVC," in *Proceedings of the 6th ACM Workshop on Information Hiding and Multimedia Security*, pp. 97–107, Innsbruck Austria, June 2018.
- [24] S. K. Kapotas and A. N. Skodras, "A New Data Hiding Scheme for Scene Change Detection in H.264 Encoded Video Sequences," in *Proceedings of the 2008 IEEE International Conference on Multimedia and Expo*, pp. 277–280, Hannover, Germany, June 2008.
- [25] H. Zhang, Y. Cao, X. Zhao, W. Zhang, and N. Yu, "Video steganography with perturbed macroblock partition," in *Proceedings of the 2nd ACM Workshop on Information Hiding and Multimedia Security-IH&MMSec'14*, pp. 115–122, Salzburg Austria, June 2014.

- [26] H. Zhang, Y. Cao, and X. Zhao, "Motion vector-based video steganography with preserved local optimality," *Multimedia Tools and Applications*, vol. 75, no. 21, pp. 13503–13519, 2016.
- [27] Y. Liu, J. Ni, W. Zhang, and J. Huang, "A Novel Video Steganographic Scheme Incorporating the Consistency Degree of Motion Vectors," *IEEE Transactions on Circuits and Systems for Video Technology*, vol. 32, no. 7, pp. 4905–4910, 2021.
- [28] Y. Wang, Y. Cao, and X. Zhao, "CEC: cluster embedding coding for H.264 steganography," *IEEE Signal Processing Letters*, vol. 27, no. c, pp. 955–959, 2020.
- [29] Y. Chen, H. Wang, K. K. R. Choo et al., "DDCA: a distortion drift-based cost assignment method for adaptive video steganography in the transform domain," *IEEE Transactions on Dependable and Secure Computing*, vol. 19, no. 4, pp. 2405–2420, 2022.
- [30] T. Shanableh, "Data hiding in MPEG video files using multivariate regression and flexible macroblock ordering," *IEEE Transactions on Information Forensics and Security*, vol. 7, no. 2, pp. 455–464, Apr. 2012.
- [31] C. Di Laura, D. Pajuelo, and G. Kemper, "A novel steganography technique for SDTV-H.264/AVC encoded video," *International Journal of Data Mining and Bioinformatics*, vol. 2016, Article ID 6950592, 9 pages, 2016.
- [32] M. M. Sadek, A. S. Khalifa, and M. G. M. Mostafa, "Video steganography: a comprehensive review," *Multimedia Tools and Applications*, vol. 74, no. 17, pp. 7063–7094, 2015.
- [33] H. Zhang, W. You, and X. Zhao, "A survey of video steganalysis," *Journal of Cyber Security*, vol. 3, no. 6, pp. 13–27, 2018.
- [34] M. Dalal and M. Juneja, "Video steganography techniques in spatial domain—a survey," in *Proceedings of the International Conference on Computing and Communication Systems*, vol. 24, pp. 705–711, 2018.
- [35] Y. Liu, S. Liu, Y. Wang, H. Zhao, and S. Liu, "Video steganography: a review," *Neurocomputing*, vol. 335, pp. 238–250, 2019.
- [36] M. Dalal and M. Juneja, "A Survey on Information Hiding Using Video Steganography," *Artificial Intelligence Review*, vol. 54, no. 8, 2021.
- [37] R. Patel, K. Lad, and M. Patel, "Study and investigation of video steganography over uncompressed and compressed domain: a comprehensive review," *Multimedia Systems*, vol. 27, no. 5, pp. 985–1024, 2021.
- [38] C. Xu, X. Ping, and T. Zhang, "Steganography in compressed video stream," in *Proceedings of the 2006 1st International Conference on Innovative Computing, Information and Control—Volume I (ICICIC'06)*, pp. 269–272, Beijing, China, September 2006.
- [39] H. A. Aly, "Data hiding in motion vectors of compressed video based on their associated prediction error," *IEEE Transactions on Information Forensics and Security*, vol. 6, no. 1, pp. 14–18, 2011.
- [40] D. Fang and L. Chang, "Data hiding for digital video with phase of motion vector," in *Proceedings of the 2006 IEEE International Symposium on Circuits and Systems (ISCAS)*, p. 4, Kos, Greece, May 2006.
- [41] S. Rana, R. Kamra, and A. Sur, "Motion vector based video steganography using homogeneous block selection," *Multimedia Tools and Applications*, vol. 79, no. 9–10, pp. 5881–5896, 2020.
- [42] L. P. Van, J. De Praeter, G. Van Wallendael, J. De Cock, and R. Van de Walle, "Out-of-the-loop information hiding for HEVC video," in *Proceedings of the 2015 IEEE International Conference on Image Processing (ICIP)*, pp. 3610–3614, Quebec, Canada, September 2015.
- [43] F. Pan, L. Xiang, X.-Y. Yang, and Y. Guo, "Video steganography using motion vector and linear block codes," in *Proceedings of the 2010 IEEE International Conference on Software Engineering and Service Sciences*, pp. 592–595, Beijing, China, July 2010.
- [44] B. Hao, L. Zhao, and W. Zhong, "A novel steganography algorithm based on motion vector and matrix encoding," in *Proceedings of the 2011 IEEE 3rd International Conference on Communication Software and Networks, ICCSN*, pp. 406–409, Xi'an, China, May 2011.
- [45] Y. Cao, X. Zhao, D. Feng, and R. Sheng, "Video steganography with perturbed motion estimation," *Lecture Notes in Computer Science*, vol. 6958, pp. 193–207, 2011.
- [46] Y. Cao, X. Zhao, F. Li, and N. Yu, "Video steganography with multi-path motion estimation," *SPIE Proceedings*, vol. 8665, 2013.
- [47] D. Ran and C. Dan, "Video steganography algorithm uses motion vector difference as carrier," *Journal of Image and Graphics*, vol. 23, no. 2, pp. 163–173, 2018.
- [48] J. Yang and S. Li, "An efficient information hiding method based on motion vector space encoding for HEVC," *Multimedia Tools and Applications*, vol. 77, no. 10, pp. 11979–12001, 2018.
- [49] G. Xuan, Y. Q. Shi, J. Gao et al., "Steganalysis based on multiple features formed by statistical moments of wavelet characteristic functions," in *Science and Technology*, M. Barni, J. Herrera-Joancomartí, S. Katzenbeisser, and F. Pérez-González, Eds., pp. 262–277, Springer Berlin Heidelberg, Berlin, Heidelberg, 2005.
- [50] C. Zhang, Y. Su, and C. Zhang, "A new video steganalysis algorithm against motion vector steganography," in *Proceedings of the 2008 4th International Conference on Wireless Communications, Networking and Mobile Computing*, pp. 4–7, Dalian, China, October 2008.
- [51] Y. Cao, X. Zhao, and D. Feng, "Video steganalysis exploiting motion vector reversion-based features," *IEEE Signal Processing Letters*, vol. 19, no. 1, pp. 35–38, 2012.
- [52] V. Holub and J. Fridrich, "Designing steganographic distortion using directional filters," in *Proceedings of the 2012 IEEE International Workshop on Information Forensics and Security (WIFS)*, pp. 234–239, Tenerife, Spain, December 2012.
- [53] L. Guo, J. Ni, W. Su, C. Tang, and Y. Q. Shi, "Using statistical image model for JPEG steganography: uniform embedding revisited," *IEEE Transactions on Information Forensics and Security*, vol. 10, no. 12, pp. 2669–2680, 2015.
- [54] Y. Yao, W. Zhang, N. Yu, and X. Zhao, "Defining embedding distortion for motion vector-based video steganography," *Multimedia Tools and Applications*, vol. 74, no. 24, pp. 11163–11186, 2015.
- [55] L. Wang, Y. Xu, L. Zhai, and Y. Ren, "An adaptive video motion vector steganography based on macroblock complexity," *Chinese Journal of Computers*, vol. 40, no. 5, pp. 1044–1056, 2017.
- [56] L. Zhai, L. Wang, and Y. Ren, "Combined and calibrated features for steganalysis of motion vector-based steganography in H.264/AVC," in *Proceedings of the 5th ACM Workshop on Information Hiding and Multimedia Security*, pp. 135–146, Philadelphia, PA, USA, June 2017.
- [57] L. Zhai, L. Wang, and Y. Ren, "Universal detection of video steganography in multiple domains based on the consistency

- of motion vectors," *IEEE Transactions on Information Forensics and Security*, vol. 15, no. c, pp. 1762–1777, 2020.
- [58] K. Wang, H. Zhao, and H. Wang, "Video steganalysis against motion vector-based steganography by adding or subtracting one motion vector value," *IEEE Transactions on Information Forensics and Security*, vol. 9, no. 5, pp. 741–751, 2014.
- [59] H. Zhang, Y. Cao, and X. Zhao, "A steganalytic approach to detect motion vector modification using near-perfect estimation for local optimality," *IEEE Transactions on Information Forensics and Security*, vol. 12, no. 2, pp. 465–478, 2017.
- [60] L. Zhai, L. Wang, Y. Ren, and Y. Liu, "Generalized Local Optimality for Video Steganalysis in Motion Vector Domain," pp. 1–13, 2021, <https://arxiv.org/abs/2112.11729>.
- [61] Y. Cao, H. Zhang, X. Zhao, and H. Yu, "Video steganography based on optimized motion estimation perturbation," in *Proceedings of the 3rd ACM Workshop on Information Hiding and Multimedia Security*, pp. 25–31, Portland, OR, USA, June 2015.
- [62] Y. Cao, H. Zhang, X. Zhao, and H. Yu, "Covert communication by compressed videos exploiting the uncertainty of motion estimation," *IEEE Communications Letters*, vol. 19, no. 2, pp. 203–206, 2015.
- [63] Y. Ren, L. Zhai, L. Wang, and T. Zhu, "Video steganalysis based on subtractive probability of optimal matching feature," in *Proceedings of the 2nd ACM Workshop on Information Hiding and Multimedia Security - IH&MMSec'14*, pp. 83–90, Salzburg, Austria, June 2014.
- [64] P. Wang, H. Zhang, Y. Cao, and X. Zhao, "A novel embedding distortion for motion vector-based steganography considering motion characteristic, local optimality and statistical distribution," in *Proceedings of the 4th ACM Workshop on Information Hiding and Multimedia Security*, pp. 127–137, Vigo, Spain, June 2016.
- [65] P. Wang, Y. Cao, X. Zhao, and B. Wu, "Motion vector reversion-based steganalysis revisited," in *Proceedings of the 2015 IEEE China Summit and International Conference on Signal and Information Processing (ChinaSIP)*, pp. 463–467, Chengdu, China, July 2015.
- [66] B. Zhu and J. Ni, "Uniform embedding for efficient steganography of H.264 video," in *Proceedings of the 2018 25th IEEE International Conference on Image Processing (ICIP)*, pp. 1678–1682, Athens, Greece, October 2018.
- [67] N. Ghamsarian and M. Khademi, "Undetectable video steganography by considering spatio-temporal steganalytic features in the embedding cost function," *Multimedia Tools and Applications*, vol. 79, no. 27–28, pp. 18909–18939, 2020.
- [68] J. Li, M. Zhang, K. Niu, and X. Yang, "Investigation on Principles for Cost Assignment in Motion Vector-Based Video Steganography," pp. 1–16, 2022, <https://arxiv.org/abs/2209.01744>.
- [69] L. Zhai, L. Wang, and Y. Ren, "Multi-domain embedding strategies for video steganography by combining partition modes and motion vectors," in *Proceedings of the 2019 IEEE International Conference on Multimedia and Expo (ICME)*, pp. 1402–1407, Shanghai, China, July 2019.
- [70] M. Guo, T. Sun, X. Jiang, Y. Dong, and K. Xu, "A motion vector-based steganographic algorithm for HEVC with MTB mapping strategy," in *Proceedings of the 2019 International Workshop on Digital Watermarking*, pp. 293–306, Chengdu, China, November 2019.
- [71] Y. Hu, W. Gong, F. Liu, L. Liu, and M. Zhu, "Large-capacity lossless HEVC information hiding based on index parameter modification," *Journal of South China University of Technology*, vol. 46, no. 5, pp. 1–8, 2018.
- [72] S. Liu, B. Liu, Y. Hu, and X. Zhao, "Non-degraded adaptive HEVC steganography by advanced motion vector prediction," *IEEE Signal Processing Letters*, vol. 28, pp. 1843–1847, 2021.
- [73] Y. Yao and N. Yu, "Motion vector modification distortion analysis-based payload allocation for video steganography," *Journal of Visual Communication and Image Representation*, vol. 74, Article ID 102986, 2021.
- [74] P. Wang, Y. Cao, X. Zhao, and H. Yu, "An adaptive detecting strategy against motion vector-based steganography," in *Proceedings of the 2015 IEEE International Conference on Multimedia and Expo (ICME)*, pp. 1–6, Torino, Italy, June 2015.
- [75] P. Wang, Y. Cao, and X. Zhao, "Segmentation Based Video Steganalysis to Detect Motion Vector Modification," *Security and Communication Networks*, vol. 2017, Article ID 8051389, pp. 1–12, 2017.
- [76] B. Li, M. Wang, X. Li, S. Tan, and J. Huang, "A strategy of clustering modification directions in spatial image steganography," *IEEE Transactions on Information Forensics and Security*, vol. 10, no. 9, pp. 1905–1917, 2015.
- [77] T. Denemark and J. Fridrich, "Improving steganographic security by synchronizing the selection channel," in *Proceedings of the 3rd ACM Workshop on Information Hiding and Multimedia Security*, pp. 5–14, Portland, OR, USA, June 2015.
- [78] W. Zhang, Z. Zhang, L. Zhang, H. Li, and N. Yu, "Decomposing joint distortion for adaptive steganography," *IEEE Transactions on Circuits and Systems for Video Technology*, vol. 27, no. 10, pp. 2274–2280, 2017.
- [79] Y. Wang, W. Li, W. Zhang, X. Yu, K. Liu, and N. Yu, "BBC++: enhanced block boundary continuity on defining non-additive distortion for JPEG steganography," *IEEE Transactions on Circuits and Systems for Video Technology*, vol. 31, no. 5, pp. 2082–2088, May 2021.
- [80] Y. Wang, W. Zhang, W. Li, and N. Yu, "Non-additive cost functions for JPEG steganography based on block boundary maintenance," *IEEE Transactions on Information Forensics and Security*, vol. 16, pp. 1117–1130, 2021.
- [81] Y. Wang, Y. Cao, and X. Zhao, "Minimizing embedding impact for H.264 steganography by progressive trellis coding," *IEEE Transactions on Information Forensics and Security*, vol. 16, pp. 333–345, 2021.
- [82] L. Li, Y. Yao, X. Zhang, W. Zhang, and N. Yu, "Video steganography based on modification probability transformation and non-additive embedding distortion," *Journal of Electronics & Information Technology*, vol. 42, no. 10, pp. 2357–2364, 2020.
- [83] Y. Su, C. Zhang, and C. Zhang, "A video steganalytic algorithm against motion-vector-based steganography," *Signal Processing*, vol. 91, no. 8, pp. 1901–1909, 2011.
- [84] K. Tasdemir, F. Kurugollu, and S. Sezer, "Spatio-temporal rich model-based video steganalysis on cross sections of motion vector planes," *IEEE Transactions on Image Processing*, vol. 25, no. 7, pp. 3316–3328, 2016.
- [85] X. Huang, Y. Hu, Y. Wang, B. Liu, and S. Liu, "Deep learning-based quantitative steganalysis to detect motion vector embedding of HEVC videos," in *Proceedings of the 2020 IEEE Fifth International Conference on Data Science in Cyberspace (DSC)*, pp. 150–155, Hong Kong, China, July 2020.
- [86] X. Huang, Y. Hu, Y. Wang, B. Liu, and S. Liu, "selection-channel-aware deep neural network to detect motion vector embedding of HEVC videos," in *Proceedings of the 2020 IEEE International Conference on Signal Processing*,

## Retraction

# Retracted: Analysis of Practical Training Characteristics and Teaching System Reform Path of College Physical Education Curriculum Based on Deep Learning

### Security and Communication Networks

Received 8 August 2023; Accepted 8 August 2023; Published 9 August 2023

Copyright © 2023 Security and Communication Networks. This is an open access article distributed under the Creative Commons Attribution License, which permits unrestricted use, distribution, and reproduction in any medium, provided the original work is properly cited.

This article has been retracted by Hindawi following an investigation undertaken by the publisher [1]. This investigation has uncovered evidence of one or more of the following indicators of systematic manipulation of the publication process:

- (1) Discrepancies in scope
- (2) Discrepancies in the description of the research reported
- (3) Discrepancies between the availability of data and the research described
- (4) Inappropriate citations
- (5) Incoherent, meaningless and/or irrelevant content included in the article
- (6) Peer-review manipulation

The presence of these indicators undermines our confidence in the integrity of the article's content and we cannot, therefore, vouch for its reliability. Please note that this notice is intended solely to alert readers that the content of this article is unreliable. We have not investigated whether authors were aware of or involved in the systematic manipulation of the publication process.

In addition, our investigation has also shown that one or more of the following human-subject reporting requirements has not been met in this article: ethical approval by an Institutional Review Board (IRB) committee or equivalent, patient/participant consent to participate, and/or agreement to publish patient/participant details (where relevant).

Wiley and Hindawi regrets that the usual quality checks did not identify these issues before publication and have since put additional measures in place to safeguard research integrity.

We wish to credit our own Research Integrity and Research Publishing teams and anonymous and named external researchers and research integrity experts for contributing to this investigation.

The corresponding author, as the representative of all authors, has been given the opportunity to register their agreement or disagreement to this retraction. We have kept a record of any response received.

### References

- [1] P. Fang, "Analysis of Practical Training Characteristics and Teaching System Reform Path of College Physical Education Curriculum Based on Deep Learning," *Security and Communication Networks*, vol. 2022, Article ID 9614356, 13 pages, 2022.

## Research Article

# Analysis of Practical Training Characteristics and Teaching System Reform Path of College Physical Education Curriculum Based on Deep Learning

Ping Fang 

Hechi University, Hechi 546300, China

Correspondence should be addressed to Ping Fang; [fangping@hcnu.edu.cn](mailto:fangping@hcnu.edu.cn)

Received 28 July 2022; Revised 22 August 2022; Accepted 1 September 2022; Published 23 September 2022

Academic Editor: Hangjun Che

Copyright © 2022 Ping Fang. This is an open access article distributed under the Creative Commons Attribution License, which permits unrestricted use, distribution, and reproduction in any medium, provided the original work is properly cited.

With the growth of the new international alignment, the establishment of multifunctional and applied universities and the training of high-quality talents have become the key tasks of all colleges and universities. With the encouragement of national policies, college physical education has gradually become one of the key subjects for students. As a novel way of pursuing learning goals, deep learning includes high-level and high-stage cognitive management strength or innovative thinking strength. With the background about the widely respected teaching about school sports education of deep learning mode, this article puts forward the analysis of practical training characteristics and educational system reform path of college physical education based on deep learning. The results of the experiment are as follows: (1) this article discusses principles and ideas of the immediate in-depth learning mode and the vacancies in the current college physical education curriculum practical teaching system, determines the research direction of the experiment, and analyzes the characteristics of school physical education practical training as well as the innovation path of the teaching system based on the in-depth learning mode, which provides a technical guarantee for the research of this article; (2) using deep learning algorithm, neural network decomposition method, and recurrent neural network algorithm, the investigation content is identified, analyzed, and calculated through experiments, which is not enough to effectively and accurately analyze the root cause of the problem; it also optimizes and improves according to specific problems, reducing unnecessary research work and time consumption.

## 1. Introduction

In today's industrialized production, due to limited production equipment and funds, the quality of the final product cannot be effectively calculated, that is, it cannot meet the requirements of the production plan. As a new testing scheme, economic data transmitter focuses on the retention test of the final value in the process of book store testing, which provides a stable and effective testing tool. Deep level learning plays an important role in today's network level learning and has been widely used in machine models. By using deep level learning, we can create an interactive transmitter and extend it to industrial manufacturing cases. The comparison of modeling results shows that compared with traditional methods, deep learning technology has the following advantages, especially

suitable for soft sensor modeling [1]. The goal of statement division is to distinguish statements in the background of interference factors. Statement separation is an important task in information processing. It is found that this is a supervised learning problem based on speech separation. It uses the relationship between speech and speaker to estimate the background noise, and uses different discrimination patterns to classify the training data. In the past decade, a lot of research work based on the supervised separation algorithm has been proposed. Recently, as deep learning is widely used in any field about speech separation, some innovations have been proposed to improve the separation performance [2]. The neural network decomposition algorithm is used to obtain representative feature factors, extract and classify feature factors, and the deep learning network feature analysis and processing tool is introduced. This

engineering example verifies the superiority of the neural network decomposition algorithm [3]. The spiritual network method and the deep learning method have been successfully applied to computer vision. This article attempts to adapt CNN for optical camera to its microwave counterpart, namely, synthetic aperture radar. As a preliminary study, the convolution neural network algorithm can help to obtain the pixel features to be extracted from the target image. The idea of this algorithm is not to use the traditional dissemination algorithm, but to use the coding feature analysis with supervisory performance to train the image features. This algorithm can effectively reduce the computational complexity. First, a series of feature maps extracted from SAR images are obtained by convolution and merging, and then these feature maps are used to train the final classifier [4]. After training the system, experiments show that the algorithm is feasible. Compared with the traditional malicious code detection based on machine learning, DBN does not need any prior knowledge in the detection process. The results show that the target algorithm is efficient and accurate. Deep learning system is mainly composed of many ways, such as transmission or neural network. Finally, the optimal hybrid model is achieved by fine tuning the whole network. After inputting the test samples into the hybrid model, the experimental results show that the detection accuracy of the proposed hybrid detection method is higher than that of other levels; the design model reduces the use of time and improves the efficiency of development [5]. This article makes a comprehensive statistical analysis on the content, layout, and the development of teaching staff of national and provincial excellent physical education courses over the years. The research results show that the development of sports quality courses in China is good, but there are also problems. For example, the overall development level is low, discipline department management is serious, and the development of internal sub disciplines is uneven. Improving the introduction of teacher team resources to promote the increase of teaching effect, evaluation, supervision, and fund guarantee system are effective ways to solve the problems existing in the introduction of teacher resource team [6]. Implementation on the club system in and out of class integration mode in college physical education curriculum is to adopt more flexible and diverse ways to implement teaching project action. This model helps to maximize its functionality to students' enthusiasm and inspire enthusiasm for learning. The physical education system for college students can not only develop a structure suitable for college students' physical exercise but can also stimulate college students' initiative to exercise and good mentality and form the habit of exercise. It helps to promote the socialization of human development. It paves the way for the society in future. In addition, this mode can maintain the enthusiasm and extensibility of college physical education teaching, promote lifelong physical education, and promote the overall development of quality education, which is the inevitable trend of college physical education development [7]. To form the best PE management system suitable for the actual situation of colleges and universities, the layered teaching mode of PE courses in colleges and universities has

been repeatedly tested and studied. In the formation of the model, quality education is the guiding ideology. This model aims to improve students' physical fitness. The starting point of this model is to deal with different students in different ways. The teaching content, means, and purpose should be closely consistent. The "one size fits all" situation must be changed, which ignores the differences in students' physique and interests. Goals at all levels have relative stability and certain variability [8]. To increase the administration quality of technical courses in sports management institutions, enriching and improving the teaching methods of technical courses in physical education institutions is necessary. Nonverbal explanation contrary to oral explanation is a common teaching method in technical courses in physical education institutions. It is a teaching method summarized and improved on the basis of various teaching methods and according to physiological principles. By observing the differences in human tissues in different groups, this design can be divided into spatial methods, sensory methods, and observation methods in principle. Their characteristics are mainly reflected in the universality and efficiency of practical teaching, as well as the high speed and ambiguity of data transmission [9]. In order to explore the system to adapt to the experimental teaching content of the high-efficiency physical education major in the twenty-first century, the present situation of laboratories in some physical education colleges and universities was studied by using the methods of questionnaire survey and expert interview. It was found that the laboratory management system was old, the laboratory instruments were old, the laboratory staff structure was unreasonable, the experimental courses and theoretical courses were equally important, and the number of comprehensively designed experiments was too small [10]. The study believes that the reform of student-centered teaching methods in China is a historical trend and a long-term process. In the past two decades, Chinese universities have advocated ability-based education and tried to learn from the modern teaching methods of famous Western business schools. However, the more important work is to lay the foundation for modern teaching methods. In the process of promoting the teaching reform of undergraduate human resource management, we should deal with these difficulties in an orderly manner, with professional orientation, curriculum system reform, and teacher training [11]. Based on the majors of civil construction and real estate management and educational curriculum design, this article analyzes the mode of practical teaching management from both internal and external aspects, and highlights the importance of combining theoretical teaching with practical ability. It mainly uses the practical teaching management mode proposed by the British reporter, investigates and collects the feedback data of the research design, and creates a practical teaching management mode that is suitable for students and can meet their needs. The experimental research summarizes the linear satisfaction index and dynamic evaluation index of students on the practical teaching management model, so as to rectify and optimize the practical teaching management system according to students' feedback information, so as to promote students' practical learning ability and improve

teaching efficiency [12]. With the development of science and technology, the information technology revolution has brought about information age. Data information improves efficiency by collecting and processing data and is widely used in many fields. In the context of data information, the traditional college teaching system reform practice analysis management system is facing new challenges and reforms. This article analyzes the teaching reform path of college teaching system reform practice analysis, which helps students' enthusiasm and stimulates learning enthusiasm [13]. In the era of deepening educational reform and promoting educational innovation, the innovation of practical teaching not only adheres to the current concept of educational reform, but also promotes the continuous improvement of the college geography management system. Taking geography teaching methods as a research goal and adopting comprehensive analysis of the geography school teaching mode, we strive to solve the problems of single teaching methods, backward construction of geography textbooks, unreasonable use of courseware, and practical courses. Therefore, we should establish a modern geography teaching concept that attaches importance to heuristic and inquiry teaching [14]. Through investigation and systematic analysis, aiming at the problems existing in the practical teaching of physical education courses in colleges and universities, this article constructs an appropriate management standard consisting of practical teaching management content standard, practical support standard, practical evaluation standard, and practical feedback standard. A set of school physical education practice teaching mode was designed, which combines theoretical knowledge with teaching practice, further improves the overall quality of teachers, creates good teaching conditions for on campus training, strengthens the construction of off-campus practice bases, strengthens the management of practical teaching in schools, and promotes students' practical achievements through face-to-face teaching [15].

## 2. Analysis of the Practical Training Characteristics of College Physical Education Curriculum Based on Deep Learning and the Reform Path of Teaching System

*2.1. Relevant Technologies and Development of In-Depth Learning.* Deep learning is supported by big data. Through automatic learning of a great quantity of sample information, we can gain the internal laws and abstract expressions of data. According to the learned internal laws and abstract expressions, we can perform corresponding tasks for different fields.

The principle of deep learning technology is closely related to the information processing mechanism of human brain visual stratification. The working mechanism of human brain is to aggregate and process the initial signal in each layer of the brain before object recognition. When people are stimulated by the outside world, they will have different degrees of psychological reactions: happy feelings, and also sad feelings; some people feel excited, some feel

depressed, some feel happy, and some feel painful. When the eye is observing the image, the retina collects the image information, which then enters the ventral visual pathway through the electrical signal, which is in charge of object recognition. Deep level research can be divided into supervised learning and unsupervised research.

Figure 1 shows the basic structure of deep learning network, which generally includes an input layer, multiple hidden layers, and an output layer.

### 2.2. Characteristics of Sports Teaching in Colleges

*2.2.1. School Sports Education Curriculum Organization.* At present, the construction of the school sports education academic model is based on the campus network, which provides support for online teaching of physical education network and builds different online teaching modules of physical education.

As shown in Figure 2, data show that the sports organization department of the school is directly led by the school leaders, who cooperate with the Communist Youth League and the student union to organize various sports activities in the school. The sports association department carries out various activities under the direct leadership of the school leaders.

An independent module is established on the homepage of the campus network to display the physical education teaching content. This module includes two parts: course information and teacher information. The internal sports module of the campus network shows students all kinds of sports activities teaching courseware, sports competition video production, taking wonderful sports photos, various project judging rules, learning the warm-up methods and physical care before physical exercise, publishing sports competition information, calling on students to sign up actively, and publishing award winning information to show the sports strength of the school.

*2.2.2. Current Needs of School Sports Education.* For the optimization of sports education studies, the teaching process should be more efficient. Second, we should use advanced network technology to deeply excavate and integrate the existing sports resources and combine sports theory with other related disciplines in combination with new educational auxiliary technology, so as to enrich students' learning content and improve the teaching efficiency of online courses. Third, teaching methods must be innovative. Teachers can carry out online teaching in a variety of ways and students are allowed to conduct offline teaching mode, improving quality of teaching.

College physical education curriculum design needs careful consideration through learner analysis and content selection, refining the classroom theme according to principles, using appropriate software practice and development, and careful designing. After that, it can be used in the classroom or network to check whether the effect evaluation can be obtained, so that college physical education



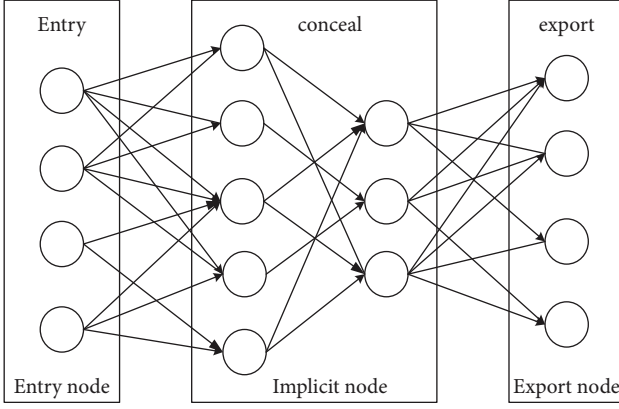


FIGURE 1: Basic structure of deep learning network.

curriculum can also be renovated on the basis of the existing evaluation.

As shown in Figure 3, the school physical education teaching system is designed with four aspects: sports education studies teaching objectives, sports education studies teaching themes, learning content analysis, and learner analysis. According to the learning situation, physical education curriculum learning strategies are formulated, so as to develop classroom resources and integrate them into learning activities. Finally, the teaching design is tested, evaluated, and applied to practice.

### 3. Algorithm Formula of Practical Training Characteristics of College Physical Education Curriculum Based on Deep Learning

**3.1. Convolutional Neural Network Algorithm.** Convolutional neural network is widely used in visual processing tasks and language processing tasks. Its main content is composed of sampling layer, initialization layer, lower sampling layer, connection layer, partition layer, and standardization layer.

When performing convolution operation in the convolution layer, it involves three common parameters: step size, filling value, and depth. Step length refers to the number of calculations required for convolution check of each pixel in the original image. It represents the distance between all data points obtained after convolution operation between the image filled by spacing pixels in a certain time and the original image. Depth refers to the time from the original image to the plane. It contains two different dimensions: one dimension represents the depth of the object and another dimension represents the distance between objects.

By improving the valid convolution algorithm, it is suitable for feature extraction in multiresolution image classification. The relationship between the feature dimension and step size obtained after the convolution layer, the filling value, the convolution kernel size, and the input feature size can be calculated by the following formula:

$$D_{\text{output}} = \frac{D_{\text{input}} - D_{\text{kernel}} + 2\text{Padding}}{S_{\text{kernel}}} + 1. \quad (1)$$

The same convolution is a convolution operation that does not change the size of the original image. The operation process of the same convolution is similar to the previous two convolution processes, with the difference in the selection of filling value. The mathematical expression is as follows:

$$n = \frac{n - D_{\text{kernel}} + 2\text{Padding}}{S_{\text{kernel}}} + 1. \quad (2)$$

A moving transformation of (2) is made, focusing on the relationship between the convolution kernel dimension and the filling value, and formula (3) is obtained:

$$\text{Padding} = \frac{1}{2} \left( \frac{n - 1}{S_{\text{kernel}}} - n + D_{\text{kernel}} \right). \quad (3)$$

The activation layer refers to the network layer composed of activation function groups after convolution operation. The characteristic map obtained by convolution operation can bring nonlinear factors to neurons after being processed by activation function, so that the depth network can have similar characteristics with the research object. The initialization function mainly includes S-type growth curve function, hyperbolic tangent function, and linear rectification function, in which the mathematical expression of S-type growth curve function is as follows:

$$y = \frac{1}{1 + e^{-x}}. \quad (4)$$

The mathematical formula expression of hyperbolic tangent function is as follows:

$$\tanh(x) = \frac{e^x - e^{-x}}{e^x + e^{-x}}. \quad (5)$$

The mathematical formula of linear rectification function is as follows:

$$y = \begin{cases} x, & x > 0 \\ 0, & \text{otherwise.} \end{cases} \quad (6)$$

The function of the full-connection layer is usually to draw the previously learned features and convert them into the sample mark space. In the PCB image defect target detection task, it mainly includes the classification of the PCB defect categories and location. The output characteristics of the full-connection layer can be calculated using the following formula:

$$h(x) = \theta(\omega^T x + b). \quad (7)$$

The parameter  $\omega$  in formula (7) is a preset weight vector. The size of  $\omega$  represents the importance of the corresponding target object in the multiobjective optimization problem. The larger  $\omega$  means that the object is more important in the problem. On the contrary, the smaller  $\omega$ -table modification object is less important;  $\theta$  is the selected activation function, which introduces the nonlinear characteristics into the network, mainly converting the input signal of a node in the convolutional neural network model into an output signal.

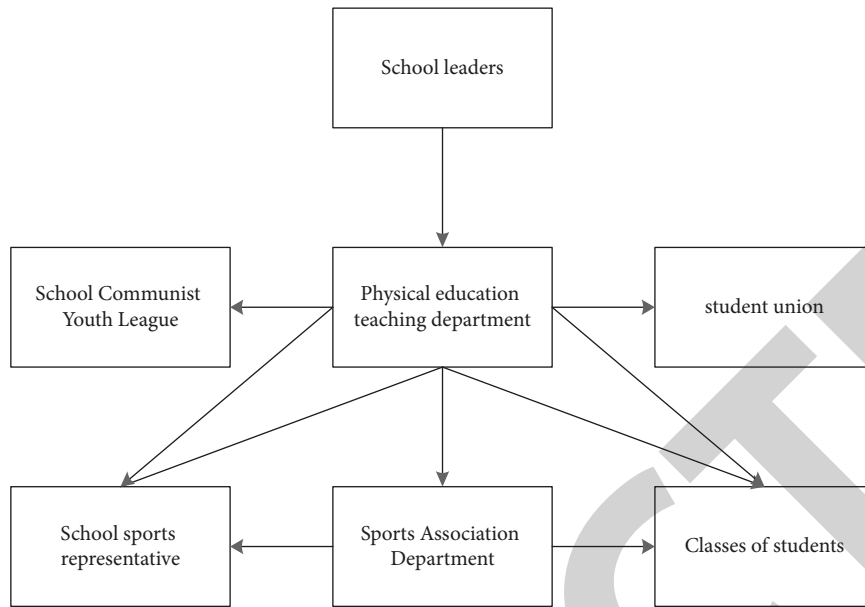


FIGURE 2: Structure of physical education teaching management in colleges and universities.

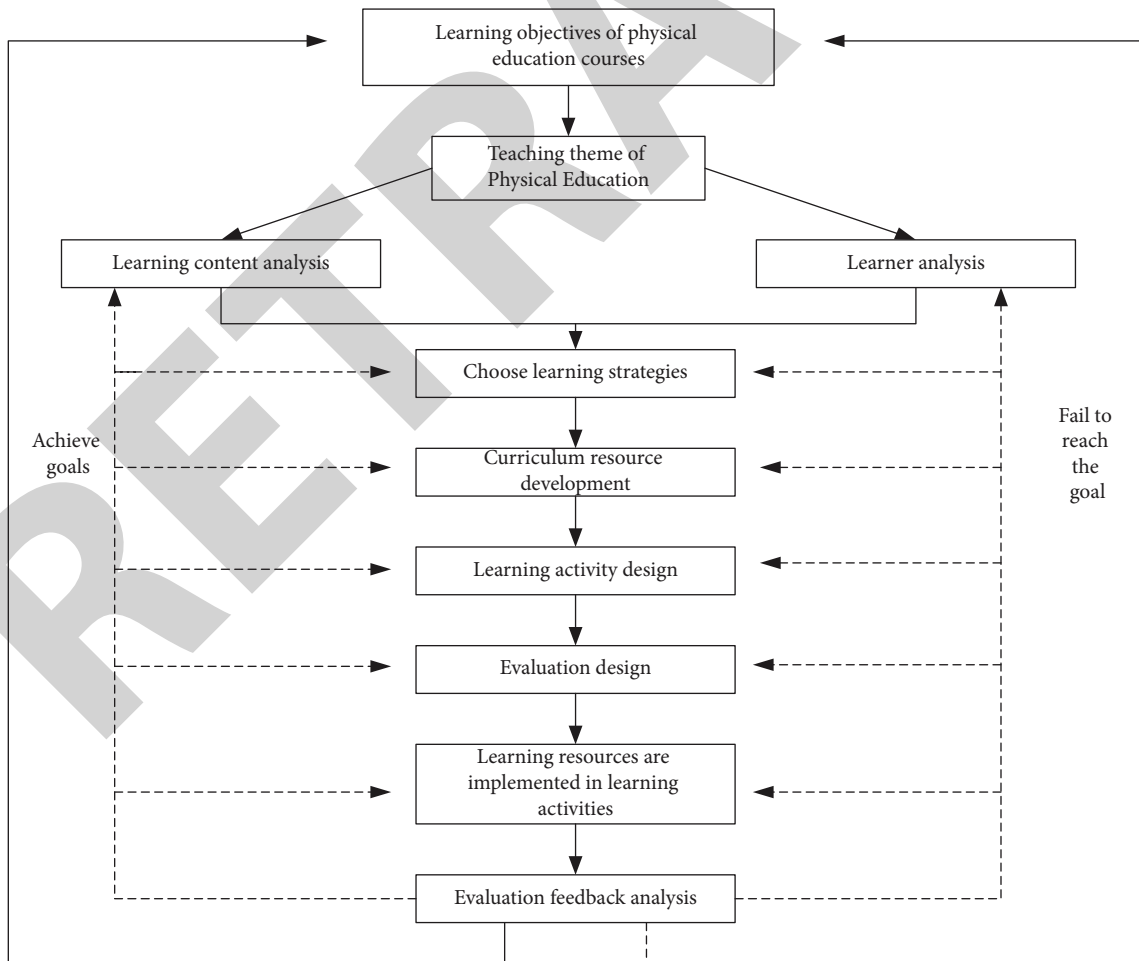


FIGURE 3: College physical education curriculum design pattern.

When designing the model of convolutional neural network, usually only a small number of full-connection layers are set because more full-connection layers may include too many neurons in the network, resulting in an increase in the amount of calculation for the model, which prolongs the calculation time spent in the training and detection stages of the network and will affect the fitting ability of the model to interested targets to a certain extent.

In order to resolve the abovementioned problems, the batch standardization layer uniformly distributes the scattered data, which is more conducive for the network to learn the hidden laws in the data. Batch standardization mainly includes the following aspects: calculating the sum and variance of the current batch data; A normalization function is designed to normalize the data of the current batch, so that the distribution of the data is within the range of (0, 1); Scale change and offset operations are performed on the data.

The mathematical expression of the formula for calculating the mean and variance of a batch of data is as follows:

$$\mu_B = \frac{1}{m} \sum_{i=1}^m x_i. \quad (8)$$

$$\delta_B^2 = \frac{1}{m} \sum_{i=1}^m (x_i - \mu_B)^2. \quad (9)$$

$\mu_B$  and  $\delta_B$  are the mean and variance obtained after batch processing, respectively. The mean reflects the average level of a group of data, and the variance reflects the dispersion of a group of data. The smaller the variance, the more stable the group of data is, and the smaller the fluctuation around the mean.

In formulas (8) and (9),  $m$  is the amount of data in the batch, and  $x$  is the input data in the current batch. The mathematical expression of the commonly used formula when normalizing the mean variance of the data is as follows:

$$x = \frac{x_i - \mu_B}{\sqrt{\delta_B^2 + \varepsilon}}, \quad (10)$$

where  $x$  is the normalized data and  $\varepsilon$  is a minimal integer to avoid denominator 0. After normalization, scale transformation and migration are carried out. The formula expression used is as follows:

$$y_i = \gamma x_i + \beta, \quad (11)$$

where  $\gamma$  is the scale factor to adjust the size of the value and  $\beta$  is the translation factor to offset the data. Scale transformation and migration operations are the core of phi table standardization.  $\gamma$  and  $\beta$  are generally obtained during network training.

**3.2. Wavelet Decomposition Algorithm.** FT is a decomposition analysis method that is widely used in time series data. This method can decompose the time-domain signal into multiple frequency-domain signals and then analyze the

overall data by analyzing the frequency-domain signals. Both time domain and frequency domain have their own unique functions and uses. This article mainly introduces three methods commonly used in time-domain and frequency-domain processing: Fourier series method, Fourier spectrum analysis method, and wavelet packet energy method. The time-domain function refers to a function that the data will change with the development of time. This method of observing and analyzing data based on time is analyzed from the time domain. FT greatly expands the means of signal analysis, and its transformation formula is expressed as follows:

$$F(\omega) = \int_{-\infty}^{\infty} f(t) e^{-i\omega t} dt. \quad (12)$$

$f(t)$  represents the time-domain signal, where  $t$  represents the time step,  $F(\omega)$  represents the frequency function (frequency signal),  $\omega$  represents the frequency component of the signal at the circular frequency, and  $F(\omega)$  is also called the image function of  $f(t)$ . Both time-domain signals and frequency-domain functions are only methods of analyzing signals, rather than saying that a signal is sometimes divided into time-domain signals and frequency-domain signals. A signal can be either a time-domain signal or a frequency-domain signal, which can be converted according to the needs of research.

Inverse Fourier transform is a transformation that transforms frequency signals into time-domain signals. Its mathematical expression is as follows:

$$f(t) = \frac{1}{2\pi} \int_{-\infty}^{\infty} F(\omega) e^{i\omega t} d\omega. \quad (13)$$

The idea of this method is to divide the larger information data into different smaller wholes from a larger part. First, it filters and classifies the initial data through filters to get the data that need to be segmented. Then, the two components are transformed by inverse wavelet transform to get a new data volume. Next, the appropriate threshold in each subband is selected to denoise the original signal.

Continuous wavelet transform is a common wavelet decomposition method. Its mathematical formula is as follows:

$$\psi_{ab}(t) = a^{-1/2} \psi\left(\frac{t-b}{a}\right). \quad (14)$$

$a$  is the scaling factor ( $a > 0$ ) and  $b$  is the translation factor. The values of  $a$  and  $b$  are adjusted to control the scale of wavelet transform and reach the peak value in the interval. The scaling factor and translation factor act on the curve equation to be deformed, and the shape of the curve can be controlled by changing the control parameters interactively, so as to obtain rich deformation effects.

The mathematical expression of continuous wavelet transform is as follows:

$$W_f(a, b) = \int_{-\infty}^{+\infty} f(t) \overline{\psi_{ab}(t)} dt. \quad (15)$$

In formula (15),  $W_f(a, b)$  represents the coherent decomposition coefficient,  $f(t)$  represents the initial source content, and  $\psi_{ab}(t)$  represents a similar function.

However, the correlation decomposition method needs to deal with all the decomposition coefficients, which not only produces unusable data but also wastes research time. Because the coherent decomposition method needs a lot of computational processing energy, a new decomposition function is constructed by the characteristics between the coherent decomposition methods. That is, the correlation between signals is used to construct a new wavelet basis function, and the parameters such as discrete expansion factor, translation factor, and orthogonal basis are adjusted according to the correlation between signals. The mathematical expression is as follows:

$$\begin{aligned} a &= a_o^j, \\ b &= ka_o^j b_o. \end{aligned} \quad (16)$$

Then, the mathematical expression of the calculation method of the function is as follows:

$$\psi_{jk}(t) = a_o^{-(1/2)} \psi(a_o^{-j}t - kb_o). \quad (17)$$

The discrete wavelet transform formula is as follows:

$$W_f(j, k) = \int_{-\infty}^{+\infty} f(t) \overline{\psi_{jk}(t)} dt. \quad (18)$$

In formula (18),  $\psi_{jk}(j, k)$  represents the coherent processing coefficient,  $f(t)$  represents the initialization data source, and  $\overline{\psi_{jk}(t)}$  represents  $\psi_{jk}(t)$  similar function.

The second step of wavelet transform is to reconstruct the wavelet coefficients and add all low-frequency signals and high-frequency signals to realize data restoration. The reconstruction method expression is as follows:

$$f(t) = cA_n l(\psi_{ik}(t)) + \sum cD_n h(\psi_{ik}(t)). \quad (19)$$

In formula (19),  $f(t)$  represents the decomposed data set,  $l(\psi_{ik}(t))$  represents the data filter, and  $h(\psi_{ik}(t))$  represents the high-efficiency filter.

**3.3. RNN Algorithm of Recurrent Neural Network.** With the wide application of artificial neural network in various fields of life, it is found that the output of traditional neural network only considers the input impact of the previous moment and does not consider the input impact of other moments. Therefore, the method based on depth research helps to improve recognition ability of a single input when dealing with multiple inputs and outputs, especially in handwritten font recognition. However, in practical applications, people have higher requirements for time series, and the traditional methods based on time series can no longer meet these requirements, which requires some new technologies to solve this problem.

As shown in Figure 4, the basic structure diagram operation of RNN greatly reduces the amount of parameter training. Where  $u$  represents the weight of the input sample at that time,  $w$  represents the input weight and  $V$  represents

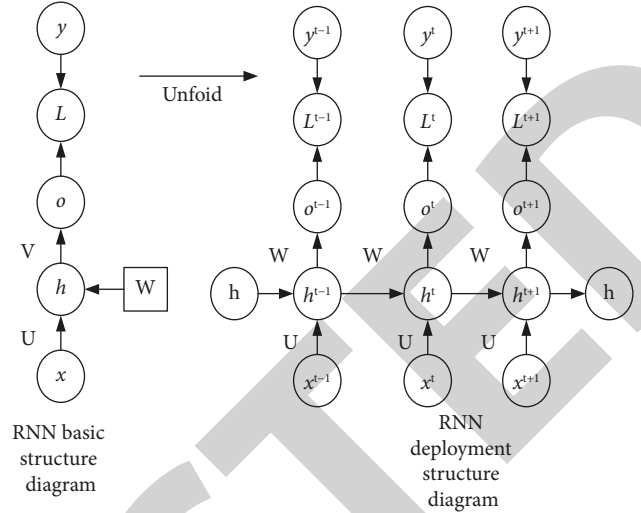


FIGURE 4: Schematic structure diagram of RNN.

the weight of the sample. An image super-resolution reconstruction algorithm based on the random walk model is proposed. The intermediate circulation structure shows that there are connections between hidden layers.

$$\begin{aligned} h_t &= f(Ux_t + Wh_{t-1} + b) \\ o_t &= Vh_t + c \\ y_t &= g(o_t). \end{aligned} \quad (20)$$

## 4. Experimental Statistical Analysis about Characteristics of Practical Training and Path of Education System on the Deep Innovation of School Sports Education

### 4.1. Analysis of Practical Training Characteristics on the Deep Innovation of School Sports Education

**4.1.1. Research of Comprehensive Quality Test of Students Both Experimental Class and Control Class before Deep Learning.** Using the test method, the physical fitness of students before the test was recorded, and the physical fitness of students in experiment group one, experiment group two, and control group before the test was tested for significant differences. The specific statistical results are shown in Table 1 and Figure 5.

Table 1 shows the statistical table comprehensive quality test analysis of pupils in the test group and the control group. The physical quality of pupils is statistically analyzed using five items: 50-meter sprint, sit ups, 800 meters, standing long jump, and change direction running.

As shown in Figure 5, the statistical chart of students' various physical qualities is shown. The statistical investigation and analysis are mainly carried out on students' 50-meter run, sit ups, 800-meter long run, standing long jump, and directional change run, and the average value changes of test group one, test group two, and control group are researched.

TABLE 1: Statistical table of comprehensive quality test analysis of pupils in the test group and the control group.

Index	Experiment group 1 Mean value	Experiment group 2 Mean value	Control group Mean value	F	P
50 meter run	72.88	74.37	73.72	0.228	0.796
Abdominal curl	75.06	73.23	75.06	0.181	0.835
800 meters	71.78	75.10	73.81	1.419	0.247
Standing long jump	72.71	72.87	73.75	0.159	0.853
Change direction run	72.41	75.63	73.58	1.120	0.331

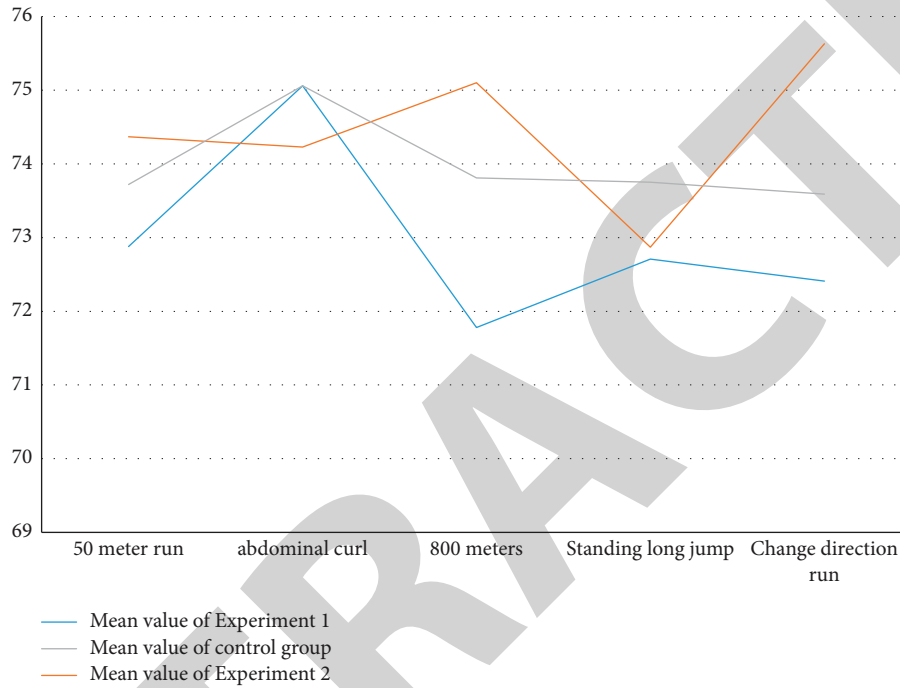


FIGURE 5: Statistical chart of students' physical fitness.

After the experiment, the data showed that values of the pupils in the experimental class 1, the experimental class 2, and the control class in the 50-meter running performance, the sit up performance, the 800/1,000-meter performance, the sitting posture forward-bending performance, and the cross direction change running performance were all less than 0.06, reflecting the differences between each group of objects.

Using the method of test, the students' sports basketball technology and technical and tactical application ability before the experiment were recorded, and the differences in both test group and the control group were investigated.

Table 2 shows the statistical table of sports basketball technology and practical application ability of students in each class. The data show that full-court passing can measure the students' basketball dribbling, passing, and high-low hand layup ability during the progress, the free throw can measure the students' single hand shoulder shooting ability, and the teaching competition can measure the students' comprehensive ability of practical basketball.

Figure 6 shows grade point average of whole field passing in the test group one is 63.75 points, the average score of the free throw is 65.94 points, the average score of the V-shaped

layup is 61.25 points, the average score of the teaching competition is 61.56 points, the average score of the whole field passing in the control class is 63.44 points, the average score of the 60 s shooting is 60.63 points, and the average score of the V-shaped basket is 60.44 points.

As shown in Table 3, the front structure level indicates that students' answer and question clues are easy to be confused, the single point structure indicates that students can take questions to heart and at least one thinking operation can connect clues and questions, and the parallel structure indicates that students can grasp most of the relevant materials.

The data show that there are differences between the experimental group and the control group in the mean value of initial tissue, single tissue, multiple tissue, coexisting tissue, and hollow tissue, and the mean value of the experimental group 2 is higher than that of the experimental group 1 and the control group, which is conducive to the comparative observation before and after the experiment and the quick statistics of the research results.

As shown in Figure 7, it is known that there is no significant difference between the five dimensions of the three groups of subjects' in-depth learning: the initial tissue

TABLE 2: Statistical table of sports basketball technology and practical application talent of pupils.

Index	Experiment group 1 Mean value	Experiment group 2 Mean value	Control group Mean value	F	P
Dribble	63.75	64.67	63.44	0.127	0.881
Pitching	65.94	60.67	60.63	2.290	0.107
Lay up	61.25	59.33	58.44	0.641	0.529
Competition	61.56	60.33	58.75	0.564	0.571

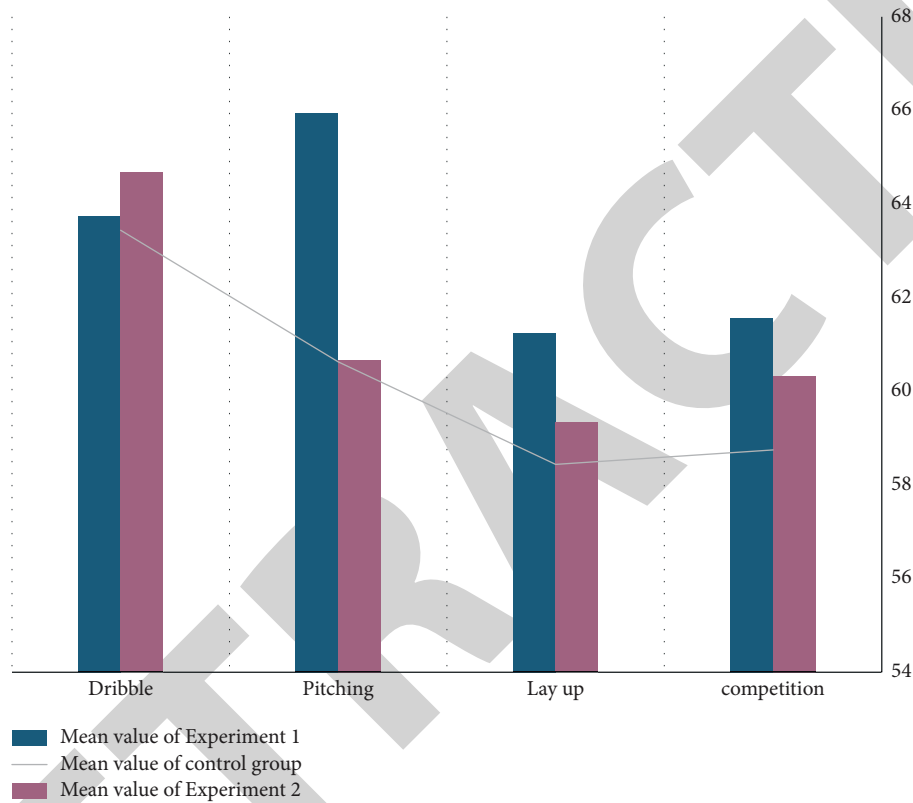


FIGURE 6: Statistical chart of basketball skills and practical ability of students in each class before the experiment.

TABLE 3: Statistics of students' in-depth learning ability.

Index	Experiment group 1 Mean value	Experiment group 2 Mean value	Control group Mean value	F	P
Initial organization	12.25	12.27	12.41	0.086	0.918
Single organization	11.41	12.03	11.81	1.370	0.259
Diverse organization	9.84	10.20	9.88	0.886	0.416
Coexisting organization	8.59	9.30	9.06	2.448	0.092
Cavitary tissue	9.44	9.57	8.94	3.002	0.055

layer, single tissue layer, multiple tissue layer, coexistence tissue layer, and void tissue layer, which indicates that the requirements are met when taking the test class 1 and test class 2 as samples for in-depth learning.

*4.1.2. Analysis of Physical Health Test of Students in the Test Group and Control Group after Deep Learning and After Deep Research.* Table 4 shows the statistical table of physical

health test analysis of pupils in the test group and the control group after deep learning. The data test indicates that the values of the test group and the control group in the five item tests are less than 0.05, indicating that the 50-meter run scores of the three groups of subjects are significantly higher than the sit ups scores.

Figure 8 shows the statistical chart of students' physical health test scores in the test group and control group after deep research. The data show that the increase in the scores

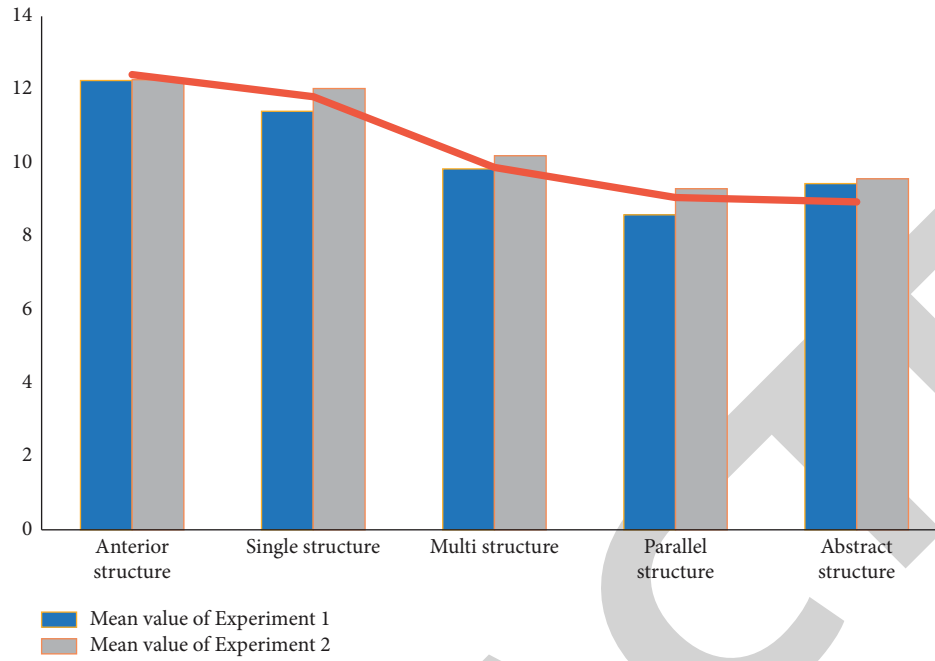


FIGURE 7: statistics of college Students' in-depth study and professional research.

TABLE 4: Statistical table of physical health test analysis of pupils in the test group and the control group.

Index	Experiment group 1 Mean value	Experiment group 2 Mean value	Control group Mean value	F	P
50-meter run	80.06	78.70	74.12	6.069	0.003
Abdominal curl	82.22	79.33	76.09	4.681	0.012
800 meters	80.78	78.83	74.22	8.426	0.011
Standing long jump	79.19	77.43	74.06	3.865	0.024
Change direction run	78.91	75.80	75.23	3.149	0.048

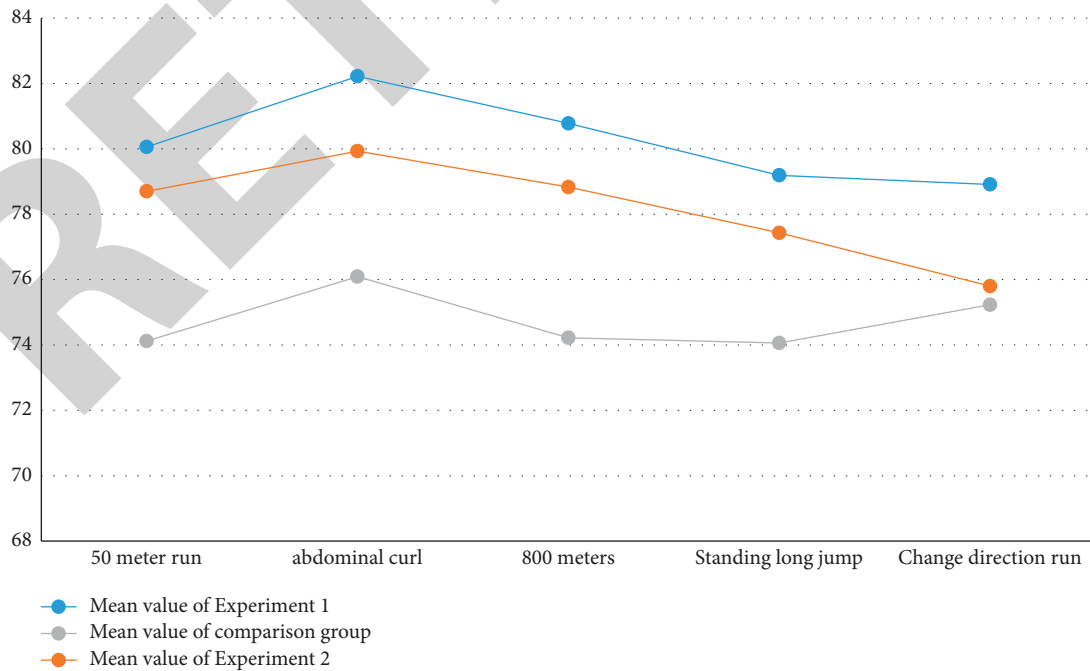


FIGURE 8: Statistical chart of students' physical health test scores in the test group and control group after deep research.



TABLE 5: Statistical table of physical education teaching objectives.

Teaching objectives	Frequency (%)	Ranking
Sports participation	91.8	1
Motor skills	89.7	2
Mental health	81.6	4
Social adaptation	85.7	3
Good health	73.4	5
Career development	59.1	6

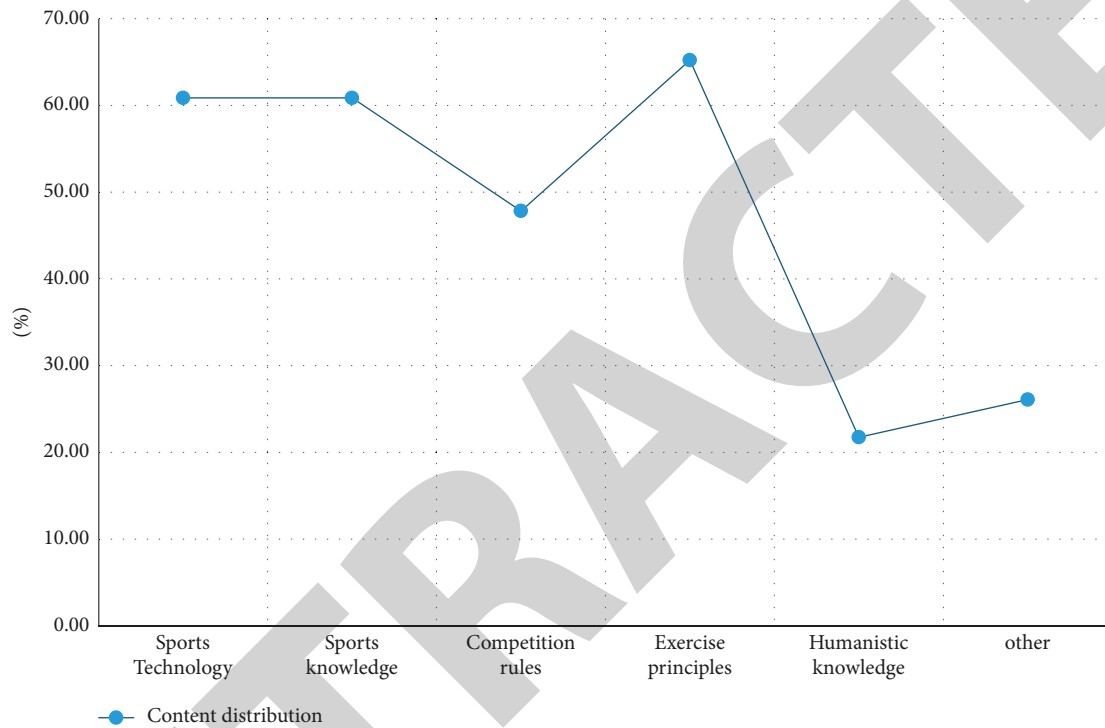


FIGURE 9: Distribution of teaching contents of sports theory.

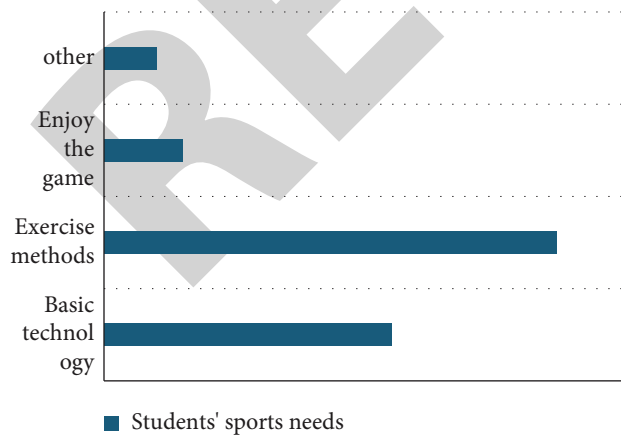


FIGURE 10: Distribution of students' sports needs.



FIGURE 11: Satisfaction degree of students' needs in physical education course hours.

of each item in the experimental group 1 is the most obvious, followed by the increase in the scores of the experimental group 2, and the smaller increase in the scores of the control

group, indicating that the practical training of physical education courses based on in-depth learning helps students better participate in the sports education mode and it greatly promotes students' physical exercise.

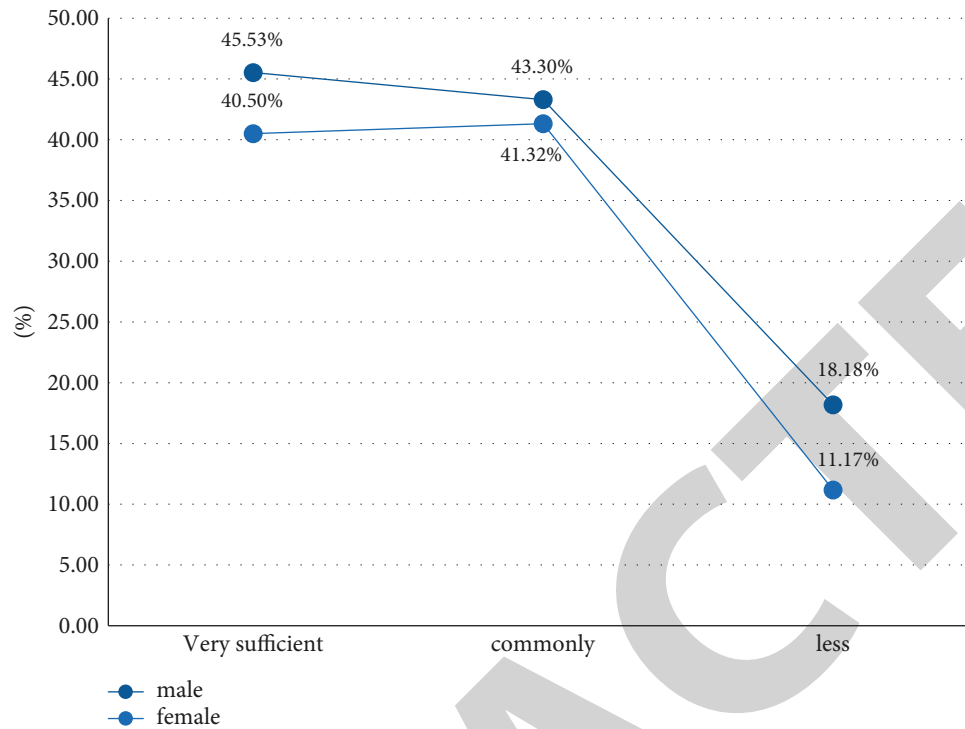


FIGURE 12: Statistical chart of the difference between male and female students' demand for physical education course hours.

**4.2. Investigation on Academic Innovation of School Sports Education with In-Depth Research.** To understand the situation of the teaching content of physical education courses in colleges and universities efficiently, it was planned that the form of questionnaire would be used to investigate the teaching of physical education courses in various colleges and universities in order to find the problems existing in school sports education academic organization content at present, analyze the reasons, and give corresponding suggestions and solutions.

Talent training focuses on the connection with the actual position, as well as the post skills and ability requirements. Under such a clear curriculum and teaching system, all courses need to be paid more attention. As an important part of the professional curriculum system in secondary vocational schools, physical education puts forward higher requirements for its educational mode. Starting with the current condition about secondary vocational education, this article analyzes the problems existing in the teaching reform of physical education and discusses the corresponding reform measures against these problems.

As shown in Table 5, through the analysis of six aspects of sports participation, sports skills, mental health, social adaptation, physical health, and career development, this article discusses the direction of college physical education model objectives and formulates frequency statistics and corresponding rankings for different college physical education teaching objectives.

The data show that more than 90% of attention of learning to sports education and skill teaching is still high and have the lowest requirements for career development. The main teaching direction is students' sports participation

and less personal guidance for students, combined with the characteristics of their careers, so that they can go to the society. It is difficult to develop sports ability and habits after participating in work.

Figure 9 shows the content distribution of sports theory teaching. The data show that the content distribution of sports theory teaching is mainly divided into sports technology, sports health knowledge, competition rules, exercise method principles, and sports humanistic knowledge. The proportion of exercise method principles is as high as 65.22%, and the proportion of sports humanistic knowledge is as low as 27.74%.

As shown in Figure 10, the data show that half of the students believe that physical education courses can be used to learn the methods needed to exercise, 33% of the students believe that physical education courses can help obtain the corresponding basic sports skills, and only 9% of the students believe that through physical education courses, they can better enjoy the game.

Figure 11 shows that according to the data of physical education class hours, nearly half of the students think that the current physical education class hours are enough, some students think that the class hours are not enough, and some students think that it is average.

Figure 12 shows the statistical analysis chart of physical education curriculum needs of male and female students. The actual investigation and analysis are carried out with three options: very sufficient, general, and less. The data show that the number of boys' actual feedback is greater than that of girls.

In the group of boys, nearly one-fifth of boys think that the amount of physical education class hours is not enough.

## Retraction

# Retracted: Evaluation of Political Classroom Teaching Quality in Universities Based on DA-BP Algorithm

### Security and Communication Networks

Received 1 August 2023; Accepted 1 August 2023; Published 2 August 2023

Copyright © 2023 Security and Communication Networks. This is an open access article distributed under the Creative Commons Attribution License, which permits unrestricted use, distribution, and reproduction in any medium, provided the original work is properly cited.

This article has been retracted by Hindawi following an investigation undertaken by the publisher [1]. This investigation has uncovered evidence of one or more of the following indicators of systematic manipulation of the publication process:

- (1) Discrepancies in scope
- (2) Discrepancies in the description of the research reported
- (3) Discrepancies between the availability of data and the research described
- (4) Inappropriate citations
- (5) Incoherent, meaningless and/or irrelevant content included in the article
- (6) Peer-review manipulation

The presence of these indicators undermines our confidence in the integrity of the article's content and we cannot, therefore, vouch for its reliability. Please note that this notice is intended solely to alert readers that the content of this article is unreliable. We have not investigated whether authors were aware of or involved in the systematic manipulation of the publication process.

Wiley and Hindawi regrets that the usual quality checks did not identify these issues before publication and have since put additional measures in place to safeguard research integrity.

We wish to credit our own Research Integrity and Research Publishing teams and anonymous and named external researchers and research integrity experts for contributing to this investigation.

The corresponding author, as the representative of all authors, has been given the opportunity to register their agreement or disagreement to this retraction. We have kept a record of any response received.

### References

- [1] H. Guan and D. Zhu, "Evaluation of Political Classroom Teaching Quality in Universities Based on DA-BP Algorithm," *Security and Communication Networks*, vol. 2022, Article ID 3391881, 10 pages, 2022.

## Research Article

# Evaluation of Political Classroom Teaching Quality in Universities Based on DA-BP Algorithm

Hui Guan<sup>1</sup> and Dongxiang Zhu<sup>2</sup> 

<sup>1</sup>*School of Marxism, Jiangxi Normal University, Jiangxi, Nanchang 330022, China*

<sup>2</sup>*School of Humanity and Law, Beijing University of Chemical Technology, Beijing 100029, China*

Correspondence should be addressed to Dongxiang Zhu; zhudx@buct.edu.cn

Received 28 June 2022; Revised 16 August 2022; Accepted 23 August 2022; Published 22 September 2022

Academic Editor: Hangjun Che

Copyright © 2022 Hui Guan and Dongxiang Zhu. This is an open access article distributed under the Creative Commons Attribution License, which permits unrestricted use, distribution, and reproduction in any medium, provided the original work is properly cited.

In order to improve the evaluation accuracy of political classroom teaching quality in universities, a DA-BP-based evaluation method of political classroom teaching quality in universities is proposed. First of all, in constructing the teaching quality evaluation system of university political courses using the framework of behavior theory, the system consists of 4 primary indicators and 15 secondary indicators. Second, the university's 2008–2013 annual teaching quality assessment scores for the teaching quality of political courses were used as the input data of the DA-BP network, and the 2013–2016 teaching evaluation scores were used as the algorithm's test data. In order to test the prediction accuracy of the DA-BP algorithm, it is compared with the GA-BP algorithm, PSO-BP algorithm, and BP algorithm. The research results show that DA-BP has higher prediction accuracy than other algorithms and can better evaluate the teaching quality of political courses.

## 1. Introduction

China has strengthened the research on the evaluation of political education for nearly three decades, and a series of documents issued at important meetings of the Party Central Committee, The Central Committee of the Communist Party of China and the State Council issued a series of documents on strengthening the quality education of college students and improving their political awareness. Several opinions of the CPC Central Committee on Strengthening and Improving Political Work, etc., have all put forward clear requirements for the evaluation of political education. In terms of research results, the book *Principles of Political Education*, edited by Professors Qiu Weiguang and Zhang Yaocan, contains a chapter on the evaluation of political education, and the book *Methodology of Political Education*, edited by Professor Zheng Yongting, also puts forward a more comprehensive and targeted evaluation method. There are also many similar works on the evaluation of political education. In addition, there are more research results in this field in academic literature, such as Yu

Manhua's "The Construction of a New Mechanism of Political Education Evaluation in Universities," Xiong Linwu's "A Trial of Political Education Evaluation in Higher Education," and Wang Maosheng's "The Scientific Connotation and Characteristics of Political Education Evaluation".

On the basis of paying sufficient attention to the evaluation of political education, China has gradually begun to refine it, including the evaluation of political education work, the evaluation of political education courses, the evaluation of the timeliness of political education, etc. [1]. So far, there has been a lot of progress. In the evaluation of the quality of political theory courses, as early as the 1980s, the idea of quality assurance was explored by some scholars in China. It was explored by some scholars in China and further disseminated in the 1990s, but it has not yet formed a large impact. Wang Anping has analyzed and researched how to improve the quality of teaching in political science courses at a macrolevel, Zhang Aijun believes that theory should be linked to practice in teaching ideology, based on classroom teaching, enriching students' theoretical knowledge reserves and strengthening the use of display, Zhang

Sennian first proposed the concept of teaching quality assurance system for political theory courses in universities that was put forward for the first time by Zhang Sennian, and the significant role of the construction of this system in improving the teaching quality of political science courses in universities was demonstrated; Gao Haisheng innovatively introduced the teaching quality monitoring system after Zhang Sennian proposed the teaching quality assurance system, upgrading the static evaluation system to dynamic. Although there are more research results for the evaluation of teaching quality of political science courses in universities, they basically stay on qualitative evaluation, without quantitative evaluation, which would make the research lack credibility and persuasiveness. Therefore, this paper applies the dragonfly algorithm (DA) to optimize the parameters of the initial connection weights  $c_j$  and  $\omega_{ij}$  and thresholds  $\varepsilon$  and  $\theta_j$  of the BP model, and proposes a DA-BP algorithm-based method for evaluating the quality of teaching in college political courses, which fills the gap of no quantitative research. From the result, we can know that the DA-BP algorithm can quickly and accurately evaluate the teaching quality, providing a new algorithm process for the subsequent evaluation of the teaching quality of college political courses.

## 2. Dragonfly Algorithm

The dragonfly algorithm (DA) is a new metaheuristic algorithm designed to solve global optimization problems by simulating the foraging and migration behavior of the dragonfly population in nature. It has the characteristics of simple implementation, few optimization parameters, short convergence time, and so on. It is widely used in various fields to optimize different problems. In this study, due to the need to combine the DA with the neural network algorithm, the band algorithm needs to have the characteristics of fast convergence and fewer steps, so the DA can well meet this demand. The original thoughts of the dragonfly algorithm comes from the simulation of group behavior of dragonflies such as predation and avoidance (Figure 1), and the flight (evolutionary) search mechanism can be expressed in five steps: separation, alignment, aggregation, food attraction, and dispersal of natural enemies [2].

In the DA, individual dragonflies forage and seek advantage through five types of behavior: collision avoidance behavior, pairing behavior, aggregation behavior, foraging behavior, and enemy avoidance behavior, which can be shown in those following formulas: the position vector update strategy for collision avoidance behavior is given in equation (1) [3].

$$S_i = - \sum_{j=1}^N X - X_i, \quad (1)$$

where  $X$  is the current position of the dragonfly individual;  $X_j$  is the position of the  $j$  th neighboring dragonfly individual, and  $N$  is the number of neighboring dragonfly individuals. The strategy for updating the position vector for pairing behavior is shown in equation (2).

$$A_i = \frac{- \sum_{j=1}^N V_j}{N}, \quad (2)$$

where  $V_j$  is the velocity of the  $j$ th neighboring dragonfly individual. The location vector update strategy for aggregation behavior is shown in equation (3).

$$C_i = \frac{- \sum_{j=1}^N X_j}{N} - X. \quad (3)$$

The location vector update strategy for foraging behavior is shown in equation (4).

$$F_i = X^+ - X, \quad (4)$$

where  $X^+$  is the food source location (the current optimal solution). The location direction update strategy for enemy avoidance behavior is as in equation (5).

$$E_i = X^- + X, \quad (5)$$

where  $X^-$  is the natural enemy location (the current worst solution). In summary of the five dragonfly group behaviors above, the step vector update strategy for individual dragonflies is shown in equation (6).

$$\Delta X_{t+1} = (sS_i + aA_i + cC_i + fF_i + eE_i) + \omega \Delta X_t, \quad (6)$$

where  $s$ ,  $a$ ,  $c$ ,  $f$ , and  $e$  are the weights of the five dragonfly group behaviors, respectively;  $\omega$  denotes the inertia weight; and  $t$  is the number of current iterations as shown in equation (7). The dragonfly position update strategy is as follows:

$$X_{t+1} = X_t + \Delta X_{t+1}. \quad (7)$$

This study adapts the optimal solution-seeking mechanism of the dragonfly algorithm as follows:

- (1) We introduce an optimization mechanism for the initial population of individuals. The initial population of dragonflies is randomly selected, and a feasible solution is obtained through the initial optimization calculation [4].
- (2) We add a local reasonableness mechanism [5]. The reasonableness review operator is added to the dragonfly algorithm, which iterates through the computational dimensions of individual dragonflies, retaining the reasonable localities after the flight and eliminating the localities that are not reasonable after the flight, to speed up the algorithm's computation rate [6].

The computational flow of the adapted dragonfly algorithm consists of 12 steps [7].

Step 1: The initialization of the calculation parameters, taking into account the short-term optimal scheduling model of the stepped power station, sets the number of dragonfly populations  $N = 40$  and the number of iterations  $\text{MAXiter} = 200$ .

Step 2: The initial population is generated by using the reservoir operating level of the stepped power station as the decision variable, based on the upper and lower

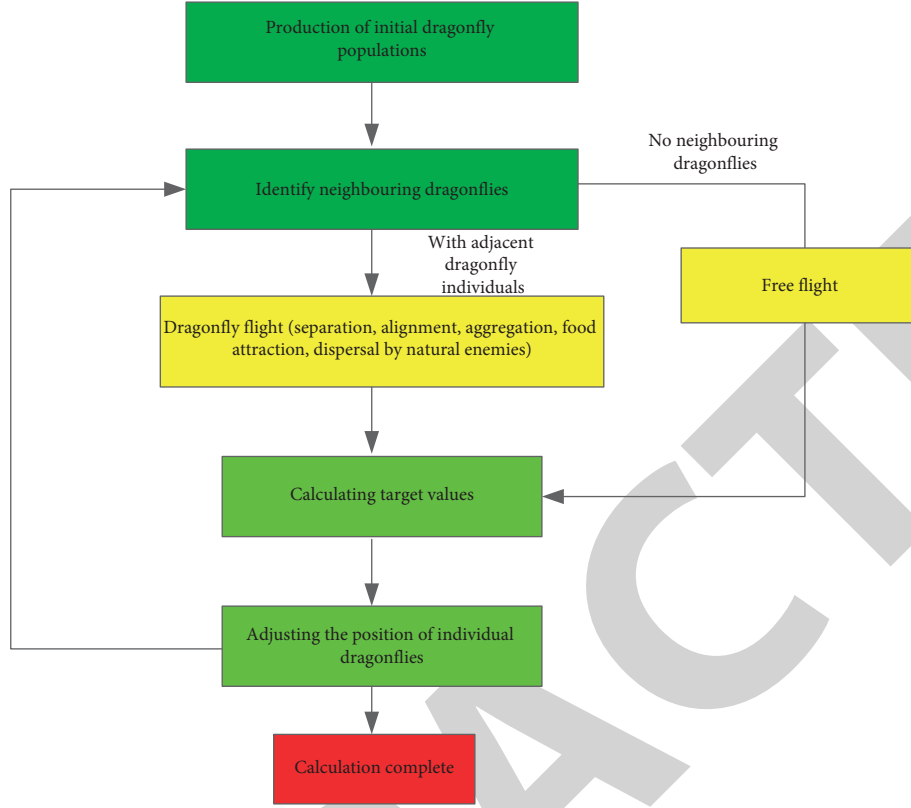


FIGURE 1: The main idea of the dragonfly algorithm for finding the best calculation.

limits of the water level operating area  $Z_{\text{Max}(i,t)}$ ,  $Z_{\text{Min}(i,t)}$  using  $\mathbf{X}_r = \mathbf{Z}_{\text{Min}(i,t)} + \mathbf{e} * (\mathbf{Z}_{\text{Max}(i,t)} - \mathbf{Z}_{\text{Min}(i,t)})$ , and the POA algorithm is used to find the optimal solution for the selected dragonfly based on the principle of single-station optimization, ensuring that at least one dragonfly in the initial population is a feasible solution. The number of iterations is  $\text{iter} = 1$ , and the dragonfly dimension is  $r = 0$ .

Step 3: We determine whether there is a neighbor of dragonfly  $\mathbf{X}_k$ . If there are neighbors, we go to step 4; otherwise, we go to step 5.

Step 4: We calculate the population evolution according to equations (1–5): separation  $S_r$ , alignment  $A_r$ , aggregation  $C_r$ , food attraction  $F_r$ , and natural enemy dispersal  $E_r$ . We calculate the step size of individual dragonfly position update according to equation (6).

Step 5: The dragonfly has no neighbors, and  $\mathbf{X}_r = \mathbf{e} * (\mathbf{Z}_{\text{Max}(i,t)} - \mathbf{Z}_{\text{Min}(i,t)})$  was used to randomize the flight of individual dragonflies to step 6.

Step 6: If  $\text{func2} > \text{func1}$  means that the change in position of the dimension is beneficial to the objective function, then the position of the current dimension is updated and  $X_t^k = X_{t+1}^k$ . If  $\text{func2} < \text{func1}$  means that the change in position of the current dimension is not beneficial to the objective function, then  $\Delta X_{kt+1} = 0$ . If  $\text{func2} < \text{func1}$ , which means that the change in position of the current dimension is not beneficial to the objective function, then  $\Delta X_{kt+1} = 0$ .

Step 7: If  $r = r + 1$ , we determine whether all the dimensions of the dragonfly have been updated, and if  $r = r_{\text{max}}$ , we go to step 8; otherwise, we go to step 4.

Step 8: We update the position of an individual dragonfly  $X_k$ ,  $\mathbf{X}_{t+1} = \mathbf{X}_t + \mathbf{X}_{t+1}$ .

Step 9: We make  $k = k + 1$  and proceed to the optimization of a new individual dragonfly. If  $k \geq N$ , then all dragonfly individuals are updated and we go to step 11. If  $k < N$ , then we go to step 3 for a loop.

Step 10: We find the best dragonfly in the current iteration, compare it with the food position, and update the food position according to whether it is better than the objective function value of the food position, let  $\text{iter} = \text{iter} + 1$ . If  $\text{iter} \geq \text{MAXiter}$ , we go to step 11; otherwise, we go to step 3.

Step 11: We return the food position of the current iteration as the best result, and the calculation is finished.

### 3. Evaluation Based on DA-BP

**3.1. BP Neural Network.** The BP neural networks are a widely used forward-looking neural network model to obtain the impact of changes on the analysis objectives when different influences are involved [8]. Increasing the number of layers can improve accuracy and reduce error, but it can also complicate the network and thus increase the training time for the network weights. Increasing the number of neurons



can be used to improve the error accuracy, and the training effect is easier to observe and adjust than increasing the number of layers [9]. Since three-layer neural networks have good function approximation and the structure is easy to design and operable, increasing the number of neurons in the hidden layer is usually preferred. According to Kolmogorov's theorem, a neural network with  $n$  input units,  $2n + 1$  intermediate units, and  $m$  output units is capable of expressing any mapping [10]. Since the input layer needs to input the data samples to score each investigator and the number of each investigator, while the output layer needs to output only the annual course quality score, so, there is only one neuron. Therefore, the neural network built in this paper uses 2 input units, 5 intermediate units, and 1 output unit, the structure of which is schematically shown in Figure 2.

If the number of layers of the input layer and output layer of the neural network is  $m$  and 1, respectively, and the number of layers of its hidden layer is  $p$ , then the formula of the neural network can be described as shown in equation (8).

$$X_{i+1} = f(X_i) = \frac{1}{1 + \exp(-\sum_{j=1}^p c_j b_j + \varepsilon)} \quad j = 1, 2, \dots, p. \quad (8)$$

The formal species  $f$  is the implied layer excitation function,  $\varepsilon$  is the threshold value of the output layer, and  $c_j$  and  $b_j$  are the connection weights from the implied layer to the output layer and the node outputs of the implied layer, respectively. [11].

Therefore, the output expression of the hidden layer nodes of the BP neural network is shown in equation (9).

$$b_j = \frac{1}{1 + \exp(-\sum_{i=1}^m \omega_{ij} + \theta_j)} \quad i = 1, 2, \dots, m, \quad (9)$$

where  $\omega_{ij}$  is the connection weight from the input layer to the hidden layer;  $\theta_j$  is the threshold value of the nodes in the hidden layer.

Since the prediction accuracy of the BP neural network is easily regulated by the initial weights, slight differences in the initial link weights may lead to very different simulation results.  $c_j$ ,  $\omega_{ij}$  and threshold  $\varepsilon$ ,  $\theta_j$  parameters are the relevant calculation coefficients of the prediction algorithm. In this paper, the DA is used to optimize the initial weights of the BP neural network and adjust its threshold.

Standard BP was used in the fields of simulation and blockchain, which itself has a more rigorous derivation process and sufficient theoretical basis, especially in the research of nonlinear systems, and has been studied and used by a large number of scholars [12]. However, through a large number of nonlinear experimental studies, it is found that there are several shortcomings as follows [13]:

- (1) Slow convergence of the learning process.

Although there are many factors that affect the convergence speed of the algorithm, the generalization ability itself is the most important factor, for example, in the selection of parameters, which, if not chosen properly, can make the training count reach

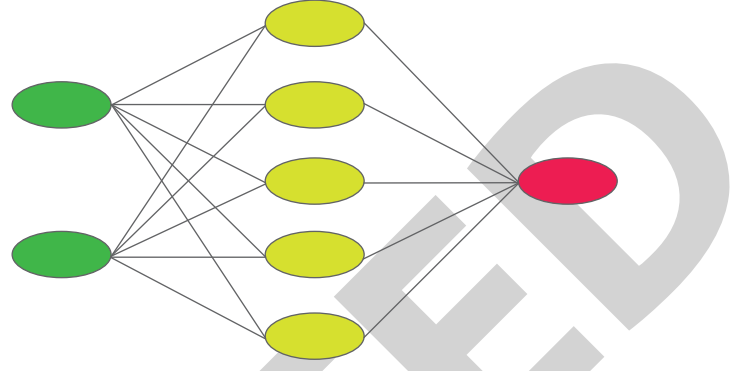


FIGURE 2: BP network topology diagram.

tens of thousands of times before the desired accuracy is achieved.

- (2) Convergence to the minimum value point is not guaranteed.

For the BP neural networks trained with gradient descent as a learning rule, the interrelated points are made up of various parabolic surfaces, all of which are extremely small individuals. Therefore, in the process of training the object under study using neural networks, it is often the case that local minima occur, and once encountered, the whole neural network will fall into a local minimum and will remain in such a state from which it cannot emerge [14].

- (3) The network structure is difficult to determine.

The structural parameters of the network include a large number of factors. Therefore, it is important to always be aware of the possibility of redundancy in building the network, and if too much of this problem occurs, the training time will significantly increase as a result.

To compensate for these shortcomings, the DP algorithm is introduced, which can solve the problems of local optimum and full learning rate. [15] The process of the DA-BP-based algorithm for evaluating the quality of teaching in college political courses is summarized as follows:

Step 1: We initialize the BP neural network model and determine the network structure. The number of layers, the type of transfer function and training function, and the number of nodes in each layer of the BP neural network are determined according to the data samples; the data are read and preprocessed, and the data are divided into the training set and the test set. [16].

Step 2: The DA algorithm uses real number encoding, the connection weights  $c_j$  and  $\omega_{ij}$  and thresholds  $\varepsilon$  and  $\theta_j$  are encoded as a whole, and the spatial search dimension of the algorithm is  $m$ . Assuming that the number of nodes in the input layer, implicit layer, and output layer is  $R$ ,  $S_1$ , and  $S_2$ , respectively, the encoding length  $S$  can be expressed as equation (10) as follows:

$$S = RS + S_1 + S_2 + S_1 S_2. \quad (10)$$



Step 3: The DA is initialized with a population size of  $N$  and a maximum number of iterations of  $T$  [17].

Step 4: We randomly initialize the step vector  $\Delta X$  and randomly generate the initial position  $X$  of the dragonfly individuals.

Step 5: We make the current number of iterations  $t = 1$ , input the training set into the BP neural network, evaluate the fitness of dragonflies according to the fitness formula (11) of dragonfly algorithm species, and rank the best solution for the current training [18], where the mean squared deviation is chosen as the fitness function, and its expression is

$$\text{fitness} = \frac{1}{k} \sum_{i=1}^k (y_i - \hat{y}_i)^2. \quad (11)$$

In the formula,  $y_i$  and  $\hat{y}_i$  are the actual and expected outputs of the  $i$ th sample, respectively, and  $k$  is the number of samples.

Step 6: We update the food source location  $X^+$  (current optimal solution) and the natural enemy location  $X^-$  (current worst solution), and update the five behavioral weights  $s, a, c, f, e$  and the inertia weight  $\omega$ .

Step 7: We update  $S, A, C, E, F$  according to equations (3–7).

Step 8: We update the step vector and position vector according to equations (8) and (9).

Step 9: If the number of iterations  $t \sim T$ , we save the most connected weights  $c_j$  and  $\omega_{ij}$  and thresholds  $\varepsilon$  and  $\theta_j$ ; otherwise,  $t = t + 1$  and we return to step 5.

Step 10: We use the connection weights  $c_j$  and  $\omega_{ij}$  and thresholds  $\varepsilon$  and  $\theta_j$  corresponding to the optimal solution and make predictions. [19].

#### 4. Empirical Analysis

This empirical study selected research data obtained from the ideology and political course teaching and research department of the School of Marxism through the end-of-year review of the course between 2008 and 2016 at a 985 university in a central province of China. At the end of each teaching term, the teaching evaluation team composed of senior teachers will score according to the students' reaction after class, the teaching progress, and the results of the teachers' assessment at the end of the year. Due to the large number of data samples, all samples have a total of 2550 groups of data. Limited by the length of the article, only some data samples are listed. The data are a true and detailed record of the teaching and learning of the school's ideology course over a period of more than ten years. Before systematically analyzing the data, it is necessary to construct an index system for evaluating the teaching quality of the university's political classroom. On the basis of the reference of previous relevant domestic studies and the teaching characteristics of this 985 university, the indexes for evaluating the teaching quality of the university's political course are constructed into a comprehensive index system of four primary indicators and 15

secondary indicators, as shown in Figure 3. The first-level indicators are as follows: adequacy of teaching preparation, effectiveness of teaching operation, strength of teaching management, and constructiveness of practical teaching. Among them, teaching preparation is the preliminary preparation and preparatory work for the formal start of teaching, which is the first important link to ensure the quality of teaching. The teaching operation stage refers to the operation of various factors in the whole teaching progress. Teaching management includes internal management and external monitoring, and is an organic combination of the two. Practical teaching, as the name implies, is practice oriented, and it usually refers to the use of practical teaching to enable students to learn theoretical knowledge in a practical and interesting atmosphere, through which the effect of heuristic teaching is achieved, and it is the students who more deeply grasp the theoretical knowledge learned in the classroom, while strengthening their own comprehensive ability and ideological quality. The adequacy of the teaching preparation is divided into the excellence of the teaching environment, the scientific nature of the teaching objectives, the rigor of the teacher selection, and the teacher's preparation for the class. The effectiveness of the teaching operation is divided into the adequacy of the teaching content, the effectiveness of the teaching methods, the manipulation of teaching skills, and the realization of teaching results. The strength of teaching management is divided into the scientific formulation of teaching policies, the adequacy of teaching policy implementation, the comprehensiveness of teaching security work, and the implementation of teaching evaluation and supervision. The constructiveness of practical teaching is divided into the directivity of practical teaching, the relevance of practical teaching content, and the adequacy of practical teaching effect.

This research uses the maximum value method to standardize the data, and according to the 1–9 scale method, the scores of each year's political teaching quality evaluation indexes are constructed according to the relative order of merit of each evaluation index by the two-by-two comparison method as shown in Table 1, and the total evaluation scores of political teaching in each year are shown in Table 2.

According to the statistical principle, the reliability and validity of the data obtained from the survey are tested to verify the credibility and effectiveness of the statistical data. Cronbach's alpha value is selected as the reliability-check index, and the KMO value and Bartlett test value are selected as the validity test index. The test results of reliability and validity are shown in Tables 3 and 4.

According to the principle of the reliability test, Cronbach's alpha value must be greater than 0.60 to pass the reliability test, so all indicators in this survey meet the reliability requirements. In terms of validity test, the author mainly tests the structural validity of the data. First, the KMO value and Bartlett sphericity value of the data are calculated to test whether they are suitable for validity test. When the KMO value is greater than 0.5 and the Bartlett sphericity test value is 0, the data are suitable for validity test. The KMO value and the Bartlett sphericity test value of the data are shown in Table 4.

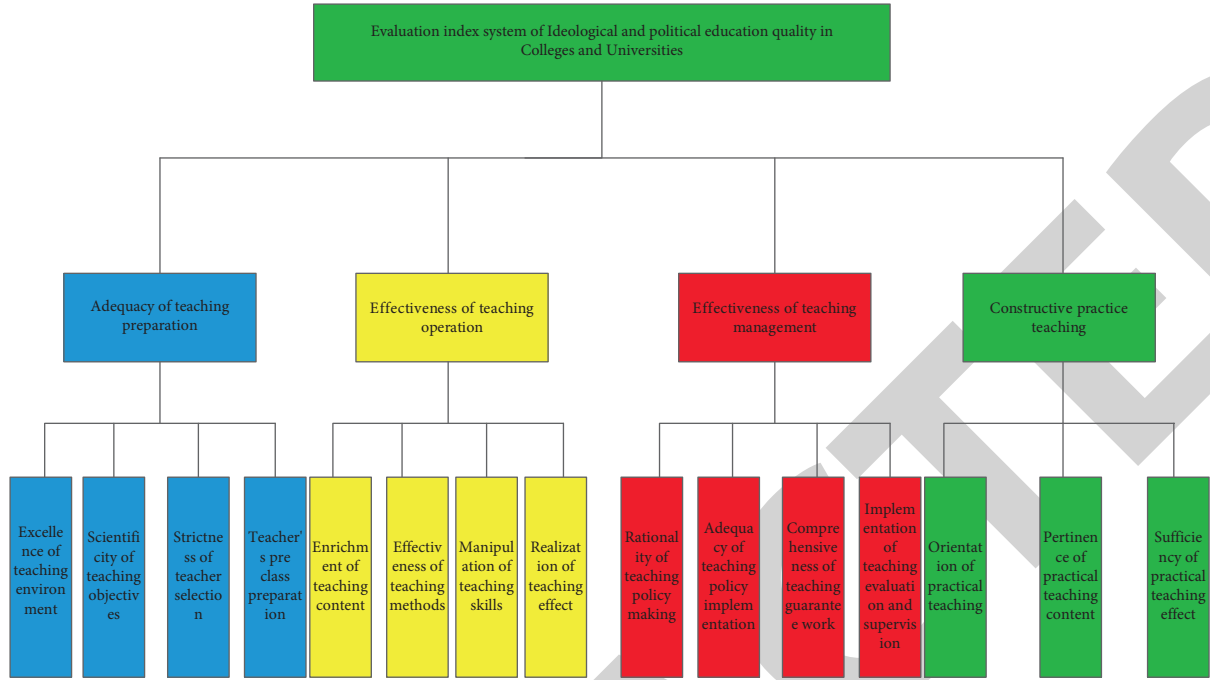


FIGURE 3: Evaluation system of teaching quality of political classroom in higher education.

TABLE 1: Scores of the indicators for evaluating the quality of teaching and learning in civic studies by year.

Indicator number	2008	2009	2010	2011	2012	2013	2014	2015	2016
1	0.0145	0.0247	0.0301	0.0417	0.0467	0.0479	0.0521	0.0546	0.0607
2	0.0264	0.0372	0.0419	0.0512	0.0527	0.0538	0.0569	0.0632	0.0649
3	0.0272	0.0530	0.0593	0.0647	0.0654	0.0674	0.0705	0.0736	0.0771
4	0.3113	0.3018	0.3297	0.3395	0.3456	0.3548	0.3874	0.4096	0.4265
5	0.2487	0.3185	0.3864	0.4245	0.4375	0.4396	0.4458	0.4780	0.4864
6	0.1921	0.2199	0.2990	0.3184	0.3288	0.3467	0.3671	0.3843	0.3976
7	0.2831	0.3017	0.3207	0.3455	0.3671	0.3789	0.3801	0.3966	0.4096
8	0.0461	0.0591	0.0842	0.1022	0.1346	0.2479	0.2633	0.3109	0.3567
9	0.0145	0.0266	0.0375	0.0515	0.0558	0.0671	0.0789	0.0804	0.1104
10	0.1961	0.2240	0.3094	0.3105	0.3249	0.3583	0.3791	0.3903	0.4116
11	0.2545	0.3099	0.3102	0.3233	0.3409	0.3502	0.3784	0.3802	0.3915
12	0.0184	0.0190	0.0222	0.0328	0.0406	0.0453	0.0497	0.0521	0.0544
13	0.0991	0.1051	0.2547	0.2674	0.2894	0.2906	0.3402	0.3579	0.3908
14	0.1874	0.2064	0.3055	0.3211	0.3577	0.3782	0.3956	0.4001	0.4214
15	0.2841	0.3011	0.3403	0.3532	0.3709	0.3921	0.4013	0.4206	0.4465

TABLE 2: Cronbach's alpha test value.

Year	Cronbach's alpha value
2008	0.707
2009	0.750
2010	0.868
2011	0.836
2012	0.670
2013	0.785
2014	0.731
2015	0.632
2016	0.836

It can be seen that the KMO value of the data is greater than 0.5, and the Bartlett sphericity test value is 0, indicating that the data validity meets the standard.

TABLE 3: KMO value and the Bartlett sphericity test value.

Kaiser-Meyer-Olkin metric	0.954
Bartlett's sphericity test	0.00

The results of the overall evaluation scores were obtained by the following equation:

$$OS = \sum_{i=1}^n S_i \cdot T_i, \quad (12)$$

where OS denotes the overall score,  $i$  denotes the number of indicators,  $S_i$  denotes the score for each indicator, and  $T_i$  denotes the weight of each indicator.

In order to test the goodness of the evaluation results of the quality of teaching in higher education political

TABLE 4: Overall evaluation scores for teaching political course by year.

Year	2008	2009	2010	2011	2012	2013	2014	2015	2016
Score	2.4035	2.6084	3.3311	3.4475	3.6586	3.9188	4.0664	4.3524	4.5561

classroom, there are two evaluation indicators, of which the RMSE is the most commonly used error analysis algorithm, followed by the indicator correlation coefficient  $R$ . The formulas are expressed as equations (13) and (14).

$$\text{RMSE} = \sqrt{\frac{1}{n} \sum_{k=1}^n (x_k - \hat{x}_k)^2}, \quad (13)$$

$$R = \frac{\sum_{k=1}^n x_k \hat{x}_k}{\sqrt{\sum_{k=1}^n x_k^2} \cdot \sqrt{\sum_{k=1}^n \hat{x}_k^2}}, \quad (14)$$

where  $x_k$  and  $\hat{x}_k$  denote the actual and predicted values of the  $k$ th sample, respectively, and  $n$  denotes the number of samples. RMSE is mainly used to measure the dispersion of the model, and  $R$  is mainly used to illustrate the degree of correlation between predicted and actual values.

According to the literature, the quality of teaching in the political classroom was classified into five levels, namely, very good, better, average, poor, and very poor, and their evaluation levels are divided as shown in Table 5.

As can be seen from Table 5, with the passage of time, the teaching supervision has become more and more perfect, and the teaching quality has also been improved accordingly, which is more in line with the facts and further verifies the authenticity of the data.

The collected data were scored by experts, and a total of 10 sets of data were obtained. The data were divided into two parts, the first 6 sets of data were used as the training set to build the DA-BP classroom teaching evaluation model, and the last 3 sets of data were used as the test set to test the correctness of the DA-BP classroom teaching evaluation model. The structure of the BP neural network is 2-5-1, the set learning rate is 0.1, the training accuracy is 10-6, and the maximum training times of the BP neural network are 20000. The hidden layer function adopts the sigmoid function, which is characterized by its differentiability, continuity of itself and derivative function, nonlinear characteristics, and fast convergence, so it is selected as the hidden layer excitation function. The prediction result of the algorithm is shown in Figure 4; as can be seen from the figure, the DA-BP algorithm more accurately predicted the actual score after 2014.

After completing the DA-BP algorithm through training to more accurately predict the teaching quality ratings of a university's political course from 2014 to 2016, the algorithm was used to continue to test the prediction accuracy of the algorithm and to continue to simulate the teaching quality ratings of the university's political course after 2016. The statistical data after 2016 also come from the university. Due to the significant role of the long-term year-end comprehensive evaluation of teaching quality in improving teaching quality, the university will maintain the year-end evaluation

TABLE 5: Classification of evaluation levels.

Rating range	Evaluation results
[4.1, 5)	Very good
[3.3, 4.1)	Better
[2.5, 3.3)	Fair
[1.7, 2.5)	Poor
[1, 1.7)	Very poor

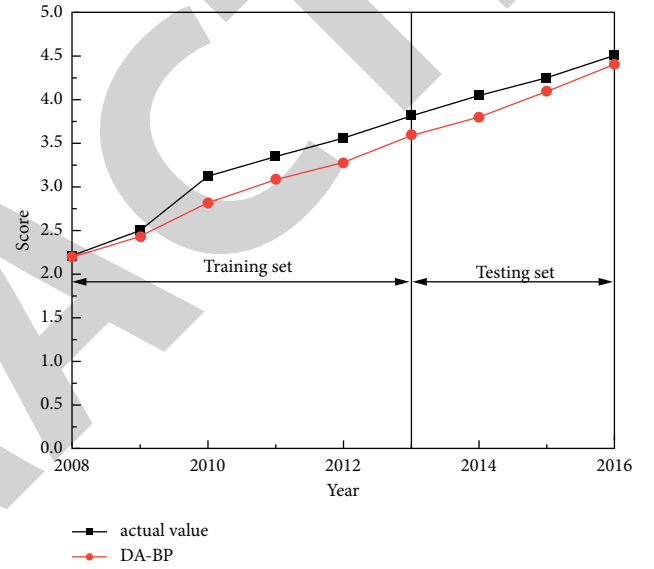


FIGURE 4: DA-BP political course teaching quality evaluation results.

until 2021. In this case, it is necessary to choose the simulation prediction method of the DA-BP algorithm, and there are three traditional prediction methods. [20].

**4.1. Single-Step Forecast.** At  $k = 1$ , each subsequent prediction step is based on the result of the previous prediction step and is a one-step prediction. The process is as follows: with a total of  $m$  predicted values and input parameters  $T_n, T_{n+1}, \dots, T_{n+m}$  in the prediction model, each input parameter is entered into the prediction model separately and the result is the predicted value of  $T_{n+m+1}$  at the next point, which is repeated in this way to predict the value of  $T_{n+m+2}$ . The value of  $T_{n+1}, T_{n+2}, \dots, T_{n+m+1}$  is used as input data to obtain the value of  $T_{n+m+2}$ .

**4.2. Multistep Prediction.** When  $k > 1$ , the previously collected data, we tentatively set  $m$  here, are input into the network together; then, the relevant values of the subsequent nodes  $T_{n+m+1}, T_{n+m+2}, \dots, T_{n+m+k}$ , multistep prediction under the background of big data output, and the prediction

result will have a large error, and the reason is mainly because of iteration and the related error in the previous step. It will continue to accumulate in the results of the next step. Yes, the error will expand step by step. When the error reaches a certain level, there may be a problem that the training network cannot achieve convergence, and the ideal optimal solution cannot be obtained.

**4.3. Rolling Forecast.** The rolling forecast is based on a single-step forecast and then predicts the follow-up after inputting the expected value. It is assumed that the observation sequence of the specific algorithm is  $T_n, T_{n+1}, \dots, T_{n+m}$ , and the output value is the observation value of  $T_{n+m+1}$ . Then, we use  $T_{n+m+1}$  and  $T_{n+1}, T_{n+2}, \dots, T_{n+m}$  as input data to evaluate and estimate  $T_{n+m+2}$ , get the output observations  $T_{n+m+2}$ , and then take  $T_{n+m+2}$  and  $T_{n+2}, T_{n+3}, \dots, T_{n+m+1}$  as the input number  $T_{n+m+3}$  for estimation continuously in this way.

Iterative feedback adjustment can realize the predictive analysis of research objects in the future.

Rolling forecasting is a combination method with a lot of advantages and strong practical significance. Therefore, this paper adopts the rolling forecast for analysis and processing. During the simulation, MATLAB software was used to call the function, and the simulation function selects the sim function. The learning rate, the number of learning times, and the number of hidden layers are set to 0.005, 10,000, and 3 according to the size of the sample data. The network is adjusted by the input of sample data. The network has been adjusted many times. When the learning rate is adjusted to 0.0001, the number of learning times is 30,000, the number of hidden layers is 5, and the number of nodes in each layer is 480, 320, 160, 160, and 320..

The simulation results and error analysis are shown in Figures 5 and 6.

The figure indicates that the absolute error of the predicted value of the DA-BP algorithm is always controlled within 0.15, which is a reasonable error. In order to further check the rationality of the error, the relative error value obtained by dividing the absolute error value by the actual value is subjected to statistical analysis, resulting in Figure 7.

It can be seen from Figure 7 that the relative error of the prediction result of the DA-BP algorithm fluctuates between 0.2% and 27%, and the maximum relative error does not exceed 27%. According to the statistical law, it conforms to the prediction accuracy and can be used for simulation.

To test the accuracy and effectiveness of the DA-BP model, DA-BP was compared with several different improved algorithms. The DA-BP algorithm was reconstructed with Python language. The logsigmoid function was selected as the hidden layer excitation function. The learning rate was set to 0.01, and the maximum number of iterations was set to 20000. The survey data from 2017 to 2020 were used as the training dataset input model for training. The parameters of other algorithms were chosen as follows: particle swarm optimization (PSO) algorithm parameters: maximum number of iterations  $T=100$ , population size  $N=10$ , learning factor  $C_1=C_2=2$ , and search interval  $[-1, 1]$ ;

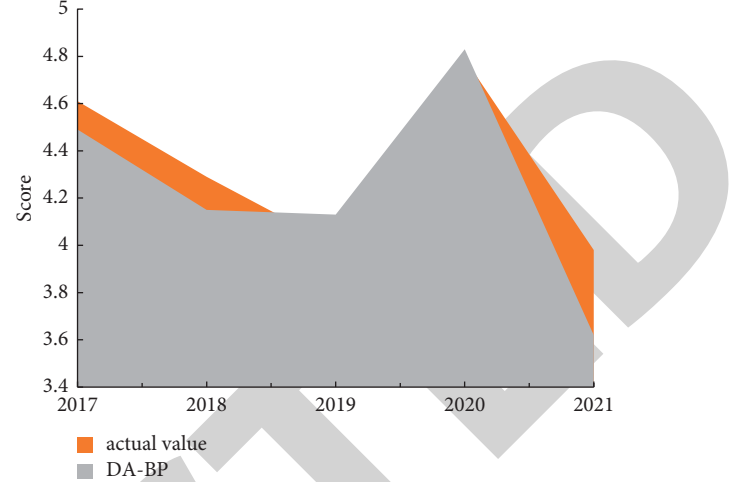


FIGURE 5: DA-BP political course teaching quality evaluation for 2017–2021.

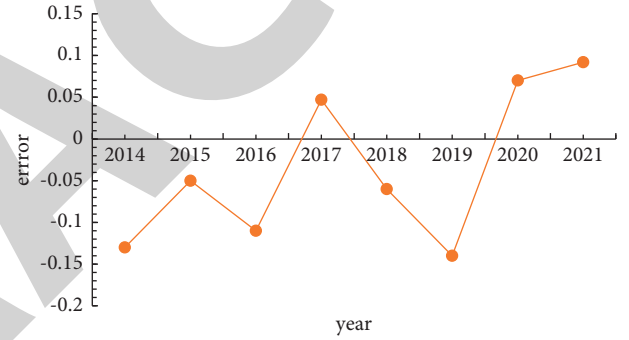


FIGURE 6: Prediction error.

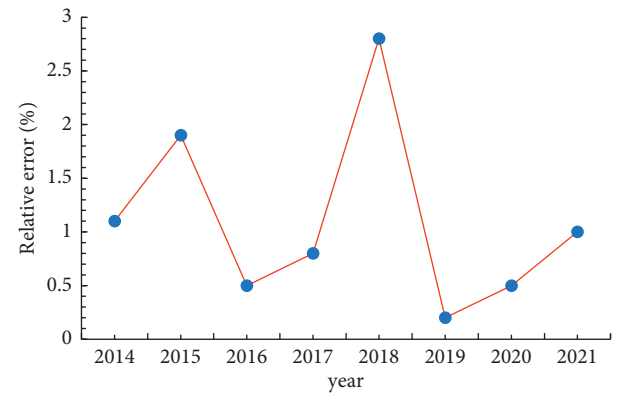


FIGURE 7: Relative error.

genetic algorithm (GA) parameters: population size  $N=10$ , maximum number of iterations  $T=100$ , crossover probability  $PC=0.7$ , and variation probability  $P_m=0.1$ ; BP neural network parameters: input layer nodes are 25, hidden layer nodes are 50, output layer node is 1, maximum training number is 1000, transfer function of hidden layer is logsig, the output layer transfer function is purelin, the training function is trainlm, the learning rate is 0.01, and the training

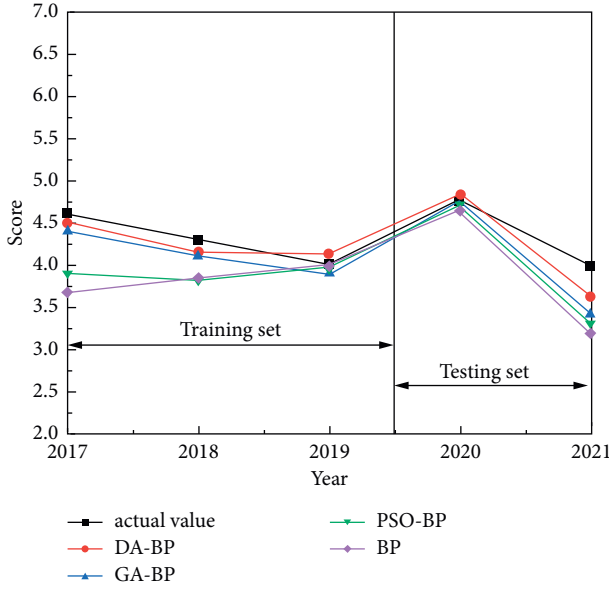


FIGURE 8: Results of teaching quality evaluation of different algorithms for political courses.

TABLE 6: Comparison of evaluation results of different algorithms.

Method	Training set		Testing set	
	RMSE	R	RMSE	R
DA-BP	0.0090	0.9871	0.0394	0.9801
GA-BP	0.0191	0.9731	0.0405	0.9694
PSO-BP	0.0185	0.9646	0.0417	0.9583
BP	0.0163	0.9528	0.0428	0.9437

error target is 0.001. The comparison results of different algorithms are shown in Figure 8 and Table 6.

As can be seen from Figure 8, except the DA-BP algorithm, the GA-BP algorithm is the most accurate in prediction. However, the minimum absolute error of the prediction result of the GA-BP algorithm is 0.20, and the minimum relative error is 30%, both higher than the DA-BP algorithm.

From Figure 8 and Table 6, it can be seen that the DA-BP algorithm outperforms the remaining three algorithms in terms of prediction accuracy, where the RMSE value calculated according to the DA-BP algorithm is the lowest and the correlation coefficient  $R$  value is the largest, which indicates that the predicted teaching quality evaluation value of the political course by the DA-BP algorithm is very close to its actual value and the DA-BP algorithm has the highest prediction accuracy. Second, it is not difficult to find that both the GA-BP and PSO-BP algorithms yielded better prediction accuracy than the BP neural network algorithm, which may be due to the fact that the first two algorithms both optimize the BP algorithm to some extent, thus improving the accuracy.

## 5. Conclusions

The DA-BP algorithm can more accurately evaluate the teaching quality of previous political courses, and more importantly, can accurately predict and evaluate the future

teaching quality, thus putting forward the following countermeasures and suggestions: (1) to strengthen the importance of college leaders and increase supervision; (2) to innovate and improve the teaching mode and teaching methods; (3) to fully utilize the enthusiasm of student subjects; (4) to strengthen student guidance in conjunction with the actual situation; (5) to clarify the purpose of teaching evaluation and evaluation indicators and the evaluation system; and (6) to strengthen case teaching to improve students' understanding and perception. This paper proposes a DA-BP-based method for evaluating the quality of teaching in college political courses in order to improve the accuracy of teaching quality evaluation in college political courses. Based on the behavioral theoretical framework and the actual teaching situation of the university, an evaluation system for the teaching quality of college political classroom teaching is constructed, the expert evaluation scores of 15 evaluation indicators related to the teaching quality of college politics classroom teaching are input into the DA-BP algorithm model, and the model outputs after training and predicts teaching quality scores. The other methods mentioned in this paper can also simulate to a certain extent, but the accuracy is not as good as the DA-BP algorithm. The teaching quality evaluation of university political classroom under the DA-BP algorithm model can be used as a reference method to provide some teaching institutions. Since the founding of New China, the state has invested a lot of energy in the political education of college students. The implementation of good political education is related to everyone, and it is imperative to have good and accurate teaching quality evaluation standards. The country hopes that every college student can receive a good and correct political education, because they are the future of the country, and they shoulder the heavy responsibility of building the country. If there is a problem with the ideology and cognition of college students, they will no longer have a sense of their national identity. If we have a sense of identity, then this will be a disaster for this country. Fortunately, various experts, scholars, and universities have gradually attached importance to political education, and at the same time, an evaluation system for the quality of education is indispensable. This paper provides a method reference for the evaluation of the quality of political teaching of college students in the future.

## Data Availability

The experimental data used to support the findings of this study are available from the corresponding author upon request.

## Conflicts of Interest

The authors declare that they have no conflicts of interest regarding this work.

## Acknowledgments

The authors would like to thank the Key Project of Beijing Educational Science Planning "Research on Engineering

## *Retraction*

# **Retracted: Modeling and Optimization Analysis of Ancient Building Construction Rule Components Based on Deep Learning**

## **Security and Communication Networks**

Received 26 December 2023; Accepted 26 December 2023; Published 29 December 2023

Copyright © 2023 Security and Communication Networks. This is an open access article distributed under the Creative Commons Attribution License, which permits unrestricted use, distribution, and reproduction in any medium, provided the original work is properly cited.

This article has been retracted by Hindawi, as publisher, following an investigation undertaken by the publisher [1]. This investigation has uncovered evidence of systematic manipulation of the publication and peer-review process. We cannot, therefore, vouch for the reliability or integrity of this article.

Please note that this notice is intended solely to alert readers that the peer-review process of this article has been compromised.

Wiley and Hindawi regret that the usual quality checks did not identify these issues before publication and have since put additional measures in place to safeguard research integrity.

We wish to credit our Research Integrity and Research Publishing teams and anonymous and named external researchers and research integrity experts for contributing to this investigation.

The corresponding author, as the representative of all authors, has been given the opportunity to register their agreement or disagreement to this retraction. We have kept a record of any response received.

## **References**

- [1] H. Ni, "Modeling and Optimization Analysis of Ancient Building Construction Rule Components Based on Deep Learning," *Security and Communication Networks*, vol. 2022, Article ID 1119059, 13 pages, 2022.



## Research Article

# Modeling and Optimization Analysis of Ancient Building Construction Rule Components Based on Deep Learning

Hao Ni <sup>1,2</sup>

<sup>1</sup>*School of Architecture and Environmental Arts, Shanghai Urban Construction Vocational College, Shanghai 201415, China*

<sup>2</sup>*Zhenjing Workshop Museum, Shanghai 201400, China*

Correspondence should be addressed to Hao Ni; nihao@succ.edu.cn

Received 28 July 2022; Revised 31 August 2022; Accepted 7 September 2022; Published 21 September 2022

Academic Editor: Hangjun Che

Copyright © 2022 Hao Ni. This is an open access article distributed under the Creative Commons Attribution License, which permits unrestricted use, distribution, and reproduction in any medium, provided the original work is properly cited.

Chinese culture is broad and profound, and successive dynasties have left many cultural treasures. Ancient architecture is a significant treasure, and it is also the core content of the inheritance of Chinese culture. Every Chinese ancient building has its own characteristics, and the creative components of each ancient building are an important part of ancient buildings. As a new learning mode of current scientific inquiry, the deep learning model includes high-level and high-stage cognitive processing ability and innovative thinking ability. Under the background of the above modeling and optimization analysis of ancient building construction rule components and the development of deep learning mode, this paper proposes the modeling and optimization analysis of ancient building construction rule components about deep studying. The results of the experiment are as follows: (1) about the concept of the deep learning technology model and the vacancy problems existing in the current situation of the design framework and optimization of ancient building construction rule components, the research direction of the experiment is determined, and through the investigation and analysis of the modeling and optimization of ancient building construction rule components based on the deep learning model, the technical guarantee is provided for the research of this paper; (2) the convolution neural network algorithm, inversion model algorithm, loss function algorithm, and optimization algorithm are used to calculate, evaluate, and analyze the research problems, and the investigation contents are identified and analyzed through experimental research. It can not only analyze the root of the research problems but also improve the specific modeling optimization problems of ancient buildings, to reduce the unnecessary loss of time and resources.

## 1. Introduction

In industrial process control, due to technical or economic constraints, it is difficult to test the accuracy of the control of a product problem and parameter variables. A new data transmitter is designed to measure product problems and control parameter variables, to provide effective and reliable process parameter evaluation and analysis. As a new deep neural network training strategy, deep learning has become a new data transmission driver method in deep study. In this study, we use the deep learning model to design the data driver and put the design model into the actual product manufacturing. The comparison of modeling results shows that compared with traditional methods, deep learning technology has the following advantages, the most suitable model architecture for software data testing. First, compared

with the original data-driven model, the deep neural network has a complex multilayer structure, which can contain more abundant information and generate better representation ability [1]. It is found that a supervised learning problem based on speech separation uses the relationship between speech and speaker to estimate the background noise and uses different discriminant patterns to classify the training data. In the past decade, many supervised separation algorithms have been proposed. However, with the improvement of scientific and technological capabilities, there is a better demand for target mechanization for supervised speech separation. Especially recently, deep learning has been introduced into the field of supervised speech separation, which has greatly accelerated the research progress and improved separation performance. The recent research on supervised speech separation based on deep learning is



summarized [2]. By adapting CNN for the optical camera to its microwave counterpart, namely, synthetic aperture radar, in order to improve the performance of the model, we design a dictionary learning algorithm based on multiscale analysis. After convolution and merging, the input SAR image is transformed into a series of characteristic images [3]. In order to improve the accuracy, we use a dynamic programming strategy to segment each category and then map each category to different networks for processing. In this framework, we use different types of age markers to encode the input face image and then use the migration learning strategy to realize the deep conversion of data. In addition, in order to characterize the relationship between the tags that make up the ordered sequence, a new loss function is defined in the age classification task training. The experiment was carried out on the population image of the widely used age estimation data set [4]. An automatic feature learning system is proposed to classify the severity of nuclear cataracts from slit lamp images. The method includes the following: one or more local filters are used to learn each hierarchical class, wherein at least one is composed of one or more lenses and one or more image patches; then a new classifier is trained in each segmentation region using gradient descent method (GLCM) and Gaussian mixture model. The classifier can be used to recognize multiple nuclear lesions produced by different categories. Using the above characteristics, support vector regression (SVR) was used to grade cataracts [5]. Compared with the achievements of China's ancient advanced architectural technology, China is still relatively backward in ancient architectural information technology. On this basis, a prototype system of three-dimensional cultural relics information system based on b/s mode is proposed and implemented, and the main technologies and methods involved in the prototype system are introduced. Finally, some application examples are given. Practice has proved that the effect is good. This platform can not only provide tools for the establishment and management of ancient building information model base but also provide accurate information for ancient building restoration, ancient building research, and ancient building virtual reality system. This paper focuses on the management method of ancient building component information and the structure of information storage database under this platform [6]. The fracture load and displacement values that may be formed in reinforced concrete structures with different cantilever types are determined by artificial neural network modeling. The key parameters of columns and beams defined in the Turkish seismic code are analyzed by nonlinear static pushover analysis, and the bearing capacity curve, failure load, and displacement are obtained. According to the variation interval of the selected parameters, a total of 64 reinforced concrete buildings are analyzed. In addition, by using the same parameters of the same model type, the statistical package of the Social Sciences (SPSS) statistical program is used for regression analysis. Therefore, the separate equations of displacement and load values are obtained, and their  $R^2$  values are calculated. Through neural network modeling, the convergence rate of displacement value is 91.77%, and the convergence rate of load value is 90.61%. The relationship

between calculated value and expected value is given [7]. Taking the ancient architectural culture of the Song Dynasty as a classic in the history of Chinese ancient architecture, a new method based on the original method was designed to form Chinese ancient architecture. The design concept of this method is to expand the regular component system of ancient buildings around the structural system and structural mode of the original ancient buildings, parameterize the components in the ancient buildings, and parameterize the elements of different modern architectural styles into the design system. In this design system pattern, it will actively generate a special file to automate the overall model of the component building. The creation of ancient buildings under the system mode retains the characteristics of traditional architectural elements and draws modern building environmental protection quality. In order to prove the feasibility of this system model, the virtual ancient building architecture model is built through specific creation rules [8]. Starting with the representative ancient buildings in Ningbo, the architectural style of ancient buildings is roughly described from the following four aspects. The first example is Baoguo temple, which has a unique structure built according to the terrain. Second, we take Tianyi Pavilion as an example to live in harmony with nature. Third, taking the old Bund architecture as an example, it introduces the western architectural culture and integrates the Chinese and Western styles. The fourth is to take the heavenly king palace as an example, which is characterized by exquisite craftsmanship and perfect and excellent artistic pursuit [9]. In the current innovative project research, researchers and architectural science and technology professionals investigated the relationship between ancient architecture and mathematics by exploring the application and expansion of numbers and geometric mathematics in the construction rules of Chinese ancient architecture. In the previous study of ancient buildings, we always hope to explain the formation of ancient buildings through the original structural rules. Now researchers try to integrate ancient architectural technology, ancient builders, and mathematical methods into an existing construction system. The research data shows that the creation theory and operation practice of ancient buildings are a whole, which cannot be divided into two parts, but cannot be divided into two parts, to complete the building system [10]. In the current particle swarm optimization (PSO) research, particles are regarded as a whole individual, and these studies are independent of the information of the dimension vector of each particle. This paper presents a visual modeling method to describe the behavior of particle dimension vector. Based on the analysis of visual modeling, the reasons for premature convergence and diversity loss of particle swarm optimization algorithm are explained, and a new improved algorithm is proposed to ensure the reasonable flight of the dimension component of each particle. At the same time, two parameters, particle distribution degree and particle dimension distance, are introduced into the algorithm to avoid premature convergence [11]. An innovative concept about the use of building modeling and optimization screening method is proposed, which forms a unique data set by selecting the corresponding data text from the overall area and some areas.

Using appropriate screening methods to obtain the data needed by the target research, in order to achieve the optimal data acquisition and reduce the loss of time, the obtained data set is used to generate the model architecture through artificial intelligence network, and the optimal parameter set is obtained through CNN model. The results of the experimental project confirm the effectiveness of this method and the modeling formation and optimization design of ancient buildings can be better achieved around the design model [12]. A modeling model around energy price reduction is designed, which mainly includes data extraction and principal component analysis of the design model and the verification of modeling functionality by using neural network technology. In order to prove the feasibility of this method, data processing algorithm and problem analysis algorithm are used to analyze the problem. This design method may lack some actual data because of the failure of functional analysis. In order to effectively study the modeling space of energy price reduction, neural network processing is used for parametric construction [13]. Hakka Tulou is listed as a world cultural heritage by UNESCO. It is a wonderful flower of ancient Chinese architecture and has high architectural, cultural, and tourism value. The high-precision and realistic three-dimensional model of cultural heritage is very important for realizing the protection, preservation, dissemination, and inheritance of cultural heritage and promoting virtual cultural tourism. Hakka Earth buildings are characterized by large volume, complex geometry, irregular shape, rich details, fragility, and vulnerability to human and natural destruction. Traditional measurement methods are difficult to obtain complete and accurate geometric information. Frequent contact in the measurement process may cause harm to cultural heritage. Ground laser scanning and other technologies are used to create realistic and fine three-dimensional models of Hakka Earth buildings [14]. DNA analysis of ancient buildings focuses on visual analysis of traditional legacy data that need to be extracted. Although the efficiency of data extraction plays an important role in the research, it is still not possible to conduct a comprehensive data research on the data DNA of ancient buildings due to the lack of practical technology. At present, there are many methods to extract DNA from data, and different methods have their own characteristics. The PCA method we use today compares these methods to optimize the original steps of each method. The research method shows that many additional data are integrated into the DNA data to be extracted, sometimes even reducing the loss of data DNA [15].

## 2. Modeling and Optimization Analysis of Ancient Building Construction Rule Components about Deep Studying

**2.1. Machine Studying and Deep Studying.** Artificial intelligence is an abstract concept, and machine learning is an algorithm that can be applied to specific scenes. Machine learning does not mean an algorithm, but a general term for a large class of specific intelligent algorithms. There are two main tasks of machine learning: first, to find an algorithm

suitable for extracting the characteristics of research objects; second, by calculating and adjusting the parameters in the algorithm, the machine learning process is simplified, as shown in Figure 1.

As shown in Figure 1, the machine learning process can be divided into five modules: selecting algorithms, initializing parameters, calculating errors, judging whether the learning is completed, and adjusting parameters. By constantly testing and optimizing parameters, the error and loss of the model can be reduced, so that the effect of the model is constantly close to the ideal state.

The emergence of artificial intelligence promotes the development of deep learning. A deep learning network model can mine information from massive data, which has a good prospect. Deep studying is a new feature method, which can obtain more useful information by analyzing and processing many samples, to improve the ability of feature representation and classification. Because it cannot express complex functions well, it has a poor effect on data feature extraction, so the generalization ability of the network is limited, and there are some limitations.

With the increase in algorithm complexity, it requires more and more network scale and computation. Therefore, how to design an efficient and feasible multilayer neural network has become an important topic. However, with the increase in the scale and complexity of the problem, simply increasing the number of layers improves functional satisfaction that cannot meet reality, because different types of data have great differences in depth, and each category has its own characteristics. Therefore, the more complex the problem is, the higher the number of layers is.

As shown in Figure 2, in deep learning, the training input only requires the original image, voice, and text information. This reduces the difficulty of processing many data sets in the training process without losing the classification performance. Therefore, this paper proposes an intelligent recognition algorithm based on a convolutional neural network (CNN) and random forest model. At the same time, the general computable feature representation can connect the work that needs more stages to be completed in traditional machine learning.

**2.2. Overview of Ancient Building Structure.** In the process of the development of human civilization, architecture is produced with the needs of the times and changes with the continuous progress of society. It accumulates a broad and profound national traditional culture and records the pace of social development.

The splendid culture of ancient China has experienced a history of 5000 years. Chinese ancient architecture is bound to become the accumulation of traditional culture, which also enjoys a considerable reputation and important position. As one of the excellent cultural heritages of the Chinese nation, Chinese traditional architecture not only has high artistic value but also has a profound cultural heritage and rich connotation. Therefore, how to better protect and make use of this precious heritage is particularly important. Ancient Chinese architecture, as a valuable asset in our

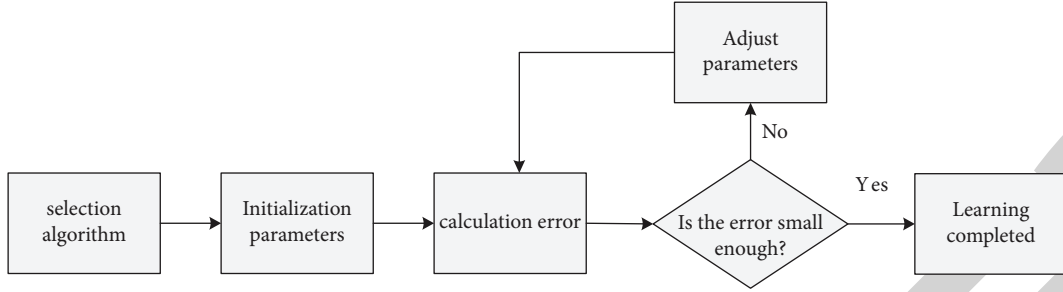


FIGURE 1: Structure of machine learning process.

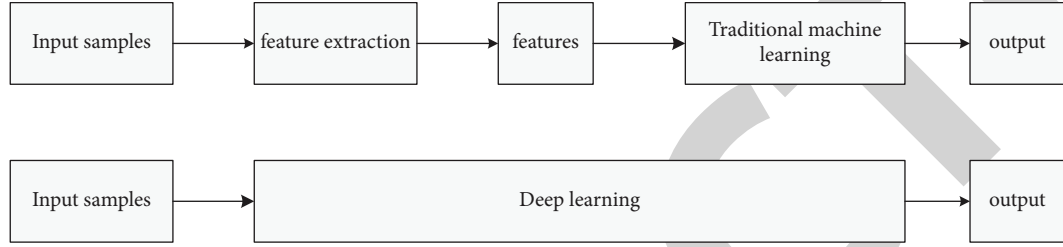


FIGURE 2: Difference between deep learning and traditional machine learning in feature engineering.

culture, has made remarkable achievements for thousands of years.

As shown in Figure 3, domain knowledge abstraction can be abstracted into different levels. The higher the level is, the more general the abstraction has, and the different levels of abstraction of knowledge have different meanings. Ancient architecture domain ontology is a complex object composed of objects of various levels and the relationships between them.

### 3. Rule Component Modeling and Optimization Algorithm Formula of Ancient Architecture Construction Based on Deep Learning

**3.1. Convolutional Neural Network Algorithm.** After each convolution check input data in the convolution layer is processed, the results obtained after each convolution check input data processing are convoluted to form the final feature map. Due to the weight sharing problem and network parameter setting problem of the convolutional neural network, the amount of calculation is too large. Receptive fields play an important role in the convolution kernel, but due to the large proportion of receptive fields in the convolution kernel, its computation is too large, which is not conducive to extracting global features from many semantic feature information. When there are only a small number of receptive fields in the convolution kernel, its computation will be large, which is not conducive to extracting local details from many semantic features. However, due to different network structures, each convolution layer will have many convolution kernels with the same or similar structure. When training, the result can be obtained by repeatedly selecting and comparing these convolution kernels, which also increases the computational cost.

$$f_{if}^{xy} = \phi \left( \sum_c \sum_{m=1}^{\epsilon} \sum_{n=1}^l w_{ijc}^{mn} f_{(i-1)c}^{(x+m)(y+n)} + b_{ij} \right), \quad (1)$$

where  $\phi$  is expressed as the activation function existing in the analysis of convolution calculation, and the primitive history of dragging Jing in the biological sense. Only when the weighted sum of the signals transmitted by the front fan Tu is too small for a specific threshold will the qualitative meridians be activated. In short, the starting function is used to design nonlinear elements, improve the cognitive ability of network models, and solve the difficulties of linear models.

$f_{if}^{xy}$  outputs the position of the variable on the  $j$  characteristic diagram of the layer;  $\epsilon$  and  $l$  represent the size of the convolution kernel;  $m$  and  $n$  represent the convolution kernel index;  $c$  represents the index of the characteristic map;  $W$  and  $b$  represent the kernel average weight and kernel deviation, respectively. Variables  $W$  and  $b$  are adjusted by training. Finally, the experimental results of this model on different data sets are given and compared with other methods. An image classification algorithm based on a local preserving projection network is proposed. In order to facilitate the following description, the convolution layer function is simplified and redefined:

$$f_p^q(x_{\text{input}}) = \phi(w_p^q \otimes x_{\text{input}} + b_p^q). \quad (2)$$

A convolutional neural network is studied by simulation. The experimental results show that the network structure can achieve high-accuracy classification tasks. The algorithm is divided into two steps. The parameters of the convolution kernel of an ordinary convolution neural network are adjusted by network model training.

The two algorithms are compared, and experiments verify that there are some differences between them. The receptive field size of hole convolution is calculated as follows:

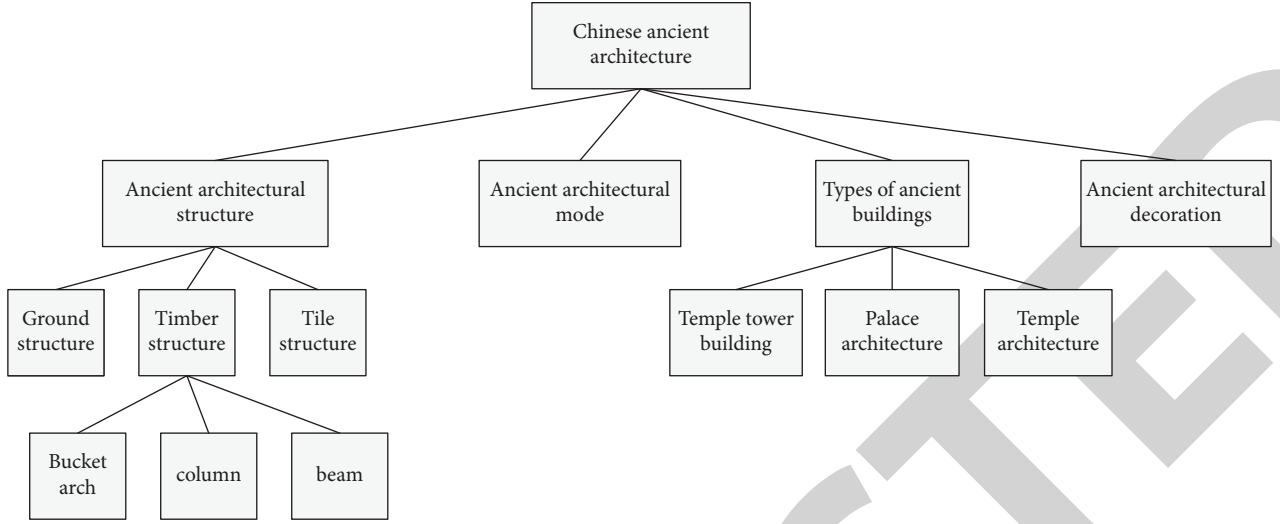


FIGURE 3: Overall structure of the ancient building component model.

$$RF = d \times (k - 1) + 1. \quad (3)$$

The parameters RF and  $d$  in formula (3) represent the size of the receptive field and convolution nucleus, respectively. When the target object is stimulated, the neural network will transmit signals to the central nervous center according to the fluctuations received. The stimulation area responded by a neuron is called the receptive field of a neuron. When  $d = 1$ , the formula is expressed as the receptive field size of ordinary convolution, and when  $d > 1$ , the formula is expressed as the receptive field size of cavity convolution.

**3.2. Inversion Model Algorithm.** The binary division of discrete or continuous attribute features in input data is as follows. Firstly, the importance of condition attributes relative to decision attributes is calculated by the information entropy method. Then the attribute subset is determined according to its importance. The cart establishment method includes traversing each attribute feature and all values of each feature, weighting the purity of the child nodes, and looking for the best partition feature from the purity weighting. The impurity weighting formula is

$$G(x_i, f_{ij}) = \frac{n_l}{n} H(X_i) + \frac{n_r}{n} H(X_r), \quad (4)$$

where  $x$  is the input variable and  $f$  is the eigenvalue of the eigenvector after segmentation. A clustering method based on the K-means algorithm is proposed for multimodal image data. Firstly,  $K$  feature points are used to segment multiple categories. Then, the least square method is used to calculate the distance between each category, where  $X_i$  and  $X_r$  represent the left and right node training sets, respectively. According to the classification and regression tree tasks, the commonly used impurity evaluation functions are

$$H(X_s) = \sum_{i=1}^c p(i) \times (1 - p(i)), \quad (5)$$

$$H(X_s) = - \sum_{i=1}^c p(i) \log(p(i)), \quad (6)$$

$$H(X_s) = \frac{1}{n_s} \sum_{i=1}^c (y_i - \bar{y}_s)^2, \quad (7)$$

$$H(X_s) = \frac{1}{n_s} \sum_{i=1}^c |y_i - \bar{y}_s|, \quad (8)$$

where  $X_s$  represents the training sample set of the node, and (5) and (6) are used to perform classification tasks;  $C$  represents the number of categories of the data set, and the probability of class  $I$  is  $p(i)$ . This method can improve the prediction accuracy of the model without adding additional calculations, and the training process of the cart is equivalent to the following mathematical optimization problem:

$$(x^*, f^*) = \operatorname{argmin}_{x, f} G(x_i, f_{ij}). \quad (9)$$

In practical application, a certain phenomenon is often formed by the correlation of various factors. However, different influencing factors may produce different results on the same thing, and these reasons are interrelated and restricted. It is difficult to find a mechanism that a single factor can fully explain all situations. Therefore, it is more effective and practical to select the best combination of independent variables in multivariate regression analysis for prediction than in univariate regression, and the prediction accuracy is also higher. The multiple linear regression equation is

$$y = \theta_0 + \theta_1 x_1 + \theta_2 x_2 + \dots + \theta_n x_n, \quad (10)$$

where  $y$  is the predicted value and  $x$  is the independent variable. Matlab software is used for fitting, and the results are analyzed and compared to obtain the optimal solution. The optimization mathematical formula expression is

$$\min Q = \sum_{i=1}^k (y - \hat{y}). \quad (11)$$

In formula (11),  $y$  is the true value and  $\hat{y}$  is the predicted value.

The application of this method in image classification and face recognition is introduced, and its development direction is prospected. The addition model is a model that accumulates several commonly used learners. Its mathematical form can be

$$F_M(x) = \sum_{i=1}^m a_i h(x; \theta_i). \quad (12)$$

Under the linear approximation model,  $\alpha$  is the weight of the  $i$ th learner. By improving the classical Kohonen network, a dynamic weighted neural network (DWNN) is proposed. The algorithm can adaptively change the weight according to the input information at the current time, which can be expressed as

$$F_M(x) = F_{M-1}(x) + a_i h(x; \theta_i). \quad (13)$$

The main idea of the AdaBoost algorithm is to add the sample weight with a large error predicted by the previous round of learners to the addition model so that the samples can get more attention in the next round of learning. The improved ADA boost algorithm is applied to multiple linear regression problems. The influence of different parameter combinations on the training effect is compared through experiments and compared with several other common methods.

**3.3. Loss Function Algorithm.** In deep learning, the neural network can reach the convergence state only when the loss value keeps approaching 0. The loss function is used to judge the advantages and disadvantages of neural networks. Therefore, different loss functions will bring different results. The calculation formula is as follows:

$$L(y, f(x)) = (y - f(x))^2, \quad (14)$$

where  $y$  is the true value and  $f(x)$  is the predicted value. The real value is the value of the physical world, which is seen by the naked eye without any error. The predicted value, the output of the model, and the output value are obtained after model training. In the analysis of the loss function algorithm, we need to train the machine learning algorithm through the prediction value  $f(x)$  and then use the prediction value obtained by the model to predict the real-world data, that is, to obtain the real data value.

The mean square error loss function calculates the loss according to the mean square deviation of the real value and the predicted value and only needs to perform the square operation, without calculating the complex power operation. The absolute value loss function is like the mean square deviation loss function, and the expression is

$$L(y, f(x)) = |y - f(x)|, \quad (15)$$

where  $y$  is the real value, and  $f(x)$  is the predicted value, but when the predicted value is equal to the real value, the absolute value loss function has discontinuities, so in practical applications, the absolute value loss function is generally not used.

In Xiangnong's information theory, the concept of crossover is mainly introduced to compare the differences between different probability distributions. This paper applies this method to the nonlinear regression prediction model and compares it with the traditional BP network. The results show that the cross entropy can describe the similarity between samples more accurately than the average entropy. Cross entropy is more suitable for predictive modeling. The calculation formula of the cross line loss function is as follows:

$$L = \sum_{i=1}^N y^{(i)} \log f^{(i)} + (1 - y^{(i)}) \log (1 - f^{(i)}). \quad (16)$$

**3.4. Optimization Algorithm.** In the optimization algorithm, the set loss function is generally called the objective function of the optimization problem. However, the neural network should distinguish the training error from the generalization error. The focus of the optimization algorithm is to reduce the training error, and deep learning pays more attention to the size of the generalization error. Therefore, even if the optimization algorithm is used, it may not guarantee that all neural networks have better generalization errors. Therefore, in the process of neural network training, we need to pay attention to the problems of overfitting and underfitting.

The random gradient descent algorithm is to reduce the value of the objective function as much as possible. Let  $f(x)$  be the index loss function about the training sample,  $n$  the amount of training data, and  $X$  the parameter vector of the neural network, and the expression of the objective function is

$$f(x) = \frac{1}{n} \sum_{i=1}^n f_i(x). \quad (17)$$

The mathematical expression for calculating the gradient of the objective function at  $x$  is

$$\nabla f(x) = \frac{1}{n} \sum_{i=1}^n \nabla f_i(x). \quad (18)$$

Compared with traditional gradient descent, random gradient descent reduces the amount of calculation in each training iteration. In each iteration, the sample index of random uniform sampling is used, and gradient  $\nabla f(x)$  is used to iterate  $x$ :

$$x \leftarrow x - \eta \nabla f_i(x). \quad (19)$$

In formula (19),  $\eta$  is the learning rate, and the amount of calculation is reduced by iterating  $X$ .  $\eta$  you need to select the appropriate value to update the independent variable in reverse along the gradient to reduce the value of the objective function. In each training iteration, only one training data sample is randomly sampled to calculate the gradient.

The random uniform sampling method is used to divide several samples into small batches and then use the small batches to calculate the gradient. This method is called small batch random gradient reduction. This paper presents a new

image edge detection algorithm based on small batch random sampling and wavelet transform. Set the objective function to  $f(x)$ , the starting time step to 0, and the time step independent variable to  $x_0$ . When each time step  $t$  is greater than 0, the small batch random gradient decreases, and the small batch  $B_t$  is formed by random uniform sampling. The gradient of the small batch  $B_t$  of time step  $t$  at  $x_{t-1}$  is

$$g_t \leftarrow \nabla f_{B_t}(x_{t-1}) = \frac{1}{|B_t|} \sum_{i \in B_t} \nabla f_i(x_{t-1}), \quad (20)$$

$$x_t \leftarrow x_{t-1} - \eta_t g_t.$$

#### 4. Statistical Analysis of Rule Component Modeling and Optimization Experiment of Ancient Architecture Construction Based on Deep Learning

**4.1. Experimental Evaluation of Deep Learning Algorithm Results.** Table 1 shows the comparison results between ts-ids and traditional machine learning test sets. The data values of naive Bayes, k-nearest neighbor, decision tree, and ts-ids are counted from four aspects: accuracy, precision, recall, and F1 value.

Table 2 shows the differences in classification accuracy of three different machine learning algorithms: naive, s-neighbor analysis, and plan tree.

From the perspective of five classifications, ts-ids is superior to traditional machine learning algorithms in most indicators, while all models perform poorly in the classification of r2l and u2r traffic. R2l and u2r are relatively small traffic in the data set. In other words, the imbalance of the data set may be the reason for the unsatisfactory training results.

As shown in Figure 4, from the comparison of F1 values of the model, except for the malicious traffic with only a small amount of data in r2l and u2r data sets, ts-ids has more outstanding performance than other traditional machine learning models.

As shown in Table 3, compared with the experimental comparison results of MP, CN, RN, LSM, etc., ts-ids has obvious advantages in classification accuracy, accuracy, recall rate, F value, and other indicators.

The accuracy, precision, recall rate, and F value of the deep learning model are better than those of the machine learning algorithm. Compared with the deep learning methods, the performance of CNN and LSTM is better in the basic deep learning model, while ts-ids is improved by 7.8% to 15.2% in accuracy, 1.3% to 8% in accuracy, 3.9% to 11.3% in recall rate, and 2.5% to 5.2% in FL value.

As shown in Figure 5, it is demonstrated that in the comparison of model F1 values, the F1 value of the ts-ids model after adding the weight balance module is almost higher than that without adding the weight balance module, especially when there is less malicious traffic in r2l and u2r data sets.

As shown in Table 4, the results of the weight balance module are compared (I). The data values of ts-id and ts-

TABLE 1: Comparison results of ts-ids and traditional machine learning test sets.

Model	Accuracy	Precision	Recall	F value
Simplicity	0.61	0.55	0.61	0.53
S-neighbor analysis	0.74	0.75	0.74	0.70
Plan tree	0.74	0.78	0.75	0.70
TS-IDS	0.83	0.81	0.79	0.77

TABLE 2: Classification effect of ts-ids and traditional machine learning test set.

Model	Classification	Precision	Recall	F value
Simplicity	Normal flow	0.59	0.92	0.72
	DOS	0.66	0.65	0.66
	Probe	0.73	0.01	0.02
	R2L	0	0	0
	U2R	0	0	0
S-neighbor analysis	Normal flow	0.67	0.97	0.80
	DOS	0.93	0.75	0.83
	Probe	0.68	0.59	0.63
	R2L	0.58	0.08	0.14
	U2R	0.70	0.10	0.18
Plan tree	Normal flow	0.64	0.97	0.77
	DOS	0.96	0.88	0.89
	Probe	0.79	0.60	0.66
	R2L	0.74	0.01	0.03
	U2R	0.22	0.07	0.13

ids + weight balance models are counted from the four aspects of accuracy, accuracy, recall, and F1 value. Compared with the previous accuracy, the accuracy, recall, and FL value have been improved.

As shown in Table 5, due to the increase in weight, the impact on accuracy caused by the category with many samples in the data set is reduced, but overall, especially for the category with a small number of samples, each index is improved.

#### 4.2. Experimental Analysis on Modeling and Testing of Regular Components of Ancient Architecture Construction under Deep Learning

**4.2.1. Analysis of Experimental Testing Environment of Ancient Buildings.** As shown in Figure 6, the monthly average temperature over the years, the monthly average maximum temperature over the years, and the monthly average minimum temperature over the years can be seen. January is the coldest, July is the hottest, January is 4.5°C, and July is 27.8°C.

As shown in Figure 7, the humidity throughout the year is basically maintained at levels 1~3. The humidity in January is level 1, and the humidity in July is level 7. April and August are wet seasons, while October to February is a dry season. The indoor temperature is also relatively high, up to 38°C. The outdoor temperature changes little, but the wind speed is small. According to the meteorological data, the environment of the building is relatively mild in winter, high in summer, and humid all year round.

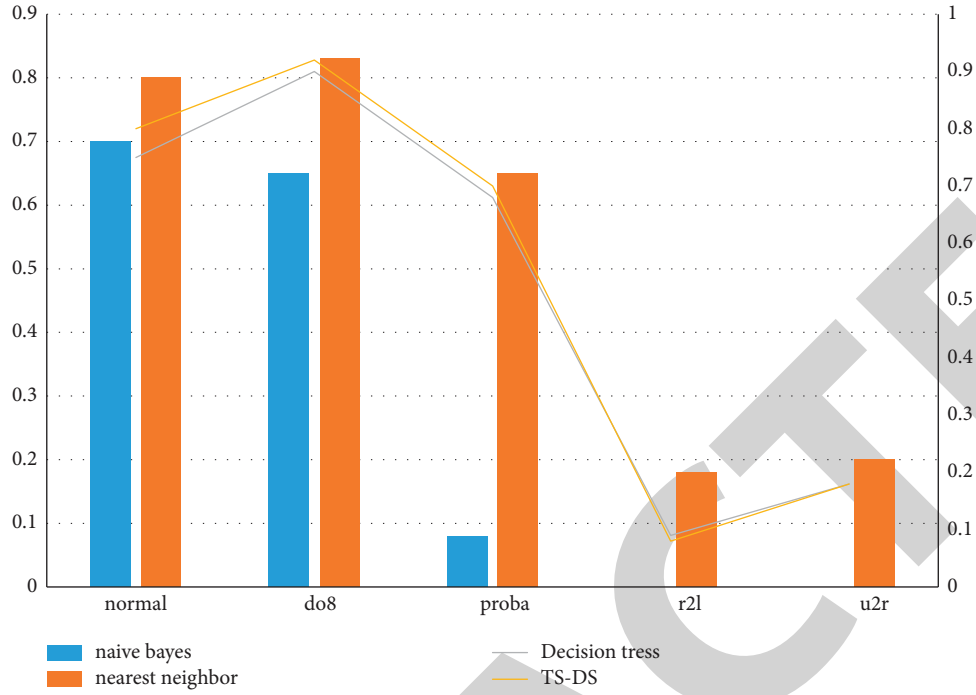


FIGURE 4: Comparison of  $F1$  value between ts-ids and traditional machine learning model.

TABLE 3: Classification effect of ts-ids and deep learning model test set.

Model	Classification	Precision	Recall	$F$ value
MP	0.73	0.75	0.73	0.73
CN	0.77	0.76	0.74	0.75
RN	0.72	0.77	0.71	0.74
LSM	0.76	0.80	0.76	0.74
TS-IDS	0.84	0.81	0.79	0.77

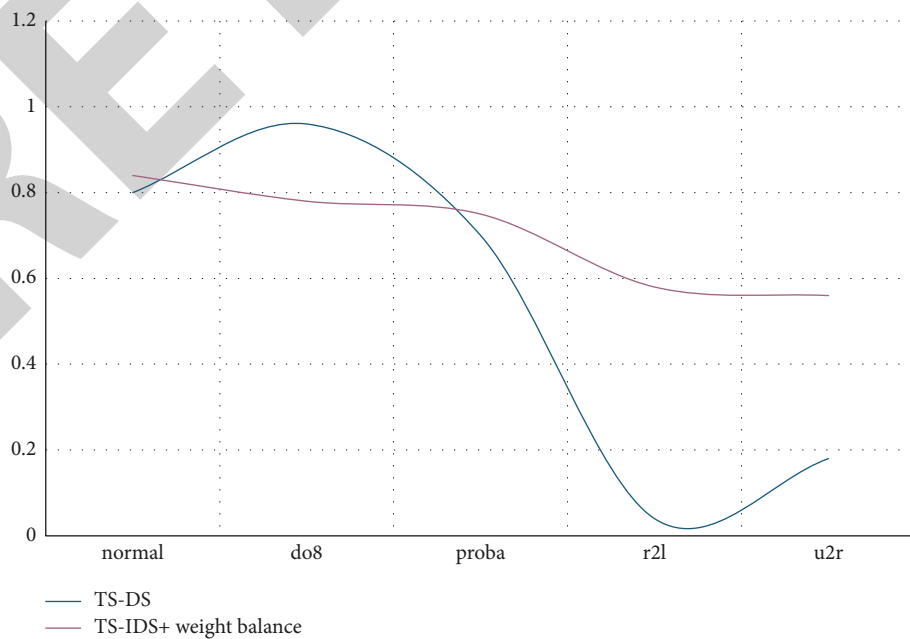


FIGURE 5: Comparison diagram of  $F1$  value of weight balance module.



TABLE 4: Comparison of weight balance module results (I).

Model	Accuracy	Precision	Recall	<i>F</i> value
TS-IDS	0.83	0.81	0.79	0.77
TS-IDS + weight balance	0.82	0.83	0.82	0.82

TABLE 5: Comparison of weight balance module results (II).

Model	Accuracy	Precision	Recall	<i>F</i> value
TS-IDS	Normal flow	0.68	0.97	0.80
	DOS	0.96	0.77	0.91
	Pro	0.90	0.62	0.68
	RL	0.94	0.01	0.02
	UR	0.56	0.07	0.13
TS-IDS + weight balance	Normal flow	0.76	0.94	0.84
	DOS	0.96	0.83	0.81
	Probe	0.78	0.72	0.71
	RL	0.81	0.45	0.57
	UR	0.58	0.43	0.49

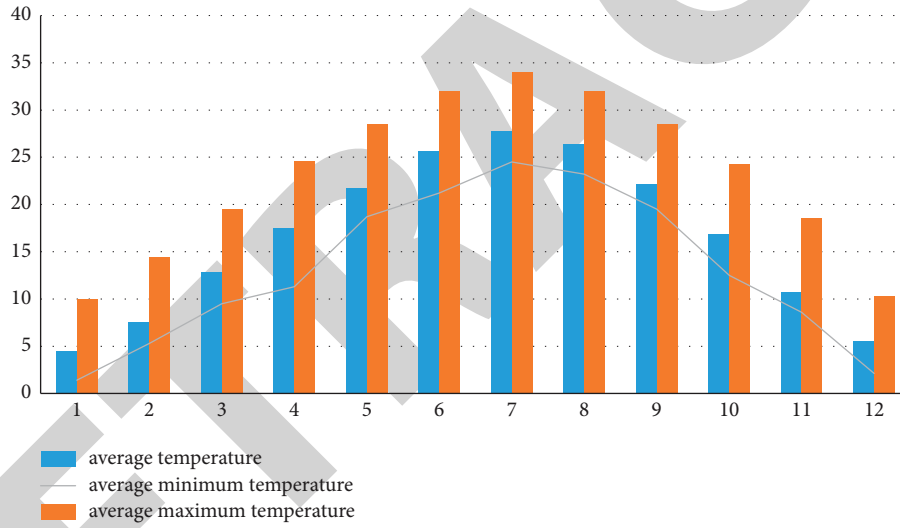


FIGURE 6: The monthly average temperature over the years.

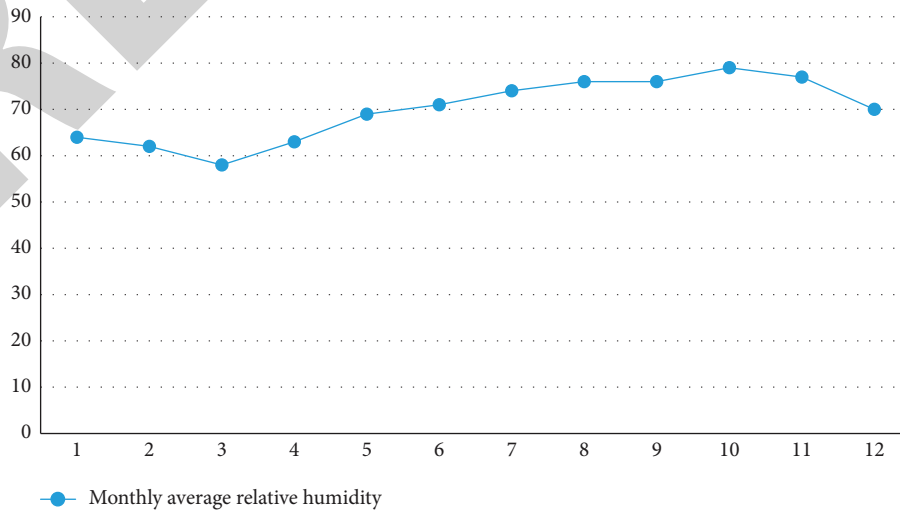


FIGURE 7: Statistical chart of monthly average phase humidity.

TABLE 6: Statistical table of time-domain characteristic parameters of striking points in different areas.

Characteristic parameters	Number	Good area			Defective area		
		Mean value	Maximum	Minimum	Mean value	Maximum	Minimum
Peak value	13	220.99	438.16	52.64	221.02	439.08	51.45
Mean value	13	1.87	3.24	0.54	2.43	4.66	0.63
Valid value	13	98.26	184.2	26.47	82.23	159.18	22.56
Standard deviation	13	22.49	37.55	5.12	24.32	41.60	5.38
Tapping time	13	1.02	1.28	0.81	1.56	1.77	1.38

TABLE 7: Normal deviation of some vertices of beam members.

Number	Deviation amount
1	2.697
2	1.554
3	2.289
4	4.356
5	2.899
6	4.569
7	5.019
8	3.497
9	3.894
10	3.269
11	1.598
12	2.731
13	4.287
14	1.366
15	3.97
16	1.98
17	3.831
18	1.036

**4.2.2. Statistical Analysis of Time-Domain Characteristics.** There are some differences in the striking force at different positions, and with the increase of the striking force value, the peak value of each characteristic parameter also increases, but compared with the time-domain characteristic parameter, its change range is small. Under the same conditions, there are some differences between round wood specimens with different sizes. Three groups of samples showed good repeatability. This is related to the distribution of internal defects in the sample, and there is a large deviation in the other two groups.

As shown in Table 6, comparing the average change of the characteristic parameters of the two areas to the impact time, the variation rate of the characteristic parameters reaches the maximum value of 52.12 and the effective value reaches the minimum value of 16.16. Knock impact time is in a defective area and knock impact time is in a good area. The optimal parameter combination and the optimal eigenvalue are obtained by using grey correlation analysis and principal component analysis and are applied to practical engineering detection.

**4.2.3. Component Deformation Detection and Analysis of Ancient Building Beam Components.** As shown in Table 7, the deformation standard member model and the original standard member model are compared and analyzed, the surface shape variables of the member are sorted out, and the

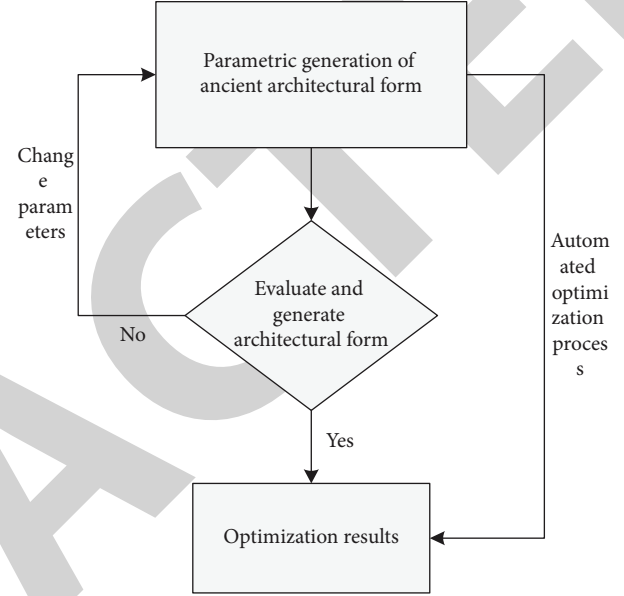


FIGURE 8: Flow chart of building parametric modeling generation system.

normal deviation of the vertex is calculated with this beam member as an example.

#### 4.3. Experimental Analysis of Optimization of Ancient Building Modeling under Deep Learning

**4.3.1. Basic Process of Ancient Modeling Optimization.** The application platform for the parametric generation and design of ancient building structures includes computer software such as digital project application plug-ins based on CATIA, GC application plug-ins based on MicroStation, processing plug-ins based on Java language platform and grasshopper plug-ins based on rhinoceros. In addition, there is a kind of program application software based on 3D modeling.

Figure 8 shows the flow chart of the building parametric modeling generation system. First, the shape parameters of ancient buildings are generated, and then the generated shape parameters are evaluated. If the parameters pass, the optimization is completed; otherwise, the parameters are changed again for evaluation and inspection.

As shown in Figure 9, the flow chart of the structural parameterization generation system reflects that the formation of structural parameters consists of picking up structural planes and generating structural planes, and the structural plane network is divided, so as to extract structural

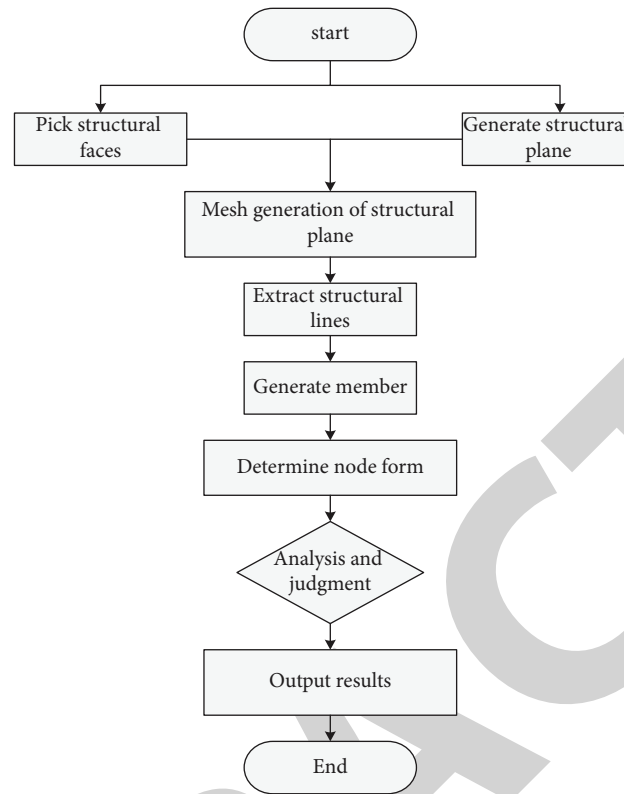


FIGURE 9: Flow chart of structure parameter generation system.

TABLE 8:  $U$  values of different insulation materials.

Material	Aluminum frame glass	Original exterior wall	Double glazing	Cotton frame	Glass fiber
$U$ value ( $\text{w/m} \times \text{k}$ )	5.70	1.76	2.65	0.89	0.65

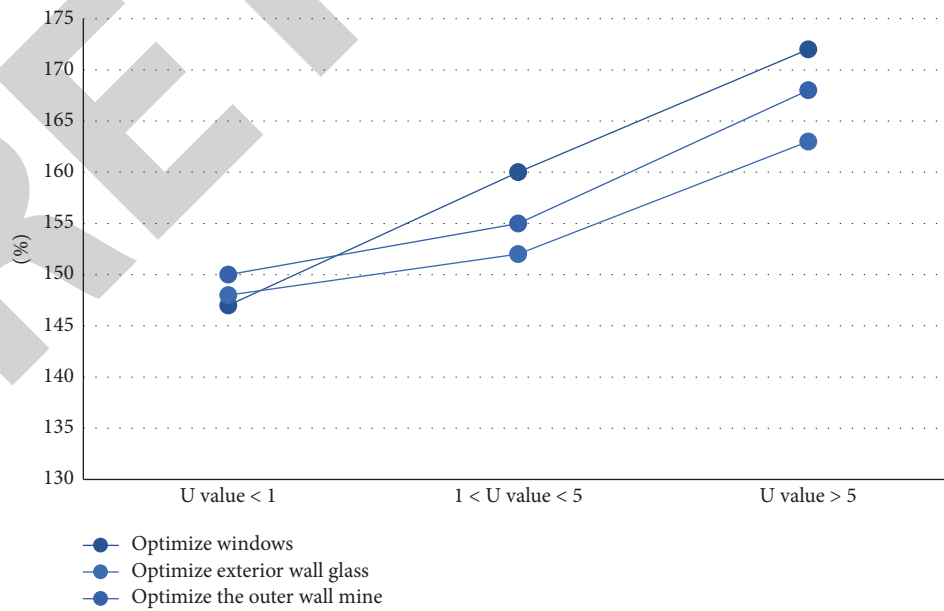


FIGURE 10: Statistical chart of comfort comparison.

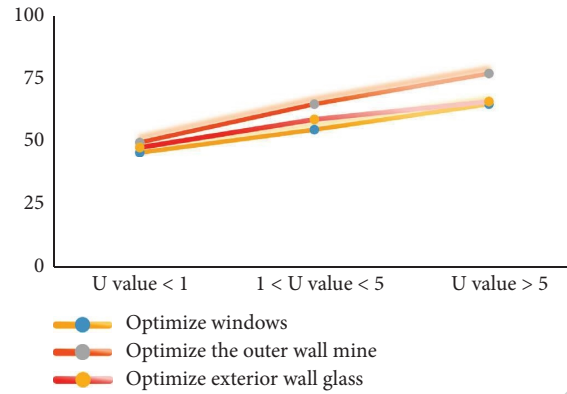


FIGURE 11: Statistical chart of total energy consumption comparison.

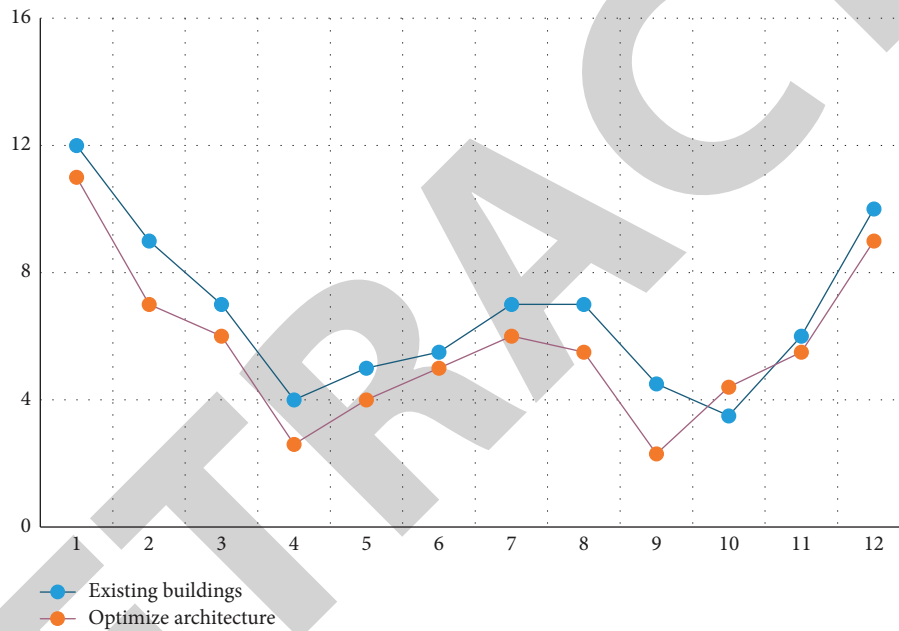


FIGURE 12: Statistical chart of comparison before and after energy-saving optimization.

lines and generate members for analysis and judgment. If the judgment is successful, the result will be output.

**4.3.2. Thermal Environment Analysis after Optimization of Ancient Building Modeling.** It is a relatively common and effective scheme to realize the energy-saving transformation of existing buildings by optimizing the enclosure structure. However, due to the characteristics of enclosure materials and environmental conditions, there are still many problems to be solved in its practical application. One of the most important is how to improve the thermal insulation performance of the building envelope. The utility model adds an energy-saving heat insulation layer on the existing building envelope, reduces the thermal conductivity of the entire envelope, and effectively blocks the cold air in winter, hot air in summer, etc. from entering the building interior, thereby reducing the intervention of auxiliary equipment,

maintaining the indoor temperature in a comfortable state, and achieving the purpose of building energy conservation.

Table 8 shows the  $U$ -value table of different thermal insulation materials statistics and the  $U$ -value data of five thermal insulation materials: aluminum frame glass, original exterior wall, double glass, cotton frame, and glass fiber.

As shown in Figure 10, the statistical chart of comfort comparison is shown. The comfort changes of optimized windows, optimized exterior wall mines, and optimized exterior wall glasses are analyzed from the three ranges of  $U \text{ value} < 1$ ,  $1 < U \text{ value} < 5$ , and  $U \text{ value} > 5$ .

Figure 11 shows the statistical chart of the comparison of total energy consumption. The energy consumption analysis of the three schemes of optimizing windows, optimizing exterior wall mines, and optimizing exterior wall glass is analyzed from the three ranges of  $U \text{ value} < 1$ ,  $1 < U \text{ value} < 5$ , and  $U \text{ value} > 5$ .

## Retraction

# Retracted: Modeling and Analysis Method of National Fitness Big Data for Basketball Projects Based on a Multivariate Statistical Model

### Security and Communication Networks

Received 1 August 2023; Accepted 1 August 2023; Published 2 August 2023

Copyright © 2023 Security and Communication Networks. This is an open access article distributed under the Creative Commons Attribution License, which permits unrestricted use, distribution, and reproduction in any medium, provided the original work is properly cited.

This article has been retracted by Hindawi following an investigation undertaken by the publisher [1].

This investigation has uncovered evidence of one or more of the following indicators of systematic manipulation of the publication process:

- (1) Discrepancies in scope
- (2) Discrepancies in the description of the research reported
- (3) Discrepancies between the availability of data and the research described
- (4) Inappropriate citations
- (5) Incoherent, meaningless and/or irrelevant content included in the article
- (6) Peer-review manipulation

The presence of these indicators undermines our confidence in the integrity of the article's content and we cannot, therefore, vouch for its reliability. Please note that this notice is intended solely to alert readers that the content of this article is unreliable. We have not investigated whether authors were aware of or involved in the systematic manipulation of the publication process.

Wiley and Hindawi regrets that the usual quality checks did not identify these issues before publication and have since put additional measures in place to safeguard research integrity.

We wish to credit our own Research Integrity and Research Publishing teams and anonymous and named external researchers and research integrity experts for contributing to this investigation.

The corresponding author, as the representative of all authors, has been given the opportunity to register their agreement or disagreement to this retraction. We have kept a record of any response received.

### References

- [1] Q. Zhao, "Modeling and Analysis Method of National Fitness Big Data for Basketball Projects Based on a Multivariate Statistical Model," *Security and Communication Networks*, vol. 2022, Article ID 2591633, 11 pages, 2022.

## Research Article

# Modeling and Analysis Method of National Fitness Big Data for Basketball Projects Based on a Multivariate Statistical Model

Qi Zhao 

Department of Physical Education, Shanghai Publishing and Printing College, Shanghai 200093, China

Correspondence should be addressed to Qi Zhao; zhaoqiww@sppc.edu.cn

Received 13 June 2022; Revised 26 July 2022; Accepted 10 August 2022; Published 21 September 2022

Academic Editor: Hangjun Che

Copyright © 2022 Qi Zhao. This is an open access article distributed under the Creative Commons Attribution License, which permits unrestricted use, distribution, and reproduction in any medium, provided the original work is properly cited.

How to start from the fitness needs of people and effectively improve the precision of the supply of public fitness services everyone is an important issue that needs to be solved first at the current stage. This requires us to proceed from the reality, conduct accurate research, and find a method that can match the current problem. In this paper, taking basketball projects in national fitness as an example, by introducing a proposition about the development of small basketball events, the corresponding big data modeling and analysis methods are studied. The research methods and research objectives involved in this paper are based on the relevant parameters of the multivariate statistical model. First, the article introduces the calculation principle of the multiple linear regression model. We introduce the concept of variance inflation factor involved in this principle and carry out the modeling and analysis of big data based on this variable. In order to illustrate the application effect of big data in this kind of research, this paper introduces three different big data technologies, including immune selection optimization algorithm, particle swarm optimization algorithm, and Elman neural network, to predict and analyze the variance inflation factor (VIF) corresponding to the small basketball project. The analysis results show that the Elman network exhibits certain advantages in terms of computing convergence time. And, as the number of calculation steps increases, the superiority of the Elman network is more obvious. As far as the prediction performance is concerned, the square of the correlation coefficient corresponding to the immune selection optimization algorithm is the largest and the sum of the squares of the residuals is the smallest, showing superior prediction performance.

## 1. Introduction

National fitness [1, 2] and healthy China is an important strategy for national development in the new era. From the internal logic point of view, the goal of national fitness is to achieve a healthy China. In addition, healthy China has become an institutional guarantee to meet the needs of the Chinese people for a better life by means of the extensive development of national fitness.

National fitness and national health involve two major elements of sports and health [3, 4], so the deep integration of the two cannot be achieved by the sports department alone. This requires multiple forces such as health care, education, culture, finance, gardening, and construction to work together to achieve the goal of deep integration [5].

With the advent of the new century, internet technology [6, 7] has achieved unprecedented development and has become an important force leading the third industrial revolution. It has produced a remarkable impact in the world, bringing a new experience to the production and life of the whole society. Among them, the big data technology involved in internet technology, or digital technology, is also widely used in all aspects of social life. With the in-depth integration of digital technology and national fitness public services, digital technology has gradually become an important form of social governance by empowering national fitness public services with precise supply, intelligent service, and intelligent governance. It also provides a strong technical support for promoting the high-quality development of China national fitness public services. In this context, all parts of the country have strengthened the informatization

construction of the national fitness public service system. This not only enhances the specific application of digital technology in the field of national fitness public services, but also improves the governance capacity and level of national fitness public services. It can be seen that the empowerment of national fitness public service governance through digital technology is of great significance for creating a social governance pattern of coconstruction, cogovernance, and sharing, and realizing the modernization of national fitness public service governance. However, the modernization of public service governance for national fitness empowered by digital technology in China is still in its infancy. Therefore, the problems of supply and demand deviation and imbalance of public services for national fitness need to be solved urgently.

Looking back at the relevant research in China in recent years, the digital governance of public services for national fitness can be roughly divided into the embryonic stage from the beginning of the 21st century to 2013 and the initial development stage from 2014 to the present.

Based on the abovementioned analysis, we can see that the modernization of public service governance for national fitness in the digital era is centered on digital technology, guided by the needs of people's livelihood and based on the relationship between supply and demand. This method can provide digital and intelligent governance services for the public service field of national fitness. This implementation can achieve the long-term goal of modernizing national governance.

However, it is undeniable that the digital governance of national fitness public services, as a complex systematic project, involves many participants. Therefore, its corresponding technical governance is more difficult. Although digital technology has been introduced into the public service governance of national fitness, due to the lag in the governance concepts of the government, society, and other multiple subjects and the lack of technological innovation capabilities, the problem of weak digital infrastructure construction in the field of national fitness public services has emerged. In addition, the bottleneck phenomenon encountered in the application of technological innovation is also more prominent. Therefore, it is necessary to solve or improve the abovementioned problems by improving the big data calculation method of national fitness.

Technologies such as big data [8, 9] and cloud computing [10, 11] are widely used in different fields such as engineering and social sciences. For example, traditional intelligence techniques are used in forecasting and research processes in various fields. In addition, statistical knowledge similar to multivariate statistical models can also be applied to the big data modeling and analysis process of national fitness. This paper takes the basketball project in national fitness as an example and first determines the main research content and research objectives of the article through a multivariate statistical model. Then, by introducing three new big data technologies, the research function obtained by the multivariate statistical model is predicted and analyzed, in order to provide suggestions for the reform and progress of national fitness.

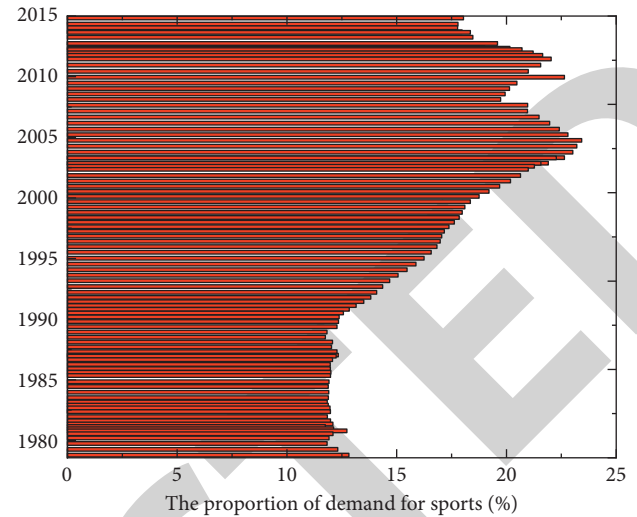


FIGURE 1: Trends in the demand for sports among the masses.

## 2. National Fitness Development in the New Era

In the new era, we should promote the transformation and upgrading of the national fitness public service system under the guidance of precise supply.

As far as the reality is concerned, problems such as unbalanced distribution of mass sports resources and insufficient supply still exist. It is mainly manifested in the lack of equalization of public services for national fitness between urban and rural areas, regions and different groups, and the inability to meet the diverse needs of the masses caused by the insufficient targeting ability of the traditional supply model. This hinders the further implementation of the national fitness strategy to a certain extent. Figure 1 shows the changing trend of the Chinese people's demand for sports in the past 30 years. As shown in Figure 1, after entering the 21st century, the Chinese people's demand for sports has gradually increased, and it has remained within a relatively high proportion.

Among them, after 2005, the desire of Chinese people to participate in fitness seems to have reached a peak. The reason for this phenomenon may be due to China's successful application for the 2008 Olympic Games.

The unbalanced economic and social development leads to the staged structural dislocation in the development of sports. Therefore, sports policies should be targeted by categories and angles. At present, a large number of innovative practice methods have been adopted in the field of sports, and comprehensive and precise interventions have been carried out in school sports, rural sports, and competitive sports. These types of interventions are based on their respective specific issues. Through accurate positioning of the problem, solutions and measures can be selected, and a series of precise solutions can be proposed.

The rapid development of high-tech means such as big data, cloud computing, and block chain has promoted the transformation and upgrading of the economy and society, and brought revolutionary innovation to traditional industries. High-tech that pays attention to individual needs



and individualized development can meet the individual sports needs of the masses in various ways. Therefore, the use of big data and other high technologies in the field of national fitness to respond to the increasingly diverse sports demands of the masses provides a technical possibility for the transformation and upgrading of the public service system for national fitness.

Finally, the development of national fitness is inseparable from the precise control and guidance of the government. The requirement of precise implementation of government policies runs through all aspects of the development of socialism with Chinese characteristics in the new era. The government's precise policy preference has achieved excellent results in promoting economic and social development, which also provides lessons for the modernization of the sports governance system. The national fitness public service, a field involving the public, has begun to implement precise policies, laying a solid foundation for the precise transformation of the national fitness public service system.

Figure 2 shows the various influencing factors of national fitness in the new era.

As shown in Figure 2, the realization of the national fitness goal is the result of the joint action of four main factors. Figure 2 shows that the main influencing factors mainly include the following four. They are the change of the main contradiction, precise intervention, government intervention, and the application of big data. Among them, the application of big data technology is the most important factor.

Data thinking [12] is the foundation and data application is the superstructure. Data analysis is a stepping stone, and its power is not limited to research itself. It is more important to apply technology at a higher level. We are committed to the multidimensional, systematic, and in-depth application of these basic knowledge. With the wide application of big data technology, the implementation of national fitness is inseparable from the blessing of this new technology. Big data technology is a platform based on artificial intelligence or intelligent algorithms. Compared with the data thinking mentioned in this section, big data technology is equivalent to an evolutionary processing of this data thinking, so that this way of thinking about problems is supported by new technologies. This approach is more reasonable and accurate.

Taking the basketball project in national fitness as an example, the specific purpose is to provide constructive opinions and reform ideas for the development strategy of China's small basketball events. To accomplish this goal, first of all, based on statistical knowledge, this paper first determines the goal and content of the research by introducing a multivariate statistical model. Then, by introducing several typical big data technologies, we compare their effects in the application of multivariate statistical models.

In order to clearly distinguish the layout of the article, here is a certain elaboration of the overall layout of the manuscript. In the third chapter of the article, we introduce the knowledge of multivariate statistical models. In the fourth chapter of the article, three typical big data techniques are introduced throughout the manuscript. The fifth part of

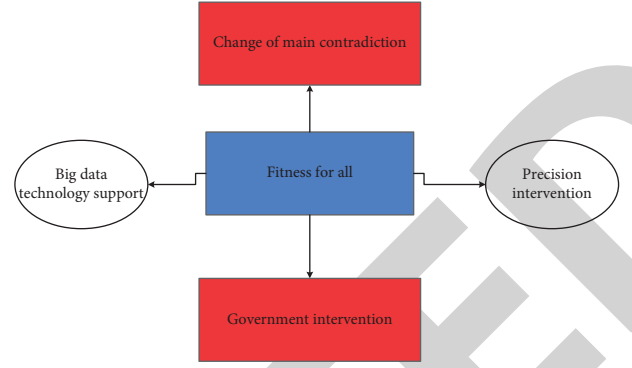


FIGURE 2: Knowledge modules in the training of data thinking.

the article shows the practical application of the theoretical research part. According to the reviewer's request, the author has added some necessary content. The specific additions are as follows.

### 3. Multiple Linear Regression Model [7, 13]

The multiple linear regression model can be expressed as follows:

$$W = \lambda_0 + \lambda_1 y_1 + \lambda_2 y_2 + \dots + \lambda_{m-1} y_{m-1} + \mu, \quad (1)$$

where  $y$  represents the dependent variable,  $y_1, y_2, \dots, y_{m-1}$  represent  $m-1$  independent variables,  $\lambda_0, \lambda_1, \lambda_2, \dots, \lambda_{m-1}$  are  $m$  unknown parameters, and  $\mu$  is an unobservable random variable with zero mean and variance  $\sigma^2$  greater than 0. It can also be called the error term. It is well known and usually assumed that  $\mu \sim N(0, \sigma^2)$ .

After the multiple regression model is initially established, whether it really explains the relationship between the predictor variable and the dependent variable needs to be tested for significance.

The decision linearity exponent  $R^2$  describes the proportion of the total change in  $Y$  that is reflected by the value of the linear function of the independent variable. The result of the coefficient of determination is between 0-1. As we all know, the larger the coefficient of determination, the better the fitting effect. The coefficient of the determination formula is as follows:

$$R^2 = \frac{SSR}{SST} = 1 - \frac{SSE}{SST} = 1 - \frac{\left( \sum_{i=1}^m (\hat{y}^{(i)} - y^{(i)})^2 \right) / m}{\left( \sum_{i=1}^m (\hat{y}^{(i)} - y^{(i)})^2 \right) / m} = 1 - \frac{MSE(\hat{y}, y)}{\text{Var}(y)}, \quad (2)$$

where MSE stands for mean squared error and SSE is called residual sum of squares. The SSR is called the regression sum, which reflects the sum of squared deviations of the linear function of the independent variable in each group of observations. The SST is called the sum of squares of the total deviation and is used to measure the degree of difference of the dependent variable itself. It can also be called the total change in data.

Before the overall mathematical experiment begins, we should first calculate the statistic  $t_i$ ; then, we can look up the  $t$

distribution table according to the given significant level  $\alpha$ , degrees of freedom  $n - k - 1$ , and get the critical value  $t_\alpha$  or  $t_{\alpha/2}$ . If  $t > t_\alpha$  or  $t_{\alpha/2}$ , the regression coefficient  $b_i$  is significantly different from 0. On the contrary, the test result is not significantly different from 0. The calculation formula of the statistic  $t$  can be expressed as follows:

$$t_i = \frac{b_i}{s_y \sqrt{C_{ij}}} = \frac{b_i}{s_{bi}}. \quad (3)$$

There are two common types of variables: quantitative variables and categorical variables. Among them, categorical variables are also called attribute variables, that is, the score of the variable is an attribute or can be classified. However, categorical variables should not be used directly in regression analysis. Because the equal spacing between discrete values assigned to categorical variables masks differences between categories. It is well known that dummy variables are one of the classic ways to solve this problem. Anyone with  $k$  attributes can be defined as a set of  $k$  dummy variables whose value is 1 or 0. This requires us to construct a dummy variable. It is worth noting that the conversion calculation discards a dummy column. Only then can we get a full rank matrix.

One of the main assumptions of multiple linear regression models is that the independent variables are not strongly correlated with each other, otherwise, multicollinearity problems will arise. A major problem with multicollinearity is that it causes the significance of the multiple linear regression coefficients to deviate from the true direction. To determine whether there is multicollinearity between two variables, the most common way is to use the VIF to correct.

The variance inflation factor refers to the ratio of the variance in the presence of multicollinearity among the explanatory variables to the variance in the absence of multicollinearity. VIF is obvious that the larger the variance inflation factor, the more severe the collinearity is. The calculation method can be expressed as follows:

$$VIF_i = \frac{1}{1 - R_i^2}. \quad (4)$$

In the formula, VIF represents the variance inflation factor of the independent variable  $x$ . It mainly represents the degree of data dispersion of this data series. The empirical judgment method shows that when  $0 < VIF < 10$ , there is no multicollinearity. When  $10 \leq VIF < 100$ , there is strong multicollinearity. When  $VIF \geq 100$ , there is severe multicollinearity.  $R_i^2$  is the coefficient of repeated measures for the regression of other independent variables when  $x_i$  represents the  $i$ th independent variable.

## 4. Big Data Modeling and Analysis Methods

**4.1. Immune Selection Optimization Algorithm.** The biological immune system is a complex adaptive system [14, 15]. The human immune system can recognize pathogens and respond to them, so it has certain abilities of learning, memory, and pattern recognition. This way is similar to an

external stimulating antigen to stimulate the human immune system to produce antibodies adapted to it. That is to say, an input variable corresponds to a unique output function. In this way, the principle and mechanism of its information processing can be described by computer algorithms to solve scientific and engineering problems. Algorithmic immunity retains some characteristics of the biological immune system and introduces them to solve optimization problems.

A population suppression process is added to the immune algorithm to control the average concentration of the population and avoid premature convergence of the algorithm to a locally optimal solution. This increases the global optimization capability.

We take the VIF involved in the previous section as a research variable and optimize it through the immune selection optimization algorithm.

A population suppression process is added to the immune algorithm to control the average concentration of the population and avoid premature convergence of the algorithm to a locally optimal solution. This increases the global optimization capability. Figure 3 is the calculation flow chart of the immune selection optimization algorithm.

A typical multipeak function is used to enhance the application of the immune algorithm. The multipeak function can be expressed as follows:

$$S(z) = \sum_{k=1}^m \left( 600(z_{k+1} - z_k^2)^2 + (1 - z_k)^2 \right). \quad (5)$$

In the formula,  $z$  represents the independent variable that meets the conditions, and  $S$  represents the value of the dependent variable after the convergence of multiple nonlinear calculations.

The global minimum point of the multimodal function is obtained when all the independent variables are 1, and the minimum value of the function is 0. The search interval for the independent variable is  $(-5, 5)$ . The specific parameter settings of the algorithm are shown in Figure 4. As shown in the figure, NP denotes the number of antibody population sizes,  $G$  denotes the maximum number of cycles, and NC represents the number of clones. As shown in Figure 4, NP is equal to 220,  $G$  is equal to 198, and NC is equal to 238.

The optimization results of 10 trials of the immune algorithm are shown in Figure 5. It can be seen from Figure 5 that the immune algorithm has a good ability to search for multidimensional and multipeak functions. Therefore, it can be applied to solve optimization problems about VIFs in multivariate statistical models.

**4.2. Particle Swarm Optimization Algorithm.** Particle swarm optimization algorithm [16, 17] is used to simulate various biological social behaviors such as biological reproduction and upgrading. This artificial intelligence algorithm consists of a finite number of particles that are unrelated to each other. These particles automatically search for a single best position and a global best position according to the optimal problem solution, according to the optimization criteria

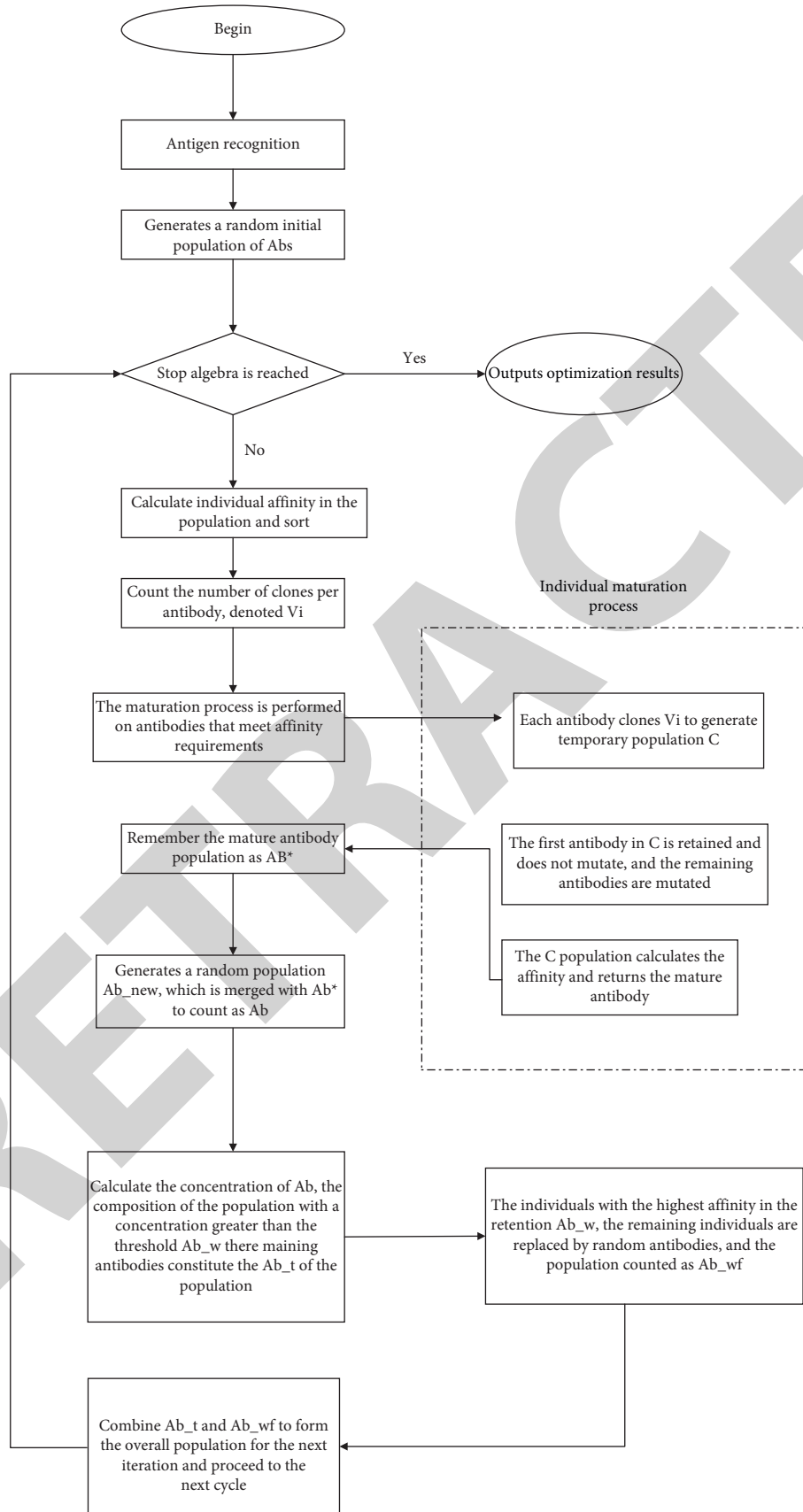


FIGURE 3: The calculation flow chart of the immune optimization algorithm.

found in nature. Each iteration the researchers got during the computation was reupdated based on the particle's position and velocity. The calculation steps for updating the relative motion trajectory of each particle can be expressed as follows.

$$\begin{aligned} L_i &= \lambda \times L_i + D_1 R_1 (Q_{\text{best}} - Y_i) + D_2 R_2 (K_{\text{best}} - Y_i), \\ K_i &= K_i + L_i. \end{aligned} \quad (6)$$

**4.3. Elman Networks.** Neural networks [18, 19] are widely used for their large-scale parallel distributed structure, learning ability, and generalization ability. The main advantages are as follows: nonlinear analysis capability, convenient input/output mapping, adaptive capability, evidence response, background information, strong fault tolerance, VLSI (very-large-scale integrated) implementation, analysis and design consistency, and neural biological analogy. This paper takes the Elman neural network as an example to describe the implementation process of traditional neural network prediction in detail.

The calculation process of the Elman network can be expressed as follows.

For the input layer, the Elman network can be represented as follows:

$$\begin{cases} x_i^0 = x_i(k), \\ s_i^1 = \sum_{j=1}^{n^0} w_{ij}^0 x_j^0(k) + \sum_{j=1}^{n^1} w_{ij}^2 c_j^0(k) \\ x_i^1 = f1(s_i^1(k)). \end{cases} \quad (7)$$

Similarly, the implicit value in the network can be expressed as follows:

$$\frac{\partial F(j)}{\partial w_{ij}^0} = - \sum_{l=1}^r \frac{\partial F(j)}{\partial y_l(j)} \cdot \frac{\partial y_l(j)}{\partial w_{ij}^0} = \sum_{l=1}^r e_l(j) \cdot f2'(s_l^3(j)) \cdot w_{lj}^1(j) \cdot \frac{\partial x_i^1(j)}{\partial w_{ij}^0}. \quad (8)$$

Through comprehensive calculation, we can get the following:

$$\left\{ \frac{\partial F(j)}{\partial w_{ij}^0} = \sum_{l=1}^r e_l(j) \cdot f2'(s_l^3(j)) \cdot w_{lj}^1(j) \cdot \chi_{ij}^i(j) \chi_{ij}^i(j) = f1'(s_i^1(j)) \cdot (x_j^0(j)) + \sum_{m=1}^{n_1} w_{im}^2 \cdot \chi_{ij}^m(j-1). \right. \quad (9)$$

The key to the nonlinear ability and learning ability of the network lies in the continuous correction of the weights. There are two methods for recurrent network training, one is the batch mode, the other is the online mode, the Elman network adopts the latter.

## 5. Example Verification and Analysis

This paper takes a small basketball project as an example to study the application of multivariate statistical models in the process of big data analysis and modeling. The small basketball is a basketball game tailored by the Chinese Basketball Association for young people. By changing the rules and equipment of adult basketball, basketball can adapt to the physical and mental development characteristics of young people of all ages. It is also a social sports project for children and teenagers that is mainly promoted by the Chinese Basketball Association. The new era of small Chinese basketball began to gradually take shape after Yao Ming became the new chairman of the Chinese Basketball Association in 2017.

Although the development of small basketball events in China is in full swing, the development of small basketball events has not kept up with the development of small basketball events, and there are still many problems in the development of small basketball events. These problems mainly include the long-term cycle of large-scale competitions held by the country; the small number of competitions; the small number of referees

and coaches; the imperfect rules and other problems. This paper analyzes the pros and cons, and opportunities threats faced in the development of small basketball events in China from a strategic perspective. Through this method, we hope to provide strategic reference and reference for promoting the scientific, stable, and sustainable development of small basketball events in China.

This paper systematically studies the internal strengths (strengths), internal weaknesses (weaknesses), external opportunities (opportunities), and external threats (threats) faced in the development of small basketball events in China. In addition, we analyze the possible strategic combinations in the development of small basketball events in China.

Among them, internal advantages and external threats are two objective facts, which will not change with the development of the event. However, internal disadvantages and external opportunities can be improved according to the nature of the event.

The direct impact matrix of the VIF of the four factors faced in the development process of Chinese small basketball events can be drawn in Figure 6.

Among them, the number of data sets corresponding to each factor is 6,000, so the total number of data sets studied in this paper is 24,000.

The direct influence matrix of VIF is composed of four main elements: influence degree, influenced degree, centrality degree, and cause degree. The measurement criteria of the influence degree of the four main elements, the degree of

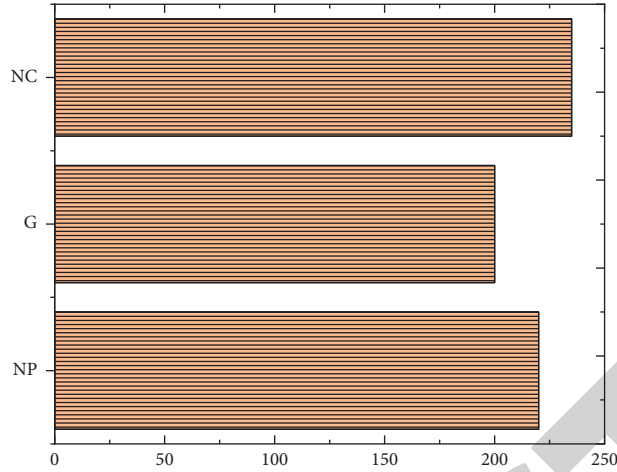


FIGURE 4: Specific application parameters of the immune algorithm.

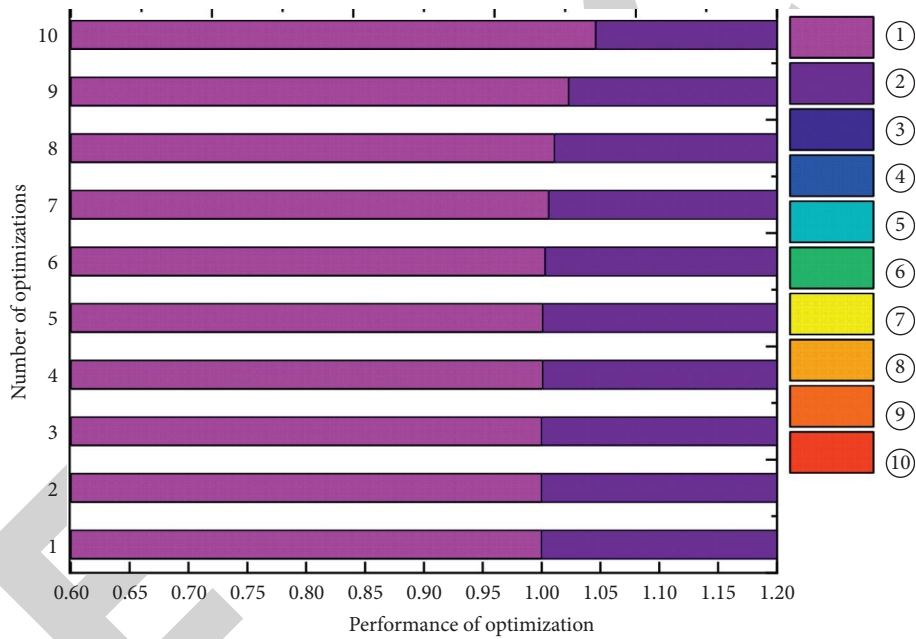


FIGURE 5: Function optimization results.

influence, the degree of being influenced, the degree of centrality, and the degree of cause, in the system can be calculated from the comprehensive influence matrix. We can add the elements of each row in the comprehensive influence matrix to get the influence degree of the corresponding variable. The sum of the influence degree and the influenced degree is the centrality degree. A large number of studies have proved that the greater the centrality, the stronger the effect on the research target. That is to say, the larger the corresponding value of VIF, the stronger the linearity of the corresponding multivariate statistical model. The difference between the influence degree and the influenced degree is the cause degree. This effect is called the causal factor of the variable. The smaller the cause degree, the smaller the influence factor is susceptible to the influence of other influencing factors, and the corresponding VIF is larger. The

variables represented by this phenomenon are called outcome factors. Figure 7 shows the VIF metrics corresponding to four factors.

As shown in Figure 7, the cause degree can reflect the categories of the influencing factors. The larger the causality degree of the influencing factor, the more the factor is the Causal Index in the influencing factor system. In addition, the smaller the causality degree of the influencing factor, it means that the factor is the Result Index in the influencing factor system. We can obtain the multivariate statistical model of the influencing factors corresponding to the four factors through the theory of the multivariate statistical model mentioned previously. We take weaknesses as an example, and the corresponding multivariate statistical model is obtained by mathematical fitting as follows:

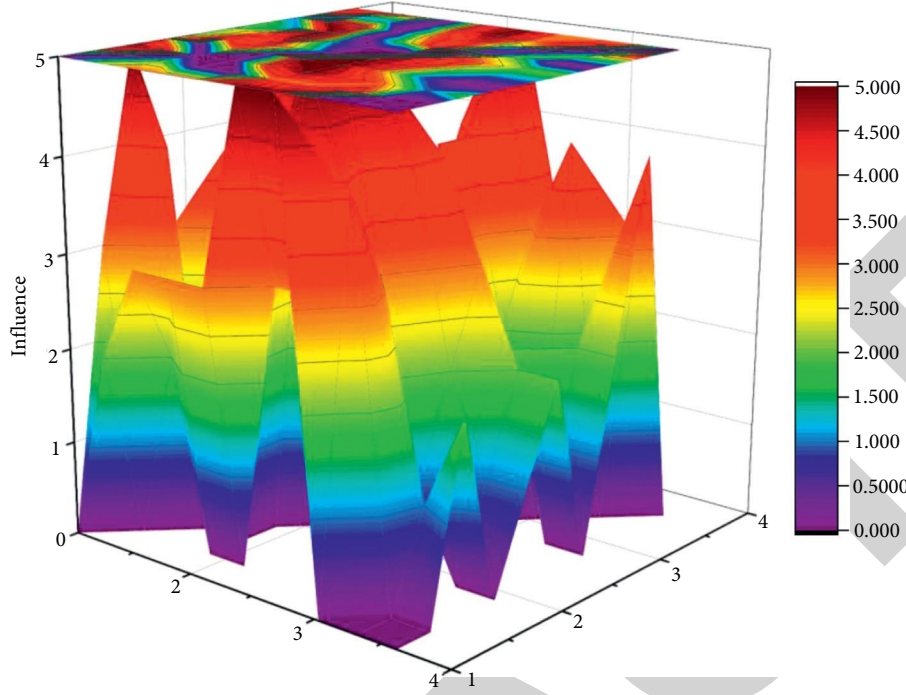


FIGURE 6: Convergence comparison of algorithms.

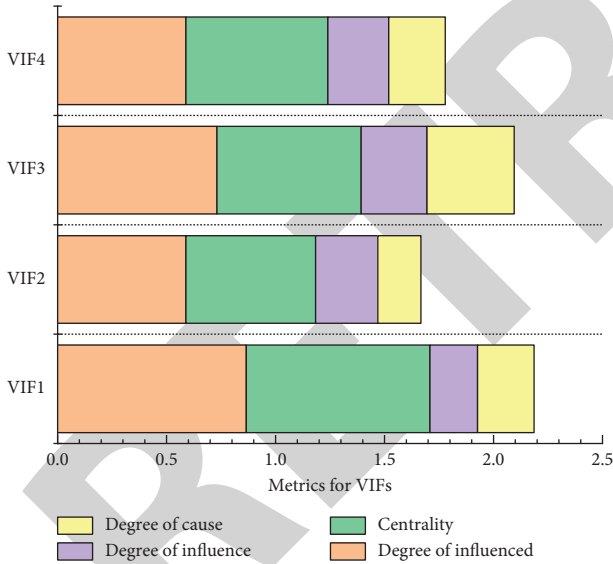


FIGURE 7: Influencing factors of new media copyright development in sports events.

$$y = 0.78 + 4.5x_1 + 3.6x_2 + 3.8x_3 + 4.9x_4. \quad (10)$$

In the formula,  $y$  represents the weaknesses corresponding to the small basketball event,  $x_1$  represents the influence degree corresponding to the factor,  $x_2$  represents the influence degree corresponding to the factor,  $x_3$  represents the centrality corresponding to the factor, and  $x_4$  represents the cause degree corresponding to the factor. And, the fitting process of formula (10) can be approximated by the fitting curve. The specific linear fitting curve is shown

in Figure 8. It can be seen from Figure 8 that for the four independent variables, for the weaknesses corresponding to the small basketball items, the linear fitting relationship is good, and the scatter points are basically distributed on both sides of the straight line.

Similar to weaknesses in the multivariate statistical model, the other three influencing factors can also find their corresponding multivariate statistical models through similar methods. Due to the limitation of the length of the article, the calculations are not explained one by one.

In order to better analyze the degree of linearity in the multivariate statistical model, three big data technologies such as immune selection optimization algorithm, particle swarm optimization algorithm, and Elman neural network are used to predict and analyze the corresponding VIF value in the multivariate statistical model. Similar to the above-mentioned analysis, we still use the corresponding internal disadvantages in the small basketball project for analysis.

It is quite necessary to predict the computational convergence ability of the three techniques before performing intelligent computation. To this end, when the calculation iteration steps of the three big data technologies are 200, 400, 600, 800, and 1000 respectively, we compare the convergence completion time of the three artificial intelligence algorithms. The specific test results are shown in Figure 9.

As can be seen from Figure 9, the Elman network has the least computation time. In addition, with the increase of the number of computational iterations, the computational superiority exhibited by the Elman network continues to increase.

Through the three abovementioned intelligent algorithms: immune selection optimization algorithm, particle swarm optimization algorithm, and Elman network, the



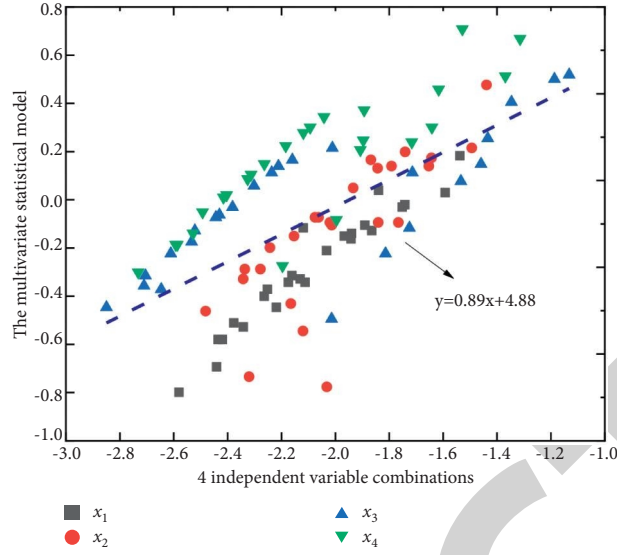


FIGURE 8: The fitting curve of the multivariate statistical model represents the relationship.

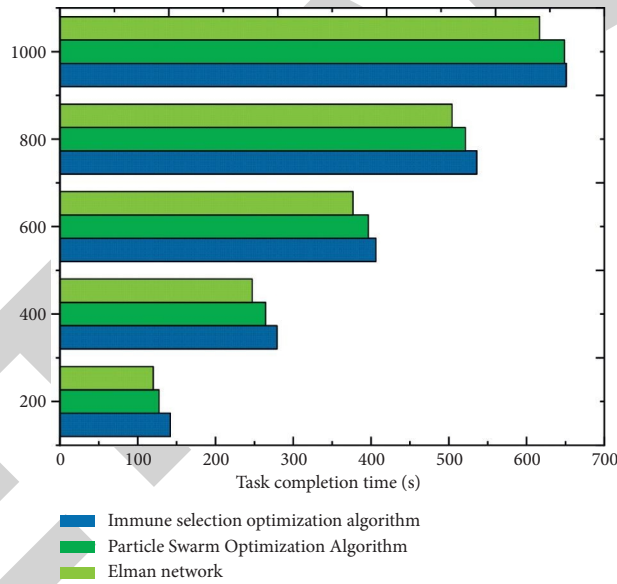


FIGURE 9: Comparison of task completion time.

corresponding VFI value in the multivariate statistical model is predicted and studied. It is well known that the squared correlation coefficient ( $r^2$ ) and root mean squared difference (RMSE) (SSE) are two typical predictors. The next step is to compare  $r^2$  and SSE of the three algorithms. The closer  $R^2$  is to 1, the smaller SSE, and the higher the prediction accuracy. Table 1 shows the prediction performance of the three artificial intelligence algorithms. Among them, the determination coefficient can be obtained by the following calculation method:

$$r^2 = \frac{[\sum_{i=1}^n (x_i - x_m)^2] - [\sum_{i=1}^n (x_i - y_i)^2]}{[\sum_{i=1}^n (x_i - x_m)^2]} \quad (11)$$

The root mean square difference can be obtained by the following calculation method:

$$RMSE = \sqrt{\frac{1}{n} \times \sum_{i=1}^n |(y_i - x_i)^2|} \quad (12)$$

It can be seen from Table 1 that compared with the three algorithms, the square of the correlation coefficient corresponding to the immune selection optimization algorithm is the largest, the maximum value is 0.9813, the root mean squared difference is the smallest, and the minimum value is 11. This shows that the prediction effect of the immune selection optimization algorithm is the best and it can be



TABLE 1: Comparison of prediction performance of three big data technologies.

Big data technology	The effect of regression analysis	
	Squared correlation coefficient ( $r^2$ )	Root mean squared difference (RMSE)
Immune selection optimization algorithm	0.9813	0.11
Particle swarm optimization algorithm	0.9473	0.21
Elman neural network	0.6851	0.36

used as a key technology for evaluating the multivariate statistical model of small basketball projects. At the same time, the multivariate statistical model introduced in this paper combined with the prediction method of big data technology provides a new processing idea for the modeling and analysis of national big data.

## 6. Conclusion

- (1) It is foreseeable that under the current social development background, if the national fitness wants to maintain a sustainable development trend, it must recognize the mainstream trend of current social development. At the same time, we should combine our own development plan, with the strong support of new technologies, change the path and method of development, strengthen concept innovation, improve our own system, and adopt scientific management and operation methods. Only in this way can the sustainable development of national fitness be guaranteed.
- (2) National fitness in the new era requires the blessing and assistance of technology. The application of big data, cloud computing, and other technologies can effectively improve the vitality of national fitness. In this paper, the multivariate statistical model is introduced to study the influence degree of the internal strengths (strengths), internal weaknesses (weaknesses), external opportunities (opportunities), and external threats (threats) corresponding to the small basketball project. The research results show that the four main factors have a good multilinear relationship with their corresponding degree of influence, degree of centrality, and degree of cause.
- (3) The article introduces three different big data technologies: immune selection optimization algorithm, particle swarm optimization algorithm, and Elman neural network, to predict and analyze the variance inflation factor VIF corresponding to the small basketball project. The prediction effect shows that for the research cases introduced in this paper, the prediction effect of the three intelligent algorithms is ranked from good to bad: immune selection optimization algorithm, particle swarm optimization algorithm, and Elman neural network. A large number of facts have proved that big data technology can be effectively applied to the eye-catching evaluation research of national fitness. At the same time, this algorithm can also provide a certain reference for the modeling and analysis of national fitness big data.

## Data Availability

The experimental data used to support the findings of this study are available from the corresponding author upon request.

## Conflicts of Interest

The authors declared that they have no conflicts of interest.

## References

- [1] F. B. Ortega, J. R. Ruiz, I. Labayen, C. J. Lavie, and S. N. Blair, "The Fat but Fit paradox: what we know and don't know about it," *British Journal of Sports Medicine*, vol. 52, no. 3, pp. 151–153, 2018.
- [2] R. T. Bartee, K. A. Heelan, and B. L. Dority, "Longitudinal evaluation of aerobic fitness and academic achievement among schoolchildren," *Journal of School Health*, vol. 88, no. 9, pp. 644–650, 2018.
- [3] K. Kaasalainen, K. Kasila, J. Komulainen, M. Malvela, and M. Poskiparta, "Changes in psychosocial factors and physical activity among Finnish working-age men in the adventures of joe Finn campaign," *The International Quarterly of Community Health Education*, vol. 39, no. 1, pp. 39–49, 2018.
- [4] E. Fuzeki, T. Engeroff, and W. Banzer, "Author's reply to lopez: comment on "health benefits of light-intensity physical activity: a systematic review of accelerometer data of the national health and nutrition examination survey (nhanes)"", *Sports Medicine*, vol. 48, no. 3, pp. 749–750, 2018.
- [5] A. S. Harrison, L. Tang, and P. Doherty, "Are physical fitness outcomes in patients attending cardiac rehabilitation determined by the mode of delivery," *Open Heart*, vol. 5, no. 2, Article ID e000822, 2018.
- [6] X. Q. Jiang, T. T. Xu, and X. J. Dong, "Campus data analysis based on positive and negative sequential patterns," *International Journal of Pattern Recognition and Artificial Intelligence*, vol. 33, no. 5, 2019.
- [7] B. Sánchez-Torres, J. A. Rodríguez-Rodríguez, D. W. Rico-Bautista, and C. D. Guerrero, "Smart campus: trends in cybersecurity and future development," *Revista Facultad de Ingeniería*, vol. 27, no. 47, pp. 104–112, 2018.
- [8] A. J. Ferrer, J. M. Marques, and J. Jorba, "Towards the decentralised cloud: survey on approaches and challenges for mobile," *ACM Computing Surveys*, vol. 51, no. 6, pp. 51–36, 2019.
- [9] S. Fatima and S. Ahmad, "An exhaustive review on security issues in cloud computing," *Ksii Transactions On Internet and Information Systems*, vol. 13, no. 6, pp. 3219–3237, 2019.
- [10] W. Zhang, X. C. Zhang, H. L. Shi, and L. Zhou, "RDDSACCGA: a reliable data distribution solution assisted by cloud computing based on genetic algorithm," *Cluster Computing*, vol. 22, no. S5, pp. 11069–11077, 2019.
- [11] P. Fraga-Lamas, M. Celaya-Echarri, P. Lopez-Iturri et al., "Design and experimental validation of a LoRaWAN fog

## *Retraction*

# **Retracted: Data Collection and Analysis of Physical Education Teaching Practice Based on Multisensor Perception**

### **Security and Communication Networks**

Received 26 December 2023; Accepted 26 December 2023; Published 29 December 2023

Copyright © 2023 Security and Communication Networks. This is an open access article distributed under the Creative Commons Attribution License, which permits unrestricted use, distribution, and reproduction in any medium, provided the original work is properly cited.

This article has been retracted by Hindawi, as publisher, following an investigation undertaken by the publisher [1]. This investigation has uncovered evidence of systematic manipulation of the publication and peer-review process. We cannot, therefore, vouch for the reliability or integrity of this article.

Please note that this notice is intended solely to alert readers that the peer-review process of this article has been compromised.

Wiley and Hindawi regret that the usual quality checks did not identify these issues before publication and have since put additional measures in place to safeguard research integrity.

We wish to credit our Research Integrity and Research Publishing teams and anonymous and named external researchers and research integrity experts for contributing to this investigation.


The corresponding author, as the representative of all authors, has been given the opportunity to register their agreement or disagreement to this retraction. We have kept a record of any response received.

### **References**

- [1] J. Tong and L. Ge, "Data Collection and Analysis of Physical Education Teaching Practice Based on Multisensor Perception," *Security and Communication Networks*, vol. 2022, Article ID 5758292, 12 pages, 2022.

## Research Article

# Data Collection and Analysis of Physical Education Teaching Practice Based on Multisensor Perception

JinFeng Tong<sup>1</sup> and Liu Ge<sup>2</sup> 

<sup>1</sup>Professional Tennis Academy of Wuhan City Polytechnic, Wuhan, Hubei 430064, China

<sup>2</sup>Zhongnan University of Economics and Law, Wuhan, Hubei 430074, China

Correspondence should be addressed to Liu Ge; z0004485@zuel.edu.cn

Received 19 June 2022; Revised 30 July 2022; Accepted 11 August 2022; Published 21 September 2022

Academic Editor: Hangjun Che

Copyright © 2022 JinFeng Tong and Liu Ge. This is an open access article distributed under the Creative Commons Attribution License, which permits unrestricted use, distribution, and reproduction in any medium, provided the original work is properly cited.

Because our country is constantly updating training standards, the first mechanism for assessing physical fitness is far from current needs. A good assessment process can help to stimulate student learning, identify strengths and weaknesses, and better improve sports knowledge. In this paper, based on the multisensor perception of physical education and teaching practice data collection and analysis, it is found that the original sensor data often have some defects, but the Kalman filter can be processed, which can make the data more accurate. After comparing the data, it can be found that each group of data basically has an error of 0.02–0.9. After processing, the data better reflect the changes in the measurement. With the reform of the professional evolution of boxers, higher requirements have been placed on athletes. The sensor can be continuously tested. According to the experiment, the basic probability of different sensors on the test paper can be found that the fused sensor data are 1/2, while the single sensor data are 1/6, and the data of a single sensor are much lower than the confidence of fused sensors, effectively improving the comprehensive ability of boxing.

## 1. Introduction

Multisensory educational equipment provides an educational tool that allows multisensory utilization to facilitate student learning. The educational tool consists of a learning board with multiple sides, at least one of which includes textured features thereon to allow tactile and kinesthetic manipulation of the board [1]. The conditions of teachers teaching physical education and health (PEH) in elementary schools and their opportunities to pursue inclusive teaching to reach all students were examined. Compilation essays are not only composed of different articles that provide knowledge from the perspective of students and teachers but also include the teaching and learning process of in situ research. The first article helps to understand how different relevant variables influence motivation to learn and how cultural aspects influence the shaping patterns of attitudes, beliefs, and values shared by students. The second article considered teachers' perspectives and examined teachers'

discourse representations of low-motivated students and associated beliefs about inclusive teaching and strategies for all students [2]. The aim was to examine preservice teachers' physical education training and its teaching effect on preschool physical education. Following the observation method, each of the 48 trainees recorded two lessons for data collection and analysis. Data analysis revealed that (a) student training needs to be re-examined and revised, (b) teachers' expectations for PE teaching in kindergarten may need to be revised, (c) components of effective teaching, such as time management, student organization, use of technology and others, need student improvement, (d) the school environment itself brings trouble to PE teaching, and (e) how preservice teachers attach importance to PE and their attitudes toward the curriculum, which not only affects the conduct of the curriculum but also the effectiveness of their teaching [3]. The industry believes that the National Vocational Standards Board (NPTS) is an important factor in improving student performance and says it needs a way to

recognize and reward good teachers. This study investigated the effectiveness of full-time sports education classes for NBCPET and non-NBCPET students and their students. All repetitive interviews with teachers included past skill training and changes in physical activity development and learning. In addition, NBCPET students did not differ significantly in the amount of time spent on moderately active physical activity (MVPA) compared to non-NBCPET students [4]. The industry believes that the National Vocational Standards Board (NPTS) is an important factor in improving student performance and says it needs a way to recognize and reward good teachers. This study investigated the effectiveness of full-time sports education classes for NBCPET and non-NBCPET students and their students. All repetitive interviews with teachers included past skill training and changes in physical activity development and learning. In addition, NBCPET students did not differ significantly in the amount of time spent on moderately active physical activity (MVPA) compared to non-NBCPET students [5]. Models such as physical education can give students a different and better experience. One of the main requirements for physical education is that students are socially active in group work where they have different roles and responsibilities. Elizabeth Cohen has made a comprehensive analysis of teamwork in the curriculum model. Although teamwork is well-known as an educational policy that facilitates learning, Noh Cohen found differences in student participation and achievement in teamwork and student identity. In this case, the curriculum describes specific situations according to the characteristics of the students, who enjoy participating in sports. It was assumed that circumstances would affect the social interaction of students in group work. It should be noted that the situation is determined contextually and culturally by students working in groups. Curriculum models such as physical education are a way of explaining the impact of situations on group performance as long as we recognize and value their importance [6]. Purpose: The purpose of this study was to examine the factors associated with the adoption of additional online teaching practices by high school physical education (PE) teachers. Methods: Semistructured and open-ended telephone interviews with 28 high school physical education teachers were used as the primary method of data collection. All teachers used or used an additional online teaching system during the study period. The Unified Theory of Acceptance and Use of Technology (UTAUT) governs the analysis of target content. Results: Four main categories were developed, including programmatic, educational, and inclusive; minimal effort from individual users and students; support schools and curriculum providers to promote exploitation; and long-term use is determined by the administrator. Discussion/ Conclusion: The results agree well with UTAUT and make it possible to place the theory in the context of secondary PE. [7]. Its purpose is to assess the beliefs of physical education teachers (PET) when teaching students with disabilities. Teachers agreed that more basic developmental training was needed. School districts should require that GPE teachers regularly attend relevant professional development training with a focus on physical education for students with

disabilities [8]. This paper analyzes the reform of university physical education information services based on artificial intelligence technology and conducts thorough and innovative research on it. AI is a leader in school transformation in data acquisition. Opportunities for decision management, education, research support, and health assessment changes. Following the requirements of education modernization, we aim to address the issues that exist in the management of physical education at the university, with a focus on intelligent and humanized education management goals [9]. With the continuous growth of colleges and universities to improve the quality of school sports management, the need for sports management is increasing. The main task of the system, to improve the quality of management and to meet the requirements of university sports management, is the student knowledge management module. Teacher experience education planning is part of student selection, student class, student management class, and student achievement [10]. Social science research and various statistical methods form an important core, but when applying statistical analysis, respondents have difficulty in completing surveys. In other words, the respondents' answers are not always correct. This study uses vague statistics that combine the natural nature of ambiguity and uncertainty in everyday statistical tasks to analyze the differences in time management between educators [11]. The biggest challenge facing electronics manufacturers is the efficient collection and analysis of quality data and rework tracking. Network-centric systems also allow data to be analyzed through engineering and management. Web-centric manufacturing execution systems collect the information needed to improve efficiency and meet customer needs and deliver these benefits in an easy-to-deploy and maintain architecture [12]. Data showing high, medium, and low responses in continuous and nonconstant patterns were generated by electromechanical equipment to determine if the same data were collected by time sampling. Are the recording intervals and recording frequencies displayed in the same way? It turns out that temporal sampling provides extremely inaccurate response estimates [13]. It provides an analytical framework to take into account the spatial conditions associated with network sensor data management algorithms. Standard data columns are considered open temporary connections. The reception will restore the area immediately. Our experiments show that robust analysis yields different results than expected. The same is true for noncommunicative and traditional methods of communication. The analytical methods proposed in this paper can be easily extended to real-time data reconstruction problems, taking into account different transmission methods, node distribution, and reconstruction methods [14]. We study the role of real-time smart sensor networks in sensory information, assuming the information is integrated into time and space. This process also helps in providing an efficient and conflict-free data delivery process to the recipient. Our results were validated by collecting data in fields with different correlation coefficients. The proposed analysis algorithm can be based on different pipeline schemes, node classification, and reconstruction methods [15]. In the existing work mentioned

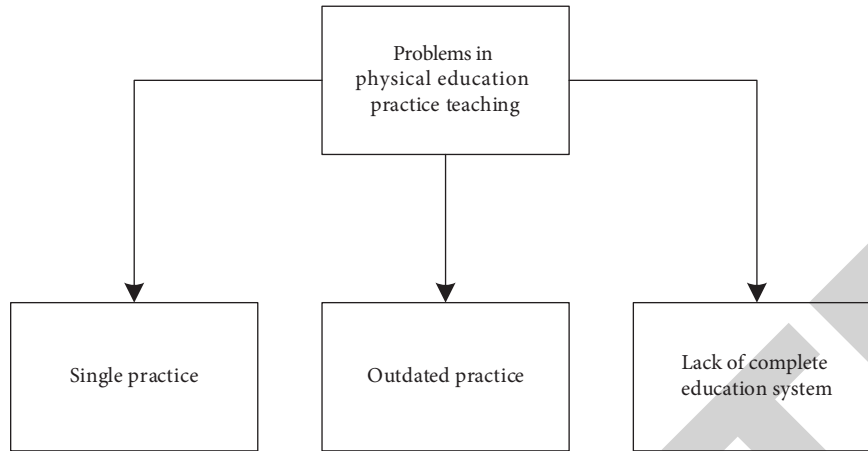


FIGURE 1: Problems existing in physical education teaching practice.

above, there are large data acquisition errors in sports data acquisition, and there are many errors in information fusion between different sensors, which lead to low accuracy of data acquisition. The results cannot correctly reflect the real effect of physical education practice, and the teaching effect is quite different. Because the content of physical education practice data is old, it cannot meet the needs of new data collection, and it cannot scientifically implement the teaching task from the analysis effect. Sports practice data collection lacks a complete collection process and analysis methods and lacks real-time analysis of corresponding data.

## 2. Physical Education Teaching Practice

**2.1. The Practical Significance of Physical Education Practice.** Physical education will face a major problem in the widespread implementation of quality education in the new era. Physical education is the main content of quality education, and physical education is the way to realize the real educational content in the process of educational modernization. In modern physical education programs, children have physical ability, physical knowledge, and aesthetics. A “perfect person” realizes the socialization of people through physical learning, creates opportunities for people to learn and creative work, and has human resources suitable for social development.

**2.2. Problems in Physical Education Practice Teaching.** The current training system includes military training, enrollment training, learning experience, experimental training, referee training, sports basic skills competition, physical education teacher basic skills assessment, trial training, and other training courses before practice. The practice of teachers’ basic skills and social questioning vary. Currently, some internships are sporadic, and the internship courses are outdated; research activities are conducted only through dissertations, and off-campus practice is limited to educational practice, summer social practice, social research, etc. It can be seen that there is a gap between the practical aspects

of talent training and society’s demand for applied talents. It is urgent to continuously reform the training practice content and curriculum system and urgently build a perfect and integrated practical training system. Only pay attention to the form, ignore the actual effect. On-site investigation by professionals found that many schools still use the old-fashioned teaching model. The equipment is outdated, not practical, and even only does superficial work, and there are very few things that can really be used in actual learning (Figure 1).

**2.3. Countermeasures to Realize the Sustainable Development of Physical Education.** Its structure largely depends on the ability to teach physical education. The development of organizational skills, health management skills, sports management skills, physical education teacher quality, and ethical standards, taking into account the integration of practical lessons into the curriculum, the structure and content of practical lessons from an extracurricular perspective, and the rules for recreation and training. Decentralized sports are conceived at the school level, sports are assessed against individual educational goals, and society needs to set rules for the athletic ability to qualify for sports. The essence of teaching practice is to combine with teaching. You can improve your training skills with the help of physical training. Most importantly, you have the opportunity to practice the skills you use, combining foundational theory with acquired skills to hone and improve your teaching skills. In practice, the internal structure should be systematic, comprehensive, and clear. The curriculum structure should include specialized knowledge, instruction, and general reading skills. Pay attention to your knowledge level and learning pattern under the conditions of modern social development, not only in the development of mathematical and legal skills and the gradual development of skills and knowledge but also in the large-scale process of advanced technology and globalization. The subject of physical education has changed many times over time (Figure 2).

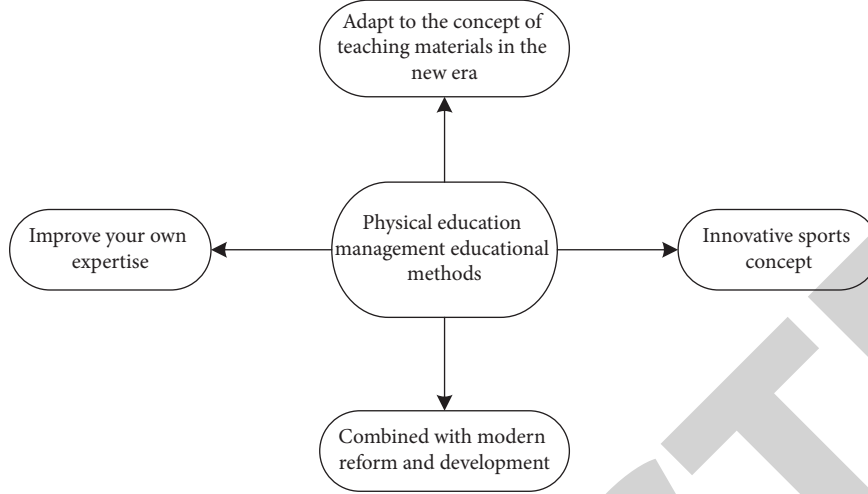


FIGURE 2: Countermeasures for the sustainable development of physical education.

- (1) Continuously improve their professional knowledge and innovate sports concepts
- (2) In combination with modern reform and development, to adapt to the teaching material concept of the new era, establish a more standardized teaching material system for physical education

**2.4. Construction and Implementation of Physical Education Practice Teaching System.** The main body is the physical education teaching ability, organizational creativity ability, health management ability, the ability to guide exercise, and the humanistic quality and behavioral norms of physical education teachers. Excavate the practical teaching content in the curriculum system and consider the construction of the practical teaching system from the perspectives of in-class and extracurricular, in-school and out-of-school, centralized and decentralized. According to the level construction, combined with the laws of physical and mental development, the laws of the formation of sports skills, according to the goals of each talent training, combined with the society's ability needs for physical education professionals; the content of practical teaching is organically divided into in-class practice, concentrated practice, and out-of-school practice. Practice three levels or three aspects to form an organic and unified whole. Through the physical education skill training course, the educational practice ability is cultivated. It mainly cultivates application ability and can combine the basic theory and skills learned to hone and improve teaching skills in teaching practice. The construction of practical course content should be systematic, complete, and hierarchical. The curriculum content system should involve professional knowledge, teaching practice, comprehensive literacy, and other aspects and angles and form a system; pay attention to the level of knowledge, the law of knowledge mastery, the development of sports skills, the law of education and teaching ability mastery, and the knowledge and ability to pass through step by step. Under the background of modern social development, extensive

high-tech technology, and the process of globalization, the physical education profession has undergone great changes with the progress of the times (Figure 3).

The main body is the ability of physical education teaching, organizational creativity, health management, ability to guide exercise, and the humanistic quality and behavioral norms of physical education teachers.

### 3. Multisensor Perception Models

**3.1. Wireless Sensor Network Coverage Model.** It is assumed that each wireless sensor node randomly deployed in the detection area has the same sensing radius. The set of wireless sensor nodes is expressed as, the coordinates of the wireless sensor nodes in this set are expressed as  $(x_i, y_i, z_i)$  detection area midpoint  $p_j$  the coordinates are expressed as  $(x_j, y_j, z_j)$  thus, from the node  $s_i$  to the point  $p_j$  the distance is defined as follows:

$$d(s_i, p_j) = \sqrt{(x_i - x_j)^2 + (y_i - y_j)^2 + (z_i - z_j)^2}. \quad (1)$$

The detection probability of the sensor node  $s_i$  to the target point  $p_j$  is as follows:

$$p(p_j, s_i) = \begin{cases} 1, & d \leq r - r_e, \\ \frac{-\lambda_1 \alpha_1^{\beta_1}}{e \alpha_2^{\beta_2}} + \lambda_2, & r - r_e \leq d \leq r + r_e, \\ 0, & \text{other.} \end{cases} \quad (2)$$

Among them,  $r$  is the detection radius of the sensor node, which is the reliability parameter measured by the wireless sensor node,  $\lambda_1, \lambda_2, \beta_1, \beta_2$  represents the relevant characteristic parameters of the wireless sensor node,  $a_1 = r_e - r + d(s_i, p_j)$ ,  $a_2 = r_e + r - d(s_i, p_j)$ . In order to reduce the computational complexity, the abovementioned formulas (2) and (3) can be simplified as follows:



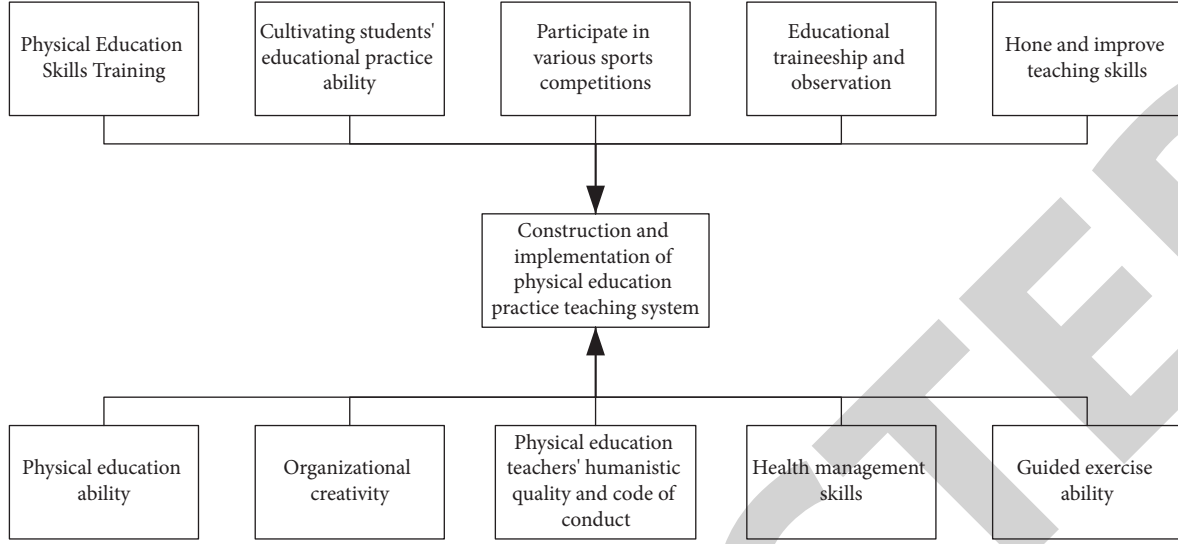


FIGURE 3: Construction and implementation of the physical education practice teaching system.

$$P_{(p,j,s_i)} = \begin{cases} 1, & d(s_i, p_j) \leq r, \\ 0, & \text{other,} \end{cases} \quad (3)$$

The common perception radius of all deployed nodes to point  $p$  in the wireless sensor network model is as follows:

$$p_u(s_{all}, p) = 1 - \prod_{i=1}^n (1 - p_{(p,s_i)}). \quad (4)$$

**3.2. Sensor Perception Model.** The sensing range of each sensor is a circular area with the location of the sensor node as the center and a radius of  $R_s$ , where  $R_s$  is the sensing radius of the node, and its size is determined by the physical characteristics of the node sensing unit. If the event occurs within the sensing radius of the node, the perceived probability is 1; if it occurs outside the sensing radius, the perceived probability is 0.

Using the Boolean perception model, the perception probability of node  $s$  to position  $p(x_p, y_p)$  can be expressed as follows:

$$C_p(s) = \begin{cases} 1, & \text{if } d(s, p) < R_s, \\ 0, & \text{other} \end{cases}, \quad (5)$$

where  $d(s, p)$  is the Euclidean distance between node  $s$  and position  $p$ .

$$d(s, p) = \sqrt{(x_s - x_p)^2 + (y_s - y_p)^2}. \quad (6)$$

**3.3. Wireless Sensor System Model and Problem Description.** In the binary sensing model of wireless sensor networks, the sensing probability  $s_i$  of sensor nodes  $P(x, y)$  to any point\* in the monitoring area  $C_{xy}(s_i)$  can be expressed as a binary function:

$$C_{xy}(s_i) = \begin{cases} 1, & \text{if } d(s_i, p) < r_s, \\ 0, & \text{otherwise,} \end{cases} \quad (7)$$

where  $d(s_i, P)$  represents the Euclidean distance between the monitoring point  $P(x, y)$  and the node  $s_i$ .

However, in practical applications, the sensing ability of sensor nodes is uncertain due to the influence of noise interference and signal strength attenuation with transmission distance. For this, a probabilistic recognition model is used, expressed as follows:

$$C_{xy}(S_i) = e^{-\lambda a^\beta}, \text{ if } r - r_e < d(s_i, P) < r + r_e, \quad (8)$$

where  $r_e = (r_e < r_s)$  represents the fault-tolerant perception radius of the node. If  $\approx 0$ , the binary perception model of formula (7) is used; if  $> 0$ , the probability perception model of formula (8) is used.  $a = d(s_i, P) - (r - r_e)$ ,  $\alpha$  and  $\beta$  represent the attenuation coefficient of the monitoring quality of the sensor node, respectively.

In addition, since each node of the sensor network works independently, any point  $P(x, y)$  in the monitoring area is perceived by the sensor node as an independent event, that is, random events  $C_{xy}(S_i)$  and  $C_{xy}(s_j)$  are independent of each other,  $i, j \in [1, N]$  and  $i \neq j$ , then the probability that the point  $P(x, y)$  is covered by the node set  $S$  is The union of  $C_{xy}(S_i)$ , expressed as follows:

$$\begin{aligned} C_{xy}(S) &= P\left\{\bigcup_{i=1}^N C_{xy}(S_i)\right\} = 1 - P\left\{\bigcap_{i=1}^N \overline{C_{xy}(S_i)}\right\} \\ &= 1 - \prod_{s_i \in S} (1 - C_{xy}(S_i)). \end{aligned} \quad (9)$$

In order to measure the coverage of the wireless sensor network to the entire monitoring area, the threshold of the perception probability of  $P_{th}$  representing the points in the monitoring area  $P(x, y)$  is defined, and the binary function  $P_{xy}(S)$  is defined as



$$P_{xy}(S) = \begin{cases} 1, & \text{if } C_{xy}(S) > P_{th}, \\ 0, & \text{otherwise.} \end{cases} \quad (10)$$

Then the total area size  $P_{XY}(S)$  monitored by all sensor nodes can be obtained as

$$P_{XY}(S) = \sum_x \sum_y P_{xy}(S). \quad (11)$$

In the two-dimensional monitoring area A, the sensor node set  $S = \{s_1, s_2, \dots, s_n\}$ , sin  $k$  node is located in the center of the monitoring area, and a suitable algorithm is needed to select a subset  $C_i$  from the node set  $S$ , so that the network coverage  $P_{XY}(C_i)$  is the largest and the number of working nodes  $|C_i|$  is the least. The problem can be formulated as

$$\text{Max} \begin{cases} f_1(x) = P_{xy}(C_i) \\ f_2(x) = 1 - \frac{|C_i|}{|S|} \end{cases}. \quad (12)$$

In addition, due to the multi-hop communication and many-to-one traffic characteristics of the sensor network, the nodes closer to the sink need not only to complete their own sensing tasks but also forward messages from peripheral nodes. Therefore, this paper considers deploying as many nodes as possible around the sink node in the set of key nodes selected in each cycle. The distribution density of nodes around the sink must be greater than the minimum distribution density threshold, with constraints

$$s.t. \pm \frac{|s_i|s_i \in C_i, d(s_i, \text{sin } k) < r_c}{\pi r_c^2} > \rho_{\min}. \quad (13)$$

**3.4. Sensor Node Perception Model.** The sensing model of the sensor node represents the sensing ability of the sensor node to the surrounding target objects, and the difference in the sensing model directly affects the solution to the coverage problem. The more commonly used node perception model is the binary perception model.

The binary sensing model in the two-dimensional plane is an ideal sensing model that is not affected by the transmission distance. The sensing range is the period, the center of the circle is the sensor node position, and the sensing radius is  $R_s$ . That is to say, the pixels within the sensing radius of the node can be monitored by the node with probability 1, otherwise, the probability is 0. Assuming that point  $P(x, y)$  is any pixel in the plane of the two-dimensional monitoring area, the probability that it is perceived by the sensor node  $s_i(x_i, y_i)$  is as follows:

$$C_p(s_i) = \begin{cases} 1, & d(s_i, P) \leq R_s \\ 0, & \text{other.} \end{cases} \quad (14)$$

Among them,  $d(s_i, p)$  is the Euclidean distance from node  $s_i$  to point  $P$  expressed as

$$d(s_i, p) = \sqrt{(x_i - x)^2 + (y_i - y)^2}. \quad (15)$$

Furthermore, consider the joint probability of pixel point  $P$  being monitored by node set  $S = \{s_1, s_2, \dots, s_N\}$  of  $N$  sensor nodes. First of all, for the convenience of representation, an event  $c_i (i \in [1, N])$  is introduced to indicate that the pixel point  $P$  is within the sensing range of the sensor node  $s_i$  which is as follows:

$$c_i: d(s_i, P) \leq R_s. \quad (16)$$

Use  $P\{c_i\}$  to represent the probability of the event  $c_i$  occurring, that is, the probability that the sensor node  $s_i$  can monitor the pixel point  $P$  which is defined as

$$P\{c_i\} = C_p(s_i) = \begin{cases} 1, & d(s_i, P) \leq R_s, \\ 0, & \text{other.} \end{cases} \quad (17)$$

Let  $\bar{c}_i$  denote the complement of  $c_i$ , that is, the probability that the pixel  $P$  is not detected by the node  $s_i$  but

$$P\{\bar{c}_i\} = 1 - P\{c_i\} = 1 - C_p(s_i). \quad (18)$$

Assuming that each node in the network area monitors any pixel point independently, that is to say, the probability that node  $s_i$  and node  $s_j (j \in 1, N)$  can cover pixel point  $P$  is as follows:

$$P\{c_i \bigcup c_j\} = 1 - P\{\bar{c}_i \bigcap \bar{c}_j\} = 1 - P\{\bar{c}_i\} \cdot P\{\bar{c}_j\}. \quad (19)$$

For the entire node set  $S$  of the network, the probability that a pixel point  $P$  is covered can be expressed as

$$C_p(s) = P\left\{\bigcup_{i=1}^N c_i\right\} = 1 - P\left\{\bigcap_{i=1}^N \bar{c}_i\right\} = 1 - \prod_{i=1}^N (1 - C_p(s_i)), \quad (20)$$

where  $C_p(s_i)$  is the node perception,  $d(s_i, p)$  is the node Euclidean distance, and  $R_s$  is the perception radius.

## 4. Research on Physical Education Teaching Practice Data Based on Multisensor Perception

**4.1. Evaluation and Analysis of Teaching Ability of Physical Education Major.** Based on the teaching characteristics of a physical education major, combined with the literature theory on pedagogy, physical education, and sports core literacy ability indicators, consult experts and scholars in related fields, discuss and exchange opinions in-depth, and design and formulate specific teaching ability evaluation indicators teaching ability. The evaluation indicators include 6 first-level indicators and 23 second-level indicators. The first-level indicators are teaching design, teaching implementation, teaching assistance, technical maintenance, teaching quality evaluation, and reflection and research skills training. Among them, the ability to design learning is divided into formulating learning plans, formulating teaching methods, formulating learning plans, using teaching tools, etc.; learning implementation ability is divided into 9 secondary indicators: student comprehension, presentation of new courses, language expression, review analysis, activity

TABLE 1: Classification of contents of physical education teaching ability.

First-level indicator	Secondary indicators
Instructional design ability	Ability to set lesson plans
	Ability to develop teaching methods
	Ability to write lesson plans
	Applied instructional media competencies
	Learn about student abilities
Teaching implementation ability	Introduce new class capabilities
	Language expression skills
	Examining analytical ability
	Action explanation and demonstration ability
	Technology leadership
Teaching assistance and technical maintenance ability	Classroom management skills
	Exercise organizational skills
	Classroom induction ability
	Technical maintenance capability
	Fixed wrong action ability
Ability to judge teaching quality	Teaching evaluation ability
	Teaching effectiveness evaluation ability
	Teaching method channel application evaluation ability
Teaching reflection skills	Self-reflection skills
	Students' learning effectiveness reflection ability
Teaching and research ability	Teaching innovation ability
	Scientific research application ability
	Information retrieval ability

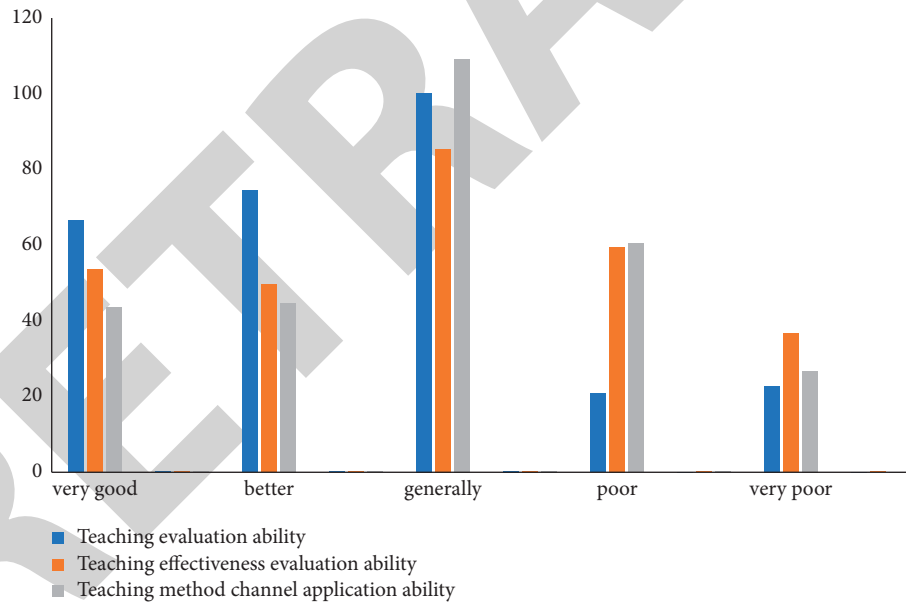


FIGURE 4: Teaching evaluation of physical education students.

report presentation, technical guidance, class management, organizational ability, and classroom implementation ability as shown in Table 1.

Judging from the educational self-evaluation of the secondary index of PE students' educational evaluation ability, 84.6% of PE students have more choices in educational evaluation ability than general options of the total, indicating that the teaching evaluation ability is strong; teaching In the effectiveness evaluation ability, 30% of the total number of people chose the general, indicating that

the students majoring in physical education have average teaching effectiveness evaluation ability. Among the options for the application ability to teach methods and channels, the general, poor, and very poor options accounted for 69% of the total number of people. This shows that physical education students are more vulnerable to weakness in the application of teaching methods (Figure 4).

According to the survey data in the table, it is greatly affected by factors such as teaching hardware conditions,

practice base cooperation, and teacher guidance, and the proportion of selected students is more than 50%, respectively, teaching hardware conditions account for 60%, practice bases account for 80% and teacher guidance accounted for 66.7%; the influence of school curriculum arrangement factors was less than 40%, accounting for 40.0%. From the perspective of teachers, the internal factors that affect the teaching ability of physical education students are far more important than external factors as shown in Figure 5.

A good assessment can motivate students to study a major and help students see the benefits and disadvantages of physical education majors, and improve the study of physical education majors.

Students (84.6%) chose in physical education the general or abovementioned options for their own teaching evaluation ability, indicating that the teaching evaluation ability is strong; in the teaching effect evaluation ability, 30% of the total number of students choose the general evaluation ability, indicating that the teaching of physical education students. The ability to judge the effect is average. Among the options for the application ability of teaching methods and channels, 69% of the total number of people choose the options general, poor, and very poor, indicating physical education students have a poor ability to apply teaching methods and approaches.

**4.2. Research on the Innovation Path of Physical Education and Cultural Communication in Colleges and Universities.** With the continuous development of information technology, information and culture are being accessed in various ways. Colleges and universities are important positions for the development and dissemination of physical education culture. In order to promote the effective dissemination of physical education culture in colleges and universities, under the background of new media, colleges and universities should have various forms, such as extra-curricular sports events, sports training, competitive competitions, and other forms. Innovate ideas, explore channels, and use new media platforms to provide simple, convenient, and diverse communication methods to spread sports culture, so as to deepen students' understanding of sports culture, effectively cultivate students' physical education and cultural literacy, and promote student development. According to the frequency of exposure to different media types in the questionnaire, we calculated the scores, weighted them, and divided them by the total number of samples to obtain the cognitive mean (see Table 2).

The research shows that among the more than 500 cases of students who are exposed to online sports information "almost every day" in the mean data survey, there are three typical ones. Among them, there are 3 typical ones. The highest proportion is mobile phone customers, accounting for 72.67%. Computer networks accounted for 23.33%. And the "almost every day" exposure to cognition means was greater than the other groups (see Table 3).

As can be seen from Table 3, from the perspective of contact time, the average value of sports cognition in the

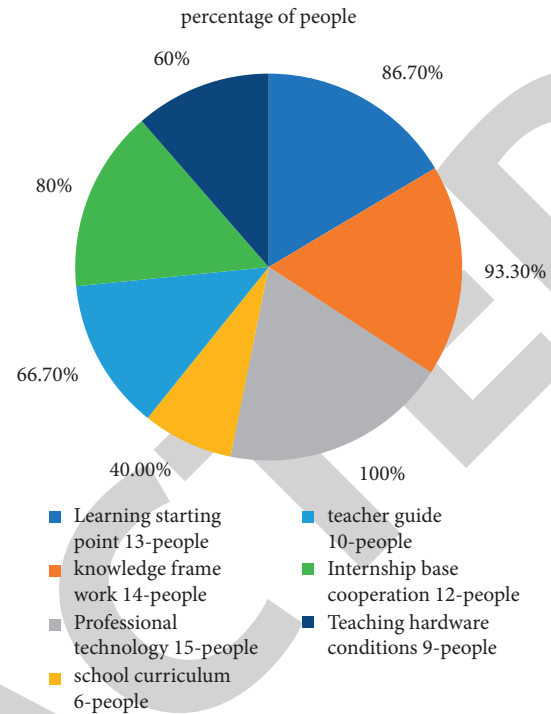


FIGURE 5: Influencing factors of teaching ability of physical education major.

sample population of "more than 3 hours" is greater than that within 0.5 hours, 0.5–1 hours, 1–2 hours, and 2–3 hours. The reason is that college students have more free time in their spare time and objectively have more contact time. With the improvement of contact time, the awareness of physical education has also deepened, and they can better understand the value of physical exercise and understand scientific exercise methods (see Table 4).

Online sports education dissemination can provide a wealth of sports information and sports knowledge, this plays a very obvious role in the understanding of sports education for most college students. Physical education awareness has a stimulating effect.

In the context of the network, the culture of physical education can be disseminated through various means such as three micro terminals, mobile TV, digital magazines and radio, and desktop test windows.

Online sports education communication can provide richer sports knowledge and information and can deepen students' understanding of sports culture, effectively cultivate students' sports cultural literacy, and promote students' all-around development effect.

**4.3. Data Processing Method Based on Kalman Filter.** From Table 5, the data collected by the sensor has a relatively large fluctuation value of around 20, such as the measured value between the third and fourth sampling points, where the difference between the measured values of the two sampling points is about 1.5. It is processed to improve the accuracy of data fusion.

It can be seen from Table 6 that the fluctuation of the data processed by the Kalman filter is relatively small, and the

TABLE 2: Contact frequency and college students' sports cognition scores.

Type	Three micro one end	Mobile TV	Digital magazines & radio	Desktop windows
Almost everyday	15.1	14.92	14.08	14.1
Often (2–3 times/worship)	14.37	13.9	12.33	12.01
Generally (1 time/worship)	12.62	11.38	11	10.21
Not in contact	12.11	10.78	10.75	10.05

TABLE 3: Contact time and college students' sports cognition scores.

Type	Three micro one end	Mobile TV	Digital magazines and radio	Desktop windows
>3 h	13.88	13.44	12.87	12.67
2 h–3 h	13.32	13.1	12.33	12.14
1 h–2 h	12.68	11.45	11.01	10.67
0.5 h–1 h	12.01	10.98	10.87	10.52
<0.5 h	11.21	10.26	9.52	9.47

TABLE 4: Sports communication has a positive effect on sports attitudes.

Frequency	Number of people	Percentage (%)
Strongly disagree	8	1.50
Not agree.	14	2.60
It does not matter	105	19.20
Identify	277	50.70
Very much agree	142	26.00

TABLE 5: Sensor raw data.

Sampling point	Measurements	Sampling point	Measurements
1	19.9	11	19.412
2	19.931	12	20.169
3	20.826	13	19.659
4	19.691	14	20.046
5	20.511	15	20.304
6	20.291	16	19.646
7	19.846	17	19.931
8	19.444	18	20.452
9	19.99	19	19.134
10	20.099	20	20.792

processed data fusion can improve the accuracy of the fusion results.

After the sensor data is processed, the measured value is more consistent with the actual ambient temperature, the data fluctuation range is smaller, and the change in the measured value is better reflected.

The fluctuation of the data processed by the Kalman filter is relatively small, and the processed data can improve the accuracy of the fusion result.

**4.4. Multisensor Sports Data Fusion.** The reform of the boxing professional process has made the competition more substantial and perfect, improved the competition level of athletes, and increased the demand for boxing coaches. The constructed boxing coach model and specific index system clarify the core quality of boxing coaches, deliberately train coaches and effectively improve the overall skill of boxing

TABLE 6: Preprocessed sensor data.

Sampling point	Measurements	Sampling point	Measurements
1	19.92	11	19.876
2	19.902	12	19.928
3	19.997	13	19.88
4	19.959	14	19.91
5	20.037	15	19.981
6	20.076	16	19.92
7	20.041	17	19.922
8	19.941	18	20.018
9	19.95	19	19.858
10	19.976	20	20.027

coaches, which is of great theoretical and practical importance in boxing competition levels. The following are examples of data processing of monitoring data by various sensors, each of which is part of the monitoring data of the laboratory environmental monitoring system, and the obtained laboratory environmental status results are shown in Figure 6. The result values of five types of sensor data fusion at different times are described.

The sample data in the table come from different times, so the representative sample data is selected. Typical sample values of different events are obtained by consulting the performance indicators of the metering equipment and the historical environmental monitoring data of the laboratory, as shown in Figure 7.

First, according to the Hamming distance between different sensor data and typical sample values, the results are shown in Figure 8.

The sum of Hamming distances for all boxing events is then calculated, and the result is shown in Figure 9.

Finally, the basic probability of different sensors for boxing events is calculated, and the results are shown in Table 7.

According to the abovementioned content, the reliability of using a single sensor data is much lower than that after fusing all sensor data, and it is feasible to use sensors to fuse laboratory monitoring data for various boxing items.

By calculating the basic probability of different sensors for boxing events, it can be found that the measurement

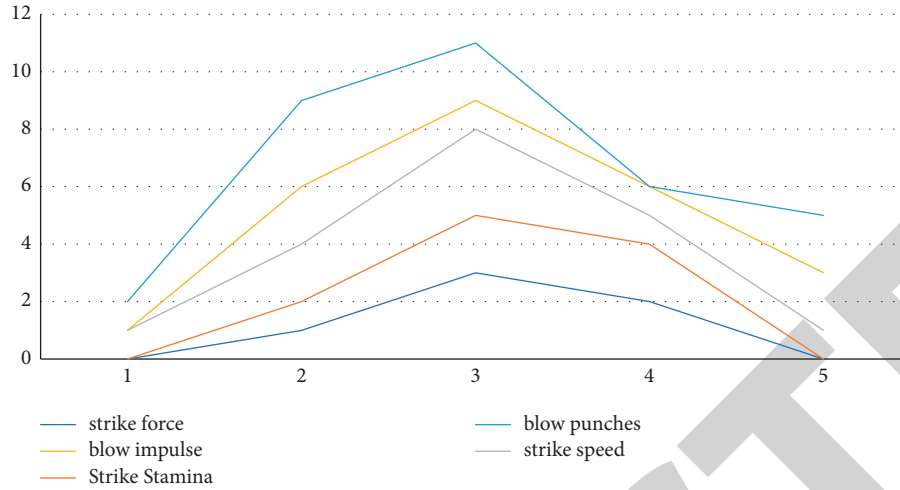


FIGURE 6: Fusion results of laboratory environmental monitoring data.

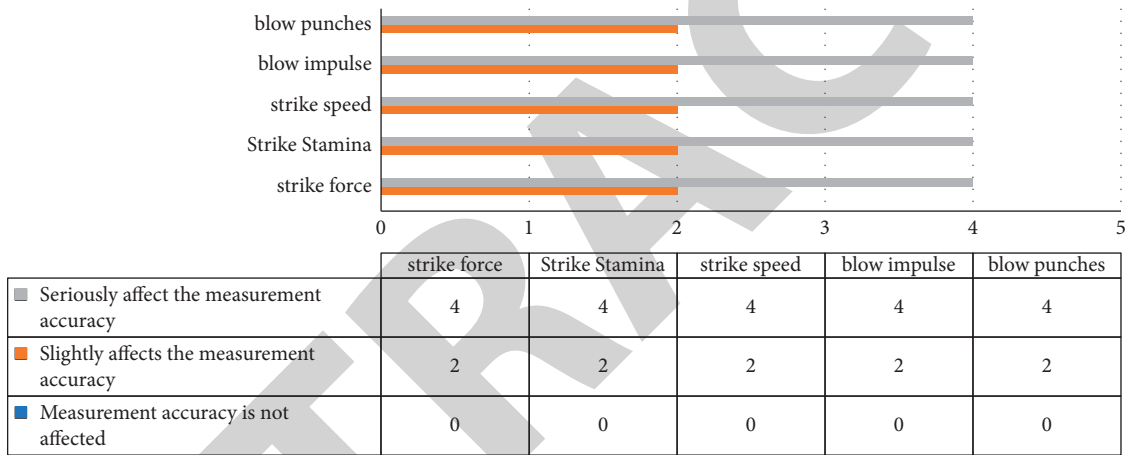


FIGURE 7: Typical sample values for different events.

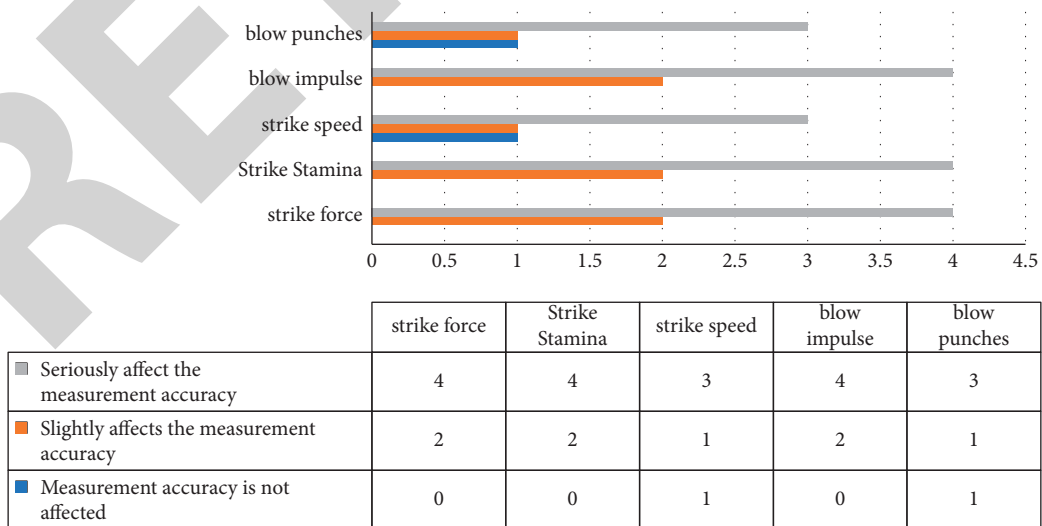


FIGURE 8: Different sensor data and typical samples worth the Hamming distance.

accuracy is not affected by 1/2, the measurement accuracy is slightly affected by 1/3, and the measurement accuracy is severely affected by 1/5. It can be found that the reliability of

single sensor data are much lower than that of fused sensor data. Experiments show that it is feasible to use sensors to fuse various experimental data of boxing.

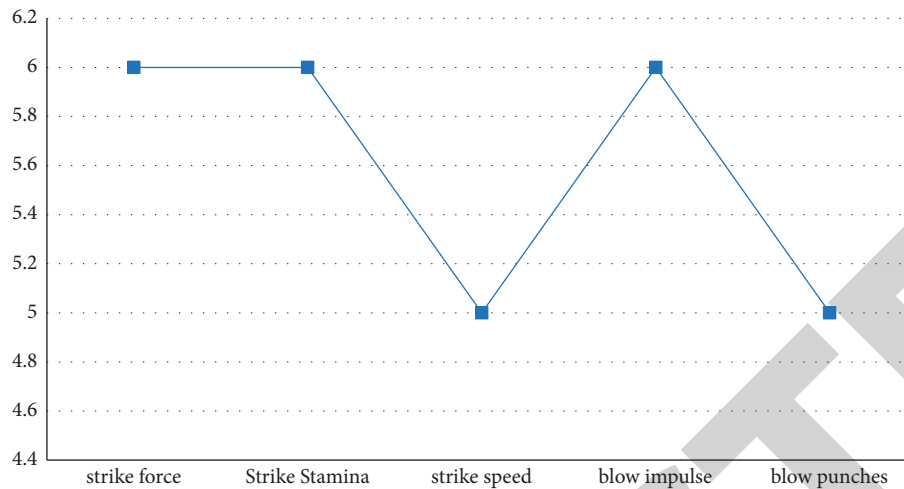


FIGURE 9: Hamming distance and sum of different events.

TABLE 7: Basic probability of events for different sensors.

Event	Strike force	Strike stamina	Strike speed	Blow impulse	Blow punches
Measurement accuracy is not affected	1/2	1/2	1/2	2/5	2/5
Slightly affects the measurement accuracy	1/3	1/3	2/5	1/3	2/5
Seriously affect the measurement accuracy	1/6	1/6	1/5	1/6	1/5

## 5. Conclusion

Chinese universities need to strengthen and improve their ability to educate PE students. At present, the physical education teaching equipment is single, the content of the curricula is outdated, there is no coherent education system, and it only focuses on the form and ignores the actual effect. With the continuous development of physical education, combined with modern reform and development, we will continuously improve our professional knowledge, innovate sports concepts, and adapt to the teaching material concepts of the new era. You can also continuously improve your own knowledge through physical education practice, combine basic theory and skill teaching practice to hone and improve teaching skills, and develop students' practical skills. Against the background of the development of modern society, the wide range of high-tech technology, and the process of globalization, the physical education major has undergone great changes with the progress of the times. It can effectively cultivate students' sports culture through WeChat, QQ, TV, and various communication methods. Literacy contributes to the all-round development of students. Understand the sports culture and make the physical education profession more diversified and standardized so that the development of my country's physical education profession can reach a new level.

## Data Availability

The experimental data used to support the findings of this study are available from the corresponding author upon request.

## Conflicts of Interest

The authors declare that they have no conflicts of interest regarding this work.

## References

- [1] C. J. Savatovich, "Multi-sensory education device," vol. 36, no. 4, pp. 412–430, 2014, US20130157247A1.
- [2] P. Astrom, "Included yet excluded: conditions for inclusive teaching in physical education and health [J]," *Department of Education*, vol. 46, no. 6, pp. 1499–1500, 2013.
- [3] P. Constantinides, "Training and teaching preschool physical education: Building in the sand [J]," in *Proceedings of the 15th National Conference of the physical education teachers association of Northern Greece*, vol. 58, no. 5, pp. 245–250, Thessaloniki, Greece, 2014.
- [4] J. Houston, *Measures of Effective Teaching: National Board Certification and Physical Education Teachers [J]*, Arizona State University, no. 6, pp. 210–217, 2014.
- [5] G. R. Skinner and M. G. Lehman, "Time and work tracker: US," vol. 84, no. 9, pp. 219–230, 1997, US5696702 A.
- [6] S. J. Brock, I. Rovegno, and K. L. Oliver, "The influence of student status on student interactions and experiences during a sport education unit," *Physical Education and Sport Pedagogy*, vol. 14, no. 4, pp. 355–375, 2009.
- [7] C. M. Killian, A. M. Woods, and K. C. Graber, "Factors associated with high school physical education teachers' adoption of a Supplemental online instructional system (iPE) [J]," *Journal of Teaching in Physical Education*, vol. 40, no. 1, pp. 1–10, 2020.
- [8] T. Guterman, "Secondary Physical Education teachers' beliefs on teaching students with disabilities at schools in Puerto

## *Retraction*

# **Retracted: Influence Analysis of Hotel and Tourism Economic Development Based on Computational Intelligence**

### **Security and Communication Networks**

Received 26 December 2023; Accepted 26 December 2023; Published 29 December 2023

Copyright © 2023 Security and Communication Networks. This is an open access article distributed under the Creative Commons Attribution License, which permits unrestricted use, distribution, and reproduction in any medium, provided the original work is properly cited.

This article has been retracted by Hindawi, as publisher, following an investigation undertaken by the publisher [1]. This investigation has uncovered evidence of systematic manipulation of the publication and peer-review process. We cannot, therefore, vouch for the reliability or integrity of this article.

Please note that this notice is intended solely to alert readers that the peer-review process of this article has been compromised.

Wiley and Hindawi regret that the usual quality checks did not identify these issues before publication and have since put additional measures in place to safeguard research integrity.

We wish to credit our Research Integrity and Research Publishing teams and anonymous and named external researchers and research integrity experts for contributing to this investigation.

The corresponding author, as the representative of all authors, has been given the opportunity to register their agreement or disagreement to this retraction. We have kept a record of any response received.

### **References**

- [1] C. Wei, J. Li, and X. Guo, "Influence Analysis of Hotel and Tourism Economic Development Based on Computational Intelligence," *Security and Communication Networks*, vol. 2022, Article ID 7549628, 9 pages, 2022.



## Research Article

# Influence Analysis of Hotel and Tourism Economic Development Based on Computational Intelligence

Canhui Wei <sup>1</sup>, Jiayu Li,<sup>2</sup> and Xiya Guo<sup>1</sup>

<sup>1</sup>School of Culture and Tourism, Luoyang Polytechnic, Luoyang 471000, China

<sup>2</sup>Modern Management School, Zhejiang Industry and Trade Vocational College, Wenzhou 330000, Zhejiang, China

Correspondence should be addressed to Canhui Wei; 202152006@lypt.edu.cn

Received 16 June 2022; Revised 23 August 2022; Accepted 26 August 2022; Published 20 September 2022

Academic Editor: Hangjun Che

Copyright © 2022 Canhui Wei et al. This is an open access article distributed under the Creative Commons Attribution License, which permits unrestricted use, distribution, and reproduction in any medium, provided the original work is properly cited.

As the main infrastructure of the tourism industry, the hotel industry is an important part of the tourism industry and one of the important symbols of the development level of the tourism industry. In recent years, with the prosperity and development of the hotel industry, it can not only effectively solve many social work problems but also contribute to the further development of the region's economy. In this paper, the convergence model and fitness function of the GSO-MCM algorithm are evaluated, and the optimal adaptive threshold of the particle swarm is given. The impact of computational intelligence on the development of hotel and tourism economy is analyzed, and the accuracy of computational intelligence method, data mining method, and fuzzy statistical method are evaluated and compared. The computational intelligence method shows better performance. The domestic tourism revenue is predicted using computational intelligence and compared with the actual value, which shows a good prediction effect. The hotel industry, an important tourism infrastructure, is an important symbol of the level of development of the tourism industry. In recent years, the rise of the hotel industry has not only effectively addressed many of the company's labor problems but also made great contributions to the region's economic growth. With this in mind, we are conducting pilot studies on data collection.

## 1. Introduction

Stochastic optimization and reverse engineering methods, especially modern evolutionary algorithms, are used in various fields because they provide current and future methods and tools to help solve problems. Despite those advantages, all swarm-based search algorithms require excessive CPU time because many candidate solutions are evaluated using expensive computational models. The focus is on reducing the cost of this computation, which makes stochastic optimization efficient and effective. Emphasis is placed on design-dependent methods and the use of alternative or similar models that can replace explicit and costly analysis tools. A literature review of several related methods was conducted following several examples illustrating the benefits of these methods [1]. The model proposed by Denuberg and his colleagues to explain the behavior of ants in their search for water provided an

unexpected inspiration for the success of the ant community. Many of the ACO's artificial ants are in trouble because they use similar circuits as real ants. The ACO supported the snowstorm back. It is hoped that future studies related to the identification of identified diseases will be identified [2]. Image classification is performed in a rule-based manner using the spatial relationships between image regions. In the specific case where image regions correspond to semantically interpretable objects, rules provide a way to demonstrate classification in a way that is familiar to humans. In the work presented here, both bottom-up and top-down information are combined to detect the instances of specific object classes. A rule-based system acts as a model for the configuration of the object space. Experimental results in the motion domain show that despite inaccurate object detection, the spatial relationship allows to effectively distinguish visually similar image categories [3]. Predicting the future based on

collected historical data is a skill that is developed in, among other things, financial planning. Performing time series analysis in the online environment of most industries has been problematic because of computer time and effort. Solutions can be found with modern computer tools, such as neural networks and genetic algorithms. Intelligent calculations that predict the time series of the energy consumption of individual and collective intelligent technologies are made in the chapter. The examples of systems and processes sensitive to each technology are reviewed in detail for quality improvement, model development, and proactive management, selecting appropriate tools and available tools [4]. Comparative mathematics is a set of expressive mathematical constructs that discuss higher-level mathematical objects other than the numbers and introduce the fields of reference mathematics and architecture for dealing with cognitively occurring complex mathematical objects. Computer science, computer intelligence, and software engineering describe vast amounts of information. Three reference algebra models are provided: conceptual algebra, system algebra, and real-time process algebra (RTPA). They describe the application of contextual mathematics to cognitive informatics and computer intelligence. Several case studies demonstrate how to model architectures and cases of iterative and recursive systems using conceptual RTPA constructive algebra and offline machine learning [5]. Cooperation issues arise when working in the economy. Firstly, it assesses the impact of basic equipment and pricing requirements on packages. They then developed a series of Stackelberg games to analyze the collaboration in a decentralized state and found that hotel guests earned more from packages than travel agents because of their higher bargaining power. Finally, volume reduction contracts based on revenue sharing are designed to work together to achieve full compliance. In this contract, the total income from loneliness is equal to the income in the middle scenario [6]. Budget hotels emerged in China in the late 1990s, however, the segment grew as fast as it did in 2003, despite the overall downturn in the Chinese hotel market. The rapid growth and strong competitiveness of the economic sector have since become the focus of attention in the hotel industry with the greatest market potential. Because of the initial development stage of China's budget hotels, most China studies can be described as descriptive, and they attempt to capture the best practices of the time. So far, there are few quantitative studies on the demand structure and pattern and product design of China's budget hotels, and further research on marketing strategies is necessary [7]. In terms of GDP, the tourism sector in Turkey generally belongs to the secondary service sector. Especially in the service sector, its share is gradually increasing. From the perspective of world trade in services, the contribution of almost 30% of trade in services to the national economy is undeniable. Given its importance in the economy, the bank offers reasonable prices, conditions, and options for restrictions on the development of tourism and other businesses. The bank has also launched a new lending assistance program to meet the needs of the sector [8]. With the rise of the mass leisure

tourism market, hotels in the resort area have been divided into two categories, namely star-rated hotels and budget hotels. In recent years, economy hotels have achieved rapid development by virtue of their location advantages in resort areas. The development of economic hotels lies in diversified competition strategies and innovative business concepts, highlighting local cultural characteristics, combining local culture, developing markets through multiple channels, and providing personalized hotel products and services [9]. Tourism is considered to be the most important industry in the 21<sup>st</sup> century because it contributes to the economic growth and development of the country. These impacts are directly and indirectly related to income and employment, reducing the balance of payment barriers, improving knowledge and transfer, and promoting foreign direct investment. Regional tourism leaks and poor relations with the local and national economies were not included in the report [10]. During the period of reform and opening up, the country's tourism industry developed rapidly with the vigorous development of the national economy. Although it started late, it has become one of the most important pillars of the national economy. Since the implementation of the new tourism law on October 1, 2013, tourism has once again become the focus of social attention. Therefore, it is of practical significance to analyze and study the influencing factors of the tourism market and explain the market changes caused by the new tourism law [11]. According to the status of the national economy in the global market, the tourism development indicators of various countries are analyzed. The question of the impact of international tourism on the national economy has been studied, both in terms of method and practical implementation, pointing out the main challenges of branch operations today [12]. The tourism industry in Qinghai Province has developed rapidly, and the influence of tourism on the local economy has been increasing, however, the scale of tourism is still small. This paper analyzes the contribution of tourism to GDP, tertiary industry, foreign exchange income capacity, tourism income dependence, and employment contribution. Through the statistical analysis of relevant data, the research conclusions are drawn, and policy recommendations to promote the further development of Qinghai's tourism industry are put forward [13]. Tourism has become one of the most popular forms of entertainment. Festival tourism projects with local cultural characteristics are very popular with tourists. Festival tourism has distinct local cultural characteristics, which can make more rational use of urban resources, promote economic development, and cultural progress, and promote the rise of tourism and the improvement of residents' living standards [14]. In a dynamic and competitive environment, tourism in each country must grow sustainably, create significant economic benefits for key stakeholders, and minimize negative environmental impacts. As a result, significant dynamics of the current tourism industry are making tourism destinations very competitive, and long-term success depends on the sustainability strategy adopted and implemented by the governing body. Conservation and management of natural

resources require long-term investment. Find ways to reduce population growth without restrictions and make decisions that harmonize the environment and the national economy [15].

## 2. Research on Hotel and Tourism Economy

*2.1. Analysis of the Current Situation of Hotel Industry Development.* With the rapid development of China's economy and the increase in the number of tourists, budget hotels, such as Yangtze River, Zhongjiang Tourism, Home Inn, Motel, GreenTree Inn, and Zhongzhou Express, are emerging. In terms of management level or hotel scale, there is still a big gap compared with the domestic first-line economic hotel brands.

*2.1.1. Under the Influence of Internal and External Factors, the Economy Hotel Industry Has Grown Rapidly.* With the deepening of the economic crisis, domestic budget hotels represented by Home Inn, Xinjiang Inn, and Seven Days took over the business, hoping to alleviate the impact of the financial crisis. Of course, the economic crisis has made travel customers more flexible in terms of demand and more price-sensitive. In addition, the share of budget hotels continues to grow as companies cut budgets in times of crisis.

*2.1.2. The Layout of Budget Hotels Is Mainly Concentrated in Hot Cities and Regions.* Generally speaking, in the case of disproportionate regional economic development, the economic development of hotels in the region is bound to appear unequal. In terms of the development of economy hotels in Hainan, developed regions, such as Haikou and Sanya, took the lead in developing economy hotels and gradually built an international tourist island in Hainan. The regional diversity has been reduced, and economy hotels still exist throughout the island.

*2.1.3. Economy Hotels Are More Respected by the Capital Market.* Due to the welfare impact brought by the listing of Jinjiang Star, Home Express Hotel and 7-day Inn, the sustainable development of the economy and the improvement of the investment environment have had a positive impact on the growth of the hotel industry. With expectations for the location of the renminbi and rising housing prices, the restaurant industry's economy has gained a lot of passive capital. The domestic budget hotel brand Longquan Star also plans to open a number of new budget hotels in the next few years, continuing to promote popular budget hotels. The development status of the hotel is shown in Figure 1.

*2.2. Research on the Relationship between Hotel Management and Economic Coordinated Development.* Because of the prosperity and development of the hotel industry in recent years, it can not only effectively solve many employment problems in the society but also contribute to the further

development of the region's economy. The main factors that affect the quality and profitability of the hotel industry should be the comfort of rooms, dining, and related travel, which are necessary for the long-term stable development of the hotel, and therefore, for the development of the hotel industry and economy of the area.

*2.2.1. The Prosperity of the Hotel Industry Can Effectively Stimulate the Growth of the Regional Economy.* The strong demand of the public for the hotel industry has increased and improved with the development of the industry, becoming the first choice for travelers. For some tourist cities, the hotel's economic resources can fully guarantee the sustainable development of the regional economy. The main source of income is the housekeeping department and catering.

*2.2.2. The Steady Development of Hotels Is the Product of Economic Development.* Economic development follows the principle of progressive prosperity theory. Hence, only sustainable economic development can ensure the prosperity of the hotel industry, especially for some cities that rely on the development of tourism. Hence, the development of hotel management has become more stringent. Hotels are built on the basis of economic sustainability. It is also an important industry that can be stabilized.

*2.2.3. The Sustainable Development of the Economy Also Lays the Foundation for the Sustainable Development of the Hotel Business.* Social reforms have brought about significant changes in regional economic growth, and relevant ministries have also formulated appropriate development plans for this purpose. The hospitality industry is also booming with the help of various ministries. With the advent of the new era, the types of hotels have become more diversified, which has effectively improved the service quality and related supporting facilities of the hotel. At the same time, it has improved the comfort and satisfaction of the residents to a certain extent, laying a foundation.

*2.3. The Role of Hotel Management in Economic Development.* The hotel service part is not included in the export trade sector, however, the added value of hotels is higher than other export trade products. Hence, one of the main sources of external income is service trade. Through the management of foreign tourists, hotels can effectively make tourists stay, eat, shop, and consume in tourist cities, thus making a lot of money and ensuring the country's income and expenditure in international trade and economy. Therefore, today's hotels are an efficient economic source for tourism and an important source of foreign exchange. Business people are one of the main customer sources of the hotel, and the hotel is an important place for business people. From a macroeconomic point of view, the more international cities and well-known hotels, the more transactions. In this period of rapid and healthy development of the market economy, hotels have become very important meeting places. Most of

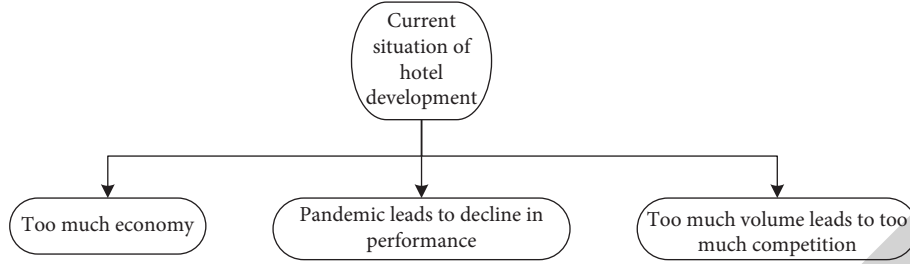


FIGURE 1: Current status of hotel development.

the transactions with a relatively large volume in a region are carried out through mutual exchanges in business hotels. It can also be said that the construction of the hotel has built a huge business platform for people. The role of hotel management on economic development is shown in Figure 2.

### 3. Computational Intelligence Algorithms

**3.1. GSO-MCM Algorithm.** (1) Deployment (initialization) of Firefly. (2) Fluorescein renewal stage. (3) Movement probability calculation stage. (4) Position change stage. (5) The field scope update stage. (6) Calculate the result through the formula.

To build a multicast tree subject to various constraints, it is necessary to invest the minimum cost and obtain a certain quality of service. There are multiple parameters and paths under multiple constraints in the network model, so that the multicast tree generation algorithm may generate a multicast routing tree for multiple QoS metrics. Firstly, the multicast tree is encoded as individuals in the search space of the GSO algorithm. The availability of encoding and decoding must be considered here. The purpose is to avoid loops in the multicast tree. A typical naming convention for an  $X$  multicast tree is as follows:

$$X = (\text{Prior}_1, \text{Prior}_2, \dots, \text{Prior}_3). \quad (1)$$

$X$  is a polynomial tree, and a priori nodes not included in the nodes of the polynomial tree are sequentially represented by "0." The previous node of the original node is itself. In the traditional GSO algorithm, firefly  $i$  moves to firefly  $j$  according to the following equation.

In the formula,  $X$  is a multicast tree, and the a priori nodes that do not belong to the multicast tree nodes are uniformly represented by "0." The prior node of the source node is itself. In the traditional GSO algorithm, the movement of firefly  $i$  to firefly  $j$  is done according to the following formula:

$$X_i(t+1) = X_i(t) + s^* \left( \frac{X_j(t) - X_i(t)}{|X_j(t) - X_i(t)|} \right). \quad (2)$$

In the formula,  $I$  represents the person who will move the position,  $j$  represents the person with a large number of fluorescein selected by probability, such as the topic  $I$  processed in a chronological order, and  $s$  represents the move step size of the multicast QoS tree, which is below some limit. During development, we will modify formula (1)

to match the formation of the mixed tree. In GSO-MCM, the motion of fire  $i$  to fire  $j$  is as follows:

$$X_i(t+1) = X_i(t) \oplus X_j(t). \quad (3)$$

The digestive process may include cycles. To avoid these loops, the newly created multicast tree must be re-encoded using the multicast tree encoding method proposed above. As for the dynamic decision range, the result is more accurate because the dynamic decision range is fixed in the multicast tree.

Loops may occur during the merge process. To eliminate these vulnerabilities, the codec multiplication method proposed above requires the re-encoding of the newly constructed data. Dynamic decision regions are mapped to multiclass trees. Therefore, GSO-MCM does not need to be updated. Furthermore, the unit of measure for GSO-MCM is the similarity between individuals in the polydisperse tree, not the common distance. Similarity is defined as the same number of previous nodes between individuals in a multi-diffusion tree. Typically, the size is set to half the raster width area.

$$N_I(t) = \{j: \text{same}(X_j(t)), X_i(t) > r_x\}. \quad (4)$$

The aggregation rate and the value of mixed wood were used as evaluation criteria. The speed of merging has two parts: the time of merging and the probability of merging. The formula for calculating the mixed cost is as follows:

$$\cos t(T(S, M)) = \omega_1^T \times \frac{PLR(T(S, M))}{\text{average}(PLRT(S, M))}. \quad (5)$$

In experiments and practical tests, the value of fluorescein is inversely proportional to the value of the price function, calculated as follows:

$$l_i = \frac{1}{\cos t(t)}. \quad (6)$$

For a continuous system, the differential equation describing the system can be expressed as follows:

$$\frac{dx}{dt} = x(t) = \Phi[x(t), u(t)], t \in R^+. \quad (7)$$

The corresponding systems are  $n$ -order,  $p$ -input, and  $m$ -output systems, which are, respectively, defined by the following equations:

$$\Phi: R^n \times R^p \longrightarrow R^n \varphi: R^n \longrightarrow R^m. \quad (8)$$

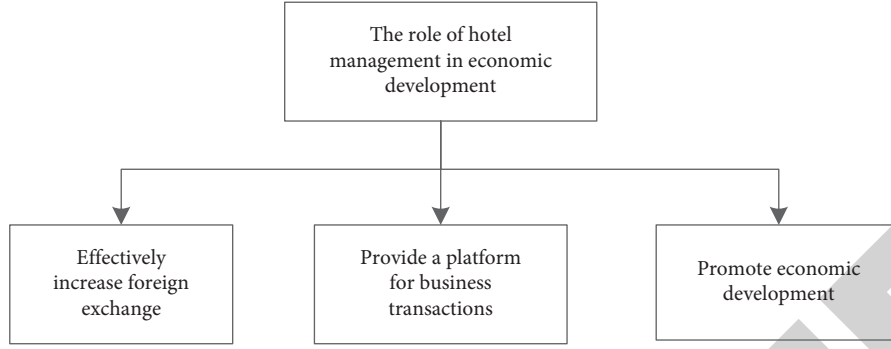


FIGURE 2: The role of hotel management in economic development.

For discrete systems, the description system can be represented by the difference equation, which is as follows:

$$\{x(k+1) = \Phi[x(t), u(t)], \quad (9)$$

where  $x(\cdot)$ ,  $u(\cdot)$ ,  $y(\cdot)$  represent the state sequence, input sequence, and output sequence of the system, respectively, and let  $u(k)$  be a uniformly bounded function. For the nonlinear system described by the formula,  $y(k)$  can establish a set of nonlinear differential equations.

$$y(k) = \Psi[x(k)]. \quad (10)$$

But solving this set of differential equations is difficult. Because of its unique properties, neural networks can be used as recognition models to identify nonlinear systems.

**3.2. Convergence Factor Model.** The particle swarm optimization algorithm originated from the modeling of social systems, and it was only in the last few years that attempts have been made to establish a mathematical foundation for the algorithm itself. So far, Clare (1999) has not demonstrated that the use of limiting factors can be applied to algorithms. PSO Clerc Demo: the mathematical algorithm analysis verifies the convergence factor model shown below.

$$k = \frac{2}{2 - \omega - \sqrt{\omega^2 - 4\omega}}, \omega = c_1 + c_2, \omega > 4, \quad (11)$$

$$x_m^{k+1} = x_m^k + v_m^k. \quad (12)$$

In early experiments and applications of the algorithm,  $v_{\max}$  was set to a maximum value, say 100,000, since the parameters were considered trivial when using the convergence coefficient model. Subsequent studies have shown the constraints of  $v_{\max}$ . The PSO algorithm is an excellent tool for minimizing numerical functions. Kennedy and Abethart (1997) extended this and introduced the discrete binary algorithm PSO. Clerc (2002) summarizes this work by examining a discrete version of the PSO algorithm and applying this work to the traveling salesman problem (TSP) with good results. The main difference between the Discrete Binary PSO algorithm and the original PSO algorithm is the difference in the equations of motion. The equation of motion for the discrete binary algorithm PSO is as follows:

$$v_m^{k+1} = v_m^k + c_1 \cdot r_1 \cdot (p_m^k - x_m^k) + c_2 \cdot r_2 \cdot (p_m^k - x_m^k), \quad (13)$$

$$\text{then } x_m^{k+1} = 1; \text{ else } x_m^{k+1} = 0. \quad (14)$$

The discrete PSO algorithm extends the capabilities of the basic PSO algorithm, especially in the class of combinatorial optimization problems.

**3.3. Fitness Function.** The choice of the fitness function directly affects the integration speed of the genetic algorithm and whether it will find the best solution, since, in general, the genetic algorithm does not use external information to search for evolution but only uses the fitness function correction. Since the complexity of fitness functions is an important element of the complexity of genetic algorithms, the development of fitness functions should be as simple as possible to reduce computational time complexity.

The fitness function is selected using the squared error measure for fitness evaluation.

$$f_k = \frac{1}{E_K} = \frac{P}{\sum_{i=k-p+1}^K (y_d(i) - y(i))^2}. \quad (15)$$

Adaptability is the key to guiding the search. To avoid early encounters and guarantee the diversity of people in the group, fitness must be adjusted linearly. Consider the above two conditions that must be satisfied in the linear fitness transformation process.

$$F' = aF + \beta. \quad (16)$$

In the formula, the dimension of  $F$  is equal to the number of individuals in the group, which can be calculated.

$$a = \frac{(c_{\text{mult}} - 1)f_{\text{ave}}}{f_{\text{max}} - f_{\text{ave}}}, \beta = \frac{(f_{\text{max}} - c_{\text{mult}}f_{\text{ave}})f_{\text{ave}}}{f_{\text{max}} - f_{\text{ave}}}. \quad (17)$$

Linear transformation bridges the gap between initial fitness and maintaining population diversity. The  $\alpha$  and  $\beta$  coefficients vary linearly.

$$(c_{\text{mult}} - 1)f_{\min} + f_{\text{max}} - c_{\text{mult}}f_{\text{ave}} < 0. \quad (18)$$

The obtained minimum value  $f_{\min} < 0$  of the adjusted fitness, at this time, needs to be adjusted. Find the following:



$$a = \frac{f_{ave}}{f_{ave} - f_{min}}, \beta = \frac{-f_{min}f_{ave}}{f_{ave} - f_{min}}. \quad (19)$$

It is an evolutionary computing technology based on the swarm intelligence method. It has given a general introduction to the PSO algorithm and given the particle update equation.

$$V_i(k+1) = wV_i(k) + c_1r_1(p_i - x_i(k)), \quad (20)$$

$$X_i(k+1) = X_i(k) + V_i(k+1)\Delta t. \quad (21)$$

It is easy to see from the equation that as the basic particle clustering algorithm repeats, more particles approach the good particles in the swarm, lose momentum, and become less active. They are reactivated and redefined as follows:

$$f = \frac{1}{n} \sum_{i=1}^n f_i, \sigma_f^2 = \frac{1}{n} \sum_{i=1}^n (f_i - f)^2, \quad (22)$$

where  $f$  is the fitness of the  $i^{\text{th}}$  particle,  $n$  is the particle swarm size,  $f$  is the average fitness of all particles, and  $\sigma_f^2$  is the variance of fitness reflects the degree of convergence of the population. The definition is as follows:

$$\tau^2 = \frac{\sigma_f^2}{\max\{(f_i - f)^2, (j = 1, 2, \dots, n)\}}. \quad (23)$$

A particle swarm system is considered immature if  $\tau^2$  is smaller than a specified lower threshold and no theoretical optimal solution or expected optimal solution to the problem has been found at present, which is the definition necessary to introduce passive particles and alienate them to some extent.

$$\frac{f_g - f_i}{\max\{(f_i - f)^2, (j = 1, 2, \dots, n)\}} \leq \theta. \quad (24)$$

The assumption is that a lower threshold is the fitness of the optimal particle. It is reactivated by applying random Gaussian interference to a specific part of particle  $i$  that satisfies the inequality.

#### 4. Analysis of the Impact of Hotel and Tourism Economic Development under Computational Intelligence

**4.1. Research on Hotel and Tourism Economy under Computational Intelligence.** In the data of hotel and tourism economy under intelligent computing, we can clearly see the economic development status of hotel and tourism industry. The evaluation accuracy of the algorithm using computational intelligence is higher, and the experiment has also carried out the confidence of other methods. The comparison results are shown in Figure 3 and Table 1.

Based on the experimental data in Figure 3, we can see that the computing intelligence computational accuracy is the highest of the three methods when the number of iterations is 50. Estimation accuracy can be 80, and the statistics are incorrect.

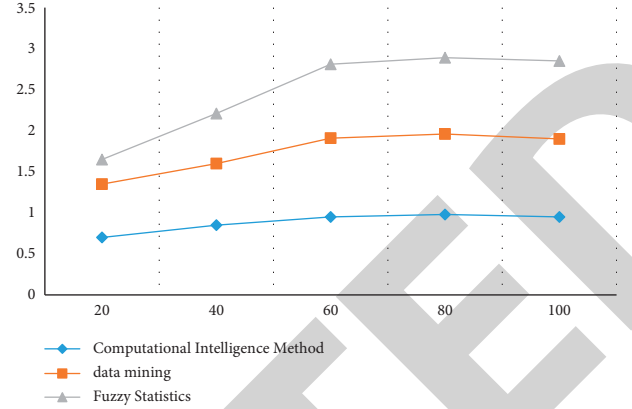


FIGURE 3: Evaluation accuracy comparison test chart.

TABLE 1: Evaluation accuracy comparison.

Number of iterations	20	40	60	80	100
Computational intelligence method	0.7	0.85	0.95	0.98	0.95
Data mining	0.65	0.75	0.96	0.98	0.95
Fuzzy statistics	0.3	0.61	0.9	0.93	0.95

Based on the data from Figure 4 and Table 2, it can be concluded that the proposed calculation algorithm model, after being carried out on a test set, can achieve an accuracy rate of 98.36% and a satisfaction level of 92.46%. What is the type with the highest indicator value among the three algorithms. The accuracy of the imprecise statistical method is 75.14%, which is the lower of the four systems, and the mining model is midtable. From the curves of these two algorithms, we can also see that the curvature of the computational intelligence score of the model is veryD stable and is on the 0.9 level. The price curve is very steep. In addition, the experimental results also show that the performance of the computational intelligence algorithm is optimal.

**4.2. Research on Hotel and Tourism Economy under Computational Intelligence.** Tourism is based on tourism resources. It provides tourism services and engages in tourism and tourism social activities. As the main tourism infrastructure, the hotel industry is an important part of tourism and an important symbol of tourism development. In recent years, because of the continuous improvement of people's living standards, tourism has become an important form of public leisure and entertainment. Domestic tourism has also developed rapidly. The forecast and actual value of domestic tourism revenue from 2017 to 2022 are shown in Figure 5 and Table 3.

The experimental data of Figure 5 shows that with increasing time, the domestic tourism revenue is increasing, showing a steady upward trend. In 2017, the domestic tourism revenue was only 1,257.9 billion yuan. At that time, we found that domestic tourism revenue rose to 3,419.4 billion yuan. It can be seen that the domestic tourism revenue is showing a steady upward trend. The error value of domestic tourism revenue using computational intelligence also showed first a trend of rising and then falling.



FIGURE 4: The performance of each algorithm on the test set.

TABLE 2: The performance of each algorithm on the test set.

Algorithm	Satisfaction	Accuracy	Error rate
Computational intelligence method	92.46%	98.36%	9.68%
Data mining	85.45%	81.28%	14.79%
Fuzzy statistics	75.14%	73.58%	19.68%

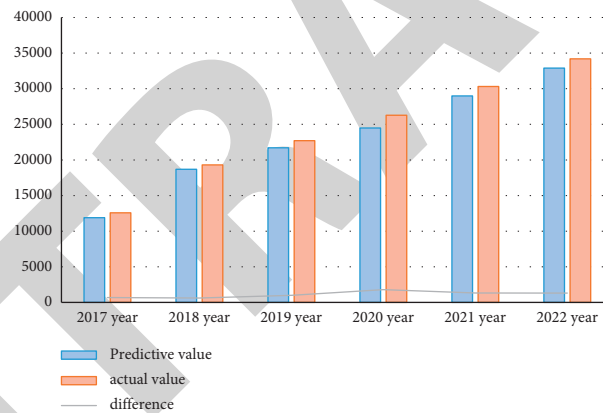


FIGURE 5: Comparison of domestic tourism revenue from 2017–2022.

TABLE 3: Forecast and actual value of domestic tourism revenue from 2017–2022.

Data mining	2017 year	2018 year	2019 year	2020 year	2021 year	2022 year
Predictive value	11893	18689	21706	24484	28988	32893
Actual value	12579	19305	22706	26276	30312	34194
Difference	683	616	1000	1792	1324	1301

The experimental data in Figure 6 shows that the largest share of revenue from tourism is accommodation payments, accounting for 52%, followed by the scenic spot ticket fee, accounting for 18%, and finally the bus fee, accounting for 15%. The hotel industry is an important part of the tourism industry and one of the most important symbols of the level of development of the tourism industry. The increase in hotel revenue is in line with the increase in tourism revenue.

**4.3. Analysis of the Impact of Tourism Economic Development.** Tourism is an important part of the service industry and plays an important role in providing employment opportunities and solving employment problems. The employment advantage of tourism relative to other industries can provide other employment opportunities. The higher the employment rate, the lower the employment threshold. The tourism industry has many levels of work. On the one hand, it needs quality management and technical talents, and on



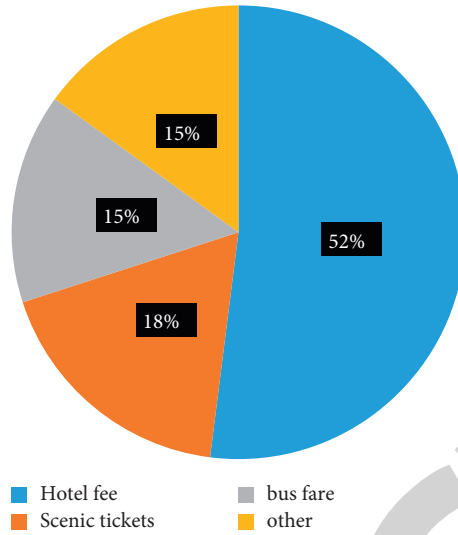


FIGURE 6: The proportion of tourism revenue.

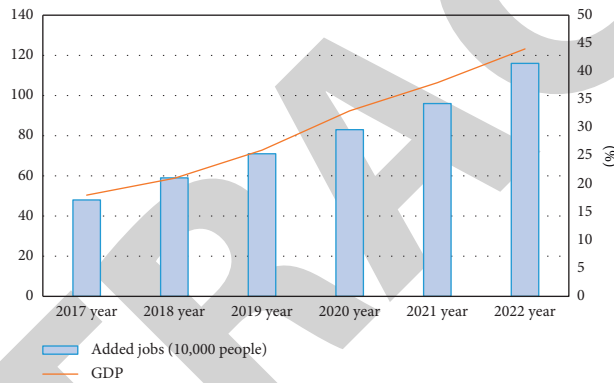


FIGURE 7: The jobs created by the tourism industry and their proportions.

TABLE 4: Jobs created by tourism and its proportion.

years	2017 year	2018 year	2019 year	2020 year	2021 year	2022 year
Added jobs	48	59	71	83	96	116
GDP	18%	21%	26%	33%	38%	44%

the other hand, it needs many jobs, especially in tourism, transportation, catering, and tourism commodities. Positions in tourist attractions, with low educational requirements and low age requirements, are helpful to young people without technical knowledge. The jobs created by tourism and its share of GDP are shown in Figure 7 and Table 4.

Through the data in Figure 7, we can see from 2010 to 2015 that the number of jobs added by the tourism industry has been increasing steadily, and the number of jobs added has also increased from 480,000 in 2017 to 1.16 million in 2022, and the proportion of tourism revenue in GDP is also rising steadily. We can also see that tourism revenue is also rising. The proportion of GDP is also increasing.

According to the data in Figure 8, we can see that with the continuous improvement of people's living standards, tourism has become an important way of public leisure and entertainment, and domestic tourism has also developed

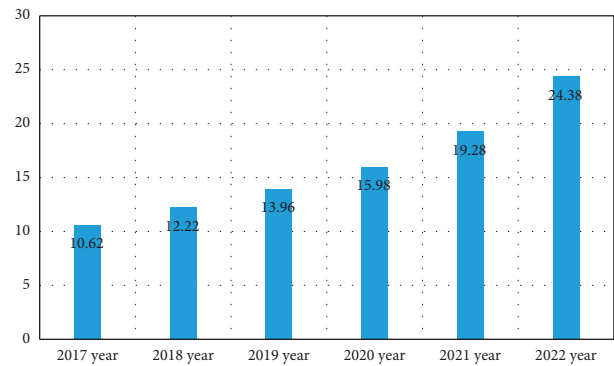


FIGURE 8: Number of tourist receptions in 2017–2022.

rapidly, showing a steady upward trend from 1.062 billion in 2017 to 2.438 billion in 2022, indicating that the domestic tourism industry has been developing toward a better trend.

## Retraction

# Retracted: Research on the Effective Fusion of Traditional Art and Old Street Culture Construction Based on Fuzzy Algorithm

### Security and Communication Networks

Received 3 October 2023; Accepted 3 October 2023; Published 4 October 2023

Copyright © 2023 Security and Communication Networks. This is an open access article distributed under the Creative Commons Attribution License, which permits unrestricted use, distribution, and reproduction in any medium, provided the original work is properly cited.

This article has been retracted by Hindawi following an investigation undertaken by the publisher [1]. This investigation has uncovered evidence of one or more of the following indicators of systematic manipulation of the publication process:

- (1) Discrepancies in scope
- (2) Discrepancies in the description of the research reported
- (3) Discrepancies between the availability of data and the research described
- (4) Inappropriate citations
- (5) Incoherent, meaningless and/or irrelevant content included in the article
- (6) Peer-review manipulation

The presence of these indicators undermines our confidence in the integrity of the article's content and we cannot, therefore, vouch for its reliability. Please note that this notice is intended solely to alert readers that the content of this article is unreliable. We have not investigated whether authors were aware of or involved in the systematic manipulation of the publication process.

Wiley and Hindawi regrets that the usual quality checks did not identify these issues before publication and have since put additional measures in place to safeguard research integrity.

We wish to credit our own Research Integrity and Research Publishing teams and anonymous and named external researchers and research integrity experts for contributing to this investigation.

The corresponding author, as the representative of all authors, has been given the opportunity to register their agreement or disagreement to this retraction. We have kept a record of any response received.

### References

- [1] M. Gong, "Research on the Effective Fusion of Traditional Art and Old Street Culture Construction Based on Fuzzy Algorithm," *Security and Communication Networks*, vol. 2022, Article ID 9616634, 9 pages, 2022.

## Research Article

# Research on the Effective Fusion of Traditional Art and Old Street Culture Construction Based on Fuzzy Algorithm

Miao Gong 

*School of Art, Xi'an International Studies University, Xi'an 710119, China*

Correspondence should be addressed to Miao Gong; [gongmiao@xisu.edu.cn](mailto:gongmiao@xisu.edu.cn)

Received 14 July 2022; Revised 8 August 2022; Accepted 17 August 2022; Published 19 September 2022

Academic Editor: Hangjun Che

Copyright © 2022 Miao Gong. This is an open access article distributed under the Creative Commons Attribution License, which permits unrestricted use, distribution, and reproduction in any medium, provided the original work is properly cited.

With the rapid development of modern science and technology, people gradually lose the importance of traditional art and old street culture, and it plays a vital role in improving the knowledge and cultural level of the people. This paper aims to effectively integrate traditional art and old street culture construction by studying fuzzy algorithms. In the era of rapid technological development, traditional culture and art must keep pace with the times and combine traditional art and old street culture through more scientific algorithms through fuzzy algorithm to solve the effective integration of traditional art and old street culture in today's society. Based on the fuzzy algorithm and visualization technology, this paper checks the meaning of traditional art and collective research by analyzing the fuzzy algorithm, uses experiments to verify the theory, refines cultural symbols, and proposes activation methods to integrate traditional art and old street culture as a whole. Through the defuzzification algorithm and the hierarchical evaluation fuzzy algorithm, people's subjective evaluation of the integration of traditional art and old street culture is calculated, and the algorithm is optimized from the above aspects, which substantially contributes to the effective integration of traditional art and old street culture. This case study can also provide new ideas for the protection of historical and cultural blocks in many cities and the integration of traditional art, remedy the dying traditional art and old street culture, and bring a glutinous feast to the construction of traditional art and old street culture.

## 1. Introduction

Due to the rapid urban construction in the past 40 years, my country's urban architecture has undergone great changes. Although people's lives have been greatly improved, it is needless to say that we have also paid a lot of traditional art and old street culture. It is quietly dying. At present, the traditional art and the old street culture cannot be better integrated with each other. There are still some problems during the integration period, and the traditional art and the old street culture have not been truly integrated through people's interest. Make full use of modern algorithms to reasonably integrate traditional art and old street culture. Based on the fuzzy algorithm [1–5], this article will integrate traditional art and old street culture and show people a “composite” old street that is in line with the development of modern society and can display traditional art. This article will use the defuzzification algorithm and the hierarchical evaluation fuzzy algorithm to reproduce the traditional art

and old street culture in people's memory and calculate the best method for the reasonable integration of traditional culture and old street construction.

## 2. Deblurring Algorithm for Night Images

When deblurring an image, the role of the blur kernel function is very important. The more accurate the calculation of the blur kernel function algorithm, the better the effect of image deblurring. However, the blur kernel can not only be obtained by calculation but also a mathematical model needs to be established according to the actual situation for calculation. Image blur [6] is roughly divided into three categories, namely defocus blur, Gaussian blur, and motion blur. These three deblurring algorithms also correspond to different types of blur kernel functions, which I will analyze in the following subsections.

### 2.1. Image Blur Type and Blur Kernel Function

#### 2.1.1. Caustics Blur and Corresponding Blur Kernel Function.

Under normal circumstances, the camera can only form a clear image for the image within a certain focal length range, but for the focal length that is thought or not within the focal length range, it cannot form a clear image, and the blurred image in this case becomes defocus blur. The imaging principle can be described as

$$\frac{1}{u} + \frac{1}{v} = \frac{1}{f}, \quad (1)$$

where  $f$  is the focal length of the lens,  $v$  is the image distance, and  $u$  is the object distance. If formula (1) does not hold, the image of the point light source is in the shape of a disk, and its energy will decrease from the center to the periphery. The blur function for caustics blur can also be described as

$$k(x, y) = \begin{cases} \frac{1}{\pi r^2}, & \sqrt{x^2 + y^2} > r, \\ 0, & \sqrt{x^2 + y^2} \leq r, \end{cases} \quad (2)$$

where  $r$  is the lens radius.

There are two optimizations for implementing this operation:

Reduce the image and then perform the convolution operation.

Split the two-dimensional Gaussian convolution into two one-dimensional Gaussian convolution operations (now do convolution horizontally and then do convolution vertically).

The first advantage of reducing the image is to reduce the resolution, so that the image can be better reflected in subsequent operations. The second advantage is set  $f(x, y)$ ,  $f(x)$ , which  $f(y)$  conforms to the standard normal distribution, that is,  $\mu = 0$ ,  $\sigma = 1$ , there are

$$f(x, y) = f(x)f(y). \quad (3)$$

but

$$\begin{aligned} g(x, y) &= \sum_{u=-r}^r \sum_{v=-r}^r s(x+u, y+v) f(u, v), \\ &= \sum_{u=-r}^r \sum_{v=-r}^r s(x+u, y+v) f(u) f(v), \\ &= \sum_{u=-r}^r \sum_{v=-r}^r s(x+u, y+v) f(v) f(u). \end{aligned} \quad (4)$$

It can be seen that the one-dimensional convolution is now performed in the horizontal direction, then the one-dimensional convolution is performed in the vertical direction, and the two-dimensional Gaussian convolution operation can be split. The most generated weights are normalized so that their sum is 1, otherwise the brightness will be reduced.

**2.1.2. Gaussian Blur and Corresponding Blur Kernel Function.** Gaussian blur can also be called Gaussian smoothing. Gaussian blur [7] is generally obtained by

calculating the pixels around each point of the image through the weighted average method [8–11]. Its blur function can be expressed as

$$k(x, y) = \frac{1}{2\pi\sigma^2} \exp\left(-\frac{x^2 + y^2}{2\sigma^2}\right). \quad (5)$$

The above formula is  $\sigma$  the standard deviation of the Gaussian function. The larger the  $\sigma$  value, the larger the radius and the worse the image clarity.

#### 2.1.3. Motion blur and corresponding blur kernel function.

When the environment is dim or the light is insufficient, in order to improve the quality of the image, we generally choose to extend the exposure time. When the exposure time of the image is prolonged, the possibility of motion blur will be greatly increased.

The function expression of motion blur can be expressed as

$$k(x, y) = \begin{cases} \frac{1}{L}, & 0 \leq |x| \leq L \cos \theta, \quad y = x \tan \theta, \\ 0, & \text{other.} \end{cases} \quad (6)$$

The above formula  $(x, y)$  is the position of the pixel,  $\theta$  is the angle between the horizontal and the moving directions, and  $L$  is the distance generated when the image moves. We can thus obtain that when the object moves at a uniform speed and in a straight line, formula (4) can be improved as

$$k(x, y) = \begin{cases} \frac{1}{L}, & 0 \leq |x| \leq L, \\ 0, & \text{other.} \end{cases} \quad (7)$$

Through the above fuzzy algorithm, the traditional art and the old street culture are preserved, and the function is used to conduct induction and integration, integrate the traditional art and the old street construction, and to learn about traditional art and old street culture.

Motion blur, as the name suggests, is the blurring effect produced by objects moving in the scene when the scene is exposed. The effect of real-time computer animation is similar to that of a camera with an infinitely short shutter time, and each (frame) picture is very clear without any motion blur. Compared with simply and rudely increasing the overall frame rate, adding motion blur not only provides an obvious sense of realism and softness to high-speed moving scenes but also avoids the significant power consumption increase brought about by high frame rates.

**2.2. Image Blur Model.** Generally, the common image blur model is the convolution model [12], but the convolution model has certain limitations; its representation can only be uniform blur, while the space-variant model cannot. It is assumed that most regions of the image conform to the convolutional blur model. The expression of the convolutional fuzzy model is

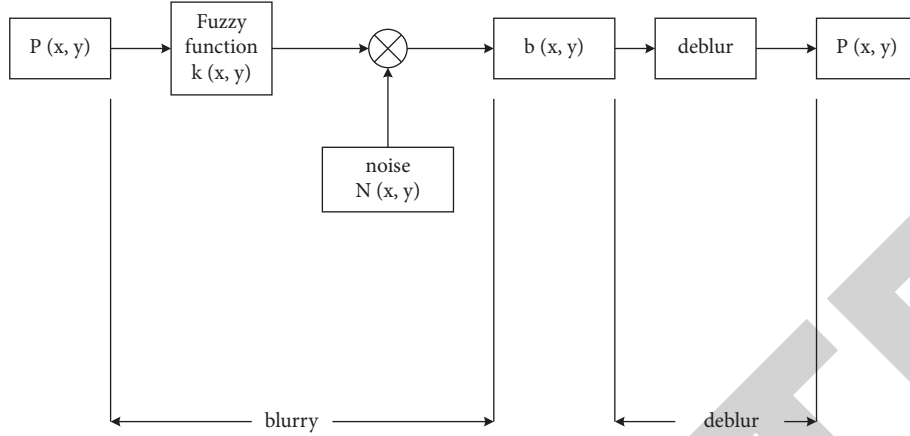


FIGURE 1: Basic flow chart of image blurring and deblurring.

$$b(x, y) = p(x, y) * k(x, y) + n(x, y). \quad (8)$$

The above formula  $b(x, y)$  represents the blurred part after convolution, which  $p(x, y)$  means that a clear blurred image needs to be restored, and the  $k(x, y)$  fuzzy kernel function,  $k(x, y)$  also known as the point spread function [13]. PSF (point spread function),  $n(x, y)$  means noise. Because when we take pictures of the old street, we will be disturbed by different factors, including motion, brightness, and noise of the old street, etc. I can only take a clear picture of the old street after eliminating these factors, and then through the hierarchical fuzzy algorithm, we can understand the types of old street art and traditional culture that people really like, so as to effectively integrate. So that these traditional arts and old street culture can be preserved.

\* represents a convolution operator.

The basic flowchart of image blurring and deblurring is as follows in Figure 1:

The interference of noise is ignored  $k(x, y)$  in the blurred image and the blur kernel function  $b(x, y)$  is assumed to be invariant in space, the above formula can be rewritten as

$$b(x, y) = p(x, y) * k(x, y). \quad (9)$$

By performing a two-dimensional Fourier transform on the formula, the formula in the region can be obtained:

$$B(x, y) = P(x, y)K(x, y). \quad (10)$$

The above expressions are the formula  $B(x, y)$  for the blurred image  $b(x, y)$  in the area and the formula  $P(x, y)$  for the clear image  $p(x, y)$  in the area is  $K(x, y)$ , and the formula of the fuzzy kernel function in the region  $k(x, y)$ . The formula at this time can also be expressed as

$$b(x, y) = p(x, y) * k(x, y) = K[p(x, y)]. \quad (11)$$

Through the above formula, we can save and reserve traditional culture and old street culture in a photographic manner, then push it in the form of data, ctivate the economic strength of historical and cultural blocks through fuzzy kernel function. Awaken people's hearts when they were young.

**2.3. Hierarchical Fuzzy Algorithms.** Since each person has unquantifiable influencing factors on traditional art and old street culture [14], we will express the influencing factors in the form of a set, and the elements are mutually exclusive and do not interfere with each other. Each influencing factor is defined as  $u_i$ , and the influencing factors are composed of each person's artistic and cultural set  $U$ , expressed as

$$U = \{u_i | i = 1, 2, \dots, n\}. \quad (12)$$

Among them,  $n$  is the set of different artistic elements and  $U$  is the set of artistic and cultural factors.

In the set  $U$ , then,  $i \neq ju_i$  with  $u_j$ . The results vary in degree of influence, that is, the degree of influence of traditional art and old street culture is different. Corresponding to each factor in the set  $u_i, i = 1, 2, \dots, nU$ , I assign the value of the influence degree of the response, which is used to reflect  $a_i, i = 1, 2, \dots, n$  the weight of each factor in participating in traditional art and old street culture [15, 16]. The influence degree value constitutes a set  $A$ , which is mathematically expressed as

$$A = \{a_i | i = 1, 2, \dots, n\}. \quad (13)$$

Among them,  $a_i$  the normalization and non-negativity conditions are satisfied, namely,

$$a_1 + a_2 + \dots + a_n = 1, \quad (14)$$

each factor in the set  $U$ , if there is a total number of appraisers  $S_{ij}S$ , the individual evaluation result is  $v_j$ , where  $S = \sum_{j=1}^m S_{ij}, i = 1, 2, \dots, n$ . According to the above, we call the  $u_i$  degree of membership to the evaluation results as  $v_j$

$$r_{ij} = \frac{S_{ij}}{S}; \quad i = 1, 2, \dots, n; j = 1, 2, \dots, m. \quad (15)$$

In this way, we can use the above data to change and integrate the influence factors of each person on traditional art and old street culture, so as to achieve a complex old street art culture that everyone likes.

After the fuzzy model of the image is established, we can consider solving a clear image. However, the fuzzy kernel function  $k(x, y)$  and noise in formula (6)  $n(x, y)$  are unknown, and his solution cannot directly solve the clear image

through convolution operation  $p(x, y)$ . Even if there is a unique solution, it is difficult to control the influence of noise  $n(x, y)$  on the image during the solution process  $p(x, y)$  because  $b(x, y)$  a slight change in the blurred image will have  $p(x, y)$  a great impact on the solution of the clear image.

Combined with the discussion points of this article, the normalization processing point is to start with the set, remove the attributes of the unimportant elements and the elements that are not comparable in the set, and retain the attributes that are helpful to the evaluation behavior. The intention of introducing the weighted average method and the product average method is always the same; the weighted average method and the product average method are  $A_i$  both representations after compounding fuzzy sets. The choice of the two is determined based on the size of the calculation amount.

### 3. Deblurring Algorithm and Hierarchical Blurring Algorithm Optimization for Night Images

The integration of traditional art and old street construction is inseparable from the old-fashioned buildings in the block. We need to optimize it based on the deblurring algorithm to make it represent the time of the block in people's memory and combine the modern society with the style and customs of the old block. How to use the fuzzy algorithm to drive the environment, economy, and history and humanities of the old block is the key to the success of the block and traditional art.

It is assumed that the constrained least squares method is used to restore the old street image. The algorithm is based on smoothness and simplifies the blurring of the image  $p$ . The optimal solution closest to the original image can be obtained  $p'$ . This problem is described by Lagrangian as follows:

$$J(p') = \lambda \left( \|b - Kp'\|^2 - \|n\|^2 \right) + \|Qp'\|^2, \quad (16)$$

where  $\lambda$  is the Lagrange coefficient. A clear image can be obtained by the above formula.

Because the hierarchical fuzzy evaluation algorithm does not involve the measurable discussion of fuzzy sets and the standard fuzzy division of the universe to a certain extent. There is no doubt that 100% of the requirements cannot be met when the core evaluation calculation is completed, and the calculated value deviates from the actual situation, even lower than the subjective evaluation value. Therefore, this section will focus on the measurability of fuzzy sets and the standard fuzzy division of the universe for optimization.

Assuming that there is a universe of discourse  $X$ , there are  $C$  and  $D$  as the fuzzy sets on the universe of discourse, and  $x$  is the element  $x \in X$  in the universe of discourse  $X$  and then define the measurability of fuzzy set  $C$  to fuzzy set  $D$  can be expressed as

$$P = \text{Poss}(D|C) = \sup_{x \in S} \left( C(x) * D(x) \right). \quad (17)$$

Among them  $P \in [0, 1]$ ,  $(*)$  is the operator.

In particular, when  $C$  is a degenerate fuzzy set  $x_0 \in X$  on the universe  $X$ , that is, only at a certain point,  $C(x_0) = 1$ , so there is

$$P = \text{Poss}(D|C) = \sup_{x \in S} \left( C(x) * D(x) \right) = D(x_0). \quad (18)$$

The above completes the relevant elaboration on the measurability of fuzzy sets. Let it be  $P(y)$  the whole fuzzy set on the universe  $Y$ , and  $x$  is the element  $x \in X$  on the universe  $X$ , that is, there is a fuzzy set  $\{A_i | i = 1, 2, \dots, r\}$ ,  $A_i \in P(y)$ , if the set satisfies:

$$\begin{aligned} & \forall i \in I, \text{Poss}(A_i | A_i) \\ & \forall i, j \in I, \max \text{Poss}(A_i | A_j) < 1 \\ & \forall x \in S, \exists i \in I, A_i(x) > 0, \sum_{i=1}^r A_i(x) = 1. \end{aligned} \quad (19)$$

It is called the  $\{A_i | i = 1, 2, \dots, r\}$  standard fuzzy partition of universe  $X$ .

Let the universe  $U = [a, b]$ ,  $a < b$ ,  $\{A_i | i = 1, 2, \dots, r\}$  of discourse be the standard fuzzy partition set of the universe of discourse, and it is stipulated that the center points of each fuzzy partition set are distributed  $[a, b]$  above, namely,

$$\begin{aligned} A_i(x) & \begin{cases} 1 - \frac{1}{d}|x - a - d(i-1)|, & a + d(i-1) \leq x \leq a + d, \\ 0, & \text{other,} \end{cases} \\ A_r(x) & \begin{cases} 1 - \frac{1}{d}|x - b|, & a + d(r-2) \leq x \leq b, \\ 0, & \text{other.} \end{cases} \end{aligned} \quad (20)$$

Among them  $d = b - a / r - 1$ , the standard fuzzy division of the universe of discourse  $U$  and the schematic diagram of the center point are shown in Figure 2.

When solving practical problems, there are fuzzy sets [17] formed by the interaction between influencing factors, and then the overall fuzzy set is constructed to include the subfuzzy sets generated by the interaction. Suppose  $U = U_1 \times U_2 \times \dots \times U_n$ , the judgment condition is

$$A_i = \mu(U_i), i = 1, 2, \dots, n. \quad (21)$$

Among them,  $A$  is composed of  $A_1, A_2, \dots, A_n$  complexes. Due to the uncertain factors in the actual problems, the situations faced are different, and the manifestations of  $A$  are various. The manifestations of  $A$  are mainly classified into two categories, namely, the weighted average method and the product average method.

$\delta_1, \delta_2, \dots, \delta_n$  As a set of weights, the weighted average method expression is

$$\mu_A(u) = \sum_{i=1}^n \delta_i \mu_{A_i}(u_i). \quad (22)$$

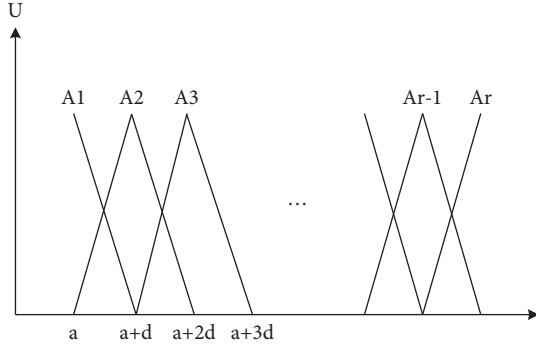


FIGURE 2: The standard fuzzy partition of the universe of discourse  $U = [a, b]$ .

$a_1, a_2, \dots, a_n$  As a set of weights, the product-average method expression is

$$\begin{aligned} \mu_A(u) &= b \left( (\mu_{A_1}(u_1))^{a_1} (\mu_{A_2}(u_2))^{a_2} \dots (\mu_{A_n}(u_n))^{a_n} \right) \\ &= b \prod_{i=1}^n \mu_{A_i}(u_i)^{a_i}. \end{aligned} \quad (23)$$

According to the modified form of  $A$  expression, any product factor of the product-average method changes proportionally and is not allowed to be 0.

Combined with the context, the infinite phenomenon does not exist in the fuzzy comprehensive evaluation model. According to the actual situation, the evaluation factor set in this paper  $a + d(i-1) \leq x \leq a + d$  takes the value of 0 when it is not in the middle, and the formula is:  $a + d(r-2) \leq x \leq b$

$$\begin{aligned} A_i(x) &\begin{cases} 1 - \frac{1}{d}|x - a - d(i-1)|, & a + d(i-1) \leq x \leq a + d, \\ 0, & \text{other,} \end{cases} \\ A_r(x) &\begin{cases} 1 - \frac{1}{d}|x - b|, & a + d(r-2) \leq x \leq b, \\ 0, & \text{other.} \end{cases} \end{aligned} \quad (24)$$

#### 4. Defuzzification Algorithms and Hierarchical Fuzzy Algorithms

Based on the image deblurring method to publicize the scenery of the old street [17–19], the current local government's propaganda of the old street culture is not enough, and it is necessary to increase the publicity live. The fuzzy algorithm will increase the publicity, increase the reputation and popularity of the old street, let more people know about the business opportunities of traditional art and old street culture [20, 21], and let the public participate in it.

**4.1. Column Simulation of Defuzzification Algorithm.** Based on the image deblurring method to publicize the scenery of the old street, the current local government's

propaganda of the old street culture is not enough, and it is necessary to increase the publicity live. The fuzzy algorithm will increase the publicity, increase the reputation and popularity of the old street, let more people know about the business opportunities of traditional art and old street culture [21], and let the public participate in it.

**4.1.1. From the Perspective of the Age of the People, The Simulation of the Fusion of Traditional Art and Old Street Culture.** The public's perspective is mainly reflected in the degree of attention paid to traditional art and old street culture in different age groups. Through the blurring algorithm and the hierarchical blurring algorithm, the people at both ends show a certain subjective thinking and independent income of adulthood, and through the view of the picture, the people based on the image de-blurring algorithm and the hierarchical blurring algorithm are compared to the old street scene. Interested age groups and numbers are shown in Table 1 and visualize its data, as shown in Figure 3.

After visualizing the data, the trend of the deblurring algorithm is roughly in line with the population distribution trend of the hierarchical fuzzy algorithm, and there is authenticity under the statistics. It is inferred in turn that the deblurring algorithm still conforms to the real situation when the subjective consciousness is not unique, so in terms of authenticity, the results given by the algorithm can be used.

**4.1.2. The People's Expectation Perspective Is a Simulation of the Fusion of Traditional Art and Old Street Culture.** The perspective of public expectation is mainly due to the subjective evaluation of the future fusion of traditional art and old street culture [22]. Taking people of different ages as an example, the algorithm-based population classification and expectations are shown in Table 2, and the simulation results are shown in Figure 4.

From the simulation results that the public is seriously lacking confidence in the future of traditional culture. In conclusion, a total of 102 people think that the future of traditional culture is relatively optimistic, but only 36 people are not very optimistic, and we still need to inherit and protect it together [23]. There are 77 people who are relatively unobjective, accounting for 35.8% of the total number. It is still a large group of people, and we must attach great importance to this point. It is highly similar to my survey results, so the calculation results of the algorithm can be used for reference.

**4.1.3. People Pay Attention to Cultural Types and Simulate the Fusion of Traditional Art and Old Street Culture.** The perspective of the type of culture people pay attention to is to quantify different types of culture, calculate the type of culture and age group concerned, and take the type of culture: agricultural culture, traditional culture, traditional festivals, traditional Chinese medicine, Chinese opera, Chinese architecture, Chinese martial arts, Chinese painting and calligraphy, folk crafts, food, and cooking [25]. The



TABLE 1: Table one or two different methods collect comparisons for different age groups.

Generation:	Under 18	19-30	30-50	Over 50	All people
Deblurring algorithm	21	110	72	12	215
Hierarchical algorithms	21	111	72	10	214

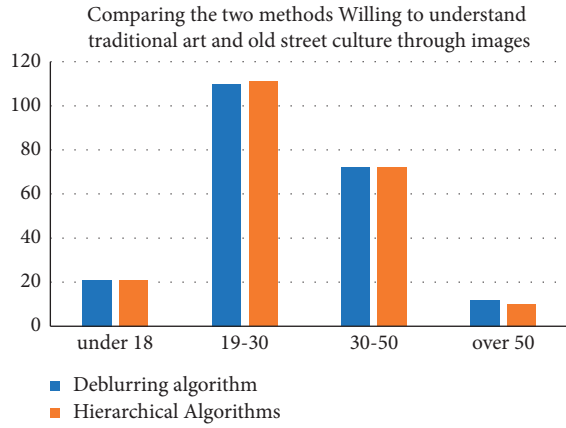


FIGURE 3: A comparison of willingness to understand traditional culture and old street art through images.

TABLE 2: The number of evaluations and the degree of expectation for the future of traditional culture.

Classification	Under 18	19-30	31-50	Over 50	Total people
Very optimistic	2	19	14	1	36
More optimistic	10	54	32	6	102
Hard to say	4	27	16	3	50
Not optimistic	5	10	10	2	27

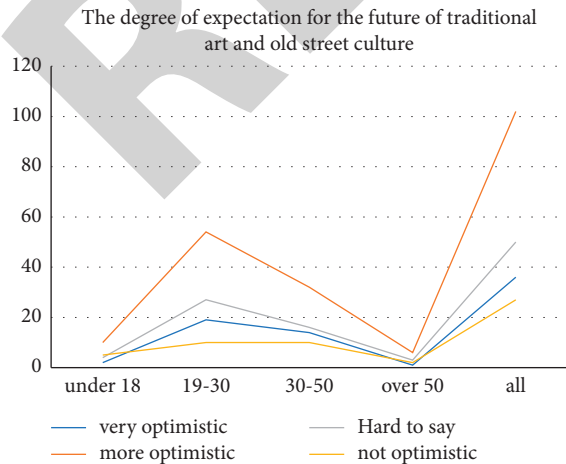


FIGURE 4: The degree of expectation for the future of traditional art and old street culture.

TABLE 3: Evaluators and types of cultures concerned.

Culture type/Age	Under 18 (%)	19-30 (%)	31-50 (%)	Over 50 (%)
Agricultural culture	4	11	20	30
Traditional culture	20	14	12	10
Traditional festival	13	10	13	15
Traditional Chinese medicine	11	15	15	17
Chinese opera	2	20	2	13
Chinese architecture	20	5	8	5
Chinese martial arts	10	5	7	0
Chinese calligraphy	5	8	3	8
Folk craft	11	2	4	2
Food and cooking	4	10	6	0
Total proportion	100	100	100	100

sampling results are shown in Table 3. The simulation results are shown in Figure 5.

From the simulation results, it can be seen that different age groups pay different attention to different cultural types. The quantitative results of teaching different people to pay attention to different cultural types are attributed to percentages and substituted into the calculation formula. The qualitative results obtained are consistent with the statistical results of a large number of experimental data and realize the core idea of fuzzy evaluation.

From Figure 5, it can be clearly understood that traditional art and literature are different for each age group based on different algorithms. Older people can understand that they pay more attention to traditional Chinese medicine and agricultural culture through calculation and comparison; adults pay more attention to traditional festivals; for most groups, those in the 18-50 age group prefer food and cooking, traditional shows, and Chinese opera. Through calculation and analysis, I can roughly conclude that we should start with traditional programs and food and cooking to attract people's interest in traditional art and old street culture.

**4.2. Big Data Analysis Method and Sampling Survey Method.** Based on traditional cultural types, I use big data analysis method and sample survey method to compare because of fuzzy algorithm and sample survey method to compare. The results of traditional art and old street culture by the public from different angles are shown in Table 4, and the visualization chart is shown in Figure 6.

As can be seen from the above Figure 6, the algorithm we used is highly consistent with the sampling survey method, which shows that the defuzzification method I used is basically the same as the hierarchical evaluation fuzzy method. It is necessary to promote it from images, videos and the Internet to gain more public attention.

#### 4.3. Algorithm Experimental Index Analysis

**4.3.1. Hierarchical Fuzzy Evaluation Algorithm Simulation Results Conformity Test.** The superiority of the algorithm is not only reflected in the fuzzy performance but also reflected

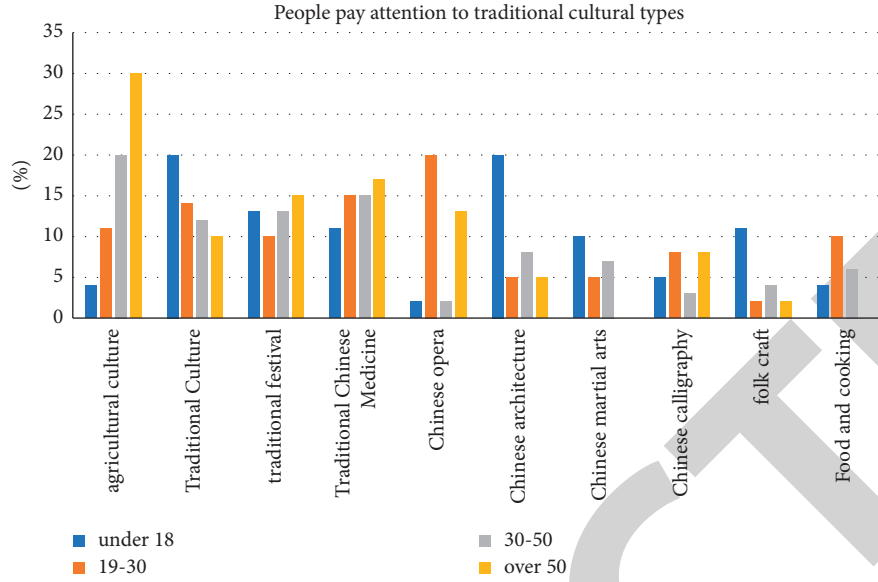


FIGURE 5: The proportion of people concerned about traditional culture.

TABLE 4: Different ways to understand traditional art and old street culture.

	Image (%)	Video (%)	Newspaper (%)	The internet (%)	Other (%)
Big data analytics	80.91	90.20	20.00	88.01	10.00
Sample survey method	79.99	91.00	19.00	89.33	11.00

TABLE 5: Algorithm compliance simulation data comparison.

Algorithm quiz results	8 7.3%	8 7.6%	8 9.5%	8 8.6%	9 1.2%
Subjective evaluation results	8 8.1%	8 7.2%	9 0.2%	8 7.8%	9 0.7%

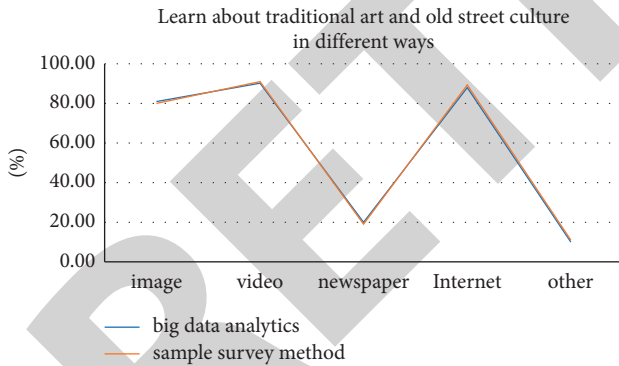


FIGURE 6: Comparison of different understanding methods.

in the consistency detection of the results. In order to achieve a reasonable effect on the judgment of the facts, this paper takes the consistency of the results of the algorithm as the test point, and the experimental data and visual charts obtained by simulation are shown in Table 5 and Figure 7, respectively. The percentage is used as the evaluation standard of the experiment. The larger the value is, the closer the conformity is to the real situation.

The simulation points are based on the individual subjective evaluation of the age of the people, the expectation of the people, and the types of traditional culture that the people pay attention to.

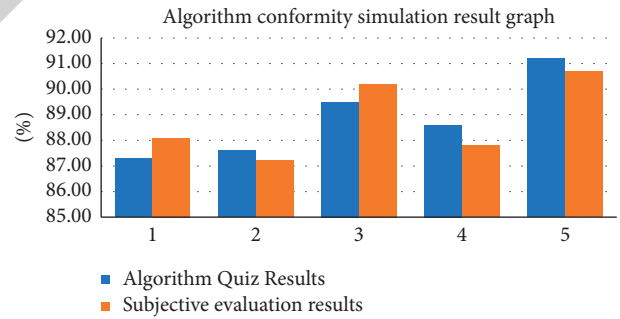


FIGURE 7: Algorithm compliance simulation results.

From the visual chart, it can be seen that the algorithm test results and the subjective evaluation have a high degree of overlap based on the fuzzy comprehensive evaluation method, and the difference between them is not more than 1%, the difference can be ignored, and the degree of compliance is considered to meet the evaluation requirements.

**4.3.2. Defuzzification Algorithm and Hierarchical Fuzzy Evaluation Algorithm Unit Calculation Time Efficiency Simulation.** Fixed experimental results are only used as a single variable to be evaluated for experimental anti-simulation. Taking the time efficiency as the evaluation standard for the calculation results reflects the simplicity of the algorithm and the simplification of complex problems.

TABLE 6: Time efficiency (T/s) per unit of calculation of similar algorithms.

To be evaluated (TB)	Deblurring algorithm	Hierarchical fuzzy evaluation method	Comprehensive evaluation method
1.0	55.1	67.3	66.2
1.5	82.3	99.2	103.5
2.0	122.7	153.7	167.3

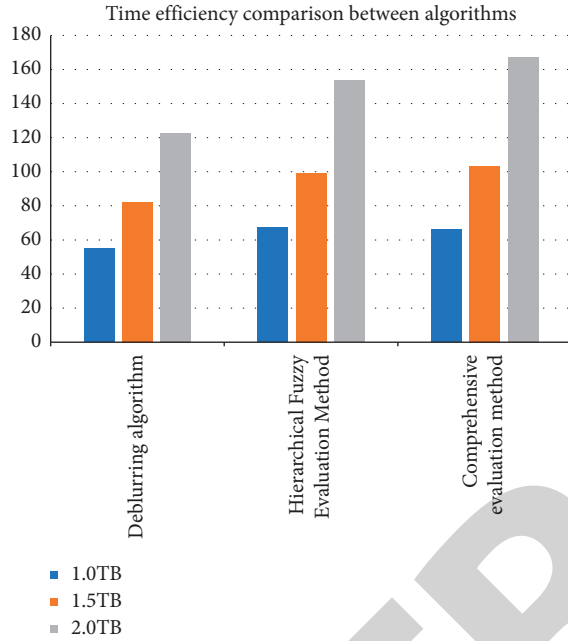


FIGURE 8: Time efficiency diagram between algorithms.

The simulation data are shown in Table 6, and the visualization chart is shown in Figure 8.

Defuzzification algorithm studied in this paper maintains an advantageous state in terms of time consumption when the evaluation results of qualitative understanding are presented in the form of data. In similar algorithms, the evaluation factor is simplified in the form of a set and a matrix, so that the evaluation factor has a regular format, and the simplified data to be evaluated can be calculated, thereby reducing the time consumption of the algorithm.

The measurability of fuzzy sets and the standard division of fuzzy sets are proposed. The reason is that if they are missing, there will be a gap between the results of the algorithm and the real situation. After the introduction of the above two links, the accuracy of the algorithm will be substantially improved; The weight of the degree is not the algorithm itself that ultimately affects the results. The function of the algorithm is only to combine the data organically and participate in the evaluation factor set of the algorithm.

## 5. Conclusion

Based on the fuzzy algorithm, I will introduce how to integrate traditional art and old street construction. With the

development of urban construction and technology, simple construction can no longer be recognized by the masses for the construction of old streets. The deblurring algorithm and the layered blurring algorithm can more intuitively and clearly show the innovative integration of traditional art and old street construction, and the traditional art and the old street that is about to disappear once again appear in people's vision. The results presented by its algorithm show that when the algorithm performs conditional derivation, the processing form is often radiative, and there is an exponential explosion of data when a single condition is derived from multiple conditions of the same type. Appropriate containment of such divergence is an important factor for the algorithm to improve time efficiency. The focus is also one of the algorithm optimization points in the future. On the basis of fuzzy algorithm, understand how to integrate traditional art and old street construction and promote the old street scenery based on the combination of traditional culture through different methods, so as to attract more people to learn about traditional art and old street culture. Create a historical and cultural block with more traditional artistic connotation and value.

According to the method of fuzzy calculation, calculate and analyze how to integrate traditional art and old street culture in today's society. As mentioned in the preface of the chapter, the blessing of fuzzy algorithms will greatly reduce the research efforts in terms of efficiency, so the research focus will naturally increase on the accuracy rate. For example, the traditional art and old street culture that people in different regions love are calculated through fuzzy calculation, and the construction and integration are carried out in different locations. While not losing traditional Chinese culture, they can develop together according to the combination of modern civilization and integrate a complete historical and cultural district.

## Data Availability

The experimental data used to support the findings of this study are available from the corresponding author upon request.

## Conflicts of Interest

The authors declare that they have no conflicts of interest regarding this work.

## Acknowledgments

This study was funded by the Key Program of China National "13th Five-Year-Plan" Program by MOE "Construction and Popularization of the General Knowledge Pedagogic System of Chinese Traditional ARTS" (DLA190427).

## References

- [1] J. L. Jin, Y. M. Wei, and J. Ding, "Fuzzy comprehensive evaluation model based on improved analytic hierarchy

## Retraction

# Retracted: Material Analysis and Application Based on Intelligent Computing in the Context of Contemporary Watercolor Painting

### Security and Communication Networks

Received 8 August 2023; Accepted 8 August 2023; Published 9 August 2023

Copyright © 2023 Security and Communication Networks. This is an open access article distributed under the Creative Commons Attribution License, which permits unrestricted use, distribution, and reproduction in any medium, provided the original work is properly cited.

This article has been retracted by Hindawi following an investigation undertaken by the publisher [1]. This investigation has uncovered evidence of one or more of the following indicators of systematic manipulation of the publication process:

- (1) Discrepancies in scope
- (2) Discrepancies in the description of the research reported
- (3) Discrepancies between the availability of data and the research described
- (4) Inappropriate citations
- (5) Incoherent, meaningless and/or irrelevant content included in the article
- (6) Peer-review manipulation

The presence of these indicators undermines our confidence in the integrity of the article's content and we cannot, therefore, vouch for its reliability. Please note that this notice is intended solely to alert readers that the content of this article is unreliable. We have not investigated whether authors were aware of or involved in the systematic manipulation of the publication process.

Wiley and Hindawi regrets that the usual quality checks did not identify these issues before publication and have since put additional measures in place to safeguard research integrity.

We wish to credit our own Research Integrity and Research Publishing teams and anonymous and named external researchers and research integrity experts for contributing to this investigation.

The corresponding author, as the representative of all authors, has been given the opportunity to register their agreement or disagreement to this retraction. We have kept a record of any response received.

### References

- [1] J. Feng and Y. Zhang, "Material Analysis and Application Based on Intelligent Computing in the Context of Contemporary Watercolor Painting," *Security and Communication Networks*, vol. 2022, Article ID 9517615, 10 pages, 2022.

## Research Article

# Material Analysis and Application Based on Intelligent Computing in the Context of Contemporary Watercolor Painting

Jianyu Feng and Yifei Zhang 

*School of Drawing and Painting, Luxun Academy of Fine Arts, Shenyang 110003, China*

Correspondence should be addressed to Yifei Zhang; [zhangyifei@lumei.edu.cn](mailto:zhangyifei@lumei.edu.cn)

Received 26 May 2022; Accepted 4 August 2022; Published 17 September 2022

Academic Editor: Hangjun Che

Copyright © 2022 Jianyu Feng and Yifei Zhang. This is an open access article distributed under the Creative Commons Attribution License, which permits unrestricted use, distribution, and reproduction in any medium, provided the original work is properly cited.

Scholars have researched the current situation and development trend of contemporary watercolor materials in terms of material intervention, material expression language, spiritual connotation in material “materiality,” and practical application of materials, which are of profound significance to the consolidation of the theoretical system of watercolor painting in China. However, how to better analyze and apply watercolor materials on the basis of intelligent computing, as well as the material analysis and application based on intelligent computing in the context of contemporary watercolor painting, still has a lack of research at present. Therefore, this study considers the analysis and application of materials based on intelligent computing in the context of contemporary watercolor painting, in an attempt to seek ways to integrate with Chinese watercolor painting and its own national art.

## 1. Introduction

In the Chinese Encyclopedia, the definition of watercolor painting is as follows: “A painting made by mixing water and watercolor pigments. Watercolor painting emerged in Europe around the end of the 15<sup>th</sup> century, formed an independent genre in England after the 18<sup>th</sup> century, and was introduced to China in the early 20<sup>th</sup> century [1]. The famous English watercolor painters include J. M. W. Turner and J. Constable. Famous Chinese watercolor painters include Guan Guangzhi, Li Jianchen, Ni Yide, Pan Sitong, Gu Yuan, and so on. Watercolor painting techniques include dry painting, wet painting, dipping, pointillism, rendering, and washing. With the help of water, watercolor painting expresses color intensity and transparency, using the masking and bleeding effect of white paper and pigment to reflect the unique artistic effects of brightness, transparency, lightness, moistening, and dripping” [2].

Watercolor painting is literally a painting made by using water as a diluent to mix colored pigments that can be diluted by water [3]. Nowadays, the number of materials used as diluent for painting is gradually increasing, and there

are more pigments that use water as a diluent, such as acrylics, water-soluble colored pencils, and illustration ink. Thus, we have to re-examine the concept of watercolor painting [4]. Watercolor painting not only does refer to the use of water to mix pigments but also has its own rich connotation and a set of techniques that are very different from other types of painting [5]. The control of the amount of water, the ratio of water to pigment, and the traces left by water on the paper all become elements of the rhythm of the picture and its embodiment. From two or three hundred years ago to today, the concept of watercolor painting has expanded, with a more profound and extensive connotation and richer content, greatly expanding the previous meaning. Moreover, contemporary watercolor art creation not only adopts watercolor but also uses gouache, acrylic, Chinese painting pigments, and partially even oil paints, fluorescent paints, textile fiber paints, oil sticks, paints, etc. There are also cases where several pigments are used in combination.

Watercolor has been developed in China for more than two hundred years, and the process has been influenced by the traditional Chinese concept of painting, forming a unique Chinese artistic landscape. In contemporary research

on the Chineseness of watercolor painting, the issue of the material language of painting has been of great concern. As various new materials have been explored and used, at the same time, traditional Chinese ink painting materials are familiar to Chinese painters, and they often apply traditional ink materials in their watercolor creative practice [6]. Painting materials are not only an expression of the medium of painting but also an artistic language. In particular, certain watercolor synthesis materials, with their own physical qualities, can highlight the spirit of Chinese aesthetics, and their own artistic values are constantly being explored, which can constantly renew our way of thinking and nourish our aesthetic sensibilities.

Since the introduction of watercolor into China, artists have never stopped exploring the relationship between watercolor and traditional ink. Watercolor painting from the West and Chinese ink painting are constantly colliding and merging conceptually, and Chinese watercolor painting naturally draws on watercolor painting materials in terms of material language. At this time, the material language was not limited by the boundaries of the painting genre but used watercolor as a vehicle to use materials according to the needs of the picture and the artist's spiritual needs. The creators kept experimenting and breaking through the use of comprehensive materials, making new breakthroughs in the language of watercolor materials while drawing on traditional Chinese painting. It is worth noting that the innovation of Chinese watercolor painting in terms of materials should, on the one hand, preserve the original language of watercolor and, on the other hand, draw nutrients from the excellent Chinese traditional culture to reflect the national characteristics and artistic values of Chinese watercolor [7].

## 2. Related Work

Materials, in our life, are everywhere. In the creation of watercolor, material analysis directly reflects the state of mind and thoughts of the creator. The analysis of painting materials is highly dynamic and contains a spiritual dimension itself, so that the painting materials are given more and more profound meanings, and their connotations and extensions are more colorful. Otieno Redon said, "Materials have their own secrets to show, they each have their own characteristics, and the wise man speaks through them." It is important to have a correct understanding of the material analysis of the painting. In fact, the creative potential of watercolor material analysis is huge, because watercolor creation is mainly a combination of water and various integrated media, which has infinitely extended expressive tension in addition to its unique natural properties. Chen Xinmao believes that material analysis cannot be regarded as a simple technique but as a specific form of expressing the spirit through the comprehensive use of various materials.

According to [8], "painting is not simply a patchwork of art forms, let alone an attempt and innovation of techniques, but a specific manifestation of the visual requirements and ideological content of painting under the inspiration of a specific artistic spirit, which can be the use of the popular media materials of the moment, or the sum of multiple

painting materials, generally and usually created within the context of specific ideological content and the painter's personal freedom of thought."

Watercolor materials themselves have certain limitations, so contemporary watercolor borrowing material analysis from Chinese ink painting is still one of the ways to effectively realize the Chinese-ness of watercolor painting. The development of watercolor material analysis cannot be satisfied only by its own inherent and monotonous attainments [9]. In addition, watercolor materials have their own material properties, which have the characteristics that they should not be covered or modified.

Material analysis is one of the important ways to express the spirit of traditional Chinese aesthetics. The study in [10] on The History of Chinese Watercolor Painting argues that the development of watercolor painting with national characteristics can be found in the tools of traditional Chinese painting materials, with the purpose of drawing on the aesthetic spirit and aesthetic style in the profound Chinese traditional art. The study in [11] argues that material analysis is, more importantly, representative of China's cultural heritage and national spirit. The study in [12] on "Transcending Again in Innovation" argues that from the actual achievements of China's previous watercolor painters, besides the material technique expression form, it is the expression of traditional cultural heritage that is the most important, so we should pay attention to the profound influence of traditional Chinese painting on watercolor. Watercolor painter Mr. Huang Tieshan said, "Chinese watercolor painters must work hard and learn to integrate traditional Chinese ink painting materials in addition to mastering the material techniques of Western watercolor painting, so as to build up Chinese watercolor painting with national spirit and artistic infectiousness, which is the road of future development of Chinese watercolor painting."

The art of painting is the expression of the deepest inner world of the mind, the catharsis and outburst of the artist's emotions, and thus, "one cannot talk about the meaning of art without its material existence in the world." From this, it can be seen that the creation of painting cannot be separated from its closely related material existence, i.e., painting materials. The use of traditional watercolor materials has evolved over time and with the history of watercolor painting.

Painting materials are the material existence of watercolor creation, and they are also the prerequisite preparation and material foundation for watercolor art creation, directly and profoundly reflecting the artistic thinking, emotional expression, and aesthetic style of the painter's works [13]. Painting materials are often used passively and mechanically, but in today's watercolor creation, the material speaking the power of media materials gradually increases and begins to rise to a height of consciousness with cultural carrier value and aesthetic properties [14].

Watercolor painting material is the aesthetic carrier for the watercolor artist to express his own thoughts and feelings, a material need for spiritual catharsis, and a cultural carrier and aesthetic experience for the spiritual monologue to be realized [9]. The painting material is a natural and



unnatural release of the artist's emotions and expressions and his or her deep feelings about everything in the world. It can be seen that the relationship between the creation of watercolor painting and materials is extremely close, and the two are interdependent, mutually reinforcing, and indispensable.

"From the perspective of the development of material media, the evolution of human art can be divided into the period of natural materials and the period of artificial materials [15]." Natural materials refer to the almost unprocessed painting materials used by the ancient ancestors when they used natural mineral pigments such as natural loess, red clay, black charcoal of burnt wood, and primitive plant pigments such as stems and leaves of plants to depict totem-like animal images, and the ancient art painted at this time can be said to be the germination of watercolor painting [16]. This natural material is simple, clumsy, and rough and maintains its original character. The art of the ancient period takes natural material as the material premise, and the artistic expression is drawn by natural factors, with a single form of subject matter and relatively poor language.

Gradually, as the production of painting materials and art production began to be separated, artificial materials gradually entered people's attention. Until the eighteenth century in Europe, watercolors were only available in a few varieties, such as brown and blue [17]. In the mid-eighteenth century, artists began to use special semi-mechanical, semi-manual ground pigments contained in pig bladders. It was not until the end of the nineteenth century that painters began to use man-made pigments packaged in ready-made tin tubes. In the early twentieth century, watercolor painting was introduced to China, and the traditional watercolor painting began [18]. The achievements of painting and the diversity of art forms to date are inextricably linked to the evolution of materials. The materials used in the creation of traditional watercolor paintings in China are simple, and the varieties of materials are not that complicated [19]. The traditional materials used in the creation of watercolor paintings are classified as follows: watercolor paper, watercolor brushes, watercolor paints, mediums, and other auxiliary tools. In short, the traditional materials used in watercolor painting include five major categories, namely, paper, brush, color, water, and other auxiliary tools.

All in all, since material analysis is one of the important ways to express the traditional Chinese aesthetic spirit, it becomes the focus of this study to strengthen the material analysis and application of intelligent computing in the context of contemporary watercolor painting.

### 3. Methods

The development of today's watercolor painting itself is complicated and difficult. The exploration of traditional watercolor language can be said to have reached a certain level, but due to certain traditional restrictions of stereotypes, the art language form is conservative and single. The stubborn insistence on the purity of the so-called art language has circled the development space of watercolor art. While the original language of watercolor should continue to

be constructed, it is worthwhile for us to think about the possible development direction of watercolor art in the future and to explore the space for the improvement and extension of the language. When the traditional art materials of the genre itself cannot meet the needs of the art environment, the art genre itself, and the artist's inner spiritual state, they will gradually turn to the direction of exploring new possibilities of using different materials to assist in the painting. The exploration and use of materials is not a blind move to develop watercolor art, but more a result of our spiritual needs.

"Nowadays, the transformation of cultural forms has become the theme of history, the old laws have been broken again and again, and the diversification of cultural dynamics has been in full swing. As a result, the original materials have become a kind of confinement, and the prosperity of art has brought about the diversification of art media as a matter of necessity, and non-traditional materials have also shown exceptional vitality because they carry a new atmosphere of the times. China's artistic achievements have today's brilliance, which is inseparable from the successful experience and fruitful results of a considerable number of artists in the application of materials." Watercolor painting and painting materials are closely related, and the breakthrough use of comprehensive materials in watercolor painting gives freedom to artists and appreciators, bringing more uncertainty and greater, unknown and unforeseen potential possibilities to watercolor art. The following is a representative list of comprehensive materials that can be used to assist in the practice of watercolor painting.

Special materials for the paper include canvas for watercolor, white cardboard, rice paper (collage), cotton cloth, wood board, vellum, and clay (paste), as shown in Figure 1.

Special materials for pens include mops, row brushes, pens, water pens, water-soluble colored pencils, oil sticks, gouache, oil pastels, brushes, and colored pastels, as shown in Figure 2.

Special materials for color include textile fiber pigments, fluorescent pigments, sequins, gold and silver, pearl powder, and paint, as shown in Figure 3.

Special materials for media are shown in Figure 4.

Other special materials for auxiliary tools include white glue, transparent tape, toothpick, tissue paper, curtain, sponge, fixing liquid, paste, framing, charcoal powder, plaster liquid, and cotton ball, as shown in Figure 5.

Special materials for other methods of media include projectors, digital cameras, electric heaters, electric drills, wind turbines, and computer Photoshop design software, as shown in Figure 6.

Let the number of watercolor painting materials consumed in the calendar year be in the order  $y_1, y_2, \dots, y_T$ ;  $\alpha$  is the weighting factor:

$$\hat{y}_{t+1} = S_t^{(1)}. \quad (1)$$

Here,  $S_t^{(1)} = \alpha y_t + (1 - \alpha)S_{t-1}^{(1)}$ . denotes an exponential smoothing value for a period  $t$  ( $t = 1, 2, \dots, T$ ).

Definition of initial value: if the number of samples is greater than, for example,  $n \geq 20$ , and if the initial value is less





FIGURE 1: Watercolor paper, white cardboard, rice paper, cotton cloth, and wooden boards.



FIGURE 2: Painting document, water-based document, pen, mop, oil painting stick, and water-soluble color pencil.



FIGURE 3: Dope-dyed fiber colors, gold color and silver color, sequins, fluorescent pigment, and acrylic colors.



FIGURE 4: Bottle medium as an example.



FIGURE 5: Variety of auxiliary tools.

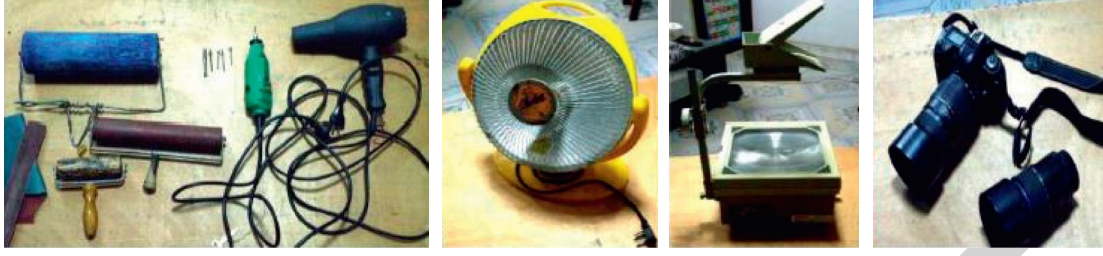


FIGURE 6: Electric hair dryer, electric drill, electric heaters, projection machine, and digital cameras.

than the subsequent value, the first data can be selected as the original data, i.e.,  $S_0^{(1)} = y_1$ . If the number of educational samples is small and the initial value has a great impact on the subsequent values, the average of the actual data in the first two cycles can be selected as the initial value  $S_0^{(1)} = (y_1 + y_2)/2$ .

Definition of weight coefficient: if the main trend in the known data is stable and the fluctuation range is small, the value of the weight coefficient should be small, for example,  $\alpha = 0.2$ . If the known data is more unstable, the data should be increased, for example,  $\alpha = 0.8$ , to make the model more sensitive. If there are few known data, multiple values can be calculated separately, and the smaller root means square error value can be selected as the actual weight coefficient.

Let  $X^{(0)}$  be the GM(1, 1) modeling sequence.

$$X^{(0)} = (x^{(0)}(1), x^{(0)}(2), \dots, x^{(0)}(n)). \quad (2)$$

$X^{(1)}$  is the 1-AGO sequence of  $X^{(0)}$ .

$$\begin{aligned} X^{(1)} &= (x^{(1)}(1), x^{(1)}(2), \dots, x^{(1)}(n)), \\ x^{(1)}(k) &= \sum_{i=1}^k x^{(0)}(i), \quad k = 1, 2, \dots, n. \end{aligned} \quad (3)$$

Let  $Z^{(1)}$  be the sequence of immediately adjacent mean generators of  $X^{(1)}$ .

$$\begin{aligned} Z^{(1)} &= (z^{(1)}(1), z^{(1)}(2), \dots, z^{(1)}(n)), \\ Z^{(1)}(k) &= 0.5x^{(1)}(k) + 0.5x^{(1)}(k-1). \end{aligned} \quad (4)$$

Here,

$$\begin{aligned} B &= \begin{bmatrix} -z^{(1)}(2) & 1 \\ -z^{(1)}(3) & 1 \\ \vdots & \vdots \\ -z^{(1)}(n) & 1 \end{bmatrix}, \\ Y &= \begin{bmatrix} x^{(0)}(2) \\ x^{(0)}(3) \\ \vdots \\ x^{(0)}(n) \end{bmatrix}. \end{aligned} \quad (5)$$

Then, the gray system values are as follows:

$$\hat{x}^{(0)}(k+1) = x^{(1)}(k+1) - x^{(1)}(k), \quad (6)$$

where

$$\hat{x}^{(1)}(k+1) = \left( x^{(0)}(1) - \frac{b}{a} \right) e^{-ak} + \frac{b}{a},$$

$$\begin{pmatrix} a \\ b \end{pmatrix} = (B^T B)^{-1} B^T Y,$$

$$B = \begin{bmatrix} -z^{(1)}(2) & 1 \\ -z^{(1)}(3) & 1 \\ \vdots & \vdots \\ -z^{(1)}(n) & 1 \end{bmatrix}, \quad (7)$$

$$Y = \begin{bmatrix} x^{(0)}(2) \\ x^{(0)}(3) \\ \vdots \\ x^{(0)}(n) \end{bmatrix}.$$

Let  $x$  be the independent variable and  $y$  be the dependent variable, and there is some linear relationship between  $y$  and  $x$ . Then, the univariate linear regression equation is

$$\hat{y} = a + \hat{b}x, \quad (8)$$

where

$$\hat{b} = \frac{n \sum_{i=1}^n x_i y_i - \sum_{i=1}^n x_i \sum_{i=1}^n y_i}{n \sum_{i=1}^n x_i^2 - (\sum_{i=1}^n x_i)^2}, \quad (9)$$

$$\hat{a} = \bar{y} - \hat{b}\bar{x}.$$

We used input matrix, output matrix, coupling matrix between the input layer and hidden layer, coupling matrix between the hidden layer and output layer, output waiting matrix, the number of neurons in the input layer, the number of neurons in the hidden layer, and the number of neurons in the output layer. The formula for determining the optimal number of neurons in the hidden layer is

$$j = \sqrt{i+k} + a, \quad (10)$$

where  $a$  is a constant between 1 and 10.

They have their own advantages and disadvantages and are interrelated and complement each other. Different methods of using different data and obtaining information are different. If an error occurs during direct deletion, useful information may be lost. If different methods and information provided in different ways are used to optimize the combination of different methods, the accuracy can be greatly improved. The combination of the new model is optimized in the form of a combination model.

Let  $x_i$  be the weighting factor of the  $i$ -th method,  $Y_{it}$  be the value of the  $i$ -th method in year  $t$ , and  $Y_t$  be the value of the combined method in year  $t$ . Then, the objective function of the combined model is given as follows:

$$\text{Min } Z = \frac{1}{n} \sum_{t=1}^n \left( \sum_{i=1}^N x_i Y_{it} - y_t \right)^2, \quad (11)$$

where  $N$  is the number of selected single methods.

The most important thing is to determine the weight coefficient to make the result of the combined model more accurate. When determining the weighting coefficient, it is important to ensure that all methods are related to one weighting coefficient, that is, all methods are related to one weighting coefficient. This paper uses genetic algorithm to solve the model, the next step of the genetic algorithm.

The first step is to set parameters. The population number of this paper is 200, the hybridization probability is 0.6, the mutation probability is 0.001, the evolution rate is 600, and the substitution rate is 0.9.

Secondly, we use numeric encoding to generate the initial total number and use the length of a single encoded string as the number of a single method.

The third stage calculates the overall adaptation according to the selected adaptation function. Since the objective function of the combined model is a minimum problem, the minimum problem must be transformed into the maximum problem when determining the fitness function of genetic algorithm.

Fourth, according to the degree of adaptation, a new generation of population formation operation with selectivity, crossover, and variability is carried out in the genetic space.

Finally, we return to step 3 until the predetermined evolutionary algebra is reached and finally get the combination of model weight coefficients.

#### 4. Experiments

In order to comprehensively evaluate the accuracy of the combination model established in this paper, according to the principle and practice of combination efficiency evaluation, at least three error characteristic indexes are generally used to comprehensively evaluate the error and the group with the smallest error is selected as the optimal combination model. This paper mainly uses the following three index error characteristics to evaluate the model:

TABLE 1: Watercolor painting materials in China (million t).

Year	Raw iron ore volume	Year	Raw iron ore volume
1992	21022	2001	21701
1993	22599	2	23143
1994	25056	2003	26139
1995	26210	2004	34634
1996	25228	2005	42049
1997	26699	2006	58888
1998	24689	2007	70665
1999	23723	2008	82401
2000	22256	2009	88122

(1) Squared sum error (SSE):

$$E_{\text{SSE}} = \sum_{t=1}^n (y_t - \hat{y}_t)^2. \quad (12)$$

(2) Mean squared error (MSE):

$$E_{\text{MSE}} = \frac{1}{n} \sum_{t=1}^n (y_t - \hat{y}_t)^2. \quad (13)$$

(3) Theil IC:

The value of Theil's inequality coefficient is usually between 0 and 1, and the smaller the value, the better the fit.

$$\text{Theil IC} = \frac{\sqrt{(1/n) \sum_{t=1}^n (y_t - \hat{y}_t)^2}}{\sqrt{(1/n) \sum_{t=1}^n y_t^2} + \sqrt{(1/n) \sum_{t=1}^n \hat{y}_t^2}}, \quad (14)$$

where  $y_t$  is the value of consumption in year  $t$ .  $\hat{y}_t$  is the real amount of consumption in year  $t$ .  $n$  is the number of samples.

We selected China's watercolor painting material data, used intelligent computing algorithm-based analysis model, and established time series analysis model for watercolor painting material analysis; the sample data are shown in Table 1.

Prior to the training of the analytical model based on intelligent computing, the sample data is processed and normalized in this study using the following approach.

$$\begin{aligned} x_i^{*P_i} &= \frac{x_i^{P_i}}{x_{i,\max} + x_{i,\min}} \quad (i = 1, 2, \dots, n), \\ o_j^{*P_i} &= \frac{o_j^{P_i}}{o_{j,\max} + o_{j,\min}} \quad (j = 1, 2, \dots, n). \end{aligned} \quad (15)$$

The minimum and maximum values of the  $i$ -th input in the sample input data are  $x_{i,\max}$  and  $x_{i,\min}$ ; the minimum and maximum values of the  $j$ -th learned output are  $o_{j,\max}$  and  $o_{j,\min}$ ; the  $i$ -th input and  $j$ -th learned output of the  $P_1$  th sample in the original data are  $x_i^{P_1}$  and  $o_j^{P_1}$ ; and the  $i$ -th input and  $j$ -th learned output of the  $P_1$  th sample after processing are  $x_i^{*P_i}$  and  $o_j^{*P_i}$ .

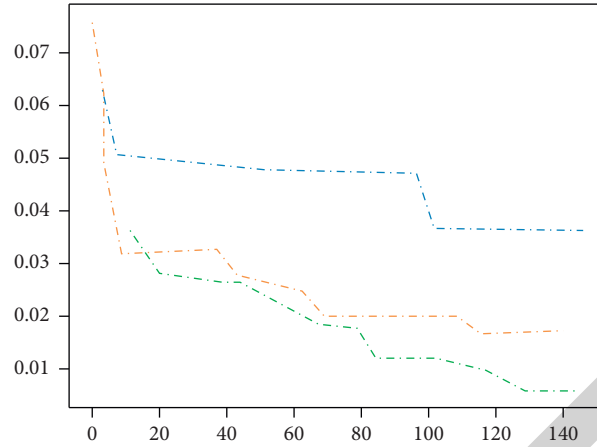
FIGURE 7: Optimization ship  $F$  network minimum error evolution curve.

TABLE 2: 2007–2009 domestic watercolor painting materials and analysis value comparison (million t).

Year	True value	RBF predicted value	Relative error (%)	DAPSO-RBF predicted value	Relative error (%)	SPSO-RBF predicted value	Relative error (%)
2007	70669	74265	5.12	72145	2.12	73382	3.86
2008	82405	86295	4.73	81689	0.85	79338	3.70
2009	72127	84545	4.08	86597	1.71	85491	3.01



FIGURE 8: Taihang Mountain Series.

The data of the first 5a is used as input for the analysis during the experiment, and the data of the 6a is analyzed. After a lot of experimental comparisons, the number of radial basis function centers of the hidden layer of the network is taken as 15, which is better, so the structure of the network is 5-15-1. Thus, there are 13 sets of sample data: the first 10 sets of data are used as training samples, while the last 3 sets of data are used as test samples; the parameters of the



FIGURE 9: Laoshan Series.

algorithm are  $c_1 = c_2 = 2.0$ , and the maximum number of iterations is 150, respectively. The minimum error evolution curve of the network during the optimization is shown in Figure 7.

From Figure 7, it can be seen that with the intelligent computing optimization analysis model, the number of iterations runs to about 10 generations and the optimization error results almost reach a stable value with a intelligent computing algorithm optimization analysis model, because the inertia weights can be adaptively adjusted.

The trained analysis is used for the analysis of the test sample, and the analysis results are shown in Table 2, and the analysis results are compared without optimization.

From the analysis results of watercolor painting materials in China from 2007 to 2009, we can see that the analysis





FIGURE 10: Liang Quan's Qi series picture.

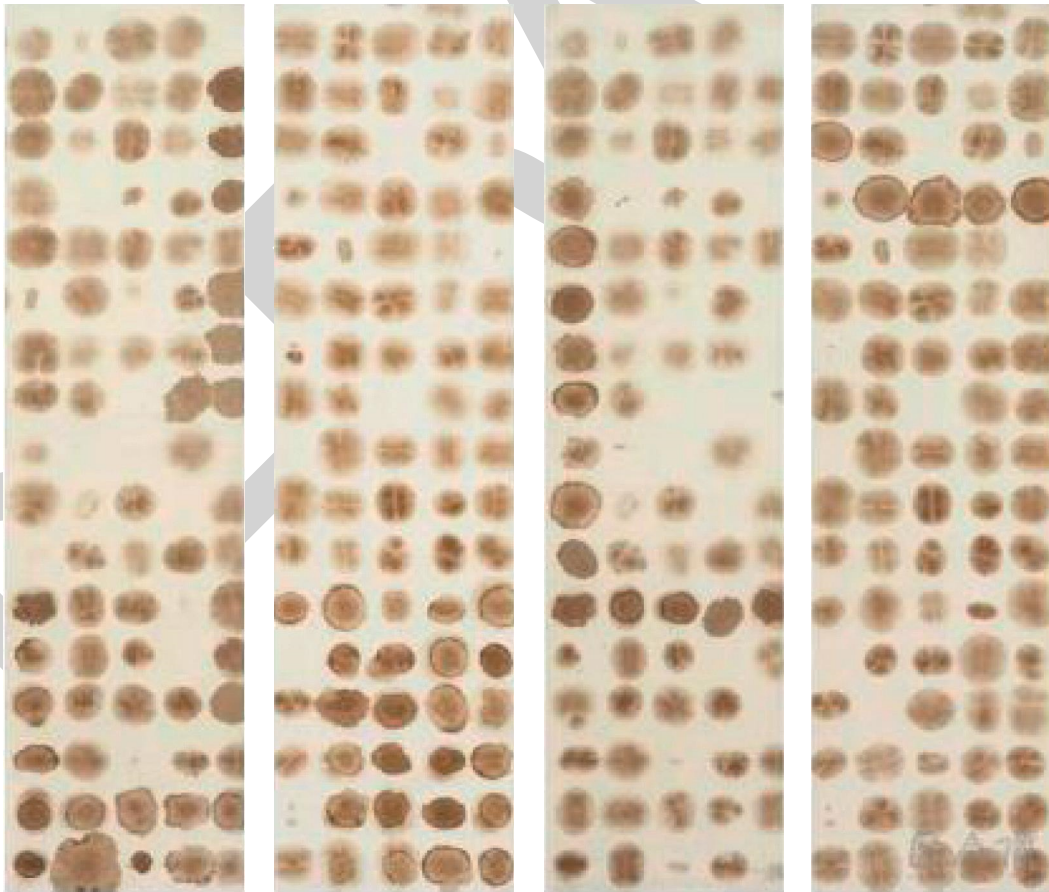


FIGURE 11: Liang Quan's Qi series picture.

results of the analysis model optimized by intelligent computing algorithm have smaller errors than those of the single network and the analysis errors of the analysis model optimized with intelligent computing are again much smaller than those of the analysis model optimized by intelligent computing algorithm, which can show that intelligent computing algorithm is effective in improving the other algorithms.

The painter Wang Gang tries to combine different materials in his paintings to create watercolor paintings with “Chinese spirit.” He uses markers or oil sticks as a base for parts of the painting before starting to lay down color. In his work “Taihang Mountain Series” (see Figure 8), the picture contains a serious and simple rhythm and spirituality. In his work “Laoshan Series” (see Figure 9), you can see that he uses a combination of materials to embody the ethereal Zen and literati interest of the East, and the picture is light and serene, as shown in Figures 8 and 9.

In the contemporary practice of material analysis in watercolor painting, new materials are constantly being expanded, injecting new vitality into the development of the Chinese-ization of watercolor material analysis.

The artist Liang Quan’s “Signs” series (as shown in Figures 10 and 11) is innovative and highly recognizable in its integrated material analysis, using “tea” mixed with watercolor paint on rice paper. In his daily life, Ambrose Liang treats tea as a kind of “practice” and leaves the effect of staining and spreading on the rice paper with irregular forms after the tea has dried, so that the picture also has the beauty of the relationship between man and nature and the feeling of unity of heaven and man. Liang Quan uses comprehensive materials to express the elements of the poetics of traditional Chinese painting, realizes the realm of “emptiness” by leaving the list of details and entering a simple and random arrangement, and presents the light and distant Zen meaning of traditional Chinese aesthetics with the white space of “managing simplicity with complexity.”

## 5. Conclusion

In conclusion, the material analysis of watercolor painting has injected a lot of vitality into the Chinese-ness of watercolor material analysis, giving watercolor works the connotation and expressive tension of the traditional Chinese spirit. The brush, ink, paper, and seal in Chinese painting materials all have their material spirits, and the painters convey the aesthetic concepts in traditional Chinese painting through the spiritual materiality of watercolor materials, which are used in watercolor painting as an artistic outlook with national cultural characteristics. The fusion of watercolor painting materials with the unique charm of watercolor painting materials has brought about its own national cultural flavor in the use of brush, ink, and paper without losing its modernity. The actual Chinese-ization of contemporary watercolor painting materials analysis is to absorb the connotation spirit of Chinese painting to reflect the artistic quality and present the artistic value of traditional Chinese aesthetics through “objects.” This paper combines intelligent computing to effectively

analyze and apply materials in the context of contemporary watercolor painting, and the results show that the application of intelligent computing technology can better analyze the materials of watercolor painting.

## Data Availability

The experimental datasets used to support the findings of this study are available from the corresponding author upon request.

## Conflicts of Interest

The authors declare that they have no conflicts of interest regarding this work.

## References

- [1] Y. Liang, “Analysis of the integration of Chinese painting techniques in watercolor painting,” *Arts Studies and Criticism*, vol. 3, no. 1, pp. 37–40, 2022.
- [2] J. Si, “On teaching methodology of figure sketching in traditional Chinese watercolor paintings,” *IPPTA: Quarterly Journal of Indian Pulp and Paper Technical - A*, vol. 30, no. 6, pp. 306–313, 2018.
- [3] Q. Liu, C. Liu, and Y. Wang, “etc. Integrating external dictionary knowledge in conference scenarios the field of personalized machine translation method,” *Journal of Chinese Informatics*, vol. 33, no. 10, pp. 31–37, 2019.
- [4] V. Pitthard, P. Finch, and T. Bayerová, “Direct chemolysis–gas chromatography–mass spectrometry for analysis of paint materials,” *Journal of Separation Science*, vol. 27, no. 3, pp. 200–208, 2004.
- [5] W. Winarno and H. Aryanto, “The efforts to increase artistic sensitivity of unesa’s art education students by painting with watercolor and wax media,” *Human*, vol. 7, no. 2, p. 129, 2016.
- [6] P. An, Z. Wang, and C. Zhang, “Ensemble unsupervised autoencoders and Gaussian mixture model for cyberattack detection,” *Information Processing & Management*, vol. 59, no. 2, Article ID 102844, 2022.
- [7] A. O. Doluda, O. S. Puklich, T. S. Romanenko, and O. S. Drobysheva, “Forensic fine art research of paintings,” *Theory and Practice of Forensic Science and Criminalistics*, vol. 18, pp. 534–542, 2018.
- [8] G. Abdel-Maksoud, Y. M. Issa, and M. Magdy, “Characterization of painting materials of presage of angel gabriel to the priest zechariah icon,” *International Journal of Engineering Research and General Science*, vol. 3, pp. 489–500, 2015.
- [9] A. Zucchiatti, A. Climent-Font, J. G. Gomez-Tejedor et al., “Building a fingerprint database for modern art materials: pixe analysis of commercial painting and drawing media,” *Nuclear Instruments and Methods in Physics Research Section B: Beam Interactions with Materials and Atoms*, vol. 363, no. NOV.15, pp. 150–155, 2015.
- [10] B. H. Berrie, M. Leona, and R. McLaughlin, “Unusual pigments found in a painting by giotto (c. 1266–1337) reveal diversity of materials used by medieval artists,” *Heritage Science*, vol. 4, no. 1, p. 1, 2016.
- [11] R. Ali, M. H. Siddiqi, and S. Lee, “Rough set-based approaches for discretization: a compact review,” *Artificial Intelligence Review*, vol. 44, no. 2, pp. 235–263, 2015.
- [12] G. Cai, Y. Fang, J. Wen, S. Mumtaz, Y. Song, and V. Frascolla, “Multi-carrier  $M$ -ary DCSK system with code index

## *Retraction*

# **Retracted: A Hybrid Model for Commercial Brand Marketing Prediction Based on Multiple Features with Image Processing**

### **Security and Communication Networks**

Received 26 December 2023; Accepted 26 December 2023; Published 29 December 2023

Copyright © 2023 Security and Communication Networks. This is an open access article distributed under the Creative Commons Attribution License, which permits unrestricted use, distribution, and reproduction in any medium, provided the original work is properly cited.

This article has been retracted by Hindawi, as publisher, following an investigation undertaken by the publisher [1]. This investigation has uncovered evidence of systematic manipulation of the publication and peer-review process. We cannot, therefore, vouch for the reliability or integrity of this article.

Please note that this notice is intended solely to alert readers that the peer-review process of this article has been compromised.

Wiley and Hindawi regret that the usual quality checks did not identify these issues before publication and have since put additional measures in place to safeguard research integrity.

We wish to credit our Research Integrity and Research Publishing teams and anonymous and named external researchers and research integrity experts for contributing to this investigation.

The corresponding author, as the representative of all authors, has been given the opportunity to register their agreement or disagreement to this retraction. We have kept a record of any response received.


### **References**

- [1] F. Wang and L. Zhao, "A Hybrid Model for Commercial Brand Marketing Prediction Based on Multiple Features with Image Processing," *Security and Communication Networks*, vol. 2022, Article ID 5455745, 10 pages, 2022.



## Research Article

# A Hybrid Model for Commercial Brand Marketing Prediction Based on Multiple Features with Image Processing

Furong Wang<sup>1</sup> and Li Zhao<sup>2</sup> 

<sup>1</sup>Business School, Shanxi Technical College of Finance and Economics, Taiyuan 712000, China

<sup>2</sup>School of Management Engineering and Business, Hebei University of Engineering, Handan 056038, China

Correspondence should be addressed to Li Zhao; zhaoli@hebeu.edu.cn

Received 4 July 2022; Revised 9 August 2022; Accepted 18 August 2022; Published 15 September 2022

Academic Editor: Hangjun Che

Copyright © 2022 Furong Wang and Li Zhao. This is an open access article distributed under the Creative Commons Attribution License, which permits unrestricted use, distribution, and reproduction in any medium, provided the original work is properly cited.

Recently, deep learning has been employed in automatic feature extraction and has made remarkable achievements in the fields of computer vision, speech recognition, natural language processing, and artificial intelligence. Compared with the traditional shallow model, deep learning can automatically extract more complex features from simple features, which reduces the intervention of artificial feature engineering to a certain extent. With the development of the Internet and e-commerce, picture advertising, as an important form of display advertising, has the characteristics of high visibility, strong readability, and easy-to-obtain user recognition. An increasing number of Internet companies are paying attention to what kind of advertising pictures can attract more clicks. Based on deep learning technology, this paper studies the prediction model of click-through rate (CTR) for advertising and proposes an end-to-end CTR prediction depth model for display advertising, which integrates the feature extraction of display advertising and CTR prediction to directly predict the probability of an advertisement image being clicked by users. This paper studies the deep-seated nonlinear characteristics through the multilayer network structure of the deep network and carries out several groups of experiments on the private display advertising data set of a commercial advertising platform. The results show that the model proposed in this paper can effectively improve the prediction accuracy of CTR compared with other benchmark models and predict whether an advertisement is clicked or not by given advertisement information and user information. By establishing a reasonable advertising click-through rate prediction model, it can help the platform estimate future revenue so as to make cooperative decisions with advertisers. For advertisers, it is necessary to evaluate the price by predicting the click-through rate and estimate the bidding price of their own advertisements.

## 1. Introduction

**1.1. Research Background and Significance.** Online advertising, also known as online marketing, Internet advertising, or web advertising, is a form of advertising marketing that uses the Internet to deliver marketing information to consumers, including e-mail marketing, search engine marketing (SEM), social media marketing, and various forms of display advertising (such as web banner advertising) and mobile advertising. Compared with traditional TV, radio, magazines and newspapers, and other types of media advertising, Internet advertising has many natural advantages, mainly reflected in coverage, accurate positioning, and wide audience and targeting clear, fast, real-

time, update, flexible, and open interaction, the cost is more economic, and so on, thus widely favored by the industry and become an important part of modern marketing media strategy for enterprises. Online advertising is a multibillion-dollar business that generates huge revenues for many Internet companies, including Alibaba, Baidu, and Google.

Since its birth, online advertising has not stopped the pace of formal innovation. From the initial agreement-based advertising, which mainly focuses on display, it has continuously enriched the display content and methods of advertising with the progress of technology [1]. Online advertising has a variety of forms. According to the characteristics of application scenarios, it can be divided into sponsored search advertising (SSA) and contextual

advertising (CA) and display advertising [2]. SSA refers to the fact that advertisers determine keywords, titles, product descriptions, and other related attributes for their products according to the characteristics and incontinence of their products and conduct independent bidding for the advertising keywords [3]. CA refers to the commercial text advertising or display advertising related to web content automatically displayed at a certain position of the web page when Internet users browse the web page [4]. Display advertisement refers to the online advertisement directly displayed in the form of text, picture, and video when users browse the web page [5]. As an important form of display advertising, display advertising has the characteristics of high visibility, strong readability, and easy-to-obtain user recognition, and its application is increasing widely.

At present, most related work is mainly based on text and picture features and uses the features calculated by statistical learning methods to estimate the CTR. In this case, people usually extract colors (RGB, LAB, or HSV), brightness, saturation, texture, histogram of oriented gradient (HOG) [6], and scale-invariant feature transform (SIFT) [7] and apply them to advertising hit rate prediction tasks.

These picture features have weak generalization ability and are only effective for specific picture advertisements. They cannot be adjusted accordingly according to the changes in application scenarios. Effective picture features need to be screened manually. In addition, each feature is independent of each other, and the correlation between features is not fully reflected in the CTR prediction process. Constructing feature combinations is one of the important ways to mine the associated information between features. The traditional methods of constructing feature combination mainly rely on manual and prior knowledge and cannot construct higher dimensional feature combination. Therefore, how to automatically extract the visual features of pictures and fully mine the correlation between features with less manual intervention is of great research significance for the prediction of display advertising CTR.

Deep learning has become one of the hottest directions in the field of machine learning in recent years and has made amazing achievements in many application fields, such as speech recognition [8], image recognition [9], and business [10]. One of the core problems solved by deep learning is to automatically extract more complex features from simple features, so it is very suitable for data expression and feature extraction in the task of display advertising CTR prediction. In this paper, deep learning technology is applied to the prediction of display advertising CTR, which automatically completes the learning and combination of features, reduces the labor consumption of feature engineering, and improves the accuracy of advertising CTR prediction. Specifically, this paper divides the original features of display advertising into two parts, picture visual features and other basic features, and the Convolutional Neural Network (CNN) [11] in deep learning is used to extract the high-level semantic features of advertising pictures and enhance the representation ability of advertising picture features; then, the deep-level internal relationship between more features is mined

through deep neural network, so as to more effectively improve the effect of CTR prediction.

*1.2. Related Work and Analysis.* The accurate prediction of advertising CTR not only helps to improve the user experience but also is one of the important revenue sources of global Internet companies. It has important commercial value and academic research value. It has become an important research field in industrial and academic circles in recent years. On the whole, feature learning and feature combination are the key factors in improving the accuracy of display advertising CTR prediction. This paper will introduce the related research work of CTR prediction from these two angles.

In the aspect of feature learning, traditional research lacks effective methods to extract the high-level semantic features of advertising pictures. The traditional picture features are manual design features, which often focus on one aspect of the image, with limited representation ability and unable to capture the key high-level semantic features of the picture [12, 13]. For example, the hog feature focuses on the edge information of the picture, the SIFT feature focuses on the interest points of the local appearance of the picture, and the local binary pattern (LBP) [14] focuses on the texture of the picture. These picture features are only effective for specific tasks and cannot be adjusted according to different application scenarios to attract users' clicks. It is difficult to design and include all visual feature items highly related to CTR. The breakthrough development of deep learning provides a new idea to solve this problem and has been successfully applied to many image recognition problems [9, 15, 16]. Among them, CNN has made amazing achievements in the image field. It directly uses the original pixels of the picture as the input and retains all the information of the input picture to the greatest extent. The image features extracted by convolution and pooling operations of convolution neural network have good generalization. It not only achieves good performance in image classification tasks but also can be well generalized to other computer vision tasks, such as object detection, semantic segmentation, and video tracking. At present, there have been many researches on how to predict the CTR of advertising by using the high-level semantic features extracted by CNN. Feature learning, an image advertising feature learning architecture based on CNN [17], uses CNN to directly learn the high-level semantic features of images with recognition from the original pixels and user click feedback and then combine the basic features from advertising information. The CTR of each advertisement is predicted by logistic regression (LR) [18]. Feature learning solves the problem of data sparsity and cold start in advertising CTR prediction by adding additional picture high-level semantic features. It is one of the earlier works to apply picture high-level semantic features to advertising CTR prediction task. The deep CTR model proposed by Chen et al. [19] combines the picture high-level semantic features extracted by the convolution neural network with the advertising context features extracted by full connection layer; after batch normalization (BN) [20], it is

fed into the fully connected network together to integrate feature extraction and CTR prediction, to realize end-to-end training. DICM [21] (Deep Image CTR Model) model uses CNN to extract high-level semantic features from candidate advertising pictures and pictures clicked by users and jointly predict the probability that an advertisement is clicked by users by combining advertising features and user features.

In the aspect of constructing feature combination, most studies solve the problem of advertising CTR prediction based on traditional models. LR model has the characteristics of simple implementation, strong interpretability, and easy parallel. It is widely used in industry. However, in the LR model, the meaning of each dimension of features is fixed and isolated, which cannot fully mine the nonlinear association between features. Therefore, the LR model needs to manually construct combined features to mine the association between features, which has many problems, such as low efficiency and unable to migrate domain knowledge. Factorization machine (FM) uses matrix decomposition, regards the weight matrix as the inner product of two identical hidden vectors, and constructs the second-order combination between any two features [22], which effectively solves the problem of feature combination under large-scale sparse data. It is widely used in recommendation system, advertising CTR prediction, and other applications. Juan et al. [23] draw on the concept of the field. Jahrer et al. [24] add domain information to features on the basis of FM and propose a domain perception decomposition machine (field aware factorization machine, FFM) model. FFM model combines features with the same or similar properties into the same domain, so the implicit vector of features is not only related to the feature itself but also related to its corresponding domain. Compared with the FM model, the FFM model learns one more layer of domain information and better excavates the implicit information in features. FM model and FFM model can be constructed with any height in theory. However, due to the computational complexity, it can only express the pairwise combination relationship between features. In addition, the FM model constructs feature combination based on the linear method, which cannot fully mine the highly nonlinear association between features. Deep learning is famous for its ability to learn deep-seated nonlinear features, which reduces the intervention of artificial feature engineering to a certain extent. Most research methods use the corresponding network structure to automatically learn the high-order combination between features. The factor decomposition machine-supported neural network (FNN) proposed by Zhang et al. [25] adds a neural network on the basis of the FM model to better mine the internal relationship between features. Qu et al. [26] proposed a product-based neural networks (PNN) model based on vector product, which uses the second-order vector integration (pair wisely connected product layer) to carry out pairwise vector product on the embedded vector of FM model and then inputs it into a fully connected neural network to effectively construct high-order feature combination. Aiming at the defect that the FM model gives the same weight to all combined features, Xiao et al. [27] proposed a factor decomposition machine model based on

the attention mechanism (Attentional Factorization Machine, AFM), introducing the popular attention mechanism [28], automatically learning different weights of second-order combined features, paying attention to feature combinations with high influence, reducing the impact of invalid or even interfering information, better mining the internal correlation between features, and playing a certain role in improving the prediction effect. The classical width and depth model is proposed by Cheng et al. [29] (Wide & Deep, WDL model), the LR model in the width part and the neural network in the depth part are jointly trained, and the final fusion model effectively constructs the low-order combination and high-order combination of features, which has been successfully used in app ranking recommended by the app store. In order to extend the second-order combination of the FM model to a high-order combination, the depth and cross-network proposed by Wang et al. [30] (Deep & CrossNetwork, DCN) uses polynomial multiplication to directly extract by depth network to comprehensively mine the internal correlation between features.

To sum up, in view of the outstanding performance of CNN in the image field, this paper uses CNN to extract high-level semantic features of images with strong generalization ability. However, the current CNN is mainly used in image classification and object recognition tasks with category labeling information training and cannot be applied to advertising image feature extraction tasks for image advertising CTR prediction. Therefore, this paper needs to improve the existing convolution neural network structure to make it suitable for the feature extraction task of advertising pictures. Learning the high-level features of advertising pictures and fully mining the correlation between features by constructing combined features is the research content of this paper. It can be seen from the above that the deep learning neural network has a high ability for feature combination and construction, which has a certain reference significance for mining the correlation between features. This paper uses its multilayer network structure to mine the nonlinear correlation between features so as to more effectively improve the accuracy of hit rate prediction.

## 2. Method

In display advertising, most of the related work is mainly based on text and picture features, and the statistical learning method is used to estimate the CTR. In this case, most of the traditional methods of extracting advertising picture features are manual extraction based on special purposes, with weak generalization ability and only effective for specific tasks, requiring manual screening of effective visual features. In addition, each feature is independent of each other, and the correlation between features is not fully reflected in the CTR prediction process. It is necessary to rely on manual experience to construct combined features, which has many problems, such as low efficiency and unable to transfer domain knowledge. Aiming at the problem that traditional methods cannot filter features quickly and effectively and fully mine the correlation between features, this paper

proposes an end-to-end CTR prediction depth model for display advertising by using deep learning technology.

**2.1. Symbol Definition and Problem Description.** In order to explain the depth prediction model of display advertising CTR proposed in this paper, the important symbols and definitions in this paper are summarized in Table 1.

**2.2. Problem Description.** In order to publish activities in the display advertising system, advertisers upload their advertising pictures and specify the targeted target of the product (user division, time, region, etc.) and the advertising budget during the event. At the same time, advertisers will also allocate a small amount of budget to purchase statistics or institutional data, learn the user's feedback mode, and carry out effective audience orientation. When users initiate a web page request, advertisers use advertising pictures and corresponding historical CTR data to estimate the CTR of this display and purchase the opportunity to present the advertisement to the current user from the advertiser according to the estimated value. In this paper,  $x$  is used to represent an advertising picture. In advertising pictures, the features are divided into two parts: basic features and picture features. The basic features are generally advertiser ID, advertiser name, advertising space ID, advertising space name, advertising category ID, creative image width, creative image height, and so on. In this paper,  $p = [p_1, p_2, \dots, p_M]$  represents the basic features of advertising picture  $x$ , where  $M$  represents the number of basic features. The visual feature of the advertising picture is the advertising creative picture of  $224 \times 224 \times 3$ , where  $224 \times 224$  represents the size of the creative picture and  $\times 3$  represents that the creative picture is a three-channel color picture; that is, there are three channels under the RGB color model in the three primary color light mode, namely, red, yellow, and blue. In this paper, the creative image is marked as the three-dimensional matrix  $G \in R^{224 \times 224 \times 3}$  of  $224 \times 224 \times 3$ , and each element value in the matrix represents the RGB three-channel color value of the pixel in the creative image. In this paper, each advertising image  $x$  is defined as a binary composed of the basic feature  $p$  and the pixel matrix  $G$  of the creative image, that is,  $X = (p, G)$ .

Suppose that the training data set  $D$  is a data set containing  $N$  advertising pictures and corresponding CTRs.  $X = \{x_1, x_2, \dots, x_N\}$  is defined as the advertising picture data set, and the corresponding CTR is  $Y = \{y_1, y_2, \dots, y_N\}$ , where  $y_i \in [0, 1]$  indicates that the real CTR of advertising picture  $x_i$  is  $y_i$ . Given  $n$  advertising pictures  $X$  and corresponding CTR  $Y$ , the specific definition of training data set  $D$  is shown in

$$D = \{(x_1, y_1), (x_2, y_2), \dots, (x_N, y_N)\}. \quad (1)$$

Among them, each sample  $(x_i, y_i) \in D_i$  indicates that the real CTR of advertising picture  $x_i$  is  $y_i$ .

Given a display advertising training data set  $D$ , the problem of estimating the CTR of display advertising can be formally defined as follows: based on the training data set  $D$ , learn a model  $f(\cdot)$  to estimate the probability  $\hat{y}$  of users

clicking on the picture advertisement on the page after opening the page; see

$$\hat{y} = f(x; \theta), \quad (2)$$

where  $f(\cdot)$  represents the CTR prediction model,  $\hat{y} \in (0, 1)$  represents the click-through probability value calculated by the prediction model  $f(\cdot)$  for a given advertising picture  $x$ , and  $\theta$  represents the relevant parameters of model  $f(\cdot)$ .

Based on the definition of the above concepts and problems, the problem definition of picture advertisement CTR prediction based on deep learning studied in this paper is given as follows: given a picture advertisement training data set  $D$ , the task of the picture advertisement CTR prediction depth model is to automatically learn a prediction model  $f^*$  with the smallest error from the training data set  $D$ , so given a picture advertisement training data set  $D$ , the task of the picture advertisement CTR prediction depth model is to automatically learn a prediction model  $f^*$  with the smallest error from the training data set  $D$ , so as to minimize the error between the predicted value  $\hat{y}$  and the real value  $y$  given by the model as shown in

$$f^* = \arg \min (\text{error}(\hat{y}, y)). \quad (3)$$

**2.3. Display Advertising CTR Prediction and Optimization Objectives.** The CTR prediction of display advertising uses the basic characteristics, including advertisers, advertising spaces, advertising categories, creative image attributes, and other pieces of information, as well as the visual characteristics of advertising pictures, to predict the probability that an advertising picture is clicked by users. Therefore, this paper defines it as a regression problem to predict the specific CTR value. The most used performance measure for regression tasks is square loss, also known as the mean square error (MSE). It uses Euclidean distance as the measurement error to represent the difference between the predicted value and the real value. The smaller the loss function is, the closer the predicted value of the model is to the real value [31]. Therefore, this paper uses the square loss to measure the error of the model. The error of a single sample is defined in

$$\text{error}(\hat{y}, y) = (\hat{y} - y)^2. \quad (4)$$

Then, the loss function of the whole data set  $D$  can be defined as

$$L(\theta) = \frac{1}{N} \sum_{i=1}^N (\hat{y}_i - y_i)^2 + \lambda \theta_2^2. \quad (5)$$

Among them,  $\theta$  represents the relevant parameters of the prediction model,  $\theta_2^2$  represents the  $L_2$  norm regular term, which is used to prevent overfitting problems in the process of parameter optimization,  $N$  represents the number of samples, and  $y_i$  represents the real value of the  $i$ th sample.

Based on the definition of (5), the overall optimization objective of the display advertising CTR prediction depth model can be given, as shown in

TABLE 1: Important symbols and meanings.

Symbol	Meaning description
$x$	Represents an advertising picture
$p$	Represents the basic characteristics of an $x$ , represented by a multidimensional vector
$G$	Represents a picture feature of $x$ , corresponding to a three-dimensional matrix $G \in R^{224 \times 224 \times 3}$ representing the pixel information of the advertising creative image. Each element value in the matrix represents the RGB three-channel color value of the pixel in the creative image
$y$	Represents the real CTR of $x$
$X$	Advertising picture dataset $X = \{x_1, x_2, \dots, x_N\}$
$Y$	Real hit rate set $Y = \{y_1, y_2, \dots, y_N\}$
$D$	Training data set $D$
$N$	Number of training set samples
$f(x; \theta)$	Advertising CTR prediction depth model $\theta$ represents the correlation of the prediction model
$\hat{y}$	Click probability predicted by the model
$L(f(x; \theta))$	Loss function of display advertising CTR prediction depth model

$$\theta^* = \arg \min \left( \frac{1}{N} \sum_{i=1}^N (\hat{y}_i - y_i)^2 + \lambda \theta_2^2 \right). \quad (6)$$

As can be seen from (6), the goal of the picture advertisement CTR prediction depth model is to solve a set of parameters  $\theta^*$  of the model, which can minimize the square loss  $L$  based on the training data set  $D$ , so that the predicted value  $\hat{y}$  calculated by the model is as close as possible to the real value  $y$ . Recognition of handwritten character strings is a process of analyzing and processing handwritten note images and segmenting and recognizing characters to obtain electronic texts. This process needs to collect a large number of data images to improve the accuracy of codes.

**2.4. Depth Prediction Model of Display Advertising CTR.** This section first gives the overall network structure of the display advertising CTR prediction depth model proposed in this paper. Then, the basic principles of different components in the network are described in detail. Finally, the algorithm flow of the display advertising CTR prediction depth model proposed in this paper is completely displayed. The residual network still satisfies the nonlinear layer and then directly introduces a short connection from the input to the output of the nonlinear layer so that the whole mapping becomes a complete mapping. This is the core formula of the residual network; in other words, the residual is an operational construction of the network, and any network that uses such an operation can be called a residual network.

**2.4.1. Model Overview.** Figure 1 shows the overall network structure of the display advertising CTR prediction depth model. As can be seen from Figure 1, the model proposed in this paper is an end-to-end prediction model integrating feature extraction of display advertising and CTR prediction. The network structure of the model can be divided into three main parts from low level to high level: (1) residual network for extracting high-level semantic features of creative image; (2) embedding layer for transforming basic features into low-dimensional real number vectors; (3) mining the fully connected network between features and the output layer to output the hit rate prediction results. The remaining sections

of this paper will introduce the specific structure and basic principles of these three parts in detail. This shows the specific operation process of ctr, which is different from the continuous and dense data in the fields of image and speech, and the local correlation in space and time is good.

**2.4.2. Residual Network.** In this paper, the residual network is used to extract the high-level semantic features of advertising creativity image. The overall network structure is shown in Figure 2. The residual network further satisfies the nonlinear layer and then directly short-circuits the output of the nonlinear layer to the output so that the entire mapping becomes the core formula of the residual network. That is, the residual of any network that uses this function can be called a residual network.

**2.4.3. Basic Feature Embedding.** In display advertising, the basic features are usually composed of a large number of discrete features and a few continuous numerical features. The embedding layer transforms a high-dimensional sparse vector into a low-dimensional real vector, which can effectively reduce the dimension of features. In this paper, the embedding layer is used to image the basic features to several low-dimensional real number vectors to alleviate the sparsity of the basic features in display advertising. The following describes the basic characteristics of the single heat coding type and the numerical coding type, respectively.

The embedding process of unique heat coding type features is shown in Figure 3, and its input is a unique heat coding vector. If the  $i$ th basic feature  $p_i$  is a unique hot coding type feature, its embedding process is shown in

$$e_i = V_i p_i, \quad (7)$$

where  $e_i \in R^K$  represents the embedding representation of the unique heat coding feature  $p_i$  learned through the embedding layer,  $K$  represents the vector dimension after embedding,  $V_i \in R^{n_i \times K}$  represents the embedding matrix, and  $n_i$  represents the dimension of the binary vector  $p_i$ .

This is a summary of the entire process of feature selection. The so-called embedded feature selection is to fit the data through some special models, then use some attributes

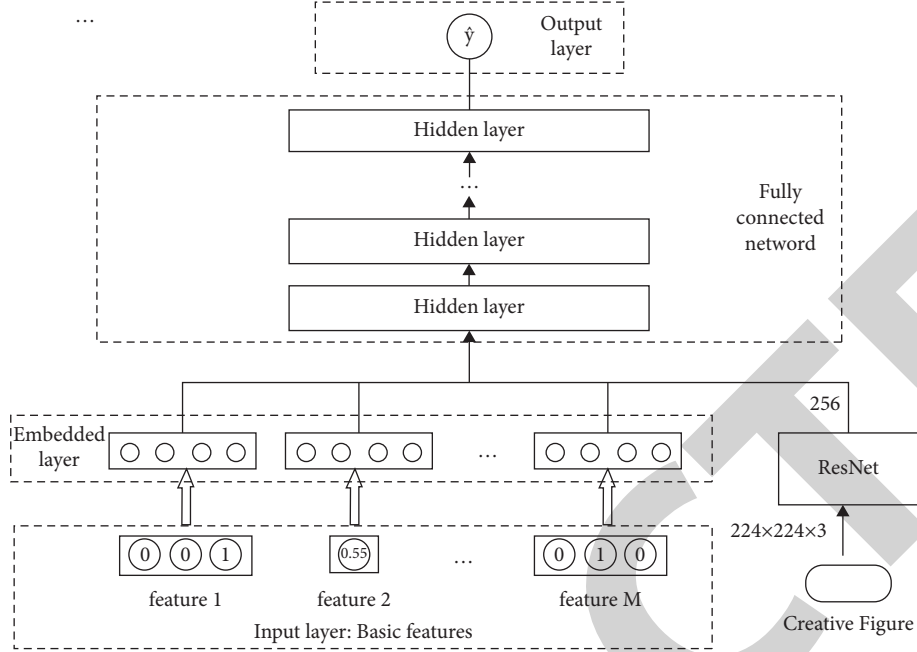


FIGURE 1: Overall network structure of display advertising CTR prediction depth model.

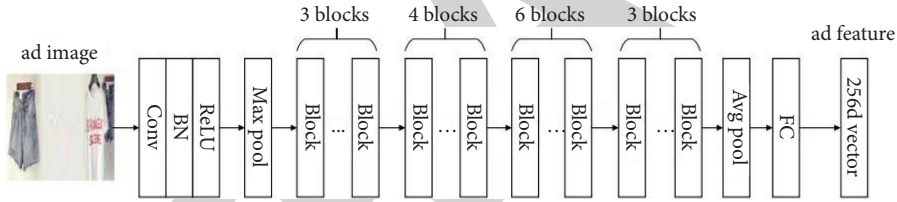


FIGURE 2: The overall network structure.

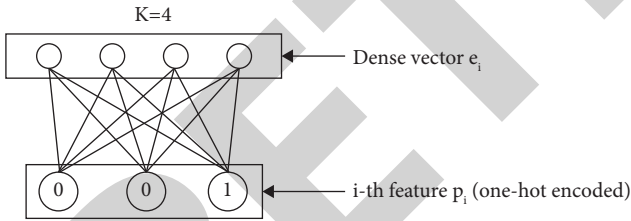


FIGURE 3: Schematic diagram of embedding layer of unique heat coding type features.

of the model itself to evaluate the features as evaluation indicators, and finally a selection is made using a packaging feature selection method. Of course, in many cases, we still stay at the stage of calculating the evaluation index, because the biggest problem of packaging feature selection is that the amount of calculation and time are the largest of the three. Assuming that the  $j$ th basic feature  $p_j$  is a numerical feature, the embedding process is shown in

$$e_j = V_j p_j, \quad (8)$$

where  $e_j \in R^K$  represents the numerical feature,  $p_j$  represents the embedded representation learned through the embedded layer,  $K$  represents the vector dimension after

embedding, and  $V_j \in R^K$  represents the embedded vector corresponding to  $p_j$ . Figure 4 shows the embedded layer of numerical features.

Connect the features of an advertising picture to generate a more comprehensive and effective feature expression  $e$  for an advertising picture  $x$ , as shown in

$$e = [e_1, e_2, \dots, e_M, e_G]. \quad (9)$$

**2.4.4. Fully Connected Network.** In this paper, a fully multilayer connected neural network is used to fully mine the nonlinear relationship between features, to improve the prediction results of CTR more effectively. There is no interconnection between neurons in the same layer. Each neuron is only connected to all neurons in the previous layer, receives the output of the previous layer, and inputs it to the next layer. The first layer is called the input layer. In this paper, the advertising picture feature  $e$  is used as the input  $a^{(0)}$  of the fully connected neural network, as shown in

$$a^{(0)} = [e_1, e_2, \dots, e_M, e_G]. \quad (10)$$

The fully connected neural network contains one or more hidden layers, and each hidden layer performs the calculation of (11) and (12):



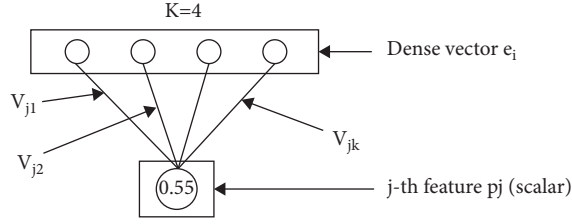


FIGURE 4: Schematic diagram of embedded layer of numerical features.

$$z^{(l+1)} = W^{(l)} a^{(l)} + b^{(l)}, \quad (11)$$

$$a^{(l+1)} = \sigma^{(l)}(z^{(l+1)}), \quad (12)$$

where  $l$  represents the depth of the hidden layer,  $\sigma^{(l)}$  represents the activation function of layer  $l$ ,  $m^{(l)}$  represents the

number of neurons in layer  $l$ ,  $z^{(l+1)} \in R^{m^{(l+1)} \times m^{(l)}}$  represents the net input of neurons in layer  $l+1$ ,  $a^{(l)} \in R^{m^{(l)}}$  represents the output of neurons in layer  $l$ , and  $W^{(l)} \in R^{m^{(l+1)} \times m^{(l)}}$  represents the weight matrix from layer  $l$  to layer  $l+1$ . Combine (11) and (12) to obtain

$$a^{(l+1)} = \sigma^{(l)}(W^{(l)} a^{(l)} + b^{(l)}). \quad (13)$$

In this way, the fully connected neural network can use its multilayer network structure to automatically learn the nonlinear correlation between features and obtain relatively high-order combined features. Among them, different hidden layers in multilayer networks are different potential representations of the input layer. They form more abstract high-level features by combining low-level features, and they can fully mine the association between features. Finally, the output definition of the fully connected network is shown in

$$h_L = \sigma^{(L)}(W^{(L)}(\sigma^{(L-1)}(W^{(L-1)} \dots \sigma^{(1)}(W^{(1)} a^{(0)} + b^{(1)})) + b^{(L-1)}) + b^{(L)}), \quad (14)$$

where  $L$  represents the number of hidden layers in the fully connected network.

Finally,  $h$  is passed through the regression layer to obtain the predicted value  $\hat{y}$  of CTR, as shown in

$$\hat{y} = Wh_L + b, \quad (15)$$

where  $W$  represents the weight matrix of the regression layer and  $b$  represents the offset vector.

**2.4.5. Optimization Algorithm.** In order to better learn the depth prediction model of display advertising CTR proposed in this paper, we use the adaptive motion estimation (Adam) algorithm with an adaptive learning rate to optimize the objective function  $L$  defined in formula (5) [32]. In this paper, the first-order moment estimation and second-order moment estimation of the gradient are calculated by the Adam optimizer, independent adaptive learning rates are designed for different parameters, and only a few parameters are needed. Firstly, the algorithm initializes the relevant parameters  $\theta$  of the prediction model, the first-order moment variable  $s$ , the second-order moment variable  $R$ , and the time step  $t$  of the Adam optimizer; Then, taking  $m$  as a minibatch, a group of samples  $\{x^{(1)}, \dots, x^{(m)}\}$  are taken, where  $x^{(i)}$  corresponds to  $y^{(i)}$ , and the sample prediction is completed according to the given CTR prediction depth model  $f(x, \theta)$ . Finally, the objective function  $L$  is calculated, and the corresponding model parameter value  $\theta$  is updated based on the gap between the predicted value and the real value so that the prediction result of the model on this minibatch of data is closer to the real CTR.

### 3. Experimental Design and Result Analysis

#### 3.1. Experimental Dataset

**3.1.1. Data Description.** The data set used in this experiment comes from the real data set of display advertising privately owned by a commercial advertising platform. During the experiment, we collected all data from November 21 to 23, 2017, including 100000 samples involving 55725 creative images. In this paper, all fields of the display advertising data set are collected to form Table 2. In the display advertising dataset of this paper, each sample contains three kinds of information: (1) the advertiser, advertising space, advertising category, and corresponding creative attributes of an advertising picture, in which the creative attributes describe the relevant information of the corresponding advertising creative image from the aspects of format, name, width, height, and URL; (2) the creative image corresponding to the advertising picture; (3) the actual CTR of the advertising picture.

Data format description and sample display based on Table 2.

**3.2. Data Preprocessing.** The purpose of data preprocessing is to convert display advertising data into recognizable input during model operation. This section introduces the data preprocessing methods of the experiment from two aspects: creative diagram and basic features.

**3.2.1. Image Feature Preprocessing.** The image advertising data set in this paper contains a variety of creative drawings of different sizes, such as  $160 \times 200$ ,  $240 \times 164$ ,  $320 \times 175$ ,



TABLE 2: Detailed data format of display advertising data set.

Serial number	Attribute field	Sample	Description
1	advertiserID	1046141401	Advertiser ID
2	advertiserName	Pink-girl European and American women's wear	Advertiser name
3	adzoneID	34492608	Adzone ID
4	adzoneName	Wireless_flow packet_online shopping_hand amoy app_hand panning focus image	Adzone name
5	maincateID	1	Maincate ID
6	maincateName	Women's wear	Maincate name
7	Date	2017-11-21	Date
8	ctr	5	CTR (%)
9	adboardID	842306140001	Adboard ID
10	adboardFormat	1	Adboard format
11	adboardName	Good looking series	Adboard name
12	adboardWidth	640	Adboard width
13	adboardHeight	200	Adboard height
14	imageUrl	TB1CfLzpL5TBuNjSspmSuuDRVXa	Image URL
15	templateID	2000000000	Template D

$520 \times 280$ , and  $640 \times 200$ . In this experiment, the bilinear interpolation method is used to uniformly adjust the original creative image of the data set to  $224 \times 224$  size and make the target image retain all the information on the original creative image as much as possible.

**3.2.2. Basic Feature Preprocessing.** The discrete features in the basic features are processed as follows: the first step is to map some data in order to reduce the data storage space and facilitate feature extraction and data operation. In this paper, the discrete features of string identification are used in statistical samples, and then the character identification is mapped to the range of natural numbers starting from zero. The second step is to reprocess the discrete features in the whole data set. When a feature string is encountered, the natural number corresponding to the string is used to replace the feature.

### 3.3. Benchmark Model and Evaluation Index

**3.3.1. Benchmark Model.** In the experiment, the display advertising CTR prediction depth model proposed in this paper is compared with six other different models. In this paper, these models are divided into two categories, traditional advertising CTR prediction model and deep learning model, and two different traditional prediction models are compared. They are as follows: (1) LM: linear regression is used to estimate the CTR, and only the basic characteristics of advertising pictures are considered in the prediction process [33]; (2) LM\_HOG: linear regression is used to estimate the CTR, and both the basic characteristics of advertising pictures and HOG characteristics are considered in the prediction process [6]. In this paper, five different depth learning models are compared in the experiment, which are as follows:

- (1) DNN\_basic: use the fully connected network to directly predict the CTR of advertising pictures and only consider the basic characteristics of advertising pictures in the prediction process.

- (2) DL\_basic: the depth prediction model of display advertising CTR proposed in Section 3 of this paper only considers the basic characteristics of advertising pictures in the prediction process. DL\_basic model can be regarded as the CTR prediction model after removing the residual network.
- (3) Feature learning: consider both the basic features of advertising images and the high-level features of images. In the data set of this paper, due to the lack of label data of click events corresponding to advertising images, this paper uses advertising images and corresponding CTRs to pretrain its convolution neural network. Then, the trained network is used to extract the high-level semantic features of creative images. Finally, combining basic features with high-level visual features and the probability of an advertisement image being clicked by users is predicted by linear regression.
- (4) DeepCTR: the CTR prediction model of display advertising based on a deep network considers the basic characteristics of advertising pictures and high-level characteristics of pictures at the same time.
- (5) DL: the depth prediction model of display advertising CTR proposed in this paper considers the basic characteristics of advertising pictures and high-level characteristics of pictures at the same time.

For the DNN\_basic model, this paper conducted many comparative experiments and finally chose to set the number of fully connected network layers as 3 and the number of neurons at each layer as 1024. For the DL\_basic model, different combinations of fully connected layers and neurons are compared when the dimension of embedded representation is 5, 10, 15, 20, 25, and 30, respectively. The experimental results show that the DL\_basic model performs best in the case of a 15-dimensional embedding representation and two fully connected layers containing 1024 neurons. For the DL model, this paper uses the Keras application module to provide the ResNet50 network with pretraining weights and fine-tune network and feature

TABLE 3: Performance comparison of different CTR prediction models on test sets.

	Model	RMSE	MAPE (%)
Traditional prediction model	LM	0.0499	85.44
	LM_HOG	0.0455	74.55
Deep learning mode	DNN_basic	0.0365	63.20
	DL_basic	0.0254	44.48
	Feature_learning	0.0375	68.25
	DeepCTR	0.0263	44.80
	DL	0.0207	35.54

extraction on this basis. Specifically, this paper uses the ResNet50 network for image classification, pretrained on the ImageNet dataset, to remove the top full connection layer and add a full connection layer containing 256 neurons for fine tuning.

During the experiment, all models were trained on the training set, and the hyperparameters of the model were adjusted through the verification set. Finally, the performance of the model was tested on the test set. In this paper, the training cycle is set to 50, the batch size is set to 120, and the learning rate was set to 0.001 and reduced to 0.1 of the original learning rate after every 10 cycles. CTR refers to the ordering of the refined layer. Therefore, the candidate ranking set of the CTR model is generally thousands of orders of magnitude. CTR is generally divided into two layers: recall and sorting. Recall is responsible for roughly selecting thousands of items from millions of items. Common algorithms include collaborative filtering and user portraits, which are sometimes called rough sorting layers; sorting is responsible for fine sorting of thousands of items recalled by the recall layer, also called the refinement layer; it calculates the underlying general technology of advertising. Under the CPC/OCPC marketing model, the estimation accuracy plays a very important role in the advertiser's traffic purchase cost and platform monetization efficiency.

**3.4. Performance Comparison Experiment.** Table 3 completely shows the experimental results of performance comparison between the DL model and the other six benchmark models in the image advertising data set of this paper.

From the experimental results, the performance of the LM model based on a single feature is the worst, indicating that the LM model has limited performance and cannot effectively learn the internal association between features. The RMSE and MAPE performance of the DNN\_basic model was significantly better than the LM model, with a relative improvement of 26.9% and 26.0%, respectively. This shows that the multilayer network structure of deep learning can effectively mine the internal correlation between features and provide great help in performance improvement. DL\_basic introduces an embedding layer to transform basic features into low-dimensional real number vectors, which has a relative improvement of 30.4% and 29.6% compared with RMSE and MAPE indexes of the DNN\_basic model.

This shows that the embedded representations learned by the embedding layer can well represent the basic features. After these embedded representations are spliced into vector inputs to the neural network, the internal associations between features can be mined more effectively.

## 4. Summary

With the development of the Internet and e-commerce, display advertising, as an important form of display advertising, has the characteristics of high visibility, readability, and easy-to-obtain user recognition; an increasing number of Internet companies are paying attention to display what kind of advertising pictures can attract more clicks.

In view of the problem that traditional methods cannot quickly and effectively screen image visual features, this paper uses CNN to extract high-level image features quickly and effectively from advertising images and images with large-scale sparse features into low-dimensional dense real vectors through the embedding layer. Thus, the visual features of images are extracted explicitly, and the sparsity of image advertising data sets is solved, which is the basis of the subsequent research.

In addition, this paper uses the multilayer network structure of a deep network to learn the deep-seated non-linear features, to solve the problem that the traditional model only considers each feature independently and does not excavate the information defects hidden between features, thus improving the accuracy of CTR estimation more effectively.

Furthermore, in order to verify the correctness and effectiveness of the model proposed in this paper, we conducted several experiments on the private image advertising data set of a commercial advertising platform. In the performance comparison experiment, the results show that the proposed model can effectively improve the prediction accuracy of advertising CTR compared with other benchmark models. The neural network layers inside DNN can be divided into three categories, input layer, hidden layer, and output layer; as shown in the following figure, the first layer is the input layer, the last layer is the output layer, and the middle layers are the hidden floor. The number of layers of a neural network is calculated in this way. The input layer is not counted. From the hidden layer to the output layer, a total of several layers represents a neural network with several layers. This kind of hierarchical network learning is a problem-solving idea, which corresponds to multistep problem solving; that is, a problem is divided into multiple steps to solve step by step, and the end-to-end data is directly obtained from the input data result. That is, without pre-processing and feature extraction, throw the original data directly into the result. Feature extraction is contained within the neural network, so the neural network is an end-to-end network.

## Data Availability

Experimental data on the results of this study can be obtained from the corresponding author upon request.

## *Retraction*

# **Retracted: Research on Segmentation Method of Greening Landscape of Urban Community Based on Improved U-Net Network**

### **Security and Communication Networks**

Received 26 December 2023; Accepted 26 December 2023; Published 29 December 2023

Copyright © 2023 Security and Communication Networks. This is an open access article distributed under the Creative Commons Attribution License, which permits unrestricted use, distribution, and reproduction in any medium, provided the original work is properly cited.

This article has been retracted by Hindawi, as publisher, following an investigation undertaken by the publisher [1]. This investigation has uncovered evidence of systematic manipulation of the publication and peer-review process. We cannot, therefore, vouch for the reliability or integrity of this article.

Please note that this notice is intended solely to alert readers that the peer-review process of this article has been compromised.

Wiley and Hindawi regret that the usual quality checks did not identify these issues before publication and have since put additional measures in place to safeguard research integrity.

We wish to credit our Research Integrity and Research Publishing teams and anonymous and named external researchers and research integrity experts for contributing to this investigation.

The corresponding author, as the representative of all authors, has been given the opportunity to register their agreement or disagreement to this retraction. We have kept a record of any response received.

## **References**

- [1] J. Sui, "Research on Segmentation Method of Greening Landscape of Urban Community Based on Improved U-Net Network," *Security and Communication Networks*, vol. 2022, Article ID 4834952, 9 pages, 2022.

## Research Article

# Research on Segmentation Method of Greening Landscape of Urban Community Based on Improved U-Net Network

Jing Sui <sup>1,2</sup>

<sup>1</sup>Kookmin University, Graduate School of Techno Design (TED), Seoul 02707, Republic of Korea

<sup>2</sup>LuXun Academy of Fine Arts, Shenyang 110003, China

Correspondence should be addressed to Jing Sui; [suijing@lumei.edu.cn](mailto:suijing@lumei.edu.cn)

Received 16 June 2022; Revised 7 July 2022; Accepted 17 August 2022; Published 14 September 2022

Academic Editor: Hangjun Che

Copyright © 2022 Jing Sui. This is an open access article distributed under the Creative Commons Attribution License, which permits unrestricted use, distribution, and reproduction in any medium, provided the original work is properly cited.

Aiming at the problem of low segmentation accuracy of greening landscape of urban community, a segmentation method of greening landscape of urban community based on improved U-Net network is proposed by adding an encoder on U-Net network. In addition, simulation is carried out on the remote sensing image data collected by GPRS network, and the effectiveness of the method is verified. The simulation results show that the result of proposed method is close to that of manual annotation. Compared with the traditional segmentation algorithm SVM and SegNet method, as well as the U-Net network before improvement, the proposed method has higher segmentation accuracy. The segmentation accuracy can reach up to 91%, the intersection ratio can reach 76%, and the mean pixel accuracy and mean intersection ratio can reach 89% and 74%, which indicates that the proposed method has certain validity and practicability.

## 1. Related Work

As a community of people's life, its environment affects people's living conditions. In recent years, with the improvement of human living standard, the requirements for community environment have been more and more strict, and more and more attention has been paid to community landscape greening space. At the same time, with the advancement of urbanization, for the requirements of sustainable urban development planning, community landscape greening space should be reasonably distributed. Therefore, whether the landscape greening space distribution in a community is reasonable is an important indicator to judge sustainable urban development. At present, there are few researches on the landscape greening space distribution of community, and there is no effective segmentation method. Therefore, with the help of deep learning image processing method, the landscape greening space distribution of community is studied. For example, Qu et al. used the combined information of SVM network and HSI spatial spectrum to realize multiscale hyperspectral image classification [1]. Zhou et al. extracted image features through K-L

transformation, mapped image features to quantum states through quantum coding, and used Hamming distance to represent image similarity. A new distance-weighted K-value classification method is proposed, which can achieve more accurate image classification [2]. Wang et al. used the symmetry theory and neural network to propose a symmetric neural network and proved the effectiveness of the algorithm by applying the classification algorithm to the classification of three-dimensional martial arts images [3]. Liu et al. introduced the idea of sparse representation into the architecture of deep learning network, thus a sparse representation classification method is proposed, which can replace the classifier of model and improve the effect of image classification [4]. Xiaoqing Zhang and Zhang adopted typical manifold learning method and local linear embedding (LLE) to construct graphs, and semisupervised classification was carried out on this basis. The classification of hyperspectral images is realized [5, 6]. On the basis of Weber's law, Kong et al. adopted multiresolution Weber local descriptor to propose a digital image forgery detection technology, which can achieve multiresolution image classification [7]. Martinez et al. used geographic processing and

remote sensing technologies to explore the effect of three image classification algorithms, MLC, SVM and RT. It is found that the three algorithms can distinguish the target successfully [8]. Among them, MLC has higher efficiency, RT has the lowest efficiency, and SVM has the highest accuracy. As can be seen, the deep learning has a good effect in the classification of image recognition, and the landscape greening space distribution of community is actually the classification of remote sensing image recognition. Therefore, using the deep learning to study the landscape greening space distribution of community, based on the urban community landscape collected by GPRS network, taking U-Net network as the basic framework, a landscape classification model can be constructed.

## 2. Basic Methods

**2.1. Overview of U-Net Network.** U-Net network is a classical full convolutional network, and it is composed of encoder and decoder, which is shown in Figure 1 [9]. The encoder is used to extract spatial features from the image, and its convolution block includes two  $3 \times 3$  convolution and maximum pooling operation. After downsampling, the filter in the convolution is doubled and connected to the decoder through convolution operation. According to the segmentation graph constructed by encoder, the decoder firstly uses  $2 \times 2$  convolution operation to upsample it, which reduces the feature channel to half of the original. Then, two  $3 \times 3$  convolution operations and one  $1 \times 1$  convolution operation are successively developed.

When the context information is transmitted to the high level, U-Net network adopts four jump connections to reduce the loss of high-resolution feature information, thus edge accuracy and resolution of final segmentation results are improved [10]. In recent years, U-Net network has been widely used to segment image because of its good segmentation effect. However, since the images used in the landscape greening space distribution of community in this paper are remote sensing images, there is often the problem of unequal target distribution. Moreover, if the standard U-Net network is used to construct classification model, the classification accuracy may be low. Therefore, in order to improve the segmentation accuracy, U-Net network needs to be improved.

**2.2. Improvement of U-Net Network.** The improvement of U-Net network mainly includes the following aspects:

- (1) To enhance the image minimum resolution receptive field, an encoder is added to original U-Net network to distinguish the input images with different levels of resolution;
- (2) To enrich context information, Concat is used in each upsampling block to fuse different levels of features;
- (3) To improve the speed of network training, all convolutional blocks are changed to deep convolutional blocks, and “one deep convolutional layer + one

batch standardization layer + one convolutional layer” is adopted to replace the traditional convolutional layer;

- (4) To ensure that downsampling can obtain more feature information, deep separable convolutional block is used to replace maximum pooling for downsampling;
- (5) To increase the receptive field of feature map, deep separable convolution of dilated convolution is adopted as the last three convolutional blocks;
- (6) To reduce the grid problem caused by dilated convolution, the dilation intervals of high and low resolution modules are set as 4 and 2, respectively.
- (7) To reduce the computational complexity and improve the segmentation accuracy, there is 512 depth adopted in the last coding block and the first decoding block to replace 1024 depth.

The structure of improved U-Net network is shown in Figure 2, and its encoding block and decoding block structures are shown in Figure 3.

## 3. Space Segmentation Model of Community Landscape Greening Based on Improved U-Net

The above improved U-Net network is adopted to construct segmentation model of community landscape greening space distribution, and the optimization method and loss function are configured. In addition, the adaptive threshold method is used to determine the thresholds of different landscape categories.

### 3.1. Network Configuration

**3.1.1. Optimization Method.** NAdam algorithm is a model optimization method proposed to improve the sensitivity of Adam optimization algorithm, in which Nesterov momentum term is added to correct the gradient in the updating process, which has better sensitivity [11]. Therefore, NAdam algorithm is adopted as model optimization method, and its formulas are as follows:

$$\begin{aligned}
 m_t &= \mu_t * m_{t-1} + (1 - \mu_t) * g_t, \\
 \hat{m}_t &= \frac{m_t}{1 - \prod_{i=1}^{t+1} \mu_i}, \\
 n_t &= \nu * n_{t-1} + (1 - \nu) * g_t^2, \\
 \hat{n}_t &= \frac{n_t}{1 - \nu} \bar{m}_t = (1 - \mu_t) * \hat{g}_t + \mu_{t+1} * \hat{m}_t, \\
 \Delta\theta &= -\eta * \frac{\bar{m}_t}{\sqrt{\hat{n}_t} + \epsilon},
 \end{aligned} \tag{1}$$

wherein formulas (1)–(3) are first-order momentum and second-order momentum, respectively; formulas (2) and formula (4) are corrected momenta;  $-\eta$  is the step size and  $\epsilon$

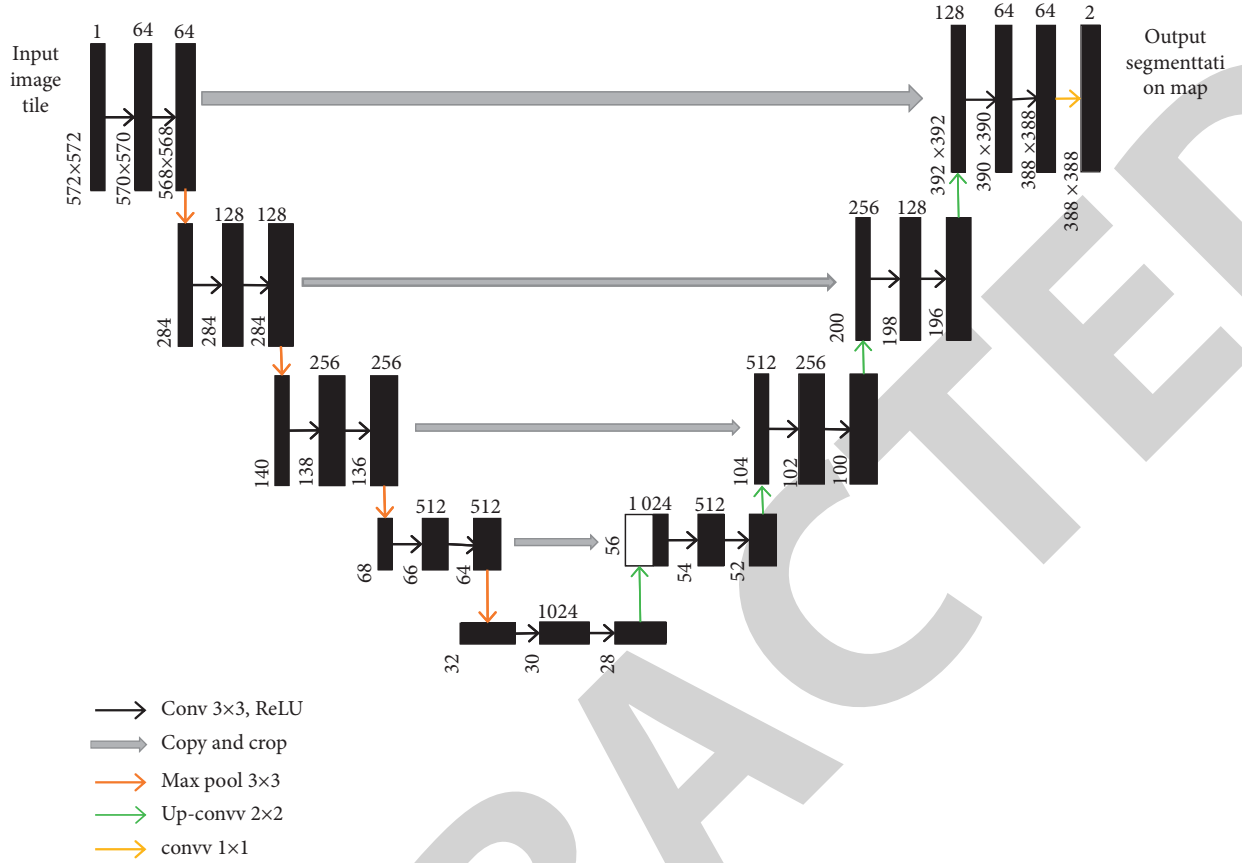


FIGURE 1: U-Net network structure.

is the lattice constant.  $g_t$  represents gradient descent value;  $\mu$  is the exponential decay rate, and its value range is  $[0,1]$ .  $m_t$  is the momentum vector.

**3.1.2. Loss Function.** The loss function directly affects the training effect of model. In image segmentation, the cross entropy function, as shown in formula (2), is mostly used as the loss function [12]. However, when sample categories are unbalanced, this loss function tends to lead to inaccurate model training results. In order to solve this problem, reference [13] introduces weight parameter  $\alpha$  to balance samples and dynamically adjust the loss function, which is defined as follows:

$$FL(p_t) = -\alpha_t (1 - p_t)^y \log(p_t). \quad (2)$$

**3.2. Adaptive Threshold.** Landscape greening space distribution of community is usually characterized by unbalanced landscape distribution and complex categories. If the same threshold judgment model is used to predict categories, it is easy to lead to large errors in the final segmentation results [14]. Therefore, adaptive threshold method is adopted to determine the optimal classification accuracy of different landscape categories. The threshold set of  $n$  classes is defined as  $T = \{t_1, t_2, \dots, t_n\}$ , and  $j^i(t)$  is the pixel accuracy of class  $i$ , then the threshold of class  $i$  can be expressed as follows:

$$t_i = \arg \max(j^i(t)). \quad (3)$$

## 4. Simulation Experiment

**4.1. Construction of Experimental Environment.** This experiment is conducted on Ubuntu 16.04 LTS operating system. The deep learning model is constructed based on Tensorflow 1.14 and Keras 2.4 frameworks. The CPU is configured as Intel (R) Core (TM) i7-6700CPU@3.40 GHz, and the memory is 16 GB. The GPU is NVIDIA GTX 1080Ti, which is implemented based on software, such as Arc GIS10.3 and MATLAB.

**4.2. Data Sources and Preprocessing.** The data in this study come from the remote sensing image data collected by a system through GPRS, which mainly contain 5 labeled large-size RGB remote sensing images [15, 16] of vegetation (No. 1), building (No. 2), water body (No. 3), road (No. 4), and others (No. 0). The image size is 4608 \* 4608, and the level is 17. Furthermore, the pixel resolution is 1.3 m, and the scale is 1 : 727.

Due to the influence of weather, geographical location, and other external factors in the process of experimental data collection, the image may have geometric distortion and atomization problems, so the image needs to be

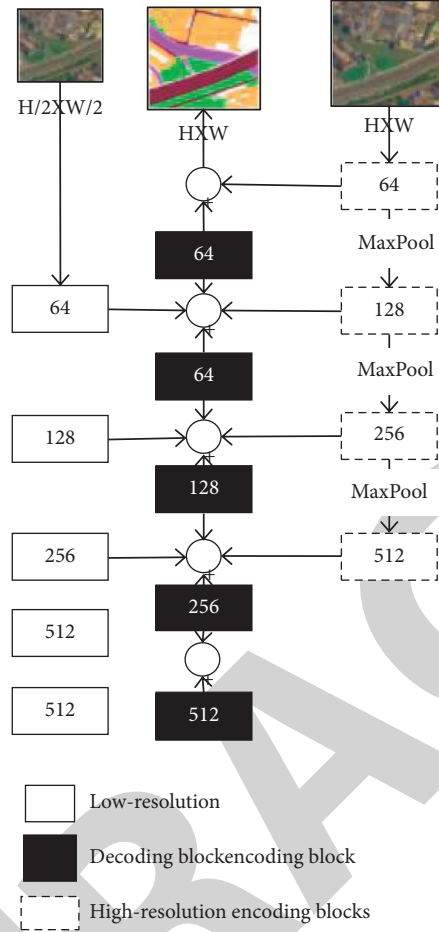


FIGURE 2: The improved U-Net network structure.

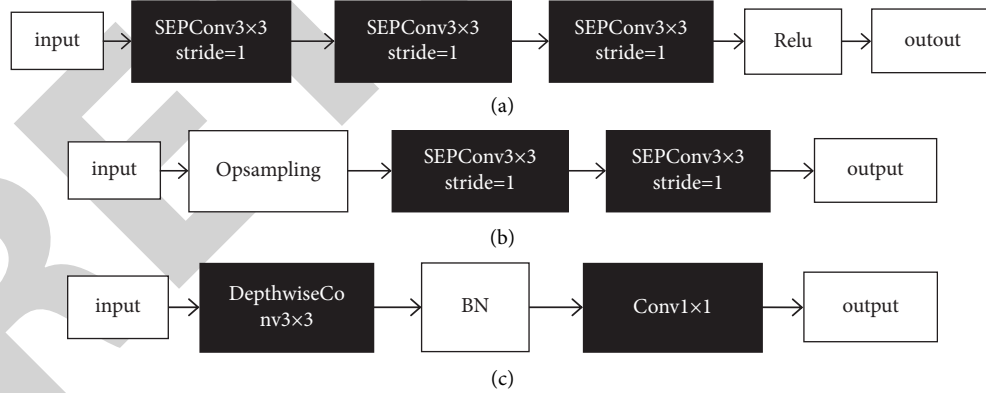


FIGURE 3: Encoding block and decoding block structure of improved U-Net network. (a) Encoding block structure (b) Decoding block structure. (c) SepConv structure.

preprocessed before experiment. According to the actual problems of remote sensing images, ENVI tool is used for geometric calibration of images, and image defogging algorithm based on channel priority is adopted for defogging treatment [17, 18]. The specific operation of defogging is as follows:

The dark channel is defined as the following formula:

$$J^{\text{dark}}(x) = \min_{c \in \{r, g, b\}} \left( \min_{y \in \Omega(x)} (J^c(y)) \right), \quad (4)$$

where  $x$  is the pixel point, and  $\Omega$  is the window in channel.

Then, the established atmospheric physical model is

$$I(x) = J(x)t(x) + A(1 - t(x)), \quad (5)$$



where  $I$  is the input image;  $J$  is the output image;  $A$  is the global atmospheric illumination intensity; and  $t$  is the transmittance, which can be calculated by the following formula:

$$\tilde{t}(x) = 1 - \omega \min_c \left( \min_{y \in \Omega(x)} \left( \frac{I^c(y)}{A^c} \right) \right), \quad (6)$$

where  $I^c$  is the input image and  $A^c$  is the global atmospheric illumination, as shown in the following formula:

$$\begin{aligned} A^c &= [A^R, A^G, A^B], \\ A^R &= \frac{\text{sum}_R}{N}, \\ A^G &= \frac{\text{sum}_G}{N}, \\ A^B &= \frac{\text{sum}_B}{N}, \end{aligned} \quad (7)$$

where  $\text{sum}_R$ ,  $\text{sum}_G$ , and  $\text{sum}_B$  represent the sum of coordinates of the brightest pixel point at 1/1000 of the total pixel point of the image found in  $J^{\text{dark}}(x)$  in the three channels of the original image. Combined with the atmospheric physical model, the defogging image can be obtained:

$$J(x) = \frac{I(x) - A}{\max(t(x), t_0)} + A. \quad (8)$$

In addition, in order to avoid over-fitting, data enhancements such as rotation, mirror image, and adding noise are performed for the data sets processed by geometric calibration and defogging.

Finally, the data sets are divided into training set and test set according to the ratio of 7:3.

**4.3. Evaluation Indicators.** There are pixel accuracy (PA), mean pixel accuracy (MPA), and mean intersection over union (MIoU) selected as indicators to evaluate performance of method, and the calculation methods are as follows [19–22]:

$$\begin{aligned} PA &= \frac{\sum_{i=0}^k P_{ii}}{\sum_{i=0}^k \sum_{j=0}^k P_{ij}}, \\ \text{MeanPA} &= \frac{1}{k+1} \sum_{i=0}^k \frac{P_{ii}}{\sum_{j=0}^k P_{ij}}, \\ \text{MIoU} &= \frac{1}{k+1} \sum_{i=0}^k \frac{P_{ii}}{\sum_{j=0}^k P_{ij} + \sum_{j=0}^k P_{ij} - P_{ii}}, \end{aligned} \quad (9)$$

where  $p_{ii}$ ,  $p_{ij}$ , and  $p_{ji}$  represent the true positive cases, false positive cases, and false negative cases, respectively.

#### 4.4. Experimental Results

**4.4.1. Model Verification.** To verify the effectiveness of proposed method, the performance of model under

different network configurations and adaptive thresholds is analyzed experimentally. Figure 4 shows the changes of model evaluation indicators with the epoch when different optimization methods are adopted. Compared with SGD method, loss of Adam and Nadam method decreases faster and accuracy increases faster. The SGD method reaches saturation in 10 epochs, and the Adam and Nadam methods reach saturation in 30 epochs. The test loss of Nadam method is closest to the verification loss, and the test accuracy is closest to the verification accuracy, indicating that using the Nadam method as a model training and optimization method has certain advantages.

Under the condition that other parameter conditions remain fixed, adaptive threshold method is adopted to train all types of data sets, and the changes of accuracy of different landscape pixels with probability thresholds are obtained as shown in Figure 5. As can be seen, the probability threshold of different categories is different. By comparing the best probability threshold of each classification, the best threshold of vegetation landscape classification can be obtained, and it is 0.6; the best threshold of road landscape classification is 0.4; the best threshold of building classification is 0.4; the best threshold of the water body classification is 0.6; and the best threshold of other classification is 0.3.

Taking roads as an example, the comparison of segmentation effects adding adaptive threshold and not adding adaptive threshold (0.5) is shown in Figure 6. As can be seen, the segmentation effect achieved by adding adaptive threshold is better.

**4.4.2. Model Comparison.** To verify the superiority of the proposed model, the segmentation results of different methods on CCF data set and BDS data set are compared. Figure 7 compares the segmentation results of proposed method with traditional classification methods SVM, SegNet, and U-Net on CCF data sets and provides manual annotation results as a reference. The SVM classification method is prone to misclassify buildings and roads, and there are many noise points in the segmentation results. Compared with SVM classification methods, SegNet and U-Net segmentation methods reduce the misclassification and noise points, but there are still problems of misclassification and missing classification of buildings and roads. The proposed method can segment all categories well, and the segmentation effect of buildings and roads is better than that of the contrast method. The reason is that when the target is segmented, the proposed method can fuse multi-scale cross features and expand the receptive field, thus the global feature during target segmentation is better extracted. On the whole, compared with the contrast method, the image segmentation result of proposed method is closer to manual annotation result, and the visual effect is the best.

Figure 8 shows the segmentation result evaluation of different methods on CCF data set. The pixel segmentation accuracy and mean intersection over union of proposed method are higher than those of contrast method for all

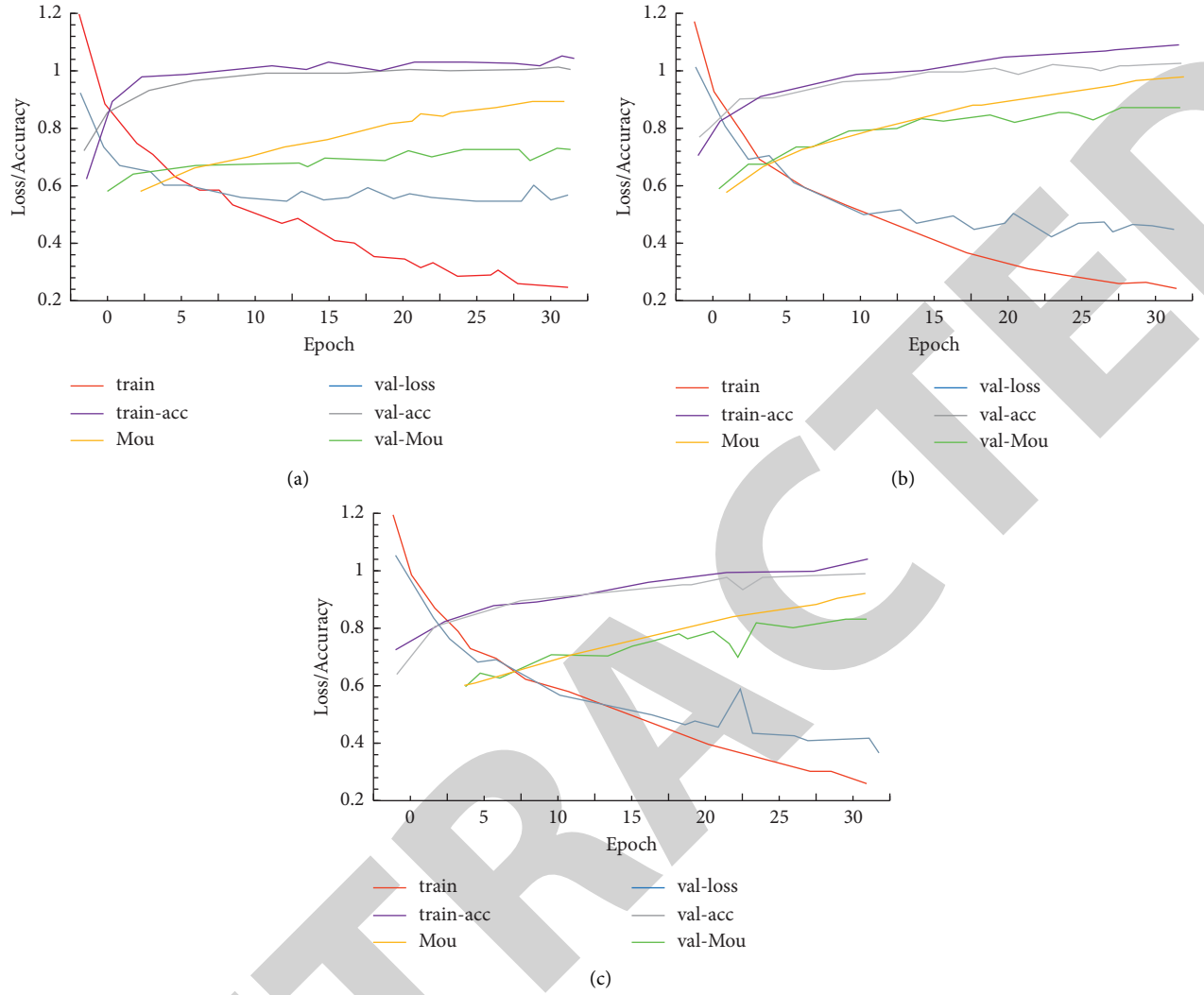


FIGURE 4: Changes of evaluation indicators of different optimization methods with epoch. (a) SGD. (b) Adam. (c) Nadam.

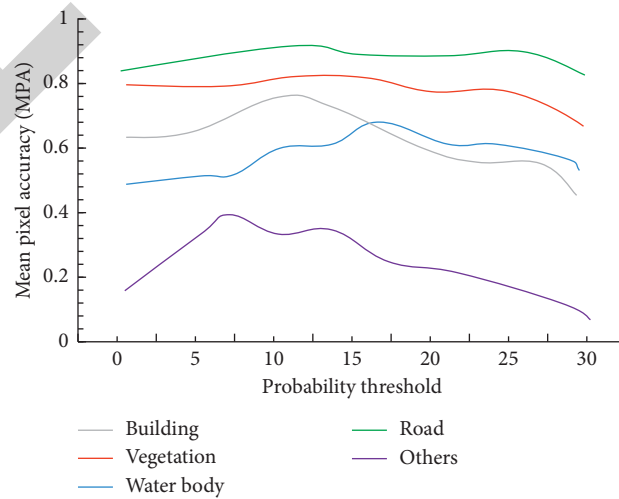


FIGURE 5: Changes of different landscapes pixel accuracy with probability threshold.

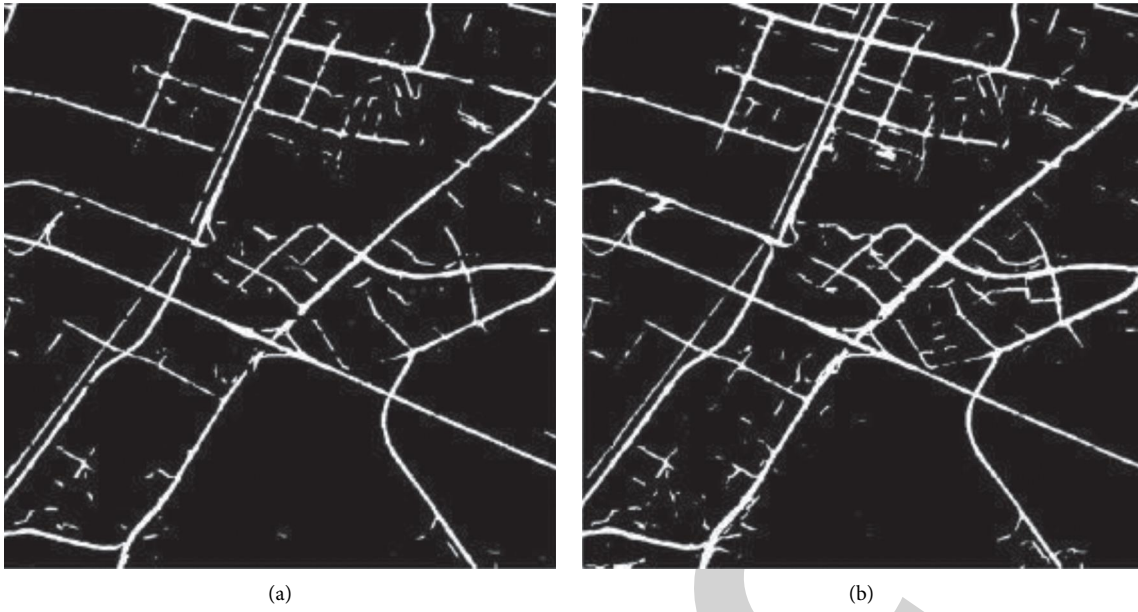


FIGURE 6: Comparison of segmentation effects. (a) Image without adaptive threshold. (b) Image with adaptive threshold.

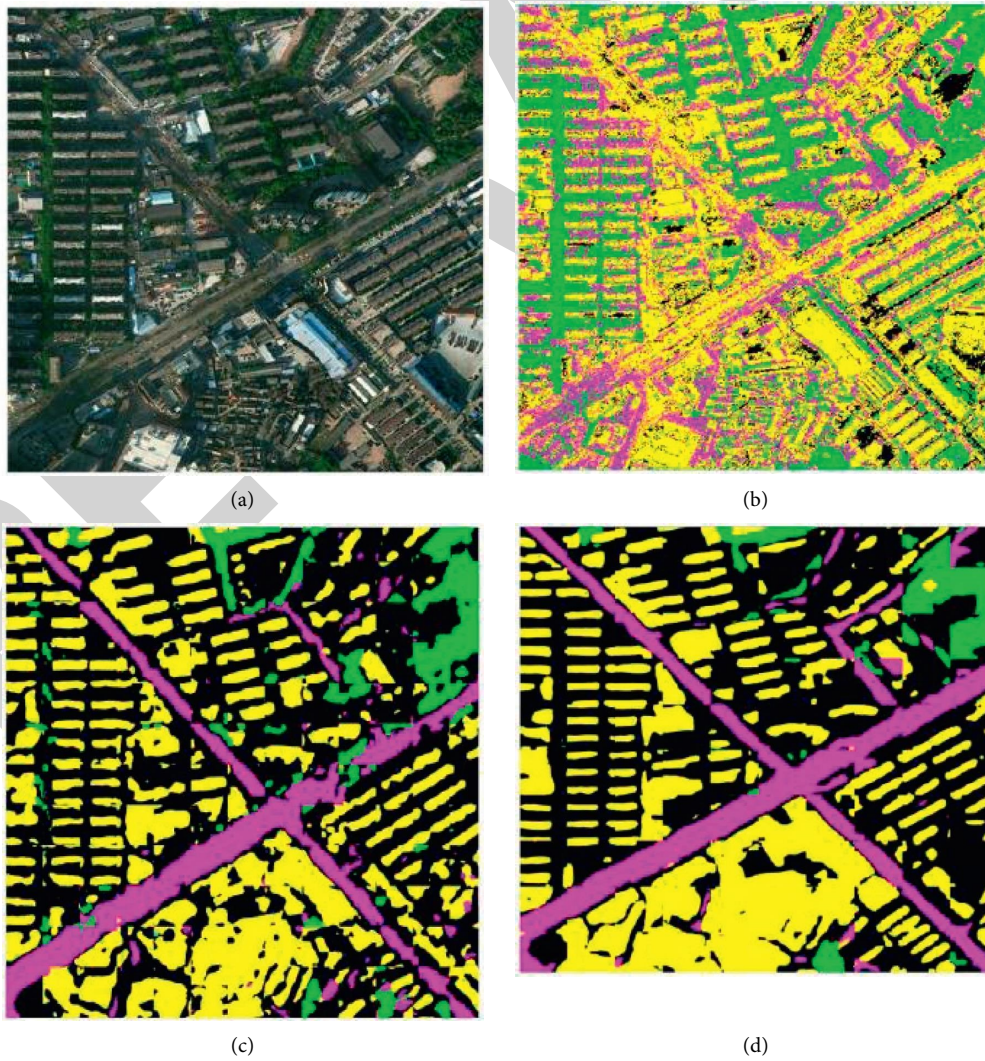


FIGURE 7: Segmentation results of different methods on CCF data set. (a) Original image. (b) SVM. (c) U-Net. (d) the proposed network.

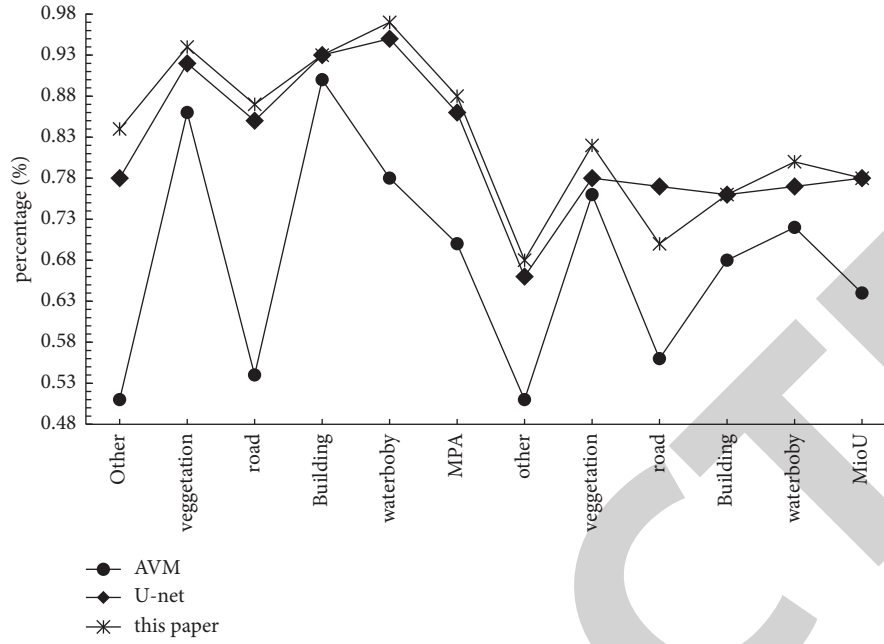


FIGURE 8: Segmentation result evaluation of different methods on CCF data set.

categories on CCF data set. Compared with SVM and U-Net methods, the mean pixel accuracy reaches 91%, which increases by 19%, 7%, and 2%, respectively. The mean intersection over union increases by 11%, 3%, and 1%, respectively, which reaches 76%. Therefore, the proposed method has good image segmentation performance and certain advantages.

## 5. Conclusion

In conclusion, the proposed landscape greening space distribution model of community based on image recognition can achieve more accurate landscape space classification of community by using improved U-Net network to segment community landscape greening. Compared with the traditional SVM and SegNet methods, as well as the improved U-Net method, the proposed method has better classification effect, and the results are closer to the manual annotation results. On data set, the mean pixel accuracy of proposed method is 19%, 7% and 2% higher than that of SVM, SegNet and U-Net methods, respectively, reaching 91%. In addition, the mean intersection over union reaches 76%. In practical application, the proposed method can also obtain good segmentation results, where the mean pixel accuracy and the mean intersection over union reach 89% and 74%, which means that the proposed method has certain validity and practicability. However, there are still some deficiencies. The improvement method used by U-Net model is supervised learning, and images need to be annotated in the early stage. Although the classification accuracy is improved to a certain extent, the overall efficiency is reduced. Therefore, the next step is to try to improve the model by using unsupervised learning method while ensuring high precision segmentation effect. [23–25].

## Data Availability

The experimental data used to support the findings of this study are available from the corresponding author upon request.

## Conflicts of Interest

The authors declared that they have no conflicts of interest regarding this work.

## References

- [1] S. Qu, X. Liu, and S. Liang, "Multi-scale superpixels dimension reduction hyperspectral image classification algorithm based on low rank sparse representation joint hierarchical recursive filtering," *Sensors*, vol. 21, no. 11, p. 3846, 2021.
- [2] N.-R. Zhou, X. X. Liu, Y. L. Chen, and N. S. Du, "Quantum K-Nearest-Neighbor image classification algorithm based on K-L transform," *International Journal of Theoretical Physics*, vol. 23, pp. 1–16, 2021.
- [3] H. Wang, Y. Zhang, and X. Fan, "Gray image segmentation algorithm based on one-dimensional image complexity," *Journal of Intelligent and Fuzzy Systems*, vol. 38, no. 6, pp. 1–10, 2020.
- [4] J E Liu, F. P. An, and M. Cristian, "Image classification algorithm based on deep learning-kernel function," *Scientific Programming*, vol. 2020, Article ID 7607612, 14 pages, 2020.
- [5] X. Zhang and S. Li, "On three species of the spider genus Pimoida (Araneae, Pimoidae) from China," *ZooKeys*, vol. 855, no. 7, pp. 1–13, 2019.
- [6] Z. Zhang, "Semi-supervised hyperspectral image classification algorithm based on graph embedding and discriminative



## *Retraction*

# **Retracted: Application and Analysis of Artificial Intelligence in College Students' Career Planning and Employment and Entrepreneurship Information Recommendation**

### **Security and Communication Networks**

Received 26 December 2023; Accepted 26 December 2023; Published 29 December 2023

Copyright © 2023 Security and Communication Networks. This is an open access article distributed under the Creative Commons Attribution License, which permits unrestricted use, distribution, and reproduction in any medium, provided the original work is properly cited.

This article has been retracted by Hindawi, as publisher, following an investigation undertaken by the publisher [1]. This investigation has uncovered evidence of systematic manipulation of the publication and peer-review process. We cannot, therefore, vouch for the reliability or integrity of this article.

Please note that this notice is intended solely to alert readers that the peer-review process of this article has been compromised.

Wiley and Hindawi regret that the usual quality checks did not identify these issues before publication and have since put additional measures in place to safeguard research integrity.

We wish to credit our Research Integrity and Research Publishing teams and anonymous and named external researchers and research integrity experts for contributing to this investigation.

The corresponding author, as the representative of all authors, has been given the opportunity to register their agreement or disagreement to this retraction. We have kept a record of any response received.

## **References**

- [1] H. Zhang and Z. Zheng, "Application and Analysis of Artificial Intelligence in College Students' Career Planning and Employment and Entrepreneurship Information Recommendation," *Security and Communication Networks*, vol. 2022, Article ID 8073232, 8 pages, 2022.

## Research Article

# Application and Analysis of Artificial Intelligence in College Students' Career Planning and Employment and Entrepreneurship Information Recommendation

Hui Zhang<sup>1</sup> and Zhuonan Zheng<sup>2</sup>

<sup>1</sup>*Institute Office, Guangdong Industry Polytechnic, Guangzhou 510300, China*

<sup>2</sup>*Human Resources Division, Guangdong Industry Polytechnic, Guangzhou 510300, China*

Correspondence should be addressed to Hui Zhang; [xb210@gdip.edu.cn](mailto:xb210@gdip.edu.cn)

Received 13 July 2022; Revised 8 August 2022; Accepted 17 August 2022; Published 13 September 2022

Academic Editor: Hangjun Che

Copyright © 2022 Hui Zhang and Zhuonan Zheng. This is an open access article distributed under the Creative Commons Attribution License, which permits unrestricted use, distribution, and reproduction in any medium, provided the original work is properly cited.

With the arrival of graduation season, the number of graduates is expanding every year, and the employment rate of college students has become one of the data that colleges and universities pay attention to. To improve the employment rate of college students, we should first educate each college student in career planning, so that they can clearly understand their own positioning and future development direction. Career planning can guide students to understand their jobs and analyze their professional fields. Faced with massive employment information, it is also a big problem for college students to search and choose information. In this paper, the personalized recommendation system for entrepreneurship is described, and the basic principles of information recommendation are described. The basic information and personal interest points of college students are represented by feature vectors, which provide a favorable theoretical support for college students' career planning and employment and entrepreneurship information recommendation. An information recommendation model under deep learning is formed. Finally, the performance of the model under the traditional algorithm and the optimized information recommendation model is evaluated, and the satisfaction of users to this system is scored so as to provide a convenient and quick information recommendation system for college students, thus indirectly improving the employment rate of graduates and providing corresponding solutions to the problem of difficult employment.

## 1. Introduction

In this era of rapid information development, the acquisition of resources is convenient and fast. College students' career planning is particularly important for their future development, which is a clear plan for their future. College students choose the learning resources and knowledge data they need to plan their future development on the Internet and make a preliminary design of themselves by using the algorithm recommended by the platform [1]. From the perspective of the Internet, this paper analyzes how college students should plan their careers and know themselves correctly from what aspects [2]. The teaching mode is to take online teaching data to reflect on offline teaching, stimulate college students' awareness of independent career

development, set teaching content according to the law of students' growth process, and carry out teaching activities aiming at cultivating students' practical ability in the process of exploration [3]. According to the online recruitment information, this paper analyzes the feasibility of career planning of Chinese college students. Taking the major of human resource management as an example, this paper studies the determination of career development path, job quality requirements, and career planning stage of Chinese college students and uses dynamic network recruitment information to adopt the rolling planning method to plan college career [4]. Career planning education strengthens the ideological and political education of college students and enhances the effectiveness, affinity, and appeal of ideological and political education. Finally, it discusses the

countermeasures of this education to college students' career planning [5]. With the continuous expansion of e-commerce, the traditional recommendation system can no longer meet the needs of current data processing. Combined with the recommendation algorithm of big data, a personalized recommendation system of e-commerce platform is constructed [6]. Data collection and processing are carried out in distance education, and gesture recognition of virtual reality is used to recommend educational information in class [7]. On the social platform, the influence of users' comments on the surrounding environment and active screening and recommendation of information are the basic user activities and services of the social software [8]. In the recommendation of students' personalized problems in the field of education, this paper puts forward a recommendation algorithm of tacit knowledge points and verifies whether the algorithm is reliable [9]. As for the increasing information and suggestions in the investment market, the portfolio model is optimized by empirical analysis according to different fuzzy information [10]. While enhancing situational awareness, it also brings many challenges to the recommendation of battlefield situation information. In the sorting stage, the situation information in the candidate set is accurately scored and sorted, and finally, the situation information with higher scores is recommended to the commander [11]. In the collaborative filtering algorithm model, users can quickly collect personalized information of users with high accuracy, which can provide a quick way for users to retrieve information [12]. In the aspect of web page design and smart phone, the system of tourism information recommendation needs to aim at the real needs of users, carry out intelligent data screening, and provide the information they want according to their preferences [13]. Label labeling is also based on the recommendation algorithm of the system, which constructs a synonymous label set for collecting synonymous labels under the definition classification, which is the result of applying the cluster seepage method to the existing resources of users [14]. The development of Internet is also important for farmers to obtain information resources. Farmers can plant grains according to accurate agricultural information to meet people's needs [15]. When recommending information, there will be a lot of mixed, fuzzy, and cross information, which will be fused according to their similarity and recommended to users [16]. There are many incomplete domains in migration learning that will be used in information recommendation systems [17]. Analyze users' information access history records, extract their whereabouts, label them according to semantic means, and finally search users for information [18]. For the generation of massive data information in the bus card, a comfortable bus route can be recommended to passengers according to their needs. The bus data card can calculate the waiting time, congestion time, and travel time between different bus stops on different bus lines at different times [19]. In the mobile environment, the group system recommendation is carried out considering the preferences of group users, and the recommendation system can also be used for restaurant recommendation according to the preferences of users

themselves [20]. On social software, the platform will also recommend people you may know according to your personal information and contacts and recommend friends among users [21]. In business activities, the personalized recommendation system also has an important application value and carries out personalized recommendation of mobile business methods [22]. Between the system and users, a system simulation model of personalized information recommendation is established, the effectiveness of the model and the sensitivity of main influencing parameters are analyzed, and the characteristics and mechanism of information recommendation between the system and users are revealed [23]. Users interact with tags. Based on the tensor decomposition method of the matrix model, especially the pyramid decomposition method, aiming at the high computational complexity of the TD model, a pairwise interactive tensor decomposition method is proposed to optimize it [24]. According to an abstract conceptual method, human preferences are recommended for new information. The recommended items are selected by using conceptual ideas, which is the user's impression of the items inferred by using label data of free classification [25].

## 2. Personalized Recommendation System

*2.1. Brief Introduction of the Personalized Recommendation System.* The personalized recommendation system has become an important tool to obtain information in this era of information crossing. It screens users' browsing records and personal information according to big data technology to predict products and information that users may like. This can greatly increase the consumption rate and click rate of customers. Personalized information recommendation needs three parts. The first step is to collect and process the information, analyze the information, and finally use the recommendation algorithm to recommend information to users. The process is shown in Figure 1.

*2.2. Types of Information Recommendation.* There are many kinds of information recommendation contents, such as entertainment, literature, and combination. Entertainment information recommendation mainly integrates information according to the praise rate and comment rate of entertainment videos that users often click on and establishes a user preference model to recommend videos to users, which also increases users' liking for apps. Literary information recommendation mainly analyzes information according to the news content and personal information that users usually watch and recommends knowledge information to users according to the analysis of news viewing content of different ages, which can accurately push the news that users want to know and the knowledge sources they want to learn. Combined information recommendation is complex, the information from different sources of users is analyzed and screened, and finally, information integration is carried out through the personalized recommendation algorithm to form different information recommendation models for each user. The information sources of combined



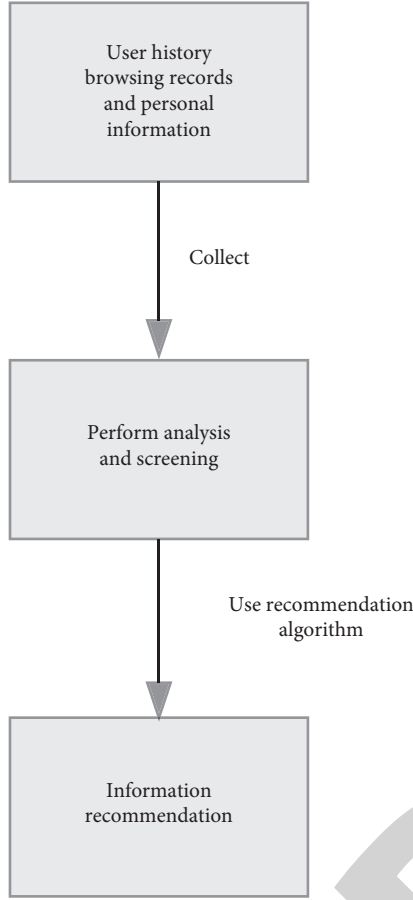


FIGURE 1: Information recommendation process.

information recommendation are more complex, and various algorithms are used to recommend so as to improve the accuracy of user preference information. The general flow of information recommendation content is shown in Figure 2.

### 3. Information Recommendation Algorithms

**3.1. Employment Recommendation Algorithm for College Students.** Collect and filter the user's information, the information content comes from different directions, and translate the information content into text information, that is, the content recommendation process is as follows.

*Step 1.* Transform the content. Each feature point of content is converted into vector points of different dimensions of the space vector, assuming that the text information after content conversion is  $i$ ,  $x_i$  is content feature point, and  $y_i$  is weight. The expression for content  $i$  is

$$\text{Content}(i) = \{x_1: y_1; x_2: y_2; \dots; x_i: y_i\}. \quad (1)$$

The feature points of the content are represented by vectors:

$$\text{Content}(i) = \{y_1, y_2, y_3, \dots, y_i\}. \quad (2)$$

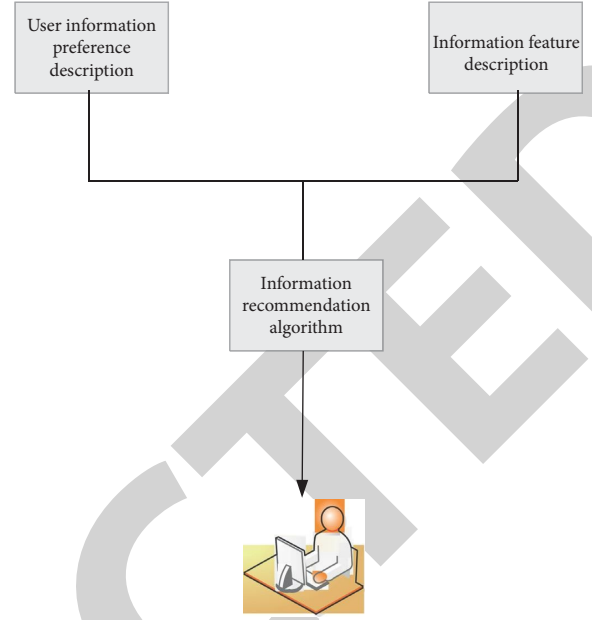


FIGURE 2: Information content recommendation process.

*Step 2.*  $N_w$  is the feature index, and the similarity relationship between content feature points is calculated. Then, different users have different preference models, and the expression is as follows:

$$W(w) = \frac{\sum_i N_w \text{content}(i)}{N_w}. \quad (3)$$

Calculate the similarity of each similarity point of the content:

$$\begin{aligned} \text{sim}(W, I) &= \cos(\vec{W}, \vec{I}) \\ &= \frac{\vec{W} \cdot \vec{I}}{|\vec{W}| \times |\vec{I}|}. \end{aligned} \quad (4)$$

*Step 3.* Generate information recommendation results. The information with the highest similarity is integrated and recommended to users.

In order to realize the career planning and employment and entrepreneurship information recommendation of college students, the information distribution model is constructed. Collect personal information from universities and output data sequences of information characteristics:

$$x = \{x_1, x_2, x_3, \dots, x_i\}. \quad (5)$$

Integrate the characteristic points of college students' personal information, that is, the expression of characteristic quantity is as follows:

$$m(x) = \frac{x_i}{\sum_{i=1}^w N_w \cdot y_i}. \quad (6)$$

The sampling model of characteristic points of college students' personal information:

$$m(k) = \frac{m(x)}{\sum_{i=1}^w y_i (n(k) \cdot y(k))}. \quad (7)$$

In the information feature point sampling model,  $k$  is the amount of employment information and  $q$  is the employment intention index.

Personal information similarities of college students' employment intentions:

$$\text{sim}(u_a, u_b) = \frac{\sum_{i \in I_a} m(x)m(k)}{\sqrt{\sum_{i \in I_a} (r_{u_a, i} - \bar{r}_{u_a})^2 \cdot \sum_{i \in I_b} (r_{u_b, i} - \bar{r}_{u_b})^2}}. \quad (8)$$

The similarity of information recommendation index between different college students is quantified by standard, and the formula is as follows:

$$\begin{aligned} E_{(i,j)} &= E_{(i)} + E_{(j)} \\ &= im(x) + jm(k^a), \\ &= \begin{cases} im(x) + jm(k^2), & k < k_0, \\ im(x) + jm(k^4), & k \geq k_0. \end{cases} \end{aligned} \quad (9)$$

Employment recommendation information is mainly matched according to the interest and hobbies of college students. By correlating the information of college students' interests and hobbies, the feature extraction model of college students' interest points is obtained:

$$\begin{aligned} y &= F(x) \\ &= (f_1(x), f_2(x), \dots, f_m(x)). \end{aligned} \quad (10)$$

The distribution expression of the spatial set of information characteristics of college students' job allocation in different fields:

$$f(m) = \{f_k | f_{ki} = 1, k = 1, 2, 3, \dots, m\}. \quad (11)$$

According to the interest and hobbies of college students, information screening is carried out to establish ambiguity functions related to their interest:

$$\begin{aligned} Q &= \sum_{k=1}^m t_{ik}, t_{jk}, \\ n_i &= \begin{cases} 1, & i = j, \\ 0, & i \neq j. \end{cases} \end{aligned} \quad (12)$$

Construct the distribution model of college students' employment interest characteristics:

$$\begin{aligned} P(U|\alpha) &= \prod_{i=1}^m n_i(U_i|0, \alpha), \\ P(V|\alpha) &= \prod_{j=1}^m n_j(V_j|0, \alpha). \end{aligned} \quad (13)$$

**3.2. Career Planning Algorithm for College Students.** College students build their own career plans according to their majors and their hobbies and fuse the characteristic

points of information to obtain an adaptive learning weight calculation formula:

$$W_k(U) = \alpha \left( \frac{1}{m} \sum_{i=1}^m \frac{\sum r_{i,j}}{\sum r_k + \bar{r}_{i,j}} \right), \quad (14)$$

$$W_k(V) = \alpha \left( \frac{1}{n} \sum_{i=1}^n \frac{\sum r_{i,j}}{\sum r_k + \bar{r}_{i,j}} \right).$$

If all the interest points of college students are counted and made into their career planning book, their interest points meet the expression:

$$\max_{i,j,m,n} \sum_{\alpha \in r_i} \sum_{\alpha \in r_j} \sum_{\alpha \in r_m} \sum_{\alpha \in n} \alpha x_{i,j,m,n} V_n. \quad (15)$$

The self-adaptive function of dividing the group size of college students in different professional fields is as follows:

$$W_k = W_k(U) [1 - W_k(V)]^{k-1}. \quad (16)$$

The deep learning method is used to search the job requirements and interest feature points of universities, and the ambiguity function of the search is as follows:

$$E_{(k)} = \sum_{k=0}^{\infty} [1 - W(k)]^k. \quad (17)$$

Average number of time slots under the deep learning method:

$$\begin{aligned} T &= E_{(k)} n_i \\ &= \frac{L}{(1 - 1/n)^{m-1}}. \end{aligned} \quad (18)$$

Interest matching function under the deep learning method:

$$\begin{aligned} E^{cv}(c_1, c_2) &= u * \text{length}(c) + v * \text{area}(\text{inside}(c)) \\ &+ \lambda_1 \int_{\text{inside}(c)} |I - c_1|^2 + \lambda_2 \int_{\text{outside}(c)} |I - c_2|^2. \end{aligned} \quad (19)$$

To sum up, the learning model of college students' career planning and employment information recommendation is

$$\begin{aligned} C &= \text{Min}\{\max(C_i)\}, \\ \sum_{j=1}^n M_j &= 1, \quad (\forall_i \in (1, n), \forall_j \in (1, m)). \end{aligned} \quad (20)$$

Optimal matching iterative representation of college students' interest feature points under deep learning model:

$$x_i(k+1) = x_i(k) + \alpha \left( \frac{x_i(k) - x_j(k)}{\|x_i(k) - x_j(k)\|} \right). \quad (21)$$

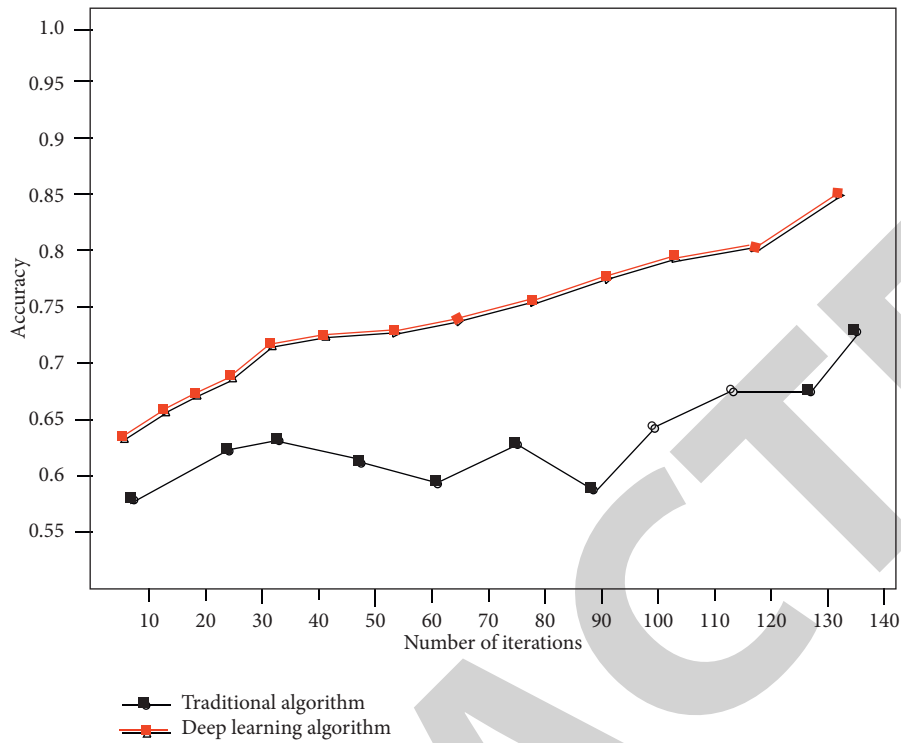


FIGURE 3: Comparison of interest matching accuracy.

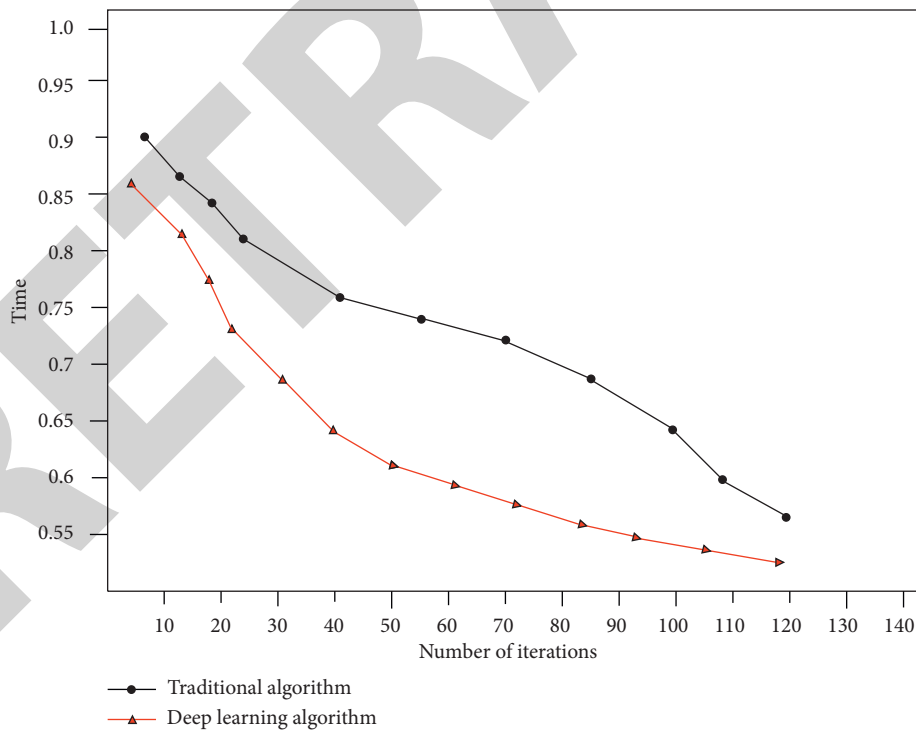


FIGURE 4: Time-cost comparison of models.

TABLE 1: Test module and method.

Test model	Method	Judgment criterion
Register/login	Perform multiple registration/login tests	Can you succeed?
Modify personal information	Submit after adding/modifying information	Is personal information in the database?
Online recommendation	Modify personal information viewing results	Can you update it in real time?
Satisfaction degree of recommended information	Satisfaction rating	Can you score?

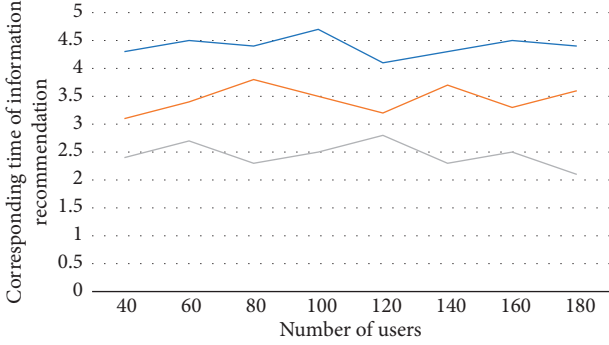


FIGURE 5: Relationship between corresponding time and node.

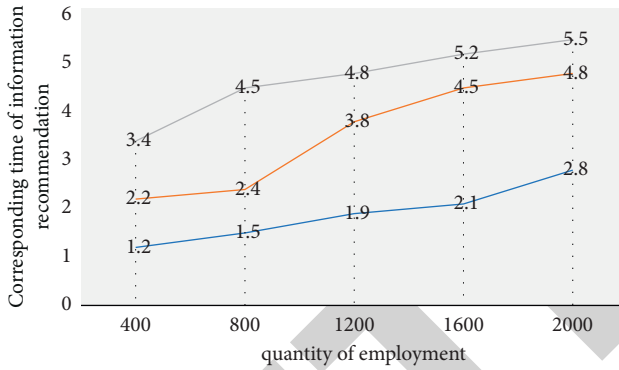


FIGURE 6: Relationship between corresponding time and employment quantity.

Finally, the satisfaction results of college students on career planning and employment information recommendation formed under the information analysis of big data:

$$F(M_j, i) = \tilde{w}_k^i * \alpha(M_j, i) + \tilde{w}_{k-1}^i * (1 - \alpha)(M_j, i). \quad (22)$$

## 4. Experimental Analyses

**4.1. Simulation Experiment.** According to the employment data statistics of fresh graduates in 2022, the traditional algorithm model and deep learning algorithm are used to match the interest characteristics of college students, and their accuracy and time-cost calculated by the employment recommendation model are compared. As shown in Figures 3 and 4, the relevant parameters are set as follows: the feature scale dataset of user interest points is  $Q = 500$ , the fuzzy matching coefficients of interest points are  $c_1 = 0.34$  and  $c_2 = 0.32$ , the distribution coefficient of personalized preference features is  $c_r = 2$ , the prediction coefficient of

TABLE 2: Information corresponding time of different nodes in the information recommendation algorithm model.

Number of nodes	Number of users							
	40	60	80	100	120	140	160	180
2	4.3	4.5	4.4	4.7	4.1	4.3	4.5	4.4
3	3.1	3.4	3.8	3.5	3.2	3.7	3.3	3.6
4	2.4	2.7	2.3	2.5	2.8	2.3	3.6	2.1

TABLE 3: Corresponding time of information with different employment quantities in the information recommendation algorithm model.

Number of users	Amount of employment information				
	400	800	1200	1600	2000
100	1.2	1.5	1.9	2.1	2.8
200	2.2	2.4	3.8	4.5	4.8
300	3.4	4.5	4.8	5.2	5.5

recommendation model is  $\mu_1 = \mu_2 = 0.01$ , and the total iteration times are 140.

**4.2. Functional Testing.** This system is mainly aimed at college students' career planning customization and employment information recommendation services. The following is a test of the functions of each module for the employment information of college students to test whether these functions can be accurately realized and how the running results are. The statistical information is shown in Table 1.

**4.3. Performance Testing.** Excellent performance is necessary for any information recommendation system. If the performance of the system is too poor, users will have a bad experience, and users will also reduce the use of the recommendation system. Four nodes of the recommendation system are tested. The total number of employment information databases is about 2,000. The relationship between recommendation information response and the number of nodes and employment information is shown in Figures 5 and 6.

Statistics of time and cost information of recommendation information model is shown in Table 2.

The time-cost of recommendation information response and the number of employment information are counted as shown in Table 3.

**4.4. Contrast Experiment.** Information screening and fusion under big data analysis, in order to compare the information recommendation system under big data analysis in many

TABLE 4: Performance comparison of the artificial intelligence employment information recommendation model.

Model	Accuracy (%)	Recall (%)	F1 (%)	MAE (%)	ROC (%)
BP	98.99	89.97	78.25	10.87	87.63
Traditional algorithm	76.84	65.43	54.72	53.48	75.49

TABLE 5: Satisfaction score data table.

Scoring point	Model	
	Deep learning model (%)	Traditional model (%)
5 scoring points per capita	3.7	65.6
10 scoring points per capita	77.9	23.7
15 scoring points per capita	18.4	10.7

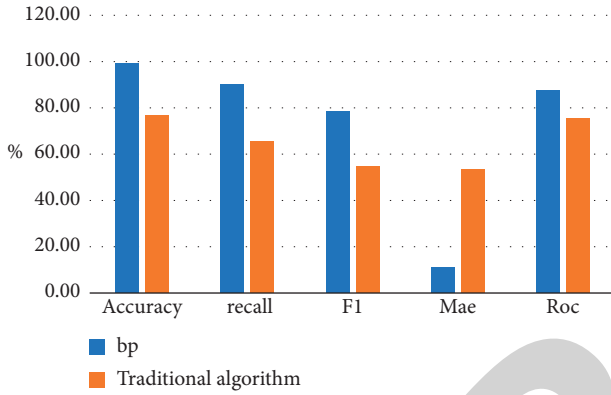


FIGURE 7: Performance comparison of the artificial intelligence employment information recommendation model.

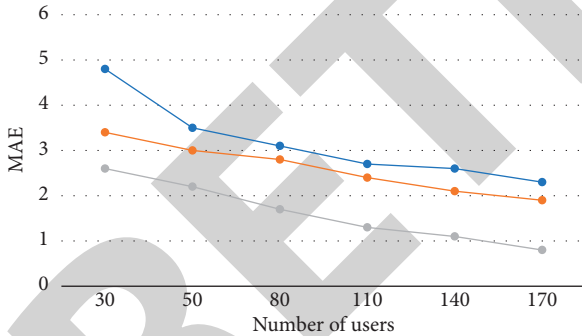


FIGURE 8: Linear relationship between number of users and MAE.

aspects, is employment information recommendation and career planning under artificial intelligence better? We make a comprehensive performance comparison of the employment information recommendation model, and the data are shown in Table 4 and Figure 7.

In order to intuitively see the applicability of the employment recommendation system to college students, we systematically score the per capita satisfaction of college students who have used the information recommendation system and compare the recommendation system using the algorithm model under deep learning with the traditional algorithm model, respectively. The experimental data are shown in Table 5.

Users carry out quality analysis and research on the information recommendation scoring points of the system and its evaluation standard MAE. The correlation between the per capita scoring points and MAE performance evaluation indicators is shown in Figure 8.

## 5. Conclusion

Our daily life is full of our personal information all the time, and the processing of data information is also the service action of our intelligent society for people's social activities. Using artificial intelligence technology, large-scale data such as college students' personal information, intended positions, and their own interest intentions are integrated and analyzed and finally provided to clients with corresponding needs and the same interest points. The research results of this paper are as follows:

- (1) The starting point of employment and entrepreneurship information recommendation algorithm is to build the recommendation strategy algorithm model through the basic personal information and interest feature points of users
- (2) Combined with the information recommendation model under deep learning, the information and users' needs can achieve an optimal matching mechanism, which greatly improves the accuracy of information recommendation and forms a good information retrieval experience for users
- (3) Taking the corresponding time of the model as the performance evaluation index of the information recommendation system, the optimized algorithm model can improve the accuracy of information recommendation
- (4) According to the user satisfaction score and the MAE value of the model, we can further see the feasibility of the information recommendation model for employment and entrepreneurship information recommendation and career planning

## Data Availability

The data used to support the findings of this study are available from the corresponding author upon request.

## *Retraction*

# **Retracted: Fault Diagnosis Method of Rotor Magnetic Field Local Demagnetization in Permanent Magnet Synchronous Motor Model Predictive Current Control System**

### **Security and Communication Networks**

Received 26 December 2023; Accepted 26 December 2023; Published 29 December 2023

Copyright © 2023 Security and Communication Networks. This is an open access article distributed under the Creative Commons Attribution License, which permits unrestricted use, distribution, and reproduction in any medium, provided the original work is properly cited.

This article has been retracted by Hindawi, as publisher, following an investigation undertaken by the publisher [1]. This investigation has uncovered evidence of systematic manipulation of the publication and peer-review process. We cannot, therefore, vouch for the reliability or integrity of this article.

Please note that this notice is intended solely to alert readers that the peer-review process of this article has been compromised.

Wiley and Hindawi regret that the usual quality checks did not identify these issues before publication and have since put additional measures in place to safeguard research integrity.

We wish to credit our Research Integrity and Research Publishing teams and anonymous and named external researchers and research integrity experts for contributing to this investigation.

The corresponding author, as the representative of all authors, has been given the opportunity to register their agreement or disagreement to this retraction. We have kept a record of any response received.

## **References**

- [1] T. Chen and B. Chen, "Fault Diagnosis Method of Rotor Magnetic Field Local Demagnetization in Permanent Magnet Synchronous Motor Model Predictive Current Control System," *Security and Communication Networks*, vol. 2022, Article ID 9344484, 13 pages, 2022.

## Research Article

# Fault Diagnosis Method of Rotor Magnetic Field Local Demagnetization in Permanent Magnet Synchronous Motor Model Predictive Current Control System

Tao Chen <sup>1</sup> and Bing Chen <sup>2</sup>

<sup>1</sup>School of Electrical Information Engineering, Henan University of Engineering, Zhengzhou 451191, China

<sup>2</sup>Henan Institute of Metrology, Zhengzhou 450000, China

Correspondence should be addressed to Tao Chen; hact@haue.edu.cn

Received 6 July 2022; Revised 9 August 2022; Accepted 17 August 2022; Published 9 September 2022

Academic Editor: Hangjun Che

Copyright © 2022 Tao Chen and Bing Chen. This is an open access article distributed under the Creative Commons Attribution License, which permits unrestricted use, distribution, and reproduction in any medium, provided the original work is properly cited.

In order to realize the reliable diagnosis of the rotor magnetic field local demagnetization fault of permanent magnet synchronous motor (PMSM) model predictive current control system, based on the establishment of the mathematical model of PMSM considering local demagnetization of rotor magnetic field and the simulation model of its model predictive current control system, a diagnosis method combining the adaptive signal extraction algorithm and Hilbert transform is proposed in this study. This method is first based on the adaptive signal extraction algorithm to extract the fault characteristic harmonics of rotor magnetic field local demagnetization fault in PMSM model predictive current control system under stationary and nonstationary operating conditions, and then, we use Hilbert transform to realize the time-frequency transformation of the extracted fault characteristic harmonics. Based on solving the problem that the weak fault characteristic signal near the fundamental wave component existing in the Hilbert–Huang transform is difficult to effectively decompose, the reliable diagnosis of the rotor magnetic field local demagnetization fault of the PMSM model predictive current control system is realized with the calculation amount less than Hilbert–Huang transform. The simulation and experimental results show that the proposed method is accurate and useful.

## 1. Introduction

Due to the fact that PMSM has the advantages of high-power density and achieving high-performance control easily, it has been widely used in electric vehicles, new energy power generation, and other fields. However, the above-mentioned fields are mostly limited by installation space, limited heat dissipation conditions, and complex motor operating conditions, it's easy to have a stronger armature reaction and high working temperature, resulting in local demagnetization fault or uniform demagnetization fault of PMSM rotor magnetic field, which affects the torque control accuracy and operational reliability of its drive system [1].

The PMSM rotor magnetic field demagnetization fault diagnosis mainly includes three basic methods: model-driven, data-driven, and high-frequency signal injection.

The artificial intelligence algorithm represented by the evolutionary algorithm is a typical representative of the model-driven method, because of its strong nonlinear processing ability, this kind of algorithm has certain advantages in the PMSM rotor magnetic field demagnetization fault diagnosis [2, 3]. However, how to reduce the amount of calculation is still an urgent problem to be solved. Another type of model-driven PMSM rotor magnetic field demagnetization fault diagnosis method is to use dynamic data processing technology to construct a rotor flux linkage observer and realize the rotor magnetic field demagnetization fault diagnosis according to the observation results. Algorithms such as luenberger observer [4], least squares method [5], extended Kalman filter [6, 7], and model reference adaptative algorithm [8] have been used to design PMSM rotor flux linkage observers, but these algorithms are



difficult to achieve a reasonable balance between the PMSM rotor flux linkage identification accuracy and identification speed due to the influence of factors such as the measurement noise, the change of motor parameters, the lack of rank of the identification model, and the difficulty in determining the adaptive rate to ensure the simultaneous convergence of multiple parameters [9]. The data-driven fault diagnosis method takes voltage, current, vibration, and noise as the analysis objects, and uses Fast Fourier Transform (FFT), Wavelet Transform (WT), and Hilbert-Huang Transform (HHT) to realize fault characteristics extraction, and then to achieve PMSM rotor magnetic field local demagnetization fault diagnosis. Fast Fourier transform, as a frequency domain analysis method that is easy to realize digitally, has been widely used in the field of PMSM rotor magnetic field local demagnetization fault diagnosis [10, 11], but it is a global transform, which is difficult to adapt to the nonstationary operating conditions of PMSM drive system. As time-frequency transform tools, wavelet transform and Hilbert-Huang transform can realize the analysis and extraction of fault characteristic signals in the nonstationary state [12, 13, 14]. However, the localization ability of wavelet transform depends on the localization property of the selected wavelet base in the time domain and frequency domain, and the wavelet basis function that takes into account the global optimum and the local optimum is difficult to reasonably determine. Hilbert-Huang transform consists of two parts: empirical mode decomposition (EMD) and Hilbert transform. It generates the required adaptive basis function through the signal itself and has better local adaptability and intuitive decomposition results when dealing with nonstationary signals. However, it is difficult to effectively decompose the weak fault characteristic signals near the fundamental wave. The high-frequency signal injection method [15, 16] takes the change of the PMSM magnetic circuit state before and after the rotor magnetic field demagnetization as the fault diagnosis criterion, which is suitable for the diagnosis and fault mode identification of both local and uniform rotor magnetic field demagnetization faults. It is necessary to superimpose the high-frequency current that varies with the degree of demagnetization, and the online diagnosis of the demagnetization fault of the rotor magnetic field cannot be realized. In a study [17], the fractal dimension was introduced into the PMSM rotor magnetic field local demagnetization fault diagnosis, and the Choi-Williams distribution in time-frequency analysis was used to extract the fault characteristic signal, the box dimension was calculated for it, and the rotor magnetic field local demagnetization fault of PMSM was determined according to the calculation results, but the calculation results of the box dimension are easily affected by the harmonics of the inverter, and the fault judgment threshold is difficult to reasonably determine.

Finite control set model predictive control (FCS-MPC) has the advantages of simple structure and good dynamic operation and is widely used in the PMSM drive and control system [18, 19, 20, 21]. FCS-MPC is a control algorithm that predicts the future state of the controlled system based on its current state and mathematical model [18]. The FCS-MPC

includes model predictive current control (MPCC) and model predictive torque control (MPTC), MPTC algorithm usually needs to determine the appropriate weight coefficient to construct the objective function [18, 19, 20], but the determination of the weight coefficient lacks effective theoretical support, and it relies on a large number of simulation and experimental data for continuous adjustment, the debugging process is complicated. In contrast, MPCC is simple to implement, the control variable can be directly measured, when constructing the objective function, only dimensionally consistent variables are included, so the weight coefficient design problem is avoided [21], and can realize high-performance PMSM drive system current control, which is beneficial to meet the requirements of PMSM drive system for wide speed regulation range, good dynamic characteristics, fast current response, and high-power density requirements [22].

There have been some studies on the diagnosis methods of PMSM rotor magnetic field local demagnetization fault based on conventional control strategies such as vector control and direct torque control in the existing literatures [2–17], but insufficient attention has been paid to the diagnosis methods of PMSM rotor magnetic field local demagnetization fault based on model predictive current control strategy. This paper proposes a fault diagnosis method for rotor magnetic field local demagnetization fault in the PMSM model predictive current control system by combining the adaptive signal extraction algorithm and Hilbert transform. First, the PMSM mathematical model considering local demagnetization fault of rotor magnetic field and the simulation model of its model predictive current control system is established. Then, based on the adaptive signal extraction algorithm, the characteristic harmonics of the rotor magnetic field local demagnetization fault of the PMSM model predictive current control system are extracted under steady and nonstationary operating conditions. And then, the Hilbert transform is used to realize the time-frequency transformation of the extracted rotor magnetic field local demagnetization fault characteristic signal, the instantaneous frequency of the extracted fault characteristic signal is obtained, and it can be used for fault diagnosis. Based on solving the problem that the weak fault characteristic signal near the fundamental wave is difficult to decompose effectively in Hilbert-Huang transform, the ability of fault characteristic signals to characterize local demagnetization fault of PMSM rotor magnetic field is improved and the reliable diagnosis of rotor magnetic field local demagnetization fault of PMSM model predictive current control system is realized.

## 2. PMSM Modeling considering Rotor Magnetic Field Local Demagnetization Fault

The modeling idea of this study is as follows: First, establishing the PMSM finite element model with different demagnetization degrees of a single permanent magnet, and then performing the spectrum analysis and the flux linkage calculation of the no-load radial air gap flux density of permanent magnet. According to the analysis and calculation results, the flux linkage equation, the stator voltage equation, and the electromagnetic torque equation of PMSM

TABLE 1: The parameters of PMSM.

Parameters	Value	Parameters	Value
Pole pairs	4	Rated speed	900 rpm
Stator resistance	0.0154 $\Omega$	$d$ axis inductance	$L_d = 2.517\text{mH}$
Rotor flux linkage	0.1732 Wb	$q$ axis inductance	$L_q = 5.99\text{mH}$

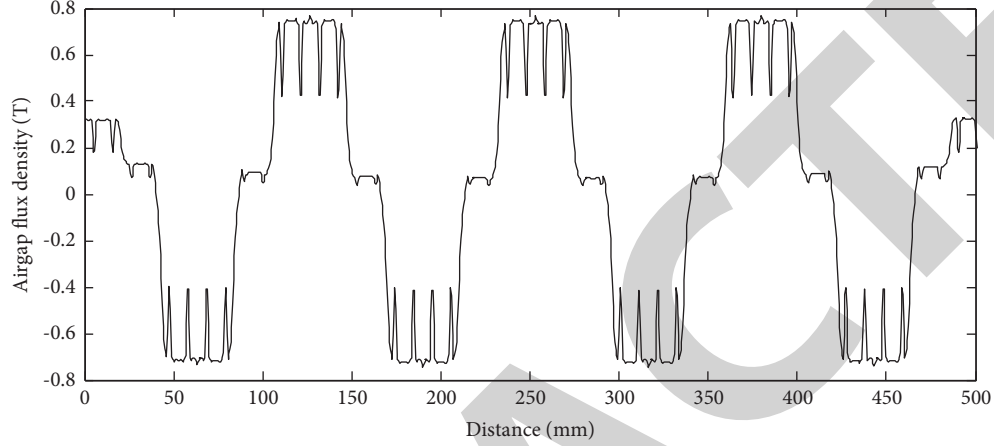


FIGURE 1: The no-load radial air gap flux density for 50% demagnetization of a single permanent magnet.

considering the local demagnetization of the rotor magnetic field are obtained, combined the above equation with the electromechanical motion equation of PMSM, the PMSM mathematical model with different local demagnetization degrees is established, which lay a foundation for establishing the simulation model of PMSM model predictive current control system considering the rotor magnetic field local demagnetization fault and studying the diagnosis method of local demagnetization fault. Table 1 shows the PMSM parameters, and Figure 1 shows the no-load radial air gap flux density for 50% demagnetization of a single permanent magnet. Figure 2(a) is the Fourier transform result of the no-load radial air gap flux density as shown in Figure 1, and Figure 2(b) is the Fourier transform result of the no-load radial air gap flux density in the permanent magnet healthy state.

The 4th harmonic in Figure 2 is the fundamental wave of the PMSM rotor no-load radial air gap flux density, the rest are integer or noninteger harmonics. As can be seen from Figure 2(a), when the rotor magnetic field is locally demagnetized, the  $k/p$  order noninteger harmonics of the air gap flux density increase significantly. Depending on this, the expression of the flux linkage in the stator armature winding generated by the fundamental wave and harmonics of the rotor air gap flux density can be obtained as [23]

$$\psi_v = \frac{2}{\pi} \left( l_{ef} \frac{\tau}{v} \right) B_v (NK_{dpv}). \quad (1)$$

In the formula,  $l_{ef}$  is the effective length of the armature core;  $\tau$  is the pitch of the motor;  $B_v$  is the  $v$ -th harmonic amplitude of the rotor flux density;  $N$  is the number of series turns of armature winding of per phase; and  $K_{dpv}$  is winding

coefficient of the  $v$ -th harmonic. Taking phase A as an example, the flux linkage in the stator winding produced by the no-load radial air gap flux density can be expressed as

$$\begin{aligned} \psi_A = & \psi_{1/4} \cos\left(\frac{\theta}{4}\right) + \psi_{2/4} \cos\left(\frac{2\theta}{4}\right) + \psi_{3/4} \cos\left(\frac{3\theta}{4}\right) \\ & + \psi_1 \cos(\theta) + \dots + \psi_{k/p} \cos\left(\frac{k\theta}{p}\right). \end{aligned} \quad (2)$$

In order to take into account the modeling accuracy and model complexity of the PMSM rotor magnetic field local demagnetization fault, the study focuses on the noninteger harmonic flux linkage that can effectively describe the local demagnetization fault, and takes the noninteger air gap flux density characteristic harmonic to  $7/4$  times. At the same time, considering that the change of the integral air gap flux density harmonics is not obvious when the rotor magnetic field is local demagnetized, only the 5th and 7th harmonics with larger amplitudes are selected in the modeling process. Based on three-phase stator winding flux linkage, through constant amplitude coordinate transformation and simplification processing, the PMSM  $dq$  axis stator flux linkage equation shown in (3) can be obtained. Substitute (3) into (4) and (5), the stator voltage equation and electromagnetic torque equation considering the local demagnetization fault of the rotor magnetic field can be obtained. Combining the above-mentioned flux linkage equation, stator voltage equation, electronic torque equation with electromechanical motion equation, the PMSM mathematical model considering the rotor magnetic field local demagnetization fault is obtained, which lays a foundation for establishing the simulation model of PMSM model predictive current

control system considering the rotor magnetic field local demagnetization fault and implementing the research on

diagnosis method of rotor magnetic field local demagnetization fault.

$$\left\{ \begin{array}{l} \psi_d = \frac{1+\sqrt{3}}{3} (\psi_{3/4} + \psi_{5/4}) \cos(\theta/4) + \frac{2}{3} (\psi_{2/4} + \psi_{6/4}) \cos(2\theta/4) + \frac{1}{3} (\psi_{1/4} + \psi_{7/4}) \cos(3\theta/4) + \psi_1 + \\ \frac{1-\sqrt{3}}{3} \psi_{1/4} \cos(5\theta/4) - \frac{1}{3} \psi_{2/4} \cos(6\theta/4) + \frac{1-\sqrt{3}}{3} \psi_{3/4} \cos(7\theta/4) + \psi_2 \cos(3\theta) + \frac{1}{3} \psi_{5/4} \cos(9\theta/4) + \\ \frac{2}{3} \psi_{6/4} \cos(10\theta/4) + \frac{1+\sqrt{3}}{3} \psi_{7/4} \cos(11\theta/4) + (\psi_5 + \psi_7) \cos(6\theta) + L_d i_d \\ \psi_q = \frac{1+\sqrt{3}}{3} (\psi_{5/4} - \psi_{3/4}) \sin(\theta/4) + \frac{2}{3} (\psi_{6/4} - \psi_{2/4}) \sin(2\theta/4) + \frac{1}{3} (\psi_{7/4} - \psi_{1/4}) \sin(3\theta/4) + \\ \frac{\sqrt{3}-1}{3} \psi_{1/4} \sin(5\theta/4) + \frac{1}{3} \psi_{2/4} \sin(6\theta/4) + \frac{\sqrt{3}-1}{3} \psi_{3/4} \sin(7\theta/4) - \psi_2 \sin(3\theta) - \frac{1}{3} \psi_{5/4} \sin(9\theta/4) - \\ \frac{2}{3} \psi_{6/4} \sin(10\theta/4) - \frac{1+\sqrt{3}}{3} \psi_{7/4} \sin(11\theta/4) + (-\psi_5 + \psi_7) \sin(6\theta), \end{array} \right. \quad (3)$$

$$\left\{ \begin{array}{l} u_d = R_s i_d + L_d di_d/dt - \omega_e L_d i_q - \omega_e \psi_q, \\ u_q = R_s i_q + L_q di_q/dt - \omega_e L_q i_d + \omega_e \psi_d, \end{array} \right. \quad (4)$$

$$T_e = p(\psi_d i_q - \psi_q i_d). \quad (5)$$

Here,  $\theta$  is electrical angle between  $d$  axis and A phase winding axis,  $\psi_d$ ,  $\psi_q$ ,  $u_d$ ,  $u_q$ ,  $i_d$ , and  $i_q$  are  $d$  axis stator flux linkage,  $q$  axis stator flux linkage,  $d$  axis stator voltage,  $q$  axis stator voltage,  $d$  axis stator current and  $q$  axis stator current respectively,  $R_s$ ,  $L_d$ , and  $L_q$  represent stator resistance,  $d$  axis stator inductance and  $q$  axis stator inductance respectively,  $\omega_e$  is rotor electrical angular speed, and  $p$  is the pole pairs of the PMSM.

### 3. Model Predictive Current Control, Adaptive Signal Extraction, and Hilbert–Huang Transform Algorithm

#### 3.1. Model Predictive Current Control Algorithm of PMSM

**3.1.1. Prediction Model.** Taking the stator current as a state variable, the PMSM current state equation can be obtained from formula (4) as

$$\left\{ \begin{array}{l} \frac{di_d}{dt} = \frac{R_s}{L_d} i_d + \omega_e \frac{L_q}{L_d} i_q + \frac{1}{L_d} u_q, \\ \frac{di_q}{dt} = \frac{R_s}{L_q} i_q - \omega_e \frac{L_d}{L_q} i_d + \frac{1}{L_q} u_q - \frac{\omega_e}{L_q} \psi_f. \end{array} \right. \quad (6)$$

If the sampling period  $T_s$  of the control system is short enough, the PMSM discrete-time model can be represented by a first-order Taylor series, which is approximately

$$\left\{ \begin{array}{l} \frac{di_d}{dt} = \frac{i_d(k+1) - i_d(k)}{T}, \\ \frac{di_q}{dt} = \frac{i_q(k+1) - i_q(k)}{T_s}. \end{array} \right. \quad (7)$$

Using (7) to discretize (6), the PMSM discrete current predictive model can be obtained as

$$\left\{ \begin{array}{l} i_d^p(k+1) = \left(1 - \frac{T_s R_s}{L_d}\right) i_d(k) + T_s \frac{u_d(k)}{L_d} + T_s \omega_e(k) \frac{L_q}{L_d} i_q(k), \\ i_q^p(k+1) = \left(1 - \frac{T_s R_s}{L_q}\right) i_q(k) + T_s \frac{u_q(k)}{L_q} - T_s \omega_e(k) \frac{L_d}{L_q} i_d(k) - T_s \omega_e(k) \frac{\psi_f}{L_q}. \end{array} \right. \quad (8)$$

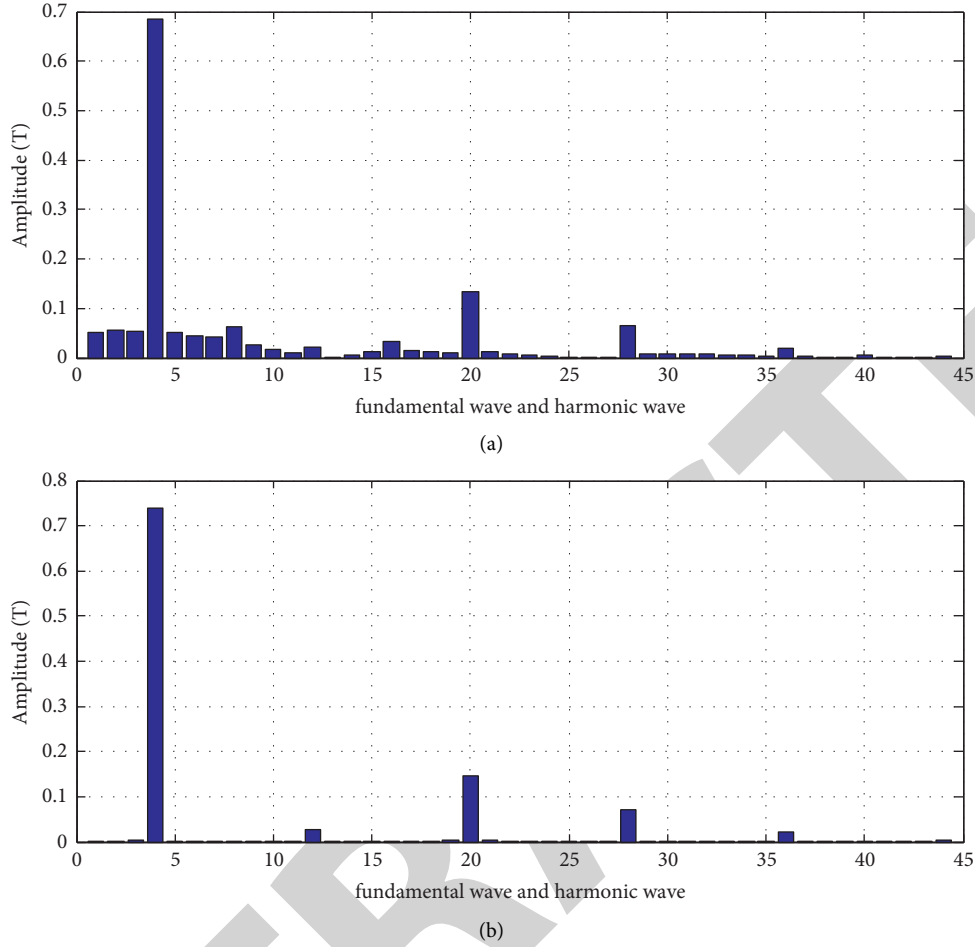


FIGURE 2: The fundamental wave and harmonic wave of no-load radial air gap flux density for 50% demagnetization of a single permanent magnet and healthy permanent magnet. (a)The fundamental wave and harmonic wave of no-load radial air gap flux density for 50% demagnetization of a single permanent magnet. (b)The fundamental wave and harmonic wave of no-load radial air gap flux density for healthy permanent magnet.

In the formula,  $T_s$  is the sampling time,  $i_d^p(k+1)$  and  $i_q^p(k+1)$  represent the  $(k+1)$ th  $d$  axis predictive current, and  $(k+1)$ th  $q$  axis predictive current, respectively.

**3.1.2. Cost Function.** The three-phase PMSM drive system has 8 voltage vectors, including 6 nonzero voltage vectors and 2 zero-voltage vectors. In the model predictive current control algorithm, in order to make the actual stator current track the reference current with high performance, it is necessary to define a reasonable cost function, and the voltage vector with the minimum cost function is usually taken as the optimal voltage vector for the next sampling period of the PMSM drive system.

In this study, the cost function is defined as

$$g_i = [i_d^* - i_d^p(k+1)]^2 + [i_q^* - i_q^p(k+1)]^2 + g[i_d^p(k+1), i_q^p(k+1)]. \quad (9)$$

In the formula,  $i = 0, 1, \dots, 7$ ;  $i_d^*$  and  $i_q^*$  represent  $d$  axis reference current and  $q$  axis reference current respectively, the last term is a nonlinear equation, its specific expression is

$$g[i_d^p(k+1), i_q^p(k+1)] = \begin{cases} \infty, & |i_d^p(k+1)| > i_{d\max} \text{ or } |i_q^p(k+1)| > i_{q\max}, \\ 0, & |i_d^p(k+1)| < i_{d\max} \text{ and } |i_q^p(k+1)| < i_{q\max}. \end{cases} \quad (10)$$

In the formula,  $i_{d\max}$  and  $i_{q\max}$  represent the limiting value of the  $d$  axis and  $q$  axis current, respectively. When the predictive current produced by a voltage vector exceeds the maximum allowable current, the cost function becomes infinite and the voltage vector cannot be used for the model predictive current control algorithm. When the predictive current is within the allowable range, only the first two terms are left in the cost function, and the optimal voltage vector that minimizes the cost function will be selected for the next control period of the PMSM drive system.

**3.2. Adaptive Signal Extraction Algorithm.** The adaptive signal extraction algorithm was proposed by Ziarani [24], Douglas et al. [25], and Barendse and Pilly [26] extended the algorithm to diagnosis of induction motor rotor broken bars and PMSM stator winding inter-turn short circuit faults,

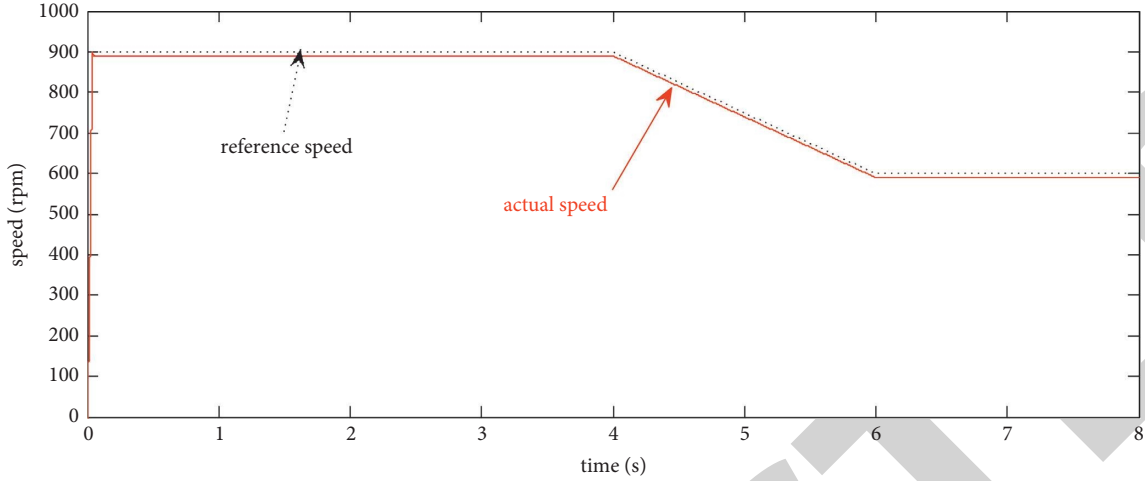


FIGURE 3: The reference speed and actual speed of the PMSM model predictive current control system.

respectively. This study applies it to fault diagnosis of PMSM rotor magnetic field local demagnetization, and gives the following derivation: Define  $i(t)$  as PMSM stator current, which includes target extraction signal  $i_o(t)$  and other signals  $i_l(t)$ , its expression is

$$i(t) = i_o(t) + i_l(t). \quad (11)$$

Assuming that the actual extracted signal of the stator current is  $i_{ext}(t)$ , the minimum square error criterion function of the  $i(t)$  and  $i_{ext}(t)$  can be minimized by the gradient descent method, and the cost function is defined as

$$J(t, \theta) = \frac{[i(t) - i_{ext}(t, \theta)]^2}{2} = \frac{1}{2} e^2(t, \theta), \quad (12)$$

where  $\theta$  is the parameter vector representing the instantaneous values of the actual extracted signal amplitude  $I(t)$ , frequency  $\omega(t)$  and phase  $\phi(t)$ . The gradient descent method provides an adjustment method to make the cost function converge to the minimum value point, and the adjustment process can be described by

$$\frac{d\theta}{dt} = -\mu \frac{\partial [J(t, \theta(t))]}{\partial \theta(t)}. \quad (13)$$

The convergence process of the cost function described by eq. (13) can generate a set of nonlinear differential equations representing the extraction process of the target extraction signal amplitude, frequency, and phase instantaneous value, and their expression is given as follows:

$$\frac{dI(t)}{dt} = \mu_1 e(t) \sin \phi(t), \quad (14)$$

$$\frac{d\omega(t)}{dt} = \mu_2 I(t) e(t) \cos \phi(t), \quad (15)$$

$$d\phi(t)dt = \mu_2 \mu_3 e(t) \cos \phi(t) + \omega(t), \quad (16)$$

$$i_{ext}(t) = I(t) \sin \phi, \quad (17)$$

where  $I(t)$ ,  $\omega(t)$  and  $\phi(t)$  represent the instantaneous values of the actual extracted signal amplitude, frequency and phase,  $e(t)$  is extraction error,  $\mu_1$ ,  $\mu_2$  and  $\mu_3$  are small positive constant, their size will determine the signal extraction accuracy and extraction speed. The adaptive extraction of the target extraction signal can be realized by solving the nonlinear differential equations (14)-(17).

**3.3. Hilbert-Huang Transform.** Literature research shows that, when the PMSM rotor magnetic field has a local demagnetization fault, the fault characteristic harmonics will be generated in the stator current [10, 11, 12, 13, 14], which is expressed as

$$f_{\text{fault}} = f_s \left( 1 \pm \frac{k}{p} \right). \quad (18)$$

Here,  $f_{\text{fault}}$  is the fault characteristic harmonics,  $f_s$  is the fundamental frequency of the stator current, and  $p$  is the pole pairs of PMSM and  $k$  is a positive integer.

As a nonlinear and nonstationary signal processing method based on instantaneous frequency, the Hilbert-Huang transform has stronger adaptability and clearer physical meaning in processing nonstationary signals [27]. As an important part of the Hilbert-Huang transformation, empirical mode decomposition (EMD) can adaptively decompose nonstationary signals into a series of single component intrinsic mode functions with definite physical significance for instantaneous frequencies according to certain screening principles, then the instantaneous frequencies of each intrinsic mode function are obtained by Hilbert transform, and the time-frequency representation of the original signal is finally obtained. The extraction process of the intrinsic mode function is as follows:

- (i) Obtain all extreme points of the original signal  $x(t)$  and their upper and lower envelopes  $e_{\max}(t)$  and  $e_{\min}(t)$ .
- (ii) Calculate the instantaneous envelope mean value,  $m_I(t) = (e_{\max}(t) + e_{\min}(t))/2$ .

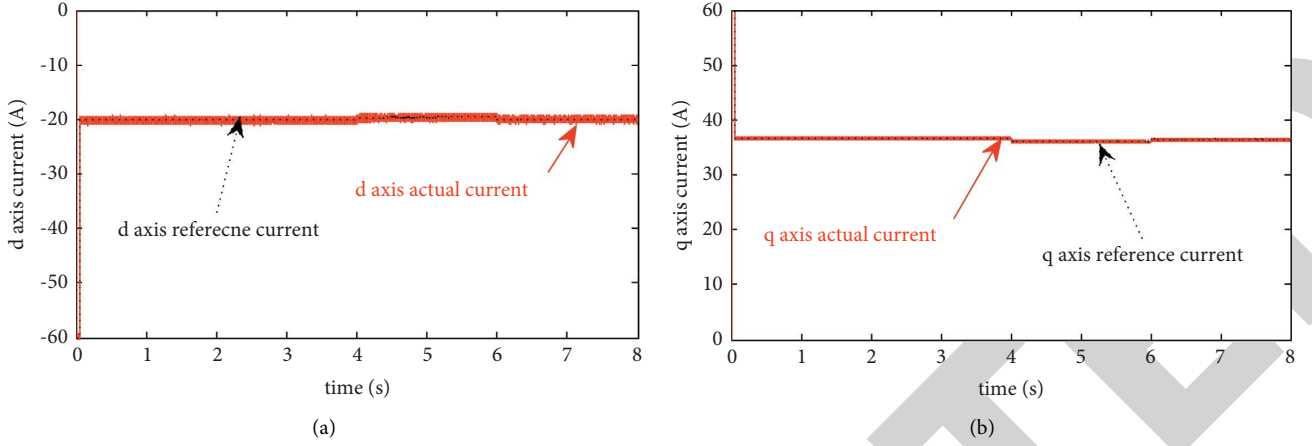


FIGURE 4: The  $dq$  axis reference current and actual current of PMSM. model predictive current control system. (a)  $d$  axis reference current and actual current. (b)  $q$  axis reference current and actual current.

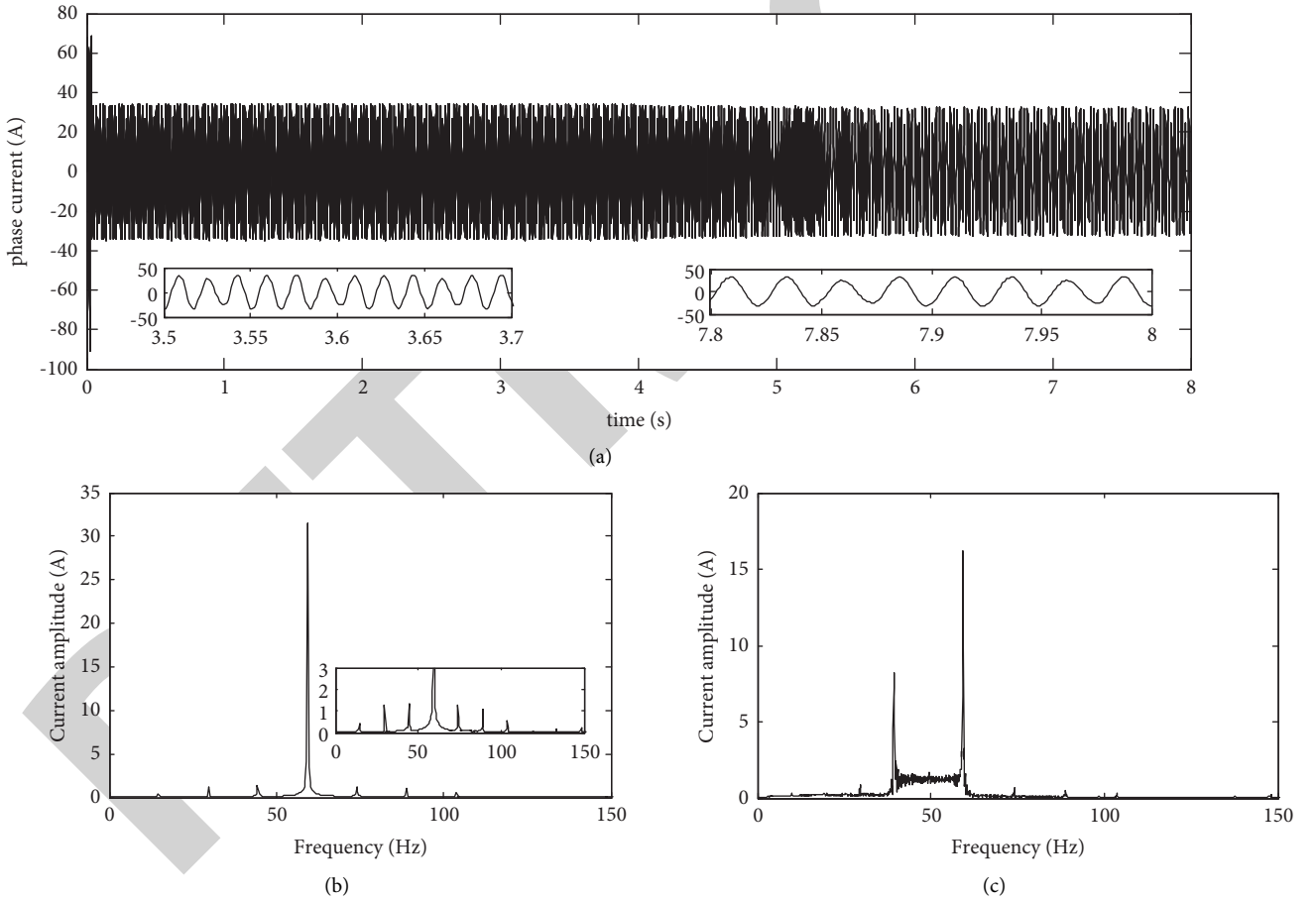


FIGURE 5: PMSM stator current and its Fourier spectrum at 50% demagnetization of a single permanent magnet. (a) Stator current. (b) Fourier spectrum of local steady-state current. (c) Fourier spectrum of the global current.

- (iii) Calculate the difference between  $x(t)$  and  $m_1(t)$ , let  $h_{11}(t) = x(t) - m_1(t)$ .  $h_{11}(t)$  generally does not satisfy the standard deviation condition described by eq. (19), it needs to be used as the original signal  $x(t)$ , and the above

extraction process is repeated. It is assumed that after  $k$  times of decomposition, the obtained  $h_{1k}(t)$  satisfies the standard deviation condition described in eq. (19), then the first intrinsic mode function  $h_{1k}(t)$  is obtained and denoted as  $C_1$ .

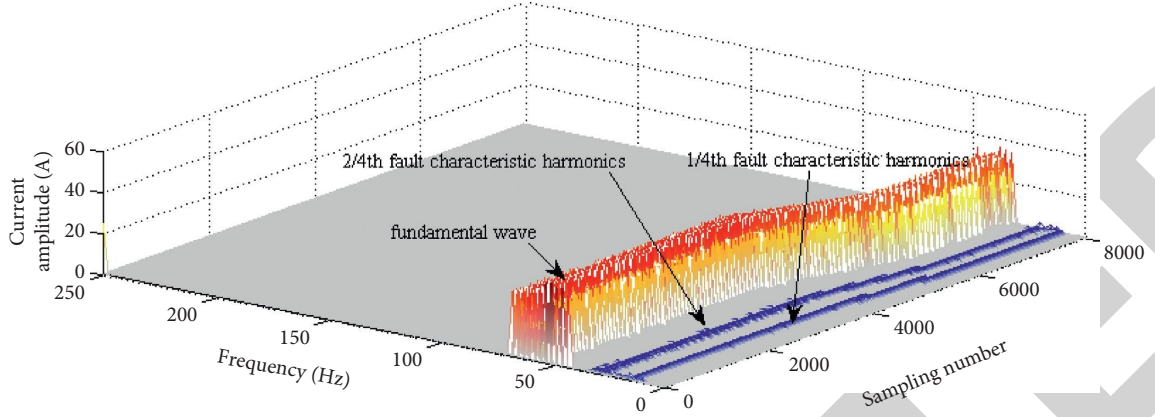


FIGURE 6: The three-dimensional time-frequency spectrum of stator phase current based on the Hilbert–Huang transform.

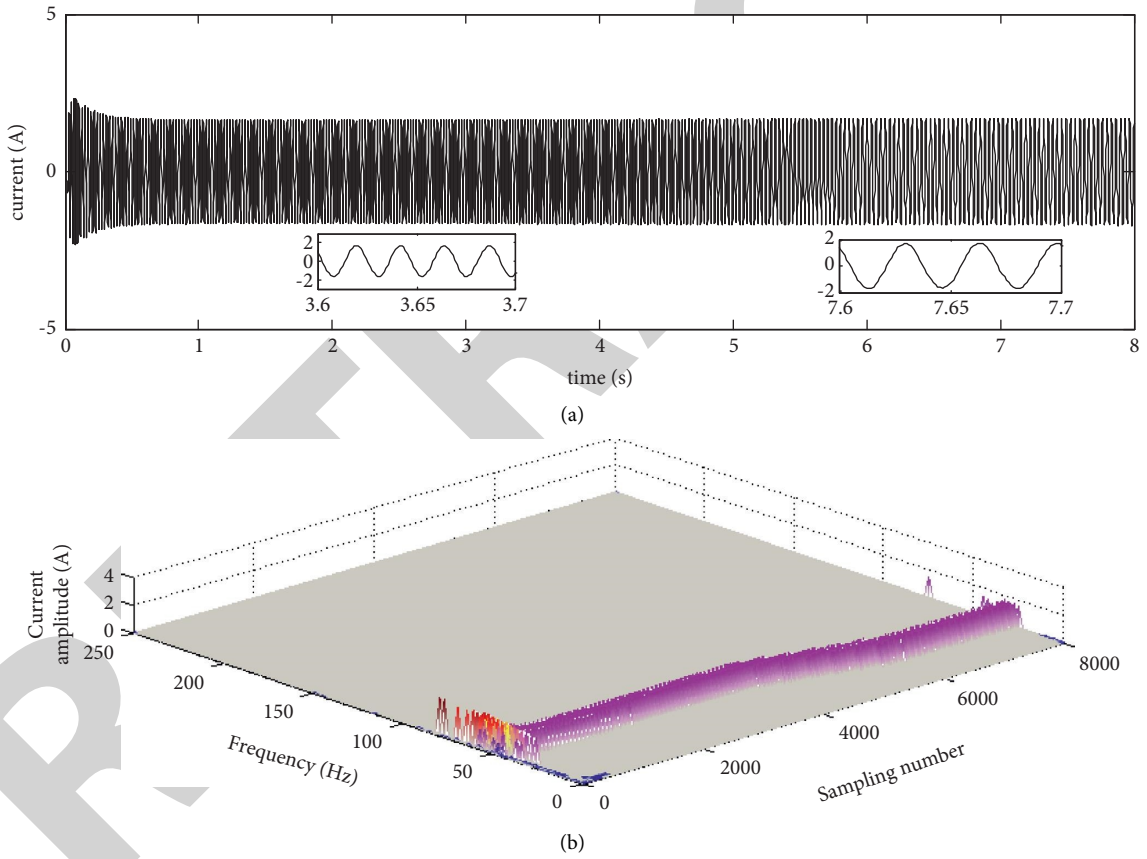


FIGURE 7: The extracted 3/4 order harmonic current based on adaptive signal extraction algorithm and its three-dimensional time-frequency spectrum based on the Hilbert transform. (a) The extracted 3/4 order harmonic current based on adaptive signal extraction algorithm. (b) Three-dimensional time-frequency spectrum based on Hilbert transform.

$$sd = \sum_{k=1}^T [h_1(k-1) - h_{1k}(t)]^2. \quad (19)$$

In the formula,  $sd$  is usually taken as 0.2–0.3.

- (iv) Let  $r_1(t) = x(t) - h_{1k}(t)$ , and let the  $r_1(t)$  be the original signal  $x(t)$ , that is,  $x(t) = r_1(t)$ .

Repeat steps (1)–(4), until the  $r_n(t)$  after  $n$  times of decomposition is smaller than the predetermined value or is a monotone function, EMD decomposition is completed, and a series of intrinsic mode functions with decreasing frequency components denoted  $C_1, C_2, \dots, C_n$  and a residual component  $r_n$  that no longer contains any frequency



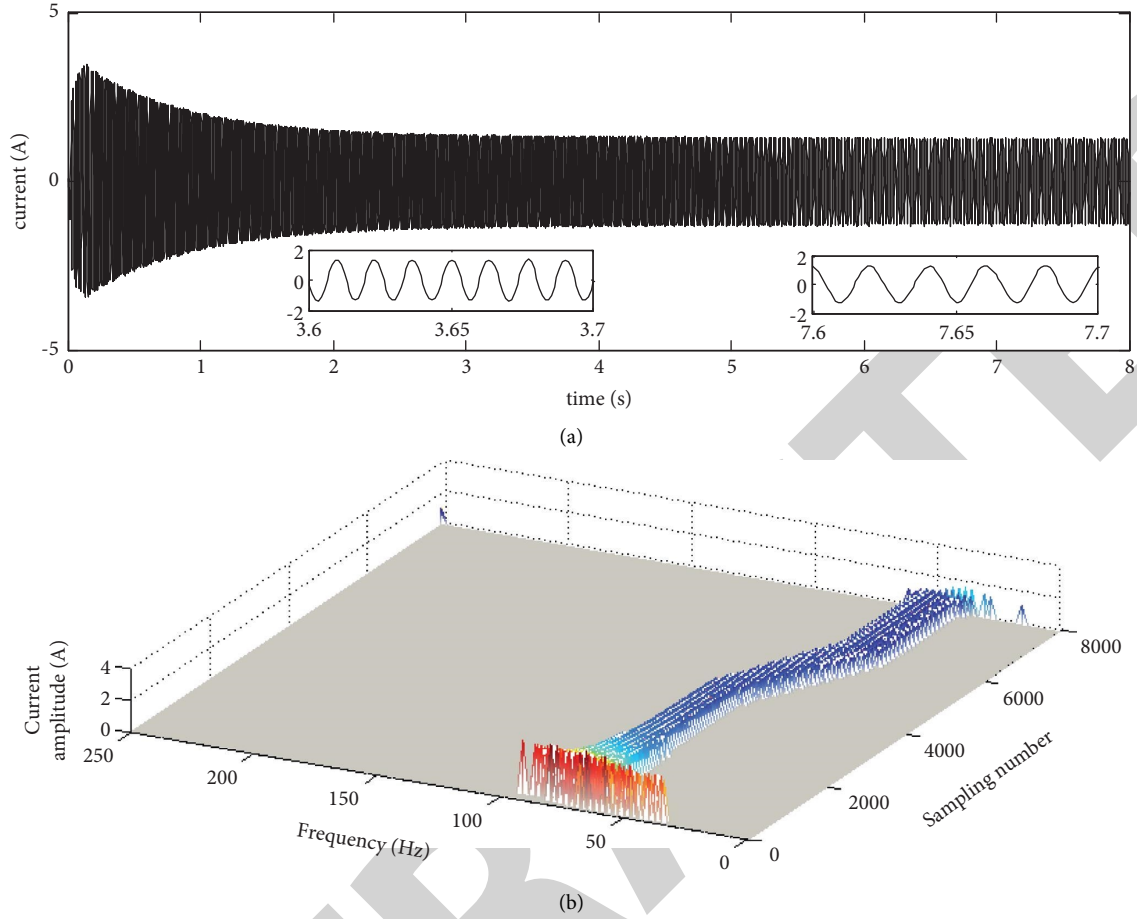


FIGURE 8: The extracted 5/4 order harmonic current based on adaptive signal extraction algorithm and its three-dimensional time-frequency spectrum based on Hilbert transform. (a) The extracted 5/4 order harmonic current based on adaptive signal extraction algorithm. (b) Three-dimensional time-frequency spectrum based on Hilbert transform.

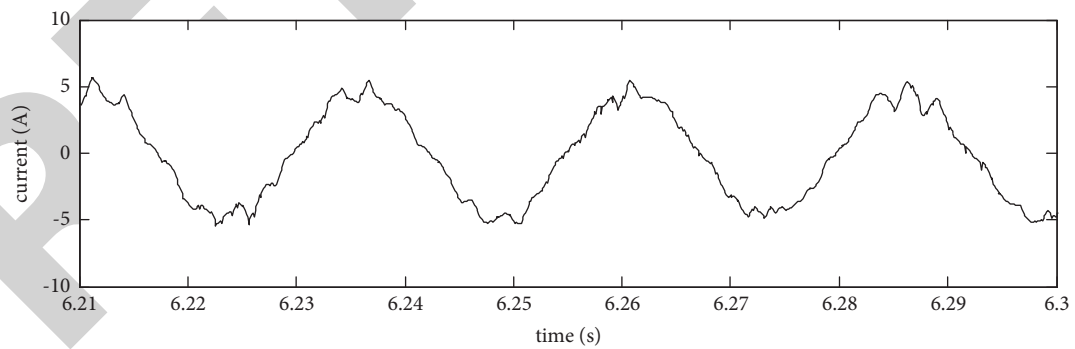


FIGURE 9: The measured stator current at the speed of 600 rpm.

information are obtained. At this time, the decomposition formula of the original signal  $x(t)$  can be expressed as

$$x(t) = \sum_{i=1}^n C_i + r_n. \quad (20)$$

After obtaining a set of intrinsic mode functions of the original signal through EMD decomposition, the

instantaneous frequency of each intrinsic mode function can be calculated by using Hilbert transform, so as to obtain the time-frequency relationship of the original signal, namely, the instantaneous frequency. However, for the weak fault characteristic signals near the fundamental wave, it is difficult to realize effectively decompose due to the limitation of its own decomposition ability, this will inevitably limit its ability to characterize local demagnetization fault and reduce

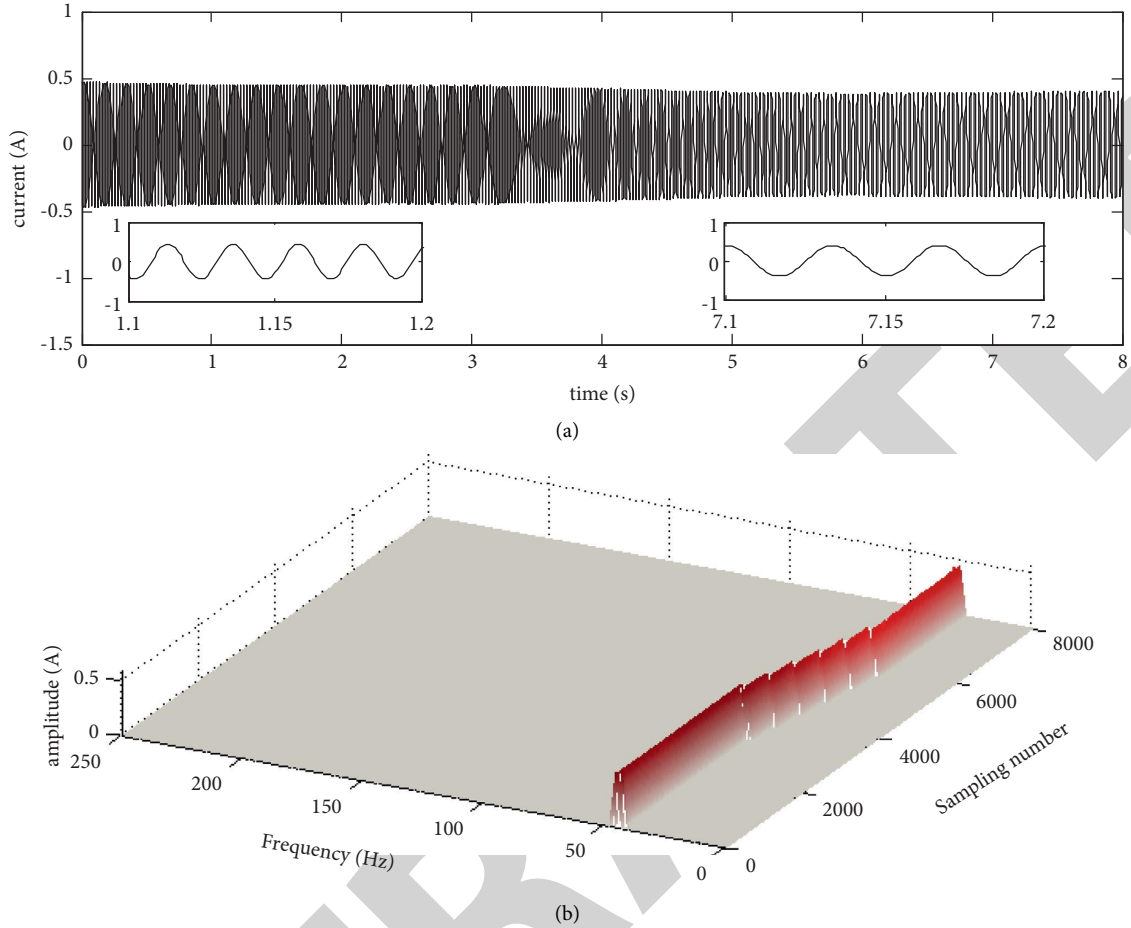


FIGURE 10: The 3/4 order fault characteristic harmonic current extracted from stator current based on adaptive signal extraction algorithm and its three-dimensional time-frequency spectrum based on Hilbert transform. (a) The 3/4 order fault characteristic harmonic current extracted from stator current. (b) Three-dimensional time-frequency spectrum.

the accuracy of fault diagnosis using this method. At the same time, the decomposition process of EMD is complicated and the calculation amount is relatively large.

#### 4. Simulation Research

The PMSM parameters used for simulation are shown in Table 1. Based on the established PMSM mathematical model considering the local demagnetization fault of the rotor magnetic field, the simulation model of its model predictive current control system is established by using MATLAB/Simulink. The simulation step size and the discrete period of the model predictive current control algorithm are both set at 0.1 ms, and the current sampling frequency is set at 1 KHz. Figure 3 shows the reference speed and actual speed of the PMSM model predictive current control system when the rotor magnetic field is in healthy state, and Figure 4 shows its  $dq$  axis reference current and actual current. It can be seen from Figures 3 and 4 that the model predictive current control algorithm can realize fast, no overshoot tracking of PMSM speed and accurate control of  $dq$  axis current, and has high speed and current control performance. The PMSM model

predictive current control system operates under the conditions shown in the reference speed in Figure 3, and sets a single permanent magnet to lose its flux density by 50%. Figure 5(a) is the PMSM stator current waveform under the above fault state, Figures 5(b) and 5(c) are the Fourier spectrum of local steady-state current (1–4 seconds data in Figure 5(a)) and global current (1–8 seconds data in Figure 5(a)), respectively. It can be seen from Figure 5(b) that when the PMSM rotor magnetic field is locally demagnetized, the fault characteristic harmonics shown in (18) appear in the stator current (integer harmonics are not considered), and the Fourier transform can obtain the frequency domain representation of the fault characteristic signal under the steady-state operating condition of the PMSM drive system, which provides a basis for rotor magnetic field local demagnetization fault diagnosis. However, in the nonstationary operating condition of the PMSM drive system, the Fourier transform cannot obtain the correct frequency and current amplitude transformation results, as shown in Figure 5(c).

Figure 6 is the three-dimensional time-frequency spectrum of the current in Figure 5 obtained based on the Hilbert–Huang transform. It can be seen from Figure 6 that the Hilbert–Huang

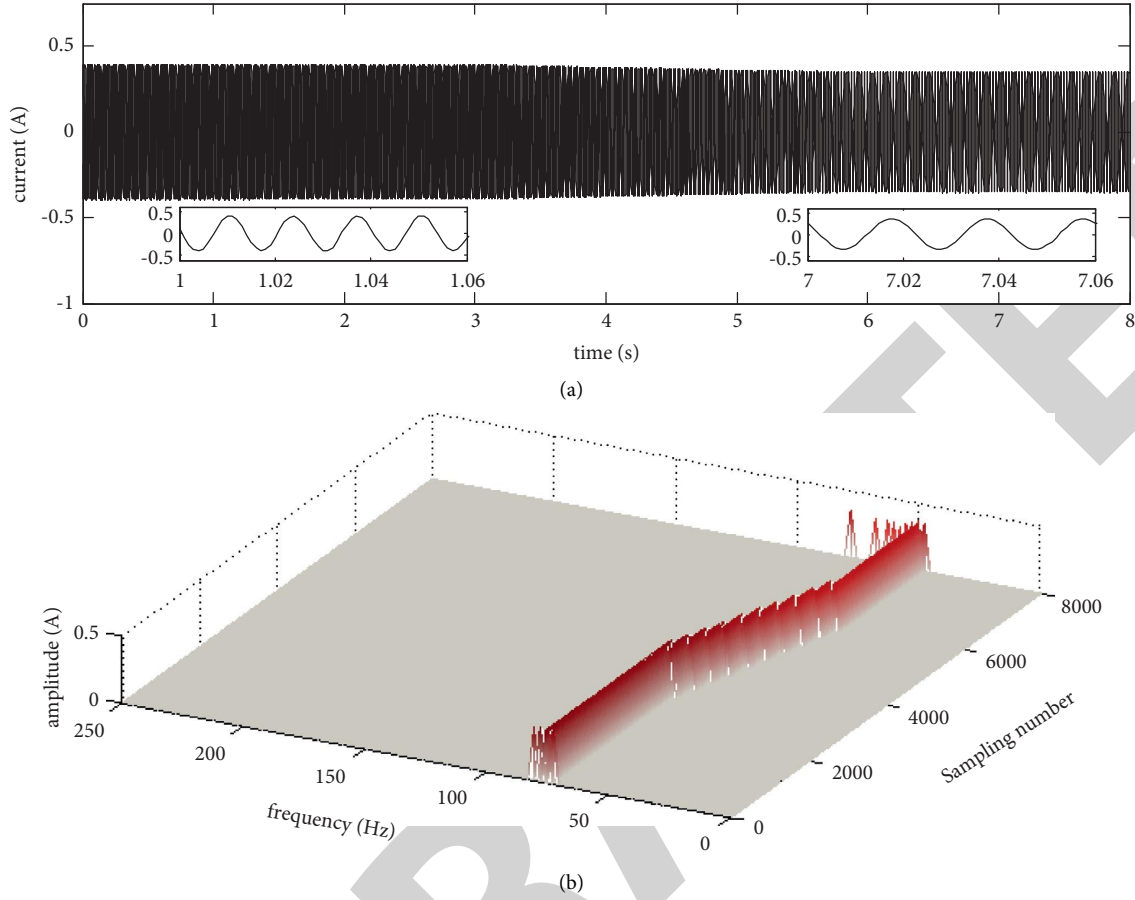


FIGURE 11: The 5/4 order fault characteristic harmonic current extracted from stator current based on adaptive signal extraction algorithm and its three-dimensional time-frequency spectrum based on Hilbert transform. (a) The 5/4 order fault characteristic harmonic current extracted from stator current. (b) Three-dimensional time-frequency spectrum.

transform can accurately decompose the current fundamental wave, the 1/4th and the 2/4th fault characteristic harmonic in stationary and nonstationary states of the PMSM drive system and obtain their instantaneous frequencies, which can be used as the basis for the diagnosis of rotor magnetic field local demagnetization fault of PMSM model predictive current control system, but it is limited by its decomposition ability, the 3/4th, 5/4th, 6/4th, and 7/4th fault characteristic harmonics close to the fundamental frequency are annihilated by the larger fundamental current and cannot be effectively decomposed, which reduces the reliability of characterizing the rotor magnetic field local demagnetization fault by fault characteristic harmonics.

In order to obtain the noninteger fault characteristic harmonics annihilated by the fundamental current, an adaptive signal extraction algorithm is introduced in this study to achieve the effective extraction of the target fault characteristic harmonics, and then the time-frequency transformation of the extracted fault characteristic signal is realized based on Hilbert transform to obtain its instantaneous frequency. Figures 7 and 8 show the 3/4th and the 5/4th fault characteristic harmonics and their three-dimensional time-frequency spectrum obtained based on the proposed method in this paper, the 6/4th and 7/4th fault

characteristic harmonics and their time-frequency spectrum are no longer given due to the limitation of this paper workload. It can be seen from Figures 7(a) and 8(a) that the adaptive signal extraction algorithm can accurately extract the target fault characteristic harmonics; the time-frequency spectrum of the extracted fault characteristic signal based on Hilbert transform is shown in Figures 7(b) and 8(b); as shown in Figures 7(b) and 8(b), the reliability of fault characteristic harmonics in characterizing local demagnetization fault of PMSM rotor magnetic field can be significantly improved, which lays a foundation for reliable diagnosis of PMSM rotor magnetic field local demagnetization fault. Meanwhile, this method has much less computation than Hilbert–Huang transform, which is convenient for online implementation.

## 5. Experimental Verifications

In order to realize the experimental verifications of the proposed method, an experimental plat of PMSM model predictive current control system was built, which mainly includes a control and drive unit, power conversion unit, signal detection and conditioning unit, protection and loading unit, etc. The system debugging interface was

designed based on the control desk to realize the online adjustment of control parameters and real-time display and storage of measurement data. The main control unit was built with dSPACE standard component system, the program code generation and loading of the PMSM model predictive current control system was completed and the SVPWM signal was generated to drive the inverter. The experimental system is loaded with an AC dynamometer, and the PMSM parameters are as follows: rated voltage is 380 V, stator resistance is  $0.28 \Omega$ ,  $dq$ -axis stator inductance is 1.273 mH, rotor flux linkage is 0.1278 Wb, and the number of pole pairs is 4.

The fault injection method is used to implement the experimental verification of the proposed diagnosis method for rotor magnetic field local demagnetization fault in the PMSM model predictive current control system. The 3/4th and 5/4th fault characteristic harmonics of the fundamental current are injected through the host computer, and the amplitude of the injected harmonics is the same as the amplitude ratio of the characteristic harmonics and the fundamental current obtained in the simulation study. The system control period and the discrete period of the model predictive current control algorithm are set at 0.1 ms, the current sampling frequency is set at 1 KHz, and the load torque is set at 3.0 Nm. Taking the dynamic running state of the PMSM model predictive current control system to verify the correctness and feasibility of the proposed fault diagnosis method, that is, the PMSM speed starts to fall from 900 rpm at the third second of the experimental data, and enters the steady state of 600 rpm at the fifth second. Figure 9 is the measured current waveform when the speed drops to 600 rpm, Figure 10 is the 3/4 order fault characteristic harmonic current extracted from stator current 9 based on adaptive signal extraction algorithm and its three-dimensional time-frequency spectrum based on Hilbert transform, and Figure 11 is the 5/4 order fault characteristic harmonic current extracted from stator current based on adaptive signal extraction algorithm and its three-dimensional time-frequency spectrum based on Hilbert transform. It can be seen from Figures 10(a) and 11(a) that the adaptive signal extraction algorithm can realize the accurate extraction of the characteristic harmonics of the rotor magnetic field local demagnetization fault in the PMSM model predictive current control system. The time-frequency spectrum of the extracted fault characteristic signal, as shown in Figures 10(b) and 11(b), can be used as a reliable basis for the rotor magnetic field local demagnetization fault diagnosis of the PMSM model predictive current control system, which greatly improves the ability of the fault characteristic signals to characterize the local demagnetization fault of the PMSM rotor magnetic field, the experimental results agree with the simulation results. Due to the heavy workload, the experiment verification of extraction and time-frequency transformation of other fault characteristic harmonics are not repeated in this study.

## 6. Conclusion

On the basis of establishing the PMSM mathematical model considering the rotor magnetic field local demagnetization fault, and the simulation model of its model predictive

current control system, a diagnosis method of rotor magnetic field local demagnetization fault in PMSM model predictive current control system is proposed in this study, the accuracy and effectiveness of the proposed method are verified by simulation and experiments, and the following conclusions are drawn:

- (i) The established PMSM mathematical model considering the rotor magnetic field local demagnetization fault can realize the accurate characterization of the abovementioned fault, which lays a foundation for establishing the simulation model of its model predictive current control system and implementing research on the diagnosis method of the local demagnetization fault.
- (ii) The PMSM drive system based on the model predictive current control algorithm can realize high-performance control of speed and current, which is beneficial to meet the system control requirements of wide speed regulation range, good dynamic characteristics, fast current response, and high-power density.
- (iii) The adaptive signal extraction algorithm can realize the effective extraction of the fault characteristic signal of the rotor magnetic field local demagnetization fault in the PMSM model predictive current control system under the stationary and nonstationary operating conditions, and effectively solve the problem existing in the Hilbert-Huang transform that the weak fault characteristic signal nearby fundamental wave component is difficult to be decomposed, which greatly improves the diagnosis reliability of the PMSM rotor magnetic field local demagnetization fault. And this algorithm has much less computation than the EMD algorithm, which is convenient for online implementation.

## Data Availability

The experimental data used to support the findings of this study are available from the corresponding author upon request.

## Conflicts of Interest

The authors declared that they have no conflicts of interest regarding this work.

## Acknowledgments

This work was sponsored in part by Henan Province Science and Technology Project (nos. 202102210293 and 192102210076).

## References

- [1] K. H. Zhao, R. R. Zhou, J. H. She et al., "Demagnetization-fault reconstruction and tolerant-control for PMSM using improved SMO-based equivalent-input-disturbance approach," *IEEE*, vol. 27, no. 2, pp. 701–712, 2022.

## *Retraction*

# **Retracted: Analysis of Management Innovation of State-Owned Enterprises in the Context of Artificial Intelligence and Market-Oriented Economic Fluctuations**

### **Security and Communication Networks**

Received 1 August 2023; Accepted 1 August 2023; Published 2 August 2023

Copyright © 2023 Security and Communication Networks. This is an open access article distributed under the Creative Commons Attribution License, which permits unrestricted use, distribution, and reproduction in any medium, provided the original work is properly cited.

This article has been retracted by Hindawi following an investigation undertaken by the publisher [1]. This investigation has uncovered evidence of one or more of the following indicators of systematic manipulation of the publication process:

- (1) Discrepancies in scope
- (2) Discrepancies in the description of the research reported
- (3) Discrepancies between the availability of data and the research described
- (4) Inappropriate citations
- (5) Incoherent, meaningless and/or irrelevant content included in the article
- (6) Peer-review manipulation

The presence of these indicators undermines our confidence in the integrity of the article's content and we cannot, therefore, vouch for its reliability. Please note that this notice is intended solely to alert readers that the content of this article is unreliable. We have not investigated whether authors were aware of or involved in the systematic manipulation of the publication process.

Wiley and Hindawi regrets that the usual quality checks did not identify these issues before publication and have since put additional measures in place to safeguard research integrity.

We wish to credit our own Research Integrity and Research Publishing teams and anonymous and named external researchers and research integrity experts for contributing to this investigation.


The corresponding author, as the representative of all authors, has been given the opportunity to register their agreement or disagreement to this retraction. We have kept a record of any response received.

### **References**

- [1] Y. Wang and L. Sun, "Analysis of Management Innovation of State-Owned Enterprises in the Context of Artificial Intelligence and Market-Oriented Economic Fluctuations," *Security and Communication Networks*, vol. 2022, Article ID 1518447, 10 pages, 2022.

## Research Article

# Analysis of Management Innovation of State-Owned Enterprises in the Context of Artificial Intelligence and Market-Oriented Economic Fluctuations

Yanwen Wang<sup>1</sup> and Lu Sun<sup>2</sup> 

<sup>1</sup>Guangdong Provincial Key Laboratory of Public Finance and Taxation with Big Data Application, Guangdong University of Finance & Economics, Guangzhou 510320, China

<sup>2</sup>School of Public Finance & Taxation, Guangdong University of Finance & Economics, Guangzhou 510320, China

Correspondence should be addressed to Lu Sun; sunlusunlu@gdufe.edu.cn

Received 20 May 2022; Accepted 8 July 2022; Published 8 September 2022

Academic Editor: Hangjun Che

Copyright © 2022 Yanwen Wang and Lu Sun. This is an open access article distributed under the Creative Commons Attribution License, which permits unrestricted use, distribution, and reproduction in any medium, provided the original work is properly cited.

At this stage, with the development of society, China's modernization level has also been greatly improved. Under the background of artificial intelligence and the impact of economic globalization, China's external economic environment is changing with each passing day. Chinese enterprises are looking for new development ways to maintain their own development vitality under the condition of artificial intelligence. State-owned enterprises are controlled by the central or local governments. On this basis, this paper mainly discusses the innovative methods of state-owned enterprise management under the background of artificial intelligence, so as to provide reference for the innovation of state-owned enterprise management.

## 1. Introduction

China has a large population, unbalanced regional development, and different levels of economic development in different regions, and the strength of SOEs is different [1]. Under the socialist market conditions, SOEs on the same line should maintain a high degree of market sensitivity, actively make use of advanced market information, actively seize opportunities, appropriately adjust internal business strategies, better improve operation and management efficiency, and stabilize their development advantages under the condition of market competition [2]. The times are advancing, science and technology are developing, and industry norms and requirements are constantly improving. In terms of SOEs, there are certain problems in their own management to varying degrees [3]. It is necessary to further strengthen the advantages and overcome the disadvantages, so as to improve the best combination of resources and improve the efficiency of resource utilization [4]. As the management of SOEs is more complex, it involves the management of people, money, and

materials. To strengthen supervision, how to stimulate the working motivation of all employees and produce  $1 + 1 > 2$  synergy is an important development issue worthy of consideration in the development of SOEs.

Under the condition of artificial intelligence, the innovative management of SOEs can make the internal financial management of enterprises consistent with the optimal scheme of enterprises, maximize the profits of enterprises, and realize the low cost and high profitability of production process. The innovation of enterprise management is also reflected in the innovation of enterprise financial management [5]. The innovation of enterprise financial management is becoming more and more important in enterprise management. At this stage, the economic development of SOEs is facing the problems of high cost and low capital turnover, which has an adverse impact on the economic benefits of enterprises. The implementation of management innovation can give full play to the function and role of enterprise financial management and play a key role in the economic development of enterprises.



However, most SOEs adopt a centralized form of management, resulting in a lack of scientific decision-making. At this stage, many managers of large enterprises in China are directly appointed by the government and adopt centralized management, resulting in many people in charge of several jobs, resulting in a lack of efficiency in decision-making, which affects the normal development of the enterprise. In addition, many enterprises have a strong political management color, and there is a personal decision-making monopoly, which seriously affects the management efficiency of enterprises, resulting in the lack of scientific and effective decision-making, and even affects the economic benefits of the company.

The design of internal institutions of SOEs lacks rationality. Because China is influenced by the planned economic system, although it has been improved after the reform and opening up, it still has the influence of the planned economic system. At the present stage, the division of labor on the management institutions of Chinese enterprises is too fine, there is crossover between functions, and the main leaders of many companies assume other positions in the company, which is not conducive to improving the effectiveness of the company, and even more so to the improvement of the company's management level, resulting in some people doing nothing in the office, while others have things to do, which to a certain extent increases the expenses of managers [6].

There is a lack of secondary innovation ability of technological innovation in SOEs. Technological innovation is one of the important core contents of an enterprise's development, and only continuous innovation can keep the development with constant vitality and vigor [7]. With the development of technology, many enterprises in China began to introduce a large number of foreign advanced technologies, but due to the backward management of Chinese enterprises, there is no way to adapt to the development of technology, resulting in the use of technology does not play its true role in the effect [8–10].

## 2. Related Work

The regulating capacity refers to the ability of the state-owned economy to participate in industries with a dominant position and to control and support pillar industries in order to promote stable growth of the national economy [11]. Safeguarding capacity, on the other hand, refers to the ability to maintain national security and social stability through control of the public security sector. This interpretation of the control capacity of the state-owned economy has also been widely adopted by domestic scholars [12].

The specific quantification and measurement of SOE control can be reflected in two aspects: "quantity" and "quality." From the perspective of "quantity," the control power of SOEs should be reflected in the scale of SOEs [13]. In other words, the employment, main business income, total output value, and total asset value of SOEs should occupy a certain proportion of the corresponding overall index. From the perspective of "quality," the control of SOEs should be reflected in a reasonable industrial layout. In [14],

the number of employees and operating income of state-owned and state-controlled enterprises were used to analyze the control power of SOEs. [15] selected the share of the gross product of SOEs in the total output value of the society and used this indicator as a measure of the control power of SOEs. In subsequent studies, domestic scholars began to measure the control power of SOEs by combining the indicators of industrial value added, total assets, total profit, main business income, and owner's equity. In order to refute the theory of "the state advancing and the people retreating," [16] used industrial enterprise data and selected the changes in the number, profit, and output value of SOEs as a measure of SOE control. However, these measures of SOEs' control are all based on the scale and do not take into account the changes in the layout of SOEs in the industry. Therefore, the most cited measure of SOE control is that of the National Bureau of Statistics (2001). This measure defines the regulation and guarantee coefficient and the vitality coefficient, and measures the control power of SOEs in three steps: in the first step, data on the proportion of state-owned owners' equity in the whole industry  $M_1$ , the proportion of state-owned assets in the whole industry  $M_2$ , and the proportion of state-owned sales revenue in the whole industry  $M_3$  are selected and given different weights according to the degree of importance, i.e., according to the formula.

$$A_j = 0.3 * M_1 + 0.3 * M_2 + 0.4 * M_3, \quad (1)$$

Measure the  $j$  th industry state-owned enterprise regulation and guarantee coefficient; select state-owned and industry-wide owner's equity growth rate  $d_1, D_1$ , state-owned and industry-wide asset growth rate  $d_2, D_2$ , state-owned and industry-wide sales revenue growth rate data  $d_3, D_3$ , and state-owned and industry-wide labor growth rate  $d_4, D_4$  data, according to the formula.

$$D_j = 0.25 * \frac{(1 + d_{1j})}{(1 + D_{1j})} + 0.2 * \frac{(1 + d_{2j})}{(1 + D_{2j})} + 0.3 * \frac{(1 + d_{3j})}{(1 + D_{3j})} + 0.25 * \frac{(1 + d_{4j})}{(1 + D_{4j})}. \quad (2)$$

Measure the vitality coefficient of SOEs in the  $j$  th industry. In the second step, the control power of SOEs in the  $j$  th industry is obtained by multiplying the regulating guarantee coefficient of SOEs in the  $j$  th industry with the vitality  $R_j$ . In the third step, different weights are assigned to different industries and summed up to obtain the overall SOE control power  $R$ .

Based on the measurement method of the National Bureau of Statistics subject group, [17] re-estimated the weights that should be assigned to the share of state-owned owner's equity, the share of state-owned assets, and the share of state-owned sales revenue in measuring the control power of SOEs in different industries. The article selected data on total market value, total assets, and main business revenue of 1287 representative industrial SOEs according to  $M = \beta_0 + \beta_1 K + \beta_2 R$ , where  $M$  represents the total market value of the enterprise,  $K$  represents the total assets of the



enterprise, and  $R$  represents the main business revenue. The weight indicators were estimated by  $\beta_1, \beta_2$  regression results.

At present, fewer domestic scholars have studied the relationship between SOEs and economic volatility in depth into the mechanism. [18] used time series data to analyze the relationship between the share of the state-owned economy and the volatility of China's economic growth over the period 1980–2012. The study used a vector autoregressive model and an error correction model, taking consumption, investment, export, and institutional factors into account in the model, and examined the impact of the declining share of the state-owned economy on the magnitude of economic growth volatility through impulse response function and variance decomposition. The results of the study indicated that the declining share of the state-owned economy was one of the important reasons for the magnitude of economic growth volatility being amplified. [19] proposed that the business objectives of SOEs are dual in nature, i.e., profit objectives and scale objectives. On the one hand, SOEs pursue the maximization of their own interests, and on the other hand, they need to coordinate the relationship between national interests, collective interests and employees' interests, and the relative weights between SOEs' profit goals and scale goals are constantly changing [20]. How to develop a scientific, reasonable, and effective management mechanism to enhance the competitiveness of state-owned enterprises has become an urgent and important problem-facing state-owned enterprises at present [21–23].

The results of the study show that the model well represents the “high volatility” characteristic of China's economic fluctuation before 2000 and the “narrowing volatility” phenomenon after 2000. Therefore, the paper concludes that the duality of SOEs' business objectives and the change of relative weights between them are one of the important reasons for the phase change of China's economic volatility around 2000.

All in all, the results show that compared with previous studies, this model can better reflect the phenomenon of “high volatility” and “narrow volatility” of China's economic fluctuations before 2000. Therefore, this paper considers that the duality of state-owned enterprises' business objectives and the change of their relative weight are one of the important reasons for the fluctuation cycle of China's economy around 2000.

### 3. Methodology

The main goal of innovative change is to adjust the economic structure in the current market and reasonably allocate all resources so as to promote the healthy development of the national economy, among which the supply-side factors include land, innovation, labor, and capital. By carrying out innovative changes, we can reasonably adjust the industrial structure of China in the form of reform, adjust and optimize the unreasonable allocation of factors, enhance the utilization rate of factors, and gradually achieve the optimal allocation. In addition, in the process of carrying out supply-side structural reform, incremental reform is often adopted when adjusting the stock of factors, which means that

promoting this reform can not only lead to a reasonable investment structure, but also expand the market effect as well as rationalize the industrial structure. In addition, innovative changes focus on the market and government being able to play a decisive role in allocating relevant resources, alleviating problems such as supply inhibition and supply constraints, meeting the growing new demands of the market economy, and tapping the potential of all types of consumption in the market.

Based on the principles of scientificity, feasibility, effectiveness and systematization, the enterprise management innovation process under the background of artificial intelligence is regarded as a continuous chain process. The structure of this paper is shown in Figure 1, which includes three stages of creativity generation, creativity transformation and creativity dissemination. Specifically, it mainly includes six key modules of creativity collection, screening, absorption, transformation, and innovation.

As shown in Figure 2(a), the traditional closed innovation model emphasizes the concept that “successful innovation requires strict internal control”; i.e., an enterprise can only obtain a strong competitive advantage through continuous and intense internal technological research and development, and ensure strict control of intellectual property rights through internal channel marketization. This kind of closed innovation was successfully verified by many large enterprises in the 20th century and before, but since the 21st century, this innovation mode of enterprises can no longer adapt to the competitive environment of informationization and globalization, so the open innovation mode combining external innovation resources and internal R&D to enhance the competitiveness of enterprises has become an inevitable trend of enterprise innovation. As shown in Figure 2(b), the open innovation model emphasizes the permeability of enterprise boundaries and the importance of external resources to enterprise innovation, interacts effectively with the external environment, promotes cooperative knowledge development and two-way flow, and realizes value co-creation by integrating all new ideas from within and outside the enterprise. In order to better understand the new innovation concept of open innovation, some domestic and foreign scholars have conducted a comparative study of two innovation models, open innovation and closed innovation, mainly in terms of staff concept, innovation ideas, R&D process, competitive advantages, intellectual property rights, organizational boundaries and innovation scope, etc. The results are shown in Table 1.

The econometric model was further set up as an individual effects model.

$$Y_{it} = \alpha S_{it} + \beta X_i + \lambda_t + \mu_i + \varepsilon_{it}, \quad (3)$$

where the explanatory variable  $Y_{it}$  denotes market economy fluctuations;  $S_{it}$  denotes the size of SOEs and all other explanatory variables;  $X_i$  denotes individual characteristics that do not change over time;  $\mu_i$  denotes the intercept specific to the  $i$ th individual;  $\lambda_t$  denotes the time-dependent characteristics that do not change with time only and can be

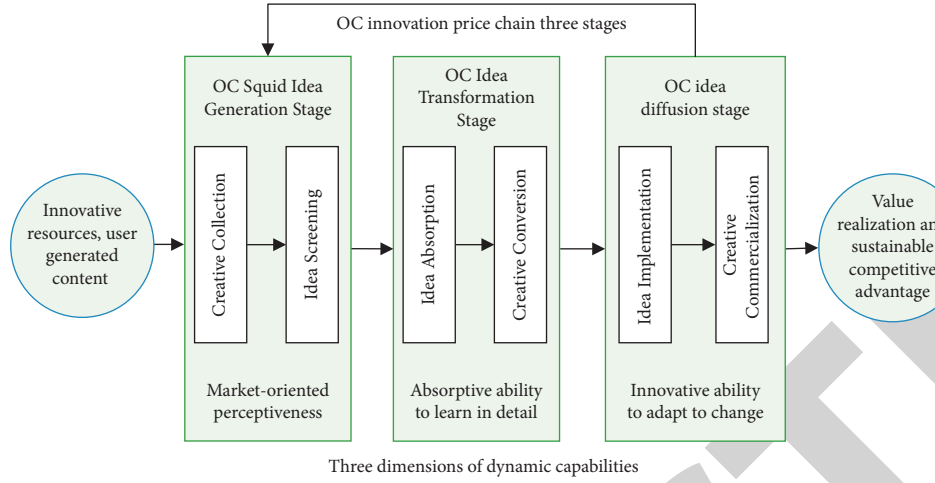


FIGURE 1: Innovation value chain model in the context of enterprise artificial intelligence.

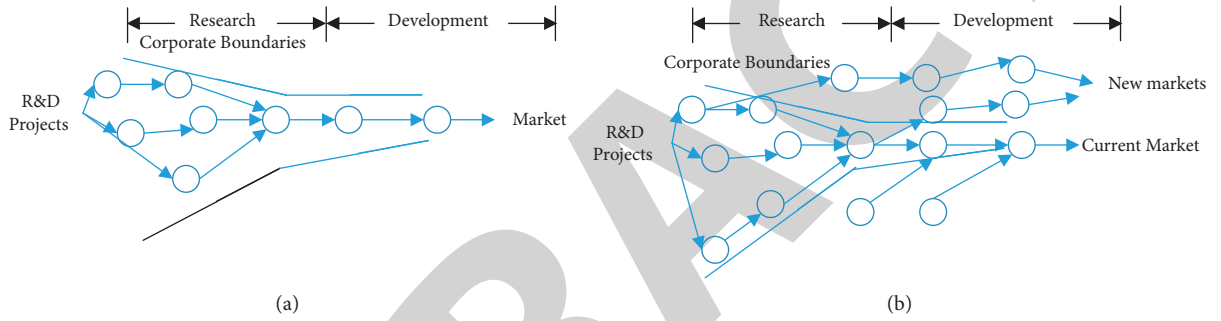


FIGURE 2: Comparison of two innovation models: (a) closed innovation and (b) open innovation.

TABLE 1: Comparison of closed innovation and open innovation.

Comparative content	Closed innovation	Open innovation
Staff philosophy	The smartest people in our industry are the internal employees who work for us	The smartest people do not all work for us, and we need to use the brightest external brains
Innovation ideology	The company wins if it has the most and best creative ideas in-house	Companies will win if they leverage internal and external creative knowledge
R&D process	The entire development process, from idea conception to implementation, is closed within the company	External R&D can create great value and should be combined with internal R&D
Competitive advantage	Be the first to turn a new idea into a new product and the first to bring it to the customer market	Having a successful business model is more important than being first to market
Intellectual property	Strictly control your intellectual property so that other companies cannot profit from your innovation	Competitiveness should be enhanced through paid use of patents or equity partnerships
Organizational boundaries	Clearly defined and impermeable	Ambiguous and permeable
Innovation scope	In-house R&D organization	All stakeholders inside and outside the company

considered as the intercept specific to period  $t$ ; and  $\mu_i + \varepsilon_{it}$  these two parts of the perturbation terms, together, constitute the compound perturbation term of the model. In the model, we assume that the regression equation for each individual has a consistent slope, and the use of a differential intercept term captures the difference between individuals.

The article sets the fluctuation of real GDP growth rate (HP) as a proxy variable for the economic fluctuation of the explanatory variable. The HP filter was used to separate the

long-term trend term and the cyclical term from the real GDP growth rate, and then the absolute value of the fluctuation part was taken to represent the magnitude of economic fluctuation.

Hodrick and Prescott argue that the trend of economic growth is flat and that in the actual economic operation, economic variables fluctuate up and down around the growth trend. Method is that the trend term of the variable  $g_t$  and the short-term fluctuation term  $c_t$  together form the time series data  $y_t$ . Thus, there are

$$y_t = g_t + c_t, \quad t = 1, \dots, T. \quad (4)$$

The moving average method principle was used to process the data, and the HP filter was constructed, which separates the trend term and the periodic fluctuation term from the time series  $y_t$ , while the fluctuation part  $g_t$  is the solution of the following problem.

$$\text{Min}\left\{\sum (y_t - g_t)^2 + \lambda \sum [(g_t - g_{t-1})(g_t - g_{t-2})]\right\}. \quad (5)$$

That is, the fluctuation term  $g_t$  is the solution of the problem when the loss function is minimized. In the above problem,  $\sum (y_t - g_t)^2$  is the measure of the fluctuation component, while  $\sum [(g_t - g_{t-1})(g_t - g_{t-2})]$  represents the “smoothness” of the data, and  $\lambda$  is called the “smoothing parameter,” which can be used to adjust the ratio between the fluctuation component and the smoothness. Because different values of the “smoothing parameter”  $\lambda$  lead to a different smoothness of the data for different filters, the issue of the value of  $\lambda$  has been the subject of controversy in the academic community. At present, when economists study quarterly data, they basically follow the findings of Hodrick and Prescott (1980, 1997) [12], where the smoothing parameter is taken as 1600. However, when studying annual data, the value of  $\lambda$  is more controversial. In this paper, we set the smoothing parameter  $\lambda = 100$  to do the HP filtering of annual GDP growth rate, and the econometric software EViews also sets the smoothing parameter to 100 by default.

The article selects state-owned enterprise control (soe) as the core explanatory variable. The control power of SOEs is calculated using equation  $soe = \alpha_1 K + \alpha_2 R + \alpha_3 Q + \alpha_4 L$ , where  $K, Q, R, L$  denote the shares of total assets, total main business income, total output value, and total employed population of industrial enterprises in the region, respectively, for state-owned and state-controlled enterprises. For the weights, they can be estimated by the linear regression equation  $M = \beta_0 + \beta_1 K + \beta_2 R$  using the data of total annual market value, total assets, and main business income of enterprises. The regression results can be obtained according to the following constraints  $\alpha_1, \alpha_2, \alpha_3, \alpha_4$ .

$$\begin{aligned} \frac{\alpha_1}{(\alpha_1 + \alpha_2)} &= \frac{\beta_1}{\beta_2}, \\ \alpha_4 &= \alpha_1, \alpha_3 = \alpha_2, \\ \alpha_1 + \alpha_2 + \alpha_3 + \alpha_4 &= 1. \end{aligned} \quad (6)$$

The reason for  $\alpha_4 = \alpha_1$  is that a large number of industrial enterprises in China currently use labor-intensive production techniques, and the weight of labor in control should be comparable to that of capital.  $\alpha_3 = \alpha_2$  is because the total output value is not directly reflected in the enterprise data.

In recent years, shocks to technology ( $tfp$ ) have increasingly become one of the main sources of macroeconomic volatility, and the article selects the change in total factor productivity as a proxy variable for technology shocks. According to the real economic cycle theory, when total factor productivity increases, labor demand increases,

leading to a rise in real wages in the market, making employment increase and output rise. The estimation of total factor productivity is done in two steps: the first step is the estimation of the capital stock. The year 1999 is chosen as the base period, the perpetual inventory method is used, fixed capital formation is selected as the investment data for that year, and the capital stock data for 1999–2017 are calculated under the assumption of geometric decline in the relative efficiency of capital goods (the estimated depreciation rate is around 10.96%). In the second step, total factor productivity is calculated. The growth accounting method is used. Assume that the aggregate production function is neutral technological progress;  $Y = A_t f(K, L)$ , further assume that the production function is flush at once, whereby the  $tfp$  growth rate or  $tfp$  level is estimated. The article takes the absolute value of the growth rate of total factor productivity to measure the magnitude of technological change.

The article also introduces investment shocks ( $I$ ), consumption shocks ( $c$ ), trade shocks ( $tr$ ), and wage factors ( $wage$ ). According to Keynesian investment theory, investment has a multiplier effect. When investment behavior occurs, it is transmitted in a chain through all sectors of the economy, and effective demand keeps expanding, which eventually leads to an increase in output several times this investment; conversely, when investment decreases, GDP also decreases several times. Therefore, the article sets up the change of investment to describe the investment shock, selects the social fixed asset investment data, uses the fixed asset price index to exclude the price factor, and calculates the growth rate. Finally, the absolute value of the growth rate data of social fixed asset investment is taken to measure the size of investment shock. According to the above analysis, a rise in investment will lead to an exponential rise in GDP, while a fall in investment will lead to an exponential fall in GDP, so the change in investment is expected to be positively correlated with GDP fluctuations. The change in consumption reflects the change in demand from domestic sources. In the theory of national income determination, consumption, as one of the four economic sectors on the demand side, plays a crucial role in macroeconomic operation. The article selects total retail sales of consumer goods, uses the retail price index to remove the price factor from the data, and then calculates the growth rate and takes the absolute value for the growth rate. It is expected that consumption changes are positively correlated with economic fluctuations. The article selects the change in total exports as a proxy variable for trade shocks, uses the annual average exchange rate, and the consumer price index to remove the price factor from the export value data, then calculates the growth rate, and takes the absolute value of the growth rate to obtain the change in exports. Wages constitute an important part of production costs of enterprises, and changes in wages will bring about changes in production costs of enterprises, which will in turn affect output and lead to economic fluctuations. The article selects the average wage of the urban unit of employment, uses the consumer price index to put forward the price factor, calculates the growth rate, and then takes the absolute value of the growth rate; it is expected that the greater the change in wages, the greater the

TABLE 2: Regression results of the dispersion method.

Variables	National sample	Northeast region	Eastern region	Western region	Central region
<i>c</i>	0.015** (0.0055)	0.002 (0.0211)	0.024*** (0.0059)	0.006 (0.0097)	0.011* (0.0049)
<i>tr</i>	0.009** (0.0034)	0.002 (0.0050)	0.018*** (0.0048)	0.005 (0.0047)	0.015* (0.0072)
<i>I</i>	0.033** (0.0093)	0.051* (0.0167)	0.002 (0.0152)	0.004 (0.0097)	0.004 (0.0202)
<i>soe</i>	-0.125* (0.063)	-0.041 (0.0332)	-0.044 (0.0129)	-0.345*** (0.0432)	0.087 (0.0245)
<i>tfp</i>	0.022 (0.0305)	0.022 (0.1233)	-0.015 (0.0359)	0.062 -0.597	0.149** (0.0447)
<i>wage</i>	0.029 (0.0038)	0.006 (0.0093)	0.002** (0.0049)	0.027* (0.0085)	0.012 (0.0182)
<i>cons</i>	0.015 (0.0052)	0.005 (0.0083)	0.005*** (0.0120)	0.025*** (0.0042)	-0.005 (0.0159)
<i>ad - R<sup>2</sup></i>	0.198	0.171	0.231	0.189	0.191

change in production costs of enterprises, which leads to more serious economic fluctuations; that is, wage growth is positively correlated with economic fluctuations.

Since the fluctuation characteristics vary from region to region and there may be omitted variables that do not change over time, the fixed-effects model regression is first performed on the national sample using the outlier method. Because the sample values can be divided into different clusters by province, observations in the same cluster may be correlated, so cluster robust standard errors are used. The regression results using the fixed-effects model are shown in Table 2.

From the results of the econometric analysis, the coefficient of the core explanatory variable *soe* on economic fluctuations is  $-0.124$ ,  $t = -2.04$ ,  $p = 0.051$ , which is significantly negative at the 10% level. Changes in consumption growth, export growth, and investment growth move in the same direction as economic volatility and are significantly positive at the 5% level. *tfp* land changes and *wage* changes have insignificant effects on economic volatility.

To examine whether there are regional differences in the impact of SOEs on economic volatility, the article also performs regression analysis on subsamples from each of the four major economic regions in China. Under the northeast sample, the regression coefficient of the core explanatory variable *soe* on economic volatility is  $-0.039$ ,  $t = -1.19$ ,  $p = 0.319$ , and the effect of SOE control on economic volatility is not significant. Changes in consumption growth, changes in export growth, changes in total factor productivity, and changes in wages fluctuate in the same direction as economic fluctuations, but the estimated coefficients are not significant. Only the estimated coefficient of the change in investment is significantly positive at the 10% level of significance. This indicates that in the case of the northeast region, economic fluctuations mainly originate from investment shocks.

The estimated coefficient of *soe* remains negative but insignificant under the eastern region sample. Changes in consumption growth and exports show a significant positive correlation with economic fluctuations, and the estimated

coefficients are significant at the 1% level of significance. The estimated coefficient of technological change changes from positive to negative, but is not significant. The estimated coefficient of wage changes is positive but insignificant. The results indicate that the main sources of economic fluctuations in the eastern region are changes in consumption and exports.

The estimated coefficient of state control changes from negative to positive,  $p = 0.743$ . Changes in consumption growth and changes in export growth move in the same direction as economic fluctuations and pass the 10% level of significance test. The estimated coefficient of technological change is significantly positive at the 5% level of significance. The effect of changes in wages and investment changes on economic fluctuations is not significant. This indicates that, for the central region, economic fluctuations mainly originate from consumption, exports, and technological changes.

Overall, in the national perspective, SOEs do have a stabilizing effect on the fluctuations of the market economy, while changes in consumption, exports, and investment are positively associated with economic fluctuations. The regression results for the sample of four major economic regions show that SOEs play an important role in stabilizing regional fluctuations in the western region; however, the stabilizing role of SOEs is not significant in the northeastern, eastern, and central regions.

To ensure that the model was used correctly, the article conducted an *F*-test on whether to use individual fixed-effects regression or mixed regression. The original hypothesis of the *F*-test was "intercept term  $\mu_i = 0$  for all individuals," which means that mixed regression should be used. The test results showed that under the national sample, the *F* statistic = 2.79,  $p = 0.0001$ ; i.e., the original hypothesis of "all  $\mu_i = 0$ " was strongly rejected, and the individual fixed-effects model and mixed regression were considered to be chosen between the individual fixed-effects model and the mixed regression.

Second, for whether to use individual random effects model regression or mixed regression, the article refers to the study of Breusch and Pagan (1980). Breusch and Pagan



propose an LM test that can test individual random effects, and the original hypothesis of this LM test is  $H_0: \sigma_u^2 = 0$ . If the original hypothesis is rejected, it indicates that individual random effects should be taken into account in the model; i.e., mixed regression cannot be performed; conversely, the model is considered acceptable for mixed regression. The test results show that  $\chi^2$  statistic = 18.38,  $p = 0.0001$ , which means that  $\sigma_u^2 = 0$  is strongly rejected, and that the former should be used for regression between the individual random effects model and the mixed regression.

If the original hypothesis holds, the random effects estimates (RE) are also consistent; moreover, the within-group estimates are more efficient than the random effects estimates. If the random effect is not the correct model, the RE is inconsistent. Therefore, if the original hypothesis holds, the in-group and random effects estimates will converge to the true parameters and the gap between them will disappear under the condition of a large sample, if the gap between the in-group and random effects estimates is too large.

Considering that there are many factors that affect the market economy volatility, the factors that have an impact on the market economy volatility cannot be exhaustively considered into the model, and all may have endogeneity problems due to omitted variables. That is, the explanatory variables are correlated with the random disturbance terms. First, the economic variables should be coherent in time, and the strength of SOEs' control in the previous period will affect SOEs' control over economic resources in the current period; second, SOEs' control in the previous period should be considered as a predetermined variable, which is related to the market economic fluctuations in the previous period but not to the market economic fluctuations in the current period. Therefore, the one-period lagged term of SOE control satisfies the assumption that it is both correlated with the explanatory variables and uncorrelated with the disturbance term.

If the estimation results of GMM are consistent, it is necessary to satisfy that there is no autocorrelation in the perturbation terms. Even when the assumption of no autocorrelation of the perturbation term holds, the first-order difference of the perturbation term still has autocorrelation. The results of the test for first-order differential autocorrelation of the nuisance term in the national sample showed that the  $z$ -statistic =  $-2.32$ ,  $p = 0.021$ , and the test for second-order differential autocorrelation showed that the  $z$ -statistic =  $1.18$ ,  $p = 0.237$ . Therefore, the original hypothesis is accepted and the nuisance term is not autocorrelated. Finally, the article also tests for overidentification of the instrumental variables.

The results of the GMM estimation show that the regression coefficient of *soe* is  $-0.0889$  with a  $p = 0.035$ . The effect of SOE control on economic volatility is negative at the 5% level of significance. That is, the estimation results suggest that SOEs do play a role in stabilizing economic volatility, which is consistent with the findings of the regression using fixed-effects model.

From Table 3 about literature analysis, we know that the control of SOEs is the ability of SOEs to control economic

TABLE 3: Regression results after replacing variables.

Variables	Estimated coefficient	Standard error	<i>t</i> -statistic	<i>p</i> -value
<i>c</i>	0.013525	0.0054221	2.52	0.019
<i>tr</i>	0.0085133	0.0032329	2.63	0.015
<i>I</i>	0.0211727	0.0090736	2.44	0.029
<i>scale</i>	$-0.1610045$	0.0687723	$-2.35$	0.026
<i>tfp</i>	197659	0.0302065	0.66	0.527
<i>wage</i>	0.0025832	0.0036605	0.75	0.487
<i>cons</i>	0.0129823	0.0049624	2.62	0.015

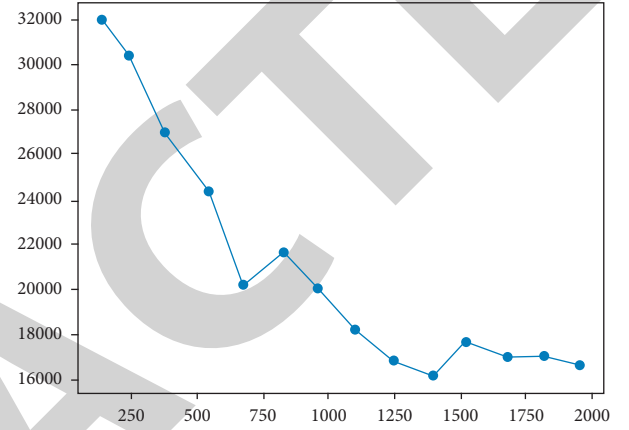


FIGURE 3: Number of state-owned and state-controlled enterprise units.

resources. The “total assets” portray the size of the enterprise from the perspective of production factors and resource possession. Referring to the study of [24], the article uses the data of industrial enterprises. This indicator is also used as a proxy variable for SOE control, and a regression analysis is conducted on the national sample as shown in the following table. It can be seen from the data that in northeast China, the economic fluctuation mainly comes from investment shock.

From the regression results after replacing the core explanatory variables, the change in consumption, change in exports, and change in investment are positively associated with economic fluctuations in the national sample and significant at the 5% level of significance, while the size of SOEs is negatively associated with economic fluctuations and significant at the 5% level of significance. Changes in technology and changes in wages do not have a significant effect on economic fluctuations. Therefore, it can be concluded that SOEs do smooth out economic fluctuations in the market; the larger the size of SOEs, the less volatile the regional economy and the smoother the economic growth.

#### 4. Case Study

Taking industrial enterprises as an example, the number of state-owned and state-controlled enterprises in China from 2003 to 2016 is shown in the following figure.

As shown in Figure 3, since 2003, the number of state-owned and state holding enterprises in China has decreased

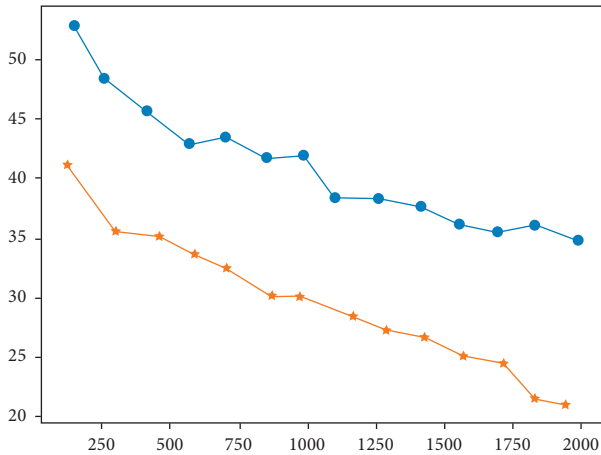


FIGURE 4: The proportion of main business income and total assets of SOEs.

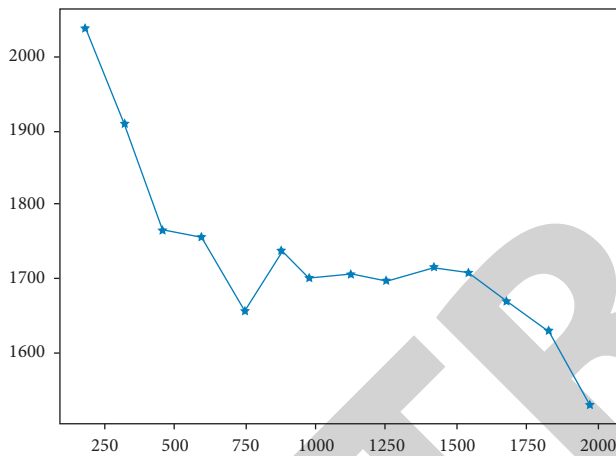


FIGURE 5: Average number of workers employed by state-owned and state-controlled enterprises.

from 34280 in 1998 to 19022 in 2016. Although the number of state-owned and state holding companies increased slightly in 2007–2008 and 2012–2015, the total number of enterprises decreased significantly. The relationship between the operating activities and total assets interest income and expenditure of the state-owned holding company is shown in Figure 4.

As can be seen from Figure 4, the proportion of core business income in total assets of state-owned and state-controlled enterprises is declining every year. From 2003 to 2016, the proportion of total assets of state-owned and state holding companies decreased from 55.99% to 38.47%; The share of core revenue decreased from 40.53% to 20.62%. It is worth noting that although the proportion of total assets and operating income of state-owned enterprises shows a downward trend, the total assets and operating income continue to grow.

On the other hand, Figure 5 shows the average employment dynamics of state-owned enterprises and state holding companies from 2003 to 2006. As shown in Figure 5, the average number of employees in state-owned and state-

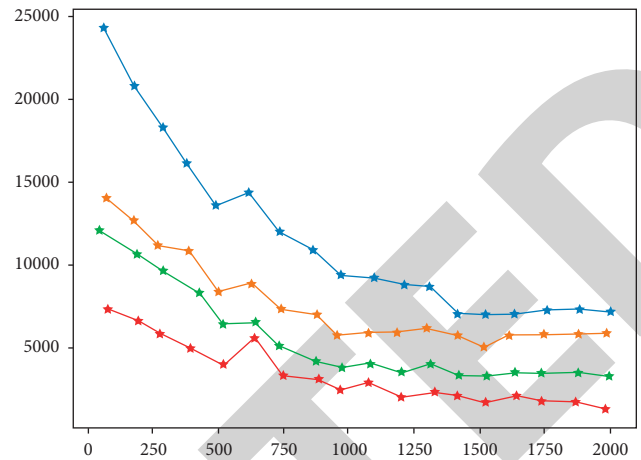


FIGURE 6: Number of units of state-owned and state-controlled enterprises.

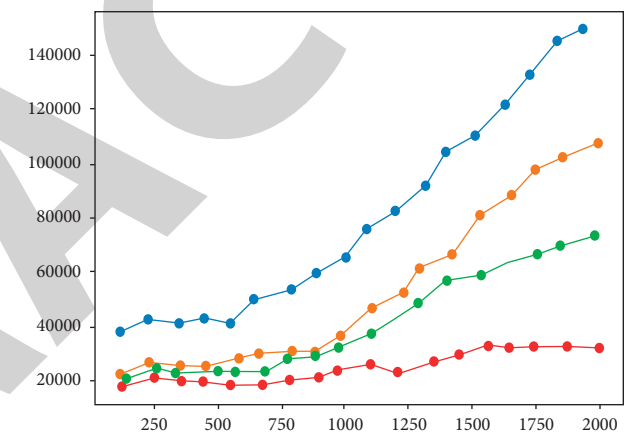


FIGURE 7: Total assets of state-owned and state-controlled enterprises.

controlled enterprises has changed little. From 2003 to 2007, the average number of employees in state-owned and state-controlled enterprises decreased slowly and remained basically unchanged after 2007. Through the study of the number of state-owned and state holding units, the proportion of total assets, the proportion of main operating income, and the average number of employees, we can draw a conclusion that the scale of China's SOEs is slowly shrinking, "the state is moving and the people are retreating".

In order to scientifically reflect the social and economic development trends of different regions of the country and provide a basis for the party and the state to formulate regional development policies.

The number of state-owned and state-controlled enterprise units in China from 1999 to 2016 is shown in Figure 6.

In the northeast, east, central, and west regions have all declined significantly overall, and the trend and speed of decline are similar. Specifically, enterprise units in the four major economic regions declined rapidly from 1999 to 2003, rebounded slightly from 2003 to 2004, declined slowly from

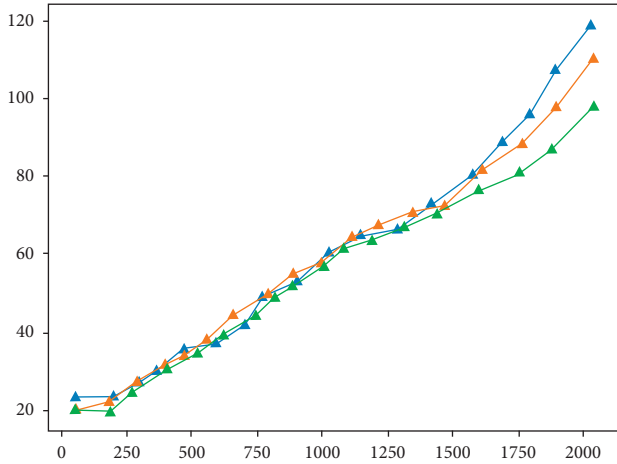


FIGURE 8: Comparison of simulation results of innovation revenue of SOEs with different time steps.

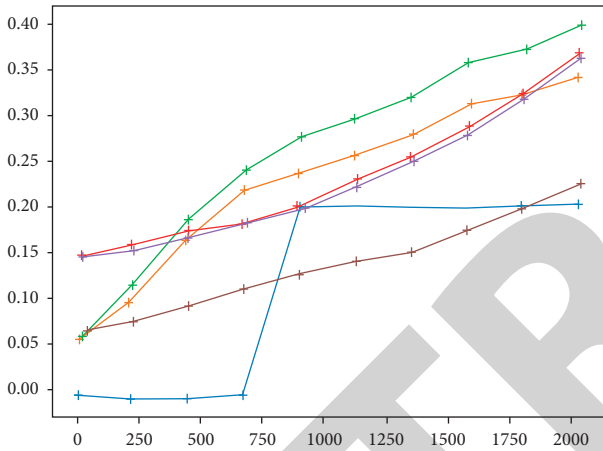


FIGURE 9: Simulation results of "the number of management ideas of SOEs" and its influencing factors.

2004 onward, and remained stable after 2012. The number of enterprises in the northeast region fell from 6,448 in 1999 to 1,406 in 2006, a decrease of 78.2%; the number of enterprises in the eastern region fell by 71.8%. Figure 7 gives the total assets of state-owned and state-controlled enterprises in the four major economic regions of China.

Therefore, we can conclude that the number of SOEs has been declining, the differences in the number of SOEs in the four major economic regions of China have been significantly reduced, and the geographical distribution of the number of enterprises tends to be even. However, SOEs in the eastern region show better profitability, and the profit income of SOEs in the eastern region still occupies the most important share of profit income of SOEs in China.

As shown in Figure 8, the simulation of the parameter "innovation revenue in the context of artificial intelligence," for example, shows that for the models with three simulation steps, there is no pathological result in the process of its operation. The system behavior is basically stable, so the model can be considered as valid.

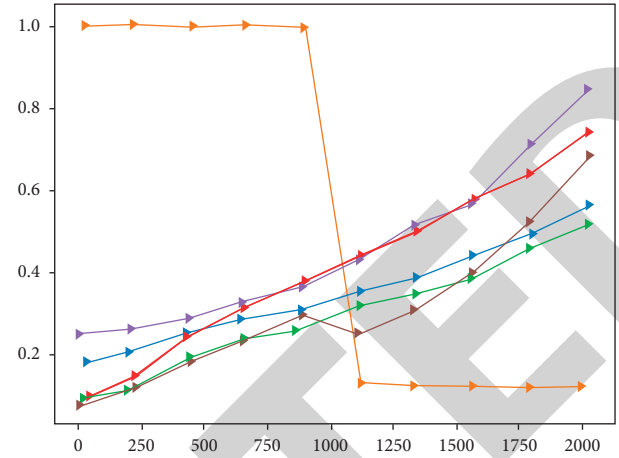


FIGURE 10: Simulation results of the number of ideas adopted and their influencing factors.

As shown in Figure 9, the number of ideas collected in the context of AI in the enterprise shows an approximately linear increase, which is positively correlated with the "number of users in the context of AI" and "users' motivation to innovate."

As shown in Figure 10, the number of creative ideas adopted by enterprises in the context of AI first shows an approximately linear increasing trend, and after a short decline after 2013, it again shows a gradually increasing development trend, which is mainly influenced by "the number of creative ideas in the context of AI," "the number of creative ideas online in the context of AI," "the quality of creative ideas in the context of AI," "the number of comments in the context of AI," "the perception of enterprises," and "the number of creative ideas online in the context of AI." The trend is mainly influenced by "the number of creative ideas in the context of AI," "the online cycle of creative ideas in the context of AI," "the quality of creative ideas in the context of AI," "the number of comments in the context of AI," and "the perceived ability of enterprises."

## 5. Conclusion

For SOEs, management innovation is an important part of enterprise innovation, and it is an inevitable trend for the development of SOEs, which can help them maintain vitality and vigor and remain invincible in the market competition. In today's economic globalization, the development of SOEs faces many opportunities and also ushers in many challenges. If SOEs want to overcome the problems encountered in their development, they need to establish perfect management mechanisms and continuously upgrade the management mode. Only by comprehensively strengthening the management and innovation of SOEs can they better dispatch and utilize resources from all sides, form a strong synergy, and create greater operational benefits. This requires continuous exploration, in-depth research, and effective response according to the changes in the market situation and SOEs' own reality, and ultimately forms a driving force. This requires continuous exploration, in-



## Retraction

# Retracted: Cultivation of Students' Independent Learning Ability in Teaching Chinese as a Foreign Language Based on the CDIO Model of Guiding Data Structures and Hidden Markov Algorithms

### Security and Communication Networks

Received 17 October 2023; Accepted 17 October 2023; Published 18 October 2023

Copyright © 2023 Security and Communication Networks. This is an open access article distributed under the Creative Commons Attribution License, which permits unrestricted use, distribution, and reproduction in any medium, provided the original work is properly cited.

This article has been retracted by Hindawi following an investigation undertaken by the publisher [1]. This investigation has uncovered evidence of one or more of the following indicators of systematic manipulation of the publication process:

- (1) Discrepancies in scope
- (2) Discrepancies in the description of the research reported
- (3) Discrepancies between the availability of data and the research described
- (4) Inappropriate citations
- (5) Incoherent, meaningless and/or irrelevant content included in the article
- (6) Peer-review manipulation

The presence of these indicators undermines our confidence in the integrity of the article's content and we cannot, therefore, vouch for its reliability. Please note that this notice is intended solely to alert readers that the content of this article is unreliable. We have not investigated whether authors were aware of or involved in the systematic manipulation of the publication process.

In addition, our investigation has also shown that one or more of the following human-subject reporting requirements has not been met in this article: ethical approval by an Institutional Review Board (IRB) committee or equivalent, patient/participant consent to participate, and/or agreement to publish patient/participant details (where relevant).

Wiley and Hindawi regrets that the usual quality checks did not identify these issues before publication and have since put additional measures in place to safeguard research integrity.

We wish to credit our own Research Integrity and Research Publishing teams and anonymous and named external researchers and research integrity experts for contributing to this investigation.

The corresponding author, as the representative of all authors, has been given the opportunity to register their agreement or disagreement to this retraction. We have kept a record of any response received.

## References

- [1] Y. Wen and S. Peng, "Cultivation of Students' Independent Learning Ability in Teaching Chinese as a Foreign Language Based on the CDIO Model of Guiding Data Structures and Hidden Markov Algorithms," *Security and Communication Networks*, vol. 2022, Article ID 7114217, 7 pages, 2022.

## Research Article

# Cultivation of Students' Independent Learning Ability in Teaching Chinese as a Foreign Language Based on the CDIO Model of Guiding Data Structures and Hidden Markov Algorithms

Ye Wen  and Shuang Peng

College of Arts, Northeast Normal University, Changchun 130024, China

Correspondence should be addressed to Ye Wen; [weny459@nenu.edu.cn](mailto:weny459@nenu.edu.cn)

Received 27 May 2022; Accepted 22 July 2022; Published 31 August 2022

Academic Editor: Hangjun Che

Copyright © 2022 Ye Wen and Shuang Peng. This is an open access article distributed under the Creative Commons Attribution License, which permits unrestricted use, distribution, and reproduction in any medium, provided the original work is properly cited.

The systematic training of metacognitive strategies in teaching Chinese as a foreign language, cultivating learners' autonomous learning ability, and improving the effectiveness of teaching Chinese as a foreign language is of great significance for realizing the overall goal of teaching Chinese as a foreign language. Therefore, this paper designs a model based on CDIO to guide the teaching of data structures and algorithms, which emphasizes students' hands-on ability, advocates learning in use, students' autonomous learning, and teamwork. Taking massive online open courses (MOOC) and small private online courses (SPOC) learning data as a sample, hidden Markov algorithm and data mining technology are used to establish a student learning behavior evaluation model to evaluate students' learning behavior in real-time. Meanwhile, teachers adjust the teaching content according to the evaluation results and enhance students' learning performance and improve teaching quality.

## 1. Introduction

As the world enters the twenty-first century, with the information age and economic globalization, language science has become more and more important. The rapid development of China's economy and its international status in the past 20 years, as well as the vast market demand, have forced both developed and developing countries to deal with China for their peace and development and national interests, and their efforts to learn Chinese are also aimed at establishing an in-depth understanding of China [1].

In Asia, Japan has been one of the hottest countries for Chinese language teaching, almost every university has a Chinese language course, and Chinese has become one of the optional foreign languages in the college entrance examination for secondary school students [2]. In South Korea, China's closest neighbor, more than one million people are learning Chinese, two-thirds of the more than 300 universities have Chinese language courses, and language institutes for learning Chinese are located in all major cities [3].

We can foresee that with the strong development of China and the accelerated development of economic globalization, we can further build a broad bridge of economic and cultural exchanges and people-to-people contact between China and foreign countries [4].

The teaching of Chinese as a second language to foreigners is not only to cultivate the communicative ability of Chinese but also to master the ability to use Chinese to listen, read, write and communicate and to shoulder the responsibility and mission of spreading Chinese culture [5].

Learner-directed learning has become a consensus in the field of language teaching, and learning-centeredness has gradually become the guiding ideology of second language teaching. The learner's subjectivity has not been fully appreciated and reflected. Only when we shift the focus of our research from "how teachers teach" to "how students learn" can we solve the problem of "how teachers teach" in a targeted way, and only then can we better improve learners' learning [6]. It is possible to better improve the learning efficiency of learners.

Therefore, in learning Chinese as a foreign language, it is meaningful to study students' learning, focus on learners, and cultivate the learning ability of foreign Chinese learners [7]. In classroom teaching, teachers tend to focus on cognitive strategies that are closely related to specific learning contents and tasks but neglect metacognitive strategy training, which makes it difficult to improve learners' strategy awareness and strategy application, and may lead to low learning efficiency [8]. The cultivation of learners' independent learning ability is one of the goals of the effectiveness of teaching Chinese as a foreign language, to achieve the overall goal of the international Chinese teaching curriculum and to realize the international promotion of the Chinese language [9].

A landmark achievement of the CDIO engineering education model is the introduction of the curriculum syllabus. The outline is a guiding document for CDIO engineering education, which specifies the objectives, contents, and specific operating procedures of the CDIO engineering education model in detail. Based on the Hidden Markov Chain Model (HMM), the evaluation index of students' learning behavior in teaching Chinese as a foreign language is constructed, and the final evaluation score of students' learning behavior is formed by combining the analytic hierarchy process.

## 2. Related Work

The ability of self-directed learning can be cultivated through various means. Researchers at home and abroad have been trying to find various ways to cultivate independent learning ability by conducting experiments and studies from various perspectives such as psychology, metacognitive theory, constructivism, and social cognitive theory [10]. At present, in the domestic foreign language teaching English, experts and scholars have commonly studied the cultivation of learners' autonomous ability, and many teachers, including primary and secondary schools and universities, have conducted research in their teaching practice and achieved good results. Lack of attention to the main role of students in teaching Chinese second language is a problem need to be solved. The independent learning of Chinese language of students can be realized by a new learning pattern of "teacher-led and student-centered combining with equal attention in and out of the classroom" [11–13]. Researchers discussed the necessity of incorporating independent reading outside the classroom into reading instruction and analyzed the effectiveness of this classroom teaching model [14, 15]. The demotivation and motivation study demonstrates that pedagogical means and methods by bridging the gap between researchers and educational practitioners are essential in learning Chinese as a foreign language.

Teachers also need to strengthen instruction in learning strategies in a variety of ways. Teachers should present a range of learning strategies that students must master for them to understand and use [16]. The following are common approaches that teachers can use in teaching a second foreign language. Teachers can guide students to develop specific, detailed plans and identify specific activities and

schedules related to their learning goals. They can also guide students to write down their learning process, methods, and experiences in a variety of appropriate ways, to self-evaluate and self-monitor their learning and to adjust their learning methods and strategies for the next stage accordingly [17, 18]. When doing exercises, pay attention to the ideas and techniques for solving various types of frequently tested questions and learn and master test-taking strategies and methods. Teachers should also guide students to make full use of resources, learn to create and grasp opportunities to use the target language, be good at using body language to improve the communicative effect, and guide the use of Internet resources for learning [19].

In this paper, a CDIO-based model is designed to guide the teaching of data structures and algorithms. Taking the MOOC + SPOC learning data of our school as a sample, the hidden Markov algorithm and data mining technology are used to establish a student learning behavior evaluation model and real-time evaluation of students' learning behavior. Learning behavior: teachers adjust teaching content according to the evaluation results and intervene in students' learning behavior to improve teaching quality. That is, it emphasizes students' practical ability and advocates learning by doing students' independent learning, and teamwork.

## 3. The Guiding Principle of the CDIO Model in Teaching

The CDIO model for teaching data structures and algorithms is based on how to combine the course with practical cases to improve students' hands-on skills. The main aspects are as follows.

*3.1. Emphasis on Practical and Hands-On Skills.* The main idea of the CDIO model is to focus on practice and operation. Only when the teaching data structure and algorithm is combined with actual cases the practical and hands-on ability can be reflected under the guidance of theory. A large number of cases will greatly improve the practical and hands-on ability [20].

*3.2. Promote Independent Learning and Problem Solving.* The CDIO model is a prerequisite and foundation for developing students' independent skills, and we should strive to improve the efficiency of teaching data structures and algorithms. Generally speaking, it is possible to use to arrange students' independent learning by listing knowledge points. Teachers must master the main points of knowledge and recommend some required reading to students, while students are required to track themselves and read the literature. One can also learn to learn by comparison. Encourage students not to blindly believe in textbooks but to understand why this view is mainstream and classical and why all other views are gradually being eliminated in practice, by actually comparing them to what was thought at the time and what was the way of understanding without distinction. The most important thing is the brainstorming method. The teacher participates equally in the students'

discussion and addresses a point of knowledge, and teachers and students freely present their views, allowing students to analyze themselves afterward, stimulating their thinking, and deepening their understanding of the point.

**3.3. Professional Competence and Teamwork.** The model recognizes the imbalance of competencies in the study team and emphasizes the best model to equip the study team to explore the competencies of the students. During learning and discussion, group members' performance should be recorded, and the best organizers and implementers should be selected through three to five rounds of observation of student readiness and mutual assessment. In a research team, it is not only important to ensure that the research direction does not deviate but also to allow members to have a process of meeting ideas, through debate, so that new ideas and new thoughts can be generated, taking into account economic performance, social impact, simplifying and streamlining as much as possible, emphasizing user interface intuition and ease of operation.

## 4. Research Framework

The assessment of student learning behavior status in this study was based on data from student learning trajectories on the MOOC + SPOC platform. HMM was used to obtain the student learning status matrix, and then the scores were calculated based on the learning behavior data evaluation method, i.e., the corresponding learning evaluation scores. Historical judgment data of more than two consecutive weeks are retained, and student learning state trends and continuous period student learning behavior evaluation scores are calculated based on these data. The HMM algorithm is used to map the observed state student learning state data to hidden state trends, and the Viterbi algorithm is used to solve for future time student learning behavior change trends and learning evaluation scores. The hidden state and continuous period of student learning behaviors are used as inputs for the process shown in Figure 1.

**4.1. Framework Model HMM Model.** Since students' learning states are more likely to be disturbed by various factors, such as the surrounding environment, psychological state, physiological cycle, and many other factors, this makes the change of students' learning states a typical random process. At the same time, the change in students' learning state is generally associated with the state of the previous period only. If it is determined by the previous state only, it is a first-order Markov model, and if it is influenced by several previous time states at the same time, it is an n-order Markov model. In Reference [21], a Markov model describes an important class of stochastic processes, which is a stochastic function that varies with time.

In a Markov model, each state represents an observable event, which limits the use of the model to certain states where the event is not easily observable [22]. For teaching, a teacher may want to determine the next state of a student's

learning behavior by looking at the student's online learning, questioning, and correctness of assignments when the next state is not yet present. This algorithm is known as HMM which predicts students' next learning state by observing their usual learning process data and the Markov hypothesis. [23].

One of the basic assumptions in HMM model is the assumption of the chi-square Markov chain, that is, the hidden state at any moment depends only on the hidden state at the previous moment.

The model obtains the probability of each observation by the current state where  $b_{ij}$  represents the probability that at any moment  $t$ , if the state is  $S_i$ , then the observation is  $O_j$ .

There are three problems in the HMM model: first is the evaluation problem, given an HMM, i.e.,  $\lambda = [A, B, \pi]$ , to calculate the probability of sequence; second is the decoding problem, given an HMM, i.e.,  $\lambda = [A, B, \pi]$ , to find the optimum sequence of states to a sequence of observations.

For the problem of early prediction and timely intervention of students' learning behavior, it is the learning problem and decoding problem of HMM. The learning problem is solved by the EM algorithm, and the decoding problem is solved by the Viterbi algorithm based on dynamic programming. Using the parametric model  $\lambda = [A, B, \pi]$  derived from the EM algorithm and the existing observed sequence of student learning states  $O = \{O_1, O_2, \dots, O_T\}$ , the most likely sequence of student learning behavior states  $I^* = \{i_1^*, i_2^*, \dots, i_T^*\}$ , i.e.,  $P(I^*|O)$  is to be maximized under the given conditions.

**4.2. Evaluation Indexes of Student Learning Behavior Analysis.** According to the construction ideas and methods of online teaching quality evaluation indexes at home and abroad, the overall evaluation indexes are divided into 2 primary indexes and 6 secondary indexes, as shown in Table 1.

The matrix was constructed using hierarchical analysis to obtain the weights. The indicators at the same level were assigned with the Starr relative importance scale (9 levels) to form a judgment matrix. Take the secondary index of learning attitude as an example, Table 2 shows its importance scale, in which the parameter levels are obtained from student questionnaires and expert ratings in reference literature [24–26].

The single-sort judgment matrix is obtained at this level:

$$B = \begin{bmatrix} 1 & 1/5 & 1/3 & 1/3 \\ 5 & 1 & 3 & 2 \\ 3 & 1/3 & 1 & 2 \\ 3 & 1/2 & 1/2 & 1 \end{bmatrix}. \quad (1)$$

Due to possible biases in perceptions, the design of student learning behavior index weights may have inconsistent biases. Therefore, we conducted a consistency test based on the hierarchical analysis method (AHP). The test formula is as follows:

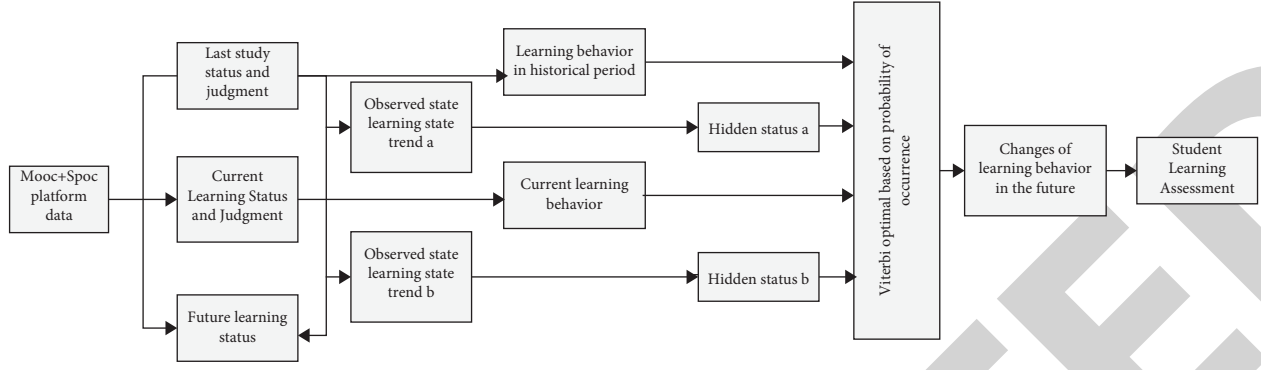


FIGURE 1: Block diagram of the learning behavior assessment.

TABLE 1: Overall evaluation indexes of learning behavior.

Primary indicators	Secondary indicators	Evaluation criteria
Learning attitude	Course access	Number of visits to the course platform
	Course learning	Length of course study, length of videos watched
	Online interaction	The number of effective postings and discussions by students
	Interaction with teachers	Students' questions, teachers' answers, and discussions
Professional ability	Assignment completion rate	The ratio of the number of completed assignments to the total number of assignments
	Assignment pass rate	The ratio of the number of graded homework questions to the total number of questions

TABLE 2: Importance ranking of secondary indicators of learning attitudes.

	1.1 course access	1.2 course learning	1.3 online interaction	1.4 interaction with teachers
1.1 course access	5	1/3	1/3	1/5
1.2 course learning	3	5	3	3
1.3 online interaction	3	1/3	1/3	3
1.4 interaction with teachers	1	1/3	1/3	1

$$CR = \frac{CI}{RI}, \quad (2)$$

where  $RI$  is the average random consistency index (see Table 3 for the values of  $RI$ ).

When  $CR \leq 0.1$ , it means that the consistency test is passed and the design can be carried out according to the results of the matrix representation; when  $CR > 0.1$ , it means that the deviation of the judgment matrix is too large and there are contradictions in the process, and the scoring needs to be modified and reconstructed until the consistency is satisfied. This hierarchical single ranking matrix is calculated to know  $CR = 0.048 \leq 0.1$ ; therefore, it passes the test [27]. In this paper, we also used AHP to test the other dimensional indicators. In this paper, the other dimensional indicators were also tested by AHP, and they all passed the consistency test, and the weights of the indicators at each level were calculated, and the total ranking of the hierarchy was thus calculated, as shown in Table 4.

## 5. Research Object

The key to the study of learning behavior analysis is as follows: first, to score the indicators for evaluating learning behavior in order to obtain the current state (current week) learning behavior evaluation; second, to obtain the related behaviors (such

as learning attitude, learning initiative, and learning effect) that reflect the learning behavior state in order to judge the trend of learning state change and then to predict the learning behavior state change according to the HMM model [28]. The formulation of this problem in the Hidden Markov Model for each parameter variable set is as follows.

The set of hidden variables (learning behavior) is as follows:

Learning attitude state set

$$I_s = \{i_1 = 1 = \text{"Active"}, i_2 = 0 = \text{"General"}\}. \quad (3)$$

Learning initiative state set

$$I_a = \{i_1 = 1 = \text{"Proactive"}, i_2 = 0 = \text{"Passive"}\}. \quad (4)$$

Learning effect status set

$$I_r = \{i_1 = 1 = \text{"Good"}, i_2 = 0 = \text{"General"}\}. \quad (5)$$

Set of observed variables (learning states) is as follows.

The set of learning attitude events  $O_s = \{o_1 = 1 = \text{"time to watch video"} \geq a_1 \text{ and "number of times to hand in notes"} \geq b_1, o_2 = 0 = \text{"time to watch video"} < a_1 \text{ and "number of times to hand in notes"} < b_1\}$ .

TABLE 3: RI values of judgment matrices of various orders.

Determine the matrix order $n$	1	2	3	4	5	6	7	8	90
RI value	0	0	0.55	0.92	1.10	1.26	1.35	1.44	1.47

TABLE 4: Total weights of learning behavior evaluation indicators.

Secondary indicators	Primary indicators		Total ranking of secondary indicators
	Learning attitude	Professional ability	
	0.675	0.325	
Learning attitude	Course access	0.078	0.055
	Course learning	0.455	0.305
	Online interaction	0.264	0.178
	Interaction with teachers	0.209	0.141
Professional ability	Assignment completion rate	0.675	0.223
	Assignment pass rate	0.332	0.112

Learn the active event set:

$$O_a = \begin{cases} o_1 = 1 = \text{"number of proactive and answer session, interactions"} \geq c_1 \\ o_2 = 1 = \text{"number of proactive and answer session, interactions"} < c_1 \end{cases}. \quad (6)$$

Learning effect event set:

$$O_r = \begin{cases} o_1 = 1 = \text{"assignment test scores"} \geq d_1 \\ o_2 = 1 = \text{"assignment test scores"} < d_1 \end{cases}. \quad (7)$$

In the specific experimental process, first, the data were transformed into a learning attitude dataset, learning initiative dataset, and learning effect dataset according to the definition of the observed dataset; then, the parameters of the student learning behavior model were obtained using the observed dataset in weeks 1–5 using the EM algorithm, and the obtained parametric model was applied to the observed dataset in weeks 6–9 for model validation. The model parameters and observed student data were then used to predict student learning behaviors over the next 10–15 weeks, and the weekly predictions were used to disrupt some students' learning [29, 30].

## 6. HMM Model Parameters Calculation

The solution to HMM model parameters is divided into two cases. The EM iterations are then performed until the values of the model parameters converge. The algorithm proceeds as follows:

One is to randomly initialize all  $\pi_i, a_{ij}, b_j(k)$ .

Second, for each sample  $d = 1, 2, \dots, D$ , the backward and forward algorithm is used to compute  $r_t^{(d)}(i), \xi_t^{(d)}(i, j), t = 1, 2, \dots, T$

Third, update the model parameters:

$$\pi_i = \frac{\sum_{d=1}^D r_1^{(d)}(i)}{D},$$

$$a_{ij} = \frac{\sum_{d=1}^D \sum_{t=1}^{T-1} \xi_t^{(d)}(i, j)}{\sum_{d=1}^D \sum_{t=1}^{T-1} r_1^{(d)}(i)}, \quad (8)$$

$$b_j(k) = \frac{\sum_{d=1}^D \sum_{t=1}^{T-1} O_t^{(d)} = v_k r_t^{(d)}(i)}{\sum_{d=1}^D r_1^{(d)}(i)}.$$

Fourth, if the value of  $\pi_i, a_{ij}, b_j(k)$  has converged, the algorithm is finished; otherwise, go back to the second step to continue the iteration.

The HMM parameters  $\pi, A$ , and  $B$  of learning attitude, learning initiative, and learning effect obtained by iteration are shown in Table 5.

## 7. Experimental Results

The prediction results of the scheme in this paper are shown in Table 6, where  $W6, W7, W8$ , and  $W9$  denote weeks 6, 7, 8, and 9, and the values in Table 6 are the probabilities of transferring states.

The prediction results obtained from the model were compared with the actual student results in weeks 6–9. Figure 2 shows the comparison of the HMM prediction results. The learning motivation prediction result shows that the HMM misfit rate is 3%, the learning method prediction result shows that the HMM misfit rate is 2.668%, and the learning effect prediction result shows that the HMM misfit rate is 1.335%.



TABLE 5: HMM model parameters.

Learning attitude	$\pi = [01], A = \begin{bmatrix} 0.68 & 0.32 \\ 0.57 & 0.43 \end{bmatrix}, B = \begin{bmatrix} 0.84 & 0.16 \\ 0.22 & 0.78 \end{bmatrix}$
Learning initiative	$\pi = [01], A = \begin{bmatrix} 0.85 & 0.15 \\ 0.19 & 0.81 \end{bmatrix}, B = \begin{bmatrix} 0.76 & 0.24 \\ 0.21 & 0.79 \end{bmatrix}$
Learning effectiveness	$\pi = [01], A = \begin{bmatrix} 0.91 & 0.09 \\ 0.10 & 0.90 \end{bmatrix}, B = \begin{bmatrix} 0.82 & 0.18 \\ 0.25 & 0.75 \end{bmatrix}$

TABLE 6: HMM prediction results.

Predicted results	W6	W7	W8	W9
Learning attitude	0.69/0.35	0.6427/0.3449	0.6355/0.3585	0.6327/0.3575
Learning initiative	0.89/0.17	0.7512/0.2497	0.6862/0.3145	0.6431/0.3587
Learning effectiveness	0.92/0.12	0.8287/0.1632	0.7539/0.2213	0.6862/0.2672

TABLE 7: Comparison of calculation results.

	1–5 weeks	6–9 weeks
Average of predicted results	77.9	79.85
Average of actual results	84.22	85.69
Consistency	91.97%	93.56%

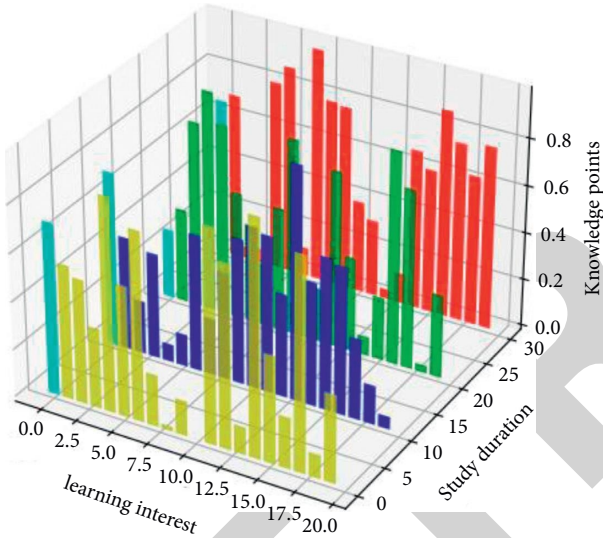


FIGURE 2: Comparison of HMM prediction results.

The validity of the model was judged by the consistency of the results. Students' scores were calculated according to the weights of student learning behavior evaluation indexes, and the predicted results were verified with the actual results for consistency, and the calibration results are shown in Table 7.

The validation analysis of the model shows that the HMM prediction model established in this paper has a certain validity.

After 4 weeks, the learning behaviors of the two groups were compared and analyzed to see if the performance of the group of students who had been disturbed by the teacher improved compared to the group of students who had not been disturbed by the teacher. The results of the learning evaluation comparison shown in Table 7, where the learning evaluation scores were calculated based on the learning evaluation indicators, and demonstrate effective improvement of students' Chinese learning performance.

## 8. Conclusion

In this paper, the evaluation indexes of students' learning behaviors in teaching Chinese as a foreign language were constructed based on the Hidden Markov Chain Model and combined with the hierarchical analysis method to form the final evaluation scores of students' learning behaviors. Based on the comprehensive scores, we determine the current state of students' learning behavior, predict the trend of students' learning behavior changes with the help of the Hidden Markov Model, and realize the early warning of students' learning behavior state, so that teachers can take disturbing measures in time to achieve the purpose of dynamic monitoring and improving students' learning state.

## Data Availability

The experimental data used to support the findings of this study are available from the corresponding author upon request.

## Conflicts of Interest

The authors declare that they have no conflicts of interest regarding this work.

## Acknowledgments

This work was supported by The National Social Science Fund of China (No. 20BY057) and the Major Program of International Chinese Education of Center for Language Education and Cooperation of Chinese Ministry of Education (No. 21YH01A).



## *Retraction*

# **Retracted: Action Recognition and Application of Table Tennis Training Based on IOT Perception**

### **Security and Communication Networks**

Received 26 December 2023; Accepted 26 December 2023; Published 29 December 2023

Copyright © 2023 Security and Communication Networks. This is an open access article distributed under the Creative Commons Attribution License, which permits unrestricted use, distribution, and reproduction in any medium, provided the original work is properly cited.

This article has been retracted by Hindawi, as publisher, following an investigation undertaken by the publisher [1]. This investigation has uncovered evidence of systematic manipulation of the publication and peer-review process. We cannot, therefore, vouch for the reliability or integrity of this article.

Please note that this notice is intended solely to alert readers that the peer-review process of this article has been compromised.

Wiley and Hindawi regret that the usual quality checks did not identify these issues before publication and have since put additional measures in place to safeguard research integrity.

We wish to credit our Research Integrity and Research Publishing teams and anonymous and named external researchers and research integrity experts for contributing to this investigation.

The corresponding author, as the representative of all authors, has been given the opportunity to register their agreement or disagreement to this retraction. We have kept a record of any response received.

### **References**

- [1] Z. Zhang, "Action Recognition and Application of Table Tennis Training Based on IOT Perception," *Security and Communication Networks*, vol. 2022, Article ID 8911564, 11 pages, 2022.

## Research Article

# Action Recognition and Application of Table Tennis Training Based on IOT Perception

Zhijian Zhang 

Guangzhou Sport University, Guangzhou, China

Correspondence should be addressed to Zhijian Zhang; 201920134354@mail.scut.edu.cn

Received 8 July 2022; Revised 28 July 2022; Accepted 11 August 2022; Published 31 August 2022

Academic Editor: Hangjun Che

Copyright © 2022 Zhijian Zhang. This is an open access article distributed under the Creative Commons Attribution License, which permits unrestricted use, distribution, and reproduction in any medium, provided the original work is properly cited.

As the national sport of our country, table tennis focuses on continuous innovation and development. Table tennis is a high-quality sport characterized by fast movement and great flexibility. Unlike other human behaviors, identifying ping pong shots is idiosyncratic and difficult. Table tennis training is extremely important, and correct training can make athletes progress. In this paper, based on the perception of the Internet of Things, the action recognition and application of table tennis training actions are carried out, and the following conclusions are drawn: (1) the training movements of table tennis are relatively complex, which has a great challenge to the action recognition technology. The action recognition technology based on IoT perception can efficiently identify table tennis training actions. (2) Analyze and study the action recognition algorithm based on IoT perception, and propose a higher recognition accuracy and more stable algorithm DTW. (3) Comparing the accuracy, loss rate, and time impact between the algorithm in this paper and the traditional recognition algorithm, it is concluded that the algorithm proposed in this paper has higher accuracy and lower loss rate than the traditional algorithm. And with good stability, it is not affected by the environment and time. The algorithm in this paper is an algorithm with better performance and more worthy of use.

## 1. Introduction

In today's era of rapid network and rapid progress in computer technology, the Internet of Things has been further developed and gradually integrated into our lives, bringing great convenience to our lives. However, the computing power of today's computers is very weak and cannot provide faster computing power to the perception layer. The perception layer network applied to information perception has potential security threats. Biometrics can add absolute features that improve security. By analyzing its safety and looking for evidence to prove it, it is proved that the protocol has high reliability and practicability [1]. IoT is supported at the core of the network, with RFID, GPS, sensors, and laser scanners as part of signal detection and collection, network layer and taskbar, network layer, and receiver layer. The application of the Internet of Things can realize the connection between things and people and things and things, so the Internet of Things is also called the new trend of the information industry. What we need to do now

is to combine practical experience, examine the environmental security system from the perspective of the Internet of Things, improve the key technologies of the Internet of Things reform system, and ensure the safe operation and healthy development of the Internet of Things [2]. A typical Internet of Things (IoT) connects all commodities with the Internet through sensing devices such as radio frequency identification (RFID) to realize intelligent identification and management of things in a specific area. The Internet of Things covers all aspects of daily life: wireless Internet access, Internet of Things video phones, and automatic gas detection are all applications of the Internet of Things. Despite the wide range of IoT applications, most people still know very little about the new technology behind it. So, this article attempts to provide readers with an opportunity to explore this mystery. By citing a large number of practical application examples of communication technologies in the Internet of Things, it fully reflects the key role played by the Internet of Things [3]. As the variety and number of devices increases, so does the amount of information on the Internet

(IoT). They do not just increase the amount of information on the web. But it also affects the transmission and processing speed on the Internet. However, the device discovery layer consolidates the data as soon as it is collected. This not only saves a large part of the area, but also shortens the processing time and realizes real-time performance. Based on this idea, this paper proposes a node discovery mapping algorithm to find connections between nodes. Exchange information, collaborate, and reduce network load between screen detection devices and improve real-time performance [4]. The Internet of Things provides us with the most intelligent calculation method, which can help us calculate what we want to know very easily and conveniently. And fully integrated into our lives, the indispensable devices in our lives such as mobile phones and computers are related to big data, but it is precisely because of this that our security is also threatened, and our personal information may be exposed out. Whether we inadvertently browse files under the line of sight of cameras or shoot confidential files with mobile phones by internal ghosts, our privacy will be invaded by big data and leaked out. Although optical-based recognition technology reduces this risk, it still cannot fundamentally solve the problem [5]. For a long time, in motor theory, it was believed that the success of any motor test with complex coordination depends first on technical and tactical training, and gradually increases (depending on age criteria) of functional task complexity. In this regard, there is still considerable potential in table tennis examinations: improving the quality of technical and tactical training, including on a large scale, perfecting the teaching control system, and turning it into a long-term reference point at all stages. Training; organize a motivational system to increase and maintain the group participating in this test to increase motivation for cognitive motor activity. This potential should be capitalized. For table tennis, improving the quality of technical and tactical training and increasing the number of participants can be ensured by: improving the content, coherence, and methodology of technical and tactical training; improving the teaching control system; and turning it into a long-term reference for all stages of training point [6]. Due to the world situation, sports and health issues are very important, we have noticed that the interest in table tennis is on the rise as a high-profile sport. Table tennis is one of the favorite sports of students. It helps develop the following skills: accuracy, speed and reflexes, explosiveness, rhythmic operational thinking, concentration, and coordination. Table tennis is recommended as the most promising sport with health benefits [7]. Before the start of the table tennis league, the athletes participating in the experiment were asked to randomly take a balance test, which was to study whether the balance of men and women was different and whether it would affect the SEBT. We tested 8 athletes in the experiment and recorded their consumption at intervals. As a result, the reach distance shows a decrease as the training progresses in all directions. Female table tennis players exhibit poorer dynamic postural control compared to male table tennis players [8]. A table tennis posture training apparatus and its use method guide and improve table tennis players' forehand, backhand, and other hitting

actions by forcing the hand to hit the ball on the correct trajectory. The equipment includes a waist belt and chest strap, or a wide waist belt, to position the vertical rigid bar support where the training guide is mounted. The training guide consists of one or two plates that can be adjusted at 6 degrees of freedom via a specially designed gimbal. There are two gimbal joints between the guide plate and the vertical pole brackets strapped to the player's torso. Players can adjust the position, direction, and angle of the guide plate according to their needs through two universal joints. Torso-mounted table tennis training device significantly improves paddle trajectory by guiding hands to return the ball to opposing players bouncing off the table [9]. Multi-ball training is an emerging method of finding immortals, combined with an innovation of Chinese table tennis technology. Combined with mathematical statistics, expert interviews, and other research methods, the multi-ball method and the single-ball method were compared in the same training content and in the same time unit and heart rate recovery (heart rate after 3 minutes of rest after exercise), to evaluate training volume and training effect by comparing and analyzing data [10]. Action representation and modeling play an important role in recognizing random action. But due to variability related to actors, camera viewpoints, durations, etc., explicit segmentation and labeling of motion are not trivial. So our training uses histogram training and can capture the movement and trajectory of athletes, while for video, a fixed value representation is required called a "Super Motion Vector" (SMV). [11]. It is extremely simple for us humans to do an action, but it is very difficult for a computer to recognize an action. Mobile cameras that shoot broadcast-quality video make this more difficult. Our main research action is in the media sector. That is, atypical graphics have a resolution. It can be demonstrated with the following video of table tennis movements. Take a method of decomposing the problem into three subproblems. The table tennis player data is first tracking the action, then generates an image to make a rough estimate of the position of the action. Action recognition systems use the stabilization results given by the stabilization process to classify actions using motion and pose features. A more advanced algorithm is proposed, which can help us solve problems that cannot be solved currently. Consistency of the template library is addressed by iteratively selecting templates to better fit the training data [12]. As one of the leading technologies of human-computer interaction, action knowledge is one of the hotspots in pattern recognition research. An accelerometer is a smart sensor. It is characterized by low power consumption, small size, low cost, and wide application. The acceleration of the cognitive activity detection process is currently divided into three levels: feature extraction, feature selection, and recognition algorithms. We propose a 3D accelerometer signal recognition algorithm that can identify various types of collisions based on the movements of tennis players on footnote maps. Data were collected with associated heart rate monitors and table tennis movements. The default acceleration threshold is similar to the fixed threshold and key features of character design and action length [13]. Whether it is possible to

recognize different actions and distinguish them accurately is very important. Now we are mainly confused whether the action recognition is affected by the direction of the recognized action. We can use the adaptive action paradigm to discern visual processes for specific actions and orientations. Under different conditions, the people conducting the experiments are used to moving back and forth and high fives. The participants then classified the ambiguous movement's action or direction of movement [14]. Computers can recognize human gestures through human-computer interaction systems like an Xbox camera. They recognize simple movements, but they do not have powerful advanced algorithms for more difficult identification. We need a robust body action recognition method that relies on DTW and use the best position between two points to identify the action. [15].

## 2. About Table Tennis Training and IoT Perception Action Recognition

**2.1. About Table Tennis.** The standardization of table tennis begins with the establishment of the ITTF constitution and competition rules, which is also a sign that table tennis has shifted from a folk sport to a competitive event. The establishment of the ITTF in 1926 made the table tennis competition gradually improved and standardized, and also greatly improved the viewing and fun of the project. Table tennis can not only develop athletes' speed, strength, agility, endurance, and other qualities, but also exercise courage, wit, courage, tenacity, and other psychological qualities, and comprehensively promote the physical health of athletes.

**2.2. Table Tennis Training and Action Analysis.** (1) Special strength training can be divided into three parts: upper body exercise, lower body exercise, and waist exercise. Core strength training is comprehensive and can be enhanced by back throwing medicine balls, standing long jumps, sit-ups, and planks. (2) Speed training needs to be combined with strength training when performing fast training. And according to the athlete's own characteristics to carry out training. You can use the table as the boundary to perform left and right footwork exercises, left and right jumping exercises, cross-step movement exercises, long and short ball movement exercises, and push-side throw exercises. (3) Endurance training quality includes general endurance and special endurance. We usually do it in part after training. We can train athletes for long-distance running, or we can also allow athletes to carry out uninterrupted spiking training, so as to further exercise the endurance of players. and physical strength. (4) Agility training. Agility training mainly trains the reflexes of the players. The stronger the reflexes of the players, the more difficult the balls can be caught. We can send the ping-pong balls in the direction we cannot figure out, and let the players catch the ping-pong balls. The ball, and then exercise the player's reflexes and agility.

Table tennis training content is shown in Figure 1.

**2.3. IoT Perception Technology.** The field of IoT detection technology mainly includes RFID receiving technology, sensor technology, two-dimensional code identification technology, and biometric identification technology (1) Radio frequency identification technology, which is a noncontact automatic identification technology that uses radio waves to automatically contact and instantly identify objects. (2) Sensor technology, as an artificial IoT technology, IoT sensors are mainly responsible for retrieving the "audio" content of objects. Sensors collect and retrieve information from information sources and process, modify, and identify the received information according to defined rules. A sensor is the input to a measurement system and usually consists of a sensor and a sensor that converts the input variable into a measurable signal. (3) Two-dimensional code identification technology. Today, the use of two-dimensional identification technology is becoming more and more popular in daily life, and it has become a simple, fast, and convenient practical identification. Black and white images are defined in horizontal and vertical plane orientations using 2D copies of multiple geometric shapes, based on specified data and information disclosure, and are automatically recognized and read by images from light-duty or scanning devices. (4) Biometric recognition technology. With the development of artificial intelligence, biological and statistical analysis methods such as facial expression analysis, speech recognition, eye measurement, and motion control are becoming more and more popular and widely used in this field. Biometrics replaces technologies designed to calculate the value and identity of human-recognized information based on physical characteristics or techniques of the human body.

The identification technology based on IoT perception is shown in Figure 2.

**2.4. Action Recognition.** Training Action Recognition Human Behavior for Table Tennis is essentially about recognizing human behavior. At this stage, researchers at home and abroad are developing more methods for table tennis ball recognition, and the use of human activity analysis has been widely used in recent years. Human discovery methods can be divided into deep knowledge and advanced traditional artificial methods. This classic approach provides a solid theoretical basis for further research into human factual analysis in tennis matches. Initially, traditional recognition of human behavior relied heavily on knowledge of objects and classifications. Artistically designed functions are used to capture different spatiotemporal motions in movies, but manually extracting functions is time-consuming and laborious, and complex to retrieve quickly from the data.

## 3. Action Recognition Algorithm for Table Tennis Training Based on IoT Perception

**3.1. Wi-Fi-Based Perceptual Recognition Technology.** We use channel state information (CSI), an information that accurately describes the channel material, for perception and

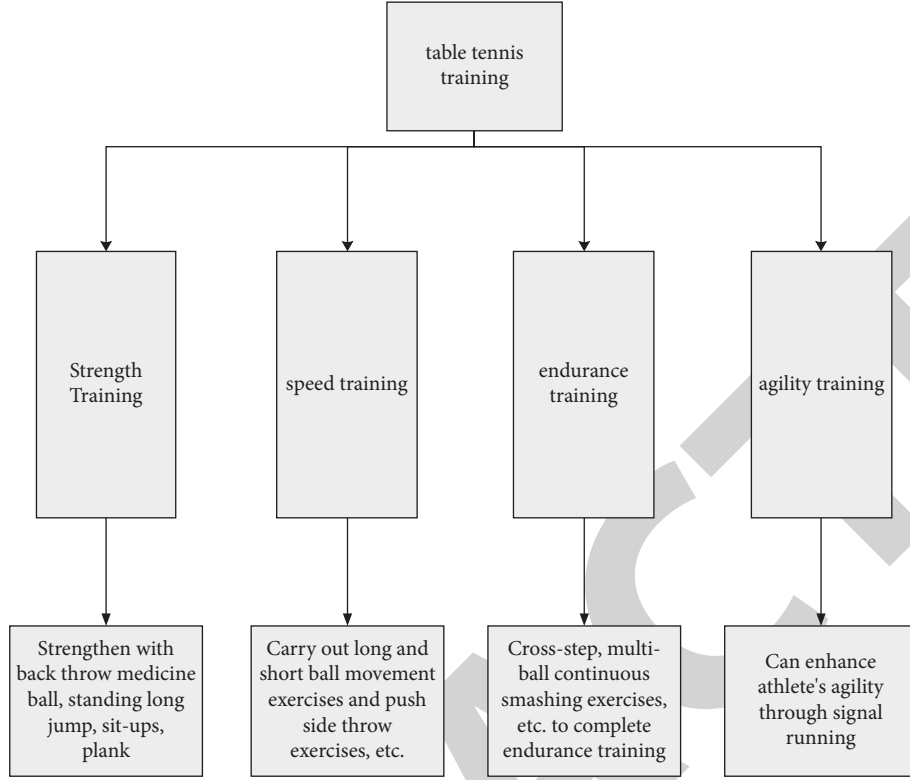


FIGURE 1: Table tennis training content.

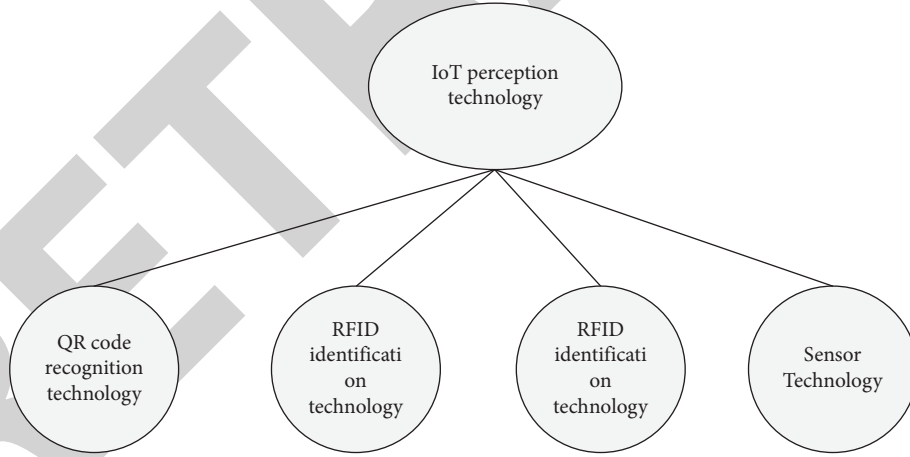


FIGURE 2: IoT perception and recognition technology.

action recognition. The key is to be able to describe the same signal propagation as the receiver, technology breaks the criteria down into several equations. If there are  $m, n$  antennas at the beginning and end, respectively, then it can be expressed by the following formula:

$$\begin{bmatrix} H_{11} & \dots & H_{1,j} \\ \vdots & \vdots & \vdots \\ H_{i1} & \vdots & H_{i,j} \end{bmatrix}, \quad i \in [1, mn], \quad j \in [1, N]. \quad (1)$$

The meaning of  $H_{i,j}$  can be called the CSI value.

The received signal of the MIMO system can be expressed as

$$Y_i = H_i X_i + N_i, \quad i = 1, 2, \dots \quad (2)$$

The meanings of  $|R_j|$  and  $\theta_j$  are the phase positions on the  $j$ -th path, the meaning of  $p$  is the total number of propagation paths, and the value of  $S$  represents the received signal. The larger the value of  $S$ , the stronger the received signal.

Calculating it gives

$$H = [H(f_1), H(f_2), \dots, H(f_N)],$$

$$N = 1, 2, 3, \dots, \quad (3)$$

$$H(f_k) = |H(f_k)| e^{j\angle H(f_k)}, \quad k \in [1, N]. \quad (4)$$

The name of  $N$  is called the number of subcarriers, and  $H(f_k)$  is the CSI value. CSI has less random noise and is more suitable for sensory research than the data from the first period.

### 3.2. RFID-Based Perception and Identification Technology

**3.2.1. Phase.** Phase is a periodic function whose period is  $0 - 2\pi$  and can be calculated as:

$$\varphi = 2\pi \left( \frac{2d}{\lambda} \right) \bmod(2\pi). \quad (5)$$

Due to the influence of the RFID hardware characteristics, the identified position will produce differences and offsets, we call it  $\varphi_n$ , and at the same time, due to the multipath effect, the identified phases will also have differences and offsets, we call it  $\varphi_e$ , so  $\varphi$  can be expressed as follows:

$$\varphi = \left( \frac{2\pi \cdot 2d}{\lambda} + \varphi_n + \varphi_e \right) \bmod(2\pi). \quad (6)$$

**3.2.2. Signal Acceptance Strength.** In RF-based scanning analysis techniques, RSSI is very easy to measure, so the received signal strength is the first to be studied and applied by experts. As the radio signal increases, the signal strength decreases with the length, which means that there is a certain correlation between signal strength and range. The signal strength of RSS during transmission can be represented by the following formula:

$$p_r = p_t \text{TG}_r^2 G_t^2 \left( \frac{\lambda}{4\pi d} \right)^4. \quad (7)$$

The meaning of  $p_t$  in the formula is the strength of the transmitted signal, the meaning of  $G_r$  and  $G_t$  is the consumption of the signal by the circuit when the signal is sent, the meaning of  $T$  is the consumption during the transmission process, the larger the value of  $p_t$ , and the stronger the strength of the signal.

Combined with the formula, the final RSSI calculation formula can be obtained:

$$\text{RSS} = 10 \lg \left( \frac{P_r}{1mW} \text{TG}_r^2 G_t^2 \left( \frac{\lambda}{4\pi d} \right)^4 \right). \quad (8)$$

**3.2.3. Doppler Shift.** The meaning of Doppler shift refers to the frequency shift of transmission and reception. We let the velocity of an object be  $v$ , the angle of antenna motion be  $a$ , and the Doppler frequency shift can be expressed by the following formula:

$$\Delta f = \frac{2v}{\lambda} \cos(a). \quad (9)$$

**3.3. Label Reflection Model.** The signal received by the reader can be simply divided into the reflected signal with the tag and the reflected signal without the tag. Since the reflected signal without the tag is not affected by any tag, that is why it is developed from the RFID automatic recall scanner for commercial use of RFID technology is now widely used in tracking and analysis systems as people move between tags, stages, and RSSI changes, but these changes are severely affected by the lack of visibility in these areas. Therefore, this method is used to study hand movements, and the influence of the circuit on the RF signal is much smaller than that of human movements.

**3.3.1. Phase Signal.** What the receiver receives is the result of the accumulation of multiple signals, so the actual received signal  $S$  can be calculated as:

$$S = \sum_{j=1}^p |R_j| e^{-i\theta_j}. \quad (10)$$

Then we can get the value of  $S_{\text{RSSI}}$ :

$$S_{\text{RSSI}} = 10 \log_2 S^2. \quad (11)$$

Phase  $\varphi$  is calculated using the following equation:

$$\varphi = \frac{2\pi \cdot 2d}{\lambda} \bmod(2\pi). \quad (12)$$

In real use, it will definitely be interfered by RFID hardware, the identified position will produce differences and offsets, we call it  $\varphi_n$ , and at the same time, due to the multipath effect, the identified phases will also have differences and offsets, we call it  $\varphi_e$ , so  $\varphi$  can be expressed as:

$$\varphi = \left( \frac{2\pi \cdot 2d}{\lambda} + \varphi_n + \varphi_e \right) \bmod(2\pi). \quad (13)$$

Using the period difference can effectively reduce the phase error and improve the accurate period performance.

**3.3.2. The Influence of Hand Movement on the Label.** When the hand crosses the tag, the tag receives a tag representing the movement of the hand, marking the two tags  $S_r$  and  $S_f$  so that the actual received signal  $S_a$  can be seen:

$$S_a = S_r + S_f. \quad (14)$$

### 3.4. Phase Preprocessing

**3.4.1. Phase Unwrapping.** The raw phase signal is a periodic function, its range is  $0 - 2\pi$  rad, and it has a chance to vary.  $\Delta N_{t,1} = N_{t,i+1} - N_{t,i}$  can be calculated using the following formula:

$$\Delta N_{t,i} = \begin{cases} 0, & |\varphi_{t,i+1} - \varphi_{t,i}| < \pi, \\ -2\pi, & \pi \leq \varphi_{t,i+1} - \varphi_{t,i} \leq 2\pi, \\ 2\pi, & -2\pi \leq \varphi_{t,i+1} - \varphi_{t,i} \leq -\pi. \end{cases} \quad (15)$$

The meaning of  $\varphi_i$  is the phase vector value of the collected original letter signal  $t$ ,  $\varphi_i = [\varphi_{t,1}, \varphi_{t,2}, \dots, \varphi_{t,n}]$ ,  $t = 1, 2, \dots, 9$ ,  $(t_i, \varphi_{t,i})$  and  $(t_{i+1}, \varphi_{t,i+1})$  the meanings of  $Z$  and  $X$  are the phase values of two continuous times.

Then the value of  $N_{t,i}$  can be calculated by the following formula:

$$N_{t,i} = \sum_{j=1}^{i-1} \Delta N_{t,j}, \quad i = 1, 2, 3, \dots, n. \quad (16)$$

**3.4.2. Phase Normalization.** Find the average of 9 pistons in a fixed position. When processing the data from the next step, the component values for each label are subtracted from the standard mean.

The acquired phase matrix can be expressed as:

$$\varphi_{m \times n} = \begin{bmatrix} \varphi_{1,1} & \dots & \varphi_{1,n} \\ \vdots & \ddots & \vdots \\ \varphi_{m,1} & \dots & \varphi_{m,n} \end{bmatrix}. \quad (17)$$

The meaning of  $m, n$  is the number of labels and the number of collection points, respectively. Calculate the mean of the rest state for each label:

$$\overline{\varphi_m} = \frac{\sum_{i=1}^n \varphi_{m,i}}{n}, \quad m = 1, 2, \dots, 9. \quad (18)$$

Typical results are obtained by subtracting the average phase balance value from the appropriate signal to read each phase.

**3.4.3. Calculate the Boundaries of Each Label.** For the length of the sliding window  $L$  we use to express, the amplitude value and frequency of the  $i$ -th window can be expressed as:

$$A_i = \sum_{k=1}^L |\phi_{i,k}|, \quad (19)$$

and

$$F_i = \sum_{k=1}^L |\phi_{i,k} - \phi_{i,k-1}|. \quad (20)$$

In the formula, the meaning of  $\phi_{i,k}$  is the  $i$ -th data point of the  $k$ -th sliding window.

The formula for calculating the difference function  $G$  is as follows:

$$G(i) = C_A |A_{i+1} - A_i| + C_F |F_{i+1} - F_i|. \quad (21)$$

**3.5. DTW Algorithm.** The DTW algorithm is an algorithm used to calculate the similarity of different datasets. Based on two independent sequences, the DTW algorithm can calculate the similarity of the two sequences, and can also combine DTW to verify and verify the two sequences. The basic idea behind the algorithm is to pick a point in one row and look for a point in another row to find the best path.

The specific calculation method is as follows:  $X = (x_1, x_2, \dots, x_n)$  and  $Y = (y_1, y_2, \dots, y_n)$  are two permutations, their length is  $m, n$ , and the DTW algorithm can calculate its minimum value., the mapping cost of  $X, Y$  can be calculated as:

$$d_{ij} = \|x_i - y_j\|. \quad (22)$$

The meaning of  $d_{ij}$  in the formula is the Euclidean distance between two points. According to the above formula, the DTW distance between the two sequences can be expressed as:

$$\text{DTW}(X, Y) = \min \sum d_w, w \in (1, 2, 3 \dots, k). \quad (23)$$

DTW is a good tool for comparing differences, the difference between  $X$  and  $Y$  can be calculated very well with the above classification formula.

**3.6. Action Recognition.** The RF-AH system uses the DTW algorithm to calculate the total distance between the known pattern and the pattern model and uses the minimum accumulation formula as the operation to display the corresponding minimum distance.

Step 1:

$$D_t(i, j) = \text{Dist}_t(i, j) + \min[D_t(i, j-1), D_t(i-1, j), D_t(i-1, j-1)]. \quad (24)$$

Step 2:

$$\xi = \arg \min(D_t), t = 1, 2, \dots, 9. \quad (25)$$

The meaning of  $t$  in the formula is the serial number of the template action sample.

## 4. Experiments Related to Action Recognition of Table Tennis Training Based on IoT Perception

In order to further explore the application and role of IoT perception in action recognition for table tennis training, we



conducted a series of experimental research and analysis on the IoT perception action recognition algorithm, so as to see the difference between the algorithms more directly and clearly and advantages and disadvantages.

**4.1. Table Tennis Action Experiment.** The skills and techniques of sports are the keys to judge whether an athlete is good or not. Table tennis is not as simple as it seems. It contains many technical movements, which cannot be done without professional training. There are many kinds of catching movements in, here we mentioned eight kinds of catching movements such as forehand attack, forehand pull, backhand pick, and so on.

In the experiment, we recruited 12 table tennis players, half male and half female. We perform action recognition on these athletes, and the specific recognition data are shown in Table 1.

**4.2. Identify Performance Evaluation Indicators.** Accuracy, recall, precision, and *F1* scales are commonly used to evaluate the performance of evaluation tasks. For binary classification activities, the origin is described as follows: In binary classification activities, rows represent actual sample categories, and columns represent suggested categories. TP number is used correctly in positive samples. FP was the quantity of false positive samples; the quantity of TN in negative film is marked correctly; there are also some examples that are wrongly predicted as negative. The details are shown in Table 2.

#### 4.3. Algorithm Improvement Comparison

**4.3.1. Algorithm Segmentation Improvement.** Careful segmentation of actions is crucial for future recognition, so we improved the DTW method, and then conducted a comparative test before and after the algorithm improvement: 5 athletes were selected. Before the algorithm improvement, the accuracy rate was not high, but after the improvement, the accuracy has significantly improved. The specific experimental results are shown in Figure 3.

From the data shown in Figure 3, we can know before the refinement of the algorithm in this paper, the accuracy of the algorithm's operational research analysis was very low and did not produce the expected results. After the algorithm is split and upgraded, the analysis accuracy of the algorithm operation is significantly improved, and the detection accuracy is significantly improved. From this, it can be concluded that our improved algorithm is efficient and can make the system more accurate.

**4.3.2. Action Segmentation Performance.** Due to the repetitive nature of bodyweight exercise, segmenting a group of actions and segmenting a phase profile containing a complete single action is necessary for correct identification. So use the number of correctly detected actions/the number of actual actions to represent the segmentation accuracy. Analysis of the system action segmentation performance

TABLE 1: Number of effective samples corresponding to each ping-pong action.

Action category	Male sample	Female sample	Total sample
Forehand attack	142	136	278
Forehand pull	144	142	286
Forehand rub	143	145	288
Forehand pick	140	139	279
Backhand stroke	148	141	289
Backhand pull	145	143	288
Backhand rubbing	143	137	280
Backhand spinning ball	142	145	287
Total	1147	1128	2275

TABLE 2: Confusion matrix of two classifications.

Category	Positive	Negative
Positive	TP	FN
Negative	FP	TN

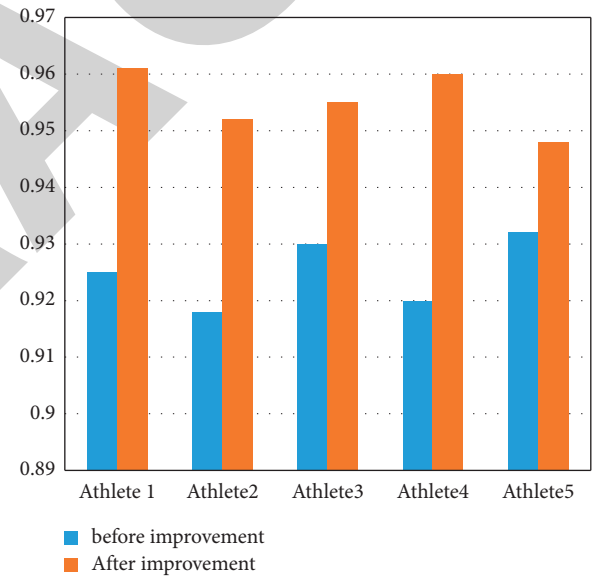


FIGURE 3: Algorithm improvement comparison.

shows that the reduction of segmentation accuracy is due to the fact that athletes may take a short rest when they are halfway through the exercise, resulting in one action being divided into two actions. The segmentation accuracy of different actions is shown in Figure 4.

#### 4.4. Ping-Pong Action Recognition Results and Analysis

**4.4.1. Confusion Matrix Experimental Analysis.** The signal features are obtained by the method of signal analysis, and the action samples are identified by the DTW algorithm. Of all the functional samples obtained, 30% were randomly selected as testing kits, and the remaining 70% were used as training kits. The DTW method, validated and analyzed, attempts to obtain a mixture matrix of all test samples, where

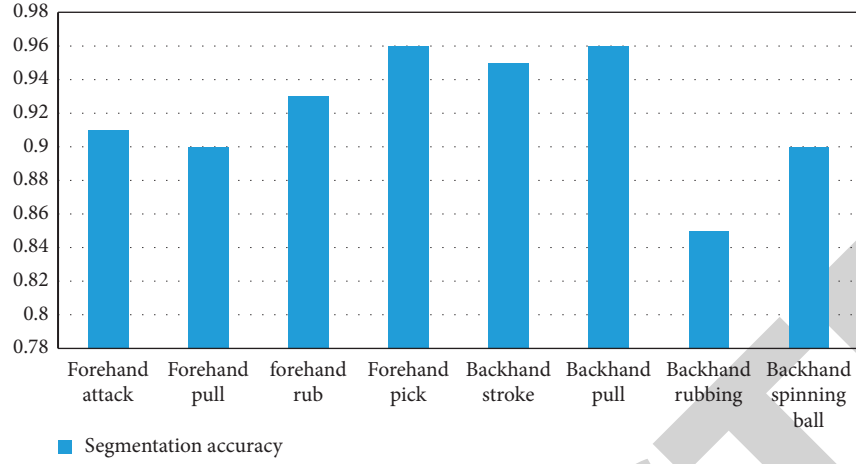


FIGURE 4: Action segmentation accuracy.

TABLE 3: DTW prediction confusion matrix.

	Forehand attack	Forehand pull	Forehand rub	Forehand pick	Backhand stroke	Backhand pull	Backhand rub	Backhand pick
Forehand attack	82	1	0	0	0	0	0	0
Forehand pull	0	85	0	0	0	1	0	0
Forehand rub	0	0	87	0	0	0	0	0
Forehand pick	0	0	0	84	0	0	0	0
Backhand stroke	0	0	0	0	85	1	0	1
Backhand pull	0	0	0	0	0	86	0	0
Backhand rubbing	0	0	0	0	0	0	84	0
Backhand spinning ball	0	0	0	0	0	0	0	86

TABLE 4: Performance evaluation results of different sensors.

	Acc	Gyro	Mag	Acc-gyro	Acc-mag	Gyro-mag	A-G-M
Accuracy(%)	92.53	88.29	92.83	96.78	96.83	96.49	97.41
Precision(%)	92.67	88.28	93.01	96.97	96.85	96.54	96.43
Recall(%)	92.54	88.34	92.84	96.80	95.83	96.49	97.42
F1-score(%)	92.51	88.28	92.85	96.78	96.83	96.50	96.42

each row is the current activity category, each column is the expected sample activity category, and records a sequence vector for the specified category. The sum of the order vector values represents the number of samples needed. The test sample matrix is shown in Table 3.

It can be seen from the error table (Table 3) that the different functions of table tennis skills can be correctly identified on the whole. Different skill activities have different recognition requirements, and some recognition results are very good.

**4.4.2. Performance Evaluation of Different Sensors.** In order to evaluate the performance of various sensors in analyzing table tennis activities, this paper conducts experiments on the detection effects of various sensors based on the DTW algorithm and uses indicators such as accuracy, precision, recall, and F1 to evaluate. Among them, Acc only uses a speed sensor, Gyro only uses a gyro sensor, Mag only uses a

magnetic field sensor, Acc-Gyro only uses a speed sensor, and Accro Gyro only uses a speed sensor. Gyro sensor and Acc-Mag are meant to go hand in hand. For magnetic field sensors, Gyro-Mag demonstrated the use of both gyroscopes and magnetic field sensors, and AGM demonstrated the use of three types of sensors simultaneously. The test results are shown in Table 4.

According to the data in Table 4, in general, more sensors can achieve better performance in capturing ping-pong movements. However, using all three sensors at the same time scored higher than otherwise.

**4.5. Influence of Multipath Effect.** RFID tags also affect the environment. Due to the existence of multilayer tags, if there are any interfering objects near the RFID system, the tags will jump and scatter, causing signal interference. Experimental and comparative data were collected in the same indoor environment with chairs and shelves placed around

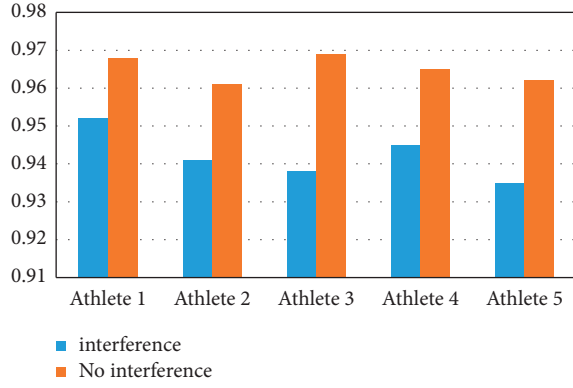


FIGURE 5: System accuracy with and without interference.

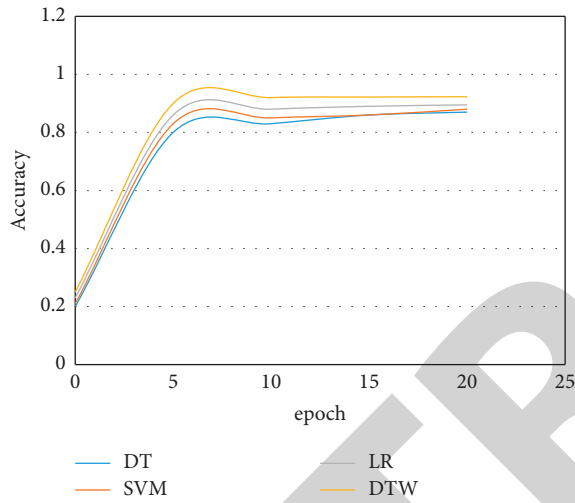


FIGURE 6: The accuracy of identifying similar actions.

the system. According to the systematic method proposed in this chapter, the signals of both cases are processed identically, and the experimental results are obtained. It can be seen that the system is basically unaffected, and the diagnosis and detection speed is slightly slower, indicating that the system is strong. The result is shown in Figure 5.

**4.6. Recognition Experiment of Similar Actions.** In order to analyze and study the recognition performance of the DTW in similar actions, this experiment compares other traditional algorithms of this algorithm in the recognition of similar actions. The ability to recognize similar actions. From the experimental data, we can know that the algorithm in this paper has better recognition ability for similar actions than other traditional algorithms. The accuracy of the algorithm in the specific experiment is shown in Figure 6.

We can know from Figure 6 of this paper that in the identification of similar actions, the algorithm in this paper has higher accuracy than other algorithms and can be stabilized, so it can be concluded that the algorithm in this paper recognizes similar actions. Compared with other

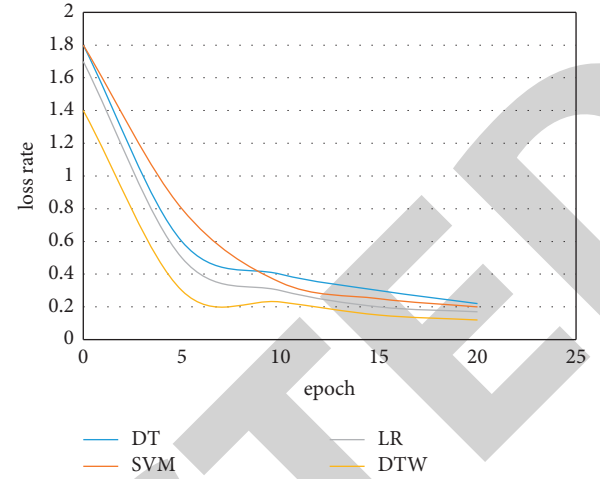


FIGURE 7: Loss rate for identifying similar actions.

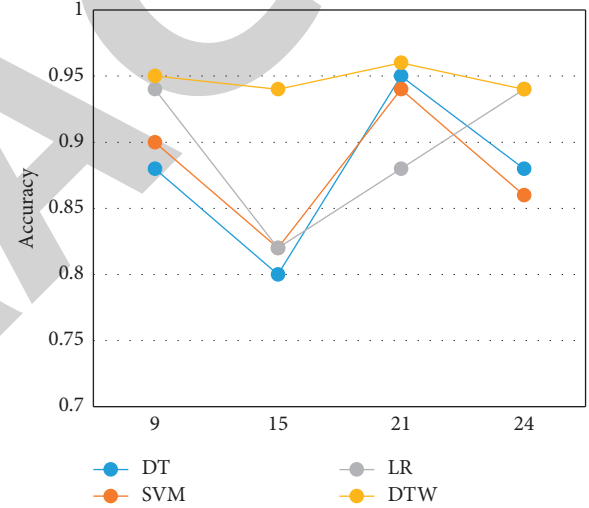


FIGURE 8: The accuracy of the algorithm at different times.

traditional algorithms, it has better recognition ability and has more outstanding performance.

The specific algorithm identification loss rate data in the experimental results are shown in Figure 7.

**4.7. Impact on the System at Different times.** To verify whether the robustness of the algorithm will be affected by time, including the impact of time on each algorithm, samples were collected in three different time periods, namely, nine o'clock, fifteen o'clock, and twenty-one o'clock. The recognition accuracy rate of each algorithm in three time periods is obtained, and the recognition accuracy rate of each algorithm in three time periods is obtained, so as to compare the time effect of the algorithm. The specific experimental result data are shown in Figure 8.

It can be seen from Figure 8 that the accuracy of the algorithm in this paper (DTW) does not change much and is relatively stable at different times, while other traditional

TABLE 5: Performance evaluation indicators.

Mode	Accuracy(%)	Precision(%)	Recall(%)	F1-score(%)	time(ms)
DT	93.93	93.96	91.93	93.93	0.379
SVM	92.97	93.27	92.99	93.03	0.143
LR	94.68	95.72	95.69	94.69	0.093
DTW	95.41	96.43	97.42	96.42	0.028

algorithms affect the cycle and the accuracy also changes accordingly. Its impact is relatively large. The experimental results confirm that the time has no effect on the algorithm in the paper, and the effect is better than the traditional algorithm, and the stability of the algorithm is highlighted in this paper.

According to Figure 8, it can be known that the accuracy of DTW in identifying actions in different time periods does not change much and is relatively stable, while other traditional algorithms are affected by the time period, the accuracy becomes fluctuating, and the impact is relatively large. The experimental results prove that the algorithm in this paper is not affected by time, and it performs quite well compared to the traditional algorithm, which highlights the stability of the algorithm in this paper.

**4.8. Comparative Test of Performance Evaluation Indicators.** The DTW diagnostic algorithm integrates three main classifiers, decision tree, auxiliary vector engine, and transport regression. This paper provides a comparative analysis of the recognition performance using the basic ping-pong algorithm. In addition to evaluating performance, accuracy, precision, retention, and F1 scale, this paper compares the average response time of each algorithm to evaluate sample sampling performance. Experimental data are shown in Table 5.

It can be seen from Table 5 that the algorithm in this paper is superior to other traditional algorithms in the four performance evaluation indicators of accuracy, precision, recall, and F1 metric. This fully proves that the algorithm in this paper has more powerful performance and higher accuracy than other algorithms and is more stable than other algorithms. It is a better and more worthwhile algorithm.

Overall, we know from the table that the performance indicators of the DTW method are better than other class classifications except for the time efficiency, and the average DTW prediction time is less than the base class prediction time. Among the individual-based classifiers, decision trees and organizational regression make good use of time, and the average prediction time is much shorter than that of support vector machines.

## 5. Conclusion

With the rapid development of IoT technology, many IoT devices appear in our daily life and are used in various fields. As a key technology of human-computer communication, the recognition of human behavior is the key to research in many fields. Table tennis is fast, complex, and similar in

structure, so it is difficult to accurately judge the movements of players. There are many traditional methods of identifying events. This recognition method relies on relatively complex vision, but has obvious shortcomings such as limited analysis range and high light output; operational knowledge based on inertial sensors can fill the gaps in vision technology. The identification method based on wireless signal is relatively new, but the development is not advanced enough, and the identification effect is not perfect. With IoT detection capabilities, activity can be identified accurately and efficiently. As an IoT discovery technology, RFID has become a research object due to its low cost, high precision, flexibility, and high stability. With the advancement of technology, the perception recognition technology of IoT is the best way to identify the future business.

## Data Availability

The experimental data used to support the findings of this study are available from the corresponding author upon request.

## Conflicts of Interest

The authors declared that they have no conflicts of interest regarding this work.

## References

- [1] L. Kou, Y. Shi, L. Zhang, D. Liu, and Q. Yang, "A lightweight three-Factor user Authentication protocol for the information perception of IoT," *Computers, Materials & Continua*, vol. 58, no. 2, pp. 545–565, 2019.
- [2] X. Guo, "Key technologies of IoT perception environment security mechanism research," *Electronics Test*, vol. 14, 2015.
- [3] D. Wei, P. Yun, and C. Wei, "Next communication technology wave Pushes IOT: possible for Earth perception," *International Journal of Advancements in Computing Technology*, vol. 4, no. 16, pp. 329–338, 2012.
- [4] Y. Fan, G. Zhao, K. C. Li et al., "SNPL: one Scheme of securing nodes in IoT perception layer," *Sensors*, vol. 20, no. 4, p. 1090, 2020.
- [5] J. Zhang, Y. Xie, W. Liu, and X. Gong, "Table recognition for Sensitive data perception in an IoT vision environment," *Applied Sciences*, vol. 9, no. 19, p. 4162, 2019.
- [6] I. Ajili, M. Malle, and J. Y. Didier, "Robust human action recognition system using Laban Movement Analysis," *Procedia Computer Science*, vol. 112, pp. 554–563, 2017.
- [7] C. Walcott, G. Moore, and T. Gurtu, "The training satisfaction of the university table tennis players of general Group[J]," *International Table Tennis Federation Sports Science Congress Co*, vol. 20, no. 5, 2010.
- [8] Y. Gu, C. Yu, S. Shao, and J. S. Baker, "Effects of table tennis multi-ball training on dynamic posture control," *PeerJ*, vol. 6, no. 1, Article ID e6262, 2019.
- [9] X. P. Zhang, "Research on effects of training for Fitting in with new Service rules in national table tennis Team of China," *Journal of Beijing University of Physical Education*, vol. 52, no. 3, pp. 393–398, 2002.
- [10] L. A. Pan, X. C. Cheng, and Q. L. Du, "Study of table tennis training system," *Advanced Materials Research*, vol. 472–475, pp. 3117–3120, 2012.

## *Retraction*

# **Retracted: Quality Evaluation and Informatization Analysis of Physical Education Teaching Reform Based on Artificial Intelligence**

### **Security and Communication Networks**

Received 26 December 2023; Accepted 26 December 2023; Published 29 December 2023

Copyright © 2023 Security and Communication Networks. This is an open access article distributed under the Creative Commons Attribution License, which permits unrestricted use, distribution, and reproduction in any medium, provided the original work is properly cited.

This article has been retracted by Hindawi, as publisher, following an investigation undertaken by the publisher [1]. This investigation has uncovered evidence of systematic manipulation of the publication and peer-review process. We cannot, therefore, vouch for the reliability or integrity of this article.

Please note that this notice is intended solely to alert readers that the peer-review process of this article has been compromised.

Wiley and Hindawi regret that the usual quality checks did not identify these issues before publication and have since put additional measures in place to safeguard research integrity.

We wish to credit our Research Integrity and Research Publishing teams and anonymous and named external researchers and research integrity experts for contributing to this investigation.

The corresponding author, as the representative of all authors, has been given the opportunity to register their agreement or disagreement to this retraction. We have kept a record of any response received.

## **References**

- [1] Y. Xu, S. Huang, and L. Li, "Quality Evaluation and Informatization Analysis of Physical Education Teaching Reform Based on Artificial Intelligence," *Security and Communication Networks*, vol. 2022, Article ID 5473153, 13 pages, 2022.

## Research Article

# Quality Evaluation and Informatization Analysis of Physical Education Teaching Reform Based on Artificial Intelligence

Yixiong Xu <sup>1</sup>, Shuai Huang <sup>2</sup>, and Lei Li<sup>1</sup>

<sup>1</sup>*School of Physical Education, Nanchang Normal University, Nanchang 330032, China*

<sup>2</sup>*South China Businesses College Guangdong University of Foreign Studies, Guangzhou 510545, China*

Correspondence should be addressed to Shuai Huang; 206019@gwng.edu.cn

Received 7 July 2022; Revised 9 August 2022; Accepted 17 August 2022; Published 30 August 2022

Academic Editor: Hangjun Che

Copyright © 2022 Yixiong Xu et al. This is an open access article distributed under the Creative Commons Attribution License, which permits unrestricted use, distribution, and reproduction in any medium, provided the original work is properly cited.

With the continuous reform of China's education and the development of the educational environment, English will no longer be the third subject for Chinese students and physical education will replace it as the third subject. The teaching mode has also gradually changed from the traditional artificial mode to the current smart education. In the context of artificial intelligence, physical education can also apply this technology to daily teaching. After physical education becomes the third subject, it is necessary to reform the existing teaching mode and conduct quality evaluation and informatization analysis. In order to achieve this effect, we use artificial intelligence action scenes to detect students' detailed actions and identify key actions and then use computer vision system to create regression models and Bayesian formulas to give the criteria for judging the subsequent training points of the computer. Then, according to the training data of each student in the training process, the quality analysis and informatization evaluation of the teaching reform of physical education are carried out. Using the action bank algorithm as the basic algorithm of feature extraction, a template research method based on multispectral clustering is proposed to facilitate its dissemination in the computer background database. Then, through experiments to compare the before and after optimization of the algorithm, the data analysis of the resolution, time consumption, and detection error of the action bank model were carried out, and it was found that the performance was improved. Then, by means of mean shift detection method and spatiotemporal action detection method, the resolution, time consumption, and detection error of the action bank model are optimized to achieve the quality evaluation and informatization analysis of physical education teaching reform.

## 1. Introduction

The logistic regression model algorithm based on artificial technology [1–4] determines the quantitative relationship between two or more variables that depend on each other, to find out the data with a strong correlation with the evaluation index. The preliminary classification of the data is completed, and then, the data mining technology is used [5–8]. By comparing the feature information of the data, the data with the same or strong correlation with the feature information of the data are mined in the same database, to achieve the preliminary mining and classification of the data, so as to facilitate the subsequent data cleaning and data mining. Changes and data purification: taking the above as the core idea, a physical education teaching reform quality

evaluation and information analysis system are established, to a certain extent, the interference of human subjective consciousness is put aside, data and evaluation indicators are used to establish a more objective evaluation behavior, based on such prerequisites, and we need to regard the algorithm model and evaluation system we have established as a system with two correlations. Using the method of data mining classification, the data related to the indicators affecting the evaluation are classified into the background database [7, 9–12], and then, to a certain extent, it is regarded as transforming into a geometric mathematical model with high flexibility [13, 14] to deal with the rigid conditions of lack of transformation ability, standing in the mathematical discussion form unnatural conditions are combined with mathematical models, and finally through the combination



of classical numbers and shapes. In this way, the indicators with strong correlation that affect the evaluation results in the evaluation system are more intuitively represented in the way of images. The evaluation system is standardized, and it is made fair. Numbers are the most concise and powerful language of reality, and the mathematical expression of everything is true, valid, and concise enough, provided the result is correct. The algorithm optimization and more scientific improvement under artificial intelligence technology are also worth looking forward to and paying attention to in the future.

## 2. Evaluation and Analysis of College English Education Informatization Degree under Big Data Technology

In this study, the quality evaluation and informatization analysis of physical education teaching reform are mainly based on artificial intelligence technology, while the data mining technology of background database based on artificial intelligence technology mainly collects and integrates various and complicated data information, to obtain more accurate and effective data. The representative data information allows us to evaluate and analyze the quality of physical education teaching reform [15–18] more objectively. Firstly, we analyze the ideas according to the data mining technology and construct the idea map. We construct the five stages in the data mining process. Based on the data mining technology of the background database under the artificial intelligence technology, the model and its algorithm are constructed, and then, the quality of physical education teaching reform is carried out.

First of all, considering the technical difficulty, most data mining tools are user-friendly, easy to understand, and easy to use, which greatly reduces the difficulty for analysts or industry evaluators to mine value from massive data. Secondly, data mining technology is the product of countless experiments and is widely recognized and accepted by everyone. It can clean, calculate, and visualize data through various built-in programs and realize automatic management and control of multitasking, which can significantly reduce the user's time and cost and reduce the workload and provide substantial help for analysts and evaluators.

Evaluation and analysis are shown in Figure 1.

At this stage, data mining is performed through artificial intelligence technology to complete the data mining work, and the generated model can be used in the follow-up to solve more complex problems.

### 2.1. Artificial Intelligence Technology Mining Learning Model and Its Algorithm

**2.1.1. Logistic Regression Model.** By introducing the logistic regression model algorithm, the correlation strength of the data collected in the students' class is calculated, and the classification function is used to classify it. After fitting the classified data, the logistic regression function is used to

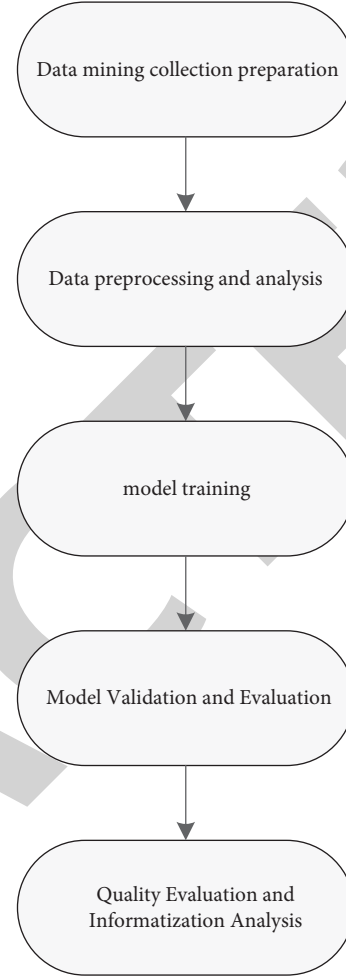


FIGURE 1: Analysis of the informatization of physical education teaching reform under artificial intelligence technology.

perform linear regression [19–21] on the basis of normalization, so that the difference between the data value and the true value obtained by the model and function becomes smaller.

The computational model experiment in the article is a special computational experiment, and its computation is nothing more than two results, either success or failure, and each experimental sample exists independently and is not disturbed, and each experiment has a fixed value. The probability of success  $p$  and then the probability of occurrence of the experimental calculation sample are assumed to conform to the Bernoulli distribution, which not only simulates the real situation of the model calculation to a great extent but also facilitates the calculation of the mathematical expectation and variance of the distribution due to the simple distribution of the results so that we can derive the log-likelihood function and find the maximum-likelihood estimate from it.

- (1) The logistic regression model algorithm mainly multiplies each attribute of the data sample participating in the experiment by the corresponding parameter value and accumulates the results we get. The formula of its model is as follows:



$$h(x) = w_0x_0 + w_1x_1 + w_2x_2 + \dots + w_mx_m. \quad (1)$$

The vectorized formula is expressed as follows:

$$h(x) = w^t x. \quad (2)$$

(2) The value of the sigmoid function is calculated.

The calculated result of the above formula into the sigmoid function is substituted. The calculated result obtained by the function calculation will be between (0, 1). The calculated value is compared with the set threshold value, which is greater than the threshold value, that is, positive class; otherwise, it is negative class, and its calculation formula is as follows:

$$g(z) = \frac{1}{1 + e^{-wx}}. \quad (3)$$

**2.1.2. Model Calculation.** Here, we assume that  $n$  samples are used for calculation training. It is known that the probability of occurrence of each assumed sample conforms to the Bernoulli distribution, and the probability of occurrence is calculated experimentally for each sample.

(1) The probability of occurrence of positive and negative classes is calculated.

$$\begin{aligned} p(y_i = 1|x_i), \\ 1 - p(y_i = 1|x_i). \end{aligned} \quad (4)$$

(2) The posterior probability of each sample is calculated.

$$p(y|x, w) = p(y_i = 1|x_i) y^i (1 - p(y_i = 1|x_i))^{1-y_i}. \quad (5)$$

**2.1.3. Log-Likelihood Function.** Due to the extremely large amount of data, in our calculation process, the model and data overfitting state will inevitably occur. To avoid this problem, here we introduce the loss function  $l(w)$ , by adding the loss function  $l(w)$  plus a penalty term for  $w$ , making the penalty a regularizer. Its calculation formula is as follows.

The impact of data purity on the results is undoubtedly the most direct. It is undeniable that such a problem does exist in this article. However, based on the diversity and quantity of data types, it is difficult to formulate a unified, specific, and standardized measurement system for the measurement of the purity of multiple types of data. Therefore, in this article, by purifying the data multiple times, the information entropy value is reduced as much as possible, and the impact of data purity on the results is minimized.

$$l(w) = \prod_{i=1}^m p(y_i = 1|x_i)^{y_i} (1 - p(y_i = 1|x_i))^{1-y_i}. \quad (6)$$

It is expanded and solved, and the derivative of  $w$  is taken:

$$\frac{\partial l(w)}{\partial w} = \sum_{i=1}^m (y_i - g(z)) x_i. \quad (7)$$

#### 2.1.4. Naive Bayes Algorithm

(1) naive Bayesian model originated from classical mathematical theory. Its stable classification efficiency and simultaneous multitask processing, especially when the amount of data information is huge, greatly improve the efficiency of classification and sorting of our data mining information. The function model is as follows:

$$C_x = \arg \max_{k \in \{1, 2, \dots, K\}} \left( P(C_K) \prod_{j=1}^n p(x_j|C_K) \right). \quad (8)$$

(2) The above formula is calculated, and the frequency is used to estimate the probability. The calculation formula is as follows:

$$p(C_K) = \frac{m_k}{m}. \quad (9)$$

(3) Here, we make reasonable assumptions about the distribution of data characteristics of the samples and calculate separately.

The naive Bayes that conforms to the multinomial distribution is calculated as follows:

$$p(x_{js}|C_k) = \frac{m_{kjs}}{m_k}. \quad (10)$$

Sometimes if the value of a feature in the sample is 0, it will seriously affect the probability distribution of the feature, so we use the Laplace smoothing to avoid this situation, namely,

$$p(x_{js}|C_k) = \frac{(m_{kjs} + \lambda)}{(m_k + \lambda)}. \quad (11)$$

The naive Bayes conforming to the Bernoulli distribution is calculated as follows:

$$p(x_{js}|C_k) = \begin{cases} p(x_{js} = 0|C_k) = 1 - p(x_{js} = 1|C_k) \\ p(x_{js} = 1|C_k) \end{cases} \quad (12)$$

The naive Bayes that conforms to the Gaussian distribution is calculated as follows:

$$f(x, \mu, \sigma) = \frac{1}{\sigma\sqrt{2\pi}} \exp\left(-\frac{(x - \mu)^2}{2\sigma^2}\right). \quad (13)$$

**2.2. Decision Tree Model and Its Data Purification.** After the data mining is collected, the data will be sorted and summarized to get a database with a huge amount of information. In our database, the invalid information we have collected is often retained. At this time, the introduction of

the decision tree model can effectively solve the data. Purity issues: decision tree model is mainly a nonparametric classifier that is simple to use and less difficult to operate. Here, we refer to the ID3 algorithm, as well as the C4.5 algorithm.

In the article, only some indicators that affect the degree of informatization in college English education are tested and the evaluation standards are formulated, but in fact, there are many factors that affect the degree of informatization in college English education. There are many indicators for reference. In this article, we only select a few of the more important reference indicators for testing, but that does not mean we are turning a deaf ear to other influencing factors. The final evaluation and analysis results must be discussed under the influence of various factors. Due to the similarity of the calculation methods, they are not tested and displayed in this study.

The commonly used algorithms in the decision tree model [22] mainly include the ID3 algorithm and the C4.5 algorithm. These two algorithms can be used to divide the data set, and the ultimate goal of the decision tree node splitting is to make the nodes that fall on each branch node. The samples are in the same category to the greatest extent possible, which means that the node purity is higher.

**2.2.1. ID3 Algorithm.** Aiming at the problem of data purity after data mining classification, we introduce the concept of information entropy [23] to measure the data purity after classification. Its calculation formula is as follows:

$$H = - \sum_{k=1}^{|y|} p_k \log_2 p_k. \quad (14)$$

$H$  represents the information entropy  $D$ , and the smaller the calculated  $H$  value, the higher the purity of the information entropy.

In this article, we only quoted a part of the cart algorithm, and we used the Gini index algorithm to improve the other part. Compared with the original algorithm, the Gini index algorithm is simpler and faster. The original algorithm is added as follows:

$$\begin{aligned} R_1(j, s) &= \{x | x^j \leq s\}, \\ R_2(j, s) &= \{x | x^j > s\}, \end{aligned} \quad (15)$$

$$c_m = \frac{1}{N_m} \sum_{x_i \in R_m(j, s)} y^i, x \in R_m, m = \{1, 2\}.$$

It can be clearly seen that our use of the Gini index algorithm is indeed more concise.

The ID3 algorithm quoted here conforms to the data gain criterion. The so-called data gain is the positive change in the original data and the classified data after the data are classified, and the gain of an indicator after the data classification is the data set. Under this condition,  $D$  represents the difference between the information entropy and the empirical conditional entropy:

$$H(D, a) = H - \sum_{v=1}^v \frac{|D^v|}{|D|} H(D^v). \quad (16)$$

### 3. Algorithm Improvement

In summary, we have made a preliminary framework for the big data technology algorithm, but there may still be deficiencies or loopholes. Next, we will optimize and improve our artificial intelligence counting algorithm to improve the computing power and accuracy of the algorithm.

**3.1. Logistic Regression Model Algorithm Optimization.** In the logistic regression algorithm, it is not excluded that the last derivative is 0. In this case, we cannot solve  $w$ , and we need to use the gradient iterative optimization algorithm to optimize the algorithm. The combination of stochastic gradient descent and batch gradient descent can help us solve the above problems by taking the derivation of the objective function.

Here, we use the batch gradient descent method to find the partial derivative of  $w$  and obtain the gradient corresponding to each  $w$ . The calculation formula is as follows:

$$\frac{\partial l(w)}{\partial w_j} = -\frac{1}{m} (y^i - h_w(x^i)) x_j^i. \quad (17)$$

Since we need to minimize the risk function, we need to update  $w$  in the negative direction of  $w$ . The calculation formula is as follows:

$$w_j^* = w_j + \frac{1}{m} (y^i - h_w(x^i)) x_j^i. \quad (18)$$

By calculating the formula, we will finally get a comprehensive optimal solution, but every change in  $w$  requires all the training data. If the data are too large, it will greatly affect the speed of  $w$  change, so we use random combined with the gradient descent method, and the calculation formula is as follows:

$$\begin{aligned} l(w) &= \frac{1}{2m} \sum_{i=1}^m (y^i - h_w(x^i))^2 \\ &= \frac{1}{m} \sum_{i=0}^m \cos t(w, (x^i, y^i)), \end{aligned} \quad (19)$$

$$\cos t(w, (x^i, y^i)) = \frac{1}{2} (y^i - h_w(x^i))^2.$$

Through the loss function of each sample, the partial derivative of  $w$  is obtained to obtain the corresponding gradient, and then,  $w$  is updated.

$$w_j^* = w_j + (y^i - h_w(x^i)) x_j^i. \quad (20)$$

**3.2. Improvement of Naive Bayes Algorithm.** Among the three classification algorithms based on the naive Bayes algorithm, the best classification effect is the multinomial

naive Bayes algorithm classification model, but the disadvantage is that the algorithm automatically defaults to the same weight of all features and ignores the features of each data. To a certain extent, it will reduce the accuracy of our data classification. Therefore, we need to combine other algorithms for related optimization. Here, we introduce the TD-IDF algorithm and improve and optimize the original algorithm before applying it to the data processing module.

The improved TDF-IDF-LD is combined into a multinomial naive Bayesian algorithm to obtain the final formula.

$$C_x = \arg \max_{k \in \{1,2,\dots,k\}} \left( \frac{m_k}{m} \prod_{j=1}^n \frac{m_{kjs} + \lambda}{m_k + s_j \lambda} \right) \quad (21)$$

$$* TF * IDF * LF * DTF.$$

**3.3. Improvement of Decision Tree Model Algorithm.** The main idea of the ID3 algorithm is a top-down greedy strategy from the root node to the leaf node. First, the information gain of each feature is calculated according to the above formula, and finally, the feature with the largest information gain is selected as the node of the decision tree. Splitting further improves the purity of the child nodes of the decision tree, and the ability to divide samples into corresponding categories is stronger, and the representativeness of such features is stronger. However, the shortcomings of ID3 are also obvious. The algorithm has a preference for attributes with a large number of values. The decision tree created only by the ID3 algorithm obviously cannot achieve the expected effect for unknown data. At this time, we use the C4.5 algorithm for collaborative calculation, so that the decision tree we create is sufficiently convincing [24].

**3.3.1. C4.5 Algorithms.** In view of the limitations of the ID3 algorithm, to minimize the adverse effects of the ID3 algorithm, we use the C4.5 algorithm for collaborative calculation. The calculation formula is as follows:

$$H(D, a)_{\text{ratio}} = \frac{H(D, a)}{H(D)}. \quad (22)$$

**3.3.2. Classification and Regression Tree Algorithm.** Classification and regression trees are a type of decision tree and are very important. It can realize the generation of classification tree and regression tree at the same time. The CART algorithm we introduce here is a binary recursive segmentation technique. The internal node of the generated decision tree has only two branches and only two categories of yes or no. Even if a feature or attribute has multiple values, it is divided into two parts.

**Create a Classification Tree.** In the recursive process of creating the split tree, the CART algorithm selects the feature with the smallest Gini index in the current data set as the node to divide the decision tree. The Gini index is similar to

the information entropy and is usually used to measure the purity of the data set D. The calculation formula is as follows:

$$Gin(D) = 1 - \sum_{k=1}^{|y|} p_k^2. \quad (23)$$

The Gini index is obtained by calculation, and the purity is estimated by observing the value of the final calculation result of the index. The smaller the value, the higher the purity.

In the process of classifying data, the Gini index is calculated for the indicator a, and the formula is as follows:

$$Gini_{\text{index}(D,a)} = \sum_{v=1}^v \frac{|D^v|}{D} Gini(D^v). \quad (24)$$

#### Create a Regression Tree

The regression tree created by CART uses the principle of least mean square variance to determine the optimal division of the regression tree, so that our final data result prediction is closest to the true value. To avoid security vulnerabilities as much as possible, first of all, we need to understand which security vulnerabilities are most likely to cause security threats to the database. The first and most direct one is that the username and password in the database are too simple, which leads to some malicious hackers. It is easy to steal user information from our database, leading to security breaches, followed by unpatched databases, insufficient authentication, and other related issues. In response to these problems, we have targeted management personnel awareness, systems, and technical means and follow the basic threat prevention guidelines, but if only from a technical perspective, we will consider the use of monitoring (DMI) system, that is, so-called database auditing systems to circumvent security breaches. Assuming that the mean squared error is calculated for a feature, and the feature with the smallest error is found, it is theoretically the optimal splitting point. The squared error formula is as follows:

$$\sum_{x_i \in R_m} (y_i - f(x_i))^2. \quad (25)$$

## 4. Based on Artificial Intelligence Technology Algorithm Evaluation Experimental Test

Traditional physical education can no longer be satisfied. In the current educational environment, based on the technology of action bank, a multidimensional analysis of physical education is carried out. Traditional sports can only provide simple action guidance for human actions under the intuitive vision of the human body. However, in the artificial intelligence motion scene, it can store the data of the human body dynamic action accurately to the frame, score, and correct the accuracy of the dynamic action and can also match the corresponding data based on the stored dynamic action data. Sports carry out intuitive information analysis and make quality evaluation. A decision tree is a tree structure consisting of nodes and directed edges. Its essence is a set of causal rules. The decision tree model we introduced

in this article is a simple and easy-to-use nonparametric classifier that does not require any assumptions on the data. Now, with the technology of action bank, the experimental simulation of the existing sports actions is carried out to compare the improvement of the action bank model compared with the traditional physical education. Now, model experiments are conducted based on a certain action data, as shown in Table 1.

The above is a demonstration of the experimental data after the model simulation experiment. It can be seen that the error correction rate of the experimental dynamic data is still maintained at more than half. Now, the same example is artificially tested, and then, the obtained data are compared, as shown in Table 2 and Figure 2.

As shown in the table, it can be intuitively found that the traditional physical education is manual inspection, so the error detection, error correction, and effective error correction are all the same, but the effective error detection of the model is more than the manual error detection by 2. From this, it can be seen that manual error detection will still be more or less affected by factors such as environment, man-made, and force majeure, while the model will not be affected by so many factors, unless there is an error in the algorithm itself, the shortcomings of the model are reflected in the correction. The error rate may be due to the lack of control data. In the future experiments, the basic behavior will be stored and the database will be improved to achieve the optimal operation of the model. Downtime is a deadlock situation that is very likely to occur in computer computing, and the possibility of server database deadlock is not ruled out. For this, we have considered setting up a framework that includes alerts and monitoring. In the event of downtime, our alert monitoring framework can detect and diagnose problems in a timely manner, reducing the possibility of data loss.

**4.1. Performance Comparison before and after Model Optimization.** Now, an example action in an artificial intelligence action scene is collected. By comparing the resolution of the experiment, the consumption of recognition time, and the number of recognition errors, it can be concluded whether the optimization of the model has a substantial effect on the model.

**4.1.1. Identification Resolution Comparison.** Comparison of unit detection volume and resolution is shown in Table 3 and Figure 3.

It can be seen from the figure that the blue one is the primary model, and the orange one is the optimized model. It can be seen intuitively that the optimized model has a significantly improved resolution than the primary model. According to the table, it can be seen that in the resolution data there is also a significant improvement in accuracy.

**4.1.2. C4.5 Algorithm and ID3 Algorithm Test.** In the previous article, based on the ID3 algorithm introduced by data processing and purification, we further optimized it and

introduced the C4.5 algorithm. We compared the advantages brought by the improvement of this algorithm through a more direct experimental test. Taking a university as an example, we use two algorithms to calculate the university's investment in physical education and compare it with the actual situation and then compare the advantages and disadvantages of the two algorithms. The calculation results are shown in Table 4, and the visualization is shown in Figure 4.

According to the visualization in Figure 4, the data results obtained by our optimized C4.5 algorithm compared with the ID3 algorithm to purify the data are compared with the actual investment of the school. The optimized C4.5 algorithm is closer to the real situation of the experiment. The existing artificial technology has a relatively complete system, and combined with the experimental tests made in this article, the artificial intelligence algorithm has been able to process data more flexibly and build a more perfect evaluation system accordingly. Then, in the future development of artificial intelligence technology, the accuracy of data and the improvement of data processing speed are worthy of attention. It will bring more convenient and substantial help to the education industry.

**4.1.3. Time Consumption Comparison of Unit Detection Amount.** In the action scene of artificial intelligence, the time requirements for detection are relatively strict, and the general detection must ensure timeliness, so that the data obtained from the detection can be effectively used.

Comparison of time consumption per unit detection amount is shown in Table 5 and Figure 5.

The figure shows that the blue one is the primary model, and the orange one is the optimized model. It can be seen intuitively that the time consumption of the optimized model is shorter, and it can better meet the requirements of the experiment for timeliness.

**4.1.4. Comparison of the Number of Recognition Errors per Unit Detection Amount.** The detection of model performance can be intuitively analyzed by the number of errors in the number of experiments. By comparing the number of errors before and after the optimization of the experimental model, the performance of the model before and after optimization can be compared, as shown in Table 6 and Figure 6.

In the figure, the blue one is the primary model, and the orange one is the optimized model. It can be seen intuitively that after the model is optimized, the number of detection errors has dropped significantly, meeting the performance requirements of the experimental model.

To sum up, the performance of the optimized model is more in line with the inspection requirements, the resolution of the experiment is optimized, and the motion data obtained by the inspection can be stored more accurately. The reduction in the number of recognition errors is an essential improvement in the performance of the model.

TABLE 1: Experimental simulation data table.

Example	Action data storage (s)	Action error detection times	Action correction times	Error correction rate (%)	Satisfaction (%)
Run	162	36	23	63.8	80.6
Shoot	195	45	30	66.7	85.3
Ping pong swing	145	33	21	63.6	96.3
Badminton swing	207	56	31	55.3	84.2
Archery	105	22	15	56.9	89.5
Shoot the ball	150	51	25	54.7	93.6
Smash	167	24	35	48.6	85.2
Swing the sword	231	61	26	68.4	86.2
Dance	164	14	19	63.6	87.7
Softball swing	176	56	26	57.4	89.3

TABLE 2: Experimental data comparison table.

	Error detection times	Error correction times	Effective error correction	Error correction rate (%)
Traditional physical education	18	9	9	100
Action bank model	16	10	7	70

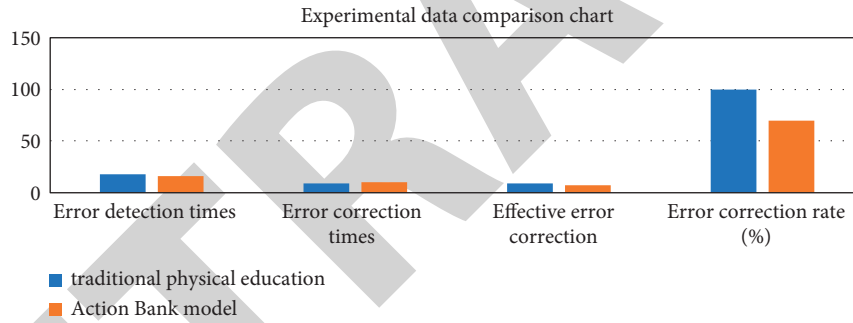


FIGURE 2: Experimental comparison diagram.

TABLE 3: Comparison of unit detection amount and resolution (%).

Teaching action	Primary model	Optimization model
Running action	69.2	70.56
Shooting action	79.3	82.01
Table tennis swing	85.2	87.21
Badminton swing	85.6	86.24
Archery	79.3	74.92
Shoot the ball	84.3	78.43
Smash	75.6	84.52
Swing the sword	73.9	89.32
Dance	87.5	79.15
Softball swing	89.6	76.34

**4.2. Performance Comparison before and after Model Optimization.** By introducing the mean shift detection method and the spatiotemporal action detection method, the action scenes of several cases are detected and analyzed, and the experimental models or algorithms are compared by comparing the resolution, time consumption, and number

of experimental errors of the experiments. Finally, it is concluded whether the performance of the action library model meets the detection requirements.

Now for the detection of the experimental resolution, based on the data collected and sorted out, the results are shown in Table 7 and Figure 7.

In the figure, the blue is the action bank model, the orange is the mean shift detection method, and the gray is the spatiotemporal action detection method. It can be seen intuitively from the figure that the blue line in the figure is the resolution data of the action bank model. Both are at the top of the datasheet, and it follows that the action bank model is superior to the other two models in terms of resolution.

The time consumption of the referenced model or algorithm is now tested to determine whether the timeliness of the model or algorithm meets the testing requirements. The testing data are shown in Table 8 and Figure 8.

In the figure, the blue one is the action bank model, the orange one is the mean shift detection method, and the gray one is the spatiotemporal action detection method. You can

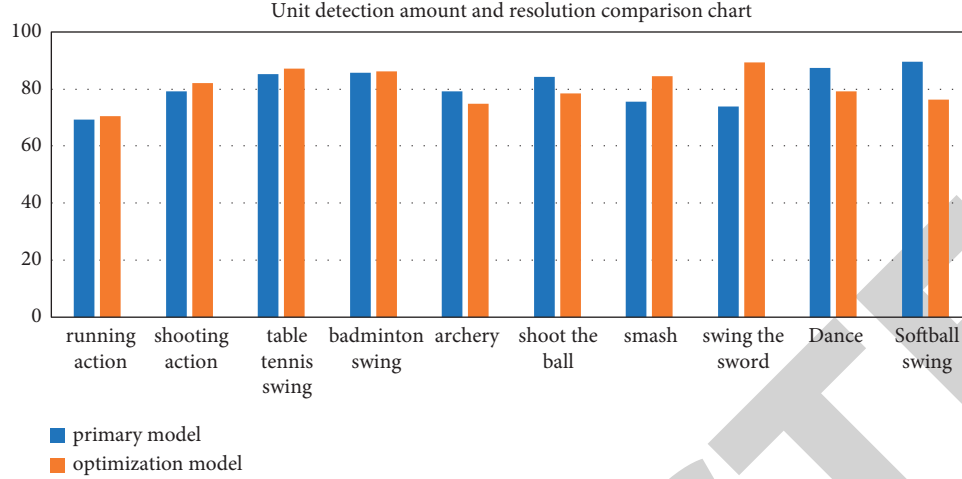


FIGURE 3: Comparison of bit detection amount and resolution.

TABLE 4: Comparison of the results of ID3 algorithm and C4.5 calculation of investment capital (unit: ten thousand yuan).

Algorithmic input	Hire a physical education teacher	Physical education equipment	Sports professional equipment	Sports e-books	Other
ID3 algorithm calculation input	22.3	72.2	88.7	11.4	7.8
C4.5 algorithmic computing input	21.9	74.8	90.6	10.1	7.5
Actual input	21.5	74.3	90.2	10.5	7.2

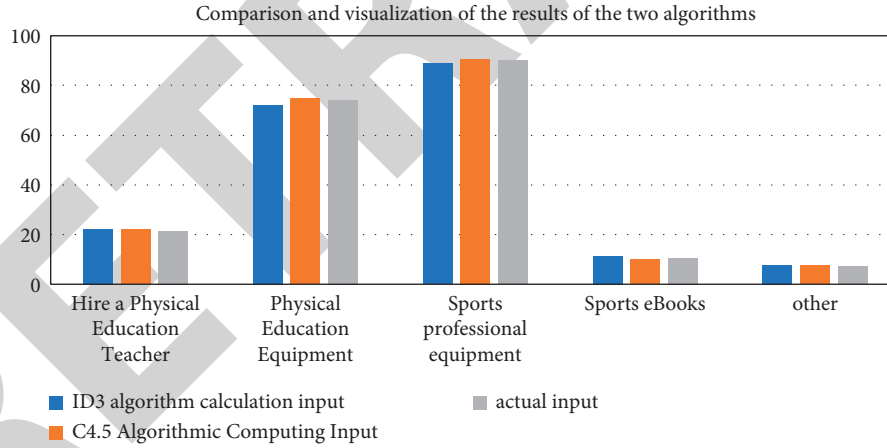


FIGURE 4: Comparison and visualization of the results of the two algorithms.

TABLE 5: Time consumption comparison of detection amount (unit: second).

Teaching action	Primary model	Optimization model
Running action	1.1	0.8
Shooting action	1.3	0.9
Table tennis swing	1.4	1
Badminton swing	1.3	0.8
Archery	1.5	0.7
Shoot the ball	1.2	0.6
Smash	1.7	1.3
Swing the sword	1.8	1.2
Dance	1.6	0.8
Softball swing	1.4	0.6

intuitively see the blue line; that is, the action bank model time consumption data is at the lowest end of the table. It can be concluded that the model is better than other models in terms of time consumption, but based on the consideration of timeliness, the time consumption of all models meets the requirements for timeliness.

To verify the accuracy of the experiment, we compare the performance, recall rate, accuracy rate, and F1 of the following three algorithms to reflect the matching degree of the three methods, as shown in Table 9 and Figure 9.

According to the data table and the comparison chart, the action bank model is better than the mean shift detection method and the spatiotemporal action detection method in

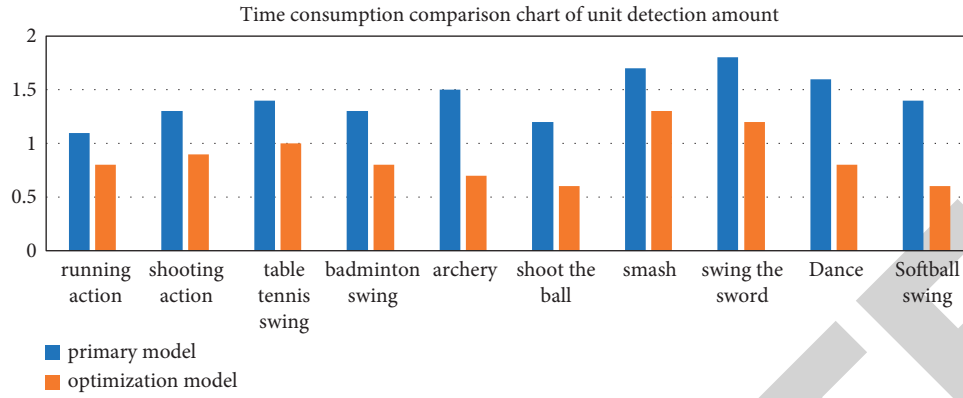


FIGURE 5: Time consumption comparison chart of detection amount.

TABLE 6: Comparison of the number of recognition errors per unit of detection.

Teaching action	Primary model	Optimization model
Running action	8	2
Shooting action	5	1
Table tennis swing	6	2
Badminton swing	12	5
Archery	7	4
Shoot the ball	11	6
Smash	9	2
Swing the sword	7	3
Dance	8	1
Softball swing	10	4

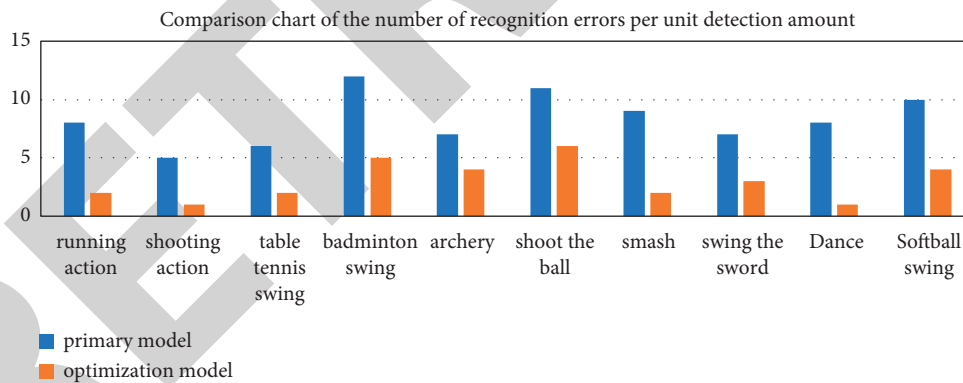


FIGURE 6: Comparison of the number of recognition errors per unit detection amount.

TABLE 7: Comparison table of resolution (%).

Teaching action	Action bank model	Mean shift detection method	Spatiotemporal motion detection
Running action	70.56	65.2	67.3
Shooting action	82.01	79.3	81.2
Table tennis swing	87.21	85.3	86.6
Badminton swing	86.24	83.3	84.3
Archery	86.43	75.6	79.4
Shoot the ball	85.43	84.2	78.6
Smash	89.46	76.3	85.2
Swing the sword	86.43	79.5	85.7
Dance	78.53	86.7	78.6
Softball swing	79.43	89.6	79.5



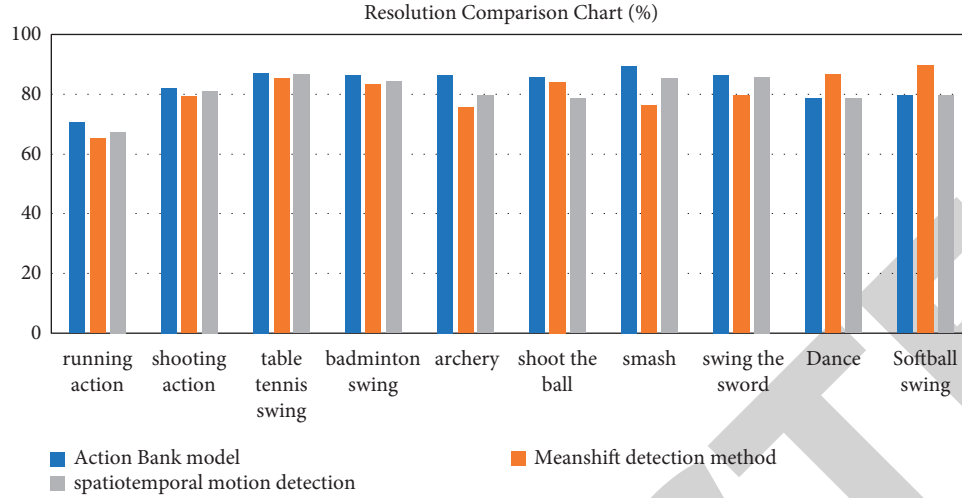


FIGURE 7: Comparison of resolutions.

TABLE 8: Comparison of test duration and consumption (unit: seconds).

Teaching action	Action bank model	Mean shift detection method	Spatiotemporal motion detection
Running action	0.8	1.1	1
Shooting action	0.9	1.3	1.1
Table tennis swing	1	1.5	1.3
Badminton swing	0.8	1.3	1.2
Archery	0.7	1.2	1.4
Shoot the ball	0.8	1.4	1.3
Smash	1.1	1.7	1.1
Swing the sword	1.4	1.3	1.5
Dance	0.9	1.1	1.4
Softball swing	0.7	1.4	1.2

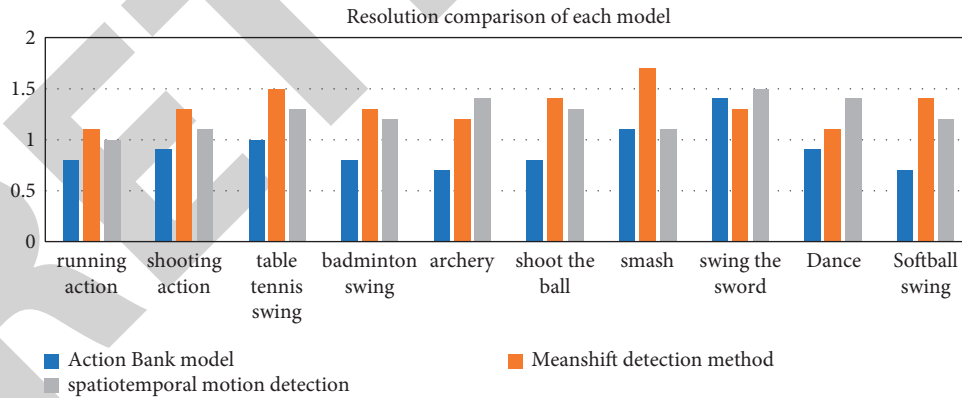


FIGURE 8: Comparison of time consumption for each model test.

all indicators. Therefore, it is trustworthy to use the action bank model as the detection algorithm.

**4.3. Quality Evaluation and Informatization Analysis.** Through the above data of error correction rate, number of errors, effective error correction, satisfaction, and other data, we can draw the following data as shown in Table 10 and Figure 10.

According to the above data, it can be seen that the satisfaction of various sports activities before the education reform is not as good as the satisfaction of various sports activities after the education reform. Based on this, we can draw the quality evaluation of physical education after the reform. According to the difference in satisfaction before and after the reform, we can draw the quality comparison before and after the reform. From the above data, it can be seen that the quality after the

TABLE 9: Data table of three methods on various indicators.

Performance	Action bank model	Mean shift detection method	Spatiotemporal motion detection
Recall	0.867	0.853	0.872
Accuracy	0.894	0.792	0.736
F1	0.874	0.857	0.785

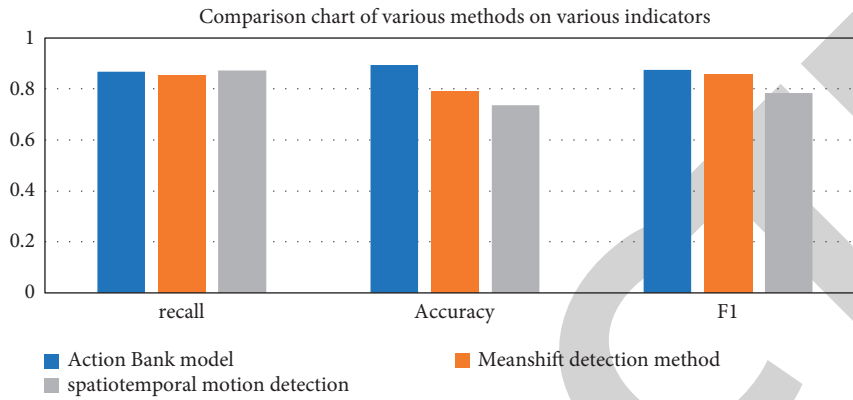


FIGURE 9: Comparison of various methods on various indicators.

TABLE 10: Satisfaction data table before and after physical education reform.

Teaching action	Satisfaction before education reform (%)	Satisfaction after education reform (%)
Running action	69.2	70.56
Shooting action	79.3	82.01
Table tennis swing	85.2	87.21
Badminton swing	85.6	86.24
Archery	79.3	74.92
Shoot the ball	84.3	78.43
Smash	75.6	84.52
Swing the sword	73.9	89.32
Dance	87.5	79.15
Softball swing	89.6	76.34

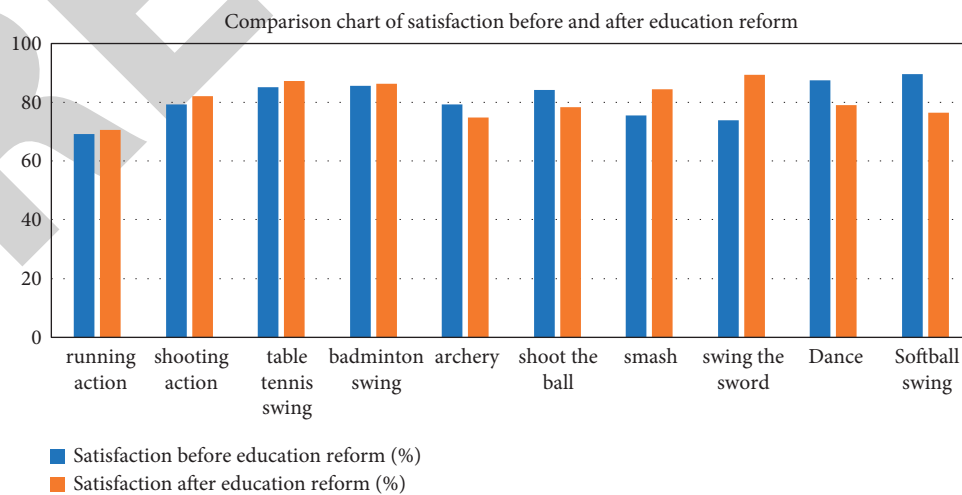


FIGURE 10: Comparison of satisfaction before and after the teaching reform.

education reform is generally higher than that before the education reform.

Information analysis can use the above action bank model, mean shift detection method, and spatiotemporal action detection method to perform information analysis on the data such as the resolution and detection duration of the pictures taken in physical education, which can ensure that the data we get are based on the correctness. The data and thus the resulting quality assessment can be convincing.

## 5. Conclusion

With the rapid development of artificial intelligence technology, there are many examples of artificial intelligence technology being applied to the education industry. It has gradually evolved into a major trend. After years of technical improvement and optimization, a large number of valuable teaching data in the artificial intelligence technology database have provided the theoretical basis and practical cases for data mining technology. The algorithm deduced based on artificial intelligence technology is introduced into the quality evaluation and informatization analysis of physical education teaching reform in this study. Compared with the traditional subjective assessment analysis and small sample sampling survey evaluation, its main advantage is reflected in data mining. Technical algorithms combine qualitative subjective events into the scope of mathematics to carry out rigorous quantitative analysis. In our simulation experiments, we mainly study the reasonable application of artificial intelligence technology algorithms to physical education teaching reform quality evaluation and information analysis test performance. If and only when we transform qualitative problems into quantitative problems under artificial intelligence technology, when there is a quantification of useless parameters for evaluation, we cleverly use the C4.5 algorithm to eliminate the useless parameters and ensure the parameters involved in evaluation and analysis. All of them have a strong correlation with the quality of physical education teaching reform, so that the evaluation results are more scientific and rigorous, close to the real situation. Then, through experimental simulation, the resolution, detection time consumption, and number of detection errors before and after the optimization of the model are compared experimentally, and experimental data are obtained, and it is concluded that the performance of the optimized model is significantly improved than that of the primary model. Meanshift detection method and spatiotemporal action detection method are compared in terms of resolution, detection time consumption, and detection error times of action library model; it is found that action bank model is superior in resolution and detection time consumption. Compared with the other two algorithms, it is weaker than the spatiotemporal detection method in terms of detecting errors. Based on the research on experimental data, this algorithm still meets the requirements of the detection performance for the experiment and also meets the requirements of the current environment. Trend development: to sum up, artificial intelligence technology is enough to provide substantial help to the evaluation and analysis

personnel in the quality evaluation of physical education teaching reform, and it also meets the requirements of the evaluation system for quantitative algorithms.

## Data Availability

The experimental data used to support the findings of this study are available from the corresponding author upon request.

## Conflicts of Interest

The authors declare that they have no conflicts of interest regarding this work.

## References

- [1] A. Ligeza, "Artificial intelligence: a modern approach," *Neurocomputing*, vol. 9, no. 2, pp. 215–218, 1995.
- [2] A. Ligeza, "Artificial intelligence: a modern approach," *Applied Mechanics and Materials*, vol. 263, no. 2, pp. 2829–2833, 2009.
- [3] N. J. Nilsson, "Artificial intelligence: a modern approach," *Applied Mechanics and Materials*, vol. 263, no. 5, pp. 2829–2833, 2003.
- [4] Z. Ghahramani, "Probabilistic machine learning and artificial intelligence," *Nature*, vol. 521, no. 7553, pp. 452–459, 2015.
- [5] D. J. Ward and D. J. C. MacKay, "Artificial intelligence: fast hands-free writing by gaze direction," *Nature*, vol. 418, no. 6900, p. 838, 2002.
- [6] M. Negnevitsky, "Artificial intelligence: a guide to intelligent systems," *Information & Computing Sciences*, vol. 48, no. 48, pp. 284–300, 2005.
- [7] T. Bench-Capon and P. E. Dunne, "Argumentation in artificial intelligence," *Artificial Intelligence*, vol. 171, no. 10–15, pp. 619–641, 2007.
- [8] A. Mellit, S. A. Kalogirou, L. Hontoria, and S. Shaari, "Artificial intelligence techniques for sizing photovoltaic systems: a review," *Renewable and Sustainable Energy Reviews*, vol. 13, no. 2, pp. 406–419, 2009.
- [9] M. D. Fethi and F. Pasiouras, "Assessing bank efficiency and performance with operational research and artificial intelligence techniques: a survey," *European Journal of Operational Research*, vol. 204, no. 2, pp. 189–198, 2010.
- [10] H. R. Nemati, D. M. Steiger, L. S. Iyer, and R. T. Herschel, "Knowledge warehouse: an architectural integration of knowledge management, decision support, artificial intelligence and data warehousing," *Decision Support Systems*, vol. 33, no. 2, pp. 143–161, 2002.
- [11] D. Hassabis, D. Kumaran, C. Summerfield, and M. Botvinick, "Neuroscience-inspired artificial intelligence," *Neuron*, vol. 95, no. 2, pp. 245–258, 2017.
- [12] C. Ramos, J. C. Augusto, and D. Shapiro, "Ambient intelligence—the next step for artificial intelligence," *IEEE Intelligent Systems*, vol. 23, no. 2, pp. 15–18, 2008.
- [13] M. Q. Raza and A. Khosravi, "A review on artificial intelligence based load demand forecasting techniques for smart grid and buildings," *Renewable and Sustainable Energy Reviews*, vol. 50, pp. 1352–1372, 2015.
- [14] J. Liebowitz, "Knowledge management and its link to artificial intelligence," *Expert Systems with Applications*, vol. 20, no. 1, pp. 1–6, 2001.

## *Retraction*

# **Retracted: Optimization and Evaluation of Oral English CAF Based on Artificial Intelligence and Corpus**

### **Security and Communication Networks**

Received 26 December 2023; Accepted 26 December 2023; Published 29 December 2023

Copyright © 2023 Security and Communication Networks. This is an open access article distributed under the Creative Commons Attribution License, which permits unrestricted use, distribution, and reproduction in any medium, provided the original work is properly cited.

This article has been retracted by Hindawi, as publisher, following an investigation undertaken by the publisher [1]. This investigation has uncovered evidence of systematic manipulation of the publication and peer-review process. We cannot, therefore, vouch for the reliability or integrity of this article.

Please note that this notice is intended solely to alert readers that the peer-review process of this article has been compromised.

Wiley and Hindawi regret that the usual quality checks did not identify these issues before publication and have since put additional measures in place to safeguard research integrity.

We wish to credit our Research Integrity and Research Publishing teams and anonymous and named external researchers and research integrity experts for contributing to this investigation.

The corresponding author, as the representative of all authors, has been given the opportunity to register their agreement or disagreement to this retraction. We have kept a record of any response received.

### **References**

- [1] Z. Wang, "Optimization and Evaluation of Oral English CAF Based on Artificial Intelligence and Corpus," *Security and Communication Networks*, vol. 2022, Article ID 4649643, 10 pages, 2022.

## Research Article

# Optimization and Evaluation of Oral English CAF Based on Artificial Intelligence and Corpus

Zhan Wang 

Foreign Language Department, Qinhuangdao Vocational and Technical College, Qinhuangdao 066100, China

Correspondence should be addressed to Zhan Wang; wangz@qvc.edu.cn

Received 1 July 2022; Revised 26 July 2022; Accepted 2 August 2022; Published 29 August 2022

Academic Editor: Hangjun Che

Copyright © 2022 Zhan Wang. This is an open access article distributed under the Creative Commons Attribution License, which permits unrestricted use, distribution, and reproduction in any medium, provided the original work is properly cited.

With the development of the times, the exchanges between countries are increasing. China is becoming a superpower, and the number of international cities is increasing. This requires the communication level of Chinese people to be improved. English, as the second largest communication language in China, should be better understood and studied. This paper makes an in-depth discussion on the optimization and evaluation of oral English CAF based on artificial intelligence and corpus and makes an experimental analysis. The results are as follows: (1) introducing oral English teaching based on artificial intelligence and oral English based on a corpus, so as to deepen the public's cognition of both and make oral English more deeply rooted in people's hearts and get attention. (2) Analyzing the algorithms of phoneme errors in spoken English. Errors in spoken English are very common. Algorithms can be used to identify them better. When evaluating spoken English, algorithms are needed to evaluate them more accurately. (3) There are many examples of the benefits of artificial intelligence to oral English teaching. By comparison, it is found that the method of evaluating using artificial intelligence is more accurate, a corpus can improve oral English, and CAF optimization is also of great help to oral English.

## 1. Introduction

The work of artificial intelligence is explained by defining intelligent agents and their functions in production systems, reaction agents, real-time conditional schedulers, neural networks, and theoretical decision systems. Proxy learning is interpreted as extending programmers' reach to unfamiliar environments and shows how this role restricts their design and promotes knowledge representation and clear thinking. Robotics and vision are only defined as elements to achieve goals [1]. The second volume of artificial intelligence manual focuses on improving artificial intelligence (AI) and its growing applications, including programming languages, CAI intelligent systems, and the application of AI in medicine, science and technology, and science and education. First of all, this book develops a programming language for artificial intelligence research and application-oriented artificial intelligence research. The discussion focuses on scientific applications, chemical applications, dependencies and assumptions, artificial intelligence, and the functionality of the

LISP programming language [2]. The work of artificial intelligence is explained by defining intelligent agents and their functions in production systems, reaction agents, real-time conditional planners, neural networks, and theoretical decision systems. Proxy learning is interpreted as extending the programmer's scope to unfamiliar environments and shows how the role limits his design to facilitate knowledge representation and clear thinking. Robotics and vision are only defined as elements to achieve goals. This book emphasizes the importance of the task environment, which is the decisive factor in correctly designing agents [3]. Almost all the literature on artificial intelligence is expressed in computer terms, full of complex matrix algebra and differential equations. Unlike many other books on computer intelligence, this shows that most ideas about intelligent systems are simple and clear. It is designed for lectures and for students with little computer skills, and readers do not need any prior knowledge related to programming language knowledge. The methods used in the book have been thoroughly tested in several courses led by the author. This paper introduces the field of

computational intelligence, including rule-based expert system, fuzzy expert system, framework expert system, artificial neural network, evolutionary computation, hybrid intelligent system, knowledge engineering, and data mining [4]. A new eyeliner/ancient phase method for measuring terms and concepts has been proposed. It combines the classification structure of words with the information of statistical database, so that it can analyze the computational evidence obtained from the data distribution of database, thus eliminating the old distance between nodes in the old space. Specifically, the proposed calculation is combined with the edge method in the edge calculation scheme and further expands from the node information calculation method. The keywords of public data collection similar to other computer models are tested [5]. Microblog has become a popular communication tool nowadays. Millions of users exchange views on different aspects of life every day. Therefore, Weibo website is a rich data source for opinion polls and emotional analysis. Since Weibo has only recently appeared, there are research articles specifically aimed at this topic. In our article, we will focus on using Twitter, the most popular microblogging platform, for emotional analysis tasks. We show how to automatically collect corpus for emotion analysis and investigation. We analyze the collected corpus and explain the phenomena found. Using a corpus, we construct an emotion classifier that can identify positive, negative, and neutral emotions in a document. Experimental evaluation shows that our proposed technology is more effective and has better performance than previous methods. In our study, we use English, but the proposed technique can be used in any other language [6]. As a medium of communication, English plays an important role in the world, which makes it more necessary to learn better spoken English. However, for many learners who learn English as a second language, speaking English seems to be more difficult than other English skills such as writing and reading. At the same time, independent college students in China have their own challenges in learning English in the first five minutes of each class [7]. Perplexed by uncertainties in learners' emotions, a survey was conducted to find out what other factors besides attitude, motivation, and language will affect language production. Causing a heated debate, the survey results lead to language barriers and lack of self-confidence. The author suggests that these can be enhanced by fuzzy learning, programmed learning, and personality matching. Finally, a flexible task system is proposed to maximize the impact of oral English teaching [8]. The purpose of this study is to find out the related factors that affect the implementation of oral English teaching assessment in rural middle schools. First, the purpose of this study is to determine the language evaluation level of schools according to the selected demographic factors. Secondly, the purpose of this study is to find out whether English teachers are familiar with the content, function, and application of oral English assessment in schools. Then, the purpose of this study is to determine the cognitive level of English teachers in schools. Then, this study further explores the relationship between oral assessment in the school environment and factors affecting

teachers' content, function, and consciousness [9]. In the current college teaching of English majors in China, it is common for many students to learn a lot of grammar knowledge and vocabulary, but they still cannot speak English accurately. Teaching methods have changed from paying attention to the grammatical structure of language to task-based teaching or communicative teaching. However, in these two approaches, fluency is the main goal of language teaching, while accuracy is often neglected. In recent years, corrective feedback has become a hot research topic in second language acquisition abroad because of its potential role in promoting oral English development [10]. This paper probes into the basic rules of oral English teaching from the perspectives of the connotation of communicative competence, the characteristics of oral communication and learners' willingness to communicate, and puts forward six suggestions on the reform of oral English teaching based on Chinese oral English and the modern teaching reality [11]. A skill is an activity aimed at improving oral fluency. This study investigates the effect of this skill on oral fluency and accuracy of 10 non-English majors. The main findings include the following: (1) compared with the former, the subjects can produce more fluent and accurate speech in the latter's conversation; (2) from the comparison of every two conversations, that is, the comparison of 4-minute conversation with 3-minute conversation, the comparison of 3-minute conversation with 2-minute conversation, and the comparison of 4-minute conversation with 2-minute conversation, the subjects showed the greatest progress from 4-minute conversation to 2-minute conversation, which indicated that the more opportunities for repetition, the more fluent and accurate the speech [12]. In the field of SLA, there are many research studies on the quality and condition of input and output, but there are few research studies on the influence of the input mode on oral output. In this experiment, the microgenetic method is used to study the influence of input methods on oral English. The results show that input patterns have different effects on oral production, and input and output frequencies play an important role in oral production. The research results are of great significance to the oral English teaching method and the measurement of oral English production [13]. In traditional English language teaching, summative assessment is widely adopted and accepted, but it is neither scientific nor reasonable. Language teaching and learning is a process, the result of which cannot be evaluated by one or two tests, especially formative assessment is a form of test that requires students to complete a task. This paper studies the significance, purpose, and principle of formative assessment and puts forward the mode and method of applying formative assessment in universities [14]. The study of corpus linguistics shows that, in actual communication, there are a large number of ready-made lexical chunks that constitute the core of the language structure. Based on the lexical approach, the present study aims to explore the effectiveness of lexical approach in improving students' oral English. The results show that teaching lexical chunks can improve students' communicative competence [15].



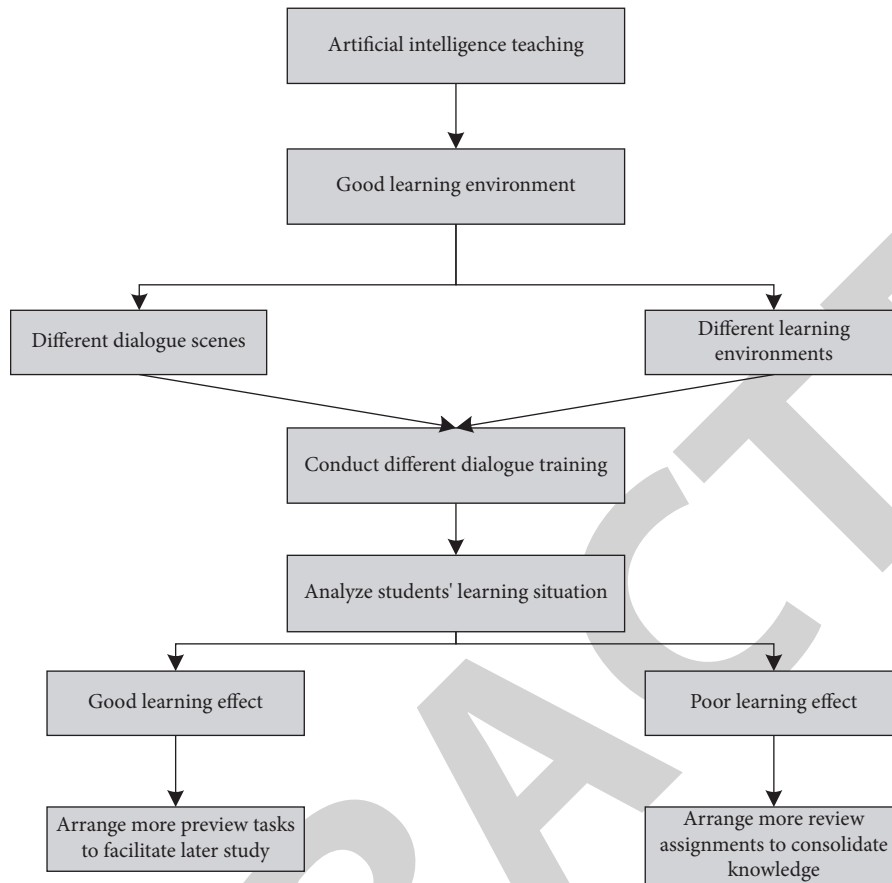


FIGURE 1: Teaching steps of learning oral English by artificial intelligence.

## 2. Artificial Intelligence and Spoken English in the Corpus

**2.1. Artificial Intelligence Robots Carry Out Oral English Teaching Activities.** As the most important part of learning English, oral English is an opportunity for students to use communicative tools skillfully. The level of oral expression will not only affect the learning effect cross-language communication, but also objectively reflect the development of students' ability to use English. In the traditional college English classroom teaching mode, teachers neglect the creation of context, students lack the opportunity to communicate, and students are ashamed to express their ambiguity. Using a language and a good environment, a robot starts a dialogue with students and creates a permanent language practice environment for them and has in-depth communication with students. At the same time, according to different dialogue scenes and different learning conditions, we should carry out different dialogue scenes, guide dialogue exercises, and analyze students' oral English communication and some hints on pronunciation and vocabulary to ensure the correct speech expression. After completing the dialogue exercise, the robot can simulate the teacher's role, summarize and evaluate the students' oral practice, and give targeted suggestions to the students. In teaching, the students' oral English level declines due to lack of practice. As an assistant in the communication activities between teachers and students,

teachers can understand students' oral ability more comprehensively and lay a good foundation for the future study. Set up practice tasks as the object of students' oral communication and provide students with various sentence patterns of oral exercises and suggestions for sentence adaptation. It is shown in Figure 1.

**2.2. Using the Artificial Intelligence Corpus to Innovate Teaching.** English teaching is the focus of teaching English and the beginning of students' learning English. In the era of rapid rise of artificial intelligence, various language platforms provide more targeted help for learners. First of all, in the teaching process, teachers will help students integrate educational resources. When students have a large amount of data, artificial intelligence can change many behaviors about learning. In addition, teachers can also sum up common words according to the vocabulary habits of each student in the system and add corresponding explanations in sentences to help students better understand the meaning of words and reduce their workload. Secondly, teachers will use intelligent technology to provide students with a better learning environment. Students are free to choose different passages and play English, which makes oral English more vivid and profound. After class, students can communicate in English. Students in daily life can scan English with their mobile phones.



**2.3. Classification of Corpus.** There are many types of corpus, and the main basis for determining the types is its research purpose and use, which can often be reflected in the principles and methods of corpus collection. Some classify corpus into four types: (1) heterogeneous: there is no specific principle for collecting corpus, and different corpus is collected and stored as it is; (2) homogeneity: only corpus with the same content type is collected; (3) systematicness: combining corpus according to predetermined principles and proportions, so that corpus is balanced and systematic and can present language facts in a given field; (4) specific: collect corpora for specific purposes only. It is shown in Figure 2.

### 3. Corpus-Based Spoken English Algorithms

**3.1. Error Determination Threshold.** Assuming that the difference between the score of the  $i$ th phoneme of the 40 phonemes of the selected TIMIT corpus language in sentence  $j$  of the TIMIT corpus language and the average pronunciation level  $\bar{p}_i$  of the phoneme is  $d_{ij}$ , the average difference between the phoneme score and the intermediate phoneme pronunciation in sentence  $j$  is

$$\bar{d}_{ij} = \frac{1}{C} \sum_{k=1}^C |p_{ij} - \bar{p}_i|, \quad (1)$$

where  $C$  is the ranking number of phoneme  $i$  in the  $j$ th sentence, thus obtaining the average difference  $D_i$  between phoneme  $i$  and the standard average level. The conclusion is that students make mistakes in pronunciation, so we can get

$$D_i = \frac{1}{M} \sum_{j=1}^M \bar{d}_{ij}, \quad (2)$$

where  $M$  is the number of TIMIT voice texts selected in actual application or experiment of the system. Formula (2) indicates that each phoneme has a corresponding threshold, which will change with the number of standard sounds provided by the scoring system. For this, we can calculate the error threshold to observe whether the pronunciation is standard or not.

$$th_i = D_i, \quad (3)$$

$$\hat{th} = \frac{1}{k} \sum_{i=1}^k D_i. \quad (4)$$

Equation (4) represents the default average overall threshold, which will be used in the following experiments, where  $k$  represents the number of phonemes.

**3.2. Phoneme Level Errors.** When detecting and judging phoneme level errors, we should first compare the difference between the learner's phoneme score  $p_i$  and the corresponding TIMIT standard speech phoneme score. Feedback judgment is given, and the formula is as follows:

$$d_i = |SP_i - ST_i|, \quad P = \begin{cases} \text{encourage,} & d_i \leq 50000, \\ \text{no suggestion,} & 50000 < d_i \leq th_i, \\ \text{suggestion,} & d_i > th_i. \end{cases} \quad (5)$$

**3.3. Continuous Evaluation.** Evaluate according to the pronunciation of spoken English. Let  $N_r$  represent the number of parts of the training set that are labeled as linked according to the uninterrupted rule and belong to different linked groups.  $N_m$  represents the number of speakers in the training set who belong to different continuous reading lengths after being labeled artificially.  $R$  stands for the linking pronunciation rate and is defined as

$$r = \frac{N_m}{N_r}. \quad (6)$$

In order to improve the reliability of the evaluation, some measures are introduced: correct recognition rate  $c$ , wrong recognition rate  $e$ , and missing rate  $\gamma$ , which are defined as follows:

$$\begin{aligned} c &= \frac{N_{\text{right}}}{(N_{\text{right}} + N_{\text{error}})}, \\ e &= \frac{N_{\text{error}}}{(N_{\text{right}} + N_{\text{error}})}, \\ \gamma &= 1 - \left( \frac{N_{\text{missed}}}{(N_{\text{right}} + N_{\text{error}} + N_{\text{missed}})} \right). \end{aligned} \quad (7)$$

The meaning of letters in the formula:  $N_{\text{right}}$  is the number of links marked by both manual and automatic linking systems in the training corpus;  $N_{\text{error}}$  is the number of training corpus labeled as linking by automatic linking labeling system but not manually labeled as linking;  $N_{\text{missed}}$  is manually labeled as linked, but the automatic linked labeling system does not recognize the number of linked. Through these three formulas, we can also calculate the measures in the corpus.

According to the hypothesis of linking category dependence, we use the same training corpus to count the three measures mentioned above.

When testing and evaluating spoken English, the practical significance of ambiguity measure is that pronunciation examples belong to or are better than different scoring levels (excellent or good), and the formula is as follows:

Fuzzy measure of "belonging to or better than good."

$$\mu(A) = \begin{cases} 0.0, & |A| = 0, \\ \left[ 1 + \left( \frac{|A| - \alpha}{\beta} \right)^{-2} \right]^{-1}, & 1 \leq |A| \leq L. \end{cases} \quad (8)$$

Fuzzy measure of "degree of superiority."

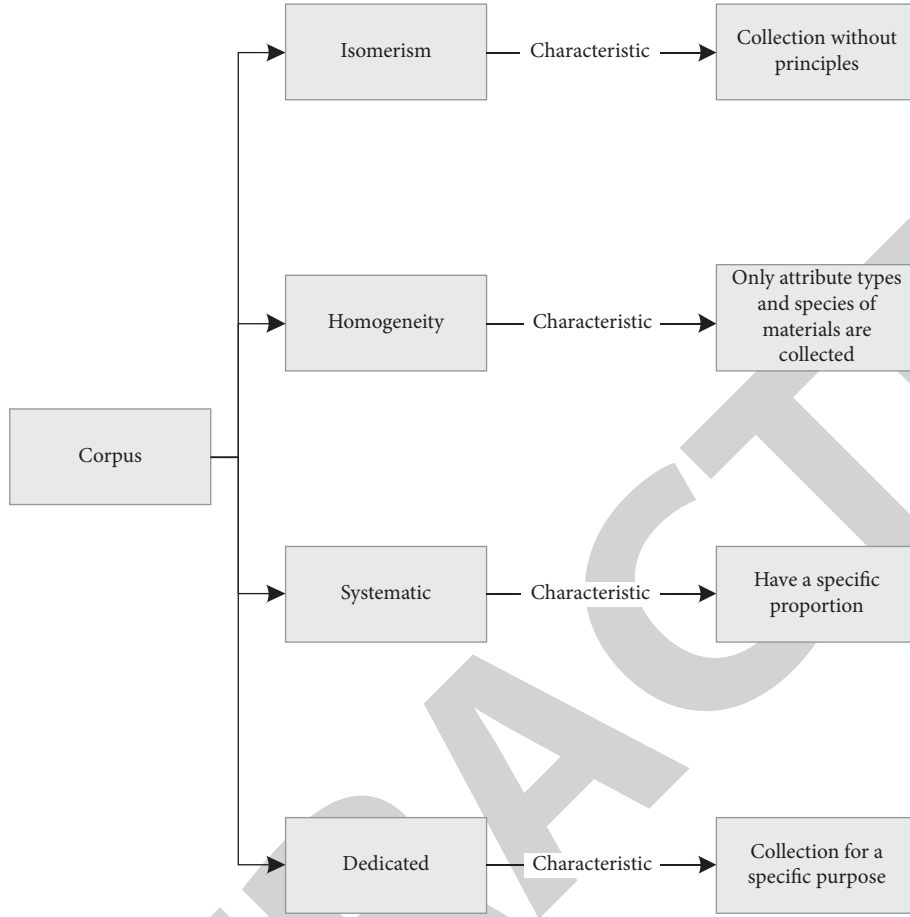


FIGURE 2: Corpus classification and characteristics.

$$\mu(A) = \begin{cases} e^{-((|A|-c)^2/2\lambda^2)}, & 1 \leq |A| \leq c, \\ 1.0, & c \leq |A| \leq L \text{ or } L < |A|. \end{cases} \quad (9)$$

For continuous evaluation, we also need to pay attention to two independent situations:

- (1) When a link is recognized by the system, the reliability of the link is defined as

$$f(x) = c[\text{Cat}(x)]. \quad (10)$$

- (2) When a link is missed by the system, the probability that the link is actually pronounced by the practitioner depends on  $\sim\gamma$ . Therefore, in this case, its reliability is defined as

$$f(x) = \sim\gamma[\text{Cat}(x)] = 1 - \gamma[\text{Cat}(x)]. \quad (11)$$

**3.4. Corpus Analysis.** Corpus is a multilanguage database, which contains a variety of information. When we need to find this information accurately in order to obtain the required data, in this paper, we study the algorithm of finding data in corpus.

Assuming that  $A$  and  $B$  are randomly assigned words in the corpus, the total oscillation amplitude of the corpus is  $W$ ,  $S$  is the period, and the actual observation frequencies are  $F(A)$  and  $F(B)$ ; the mutual information value is calculated as follows:

$$I(a, b) = \log_2 \frac{P(a, b)}{P(a) \cdot P(b) \cdot 2S} = \log_2 \frac{F(a, b) \cdot W}{F(a) \cdot F(b) \cdot 2S}. \quad (12)$$

$F(A)$  is the observation frequency of word-controlled structure,  $F(B)$  is the observation frequency of word-controlled structure, and  $F(A, B)$  is the speech dual frequency of two parts, and its value can be calculated in the following formula:

$$I(a, b) = \log_2 \frac{W \cdot F(a, b)}{F(a) \cdot F(b)}. \quad (13)$$

If the total size of the corpus is  $W$  and the frequency of observation of a certain collocation word in the corpus is  $C1$ , the average frequency of occurrence of the collocation word in each word position is calculated as  $C1/W$ . 1 is the lexical position occupied by node words, but this paper can calculate for lexical chunks and similar sentence patterns, so the lexical position may not be 1 in the design. However, when considering the co-occurrence probability of a node word with the observation frequency of  $N$ , the probability  $P$  is calculated as follows:

TABLE 1: The influence of CAF triplet on English learning.

CAF triplet	First-class index	Secondary index
Complicated vocabulary and sentence patterns	Complicated vocabulary Syntactic complexity	Form-symbol ratio, vocabulary frequency change rate Sentence length, subordinate sentence ratio
Oral accuracy	Error ratio Speed Pause	Pronunciation error ratio, word error ratio Speech speed, pronunciation speed, and phonation time ratio Pause frequency, pause duration
Oral fluency	Repetition Self-modification Hesitate	Repeated superposition, paragraph chunk Modification times, modification bands Frequency and length of hesitation

$$P = \frac{C_1 \cdot (2S + 1)}{W} \cdot \frac{N}{W}. \quad (14)$$

The expected frequency of co-occurrence of collocation words is as follows:

$$SD = \sqrt{(2S + 1) \cdot N \cdot \left(1 - \frac{C_1}{W}\right) \cdot \frac{C_1}{W}}. \quad (15)$$

The standard deviation of collocation distribution is as follows:

$$E = \frac{C_1 \cdot (2S + 1) \cdot N}{W}. \quad (16)$$

The Z value is as follows:

$$Z = \frac{C_2 - E}{SD}. \quad (17)$$

#### 4. Research on Oral English Optimization and Evaluation

**4.1. The Influence of CAF on Oral English.** At present, CAF is an important standard for testing foreign language output. When developing CAF, we have grasped the test level and error analysis. CAF is an important and interesting research topic in oral English output and English language development and has many influences on oral English and English learning. According to our investigation, the influence of CAF on English learning is shown in Table 1.

The effects of CAF on English learning and oral English are as follows: complexity and accuracy (writing, dictation, reading, shorthand, etc.); complexity and fluency (speaking, reading aloud, pause, dictation, etc.); and accuracy and fluency (speaking, interpreting, reading, visual translation, etc.). Its influence on it is shown in the table. From the first index, it has influence on lexical complexity, syntactic complexity, error ratio, speed, pause, and repetition of oral English. From the second index, each first index corresponds to the corresponding second index, which is also the key to the influence of CAF on oral English. In this regard, we have made a survey on the influence of CAF on oral English. By comparing the oral English level before applying CAF optimization with the scores before and after using CAF (out of one point in all aspects), we can get the comparison as shown in Figure 3.

Figure 3 introduces the comparison of scores in various aspects of oral English before and after using CAF. Whether

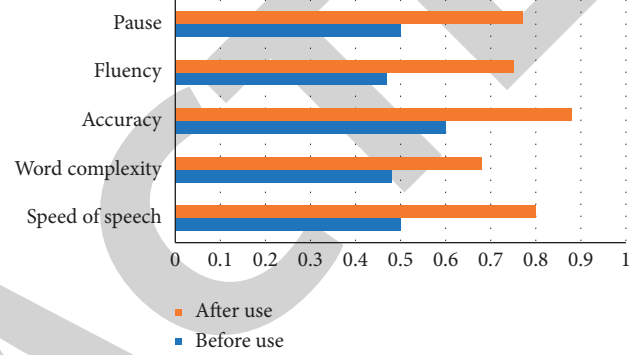


FIGURE 3: Comparison of scores in various aspects of oral English before and after using CAF.

CAF is helpful to oral English learning needs experimental comparison. We mainly compare five aspects: speed, word complexity, accuracy, fluency, and pause. The scores in five aspects are higher after using CAF than before using CAF. I have a better understanding of oral English in the next study of this paper.

From the figure, we can see that, after using CAF optimization, the oral English score has obviously increased a lot compared with that before using CAF, and the accuracy has increased to 0.88, which is the highest score. The score before using CAF is also the highest before using all the data, and the lowest score after using CAF optimization is also 0.68 of the word accuracy. From the figure, we can see that CAF optimization is positive for the adjustment of oral English, and it is of great help to oral English.

**4.2. Research on the Influence of Artificial Intelligence on Oral English Learning Evaluation.** The general trend is to introduce artificial intelligence into English teaching. Artificial intelligence is actually a science that simulates human intelligence by computer. With the rapid development of the information age, the development of computer technology also affects the progress of society. The use of artificial intelligence is actually what they are most interested in. Intellectual property rights have changed people's production and living habits and played an irreplaceable role in education and teaching. There is no doubt about the importance of language as a basic tool for human communication. Artificial intelligence technology, speech processing, machine translation, and speech recognition are inseparable

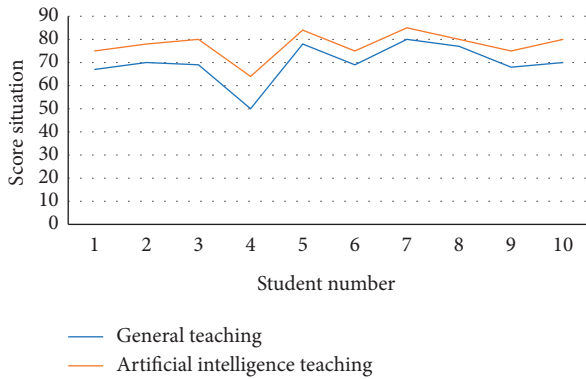


FIGURE 4: Comparison of students' scores in two teaching methods.

from human language learning. Therefore, it is meaningful to use artificial intelligence technology to learn and develop human language. English is the second language in China, and lack of English communication ability is a difficult problem in personnel training in every school stage, and the influence of English teaching in primary schools is ignored. It is an academic topic discussed by experts and scholars, and it is also a difficult problem for teachers, parents, and students. To sum up, the practical application of artificial intelligence technology should be increased in intermediate English teaching, and the revolutionary power provided by artificial intelligence technology will affect the practice of intermediate English teaching. In oral English learning, artificial intelligence products have rich language resources and many functions such as reading samples, student guidance, student repetition, reading aloud, and pronunciation correction. The purpose of developing artificial intelligence products is to enable students to master correct pronunciation in a short time, so as to achieve a higher English level. The software can classify and arrange the existing oral resources, set different levels, and then start testing students and provide corresponding learning resources according to the students' oral test results. In this regard, we put a group of students in different learning environments to study for a period of time. The teaching content and teaching time are the same, but the teaching methods are different. After studying for a period of time, we compare the learning situation and the score distribution as shown in the figure.

Figure 4 shows the results of ten students in two learning environments. In a normal learning environment, their academic performance is not as good as that in the AI learning environment. The highest score for AI is 85. The lowest score is only 80 points in the normal learning environment, and the lowest score is only 50 points. At present, the oral English test mainly includes self-introduction, reading articles, situational questions, listening to essays, and answering questions. It can be seen that the main problems we encounter when implementing smart assessment are speech recognition and content understanding. In order to be evaluated automatically, it must be completed from two angles: oral presentation and reviewer's content. When evaluating expressions, we should first capture the paragraphs of the speech tester and then analyze the

captured contents to obtain features and comprehensively evaluate them from the aspects of sound quality, color, and pitch and finally summarize a reasonable single result to get the result. For example, the content of self-statement must be verified, and the scoring principle is more complex. It is necessary for the scoring system to use natural language processing, collect multiple sets of data for averaging processing, and obtain the comparison of the scoring accuracy between artificial intelligence evaluation and ordinary evaluation in timbre, tone, sound quality, and self-introduction as shown in Figure 5.

Figure 5 is mainly through the comparison of two evaluation methods. In the evaluation and comparison, we should pay attention to accuracy. In the general evaluation, human emotional factors account for a larger impact. At this time, we need to use the evaluation method of artificial intelligence to make a fair evaluation. The evaluation of artificial intelligence is based on the set scoring standard, which is more scientific. Through Figure 3, we can also get that the evaluation accuracy of artificial intelligence is higher than that of ordinary evaluation methods. This paper can better study the evaluation of oral English.

According to Figure 5, we know that the accuracy of artificial intelligence evaluation is higher than that of ordinary evaluation in the most important aspects of evaluation. The accuracy of ordinary evaluation in timbre is 0.6, and that of artificial intelligence evaluation is 0.86; the general evaluation of sound quality is 0.67, and the artificial intelligence is 0.89; the general evaluation of tone is 0.78, and the artificial intelligence evaluation is 0.95; in self-introduction, the accuracy of general evaluation score is 0.56, and artificial intelligence is 0.85. From the above data, it can be shown that the artificial intelligence evaluation method is better than the ordinary evaluation in oral English.

**4.3. A Corpus-Based Study of Oral English.** There are a lot of data in the corpus, and spoken English is a very common language, which needs a lot of vocabulary and sentence patterns. At this time, the knowledge support in corpus is very needed, but it is inconvenient to find too much data. Therefore, according to the word list, Nation (2001) divides words into four groups. The first two groups are 2,000 high-frequency words. The third group is academic vocabulary, which is mainly used in a written form. The fourth group is low-frequency words commonly found in written and spoken styles. Table 2 is obtained by investigating the vocabulary in the corpus.

The figures in Table 2 show that the first two types of high-frequency words account for the majority of Chinese students, among which the coverage rate of the first type is 82.14%, and the minimum incidence rate of academic words is 4.89%. With the investigation, it is found that the distribution of high-frequency words in different corpora is as follows.

Table 3 shows that there are many high-frequency words distributed in the corpus in different environments. In order to find the required information and words quickly, we conducted a survey on the vocabulary used by various



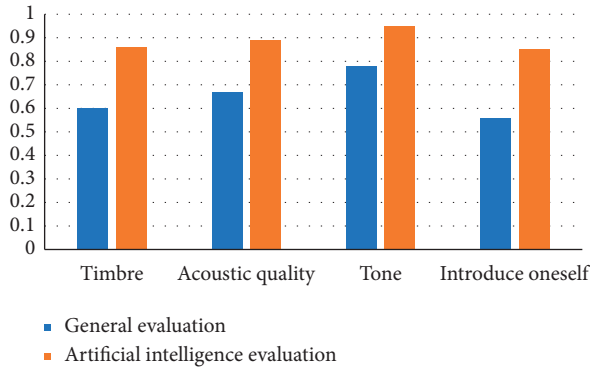


FIGURE 5: Comparison of scoring accuracy between two evaluation methods.

TABLE 2: Distribution of high-frequency words in HVC.

Vocabulary	Quantity
The first category	19,926
Category II	1543
Academic category	1186
Low frequency use	1603
All	24258

TABLE 3: Distribution of high-frequency words in different environments.

Vocabulary	HVC (%)	Local spoken English (%)	Local English writing (%)
High-frequency words	88.5	85	80
Academic category	4.89	5	10
Low-frequency words	6.61	10	10

groups of people in oral English. In the HVC corpus, high-frequency words account for 88.5%, academic words account for 4.89%, and low-frequency words account for 6.61%. In the local spoken language, high-frequency words account for 85%, academic words account for 5%, and low-frequency words account for 10%. In spoken English, locals use lower high-frequency words than Chinese people, and academic and low-frequency words are higher than Chinese people. Locals are more familiar with oral English.

The distribution of high-frequency words in the corpus is shown in Table 3. In foreign environments, the proportion of high-frequency words in spoken language is lower than that in China, but higher in the other two items, which also shows that local people are relatively more accustomed to using low-frequency and academic words. We have also investigated the benefits of corpus for oral English, such as providing words for oral English better and making oral English more fluent. The public's percentage of the benefits of corpus is as follows:

According to Figure 6, it can be seen that, in the eyes of the public, the benefits of the corpus for oral English mainly

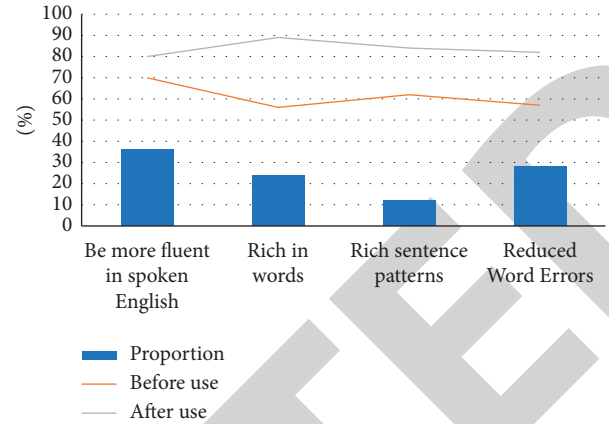


FIGURE 6: Comparison of the benefits of corpus to English compared with the situation after using corpus.

includes the following four aspects: more fluent oral English accounts for 36% at most, rich words account for 24%, rich sentence patterns account for 12%, and reduced word errors account for 28%. The comparison between before and after the use of the corpus also shows that the oral English scores have risen greatly after the use of the corpus.

**4.4. Influence of External and Self on Oral English.** Besides oral English, external influences are also important. In education, students have less time to practice speaking English. Most students have no way to communicate with foreigners, and of course, there is no environment to communicate in English. The only English communication takes place is in class, and there is no atmosphere conducive to communication after returning home. In today's quality education, testing is still the main means to measure and evaluate students. To pass the exam, you need to master grammar, vocabulary, reading, and writing skills, but students miss the opportunity of oral communication training in class. Many teachers insist that mastering grammar, vocabulary, and sentence structure are the only way to get good test scores, but ignore listening and speaking. Teachers have different language abilities. Senior high school exams have relatively low requirements for senior high school students' oral English, which leads to the decline of many middle school teachers' oral English ability. Daily oral communication mainly takes place in the classroom, which is limited to the classroom, that is to say, teachers' oral games also have certain limitations. Finally, teachers' oral level affects the development of students' oral ability. Students themselves have many emotional changes when learning oral English because oral English is not a rigid study but to communicate with others, and personality has a great influence on it. We conducted a survey on people with poor oral English and found out their differences in personality and their influence on oral English, as shown in Figure 7.

Figure 7 shows several states that affect spoken English, such as shyness, indifference, conformity, and inferiority complex. For the study of oral English, these psychology will affect its exertion. At present, the most serious influence on

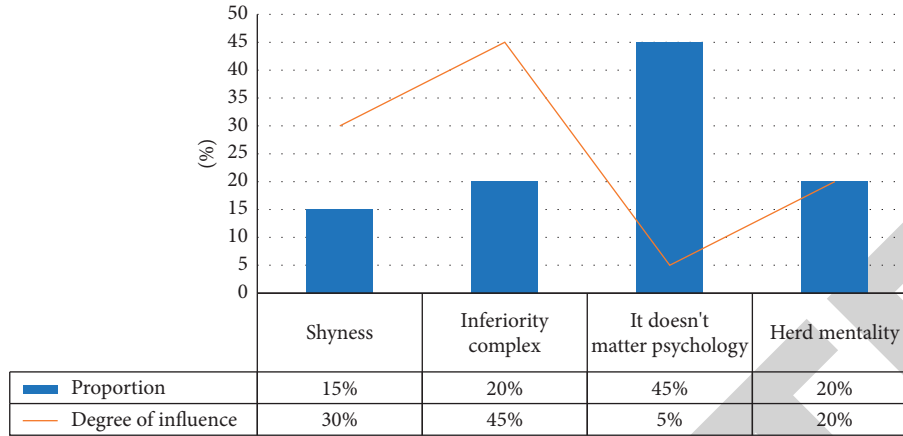


FIGURE 7: Psychological proportion and influence degree of losers in oral English learning.

spoken English is inferiority complex. For inferiority complex, their self-confidence is frustrated and they dare not to speak and communicate. For oral English, the most important thing is to use it frequently, as practice makes a person perfect. Inferiority complex cannot be changed for a while and needs long-term treatment, so it has the greatest impact on oral English.

For psychological differences as shown in Figure 7, the unsuccessful psychology of learning oral English mainly includes the following four aspects: shyness exists in many beginners, such as shy girls and introverted boys. These colleagues are nervous, stuttering, quiet, and vague when communicating. They are always afraid of laughing at themselves when they say the wrong thing. Sometimes they blush and bow their heads, especially some students from rural families. Accounting for 15%, the reason for inferiority complex is weak cognitive ability. Some students have this inferiority complex even if they fail for the first time, while other students stutter. Ambiguous voice, clumsy pronunciation, and answers full of sick sentences have long been unmatched by others. These people account for 20%, and their psychology does not matter. Students with this psychology often think that their grades are not applicable to themselves, and whether they can say it does not matter. It is enough to know words, write and spell, and whether they can say it does not matter. Such people account for 45% at most. Herd mentality: this kind of psychology thinks that many people cannot speak English, everyone does not learn it, and they do not have to learn it themselves, which accounts for 20%.

**4.5. Comparison of Comprehensive Oral English Fluency.** We have studied above the influence of CAF optimization, artificial intelligence, and corpus on oral English, all of which have positive effects on oral English. We have conducted below mixed experiments to observe the comparison of these items on oral English fluency and the comparison when they are mixed.

According to Figure 8, we can see that the fluency scores of oral English are different under various methods. The

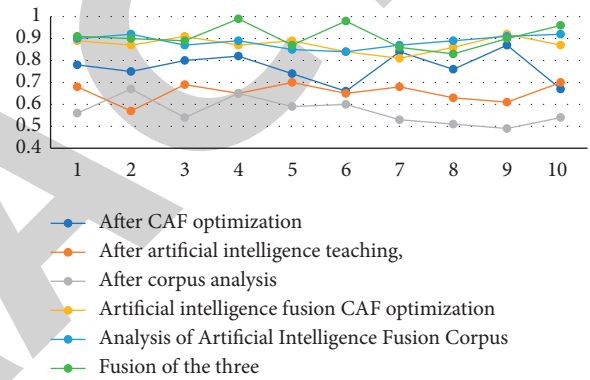


FIGURE 8: Scoring of oral English fluency by various methods.

single method is far worse than the hybrid method. When using corpus analysis and artificial intelligence alone, the average fluency score is only about 0.65, and when using the combination of the three, the average fluency score reaches 0.94.

## 5. Conclusion

This paper makes an in-depth analysis of the optimization and evaluation of oral English CAF based on artificial intelligence and corpus. As the society moves towards internationalization, oral English becomes more and more important. It is necessary to study oral English by combining artificial intelligence, corpus, and CAF, but their roles in oral English are not exactly the same. This paper introduces this, and the oral English combined by several is fully explained. This paper introduces the algorithm of evaluating and determining accuracy in spoken English and introduces its definition, so that readers can fully understand the importance of spoken English and the research in artificial intelligence corpus.

## Data Availability

The experimental data used to support the findings of this study are available from the author upon request.

## Retraction

# Retracted: Enterprise Credit Security Prediction and Evaluation Based on Multimodel Fusion

### Security and Communication Networks

Received 8 January 2024; Accepted 8 January 2024; Published 9 January 2024

Copyright © 2024 Security and Communication Networks. This is an open access article distributed under the Creative Commons Attribution License, which permits unrestricted use, distribution, and reproduction in any medium, provided the original work is properly cited.

This article has been retracted by Hindawi following an investigation undertaken by the publisher [1]. This investigation has uncovered evidence of one or more of the following indicators of systematic manipulation of the publication process:

- (1) Discrepancies in scope
- (2) Discrepancies in the description of the research reported
- (3) Discrepancies between the availability of data and the research described
- (4) Inappropriate citations
- (5) Incoherent, meaningless and/or irrelevant content included in the article
- (6) Manipulated or compromised peer review

The presence of these indicators undermines our confidence in the integrity of the article's content and we cannot, therefore, vouch for its reliability. Please note that this notice is intended solely to alert readers that the content of this article is unreliable. We have not investigated whether authors were aware of or involved in the systematic manipulation of the publication process.

Wiley and Hindawi regrets that the usual quality checks did not identify these issues before publication and have since put additional measures in place to safeguard research integrity.

We wish to credit our own Research Integrity and Research Publishing teams and anonymous and named external researchers and research integrity experts for contributing to this investigation.

The corresponding author, as the representative of all authors, has been given the opportunity to register their agreement or disagreement to this retraction. We have kept a record of any response received.

### References

- [1] L. Zhang, J. He, and Z. Zhao, "Enterprise Credit Security Prediction and Evaluation Based on Multimodel Fusion," *Security and Communication Networks*, vol. 2022, Article ID 2754302, 12 pages, 2022.



## Research Article

# Enterprise Credit Security Prediction and Evaluation Based on Multimodel Fusion

Lei Zhang <sup>1,2</sup>, Jie He <sup>2</sup>, and Zihao Zhao <sup>2</sup>

<sup>1</sup>School of Economics and Management, Chongqing Jiaotong University, Chongqing 400074, China

<sup>2</sup>School of Mathematics and Statistics, Chongqing Jiaotong University, Chongqing 400074, China

Correspondence should be addressed to Lei Zhang; zhangleicqjtu@163.com

Received 13 April 2022; Revised 23 July 2022; Accepted 29 July 2022; Published 29 August 2022

Academic Editor: Yuchuan Luo

Copyright © 2022 Lei Zhang et al. This is an open access article distributed under the Creative Commons Attribution License, which permits unrestricted use, distribution, and reproduction in any medium, provided the original work is properly cited.

Based on the industry data and enterprise data from tens of thousands of small and medium-sized enterprises, a deep learning and machine learning model of credit prediction is constructed through the division of data sets, processing, and integration of models. At first, with the help of two characteristic selection methods, several subsets separated from the dataset are analyzed based on convolutional neural network as coarse prediction. Then, combined with the tree model, the precise prediction is further made for the enterprise credit evaluation. Finally, the model fusion is carried out to obtain high-precision results. In the simulation experiment, this paper takes a data set of 14,366 small and medium-sized enterprise credit evaluations as the analysis samples to verify the results. The accuracy of the model is 97%, which is far more than 93% of single model with metadata set.

## 1. Introduction

According to statistics, by the end of 2018, the number of small and medium-sized enterprises in China has exceeded 30 million, and the number of individual industrial and commercial households has exceeded 70 million, taking over more than 50 percent of the country's tax revenue, 60 percent of GDP, and 70 percent of technology innovation. The achievements and employment of more than 80 percent of the workforce play an increasingly important role in supporting the national economy. The difficulty of financing and loans for small and micro-businesses is particularly acute, and the risks and challenges they face are severe and complex.

The credit evaluation of small and medium-sized enterprises uses the machine learning models and algorithms to carry on the statistics of enterprises themselves. Calculation and qualitative analysis are used to predict whether an enterprise can be included in the trust-breaking enterprises. Existing credit evaluation models and subset selection models can be roughly divided into traditional statistical models, machine learning models, subset selection of characteristic numerical attributes, and subset selection

based on models. The earliest credit evaluation models are generally based on classical statistical theory, which mainly includes logistic regression, linear regression, and Naive Bayesian classification. In recent years, with the rapid progress of computing capability and algorithm as well as the substantial increase in data scale, methods in the fields of machine learning and deep learning have been used in enterprise credit evaluation and achieved excellent results. At present, the representatives of data mining models include SVM, K means, decision tree, artificial neural network, and artificial neural network of long- and short-term memory. In this paper, deep learning, machine learning, and other methods are used to predict high-precision model results, so as to provide a good reference for real enterprise credit evaluation system.

For the credit evaluation of small and medium-sized enterprises in reality, an enterprise with a relatively high credit evaluation score will be relatively easier in bank lending, private financing, and government support in reality. On the other hand, it also provides direction and guidance for companies with low ratings to some extent. Liu et al. [1] studied the financial market in China, Yoshino and Taghizadeh-Hesary [2] studied the financial market of the

whole Asia, and the research results show that the financial center must be in Asia in the future. Hu et al. [3] proposed a hybrid integration model based on support vector machine, which randomly sampled the feature space and then trained the model with support vector machine. However, the accuracy was not good, and the random sampling and decision tree model could not make use of all the sample space. Gregori et al. [4] proposed a multi-criteria credit rating model for the financing of small and medium-sized enterprises, but the ductility of this model was not good enough. Zhang et al. [5] used the fuzzy BP neural network to predict investment risks, and the overall effect of the model was good. Some studies utilize back propagation neural network [6, 7] to study the risk of financing and credit risk of enterprise supply chain. Fonseca et al. [8] compared the effectiveness of fuzzy neural network and BP neural network in discriminating the credit rating of small and micro-enterprises, and the result showed that the fuzzy neural network is more effective. Li et al. [9], improved the method of XGBoost algorithm and proposed fuzzy XGBoost on the basis of adding fuzzy membership degree. Zhou et al. [10] also proposed some solutions on fuzzy algorithm. Zhang et al. [11, 12] put forward a large-sample mixed credit evaluation model based on similar sample merge and a three-stage mixed credit evaluation model based on multi-attribute subset selection strategy, respectively, in 2018 and 2019. Sun et al. [13] put forward a series of solutions to the problem of uneven distribution in terms of credit evaluation.

For the small and medium-sized enterprise credit evaluation models based on subset selection strategy of feature's numerical attributes above, most of them just simply remove the redundant features from metadata, and put a subset in one or more basic models to train. But they did not further pursue higher accuracy, nor did they compare and verify the results of selected subsets based on different base models. Is the accuracy of the selected subset training model higher than that of the metadata-trained model? Is there any difference among different subsets? If the data are redundant, does that mean the redundant data are completely useless? Can subsets highlight local features of the feature space? Can an algorithm be used to mine the relationships among data? Is it possible to achieve higher accuracy through model fusion? These are the emphases of this paper.

In order to carry out data mining, first, data should be preprocessed, outliers should be proposed, and the missing values should be filled. Next, even if the noise samples are processed, the metadata often contains data redundancy. The redundant data often cannot further improve the accuracy of the model and sometimes even prevent the model from reaching better accuracy. Last, train and verify the model. The speed of model training can be further accelerated by the selection of features and the reduction of training samples.

Aiming at the shortcomings of existing research, this paper proposes a multimodel hybrid integration model based on convolutional neural network. The main innovations are as follows:

- (1) This paper summarizes the methods and principles needed in models firstly and then combines different subset division methods: correlation coefficient and GBDT subset division. Random forest model is constructed to verify the subsets after division to ensure that the accuracy will not drop too much.
- (2) On the basis of dividing four subsets, the convolutional neural network is used to explore the relationship between data and the four channels of the convolutional network. Use three models including extreme gradient boosting, light gradient boosting machine, and CatBoost to train, respectively, the four subsets and the four-channel convolutional neural network.
- (3) Bayes ridge regression was used to fuse the advantages of all single models in different subsets with convolutional neural network channels, and a more robust model is trained whose prediction result is more uniformly distributed and more in line with the real credit evaluation situation with an accuracy of up to 97%, which is much higher than 93% of single model with metadata set.

## 2. Enterprise Credit Evaluation Methods and Technologies

This section first introduces the theory and technology that can explain the credit evaluation of small and medium-sized enterprises, the evaluation method of model performance, the volume neural network, and the machine learning tree model.

**2.1. Evaluation Method.** In this paper, to evaluate the effectiveness of the model, we use AUC (area under curve) as the evaluation metric. AUC is an evaluation index for binary classification models, and its actual meaning is the area under the ROC (receiver operating characteristic) curve. AUC considers the classifier's ability to classify positive and negative examples, and can still make a reasonable evaluation of the classifier in the case of unbalanced samples.

The ROC curve is generated based on the ground-truth class and predicted probability of the sample. The horizontal axis is FPR (false-positive rate), and the vertical axis is TPR (true-positive rate), as shown in equation (1). Among them, TPR represents the proportion of all samples whose true class is 1, and the predicted class is 1; and FPR represents the proportion of all samples whose class is 0, and the predicted class is 1.

$$TPR = \frac{TP}{TP + FN}, FPR = \frac{FP}{FP + TN}, \quad (1)$$

where TP (true positive), FN (false negative), FP (false positive), and TN (true negative) are generated by confusion matrix. We use the AUC\_ROC\_SCORE [14] function in scikit-learn to calculate the AUC value.

## 2.2. Credit Prediction Technologies

**2.2.1. Random Forest.** Bagging [15] gives datasets including  $m$  samples. We randomly take out a sample and put it into the sample set, and then put this sample back into the initial data set. It is still possible to select the sample in the next sampling, and then a sample set of  $m$  samples is obtained after  $m$  cycles.

Random forest (RF) [16, 17] is an extension of bagging. On the basis of building bagging integration based on decision learning, RF further introduces random attribute selection in the training process of decision tree. To be specific, the traditional decision tree selects the most attribute in the current node when selecting and dividing attributes, whereas in RF, for each node of the base decision tree, a subset containing  $k$  attributes is selected randomly from the attribute set of this node, and then selected an optimal attribute user to divide from this subset.

Random forest is used to test whether the error of subset division is too large. Random forest model is a model based on variance, so it is very difficult to fit the predicted results, and it is a good model to test the selection of characteristic subset.

**2.2.2. Convolutional Neural Network.** Convolutional neural network (CNN) is a feedforward neural network, whose artificial neurons can respond to a part of the surrounding units in the coverage range and perform well in regular data processing [18–21].

Convolutional neural network is composed of one or more convolutional layers and the top fully connected layer, and also includes associated weight and pooling layer at the same time. This structure enables convolutional neural network to utilize the two-dimensional structure of the input data. Compared with other deep learning structures, convolutional neural networks can provide better results in image and speech recognition and can also be trained using a backpropagation algorithm. Compared with other deep and feedforward neural networks, convolutional neural networks require fewer parameters to be considered, which makes it an attractive deep learning structure.

**2.2.3. Decision Tree Model.** Decision tree [22] and its advanced models are the kind of algorithms that divide the input space into different regions, and each region has its own weighted parameters. In machine learning, decision tree is a prediction model. It represents a mapping relationship between object attributes and object values. Each node in the tree represents an object. The join node represents a small region divided into a decomposition space, and each branch fork path represents a possible attribute value—the node weight. Each leaf node represents the value of the object represented by the path from the root node to the leaf node.

Let  $\hat{y}_i^{(t)}$  represent the predicted value of the  $i$  th example in the  $t$  th tree,  $\omega(f_t)$  is the size of the  $t$  th tree,  $f_t(x_i)$  is the weight value of the leaf node corresponding to the  $i$  th

training sample in the  $t$  th tree, and  $L^{(t)}$  is the target function of the  $t$  th tree.

$$L^{(t)} = \sum_{i=1}^n l(y_i, \hat{y}_i^{(t-1)} + f_t(x_i)) + \omega(f_t). \quad (2)$$

For  $f_t(x_i)$ , Taylor quadratic expansion is used, where  $g_i$  is the first gradient of the loss function to  $\hat{y}_i^{(t-1)}$  and  $h_i$  is the second gradient of the loss function to  $\hat{y}_i^{(t-1)}$ .

$$L^{(t)} = \sum_{i=1}^n \left[ l(y_i, \hat{y}_i^{(t-1)}) + g_i f_t(x_i) + \frac{1}{2} h_i f_t^2(x_i) \right] + \omega(f_t). \quad (3)$$

The loss function value of tree  $t-1$  in front of the  $t$  th tree is known, and  $\tilde{L}^{(t)}$  is an approximate value, so

$$\tilde{L}^{(t)} = \sum_{i=1}^n \left[ g_i f_t(x_i) + \frac{1}{2} h_i f_t^2(x_i) \right] + \omega(f_t). \quad (4)$$

$I_j = \{i | x_i = j\}$  is defined as the mapping of the  $i$  th sample to the  $j$  th cotyledon node

$$\tilde{L}^{(t)} = \sum_{i=1}^n \left[ g_i f_t(x_i) + \frac{1}{2} h_i f_t^2(x_i) \right] + \gamma T + \frac{1}{2} \lambda \sum_{j=1}^T w_j^2 \quad (5)$$

$$= \sum_{j=1}^T \left[ \left( \sum_{i \in I_j} g_i \right) w_j + \frac{1}{2} \left( \sum_{i \in I_j} h_i + \lambda \right) w_j^2 \right] + \gamma T.$$

Take the first derivative of  $w_j$  from  $\tilde{L}^{(t)}$ , set it to 0, and get

$$w_j^* = \frac{\sum_{i \in I_j} g_i}{\sum_{i \in I_j} h_i + \lambda}. \quad (6)$$

Bring the  $w_j^*$  back into the upper form:

$$\tilde{L}^{(t)} = -\frac{1}{2} \sum_{j=1}^T \frac{\left( \sum_{i \in I_j} g_i \right)^2}{\sum_{i \in I_j} h_i + \lambda} + \gamma T. \quad (7)$$

So, we can get the solution of the objective function.

## 3. Data Processing of Credit Assessment Model

**3.1. Data Preprocessing.** In this paper, the data which come from the Statistics Bureau of Shandong Province include enterprise type, the registration authority, the enterprise status, the total amount of investment, registered capital, industry code, industry, business category, the jurisdiction of the organs, the value-added tax, corporate income tax, stamp duty, education, urban construction tax and the rest in early and late, a series of registration time correlation of dynamic data, a total of 200 or so.

According to the obtained data, make feature combination as far as possible, for example, subtract all year-end values from the initial values of last year, so as to construct new features and expand the sample space of training set. However, combining as many features as possible also brings some problems. If data redundancy occurs, then based on the tree model, there are two very important features that are

very good for predicting the analytic hyperplane, but if the similarity of these two features is very high, data redundancy will occur. In a word, if the weight of split points of the tree model for these two features is very low, it will deteriorate the effect of the model. From this point of view, feature selection becomes quite important for the tree model.

**3.2. Feature Selection—Using Random Forest to Test the Feasibility.** Filter-based feature selection, also known as filtering method, scores every feature according to the divergence or relevance of each feature score, and set a threshold or the number of thresholds that are about to be selected and then select features. The steps for using a filter in this article are as follows:

The correlation coefficient method: Calculate the correlation sparsity among the features, and the features with larger Pearson coefficient are selected according to the threshold.

Directly delete features whose variance does not meet the threshold; directly delete one of the two corresponding features with a large Pearson coefficient.

**3.2.1. The Correlation Coefficient Method.** For the correlation between the two characteristics of  $A$  and  $B$ , we can obtain the correlation degree  $r_{A,B}$  by calculating the correlation coefficient of  $A$  and  $B$  (also called Pearson product moment coefficient, Pearson's product moment coefficient).

$$r_{A,B} = \frac{\sum_{i=1}^n (a_i - \bar{A})(b_i - \bar{B})}{n\sigma_A\sigma_B} \quad (8)$$

$$= \frac{\sum_{i=1}^n (a_i b_i) - n\bar{A}\bar{B}}{n\sigma_A\sigma_B},$$

where  $n$  is the number of tuples;  $a_i$  and  $b_i$  are the values of tuples  $i$  on  $A$  and  $B$ , respectively;  $\bar{A}$  and  $\bar{B}$  are the mean values of  $A$  and  $B$ , respectively;  $\sigma_A, \sigma_B$  are the standard deviations of  $A$  and  $B$ , respectively; and  $\sum (a_i b_i)$  is the cross product of  $A$  and  $B$  (for each tuple, the product within the element is used), Pearson greater than zero means a positive correlation, indicating that one value increases as another value increases; A negative value of Pearson indicates that one value decreases as the other increases. The larger the value is, the stronger the correlation is, and the stronger the correlation is, the more obvious the data redundancy is.

Based on the analysis of enterprise type, registration authority, enterprise status, registered capital, industry code, industry category, jurisdiction authority, and other category characteristics, only part of the data with high correlation is retained here, and it can be found that there is a certain correlation between industry category and industry code, jurisdiction authority, and registration authority. As shown in Figure 1, especially for tax characteristics, there is an obvious correlation between value-added tax and education expenses, and between value-added tax and urban construction tax.

Based on Pearson coefficient, a thermal diagram can be made to further determine the specific relevant values. As shown in Figure 2, there are three features with high correlation: value-added tax, urban construction tax, and education fee. Taxpayers in the urban construction tax are 7%. The construction tax in county towns is 5%. Elsewhere, the city construction tax is 1%. The surcharge of education expenses is (VAT + consumption tax actually paid) × 3%. Based on this, further feature engineering is carried out and further data relationship is mined.

Cross-features can be made for features with medium or low correlation, such as Pearson coefficient interval  $[0.2, 0.5]$ , so as to obtain certain cross-new features, so as to achieve the best effect of the model.

In order to avoid data redundancy caused by highly correlated features, we divide the data set with high correlation coefficient into  $m$  subsets, and the union of all subsets is  $N$ -dimensional data. Then, the model is trained in turn, and finally the model is fused to get the best data effect. The features with high correlation coefficient in the metadata are split into two subsets, where the metadata is divided into subsets 1 and 2. The results of random forest test are shown in Table 1.

According to the comparison of the results in Table 1, although the accuracy of both subset 1 and subset 2 is lower than that of metadata set, they avoid cleverly data redundancy and have only a small difference in accuracy. Therefore, the division of data set can be considered reasonable.

**3.2.2. Tree Model Selection.** Tree model selection is a model-based selection method and not based on the basic attributes of numerical values. The tree model divides the nodes based on the Gini index of information theory to get the index value of the features.

Assuming that the proportion of class  $K$  samples in the current sample set  $D$  is  $p_k$  ( $k = 1, 2, \dots, |Y|$ ), the Gini index of  $D$  is defined as shown in

$$\text{Gini}(D) = \sum_{k=1}^{|Y|} \sum_{k' \neq k} p_k p_{k'} = 1 - \sum_{k=1}^{|Y|} p_k^2. \quad (9)$$

Intuitively,  $\text{Gini}(D)$  reflects the probability that two samples are randomly drawn from data set  $D$  with different category markers. So, the smaller the  $\text{Gini}(D)$  is, the higher the improvement in data set  $D$  is made. In the set of candidate attributes, the attribute with the lowest Keeny index is selected as the dividing attribute.

The metadata is divided into a subset 3 and a subset 4, where subset 3 is considered as an important feature in the GBDT model, and subset 4 is not considered important to the GBDT model. Using random forest to test the subsets, the test results are shown in Table 2.

As shown in Table 2, the accuracy deviation between the two subsets is not significant and can be regarded as reasonable. The above two different methods are as follows: the first is based on mathematical relations, and the second is based on model selection. Due to certain deviations of



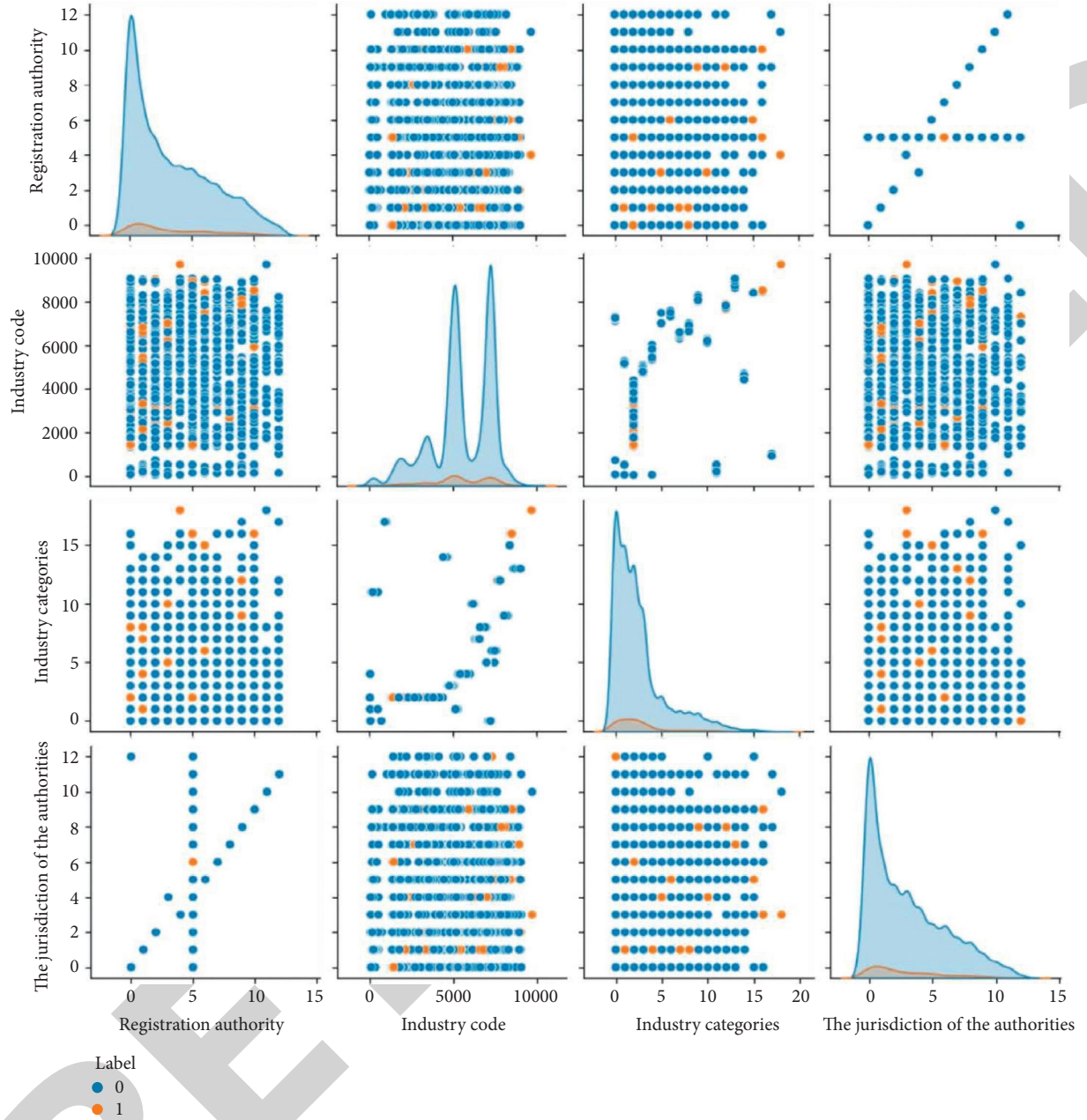


FIGURE 1: Feature space distribution.

results, the uncertainty of performance of feature selection method exists. Therefore, this paper will try to achieve higher scores by comparing different methods and different subsets longitudinally, and, at the same time, with undivided subsets. And use only the correlation coefficient method and GBDT selection method, after which there will be subset 1, subset 2, subset 3, and subset 4. When the sample space is segmented, the segmented sample space pays more attention to the local sample space of the features than the global sample space. So, the precision of the single model will decrease, but the precision of the whole model should be guaranteed not to be lost simultaneously. In the following research, we use stacking model fusion method to make full

use of each data and construct the model to take better care of the global sample.

#### 4. Design of Credit Evaluation Model

After processing the outlier data and the feature, we divide the metadata into four channels by using the correlation coefficient and GBDT, and get the sub-data set of the four channels, using convolutional neural network to capture the interaction among the data as a prediction, and different channels correspond to different rough predictions. The corresponding rough predictions of four channel results are taken as the characteristics of XGB, LGB, and CB. Make

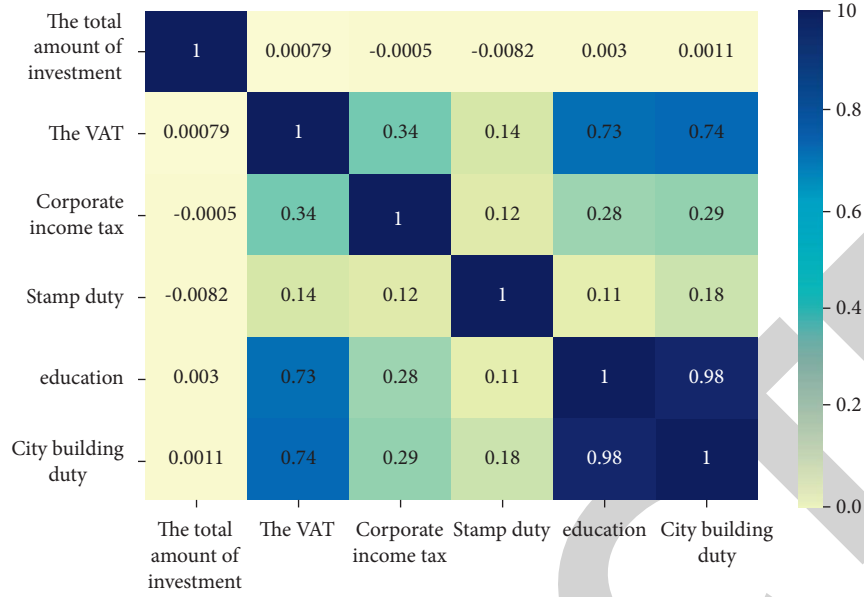


FIGURE 2: Correlation coefficient of tax characteristics.

TABLE 1: The correlation coefficient method.

Model accuracy	Metadata	Subsets 1	Subsets 2
Random forest	91.139%	89.255%	91.051%

TABLE 2: Tree model selection.

Model accuracy	Metadata	Subset 3	Subset 4
Random forest	91.139%	91.139%	88.911%

predictions correspondingly and respectively, and 12 fine prediction results are obtained after model fusion. The specific operation process is shown in Figure 3.

**4.1. Convolutional Neural Network Seeks Data Representation.** Combined with the actual data, the data sets collected by enterprises often have a lot of missing data. So, missing values must be filled in before using neural network model. Encode the data to meet the input of the convolutional neural network, and attempt to find the data mining point from the angle of the relationship between the numerical representations of the data.

Due to the small amount of data and the low dimension of two-dimensional matrix, a relatively simple convolutional neural network structure is used. The parameters of convolutional neural network are shown in Table 3.

The results of the four-channel experiment were obtained by plotting, respectively. showing the loss and AUC of binary cross-entropy and the loss and AUC of the verification set.

As shown in Figure 4, in the case of constant iteration of convolutional neural network, the loss function value of training set and verification set is close to the value of AUC, so it can be considered that the convolutional neural network has learned the preliminary representation of data.

**4.2. Multi-Subset Comparison—Tree Model Prediction Results.** In the algorithm of the decision tree model, the tree model can use the missing value to calculate the

missing value direction. Even in the face of the missing value, the tree model still has good accuracy, so three models are used, respectively, XGBoost, LightGBM, and CatBoost.

The three tree models are all based on boosting idea. The tree growth strategy of XGBoost is width-first growth, which has the advantage of accurate node segmentation of the model, but the model often grows nodes that are not beneficial to the accuracy of the model. LightGBM's tree growth strategy that is depth-first, which has the advantage of fast model speed and will not grow for nodes that do not benefit much from model accuracy. CatBoost's tree growth strategy is to generate symmetric binary trees. The model is insensitive to parameter adjustment and has the highest robustness, but consumes the most space.

According to the model accuracy, as shown in Table 4, the data accuracy of the LightGBM model is the best. It can be seen that even subsets 2 and 4 have certain effects, and they are not useless data that completely lose characteristic expression.

In order to verify the improved effect of adding CNN channel, the data distribution without CNN channel is shown in Figure 5.

Figure 5 shows the accuracy broken line graph and numerical distribution graph of prediction results of tree model. Three broken lines of Figure 5(a) represent different tree models, and Figures 5(b)–5(d) represent different distribution maps of four subsets, respectively. This step is to highlight that different subsets corresponding to different models have different model results, to show that the discrimination degree of feature selection method is effective, and to show that

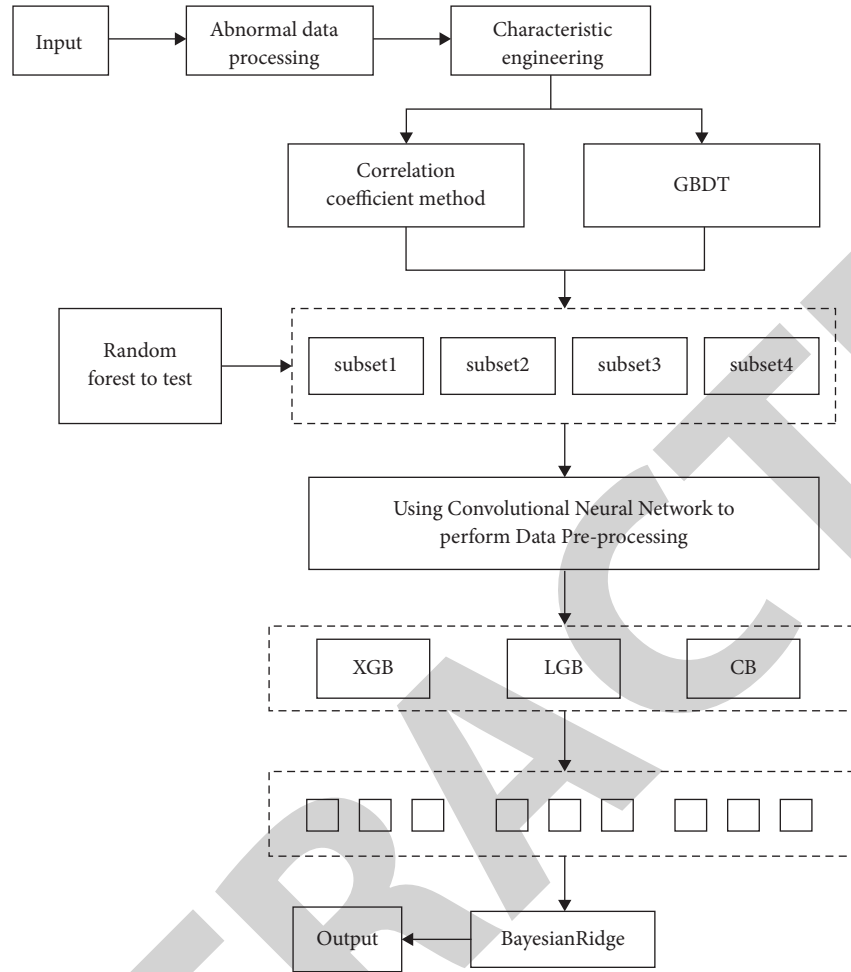


FIGURE 3: Model flow diagram.

TABLE 3: Convolutional neural network parameters.

Model	Input layer	Hidden layer	Output layer	Learning rate	Number of times
CNN	$(k \times m)$ ; sigmoid	$2 \times, 2 \times \text{conv}; 2 \times \text{MaxPooling}$	1; sigmoid	0.01	50

the model can learn different advantages and disadvantages of data according to different feature spaces.

- (1) As shown in Figure 5, the distribution of the LGB model has the best acceptability, but the prediction score of the LGB model is mainly in  $[50, 100]$ , and there is no uniform distribution of models such as XGB and CB; also, the high frequency ratio is too high. However, the advantage of the LGB model is that its data distribution is relatively close to the real distribution, and the companies with high scores are relatively concentrated, while the scores of small and medium-sized enterprises with low scores are relatively scattered.
- (2) XGB is in a state of serious two-level differentiation. The advantage of XGBoost is the data with high scores are concentrated at about 80 points instead of 90. The area of  $[60, 100]$  is close to the normal distribution; that is, XGBoost can be well-

distributed A company with a predicted score of  $[60, 100]$ .

- (3) CB is also in a state of serious polarization. CatBoost has the same advantages in subsets 1 and 3 as XGBoost, but the distribution of subset 3 and subset 4 is similar to that of neural network, and the data are very discrete.

**4.3. After Adding the CNN Channel—Tree Model Prediction Results.** Now add the CNN channel to try to achieve better accuracy. The distribution is shown in Figure 6.

The model fusion used here is to merge the advantages of a single model while discarding the shortcomings, so as to obtain a better model to evaluate the credit score of SMEs.

- (1) After applying the CNN channel, it can be found that the distribution is significantly more concentrated



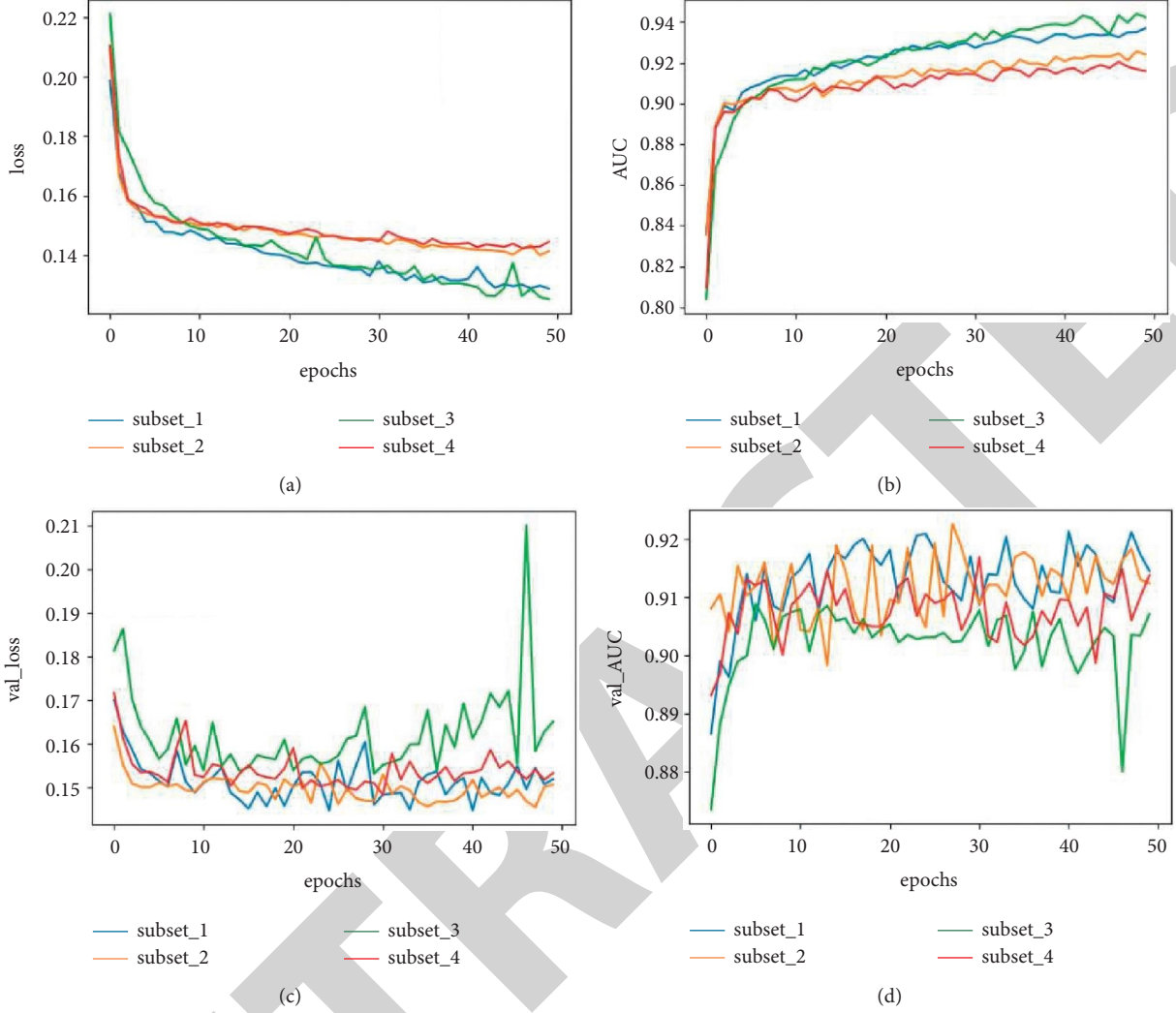


FIGURE 4: Convolutional neural network learning process. (a) Loss. (b) AUC. (c) Val\_loss. (d) Val\_AUC.

TABLE 4: Tree model accuracy.

Accuracy	Metadata (%)	Sub 1 (%)	Sub 2 (%)	Sub 3 (%)	Sub 4 (%)
LGB	93.723	92.933	91.552	92.310	92.091
XGB	93.225	92.703	92.625	92.760	92.493
CB	92.416	86.295	89.814	92.359	83.787
<i>With CNN channel</i>					
CNN-LGB	92.649	91.896	90.907	91.146	92.325
CNN-XGB	92.188	92.328	92.384	92.570	91.858
CNN-CB	92.334	92.040	88.464	91.960	86.718

and more stable, and the distribution of prediction is more reasonable.

- (2) For the utilization of metadata, it can be seen that the distribution of each model of metadata is closer to each model of subset 1. Although other local details on the data set cannot be highlighted, the overall distribution is taken good care of relatively.

#### 4.4. Credit Assessment Model Integration

**4.4.1. Stacking Ensemble, Multi-Model Comparison.** Stacking absorbs the idea of neural networks. In a neural network,  $n$  units of the last hidden layer of the neural network are mapped to a unit on the output layer. The activation function may be sigmoid or ReLU. In stacking,  $n$  neural network units correspond to  $n$  base models (such as NN, LightGBM, XGBoost, and CatBoost), where the activation functions correspond to linear regression, logistic regression, or Bayesian ridge. And finally it outputs the result.

Stacking algorithm framework is as follows.

- (1) Select the base model, for example, XGBoost, LGB, random forest, SVM, KNN and other basic algorithm models, assuming that  $n$  base models are used.
- (2) Use K fold to divide the training set into  $m$  folds, and they are marked as  $\text{Train}_1$  to  $\text{Train}_m$ .
- (3) Suppose training the  $k$ -th model. Start from  $\text{Train}_1$ , and divide this into a validation set. Use  $\text{Train}_2$  to

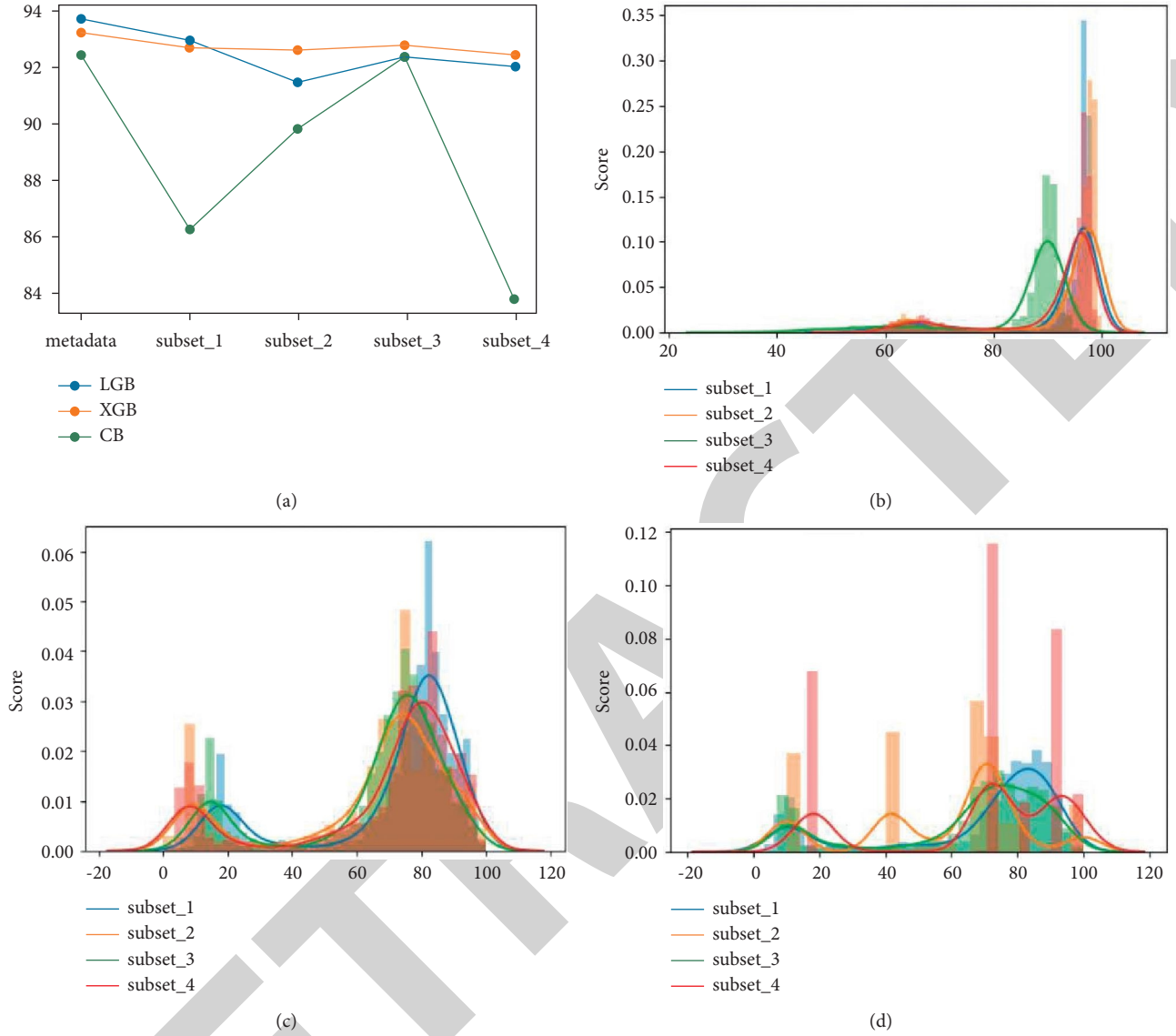


FIGURE 5: Distribution of tree models without CNN channels. (a) Tree model accuracy. (b) LGB result distribution. (c) XGB result distribution. (d) CB result distribution.

Train<sub>m</sub> to train the model, then predict Train<sub>1</sub>, and keep the prediction results. Then, take Train<sub>2</sub> as the validation set, use Train<sub>1</sub> and Train<sub>3</sub> to Train<sub>m</sub> for modeling, and predict Train<sub>2</sub>, then keep the results, and so on, until all Train<sub>1</sub> to Train<sub>m</sub> are predicted once the establishment of the k-th base model is completed.

- (4) In the base model established in step 3, each model separately predicts the data set and retains the results, and then averages the prediction results  $m$  times as the base model prediction result of the k-th column.
- (5) Select the  $(k+1)$ -th base model and repeat the above operations from equations (2)–(4). Get the result of the  $(k+1)$ -th model until the training of  $n$  base models is completed.
- (6) If there are  $n$  base models,  $n$  columns of new feature expressions will be generated, that is,  $n$  single model

prediction results. Similarly, the prediction data set also has  $n$  columns of new feature expressions. There are totally  $n \times m$  prediction results.

- (7) The above 6 steps are used as the input unit of stacking, and the set model is used to predict and output all the units of the first layer.

In this article, NN, LGB, XGB, and CB are the base model of stacking, and K fold has 5 fold. The selection of output model in stacking is shown in Table 5.

According to the results in Table 5, the accuracy of Bayesian regression is generally higher than that of linear regression or logistic regression. Therefore, the stacking output model chosen here is Bayesian ridge regression instead of linear regression or logistic regression. The distribution of the final model is shown in Figure 7.

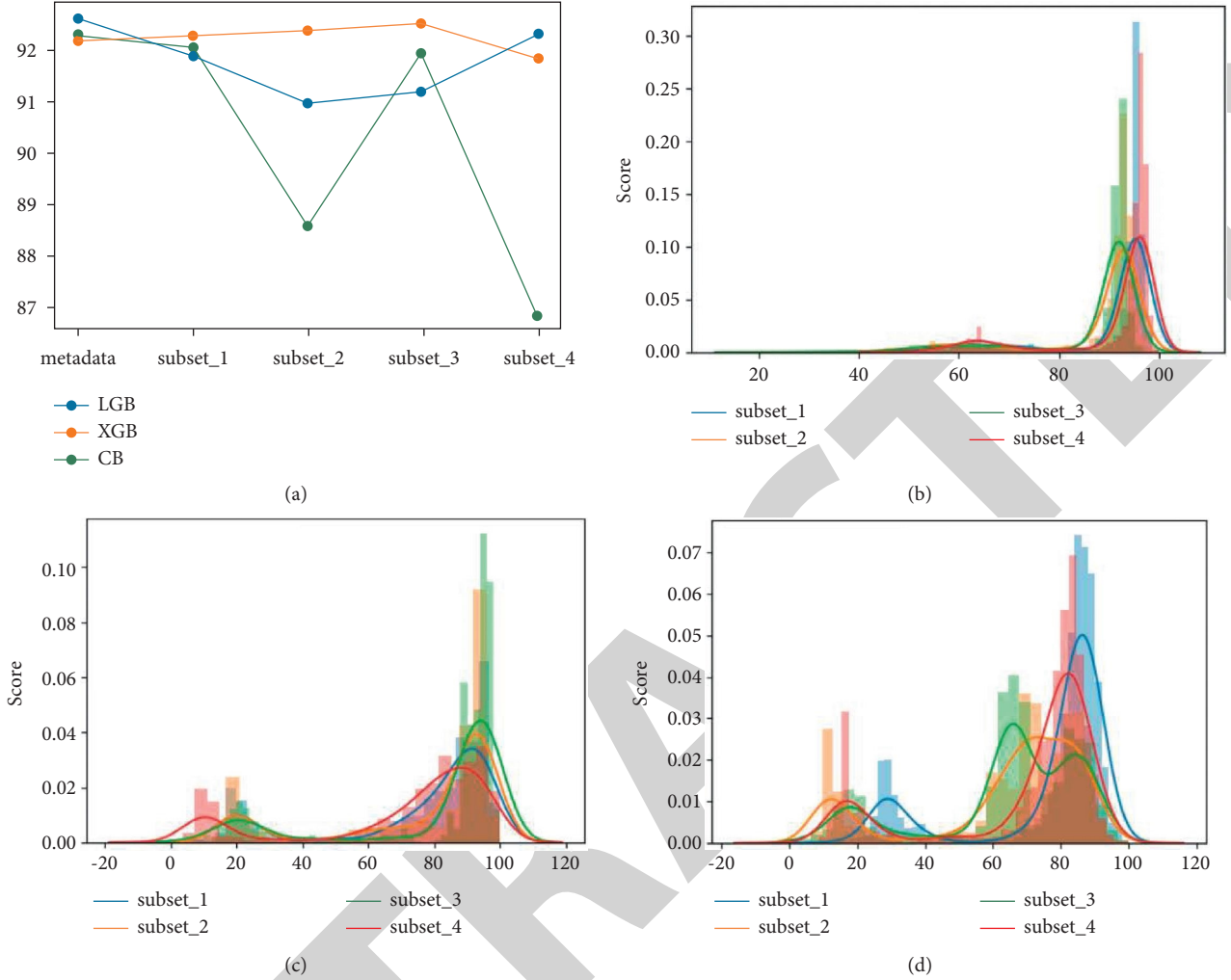


FIGURE 6: Distribution of tree models with CNN channels. (a) Tree model accuracy. (b) CNN-LGB result distribution. (c) CNN-XGB result distribution. (d) CNN-CB result distribution.

TABLE 5: Stacking model accuracy.

Stacking output	Linear regression (%)	Logistic regression (%)	Bayesian ridge (%)
Metadata	95.245	69.477	95.267
Subset 1	94.831	67.437	94.838
Subset 2	93.813	59.437	93.812
Subset 3	96.500	78.353	96.503
Subset 4	93.675	59.138	93.675
All subsets	96.746	77.884	96.749
With CNN channel	97.122	77.221	97.130

It can be seen from Figure 7 that stacking improves the problem that the distribution range of the LGB single model is [50, 100], there are no data that are too concentrated around 90 points, and it will not be like LGB model that the evaluation scores are too concentrated around 95. Stacking makes the distribution of the model more uniform and more close to the actual distribution of business forecasts.

Moreover, the distribution of the model fused by four subsets is better than that of the model fused by metadata, and the accuracy of the verification set reaches 96.749%.

After applying the CNN channel, the accuracy is further improved to 97.130%, which is a great increase over metadata. Every 1% increase up to 95% accuracy is difficult. This shows that although the model is divided into four subsets, the accuracy of a single model is not good enough because a different feature space has different targeted regions; that is to say, the divided subsets can highlight local details instead of global accuracy. Using the stacking method, the advantages of the model trained on the subset can be well combined and disadvantages can be discarded, which

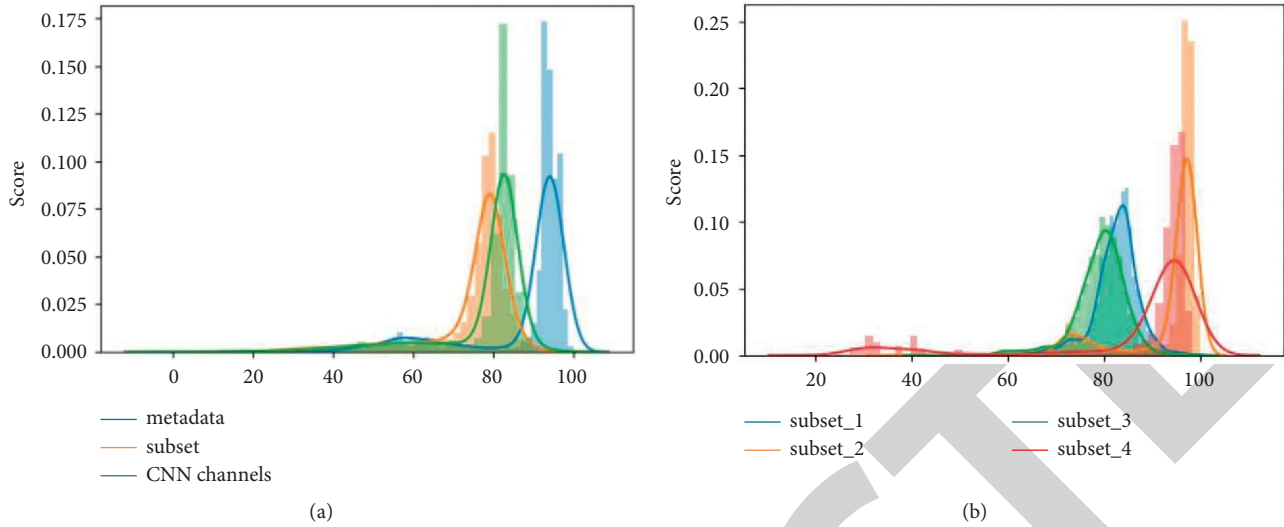


FIGURE 7: Weighted fusion comparison. (a) Weighted metadata. (b) Weighted subset.

contributes to an excellent result. This is the so-called removing the dross and choosing the essence. It is believed that the prediction effect of enterprise credit evaluation based on the integration of multiple models is good, and it provides a good reference for enterprise credit evaluation.

## 5. Conclusion

The data used in this experiment contain the data of 14366 enterprises. Each data item records the features of 274 dimensions including enterprise type, registration authority, enterprise status, total investment, registered capital, industry code, industry category, enterprise category, value-added tax, enterprise income tax, and stamp tax. The credit evaluation of SMEs has very important practical value and theoretical significance for commercial banks and credit institutions.

Existing researches often screen out subsets with good quality based on related theoretical results and then conduct training and verification on a single model. Although it can play a certain role, it does not take into account the differences among the individual models and the advantages of the models. This paper uses the method based on numerical selection and model selection to construct the subset, and makes full use of the insufficient data, then puts them in another subset, and verifies all the subsets with the base model respectively, and finally merges all the models to obtain very accurate high SME credit evaluation results.

Compared with existing related researches, this article has the following characteristics: observe the distribution of data; find outliers in the data; use metadata set data as much as possible; carry out feature engineering; and analyze the relationship among data. Simulate as much as possible the situation of credit evaluation in real enterprises, avoid data redundancy, and use separate metadata sets. Because data redundancy is not completely redundant, in order to mine the data features as many as possible, the correlation

coefficient and GBDT are used to divide the data, and then the random forest test model is used. Encode the data so that it conforms to the input mode of the convolutional neural network. Through the convolutional neural network, find the relationship among the data. The four subsets are input into four different convolutional neural networks to obtain four coarse prediction channels. Aiming at the 12 training results of all models, the Bayesian regression is used to fuse the training results of single models, and a particularly high precision result is obtained, with an accurate value of 97.13%.

From the point of empirical results, the effect of multimodel fusion model established by this paper is better, compared with other algorithms and traditional methods, it shows that it can help more creditworthy enterprises to more effectively and more fairly get loans, and it can better help bank enterprise risk assessment, reduce the rate of bad debts, and promote whole credit business benign development thereby.

The simulation results show that the model has achieved good results in SMEs credit risk assessment, improving the efficiency and accuracy of assessment, and can make accurate and reliable assessment in SMEs financing, loan, and other scenarios. It is of great significance to the financing, risk management, and financial service supervision of small and medium-sized enterprises. Its application prospect is very broad, and it has certain practical application significance and theoretical research value.

## Data Availability

The data used to support the findings of this study can be obtained from the corresponding author (zhangleicqjtu@163.com).

## Conflicts of Interest

The authors declare that they have no conflicts of interest.

## *Retraction*

# **Retracted: Image Analysis Method of Substation Equipment Based on Convolutional Neural Network**

### **Security and Communication Networks**

Received 26 December 2023; Accepted 26 December 2023; Published 29 December 2023

Copyright © 2023 Security and Communication Networks. This is an open access article distributed under the Creative Commons Attribution License, which permits unrestricted use, distribution, and reproduction in any medium, provided the original work is properly cited.

This article has been retracted by Hindawi, as publisher, following an investigation undertaken by the publisher [1]. This investigation has uncovered evidence of systematic manipulation of the publication and peer-review process. We cannot, therefore, vouch for the reliability or integrity of this article.

Please note that this notice is intended solely to alert readers that the peer-review process of this article has been compromised.

Wiley and Hindawi regret that the usual quality checks did not identify these issues before publication and have since put additional measures in place to safeguard research integrity.

We wish to credit our Research Integrity and Research Publishing teams and anonymous and named external researchers and research integrity experts for contributing to this investigation.

The corresponding author, as the representative of all authors, has been given the opportunity to register their agreement or disagreement to this retraction. We have kept a record of any response received.


### **References**

- [1] J. Zhang, Y. Liu, L. Yuan, and H. Jia, "Image Analysis Method of Substation Equipment Based on Convolutional Neural Network," *Security and Communication Networks*, vol. 2022, Article ID 1718514, 10 pages, 2022.



## Research Article

# Image Analysis Method of Substation Equipment Based on Convolutional Neural Network

Jingjing Zhang <sup>1</sup>, Yuxin Liu,<sup>1</sup> Lin Yuan,<sup>2</sup> and Haowei Jia<sup>3</sup>

<sup>1</sup>School of Electrical Engineering, Zhengzhou Railway Vocational & Technical College, Zhengzhou 450052, China

<sup>2</sup>Beijing Institute of Science and Technology, China Railway Beijing Group Co., Ltd, Beijing 100081, China

<sup>3</sup>Power Supply Maintenance Technology Center,  
Zhengzhou East High Speed Rail Infrastructure Section of China Railway Zhengzhou Group Co., Ltd, Zhengzhou 450052, China

Correspondence should be addressed to Jingjing Zhang; [zhangjingjing@zzrvtc.edu.cn](mailto:zhangjingjing@zzrvtc.edu.cn)

Received 20 June 2022; Revised 18 July 2022; Accepted 29 July 2022; Published 27 August 2022

Academic Editor: Hangjun Che

Copyright © 2022 Jingjing Zhang et al. This is an open access article distributed under the Creative Commons Attribution License, which permits unrestricted use, distribution, and reproduction in any medium, provided the original work is properly cited.

Due to the continuous development of computer technology to promote the continuous progress of substation automation technology, the current substation equipment is diverse and there are many interferences, making the accuracy of the image processing algorithm to be low, and there is a lack of a complete automatic processing system. Convolutional neural networks (CNNs) are one of the most important breakthroughs in artificial intelligence in the last decade, especially in the field of image recognition, and have made important research achievements. In this study, we apply CNNs to substation equipment image processing, a method that performs feature extraction for recognition through substation equipment images. The research focuses on the expansion of the image sample set, the automatic training method based on recognition rate, and the voting strategy based on integrated learning, which not only improves the training efficiency of the model but also increases the recognition rate, and the proposed method is of high practicality.

## 1. Introduction

Since the 20th century, computer technology has contributed to a great improvement in the way all sectors of society produce. The traditional way of manually manning substations has been made possible by the continuous advancement of automation technology, which has made it possible for unmanned substations, and through which companies hope to change the current backward status quo of substations. In this social environment, video monitoring systems have received widespread attention, and more and more people are devoted to the study of video monitoring, which has become a hot research topic today.

Substation video surveillance systems need to detect and identify specific targets in the surveillance video taken by inspection robots [1], and the analysis of specific targets to predict and understand the significance of their behavior. At its core, it analyses the behavior of targets and events by processing the original video image through a series of

algorithms such as feature extraction [2], image segmentation, image target detection and tracking, and image classification and recognition. In order to improve these hardships, we need to improve the operational efficiency and quality of substation equipment. Robot-based automatic inspections are implemented to fix the video images collected by robots. Tracking and identification can then understand the operating status of each equipment in the substation and improve the safety and reliability of the operation and maintenance of the substation.

Existing video image target detection and tracking algorithms have a low accuracy rate due to poor image quality from a distance, the complexity of the outdoor environment, and the presence of multiple interferences [3]. Therefore, the existing video surveillance system cannot be effective for video content analysis, understanding, processing, providing solutions to complex power problems, and meeting the security requirements of today's unattended substations. In summary, the power

system is in urgent need of basic and applied theories based on intelligent image tracking and image recognition of substation equipment.

Power equipment condition detection includes infrared detection technology, dissolved gas analysis in oil, and partial discharge detection methods. A large number of empirical studies have shown that most electrical equipment will show temperature changes when faults occur [4]. Infrared inspection technology is the only way to reveal the operating status of power equipment through visualization of equipment temperature information and can be used for nonstop, regular, or real-time inspection of power equipment, with noncontact, fast, and safe features. The current substation equipment infrared image analysis is still mainly manual, the influence of human factors in this method is large, and there is the problem of low efficiency of image analysis. Due to the limitations of infrared detection technology itself and the complexity of power equipment, the operation status of power equipment can no longer be judged by infrared detection technology alone. With the development of artificial intelligence and computer image recognition technology, the combination of substation equipment and image processing technology has become a new breakthrough [5].

The field of artificial intelligence has evolved rapidly over the past decade, with deep learning [6] (DL) being one of the fastest growing machine learning methods. DL is formed by using multiple simple neurons to form a multilayer network and adjusting the input according to the nonlinear relationship between the input and output. DL is essentially a complex function that extracts features [7] from an input sample and reflects its power. In recent years, DL has led to many research results in areas such as video tracking and video recognition [8]. When DL is integrated into the remote video monitoring system of substations to automatically track and identify the status of video monitoring equipment, it can greatly improve the accuracy of automatic equipment status identification, realize the automatic detection function of substations, ensure the operation of substations, and improve maintenance efficiency. On the other hand, in the complex outdoor environment, various interferences may occur, resulting in blurred and otherwise inaccurate video from the substation. Deep learning technology has strong feature extraction ability in image recognition and has strong generalisation ability. Therefore, in this study, DL was combined with image processing technology and category detection and pointer reading of substation images was introduced. The theoretical and applied research on image tracking in substations and image recognition based on DL and image feature extraction is of great research importance and has many potential applications.

As early as 1989, LeCun et al. published a study on CNNs and named the structure LeNet5 [9], which has a very high recognition rate for image figures. However, due to the small number of layers, this model structure did not show good recognition results for image data with many image features. However, with the improvement of computer hardware, multilayer CNNs and DL have become a current research hotspot. The network structure has greatly reduced the complexity of the network structure and reduced the

requirements for hardware, making the network model accessible to an increasing number of people and facilitating its widespread dissemination. Multilevel CNN model can use images directly as outputs, avoiding the complex process of feature extraction [10] and data reconstruction found in image processing algorithms. CNN is a multilayer perceptron specially designed for the recognition of two-dimensional shapes and has highly undistorted characteristics for the translation, rotation, scaling, and offset of objects in images.

DL is a CNN with hidden layers. In supervised learning, as long as the sample data are manually labelled [11, 12], the deep CNN can automatically extract features from a specific target in the substation image according to the labelling, recognise, analyse, and understand the target, achieve remote intelligent inspection instead of manual inspection to transcribe meter values, analyse the status of a specific monitoring object on-site, and upload the results of the analysis (standard information, pictures, or video information). The results of the analysis (standard information, pictures, or video information) are uploaded to the unified video monitoring platform of the power grid to meet the requirements for monitoring the safety and production of individual meters in smart substations.

The use of CNN methods for target identification is subject to interference from many sources, and the inaccuracy of one parameter may lead to a significant reduction in the final recognition rate, with too many uncontrollable factors. Therefore, can we consider combining CNN methods with other machine learning algorithms, reducing the requirement for neural network tuning, allowing for a certain amount of error in the neural network, and by combining several algorithms, even higher recognition results can be achieved. In this study, CNNs are introduced to the processing of substation equipment images, combining them with traditional image processing methods for feature extraction, classification, and recognition of substation equipment images. The research focuses on the expansion of the image sample set, the automatic training method based on recognition rate, and the voting strategy based on integrated learning, which not only improves the training efficiency of the model but also increases the recognition rate, and the proposed method is of high practicality.

## 2. CNN Models

**2.1. Model Introduction.** As an important branch of machine learning, DL has broken the bottleneck in the development of artificial intelligence based on the construction of multi-implicit layer machine learning models and learning more effective features through massive data and has promoted technological development in many fields. The idea of DL was first introduced by Geoffrey Hinton [13].

In the 1980s, the LeNet5 network model was proposed. Due to the limitations of the computer hardware level at that time, the number of layers of the LeNet5 model was limited. When working with complex image recognition, the recognition effect of the model is not good. With the computer hardware available at the time, algorithms such as support



vector machines (SVMs) performed better than CNNs. However, shallow machine learning algorithms have their limitations, as they have fewer parameters than DL, and this has led to a major bottleneck in the accuracy of the shallow algorithms, which has prevented them from being used on a large scale.

However, technology has always been developing, and after entering the 21st century, computer hardware has been developed rapidly, with the emergence of various high-performance CPUs and GPUs, which has paved the foundation for the development of DL. High-performance computer hardware solves the problem of computation, and excellent CNN algorithms solve the problem of algorithms. As a result, CNNs have grown exponentially. The number of network layers is also increasing, successfully achieving better and better results in image recognition, speech recognition, financial prediction, and judgement. In the 2012 ImageNet competition, deep CNNs were a hit in the field of image recognition, surpassing the SVM algorithm by a huge margin and attracting great attention from scholars at home and abroad.

CNNs [14, 15] are an important algorithm in DL, whose main features are reflected in three aspects: (1) having local awareness, using local connections between adjacent neurons instead of full connections, i.e., having convolutional layers that perform convolutional operations with the data. (2) Using weight sharing and greatly reducing the parameters required for training. (3) Using pooling operations to achieve dimensionality reduction and reduce the occurrence of overfitting. This makes the network more tractable and robust. Based on the above characteristics, CNNs have gained extensive attention, research, and application in image classification problems. LeNet-5 CNN has an excellent performance in classifying MNIST handwritten digital dataset [16, 17], which opened a new phase of CNN in the field of image classification, and since then, AlexNet [18], VGGNet [19], GoogleNet [20] and other CNNs have been proposed, which have made great progress in image classification and recognition.

## 2.2. Model Structure

**2.2.1. The LetNet-5 Model.** The convolutional neural network is mainly composed of an input layer, a convolutional layer, a pooling layer, a fully connected layer, and an output layer. The neural network is to alternately connect several convolutional layers and pooling layers, that is, a convolutional layer is connected to a pooling layer, and the pooling layer is connected to a convolutional layer. The network structure of the convolutional neural network model LetNet-5 is shown in Figure 1.

The convolutional layer is the core component of a CNN and consists of a series of convolutional kernels. The convolutional operation is as follows:

$$C_{p,j}^{(l)} = f \left( \sum_{l \in M_j^{(l-1)}} \sum_{(u,v) \in k^{(l)}} \left( W_{ij(u,v)}^{(l)} \otimes X_{p,j}^{(l-1)}(x+u, y+v) + b_j^{(l)} \right) \right), \quad (1)$$

where  $C_{p,j}^{(l)}$  is the feature image prime value of the  $p$  training sample in layer  $l$ .  $W_{ij(u,v)}^{(l)}$  denotes the convolution kernel in layer  $l$ ,  $u$  and  $v$  are its step size,  $b_j^{(l)}$  is the bias,  $X_{p,j}^{(l-1)}$  is the feature map in layer  $l-1$ ,  $M_j^{(l-1)}$  is the input mapping in layer  $l-1$ , and  $l$  is the current layer activation function.

The output of the convolutional needs to be nonlinearly mapped by excitation functions such as sigmoid, tanh, and ReLU. The sigmoid and tanh functions are similar and are expressed as follows:

$$\begin{aligned} f(x) &= \frac{1}{1 + e^{-x}}, \\ \tanh(x) &= \frac{2}{1 + e^{-2x}} - 1. \end{aligned} \quad (2)$$

The images of these two functions are shown in Figure 2.

As can be seen in Figure 2, the tanh function converges more quickly than the sigmoid function. Both activation functions suffer from soft saturation, i.e., when the input falls into the saturation zone, it tends to cause the gradient to disappear, thus making the model training slower. The ReLU function is more expressive than the above activation functions, and the gradient of the non-negative interval of ReLU is constant, which can overcome the problem of gradient disappearance, thus maintaining the convergence speed of the model in a stable state. Therefore, the ReLU excitation function is widely used in CNNs with the expression  $f(x) = \max(0, x)$  and its image is shown in Figure 3.

The pooling layer is located in the middle of successive convolutional layers and its main role is to reduce the amount of image data, while ensuring that local features do not change. It speeds up CNN training and also prevents overfitting. Max pooling calculates the maximum value of a local region in the feature map and uses this value as the pooled result. Average pooling is the calculation of the average of the image regions and takes this as the resultant value.

The CNN training has two stages: the forward propagation of the signal and the backward propagation of the error. First, the network weights are initialised and the input infrared image data are passed through convolutional, pooling, and fully connected layers to obtain the output value. The backward propagation refers to the construction of the error function, when the degree of error between the output value and the target value exceeds the set threshold, the error is propagated backwards into the network, and the network weights parameters are adjusted according to the loss function and gradient descent method for another training until the end of training, and its training process is shown in Figure 4.

**2.2.2. Underfitting and Overfitting.** Fitting is the process of taking some discrete data and adjusting the parameters of the function through an algorithm to minimise the sum of the distance between the fitted function value and the data points. The resultant function has the smallest distance between the point set and these discrete data. The effect of underfitting is that the recognition effect of the trained

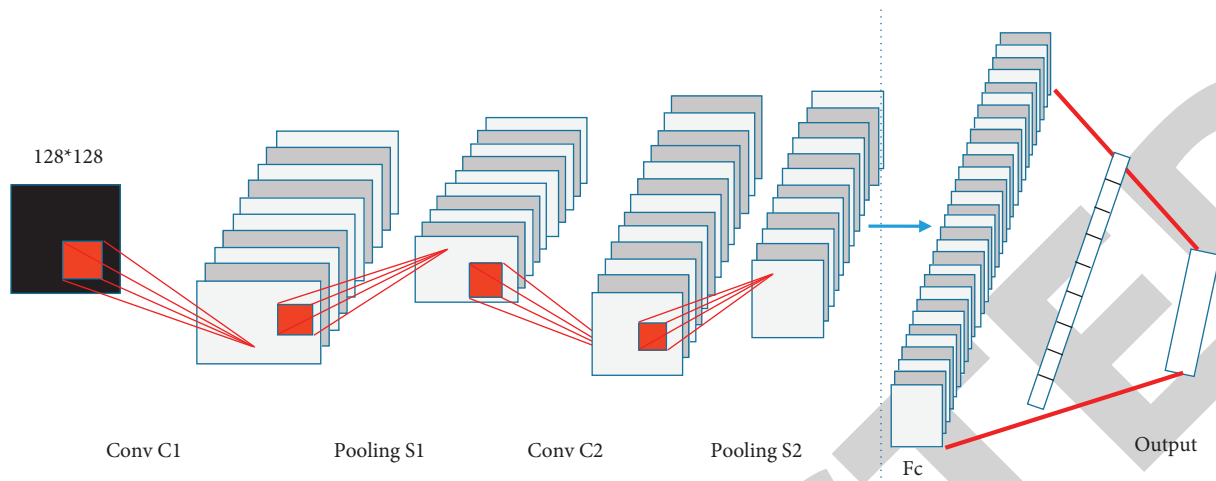


FIGURE 1: CNN structure.

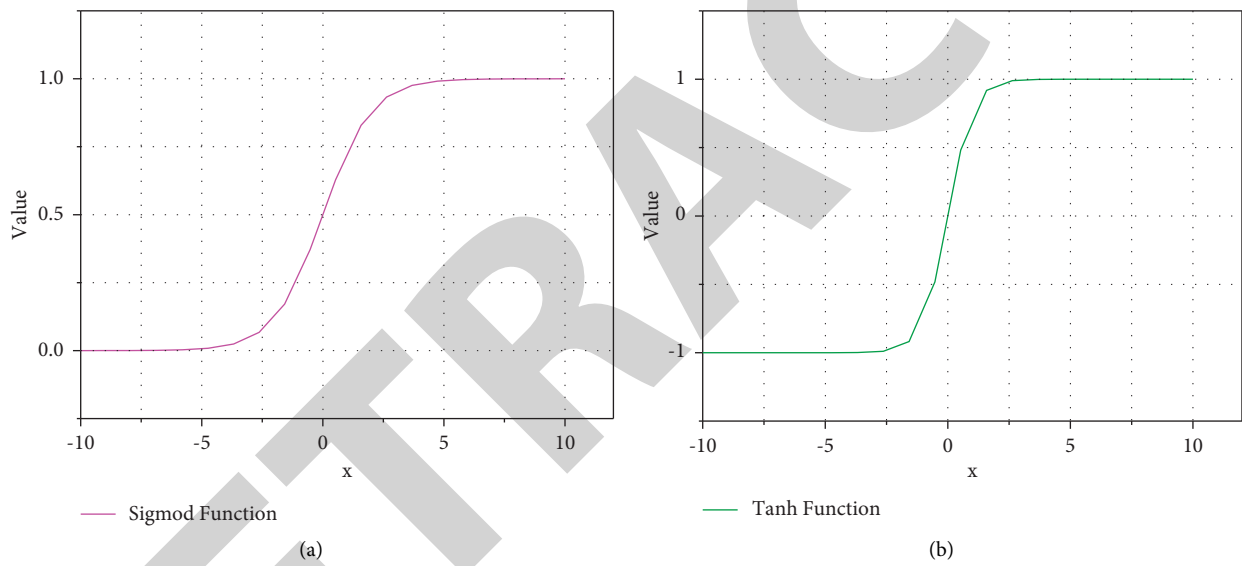


FIGURE 2: Images of sigmoid and tanh functions. (a) Sigmoid. (b) Tanh.

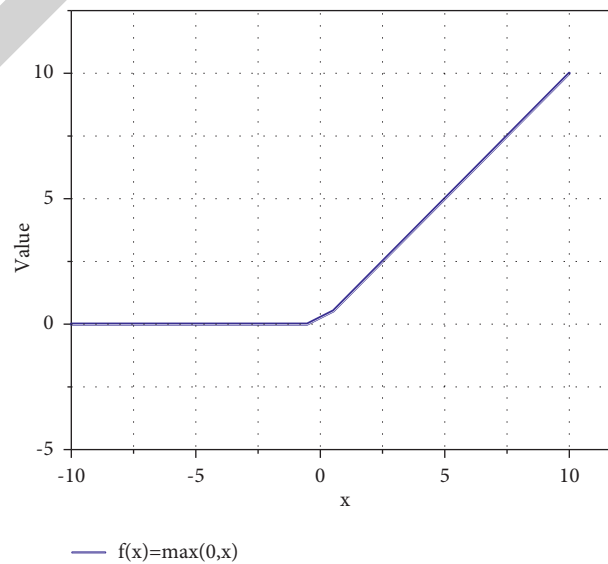


FIGURE 3: ReLU excitation function image.

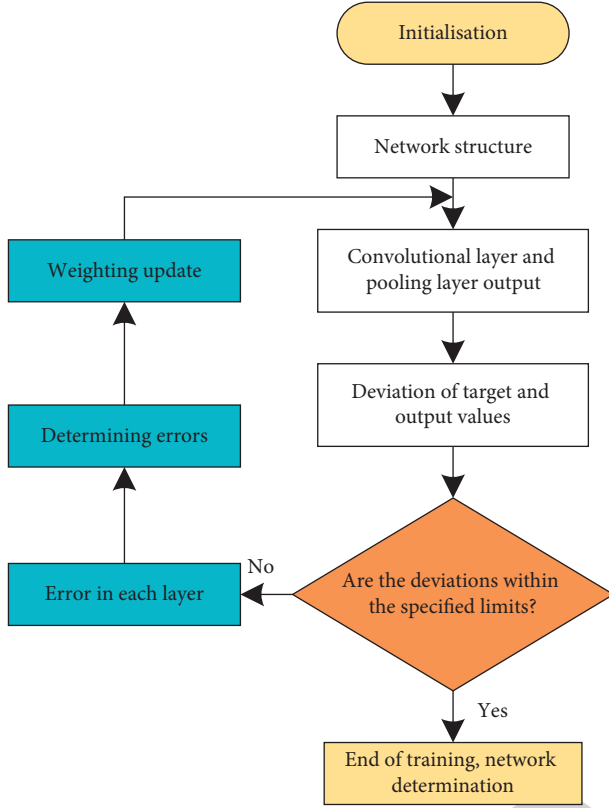


FIGURE 4: Schematic diagram of the CNN training process.

model in the training set and the test set is not good. There are two methods to solve the problem of underfitting, one is to increase the amount of data, and the other is to reduce the complexity of the designed neural network.

Overfitting is manifested by the fact that as the number of training sessions increases, the trained model performs very well in the training set but flattens out in the test set. The reason for this is the inappropriateness of supervised learning, where the backpropagation algorithm iterates backwards to modify the parameters and learn features such as noise as if they were correct. However, the effect of these noisy features should actually be reduced.

### 3. Data Processing

Most of the traditional instrumentation type recognition projects are pointer recognition for a certain type of instrumentation community, or require manual selection of a certain type of instrumentation and then inputting image data for reading. But for intelligent substations and inspection robots, this type of method is not applicable, the inspection robot cannot automatically get the type of instrumentation equipment, and manual operation is too cumbersome. Therefore, we need the inspection robot to “learn” how to recognise which type of instrument the image data collected is, so that the image data can be recognised using the appropriate template and data.

In the present day, computer hardware is developing very fast and is sufficient to support the computational load of deep neural networks in multiple layers. In recent years,

the results of DL in the field of image recognition are well known, so in this study, we will use deep neural networks to identify the type of substation equipment from the image data collected by the inspection robot.

**3.1. Data Set Expansion.** Deep neural networks have a strong fitting capability due to their deeper neural network layers. If the training set is small, it will lead to an overfitting condition, which will inevitably lead to weak generalisation. The results are often unsatisfactory when testing instrumentation data that is in outdoors and a highly variable environment.

However, in the case of outdoor smart substations, there are safety hazards or environmental factors that prevent us from obtaining sufficient data sets. To solve the problem of inadequate data sets, this study uses background replacement, rotation, affine, translation, and noise addition to expand the image data set.

**3.1.1. Image Background Replacement.** The backgrounds and environments, in which instrumentation devices are located, vary little. In order to achieve the diversity and complexity of the image background, the replacement of the background of the instrumentation equipment is achieved by means of image processing. The image augmentation method of background replacement is used for several reasons:

- (1) The background replacement requires a large amount of calculation and has a high success rate, which can lead to a high time complexity if the initial trial data volume is large.
- (2) After the background replacement, the instrument is placed at randomly chosen coordinates, and a richer amount of data can be obtained.
- (3) The manual workload is greatly reduced due to the smaller amount of data and the manual screening of the meter scene replacement if errors occur.

Figure 5 shows the replacement effect after the resolution of the background image was modified to 1000 \* 1000.

**3.1.2. Image Panning and Expansion.** The position, in which the meter is located in the data captured by the inspection robot, is uncertain. When we manually capture image data, we often shoot the meter data in the centre of the image, which is not desirable for later generalisation to identify the input data of the inspection robot. We therefore need to manually perform a translation transform for the dataset so that the meters will exist anywhere in the image, not only expanding the dataset but also enabling the final neural network model to be generalised much more.

The translation transform is a simple transformation where all points on an image are moved horizontally along the  $x$  and vertically along the  $y$  according to a given offset, and is given by

$$\begin{cases} x = x_0 + \Delta x, \\ y = y_0 + \Delta y. \end{cases} \quad (3)$$

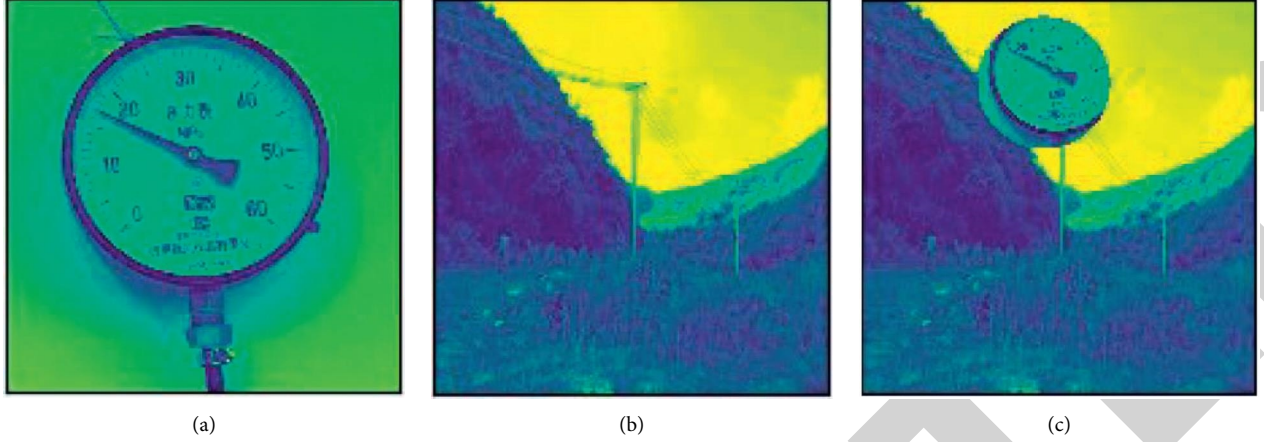


FIGURE 5: Image background substitution effect. (a) Original image, (b) background image, and (c) background replacement.

The equation can be expressed in terms of matrix transformations:

$$\begin{bmatrix} x \\ y \\ 1 \end{bmatrix} = \begin{bmatrix} 1 & 0 & \Delta x \\ 0 & 1 & \Delta y \\ 0 & 0 & 1 \end{bmatrix} \begin{bmatrix} x_0 \\ y_0 \\ 1 \end{bmatrix}. \quad (4)$$

After panning, the choice was made to use white to fill in the excess panned out in order to reduce the distracting elements in the image; in practice, black would cause a greater amount of noise.

**3.1.3. Image Rotation Expansion.** The instrument can be panned to one side by a translation transformation, but there is no guarantee that the instrument will be at a particular position in the graph when the inspection robot is actually collecting data. If the devices in the image dataset used are all at a particular location, then the deep neural network model trained using this dataset will not be available for some of the images acquired by the inspection robot. The CNN model may not achieve accurate recognition, i.e., the depth model does not have excellent generalisation capabilities. In order to make the training model have better generalisation ability and solve the impact of insufficient data sets on model training, image rotation and translation methods are used to analyse the data. At the same time, it can increase the diversity of samples and effectively increase the generalisation ability of training results.

Each image is rotated and transformed to expand the dataset by a factor of eight, which greatly expands the dataset, and after translation and rotation, the positions of the substation images are present at various locations in the image, increasing the diversity of the dataset.

## 4. Experimental Results and Analysis

### 4.1. Experimental Preparation

**4.1.1. Network Structure and Parameter Setting.** The issue regarding the choice of convolutional kernel size in each convolutional layer is different for different classes of

substation equipment images. A large convolutional kernel can easily extract the overall features of the instrument but ignore some detailed features, while a small convolutional kernel, in contrast, can extract detailed feature information but may ignore the overall information of the instrument. The main problem in the structural design is the confirmation of the hidden layer structure, and the relevant parameters designed in this process include the convolution kernel. The size of the feature maps, the size of the pooling kernel, the number of iterations, and the number of batches are influencing factors.

The pixel values of the normally acquired image data are relatively high, but for recognition, such high precision image data are not required and are very consuming in terms of training difficulty and time spent. Therefore, if the image data are uniformly sized at  $128 * 128$  when inputting the acquired data, the main features will be preserved and the training speed will be significantly increased.

**4.1.2. Selection of the Number of Feature Maps.** The number of feature maps in the hidden layer  $n$  means that the image uses  $n$  different  $N * N$  convolution kernels during the convolution machine operation or  $nM * M$  pooling kernels during pooling. In general, the number of feature maps is chosen based on personal experience, but for those using the software, it is not possible to set the number of different layers for each type of image data through experience. Therefore, in this study, the number of feature maps in the convolution and pooling layers are selected automatically from the experimental results, thus avoiding the complicated operation of the staff and improving the recognition rate reduction due to inexperience.

**4.1.3. Initialisation of Weights.** The initialization operations are first performed on the weight matrices in the convolutional and fully connected layers. The multiple iterations of a deep neural network are designed to continuously modify the values in this weights matrix, and therefore, the initialization of weights affects the final recognition rate. If

the range of variation in the initialization of the weights is too large, it will result in more iterations being required to achieve optimal recognition. In this study, the set range of the aggregated weights is  $[-1, 1]$ , and all values in the weight matrix of  $N * N$  are taken randomly from this range. Because the range is small, the number of iterations required is not too large, which greatly improves the speed of computation and achieves the “optimal solution” as quickly as possible.

**4.1.4. Selection of the Activation Function.** The activation function used in this study is ReLU, which is a modified version of ReLU, and is used to solve the problem of necrosis. The main difference with ReLU is that instead of having a value of 0 when  $x < 0$ , it becomes  $ax$ , where  $a$  is a smaller value, in this study  $a = 0.15$ .

$$ReLU(x) = \begin{cases} x, & x > 0, \\ ax, & x \leq 0. \end{cases} \quad (5)$$

**4.2. Parameter Settings.** The parameter settings of the CNN in the study are listed in Table 1.

For the above parameters, the model is randomly reset each time it is executed, and the parameters are saved. If the result of this training does not reach the set recognition rate, it will be reset once again and with different parameters than previously saved until the recognition results reach the set threshold. The neural network model can therefore be applied to the training of any type of substation image data.

**4.3. Experimental Results.** The experimental dataset consisted of 8000 image data and a total of 47 runs of the neural network structure with different parameters.

The relationship between the recognition rate of the CNN model used and the number of different iterations is listed in Table 2.

A visual comparison of the recognition rate of the CNN for different numbers of iterations of the substation equipment image is shown in Figure 6. In Figure 6, the best recognition rate of the substation equipment image is achieved when the number of iterations is 8.

In this training process, the recognition rate of the training set and the recognition rate of the test set are listed in Table 3.

A comparison of the recognition rate data between the training set and the test set for nine different iterations of the substation equipment images is shown in Figure 7.

It can be seen that at iteration number 1, the recognition rate of the image is too low and the model is not performing as it should at this point and there is no value in the study at this point. The recognition time data for single images with iterations 5–9 are listed in Table 4.

A visual comparison of the recognition times of the training and test sets for a single image at different numbers of iterations is shown in Figure 8.

TABLE 1: Parameter settings of the CNN.

Weighting	Normal distribution initialization [0, 1]
Learning_rule	Sad
Learning_rate	0.015
Leanring_momentum	0.9
Weight_decay	0.001
n_iter	1–9
n_stable	10
f_stable	0.001
valid_size	0.1
Verbose	True

TABLE 2: Recognition rate data for different number of iterations.

Number of iterations	Recognition rate (%)
1	93.6
2	97.1
3	97.2
4	97.9
5	98
6	98
7	96.9
8	98.57
9	98.5

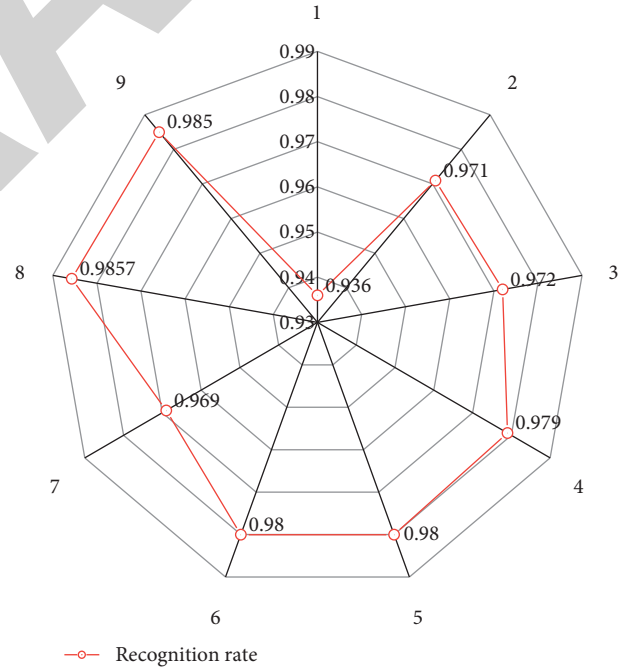


FIGURE 6: Visual comparison of recognition rates of substation equipment images with different iterations.

**4.4. Result Analysis and Recognition Rate Optimization.** The maximum number of iterations was set to 9. However, in some structures, 9 iterations did not reach the optimal number of iterations for the structure, and the training time increased significantly as the number of iterations increased. The model running time and the model recognition accuracy are comprehensively considered. When the number of iterations is set to 9, the recognition accuracy of the model is



TABLE 3: Recognition rate data of the training set and test set for different number of iterations of substation equipment images.

Number of iterations	Train score (%)	Test score (%)
1	93.5	94.5
2	97.2	98.1
3	97.3	97.2
4	97.6	97.5
5	98.1	97.2
6	97.9	97.4
7	96.7	96.2
8	98.6	97.8
9	98.3	97.4

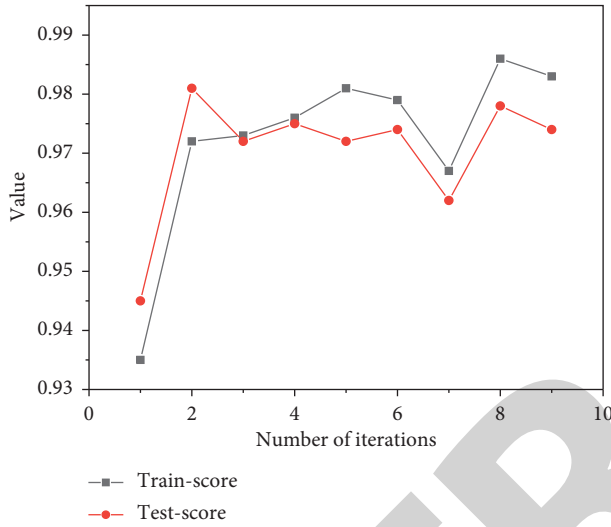


FIGURE 7: Comparison of recognition rates between training and test sets with different iterations.

TABLE 4: Comparison of recognition times (s) for individual images.

Number of iterations	Train score	Test score
5	0.24	0.21
6	0.26	0.23
7	0.27	0.24
8	0.29	0.25
9	0.30	0.27

the best and the running time at this time has less impact on the model. The main idea of integrated learning [21, 22] is to build three neural network structures with high performance and diversity and to combine the three learners to recognise images through a voting strategy. High performance means that each neural network has a relatively high recognition rate, without using multiple “weak learners” for learning.

The voting strategy is often used for prediction of classification problems, and the core idea is that the few follow the many. The prediction category is assumed to have  $N$  classes, and after using multiple neural network models with different parameters to make predictions, the final classification category is based on the one with the highest number of identified classes.

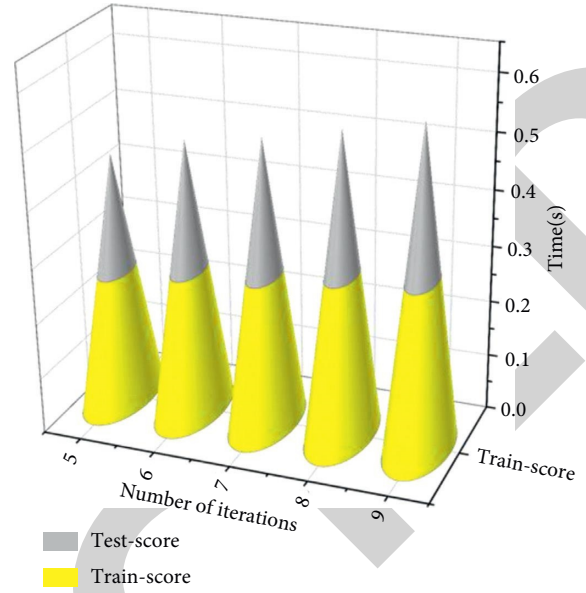


FIGURE 8: Comparison of recognition time for a single image with different number of iterations.

TABLE 5: Five times recognition results of the three neural network models.

Category	Model 1 (%)	Model 2 (%)	Model 3 (%)
1	98.7	98.6	98.4
2	98.6	98.7	98.5
3	98.8	98.5	98.3
4	98.7	98.5	98.3
5	98.7	98.7	98.5

After training the neural network 47 times with different structures, the three neural network models with the highest recognition rates were selected among them and their recognition data are listed in Table 5. Each neural network was experimented five times and the average value was selected as the final result.

The five recognition results for the three neural network models are shown in Figure 9.

The average recognition rates of the three models were 98.7%, 98.6%, and 98.4%, respectively. Using the voting method strategy to combine the three results, the recognition rate data under five experiments are listed in Table 6. Where time conditions allow and the computer configuration is high, an attempt to increase the upper limit of the number of iterations should result in even higher recognition rates. Integrated learning refers to the construction and combination of multiple learners to complete a learning task, sometimes referred to as multiclassifier systems, committee-based learning, etc., and can often achieve significantly better generalisation performance than a single learner. This method is particularly effective for “weak learners.”

As seen in Table 6, the most this recognition rate reached 99.4%. As the computer configuration increases, the upper limit of the number of iterations is also increased, and the use of the voting method strategy further improves the

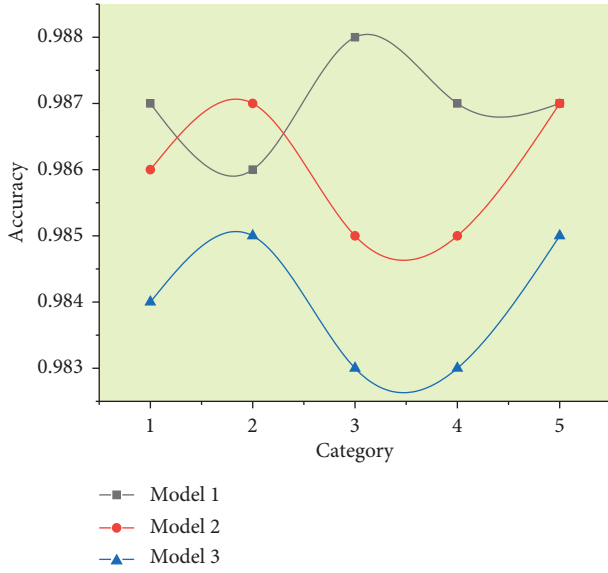


FIGURE 9: Comparison of the five recognition results of the three neural network models.

TABLE 6: Recognition rate data for the voting method strategy for five experiments.

Category	Accuracy (%)
1	99.3
2	99.4
3	99.4
4	99.3
5	99.4

recognition accuracy of the substation equipment. The recognition time for a single image can be controlled compared to previous algorithms, demonstrating the effectiveness of the proposed method.

## 5. Conclusion

Due to the complexity of the current substation environment, the variety of existing equipment and the presence of multiple interferences make the accuracy of image processing algorithms low. This study applies convolutional neural networks to the analysis of substation equipment images, using image translation and rotation methods to expand the sample set and replace the image background. Experiments are carried out on substation equipment images acquired by inspection robots, using automatic training methods for neural networks and an integrated learning voting strategy for substation equipment image recognition. The proposed method improves the training efficiency of the model and achieves a higher recognition rate by combining three strong learners through the voting rule, with an optimal substation equipment image recognition rate of 99.4%. The proposed method is ideal for substation image recognition experiments, but there are more factors that may interfere with the recognition of real devices.

## Data Availability

The experimental data used to support the findings of this study are available from the corresponding author upon request.

## Conflicts of Interest

The authors declare that they have no conflicts of interest.

## References

- [1] M. Yang, S. Ji, W. Xu et al., "Detecting Human Actions in Surveillance Videos," vol. 65, no. 3, pp. 128–132, 2011.
- [2] A. Rehman and T. Saba, "Features extraction for soccer video semantic analysis: current achievements and remaining issues," *Artificial Intelligence Review*, vol. 41, no. 3, pp. 451–461, 2014.
- [3] W. Hu, *Research on Target Detection and Tracking Algorithms Based on Video Images*, Changjiang University, Jingzhou, Hubei, China, 2017.
- [4] H. Y. Zhang, *Research on Some Key Technologies for Early Warning and Prediction of Current-Carrying Faults in Power Equipment*, Zhejiang University, Hangzhou, Zhejiang, China, 2014.
- [5] H. Zhuang li, H. Tong, and Z. Yihui, "Fast image recognition of transmission tower based on big data," *Protection and Control of Modern Power Systems*, vol. 3, no. 3, pp. 149–158, 2018.
- [6] Y. Lecun, Y. Bengio, and G. Hinton, "Deep learning," *Nature*, vol. 521, no. 7553, pp. 436–444, 2015.
- [7] M. Ranzato and Y. LeCun, "A sparse and locally shift invariant feature extractor applied to document images document Analysis and Recognition," vol. 2, pp. 1213–1217, in *Proceedings of the ICDAR 2007. Ninth International Conference on*, vol. 2, pp. 1213–1217, IEEE, Curitiba, Brazil, September 2007.
- [8] Y. Pan, T. Mei, T. Yao, and Y. Rui, "Jointly modeling embedding and translation to bridge video and language," *Computer Science*, vol. 3, no. 6, pp. 4594–4602, 2015.
- [9] Y. Lecun, K. Kavukcuoglu, and C. Farabet, "Convolutional networks and applications in vision," in *Proceedings of the 2010 IEEE International Symposium on Circuits and Systems*, vol. 14, no. 5, pp. 253–256, IEEE, Paris, France, May 2010.
- [10] D. J. Hurley, M. S. Nixon, and J. N. Carter, "Force field feature extraction for ear biometrics," *Computer Vision and Image Understanding*, vol. 98, no. 3, pp. 491–512, 2005.
- [11] C. Quan and F. Ren, "Unsupervised product feature extraction for feature-oriented opinion determination," *Information Sciences*, vol. 272, no. 3, pp. 16–28, 2014.
- [12] D. Erhan, Y. Bengio, A. Courville, P. A. Manzagol, and P. Vincen, "Why does unsupervised pre-training help DL?" *Journal of Machine Learning Research*, vol. 11, no. 3, pp. 625–660, 2010.
- [13] G. Hinton, S. Osindero, M. Welling, and Y. W. Teh, "Unsupervised discovery of nonlinear structure using contrastive backpropagation," *Cognitive Science*, vol. 30, no. 4, pp. 725–731, 2006.
- [14] B. Chen, H. Li, W. Luo, and J. Huang, "Image processing operations identification via CNN," *Science China Information Sciences*, vol. 63, no. 3, pp. 31–45, 2020.
- [15] L. Zhang, Z. Sheng, Y. Li, Q. Sun, Y. Zhao, and D. Feng, "Image object detection and semantic segmentation based on



## *Retraction*

# **Retracted: Construction of Student Mental Health Education Expert Platform Based on Cloud Native Model**

### **Security and Communication Networks**

Received 26 December 2023; Accepted 26 December 2023; Published 29 December 2023

Copyright © 2023 Security and Communication Networks. This is an open access article distributed under the Creative Commons Attribution License, which permits unrestricted use, distribution, and reproduction in any medium, provided the original work is properly cited.

This article has been retracted by Hindawi, as publisher, following an investigation undertaken by the publisher [1]. This investigation has uncovered evidence of systematic manipulation of the publication and peer-review process. We cannot, therefore, vouch for the reliability or integrity of this article.

Please note that this notice is intended solely to alert readers that the peer-review process of this article has been compromised.

Wiley and Hindawi regret that the usual quality checks did not identify these issues before publication and have since put additional measures in place to safeguard research integrity.

We wish to credit our Research Integrity and Research Publishing teams and anonymous and named external researchers and research integrity experts for contributing to this investigation.

The corresponding author, as the representative of all authors, has been given the opportunity to register their agreement or disagreement to this retraction. We have kept a record of any response received.

### **References**

- [1] S. Jin, "Construction of Student Mental Health Education Expert Platform Based on Cloud Native Model," *Security and Communication Networks*, vol. 2022, Article ID 5301723, 15 pages, 2022.

## Research Article

# Construction of Student Mental Health Education Expert Platform Based on Cloud Native Model

Song Jin 

Guangxi Normal University for Nationalities, Chongzuo 532200, China

Correspondence should be addressed to Song Jin; jinsong@gxnun.edu.cn

Received 7 June 2022; Revised 14 July 2022; Accepted 21 July 2022; Published 27 August 2022

Academic Editor: Hangjun Che

Copyright © 2022 Song Jin. This is an open access article distributed under the Creative Commons Attribution License, which permits unrestricted use, distribution, and reproduction in any medium, provided the original work is properly cited.

After completing the function and performance requirements of the system, the architecture design of the college students' mental health expert platform is carried out. The overall design of the platform is introduced as a whole, including the logical architecture, topology architecture, and functional architecture of the system. Due to the particularity of the college student's mental health expert platform, the framework design of the server and the client is made from the system framework level. Then, it introduces the logical design and physical design of the system database, and finally introduces the detailed design of the core function modules in detail. The corresponding weights of each index in the index system are obtained through AHP, and the evaluation model of the mental health expert platform based on AHP is obtained. After testing, it proved that the platform construction was successful. After investigation, more and more students come to the platform for help, and the students believe that functions such as appointment consultation and online consultation should be added.

## 1. Introduction

Modern students are prone to emotional and psychological changes such as inferiority complex, anxiety, and tension due to various pressures. Under the pressure of various aspects of studies, family, and society, students have autism, Internet addiction, running away from home, and other consequences [1–3]. Therefore, it is necessary to carry out the correct psychological education of students to effectively avoid this situation. Many adolescents' psychological problems are not fully recognized by schools and families. Therefore, it is very important to vigorously carry out the work of youth mental health education. According to the World Health Organization, nearly half of the world's population suffers from mental illness that affects their self-esteem, relationships, and ability to function in everyday social life. Individual mental health problems can also affect physical health and lead to poor mental state [4]. A series of social problems have thus occurred. Psychological problems such as depression, anxiety, and schizophrenia are prevalent among young people and college students. With the development and progress of modern education, colleges and

universities pay more and more attention to the mental health of college students. College students have more problems of mental health. The reason is that after entering the university, great changes take place in their living environment, interpersonal relationships, personal roles, and learning methods. If the adjustment is not in place or the adjustment is wrong, it is easy to have problems in some aspects. If these problems cannot be solved in time, it will bring in other psychological problems. It will also directly affect the students' future university life and life in general [5].

For example, the Yao Jiaxin and Ma Jiajue incidents that shocked the whole country have aroused everyone's attention to the mental health of college students. The mental health of college students is not only closely related to the healthy growth of the students themselves but also to the future development of the whole country and society. Therefore, it should pay attention to the mental health development of college students [6, 7]. Timely discovery of students' mental illness and timely and correct guidance of students help to overcome psychological obstacles. Early prevention and treatment of mental illness is one of the most

important tasks of higher education. Mental health refers to a person having a healthy mind. This is affected by many aspects such as culture, family, social atmosphere, education level, and physical health. Every year, October 10th is celebrated as World Mental Health Day. The day is devoted to raise awareness of mental health issues by the UN's mental health and WHO initiative.

With the increasingly prominent mental health problems of college students, the student mental health education and management institutions, such as student mental health education and counseling centers in colleges and universities, have extensively carried out mental health knowledge publicity and education. The school also patiently counsels students with psychological problems and establishes a psychological crisis prevention mechanism to avoid the occurrence of psychological crisis events for students. The main forms are surveys and statistical analysis of mental health problems. By carrying out a series of publicity and education activities such as the Mental Health Festival and devising mental health education courses, a four-level work network will be established to pay attention to students with psychological abnormalities and provide timely feedback. Although college management and institutions have begun to pay attention to the mental health of college students, the following problems still exist [8, 9].

- (1) The proportion of college students who actively seek help is very small. According to a survey report by a consulting agency, among the college students, 23% have mental illnesses requiring psychological treatment, and 26% have minor psychological problems requiring psychological counseling. However, only 3% of students actively seek psychological counseling and help in mental health counseling institutions for college students. From these statistics, it can be seen that the hidden dangers of college students' mental health are particularly prominent.

Figure 1 shows the proportion of students with mental illnesses who need psychological treatment and minor psychological problems who need psychological counseling in the past ten years.

Figure 2 shows the change pattern of students who actively and passive seek psychological counseling and help from college students' mental health counseling institutions in the past ten years.

- (2) There are few information system platforms.

There is no single channel for effective documentation and communication. At present, most psychological counseling institutions set up in colleges and universities do not have effective information-based means to provide psychological counseling to college students, and schools often maintain a face-to-face counseling model. Although some colleges and universities also use some psychological counseling software, the school is only used as a psychological file preservation and psychological counseling record tool. It is used for preliminary psychological assessment and by counselors to

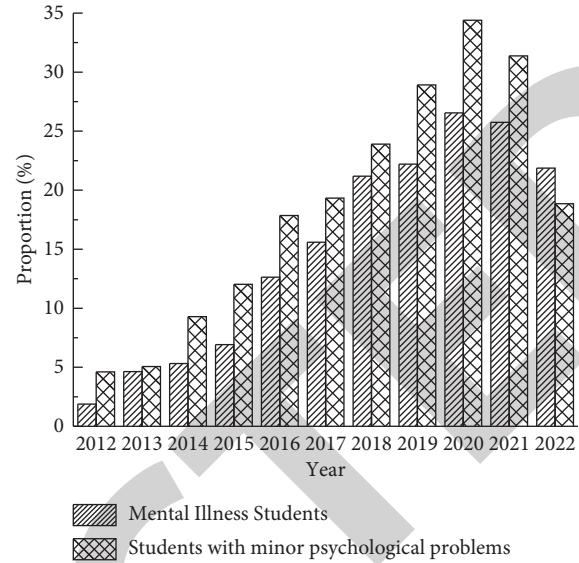


FIGURE 1: Percentage of students requiring psychotherapy and counseling.

record the psychological counseling records of college students. Irrespective of the configuration of software and hardware or the utilization rate of psychological counselors in colleges and universities, it cannot be effectively used. This greatly reduces the role of psychological counseling institutions in colleges and universities.

- (3) There is a lack of effective counseling tracking for college students who receive psychological counseling. It is a step-by-step process for college students to receive psychological counseling, and it is necessary to establish an effective file for each student who receives psychological counseling. If there is no information system to store the psychological counseling cases of college students, it will often lead to serious bias in the results of psychological counseling.

Such problems can be solved by means of information technology. Through the construction of an information system, the mental health counseling of college students is brought into online management. At the same time, through the use of mobile Internet technology, college students' mental health consultation can be conveniently conducted anytime and anywhere through mobile phones, pads, and other mobile devices.

The construction of student mental health education expert platform mainly has the following research significance and purpose [10].

By building an expert platform for students' mental health education, teachers can better understand the psychological problems of college students. Teachers can understand college students' personality, psychological characteristics, values, social adaptation, and other attributes. This is beneficial for teachers to better guide college students, so as to achieve the effect of teaching students in accordance with their aptitude. At present, college students

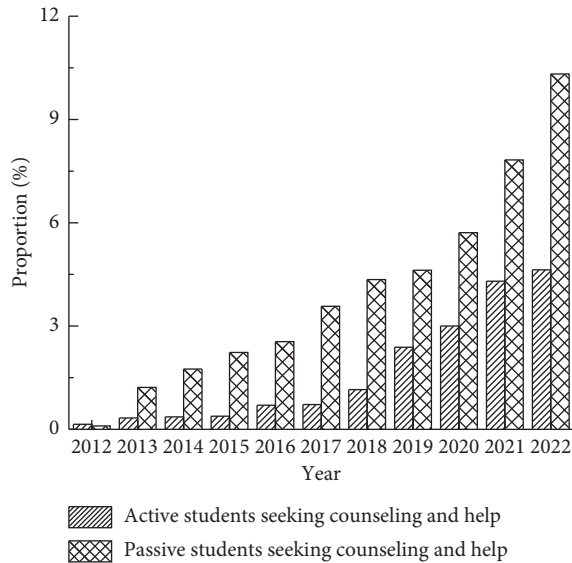


FIGURE 2: Active and passive students seeking counseling and help.

are in a special period of development. Especially, this year's students are born after 1995; their psychology is relatively fragile. Even the post-00 students who are more vulnerable are about to usher in. The changes in physical and psychological activities are rapid, and among them, only children account for a large proportion. They have not experienced tempering since childhood, and their psychological endurance is relatively fragile. The psychological problems exposed in school, interpersonal communication, and life are also increasing day by day. It is very common in daily life for students to escape when they are frustrated.

In recent years, the student mental health education expert platform has been widely used in colleges and universities, and it mainly plays four roles. It is used to comprehensively grasp and understand the mental health status of students. Students who need timely detection of psychological abnormalities provide effective guidance and treatment. It has played a role in promoting mental health, helping students to understand the manifestations of mental problems and enhancing their awareness of mental health care. Mental health education-related research can be conducted using mental health tests.

The platform can assess the psychological development of students. Only through scientific and information-based psychological assessment can schools accurately and timely identify some high-risk groups or individuals with psychological problems among students. Obtain relevant psychological information and mental health data through the platform, so as to carry out guidance on these psychological problems and timely correct prevention of these psychological crises. The prevention of psychological problems or psychological disorders can lead to the occurrence of emergencies. The process of testing students' psychology and feeding back the results of the evaluation, as well as the process of returning to the students who showed abnormality in the psychological test, is also to publicize and popularize the knowledge of mental health among the students. Students need to be actively concerned about their

own mental health issues. The mental health test system is beneficial to guide students to face various psychological troubles correctly and effectively enhance their ability to resist pressure and adapt to society.

## 2. Related Theories

**2.1. Cloud Native.** Cloud-native technologies represented by containers, microservices, and integration of development, operation, and maintenance have reconstructed software development and operation and maintenance models.

Users can build fault-tolerant, easy-to-manage, and observable applications. Cloud native is a set of technology systems and methodologies, a method of building and running applications. Cloud native is a compound word. Cloud means that the application is in the cloud. Native means that the application runs on the cloud. This technology breaks through the shackles of the data center, makes full use of the elasticity and distributed advantages of the cloud platform, and runs in the best posture. Cloud native includes four elements: microservices, containerization, DevOps, and continuous interaction [11–13].

- (1) Microservices are an architectural solution for building application services. Microservices can split application services into multiple core functions. The monolithic solution and the microservice architecture model are shown in Figure 3. Each service corresponds to a function, which can be deployed and built separately, and different services will not affect each other in the event of work or failure. When things go wrong with a service-oriented architecture, just tweaking the microservices used for deployment can fix the problem. Just a little tweaking will do the trick. The advantages of microservice architecture are service decoupling, stronger cohesion, and easier change. The division of services is based on domain-driven design.
- (2) Virtualization technology provides system administrators with great flexibility, but there are problems such as poor performance and low resource utilization. Containers are a new type of virtualization technology that breaks through the bottleneck of traditional virtualization technologies. Docker is the most widely used container engine and is widely used in the infrastructure of companies such as Cisco and Google. Based on LXC technology, containerization provides implementation guarantees for microservices and plays a role in application isolation. Kubernetes is a container orchestration system for container management and load balancing between containers.
- (3) DevOps is a methodology for the integration of development operations and maintenance.

In the life cycle of system applications and services, system developers develop operation and maintenance tools. For example, a large part of the development tools of Google SRE is for operation and maintenance,

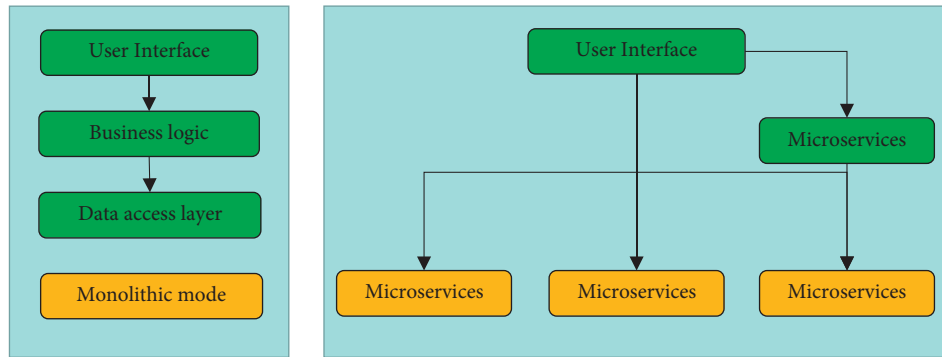


FIGURE 3: Monolithic solution and microservice architecture model.

which makes the operation and maintenance process highly automated and intelligent, and improves the operation and maintenance efficiency. DevOps promotes a change in the way of thinking at work. DevOps pays attention to the diversity of business and people, and provides support for the rapid increase of business value. DevOps emphasizes common goals and takes user value as the only evaluation criterion. It is conducive for the integration of communication and collaboration between technical development, technical operation and maintenance, quality assurance, and other departments. This in turn ensures the timely realization of product functions and ensures successful deployment and stable use.

- (4) Continuous Delivery refers to the software development process, i.e., from the original requirements to the final product development process. It actually refers to the process of testing in a production-like environment after integration and providing timely feedback. Continuous delivery ensures that software is stable and continuously maintained in a state of being released at any time. It allows software to be built, tested, and released faster and more frequently. It can shorten the development time, reduce the development cost, and reduce the risk.

The IT world is undergoing a transformation in order to adapt to rapidly changing IT business needs. Through the cloud native technology system and methodology, users can develop, test, and deploy applications in various fields. Improvements and enhancements are made in each link. Enterprise applications go live faster and ideas come to life faster. It makes it easier to improve business efficiency. Based on the microservice architecture, the cloud native architecture adopts the open source stack for containerized design. With the help of the agile development management model, DevOps supports continuous iteration and intelligent operation and maintenance. The elastic scaling and dynamic scheduling functions of the cloud platform can be used to optimize resource utilization. The cloud native architecture system is shown in Figure 4.

**2.2. Mental Health Concept.** Mental health is a modern civilization concept expanded and sublimated from the connotation of human “health.” Mental health refers to the ability of

the subject to adapt well and to fully develop his or her physical and mental potential. Maintaining the mental health of college students is actually a systematic mental health work. In other words, maintaining the mental health of college students is the ultimate goal, and effective psychological counseling is the way and means to achieve mental health. Regarding mental health, at present, there is no consensus in the academic circles at home and abroad, and there is no generally accepted definition [14].

In 1946, the Third International Congress of Mental Health defined mental health as follows. The so-called mental health refers to the development of the individual's state of mind to the best state within the range that does not contradict the mental health of others physically, intellectually, and emotionally. In 1958, the psychologist Inglis proposed that mental health refers to an ongoing psychological condition. Under that circumstance, the person concerned can make a good adaptation, has the vitality of life, and can give full play to his or her physical and mental potential. It is a positive, rich situation that goes beyond being free from mental illness. College is an important stage of development from adolescence to adulthood. The psychological characteristics of contemporary college students mainly include the following four aspects.

- (1) Students have a strong sense of respect and self-realization

Today's college students are too much loved by their parents. The social environment of reform and opening up has created favorable conditions for it. Many college students have experienced the trials of life, like greenhouse flowers. Students of this type have high self-evaluation. This awareness can make it stand out and inflate confidence. They only want to socialize and play with their peers, and they tend to stay away from people of different generations.

- (2) Strong self-esteem, sensitive to interpersonal relationships

Contemporary college students have very strong self-esteem and do not want to be ignored. They want to be respected and trusted by others, but they tend to be resistant to others' education. The strongest feeling in the psychological counseling of college students is that more than 80% of the psychological problems are related to interpersonal relationships



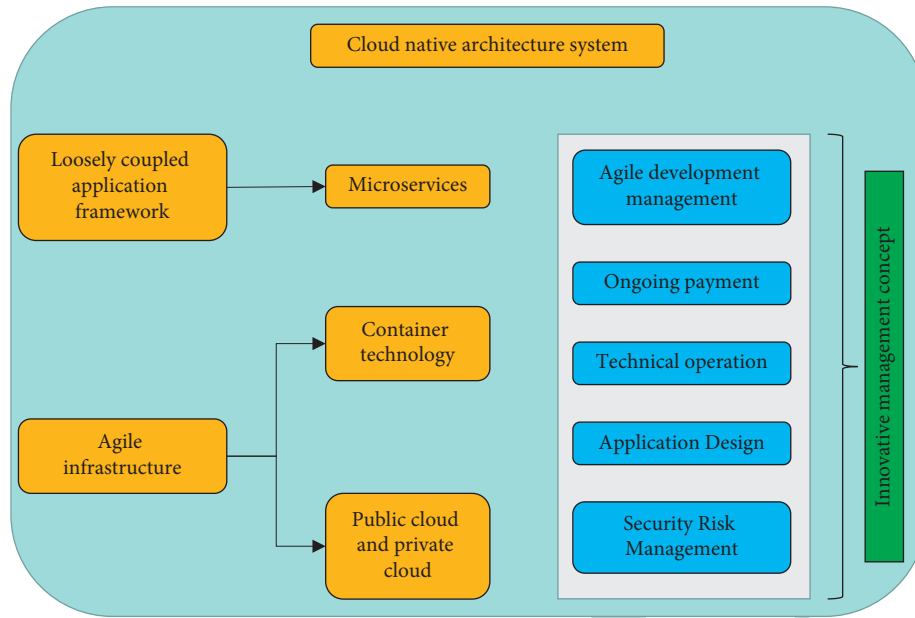


FIGURE 4: The cloud native architecture system.

(including making friends, love, etc.). Modern college students explore their own way of life and values by themselves without “infringing” the unspoken rules of each other’s fields.

(3) Lack of willpower

The age of college students determines that they are in an important period of willpower formation. College students generally lack strong willpower, and they can easily face the general study and daily life. But in the face of key issues, it is possible to show indecision and conformity.

(4) Students have strong creativity but lack the spirit of hard work

There are many ways for modern college students to obtain information. Guided by a variety of information, students are very creative. Modern college students generally lack the ability of self-reliance and the spirit of bearing hardships and standing hard work. All psychological phenomena and mental states related to college students may be problems that affect college students’ mental health. In a word, all psychological phenomena and mental states related to college students may be problems that affect college students’ mental health. Therefore, it is urgent to strengthen the mental health education of college students. This is not only related to the normal study, life, and success of individual college students but also affects the overall quality of a group of talents in the new century in China.

practice. This statement is actually a scientific summary and generalization of the psychological nature of human beings. Psychology first came from Greek. It represents the universal law of spirit or the soul of science. Modern psychology defines psychology as a discipline that mainly studies the laws of the occurrence and development of human psychology [15].

As a new discipline, psychology has a very short history, but this does not mean that the process of psychological development is also very short. In fact, psychology has a very long past. The study of psychology can be traced back to ancient philosophical thought. Religion and philosophy have long ago engaged in in-depth discussions about the relationship between mind and body and how human knowledge arises. Many famous philosophers in ancient times have a lot of expositions on the mind. These philosophers mainly include Aristotle, Wang Chong, Plato, and so on. Modern psychology was born in 1879. In the same year, the world’s first psychology laboratory was established in Leipzig by the German psychologist Wundt, and psychology was officially born as an independent discipline. Since then, psychology has been freed from the shackles of philosophy and has become a truly independent discipline, beginning the real history of psychology. Wundt’s Psychology Laboratory focuses on perceptual psychological processes. Because Wundt is also a well-known physiologist, he mainly uses the experimental techniques of physiology in his research. So he called his research “physiological psychology.” The study of psychology in China originates in the late Qing Dynasty. At that time, it is popular to set up new schools and reform the education system, so it is the first to offer psychology courses in normal colleges and universities. The textbooks used at the time were translated Japanese and Western works. In 1907, “Introduction to Psychology” was translated from English to Chinese by Wang Guowei. In 1917, Peking University established the first psychology laboratory in

**2.3. Psychology and the Concept of Psychology.** In dialectical materialism, psychology is the active reflection of the objective reality produced by the brain in the process of

China. In 1918, China published the earliest psychology book, "The Outline of Psychology." In 1920, China established its first psychology department at Nanjing Higher Normal School.

With the continuous progress of science and technology and the needs of practical life, psychology has developed rapidly in the world, and it mainly has the following characteristics.

- (1) There are too many schools. Shortly after the emergence of psychology, various schools have sprung up like mushrooms after rain, such as schizophrenia, behaviorism, and so on. Although these schools have more or less certain limitations, they also have certain rationality. They carried out in-depth research on psychological phenomena from different aspects and promoted the development of psychology. There were many schools of great influence at that time, such as the humanistic school, the neo-behaviorism school, and so on. Compared with traditional schools, these schools have been greatly improved. For example, they no longer confront each other, but infiltrate and integrate with each other. The emergence of these schools marks the continuous maturation of psychological science and is developing in a unified direction.
- (2) The subdisciplines of psychology have grown dramatically. Compared with traditional psychology, contemporary psychology has a particularly obvious change. That is, the scope of contemporary psychological research is getting wider and wider, and the categories of research are also becoming numerous. If psychology is a big tree that is thriving, then reflexology and reflectionism are the two big branches of this big tree. Reflexology mainly studies social psychology, while reflectionism is the study of individual psychology. There are many small branches growing on these two large branches. For example, in the large branch of individual psychology, child psychology, juvenile psychology, youth psychology, geriatric psychology, military psychology, labor psychology, and so on have emerged. According to incomplete statistics, there are more than 100 branches of psychology at this stage. Different branches study different psychological phenomena in different fields. They, respectively, discussed the laws of people's mental activities in their fields to a certain extent.
- (3) The fields in which psychology can be applied are very broad. In modern society, many psychological research results have certain applications in all walks of life, such as education, military, medical, and other industries. Moreover, psychology can also be applied to many cutting-edge science and technology departments, such as artificial intelligence, bionics, which can fully demonstrate the vitality and true value of psychology.

**2.4. Mental Health Concept.** Mental health is a modern civilization that is sublimated and expanded from human physical health. The traditional understanding of health only refers to physical health, which is one-sided. WHO expanded the concept of health in 1989. Health includes a person's physical, psychological, and social well-being and moral character. More and more people are coming to accept the idea that mental health represents half or more of a person's health. From the above discussion of health, it can be seen that in order to achieve good health, not only should we pay attention to hygiene but also pay attention to psychological hygiene [16, 17].

Mental health is a concept derived from mental health. Mental health refers to a very optimistic state of mind. Mental health generally refers to all the maintenance of mental health activities and the study of mental health as a discipline. In the early twentieth century, American Bills advocated the modern mental health movement. The systematic mental health work is actually to maintain the mental health of college students.

The psychological characteristics of Chinese college students mainly include the following aspects.

- (1) College students in modern society can no longer be confined by certain fixed philosophical thoughts or values and ideologies like those in early society. Modern college students pay great attention to their own feelings and judgments, as well as their experience of reality. They gradually form their own unique value orientation in these feelings and judgments. Although college students in modern society have more information and knowledge than previous college students, their feelings and experiences in real life are far less experienced than those of previous college students.
- (2) The most common phenomenon in the process of psychological counseling for college students is that most of the psychological problems are inextricably linked with interpersonal relationships. Moreover, among college students, there is an unspoken rule of not infringing on each other's fields, and they are exploring their own way of life and values under this unspoken rule.
- (3) Many college students want to be more unrestrained in college, and they try every way to get rid of their troubles. Only after experiencing distress, pain, and anxiety can people overcome the psychological crisis deep in their hearts, so that people can truly grow up. Although, on the surface, modern college students seem to live very casually, without any troubles at all, in fact, their hearts are full of troubles. In this way, there is a big difference between the deep inside of the college students and their external performance. Generally, on the surface, they appear to be carefree, but students are actually troubled inside. All mental transitions and psychological



phenomena related to college students may have an impact on the mental health of college students to a certain extent.

### 3. Construction of College Students' Mental Health Expert Platform

#### 3.1. The Overall Structure of College Students' Mental Health Expert Platform

*3.1.1. The Logical Structure of College Students' Mental Health Expert Platform.* According to the actual business needs of the college student mental health education expert platform, combined with the existing technology accumulation, after analyzing the logical architecture, the logical architecture of this platform construction is obtained, as shown in Figure 5 [18].

(1) *Data Storage Layer.* The data in the mental health management system of college students include structured data and text data. Structured data are stored in the relational database MySQL. All other storage, such as text files, is on the SAN. Since there are many relational queries and transaction processing involved in the system, it is necessary to choose a relational database to better meet the requirements.

(2) *Data Access Layer.* This layer is the middle layer between the processing business logic layer and the data storage layer. The database access layer needs to meet the requirements of accessing relational databases and file storage. Accessing the relational database requires JDBC, and the upper layer maps business logic entities to the database table structure through the mybatis framework. Access to disk storage requires disk read and write operations through the FileUtil framework.

(3) *Business Logic Layer.* It is necessary to use Spring and SpringMVC to implement the business logic layer, and all business logic is processed in this layer. The business logic layer obtains data through the data access layer, and then operates on the data in combination with business logic. At the same time, the operation results are stored in the data storage using the data access layer, and the business processing results are transmitted to the presentation layer through the interface layer.

(4) *Interface Layer.* The role of the interface layer is to directly transmit data in the presentation layer and the business logic layer. The interface layer encapsulates the data results of the business logic layer and then transmits them. The client obtains the data of the business layer by calling the interface of the interface layer for presentation.

(5) *Presentation Layer.* The platform adopts a cloud-native framework. For some pages, the webview is used to load html5 for display, and the hybrid development mode of hybrid can ensure that the operating efficiency of the platform is greatly improved.

*3.1.2. Topological Structure of College Students' Mental Health Expert Platform.* The college students' mental health management system uses two servers as application server clusters. Load balancing is done by nginx on these two servers. When the traffic volume is too large, the requests can be divided into two servers, which can ensure the high availability of the system.

The SMS and e-mail server is a single server that handles all requests to send SMS and emails. The SMS server needs to be externally connected to the SMS gateway provided by the supplier. Therefore, a specific network route needs to be opened to ensure that the external network can be accessed.

Since both the application server and the database server are deployed on the intranet of Qilu Normal University, the network environment is not necessarily the intranet when college students access the college students' mental health management system through mobile phones. Therefore, it is necessary to do internal and external network mapping on the firewall. When college students are on the external network, they can access the internal network system through firewall mapping. When college students are in the intranet, they can directly access the system.

*3.1.3. The Functional Structure of College Students' Mental Health Expert Platform.* After a detailed demand analysis of the college students' mental health management system, it can be understood that the functional modules of the system can be analyzed from two aspects. It is analyzed from the role of college students and the role of psychological counseling teachers. The functions of college students' roles in the mental health management system mainly include psychological assessment, online consultation, appointment, and viewing related articles. The main functions used by psychological counselors in the system are evaluation management, questionnaire management, online consultation, and appointment management. At the same time, it must have the ability to publish mental health-related articles.

*3.2. Framework Design of College Students' Mental Health Expert Platform.* Since the server and client are separate architectures, both the server and the client can interact with data through interfaces. Therefore, the server and client need to be architected separately [19].

From the perspective of logical architecture, the server-side covers the data access layer, business logic layer, and interface service layer. Therefore, J2EE's Spring, SpringMVC, and myBatis frameworks can be used as the technical framework of the server when selecting the server-side architecture. The specific operation logic is that myBatis is responsible for the data access layer. Spring is responsible for the management of all beans, and SpringMVC implements the business logic layer.

Each entity must have a corresponding Model object. The return result of each interface must have a corresponding DTO object, and the Model object corresponds to the table structure of the database. The DTO object corresponds to the JSON object returned by the data interface.

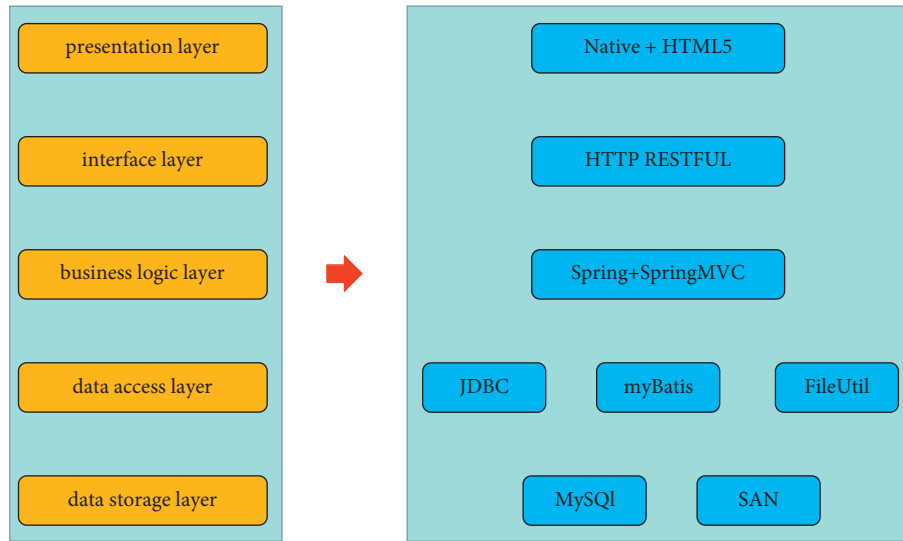


FIGURE 5: Logical architecture of platform construction.

When the data access layer performs database operations, all parameter transfer and return result objects are transmitted by the Model object.

Since SpringMVC is used as the implementation of the business logic layer, according to the characteristics of SpringMVC, the business processing process can be standardized. The steps for the business layer to process client requests are described below.

- (1) The platform sends requests to the Controller layer, and the request methods can be divided into GET and POST. PUT and DELETE operations can be ignored here. Need to follow RESTFUL style architecture. All parameters must be able to be data bound so that the controller in the background can receive the parameter data passed by the platform client.
- (2) After the controller receives the client request, it first parses the parameters. The request is forwarded to the corresponding Service layer for processing according to the actual business logic.
- (3) Service is the core class for processing business, and all business logic implementations are done by Service. If the service's business processing logic needs to interact with the database, the service will access and request database data through DAO.
- (4) The DAO layer utilizes the functionality provided by myBatis for database access. The data returned by the database need to be wrapped into a Model entity.
- (5) The data returned by DAO needs to be encapsulated in the format required by the Service.
- (6) After the Service layer receives the data returned by DAO, it performs operations according to the actual business logic, and then extracts the data from the Model.
- (7) The Service encapsulates the data into the required DTO and returns it to the Controller.
- (8) If the data returned by the Controller requires the cooperation of multiple Services, the Controller can also encapsulate multiple DTO objects into the final required DTO objects.
- (9) The Controller will return the data to the platform client according to the DTO format finally required by the client.

After the server-side framework is determined, all functional modules must follow this step to complete the code development. The entire project can maintain a consistent style, which greatly improves the readability of the code and future scalability.

**3.3. Network Layer Design.** The network layer mainly implements the client's network request through the Volley network transmission framework. The Volley framework can handle both synchronous and asynchronous network requests. Volley is said to possess the advantages of AsyncHttpClient and Universal-Image-Loader in one. It can perform HTTP communication as easily as AsyncHttpClient, or load pictures on the network as easily as Universal-Image-Loader. In addition to being simple and easy to use, Volley has also undergone significant adjustments in performance. Its design goal is to be very suitable for network operations with a small amount of data but frequent communication. Since the network transmission of the college students' mental health management system does not involve a large number of file download operations, it is appropriate to choose Volley as the network layer transmission framework [20–22].

Combined with the specific needs of college students' mental health management system, college students and psychological counselors have different functions when using the platform. And the number of first-level functional modules is limited, so it can be implemented by ViewPager. This time we introduce the solution of using ViewPager to implement Tab because the Views of all Tab pages of ViewPager are generated in MainActivity.

**3.4. Database Design of College Students' Mental Health Expert Platform.** When designing a database, it must first analyze the entities in the system. The simplest and most convenient entity extraction method is to discover the noun method. The nouns involved in the requirements are extracted for further analysis. The nouns obtained from the demand include college students, psychological counseling teachers, psychological assessment questions, psychological assessment records, questionnaires, questionnaire records, consultation messages, appointment records, message records, announcement information, article information, personal information, etc. By extracting these nouns and analyzing the relationship between entities, the E-R entity relationship of the system can be obtained.

After completing the logical design of the database, and knowing the table structure of the database, it is necessary to determine the naming conventions of the database, tables, and fields to be used in the physical design stage to choose the appropriate storage engine, and choose the appropriate data type for the fields in the table. Only in this way can a complete database structure design be established.

#### 4. Functional Design of College Students' Mental Health Education Expert Platform

The platform function design mainly includes the following parts, as shown in Figure 6.

**4.1. Forum Module.** The forum module of the college student's mental health education expert platform includes four areas: chatting, sharing skills, asking for help, and forum construction [23].

- (1) The chatting area contains three sub-modules. Focus on the current news, policies, and hotspots of college students' mental health education.
- (2) In the face of college students' mental health education teaching and case processing, it is necessary to collect more opinions and ideas of the student group.
- (3) Strategies, methods, suggestions, etc., of college students' mental health education knowledge sharing, no matter how simple or complex, whether they are operable or not, as long as they are their own words, they can be published here.

The Qiao Shared Area contains two sub-modules.

- (1) Explicit knowledge of college students' mental health education  
Theoretical knowledge about college students' mental health education and teaching, the use methods and rules of testing instruments, etc., can be informed to other college students' mental health education teachers and experts in the current module to share knowledge.
- (2) Teaching tips and tricky questions.  
This module focuses on the sharing of tacit knowledge of college students' mental health education teachers and experts. Experience or method

guidance can be given to some new teachers who do not know how to explain the theoretical knowledge or specific cases that they do not know how to deal with.

The Helpdesk area contains two sub-modules.

- (1) Explicit Knowledge of College Students' Mental Health Education  
If you do not understand the theoretical knowledge of college students' mental health education and teaching, the use of methods and rules of testing instruments, etc., you can ask for help in the current module.
- (2) Teaching Tips and Tough Issues  
This module focuses on the sharing of tacit knowledge of college students' mental health education teachers and experts. Students can seek help for some theoretical knowledge that they do not know how to explain in teaching or specific cases that they do not know how to deal with.

**4.2. Expert Tree Module.** The expert information not only introduces the names, genders, and contact information of experts and scholars but also collects the learning experiences, research results, and participation in scientific research projects of experts and teachers from an objective perspective. This module page contains five sub-modules: keyword search, expert category, expert personal information, expert experience learning, and expert talks. Expert maps store expert description documents. Experts are classified according to their professional knowledge. Teachers and experts of mental health education for college students can get in touch with experts in the field through the expert map. For example, when college students' mental health education teachers encounter problems in practice, they can find experts in this field to communicate with them through the expert map. Topic and expert association maps can locate the connections between knowledge and experts.

**4.3. The Resource Area Module.** The resource area module of the knowledge sharing platform for college students' mental health education mainly includes five submodules: teaching cases, teaching videos, teaching reflection, experience skills, and intractable diseases.

**4.3.1. Teaching Sample.** It can display excellent teaching cases of college students' mental health education.

**4.3.2. Teaching Video.** It can display excellent teaching videos of college students' mental health education.

**4.3.3. Teaching Reflection.** Excellent college students' mental health education teachers and experts make daily reflections on their own teaching methods and methods of dealing with college students' mental health cases.

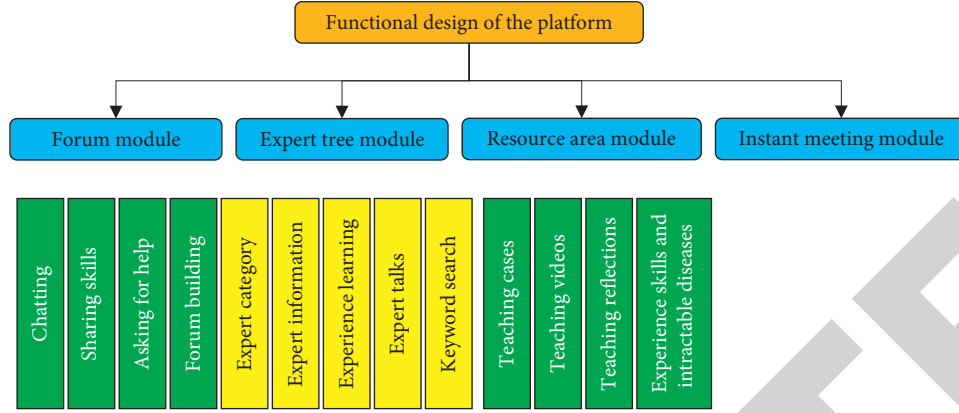


FIGURE 6: Platform functional design framework.

**4.3.4. Experience Skills and Difficulties.** It mainly includes excellent college students' mental health education teachers, experts' daily teaching experience, case analysis and processing experience, skills, and methods of communicating with students.

**4.4. Message Board Module.** The message board module of the knowledge sharing platform for college students' mental health education is a section that provides a platform for members and non-members to communicate with each other. It can enhance mutual communication, trust, and promote sharing. In this section, every member and expert can leave messages to each other. It can be a blessing to others, a promise, a greeting to everyone, and so on. It can not only enhance mutual trust but also create a good environment for sharing and lay a firm foundation.

**4.5. Instant Meeting Module.** When college students encounter problems and difficulties in mental health education, they can invite other teachers and experts on the platform to talk, analyze, and summarize, and come up with favorable treatment methods and approaches. In this module, experts can also be selected. Students can choose and appoint experts for the problems in teaching and cases that you encounter. In this way, the difficulties in reality can be better solved, and the problems in teaching and cases can be better solved.

After investigation, schools that adopted the platform in the follow-up achieved better results in helping students' mental health. More and more students have come to the platform to seek help. However, the students believed that they should also combine the school's own resources and the needs of the students to develop special functional sections. After research, the students believe that functions such as appointment consultation and online consultation should also be added. The student support rate for each function is shown in Figure 7.

## 5. Construction of Evaluation Index System of Mental Health Expert Platform

On the basis of literature research and actual investigation, establish the first-level indicators for evaluation of the mental health expert platform. The constituent

elements under the first-level index category are summarized and refined to form the second-level index. Then, the hierarchical structure of the evaluation indicators can be completed and the construction of the evaluation system of the mental health expert platform can be realized [24].

The first-level indicator to be determined is the mental health expert platform (A1). The other three first-level indicators are defined as user experience (A2), content construction (A3), and service functions (A4). From the first-level indicators of the mental health expert platform, five elements of developer identity (b1), related platforms (b2), release year (b3), platform developed technology (b4), and update frequency (b5) can be extracted as second-level indicators. Six indicators of frequency of use (b6), total usage platform rating (b7), operational convenience (b8), total number of students (b9), number of registrants (b10), and functional pertinence (b11) are selected as the secondary indicators under user experience. Five indicators of overall style (b12), typesetting layout (b13), content timeliness (b14), content division (b15) and content diversity (b16) are extracted as secondary indicators under content construction. Four indicators of online consultation (b17), expert services (b18), health records (b19), and extended functions (b20) are extracted as secondary indicators under the service function.

First, the judgment matrix  $A$  is established as follows:

$$A = \begin{bmatrix} 1 & 3 & 5 & 7 \\ 1/3 & 1 & 2 & 5 \\ 1/5 & 1/2 & 1 & 3 \\ 1/7 & 1/5 & 1/3 & 1 \end{bmatrix}. \quad (1)$$

The feature vector  $W$  can be expressed as

$$W = \begin{bmatrix} 0.4729 \\ 0.2844 \\ 0.1699 \\ 0.0729 \end{bmatrix}. \quad (2)$$

Equation (3) can be obtained by multiplying the judgment matrix and the eigenvector  $W$ .

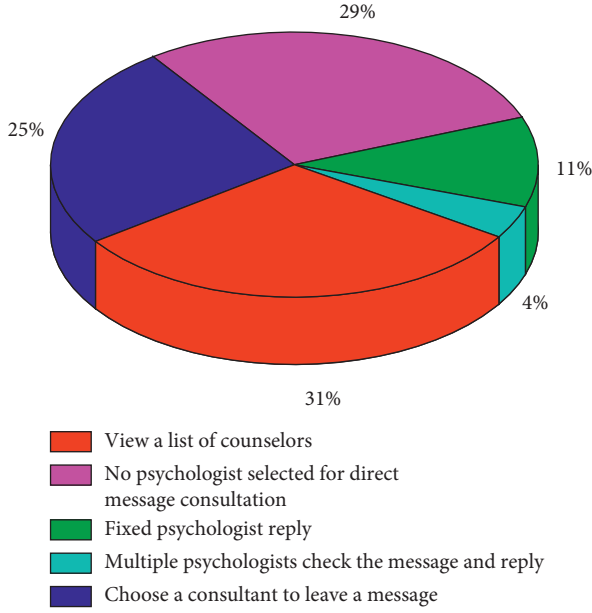


FIGURE 7: The student support rate for each function.

$$AW = \begin{bmatrix} 1 & 3 & 5 & 7 \\ \frac{1}{3} & 1 & 2 & 5 \\ \frac{1}{5} & \frac{1}{2} & 1 & 3 \\ \frac{1}{7} & \frac{1}{5} & \frac{1}{3} & 1 \end{bmatrix} \begin{bmatrix} 0.4729 \\ 0.2844 \\ 0.1699 \\ 0.0729 \end{bmatrix} = \begin{bmatrix} 2.6859 \\ 1.1463 \\ 0.6254 \\ 0.2540 \end{bmatrix}. \quad (3)$$

The maximum eigenvalue  $\lambda_{\max}$  and CI value can be obtained.

$$\begin{aligned} \lambda_{\max} &= 4.1289, \\ \text{CI} &= 0.0729. \end{aligned} \quad (4)$$

By looking up the table, when  $n=4$ ,  $\text{RI} = 0.89$ . Therefore, equation (5) can be obtained.

$$\text{CR} = 0.0191 < 0.1. \quad (5)$$

Therefore, the judgment matrix has good consistency.

The calculation steps of the maximum eigenroot  $\lambda_{\max}$  of the judgment matrix are as follows [25].

$$M_i = \prod_{j=1}^n c_{ij}. \quad (6)$$

The  $n$ th root of  $M_i$  can be calculated as

$$\bar{W}_i = \sqrt[n]{M_i}. \quad (7)$$

By normalizing the vector  $W(-)$ , we can get

$$W_i = \frac{\bar{W}_i}{\sum_{j=1}^n \bar{W}_j}. \quad (8)$$

The maximum eigenroot of the judgment matrix can be calculated as

$$\lambda_{\max} = \sum_{i=1}^n \frac{(CW)_i}{nW_i}, \quad (9)$$

where  $(CW)_i$  is the  $i$ th element of the vector  $CW$ .

Similarly, the judgment matrix of the first-level index layer can be obtained as

$$B_1 = \begin{bmatrix} 1 & 2 & \frac{1}{7} & \frac{1}{5} & \frac{1}{3} \\ \frac{1}{2} & 1 & \frac{1}{9} & \frac{1}{7} & \frac{1}{7} \\ 7 & 9 & 1 & 3 & 5 \\ 5 & 7 & \frac{1}{3} & 1 & 2 \\ 3 & 5 & \frac{1}{7} & \frac{1}{2} & 1 \end{bmatrix},$$

$$W_1 = \begin{bmatrix} 0.0585 \\ 0.0362 \\ 0.5227 \\ 0.2419 \\ 0.1406 \end{bmatrix},$$

$$B_2 = \begin{bmatrix} 1 & 3 & 7 & 2 & 5 & 5 \\ \frac{1}{3} & 1 & 5 & \frac{1}{2} & 3 & 3 \\ \frac{1}{7} & \frac{1}{5} & 1 & \frac{1}{5} & \frac{1}{3} & \frac{1}{3} \\ \frac{1}{2} & 2 & 5 & 1 & 3 & 3 \\ \frac{1}{5} & \frac{1}{3} & 3 & \frac{1}{3} & 1 & 1 \\ \frac{1}{5} & \frac{1}{3} & 3 & \frac{1}{3} & 1 & 1 \end{bmatrix},$$

$$\begin{aligned}
 W_1 &= \begin{bmatrix} 0.3959 \\ 0.1757 \\ 0.037 \\ 0.234 \\ 0.0787 \\ 0.0787 \end{bmatrix}, \\
 B_3 &= \begin{bmatrix} 1 & \frac{1}{5} & \frac{1}{7} & 3 & 2 \\ 5 & 1 & \frac{1}{7} & 5 & 3 \\ 7 & 3 & 1 & 9 & 8 \\ \frac{1}{3} & \frac{1}{5} & \frac{1}{3} & 1 & \frac{1}{2} \\ \frac{1}{2} & \frac{1}{3} & \frac{1}{5} & 2 & 1 \end{bmatrix}, \\
 W_1 &= \begin{bmatrix} 0.0922 \\ 0.2504 \\ 0.5488 \\ 0.0417 \\ 0.067 \end{bmatrix}, \\
 B_4 &= \begin{bmatrix} 1 & \frac{1}{5} & \frac{1}{3} & \frac{1}{7} \\ 5 & 1 & 2 & \frac{1}{3} \\ 3 & \frac{1}{2} & 1 & \frac{1}{5} \\ 7 & 3 & 5 & 1 \end{bmatrix}, \\
 W_1 &= \begin{bmatrix} 0.0563 \\ 0.2388 \\ 0.131 \\ 0.5738 \end{bmatrix}. \tag{10}
 \end{aligned}$$

The maximum eigenvalue of the second index is shown in Figure 8.

After calculation, the CR values of the first-level index layer matrix are all less than 0.1. Therefore, all judgment matrices have good consistency. Through the calculation of the weights of all levels of the index system relative to the total target weight, the composite weight of the index system is finally obtained, as shown in Figure 9.

In general, the weight of mental health expert platform indicators is relatively heavy. When designing and developing a relevant mental health professional platform, the risk of possible personal information leakage should be considered. Through the establishment of a reasonable identification and identification mechanism, access control and communication technology encryption processing and ensuring the user's mental health needs are realized. At the same time, it realizes basic information security protection and reduces the

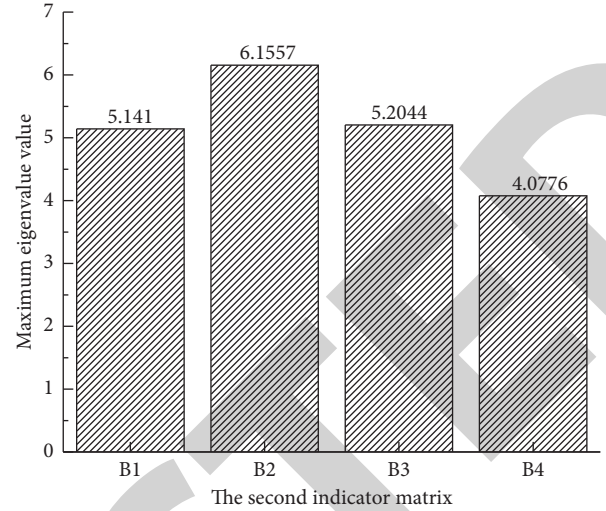


FIGURE 8: The maximum eigenvalue of the second index.

concerns of users with mental health needs in terms of information security. Overall, the build of the platform is a success.

## 6. Suggestions for Improving the Platform

**6.1. Pay Attention to Student Experience and Improve Content Construction.** User experience and content construction appear as two independent first-level indicators, but in practice, the elements of user experience and content construction overlap. User experience and content creation are actually two sides of the same problem. One problem is that of quality management. The two aspects are the quality management problem from the user's point of view and the quality management problem from the design developer's point of view. The needs of users are changing, and whether a platform builder can follow-up or even lead to the needs of users in a timely manner is an important criterion for judging a platform builder. As far as mental health services are concerned, the current development of the mental health expert platform is facing a dilemma because the mental health expert platform is seriously homogenized in terms of service methods and service content. In the actual survey, the basic service mode of most mental health expert platforms provides users with basic mental health knowledge science, online tests, and mental health questions and answers.

**6.2. Develop Social Features.** From the user's point of view, when individual users seek mental health knowledge services through the platform, it is easy to get feedback and experiences from other users on related psychological issues. The feedback and experience of this kind of related psychological problems have positive effects on patients with the same disease. Mental health services are services that value speaking and communication. Faced with emotional problems, anxiety, social pressure, and other mental health problems and diseases, finding a way to communicate freely with people is often a good medicine to solve their psychological problems.



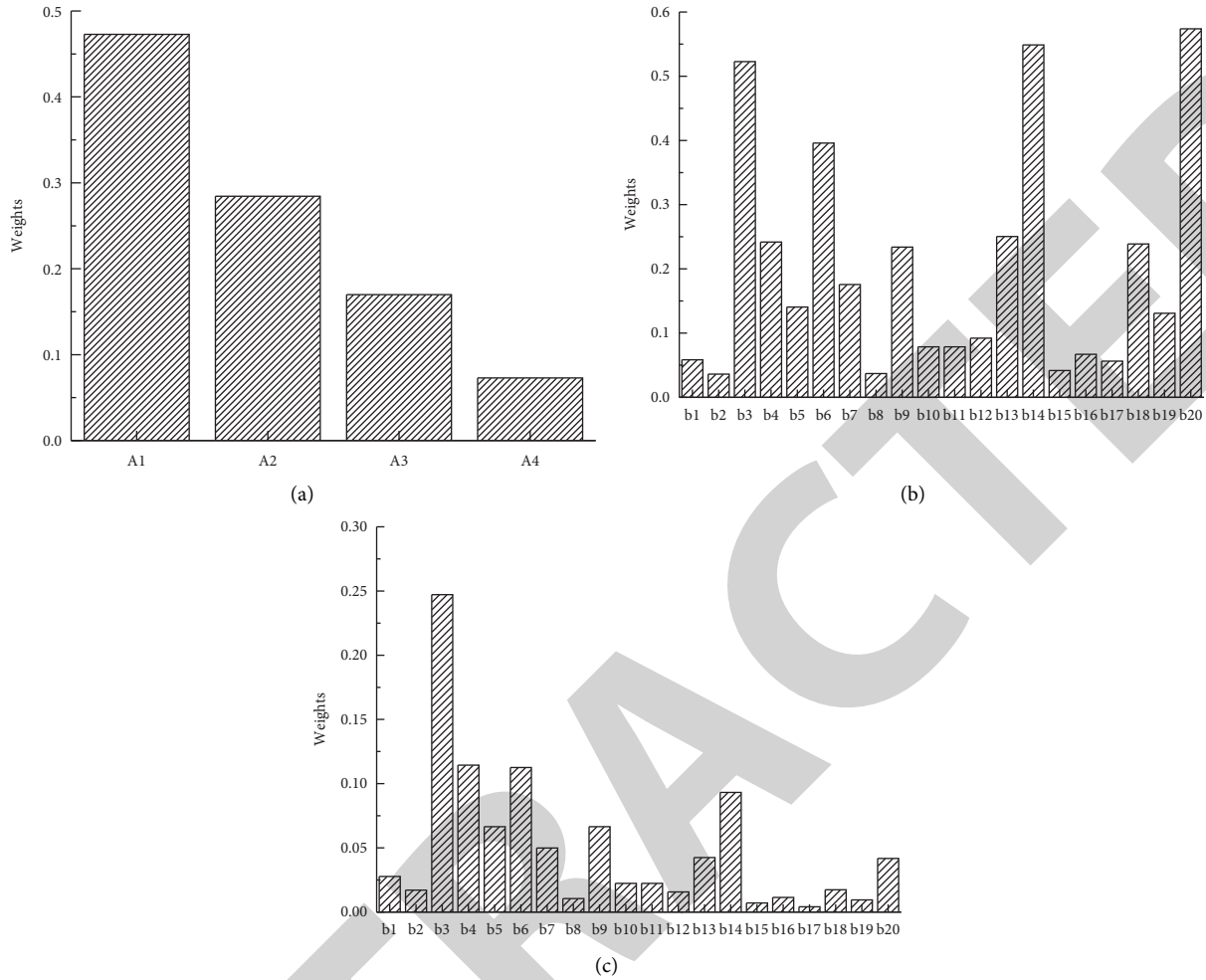


FIGURE 9: Weights of primary indicators, secondary indicators, and composite weights (a) The weight of the first-level indicator. (b) The weight of the secondary-level indicator. (c) Composite weights.

From the perspective of developers, while improving content construction and optimizing user experience, they should seek innovation in service functions. Adding social functions is a feasible attempt to extend the functions of the platform. Excellent community building and user management can significantly improve user stickiness and usage habits. The construction of good social functions can help mental health service agencies retain a group of loyal users with mental health needs.

**6.3. Pay Attention to the Safety of the Mental Health Expert Platform.** Different from the previous understanding, after the evaluation and research on the mental health expert platform, it is found that there are hidden dangers in the confidentiality of communication and the security of content in the mental health category in the mobile environment. The establishment of the security mechanism here is the same as the requirements for the construction of the Xinlu Health Knowledge Service website. When designing and developing a related mental health platform, the risk of possible medical information leakage should be taken into consideration. It is necessary to establish a reasonable

identification and identification mechanism, realize access control and encryption processing of communication technology, to ensure the mental health needs of users. At the same time, it realizes basic information security protection and reduces the concerns of users with mental health needs in terms of information security.

## 7. Conclusion

Around the platform design, firstly, the overall design of the system is introduced as a whole. It includes the logical architecture, topological architecture, and functional architecture of the system. Due to the particularity of the mental health management system for college students, the server and Android client are designed from the system framework level. Then, the logical design and physical design of the system database are introduced. Finally, the detailed design of the core functional modules is introduced in detail, and the design of the mental health management system for college students has been completed.

The server-side technology of the platform adopts the J2EE open source framework, which ensures that the college student mental health expert platform has scalability and



easy maintenance. Although as a platform for colleges and universities, due to the consideration of distributed deployment in the system design, the performance has also reached the level of Internet applications. It is guaranteed that the system does not need to expand hardware to improve system performance within five years.

After investigation, schools that adopted the platform in the follow-up achieved better results in helping students' mental health. More and more students have come to the platform to seek help. However, the students believed that they should also combine the school's own resources and the needs of the students to develop special functional sections. Overall, the build of the platform is a success.

## Data Availability

The data used to support the findings of this study are available from the author upon request.

## Conflicts of Interest

The author declares that there are no conflicts of interest or personal relationships that could have appeared to influence the work reported in this paper.

## References

- [1] S. B. Oswalt, A. M. Lederer, K. Chestnut-Steich, C. Day, A. Halbritter, and D. Ortiz, "Trends in college students' mental health diagnoses and utilization of services, 2009–2015," *Journal of American College Health*, vol. 68, no. 1, pp. 41–51, 2020.
- [2] C. Son, S. Hegde, A. Smith, X. Wang, and F. Sasangohar, "Effects of COVID-19 on college students' mental health in the United States: interview survey study," *Journal of Medical Internet Research*, vol. 22, no. 9, Article ID e21279, 2020.
- [3] R. Corona, V. M. Rodríguez, S. E. McDonald, E. Velazquez, A. Rodriguez, and V. E. Fuentes, "Associations between cultural stressors, cultural values, and latina/o college students' mental health," *Journal of Youth and Adolescence*, vol. 46, no. 1, pp. 63–77, 2017.
- [4] W. Fu, S. Yan, Q. Zong et al., "Mental health of college students during the COVID-19 epidemic in China," *Journal of Affective Disorders*, vol. 280, pp. 7–10, 2021.
- [5] S. Griggs, "Hope and mental health in young adult college students: an integrative review," *Journal of Psychosocial Nursing and Mental Health Services*, vol. 55, no. 2, pp. 28–35, 2017.
- [6] S. K. Lipson, E. G. Lattie, and D. Eisenberg, "Increased rates of mental health service utilization by U.S. College students: 10-year population-level trends (2007–2017)," *Psychiatric Services*, vol. 70, no. 1, pp. 60–63, 2019.
- [7] E. G. Lattie, E. C. Adkins, N. Winkvist, C. Stiles-Shields, Q. E. Wafford, and A. K. Graham, "Digital mental health interventions for depression, anxiety, and enhancement of psychological well-being among college students: systematic review," *Journal of Medical Internet Research*, vol. 21, no. 7, Article ID e12869, 2019.
- [8] J. Chang, Y. Yuan, and D. Wang, *Nan fang yi ke da xue xue bao= Journal of Southern Medical University*, vol. 40, no. 2, pp. 171–176, 2020.
- [9] C. Karatekin, "Adverse childhood experiences (ACEs), stress and mental health in college students," *Stress and Health*, vol. 34, no. 1, pp. 36–45, 2018.
- [10] S. Kim, D. Sinn, and S. Y. Syn, "Analysis of college students' personal health information activities: online survey," *Journal of Medical Internet Research*, vol. 20, no. 4, p. e132, 2018.
- [11] N. Kratzke and P. C. Quint, "Understanding cloud-native applications after 10 years of cloud computing - a systematic mapping study," *Journal of Systems and Software*, vol. 126, pp. 1–16, 2017.
- [12] D. Gannon, R. Barga, and N. Sundaresan, "Cloud-native applications," *IEEE Cloud Computing*, vol. 4, no. 5, pp. 16–21, 2017.
- [13] I. Pelle, J. Czentye, J. Dóka, and B. Sonkoly, "Towards Latency Sensitive Cloud Native Applications: A Performance Study on aws," in *Proceedings of the 2019 IEEE 12th International Conference on Cloud Computing (CLOUD)*, pp. 272–280, IEEE, Milan, Italy, July 2019.
- [14] J. Ye, C. Wang, A. Xiao et al., "Physical restraint in mental health nursing: a concept analysis," *International journal of nursing sciences*, vol. 6, no. 3, pp. 343–348, 2019.
- [15] J. S. Nevid, *Essentials of Psychology: Concepts and applications*, Cengage Learning, Boston, Massachusetts, United States, 2021.
- [16] A. F. Jorm, "The concept of mental health literacy [J]," *International Handbook of Health Literacy: Research, Practice and Policy across the Life-Span*, pp. 53–66, 2019.
- [17] K. Denecke, S. Vaaheesan, and A. Arulnathan, "A mental health chatbot for regulating emotions (SERMO) - concept and usability test," *IEEE Transactions on Emerging Topics in Computing*, vol. 9, no. 3, pp. 1170–1182, 2021.
- [18] A. S. Haider and S. Al-Salman, "Dataset of Jordanian university students' psychological health impacted by using e-learning tools during COVID-19," *Data in Brief*, vol. 32, Article ID 106104, 2020.
- [19] G. Marques, N. Drissi, I. d l T. Díez, B. S. de Abajo, and S. Ouhbi, "Impact of COVID-19 on the psychological health of university students in Spain and their attitudes toward Mobile mental health solutions," *International Journal of Medical Informatics*, vol. 147, Article ID 104369, 2021.
- [20] J. M. Quintero Johnson, G. Yilmaz, and K. Najarian, "Optimizing the presentation of mental health information in social media: the effects of health testimonials and platform on source perceptions, message processing, and health outcomes," *Health Communication*, vol. 32, no. 9, pp. 1121–1132, 2017.
- [21] T. D. Meyer, R. Casarez, S. S. Mohite, N. La Rosa, and M. S. Iyengar, "Novel technology as platform for interventions for caregivers and individuals with severe mental health illnesses: a systematic review," *Journal of Affective Disorders*, vol. 226, pp. 169–177, 2018.
- [22] R. Kayano, E. Y. Y. Chan, V. Murray, J. Abrahams, and S. Barber, "WHO thematic platform for health emergency and disaster risk management research network (TPRN): report of the kobe expert meeting," *International Journal of Environmental Research and Public Health*, vol. 16, no. 7, p. 1232, 2019.

## *Retraction*

# **Retracted: Analysis of Artistic Creation and Design Methods in Universities Based on Augmented Reality and 5G Communication Technology**

### **Security and Communication Networks**

Received 26 December 2023; Accepted 26 December 2023; Published 29 December 2023

Copyright © 2023 Security and Communication Networks. This is an open access article distributed under the Creative Commons Attribution License, which permits unrestricted use, distribution, and reproduction in any medium, provided the original work is properly cited.

This article has been retracted by Hindawi, as publisher, following an investigation undertaken by the publisher [1]. This investigation has uncovered evidence of systematic manipulation of the publication and peer-review process. We cannot, therefore, vouch for the reliability or integrity of this article.

Please note that this notice is intended solely to alert readers that the peer-review process of this article has been compromised.

Wiley and Hindawi regret that the usual quality checks did not identify these issues before publication and have since put additional measures in place to safeguard research integrity.

We wish to credit our Research Integrity and Research Publishing teams and anonymous and named external researchers and research integrity experts for contributing to this investigation.

The corresponding author, as the representative of all authors, has been given the opportunity to register their agreement or disagreement to this retraction. We have kept a record of any response received.

## **References**

- [1] Y. Li, "Analysis of Artistic Creation and Design Methods in Universities Based on Augmented Reality and 5G Communication Technology," *Security and Communication Networks*, vol. 2022, Article ID 4005210, 10 pages, 2022.

## Research Article

# Analysis of Artistic Creation and Design Methods in Universities Based on Augmented Reality and 5G Communication Technology

Ying Li 

Hainan Tropical Ocean University, Sanya 572022, China

Correspondence should be addressed to Ying Li; [liying@hntou.edu.cn](mailto:liying@hntou.edu.cn)

Received 7 June 2022; Revised 19 July 2022; Accepted 29 July 2022; Published 25 August 2022

Academic Editor: Hangjun Che

Copyright © 2022 Ying Li. This is an open access article distributed under the Creative Commons Attribution License, which permits unrestricted use, distribution, and reproduction in any medium, provided the original work is properly cited.

In order to enhance the research of art design in colleges and universities, based on the theory of augmented reality, 5G communication technology is used to conduct targeted analysis of art design and creation in colleges and universities. Through the research of feature parameter extraction, parameter consistency test, and optimization algorithm analysis on the relevant data of the art design in colleges and universities, the deficiencies of art design and creation in colleges and universities are pointed out, and relevant solutions are adopted. The results show that with the increase of distribution distance, the curve of the  $z$  value shows a linear change trend. The curve corresponding to a value has an obvious polynomial change rule. Through the analysis, it can be seen that the influence of two parameters on augmented reality needs to be considered comprehensively. As the number of iterative steps increases, the consistency curve of augmented reality shows an obvious linear downward trend. However, the increase of parameter  $m$  can improve the data changes of augmented reality consistency, and the research shows that parameter  $m$  can further promote the consistency changes of augmented reality. The gradual increase of index  $P_n$  leads to a gradual decline in data  $P_c$ , while the parameter  $P_x$  has an opposite effect on data  $P_c$ . Therefore, in order to obtain targeted data and results of 5G communication technology, it is necessary to comprehensively consider the influence of the two factors. Finally, the optimization model based on augmented reality and 5G communication technology is used to analyze and predict the relevant characteristic data of university art design, so as to verify the accuracy of the model. The research results can provide support for the application of augmented reality and 5G communication technology in other art fields.

## 1. Introduction

Augmented reality and 5G communication technology have been widely applied in various fields: urban visualization research [1], tourism promotion [2], teaching methods [3], computer storage [4], tracking display [5], and so on. In view of the problems existing in the process of image output, Shishova et al. [6] proposed an optimization model based on augmented reality theory. In this model, feature parameters were extracted from the image to obtain the corresponding optimization data, and the optimal solution of the corresponding graph was obtained through calculation. 5G communication technology can be used for the adjustment and optimization of high-power voltage dividers [7]. A series of measures were adopted to analyze the parameters and data of the model, and experiments were used to verify it. 5G

communication technology also has broad application prospects in signal processing [8], and relevant data can be used to verify and analyze the model. First, the augmented reality algorithm was used to further extract and analyze the data of the model, so as to obtain the extracted data. Then, the collected data were imported into the optimization model, so as to carry out optimization parameter calculation. Finally, relevant graphs were analyzed and verified by using the above methods.

The above studies mainly focus on the application of augmented reality and 5G communication technology from urbanization, information technology, and other aspects. Aiming at the problems existing in artistic creation in colleges and universities, this paper first extracts and analyzes the data on artistic creation in colleges and universities based on the relevant theories of augmented reality. A series

of consistency tests were carried out to simulate and verify the accuracy of the test data, and then 5G communication technology was used for further analysis of the above data. The method of data collection is used to obtain the relevant information of college art creation and design methods, and the solutions are put forward to solve the existing problems. Therefore, based on the theory of augmented reality and 5G communication technology, it can provide relevant data support for artistic creation in colleges and universities, so as to provide a guarantee for the application of augmented reality and 5G communication technology in other fields.

## 2. Related Theory Based on Augmented Reality

**2.1. Feature Extraction in Augmented Reality.** Augmented reality technology is a clever fusion of virtual information and the real world, widely using multimedia, three-dimensional modeling, real-time tracking and registration, intelligent interaction, sensing, and other technical means [9, 10]. The audience can overlap the real world and the virtual scene generated by the computer into one body only by using corresponding external devices. Augmented reality technology synchronizes the changes of images, sound, and touch in the virtual scene to the real world with real-time interaction, which greatly enhances the fun and product characteristics. Add positioning virtual objects in three-dimensional space, advanced technology, and wide application prospects, so it has super practicability.

In order to further analyze and study the related content of the augmented reality system, the working process of the augmented reality system is drawn, as shown in Figure 1. From the figure, we can see the specific workflow of the augmented reality system as follows: first, the real scene and virtual scene are imported into target recognition and scene rendering, respectively, for parameter extraction and analysis, and then the extracted parameters are imported into tracking registration and 3D registration. In this way, the tracking parameters can be further registered, extracted, verified, and analyzed, and the corresponding characteristics of the parameters can be obtained. Then, the targeted features are introduced into the module combining real scenes and virtual scenes so that we can get the corresponding data of real scenes and virtual scenes based on the augmented reality system. Finally, the data is imported into the display device module. In the display device module, the relevant data of the augmented reality system can be further analyzed and extracted through the comprehensive effect of the display system, users, and human-computer interaction interface, and finally, the relevant data can be exported.

In order to further study the image processing process of augmented reality technology, the graphic analysis and extraction process based on augmented reality theory is obtained by extracting and analyzing different kinds of graphic features, as shown in Figure 2. We can see from the figure that image extraction and processing can be divided into two modules: local feature extraction and quantization module and global feature extraction and quantization module. The specific calculation and processing process is as follows: first, the image is imported into the local feature

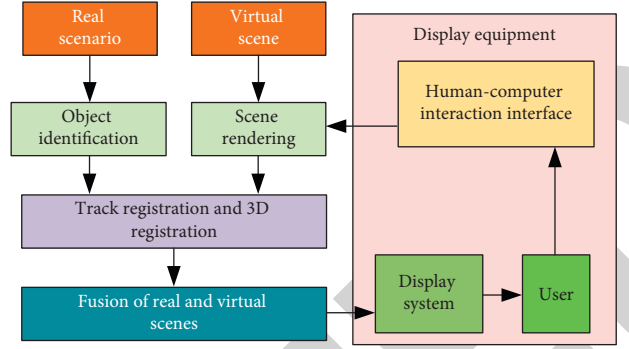


FIGURE 1: Workflow flowchart of augmented reality system.

extraction and quantization module, and the local feature extraction module is used to further extract the relevant features of the image. It mainly extracts pixel, size, and color of graph and then imports extracted parameters into local feature extraction and quantization module and global feature extraction quantization module. In the quantization module of local feature extraction, feature points are first screened after data is imported, and targeted feature points are selected for further analysis. The purpose of this is to realize the application of augmented reality technology in local features but also to be able to remove the influence of redundant interference factors. Then it is imported into the local feature generation module, so as to obtain the local feature data of the image and then edit and verify the corresponding position points so that the obtained image can better reflect the targeted features of the image. In the global processing module, the feature points are screened and extracted first, and then the feature points of the image are reduced in dimension. This is mainly in order to be able to grasp and analyze the global data and images. Finally, through extraction and further analysis, scalable quantitative images can be obtained, and the corresponding results will be output at last [11, 12].

For any evaluation attribute  $y$ , the probability of an important point appearing in a region  $S$  of the  $y$  distribution is

$$p(c = 1|y \in B) = \frac{p(y \in B \cap c = 1)}{p(y \in B)}, \quad (1)$$

where  $p$  is the probability of appearance of feature points,  $B$  is the corresponding set of feature points, and  $c$  is the characteristic parameter value.

In order to verify and explain whether there are matching points for each feature point in the training sample, a binary decision function  $k$  is defined by assigning corresponding values to binary label  $c_n$  as follows:

$$\begin{aligned} \hat{p}(y \in B|c = 1) &= \frac{\sum_{n=1}^N k(y_n \in B)c_n}{N} \\ &= \hat{p}(y \in B) = \frac{\sum_{n=1}^N k(y_n \in B)}{N}, \end{aligned} \quad (2)$$

where  $\hat{p}(y \in B|c = 1)$  is the probability of optimizing feature points,  $N$  is the number of samples, and  $c_n$  is a binary label.

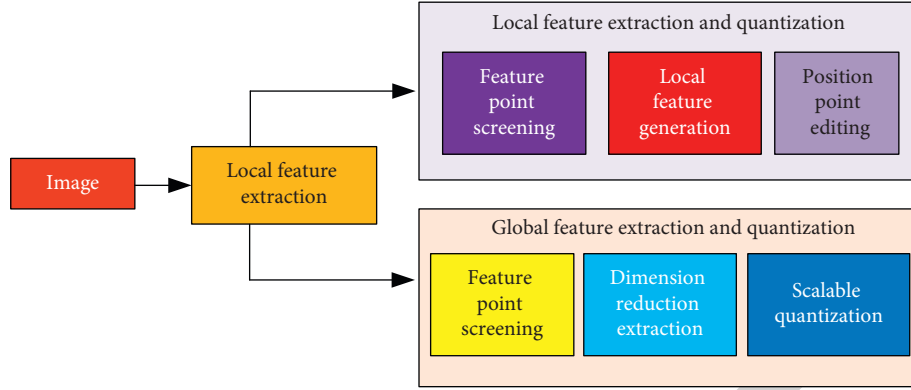


FIGURE 2: Graphic feature extraction and quantization flow chart based on augmented reality.

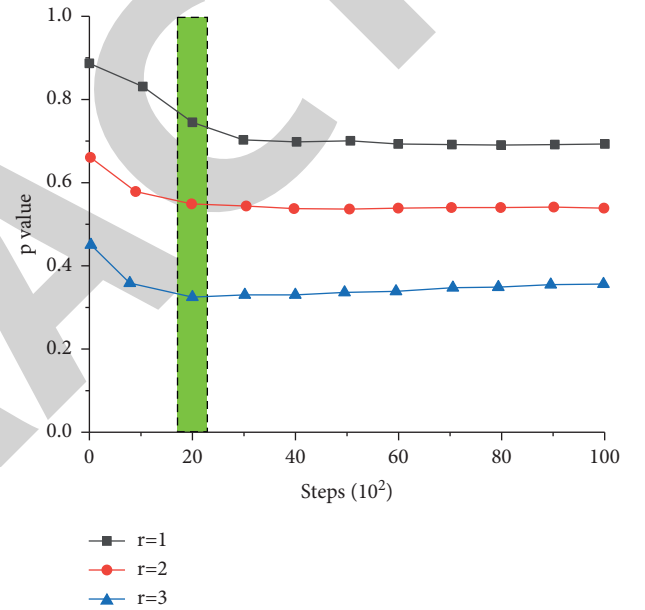
Thus, the probability of matching points in the region where each attribute is located can be obtained, and the importance score of feature points can be obtained by multiplying the probability of each attribute as follows:

$$r = \hat{p}(c = 1|\sigma \in S) \dots \hat{p}(c = 1|d \in D), \quad (3)$$

where  $D$  is the corresponding set of  $d$  and  $d$  is the parameter of importance score.

Based on the above analysis, we can see that the extraction probability is different under different  $r$  values. Therefore, in order to further analyze the influence of different  $r$  values on the extraction probability, we draw the curve of  $r$  value changing with the extraction probability under different iteration steps, as shown in Figure 3. It can be seen from the figure that the extraction probability is different under different  $R$  values, which can be divided into two stages according to the changing trend. When the number of iteration steps ranges from 0 to 2,000, the corresponding curve shows a trend of gradual decline as the number of iterations increases, and the slope of the decline curve gradually approaches zero. When the number of iteration steps exceeds 2,000, the curve enters the second stage. In the second stage, the curve shows a relatively gentle trend of change, and with the increase of iteration steps, the corresponding value shows an approximate constant trend of change. This shows that when the number of contemporary steps reaches a certain level, the corresponding extraction probability tends to be stable, and such curve changes can better meet the requirements of image extraction based on augmented reality technology. From different  $r$  values, it can be seen that with the gradual increase of the  $r$  value, the corresponding extraction probability data shows a trend of gradual decline. This shows that there is an obvious inverse proportional decreasing relationship between the  $r$  value and corresponding probability change. It is worth noting that the spacing between the corresponding trends is basically the same, which indicates that the change of the  $r$  value has obvious linear characteristics.

**2.2. Consistency Checking for Augmented Reality.** Based on the above analysis, we can see that augmented reality technology can be widely used in different fields. In order to

FIGURE 3: The probability change diagram is extracted under different  $r$  values.

further illustrate the content of the consistency test of augmented reality technology [13, 14]. First, the quantized local features are used for feature matching to obtain the matching relationship between the optimized image sample and the query image. Then, the correlation algorithm relative to augmented reality is used for geometric verification [15, 16]. Compared with the consistency verification of traditional augmented reality algorithms, the geometric verification method based on the matching pair ratio theory of augmented reality carries out the consistency verification of statistical distributed data, which has a great speed advantage.

$$Z_{ij} = \ln \frac{\|x_i - x_j\|}{\|y_i - y_j\|}, \quad (4)$$

where  $x_i$  is the coordinate of point  $i$  of the first image,  $x_j$  is the coordinate of point  $j$  in the first image,  $y_i$  is the coordinate of



point  $i$  in the second image, and  $y_j$  is the coordinate of point  $j$  in the second image.

The geometric verification method based on augmented reality is to judge the geometric similarity of two kinds of data by using the concentration degree of matching distance distribution. The basic idea of the geometric verification method based on augmented reality is that if two images have the same object, the graph model composed of points of interest on the same object has similarities. The matching interest point pair of two images is the position point after decoding. The function of position point coding is to reduce the length of the descriptor and save storage space. Then, using the method of hypothesis testing, the matching distance can be counted into a distribution broken line graph according to the size of the value. Then, the chi-square test is used to test the probability distribution model, and the corresponding expression of the probability distribution model is as follows:

$$f_z(z; a) = 2 \left( \frac{ae^z}{e^{2z} + a^2} \right)^2, \quad (5)$$

where  $f_z(z; a)$  is the probability distribution function and  $a$  and  $z$  are parameters of the corresponding distribution model.  $a^2 = \sigma_x^2 / \sigma_y^2$ ;  $\sigma_x^2$  and  $\sigma_y^2$  are the variances of the distribution of interest points of images  $X$  and  $Y$ , respectively.

Through the above formula and analysis, we can see that  $a$  and  $z$  have a great influence on the exponential result of a probability distribution. In order to further study the influence degree of  $z$  and  $a$  parameters on probability distribution indexes, the influence curves of probability distribution under two different indexes were drawn, as shown in Figure 4. It can be seen from the figure that the influence and change trend of probability distribution under different indexes are different, which indicates that different distribution distances of probability parameters have a certain influence on the probability distribution index. The details are as follows: from the changing trend of the  $z$  value, we can see that the curve shows a typical four-stage changing trend: (1) when the distribution distance is between 0 and 28, the corresponding curve tends to be gentle. In this stage, the fluctuation of probability distribution index data is relatively small, and the overall performance is a gentle change trend. (2) When the distribution distance is between 28 and 45, the probability distribution curve shows a trend of rapid increase, and the corresponding slope is approximately constant, which indicates that this stage has typical linear characteristics. (3) When the corresponding distribution distance is between 45 and 78, the curve still shows a linear change characteristic, but the linear change curve decreases compared with the previous stage. With the gradual increase of the distribution distance, the corresponding probability distribution index gradually improves. (4) When the distribution distance exceeds 78, the curve shows a rapid linear increase trend again, and the increase slope is basically consistent with the second stage. Through the above analysis, we can see that the influence process of the  $z$  value on the probability distribution shows obvious linear characteristic changes, but on the whole, it belongs to

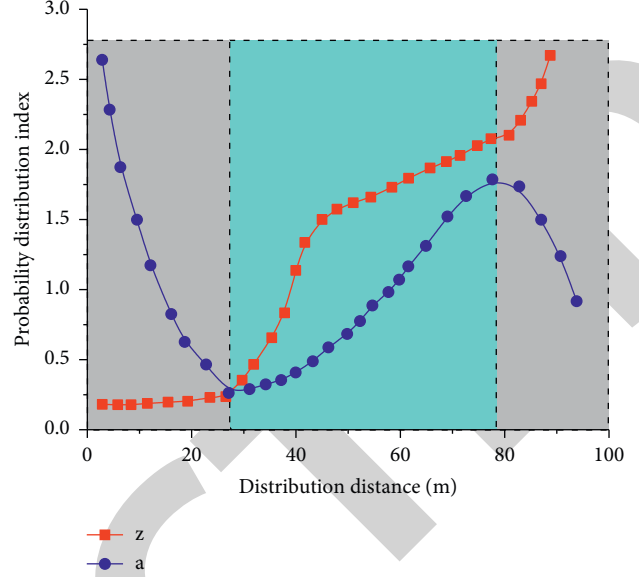


FIGURE 4: Influence diagram of  $z$  and  $a$  on probability distribution index.

multilinear characteristic distribution. From the influence of parameter proximity to  $a$  on the curve of a probability distribution, it can be seen that this area presents a typical polynomial distribution. According to the change rule of the curve, it can be divided into three stages: in the first stage, the curve declines gradually with the increase of the distribution distance, and the corresponding slope of the curve shows a trend of gradual decline. When the distribution distance exceeds 28, the corresponding curve shows a trend of gradual increase, and the slope of the corresponding curve changes approximately linearly. Finally, when the distribution distance exceeds 78, the corresponding curve gradually decreases, indicating that the probability distribution curve under the action of a value shows a fluctuation change on the whole.

By constructing the distance matrix between matching points and calculating the feature points and feature vectors of the matrix, the following formula is used to eliminate the number of matching errors.

$$m = 1 + \frac{\mu}{\sum \max d(x)} 2 \left( \frac{ae^z}{e^{2z} + a^2} \right)^2, \quad (6)$$

where  $\mu$  is the dominant eigenvalue,  $d(k)$  is the distance between the  $k$ -th matching pair, and  $m$  is the number of eigenmatrixes.

For each correct matching pair, the following formula is used to calculate the data score based on augmented reality:

$$\omega(r) = \cos\left(\frac{\pi r}{2}\right), \quad (7)$$

where  $r$  is the ratio parameter and  $\omega(r)$  is the score function.

The final retrieval result can be obtained by summing up all the correct matching pairs  $\omega(r)$  and reordering the relevant data with the score function.

Through the above analysis, it can be seen that the change of parameter  $m$  value will affect the consistency test results of augmented reality theory to a certain extent, thus having a great impact on relevant data. In order to further analyze the influence of parameter  $m$  on augmented reality, the variation relationship between parameter  $m$  and the score is drawn, as shown in Figure 5. As can be seen from the figure, with the increase of iteration steps, the corresponding value of augmented reality shows a trend of gradual decline. And it can be seen from the first-order polynomial fitting that the change relation of the curve approximately presents a linear decline, indicating that the increase in the number of iterations can further reduce the corresponding parameters of augmented reality consistency. As can be seen from parameter  $m$ , with the gradual increase of parameter  $m$ , the corresponding augmented reality consistency data also shows an increasing trend. This shows that parameter  $m$  plays a positive role in promoting augmented reality. The slope of different parameter  $m$  is different; from large to small, it is  $10 > 20 > 30 > 40$ .

**2.3. Algorithm Description of Augmented Reality.** The description algorithm based on augmented reality is very complex and has a large amount of computation and memory consumption, so it is not suitable for running on intelligent terminals with limited performance [17, 18]. The algorithm based on augmented reality theory is a feature point detection and description algorithm based on visual information. In the feature point detection part, directional feature points are used to detect the algorithm of augmented reality theory, and in the feature extraction part, rotational invariant feature points are used to describe the iterative content of the algorithm. This prompts us to further optimize and evaluate the relevant algorithms in the actual use process. The optimized algorithm has the characteristics of fast computing speed and small memory and can work well on a mobile platform, so as to meet the real-time requirements of augmented reality [19]. The augmented reality algorithm mainly adds the corresponding feature points to the corresponding direction algorithm, and the corresponding steps are as follows:

- (1) Calculate the  $(p+q)$  order moment of the neighborhood of augmented reality feature points as follows:

$$m_{p,q} = \sum_{x,y} x^p y^q g(x, y), \quad (8)$$

where  $m_{p,q}$  is the corresponding matrix and  $x^p$  and  $y^p$  are the corresponding matrix parameters.

- (2) Calculate the centroid of the neighborhood of feature points as follows:

$$C = (C_x, C_y) = \left( \frac{m_{10}}{m_{00}}, \frac{m_{01}}{m_{00}} \right), \quad (9)$$

where  $C$  is the calculated data of the center of mass. The distribution of  $C_x$  and  $C_y$  is the data of the

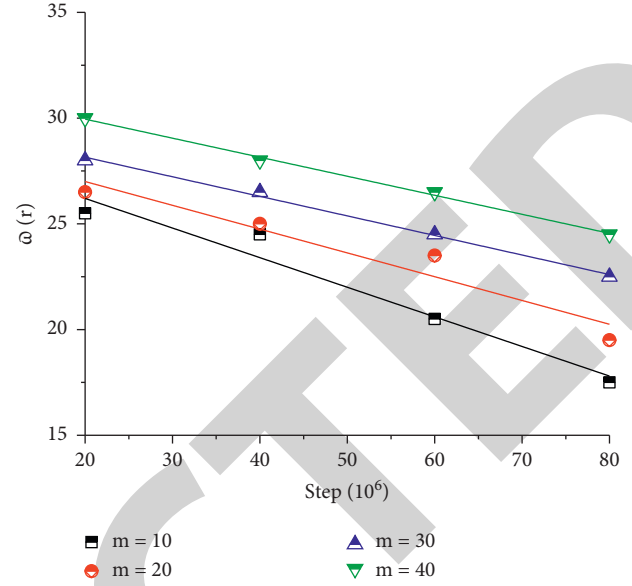


FIGURE 5: Parameter  $m$  to augmented reality consistency check diagram.

corresponding center of mass along the  $x$  and  $y$  axes.  $m_i$  ( $i=0,1$ ) is the corresponding parameter.

- (3) Calculate the direction of the center of mass  $\theta$  as follows:

$$\theta = \arctan \left( \frac{m_{10}}{m_{01}} \right). \quad (10)$$

If the centroid is defined as the main direction of feature points in augmented reality, the corresponding feature points can be extracted according to this direction.

In order to further analyze the influence of different parameters on centroid feature points, corresponding change curves of centroid feature points under three different parameters are drawn, as shown in Figure 6. It can be seen from the figure that the parameter  $\theta$  gradually increases with the increase of centroid distance, and the corresponding trend shows typical nonlinear variation characteristics. And the increasing rate of the corresponding centroid feature point data shows a trend of gradual improvement. As can be seen from the parameter  $C_y$ , the feature point of the centroid shows a fluctuating trend with the increase of the centroid distance, that is, it increases slowly at first and then gradually decreases. It can also be seen from the influence of parameter  $C_x$  on the feature points of the center of mass. When the distance of the center of mass is between 0 and 150, the data of the corresponding feature points of the center of mass is zero. When the centroid distance is over 450, the corresponding centroid feature point data shows a trend of slow increase at first, while when the centroid distance is over 450, the corresponding data shows a trend of rapid increase.



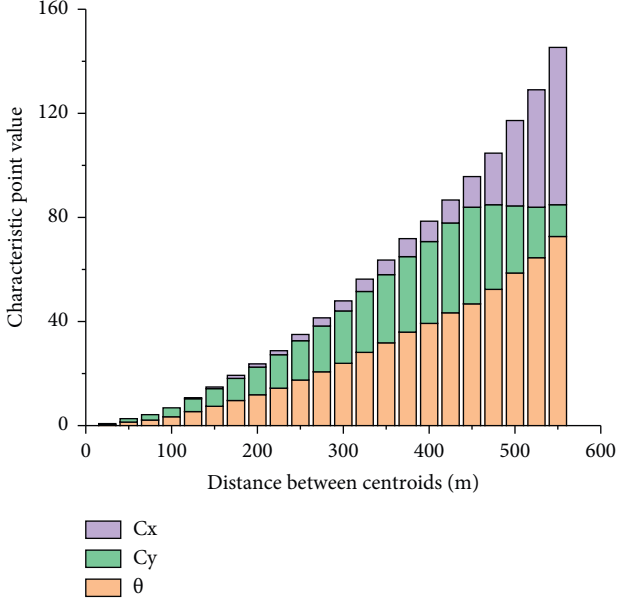


FIGURE 6: Augmented reality histogram of centroid versus feature points.

### 3. Related Theories of 5G Communication Technology

As a new mobile communication network, 5G communication technology will not only solve interpersonal communication but also provide users with augmented reality, virtual reality, ultra-high-definition video, and other content [20]. The communication between people and things and between things should also be solved to meet the needs of IOT [21]. In this 5G network system model, it is assumed that the network slice is a collection of virtual nodes and virtual links created by the network infrastructure provider. It is operated by the service provider to provide customized services so that the problem of cache resource allocation optimization is transformed into the problem of revenue maximization for the network infrastructure provider.

In order to further analyze the process related to 5G communication technology in the augmented reality system, the relevant workflow of 5G communication technology is obtained through analysis and sorting, as shown in Figure 7. Based on the above analysis, we can see that the workflow of the system is as follows: first, the data processed by the 5G communication network is imported into the 5G management module. The optimized 5G communication technology corresponding data is obtained through further analysis of business design, instance programming, and operation management modules in the 5G manager and then imported into the 5G function selection module. The 5G communication function selection module consists of three sub-modules, and each submodule is composed of two parts: access 5G and core 5G. Through further iteration and analysis of these six parts, data can be further identified. It is then imported into the virtualization build manager, which further arranges and analyzes the data through the

virtualization manager choreographer. On this basis, the data calculated by 5G communication technology will be imported into the basic design of the 5G network. Through further analysis of different resources such as computing resources, network resources, and storage resources, the obtained data can meet the requirements of 5G communication technology. In view of a series of problems existing in different modules of 5G communication technology, different methods are needed to analyze and evaluate 5G communication modules.

The traditional model only considers one network infrastructure provider and multiple service providers, and each service provider provides only one network data [22]. In order to better allocate virtual resources among multiple network data, based on the above research, optimization and evaluation of 5G communication technology based on augmented reality theory can be adopted, as shown below.

The data that network data  $k$  should input to node  $i$  within unit time  $T$  can be represented by  $M$ . Therefore, the corresponding data that network data  $k$  should input to all nodes within unit time  $T$  can be expressed as follows:

$$P_k = \sum_{i=1}^N MT, \quad (11)$$

where  $P_k$  is the total amount of data,  $T$  is time, and  $M$  is the input data.

The data provided by all network database stations to the network infrastructure can be expressed as follows:

$$P = \sum_{k=1}^M P_k = \sum_{k=1}^M \sum_{i=1}^N MT, \quad (12)$$

where  $P$  is the total amount of data of different 5G base stations. The two different evaluation indicators are as follows:

- (1) Cache energy consumption index: Cache energy consumption index is mainly due to the energy consumption caused by content cache and content update. Therefore, the cache energy consumption index can be expressed as follows:

$$P_n = \rho_n E_n = \rho_n \sum_{k=1}^M \sum_{i=1}^N aMvT, \quad (13)$$

where  $a$  represents the energy consumption of content cache or content update per unit cache capacity,  $v$  represents the number of content updates per unit time  $T$ , and  $\rho_n$  represents the energy consumption of content cache or content update per unit capacity. In order to avoid overload of the cache energy consumption index in the cache nodes, the 5G network optimization model sets a content update limit  $V$ , which represents the maximum update times per unit time, that is,  $v \leq V$ .

- (2) Response energy consumption index: The response energy consumption cost is mainly caused by the response and service users' content requests. The

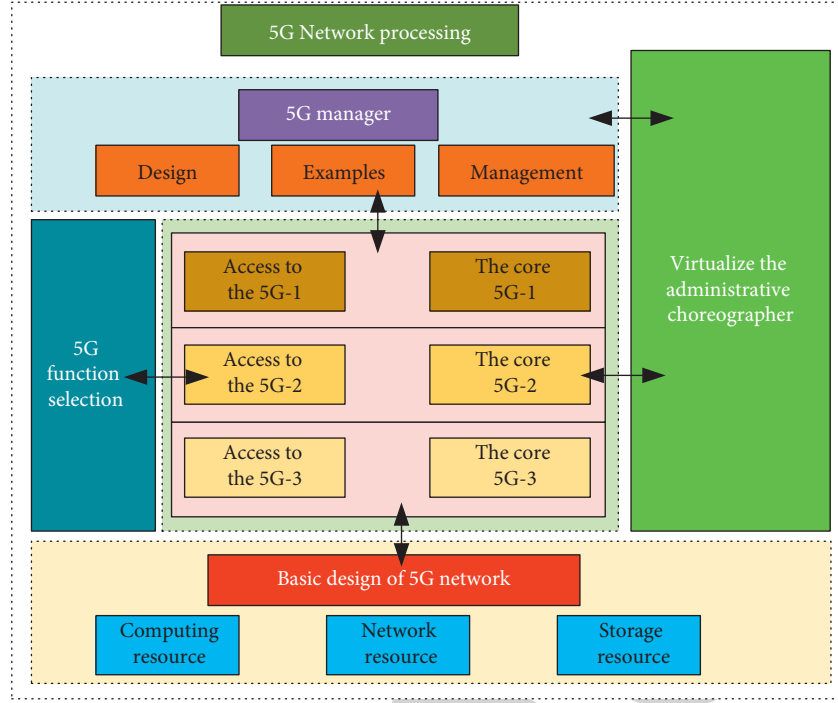


FIGURE 7: A calculation flowchart of 5G communication technology.

energy consumption index can be expressed as follows:

$$P_x = \rho_x E_x = \rho_x \sum_{k=1}^M \sum_{i=1}^N bM\gamma T, \quad (14)$$

where  $b$  is the energy consumption,  $\gamma$  is the content response, and  $\rho_x$  is the energy consumption index. In order to avoid the overload of cache nodes in the calculation process, the model also sets the limit of content response times  $R$ , which represents the maximum number of content responses. When  $\gamma \leq R$ , the corresponding model works within the allowed range of settings.

$$\begin{aligned} P_c &= P_n + P_x = \rho_n E_n + \rho_x E_x \\ &= \rho_x \sum_{k=1}^M \sum_{i=1}^N bM\gamma T + \rho_n \sum_{k=1}^M \sum_{i=1}^N aMvT. \end{aligned} \quad (15)$$

In order to further analyze the change rules of 5G communication technology under different factors, the 5G communication change curves under different factors are drawn, as shown in Figure 8. It can be seen from the figure that with the gradual increase of indicator  $P_n$ , the corresponding  $P_c$  data shows a trend of gradual decline, indicating that the increase of  $P_n$  will have a negative impact on the data  $P_c$  of 5G communication technology. It can be seen from the parameter  $P_x$  that with the gradual increase of parameter  $P_n$ , the corresponding  $P_c$  data shows a trend of rapid increase. This indicates that with the increase of parameter  $P_x$ , the corresponding 5G communication technology data  $P_c$  has an obvious upward trend. Therefore, it can be seen from the figure that the influences and functions expressed by  $P_x$  and

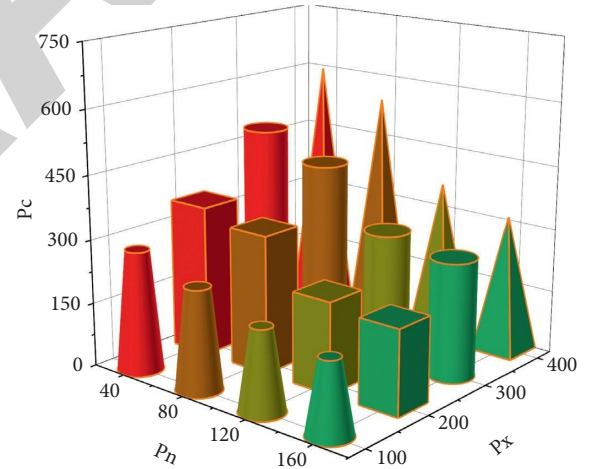


FIGURE 8: Graph of 5G communication technology changes under different factors.

$P_n$  are opposite. For data  $P_c$  with 5G communication technology, we need to comprehensively consider the influence of two factors on data  $P_c$ , so as to obtain targeted data and results.

#### 4. Application of Augmented Reality and 5G Communication Technology in University Art

**4.1. The Basic Content of Artistic Creation and Design Methods in Colleges and Universities.** As an important form of humanistic training in colleges and universities, art creation and design methods in colleges and universities are very

important for college education. Art in colleges and universities can be divided into the cultivation of artistic creation ideas and the training of artistic design methods. However, at present, there are a series of problems in artistic creation and design in colleges and universities, which to some extent restrict the further development of art in colleges and universities. These problems must be solved for college education, as shown below:

- (1) Curriculum innovation needs to be improved: at present, the curricula related to artistic creation and training in colleges and universities are relatively new and have not been updated for a long time. This will restrict the artistic creation and development of colleges and universities, making the cultivation of artistic talents in colleges and universities lag behind the times for a long time, indicating that college education is not at the forefront of the times. Therefore, we need to improve the lack of innovation in the process of artistic creation in colleges and universities so that the artistic creation of colleges and universities can walk at the forefront of the times.
- (2) Lack of teaching resources: Colleges and universities pay attention to the cultivation of science and technology for a long time, resulting in a lack of attention and investment in the faculty of art in colleges and universities, resulting in a serious shortage of teachers in the field of art in colleges and universities. Moreover, it is worth explaining that there are obvious differences in the faculty of art in colleges and universities in different regions. The faculty of art in colleges and universities in developed areas is much higher than that in remote areas. This is a serious problem that needs to be solved.
- (3) Relatively little art teaching: Art teaching covers a wide range of fields, requiring targeted research on different details and modules. At present, colleges and universities mainly focus on the popular art field to carry out relevant teaching and scientific research, which leads to a gradual lack of research in the relatively unpopular art research direction. As a result, the field of art creation and research in colleges and universities is becoming smaller and smaller. This is not conducive to the development of the art field in universities.
- (4) Relatively low practical application: Universities are mainly engaged in theoretical research in the field of art, mainly focusing on the conceptual teaching of artistic creation and design methods, while the analysis and teaching of the practical application of artistic creation are relatively small. As a result, college students cannot organically combine the theory and practical application in the field of art. As a result, the study enthusiasm of the art field in colleges and universities gradually decreases.

Aiming at a series of problems in artistic creation, in order to further analyze the specific content of artistic

creation and design, the research in the field of artistic creation and design can be divided into five parts: curriculum innovation, teaching resources, teaching content, faculty, and art application. In order to more accurately analyze the five parts of college art creation, the pie chart of college art creation and design is obtained by summarizing relevant data in the field of college art creation and design, as shown in Figure 9. From the figure, we can see that art application accounts for the highest proportion, about 40%, while the corresponding proportion of teachers is 20%. Teaching content accounted for more than 16%, teaching resources accounted for about 13%, and curriculum innovation accounted for the lowest proportion, only 10%.

*4.2. Application of Augmented Reality and 5G Communication Technology in College Art Creation and Design.* Through the above analysis, we can see that there are some problems in college art creation and design methods. In order to better analyze and solve the problems in college art creation, Based on the theory of augmented reality, 5G communication technology is used to carry out targeted research and analysis on the art design and creation of colleges and universities, so as to get the corresponding solutions. In order to further improve the application of augmented reality and 5G communication technology to college art creation and design, first, we extracted the relevant data of artistic creation in colleges and universities. Then the extracted data is tested for consistency under augmented reality, and then the corresponding augmented reality algorithm and model are obtained. Finally, 5G communication technology is used to analyze and evaluate the data and algorithms obtained above, so as to find out the problems existing in the artistic creation of colleges and universities and provide targeted solutions.

Through the analysis of art creation based on augmented reality and 5G communication technology, the corresponding analysis curve of art creation and design is obtained, as shown in Figure 10. From the figure, we can see that four different factors have different influences on artistic creation in colleges and universities. First, it can be seen from parameter  $C_x$  that with the gradual increase of parameter samples, the corresponding curve shows a trend of gradual increase, and the trend is linear. When it reaches the maximum value of 500, the corresponding curve shows a relatively slow change trend with the further increase of the number of iterations and gradually declines to the lowest point of 50. As can be seen from the parameter  $C_y$ , with the gradual increase of samples, the corresponding art index of colleges and universities shows a trend of slow decline, which also conforms to the linear change. Overall, there was a drop of nearly 80% from highest to lowest. As can be seen from the parameter  $P_m$ , the corresponding art index data as a whole remains within the range of about 300. This shows that parameter  $P_n$  has good stability for artistic creation in colleges and universities. Finally, through parameter  $P_x$ , it can be seen that with the increase of samples, the corresponding art data of colleges and universities show a trend of gradual improvement. The corresponding data increase is about 90%.

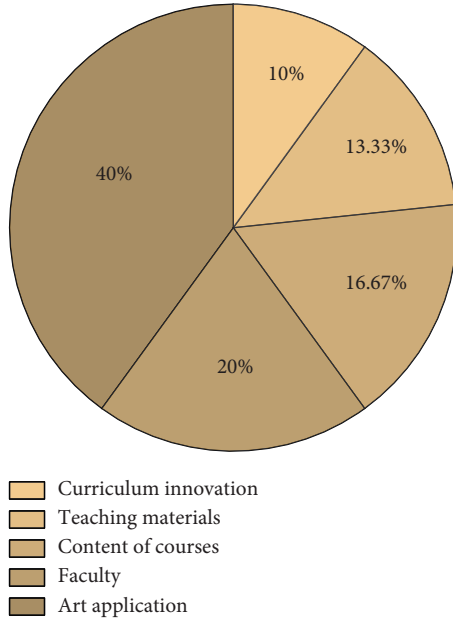


FIGURE 9: Pie chart of college art creation and design.

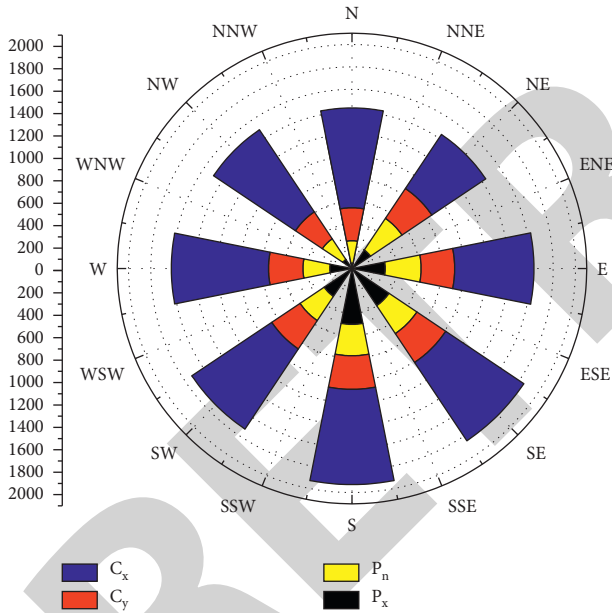


FIGURE 10: Analysis diagram of art creation and design in colleges and universities under the combined effect of augmented reality and 5G communication technology.

## 5. Discussion

The above research shows that art in colleges and universities based on augmented reality and 5G communication technology has different forms of expression in creation and design methods. In order to study the influence of augmented reality and 5G communication technology on artistic creation in colleges and universities, the corresponding prediction curve of artistic creation research in colleges and universities is drawn, as shown in Figure 11. As can be seen from the figure, with the increase in iteration times, the

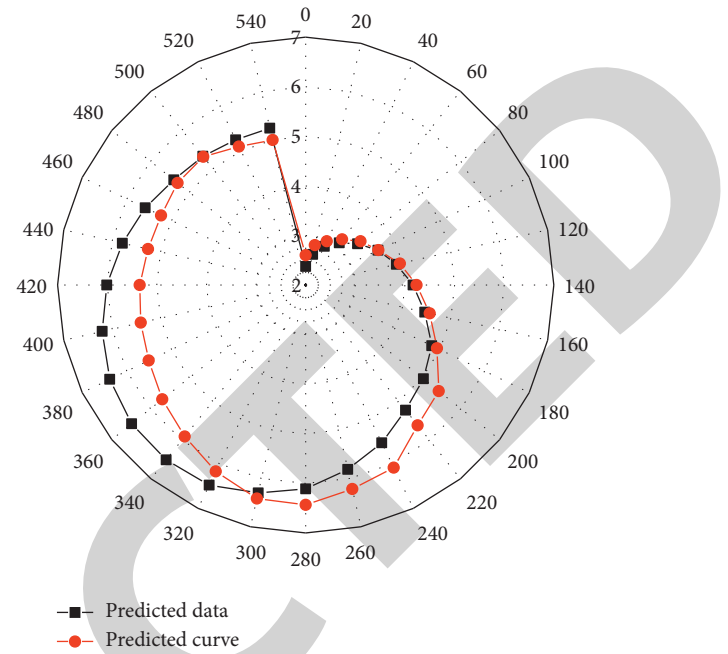


FIGURE 11: A forecast of augmented reality and 5G communication technology in the field of art creation in colleges and universities.

corresponding data of artistic creation in colleges and universities shows a trend of increasing first and then decreasing. The prediction curve of the corresponding optimization model shows the same change trend, indicating that the model can well describe and analyze the art field in colleges and universities. At the same time, it also shows that 5G communication technology based on augmented reality can be used to describe the artistic creation and design of colleges and universities.

## 6. Conclusion

- (1) The variation trend of extraction probability under different  $r$  values mainly includes the slow decline stage and the stable stage. And the extracted probability curve shows a trend of gradual decline with the increase of the  $r$  value. Relevant studies show that there is an obvious inverse proportional decreasing relationship between the  $r$  value and corresponding probability change.
- (2) With the increase of centroid distance, the parameter  $\theta$  increases nonlinearly. The parameter  $C_y$  showed a trend of slow increase and then a gradual decline. Parameter  $C_x$  shows a trend of slow increase at first and then rapid increase. Therefore, the influence degree of different parameters on the centroid characteristic data is  $\theta > C_x > C_y$ .
- (3) The influence of different factors on college art creation is shown as follows: the curve corresponding to parameter  $C_x$  shows a linear increase at first and then a linear decline. The parameter  $C_y$  showed a linear change with a slow decline. Parameter  $P_n$  has very good stability to art index data.

## Retraction

# Retracted: Improving and Evaluating Business Management in the Digital Economy Based on Data Analysis

### Security and Communication Networks

Received 8 August 2023; Accepted 8 August 2023; Published 9 August 2023

Copyright © 2023 Security and Communication Networks. This is an open access article distributed under the Creative Commons Attribution License, which permits unrestricted use, distribution, and reproduction in any medium, provided the original work is properly cited.

This article has been retracted by Hindawi following an investigation undertaken by the publisher [1]. This investigation has uncovered evidence of one or more of the following indicators of systematic manipulation of the publication process:

- (1) Discrepancies in scope
- (2) Discrepancies in the description of the research reported
- (3) Discrepancies between the availability of data and the research described
- (4) Inappropriate citations
- (5) Incoherent, meaningless and/or irrelevant content included in the article
- (6) Peer-review manipulation

The presence of these indicators undermines our confidence in the integrity of the article's content and we cannot, therefore, vouch for its reliability. Please note that this notice is intended solely to alert readers that the content of this article is unreliable. We have not investigated whether authors were aware of or involved in the systematic manipulation of the publication process.

Wiley and Hindawi regrets that the usual quality checks did not identify these issues before publication and have since put additional measures in place to safeguard research integrity.

We wish to credit our own Research Integrity and Research Publishing teams and anonymous and named external researchers and research integrity experts for contributing to this investigation.

The corresponding author, as the representative of all authors, has been given the opportunity to register their agreement or disagreement to this retraction. We have kept a record of any response received.

### References

- [1] L. Sun and Y. Wang, "Improving and Evaluating Business Management in the Digital Economy Based on Data Analysis," *Security and Communication Networks*, vol. 2022, Article ID 5908877, 7 pages, 2022.

## Research Article

# Improving and Evaluating Business Management in the Digital Economy Based on Data Analysis

Lu Sun <sup>1</sup> and Yanwen Wang <sup>2</sup>

<sup>1</sup>School of Public Finance & Taxation, Guangdong University of Finance & Economics, Guangzhou 510320, China

<sup>2</sup>Guangdong Provincial Key Laboratory of Public Finance and Taxation with Big Data Application, Guangdong University of Finance & Economics, Guangzhou 510320, China

Correspondence should be addressed to Yanwen Wang; wangyanwen@gdufe.edu.cn

Received 7 June 2022; Accepted 1 August 2022; Published 25 August 2022

Academic Editor: Hangjun Che

Copyright © 2022 Lu Sun and Yanwen Wang. This is an open access article distributed under the Creative Commons Attribution License, which permits unrestricted use, distribution, and reproduction in any medium, provided the original work is properly cited.

In the new economic situation, enterprises formally enter the transition period of “think power differentiation and gap,” big data, artificial intelligence, digital empowerment, and other new digital economy has a positive effect on improving technical means and reducing operating costs, but the digital economy also forces enterprises to improve their strategies at a multiplier speed. The strategic decision of enterprises is to de-enterprise, from pursuing a single business operation benefit to winning competitive advantage by creating a platform ecosystem; the enterprise organization management mode is shifting from vertical management to horizontal collaborative management, and the organization structure is developing dynamically flat. This requires enterprises to pay attention to the role of data analysis in daily operations and management, promote the establishment of a data-driven corporate culture, make full use of digital technology, modularize production links or departments with similar functions or services, and promote the transformation of organizational structure. By unifying the output of products or services to the outside world; at the same time, improve the corporate performance model, shift from result-oriented to process-oriented assessment, and implement a personalized, authority, and accountability system. Shift from result-oriented to process-oriented assessment and implement a personalized incentive model that matches authority, responsibility, and benefits.

## 1. Introduction

In the new economic situation, knowledge and technology have become an important force to change the world, and the digital economy and the Internet have become a major trend [1]. However, most enterprises still choose the traditional management model in the process of business management, which leads to poor communication of information and data within the enterprise and affects the efficient development of the enterprise. In the current digital economy situation, Internet technology is constantly spreading [2]. The work that originally required a lot of manual input can now be done through a simple program; interlayer information transfer can be achieved on the corresponding information management platform; market research can also be achieved through computer development programs on a network platform, saving a lot

of time and effort while ensuring the accuracy of data transmission [3–5].

Corporate culture is a benign conduit for the combination of culture and economy, and the current scholarly view of corporate culture includes spiritual culture, group norms, and organizational ideas. Unlike corporate culture that focuses on the spiritual dimension, corporate managerial culture is more pragmatic and focused [6–8], accompanying management activities and permeating all aspects of corporate decision making, operational organization, motivational model, and leadership model.

This paper argues that management culture refers to the management ideology developed in the practice of strategic decisions, organizational models, and personnel management activities, as well as the accompanying institutional and organizational design, in order to achieve the strategic goals of the enterprise and maximize the efficiency of the



enterprise organization's resource allocation in the context of limited resources [9, 10]. He argues that the digital economy differs from the traditional economy in that its development is an open market from the very beginning, which makes it easier to form a virtuous circle of effective markets, fierce competition, and constant innovation. Only through high-quality scientific decision-making can we make full use of digital technology to improve production quality and efficiency, enhance the production capacity of enterprises, and meet the personalized and customized needs of consumers in the digital economy. On the basis of their own products, companies also need to make a comprehensive analysis and research judgments on the marketing of consumer demand preferences, product sales dynamics, competitors' market information and other massive and frequently changing data, so as to sign a more competitive pricing strategy and more attractive marketing plan, enhance the competitiveness of the enterprise market, and create value for consumers.

Second, corporate management culture needs more cooperation and open space. This is because the application of digital information technology enables companies to connect more market players and consumers and create value through open platforms, collaboration, and other organizational management models. Another important value of the digital economy is that users' personalized needs can be responded to quickly, and positive feedback is provided to the market supply capacity through demand satisfaction, thus promoting the operation of the production and consumption cycle. Therefore, in the digital economy, the most valuable companies are those that can openly collaborate to meet consumers' personalized needs and bring about a huge network effect, rather than traditional companies that concentrate a large amount of resources in one place.

Finally, the enterprise management culture should have the gene and power of continuous innovation. The in-depth application of technological practices such as big data and cloud computing has enabled the flow and reorganization of production factors to be carried out frequently at low cost and high efficiency, with new creations and ideas emerging and innovative products popping up all the time. In response to these innovative changes, Ref. [11] argued that the technological and economic paradigm shift brought about by innovation has led to new economic forms and economic structures. Reference [12] states that in the real world, companies manufacture products and sell them; in the online future, companies produce what consumers decide to buy, and small-volume, personalized production becomes a reality. This, together with the rapid development of digital technology itself, is driving the emergence of new products, new business models, and even new industries.

In today's era, the competition of enterprises is becoming increasingly fierce, and in the fierce market competition, enterprises must do a good job of management in order to stabilize their position. At present, the level of information technology in China is improving, and various advanced technologies are widely used in development and construction. Therefore, this paper analyzes the importance

of data analysis in enterprise management and proposes corresponding methods and measures to improve the quality level of data analysis work, hoping to be a reference and help for the future management of enterprises.

## 2. Related Work

The "digital economy" is a relative expression based on concepts such as the Internet and big data. In general, the basic characteristic of the "digital economy" is the focus on the use of knowledge and technology. This is mainly due to the influence of Internet technology. At the same time, in the digital economy. The huge economic benefits of knowledge and technological innovation are indispensable. Estimation. Therefore, giving full play to the advantages and competitiveness of knowledge and technology is the current way forward for all business management. In the Internet era, the "digital economy" is a virtual and physical form of economy. By constantly using various factors in the market, it is possible to break through traditional possibilities and achieve new breakthroughs in the process of economic development.

The digital economy has profoundly influenced economic and social development, reshaped business operation models, and driven the evolution of business management culture. Compared with agricultural and industrialized economies, the digital economy has unprecedented resource allocation, penetration integration and synergy capabilities, and promoting total factor productivity. The information flow mode of enterprises in the digital economy changes from one-way communication to network-based communication; enterprise value creation changes from tangible products to intangible data creation, and the business philosophy changes from stable profit acquisition to sustainable competitive winning [13]. Enterprise management culture must adapt to these new changes, promote the efficient flow of information, give full play to the value of employees, enhance market resilience, and improve the overall competitiveness of enterprises [14].

Supervision belongs to a very important role of data analysis in business management, the data analysis department in the enterprise data or information collection process, it will be able to more comprehensively know the development of the industry and the actual operation of the enterprise, so that after understanding the context and scope of the relevant data, the data analysis department can effectively assume the enterprise's various aspects of Supervision and management work. In view of the various problems in the development process of the enterprise, timely and effective measures can be taken to solve them, and some problems can also be prevented in time through the corresponding data analysis, and a corresponding problem prevention mechanism can be established, so as to effectively promote the improvement of the efficiency of the enterprise [15].

The difficulty of this work is high, so in order to complete this series of demanding, complex and difficult work, the analysts of the relevant departments need to have a certain amount of analysis of the basic conventional knowledge, but



also to have the corresponding analytical ability, theoretical knowledge, which, to some extent, requires the staff of the data analysis department to improve their quality level [16]. As the staff should master the method of data analysis and clarify the key steps before and after, on the other hand, they should also have the ability to summarize and analyze the data and certain writing skills. Thus, during the work of the data analysis department, it is inevitable that the relevant staff will be motivated to take the initiative to learn and continuously learn to improve their professional knowledge and skill level, so as to protect their own position in the enterprise, thus effectively improving the overall quality level of the staff [17].

China adheres to the socialist market economy system and has developed a way of economic development that is suitable for its national conditions. China mainly adopted the planned economy system in the early stage of economic construction, which consolidated the ideology of some management talents and formed administrative characteristics [18]. Especially in some regions, the government ideology was more serious, which made some enterprises maintain a strong administrative color in enterprise management. Management agencies overlapped and personnel was inefficient; after the reform and opening up, influenced by the international economic environment, a number of rigid and backward enterprises were gradually eliminated and began to reform their own enterprise management mode, and the domestic economic development potential was gradually enhanced. However, in the digital economy situation, many managers still resist the development of enterprise reform, rely too much on the traditional enterprise management model, and lack the acceptance of knowledge and technological innovation, which restricts the development of enterprise operation. At the same time, there is a problem of turnover of old and new personnel in enterprises [19]. Therefore, the lack of talent support in the transformation of the enterprise management model in the digital economy will become a key issue affecting the economic development and transformation of domestic enterprises.

### 3. Method

The meta-analysis method is a quantitative analysis method for reexamining previous studies, and according to the meta-analysis technique for sample. In this study, the following criteria were followed in the data selection process: (1) The data included in the study must be empirical studies using publicly available data, and the  $r$ -value of the relationship between CSR and corporate performance must be included in the study; (2) The data included in the study must include indicators related to CSR and corporate performance in the dependent and independent variables and in the moderating variables; (3) The data included in the study must be independent samples, and if there are cases where the samples in the study are the same, similar or intersecting, limited data with detailed sample size or research content will be included in the study; (4) For the definition of variables, the data selection process follows the following criteria studies;

(5) Data with vague variable definitions or variable definitions that are not within the scope of this study will be excluded if the data cannot be transformed and processed.

As shown in Figure 1, compared with the vertical organization model, the flat matrix organization model enables enterprises to effectively integrate internal and external resources based on objectives, provide quality products or services, respond to market changes in an agile manner, reduce trial and error costs, and resolve risks caused by uncertainty, which brings great benefits to enterprises.

The data coding for the meta-analysis consisted of two levels of content: sample information and effect values. Before formally coding the data, a coding manual was first developed to provide a reference for subsequent coding, and the coding manual was developed and its content was determined in communication with the supervisor to determine the accuracy of coding. When coding the sample information, we mainly included the direct information data in the sample data, and the coding catalog includes: basic information of the sample data, such as author, sample title, publication year, publication journal, data type, and sample size, sample data characteristics, such as country, industry and enterprise characteristics data, and target variables, such as enterprise performance and its measurement; in the coding of the main effect values, the correlation coefficients between enterprise environmental responsibility and performance were used. In the coding of the main effect values, the correlation coefficients between CSR and performance are used as the basic indicators, as well as other statistics that can be converted to correlation coefficients, such as  $t$ -values,  $F$ -values, and chi-square values.

At the same time, common data problems were also coded using the corresponding methods, specifically: first, if there were multiple correlation coefficients between the two in the same piece of data, according to the variables defined as the same subject and no indistinguishable, the study was included according to the mean value of all correlation coefficients. Second, for the same piece of data in the environmental responsibility or enterprise performance in the same piece of data, all of them are coded, screened, and processed in the data collation process. Third, for other statistics that can be transformed for correlation coefficient  $r$ , all are coded and transformed for effect values, and the specific transformation methods are described in the effect size transformation; fourth, for the missing values in the study, except for the relationship between CSR and corporate performance, the coding is blanked, and only the main effects are studied without the moderating effects.

In this paper, the effect value used in the study of the relationship between CSR and corporate performance in the main effect is Fisher's  $z$  value, which is converted from the correlation coefficient  $r$ . The conversion of the effect value consists of two parts: first, if the correlation coefficient  $r$  exists in the sample data, it is directly converted to Fisher's  $z$  value through the calculation formula; second, for other statistics such as  $t$  value,  $F$  value, chi-square value and regression coefficient in the sample data for the relationship between the two, it is transformed into Fisher's  $z$  value after the conversion of the correlation coefficient  $r$ . Table 1 shows

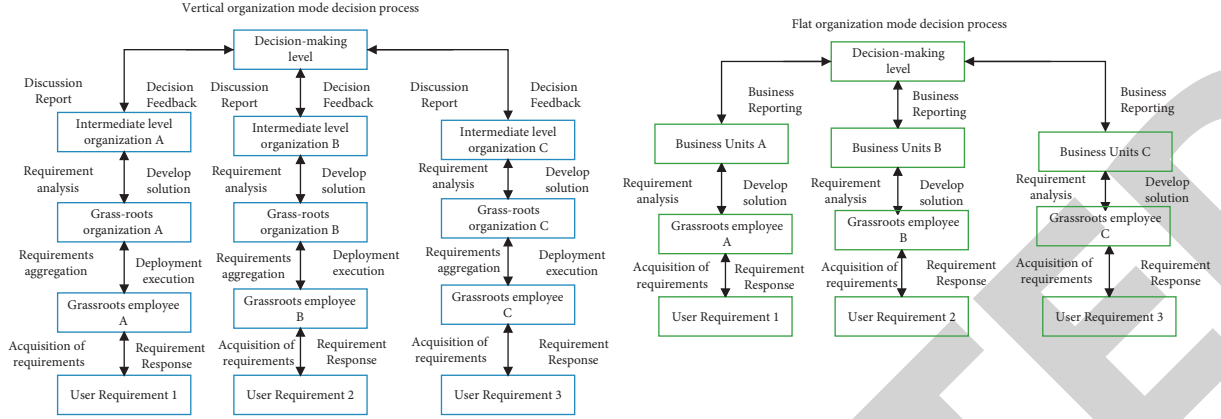


FIGURE 1: Differences in market demand response patterns across organizational forms.

TABLE 1: Effect value conversions.

Statistical value	Calculation method
$t$ -value	$r = \sqrt{t^2/t^2 + df}$ , where $df = N_e + N_e - 2$
$F$ -value	$r = \sqrt{F/F + df}$ , where $df = N_e + N_e - 1$
Cardinality value	$r = \sqrt{x^2/N_e + N_e}$
Regression coefficient	For the value of regression coefficient $\beta$ , if $-0.5 < \beta < 0.5$ , the following formula can be used for conversion $r = \beta * 0.98 + 0.05 (\beta \geq 0); r = \beta * 0.98 - 0.05 (\beta < 0)$

TABLE 2: Effect value conversion.

Statistical quantities	Calculation method
Corrected correlation coefficient	$r' = r / \sqrt{r_{xx} r_{yy}}$ , where $r_{xx}$ is the reliability of the independent variable, $r_{yy}$ is the reliability of the dependent variable
Fisher's $z$	$z = 0.5 \ln(1 + r/1 - r)$
Weighted average $z$	$\bar{z} = \sum (n_i - 3)z_i / \sum (n_i - 3)$ , where the sampling standard error is $SE_z = 1/\sqrt{(N - 3)}$ , weight $W_i = 1/SE = n - 3$ $\bar{r} = e^{2\bar{z}} - 1/e^{2\bar{z}} + 1$
Final effect value	$SE_r = \sqrt{1/SE W_i}$
Full sample sampling error	$Sig. = SE_z / SE_r$
Final effect value sig	$CI = \bar{z} \pm 1.96/SE_r$
95% confidence interval	
Variance of effect values	$S_r^2 = \sum (r_i - \bar{r})^2 / \sum n_i$ , where, $\bar{r} = \sum r_i / \sum n_i$
Sampling error variance	$S_e^2 = \sum (1 - \bar{r}_i)^2 / (n_i - 1) n_i / \sum n_i$
Q-value	$Q = W_i ES_i^2 - W_i^2 ES_i^2 / \sum W_i$

the correlation coefficient  $r$  conversions for  $t$ -values,  $F$ -values, chi-squared values, and regression coefficients. Table 2 shows the calculation of other statistics in the meta-analysis process.

The tests for publication bias are mainly qualitative and quantitative. The funnel plot method is based on whether the graph is centrally symmetric, and symmetry indicates that

TABLE 3: Begg's test.

Adj.Kendall's score ( $P - Q$ )	Std. dev. of score	Number of studies	$z$	$P_r >  z $
148	133.98	55	1.12	0.278

TABLE 4: Egger's test.

Std.Err	Coef.	Std.Err.	$t$	$P <  t $	[95%Conf.Interval]
slope	0.717055	0.562994	1.29	0.209	-0.412587 1.846657
biss	1.246767	1.358283	0.93	0.377	01.486578 3.960352

there is no publication bias between studies, while asymmetry indicates that there is publication bias between studies; the loss of safety coefficient is mainly observed whether the  $n$  value is greater than 0, and there is no publication bias if it is greater than 0, and vice versa.

In Tables 3 and 4, the results of the tests for publication bias of the sample data. The results in Table 3 show that the adjusted statistic  $z$  value is 1.12, which rejects the original hypothesis of publication bias; the results of the Egger's linear correlation test in Table 4 show that the corresponding  $P$  value of the bias variable is  $0.366 > 0.05$ .

The current situation of the development of business management is further analyzed using the hierarchical analysis method, and relevant countermeasures to promote the development of business management are proposed based on the analysis results.

The target layer  $G$  selects the most suitable online marketing development model for the enterprise; the criterion layer  $C$  consists of business management influencing factors, mainly including personalized demand  $C_1$ , logistics cycle  $C_2$ , brand awareness  $C_3$  and website content  $C_4$ ; the program layer  $P$  consists of different models of food online marketing programs, mainly including social online marketing model  $P_1$ , enterprise self-built website model  $P_2$ , and e-commerce platform model  $P_3$  (The constructed index hierarchy is shown in Figure 2).

On the basis of the index hierarchy, a two-by-two comparison of the elements present in the hierarchy is made to construct a judgment matrix. Using the judgment matrix,

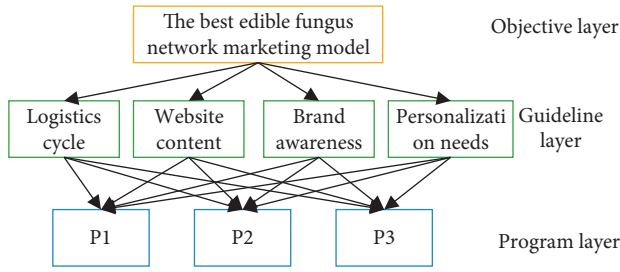


FIGURE 2: Hierarchical structure.

we calculate the weights corresponding to the indicators, and the indicators with higher weights are the main factors affecting the development of business management.

### 3.1. Pre-Production Link

**3.1.1. Low Level of Supervision.** However, at present, there are still problems of poor product quality and low market supervision in areas such as enterprise sales and production in China, and some vendors do not comply with the enterprise product management law and sell poor-quality products to users. Enterprise managers can not accurately identify the quality of products of good and bad quality, so that their own interests are damaged and reduce the motivation of users.

**3.1.2. Lack of Quality Inspectors and Quality Products.** The basis of enterprise research and production is quality products, and product quality directly affects the quality of finished products of the enterprise. Cultivating enterprises is a high-risk, high-investment work, most of the enterprise technology and equipment is difficult to support the cultivation of high-quality enterprise products. Coupled with the relatively small number of enterprise research institutes in China so far, there is a lack of technical personnel, backward equipment and insufficient funds, resulting in the industrial development of enterprises and product cultivation is relatively late.

### 3.2. The Production Chain

**3.2.1. Sloppy Management and Low Technical Level.** Most of the enterprises in China are in the primary stage of production, and manual operation is the main way of enterprises. Specifically, see Figures 3 and 4.

Analysis of Figures 3 and 4 shows that the statistics of users according to their education level show that most of the users engaged in enterprise production have a junior high school education, and the statistics of users according to their age show that most users are between 41 and 50 years old. In the family model, due to the limited education level, users have less knowledge about the enterprise, which leads to the constant stagnation of the enterprise industry development.

The methods of users' enterprises in the family mode come from daily accumulation and summary, and they

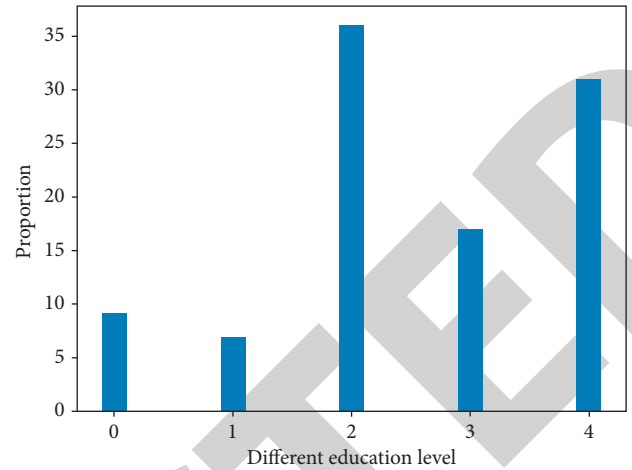


FIGURE 3: Classification of educational levels.

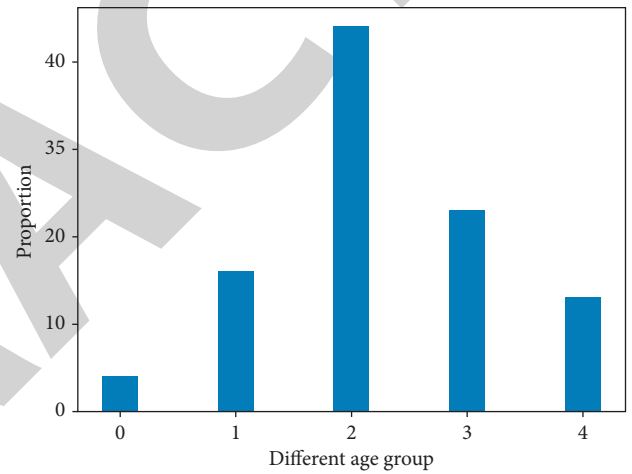


FIGURE 4: Age group division.

master less enterprise expertise, especially lacking knowledge of enterprise product purchase, which makes it easy to buy inferior products. At present, the level of regulation of China's enterprise market is low, and there are fewer purchase channels, using inferior products to cultivate the enterprise, the yield and quality are poor, which adversely affects the user income.

## 4. Case Study

The development status of a city's business management is used as an example to analyze the current situation of China's enterprise network marketing development. Factory enterprises, bases, and individual households are the main forms of enterprise production in a city, mainly distributed in several districts and counties. Sales and production of enterprises of different varieties vary, but overall production tends to be stable.

In recent years, enterprise factory has been developed in a city. Compared with the traditional way, the economic efficiency and production level of enterprise factories are higher, which facilitates the application of new

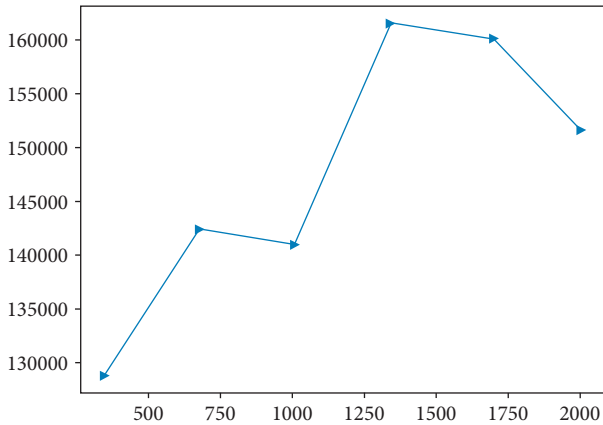


FIGURE 5: Enterprise production in a city from 2017 to 2022.

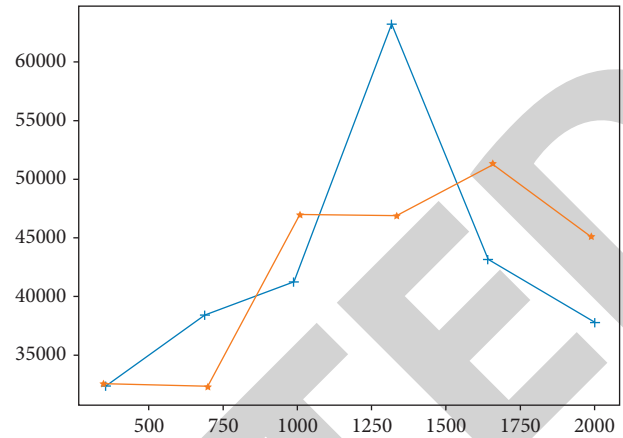


FIGURE 7: Production of a city from 2017 to 2022.

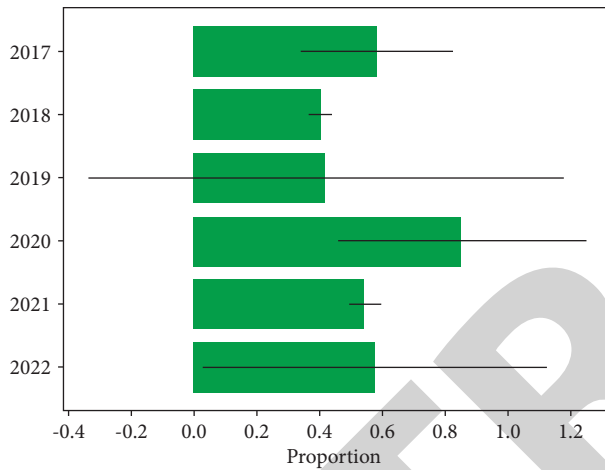


FIGURE 6: Proportion of the production of edible fungi in the country from 2017 to 2022.

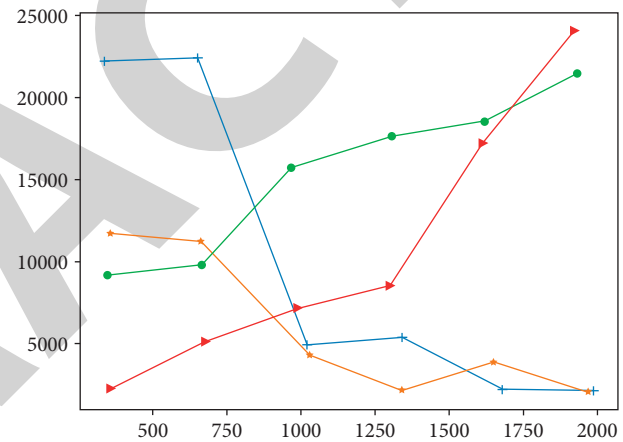


FIGURE 8: Enterprise production in a city from 2017 to 2022.

technology as well as the promotion of new varieties and keeps the supply market stable, which is an inevitable trend for the development of enterprise industry in the country.

As of 2021, the annual output of enterprises in a city is up to 16.2 million tons, and the varieties of enterprises are up to more than 20. The output of a city enterprise is shown in Figure 5, and the proportion of the output of enterprises in the country is shown in Figure 6.

Analysis of the data in Figures 5 and 6 shows that the enterprise production in a city from 2017 to 2020 has been rising, but from 2020 to 2022 there is a decreasing trend; compared with the enterprise production in 2017, the enterprise production in 2022 increased by about 20%, in contrast, the enterprise production in a city in the national enterprise production in the proportion of the decreasing trend.

The number of enterprise varieties in a city in 2022 is the same as the number of enterprise varieties in 2021, and the production is about 15.28 million tons, which accounts for 95.12% of the total production of enterprises in a city, which is the highest and most common sales volume in a city

market. According to the production of a city from 2017 to 2022, the enterprise varieties can be divided into three categories, the first category of enterprises with the production of annual growth and production of a larger number of characteristics. The proportion of production in the total output of enterprises in the city is large, and the output fluctuates from around 30,000 tons to 50,000 tons on average every year, and the output of a city from 2017 to 2022 is shown in Figure 7.

As can be seen from Figure 7, the production has the highest values in 2020 and 2021, and the production has been increasing steadily in other years. Figure 8 shows the production of different types of enterprises in a city from 2017 to 2022.

The second category of enterprises refers to the varieties with good industrial production technology and rapid growth in production in the last two years. Analysis of the data in Figure 8 shows that compared with the output in 2017, the output in 2022 has doubled. The third type of enterprises, showing the characteristics of decreasing production year by year, had the most production in 2017 and 2018 in Zhonghe, but the production gradually became less after 2019.

## Retraction

# Retracted: Dance Movement Recognition Based on Modified GMM-Based Motion Target Detection Algorithm

### Security and Communication Networks

Received 10 October 2023; Accepted 10 October 2023; Published 11 October 2023

Copyright © 2023 Security and Communication Networks. This is an open access article distributed under the Creative Commons Attribution License, which permits unrestricted use, distribution, and reproduction in any medium, provided the original work is properly cited.

This article has been retracted by Hindawi following an investigation undertaken by the publisher [1]. This investigation has uncovered evidence of one or more of the following indicators of systematic manipulation of the publication process:

- (1) Discrepancies in scope
- (2) Discrepancies in the description of the research reported
- (3) Discrepancies between the availability of data and the research described
- (4) Inappropriate citations
- (5) Incoherent, meaningless and/or irrelevant content included in the article
- (6) Peer-review manipulation

The presence of these indicators undermines our confidence in the integrity of the article's content and we cannot, therefore, vouch for its reliability. Please note that this notice is intended solely to alert readers that the content of this article is unreliable. We have not investigated whether authors were aware of or involved in the systematic manipulation of the publication process.

In addition, our investigation has also shown that one or more of the following human-subject reporting requirements has not been met in this article: ethical approval by an Institutional Review Board (IRB) committee or equivalent, patient/participant consent to participate, and/or agreement to publish patient/participant details (where relevant).

Wiley and Hindawi regrets that the usual quality checks did not identify these issues before publication and have since put additional measures in place to safeguard research integrity.

We wish to credit our own Research Integrity and Research Publishing teams and anonymous and named external researchers and research integrity experts for contributing to this investigation.

The corresponding author, as the representative of all authors, has been given the opportunity to register their agreement or disagreement to this retraction. We have kept a record of any response received.

### References

- [1] J. Tian and X. Yang, "Dance Movement Recognition Based on Modified GMM-Based Motion Target Detection Algorithm," *Security and Communication Networks*, vol. 2022, Article ID 6023784, 12 pages, 2022.



## Research Article

# Dance Movement Recognition Based on Modified GMM-Based Motion Target Detection Algorithm

Jing Tian<sup>1</sup> and Xiaoqiang Yang<sup>2</sup> 

<sup>1</sup>Zhengzhou Tourism College, College of Arts and Culture, Zhengzhou 451464, China

<sup>2</sup>Hainan University School of Music and Dance, HaiKou 570228, China

Correspondence should be addressed to Xiaoqiang Yang; 991593@hainanu.edu.cn

Received 21 June 2022; Revised 29 July 2022; Accepted 4 August 2022; Published 22 August 2022

Academic Editor: Hangjun Che

Copyright © 2022 Jing Tian and Xiaoqiang Yang. This is an open access article distributed under the Creative Commons Attribution License, which permits unrestricted use, distribution, and reproduction in any medium, provided the original work is properly cited.

Under the synergistic development of social economy and science and technology, the intelligent teaching of dance has become more and more popular. This teaching method can not only decompose dance movements more specifically, which is easy for students to understand and master, but also get rid of the time and space limitation in traditional dance teaching and provide more independent learning opportunities for students. The problem of low accuracy of dance movement recognition due to complex gesture changes in dance movements is addressed. To this end, this paper proposes a modified motion target detection algorithm based on GMM. The dance movement recognition algorithm first extracts the features of dance movements through a feature pyramid network, then uses a multi-feature fusion module to fuse multiple features to improve the algorithm's estimation of complex postures, and finally completes the recognition of dance movements. Experiments show that our method can maintain a certain recognition rate in the case where the background and target are easily confused, and can effectively improve the dance action recognition accuracy, thus realizing the action correction function for dancers. This also verifies the effectiveness of the action recognition algorithm for dance movement recognition.

## 1. Introduction

Human pose estimation is a key technique in the field of human action recognition, which is based on the principle of recognizing human pose by extracting features in images [1]. This technique can be used in intelligent dance-assisted training to obtain a skeleton map of the dancer's posture by extracting features from the dancer's image. Thus, the dancer's dance movements are recognized, and the dancer's posture is evaluated and corrected [2].

As an aid to human eye vision and an important component of automated systems, computer vision is widely used in medical and transportation fields [3]. Compared with the human eye, the advantage of computer vision is that it has much higher computational power than the human brain and higher analysis capability for complex images [4]. Action recognition in dance video images is an important application area of computer vision technology, which can

be applied to many scenarios, such as competition arbitration, introductory learning for dancers, and movement correction for professional dancers [5, 6].

Compared with low-level action recognition such as gesture recognition and simple limb action recognition, dance action recognition has penetrated into the level of motion recognition [7, 8]. Therefore, when simple limb localization algorithms are applied to dance movement recognition, it is usually difficult to obtain high recognition accuracy [9, 10]. The difficulties of dance movement recognition mainly include the following three points.

Dance movements are complex and variable. From the most basic action elements such as "lifting," "sinking," "rushing," and "leaning" to the coherent and complex actions such as "standing beat swallow," "pouncing step," "cloud step," and "turning over," there is a great degree of freedom [11, 12]. Therefore, it is more difficult to identify each movement accurately.

Obscuration in dance is a serious problem. If there is only one dancer, some of the dancer's limbs may be obscured by themselves, making it difficult to identify the position of certain limbs; if there are multiple dancers, the dancers will obscure each other [13, 14]. In particular, the dancers' clothes are loose, such as long dresses with skirt support, so the obscured area will be larger. In addition, the angle of the photo or video can also cause some obstacles to the recognition of dance movements [15].

The coherence of dance movements is strong. In simple body movements, the coherence of the movements is weak. Generally, everyday body movements change slowly and each body movement remains the same over a period of time. However, in dance, all movements are coherent and fluid, and fewer movements remain stationary. Therefore, it is more difficult to accurately detect the boundaries of each dance movement in time.

Early human posture estimation mainly focused on human contour features or part models. For example, the literature [16, 17] designed a human pose estimation algorithm based on part detection by extracting edge force field features through boosting classifier. Literature [18, 19], on the other hand, proposed an appearance model combining histogram of oriented gradients (HOG) and color features for human pose estimation. However, due to the complex variation of human pose, the traditional methods are difficult to achieve effective pose estimation [20, 21]. Therefore, deep learning-based methods are gradually used for human pose estimation. In 2015, deep learning-based human pose estimation algorithms started to return to the human skeleton heat map [22]. In 2016, a research team from the University of Michigan [23] designed an hourglass-like neural network structure for extracting multi-scale features for human pose estimation. In 2017, the literature [24] proposed an approach using partial affinity domain to obtain human skeleton maps. In addition, numerous deep learning-based algorithms for human pose estimation have been proposed, all of which can be used for dance movement recognition to assist dancers' training [25]. The rapid change of dancers' movements and the variability of their postures pose a challenge for dancer-assisted training intelligence.

To this end, a dance movement recognition algorithm based on multi-feature fusion is designed in the paper for learning complex and variable dancer movement recognition.

## 2. Motion Recognition System

The motion recognition system in this paper consists of a human detection module, a pose and feature detection module, and a motion recognition module. First, a modified GMM-based motion target detection algorithm is used to detect and segment the moving human body from the video. For the detected binarized human region, the pose, pose change rate, and human position change information are extracted, and the pose evaluation function is introduced to improve the accuracy of pose detection. In the process of action recognition, an action recognition algorithm based on multi-feature fusion is proposed in this paper. The algorithm

not only analyzes the shape features of human appearance, but also fuses the motion features of human body, so the recognition results are more accurate. The algorithm is easy to understand and implement, with a small amount of operations and fast recognition speed. The flow of the whole algorithm is shown in Figure 1.

**2.1. Human Body Detection.** The first step in human motion recognition is to detect and segment the human body in motion or at rest. Due to the various colors and textures of human clothing, the uncertainty of human posture, and the uncertainty of the visual background, there is still no feasible method to detect the human body from static images. Therefore, this paper uses motion detection to extract human targets in video images.

Background subtraction (BS) is a general and widely used technique for generating foreground masks (i.e., binary images containing pixels belonging to moving objects in the scene) by using a static camera. BS is the most commonly used method for detecting motion targets, and it can detect motion targets in indoor environments very well. It is found that the GMM background model adopts a global uniform update strategy, which highlights its shortcomings in dealing with complex target motion forms. The main manifestation is that the suspended motion targets are absorbed as part of the background, resulting in incomplete extracted motion targets such as people. This absorption phenomenon is unavoidable due to the need for an adaptive background model to handle slow background changes (e.g., illumination). Therefore, the results of motion segmentation and the recognition of the target can be used to guide the background update. For example, if the motion target  $O_{(ij)}$  is a human object, the corresponding background update confidence  $f_{Bg}$  takes the value of 0, and the pixels at that point do not participate in the background update; otherwise, the corresponding background update confidence  $f_{Bg}$  takes the value of 1, and the pixels at that point participate in the background update. The region-based background update strategy avoids pose false detection caused by local human motion and improves the accuracy of action recognition using pose changes.

**2.2. Motion State Characterization.** Different features reflect the characteristics of human motion states from different perspectives. When selecting features, we should consider not only their distinguishability, but also the difficulty of their extraction. The object of this paper is the whole human body, including the limbs, and the goal of the study is to identify the typical daily movements (standing up, lying down, etc.) and sudden abnormal movements (falling down) in a complex environment. Therefore, the key features related to the shape and movement of the human body as a whole are considered in the human motion state characterization. In this paper, we adopt the idea of feature fusion to characterize the human motion state by fusing multiple features, because there are shortcomings in using appearance-based shape features alone or motion features alone.



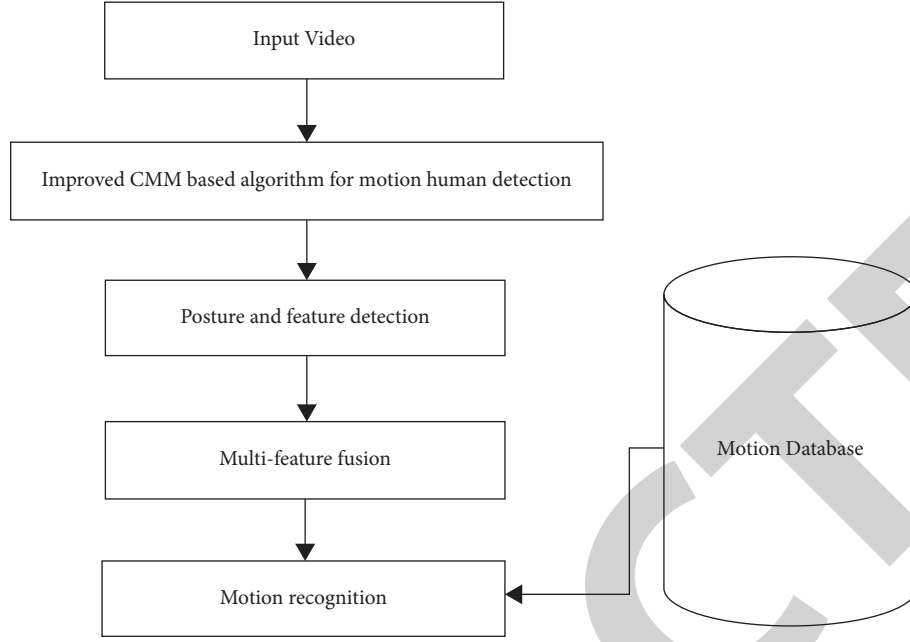


FIGURE 1: Action recognition system based on multi-features fusion.

**2.2.1. Posture Features.** Human motion in the home environment consists mainly of several key pose transformations, so this paper selects the overall human pose information to describe the human motion state based on appearance and shape. Model-based pose acquisition can describe complex poses, but the model is difficult to initialize, computationally intensive, and prone to local minima, making it difficult to find globally optimal and robust parameters. Therefore, this paper chooses the human body width and height ratio, which is invariant to the target size and distance and has little influence on the viewpoint, to describe the human body's pose characteristics.

**2.2.2. Pose Change Rate Feature.** The posture of the human body always changes smoothly in normal daily movements, but the rate of posture change can be dramatic when a sudden abnormal (fall) situation occurs. In this paper, the motion feature of the rate of change of posture is introduced to detect the fall of a person. In the two actions of falling and lying down, the critical posture change process is similar and the posture change rate is different.

**2.2.3. Position Change Feature.** It is impossible to determine whether the human body is walking or standing by only relying on the selected posture features and their posture change rates. In these two kinds of movements, the human posture changes from the standing posture to the standing posture, and the introduction of the motion information of position change can solve this problem. Then, how to determine whether the position of the "human target" changes? After region segmentation, we can obtain the position of the moving human target in the image coordinate system (coordinates of the top left

vertex of the smallest rectangle containing the foreground target) and compare the positions of the two frames before and after to determine whether the target position has changed.

### 2.3. Attitude and Feature Detection

**2.3.1. Pose Feature Detection.** The basic postures of human daily actions are defined as stand, sit, and lay, and the set of postures  $P$ .

$$P = \{s, \tan d, \text{sit}, \text{lay}\}. \quad (1)$$

The currently detected pose  $p(t) \in P$  is considered to be detected only when the human body is in motion, so the human body is considered to remain in the same pose when there is no motion information.

Since the motion body detection is a high-dimensional signal, it is not easy to recognize the pose in this high-dimensional space, and feature transformation is needed for later classification. The body posture ratio  $k$  is calculated for different postures in 900 daily actions, and the threshold value of  $k$  is set to distinguish between standing, sitting, and lying postures based on the minimum probability of misjudgment criterion, as described in Table 1.

One of the problems found in the experiments that affects the accuracy of posture is the false detection of posture. For example, when the human arm is unfolded, the standing posture is mistakenly detected as a sitting posture, as shown in Figure 2.

By constructing a posture evaluation function to eliminate the misjudgment of posture due to "unusual" human movements, define the posture evaluation function  $S$  as in equation.

TABLE 1: Thresholds for different actions.

Gesture	Stand	Sit	Lay
Threshold $k$	$k \geq 1.8$	$1.8 > k \geq 0.7$	$k < 0.7$



FIGURE 2: Posture detection.

$$S = \frac{\sum F_g}{S(T)}, \quad (2)$$

$$Q = \frac{k(t-1)}{k(t)}. \quad (3)$$

where  $\sum F_g = \sum_{(x,y) \in T} I(x, y)$ . is the area of the foreground image of the moving human body and  $S(T) = W * H$ . is the area of the smallest external rectangle of the foreground image. From the expression of the evaluation function, we can see that the value of the function varies in the range  $[0, 1]$ . The value of the evaluation function is highest when  $\sum F_g = S(T)$ , and becomes very low when the human arm is expanded. If the pose evaluation function is low, it is considered as an undefined pose and is not involved in action recognition.

The pose recognition algorithm in Haritaoglu compares the pose recognition algorithm in this paper with the algorithm in Haritaoglu. The pose recognition algorithm in Haritaoglu projects the foreground image of a moving human body in the  $x$ -axis and  $y$ -axis directions, and matches the projected contour lines with the training contour line templates of different poses to obtain the human pose. The pose recognition rates of the two algorithms are comparable, but in terms of complexity, Haritaoglu's algorithm is more complex than the one in this paper.

**2.3.2. Pose Change Rate Detection.** Define the ratio of the body posture ratio of the previous frame to the body posture ratio of the current frame as the inter-frame change rate of human posture, denoted by  $Q$ , i.e.,

$Q$  characterizes how quickly a person's posture changes: when a person maintains the same posture,  $Q$  is close to 1; when a person sits or lies down normally,  $Q$  increases slowly; when a person falls,  $Q$  increases rapidly. Thus, the rate of change of the human posture ratio can be used to detect the falling action. The rate of change of human posture during normal movement  $Q < 1.5$  is obtained statistically.

**2.3.3. Position Detection.** The position of the human body in the image coordinate system is defined as  $P(t, i)$ , and the position of the human body changes using the Euclidean distance metric, i.e.,  $k(t, i) = \|P(t+1, i) - P(t, i)\|$ ; when  $k(t, i)$  is greater than the threshold value  $K_s$ , the human body position is in motion. The discriminant method is

$$\text{if } k(t, i) > K_s, \text{ then Action} = 1; \text{ else Action} = 0; \quad (4)$$

In order to accurately determine whether the position of the human body has changed and to improve the robustness of the algorithm, the concept of confidence is introduced. The confidence level is used to measure the degree to which the human target is in motion and ranges from 0 to 40. A confidence level of 0 means that the human body is definitely in motion and a confidence level of 40 means that the target is definitely not in motion. If  $\text{Action} = 0$ , then the confidence

TABLE 2: Condition setting of different actions.

$a(t)$	Action		Conditions		
	$p(t)$	$p(t-1)$	$Q$	UAction	
Walk	Stand	Stand	$< 1.5$	$\leq 0.5$	
Sit down	Stand	Sit	$< 1.5$	—	
Stand up	Sit	Stand	$< 1.5$	—	
Lay down	Sit, stand	Lay	$< 1.5$	—	
Get up	Lay	Sit, stand	$< 1.5$	—	
Fall down	Stand, sit	Sit, lay	$\geq 1.5$	—	
Stand still	Stand	Stand	$< 1.5$	$> 0.5$	

level of the target is increased by 1; otherwise, the confidence level is zero. Given a confidence threshold, the target is considered to be in a nonmotion state when the confidence level is greater than the threshold, which is set to 20 in the text. The confidence level is defined as CAction, the initial value of CAction is 0, and the confidence level is normalized to UAction. If UAction is greater than 0.5, the human position changes and vice versa, and there is no change. The specific method is

$$\begin{aligned}
 &\text{if Action} = 0, \text{ then CAction} \\
 &\quad + +; \text{ else CAction} = 0; \\
 &\text{if CAction} \geq 40 \text{ then CAction} = 40 \\
 &\quad \text{UAction} = \text{CAction}/40.
 \end{aligned} \tag{5}$$

**2.4. Action Recognition.** Define the daily actions of a person: walk, sit down, stand up, lay down, get up, fall down, and standstill, which form the action set A.

$$A = \{\text{walk, sit down, stand up, lay down, get up, fall down, stand still}\}. \tag{6}$$

The current detected action  $a(t) \in A$ . According to the regularity that different human actions are composed of different postures, this paper detects human actions by using the posture change combined with the frame-to-frame change rate feature and the position change feature, as shown in Table 2.  $p(t)$  denotes the posture at moment  $t$ , and  $p(t-1)$  denotes the posture at moment  $t-1$ .

In order to filter out meaningless or undefined actions, this paper introduces a threshold model of the minimum number of frames of pose duration. The threshold model gives the bottom line for performing action judgments, and action judgments are performed only when the number of pose duration frames of the observed sequence is greater than the threshold; otherwise, the observed sequence is considered as a meaningless or undefined action. According to this criterion, the minimum number of frames that can be statistically obtained to describe the pose of each action is 10; i.e., the threshold value in the threshold model is 10 frames (the video image acquisition rate is 30 frames/s). This method is able to eliminate the false detection of motion due to noise.

**2.5. Dance Video Image Motion Pose Extraction and Joint Modeling.** With the development of human behavior recognition field and the depth of research tasks, from the initial recognition of simple single actions under restricted

conditions to the complex group behavior recognition in real natural scenes nowadays, both the information acquisition equipment and algorithm capability have posed serious challenges. As an important part of the behavior recognition process, the result of feature extraction largely affects the real time and accuracy of the behavior recognition effect. As a classical problem in the field of computer vision and machine learning, feature extraction is different from feature extraction in image space, and the feature representation of human action in video not only describes the human form in image space, but also must extract the human appearance and posture changes, which extends the feature extraction problem from two-dimensional space to three-dimensional space-time, which greatly increases the complexity of behavior mode expression and subsequent recognition tasks. At the same time, it also broadens the thinking of vision researchers in terms of solution ideas and technical methods. Human features are the information that can be extracted from the underlying video sequence to characterize the target behavior, such as color, contour, texture, depth, or human motion direction, speed, trajectory, as well as spatiotemporal interest points and spatiotemporal context.

## 2.6. Identifying Action Features Using Pose Feature Extraction Method

**2.6.1. Dancer's Action Recognition Feature Classification.** There are great differences between the dance movements of dancers and the daily movements of ordinary people, and many movements require dancers to use their arms and legs to complete, so when selecting the target area for background recognition, it is necessary to grasp the whole body movement information of dancers to accurately identify their movements. Dancer's movement recognition can be divided into several categories: static features, mainly in the form of dancer's human target size, color, body contour, depth, etc., which can convey the overall information of dancer's movement, such as the current basic shape that can be derived from the dancer's contour features; dynamic features, mainly in the form of dancer's movement speed, direction, and trajectory, which can reflect the dancer's movement path. The identification of these features can calculate the movement direction characteristics of the dancer and create conditions for modeling; spatiotemporal features are mainly manifested as spatiotemporal shapes, points of interest, etc.; descriptive features include the scene the dancer is in, surrounding objects, posture, etc.

**2.6.2. Dancer Pose Feature Extraction.** The pose feature extraction method can be used in conjunction with a pose estimation sensor, which is commonly used in the field of motion tracking and robot vision to determine the directional points of a dancer's motion. It can use the optical flow value in the pose estimator to filter the background information in the image to obtain the dancer's joint coordinate region, and can eliminate the occlusion and influence of factors such as the dancer's clothes on the dancer's motion as shown in Figure 3.

**2.7. Dancer Joint Point Recognition Modeling Using Kinect.** The Kinect method is used to consider the human body as an axis composed of 25 joint point coordinates, and the human skeletal structure of the dancer is built with these joint points to obtain the human skeletal model of the dancer as shown in Figure 4.

From the model, it can be seen that the dancer's joint points are mainly distributed in the extremities. There is one joint point in the center of the head, neck, spine, and shoulder, and the most concentrated joint points are located in the upper limbs. The left upper limb has joint points. The principle of using these joint points to build the model is to accurately record the movement of each joint point during the dancers doing various movements, accurately identify each movement of the dancer, and thus output the correct skeleton of the dancer's movements. With the skeleton model of dancers' movements, the recognition accuracy and efficiency of the computer vision system for dancers' movements can be significantly improved, and the whole recognition process is shown in Figure 5.

### 3. Dance Movement Recognition

The new algorithm uses a feature pyramid network (FPN) for feature extraction, then deepens the extraction for different scale features, and finally upsamples each feature to the original image size for feature fusion, as shown in Figure 6. The residual block in the figure indicates the residual module as shown in Figure 7.

**3.1. Feature Pyramid-Based Backbone Network.** The shallow features in  $C_1, C_2, C_3$  have a high spatial resolution. However, the semantic information contained is not sufficient, while the opposite is true for the deeper features in  $C_4, C_5$ .

Based on the FPN backbone network, as shown in Figure 8, it is difficult to identify human pose key points in complex environments, such as occluded hidden key points. The localization of such complex key points usually requires richer feature information, for which a multi-feature fusion module is designed in the paper.

**3.2. Multi-Feature Fusion Module.** The FPN-based backbone network is used to identify the estimation of simple key points, and the multi-feature fusion module is used to handle the estimation of more complex key points, whose structure is shown in Figure 9. To obtain better local features,

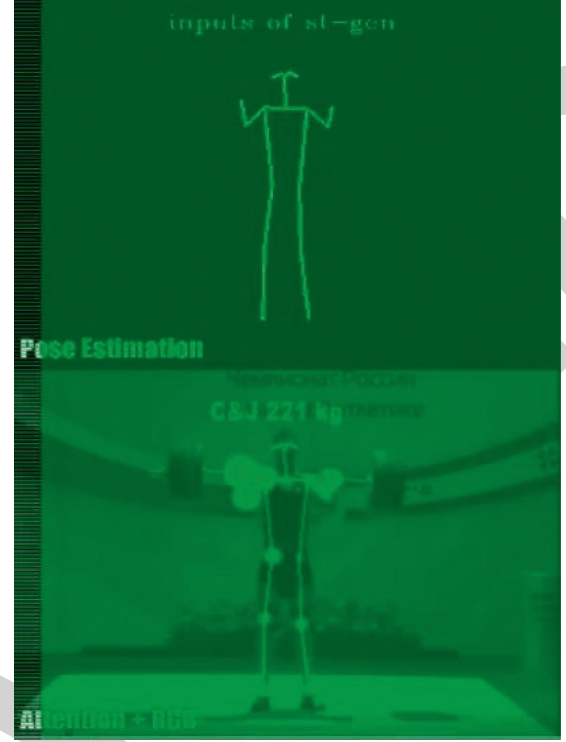


FIGURE 3: Dancer's posture characteristics.

this paper enhances the feature resolution at each stage by upsampling operation. Finally, the individual features from the FPN are fused into the CONCAT operation.

During the training process, the FPN extracts features and returns the human skeleton key points, and simple key points will be basically completed in the FPN stage. For complex key points, such as occlusion and hiding, the multi-feature fusion module will further deepen the learning of features from each layer of the FPN and fuse them, and finally return to the human skeleton heat map.

**3.3. Loss Function.** Human pose estimation is a regression problem, and the common loss functions in regression problems are L1 loss function and L2 loss function. The dancer movement recognition in this paper adopts the regression of the key points of the dancer's skeleton, so the algorithm in this paper adopts the loss function of L2 parametric optimized Euclidean distance, as shown in (1).

$$L(\theta) = \frac{1}{2N} \sum_{i=1}^N \|F(X_i; \theta) - F_i\|_2^2, \quad (7)$$

where  $\theta$  denotes the dancer movement recognition network parameters to be optimized;  $N$  is the total number of dancer images involved in the learning training;  $X_i$  denotes the current learning dancer image sample  $i$ ;  $F_i$  denotes the heat map of the  $i$ -th dancer image; and  $F(X_i; \theta)$  denotes the key points of the dancer skeleton regressed by the model heat map of the key points of the dancer's skeleton regressed by the model.

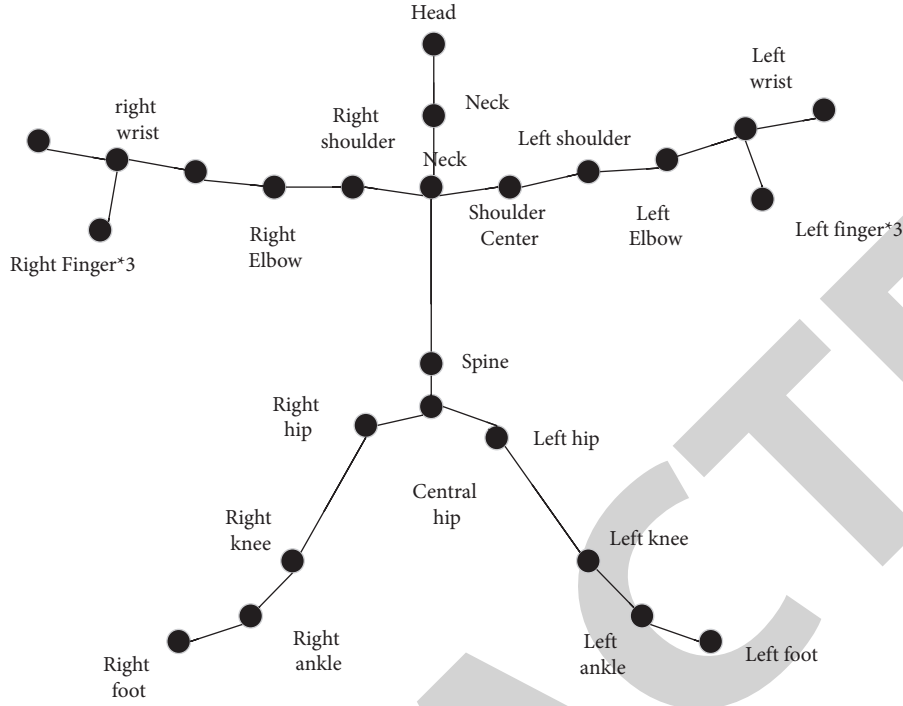


FIGURE 4: Dancer's joint point recognition model by 2 Kinect method.



FIGURE 5: Dancer's joint point recognition process.

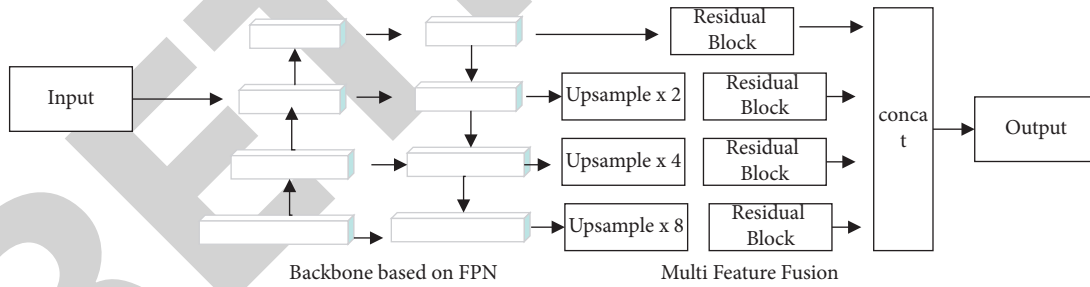


FIGURE 6: Dance movement recognition.

#### 4. Long-Time Target Tracking Algorithm

The extraction of features directly affects the accuracy and efficiency of target tracking. Given a new image frame, two filtering templates, target position and scale prediction, are learned based on HOG and texture features, respectively. The filtering output is calculated using (2).

$$f(z) = \gamma_{HOG} f_{HOG}(z) + \gamma_{tex} f_{tex}(z). \quad (8)$$

The contribution of the two feature responses is  $\gamma_{HOG}$ ,  $\gamma_{tex}$ , and the calculation rule is shown in (3) and satisfies  $\gamma_{HOG} + \gamma_{tex} = 1$ .

$$\begin{cases} \gamma_{HOG} = \frac{f_{HOG}(z)}{f_{HOG}(z) + f_{tex}(z)}, \\ \gamma_{tex} = \frac{f_{tex}(z)}{f_{HOG}(z)/(f_{HOG}(z) + f_{tex}(z))}. \end{cases} \quad (9)$$

The filtered response values of the two features are linearly weighted and fused using (3), and the maximum response value after fusion is used to determine the target region.

In this paper, a simple and effective region suggestion generation scheme, EdgeBox, is chosen to generate candidate regions for the whole image and calculate their

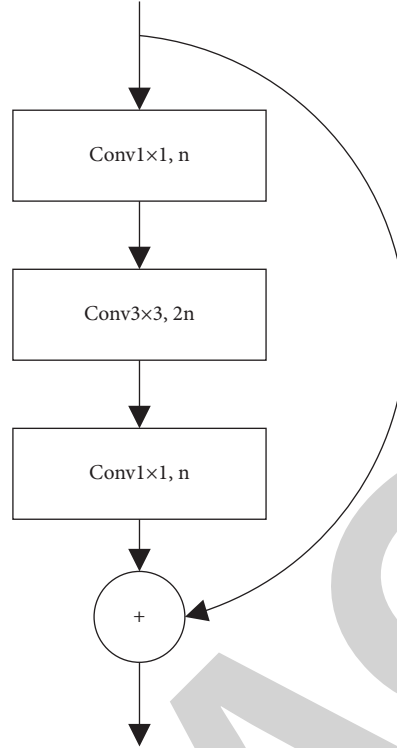


FIGURE 7: Dance movement recognition residual module.

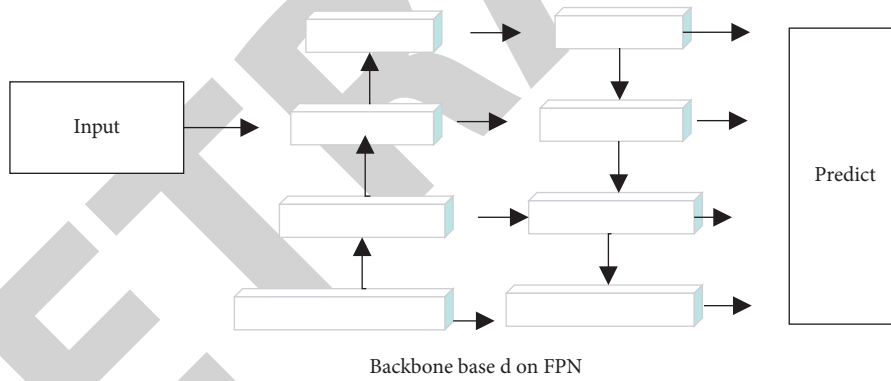


FIGURE 8: Backbone network.

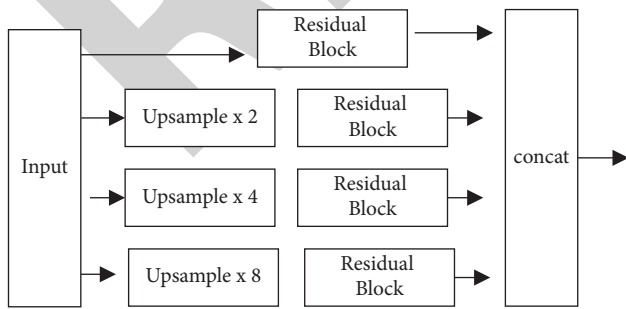


FIGURE 9: Multi-feature fusion structure diagram.

confidence scores, and the candidate region with the highest confidence is the retracing result. For an image, the edge information is used to determine the bounding box of

the object. Based on the number of contours within the bounding box and the number of contours overlapping with the edges of the bounding box, the bounding box is scored and the candidate region information is determined according to the order of the scores. The candidate regions generated by EdgeBox include two types, one near the predicted target (denoted by  $B_s$ ) and one for the whole image region (denoted by  $B_h$ ).  $b$  is a candidate bounding box in  $B_s$  or  $B_h$ . Define  $g(b)$  as the maximum filter response, and detect the tracking result by checking whether  $g(b)$  is lower than the given threshold  $T1$ , which is less than the threshold value to indicate tracking failure and start the retracing procedure. In the normal tracking process, the filter template of the previous frame is generally used to find the target position of the current frame. However, during retracing, the tracking result of the previous frame

TABLE 3: Number and complexity of training set images for each movement.

Dance action name	Number of training set images	Action complexity
Lift	185	1
Sink	210	1
Charge	122	2
Cloud step	108	1
Turn over	150	2
Stand up and shoot the swallow	188	3

Cross your arms	98.86	0	0	0	0	1.14
Raise high	0	84.3	3.93	0	3.93	7.84
One arm open	0	0	94.2	0	1.93	3.85
Wave your hand	0	3.7	3.7	85.2	0	7.4
Open both arms	0	1.78	0	0	96.4	1.78
Walking	0	0	2.8	1.4	0	95.8
	Cross your arms	Raise high	One arm open	Wave your hand	Open both arms	Walking

FIGURE 10: Confusion matrix of 6 dance movements.

is no longer reliable, so it is necessary to select a reference image from the label library as the retracking head (the first frame is used as the retracking head by default). The confidence level of all images in the label library is read, and the Euclidean distance between a candidate frame ( $b_t^i$ ) and these images ( $b_{t-j}$ ,  $j = 1 \rightarrow t$ ) is calculated for the current frame.

$$D(b_t^i, b_{t-j}) = \exp\left(-\frac{1}{2\sigma^2}\|(x_t^i, y_t^i) - (x_{t-j}, y_{t-j})\|^2\right), \quad (10)$$

$\sigma$  is the initial target size diagonal length. Based on the confidence, Euclidean distance, the best element is found as the retracking head and trained online to update the filtering model and regain the normal tracking pattern, so that the algorithm maintains high robustness and efficiency in long-time tracking.

$$\arg \min_{i,j} \beta g(b_t^i) + (1 - \beta) D(b_t^i, b_{t-j}), \quad (11)$$

$$g(b_t^i) > T_1.$$

The  $\beta$  in (5) is a weight parameter that adaptively adjusts the confidence, the contribution of the Euclidean distance. If  $\{g(b)|b \in B_s\}$  is greater than  $g(z)$  (the confidence level of the current template), the new target size ( $w_t, h_t$ ) is defined as

$$(w_t, h_t) = \alpha(w_t^*, h_t^*) + (1 - \alpha)(w_{t-1}, h_{t-1}), \quad (12)$$

It can also be expressed as

$$(w_t, h_t) = (w_{t-1}, h_{t-1}) + \alpha((w_t^*, h_t^*) - (w_{t-1}, h_{t-1})), \quad (13)$$

$(w_t^*, h_t^*)$  indicates the width and height of the maximum confidence candidate region, and  $(w_{t-1}, h_{t-1})$  is the width and height of the previous tracking target [26–28].



TABLE 4: Recognition results.

Movement type	Accuracy (%)
Arms crossed	98.9
Arms raised	85.3
One-hand wave	95.2
One arm open	85.1
Both arms open	96.9
Walking	95.8

## 5. Results and Analysis

**5.1. Algorithm Validation.** In order to better verify the accuracy of the dance movement recognition method designed in this paper, two data sets, PASCAL VOC2011-val set and Stanford 40 actions, are more commonly used, and the collected dance images were used to conduct the experiments. All experiments were performed on a computer with Intel Core i7-4790 CPU and 16 GB RAM and Windows 10 operating system based on Visual Studio 2010 development platform and OpenCV2.4.3 programming environment [29, 30]. The complexity of each dance movement and the number of images in the training set are shown in Table 3.

To verify the effectiveness of the algorithm, all heat maps are visualized as shown in Figure 8. The left image is the input image, the middle image is the singer's skeletal key point heat map, the right image is the computed singer heat map, and the right image is the maximum probability key point and key point limb region obtained from the computed singer heat map. The algorithm is trained and recognized, the accuracy on the training set and test set is shown in Figure 10, and the recognition accuracy on the specific test set is shown in Table 4.

From Table 4, it can be seen that the average recognition accuracy of this research method on the test set is more than 92%, and the overall recognition accuracy is high, but the recognition accuracy of arm raising and one-hand waving does not reach 85%. The reason is that the amplitude of the arm is larger for the arm raise and one-handed wave compared with the other four actions, and the status of the other hand is uncertain when waving with one hand, thus reducing the accuracy of the algorithm [31, 32]. In addition, the arm raise and one-hand wave movements may have certain deviations due to the distance between the human body and the camera and the different shooting angles, resulting in recognition errors. Therefore, the recognition accuracy of these two actions is low. In addition, the difference of data set is also the reason for the low recognition rate of arm raising and one-hand waving by this algorithm. One arm open and arm raise movements are less frequent than other movements in dance, so they have some influence on the recognition accuracy of the algorithm.

The recognition accuracy of each dance movement is shown in Table 5. To avoid the influence of chance on the experimental results, the number of test set images for all movements is 100.

From the experimental results, it can be seen that the accuracy of the dance action recognition method proposed in this paper is above 70% for all kinds of dance actions, and

TABLE 5: Action recognition accuracy test results.

Dance action name	Accuracy (%)
Lift	88.62
Sink	92.35
Charge	86.35
Cloud step	72.22
Turn over	85.98
Stand up and shoot the swallow	73.15

TABLE 6: Comparison of recognition accuracy of different algorithms.

Method	Accuracy (%)
Residual network four-channel algorithm	79.2
Calculating $H_u$ moment algorithm	89.9
Our method	92.7

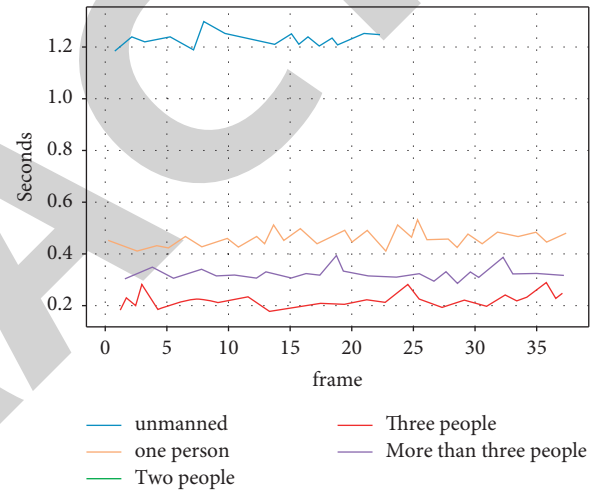


FIGURE 11: HOC algorithm efficiency.

the highest can be above 90%. Under the condition of similar motion complexity, the accuracy rate of dance motion recognition is higher; under the condition of the same number of images in the training set, the lower the complexity, the higher the accuracy rate of motion recognition.

In order to solve the problem of low recognition accuracy caused by the differences in data sets, this study constructed confusion matrices for the above six dance movements in the data set processing, as shown in Figure 10, to ensure that the number of each movement data set is basically the same, and then used this algorithm for recognition. According to the recognition results, the classification accuracy of all six dance movements reached over 90%, indicating that increasing the number of data sets of arm raising and one-handed waving movements through the confusion matrix can effectively reduce the influence of human differences on the recognition results and improve the recognition accuracy.

**5.2. Comparison of Algorithms.** As can be seen from Table 6, the accuracy of our algorithm is higher, reaching more than 92%, which indicates that the present algorithm is more ideal

for recognition of dance movements and has a higher accuracy rate. In addition, it is known by the experimental time that the present algorithm runs at 0.75 frames/s on the Tesla P4 graphics card and can recognize multi-person movements in a single picture.

To further verify the recognition efficiency of the algorithm, we tested it in scenes with 0 to multiple people, respectively, and found that the time spent by the algorithm gradually increases with the number of people in the image, but the magnitude is small. The running time of the Hoff orientation calculator (HOC) algorithm increases linearly with the number of people, as shown in Figure 11. In contrast, the running time of the algorithm in this study essentially did not increase significantly. This indicates that the present algorithm is more efficient and the algorithm performs better.

## 6. Conclusion

Dance video image recognition should take into account the influence of dance background, costume, etc., on action recognition, as well as the obscuration and self-obscuration in the dancer's own movements, and an action recognition technique that can accurately and completely record and reflect the dancer's action information should be used in order to obtain the dancer's body static information and action information. The practical test verifies the feasibility and high efficiency of the method, and the design can be widely applied to the visual perception interaction between human and service robots in the future, so that the robots can understand human actions better and faster, and engage in general service work according to human behaviors.

## Data Availability

The experimental data used to support the findings of this study are available from the corresponding author upon request.

## Conflicts of Interest

The authors declared that they have no conflicts of interest regarding this work.

## References

- [1] Y. Liu, M. Fan, and W. Xu, "Recognition method of dance rotation based on multi-feature fusion," *International Journal of Arts and Technology*, vol. 13, no. 2, pp. 91–107, 2021.
- [2] G. Li, Z. Y. Wang, J. Luo, X. Chen, and H. B. Li, "Spatio-context-based target tracking with adaptive multi-feature fusion for real-world hazy scenes," *Cognitive Computation*, vol. 10, no. 4, pp. 545–557, 2018.
- [3] A. Zhao, L. Qi, J. Dong, and H. Yu, "Dual channel LSTM based multi-feature extraction in gait for diagnosis of Neurodegenerative diseases," *Knowledge-Based Systems*, vol. 145, pp. 91–97, 2018.
- [4] S. Koehne, A. Behrends, M. T. Fairhurst, and I. Dziobek, "Fostering social cognition through an imitation-and synchronization-based dance/movement intervention in adults with autism spectrum disorder: a controlled proof-of-concept study," *Psychotherapy and Psychosomatics*, vol. 85, no. 1, pp. 27–35, 2016.
- [5] J. Young, "The therapeutic movement relationship in dance/movement therapy: a phenomenological study," *American Journal of Dance Therapy*, vol. 39, no. 1, pp. 93–112, 2017.
- [6] S. C. Koch, L. Mehl, E. Sobanski, M. Sieber, and T. Fuchs, "Fixing the mirrors: a feasibility study of the effects of dance movement therapy on young adults with autism spectrum disorder," *Autism*, vol. 19, no. 3, pp. 338–350, 2015.
- [7] E. Shuper Engelhard, "Dance movement psychotherapy for couples (DMP-C): systematic treatment guidelines based on a wide-ranging study," *Body, Movement and Dance in Psychotherapy*, vol. 14, no. 4, pp. 204–217, 2019.
- [8] R. Melhuish, C. Beuzeboc, and A. Guzmán, "Developing relationships between care staff and people with dementia through Music Therapy and Dance Movement Therapy: a preliminary phenomenological study," *Dementia*, vol. 16, no. 3, pp. 282–296, 2017.
- [9] M. Shim, R. B. Johnson, S. Gasson, S. Goodill, R. Jermyn, and J. Bradt, "A model of dance/movement therapy for resilience-building in people living with chronic pain," *European Journal of Integrative Medicine*, vol. 9, pp. 27–40, 2017.
- [10] R. T. H. Ho, J. K. K. Cheung, W. C. Chan, I. K. M. Cheung, and L. C. W. Lam, "A 3-arm randomized controlled trial on the effects of dance movement intervention and exercises on elderly with early dementia," *BMC Geriatrics*, vol. 15, no. 1, pp. 127–128, 2015.
- [11] K. E. Raheb, M. Stergiou, A. Katifori, and Y. Ioannidis, "Dance interactive learning systems: a study on interaction workflow and teaching approaches," *ACM Computing Surveys*, vol. 52, no. 3, pp. 1–37, 2020.
- [12] S. Lyons, V. Karkou, B. Roe, B. Meekums, and M. Richards, "What research evidence is there that dance movement therapy improves the health and wellbeing of older adults with dementia? A systematic review and descriptive narrative summary," *The Arts in Psychotherapy*, vol. 60, pp. 32–40, 2018.
- [13] B. Levine and H. M. Land, "A meta-synthesis of qualitative findings about dance/movement therapy for individuals with trauma," *Qualitative Health Research*, vol. 26, no. 3, pp. 330–344, 2016.
- [14] S. Wiedenhofer and P. D. S. C. Koch, "Active factors in dance/movement therapy: specifying health effects of non-goal-orientation in movement," *The Arts in Psychotherapy*, vol. 52, pp. 10–23, 2017.
- [15] O. K. N. Streater, "Truth, justice and bodily accountability: dance movement therapy as an innovative trauma treatment modality," *Body, Movement and Dance in Psychotherapy*, vol. 17, no. 1, pp. 34–53, 2022.
- [16] R. Preda, "Power dynamics in dance movement therapy," *Body, Movement and Dance in Psychotherapy*, vol. 17, no. 1, pp. 71–80, 2022.
- [17] S. Lotan Mesika, H. Wengrower, and H. Maoz, "Waking up the bear: dance/movement therapy group model with depressed adult patients during Covid-19 2020," *Body, Movement and Dance in Psychotherapy*, vol. 16, no. 1, pp. 32–46, 2021.
- [18] K. Michels, O. Dubaz, E. Hornthal, and D. Bega, "Dance Therapy" as a psychotherapeutic movement intervention in Parkinson's disease," *Complementary Therapies in Medicine*, vol. 40, pp. 248–252, 2018.
- [19] O. Alemi, J. Françoise, and P. Pasquier, "GrooveNet: real-time music-driven dance movement generation using artificial neural networks," *Networks*, vol. 8, no. 17, p. 26, 2017.

## *Retraction*

# **Retracted: Evaluation and Analysis of the Informatization Degree of College English Education Based on Big Data Technology**

### **Security and Communication Networks**

Received 26 December 2023; Accepted 26 December 2023; Published 29 December 2023

Copyright © 2023 Security and Communication Networks. This is an open access article distributed under the Creative Commons Attribution License, which permits unrestricted use, distribution, and reproduction in any medium, provided the original work is properly cited.

This article has been retracted by Hindawi, as publisher, following an investigation undertaken by the publisher [1]. This investigation has uncovered evidence of systematic manipulation of the publication and peer-review process. We cannot, therefore, vouch for the reliability or integrity of this article.

Please note that this notice is intended solely to alert readers that the peer-review process of this article has been compromised.

Wiley and Hindawi regret that the usual quality checks did not identify these issues before publication and have since put additional measures in place to safeguard research integrity.

We wish to credit our Research Integrity and Research Publishing teams and anonymous and named external researchers and research integrity experts for contributing to this investigation.

The corresponding author, as the representative of all authors, has been given the opportunity to register their agreement or disagreement to this retraction. We have kept a record of any response received.

## **References**

- [1] Z. Wang, "Evaluation and Analysis of the Informatization Degree of College English Education Based on Big Data Technology," *Security and Communication Networks*, vol. 2022, Article ID 2420071, 11 pages, 2022.

## Research Article

# Evaluation and Analysis of the Informatization Degree of College English Education Based on Big Data Technology

Zongying Wang 

*School of Foreign Languages, East China University of Technology, Nanchang 330013, China*

Correspondence should be addressed to Zongying Wang; [zywang@ecut.edu.cn](mailto:zywang@ecut.edu.cn)

Received 29 June 2022; Revised 19 July 2022; Accepted 29 July 2022; Published 21 August 2022

Academic Editor: Hangjun Che

Copyright © 2022 Zongying Wang. This is an open access article distributed under the Creative Commons Attribution License, which permits unrestricted use, distribution, and reproduction in any medium, provided the original work is properly cited.

Since the 21st century, thanks to the continuous achievements in the computer field, the Internet technology has developed rapidly in just a few years until it has swept the world. In the torrent of the information age, big data technology came into being. The application of big data technology is extremely high, and it is widely used in many industries. Based on the excellent performance of big data technology in the education industry, this paper will discuss the application of big data technology in the evaluation and analysis of college English education informatization. Under the condition that the evaluation standard is relatively abstract, the traditional method of evaluating through the subjective perspective of human beings has a large interference surface, and it is difficult to make the evaluation work substantive, data-based, and fair, which directly leads to evaluation and analysis work being difficult to carry out. Based on the abovementioned situation that the evaluation and analysis are relatively limited, this article will introduce the role of the big data technology algorithm model in the evaluation and analysis work. Through big data technology algorithms, qualitative problems that are difficult to evaluate are converted into quantitative problems that are easier to analyze and compare and then get rid of the limitations faced by traditional evaluation algorithms. The interference caused by human subjective factors to evaluation and analysis should be reasonably avoided as much as possible. This makes the evaluation and analysis results more objective and fair. This article is mainly based on the relevant algorithms under the big data technology to mine, classify, and purify the data with strong correlation with the important relevant indicators that affect the degree of college English informatization and carry out the experimental calculation of the evaluation of the relevant indicators. The results are as follows: we provide a reliable basis for the evaluation of the degree of informatization in college English and then conduct more scientific and rigorous evaluation and analysis. In the future development of big data technology, the database will be continuously supplemented with valuable teaching data, so that the results of big data technical analysis are more and more consistent with the real situation.

## 1. Introduction

The logistic regression model algorithm based on big data technology [1–4] determines the quantitative relationship between two or more variables that depend on each other, so as to find the data with strong correlation with the evaluation index. Complete the preliminary classification of the data and then use data mining. The technology [5–8] mines the data with the same or strong correlation with the data feature information in the same database by comparing the data feature information, so as to achieve the preliminary mining classification of the data, so as to facilitate the subsequent data cleaning, data changes, and data purification. Taking the

above as the core idea, try to establish an evaluation system for the degree of informatization in college English education. To a certain extent, put aside the interference of human subjective consciousness and use data and evaluation indicators to establish a more objective evaluation behavior. Based on such prerequisites, it is necessary for the algorithm model and the evaluation system we established to be regarded as systems with two correlations. Using the method of data mining classification, the data related to the indicators affecting the evaluation are classified into the database [9–13], and then to a certain extent, the data related to the evaluation indicators are classified. In order to transform it into a geometric mathematical model with high flexibility to

deal with the rigid conditions of lack of transformation ability, the unnatural conditions of the mathematical discussion form are combined with the mathematical model, and finally, the combination of classical numbers and shapes is used to form images [14, 15]. A more intuitive performance evaluation system is with strong correlation indicators that affect the evaluation results. Standardize the evaluation system and make it fair. Numbers are the most concise and powerful language of reality, and the mathematical expression of everything is true, valid, and concise enough, provided the result is correct. The algorithm optimization and more scientific improvement under the big data technology are also worth looking forward to and paying attention to in the future.

Downtime is a deadlock situation that is very likely to occur in computer computing, and the possibility of server database deadlock is not ruled out. For this, we have considered setting up a framework that includes alerts and monitoring. In the event of downtime, our alert monitoring framework can detect and diagnose problems in a timely manner, reducing the possibility of data loss.

## 2. Evaluation and Analysis of College English Education Informatization Degree under Big Data Technology

This paper mainly evaluates and analyzes the informatization degree of college English education under the big data technology, while the data mining technology based on the big data technology mainly collects and integrates various and complicated data information and then obtains more accurate and representative data information so that we can more objectively evaluate and analyze the degree of university education informatization [16–19]. Firstly, we analyze the ideas according to the data mining technology and construct the idea map. We construct the five stages in the big data mining process. Based on the big data mining technology, we construct the model and its algorithm and then evaluate the informatization degree of college English education, as shown in Figure 1.

At this stage, data mining is done through big data technology, and the generated model can be used later to solve more complicated problems.

In order to avoid security vulnerabilities as much as possible, first of all, we need to understand which security vulnerabilities are most likely to cause security threats to the database. The first and most direct one is that the username and password in the database are too simple, which leads to some malicious hackers. It is easy to steal user information from our database, leading to security breaches, followed by unpatched databases, insufficient authentication, and other related issues. In response to these problems, we have targeted management personnel awareness, systems, and technical means and follow the basic threat prevention guidelines, but if only from a technical perspective, we will consider the use of monitoring (DMI) system, which is so-called database auditing systems, to circumvent security breaches.

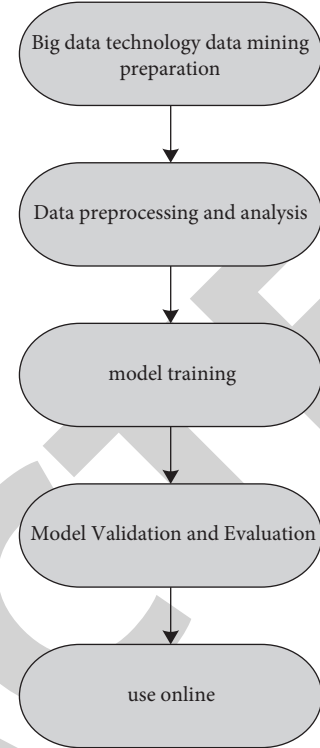


FIGURE 1: Analysis of college English education informatization under big data technology.

### 2.1. Big Data Technology Mining Learning Model and Its Algorithm

**2.1.1. Logistic Regression Model.** This paper mainly discusses the evaluation of the informatization degree of college English education based on the big data technology algorithm. Here, we introduce the logistic regression model algorithm to calculate the correlation strength of the correlation data with the relevant indicators and then make a preliminary classification of our data. We use this model to fit the data, and the logistic regression we use is normalized on the basis of linear regression [20–22]. It minimizes the difference between the data value predicted by the model and related algorithms and the real value.

The logistic regression model algorithm mainly multiplies each attribute of the data sample participating in the experiment by the corresponding parameter value and accumulates the results we get. The formula of its model is

$$h(x) = w_0x_0 + w_1x_1 + w_2x_2 + \dots + w_mx_m. \quad (1)$$

The vectorized formula is expressed as

$$h(x) = w^t x. \quad (2)$$

Calculate the value of the sigmoid function as follows.

Substitute the calculated result of the above formula into the sigmoid function. The calculated result obtained by the function calculation will be between (0, 1). The calculated value is compared with the set threshold value, which is greater when the threshold value is positive class; otherwise it is negative class, and its calculation formula is as follows:



$$g(z) = \frac{1}{1 + e^{-wx}}. \quad (3)$$

**2.1.2. Model Calculation.** Here, we assume that  $n$  samples are used for calculation training. It is known that the probability of occurrence of each assumed sample conforms to the Bernoulli distribution, and the probability of occurrence is calculated experimentally for each sample.

Calculate the probability of occurrence of positive and negative classes:

$$\begin{aligned} p(y_i = 1 | x_i), \\ 1 - p(y_i = 1 | x_i). \end{aligned} \quad (4)$$

Calculate the posterior probability of each sample:

$$p(y | x, w) = p(y_i = 1 | x_i) y^i (1 - p(y_i = 1 | x_i))^{1-y_i}. \quad (5)$$

The computational model experiment in the article is a special computational experiment, and its computation is nothing more than two results, either success or failure, and each experimental sample exists independently and is not disturbed, and each experiment has a fixed value. The probability of success  $p$  and then the probability of occurrence of the experimental calculation sample are assumed to conform to the Bernoulli distribution, which not only simulates the real situation of the model calculation to a great extent, but also facilitates the calculation of the mathematical expectation and variance of the distribution due to the simple distribution of the results.

**2.2. Log-Likelihood Function.** Due to the extremely large amount of data, in our calculation process, the model and data overfitting state will inevitably occur. In order to avoid this problem, here we introduce the loss function  $l(w)$ , by adding the loss function  $l(w)$  plus a penalty term for  $w$ , making the penalty a Regularizer. Its calculation formula is as follows:

$$l(w) = \prod_{i=1}^m p(y_i = 1 | x_i)^{y_i} (1 - p(y_i = 1 | x_i))^{1-y_i}. \quad (6)$$

Expand and solve for it and take the derivative of  $w$

$$\frac{\partial l(w)}{\partial w} = \sum_{i=1}^m (y_i - g(z)) x_i. \quad (7)$$

**2.3. Naive Bayes Algorithm.** Naive Bayesian model originated from classical mathematical theory. Its stable classification efficiency and simultaneous multitask processing, especially when the amount of data information is huge, greatly improve the efficiency of classification and sorting of our data mining information. The function model is as follows:

$$C_x = \arg \max_{k \in \{1, 2, \dots, k\}} \left( P(C_k) \prod_{j=1}^n p(x_j | C_k) \right). \quad (8)$$

The above formula is calculated, and the probability is estimated by frequency. The calculation formula is as follows:

$$p(C_k) = \frac{m_k}{m}. \quad (9)$$

Here, we make reasonable assumptions about the distribution of data characteristics of the samples and calculate separately.

The naive Bayes model that conforms to the multinomial distribution is calculated as follows:

$$p(x_{js} | C_k) = \frac{m_{kjs}}{m_k}. \quad (10)$$

Sometimes if the value of a feature in the sample is 0, it will seriously affect the probability distribution of the feature, so we use Laplace smoothing to avoid this situation, namely,

$$p(x_{js} | C_k) = \frac{(m_{kjs} + \lambda)}{(m_k + \lambda)}. \quad (11)$$

For the Naive Bayes model conforming to the Bernoulli distribution, the formula is as follows:

$$p(x_{js} | C_k) = \begin{cases} p(x_{js} = 0 | C_k) = 1 - p(x_{js} = 1 | C_k), \\ p(x_{js} = 1 | C_k). \end{cases} \quad (12)$$

The naive Bayes model that conforms to the Gaussian distribution is calculated as follows:

$$f(x, \mu, \sigma) = \frac{1}{\sigma \sqrt{2\pi}} \exp\left(-\frac{(x - \mu)^2}{2\sigma^2}\right). \quad (13)$$

**2.4. Decision Tree Model and Its Data Purification.** After the data mining is collected, the data will be sorted and summarized to get a database with a huge amount of information. In our database, the invalid information we have collected is often retained. At this time, the introduction of the decision tree model can effectively solve the data (purity issues). Decision tree model is mainly a nonparametric classifier that is simple to use and less difficult to operate. Here, we refer to the ID3 algorithm, as well as the C4.5 algorithm.

The commonly used algorithms in the decision tree model [23] mainly include the ID3 algorithm and the C4.5 algorithm. These two algorithms can be used to divide the data set, and the ultimate goal of the decision tree node splitting is to make the nodes that fall on each branch node. The samples are in the same category to the greatest extent possible, which means that the node purity is higher.

A decision tree is a tree structure consisting of nodes and directed edges. Its essence is a set of causal rules. The decision tree model we introduced in this article is a simple and easy-to-use nonparametric classifier that does not require any assumptions on the data.

**2.4.1. ID3 Algorithm.** Aiming at the problem of data purity after data mining classification, we introduce the concept of information entropy [24] to measure the data purity after classification. Its calculation formula is as follows:

$$H = - \sum_{k=1}^{|y|} p_k \log_2 p_k. \quad (14)$$

$H$  represents the information entropy  $D$ , and the smaller the calculated  $H$  value, the higher the purity of the information entropy.

The impact of data purity on the results is undoubtedly the most direct. It is undeniable that such a problem does exist in this article. However, based on the diversity and quantity of data types, it is difficult to formulate a unified, specific, and standardized measurement system for the measurement of the purity of multiple types of data. Therefore, in this article, by purifying the data multiple times, the information entropy value is reduced as much as possible, and the impact of data purity on the results is minimized.

The ID3 algorithm quoted here conforms to the data gain criterion. The so-called data gain is the positive change of the original data and the classified data after the data is classified, and the gain of an indicator after the data classification is the data set. The difference between the information entropy and the empirical conditional entropy of  $D$  under this condition is

$$H(D, a) = H - \sum_{v=1}^v \frac{|D^v|}{|D|} H(D^v). \quad (15)$$

### 3. Algorithm Improvement

In summary, we have made a preliminary framework for the big data technology algorithm, but there may still be deficiencies or loopholes. Next, we will optimize and improve our big data counting algorithm to improve the computing power and accuracy of the algorithm.

**3.1. Logistic Regression Model Algorithm Optimization.** In the logistic regression algorithm, it is not excluded that the last derivative is 0. In this case, we cannot solve  $w$ , and we need to use the gradient iterative optimization algorithm to optimize the algorithm. The combination of stochastic gradient descent and batch gradient descent and derivation of the objective function can help us solve the above problems. Here, we use the batch gradient descent method to find the partial derivative of  $w$  and get the gradient corresponding to each  $w$ . The calculation formula is as follows:

$$\frac{\sigma l(w)}{\sigma w_j} = \frac{1}{m} (y^i - h_w(x^i)) x_j^i. \quad (16)$$

Since we need to minimize the risk function, we need to update  $w$  in the negative direction of  $w$ . The calculation formula is as follows:

$$w_j^* = w_j + \frac{1}{m} (y^i - h_w(x^i)) x_j^i. \quad (17)$$

By calculating the formula, we will finally get a comprehensive optimal solution, but every change of  $w$  requires all the training data. If the data is too large, it will greatly affect the speed of  $w$  change, so we use randomly the gradient descent method which is combined, and the calculation formula is as follows:

$$\begin{aligned} l(w) &= \frac{1}{2m} \sum_{i=1}^m (y^i - h_w(x^i))^2 \\ &= \frac{1}{m} \sum_{i=0}^m \text{cost}(w, (x^i, y^i)), \end{aligned} \quad (18)$$

$$\text{cost}(w, (x^i, y^i)) = \frac{1}{2} (y^i - h_w(x^i))^2.$$

Obtain the corresponding gradient by taking the partial derivative of  $w$  through the loss function of each sample, and then update  $w$ :

$$w_j^* = w_j + (y^i - h_w(x^i)) x_j^i. \quad (19)$$

**3.2. Improvement of Naive Bayes Algorithm.** Among the three classification algorithms based on the naive Bayes algorithm, the best classification effect is the multinomial naive Bayes algorithm classification model, but the disadvantage is that the algorithm automatically defaults to the same weight of all features and ignores the features of data. To a certain extent, it will reduce the accuracy of our data classification. Therefore, we need to combine other algorithms for related optimization. Here, we introduce the TD-IDF algorithm and improve and optimize the original algorithm before applying it to the data processing module.

Combine the improved TDF-IDF-LD into a multinomial naive Bayesian algorithm to get the final formula:

$$C_x = \arg \max_{k \in \{1, 2, \dots, k\}} \left( \frac{m_k}{m} \prod_{j=1}^n \frac{m_{kjs} + \lambda}{m_k + s_j \lambda} \right) * \text{TF} * \text{IDF} * \text{LF} * \text{DTF}. \quad (20)$$

**3.3. Improvement of Decision Tree Model Algorithm.** The main idea of the ID3 algorithm is a top-down greedy strategy from the root node to the leaf node. First, the information gain of each feature is calculated according to the above formula, and finally the feature with the largest information gain is selected as the node of the decision tree. Splitting further improves the purity of the child nodes of the decision tree, and the ability to divide samples into corresponding categories is stronger, and the representativeness of such features is stronger. However, the shortcomings of ID3 are also obvious. The algorithm has a preference for attributes with a large number of values. The decision tree created only by the ID3 algorithm obviously cannot achieve the expected effect for unknown data. At this time, we use the C4.5



algorithm for collaborative calculation, so that the decision tree we create is sufficiently convincing [25].

**3.3.1. C4.5 Algorithm.** In view of the limitations of the ID3 algorithm, to minimize the adverse effects of the ID3 algorithm, we use the C4.5 algorithm for collaborative calculation. For attribute preference problem, the calculation formula is

$$H(D, a)_{\text{ratio}} = \frac{H(D, a)}{H(D)}. \quad (21)$$

**3.3.2. Classification and Regression Tree Algorithm.** Classification and regression trees are a type of decision tree and are very important. The generation of classification tree and regression tree can be realized at the same time. The CART algorithm we introduce here is a binary recursive segmentation technique. The internal node of the generated decision tree has only two branches and only two categories of yes or no. Even if a feature or attribute has multiple values, it is divided into two parts.

Create a classification tree: in the recursive process of creating the split tree, the CART algorithm selects the feature with the smallest Gini index in the current data set as the node to divide the decision tree. The Gini index is similar to the information entropy and is usually used to measure the purity of the data set D. The calculation formula is as follows:

$$\text{Gin}(D) = 1 - \sum_{k=1}^{|y|} p_k^2. \quad (22)$$

The Gini index is obtained by calculation, and the purity is estimated by observing the value of the final calculation result of the index. The smaller the value, the higher the purity.

In the process of classifying data, the Gini index is calculated for the indicator a, and the formula is as follows:

$$\text{Gini}_{\text{index}(D, a)} = \sum_{v=1}^v \frac{|D^v|}{D} \text{Gini}(D^v). \quad (23)$$

Create a regression tree: the regression tree created by CART uses the principle of least mean square variance to determine the optimal division of the regression tree, so that our final data result prediction is closest to the true value. Assuming that the mean squared error is calculated for a feature, and the feature with the smallest error is found, it is theoretically the optimal splitting point. The squared error formula is

$$\sum_{x_i \in R_m} (y_i - f(x_i))^2. \quad (24)$$

In this article, we only quoted a part of the cart algorithm, and we used the Gini index algorithm to improve the other part. Compared with the original algorithm, the GIN index algorithm is simpler and faster. The original algorithm is added as follows:

$$R_1(j, s) = \{x \mid x^j \leq s\},$$

$$R_2(j, s) = \{x \mid x^j > s\},$$

(25)

$$c_m = \frac{1}{N_m} \sum_{x_i \in R_m(j, s)} y_i^j, x \in R_m, m = \{1, 2\}.$$

## 4. Experiment and Test Based on Big Data Technology Algorithm Evaluation

This article mainly evaluates and analyzes the informatization degree of college English education based on big data technology. Here, we will consider the selection of student learning environment, information equipment construction, teaching equipment, voice environment, and other indicators to use our proposed big data technology algorithm for experimental testing.

**4.1. Feasibility Experiment Test of Big Data Technology Algorithm.** Since the degree of feasibility of the algorithm proposed in our article is still unknown, in order to ensure that the test results obtained by our subsequent experimental tests based on this algorithm are more credible, we first test the feasibility of the algorithm. Taking a university as an example, we will conduct experiments on the hardware facilities of a university based on the traditional evaluation method of the results calculated by the big data counting algorithm and compare and analyze the obtained results. The comparison results are shown in Table 1, and the visualization is shown in Figure 2.

Through our big data counting algorithm and artificial traditional algorithm to calculate some indicators of a university's hardware facilities construction, it can be clearly observed that the results obtained by our big data algorithm are highly consistent with the results obtained by traditional artificial algorithms, and there are slight differences. We can think that our proposed big data technology algorithm is still feasible in the experiment, and the high accuracy is in line with the real situation. You can continue to participate in follow-up testing.

**4.2. Big Data Technology Algorithm Optimization Test.** This paper mainly evaluates and analyzes the degree of college English informatization, which requires us to take into account the important indicators that affect the degree of college English informatization, such as college English education funding, English e-book resources, and student learning environment. Use our big data technology algorithm to quantitatively analyze the important influencing factor indicators, and compare the experimental results obtained with the real situation to reflect the advantages of the optimization algorithm.

**4.2.1. C4.5 Algorithm and ID3 Algorithm Test.** In the previous article, based on the ID3 algorithm introduced by data processing and purification, we further optimized it and

TABLE 1: Comparison of experimental results between big data algorithm and artificial traditional algorithm.

	Number of computers	Number of multimedia classrooms	Amount of professional experimental equipment	Amount of professional practice equipment
Big data algorithm	1237	136	109	223
Artificial traditional algorithm	1224	139	117	219

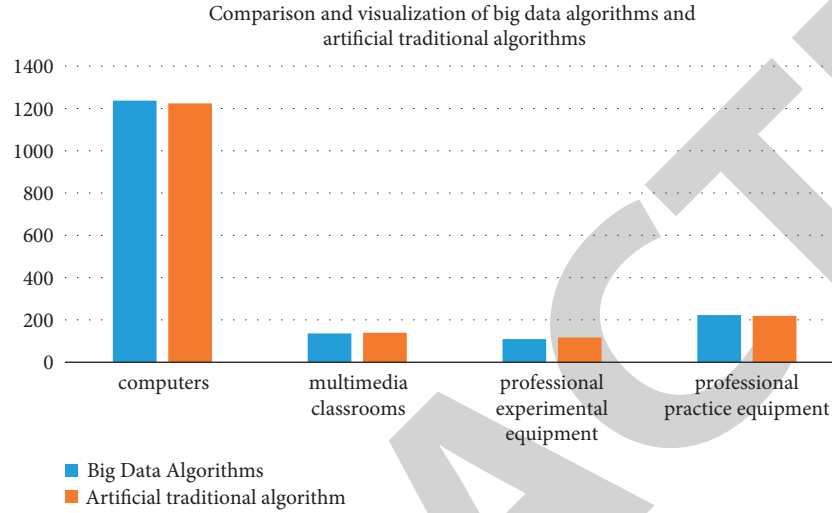


FIGURE 2: Visualization diagram of big data algorithm and artificial traditional algorithm.

introduced the C4.5 algorithm. We compared the advantages brought by the improvement of this algorithm through a more direct experimental test. Taking a university as an example, we use two algorithms to calculate the university's investment in English education and compare it with the actual situation, and then we compare the advantages and disadvantages of the two algorithms. The calculation results are shown in Table 2, and the visualization is shown in Figure 3.

According to the visualization in the above figure, the data results obtained by our optimized C4.5 algorithm compared to the ID3 algorithm after data purification are compared with the actual investment of the university, and the optimized C4.5 algorithm is closer to the real situation of the experiment.

**4.2.2. Classification Tree and Regression Tree Algorithm Test.** In this article, we have created the classification tree and regression tree model algorithms, respectively. Here, we will use the collection of English e-books in the university library as an indicator to use the two algorithms for experimental comparison. The experimental results are shown in Table 3. The visualization is shown in Figure 4.

According to the visual display of the experimental results in the figure, there are differences within a certain range between the two algorithms we use, respectively, but the degree of error is extremely small and can be basically ignored. Both algorithms have excellent data processing and analysis capabilities.

**4.2.3. Simulation Test of Unit Computation Time Efficiency of the Stochastic Gradient Descent Method.** Since the amount of data is too large, we need to test the time-consuming comparison of different algorithms when processing the same unit capacity of data. Here, we introduce the control variable method to fix the difference of irrelevant variables brought by the experimental equipment and only change the type of the algorithm and carry out the experiment with a single variable. As a simulation test, taking the time efficiency as the evaluation standard for the calculation results reflects the simplicity of the algorithm and the simplification of complex problems. The test result data is shown in Table 4, and the visual chart is shown in Figure 5.

Considering the efficiency of the three algorithms used in this paper for data processing, we will transform qualitative problems into quantitative problems for experimental testing. The evaluation results of qualitative understanding are presented in the form of relatively intuitive data. The time consumption remains high in an advantageous state. In similar algorithms, the measurement to be measured is simplified, and the simplified data to be measured is calculated, thereby reducing the time consumption of the algorithm. Minimize the time consumption of the algorithm due to the huge amount of data, and reduce the algorithm speed.

In the article, only some indicators that affect the degree of informatization in college English education are tested and evaluation standards are formulated, but in fact, there are many factors that affect the degree of informatization in college English education. There are many indicators for

TABLE 2: Comparison of the results of ID3 algorithm and C4.5 calculation of investment capital (unit: ten thousand yuan).

	Hire an English teacher	English teaching equipment	English professional equipment	E-books in English	Other
ID3 algorithm calculation input	22.3	72.2	88.7	11.4	7.8
C4.5 algorithmic computing input	21.9	74.8	90.6	10.1	7.5
Actual input	21.5	74.3	90.2	10.5	7.2

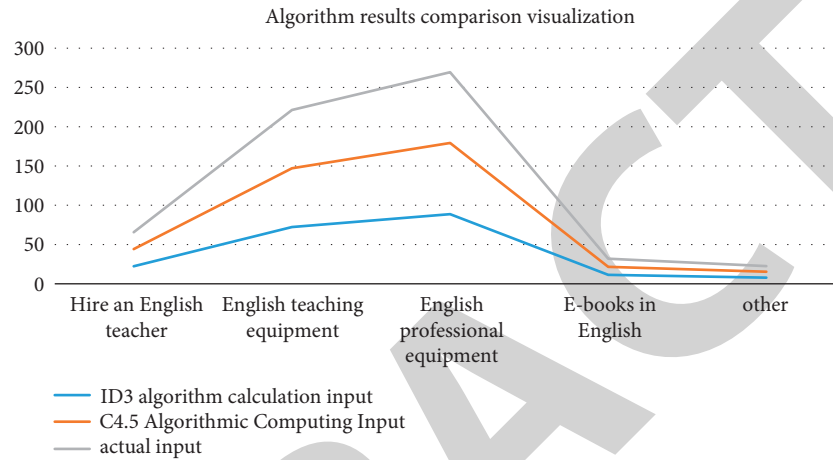


FIGURE 3: Comparison and visualization of the results of the two algorithms.

TABLE 3: Library's English e-book collection data.

	English reading and writing	English listening and speaking	English extracurricular readings	Other literature
Classification tree algorithm	1648	2071	3011	1024
Regression tree algorithm	1692	2104	3048	1133

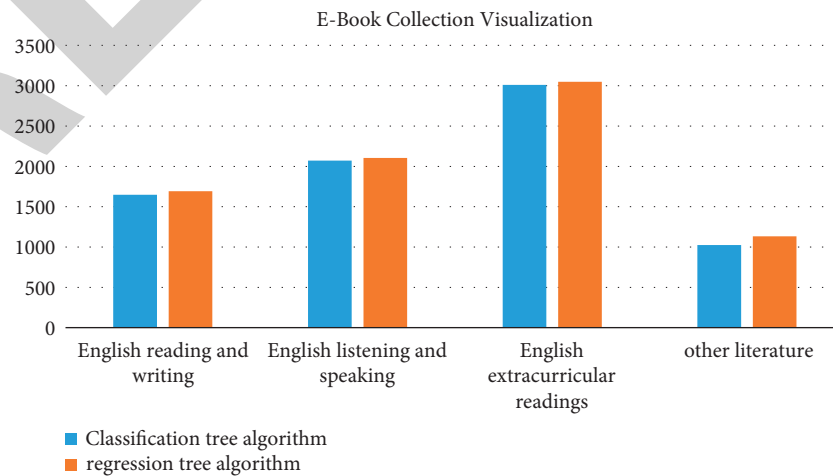


FIGURE 4: Visualization of e-book collections.

TABLE 4: Time efficiency (T/s) of different algorithm units calculation amount.

To be evaluated (TB)	Batch gradient descent	Stochastic gradient descent	Logistic regression algorithm
1.0	57.2	71.5	51.7
1.5	88.7	99.2	80.2
2.0	119.5	153.7	104.9

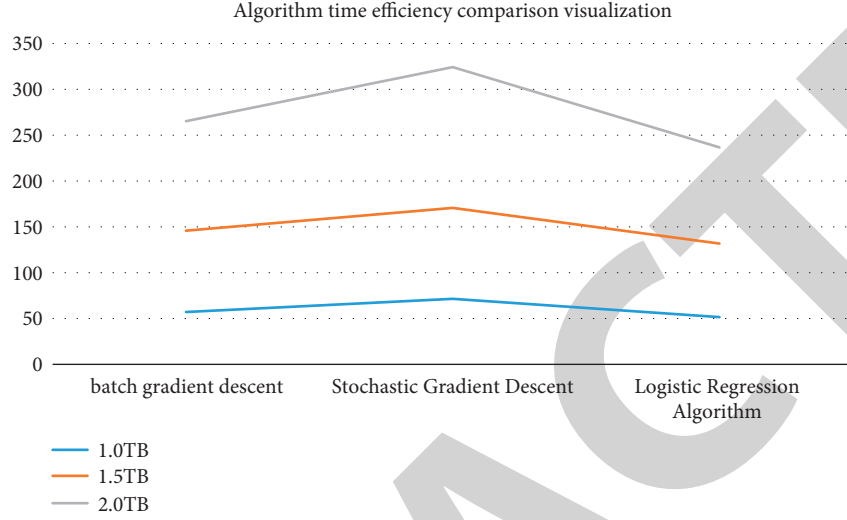


FIGURE 5: Comparison of time efficiency of algorithms.

reference. In this article, we only select a few of the more important reference indicators for testing. But that does not mean we are turning a deaf ear to other influencing factors. The final evaluation and analysis results must be discussed under the influence of various factors. Due to the similarity of the calculation methods, they are not tested and displayed in this paper.

**4.3. Evaluation Experiment of College English Education Informatization Degree Based on Big Data Technology Algorithm.** In summary, after the feasibility and optimization tests of our algorithm have been carried out, we use the algorithm to conduct experiments on the evaluation and analysis of college English education informatization. Here, we select three indicators, learning environment, English e-books, and language environment, to evaluate the degree of English informatization in a university.

**4.3.1. Learning Environment Assessment Experiment.** Aiming at the pros and cons of students' learning environment, it can reflect the degree of college English teaching informatization to a certain extent. Taking a university as an example, we use the big data technology algorithm proposed by us to make the evaluation criteria for students' different learning environments evaluation and compared it with human subjective evaluation. The experimental results are shown in Table 5, and the visualization is shown in Figure 6.

To a certain extent, the evaluation of students' learning environment in school reflects the degree of informatization of the university's learning environment construction. There

is a certain difference between the experimental results obtained using our big data technology and the human subjective evaluation. However, considering that human subjective evaluation is influenced by human subjective psychological differences, the error brought about by the evaluation results is relatively large. We can think that the evaluation results made by big data algorithms are fairer and more accurate.

**4.4. Derivative Simulation of Similar Algorithms.** The big data technology algorithm needs to perform weighted calculation on the evaluation index factor set when mining the correlation data of participation evaluation indicators, which brings certain challenges to the derivative performance of the algorithm. The ability to derive a single impact factor into multiple impact factors is a necessary ability of the algorithm when the conditions for participating in the evaluation in the actual calculation process are insufficient or the conditions for participating in the evaluation are single. The starting point of this simulation is to derive the number of participating factors after the basic evaluation factor is tested by the algorithm. The evaluation factor data of similar algorithm tests are shown in Table 6, and the data visualization chart is shown in Figure 7.

When the big data technology algorithm explored in this article has a single or insufficient condition among similar algorithms, the ability to derive the known condition is twice that of the original condition. Compared with similar algorithms under the same conditions, the derivation ability of the participating factors is only about 1.5 times of the

TABLE 5: Learning environment assessment.

	Health	Learning atmosphere	Openness	Degrees of freedom	Resources
Big data evaluation	8	7	6	9	7
Human subjective assessment	7	5	7	8	6

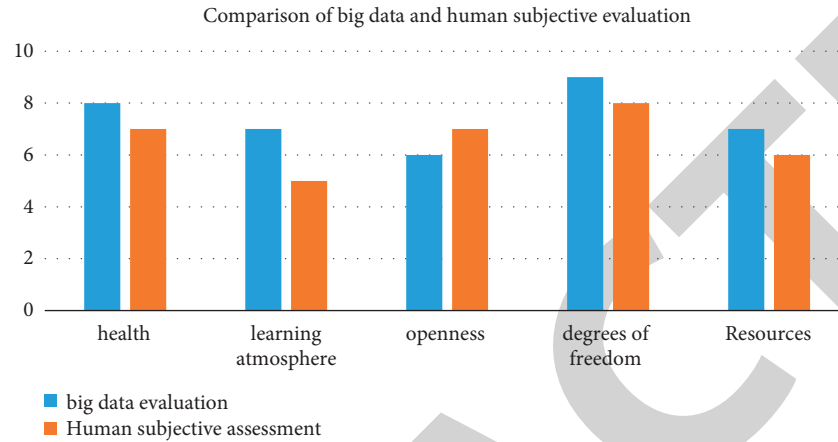


FIGURE 6: Learning environment assessment visualization.

TABLE 6: Algorithm condition derived performance data table.

Basic evaluation factor	Big data evaluation method	Factor analysis evaluation method	Subjective assessment
10	21	18	16
15	37	36	34
25	58	54	51

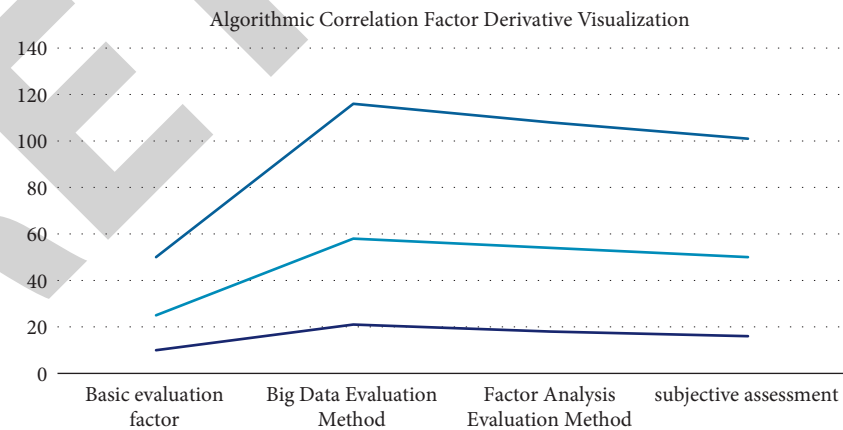


FIGURE 7: Simulation diagram of algorithm related factors derived performance.

original factor. When faced with the actual situation, the evaluation factors often appear in the order of ten. The stronger the derivative ability of the factors participating in the evaluation, the more comprehensive the expanded evaluation factor set, which provides the accuracy of the big data technology algorithm in this article (data help).

Because the existing big data technology has a relatively complete system, and combined with the experimental tests made in this article, the big data algorithm has been able to process data more flexibly and build a more perfect evaluation system accordingly. Then, in the future development of big data technology, it is worth paying attention to the



improvement of data accuracy and data processing speed. It will bring more convenient and substantial help to the education industry.

## 5. Conclusion

With the rapid development of big data technology, there are many examples of big data technology being applied to the education industry. It has gradually evolved into a major trend. After years of technical improvement and optimization, a large amount of valuable teaching data in the database has provided theoretical basis and practical cases for big data mining technology. The algorithm deduced based on big data technology is introduced into the evaluation and analysis of the informatization degree of college English education. Mining and technical algorithms combine qualitative subjective events into the scope of mathematics to carry out rigorous quantitative analysis. In our simulation experiments, we mainly study the rational application of big data technology algorithms to the evaluation and analysis of the degree of informatization in college English education performance. If and only when we transform qualitative problems into quantitative problems under big data technology and quantify useless parameters for evaluation, we cleverly use the C4.5 algorithm to eliminate useless parameters and ensure the parameters are involved in evaluation and analysis. All of them have a strong correlation with the informatization of college English education, so that the evaluation results are more scientific and rigorous, close to the real situation. To sum up, the big data technology is enough to provide substantial help to the evaluation and analysis personnel in the evaluation of the informatization degree of college English education, and it also meets the requirements of the evaluation system for quantitative algorithms.

First of all, considering the technical difficulty, most data mining tools are user-friendly, easy to understand, and easy to use, which greatly reduces the difficulty for analysts or industry evaluators to mine value from massive data. Secondly, data mining technology is the product of countless experiments and is widely recognized and accepted by everyone. It can clean, calculate, and visualize data through various built-in programs and realize automatic management and control of multitasking, which can significantly reduce the user's time and cost and reduce the workload, and provide substantial help for analysts and evaluators.

## Data Availability

The experimental data used to support the findings of this study are available from the author upon request.

## Conflicts of Interest

The author declares no conflicts of interest regarding this work.

## Acknowledgments

This work was sponsored in part by 14th Five-Year Plan of Jiangxi Education Science (21YB082) and Fuzhou Social Science (20SK20).

## References

- [1] A. McAfee and E. Brynjolfsson, "Big data: the management revolution," *Harvard Business Review*, vol. 90, no. 10, pp. 60–128, 2012.
- [2] H. R. Varian, "Big data: new tricks for econometrics," *The Journal of Economic Perspectives*, vol. 28, no. 2, pp. 3–28, 2014.
- [3] D. Howe, M. Costanzo, P. Fey et al., "Big data: the future of biocuration. [J]," *Nature*, vol. 455, no. 7209, pp. 47–50, 2008.
- [4] V. Marx, "Biology: the big challenges of big data [J]," *Nature*, vol. 498, no. 7453, pp. 255–260, 2013.
- [5] Z. Zhu, "Application of data mining technology in the information technology of college English teaching [J]," *Advance Journal of Food Science and Technology*, vol. 5, no. 7, pp. 969–975, 2013.
- [6] Y. R. Shiau, C. H. Tsai, and Y. H. Hung, "The application of data mining technology to build a forecasting model for classification of road traffic accidents [J]," *Mathematical Problems in Engineering*, vol. 2015, pp. 170635.1–170635.8, 2015.
- [7] H. Tang, J. Zhou, D. Liao, and R. Liu, "Research on data mining and visualization technology for numerical simulation data based on the PDM platform," *Journal of Computational and Theoretical Nanoscience*, vol. 9, no. 9, pp. 1193–1199, 2012.
- [8] G. Ji, "The research of decision tree learning algorithm in technology of data mining classification [J]," *Journal of Convergence Information Technology*, vol. 7, no. 10, pp. 216–223, 2012.
- [9] S. F. Altschul, T. L. Madden, and A. A. Schffer, "Gapped BLAST and PSI-BLAST: a new generation of protein database search programs," *Nucleic Acids Research*, vol. 25, no. 17, pp. 3389–3402, 1997.
- [10] S. Altschul, "Gapped BLAST and PSI-BLAST: a new generation of protein database search programs," *Nucleic Acids Research*, vol. 25, no. 17, pp. 3389–3402, 1997.
- [11] S. T. Sherry and M. Kholodov, "dbSNP: the NCBI database of genetic variation," *Nucleic Acids Research*, vol. 29, no. 1, pp. 308–311, 2001.
- [12] K. Hofmann, P. Bucher, L. Falquet, and A. Bairoch, "The PROSITE database, its status in 1999," *Nucleic Acids Research*, vol. 27, no. 1, pp. 215–219, 1999.
- [13] K. Higo, Y. Ugawa, M. Iwamoto, and T. Korenaga, "Plant cis-acting regulatory DNA elements (PLACE) database: 1999," *Nucleic Acids Research*, vol. 27, no. 1, pp. 297–300, 1999.
- [14] M. Marcotte, C. J. Toupin, and M. Le Maguer, "Mass transfer in cellular tissues. Part I: the mathematical model," *Journal of Food Engineering*, vol. 13, no. 3, pp. 199–220, 1991.
- [15] A. Wilson, "The mathematical model [J]," *Canadian Medical Association Journal: Canadian Medical Association journal = journal de l'Association medicale canadienne*, vol. 139, no. 6, p. 479, 1971.
- [16] W. Zheng, "Comparative analysis of the informatization degree of regional economy [J]," *Research on Quantitative Economy and Technology Economy*, no. 01, pp. 27–29, 2001.
- [17] F. Chen, "Discussion on gray evaluation of enterprise management informatization [J]," *China Management Informatization: Comprehensive Edition*, vol. 9, no. 2, p. 2, 2006.
- [18] J. Zheng, L. Qi, and Y. Qi, "A correlation analysis between the degree of informatization and economic development in my country [J]," *Journal of Harbin University of Science and Technology*, vol. 7, no. 4, p. 4, 2002.

## *Retraction*

# **Retracted: Big Data Analysis and Modeling of Higher Education Reform Based on Cloud Computing Technology**

### **Security and Communication Networks**

Received 26 December 2023; Accepted 26 December 2023; Published 29 December 2023

Copyright © 2023 Security and Communication Networks. This is an open access article distributed under the Creative Commons Attribution License, which permits unrestricted use, distribution, and reproduction in any medium, provided the original work is properly cited.

This article has been retracted by Hindawi, as publisher, following an investigation undertaken by the publisher [1]. This investigation has uncovered evidence of systematic manipulation of the publication and peer-review process. We cannot, therefore, vouch for the reliability or integrity of this article.

Please note that this notice is intended solely to alert readers that the peer-review process of this article has been compromised.

Wiley and Hindawi regret that the usual quality checks did not identify these issues before publication and have since put additional measures in place to safeguard research integrity.

We wish to credit our Research Integrity and Research Publishing teams and anonymous and named external researchers and research integrity experts for contributing to this investigation.

The corresponding author, as the representative of all authors, has been given the opportunity to register their agreement or disagreement to this retraction. We have kept a record of any response received.

### **References**

- [1] Z. Tang, "Big Data Analysis and Modeling of Higher Education Reform Based on Cloud Computing Technology," *Security and Communication Networks*, vol. 2022, Article ID 4926636, 11 pages, 2022.



## Research Article

# Big Data Analysis and Modeling of Higher Education Reform Based on Cloud Computing Technology

Ziye Tang <sup>1,2</sup>

<sup>1</sup>School of Public Administration, Central China Normal University, Wuhan 430079, China

<sup>2</sup>Qiannan Polytechnic for Nationalities, Qiannan 558022, China

Correspondence should be addressed to Ziye Tang; ziyetang@mails.ccn.edu.cn

Received 21 June 2022; Revised 14 July 2022; Accepted 21 July 2022; Published 19 August 2022

Academic Editor: Hangjun Che

Copyright © 2022 Ziye Tang. This is an open access article distributed under the Creative Commons Attribution License, which permits unrestricted use, distribution, and reproduction in any medium, provided the original work is properly cited.

In view of the current educational environment, the development of higher education cannot be separated from the support of information technology. The era of big data has had various impacts on higher education and accelerated the development of higher education. Cloud computing technology has good application prospects for the data analysis and mathematical modeling content involved in the reform of higher education. This study analyzes and calculates the concerns of the four main contents involved in the educational reform of a higher education institution as the research object. In order to quantify the application effects of different cloud computing technologies, the paper introduces three typical cloud computing technologies to analyze the research data and establish related mathematical models. The results show that the prediction accuracy based on the immune cloning algorithm is the best. Based on the calculation results, it can be found that the corresponding data of the two main contents of teaching scene setting and teaching quality detection show an obvious polynomial function relationship.

## 1. Introduction

The traditional teaching model [1, 2] is a one-to-many classroom teaching pattern. That is, the instructor instills knowledge unilaterally to the recipient face-to-face in a fixed place and time. This model of teaching is limited by time and space and has been used to this day. At present, much of our university education still follows the traditional teaching model, i.e., uniform classes and uniform examinations. It is difficult to explore students' differences and interests in this "one size fits all" model, resulting in a lack of innovation in the final talent produced [3]. China has always advocated the concept of education according to the needs of the individual, but it is difficult to achieve this due to the limitations of educational resources and traditional teaching models.

After years of development, many universities have formed a unique way of development. However, they are still accustomed to investing only in the construction of hardware and improvement of teaching quality, ignoring the importance of modern education management [4]. This leads to an overall low level of educational management that

does not meet the basic development needs of the new-age students. For example, the awareness of information technology education management is weak, and the scope and strength of information technology construction are limited [5, 6]. The development of an education management information systems is not in place. When a bottleneck is encountered at work, development work is put on hold. The education management system is not sound, and the education management work lacks norms and standards. The construction of education management team is insufficient, and the information operation level of managers is low, so they cannot carry out management work effectively. This shows that the status quo of higher education management informatization cannot meet the needs of higher education reform. Therefore, the construction of higher education management information technology is urgent.

With the rapid development of technology and great progress in the twenty-first century, mankind has entered a new era of intelligence. Artificial intelligence has entered all corners of human social life, and the development of artificial intelligence has become a major strategic opportunity

for various countries at present. How to occupy the technological frontier of the development of artificial intelligence and turn it into an important breakthrough for China to lead the world in the future has become a priority task at present. The era of artificial intelligence requires not only capturing breakthroughs in technological advances but also cultivating specialized talent. Therefore, in this context, it is also of utmost importance to plan and develop the artificial intelligence education system, further promote the change in higher education, and jointly speed up the development of artificial intelligence, high-speed Internet and education big data, and other related disciplines [7, 8].

Currently, with the rapid development of information technology such as the Internet, cloud computing, and cloud storage, the speed of data update and dissemination has increased exponentially. The challenge of how to store, process, and share this data is enormous. It is in this context that big data emerged. Big data [9, 10] is not limited to digital but includes video, text, images, and audio in many forms. Big data is widely used in higher education reform, and the application of big data technology has also accelerated the process of education reform.

With the further development and advancement of technology, innovative technologies [11, 12] such as big data, cloud computing, and artificial intelligence are widely used in different fields such as science and technology. For example, traditional smart technologies [13, 14] are used in the prediction and research process in various fields. By simulating the replication process of human chromosomes, the genetic algorithm forms a new nonlinear optimization algorithm, which optimizes the fixed weights and thresholds in the traditional neural network. In this way, the calculation purpose of finding the optimal solution is achieved. The particle swarm optimization algorithm completes the nonlinear calculation process by simulating the social behavior of different quasi-groups. By setting a certain optimal value threshold, the algorithm finds the individual optimal solution and the global optimal solution through the movement of particles. At the same time, compared with genetic algorithms, particle swarm optimization has stronger adaptability.

Similarly, big data and cloud computing technologies can be applied to analysis and modeling efforts for higher education reform. In this study, from the perspective of big data technology, by introducing several conventional artificial intelligence techniques, we will make a nonlinear mathematical model prediction from several aspects of the curriculum, teaching content, teaching scenario setting, and teaching quality detection involved in higher education. And by comparing the predictive performance of several intelligent algorithms, we can provide suggestions on the process of educational change in Chinese higher education.

## 2. Exploration of Higher Education under Cloud Computing and Big Data Analysis

Higher education in the era of big data and artificial intelligence should use the analysis function of big data and pay more attention to teaching according to students'

differences for one-to-one independent training [15, 16]. At the same time, we also need to provide a precise training platform for the development of students' innovation and cooperation.

At present, much of our university education still follows the traditional teaching model, i.e., uniform classes and uniform examinations. It is difficult to explore students' differences and interests in this "one size fits all" model. Big data provides a more comprehensive picture of each student by collecting, analyzing, and providing feedback on a variety of campus educational data. However, the educated are living individuals whose interests may change over time. Therefore, we need to continuously change and adjust our teaching plan according to the actual situation after receiving the data.

However, if we want to successfully implement the above reform of the new teaching model of higher education based on big data technology, it is inseparable from the supporting role of data informatization [17, 18]. With the continuous promotion of information technology construction, related work has penetrated all aspects of teaching, research, service, management, culture, and life. There is a large gap between the rough information technology operation and maintenance services, passive network security supervision, and the demands of teachers and students. Similarly, big data in higher education is also built based on information technology. Figure 1 shows the framework of campus big data governance support platform construction.

As shown in Figure 1, the smart campus integrates teaching, research, and management based on the digital campus. Based on mobile Internet and intelligent sensing network and supported by big data and cloud computing [19, 20], the gap between the virtual campus and the physical campus is narrowing, and the activities of school teachers and students have covered the old physical space and the emerging digital space. Campus security, on-campus management, teacher and student classrooms, learning modes, teaching methods, and office processes will all be gradually made smart.

In the context of a smart campus, the information technology within the university is becoming more and more mature, which brings a lot of convenience for various information processing. The management of information no longer takes a lot of time to carry out the process of issuing many documents. Compared with traditional teaching, the reform of university education based on cloud computing can be taught by a coordinated and unified approach of online courses and practical courses. Web courses can use a variety of technologies to present and process the teaching content, including language, text, pictures, and other delivery methods. The special course content can be carried out in the form of online teaching lectures, which not only can eliminate many objective conditions, but also can be independent of time and geographical influence. This can fully reflect the distribution characteristics of various types of information for students.

In the era of big data, teachers are the initiators and organizers of teaching, and they play a key role in the middle of whether online teaching can be realized and how effective

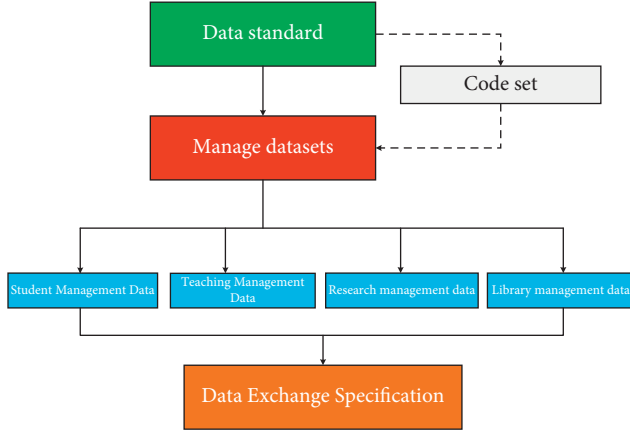


FIGURE 1: Construction framework of the campus big data governance support platform.

it can be. In the information age, students have access to a wide variety of online information, which includes information that is both beneficial and unhelpful to them. If students are not properly guided in this process, they are likely to spend a lot of time-consuming poor quality information and thus ignore useful information. Therefore, in the face of a large amount of online information, the teacher's job is no longer just to impart knowledge, but to guide students on how to search and identify useful information, so that they can feel the charm of independent learning, which undoubtedly puts higher demands on the teacher's ability. Therefore, teachers are required to familiarize themselves with online knowledge learning one step ahead of time, and then guide students in independent learning. The teacher should help students when they encounter problems so that they can eventually develop the ability to learn independently.

In the era of big data, higher education management based on information tools is the focus of educational reform efforts. Facing the shortcomings of current higher education management, colleges and universities should base on the actual development needs of students, strengthen the information construction of higher education management through various means, and give full play to the advantages of big data technology and information technology. This requires schools to provide more comprehensive education management services for students by starting from various aspects such as education management system, education management reform, faculty construction, and financial investment.

The original goal of cloud computing is the management of resources. However, the management is mainly of computing, storage, and network resources. Big data technology, or artificial intelligence algorithms, is an important part of the cloud computing platform, and is mainly responsible for the scheduling work in cloud computing. Limited by the length of the article, this article is based on the application of artificial intelligence algorithms in cloud computing. However, it should be pointed out that the implementation of cloud computing is the result of the interaction of various computing modules. This approach is

also applicable to reform applications in higher education. In order to specifically illustrate the application effect of big data technology in higher education reform, taking the education reform of a higher education institution as an example [21, 22], we compare the attention of the main content of curriculum setting, teaching content, teaching scene setting, and teaching quality inspection involved in this reform. In order to complete the above-mentioned prediction tasks, the following study systematically expounds on the application of big data technology in this education reform by introducing three cloud computing methods: immune cloning algorithm, fuzzy neural inference system, and Elman network. In addition, we can also obtain the model equation between any two or more main contents by means of mathematical fitting.

It should be noted that cloud computing is carried out on the basis of big data. That is to say, the big data-driven environment is the data matrix of cloud computing. Without the help of big data, it is impossible to build a cloud computing platform smoothly.

In order to clearly express the application effect of cloud computing technology in education reform, we have elaborated the following ideas. Section 3 mainly introduces several computing methods of cloud computing. The article compares the application of three cloud computing methods through Section 4, and obtains the model equation between teaching scene setting and teaching quality detection through the mathematical fitting.

### 3. An Introduction to Cloud Computing Methods

**3.1. Immune Cloning Algorithm [23, 24].** The biological immune system is a complex adaptive system. The human immune system can recognize pathogens and respond to them, so it has certain abilities of learning, memory, and pattern recognition. This way is similar to an external stimulating antigen to stimulate the human immune system to produce antibodies adapted to it. That is to say, an input variable corresponds to a unique output function. In this way, the principle and mechanism of its information processing can be described by computer algorithms to solve scientific and engineering problems. Algorithmic immunity retains some characteristics of the biological immune system and introduces them to solve optimization problems.

A population suppression process is added to the immune algorithm to control the average concentration of the population and avoid premature convergence of the algorithm to a locally optimal solution. This increases the global optimization capability.

A typical multi-peak function is used to enhance the application of the immune algorithm. The multi-peak function can be expressed as follows.

$$g(y) = \sum_{i=1}^{n-1} \left( 100(y_{i+1} - y_i^2)^2 + (1 - y_i)^2 \right). \quad (1)$$

In the formula,  $g(y)$  represents the fitness function involved in the immune algorithm.

The global minimum point of the multimodal function is obtained when all the independent variables are 1, and the minimum value of the function is 0. The search interval for the independent variable is  $(-10, 10)$ . The optimization results of five times of immune algorithm trial calculation are shown in Figure 2. It can be seen from Figure 2 that the immune algorithm has a good ability to search for multi-dimensional and multi-peak functions.

In the process of building a multi-dimensional support vector machine prediction model, the values of the control parameters need to be specified artificially to control the parameter values to achieve the minimum sample training error and the best multi-dimensional support vector machine model generalization accuracy.

In the model training phase, the overall error function of the set of training samples is defined as the optimization objective, and the same insensitive loss function is used for the errors of individual samples. The training samples are divided into learning samples and test samples, and the expression of the normalized objective function is:

$$(C^*, \varepsilon^*, \sigma^*) = \underset{C, \varepsilon, \sigma}{\operatorname{argmin}} L_{\text{all}}(C, \varepsilon, \sigma), \quad (2)$$

$$L_{\text{all}}(C, \varepsilon, \sigma) = \sum_{m=1}^k \sum_{i=1}^{k_m} L(u_i),$$

where  $L_{\text{all}}(C, \varepsilon, \sigma)$  denotes the overall training loss function,  $k$  denotes the number of aliquots of the sample,  $k_m$  denotes the number of each copy after  $k$  aliquots of training samples, and the superscript asterisks indicate the optimal parameters obtained.

After the training of the prediction model based on the immune algorithm is completed, that is, after the optimal engineering parameters are obtained by the immune algorithm, the calculation process of the entire artificial intelligence algorithm can be considered to be completed. Figure 3 shows the operation process of the immune algorithm cloning algorithm.

The range of the error value can be judged by the inversion theory of the immune algorithm. The specific error function can be expressed as follows.

$$x^* = \underset{x}{\operatorname{argmin}} \operatorname{aff}(x), \quad (3)$$

$$\operatorname{aff}(x) = [f_u(x) - u]^2 + [f_v(x) - v]^2.$$

In the formula,  $x$  is the parameter vector to be inverted,  $f_u(x)$  is the predicted convergence value of the immune cloning algorithm model,  $f_u(x)$  is the predicted value of the immune algorithm model,  $u$  is the measured value of the No. 1 site, and  $v$  is the measured value of No. 2 site.  $\operatorname{aff}$  is the affinity function (minimization problem).

In the optimization process of the immune cloning algorithm, in order to expand the search range and efficiency of the parameters, the parameters to be optimized are mapped exponentially, that is, the value range of the parameters in the population is the natural logarithm of the actual value range. The concrete realization model equation of this calculation process is as follows.

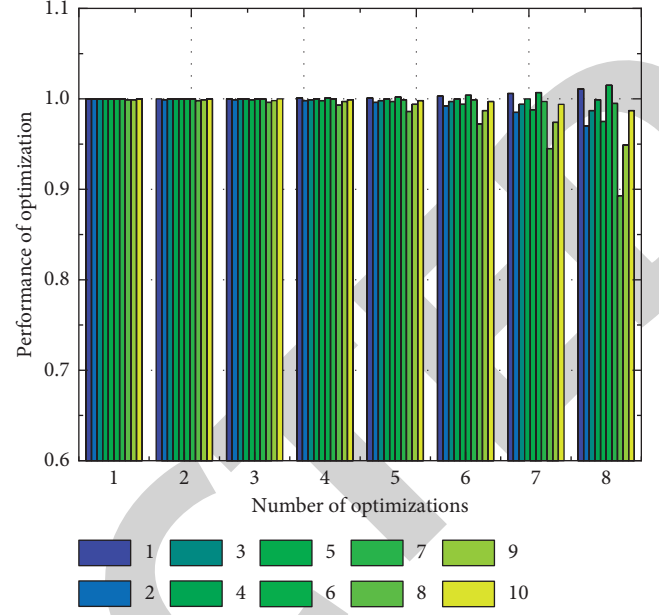


FIGURE 2: Function optimization results.

$$Q' = \exp(Q). \quad (4)$$

In the formula:  $Q$  is the value of each individual. The affinity calculation adopts the individual value after index mapping.  $\exp(Q)$  represents the form of an exponential function of a variable.

The specific operation steps of the immune cloning algorithm are shown in Figure 3. As shown in Figure 3, the immune algorithm achieves certain computational goals by setting certain preconditions. Algorithms can then obtain their own unique principle calculation equations through built-in nonlinear calculation rules. Finally, several parameters to be determined in the immune algorithm can be determined through a certain optimal condition setting method.

### 3.2. Prediction Based on Fuzzy Neural Inference System.

The neural reasoning system [25] is a system composed of three components, which mainly include (1) rule base (2) database (3) reasoning system. In the fuzzy neural inference system, the input parameters consider different fuzzification and defuzzification methods and strategies and have various rules. This intelligent algorithm can choose from many sets of member functions to ensure the effect of fuzzy logic on the input data. The fuzzy inference system can be divided into three inference modes according to the “if-then rule” inference operation. These inference modes are Mamdani system, Sugeno system, and Tsukamoto system, respectively. Sugeno system is considered to be the most popular candidate for sample-based fuzzy modeling and facilitates the use of adaptive techniques. In a one-dimensional Sugeno system, a typical rule set with two computational rules for fuzzy inference can be expressed as follows.

When  $x=A1$ ,  $y=B1$ , then the fuzzy neural inference system can get:

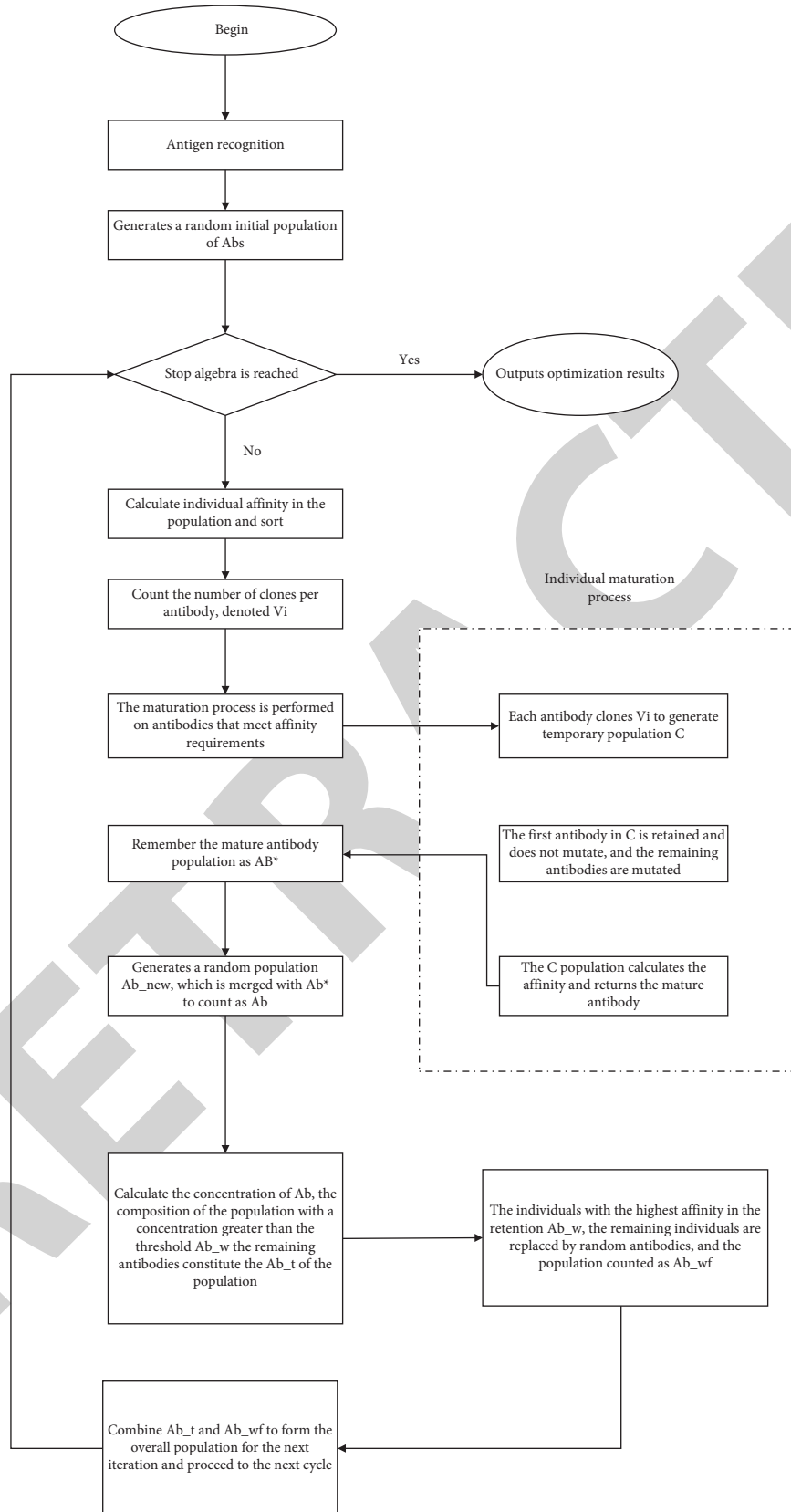


FIGURE 3: Flowchart of immune cloning algorithm.



$$f_1 = \alpha_1 x + q\beta_1 y + \eta_1. \quad (5)$$

In the formula,  $f_1$  represents the function value obtained by the fuzzy neural inference system,  $\alpha_1$ ,  $\beta_1$ , and  $\eta_1$ , respectively, represent the undetermined coefficients related to the function output.

Similarly, when  $x = A_2$ ,  $y = B_2$ , then the fuzzy neural inference system can get:

$$f_2 = p_2 x + q_2 y + r_2. \quad (6)$$

In the formula,  $f_2$  represents the function value obtained by the fuzzy neural inference system,  $\alpha_2$ ,  $\beta_2$ , and  $\eta_2$ , respectively, represent the undetermined coefficients related to the function output.

Figure 4 is a schematic diagram of the workflow of the fuzzy neural network prediction system.

**3.3. Prediction Based on Elman Network.** Neural networks are widely used for their large-scale parallel distributed structure, learning ability, and generalization ability. The main advantages are nonlinear analysis capability, convenient input/output mapping, adaptive capability, evidence response, background information, strong fault tolerance, VLSI (Very Large Scale Integrated) implementation, analysis and design consistency, and neural biological analogy. This study takes Elman neural network as an example to describe the implementation process of traditional neural network prediction in detail.

The calculation process of the Elman network can be expressed as follows.

For the input layer, the Elman network can be represented as follows.

$$x_i^0 = x_i(k). \quad (7)$$

For the hidden layer, the Elman network can be expressed as follows.

$$\begin{cases} s_i^1 = \sum_{j=1}^{n^0} w_{ij}^0 x_j^0(k) + \sum_{j=1}^{n^1} w_{ij}^2 c_j^0(k), \\ x_i^1 = f_1(s_i^1(k)). \end{cases} \quad (8)$$

For the association layer, the Elman network can be expressed as follows.

$$\begin{cases} s_i^2(k) = x_i^1(k-1), \\ c_i(k) = s_i^2(k). \end{cases} \quad (9)$$

For the output layer, the Elman network can be represented as follows.

$$\begin{cases} s_i^3(k) = \sum_{j=1}^{n_1} w_{ij}^1 x_j^1(k), \\ y_i(k) = f_2(s_i^3(k)). \end{cases} \quad (10)$$

The key to the nonlinear ability and learning ability of the network lies in the continuous correction of the weights. There are two methods for recurrent network training, one is batch mode, and the other is the online mode, Elman network adopts the latter.

## 4. Example Verification and Analysis

As mentioned in the second section of the article, this study uses the corresponding concerns of the four main aspects involved in the teaching reform of a certain institution of higher learning as the research data for research. The prediction effect of the three cloud computing methods mentioned above is mainly analyzed. In addition, by comparing the relevant data corresponding to the four main aspects, we can also obtain the model equations of any two main aspects.

These data mainly include the attention corresponding to four main aspects. For the data collection of the educational reform of a certain institution of higher learning, the number of data for each item is 5800 groups. The number of data in four data groups is as high as 23200 groups.

For the content of the curriculum, big data technology can use information collection and big data analysis to group the students enrolled in the major categories according to their learning willingness and career planning. In addition, it can also plan a professional orientation for each student through questionnaires and analysis of students' class performance. In addition, this model can set up an optimized curriculum system that is conducive to their academic development according to different professional orientations.

For teaching content, big data technology relies on Internet big data, continuously integrates the content of other related disciplines, and continuously integrates foreign advanced knowledge content. In addition, on the basis of existing educational resources, this technology can expand the proportion of course cases that solve international-related problems, and truly improve students' professional quality and technical level in dealing with international problems.

For the setting of teaching scenarios, various new methods and technologies in the era of artificial intelligence are the entry point to change the barriers of the old education system. Through the combination and application of various teaching methods, higher education courses can go out of traditional classrooms. This approach allows students to make the most of every minute around them. In addition, it has established comprehensively diversified and multi-level online teaching resources through introduction or creation.

For teaching quality detection, big data technology can use the Internet and big data to closely combine education evaluation with artificial intelligence by tracking and monitoring the whole process of teaching and learning. At the same time, it can analyze various student learning behavior data obtained from the network and the terminal, and realize comprehensive evaluation based on the data.

The three artificial intelligence techniques discussed above are mostly used in this section to conduct research on higher education reform modeling, which may serve as a theoretical foundation for the analysis and modeling of future higher education models. The suggested model is capable of predicting, analyzing, and computing attention data in curriculum development, teaching content, teaching scenario development, and teaching quality detection.

The comprehensive impact matrix among the four main contents involved in higher education reform can be drawn in



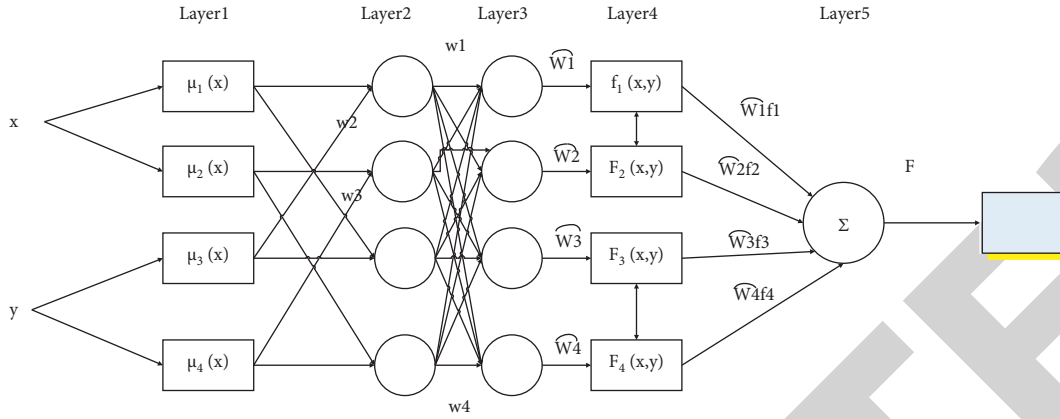


FIGURE 4: Elman network structure diagram.

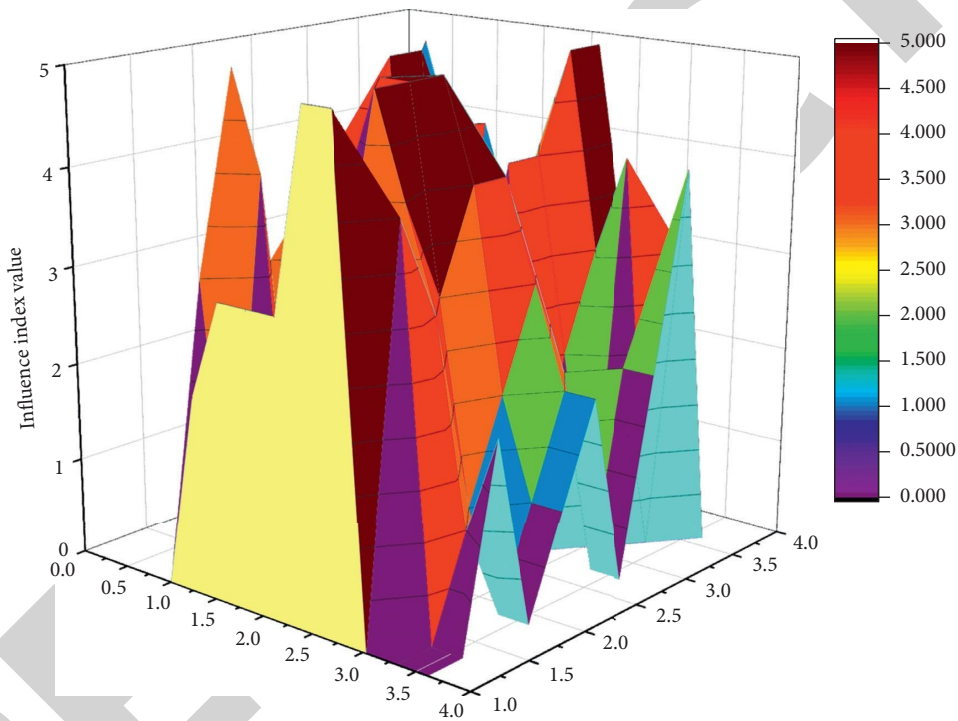


FIGURE 5: Influence index value of four main contents.

Figure 5. It can be found from Figure 5 that the influence degree of each main content is different, and the difference is large. This illustrates the need to add artificial intelligence-like techniques to the prediction process for such problems. As shown in Figure 5, we can also find that the predicted values of the four main impact indicators have good continuity and derivation. This also shows from the side that the prediction effect based on the cloud computing method is relatively complete, and can approximately reflect the distribution law of the original data.

The elements of each row in the comprehensive influence matrix are added to obtain the corresponding influence degrees of curriculum setting, teaching content, teaching scene setting, and teaching quality detection. The sum of the degree of influence and the degree of being influenced is the degree of centrality. The greater the degree of centrality, the stronger the effect of this research project on the research target. The

difference between the degree of influence and the degree of being influenced is the degree of cause. The smaller the causal degree, the more likely the influencing factor is to be influenced by other influencing factors, which is called the result factor. Figure 6 is a graph showing the variation curve of the degree of cause corresponding to the detection of teaching quality with the calculation time step.

The degree of cause can reflect the categories of influencing factors. The larger the causality degree of the influencing factor, the more the factor is the causal index in the influencing factor system. The smaller the causal degree of the influencing factor, the more the factor is the result index in the influencing factor system. As shown in Figure 6, as the calculation time step increases, the cause degree corresponding to the teaching quality detection increases first and then decreases, and when the time step is

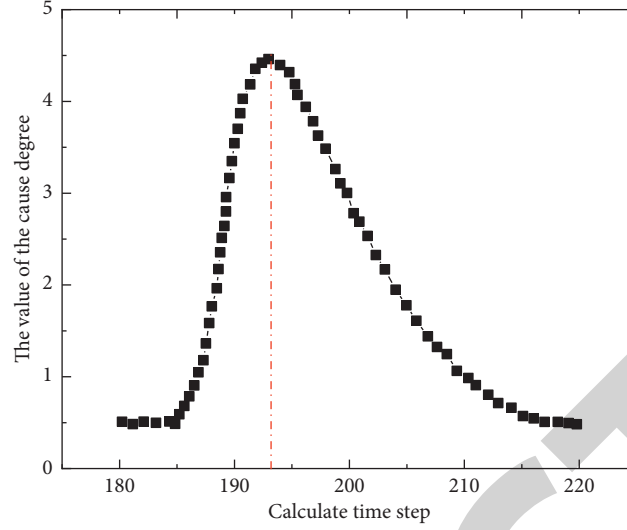


FIGURE 6: Influencing factors of four feature columns.

approximately equal to 195, the value of the cause degree reaches the maximum value. Its maximum value is about 4.5.

When the number of big data computing steps is 4000, 8000, 12000, 16000, and 20000, respectively, we compare the calculation completion time of the three algorithms: immune cloning algorithm, fuzzy neural inference system, and traditional Elman network. The specific test results are shown in Figure 7.

It can be seen from Figure 7 that compared with the three methods of immune cloning algorithm, fuzzy neural reasoning and traditional Elman network, the corresponding computing time of immune cloning algorithm is shorter, and the prediction is better. As the time required to complete the task increases, the difference in the completion time corresponding to the three algorithms becomes more and more obvious. Among them, the advantages shown by the immune algorithm are more obvious.

It is well known that among the evaluation indicators of various prediction algorithms, the coefficient of determination ( $r^2$ ) and the root mean square error (RMSE) are the two most representative important indicators. In order to quantify the prediction effects of the three types of cloud computing, the attention corresponding to the four main contents of curriculum setting, teaching content, teaching scene setting, and teaching quality detection is used as the predictive index. Then through the nonlinear calculation process, the application effects of the three calculation methods are compared. The corresponding coefficient of  $R^2$  and RMSE are obtained as shown in Figures 8-9. In order to clearly express the calculation method of statistical variables, we can get the calculation method of root mean square difference.

$$\text{RMSE} = \sqrt{\frac{1}{n} \times \sum_{i=1}^n (y_i - x_i)^2}. \quad (11)$$

It should be pointed out that FNSR stands for fuzzy neural reasoning system, ICSA stands for immune algorithm optimization, and ELMAN stands for Elman network.

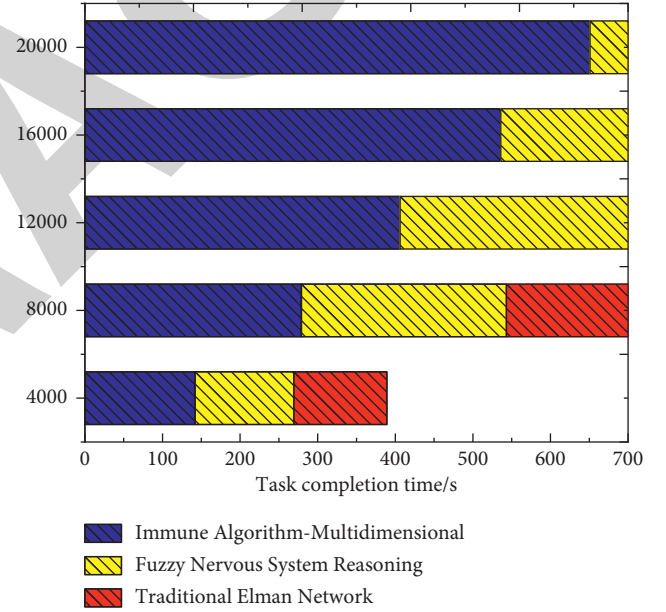


FIGURE 7: Comparison of task completion time.

It can be seen from Figures 8 to 9 that the coefficient of determination and the root mean square difference show a negative correlation. That is, a larger coefficient of determination corresponds to a smaller RMSE, and vice versa. For the four main contents of higher education, the coefficient of determination corresponding to ICSA is the closest to 1, and the root mean square difference is the smallest. So its prediction performance is better.

As shown in Figure 10, we use the ICSA algorithm to predict the causality of the two main contents of teaching scene setting and teaching quality detection. And a scatter plot can be drawn as follows. As shown in Figure 10, the corresponding value of the cause degree of the teaching scene setting and the teaching quality detection is approximately a polynomial function. The polynomial function

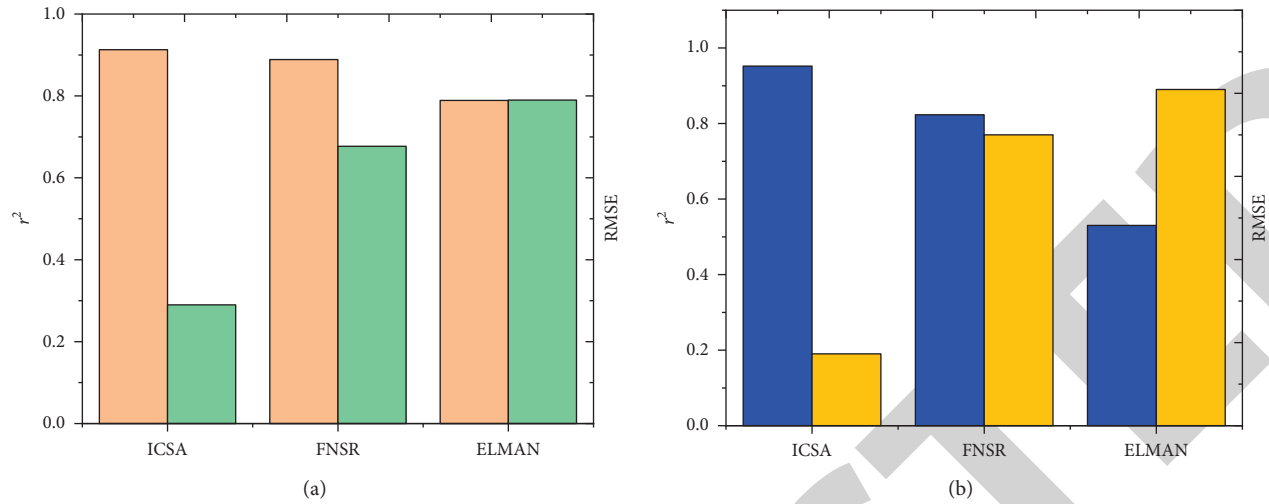


FIGURE 8: Predictive indicators corresponding to curriculum setting and teaching content. (a) Predicted performance for course offering content. (b) Predictive performance for instructional content.

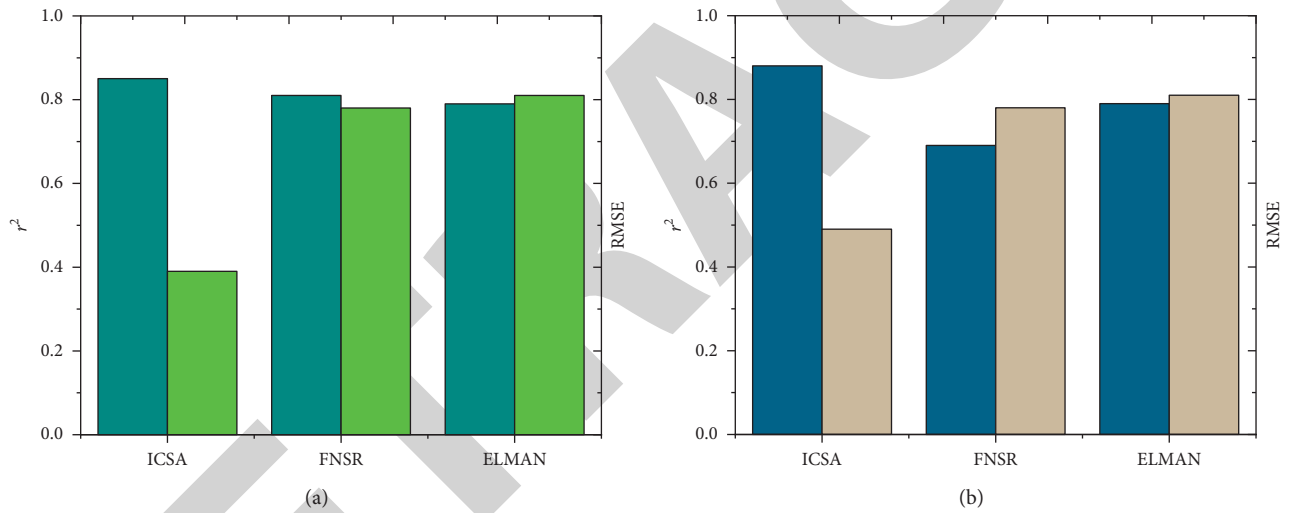


FIGURE 9: Predictive indicators corresponding to teaching scene settings and teaching quality. (a) Predictive performance for setting content for instructional scenarios. (b) Prediction performance for teaching quality detection content.

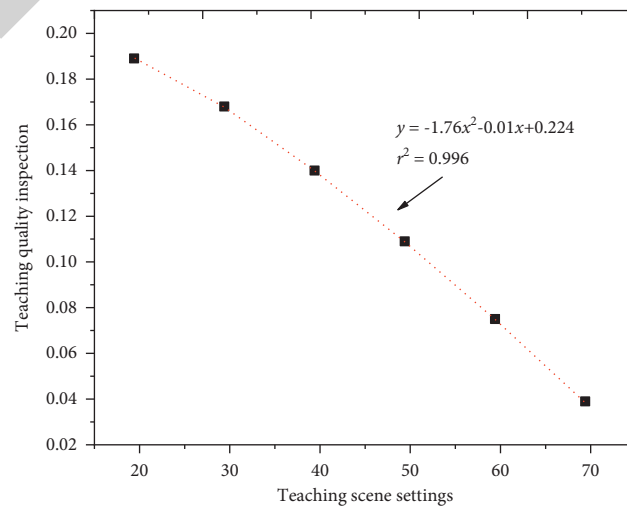


FIGURE 10: Mathematical connection between the two main contents of higher education.

relationship corresponding to the cause degree of teaching scene setting and teaching quality detection can be expressed as follows.

$$y^2 = 1.76x^2 - 0.01x + 0.224. \quad (12)$$

## 5. Conclusion

The development of higher education is inseparable from the support of new information technology, so the impact of the era of big data on higher education is multi-faceted. The innovation model based on big data has also accelerated the reform process of higher education. This study studies the application effect of different algorithms or technologies in the reform of higher education by studying the intelligent algorithm part of the cloud computing program. Three typical intelligent algorithms are introduced to conduct predictive research on the four main aspects involved in higher education reform. The results show that the prediction effect based on the immune cloning algorithm is the best. In addition, through the method of mathematical fitting calculation, it can be found that the causal relationship between the two main contents of teaching scene setting and teaching quality detection approximately presents a polynomial function relationship.

## Data Availability

The experimental data used to support the findings of this study are available from the corresponding author upon request.

## Conflicts of Interest

The authors declared that they have no conflicts of interest regarding this work.

## References

- [1] J. You, C. J. Craig, and S. Oh, "Challenges in the new roles of physical education as liberal education in higher education," *Quest*, vol. 71, no. 1, pp. 51–65, 2019.
- [2] S. Stein, "Beyond higher education as we know it: gesturing towards decolonial horizons of possibility," *Studies in Philosophy and Education*, vol. 38, no. 2, pp. 143–161, 2019.
- [3] N. M. Xie, R. Z. Wang, and N. L. Chen, "Measurement of shock effect following change of one-child policy based on grey forecasting approach," *Kybernetes*, vol. 47, no. 3, pp. 559–586, 2018.
- [4] S. Milton, "Syrian higher education during conflict: s," *International Journal of Educational Development*, vol. 64, pp. 38–47, 2019.
- [5] B. Barakat and R. Shields, "Just another level? Comparing quantitative patterns of global expansion of school and higher education attainment," *Demography*, vol. 56, no. 3, pp. 917–934, 2019.
- [6] S. B. Liu, M. M. Liu, H. Jiang, Y. Lin, and K. Xu, "International comparisons of themes in higher education research," *Higher Education Research and Development*, vol. 38, no. 7, pp. 1445–1460, 2019.
- [7] X. Xu, D. Li, M. Sun et al., "Research on key technologies of smart campus teaching platform based on 5G network," *IEEE Access*, vol. 7, pp. 20664–20675, 2019.
- [8] P. Chea, "Does Higher Education Expansion in Cambodia Make Access to Education More Equal?[]," *International Journal of Educational Development*, vol. 70, 2019.
- [9] M. Z. Latif, I. Hussain, R. Saeed, M. Qureshi, and U. Maqsood, "Use of smart phones and social media in medical education: trends, advantages, challenges and barriers," *Acta Informatica Medica*, vol. 27, no. 2, pp. 133–138, 2019.
- [10] R. M. Myers and A. L. Griffin, "The geography of gender inequality in international higher education," *Journal of Studies in International Education*, vol. 23, no. 4, pp. 429–450, 2019.
- [11] D. D. Jiang, Y. Q. Wang, Z. H. Lv, S. Qi, and S. Singh, "Big data analysis based network behavior insight of cellular networks for industry 4.0 applications," *IEEE Transactions on Industrial Informatics*, vol. 16, no. 2, pp. 1310–1320, 2020.
- [12] S. S. Kamble and A. Gunasekaran, "Big data-driven supply chain performance measurement system: a review and framework for implementation," *International Journal of Production Research*, vol. 58, no. 1, pp. 65–86, 2020.
- [13] Z. H. Sun, K. D. Strang, and F. Pambel, "Privacy and security in the big data paradigm," *Journal of Computer Information Systems*, vol. 60, no. 2, pp. 146–155, 2020.
- [14] Z. Li and H. Wang, "Intelligent Guiding Model Based on Environment Perception and Posture Recognition[C]," in *Proceedings of the 2021 Third International Conference on Inventive Research in Computing Applications (ICIRCA)*, pp. 1152–1155, IEEE, Coimbatore, India, 2021.
- [15] X. Li and R. Law, "Network Analysis of Big Data Research in Tourism[]," *Tourism Management Perspectives*, vol. 33, 2020.
- [16] D. J. Kim, J. Hebler, V. Yoon, and F. Davis, "Exploring determinants of semantic web technology adoption from IT professionals' perspective: industry competition, organization innovativeness, and data management capability," *Computers in Human Behavior*, vol. 86, pp. 18–33, 2018.
- [17] M. J. Sanders, R. Bruin, and C. T. Tran, "How to make a standard inhaler device into a 'smart' inhaler that teaches technique[]," *Journal of Aerosol Medicine and Pulmonary Drug Delivery*, vol. 31, no. 2, p. A14, 2018.
- [18] P. K. Wu, C. Wu, and Y. Y. Wu, "Reforming path of China's fertility policy in stabilizing demographic dividends perspective," *Social Indicators Research*, vol. 137, no. 3, pp. 1225–1243, 2018.
- [19] I. Ahmad, G. Ahmed, S. A. A. Shah, and E. Ahmed, "A decade of big data literature: analysis of trends in light of bibliometrics," *The Journal of Supercomputing*, vol. 76, no. 5, pp. 3555–3571, 2020.
- [20] V. G. Ravindhren and S. Ravimaran, "CCMA-Cloud critical metric assessment framework for scientific computing," *Cluster Computing*, vol. 22, no. S5, pp. 11307–11317, 2019.
- [21] A. M. Aleixo, S. Leal, and U. M. Azeiteiro, "Conceptualization of sustainable higher education institutions, roles, barriers, and challenges for sustainability: an exploratory study in Portugal," *Journal of Cleaner Production*, vol. 172, pp. 1664–1673, 2018.
- [22] C. Senior, D. Fung, C. Howard, and R. Senior, "Editorial: what is the role for effective pedagogy in contemporary higher education?[]," *Frontiers in Psychology*, vol. 9, p. 1299, 2018.
- [23] Y. Jing and Z. H. Zhang, "A study on car flow organization in the loading end of heavy haul railway based on immune clonal

## *Retraction*

# **Retracted: Application Exploration of Scenario Logistics Ecosystem Based on beyond 5G and IoT Architecture**

### **Security and Communication Networks**

Received 26 December 2023; Accepted 26 December 2023; Published 29 December 2023

Copyright © 2023 Security and Communication Networks. This is an open access article distributed under the Creative Commons Attribution License, which permits unrestricted use, distribution, and reproduction in any medium, provided the original work is properly cited.

This article has been retracted by Hindawi, as publisher, following an investigation undertaken by the publisher [1]. This investigation has uncovered evidence of systematic manipulation of the publication and peer-review process. We cannot, therefore, vouch for the reliability or integrity of this article.

Please note that this notice is intended solely to alert readers that the peer-review process of this article has been compromised.

Wiley and Hindawi regret that the usual quality checks did not identify these issues before publication and have since put additional measures in place to safeguard research integrity.

We wish to credit our Research Integrity and Research Publishing teams and anonymous and named external researchers and research integrity experts for contributing to this investigation.

The corresponding author, as the representative of all authors, has been given the opportunity to register their agreement or disagreement to this retraction. We have kept a record of any response received.

### **References**

- [1] W. Yao and Y. Li, "Application Exploration of Scenario Logistics Ecosystem Based on beyond 5G and IoT Architecture," *Security and Communication Networks*, vol. 2022, Article ID 5797503, 11 pages, 2022.

## Research Article

# Application Exploration of Scenario Logistics Ecosystem Based on beyond 5G and IoT Architecture

Wei Yao  and Yudong Li

*School of Business, Macau University of Science and Technology, Macau 999078, China*

Correspondence should be addressed to Wei Yao; 2009853fbg20001@student.must.edu.mo

Received 23 June 2022; Revised 12 July 2022; Accepted 18 July 2022; Published 19 August 2022

Academic Editor: Hangjun Che

Copyright © 2022 Wei Yao and Yudong Li. This is an open access article distributed under the Creative Commons Attribution License, which permits unrestricted use, distribution, and reproduction in any medium, provided the original work is properly cited.

With the continuous expansion of my country's logistics market, the business scale and management scale of logistics enterprises are increasing day by day. Smart logistics enterprises realize the "three streams in one" of the logistics industry through informatization and intelligent management, which greatly improves the service efficiency and quality of logistics enterprises. However, there are still many problems in this intelligent logistics mode. In this context, we conduct research experiments on the logistics ecosystem of IoT architecture scenarios and draw conclusions through experiments: (1) logistics development in IoT building scenarios. The environment includes natural environment, economic environment, political environment, etc. The economic environment plays an important role in driving logistics demand and promoting logistics growth. The political environment helps to improve the logistics infrastructure and ensure the healthy development of logistics. (2) The most important cost of the logistics industry is that transportation costs account for 67% of the entire logistics cost, followed by cargo storage accounting for 16% of the cost, and smart express cabinets accounting for 13% of the cost. From this, we can see the highest cost out of the logistics system under the Internet of Things is the transportation cost. As a unity is closely linked to the economy and interdependent, logistics is the driving force to promote the development of economic integration. In order to ensure the sustainable development of the economy, it is necessary to continuously improve the service level of logistics, reduce logistics costs, improve operation efficiency, strengthen the linkage development with other industries, and enhance the competitiveness of logistics. We launched an investigation against this background and researched the logistics system under the scenario logistics ecosystem of beyond 5G and IoT architecture.

## 1. Introduction

Self-interference cancellation invalidates a long-standing fundamental assumption in wireless, network design that radios can only operate in half-duplex mode on the same channel. This is a serious global problem that will only get worse with 5G. Self-interference suppression complements and supports the development of 5G technologies for denser heterogeneous networks and can be used in wireless communication systems in a variety of ways, including increased channel capacity, virtualized spectrum, random division duplex (ADD), new relay solution, and enhanced interference coordination. Due to its core nature, eliminating self-interference will have a huge impact on 5G networks and beyond [1]. A computationally efficient multi-carrier

waveform for next-generation wireless communication systems is introduced. In the proposed technique, we first divide resource blocks (RBs) into two groups, namely, odd and even groups. The filter operation will then be applied to only these two groups, whereas the standard UFMC system will apply the filter operation to each individual RB. This reduces the number of inverse Fourier transforms and filtered convolutions, thereby reducing complexity, which is especially important for a large number of subcarriers. The results show that the proposed scheme outperforms the OFDM system while maintaining the same performance level as the standard UFMC system [2]. Driven by the rapidly escalating wireless capacity requirements of advanced multimedia applications and the dramatic increase in user access requirements required by the Internet of Things



(IoT), fifth-generation (5G) networks face challenges in supporting large-scale heterogeneous data traffic. Non-orthogonal multiple access (NOMA), recently proposed for the 3rd Generation Partnership Project Long-Term Evolution Advanced (3GPP-LTE-A), constitutes a promising technology that can address the above challenges in 5G networks [3]. Wireless engineers and business planners often ask questions about where, when, and how mmWave will be used for 5G and beyond. Since next-generation networks are not just a new wireless access standard, but network integration for vertical markets with multiple applications, the answer to this question depends on the scenarios and use cases to be deployed. Four examples of 5G mmWave deployments are presented, along with a chronological description of possible deployment scenarios and use cases, including expected system architectures and hardware prototypes. A third example is a millimeter-wave mesh network used as a micro-Ra [4]. Nonorthogonal multiple access (NOMA) is expected to play a key role in heterogeneous networks beyond fifth-generation (5G) wireless systems. The unparalleled advantages of NOMA and the multi-layered architecture of HetNets have the potential to significantly improve the performance of cellular networks. Inspired by this possibility, a new resource optimization scheme is presented for efficient cellular device association and optimal power control in NOMA-enabled HetNet, so a joint solution is difficult to obtain [5]. The Internet of Things (IoT) technology permeates diverse application areas, relying on sensing and actuating devices that share, process, and present meaningful real-world information. This paper focuses on one of the main functions of IoT, that is, virtualization, and proposes an IoT solution for wide-area measurement systems, which introduces virtualized phasor measurement resources. Such solutions aim to create a programmable intelligent environment that promotes interoperability, reusability, and flexibility of 5G services. The performance of the system is evaluated against generated traffic and latency to understand which scenarios can benefit from its deployment [6]. An integrated IoT architecture is introduced to deal with cyber-attacks, based on the developed deep neural network (DNN) with rectified linear units. The developed DNN-based IoT architecture introduces a new approach. For online monitoring of AGVs to defend against cyber-attacks, it is inexpensive and easy to implement, rather than traditional cyber-attack detection schemes in the literature. The proposed DNN is trained based on experimental AGV data representing the true state of the AGV and different types of network attacks, including random attacks, ramp attacks, impulse attacks, and sinusoidal attacks in which the attacker injects the Internet network [7]. The penetration of the Internet of Things (IoT) has grown significantly, along with increased capacity and reduced communication costs, as well as rapid technological advancements. At the same time, big data and real-time data analytics are becoming increasingly important, and this growth in data and infrastructure must be accompanied by software architectures that allow it to be exploited. While there are various proposals focused on leveraging IoT at the edge, fog, and/or cloud level, it is not easy to find a software

solution that leverages all three layers, not only maximizing the use of context and contextual analysis of each layer data, but also bidirectional communication between adjacent layers [8]. In order to improve the utilization efficiency of Internet of Things (IoT) and cyber-physical system technologies, it is recommended to strengthen collaboration in data transmission. These applications receive data from multiple sensors; therefore, efficient data acquisition systems must be added. The research work proposes the use of a reconfigurable FIFO design for data acquisition. The optimal algorithms for FIFO tasks in offline situations are first provided, and then the architecture is synthesized using an FPGA board [9]. Firstly, the architecture of direct control of IoT devices through mobile phones and the characteristics of IoT architecture, based on independent background services, are analyzed, and the core content of IoT scenario evolution is proposed, namely, independent servers and independent services. Then, on this basis, we developed a WeChat-based smart equipment platform and IoT architecture, and elaborated its implementation process and working mechanism of its components [10]. Take logistics students as the experimental objects, after three years of exploration and practice, through the construction of multi-dimensional ecological experience field, a large number of teaching activities, the construction of talent pool, and the implementation of the sophomore tutor system. This reform has successfully resolved students' misunderstandings about logistics, activated students learning potential, improved students' logistics skills and various soft powers, and improved the satisfaction of enterprises. At the same time, the reform has also greatly enhanced the strength of the teaching staff [11]. The article introduces the concept of GPS in the logistics ecosystem, summarizes the current application of GPS in small and medium-sized logistics enterprises, analyzes the problems existing in the application of GPS technology in small and medium-sized logistics enterprises, puts forward the application of GPS in small and medium-sized logistics enterprises in the future, and made some suggestions [12]. Logistics agents shoulder the mission of logistics development in their respective market segments and jointly form an industrial ecosystem of mutual benefit and coexistence through the connection of the logistics ecological chain. Based on the ecosystem metaphor, the concept of logistics ecosystem is proposed, the evolution equation of logistics growth curve is established, and the characteristic mechanism of self-organization evolution under the combined action of internal and external forces and positive and negative feedback is analyzed, and has established the complex logistics development equation and analyzed the evolution mechanism and curve of the scientific understanding and management of regional logistics [13]. Ecosystem theory provides a new perspective for the study of logistics market and third-party logistics enterprises. By studying the basic theory of ecosystem, it analyzes the competition and synergy between the integrated logistics market, regional logistics market, and specialized logistics market, as well as the optimal distribution of third-party logistics activities in the logistics market. Based on the ecosystem theory, this paper studies the evolution of

competition and cooperation among third-party logistics companies, and proposes an ecosystem structure model for third-party logistics companies' competition and partnership management [14]. With the global economic integration and the development of Internet technology, the traditional logistics ecosystem has encountered problems such as low level of industrialization and backward management methods. Through a series of studies and investigations, the application of Internet technology to the logistics ecosystem of short-cycle products will help to solve the above problems. Therefore, in the research process, the NSGA-II algorithm is used to optimize the traditional logistics ecosystem, and the Internet technology is used to build a new intelligent short-cycle agricultural product supply chain logistics system, which verifies the necessity and importance of its construction. In order to promote the development of the bioflow ecosystem, some Internet technologies need to be introduced [15].

## 2. Scenarios of IoT Architecture

### 2.1. Proposition and Demand of IoT Service Grid Architecture

- (1) The "Internet of Things system microservice abstraction model" is proposed, including the overall abstraction of the Internet of Things system and the abstraction of the internal structure of microservices. The specification for the Internet of Things system defines the abstract model of microservices.
- (2) Integrating microservices in IoT systems requires the description of service APIs at the syntactic and semantic levels, and its microservice description model is used for writing new microservices or for microservice discovery and recommendation.

Different IoT devices, different connection methods, multiple platforms, poor interoperability of devices and products from different manufacturers, and lack of compatible design and development models in application development are the reasons for the differences in IoT services. Furthermore, with the proliferation of IoT devices, the scope and complexity of services increase significantly, making it difficult to manage the interaction of different microservices in an IoT system. Current high-performance design and development models for centralized cloud services and management models for network services are not suitable for true IoT infrastructure. These factors have led to the proposal and creation of an IoT service network architecture. In an IoT-centric service network architecture, the distribution model and abstraction of microservices, service description and detection methods, and security requirements are all different from traditional service networks.

**2.1.1. IoT Microservice Abstraction.** In the field of traditional Web, all microservices are located in the cloud, which is an abstraction of modular applications. In the Internet of Things system, devices can display their capabilities through service interfaces, and microservices can be connected to devices, cloud peripherals or gateway components, and the larger Internet cloud. Improve the flexibility of system development,

improve the interaction between services, simplify the development of Internet of Things applications, clarify the concept of "Internet of Things" integrated microservices, and finally form "Internet of Things Microservices Network." It requires the integration of "Internet of Things" and "Microservices." "Microservice abstraction model grid" is widely available for download via the Internet and free from internal microservices, and the IoT traditional abstract microservice system is the basis for developing IoT prototype services.

**2.1.2. IoT Microservice Description and Discovery.** By providing a survey processing service, the caller of the service knows the process by which we invoke the shortcut when it is removed from the list of available services on the registry. When a service is called, the back of the call is also called a microservice. Therefore, the service description is very simple and usually only includes the name of the required service tool and the information provided by the service provider, which can only be used to find the work place of the service, but cannot be used.. Microintegration of IoT systems requires the definition of an API service in terms of integration and interpretation, while microservices define a new way of writing or discovering and suggesting small services. The identity and nature of IoT micro-employees correspond to service characteristics based on information from customers and the performance, description, and quality of the requested service.

**2.2. IoT Service Grid Architecture Design.** The IoT-centric service network architecture aims to establish IoT as a core block of services and service brokers, implement a consistent microservice management system, and reap the benefits of microservices deployed in the cloud. The consistent architecture agent forms a service management grid, connects, protects, manages, and controls complex and efficient microservice distribution, and introduces inter-service communication management for deployed microservices, allowing developers to focus only on basic service functions. Microservices themselves are not common services management problem such as service discovery and secure communication. Extensive and advanced microservices will link broker organizations, enabling IoT systems to integrate cloud, connectivity, applications, and services to provide IoT services. Develop and explain the general and secure architecture of IoT service networks. The IoT service network architecture is shown in Figure 1. At the level, the architecture is divided into edge layer, edge cloud layer, middle cloud layer, and infrastructure layer. The infrastructure layer is divided into a data layer and a control layer. A system based on this architecture consists of microservices and microservice agents with different functions. The features and characteristics of the IoT service network architecture are described below.

**2.3. IoT Microservice Description and Discovery.** The descriptive service model is used to map and use IoT e-replication terminology for microservices. During the standard service search process, when a service receives a service call through

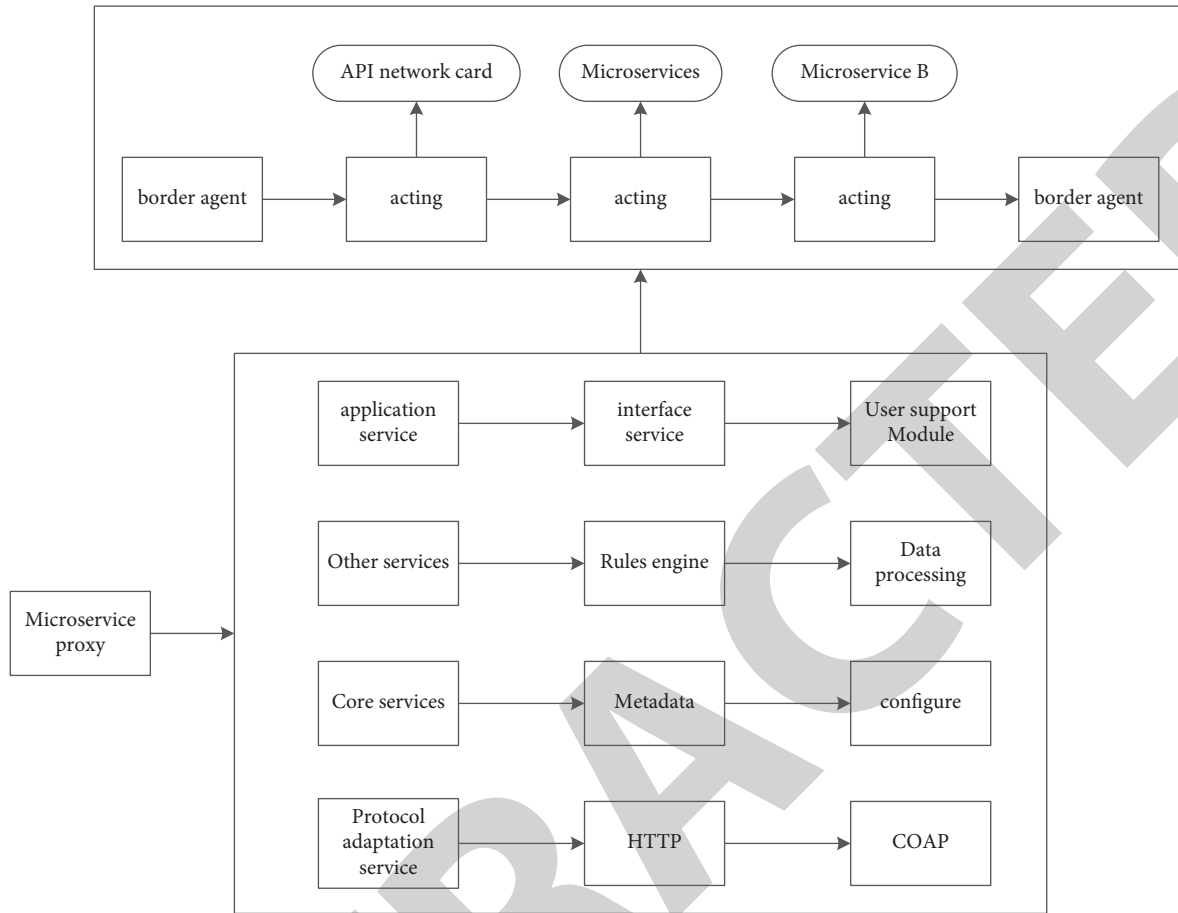


FIGURE 1: The overall architecture of the Internet of Things network.

the service log, the server preidentifies the process. When a service is invoked, the billing solution is determined and the handler is identified by the server. Therefore, the described copy of the service is simple and often contains so much information that the name and location of the media service network resource are required. For example, a project advisor (see Service Registration) includes a service description model, network number, and service (service name, serial number, and version number). Some lists can be deleted in SOW, but other files cannot be added. In IoT systems, the integration of API microservices requires the development of syntax and semantics. Service descriptions can also be used to investigate and approve or author new existing services. The descriptive service model is used to map and use IoT e-replication terminology for microservices. In the standard service search process, when a service receives a service call through the service log, the server preidentifies the process, when a service is called, the billing solution is determined, and the processor is identified by the server. Therefore, the described copy of the service is simple and often contains so much information that the name and location of the media service network resource are required. For example, a project advisor (see Service Registration) includes a service description model, network number, and service (service name, serial number, and version number). Some lists can be deleted in SOW, but other files cannot be added.. In IoT systems, the integration of API microservices

requires the development of syntax and semantics. Service descriptions can also be used to investigate and approve or author new existing services. The description model of IoT services is shown in Figure 2.

### 3. Beyond 5G Algorithms

**3.1. 5G Network Soft Slicing.** Network slicing is an intelligent connectivity service that provides customers with customized end-to-end 5G networks based on logical and physical resources, including slices of multiple subnets such as core subnets, transmission subnets, and wireless subnets. An example of a network segment is an end-to-end logical network that includes many network functions, resources, and connections. Depending on the required services and resources, network slicing can provide flexible network management. The network component management system can design network component models that meet network characteristics and SLA requirements, including slice implementation and tuning capabilities, and implement SLA through NSI runtime monitoring. Based on advanced cloud management technology, NSM has enhanced functions, supported network partitioning, and optimized operation and maintenance services. The description of the slice network can be transformed into a physical G network, which is defined as follows:

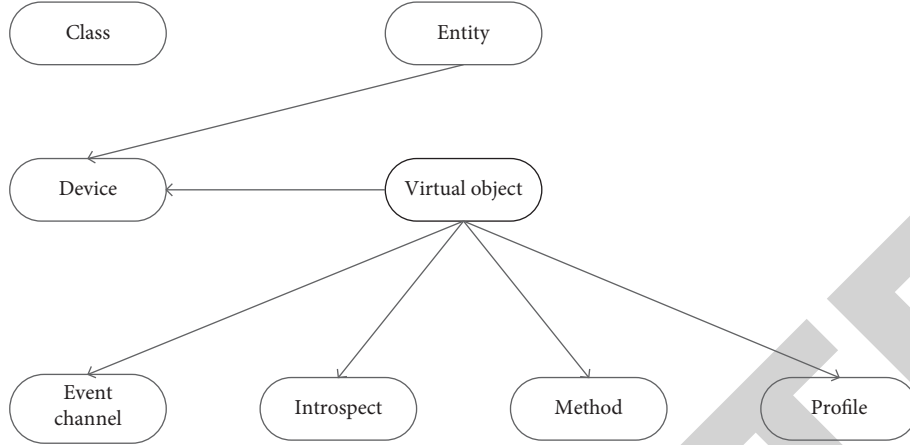


FIGURE 2: IoT service description model diagram.

$$SLICE_{MAP} = (N_{MAP}, E_{MAP}, R, B, D). \quad (1)$$

Network slicing is a multiobjective optimization problem. In order to reduce the UPF, it is necessary to organize as many hops as possible in the core network to make full use of network resources and increase revenue. Therefore, resource weights are proposed.

$$R(G^V, t) \propto \sum_{n^v \in N^V} CPU(n^v) + \beta \sum_{l^v \in E^V} BW(L^V). \quad (2)$$

Orchestration overhead represents the cost of successfully orchestrating a network slice. Since it consumes the underlying resources of the physical network, it is calculated as follows:

$$C(G^V, t) = \gamma \sum_{n^v \in N^V} CPU(n^v) + \delta \sum_{l^v \in E^V} BW(L^V). \quad (3)$$

According to (2) and (3), the cost and benefit ratio of the underlying network can be obtained as follows:

$$\tau = \lim_{T \rightarrow \infty} \frac{\sum_{t=0}^T R(G^V, t)}{\sum_{t=0}^T C(G^V, t)}. \quad (4)$$

The security and reliability of sliced networks depend on the isolation mechanism of slices. Each component can be thought of as a collection of individual resources provided by different network devices. Insulation grades and strengths vary depending on cutting requirements and operating conditions. In this paper, the Bayesian estimation method is used to calculate the insulation coefficient of the mesh wafer, and the calculated probability is

$$p(R_{IJ} | x, y) = \frac{p(R_{IJ} | x, y)}{p(x, y)}. \quad (5)$$

Then according to the density function,

$$B(x, y) = \int_0^1 R_{ij}^{x-1} (1 - R_{IJ})^{y-1}. \quad (6)$$

Push

$$p(R_{IJ} | x + 1, y) = \frac{R_{ij}^x (1 - R_{IJ})^y}{B(x + 1, y)}. \quad (7)$$

Then, its mathematical trust factor is

$$E(R_{IJ}) = \frac{x + 1}{x + 1 + y}. \quad (8)$$

From this, it can be deduced that the calculation formula of the isolation factor of node  $G_i$  is

$$R_i = \frac{1}{n} \sum_{j=1}^n E(R_{IJ}). \quad (9)$$

The goal of the segment mapping algorithm is to dynamically configure the use of network shards to require limited network resources and reduce the impact of additional traffic changes on network performance. The specific steps of the synchronization strategy are as follows: consider providing a slice of  $K$  sources for each match. Step 2: randomly create an  $N$ -dimensional particle  $K$  as the initial population (the actual number of eye slices is used as a constant throughout the test). Step 3: calculate the fitness function value according to the speed and bandwidth resources of the vLink, and calculate the particle separation current as the limit. If the constraints are met, the maximum value of the conditional function is the current optimal decision, namely,  $H$ . The decision vector represents the current method of allocating resources to network segments that maximizes resource utilization while isolating the network. Step 4: update the properties of the particle according to the particle's velocity and position information, and then recalculate the value of the fitness function. Step 5: decrease the number of repetitions by one until the particle passes  $N$  times and recovers the optimal solution. If the network entity has completed the data transmission task, enter the next round of data transmission; otherwise return to Step 3.

3.2. Distributed Edge Computing Network Slicing. 5G radio access network edge computing and core network edge



computing are an important step in network slicing. According to the collaborative terminal call control feature of the police system, a distributed service cluster (MECS) should be used to provide simultaneous recording, and viewing and retrieval of audio, video, and video data streams. The integration of MECS is the key to realize group service. Based on the characteristics of group communication, the traditional centralized domain terminal is changed to a distributed MECS server group to realize group call fusion, signal management, and data synchronous transmission. Integrated control includes integrated technology and synchronous power distribution control technology. Integration technologies can use the best tools to perform tasks such as control, balancing, configuration, mode selection, and queuing. Parallel control ensures the cohesion of MECS states, i.e., a multi-agent network, and creates a distributed and consistent MECS model to manage operations. In a network of node size  $N$ , each node is represented as an  $n$ -dimensional first-order dynamic system, and nodes use an interactive state information mechanism to declare the dynamic behavior of the  $i$ -th node.

$$\frac{dx_i}{dt} = c \sum_{j=1}^n a_{ij} I(x_j(t) - x_i(t)) + u_i(t),$$

$$u_i(t) = -cd_i(t) I(x_j(t) - s(t)),$$

$$s(t) = s_{mT}, mT \leq t < (m+1)T.$$

As reported in the literature, the network system achieves constrained coherence by feeding back to the input  $u_i(t)$ . When the system reaches coherent equilibrium, the system jointly reaches state  $s(t)$ , interconnecting all network nodes and controlling them simultaneously. Network segments of different types and users should be isolated as much as possible to ensure security. This form is disruptive and creates a security risk when virtual hosts are mapped to physical servers and multiple virtual hosts are mapped to the same physical server. Therefore, the insulation protection level for a specific part is the weighted sum of the operating insulation level and the insulation protection level, defined as

$$Eva = \alpha Per + \beta Sec. \quad (11)$$

Networks should be segmented and divided into different types of users to ensure as complete security as possible. When a virtual host is mapped to a physical server, if multiple virtual hosts are configured on the same physical server, the shards will be split.

Determining the performance isolation level, the ratio of the virtual resources is required by the network slice to the remaining resources of the physical server; that is, the more virtual resources required, the less resources remaining in the physical server, and the worse the performance level:

$$Per = \gamma \frac{B_i}{B_i^v} + \delta \frac{D_i}{D_i^v}. \quad (12)$$

For an INS, the more physical resources the INS shares with it, the greater the potential for security threats. Therefore, the security isolation level is defined as the ratio of link resources of virtual network fragment nodes to actual dedicated physical nodes and links; the higher the coefficient, the more resources the slice covers for physical nodes and channels, and the higher the security risk:

$$Sec = \varphi \frac{N_i}{N_i^v} + \varepsilon \frac{L_i}{L_i^v}. \quad (13)$$

Substitute (12) and (13) into (11) to obtain the calculation formula of the security isolation evaluation value of network slice:

$$Eva = \alpha \left( \gamma \frac{B_i}{B_i^v} + \delta \frac{D_i}{D_i^v} \right) + \beta \left( \varphi \frac{N_i}{N_i^v} + \varepsilon \frac{L_i}{L_i^v} \right). \quad (14)$$

### 3.3. M2M Scheduling Algorithm Based on Q-Learning.

- (1) Preprocessing and query. The preprocessing is run only once to create the M2M data structure for path search. If the map changes slightly later, the M2M data structure can be updated.
- (2) After preprocessing, once the search task is determined, the query program can be executed in a very short time.
- (3) Summarize and synthesize the returned opinions, and then send them to relevant experts after quantitative statistical analysis. Each member receives a copy of the questionnaire results.
- (4) After seeing the results, ask members to propose their proposals again. The results of the first round often inspire new proposals or change some people's original views.

The proposed distributed Q-learning uplink timing algorithm uses each capable group leader as an agent, interacts with the agent as a mobile network environment, and tries to maximize the overall performance. Each agent can independently select the agent whose  $RB$  resource sends information and captain. The function performed at each timing time  $t$  can be expressed as follows:

$$a_t = \{0(\text{no-access}), RB_1, RB_2 \cdots RB_m\}. \quad (15)$$

The learning algorithm only considers one state in the learning process, namely, time. The team leader actively learns based on one state at a time, and the learning process ends when the optimal scheduling policy is reached. Also,

the state of the channel does not change. A number of learning processes can be used to derive optimal scheduling policies for different team leaders' access conditions. The additional cost function is defined as follows:

$$B_{RB_L} \log_2(1 + SINR_{RB_L}). \quad (16)$$

At design time  $t$ , function  $a$  is selected according to the activity selection strategy to obtain the reward ability of data  $r$ , and the  $Q$  value corresponding to function  $a$  in the  $Q$  value table is updated according to the reward value.

$$Q(a_t) = (1 - a) Q(a_t)^t + r_t. \quad (17)$$

Among them,  $AB$  represents the  $Q$  value of the group leader agent before and after performing action  $C$ , respectively. Throughout the learning process, the possibility of conflicting actions is reduced, the learning speed is increased, and the convergence speed is accelerated. Redefine the reward function using a conflict resolution mechanism:

$$r_t = \sum_{i=1}^m B_{RB_L} \log_2(1 + SINR_{RB_L}). \quad (18)$$

The global  $Q$  value at time  $T$  is a linear combination of each group length, as shown in the following formula:

$$Q_t(a_t) = \sum_{i=1}^n Q_i(a_t), \quad (19)$$

where  $a$  is a set of action vectors for all performed within training epoch  $t$  and the global value of  $Q$  represents the action selected by each team leader in a cell. The sum of the corresponding values  $Q$  is one of the Performance Indicators for the given algorithm. The set of strategic actions taken by all team leaders according to the total value of  $Q$  for each training period, and the set of actions for each team leader corresponds to the maximum global value of  $Q$ . The optimal resource allocation strategy  $RB$  is selected as follows:

$$V^\pi = \max_{a \in A} (Q(a_t)), \quad (20)$$

$a$  is the set of all executed action vectors in the learning cycle  $t$ , and  $Q$  is the action selected by each team leader in the cell, which is one of the performance indicators of this algorithm, reflecting the set of strategic actions taken by all team leaders in the cell.

#### 4. Exploration of Scenario Logistics Ecosystem Application of beyond 5G and IoT Architecture

**4.1. Beyond 5G Smart Logistics Ecosystem.** With the continuous improvement of the digitization, informatization, and intelligence of logistics enterprises, the China Federation of Logistics and Purchasing predicts that by 2025, the scale of my country's intelligent logistics industry will exceed one trillion yuan. For most intelligent logistics operations, with the help of retail terminal platforms, Internet, and other advantageous enterprises, in addition to intelligently upgrading traditional logistics enterprises, they also make

use of intelligent industries. For example, JD.com and China Federation of Logistics and Purchasing jointly released the "2025 China Smart Logistics Blue Book," creating a new model of smart logistics by establishing logistics subgroups. In particular, several unmanned warehouses, drones, and unmanned vehicles will be deployed, and a new model of "unmanned commercialization" will be realized through the combination of artificial intelligence and robotics. In terms of transportation and distribution, JD.com has cooperated with the Beidou-6 satellite navigation system, and more than 6,000 self-driving cars use the Beidou navigation system smart bracelet to help salespeople. At the same time, JD.com signed a cooperation agreement with Xi'an Aerospace to build the country's largest comprehensive intelligent logistics base and develop a comprehensive system of all links of the intelligent supply chain. The development scale of 5G smart logistics is shown in Figure 3 and Table 1.

According to the experimental data in Figure 3, we can conclude that the scale of the 5G smart logistics market continues to expand, and the technical capabilities of participating institutions continue to increase. According to the statistics of China Association of Logistics and Purchasing, by the end of 2020, the total amount of social logistics in my country will reach 300.1 trillion yuan, an increase of 3.5% over last year. The revenue of logistics enterprises reached 10.5 trillion yuan, a year-on-year increase of 2.2 percentage points. Among them, the 5G smart logistics industry is in strong demand, with a market size of 590 billion yuan. We can also see that the scale of the 5G smart logistics industry is showing a steady growth trend.

According to the experimental data in Figure 4 and Table 2, we can get that in the 5G smart logistics system, the accuracy can reach 89.22%, the rate can reach 81.94%, and the error rate is only 34.56%; in the traditional logistics system, the accuracy can reach 68.33%, the rate can reach 65.67%, and the error rate reached 53.41%. We can see that the 5G smart logistics system is faster than the traditional logistics system in terms of accuracy and speed, and the error rate is much more stable.

**4.2. Scenario Logistics Ecosystem of IoT Architecture.** The logistics development environment in the IoT architecture scenario includes natural environment, economic environment, political environment, etc. The economic environment plays an important role in stimulating logistics demand and facilitating its growth. Logistics Infrastructure and Logistics Delivery: This section describes the efficient development of the IoT in combination with the economic and political environment, and more intuitively reflects the logistics environment conditions within the IoT architecture.

From the experimental data in Figure 5, we can find that with the increase of time, the national IoT logistics GDP has been in a steady upward trend. In 2016, the logistics GDP reached 800 billion yuan, and in 2020, the logistics GDP reached a maximum of 1,600 billion yuan; and we found that the growth rate of GDP under the IoT architecture has been accelerating, reaching 23.06% in 2018. After 2018, the growth



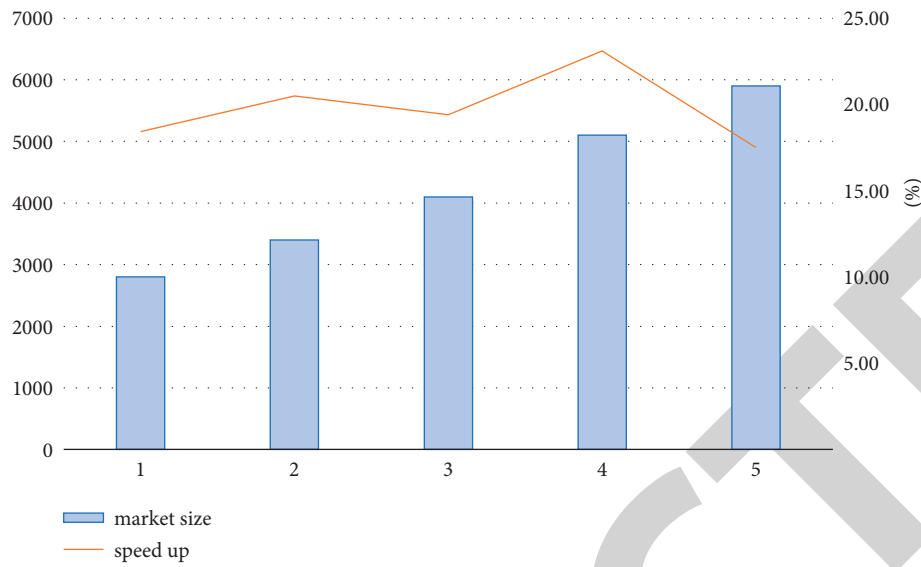


FIGURE 3: Market scale of my country's 5G smart logistics industry from 2016 to 2020.

TABLE 1: Market scale of my country's 5G Smart Logistics Industry from 2016 to 2020.

Years	Market size	Speed up (%)
2016	2800	18.43
2017	3400	20.49
2018	4100	19.41
2019	5100	23.10
2020	5900	17.50

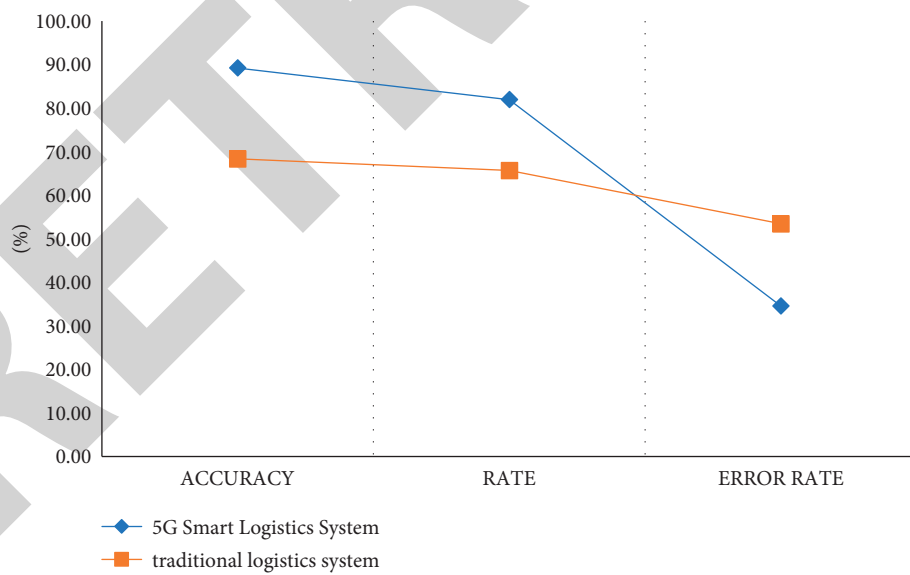


FIGURE 4: Comparison of different logistics models.

TABLE 2: Comparison of different logistics models.

Different logistics models	Accuracy (%)	Rate (%)	Error rate (%)
5G smart logistics system	89.22	81.94	34.56
Traditional logistics system	68.33	65.67	53.41

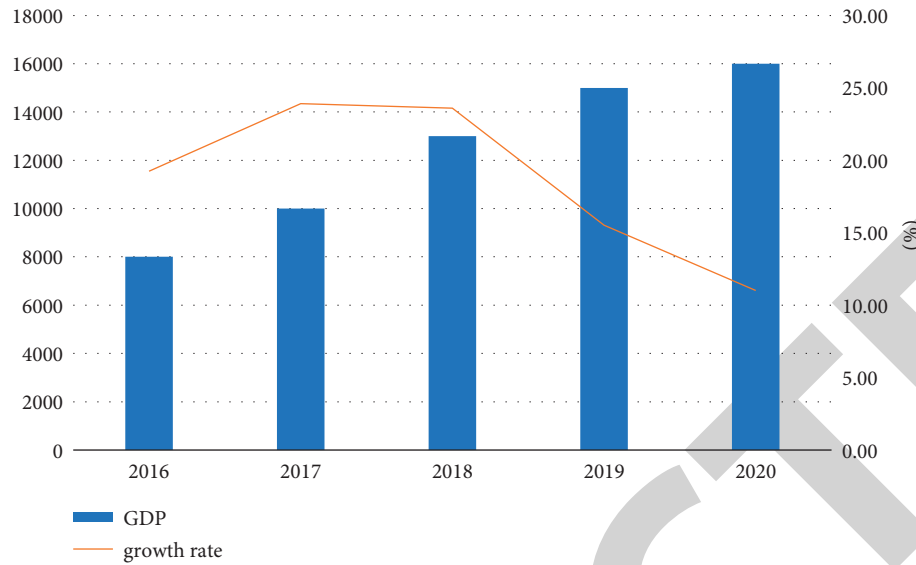


FIGURE 5: National IoT logistics GDP and growth rate from 2016 to 2020.

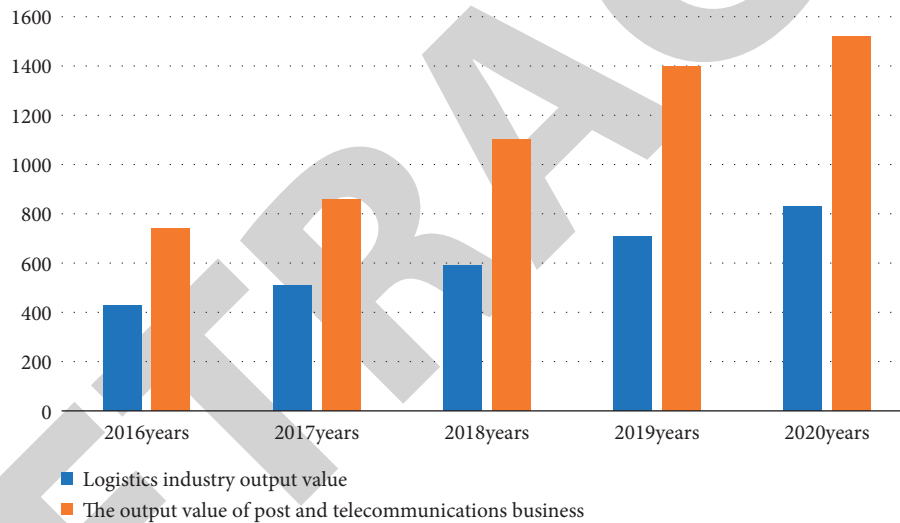


FIGURE 6: Logistics output value under the IoT architecture from 2016 to 2020.

rate began to decline. In 2020, the growth rate was only 11.01%.

From the experimental data in Figure 6, it can be seen that the development of logistics under the IoT architecture mainly includes the production cost of the logistics industry, and the volume of the post and telecommunications industry is the volume of the logistics company. The business volume of the post and telecommunications company can be used to replace the business volume and quantity of the logistics company. With the growth of time, the output value of the logistics industry and the output value of post and telecommunications business are showing a steady upward trend. By 2020, the overall value of the logistics industry of the Internet of Things will reach 235 billion yuan, and the output value of the logistics industry will be 83 billion yuan. The output value is 152 billion yuan.

**4.3. Application Exploration of Logistics Ecosystem.** In traditional warehouse buildings, it is often necessary to manually scan goods and store data, resulting in low work efficiency. At the same time, storage sites are sometimes dominated by chaos and lack of process monitoring. As the industry enters the ecosystem, it will be possible to develop an intelligent inventory management system that improves the basic efficiency of goods, expands inventory capacity, reduces labor intensity and labor costs, and conducts real-time monitoring and monitoring of the in and out of goods time, improving delivery security and complete pickup. The system completes product warehousing, inventory allocation, selection, and delivery, as well as data query, backup, statistics, reporting, report management, and other system-wide tasks. The cost of logistics industry is shown in Figure 7.

According to the experimental data in Figure 7, we can conclude that the most important cost of the logistics

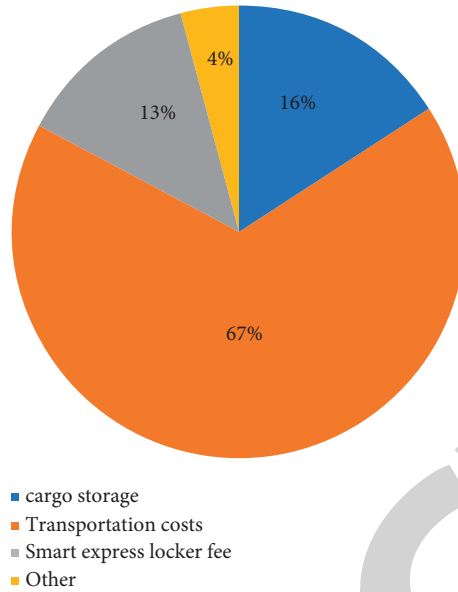


FIGURE 7: IoT logistics industry cost diagram.

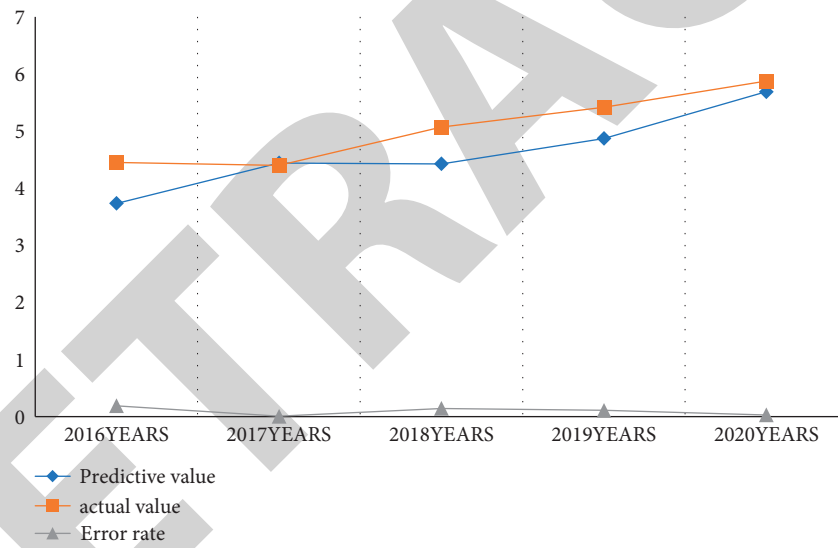


FIGURE 8: Comparison between the predicted value of logistics demand and the actual value.

TABLE 3: Comparison between the predicted value of logistics demand and the actual value.

Years	Predictive value	Actual value	Error rate
2016	3.7345	4.4518	0.1921
2017	4.4407	4.3998	0.0092
2018	4.4257	5.0703	0.1456
2019	4.8707	5.4139	0.1115
2020	5.6877	5.8757	0.0330

industry is that the transportation cost accounts for 67% of the entire logistics cost, followed by the cargo storage accounting for 16% of the cost, and the cost of smart express cabinets 13%; from this, we can see that the highest cost of the logistics system under the Internet of Things is the transportation cost.

According to the experimental data in Figure 8 and Table 3, we can see that the value of logistics demand shows a steady upward trend with the increase of time, the predicted value is also increasing, and the accuracy of the prediction is gradually improved. After 2018, the accuracy is relatively high. The five-year average error rate from 2016 to 2020 is

## Retraction

# Retracted: Visual Feature Evaluation of Shenyang Greenway Landscape Based on Deep Learning

### Security and Communication Networks

Received 8 August 2023; Accepted 8 August 2023; Published 9 August 2023

Copyright © 2023 Security and Communication Networks. This is an open access article distributed under the Creative Commons Attribution License, which permits unrestricted use, distribution, and reproduction in any medium, provided the original work is properly cited.

This article has been retracted by Hindawi following an investigation undertaken by the publisher [1]. This investigation has uncovered evidence of one or more of the following indicators of systematic manipulation of the publication process:

- (1) Discrepancies in scope
- (2) Discrepancies in the description of the research reported
- (3) Discrepancies between the availability of data and the research described
- (4) Inappropriate citations
- (5) Incoherent, meaningless and/or irrelevant content included in the article
- (6) Peer-review manipulation

The presence of these indicators undermines our confidence in the integrity of the article's content and we cannot, therefore, vouch for its reliability. Please note that this notice is intended solely to alert readers that the content of this article is unreliable. We have not investigated whether authors were aware of or involved in the systematic manipulation of the publication process.

Wiley and Hindawi regrets that the usual quality checks did not identify these issues before publication and have since put additional measures in place to safeguard research integrity.

We wish to credit our own Research Integrity and Research Publishing teams and anonymous and named external researchers and research integrity experts for contributing to this investigation.

The corresponding author, as the representative of all authors, has been given the opportunity to register their agreement or disagreement to this retraction. We have kept a record of any response received.

### References

- [1] T. Pan and M. Jiang, "Visual Feature Evaluation of Shenyang Greenway Landscape Based on Deep Learning," *Security and Communication Networks*, vol. 2022, Article ID 8730399, 11 pages, 2022.

## Research Article

# Visual Feature Evaluation of Shenyang Greenway Landscape Based on Deep Learning

Tianyang Pan  and Min Jiang 

*Architectural Art Design Institute, LuXun Academy of Fine Arts, Shenyang 110003, China*

Correspondence should be addressed to Min Jiang; [jiangmin@lumei.edu.cn](mailto:jiangmin@lumei.edu.cn)

Received 25 May 2022; Accepted 11 July 2022; Published 19 August 2022

Academic Editor: Hangjun Che

Copyright © 2022 Tianyang Pan and Min Jiang. This is an open access article distributed under the Creative Commons Attribution License, which permits unrestricted use, distribution, and reproduction in any medium, provided the original work is properly cited.

At present, the research on the visual characteristics of greenway landscape is mostly focused on the evaluation of beauty degree, landscape preference, and recreation preference and mainly on the overall macroscopic evaluation of a single greenway or typical spatial research in some areas, while less attention is paid to the overall characteristics of urban greenway landscape and the differences in visual characteristics of different types of greenway landscape. The emergence of new data and new technologies such as street view, Baidu map, and deep learning provides the possibility to study the visual characteristics of greenway landscapes in large scale and full sample. The study of greenway landscape based on large deep learning can effectively refine the overall pattern of visual characteristics of greenway landscape and reveal the differences of visual characteristics of different types of greenways and their key factors, so as to provide support for the planning and design of greenway landscape and landscape appearance enhancement.

## 1. Introduction

In recent years, many problems such as fragmentation of natural ecological pattern, homogeneity of urban landscape, and lack of regional characteristics have gradually emerged. In order to effectively cope with the above problems, Shenyang City prepared and adopted the “Shenyang City Greenway System Construction Plan” as early as 2012, laying out greenways in the urban green space system and positioning them as “an important part of the urban ecosystem, scenic tourism system, and comprehensive transportation system, with leisure and fitness and tourism functions as the main functions, taking into account the transportation and commuting functions. Subsequently, they also issued a document proposing to steadily promote the construction of urban greenways and promote the formation of a green development and lifestyle. Since 2017, Nanjing, Wuhan, Shanghai, Guangdong and many other places have actively promoted the construction of greenways and made positive progress. To further promote the formation of green development and lifestyle, they will clearly continue to improve

the construction standards of greenway projects to further enhance the leading green and healthy living style. The construction of suitable regional characteristics of the greenway landscape has become an important element of the current urban green development.

With the rapid advancement of greenway construction in Shenyang, the visual resources of greenways have been fully utilized while there are also excessive excavation and destruction. Due to the excessive pursuit of visual attraction in the construction of a single greenway, the inconsistency between the new greenway and the existing greenway and the overall landscape of the city is increasingly prominent. At the same time, some of the earlier completed greenways due to the imbalance of management and care and other issues lead to the decline of visual landscape quality, and gradually with the overall appearance of the city, while the repair of the destroyed greenway landscape is also arbitrary, the new repair landscape visual features difficult to integrate into the overall landscape of the greenway landscape. The reason for this is that there is a lack of understanding of the overall features and visual characteristics of the greenway

landscape and the commonalities and differences, and a lack of theoretical guidance in the practice of visual resources mining and utilization, visual attraction elements restoration and enhancement, which leads to the construction of greenway visual landscape construction arbitrarily. In view of the above, there is an urgent need to clarify the commonality and differences of visual characteristics of the current urban greenway landscape, and to clarify the color of the greenway landscape, so as to guide the unity of the landscape construction of the greenway and its coordination with the overall landscape of the city.

Landscape vision is a composite concept, as the conception and formal expression of landscape design, has an important impact on the audience's associative experience and consciousness perception. The current domestic and international research on landscape vision is mostly about the perceptual cognition of physical landscape objects, reflecting people's consensus landscape consciousness. At the same time, the study in [1] believes that through the generalization and refinement of the typical characteristics of specific objects, a single landscape design element that can reflect the local characteristics, reflect the spirit of the region and be understood by the local public can be regarded as a "landscape visual" unit, and the imagery structure is inseparable from the traditional Chinese aesthetic. It is important to understand and construct the structure of imagery in landscape design.

In order to comprehensively evaluate the visual characteristics of greenway landscape, this paper evaluates greenways from multiple levels of greenway landscape characteristics, from point to line to surface, in multiple dimensions. The evaluation analysis is carried out from two aspects of the composition of the visual elements of greenway landscape and the diversity of the composition of the elements to reveal the overall composition characteristics of the visual elements of greenway landscape in Shenyang, the differences in the characteristics of the visual elements of different levels and types of greenway landscape, and the specific composition characteristics of different visual elements in each greenway. The spatial distribution sequence characteristics in different types of greenway landscapes are evaluated from three aspects: green view rate, sky and water bodies, and the number and magnitude of changes of the ups and downs of each visual element in the greenways are compared and analyzed so as to reveal the spatial sequence changes of the visual elements of greenway landscapes. The overall spatial accessibility characteristics of all greenways are studied and correlated with three kinds of positive services, namely, green view rate, landscape vignettes and post buildings, and two kinds of negative interferences, namely, peripheral buildings and peripheral utility pole billboards, to reveal the relationship between the quality of visual services of different types of greenway landscapes and the accessibility of residents, so as to provide reference for the improvement of visual services of greenway landscapes. Based on the above research results, suggestions and strategies for the optimization of greenway landscape enhancement are proposed around the visual elements of greenway landscape and their spatial distribution sequence characteristics and the accessibility of residents' space.

## 2. Related Work

In recent years, foreign visual landscape research has conducted a number of empirical studies on visual landscape quality, preferences, and impacts using new data and technologies. The visual quality of 20 scenic-eligible roadway landscape features was assessed using color slide photography, combined with design procedures in [2]. The study in [3] investigated the influence of public art on the visual character and affective evaluation of landscapes by having undergraduate and graduate students view landscapes with or without public art in turn and rating the visual character and affective evaluation of each landscape, with results showing that the affective quality of public art had a greater impact on the landscape. The study in [4] assessed the visual quality of landscapes in historic areas using a photo questionnaire method based on a range of indicators, such as landscape visual legibility, consistency, complexity, temporality, continuity, historicity, visual scale, and spatial perception. The study in [5] evaluated the visual quality of landscapes by analyzing the visual preferences of residents through social media Instagram photos, a platform dedicated to uploading and discovering visual content (e.g., photos and videos), which can be a tool for analyzing community preferences and a new approach in the field of landscape. The study in [6] explored the relationship between the visual characteristics of the landscape and the large-scale landscape in Taiping District, Peninsular Malaysia as a study. The landscape characteristics of Taiping, Perak and surrounding areas are evaluated to understand the changes in the landscape.

Chinese scholars started their research on greenway landscape visualization late, and now mainly focus on the study of greenway landscape visual perception and preference. The study in [7] studied the influencing factors of greenway cycling perception from three aspects: social characteristics, behavioral characteristics and landscape element characteristics, and extracted the cycling perception characteristics of different types of greenways by semantic evaluation method and picture analysis method, and found that different types of greenways have different landscape visual structures. The study in [8] reveals the differences of visual characteristics of different cities and their landscape types, and provides a lot of rich research support for urban landscape style camping. The study in [9] proposed that the Guidelines for Greenway Planning and Design were introduced at the national level, but confined to the differences in local characteristics, cities have introduced more detailed and more geographically distinctive standards for greenway landscape construction. For example, the study in [10] evaluated the current situation of greenways in Zengcheng, Guangdong, and divided the composition of greenways into six parts: slow walking system, greening system, service facility system, traffic interchange system, signage system, and lighting system. The study in [11] classified the greenway elements in Shenyang into three categories, namely, mountain elements, water elements, and urban park elements. The study in [12] compared the sustainability performance and visual preference of landscape elements in the



landscape and proposed the design of landscapes with highly sustainable elements and visual preference. The study in [13] took Zijinshan National Forest Park as the research object, and carried out landscape visual evaluation of 15 sites according to subjective and objective evaluation weighting, and analyzed the best and worst landscape visual conditions by combining subjective and objective methods for equal proportional weighting analysis, and this evaluation system is comprehensive and operable in the protection and development of landscape visual resources.

In recent years, with the rapid development of new data and new technologies, the study of visual characteristics of landscape has made new breakthroughs in many aspects, such as research scale, research object, and research methods. The study in [14] conducted a relevant experiment in California, USA, by means of real-time photography, and obtained streetscape photographs of a street intersection in four directions: east, west, north, south, and west, quantitatively calculated the proportion of vegetation in the photographs and used it as the green view rate value of the point for the first time. Subsequently, the study in [15] improved the experiment of [16] by using Google panoramic photos to extend the view of the observer, and their acquisition included more angles of panoramic photos, and the computer automatically extracted the photo bands to obtain the green field of panoramic photos. With the introduction of Google Street View maps, it was found that the richness of information contained in Google panorama maps could bring new possibilities for urban studies. The study in [17–20] performed semantic segmentation and street view element target recognition on Google's street view panoramic photos, identified trees, buildings, sky, and road surface of all photos, and used metrics such as field of view and shape to generalize and quantify the visual quality of the landscape.

In China, the study in [21] extracted the spatial distribution characteristics of street green view rate based on Baidu Street View data and explored the objective perception level of street green space, meanwhile, the actual perceived degree of street green space was studied by overlaying street green view rate and real-time population heat, so as to complete the evaluation of street green space maintenance and enjoyment. Based on street images, the study in [22] presented the application of newly developed deep convolutional neural networks in landscape analysis. Using the trained deep convolutional neural network model, different urban features can be accurately identified from the street images. The study in [23] used Baidu Street View photos and Microsoft machine learning algorithm to measure the street greenway landscape in the central city of Zhoushan Islands as the research object, and summarized the landscape type composition and landscape spatial distribution in the area. [24] introduced the quantitative evaluation method of street space evaluation index, and measured the street evaluation index of Beijing and Shanghai through objective element composition analysis and users' subjective evaluation by using the image data of street microscale. The study in [25] crawled the large-scale streetscape data of Shanghai and extracted the greening visibility based on machine learning

algorithm, and carried out the overlay analysis with the street accessibility based on spatial network analysis. By comparing with the greening rate based on satellite remote sensing images, we found that the greening rate obtained from the calculation based on remote sensing images could not accurately show the greening exposure in citizens' daily life.

Numerous studies have shown that processing streetscape mapping datasets with the help of deep learning is a very effective and objective data work to help planners and urban researchers understand streetscapes from a human perspective. Most of the traditional landscape evaluation studies rely on small sample size surveys and limited data sources, which are not only laborious, expensive, and time-consuming to acquire, but also these data sources can hardly meet the research needs of measuring human perception of landscape on a large scale. With the rapid development of new technologies and data represented by computer technology and multisource urban data, the popularity of street view data represented by Baidu Street View and Google Street View has provided new possibilities for high-precision large-sample street view visual feature research.

### 3. Methods

The Greenway Planning and Design Guidelines (Jiancheng letter [2016] No. 211) classifies the greenway composition into five categories: greenway trail system, greenway greening, service facilities, municipal facilities, and signage facilities. Among them, the greenway trail system is mainly for walking paths, bicycle paths, comprehensive paths and traffic connection points; service facilities are mainly for buildings, such as stations, visitor service centers, and recreational facilities, such as activity sites, resting places, and environmental health facilities such as garbage bins; municipal facilities are mainly for pipeline networks, ditches, etc.; signage facilities are for signs, interpretation, warnings, and other signs; road greening is mainly for trees and shrubs and herbaceous plants. According to the visual classification of visual landscape, the above greenway composition can be classified as visual landscape of carriageway, pedestrian path, station building, landscape sketches, shrubs, and herbaceous plants. At the same time, a certain amount of water and sky can be seen in the Shenyang greenway recreation view. Therefore, in this study, combining with the actual situation of Wuhan greenway, the landscape elements of the greenway are divided into eight categories: sky, trees and shrubs, carriageway, pedestrian path, herbaceous plants, water body, landscape sketches, and station buildings. In addition, there are other landscape visual elements in the actual streetscape pictures, mainly stairs and billboards in the greenway surroundings, etc. This study identifies these nongreenway landscape elements also as streetscape recognition objects (see Table 1) and analyzes them as greenway landscape visual interference elements.

The general technical route of this paper is shown in Figure 1.

The visual feature extraction network of greenway landscape established in this paper includes a shared

TABLE 1: Classification of greenway landscape elements.

System name	Elements	Greenway Baidu street view element extraction	Greenway landscape visual elements	Visual interference elements
Greenway tour warp system	Pedestrian paths	Carriageway, walkway	Carriageway	Surrounding buildings
	Bicycle paths		Walkway	
	Comprehensive walking and cycling paths			
Greenway greening	Traffic connection point	Herbaceous plants of trees and shrubs	Herbaceous plants of trees and shrubs	Surrounding poles
	Greenway greening			
	Management service facilities		Sky	
Service facilities	Supporting commercial facilities	Stagecoach buildings, sky, water bodies, landscape vignettes, cars, surrounding buildings, surrounding poles, surrounding billboards	Water bodies	Surrounding billboards
	Recreation and fitness facilities			
	Science education facilities			
Municipal facilities	Safety and security facilities	Stagecoach buildings, sky, water bodies, landscape vignettes, cars, surrounding buildings, surrounding poles, surrounding billboards	Stagecoach buildings	Surrounding billboards
	Environmental health facilities			
	Environmental lighting facilities			
Signage facilities	Electricity and telecommunications facilities	Stagecoach buildings, sky, water bodies, landscape vignettes, cars, surrounding buildings, surrounding poles, surrounding billboards	Landscape vignettes	Surrounding billboards
	Water supply and drainage facilities			
	Other			
Signage facilities	Instruction facilities	Stagecoach buildings, sky, water bodies, landscape vignettes, cars, surrounding buildings, surrounding poles, surrounding billboards		Surrounding billboards
	Warning signs			

VGG-like convolutional network coding layer and two decoding layers, which are the feature point detector decoding layer and the descriptor decoding layer, respectively. Referring to Superpoint's network model structure, the parts of the coding layer and descriptor are retained, the activation function is improved, and the detector decoding layer, training process, and loss function are different. The overall network framework is shown in Figure 2.

A VGG-like convolutional backbone network is used as an encoder, which serves to dimensionalize the image and facilitate feature extraction. The encoding layer consists of a convolutional network layer, a pooling layer and a nonlinear activation function. The coding layer uses three maximal pooling layers to change the original image size  $H \times W$  to  $H_c = H/8, W_c = W/8$ . The activation function is a leaky ReLU activation function.

The feature point detector decoder layer performs a two-layer convolution operation on the shared feature map to turn the feature map into  $H/8 \times W/8 \times 64$ . The feature map is operated by Softmax so that the feature map takes values between 0 and 1, and feature points taking values close to 1 indicate that the location is a real feature point. Then, after dimensional transformation, the feature point map with the same size as the original image is output and used to calculate the loss function of the feature point detection layer.

The descriptor decoding layer up-samples the feature map of descriptors by 3 times of interpolation, and then

normalizes the feature map values to unit length using L2 parametric, and outputs a dense descriptor of  $H/8 \times W/8 \times 256$ , which is used to compute the loss of descriptors with the feature map output by the feature point detector.

The training of the model is performed based on the single-strain transformation of the image and the noise addition. The single-response change is the mapping relationship from one plane to another, including affine change, perspective transformation. A random single-strain change is applied to the original image  $I$  to obtain  $I_h$ , and then a loss function is calculated for both to achieve the effect of self-supervised learning.

The loss function is expressed as

$$L(P, PhD, Dh, H) = \lambda_1 L_d + \lambda_2 L_p, \quad (1)$$

where  $\lambda_1, \lambda_2$  is the weight parameter,  $P, Ph$  are the feature maps of the original  $I$  and the transformed  $I_h$  maps,  $D, Dh$  are the descriptors of the two maps, and  $L_d, L_p$  are the descriptors and the loss function of the detector, respectively. After transformation, random noise is added to  $I, I_h$  including Gaussian noise, random brightness variation, pretzel noise, and fuzzy treatment to enhance the model performance.

The training principle of feature points is derived from the Expectation Maximization (EM) algorithm, and the main steps are shown in Figure 3. In the training process, the target feature points are processed as follows: ① detects the point  $K$  in the original figure  $I$ , and projects the point  $K$  onto

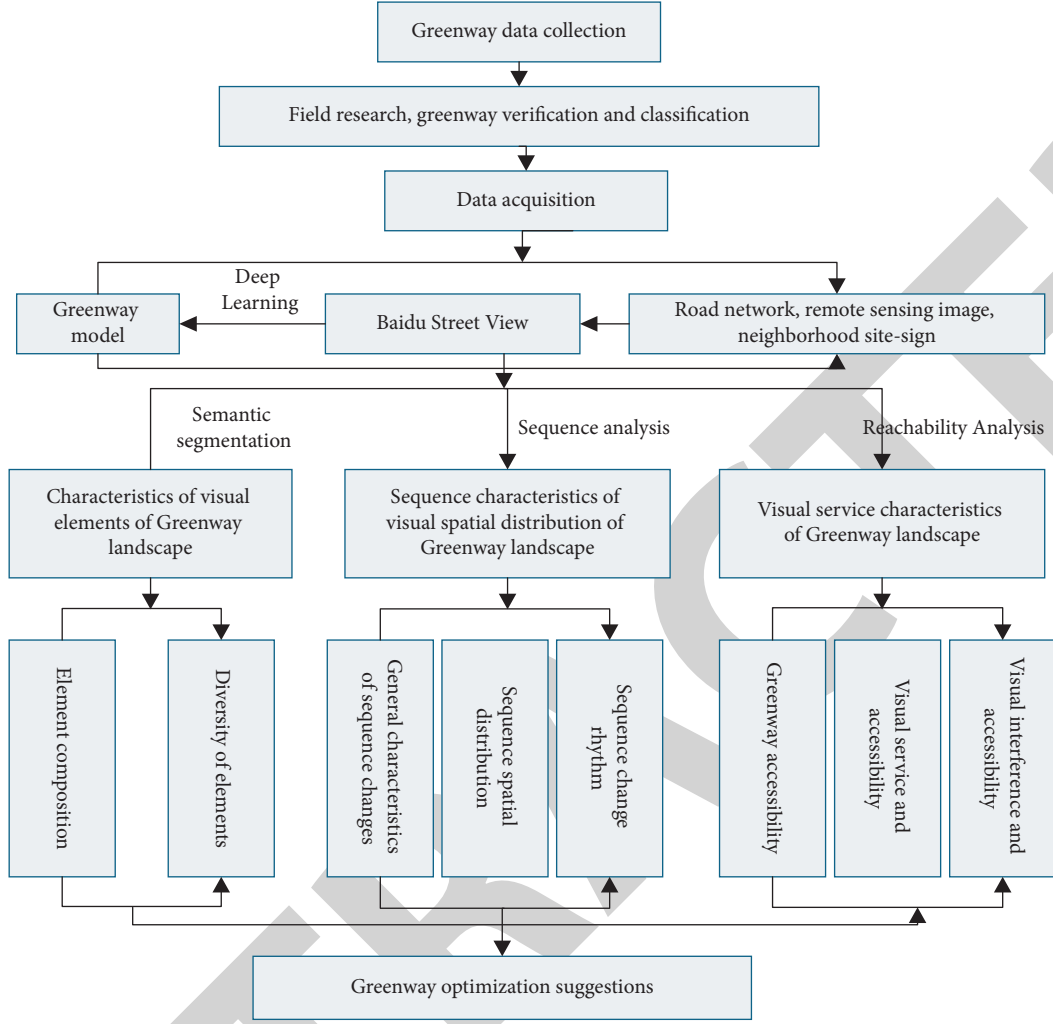


FIGURE 1: Technology roadmap.

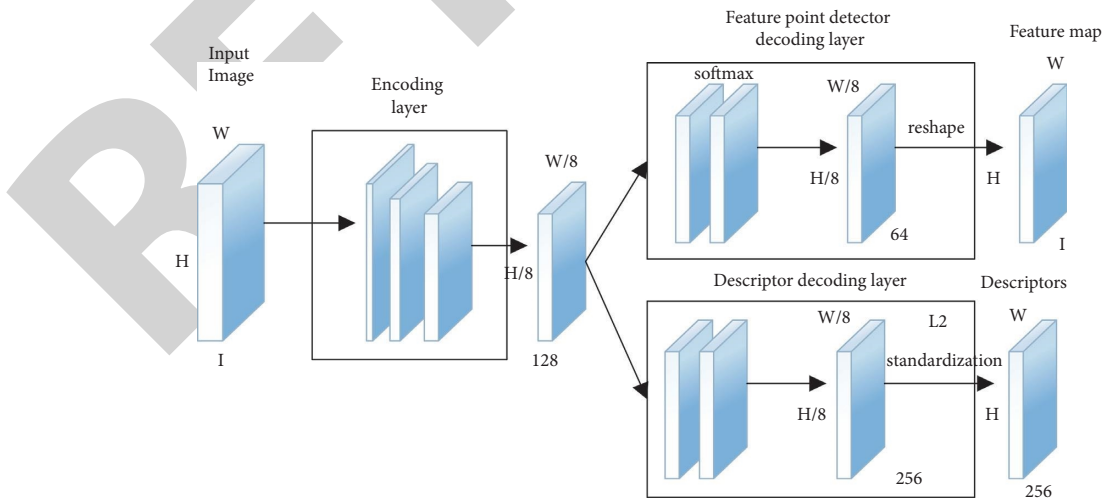


FIGURE 2: Architecture of the feature extraction network.

$I_h$  according to the imposed single-strain transform to form  $K_{proj}$ . ② Two ways are used to match the detected points  $K_h$  on the transformed points  $K_{proj}$  and  $I_h$ , which are 2D

coordinates and descriptors, respectively, both using nearest-neighbor matching to form two pairs of matched point sets. ③ Form the target point  $K'_h$  by the matched point set,

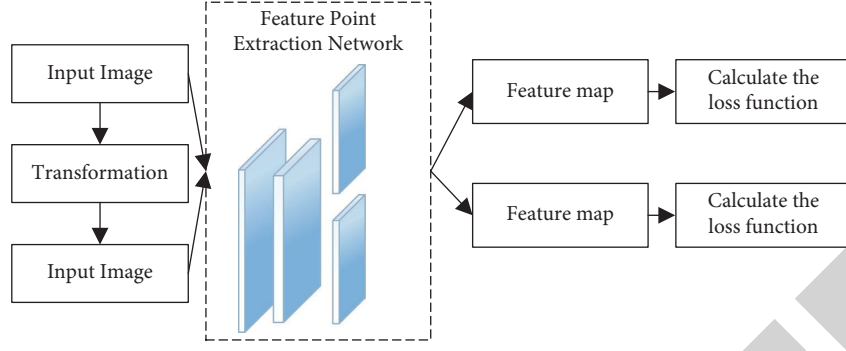


FIGURE 3: Feature training procedures.

and then project it to the original figure  $I$  to form  $K'$  according to the inverse transformation of the single-response transform, and form a pair of point sets with  $K'_h$  for calculating the loss function.

The loss function of the detector part is expressed by applying the negative log-likelihood method as

$$L_p = -\frac{1}{2} (\log P[K'] + \log P_h[K'_h]), \quad (2)$$

where  $P[K'], P_h[K'_h]$  denotes the distribution of detected feature points on  $I, I_h$ , respectively.

Given the  $I, I_h$  two images to be trained, the true feature points  $K', K'_h$  are extracted by the following steps:

- (1) The set of feature points  $K', K'_h$  is extracted from the images by two different pooling operations, denoted as

$$\begin{aligned} K &= \text{maxpool}_{32 \times 32}(P), \\ K_h &= \text{maxpool}_{16 \times 16}(p_h). \end{aligned} \quad (3)$$

The feature points are selected in two different sizes,  $32 \times 32$  and  $16 \times 16$ , so that the feature points can be distributed to cover the whole map but not too dense. The image is pooled to return an array of coordinates of feature points  $(x_i, y_i)$ .

- (2) A single-response transformation  $K_{\text{proj}} = \overline{KH}$  is performed on  $K$ . Points that are beyond the image boundary are discarded,  $D_{\text{proj}}, D_h$  for the descriptor of  $K_{\text{proj}}, K_h$ .
- (3) Matching is performed on  $I_h$  according to the descriptors and coordinate relations, respectively, denoted as

$$\begin{aligned} \text{dist}_{\text{geom}}, \text{idx}_{\text{geom}} &= \text{match}_{\text{geom}}(K_{\text{proj}}, K_h), \\ \text{idx}_{\text{desc}} &= \text{match}_{\text{desc}}(D_{\text{proj}}, D_h). \end{aligned} \quad (4)$$

The function of  $\text{match}_{\text{geom}}$  is to perform nearest-neighbor matching on  $K_{\text{proj}}, K_h$  based on Euclidean distance, returning the distance between matching points and the index of the point.  $\text{idx}_{\text{geom}}$  gives the index of  $K_{\text{proj}}$  the most matched point on the descriptor.

- (4) The coordinates of the possible true feature points on  $I_h$  are expressed as

$$K'_h = \text{mean}(K_{\text{proj}}(i), K_h[\text{idx}_{\text{geom}}(i)]). \quad (5)$$

From the above equation, it can be seen that the possible true feature points  $K'_h$  are obtained by taking the mean value of  $K_{\text{proj}}$  and the matching  $K_h$ , and then this is inverted by the single-strain transformation and projected back onto the original graph to obtain  $K'$ .  $K', K'_h$  obtained after the above steps is used to calculate the loss function equation (2).

The loss function in the descriptor part consists of two parts, denoted as

$$L_d(D, D_h, K, K_h, H) = L_{\text{desc}} + L_{\text{wrong}}. \quad (6)$$

Let  $g_i = D_{\text{proj}}(i) D_h^T(\text{idx}_{\text{geom}}[i])$ , the above equation is the dot product between the feature point descriptors matched according to the coordinate Euclidean distance. The descriptors are normalized, so the dot product is equal to the cosine similarity.  $L_{\text{desc}}$  Maximize the similarity of each pair of feature point descriptors, expressed as

$$L_{\text{desc}} = \frac{1}{N_{\text{desc}}} \sum_j (1 - g_j). \quad (7)$$

$L_{\text{wrong}}$  has the opposite effect and aims to minimize the similarity of the mis-matched feature point descriptors, denoted as

$$L_{\text{wrong}} = \frac{1}{N_{\text{wrong}}} \sum_j (1 - g_j). \quad (8)$$

## 4. Experiments

To analyze the diversity characteristics of the visual element composition of the greenway landscape, this study used the entropy index to calculate the reflection. The entropy index to measure diversity has been widely used in several scenarios, especially in-built environment studies. Its calculation formula is

$$D_i = - \sum_{i=1}^R p_i \times \ln p_i, \quad (9)$$

where  $D_i$  is the element diversity of the  $i$ th Baidu street-scene,  $R$  is the total number of landscape element types, where  $p_i$  refers to the proportion of the  $i$ th element in the greenway to the total number. The diversity value is between 0 and 1, and the larger it is, the higher the diversity of the greenway is.

In order to analyze the spatial distribution sequence characteristics of visual elements in each greenway, this study takes 500 m as a sequence analysis unit, starts from one end of a greenway (starting point or end point), calculates the average value of visual proportion of all elements in this unit, and uses this to represent the characteristic value of visual elements in this unit section of the greenway.

The formulae for the magnitude of change and frequency of change, respectively, are

$$P = \frac{f + g}{L}, \quad (10)$$

where  $P$  is the frequency of sequence change.

$$H = \frac{\sum_{i=1}^n |F_i - F_{i-1}|}{f + g}, \quad (11)$$

where  $H$  is the magnitude of the sequence variation,  $F$  is the extreme value in the sequence (the value of the crest or trough in the sequence).

To further analyze the accessibility of residents to the visual element services of the greenway landscape, this study first calculates the accessibility of each greenway landscape street spot, and then correlates the accessibility results with the percentage of visual elements to obtain the service efficiency of the visual elements of the greenway, so as to further clarify the key characteristics of the greenway landscape such as high service low accessibility and low service high accessibility. Research shows that 0–1.5 km is a suitable range for residents to use public facilities and green space, so in this paper, to study the relationship between greenway services and accessibility, the number of residential neighborhoods covered within the 1.5 km buffer zone of greenway street points is calculated as a benchmark, and the higher the number of neighborhoods, the higher the accessibility value. The correlation analysis of the visual element services and their accessibility of the greenway landscape is based on the cross-quadrant axis characterized by the Excel software with scattered distribution, where the origin of the quadrant axis is the intersection of the visual element characteristic values and the accessibility mean values.

The results of the statistical analysis of the visual elements of 29 greenway landscapes in Shenyang (Figure 4) show that the sky is the main visual element of the greenway landscape in Shenyang, with the highest percentage of 43%; road trees and shrubs have the second highest percentage, with 17%; pedestrian paths, herbaceous plants, post buildings, landscape artifacts, and water elements have lower

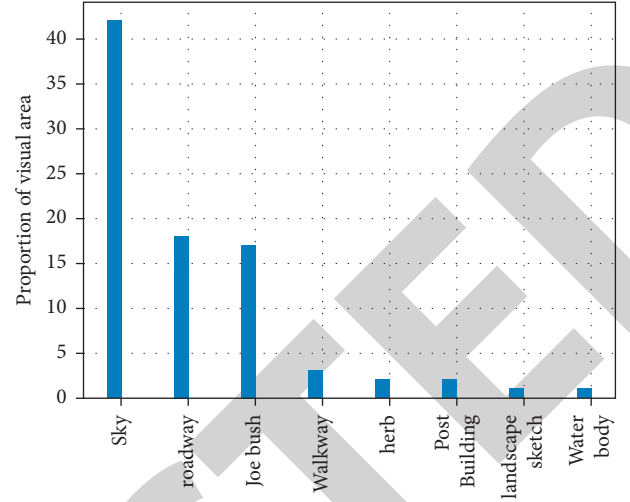


FIGURE 4: Visual proportion of greenway landscape elements.

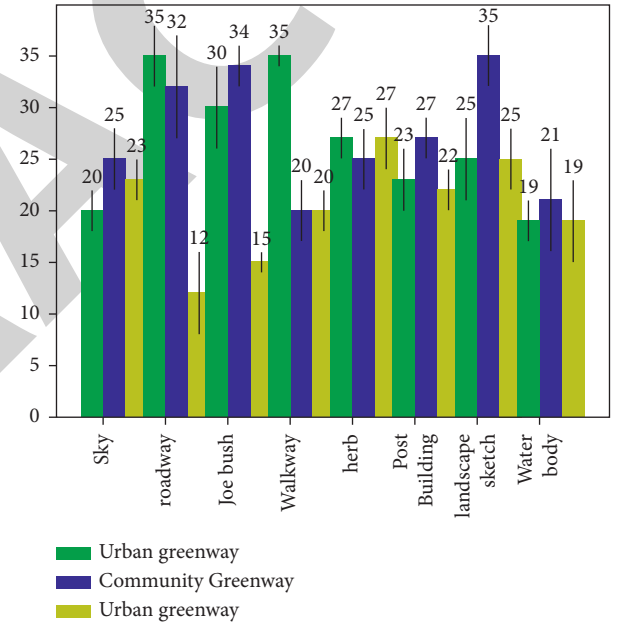


FIGURE 5: Percentage of visual area of greenway landscape elements of different levels.

percentages in turn and are relatively small, with less than 5%.

Looking at the different classes (Figure 5), the visual share of sky in urban greenways, community greenways, and urban greenways increased in order, while the share of trees and shrubs decreased in order, and the share of trees and shrubs in urban greenways was significantly higher than the other two types. The visual proportions of pedestrian paths and stagecoach buildings in urban greenways were higher than those of urban and community greenways, while the visual proportions of vehicular paths in urban greenways were lower than those of the other two types of greenways. The percentage of herbaceous plants in urban greenways is significantly higher than that of community greenways and urban greenways.

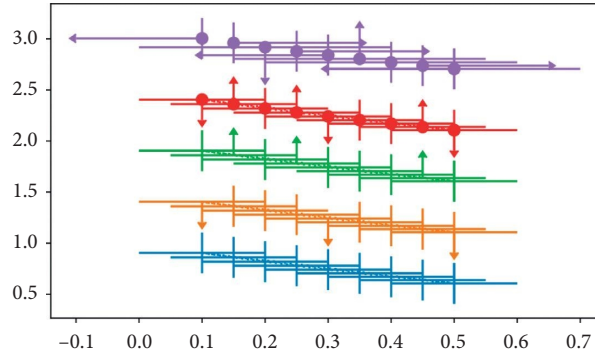


FIGURE 6: The visual proportions of different types of greenway landscape elements.

TABLE 2: Whitehorse road landscape elements index.

Observation type	Number of photos	Number of people	Number of motor vehicles	Building area ratio (%)	Green view rate (%)	Road area ratio (%)	Sky area ratio (%)
Working day-isometric mean	88	0.9	0.18	2.99	39.5	29.29	20.95
Working day-node average	117	0.15	0	5.86	50.25	9.58	24.13
Rest day-isometric mean	88	2.3	0.09	5.33	40.36	20.49	22.55
Rest day-node average	115	0.67	0.03	5.52	53.77	9.24	19.56

TABLE 3: Listening road landscape elements indicators.

Observation type	Number of photos	Number of people	Number of motor vehicles	Building area ratio (%)	Green view rate (%)	Road area ratio (%)	Sky area ratio (%)
Working day-isometric mean	45	1.97	1.35	9.12	45.23	23.49	5.79
Working day-node average	27	1.89	1.91	5.97	48.89	17.79	0
Rest day-isometric mean	41	3.98	0.98	7.62	48.81	17.99	8.36
Rest day-node average	25	4.23	1.55	4.92	57.68	12.30	10.13

TABLE 4: Forest road landscape element indicators.

Observation type	Number of photos	Number of people	Number of motor vehicles	Building area ratio (%)	Green view rate (%)	Road area ratio (%)	Sky area ratio (%)
Working day-isometric mean	182	1.31	0.32	3.34	51.89	20.67	14.89
Working day-node average	206	0.52	0.21	5.77	54.23	14.98	16.03
Rest day-isometric mean	187	2.21	0.6	3.89	51.36	1.97	15.32
Rest day-node average	212	1.13	0.25	4.85	56.03	14.32	15.69

The results of the visual proportion of landscape elements in different types of greenways (Figure 6) show that among the six types of greenways, the visual proportion of sky in mountainous greenways is the highest among all types of greenways, and the opposite is true for trees and shrubs, which are the lowest. The sky visual area share of countryside

and field-type greenways is relatively high, while the sky visual area share of urban, riverfront, and lagoon type greenways is the lowest, but the visual area share of trees and shrubs of lagoon type greenways is the highest among all types of greenways. The percentage of vehicular paths in the field-type greenways is significantly lower than that of other



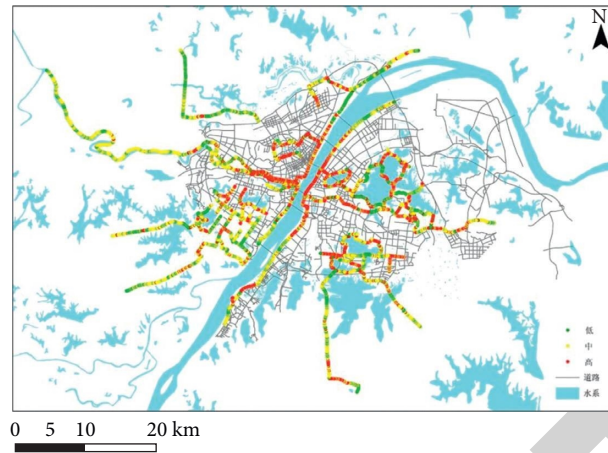


FIGURE 7: Features of visual diversity of greenway landscape.

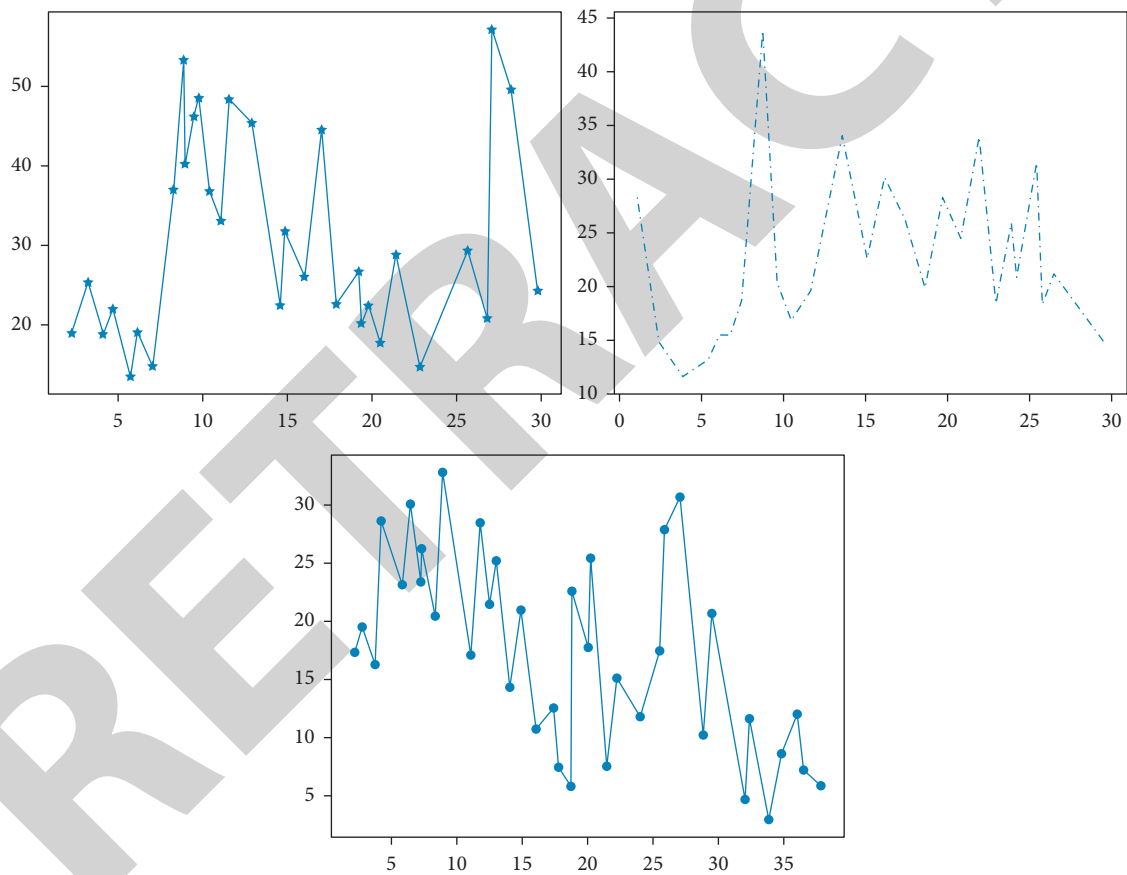


FIGURE 8: Green visibility series of riverside greenways.

greenways, while the visual percentage of pedestrian paths and herbaceous plants is significantly higher than that of other types of greenways. The proportion of stagecoach buildings is significantly higher in riverfront, lake, and urban greenways than in countryside, field, and forest greenways.

With the help of software, the number of people, the number of motor vehicles, and the elemental area rate in the recorded photos can be quantified and analyzed. The

number of people and vehicles can reflect the activity status and motor vehicle interference status of the site (Tables 2–4). The element area rate can reflect the visual structure of the landscape. Also, the comparison of node data and isometric record data can reflect the rider preference.

White Horse Road is a theme road created by artistic design, with a very good location, and has been praised since its opening, among which the Peach Blossom Island and the

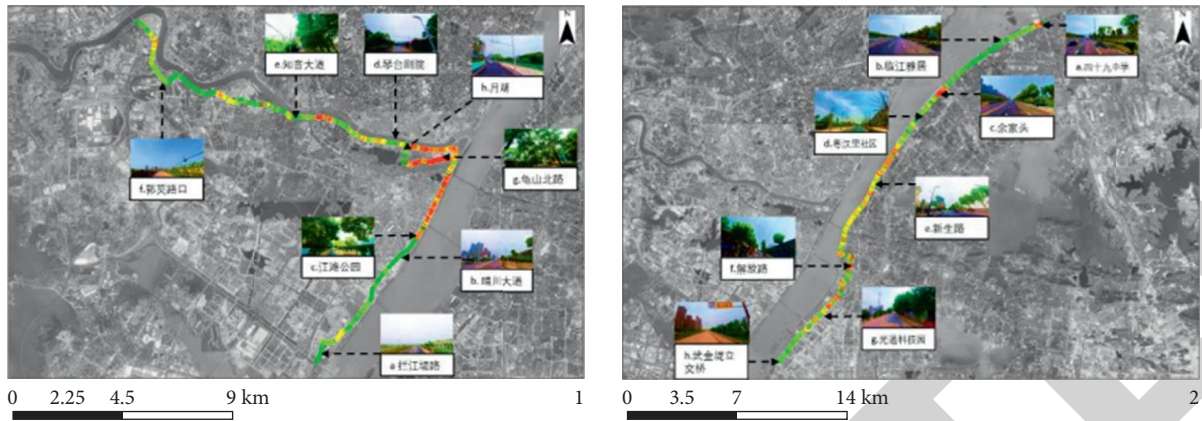


FIGURE 9: Spatial distribution of green visibility of riverside greenways.

Ten Mile Promenade have received more attention. But probably because the construction is not yet complete, the amount of activity is not very large.

Listen to the Tao Road is the earliest section of the East Lake, in line with the scale of pedestrian activity, but is also full of historical and cultural heritage. However, the frequency of motor vehicles in this theme path is high, which may cause some interference to the slow-moving activities, the element area ratio does not vary much between different time periods, nodes, and recorded photos.

Forest Road is the longest path and the most complex system in this study, but also the richest one in landscape. From the data, isometric records and node photos produce large differences in activity. Combined with its landscape element ratio, the overall green view is high, and it is a greenway dominated by natural landscape; in comparison, the proportion of buildings in the nodes is slightly higher.

In order to conduct a hierarchical analysis of the greenway landscape visual element diversity index (Figures 7–9), this study used the natural interruption method to classify the entropy index calculation results into three levels: low (0–0.12), medium (0.12–0.33), and high (0.33–1), and visualized them in GIS software for spatial analysis. The results show that the high values of diversity of visual elements composition of greenway landscape are mainly distributed in the central urban areas along the river and lake, and generally show the characteristics of high in the main urban areas and low in the suburban areas. Specifically, the diversity values of visual elements of greenway landscape along the intersection of Yangtze River and Han River are significantly higher than those of other areas.

The overall variation in the sequence of green views for the riverfront-type greenways (Figure 8) is large and the number of changes is high.

## 5. Conclusion

In summary, the continuous organization of visual elements is not only the key to enriching the linear landscape space of

the greenway and enhancing the recreational experience, but also an important means to enhance the coordination between the landscape appearance of the greenway and the surrounding environment and to strengthen the sense of organic order. Shrubs, skies, landscape vignettes, etc. are key elements affecting the visual space characteristics of the greenway, determining the visual space of the enclosed and permeable, virtual and real, light and dark characteristics. Space can also be added through the landscape vignette, so that the visual picture of the greenway landscape presents a different scene. You can also control the sequence of water surface changes to increase the diversity and interest of the greenway space.

## Data Availability

The experimental data used to support the findings of this study are available from the corresponding author upon request.

## Conflicts of Interest

The authors declare that they have no conflicts of interest regarding this work.

## References

- [1] Yuji, S. Osaki, K. Yoshikawa, and Tanaka, "Analysis and evaluation of landscape based on social media\ncase studies in tourist area," *Proceedings of The City Planning Institute of Japan, Kansai Branch*, vol. 15, pp. 13–16, 2017.
- [2] Ł. Sarnowski, Z. Podgórski, and D. Brykała, "Planning a greenway based on an evaluation of visual landscape attractiveness," *Moravian Geographical Reports*, vol. 24, no. 3, pp. 55–66, 2016.
- [3] H. L. Liu, T. Taniguchi, Y. Tanaka, K. Takenaka, and T. Bando, "Visualization of driving behavior based on hidden feature extraction by using deep learning," *IEEE Transactions on Intelligent Transportation Systems*, vol. 18, no. 9, pp. 2477–2489, 2017.
- [4] K. Malik and C. Robertson, "Landscape similarity analysis using texture encoded deep-learning features on unclassified

## *Retraction*

# **Retracted: Application of Fuzzy Analytic Hierarchy Process in the Quality Monitoring and Evaluation of College Teachers and the Construction of Index System**

### **Security and Communication Networks**

Received 26 December 2023; Accepted 26 December 2023; Published 29 December 2023

Copyright © 2023 Security and Communication Networks. This is an open access article distributed under the Creative Commons Attribution License, which permits unrestricted use, distribution, and reproduction in any medium, provided the original work is properly cited.

This article has been retracted by Hindawi, as publisher, following an investigation undertaken by the publisher [1]. This investigation has uncovered evidence of systematic manipulation of the publication and peer-review process. We cannot, therefore, vouch for the reliability or integrity of this article.

Please note that this notice is intended solely to alert readers that the peer-review process of this article has been compromised.

Wiley and Hindawi regret that the usual quality checks did not identify these issues before publication and have since put additional measures in place to safeguard research integrity.

We wish to credit our Research Integrity and Research Publishing teams and anonymous and named external researchers and research integrity experts for contributing to this investigation.

The corresponding author, as the representative of all authors, has been given the opportunity to register their agreement or disagreement to this retraction. We have kept a record of any response received.

## **References**

- [1] X. Shi, "Application of Fuzzy Analytic Hierarchy Process in the Quality Monitoring and Evaluation of College Teachers and the Construction of Index System," *Security and Communication Networks*, vol. 2022, Article ID 5124433, 11 pages, 2022.

## Research Article

# Application of Fuzzy Analytic Hierarchy Process in the Quality Monitoring and Evaluation of College Teachers and the Construction of Index System

Xiaoyan Shi 

Personnel Department of Jiangsu Maritime Institute, Nanjing 211170, China

Correspondence should be addressed to Xiaoyan Shi; 20070912@jmi.edu.cn

Received 7 June 2022; Revised 12 July 2022; Accepted 19 July 2022; Published 18 August 2022

Academic Editor: Hangjun Che

Copyright © 2022 Xiaoyan Shi. This is an open access article distributed under the Creative Commons Attribution License, which permits unrestricted use, distribution, and reproduction in any medium, provided the original work is properly cited.

In view of the relevant problems existing in the faculty of colleges and universities, in order to further analyze the deficiencies existing in the quality monitoring and index system of the faculty of colleges and universities. Based on the method and theory of fuzzy analytic hierarchy process, this study evaluates the quality monitoring results of university teachers, and researches the establishment of the index system of university teachers. The results show that  $k$  of different parameters increases slowly at first and then tends to be stable with the increase of iteration time. However, different parameters show different variation relations at higher iteration time. When  $k$  is 15, it can be used for targeted analysis of model index  $CR_1$ . It can be seen from the weight analysis chart of quality monitoring of college teachers that the highest proportion is work pressure, while the lowest proportion is working environment. The research shows that the work pressure has the greatest influence on the quality monitoring analysis of college teachers. The construction diagram of the index system of college teachers shows that the fuzzy analytic hierarchy process can better reflect the quality system and index system of college teachers. Relevant research results can provide theoretical support for the application of fuzzy analytic hierarchy process in the research of college teachers.

## 1. Introduction

Fuzzy analytic hierarchy process has been widely used in different fields. In terms of transportation, aiming at the problems existing in safety and reliability of roads and bridges, a new optimization model based on fuzzy analytic hierarchy process theory was proposed in [1]. The model obtains the operation data of different vehicles by using the method of hierarchical analysis, and then imports the corresponding data into the target module. Through further iterative calculation of the target module, the relevant indexes and corresponding factors that quantitatively describe the bridge safety were obtained. Through the analysis of different factors to find out the most important factors, which were imported into the model function, so as to evaluate the safety of the model related indicators. The optimization model can carry out targeted analysis on expressways and other vehicles. In order to verify the accuracy of the model, a local vehicle was used for verification. The

final results show that the optimization model based on analytic hierarchy theory can accurately characterize the safety and reliability of traffic transportation. In view of the relevant problems existing in the construction of the Internet, as well as for the targeted evaluation and analysis of the Internet, an atomization method based on the theory of fuzzy analytic hierarchy process was proposed in [2]. The method firstly iteratively analyzes the evaluation data of the Internet, and then obtains the optimized corresponding parameters, and then imports the data into the fuzzy hierarchy analysis function. This function can not only analyze the data, but also predict and study the computing rules of the Internet through the change trend of the data. The research shows that the Internet atomization calculation method based on fuzzy analytic hierarchy process model can provide theoretical support for Internet decision-making and operation, so as to make targeted evaluation for the development of the Internet. Finally, the model was verified by Internet data, and the atomization method and function

of fuzzy analytic hierarchy process after model optimization were obtained. Fuzzy analytic hierarchy process is not only widely used in traffic computation and Internet, but also in engineering. In view of the relevant safety problems existing in coal mine engineering, a fuzzy analytic hierarchy process method was used to explore and evaluate the safety and stability of coal mine [3]. The model first divides coal mine safety into four different grades, which were based on the seismic conditions, geological causes, natural environment, and other factors of the coal mine. This grade was explored by considering the application prospect of engineering comprehensively. Based on the classification of the original model, targeted evaluation and research on coal mine safety of different grades can be divided into different grades according to different research content. And the different levels were interchangeable. Finally, the relevant database of coal mine safety was established, the evaluation data in the database was imported into the fuzzy analytic hierarchy process model for analysis, and the stability of coal mine safety was studied in combination with the evaluation grade. In order to verify the accuracy of the model, a coal mine in Iran was used to verify the safety and reliability of the model. In order to explore the application of fuzzy hierarchy analysis method in multi-function printer, the fuzzy hierarchy analysis model was firstly used to analyze the relevant functions of multi-function printer [4]. The corresponding discriminant index was obtained through analysis, and the discriminant index mainly includes printing speed, printing effect, and printing cost. Then, different discriminant indexes were brought into the fuzzy analytic hierarchy process function, so as to carry out the calculation of related evaluation indexes. As the data with evaluation indexes were imported into the optimization model, the iterative results can be used for optimization analysis of the fuzzy hierarchy analysis model. Finally, the indexes of the multi-functional printer can be analyzed and optimized, so that the optimized indexes can well explain the performance of the multi-functional printer. At last, 1000 samples were used to calculate the model to demonstrate the accuracy of the optimized model.

Based on the theory of fuzzy hierarchy analysis, this paper adopts the method of model analysis to study the faculty team in colleges and universities. This study mainly focuses on the analysis of quality monitoring and evaluation and index system construction of college teachers. The experimental curves and corresponding fitting parameters verify the accuracy of the model, and the relevant research results can provide a theoretical basis for the application of fuzzy analytic hierarchy process in college teachers.

## 2. Fuzzy Analytic Hierarchy Process

*2.1. Related Theory of Analytic Hierarchy Process.* Fuzzy analytic hierarchy process can be used to quantify the evaluation index, and the model can provide the basis for choosing the optimal scheme, so it has been widely used [5, 6]. The analytic hierarchy process is characterized by making use of less quantitative information to make the thinking process of decision-making mathematical on the

basis of in-depth analysis of the nature, influencing factors and internal relations of complex decision-making problems. However, analytic hierarchy process has the following defects: (1) it is very difficult to test whether the judgment matrix is consistent, and there is a lack of certain scientific basis for the criterion to test whether the judgment matrix is consistent. (2) The consistency of judgment matrix is significantly different from the consistency of original computational thinking. (3) In fuzzy analytic hierarchy process, triangle fuzzy number cannot be used for quantitative analysis of pairwise comparison and judgment between different factors.

The basic principle of analytic hierarchy process is to list the expected purpose of solution according to the characteristics and related requirements of the actual events encountered in the actual operation. Then, according to the needs of the careful and detailed analysis of the possible related factors, analysis, comparison, research to carry out a hierarchical comparison of each factor, to establish the weight coefficient. Then, the important factor relative to the upper target layer is calculated. The principle of analytic hierarchy process is shown in Figure 1.

Through the system hierarchy analysis schematic diagram, we can see that the analytic hierarchy process can be mainly divided into four aspects, respectively, the target layer, the criterion layer, the sub-criterion layer, and the scheme layer. Different layers contain different subsets and content. The principle of analytic hierarchy process is as follows: firstly, relevant data are imported into the decision-making target module in the target layer, and the data are preliminarily analyzed and discriminated. The discriminant data is imported into the specific criterion module in the criterion layer. Different specific criterion modules correspond to different criterion areas, respectively. The data in the specific criteria area is imported into the sub-criteria module for further iteration update and analysis, and then different schemes are selected for calculation, and finally the obtained results are output.

The basic execution steps of analytic hierarchy process are as follows [7, 8]:

- (1) clear objectives and construct hierarchical analysis model: through research and analysis of the expected objectives, clarify the relationship between the listed factors in the system events.
- (2) Constructing judgment matrix: the core of analytic hierarchy process is to make quantitative comparison between different factors and determine the weight coefficient of factors of this layer to criteria of the next layer by comparison. The factors affecting the judgment and evaluation of college teachers, especially the analysis of quality monitoring and evaluation and the construction of index system, are also complex and changeable. Moreover, it is worth noting that many influencing factors can only be described by qualitative analysis method, which is difficult to be directly expressed by quantitative indicators. Therefore, for the evaluation and index system construction of quality monitoring of college



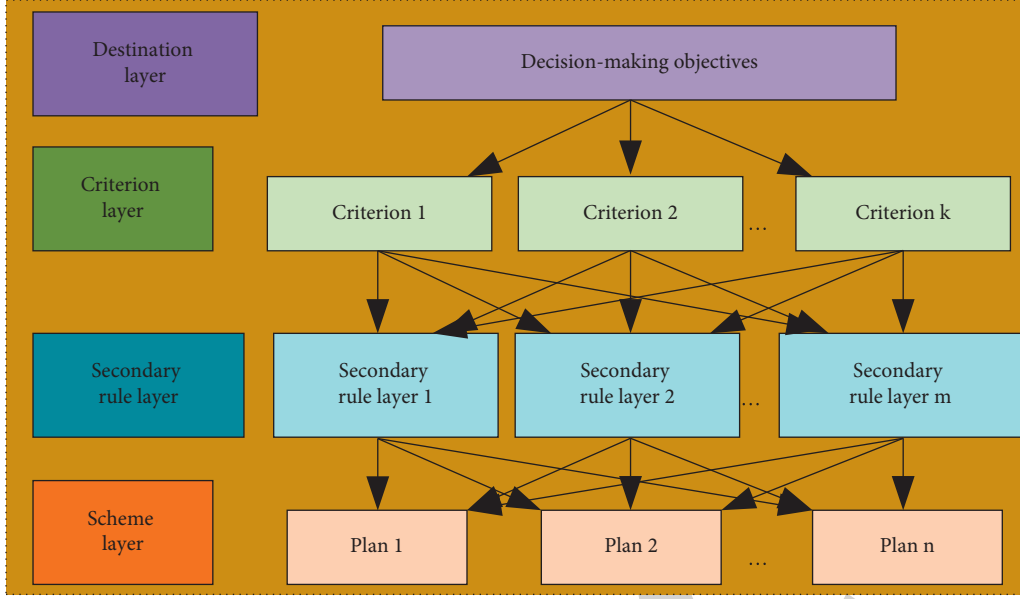


FIGURE 1: Schematic diagram of analytic hierarchy Process.

teachers, it is necessary to adopt a variety of different schemes for comparative analysis. Thus, the weight and influence of specific indicators can be determined more accurately. In order to determine the research content of the objective function more accurately, it is necessary to determine the judgment matrix  $M$  of the objective function first, as shown below.

$$M = \begin{bmatrix} a_{11} & \cdots & a_{1n} \\ \vdots & & \vdots \\ a_{n1} & \cdots & a_{nn} \end{bmatrix} = \begin{bmatrix} 1 & \cdots & w_1/w_n \\ \vdots & & \vdots \\ w_n/w_1 & \cdots & 1 \end{bmatrix}, \quad (1)$$

where,  $a_{ij}$  is the relative importance of the target,  $w_i$  is the weight of  $(i)$ .

In order to analyze the calculation process of the judgment matrix more briefly, it is necessary to normalize the data of the judgment matrix, so as to obtain the weight coefficient  $w_i$ :

$$w_i = \frac{\bar{w}_i}{\sum_{i=1}^n \bar{w}_i}, \quad (2)$$

where,  $\bar{w}_i$  is the average value of the weight.

- (3) Consistency test of evaluation matrix: The purpose of consistency test of evaluation matrix is to judge whether the internal connection between the two factors is consistent. Generally speaking, if the judgment matrix  $A$  satisfies:  $a_{ij} = a_{ik} \times a_{kj}$   $i, j, k = (1, 2, \dots, n)$ , then, the matrix  $A$  must be completely consistent, and the consistency test formula is as follows:

$$\sum_{i=2}^n \lambda_i = n - \lambda_{\max}, \quad (3)$$

where,  $n$  is the number of samples;  $\sum_{i=2}^n \lambda_i$  is the cumulative value of linear parameters;  $\lambda_i$  is a linear parameter, and  $\lambda_{\max}$  is the maximum value of the linear parameter. In this case, the judgment matrix is usually inconsistent. If the inconsistency is within the allowable deviation range, we can consider the matrix to be reasonable. However, if the judgment matrix exceeds the general allowable range, the availability of the calculated index weight will be reduced, which requires us to adjust the judgment matrix immediately and continuously until the consistency meets the allowable range.

The consistency verification test parameters are represented by  $CI$  and  $CR$ . The goal of  $CI$  index analysis is to study the relative analysis error between the analytic hierarchy process calculation results and corresponding test results. The objective of  $CR$  index analysis is to study the absolute analysis error between the analytic hierarchy process calculation results and corresponding test results.

$$CI = \frac{\lambda_{\max} - n}{n - 1}, \quad (4)$$

$$CR = \left| \frac{CI}{RI} \right|,$$

where,  $RI$  is the index of average random consistency analysis. A large number of scientific studies have found that when  $CR < 0.10$ , it meets the consistency requirement and meets our needs. When  $CR > 0.10$ , it is necessary to analyze the factors, modify the comparison matrix, re-check the values of the elements of the judgment matrix, return to the first step, and constantly adjust the factor values until the consistency of the final results meets the requirements.

In order to better reflect the research errors of the judgment indicators  $CI$  and  $CR$  on the test data, the data change curves under two different judgment indicators are drawn, as shown in Figure 2.



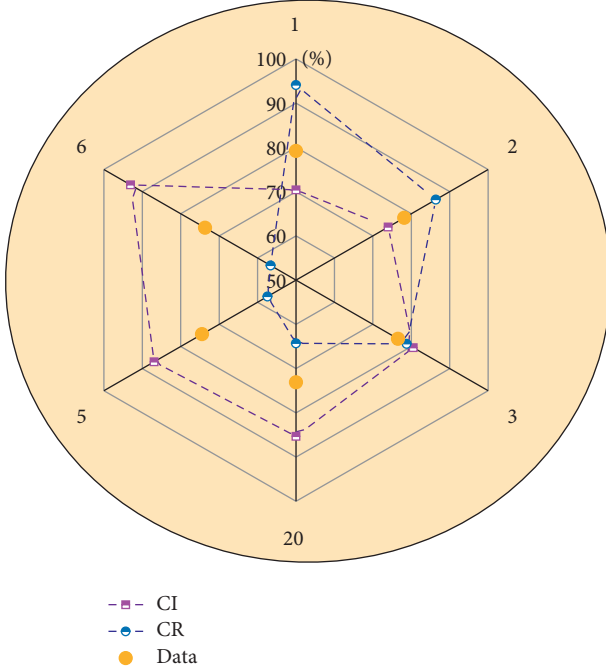


FIGURE 2: Change diagram of different judgment indexes.

It can be seen from the variation diagram of different indicators that the curve corresponding to  $CI$  judgment indicator shows a gradually increasing trend as the number of iterations increases. When the number of iterations is 1, the value of the judgment index of drinking is only 71%, while when the number of iterations increases to 6 times, the corresponding value is more than 90%. It indicates that the increase of iteration times can improve the proportion accuracy for judging index  $CI$ . The proportion of  $CR$ , the corresponding iteration index, shows a trend of gradual decline with the increase of the number of iterations. When the number of iterations is 1, the corresponding proportion data reaches 95%, while when the number of iterations is 6, it has decreased to below 60%. It indicates that the proportion accuracy of  $CR$  can be reduced with the increase of iteration times. The two different iterations have different trends, The corresponding test shows a relatively stable trend of change, and the corresponding test data mainly concentrated in the range of 70% to 80%. It indicates that the data change of the experimental data is relatively small in the process of operation, and neither of the two iteration indexes can better reflect the change trend of the data. Therefore, it is necessary to comprehensively consider the influence of the two iterative indicators, and then, get an accurate iterative method to represent the data changes of the comprehensive quality of college teachers under analytic hierarchy Process.

**2.1.1. Hierarchical Analysis of the Sequence and Data Consistency Test.** After obtaining the relevant data of college teachers, the data are tested step by step from high level to low level so as to verify the consistency of the data. The corresponding sequence  $CR_1$  can be calculated as follows:

$$CR_1 = \frac{\sum_{j=1}^m a_j CI_j^{(a)}}{\sum_{j=1}^m a_j RI_j^{(a)}} = \frac{a^T CI^{(a)}}{a^T RI^{(a)}}, \quad (5)$$

where,  $a_j$  and  $a^T$  are the correlation coefficients of the calculation formula, and  $k$  is the influence parameter of the index. When  $CR^{(k)} < 0.1$ ,  $k = 1, 2, \dots, p$ , unity is very satisfactory. When  $CR$  is greater than or equal to 0.10, we should reassign the judgment matrix and recalculate the process until the final result is consistent to our satisfaction.

Thus, the corresponding mutual recursive formula can be obtained:

$$CR_1^{(k)} = \frac{\sum_{j=1}^{n_{k-1}} w_j^{(k-1)} CI_j^{(k-1)}}{\sum_{j=1}^{n_{k-1}} w_j^{(k-1)} RI_j^{(k-1)}} = \frac{(w^{(k-1)})^T CI^{(k-1)}}{(w^{(k-1)})^T RI^{(k-1)}}. \quad (6)$$

In order to better analyze the influence degree of influence parameter  $k$  on  $CR_1$  parameter, the index change curves under different influence parameter  $k$  were drawn, as shown in Figure 3.

According to the influence diagram of different parameter  $k$  on  $CR_1$  index, it can be seen that with the gradual increase of iteration time, the values of different parameter  $k$  show different variation trends. When  $k$  is equal to 30, the curve rises slowly, then remains constant, and finally tends to fall. When  $k$  is equal to 0, the corresponding curve rises slowly at first and then tends to be stable. When the parameter  $k$  is less than zero, the corresponding parameters all show a trend of slow rise at first, then keep constant, and finally increase. It indicates that the decrease of parameter  $k$  can further promote the increase of the corresponding value of  $CR_1$  index. It can be seen from the above calculation that the specific value of  $CR_1$  can be described by the variation parameters between  $k = -10$  and  $k = -20$ , and the specific determination method needs further analysis and research.

**2.2. Fuzzy Analysis Theory.** The research content of fuzzy analysis theory should not only consider the nature and characteristics of the research object itself, but also combine fuzzy theory with all kinds of quantitative problems in reality [9, 10]. In order to use fuzzy mathematics to judge the specific target problem, the model is analyzed and verified by combining qualitative analysis and quantitative analysis, so as to get a scientific and reasonable solution. The characteristics of fuzzy theory are shown as follows: (a) the extension of fuzzy theory has obvious uncertainty; (b) understanding of fuzzy theory is subjective to a certain extent; (c) fuzzy theory is the opposite, but not the opposite, of precision theory; (d) fuzzy theory is conceptually unclear.

Fuzzy set is a simple concept of fuzzy theory. Fuzzy set and its corresponding boundary conditions are not clear, fixed, and indistinguishable. There are many expressions of fuzzy set  $A$ , which can be summarized as follows:

$$A = \left\{ \frac{\mu_A(x)}{x}, x \in X \right\} = \sum_{i=1}^n \frac{\mu_A(x_i)}{x_i}, \quad x \in X, \quad (7)$$

where,  $\mu_A(x)$  is the membership function of the fuzzy set. Set  $A$  is the fuzzy set,  $\mu_A(x)$  is the membership function of the

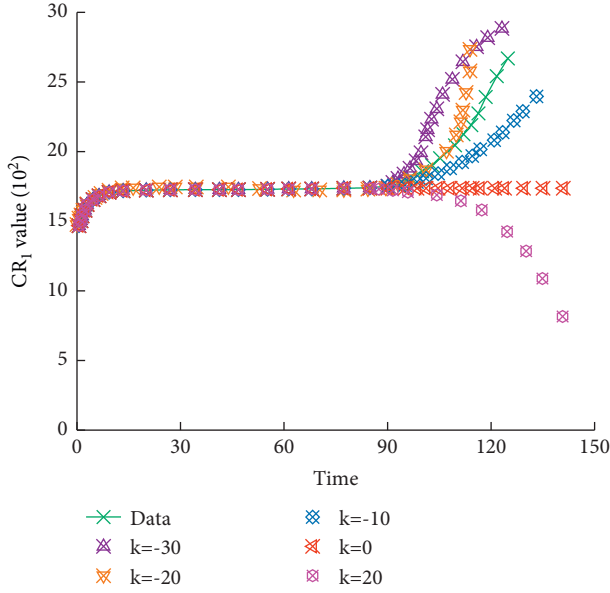


FIGURE 3: Diagram of the influence of parameter ( $k$ ) on  $CR_1$  index.

fuzzy set we need. The membership function is biased to both ends of its range space and reflects the coupling degree of the case to the fuzzy set one by one. If the membership function value is just at the two endpoints of the function range, the fuzzy set can be reduced to a common mathematical qualitative set.

In fuzzy theory, there are many ways to determine the membership function. In order to get a consistent recognition conclusion, the membership function needs to be modified and optimized for many times [11, 12]:

- (1) determination analysis method: determination analysis method is generally applicable to the case of large dispersion of model data, and the reliability of model specimens is relatively low.
- (2) Fuzzy statistical method: the method of calculation through the use of model statistical formula. Fuzzy statistical method is an objective method, which is mainly determined based on the objective existence of membership degree on the basis of fuzzy statistical test. The so-called fuzzy statistical test consists of the following four elements: (a) domain, (b) fixed element, (c) set, and (d) fuzzy set.

$$\mu_{A_i}^p = \begin{cases} 1, & u \in A_i, \\ 0, & u \notin A_i. \end{cases} \quad (8)$$

where,  $\mu_{A_i}^p$  is the fuzzy statistical coefficient, and  $A_i$  is the fuzzy region. The instructions have been given that  $u$  must belong to and only belong to one of the sets  $A_1$ ,  $A_2$ , and  $A_m$ . The corresponding membership degree can be expressed as:  $\mu_{A_i}(u) = \sum_{p=1}^n \mu_{A_i}^p / n$ .

- (3) Membership function determination method: in order to be more accurate and quantifiable, the common distribution function is often used as membership function to express the fuzzy set,

including triangle membership function and quadrilateral membership function, two kinds of corresponding function relations.

$$\mu_A(x) = \begin{cases} x - \frac{b}{a-b}, & x \in [b, a], \\ c - \frac{x}{c-a}, & x \in [a, c], \\ 0, & x \in R - [b, c], \end{cases} \quad (9)$$

$$\mu_A(x, a, b, c, d, H) = \begin{cases} I(x), & x \in [a, b], \\ H, & x \in [b, c], \\ D(x), & x \in [c, d], \\ 0, & x \in R - [a, d], \end{cases}$$

where,  $\mu_A(x)$  is triangular membership function;  $\mu_A(x, a, b, c, d, H)$  is the quadrilateral membership function;  $D(x)$  is the function on the interval  $[c, d]$ . The  $a \leq b \leq c \leq d$ ,  $0 \leq H \leq 1$ ,  $0 \leq I(x) \leq 1$ . In order to explore the influence of different parameters in the quadrilateral membership function on the model, the sensitivity curves of the model under different parameters were drawn, as shown in Figure 4.

It can be seen from the sensitivity analysis diagram of function with different parameters that the sensitivity of function with four different parameters is different, as shown below: with the increase of iteration time, the sensitivity of parameter  $a$  firstly slowly increases to the highest point and then gradually shows an approximate linear trend of slow decline. With the increase of iteration time, parameter  $b$  presents a trend of slow decline. The slope of the corresponding function curve decreases gradually at first, and finally tends to 0. It shows that with the increase of iteration time, the sensitivity of parameter  $b$  to membership function decreases gradually. It can be seen from the variation curve of parameter  $c$  that the gradual increase of iteration time will make the corresponding curve also show a relatively large downward trend. Moreover, the decrease range of parameter  $b$  exceeds the corresponding iteration range, indicating that parameter  $c$  has the characteristics of large influence and short iteration time. The change curve of parameter  $d$  shows two typical trends. The first one is the trend of rapid decline, and the second one is the trend of approximate linear increase when it reaches the lowest point. This indicates that the function has typical piecewise points, and that parameter  $d$  can be used for sensitivity analysis of different membership functions.

**2.3. Fuzzy Analytic Hierarchy Process.** The fuzzy analytic hierarchy process can analyze different dimensions and calculate the influence degree of each factor on the overall objective [13, 14]. In order to further explain the calculation process of fuzzy analytic hierarchy process, the corresponding fuzzy analytic hierarchy process is drawn, as shown in Figure 5. Different calculation forms in the state

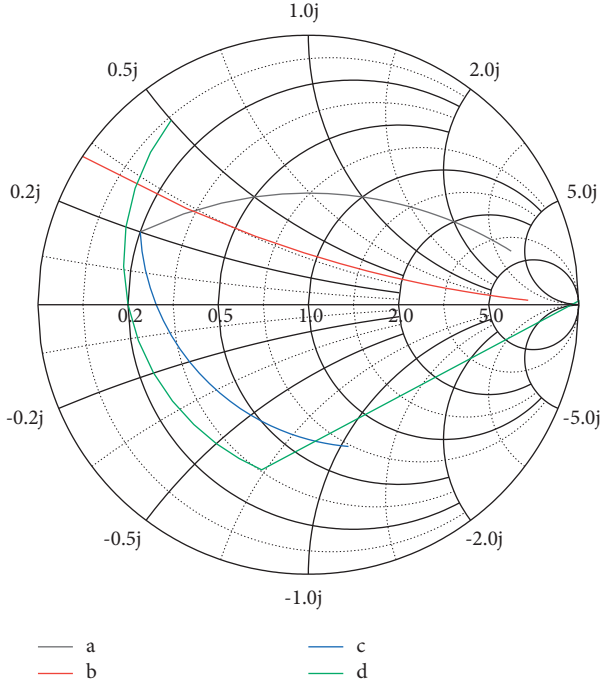


FIGURE 4: Sensitivity analysis diagram of different parameters to membership function.

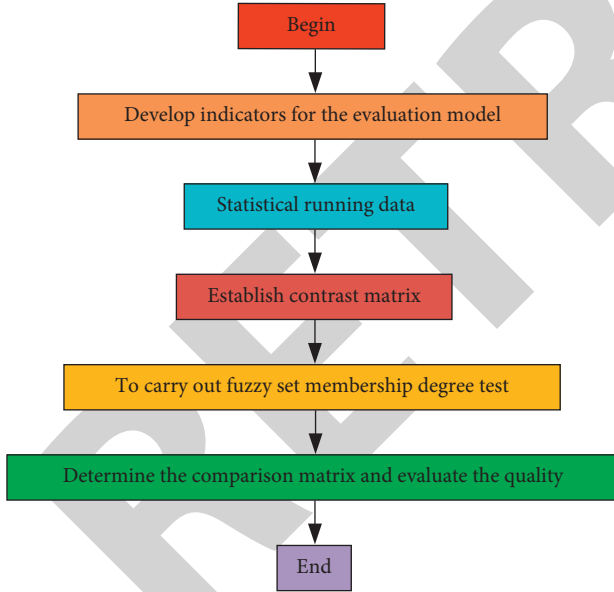


FIGURE 5: Flow chart of fuzzy analytic hierarchy process.

comprehensive evaluation module are shown as follows: (a) prominent main factor type: after identifying the main influencing factors, further strengthening them will further weaken the other indicators and continuously reflect the distinction and contrast; (b) comprehensive constraints: the original indicators are modified so as to have a restrictive effect; (c) weighted average type, in which the contribution rates of different indicators to evaluation objectives are represented by weights.

It can be seen from the flow chart of fuzzy hierarchy analysis that, firstly, relevant data obtained from membership function analysis theory are imported into the indicator analysis module of the established evaluation model. Calculate and analyze the relevant data through the indicator statistics of the evaluation model, and then, import the obtained analysis data into the corresponding comparison matrix. The membership test and sensitivity analysis of fuzzy function can be realized by checking the comparison matrix. When the calculation result of membership function exceeds the sensitivity requirement, the quality test data can be determined through the comparison matrix, and the corresponding theoretical analysis and evaluation can be carried out. Finally, the relevant data of quality inspection and evaluation and index system construction of college teachers are derived. The corresponding fuzzy analytic hierarchy process mainly includes fuzzy transformation and fuzzy calculation model.

Fuzzy transformation: fuzzy transformation requires the comprehensive expansion of the evaluation basis of weighted summation through the calculation of fuzzy theory and fuzzy set, so as to establish the corresponding evaluation index set  $U$ , and the final evaluation results are shown as follows.

$$B = A \odot B = (a_1, a_2, \dots, a_n) \odot \begin{bmatrix} r_{11} & r_{12} & \cdots & r_{1m} \\ r_{21} & r_{22} & \cdots & r_{2m} \\ \vdots & \vdots & \ddots & \vdots \\ r_{n1} & r_{n2} & \cdots & r_{nm} \end{bmatrix}, \quad (10)$$

where  $B$  is the fuzzy vector, and  $A$  is the fuzzy vector in the evaluation index set  $U$ .

Fuzzy calculation model: for fuzzy comprehensive evaluation method, fuzzy analytic hierarchy process is adopted to evaluate, and comprehensive evaluation is carried out one by one:

- (1) establishment of factor set  $U$  of the underlying evaluation index: the underlying evaluation index set is  $U$ , and each weight vector together forms a fuzzy vector  $A$ , so as to explain the different importance of each index.
- (2) The establishment of evaluation set  $V$ : to construct a scientific and reasonable fuzzy evaluation set  $V$ , so that the results can be accurately reflected in the evaluation set.
- (3) Establishment of evaluation matrix of underlying indicators: element calculation method is as follows.

$$u_i: R(u_i) = \frac{r_{i1}}{v_1} + \frac{r_{i2}}{v_2} + \cdots + \frac{r_{im}}{v_m}. \quad (11)$$

Through fuzzy evaluation, the fuzzy evaluation matrix on  $U \times V$  is constructed as follows:

$$R = \begin{bmatrix} r_{11} & r_{12} & \cdots & r_{1m} \\ r_{21} & r_{22} & \cdots & r_{2m} \\ \vdots & \vdots & \ddots & \vdots \\ r_{n1} & r_{n2} & \cdots & r_{nm} \end{bmatrix}. \quad (12)$$

- (4) State comprehensive evaluation:  $B$  is obtained by fuzzy transformation according to  $A$  and  $R$ . The maximum membership criterion of modular mathematics is reversely applied to obtain comprehensive evaluation after calculation. The calculation is as follows:

$$B = A \odot B = (a_1, a_2, \dots, a_n) \odot \begin{bmatrix} r_{11} & r_{12} & \cdots & r_{1m} \\ r_{21} & r_{22} & \cdots & r_{2m} \\ \vdots & \vdots & \ddots & \vdots \\ r_{n1} & r_{n2} & \cdots & r_{nm} \end{bmatrix} \quad (13)$$

$$= (b_1, b_2, \dots, b_n).$$

In order to further analyze the solution process of vector  $B$ , change curves of different vectors were drawn, as shown in Figure 6. From the variation trend of different vectors, we can see that  $A$  and  $R$  vectors have different influence degrees on index  $B$  and have typical segmentation characteristics. First of all, it can be seen from the change curve of vector  $A$  that this line segment has typical segmenting characteristics. When the iteration speed is between 0 and 1800, the curve corresponding to the matrix value of vector  $A$  and that of vector  $B$  have basically the same change trend. With the increase of iteration speed, the corresponding curve gradually reaches the highest point, and then with the further increase of iteration speed, the corresponding curve value drops rapidly, with typical segmentation characteristics. It can be seen from the change curve of vector  $R$  that the corresponding matrix data shows a slow increasing trend with the increase of the number of iterations. However, when the iteration rate exceeds about 1800, it shows a rapid increasing trend, while when the iteration rate exceeds 2000, it shows a sudden slight decrease. It can be seen from the change curve of vector  $B$  that the curve has a typical increasing trend. With the increase of iteration speed, the corresponding matrix values show a linear changing trend. The slope of the corresponding curve still shows an increasing trend, indicating that the increase of iteration speed can make the matrix data increase rapidly. The iterative data of matrix vector  $B$  can be obtained through vector  $A$  and  $R$ , and it can be seen from the data that the process of solving vector  $B$  by vector  $A$  and vector  $R$  is not a simple calculation, but a complex iterative solution.

### 3. Application of Fuzzy Analytic Hierarchy Process in College Teachers

The construction of college teachers is very important for the development of higher education. In order to explore the evaluation method of quality monitoring of college teachers and the construction process of corresponding index system, the construction of college teachers is analyzed and researched based on fuzzy analytic hierarchy process [15, 16]. Thus, the analysis process of the quality of college teachers under different evaluation factors is obtained, as shown in Figure 7.

It can be seen from the quality evaluation chart of statistical indicators under different evaluation factors that

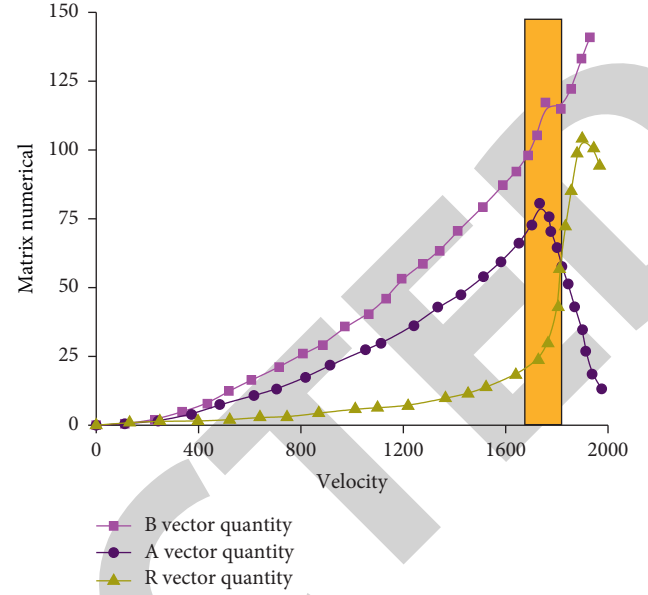


FIGURE 6: Change process diagram of vector ( $B$ ).

quality evaluation can be divided into three parts: the first part is determining function, the second part is iterative solution, and the third part is the comparison of corresponding indicators. The specific analysis process is as follows: firstly, the relevant indicators of quality monitoring in the faculty of colleges and universities are imported into the relevant modules of the criterion layer. By determining the iterative relations in the function criterion layer, the relevant parameters of the model are solved, and then, the corresponding judgment basis is obtained. The corresponding judgment function is obtained through the correlation coefficient of the function, and then, the judgment function is imported into the solution module, and consistency test and model reconstruction are carried out at the same time. Through the iterative process of consistency test and model reconstruction, the influence range and degree of the judgment matrix in the faculty of colleges and universities are obtained. Finally, the corresponding scope of influence and indicators are imported into the comparison module, and the relevant quality evaluation data is finally exported through the circulation function of the modules such as consistency test, quality detection evaluation, and index system evaluation again.

**3.1. Quality Monitoring and Evaluation of College Teachers.** The quality inspection of college teachers is an important part of the construction of college teachers. In order to quantitatively analyze the problems existing in college teachers, different indicators are used to analyze them [17, 18]. The first-level indicators mainly include: professional ethics, professional quality, research tasks, research summary, and research environment [19, 20]. The corresponding secondary indicators mainly include: ethics, professional attitude, faculty, theoretical basis, teaching ability, work pressure, physical and mental health, scientific research achievements, teacher evaluation, working environment, research pressure, and

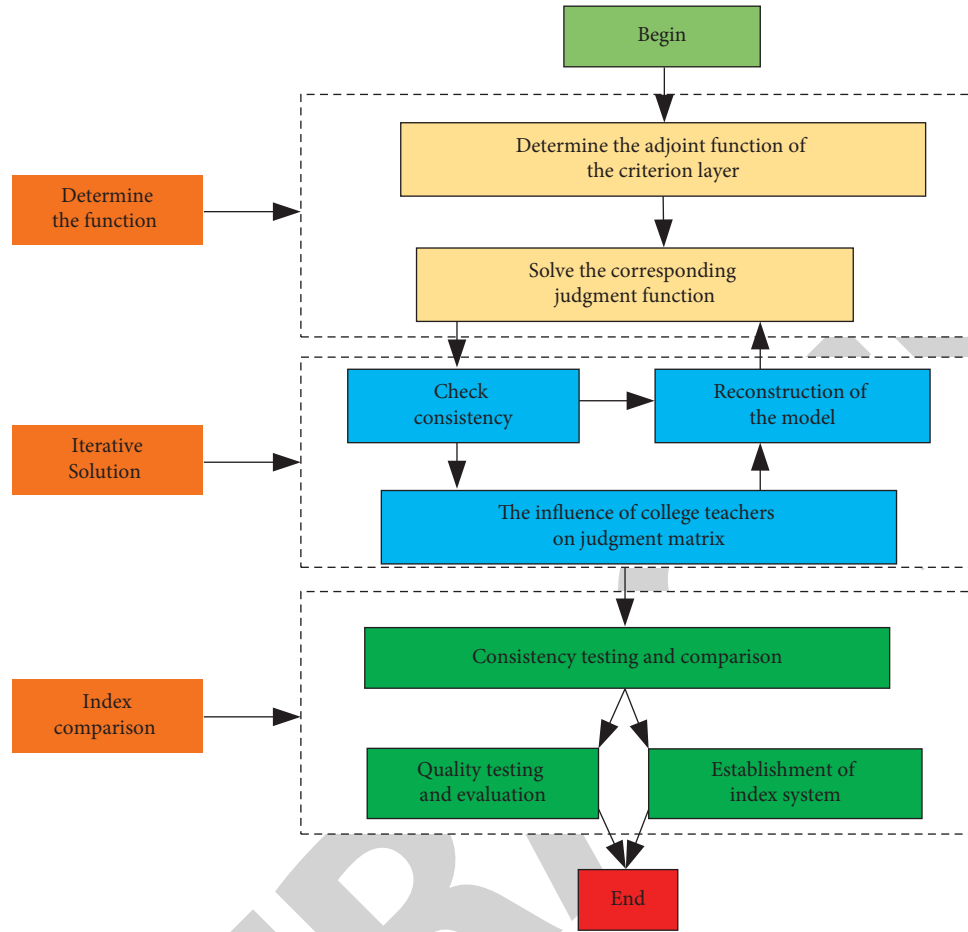


FIGURE 7: Quality evaluation chart of university teachers under different evaluation factors.

other indicators. In order to better analyze the influence weight of different levels of indicators on the quality of college teachers,  $CR$  and  $CI$  indicators in fuzzy analytic hierarchy process are used to monitor and analyze college teachers. The specific results are shown in Figure 8, and the relevant results are shown in Table 1.

According to the weight analysis chart of quality monitoring of university teachers under different indicators, we can see that the weight of scientific research task is 0.36, and the weight of scientific research summary is 0.272. The corresponding weight of professional ethics is only 0.21, professional quality is 0.13, and the corresponding research environment is the lowest 0.03. Different first-level indicators can be subdivided into different second-level indicators. The first-level indicators are analyzed by using  $CI$  weights, while the corresponding second-level indicators are described by using  $CR$  weights. Then, through the second-level indicators, we can see that the weight of work pressure is 0.21, accounting for the highest proportion, while the lowest proportion is the work environment in the scientific research environment, which is only 0.01, indicating that work pressure has the greatest impact on the quality monitoring of university teachers.

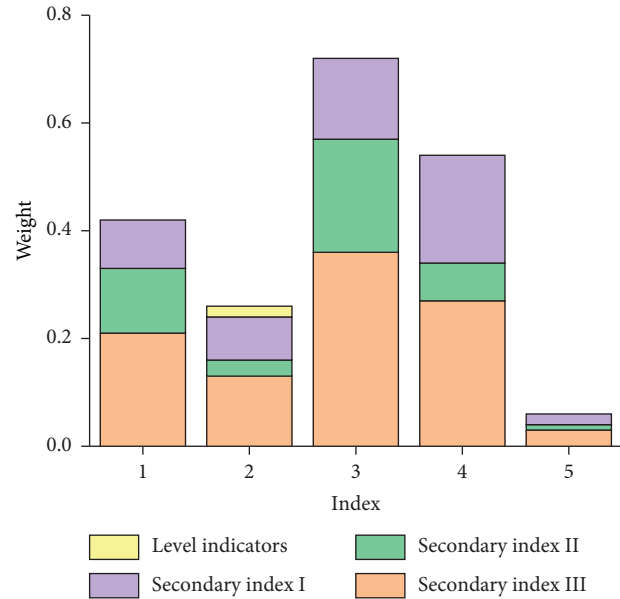


FIGURE 8: Weight analysis chart of quality monitoring of college teachers under different indicators.



TABLE 1: Summary of quality monitoring under different indicators.

Number	Level indicators	CI weight	Secondary indicators	CR weight	Comprehensive order
1	Professional ethics	0.21	Ethics	0.12	5
			Professional attitude	0.09	6
2	Professional quality	0.13	Faculty	0.03	8
			Theoretical basis	0.08	7
			Teaching ability	0.02	9
3	Research tasks	0.36	Work pressure	0.21	1
			Physical and mental health	0.15	2
4	Research summary	0.27	Scientific research achievements	0.07	4
			Teacher evaluation	0.20	3
5	Research environment	0.03	Working environment	0.01	11
			Research pressure	0.02	10

TABLE 2: College index system construction summary table.

Vector	Factor	Index	Weight	Coefficient
B	Professional quality	1-Team structure $B_1$	0.07	0.961
		2-Concept of knowledge $B_2$	0.02	0.923
		3-Professional proficiency $B_3$	0.03	0.943
	Younger age of the team	4-Education level $B_4$	0.12	0.912
		5-School age indicators $B_5$	0.13	0.972
		6-Professional title appraisal $B_6$	0.04	0.962
A	Knowledge level	7-Disciplinary knowledge $A_1$	0.13	0.892
		8-Pedagogical knowledge $A_2$	0.11	0.914
		9-Knowledge $A_3$	0.01	0.887
	Professional ability	10-Teaching design $A_4$	0.03	0.789
		11-Classroom harmony $A_5$	0.04	0.862
		12-Information development $A_6$	0.06	0.785
R	Psychological quality	13-Quality-oriented education $R_1$	0.11	0.956
		14-Heart health $R_2$	0.04	0.936
		15-Communication $R_3$	0.06	0.978

**3.2. Construction of Index System of College Teachers.** In view of the problems existing in the quality monitoring process of college teachers, fuzzy analysis method is adopted to calculate, and relevant calculation results are obtained. However, the construction of the index system of college teachers also needs to be analyzed by relevant algorithms [21, 22]. Therefore, in order to explore the relevant content of index system construction in the faculty of colleges and universities, the fuzzy vector analysis method based on the fuzzy hierarchy analysis theory is adopted to calculate and analyze the relevant data. The specific results are shown in Table 2, and the corresponding index system construction analysis is shown in Figure 9.

The index system under different factors mainly includes professional quality, younger age of the team, knowledge level, professional ability, and psychological quality, etc., In order to better analyze the construction of the index system of college teachers, we divided the relevant factors into specific categories, each representing three different aspects. By introducing it into fuzzy analytic hierarchy process, corresponding weight analysis can be obtained. Figure 9 shows the construction of relevant index system in the faculty of colleges and universities. We can see that the data

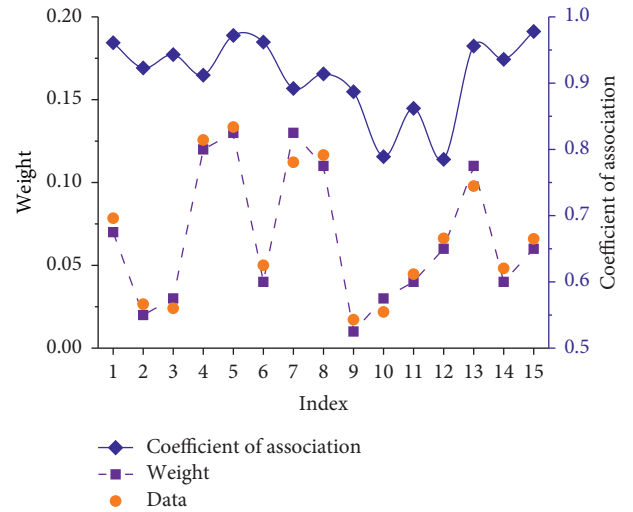


FIGURE 9: Analysis chart of index system construction in colleges and universities.

obtained by weight analysis method for the construction of the index system of colleges and universities are basically consistent with the experimental data. It stays within the



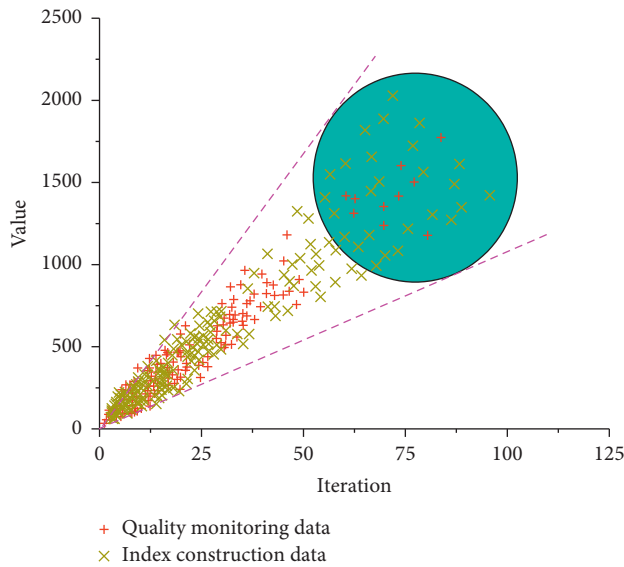


FIGURE 10: Evaluation and analysis chart of model with different indexes.

range of 0 to 0.15, and the corresponding relationship obtained by fuzzy analytic hierarchy process is generally high, the correlation coefficient is higher than 0.7, mainly concentrated around 0.9, indicating that the analytical method has a good accuracy in the research on the quality system and index system of college teachers.

#### 4. Discussion

Finally, in order to further analyze the impact of different data on model evaluation, the impact range of quality monitoring data and index construction data on the model is counted, as shown in Figure 10. It can be seen from the data that the changes of the two kinds of data remain in a linear range as a whole. When the number of iterations exceeds 50, the corresponding iteration parameters are relatively small. The parameters of the two models are mainly concentrated in the range of 0–25, while the corresponding data remain in the range of 0–2500 as a whole, indicating that the fuzzy analytic hierarchy model under the two data has relatively good linear characteristics.

#### 5. Conclusion

- (1) The proportion of the two different judgment indexes to model parameters is different. With the increase of iterations, the *CI* of judgment indexes shows a trend of gradual improvement. While the iteration index *CR* showed a trend of gradual decline, it can be seen that neither of the two iteration indexes can better reflect the change trend of the data. Judgment indexes and iteration indexes need to be considered comprehensively.
- (2) Different parameters lead to different sensitivity analysis of functions according to their different influences on the model. Parameters *a*, *b*, and *c* can

only reflect the local characteristics of model parameters, while parameter *d* shows obvious stage characteristics.

- (3) The staged characteristics of vector *A* and vector *R* on the iteration speed indicate that the analysis of vector on the model shows certain nonlinear characteristics. It can be seen from the vector curve that the complex iterative solution method is needed to obtain vector *B*.

#### Data Availability

The experimental data used to support the findings of this study are available from the corresponding author upon request.

#### Conflicts of Interest

The authors declared that they have no conflicts of interest regarding this work.

#### Acknowledgments

This work was funded by Jiangsu Higher Education Society of Higher Education Education Reform Research Project (2019JSJG507).

#### References

- [1] Y. Yang, Y. Chen, and Z. Tang, "Analysis of the safety factors of municipal road undercrossing existing bridge based on fuzzy analytic hierarchy process methods," *Transportation Research Record Journal of the Transportation Research Board*, vol. 10, no. 3, pp. 736–749, 2021.
- [2] R. Verma and S. Chandra, "Interval-valued intuitionistic fuzzy-analytic hierarchy process for evaluating the impact of security attributes in fog based internet of things paradigm," *Computer Communications*, vol. 175, no. 4, pp. 369–382, 2021.
- [3] K. Vahid, S. Aref, and S. Adel, "Hybrid fuzzy-analytic hierarchy process (AHP) model for porphyry copper prospecting in simorgh area, eastern lut block of Iran," *Mining*, vol. 2, no. 10, pp. 1245–1262, 2022.
- [4] R. Kasin and K. Peerapat, "Integrated fuzzy analytic hierarchy process and technique for order of preference by similarity to ideal solution for additive manufacturing printer selection," *Journal of Materials Engineering and Performance*, vol. 30, no. 9, pp. 6481–6492, 2021.
- [5] F. M. Kasie and G. Bright, "Integrating fuzzy case-based reasoning, parametric and feature-based cost estimation methods for machining process," *Journal of Modelling in Management*, vol. 26, no. 10, pp. 7269–7284, 2021.
- [6] C. Kim and J. S. Won, "A fuzzy analytic hierarchy process and cooperative game theory combined multiple mobile robot navigation algorithm," *Sensors*, vol. 20, no. 10, pp. 2827–2836, 2020.
- [7] A. O. Knay and B. T. Tezel, "Modification of the fuzzy analytic hierarchy process via different ranking methods," *International Journal of Intelligent Systems*, vol. 52, no. 3, pp. 439–451, 2021.
- [8] X. Liu, "Evaluation of influencing factors of intellectual property protection based on fuzzy analytic hierarchy

## *Retraction*

# **Retracted: Data-Driven Winter Landscape Design and Pleasant Factor Analysis of Elderly Friendly Parks in Severe Cold Cities in Northeast China under the Background of Artificial Intelligence**

### **Security and Communication Networks**

Received 26 December 2023; Accepted 26 December 2023; Published 29 December 2023

Copyright © 2023 Security and Communication Networks. This is an open access article distributed under the Creative Commons Attribution License, which permits unrestricted use, distribution, and reproduction in any medium, provided the original work is properly cited.

This article has been retracted by Hindawi, as publisher, following an investigation undertaken by the publisher [1]. This investigation has uncovered evidence of systematic manipulation of the publication and peer-review process. We cannot, therefore, vouch for the reliability or integrity of this article.

Please note that this notice is intended solely to alert readers that the peer-review process of this article has been compromised.

Wiley and Hindawi regret that the usual quality checks did not identify these issues before publication and have since put additional measures in place to safeguard research integrity.

We wish to credit our Research Integrity and Research Publishing teams and anonymous and named external researchers and research integrity experts for contributing to this investigation.

The corresponding author, as the representative of all authors, has been given the opportunity to register their agreement or disagreement to this retraction. We have kept a record of any response received.

### **References**

- [1] P. Shan and W. Sun, "Data-Driven Winter Landscape Design and Pleasant Factor Analysis of Elderly Friendly Parks in Severe Cold Cities in Northeast China under the Background of Artificial Intelligence," *Security and Communication Networks*, vol. 2022, Article ID 8218468, 11 pages, 2022.

## Research Article

# Data-Driven Winter Landscape Design and Pleasant Factor Analysis of Elderly Friendly Parks in Severe Cold Cities in Northeast China under the Background of Artificial Intelligence

Pengyu Shan  and Wan Sun

*College of Arts, Northeastern University, Shenyang, Liaoning 110819, China*

Correspondence should be addressed to Pengyu Shan; [shanpengyu@mail.neu.edu.cn](mailto:shanpengyu@mail.neu.edu.cn)

Received 16 June 2022; Revised 14 July 2022; Accepted 22 July 2022; Published 17 August 2022

Academic Editor: Hangjun Che

Copyright © 2022 Pengyu Shan and Wan Sun. This is an open access article distributed under the Creative Commons Attribution License, which permits unrestricted use, distribution, and reproduction in any medium, provided the original work is properly cited.

Urban parks not only combine the greening of the city with the natural landscape but also are places for people's daily fitness, leisure, entertainment, and activities to meet their psychological needs. At present, the design of our country's northeast severe cold city park is not perfect, which cannot fully highlight the regional characteristics and show the local winter natural landscape. Under the background of the lagging development of the northeast severe cold city park, we use artificial intelligence technology and data-driven algorithm to design a new northeast severe cold city elderly friendly park. The experimental results are as follows: (1) we analyze the development trend of population aging in our country. As the main demanders of urban parks, the elderly determined the research direction of the experiment, investigated the needs of different people for the park, and designed the function of the park according to the needs of the park. (2) On the basis of retaining the traditional garden design, show artificial intelligence technology in the design of urban parks and transforming the urban park design with intelligent construction can not only let tourists have better entertainment and exercise but also enable residents to better invest in the park surroundings. Intelligent park design can not only show the unique park landscape but also relieve the pressure of tourists.

## 1. Introduction

As the child of the scientific field in the new era, artificial intelligence technology can be seen in every industry. Of course, artificial intelligence also wants to show itself in the field of literature and art. This article mainly introduces the development and exploration of literature and art under the background of artificial intelligence technology. Through the big data survey and questionnaire collection and analysis, this paper investigates and analyzes the learning situation of Chinese subjects of middle school students and studies their reading situation and analysis ability from the perspective of students. The data survey and analysis show that 10% of the students have good literary reading and analysis ability, and more than 70% of the students have general literary reading and analysis ability. Fifteen percent of the students are poor

in literary reading and analysis. Through the combination of artificial intelligence technology, it is found that it can better cultivate students' literary learning style and improve their reading and analysis ability [1]. The development of artificial intelligence technology has brought many benefits to various fields, including education. This article explores how artificial intelligence brings opportunities for improving the studying process and burgeon creative educational methods, such as hybrid teaching. On this basis, the author attempts to put forward some preliminary suggestions: the combination of artificial intelligence technology and Chinese learning and reading [2]. With the development of artificial intelligence technology and the popularization of smartphones, the marketing mode of mobile client has become a new way for enterprises to promote the garment industry. This method can help consumers better choose products and promote

consumption. With the continuous improvement of China's international status, the development and construction of traditional garment customization application under the background of artificial intelligence is of great significance [3]. With the gradual development of artificial intelligence technology, the design of environmental art combined with artificial intelligence technology has been effectively recognized. How to realize the integration of artificial intelligence technology and environmental art design in the research is a new direction of artificial intelligence technology research. This paper mainly introduces how to integrate the two. The first step is to analyze the current social situation and existing problems of the environmental art design, compare the application of some artificial intelligence technology in environmental art design and the artificial environment with the traditional artificial intelligence model, and then collect and analyze the data through the experiment of artificial intelligence. The experimental analysis shows that the model constructed by artificial intelligence technology is more accurate and clearer than the traditional artificial construction model. Even the simulated three-dimensional image is more practical and realistic, which also shows that it has been widely used in reality [4]. To establish and create a safe computer network environment, the application of artificial intelligence in computer network technology under the background of big data is analyzed. First, introduce artificial intelligence and understand its development surrounded by big data. Then, it analyzes the current development status of artificial intelligence and defines the application direction of artificial intelligence technology in the field of computer network and communication problem-solving. Finally, the expert system, artificial neural network technology, data mining technology, autonomous agent technology, security management technology, problem-solving technology, expert knowledge base technology, and computer network fuzzy information processing technology are analyzed. This goal is to solve the difficulties by showing the characteristics and advantages of artificial intelligence technology, which provides a powerful shield for the security of computer network system [5]. Many studies have documented the link between the Arctic Oscillation (AO) and the frequency of winter extreme temperatures in East Asia. The explanation of the imbalance is that compared with the due north polar oscillation, the central point of the anti-Arctic Oscillation extends around, which is convenient and helpful to establish a closer relationship with the frequency of extreme weather. Therefore, the relationship between the number of extreme weather and anti-Arctic oscillation was more significant years ago. In addition, there is another view that heat flow expansion will be formed in the upper part of the airflow at the same time as the anti-Arctic Oscillation. Therefore, the kinetic energy of the anti-Arctic Oscillation better reflects the large-scale changes in extreme weather [6]. This is the kinetic energy evolution process of the cold and hot flow in Northeast China on July 19, 2010. The main causes and formation process of heat flow expansion in the severe cold area of Northeast China are discussed and studied. Research shows that as the air temperature rises, air molecules begin to

vibrate and move more, usually creating more distance between them, resulting in heat flow expansion. This study is particularly interested in assessing the role of thermal advection in the development of cold vortex bar clinic. The results show that the rising of air in relatively warm regions and the sinking of air in relatively cold regions are conducive to the release of turbulent extended exergy (eT), which is then converted into turbulent kinetic energy (KT). This process occurs in the formation and enhancement of cold vortices. In addition, the barotropic energy conversion is another important process of KT growth, which gradually increases after the cold vortex begins. In addition to friction consumption, the KT flux in the vertical direction will also consume part of KT. ET flux, baroclinic energy conversion, and diabatic generation are favorable factors for ET growth, but due to the release of a large amount of ET, the growth of ET decreases with time. In the process of cold vortex formation, the energy conversion process in the lower troposphere, including baroclinic and barotropic energy conversion, ET to KT energy conversion, and ET flux, is stronger than those in other regions. This explains the effect of excessive temperature between air molecules on heat flow expansion. Finally, temperature is a monotonic function of the average molecular kinetic energy of matter. When the temperature in the air rises, the air molecules begin to vibrate with each other and move at high speed [7]. Many studies have documented the link between the Arctic Oscillation (AO) and the frequency of winter extreme temperatures in East Asia. This paper explains the imbalance of extreme cold weather in the severe cold area of Northeast China and then deeply analyzes the causes of this extreme weather. The results show that the cause of this extremely cold weather is directly proportional to the occurrence of the Arctic Oscillation. If the occurrence of the Arctic Oscillation is not significant, the occurrence of this extremely cold weather is not significant. If the occurrence of the Arctic Oscillation is significant, it also indicates that the occurrence of the extremely cold weather is significant. The existence of this relationship can be explained by that compared with the proportional Arctic Oscillation, the inverse Arctic Oscillation extends from the center to all around, which is more helpful to compare with the frequency of extreme weather. Therefore, the frequency of extremely cold weather was more closely related to the Arctic Oscillation years ago. In addition, it is also said that when the extremely cold weather is inversely proportional to the Arctic Oscillation, there is a transverse vortex around the large airflow, which occurs in the center of the Arctic Oscillation. Therefore, the negatively correlated Arctic Oscillation can better reflect the instantaneous changes in the surrounding weather, which is closely related to the occurrence of extremely cold weather [8]. The evolution of summer temperature in China in the recent 40 years is diagnosed by rotating principal component (RPC) method, and an index reflecting the cold summer in Northeast China is obtained. The time lag correlation analysis is carried out with the 500 hPa potential height in the northern hemisphere and the Global SST. The low temperature in Northeast China usually starts from May and lasts for about one year, forming a "cold summer year." In

addition, the monthly average temperature in June of the previous year and June of the next year is significantly higher than the normal value. The results show that these characteristics are closely related to the atmospheric circulation anomaly in the “cold summer year.” The monthly average 500 hPa potential height in Northeast China from April to April of the next year is lower than the normal value while the data in the previous June and the second June are significantly higher than the normal level [9]. Using the reanalysis data of daily potential height from 1981 to 2010 (a total of 30 years) released by NCEP/NCAR, the Northeast China cold vortex (cvonc) is inverted and analyzed, the average state of cvonc is extracted and analyzed, the deviation index of cvonc is defined, and the rationality of describing the intensity of cvonc is discussed. The results show that (1) when cvonc is at 500 hPa, the probability distribution of block center potential height is similar to Gaussian regression normal distribution, and the result value obtained from Gaussian distribution has some corresponding characteristics. (2) The deviation index of cvonc is defined according to the average state of cvonc, which can not only represent the degree that cvonc deviates. On the whole, it also reflects some problems in some areas, which means that it can directly some strength characteristics [10]. Due to the special climate of winter city, winter city has a greater impact on the life of the elderly than other cities. Therefore, the design of new urban parks is the primary task of park designers [11]. By studying the needs of the parks near the residence of the elderly, the design of urban parks is gradually improved, making the design more humanized, systematic, and comprehensive. Exploring the urban park design plays an important role in the elderly, making the landscape space more suitable for the physiological and psychological needs of the elderly [12]. Ecological waterfront park landscape is an important resource for urban development and plays an important role in improving urban landscape. Taking the design of Wuhan Shahu Park as an example, this paper deeply conveys the urban ecological landscape design concept and technology; puts forward the ecological landscape design concept of unique, humanized, and renewable resources; and combines the historical context of the Heritage Park. It provides a certain reference for waterfront ecological landscape design [13]. Nanhai Forest Scenic Park covers an area of 370000 hectares. Every year, 20 million tourists come here for cross-country skiing, downhill skiing, hiking, and cycling. It is also home to surviving plant species and rare fauna such as goat horns and lynx. Recent pressures include the increasing concentration of skiing traffic at higher altitudes and more skiing due to the shortage of snow resources elsewhere [14]. This paper investigates the current situation of landscape design for the elderly in three community parks: Jingang Park, Feifeng Mountain Olympic Park, and Labor Park in Fuzhou. Combined with the physiological and psychological characteristics of the elderly, this paper analyzes the disadvantages of the design of Fuzhou elderly community park. Combined with community construction and horticultural treatment, a reasonable spatial layout and barrier-free design

are proposed to suit the elderly activities in Fuzhou Community Park [15].

## 2. Winter Landscape Design of Elderly Friendly Park under the Background of Artificial Intelligence

*2.1. Development of Artificial Intelligence.* The development of artificial intelligence technology has experienced technological innovation. It has been developed for more than 70 years, and it has stored immeasurable potential. Its development process can be distinguished from development time and technology. From the perspective of time evolution, the development of artificial intelligence technology can be divided into initiation stage, birth stage, golden period, first trough, peak period, second trough, and current development stage. Technically speaking, artificial intelligence can be developed into solving intelligence, perceptual intelligence, and cognitive intelligence.

*2.2. The Elderly Are Divided According to Age Standards.* The issue of population aging proposed at the United Nations in 1982 can be judged by the age of 60. Through the investigation and evaluation of the quality of the global human body and the aging of the population by the United Nations health organization, it further puts forward the standard for the differentiation of the age of the elderly. (1) The elderly aged between 60 and 74 are young and old. This age group is because their daily activities are relatively less than before. Due to the growth of age, in addition to their basic material needs, they also need to meet their spiritual and cultural needs; (2) the elderly aged between 75 and 89 are called the elderly. Most of the elderly in this age group basically do not carry out dynamic activities because their physical strength and intelligence are not as good as before. Their daily activities usually focus on walking in parks and communities; (3) those aged 90 and above become elderly people. Because they are basically self-cultivation at home, they are elderly, and partly because they cannot take care of themselves and need the care of their families.

*2.3. Town Park.* So far, there is no accurate and unified definition of the concept of urban park. There are many explanations from different angles. The encyclopedia points out that urban parks are a kind of urban green space. Urban parks are directly funded by the government or public organizations to provide public places for people to rest, entertainment, and play. Compared with other cities and towns in Northeast China, the development of parks and facilities in cities and towns is relatively old, and the development of parks is not balanced. Therefore, focusing on the cold cities in Northeast China, this paper designs the winter landscape of the elderly friendly park under the background of new artificial intelligence, which is convenient for the elderly to enjoy and play.

**2.3.1. Definition of Park Landscape Facilities.** Park landscape facilities refer to all public equipment in the park that can serve the people or have a specific function. The landscape facilities of Gong Park are indispensable to a park, which endows the park with functionality and uniqueness, which not only enhances the spatial quality of urban parks but also enhances people's economy of life.

**2.3.2. Division of Park Landscape Facilities.** The park landscape facilities are divided into (1) necessary landscape transportation facilities, such as the entrance and exit of a park and the park road. The entrance and exit of the park are the necessary passages of the park. The entrance and exit of the park must be simple and unobstructed and provide simple service facilities for tourists; (2) the activity places of the park landscape are combined with artificial intelligence to build new entertainment facilities to serve the masses. For example, replacing the traditional service staff with AI machines not only promotes artificial intelligence but also attracts the masses to play, launch intelligent shooting machines, and record themselves at a certain time. As the main places to rest, pavilions and chairs are also valuable heritage in Chinese traditional park culture and essential elements of modern gardens. Because the traditional pavilion seats are small in size and high in position, they are not suitable for the elderly, so special tables and chairs should be built for the convenience of the elderly; (3) the service facilities of the park shall include public toilet facilities and landmark landscape signs. Many parks are equipped with a small number of toilets, which makes it inconvenient to use. For the convenience of special elderly people, public toilets should be equipped with special barrier-free toilets. As the guiding route, transmitting information, and warning function of the park, the design of symbolic landscape signs should meet the characteristics of simplicity and easy to understand.

### 3. Artificial Intelligence Data-Driven Algorithm

**3.1. Research Model of Artificial Intelligence Machine.** What is support vector machine? In short, the initial definition of support vector machine is to find a hyperplane in a sample hyperspace. The learning purpose of support vector machine is to find a hyperplane with the largest interval.

The mathematical expression is

$$\min \frac{1}{2}|w|^2, \quad (1)$$

$$\text{s.t. } y_i(w^x x_i + b) \geq 1.$$

The optimization formula (1) solves the required hypersector, and the mathematical expression is

$$\min \frac{1}{2}|w|^2 + C \sum_{i=1}^m X\zeta_i, \quad (2)$$

$$\text{s.t. } y_i(w^x x_i + b) \geq 1 - \zeta_i, \quad \zeta_i \geq 0, i = 1, 2, \dots, m.$$

This choice of  $C$  also has a significant influence on the generalization expression of support vector machine. When  $C=0$ , support vector machine cannot achieve the effect of classification. When  $C$  is infinite, all samples are forced to meet the constraints of formula (1). Therefore, choosing an appropriate value for  $C$  exists a deep influence on the generalization performance of sustain vector machine.

As shown in Table 1, some common nuclear parameters are recorded. However, in practical applications, the parameters of SVM are mostly linear, and the data are inseparable. Therefore, most support vector machines are nonlinear. Support vector machine involves many parameters, one of which is the kernel parameter.

Convolutional neural network turns the full connection of neural network into partial connection and adds some weight sharing strategies. However, the learning method of convolutional neural network is still back-propagation algorithm.

Define a loss function between neural networks for simulation learning. There are two kinds of loss functions, one is mean square deviation, and the expression is

$$C(w, b) = \frac{1}{2m} \sum_{i=1}^m |y_i - f(x_i)|^2. \quad (3)$$

Cross-entropy expression:

$$C(w, b) = \frac{1}{2m} [y_i \ln f(x_i) + (1 - y_i) \ln (1 - f(x_i))]. \quad (4)$$

**3.2. Artificial Intelligence Machine Optimization Algorithm.** In the process of mathematics learning, optimization algorithm is an ancient but very practical mathematical skill in solving problems. In real scientific inquiry or life, many problems can be reduced to optimization problems, for example, the location of buildings, the path planning of road construction, and the investment of stocks and bonds. The first thing to learn about artificial intelligence technology is artificial intelligence machine optimization algorithm. Most AI machine learning algorithms involve optimization.

Gradient descent means: gradient descent means is a very classic and practical optimization method. When the function is not convex, the solution uncertainty of ladder descent method is the best solution, but when the action is concave, the solution must be the optimal solution. The expression of gradient descent method is

$$x^{k+1} = x^k + \lambda(-\nabla f(x^k)), \quad (5)$$

where  $-\nabla f(x^k)$  indicates the current location,  $x^k$  represents negative gradient direction, and  $\lambda$  represents the step size.

In learning machine model, in order to maintain the balance between the speed and accuracy of machine model learning algorithm, multiquantity gradient descent method and contingent gradient descent method are proposed. It can be seen that the advantages and disadvantages of the two algorithms also echo each other. The solution obtained by



TABLE 1: Common kernel parameters of vector machine.

Name of kernel function	Expression	Superparameter
Linear kernel	$K(x_i, y_i) = x_i^T y_i$	—
Polynomial kernel	$K(x_i, y_i) = (x_i^T y_i)^d$	$d \geq$ is the degree of polynomial
Gaussian kernel	$K(x_i, y_i) = \exp(- x_i - x_j ^2 / 2\sigma^2)$	$\sigma > 0$ is the bandwidth of Gaussian kernel
Laplace nucleus	$K(x_i, y_i) = \exp(- x_i - x_j /\zeta)$	$\sigma > 0$

the multiquantity gradient descent method is more global, but the efficiency is low. The probabilistic gradient descent method only solves the local optimal solution. When exploring problems, the combination of the gradient method and the probabilistic method not only meets the advantages of the probabilistic method but also meets the decline of the quality in the process of solving the problem.

The learning idea of Newton method is to expand the second-order Taylor expansion at the point to be calculated and then find the next point based on the point to be calculated. The mathematical expression is

$$f(x) = f(x^k) + \nabla f(x^k)(x - x^k) + \frac{1}{2}(x - x^k)^T \nabla^2 f(x^k)(x - x^k). \quad (6)$$

Take the derivative of formula (6) and make the derivative 0 as

$$\nabla f(x^k) + \nabla^2 f(x^k)(x - x^k) = 0. \quad (7)$$

Formula (7) is further improved to obtain the iterative formula of Newton method, and its expression is

$$x^{k+1} = x^k - \nabla^2 f(x^k)^{-1} \cdot \nabla f(x^k). \quad (8)$$

If the objective function of the solution is required to be a quadratic function, because the expansion of Taylor formula is a quadratic polynomial, when starting from a certain point, it only takes one step of circulation to reach the minimum value of  $F(x)$ .

Conjugate gradient method: let  $A$  be an order symmetric positive definite matrix  $n \times n$ , and let  $X$  and  $Y$  be  $n$ -dimensional vectors. If formula (9) holds, then  $X$  and  $Y$  are in common with respect to  $A$ .

$$X^T A Y = 0. \quad (9)$$

**3.3. Artificial Intelligence Machine Quantum Genetic Algorithm.** What is quantum genetic algorithm? The definition of quantum genetic algorithm is that in computer learning, the smallest unit of stored information is byte. If it is not 1, it is 0. In quantum computer, the smallest unit of information storage is qubit, either 1 or 0, or the superposition of 1 and 0. The expression of qubits is as follows:

$$|\psi\rangle = \alpha|0\rangle + \beta|1\rangle, \quad (10)$$

$$|\alpha|^2 + |\beta|^2 = 1. \quad (11)$$

If you want to change the value of qubits, you can change it through quanta  $\alpha$  and  $\beta$ . Value of quantum gate satisfaction  $UU^+ = U^+U$ , and  $U^+$  is the common matrix of  $U$ . The quantum gate updates the qubit through formula (12) and sets the new qubit as  $[\alpha'/\beta']$ , and the expression is

$$\begin{bmatrix} \alpha' \\ \beta' \end{bmatrix} = U \begin{bmatrix} \alpha \\ \beta \end{bmatrix}. \quad (12)$$

Superparameter optimization of genetic algorithm: the essence of the so-called hyperparameter is to find a set of suitable parameters for the learning of machine model, which can make the generalization ability of the machine model the strongest. However, the search for parameters is not random but to optimize the problem into a model and find parameters through optimization. The optimization parameter expression is

$$\lambda^* = \arg \min Err(x_{\text{test}}, A_\lambda(x_{\text{train}}, \theta)). \quad (13)$$

It is to select a set of good hyperparameters in the hyperparameter space (that is, select an optimal one and a set of hyperparameters after decoding) to minimize the generalization error of the machine learning model on the test set. However, the superparameter selection space is generally large or even infinite, and we usually do not know much about the superparameter selection space. Therefore, using optimization algorithm to solve this problem is a more effective idea.

**3.4. Artificial Intelligence Data-Driven Parameter Optimization.** Because the evolutionary algorithm is very effective in solving the cost of black box function, especially in solving hyperparametric optimization problems and machine learning models, the efficiency of the traditional population-based evolutionary algorithm is very low. Therefore, a data-driven optimization algorithm is suggested. This basic view of data-driven optimization is to use the estimation information of the solution to establish a regression model in the iterative optimization process. Regression model is also called agent model. Its main function is to predict which possible optimal solution in each iterative algorithm and then estimate these possible optimal

TABLE 2: Details of Ackley function to be optimized.

Type	Minimize
Decision variable value	$x_i \in [-30, 0, 30, 0]$
Global minimum	$x_i = 0, \forall i \in \{1, 2, \dots, N\}, f(x) = 0$
Function	$f(x) = 20 - 2 - \exp(-0.2\sqrt{1/N} \sum_{i=1}^N X_i^2) + e - \exp(1/N \sum_{i=1}^N \cos(2\pi x_i))$

solutions by using the actual objective function so as to reduce the number of objective function estimation.

**3.4.1. Gaussian Process Regression.** Gaussian process regression is used to define the traditional Gaussian process to the Gaussian distribution in time. The mathematical expression is

$$f(x) \sim \text{GP}(0, k(x, x')). \quad (14)$$

In formula (14),  $k(x, x')$  is the covariance function, and the commonly used covariance function expression is

$$k(x, x') = \exp\left(-\frac{1}{2}\|x_i - x_j\|^2\right). \quad (15)$$

How to carry out regression modeling through Gaussian process:

Suppose there is a training set  $D = \{(x_1, y_2), (x_2, y_2), \dots, (x_n, y_n)\}$ , now we need budget points  $x_{n+1}$  and budget value at  $y_{n+1}$ :

$$f_{n+1} \sim \text{GP}\left(\begin{pmatrix} K & k^T \\ k & k(x_{n+1}, x_{n+1}) \end{pmatrix}\right). \quad (16)$$

The distribution of  $f_{n+1}$  can be deduced from formula (16), and the expression is

$$p(f_{n+1} | D, x_{n+1}) = \text{GP}(u((x_{n+1}), \delta^2(x_{n+1}))). \quad (17)$$

In formula (17),  $u((x_{n+1}) = kK^{-1}f_{1:n}, \delta^2(x_{n+1}) = (k(x_{n+1}, x_{n+1}) - kK^{-1}k^T)$ . If there is a homogeneity problem, that is, when the decision variables have the same impact on the final solution result, the covariance function of formula (18) is usually selected:

$$k(x_i, x_j) = \exp\left(-\frac{1}{2\theta^2}\|x_i - x_j\|^2\right). \quad (18)$$

If there is a heterogeneity problem, that is, when the decision variables have different effects on the final solution result, the covariance function of formula (19) is usually selected, and the expression is

$$k(x_i, x_j) = \exp\left(-\frac{1}{2}(x_i, x_j)^T \text{diag}(\theta)^{-2}(x_i - x_j)\right). \quad (19)$$

In addition to the above two kernel functions, there is also a classical kernel function, which is expressed as

$$k(x_i, x_j) = \frac{1}{2^{\ell-1}\Gamma(\ell)} \left(2\sqrt{\ell}\|x_i, x_j\|^\ell H_\ell\left(2\sqrt{\ell}\|x_i, x_j\|\right)\right). \quad (20)$$

TABLE 3: Details of SVM to be optimized.

Superparameter	Type	Selection interval
C	Continuity	[1.0,1000.0]
$\partial$	Continuity	[0.00001,1.0]

#### 4. Winter Landscape Design and Pleasant Factor Analysis of Elderly Friendly Parks in Severe Cold Cities in Northeast China Based on Data-Driven Parameter Optimization

**4.1. Experimental Analysis of Data-Driven Parameter Optimization.** The hyperparametric optimization based on multiple regression function is compared with the classical Bayesian algorithm. The experimental test shows that the hyperparametric optimization based on Mars increases the time productivity to a great degree on the premise of ensuring the solution quality.

The first basic problem is Ackley function. At present, finding the extreme value of this function is a recognized challenge in the field of optimization. Some detailed instructions can be found in Table 2.

The second problem is about sorting out the random parameters of the support vector machine. In the second problem, we only need to optimize the parameters of core bandwidth 8 and core positive side coefficient C. Detailed information is given in Table 3.

As shown in Tables 3 and 4, the random parameters of the support vector machine and the details to be optimized are given.

The third question is about sorting out random hyperparameters. I think of how to sort out random hyperparameters. The details in Table 3 are as follows.

**4.2. Investigation and Analysis of Population Aging.** According to the survey data obtained from Table 5, the number of the world's elderly population over the age of 60 has reached 720 million, accounting for 12% of the world's population and growing at the rate of 90 million per year. It is expected that by 2050, the number of elderly people in the world will increase to 2.064 billion, accounting for 22% of the world's population.

As shown in Figures 1 and 2, the development situation of China's 60-year-old population from 2000 to 2050, and the comparison between China and the world population development situation from 1950 to 2050 shows that the aging proportion of China's population is increasing.

The rate of population aging in China is higher than that in other countries. China has always been a populous country in the world. In recent decades, social economy

TABLE 4: RF details to be optimized.

Superparameter	Type	Selection interval
Minimum number of partition templates	Dispersed	Integer range [2, 40]
Minimum number of samples required	Dispersed	Integer range [2, 20]
Bootstrap	Dispersed	Integer range [2, 20]
Standard	Dispersed	True or false
Standard	Dispersed	Gain or entropy

TABLE 5: Development trend of the world's elderly population.

years	Population (100 million)	Proportion over 65 (%)	Proportion of quantity over 60 (%)	Average life span	Population growth rate (%)
1950	25.15	5.1	8.04	46.0	17.7
1960	36.69	5.4	8.34	54.8	20.8
1970	44.49	5.9	8.49	58.0	17.2
1980	52.46	6.2	9.25	9.25	16.2
1990	56.78	6.5	9.51	62.6	15.7
2000	61.23	6.8	9.93	64.9	12.7
2020	82.05	8.7	14.27	70.5	9.5

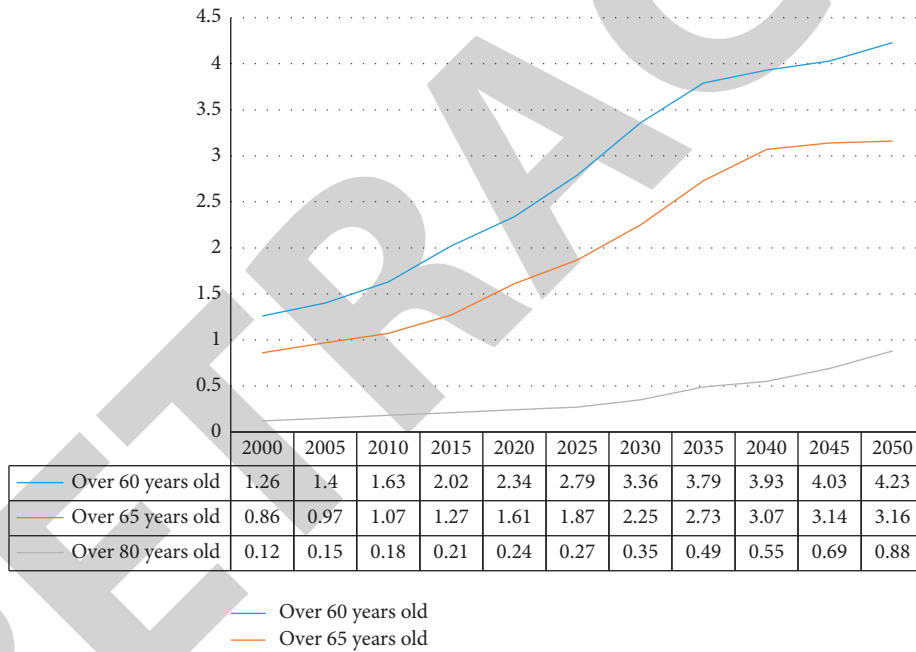


FIGURE 1: Development situation of 60-year-old population from 2000 to 2050.

has developed rapidly, living standards and medical standards have improved, people's life expectancy has been prolonged, and mortality has been reduced; at the same time, the family planning policy has been implemented since 1979, which has reduced China's birth rate. The combined effect of low birth rate and low mortality has led to the development of rapid population aging in China.

**4.3. Investigation and Design Analysis of Winter Tree Species in the Park.** According to the survey and statistics, the cultivated plants in northeast urban parks are mainly evergreen trees and shrubs.

As shown in the data survey in Table 6, the green vegetation of urban parks in the severe cold area of Northeast China is relatively rare, including evergreen broad-leaved trees, and almost none. According to the research and investigation, the greening of parks in the severe cold area of Northeast China is usually dominated by deciduous trees, and the proportion of green forest vegetation should be controlled at about 25%. It can not only meet the needs of tourists but also make the park lack of green landscape.

**4.4. Analysis of Public Service Facilities in Parks.** The equipment design of the urban park is also a part of the park environment. In the design of the urban park, the level of

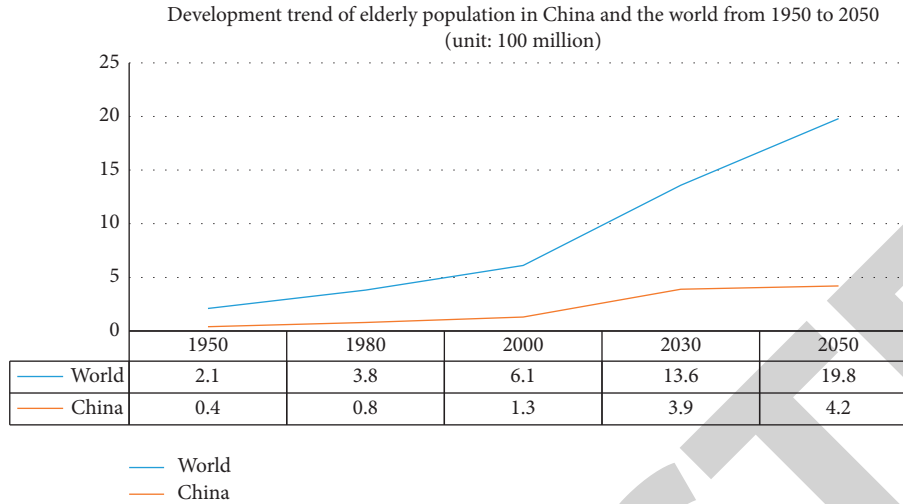


FIGURE 2: Comparison of the development situation of the elderly population between China and the world from 1950 to 2050.

TABLE 6: Common tree species in northeast urban parks.

	Serial number	Plant name	Section	Latin name
Evergreen tree	1	Juniper	Baike	Sabina chinensis
	2	Cedar	Pinaceae	Cedrus deodara
	3	Chinese pine	Pinaceae	Pinus tabulaeformis
	4	White-barked pine	Pinaceae	Pinus bungeana
Deciduous trees	5	Elm	Ulmaceae	Ulmus pumila
	6	Ailanthus	Bitter wood	Ailanthus altissima
	7	Koelreuteria paniculata	Nonpatients division	Koelreuteria paniculata
	8	Dryland willow	Salicaceae	Salix matsudana
Evergreen shrub	9	Euonymus japonicus	Celastraceae	Euonymus japonicus
	10	Yucca gloriosa	Phoenix tailed orchidaceae	Yucca gloriosa
	11	Longbai	Baike	Juniperus chinensis
	12	Crape myrtle	Lysimachiaceae	Lagerstroemia indica
Deciduous shrub	13	Pomegranate	Pomegranate	Punica granatum
	14	Lilac	Oleaceae	Syringa oblata
	15	Gold and silver woo	Loniceraceae	Lonicera maackii
	16	Winter Jasmine	Oleaceae	Jasminum nudiflorum

public equipment and facilities shows the service quality and civilization provided by the park to tourists from the side. The matching of public facilities in the park is another public facility landscape in addition to the natural landscape and construction landscape, and its design also reflects another taste of the urban park.

Through investigation and analysis, it is found that people's low utilization rate of urban parks in winter is not because people prefer to move in indoor space. It is difficult to resist the wind, and cold is only one of the factors. Another important factor is that the public service facilities of urban parks are not perfect, and there is no humanized design based on the needs of users. The data show that in the current environment, only 21% of people will choose to take regular outdoor activities. If we improve the construction of public facilities, 63% of people will be willing to choose outdoor activities.

As shown in Figures 3 and 4, the design of urban parks is people oriented. Designers should look at it from the perspective of users. They need to meet the users' needs for the

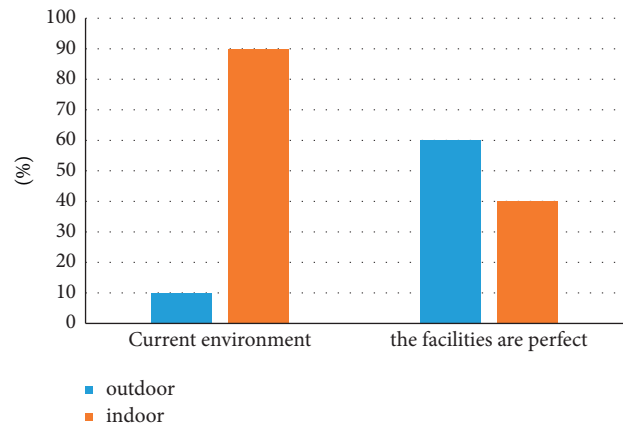


FIGURE 3: Selection of winter venues.

functions and life of the park and also need to meet the users' visual enjoyment, emotional pleasure, and spiritual resonance in the park so as to integrate users with the park and

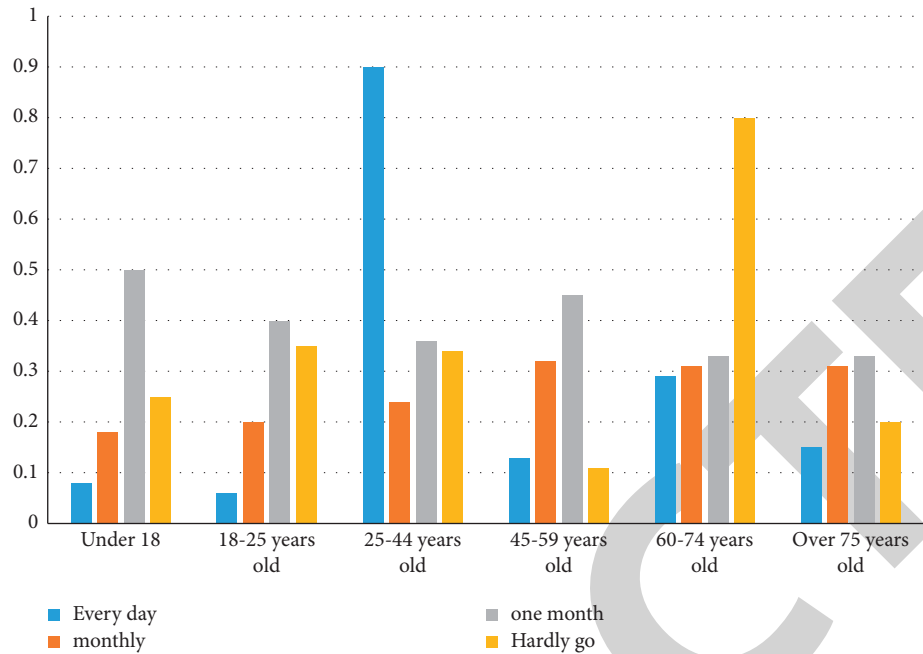


FIGURE 4: Frequency of park use by age group.

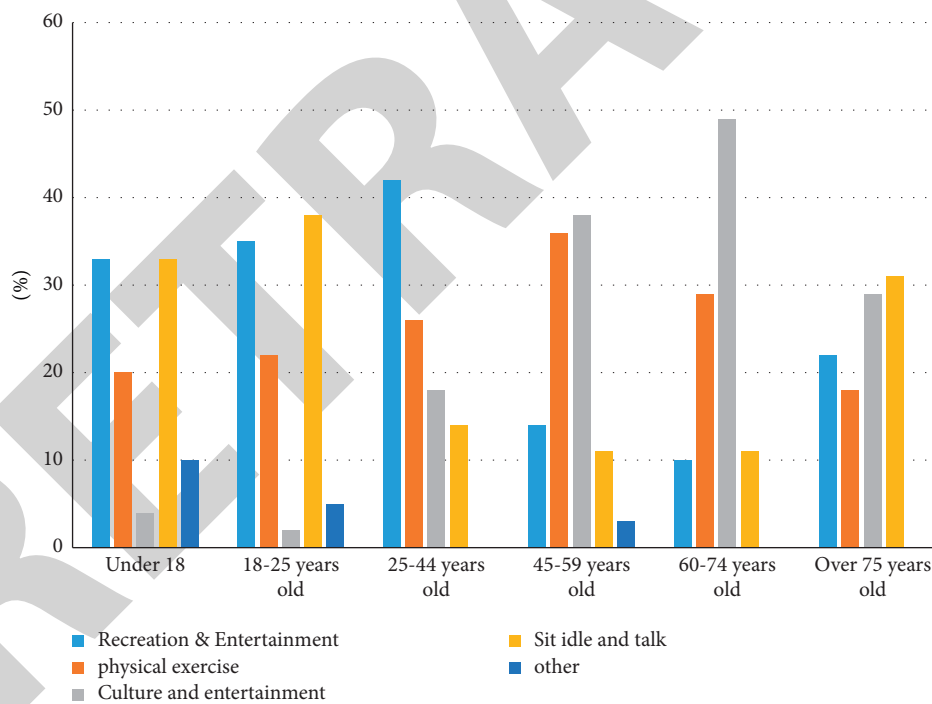


FIGURE 5: Main activities of users of different ages in the park.

show a harmonious relationship. As long as the above requirements are met, designers can design popular urban parks.

As shown in Figure 5, different types of places are very necessary in the design of urban parks. Due to some minor inconveniences, the proportion of 75-year-olds on vacation, traveling, and chatting has increased. The park must have quiet entertainment areas and communication places. The security design of such websites should be considered.

Although the younger generation rarely go to the park, it is also useful to bring them an entertainment space in winter and attract them to go out of the house and get close to nature. In order to meet the needs of young people for leisure, sightseeing, communication, and play, urban parks should create different spaces, both open and comfortable environment and warm and private semienclosed space.

As can be seen from Figure 5, the most frequently used urban parks are the young elderly aged 60–74 and 50% of

TABLE 7: Impact of environment, public infrastructure, and residents' satisfaction.

Variable name	Very satisfied (%)	Satisfaction (%)	General (%)	Dissatisfied (%)	$\chi^2$	$P$
Landscape aesthetics	20.65	28.39	20.00	13.55	11.56	0.02
Biodiversity	25.81	23.23	21.94	17.42	5.84	0.21
Park characteristic line	23.23	24.52	22.58	15.48	5.12	0.27
Acoustic environment	27.10	17.42	23.23	18.71	3.22	0.52
Air quality	27.10	23.23	14.84	21.29	7.94	0.09
Human comfort	23.87	26.45	20.65	16.77	5.31	0.25
Psychological security	20.65	23.23	21.29	18.06	15.22	0.04
Sports fitness	20.65	21.29	23.23	20.00	3.71	0.44
Humanistic atmosphere	22.58	27.10	17.42	18.71	8.26	0.08
Marking facilities	15.48	21.94	25.16	20.65	3.09	0.54
Cultural education	19.35	23.87	22.58	16.77	4.55	0.33
Safety protection	24.52	19.35	23.87	19.35	3.59	0.46
Public infrastructure	15.48	16.13	27.10	26.45	5.66	0.22
Traffic convenience	21.29	25.81	29.03	14.84	1.30	0.86
Site flatness	23.23	23.23	23.23	18.71	10.33	0.03
Site sanitation and plant conservation	19.35	23.23	20.00	16.13	14.13	0.007

TABLE 8: Regression analysis of influencing factors of residents' satisfaction.

Project	Influence factor	$B$	Wals	$P$	Exp ( $B$ )
Demographic characteristics	Educational level	-0.30	2.66	0.10	0.75
	Tour frequency	0.07	0.13	0.72	1.07
Tourist motivation	Natural scenery	0.82	4.07	0.04	2.27
	Other	0.53	1.68	0.20	1.70
	Psychological security	0.47	8.98	0.00	1.61
Environment and public services	Site flatness	0.13	0.72	0.40	1.14
Overall model test	Site sanitation and plant conservation	0.10	0.50	0.48	1.11
	Constant	-3.21	9.91	0.00	0.04

the young elderly often enter urban parks in winter. Secondly, of middle-aged people, more than 80% will enter the park at least once a month. Their main activities in the park include culture, entertainment, and physical exercise.

**4.5. Analysis of Pleasant Factors in Urban Parks.** As shown in Tables 7 and 8, the "complete satisfaction" of acoustic environment and air quality is 27.1%, which is higher than that of other systems (see Table 7). The quality of the air environment and people's comfort are more than 5%, so we are satisfied with the air environment and comfort of the park. Chi-square test showed that ecological diversity, garden characteristics, decibel environment, air environment, and other indicators failed to pass the significance test ( $P > 0.05$ ), indicating that biodiversity, garden characteristics, acoustic environment, air quality, and other factors did not affect residents' satisfaction. Landscape and aesthetic flatness have a significant impact on residents' satisfaction ( $P < 0.05$ ), and safety, health, and site maintenance have a significant impact on residents' satisfaction ( $P < 0.01$ ).

Eight independent variables such as education level, tour frequency, and natural scenery were included in the regression to test their significance. Logistic regression was used to analyze the influencing factors of residents'

satisfaction. It is shown in Table 8. Among them, the natural landscape in winter has a profound impact on tourists' satisfaction. In addition, psychological safety is also affecting tourists' satisfaction, both of which are positively correlated.

## 5. Conclusion

Firstly, understand the development process of artificial intelligence technology, the division of the development process and its concept, as well as the research direction and background of the subject. Then, it introduces the division standard of the elderly, confirms the research purpose of this paper, and introduces the definition of the urban park and how to design an urban park combined with the special winter landscape in Northeast China. Then, it introduces the artificial intelligence data-driven algorithm, mainly including the construction of the artificial intelligence machine research model, artificial intelligence machine optimization algorithm, artificial intelligence machine quantum genetic algorithm, and the artificial intelligence machine data-driven optimization. Finally, the data-driven parameter optimization experiment is carried out, the development trend of population aging is investigated, the vegetation of urban parks in Northeast China is investigated and screened, and the public facilities and park demand of urban parks are analyzed and investigated.



## *Retraction*

# **Retracted: Research on the Cultivation of College English Listening, Speaking, Reading, and Writing Ability by VR Technology**

### **Security and Communication Networks**

Received 26 December 2023; Accepted 26 December 2023; Published 29 December 2023

Copyright © 2023 Security and Communication Networks. This is an open access article distributed under the Creative Commons Attribution License, which permits unrestricted use, distribution, and reproduction in any medium, provided the original work is properly cited.

This article has been retracted by Hindawi, as publisher, following an investigation undertaken by the publisher [1]. This investigation has uncovered evidence of systematic manipulation of the publication and peer-review process. We cannot, therefore, vouch for the reliability or integrity of this article.

Please note that this notice is intended solely to alert readers that the peer-review process of this article has been compromised.

Wiley and Hindawi regret that the usual quality checks did not identify these issues before publication and have since put additional measures in place to safeguard research integrity.

We wish to credit our Research Integrity and Research Publishing teams and anonymous and named external researchers and research integrity experts for contributing to this investigation.

The corresponding author, as the representative of all authors, has been given the opportunity to register their agreement or disagreement to this retraction. We have kept a record of any response received.

## **References**

- [1] Z. Zeng, "Research on the Cultivation of College English Listening, Speaking, Reading, and Writing Ability by VR Technology," *Security and Communication Networks*, vol. 2022, Article ID 4241870, 9 pages, 2022.

## Research Article

# Research on the Cultivation of College English Listening, Speaking, Reading, and Writing Ability by VR Technology

Zhen Zeng 

*School of Applied Foreign Languages, Xinyang Vocational and Technical College, Xinyang 464000, China*

Correspondence should be addressed to Zhen Zeng; [zengzhen@xyvtc.edu.cn](mailto:zengzhen@xyvtc.edu.cn)

Received 1 June 2022; Revised 12 July 2022; Accepted 20 July 2022; Published 12 August 2022

Academic Editor: Hangjun Che

Copyright © 2022 Zhen Zeng. This is an open access article distributed under the Creative Commons Attribution License, which permits unrestricted use, distribution, and reproduction in any medium, provided the original work is properly cited.

With the development of VR technology, it is possible to apply innovation to English teaching, and realize new breakthroughs and innovations in English teaching. In the background of information technology widely used in teaching, VR technology has become a very popular new technology because it can promote teaching better and make teaching effect more obvious; Through VR technology in English learning in listening, speaking, reading, and writing mode, we summarize the application of this technology in education industry at home and abroad, and put forward the purpose and significance of this research. Firstly, through the listening, speaking, reading, and writing mode of VR technology in English learning; In order to better evaluate the performance comparison under different modes, the score and weight distribution method are carried out for listening, speaking, reading, and writing. Secondly, by evaluating the value of  $E(X)$  in the nonexisting combination mode, the corresponding optimal proportion distribution scheme can be obtained. Finally, by comparing the scores of 8 groups of people under VR technology and statistical learning mode, the results show that VR technology has obvious advantages in improving listening, speaking, reading, and writing scores.

## 1. Introduction

2016 is called “the first year of VR.” Since 2016, China’s VR industry has started to develop rapidly, but it is also facing serious talent problems and unequal development [1]. By analyzing the current situation of VR industry chain structure in China, this paper expounds the demand direction of VR talents in China from three fields: technology production, content creation, and operation planning [2, 3]. This paper examines the possibility of training talents in reality from the perspective of the links among schools, public authorities, and enterprises. With the rapid development of Internet technology, the tradition of terminal equipment general education and the modern network autonomous learning new musical instrument training classroom complement and strengthen each other, especially in the learning resources of students, whether it is the allocation of working hours, that is, anyone can learn more selectivity and stability at their own rhythm [4]. However, self-sufficient online education for college students remains

a challenge. English learning is becoming more and more important in all stages of people’s learning and development, especially in compulsory education and higher education [5]. However, in real life, many students have obstacles in English learning and development [6]. In clarifying the needs of talents and establishing an effective talent training mechanism, VR technology is used to cultivate college English listening, speaking, reading, and writing skills [7]. The combination of VR technology and college English listening, speaking, reading, and writing can not only promote the development of VR technology but also help people to learn English [8, 9].

English learning has been accompanied by the growth of students. Most students begin to contact English from preschool education or primary school. Junior high school English has become an essential hard test subject, and most students learn English more or less. At the stage of higher education, English is also an extremely important language and subject, but at the stage of university, many students encounter bottlenecks in learning English, and even English

has become a major obstacle in many students' learning career. Constantly, exploring new and more suitable ways of learning English for modern students has become a major trend of development.

After the epidemic, online learning has become a new way of learning. During the online teaching period, QQ, WeChat, and Nail have become the learning tools chosen by most students and teachers. Superstar Erya network course platform, university MOOC, rain class, and BILIBILI software have become learning tools for many students to learn to watch more learning content [10]. However, for many students, online learning lacks self-control and online learning conditions, and online learning is still developing.

Virtual reality is called VR for short [11, 12]. VR was put forward by Haron Lanier, founder of VPL in the early 1980s. This is a technology that can make full use of the graphics system on the computer and various interface devices (such as reality and control) for interactive 3D environment diving. In computer technology, computers and interactive 3D environments are called virtual environments (virtual environments are called EVs). Virtual reality technology is supported by virtual reality simulation platform (VRP) [13]. VR technology can be widely used in urban planning, interior design, bridge and road design, real estate sales, tourism and education, hydropower, geological disasters, education and training, and other fields to provide practical solutions [14]. We boldly innovate and combine VR technology with college English listening, speaking, reading, and writing, which not only promotes the development of VR technology but also helps students make progress in English learning. It is shown in Figures 1–3.

## 2. VR Technology Research Model

VR technology research model is an improved probabilistic recommendation model based on different aspects of application [15]. The traditional probabilistic estimation model simply estimates the influence of parameters on events, but only estimates it theoretically or experimentally, ignoring the complexity of events in real life, so it can only be a theoretical or unpractical algorithm. In order to solve this problem, based on the traditional probability estimation model, VR virtual technology is added to help solve the problem that the experiment does not conform to reality. It provides a reasonable method model for improving college English listening, speaking, reading and writing. The structure of VR technology research model is shown in Figure 4.

In Figure 4, VR technology is used to evaluate English listening, speaking, reading, and writing. This proportional

distribution scheme is a reasonable distribution of proportional standards in experimental exam-oriented education. Therefore, this distribution scheme meets various requirements such as teaching content distribution and teaching examination. For professional examinations, the ratio of each item can be adjusted, and the corresponding preference can be improved.

The influence of VR on English listening, speaking, reading, and writing is evaluated by calculating the moment estimator. According to the corresponding expression, it is as follows.

When a single project is evaluated continuously, the evaluation method is as follows:

$$\begin{aligned}\alpha_m &= \int_{-\infty}^{+\infty} x^m f(x; \theta_1, \dots, \theta_k) dx, \\ \mu_m &= \int_{-\infty}^{+\infty} (x - E(X))^m f(x; \theta_1, \dots, \theta_k) dx.\end{aligned}\quad (1)$$

When a single project is evaluated discrete, its evaluation method is as follows:

$$\begin{aligned}\alpha_m &= \sum_{i=1}^n f(x_i; \theta_1, \dots, \theta_k), \\ \mu_m &= E(X - E(X))^m = \sum_{i=1}^n (X_i - E(X))^m \\ &\quad \cdot P(X = X_i, \theta_1, \dots, \theta_k).\end{aligned}\quad (2)$$

For  $\theta_1, \dots, \theta_k$  dependent, when the sample size is relatively large,  $\alpha_m$  shows:

$$\alpha_m = \alpha_m(\theta_1, \dots, \theta_k) \approx \sum_{i=1}^n \frac{X_i^m}{n}. \quad (3)$$

When  $m = 1, \dots, k$ , the (3) can be converted to the following:

$$\alpha_m(\theta_1, \dots, \theta_k) = \alpha_m, (m = 1, \dots, k). \quad (4)$$

The whole sample is evaluated by sample matrix, and the whole moment is called unbiased estimation. The corresponding unbiased estimation is explained for the first-order origin moment  $\alpha_{n1}$  and the second-order center moment  $m_{n2}$ :

$$E(\alpha_{n1}) = \frac{1}{n} E\left(\sum_{i=1}^n X_i\right) = \frac{1}{n} \sum_{i=1}^n E(X) = \alpha_1. \quad (5)$$

The estimation of the second-order central moment is shown as follows:

$$\begin{aligned}E(m_{n1}) &= \frac{1}{n} E\left(\sum_{i=1}^n (X_i - \bar{X}_n)^2\right) = \frac{1}{n} E\left(\sum_{i=1}^n (X_i^2 - 2X_i\bar{X}_n + 2\bar{X}_n^2)\right), \\ &= \frac{1}{n} \sum_{i=1}^n E(X_i^2) - \frac{1}{n} \bar{X}_n E\left(\sum_{i=1}^n X_i\right) + E(\bar{X}_n^2) = \frac{1}{n} \sum_{i=1}^n E(X_i^2) - E(\bar{X}_n^2).\end{aligned}\quad (6)$$

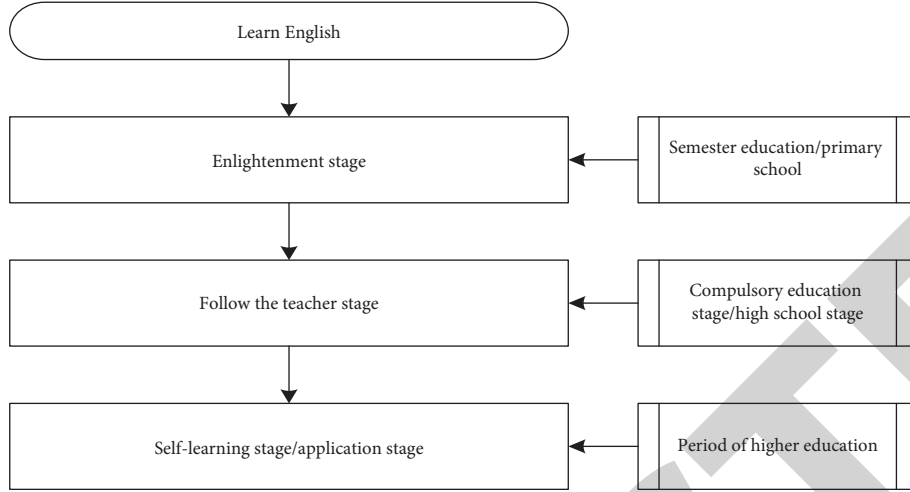


FIGURE 1: English learning at different stages.

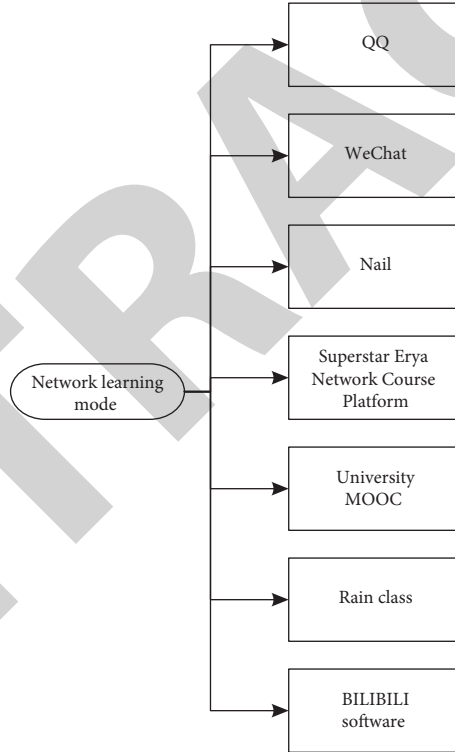


FIGURE 2: Students' learning methods during the epidemic network period.

Expect the probability distribution in Table 1, assuming an average distribution, and the formula is shown as follows:

$$E(X_1) = \frac{(X_1 + X_2 + X_3 + X_4)}{4}, \quad (7)$$

$$E(\theta) = E(X_1). \quad (8)$$

In the process of English teaching, the probability analysis of listening, speaking, reading, and writing is carried out, assuming that the distributions are  $\{X_1, X_2, X_3, X_4\}$ , as shown in Table 1.

Under the same number of people in the previous period, different proportions are set to get different expectations, as shown in Table 2.

In Table 2, the scores of listening, speaking, reading, and writing are assigned, and the proportion method or weight below the scores. The score is multiplied by the weight and accumulated to obtain the corresponding  $E(X)$  value. Different  $E(X)$  values are evaluated to get the corresponding optimal proportional structure. In Table 2, the value of  $E(X)$  is too large or too small. It is reasonable to choose an intermediate value.

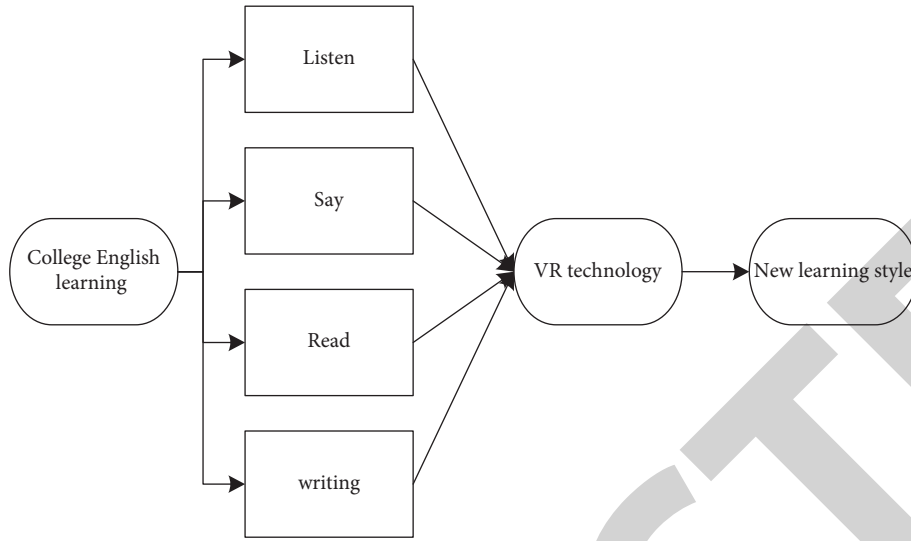


FIGURE 3: VR combined with a new way of English learning.

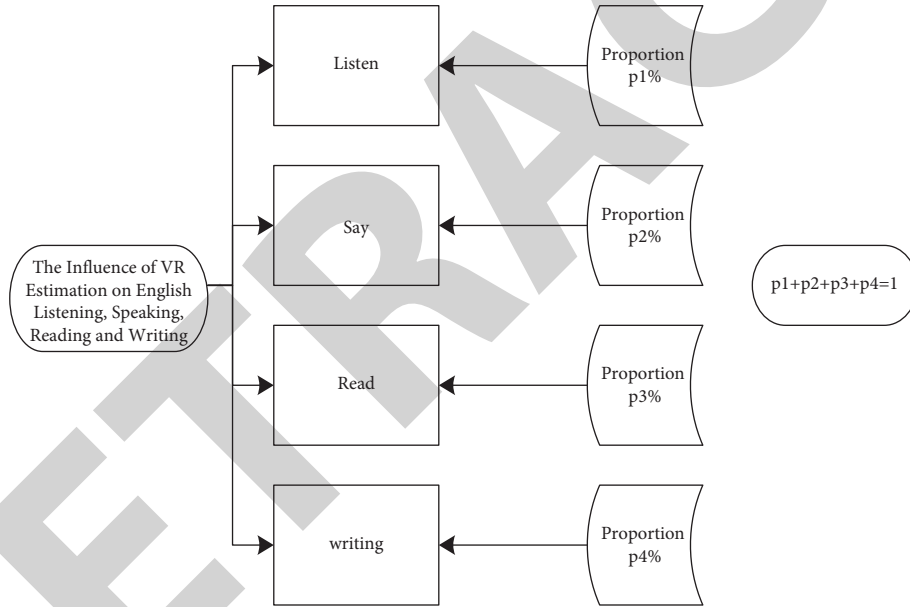


FIGURE 4: The influence of VR estimation on English listening, speaking, reading, and writing.

TABLE 1: VR affects the probability of English listening, speaking, reading and writing.

Category	Listen	Say	Read	Writing
Proportion	X1	X2	X3	X4

TABLE 2: Expected values under different examples.

Sample	Listen	Say	Read	Writing	E(X)
Sample 1	10 30%	49 30%	2 30%	39 10%	22.2
Sample 2	40 20%	30 30%	15 30%	15 20%	20.5
Sample 3	90 20%	5 30%	3 30%	2 20%	20.8

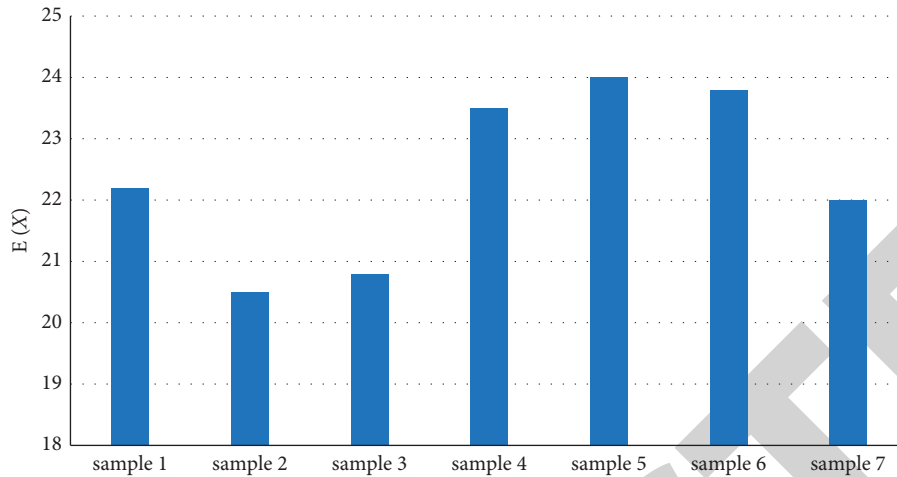


FIGURE 5: Values of different journals.

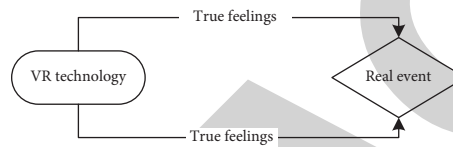


FIGURE 6: VR experience process.

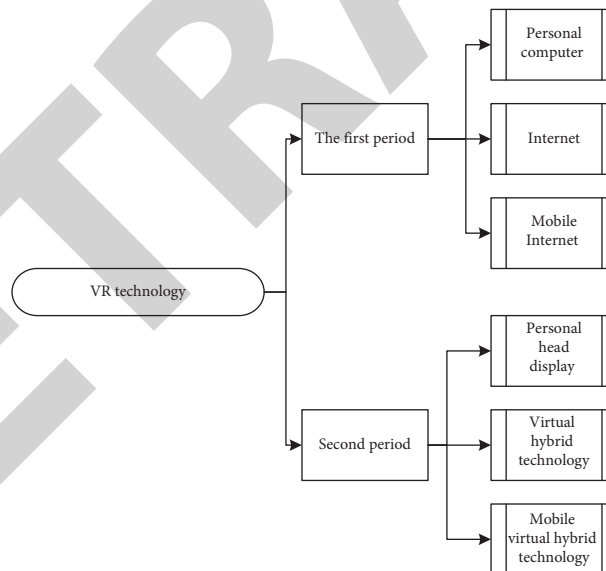


FIGURE 7: Development of VR in different periods.

When the personnel relationship with different proportional relationships is set at any time, different journal values are generated, as shown in Figure 5:

### 3. English Learning Methods Based on VR Technology

**3.1. English Learning Process.** VR technology can create and experience the computer simulation technology of virtual

world, and can give users a real immersive experience, as if they were in an event. It is shown in Figure 6.

The first period of VR technology brought people personal computers, Internet, and mobile Internet. The second period will bring people personal head display, virtual hybrid technology, and mobile virtual hybrid technology. It is shown in Figure 7.

Just as the Internet has developed to enable everyone to use electronic computers, VR technology will also develop to



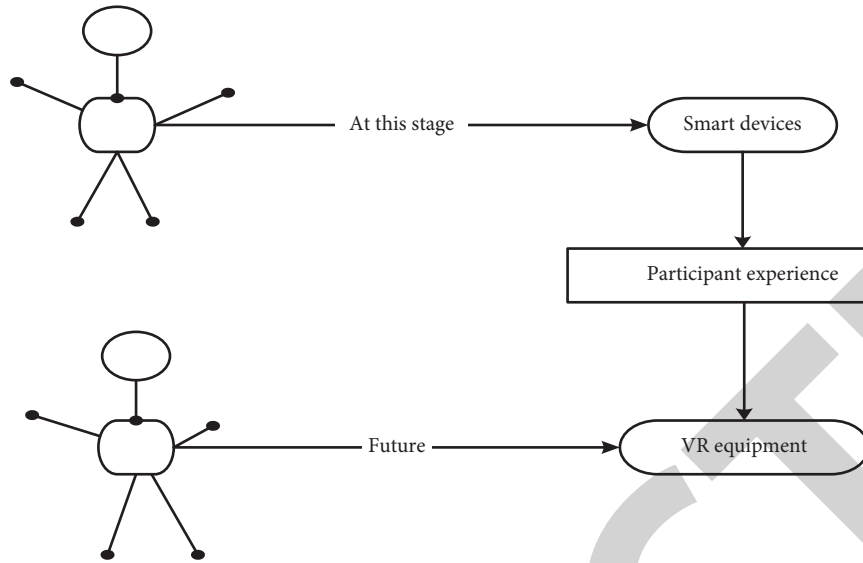


FIGURE 8: VR intelligent process.

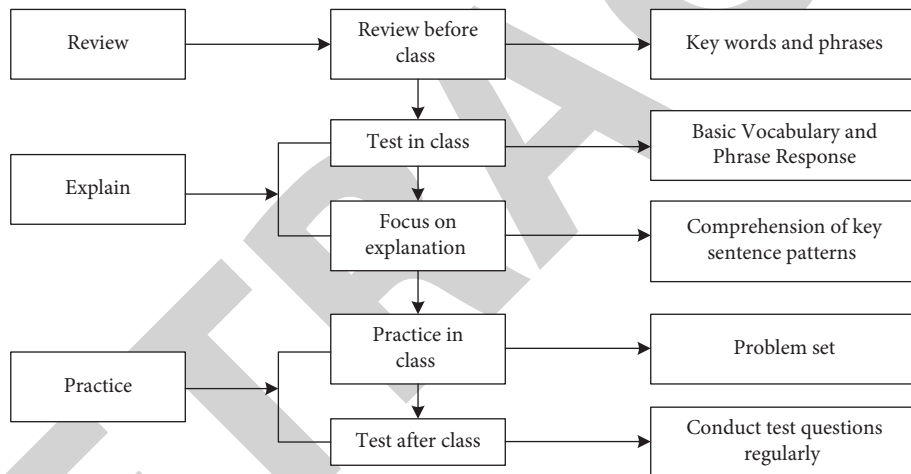


FIGURE 9: Traditional classroom teaching design.

TABLE 3: Achievement statistics under traditional English learning mode.

Sample	Listen	Say	Read	Write	Total
No 1	18.6	12.6	13.5	20.6	65.3
No 2	19.4	13.4	14.2	18.6	65.6
No 3	18.8	12.4	13.2	21.3	65.7
No 4	19.6	11.6	11.2	20.1	62.5
No 5	17.6	12.8	12.4	18.9	61.7
No 6	18.8	14.3	13.6	17.3	64
No 7	20.7	12.7	12.8	18.4	64.6
No 8	20.2	12.3	13.1	18.3	63.9

enable everyone to own and use VR machines and equipment in the future. This is the irresistible development direction of scientific and technological progress, and VR technology will be applied to people's lives, including intelligent English learning. It is shown in Figure 8.

According to the report, in the era of artificial intelligence, mixed reality and immersive experience are playing an increasingly important role in modern education. VR

technology can help us learn at a lower cost, in a shorter time and more effectively. These data show that the test scores of students who use immersion technology will increase by 22%. With the continuous popularization of educational internationalization and the rapid growth of English education demand, the integration of VR technology into learning is bound to become an important step in the reform and modernization of college English education industry.

TABLE 4: Achievement statistics under VR English learning mode.

Sample	Listen	Say	Read	Write	Total
No 1	19.3	14.9	14.8	22.3	71.3
No 2	20.6	15.3	15.1	20.6	71.6
No 3	19.8	13.5	14.6	23.5	71.4
No 4	21.3	13.2	13.4	21.2	69.1
No 5	19.5	13.6	14.5	19.5	67.1
No 6	19.8	15.2	15.9	19.3	70.2
No 7	21.8	14.8	14.6	19.6	70.8
No 8	21.9	13.7	15.2	19.7	70.5

### 3.2. Advantages of VR Technology

**3.2.1. Learners' Practical Experience.** Virtual reality technology gives College English learners an immersive feeling that traditional educational media cannot achieve, and can significantly improve the conversion rate of knowledge. With the 360-degree panoramic screen, you can meet Americans in English, just like you do in your native language environment. On-the-spot learning scene enables students to have a deeper understanding of how spoken English is used in real life, which significantly improves learning efficiency and achieves higher English learning results.

**3.2.2. Learners Have More Authentic and Interesting Conversations and More Authentic English and American Language Environments.** VR technology simulates the English and American real-life language environment, so that college English learners can feel the foreign language atmosphere, cultivate their interest in learning, and improve their learning initiative. After many simulations of facing foreigners in real life, students can communicate with foreigners more skillfully, and even after going abroad, students can speak English fluently.

**3.2.3. Innovate Learning Mode to Attract Students and Parents.** The educational ideas in 1980s and 1990s, which grew up in the Internet age, have also changed obviously. Due to the high utilization rate of digital education and the influence of education in Europe and America, children's thinking on education has become more profound and systematic. It is more important to improve the quality of interactive experience education and professional knowledge. VR technology is a new way for college English listening, speaking, reading, and writing.

**3.2.4. The Present Situation and Future of VR Education Applied to English.** VR is used to learn architecture, organizational structure, virtual hypothesis, and video courses, but VR technology is rarely applied. VR technology is very difficult to get the recognition of students, teachers and parents, not to mention changing the way of education. The fundamental problem is that many VR technicians want to apply the past education methods and methods directly to VR technology. In fact, it is to put a new shell on the old way. The application of VR technology to education is not "decoration," but a complete change in modern language education methods.

## 4. Comparison of the Application of VR Technology in English Teaching

**4.1. Traditional Classroom Teaching Design.** In traditional classroom teaching, the corresponding content is usually displayed with the help of electronic whiteboard and office software PPT. The specific implementation steps in the classroom are shown in Figure 9:

**4.2. Application of VR in English Teaching.** This paper selects some contents in college English to practice and apply English listening, speaking, reading and writing under VR technology, after two years, all the subjects have completed the study of English teaching content, and have a certain familiarity with the teaching materials. All the experimental contents are carried out in the form of review lessons. All the subjects meet the requirements of the subjects, have the same educational and cultural background, and have the same basic English level. 80 of them were tested, and 10 of them were averaged in one group. The scores of listening, speaking, reading, and writing are 30, 20, 20, and 30, respectively. Traditional teaching and VR English teaching are shown in Tables 3 and 4.

Table 3 shows the distribution of listening, speaking, reading, and writing scores in traditional English teaching, and Table 4 shows the distribution of listening, speaking, reading, and writing scores in English teaching using VR technology. The two tables are divided into 8 groups of students for testing, and the scores of these 8 groups of students are random. After the implementation of VR technology, the overall level of English has been improved, which fully demonstrates the advantages and significance of adopting VR technology in English teaching practice. It can be seen from Tables 3 and 4 that VR English learning mode has improved compared with traditional English learning results, and the effect of improving scores is obvious, as shown in Figure 10.

It can be seen from Figure 10 that the learning effect after adopting VR technology has been obviously improved, especially in the fourth group, with an average score of 6.6 points. This group has poor grades, but there is much room for improvement. Therefore, VR technology has a good learning effect on English learning.

The following is a comparison from various aspects of listening, speaking, reading, and writing. Through experimental teaching, students' mastery of listening, speaking, reading, and writing questions has also been improved.

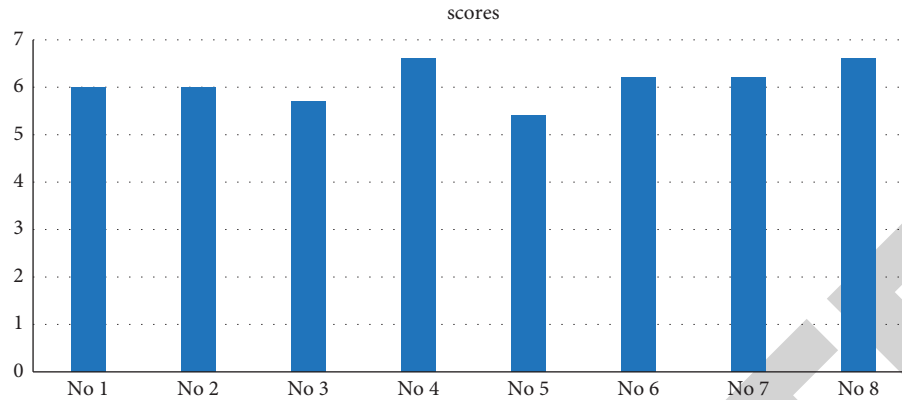


FIGURE 10: VR and the total score improvement of traditional learning.

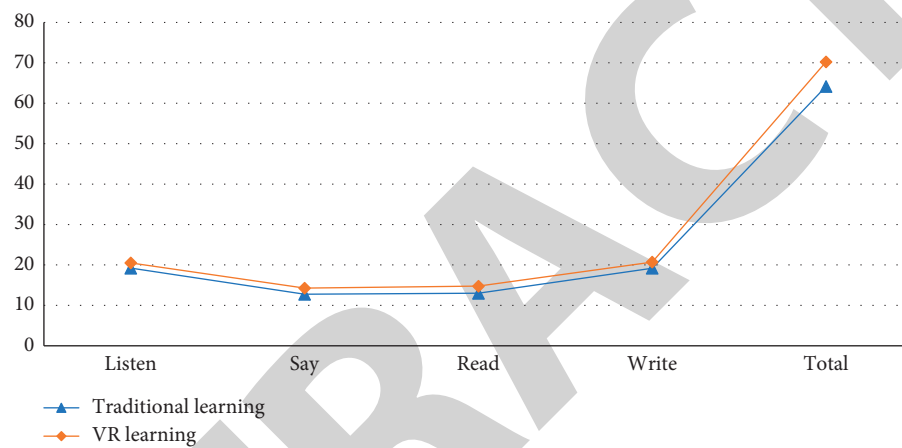


FIGURE 11: Comparison of VR and traditional learning achievements.

Because all grammar knowledge points of questions are collected, students need to rely on classroom explanation to make them.

Understanding and mastering the data comparison of this question shows that different groups of students have basically the same mastery of this question. The improvement of each method of listening, speaking, reading, and writing is shown in Figure 11.

## 5. Conclusion

To sum up, it is feasible to apply VR technology reasonably to English listening, speaking, reading, and writing. Using VR model can effectively help to apply it to English learning, and students' academic achievements and learning enthusiasm can be improved. VR technology will continue to develop in the future.

## Data Availability

The experimental data used to support the findings of this study are available from the corresponding author upon request.

## Conflicts of Interest

The author declares that there are no conflicts of interest regarding this work.

## References

- [1] Y. Wang, "Current situation research on integrated development and application of China's "publishing + VR/AR"[J]," *Publishing Research Quarterly*, vol. 37, no. 2, 2021.
- [2] B. Liu and W. Zhou, "Research on China's AR/VR industry transformation strategies in the context of domestic and foreign market changes," *E3S Web of Conferences*, vol. 235, no. 17, Article ID 03037, 2021.
- [3] X. Li and X. Hu, "Current status of ceramic industry and VR technology used in ceramic display and dissemination," *Scientific Programming*, vol. 2021, no. 12, pp. 1–8, Article ID 7555550, 2021.
- [4] L. Niu, "Retracted article: the conversion of traditional arts and crafts to modern art design under the background of 5G mobile communication network," *Personal and Ubiquitous Computing*, vol. 25, no. S1, pp. 15–11, 2021.

## Retraction

# Retracted: Value Assessment for a Theory-Oriented Flipped Classroom of Physical Education Based on Multi-Source Data Analysis

### Security and Communication Networks

Received 8 August 2023; Accepted 8 August 2023; Published 9 August 2023

Copyright © 2023 Security and Communication Networks. This is an open access article distributed under the Creative Commons Attribution License, which permits unrestricted use, distribution, and reproduction in any medium, provided the original work is properly cited.

This article has been retracted by Hindawi following an investigation undertaken by the publisher [1]. This investigation has uncovered evidence of one or more of the following indicators of systematic manipulation of the publication process:

- (1) Discrepancies in scope
- (2) Discrepancies in the description of the research reported
- (3) Discrepancies between the availability of data and the research described
- (4) Inappropriate citations
- (5) Incoherent, meaningless and/or irrelevant content included in the article
- (6) Peer-review manipulation

The presence of these indicators undermines our confidence in the integrity of the article's content and we cannot, therefore, vouch for its reliability. Please note that this notice is intended solely to alert readers that the content of this article is unreliable. We have not investigated whether authors were aware of or involved in the systematic manipulation of the publication process.

Wiley and Hindawi regrets that the usual quality checks did not identify these issues before publication and have since put additional measures in place to safeguard research integrity.

We wish to credit our own Research Integrity and Research Publishing teams and anonymous and named external researchers and research integrity experts for contributing to this investigation.

The corresponding author, as the representative of all authors, has been given the opportunity to register their agreement or disagreement to this retraction. We have kept a record of any response received.

### References

- [1] N. Li, "Value Assessment for a Theory-Oriented Flipped Classroom of Physical Education Based on Multi-Source Data Analysis," *Security and Communication Networks*, vol. 2022, Article ID 6540710, 9 pages, 2022.

## Research Article

# Value Assessment for a Theory-Oriented Flipped Classroom of Physical Education Based on Multi-Source Data Analysis

Na Li 

Shandong Institute of Physical Education, Jinan, Shandong 250102, China

Correspondence should be addressed to Na Li; [lina@sdpei.edu.cn](mailto:lina@sdpei.edu.cn)

Received 27 April 2022; Accepted 18 July 2022; Published 8 August 2022

Academic Editor: Hangjun Che

Copyright © 2022 Na Li. This is an open access article distributed under the Creative Commons Attribution License, which permits unrestricted use, distribution, and reproduction in any medium, provided the original work is properly cited.

In order to overcome the problem of students' boredom in physical education theory classes in general, and to give full play to the role of assessment in guiding, diagnosing, motivating and proving, this paper analyses the multi-source data generated during the teaching process, which can predict students' subsequent learning status. Based on the collection and processing of data from multiple sources, this study takes the PE course as an example and predicts the course performance based on multiple dimensions; and carries out empirical analysis with the actual course performance through numerical correlation, ranking correlation and the bottom band. The analysis was compared with actual course grades through numerical correlation, ranking correlation and bottom band warning coverage of students. The results of the study show that the earliest grade prediction using taught courses has the highest student warning coverage; the highest grade prediction based on unit tests has the highest numerical relevance and ranking relevance; and the highest grade prediction based on unit tests has the highest student warning coverage.

## 1. Introduction

Since the 21st century, with the continuous progress and development of information technology in education, how to integrate computer-related technology with the field of physical education has gradually formed an important research direction [1]. Smart education based on modern information technology has received great attention at the national level. In the field of professional sports theory courses, the rapid development of the Internet and various digital terminals has promoted big data research, and data analysis has shown great potential in improving the quality of education, optimising the learning process and improving the learning experience [2, 3]. Educational data analytics is used as a supporting technology for building smart education, for understanding and optimising the learning process and learning context [4]. Learning analytics is used to monitor and evaluate the learning process [5–7]. Al Afi and Rao Naidu [8] constructed a personalized adaptive online learning analysis model based on online teaching data, which can be applied to personalized resource delivery and learning result analysis. The use of process evaluation

based on big data can effectively promote adaptive development of learners. Cross-domain correlation and data analysis based on educational big data from multiple data sources can uncover hidden phenomena and patterns in the teaching and learning process, which is conducive to assisting decision-making in physical education [9].

According to the students interviewed, the process performance assessment enables students to understand their learning situation in a timely manner and guide their learning behaviour correctly, especially that a test paper is no longer used to assess the degree of knowledge mastery [10–12]. In particular, instead of using a test paper to assess knowledge mastery, students' attitudes, values, behaviours and abilities are included in the assessment, and a "point system" is used to record students' learning behaviour, which effectively guides their learning behaviour. Students' satisfaction with the indicators of "classroom participation, classroom order, classroom communication and cooperation" is high, with an average score of 4.5 or above. The classroom atmosphere is particularly good, as every student has the opportunity to participate in the classroom. Students' satisfaction with the indicators of "knowledge

acquired, emotions developed and skills learnt” is high, with an average score of over 4.6. Information technology application skills have been improved to different degrees [13].

Big data in education records data on students’ basic information, campus life, classroom learning and extra-curricular learning, which can be used to assess current academic status as well as to predict students’ future performance and academic early warning [14–17]. The research and application of big data in education is entering a phase of rapid development, but there are still the following problems: (1) the extent of data in education is further strengthened, and the variety and total amount of data is increasing, but the education and teaching mode has not changed substantially as a result, and smart education based on big data in education still has a long way to go. This paper aims to collect and analyse data from multiple sources in the teaching and learning process to investigate the learning status and effectiveness of students and to predict the learning status of students in the course. The course is based on the collection and processing of data from multiple sources.

*1.1. Data Collection.* Make full use of modern information technology to further optimise the structure of classroom teaching, so that students can learn and communicate in class, reducing the time for teachers to teach in class and increasing the time for tutorials and question and answer sessions in class, further optimising the structure of classroom teaching and improving the efficiency and quality of teaching [18]. This will reduce the time spent on lectures and increase the time spent on question and answer sessions, further optimising the classroom teaching structure and improving the efficiency and quality of classroom teaching [19].

Improve the classroom learning behaviour contract to guide students’ independent learning and self-management [19]. The classroom teaching management system should not be a cold rule, but a classroom learning behaviour contract agreed upon by teachers and students, with clear boundaries of classroom behaviour standards for better fulfilment of the contract [20].

Adding evaluation criteria for cooperative group learning and strengthening guidance and monitoring of the learning process in learning groups [21]. In order to promote cooperative learning in learning groups and to supervise communication, discussion, collaboration and reflection among peers, improvement measures are as follows: (a) guide learning groups to draw up a common learning contract and evaluation criteria, and to conduct self-assessment and mutual assessment of group members; (b) explain and explain group assignments and ways and means of completing them; (c) guide (c) guiding learning groups to make full use of each other’s strengths and resources to complement each other’s weaknesses; (d) adding evaluation criteria for group work sharing and collaboration to encourage mutual monitoring among learning groups.

The same correlation analysis was conducted for the 2013 year group. The correlation values between Physical Education courses and other core course for the 2013 and 2014

years were extracted and constructed into Table 1, and the values were averaged for both years [22]. From Table 2 can be seen that the three courses with the highest correlations are Computer Networking, Physical Education and Object-Oriented Programming, indicating that they have the greatest influence on each other. However, the Physical Education course was offered before Physical Education and Computer Networking, and these courses with later chronology cannot be used as a basis for prediction. Therefore, Table 1 selects the three pre-trending courses that are ahead of the chronological order as the basis for prediction, and the values of their correlation coefficients are averaged and then normalised to form the corresponding weighting coefficients.

The way in which a course grade is predicted from an existing core course grade is shown in equation (1):

$$ForrScore = \sum_{i=1}^m (q'_i \times Score_i). \quad (1)$$

In equation (1), the Forr Score represents the individual grade for the predicted course and is calculated by multiplying the weighting factor  $q'_i$  with the previous trend course grade and summing.

The predicted grades for the PE course are obtained by equation (1) and ranked within the group. The students who are lagging behind in their predicted performance (e.g. the last 15% of students, 12 students, whose numbers and names have been treated accordingly to protect their rights) can be identified [23].

This group of students can be educated in advance by communicating with the class teacher and the lecturer, and by providing focused attention and intervention during the teaching process to strengthen the process of control.

*1.2. Reversing the Classroom Model Set-Up.* The Technology Acceptance Model (TAM) was proposed by Davis in 1989, as shown in Figure 1, and includes perceived usefulness, perceived ease of use, attitude towards use and behavioural intention [24]. Numerous empirical studies have found that TAM mostly explains differences in usage intentions and behaviour. Perceived usefulness and perceived ease of use are the main measures of technology acceptance behaviour, with perceived usefulness being the user’s perceived ability to bring performance to the job, perceived ease of use being the user’s perceived ease of use of the technology, and attitude towards use being the mediating variable between perceived usefulness and perceived ease of use, which acts to influence behavioural intentions and thus the actual behaviour of the user [25]. TAM indicates that the user’s The higher the perceived ease of use and perceived usefulness, the more positive their attitudes towards use will be, and the stronger the influence of perceived usefulness and perceived ease of use in the early stages of learning and behaviour [26]. The flipped classroom uses a platform for online learning and discussion, therefore, TAM was chosen as the theoretical support to determine students’ acceptance of the flipped classroom.



TABLE 1: Correlation statistics between physical education courses and core courses of the major for both cohorts.

	Operating system (level 14)	Operating system (level 13)	Average value	Forward normalization
C language programming	0.18	-0.06	0.06	0.09
Data structure	0.17	0.39	0.28	0.41
Object oriented programming	0.21	0.48	0.34	—
Operating system	0.22	0.34	0.28	—
Database principle	0.19	0.41	0.3	—
Algorithm design and analysis	0.5	0.2	0.35	—
Computer network	0.45	0.27	0.36	—

TABLE 2: Correlation analysis between the core courses of the major for the class of 2014.

Correlation coefficient	C language programming	Data structure	Object oriented programming	Operating system	Database principle	Algorithm design and analysis	Software engineering	Computer network
C language programming	1	0.33	0.26	0.18	0.12	0.16	0.18	0.33
Data structure	0.33	1	0.22	0.17	0.1	0.02	0.1	0.2
Object oriented programming	0.26	0.22	1	0.21	-0.03	0.31	0.42	0.45
Operating system	0.18	0.17	0.21	1	0.22	0.19	0.5	0.45
Database principle	0.12	0.1	-0.03	0.22	1	0.14	0.28	0.15
Algorithm design and analysis	0.16	0.02	0.31	0.19	0.14	1	0.48	0.37
Software engineering	0.18	0.1	0.42	0.5	0.28	0.48	1	0.6
Computer network	0.33	0.2	0.45	0.45	0.15	0.37	0.6	1

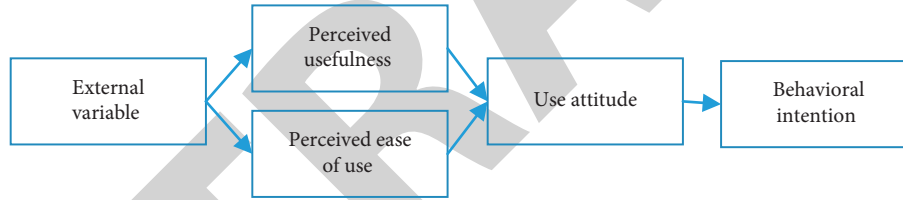


FIGURE 1: Technology acceptance model (TAM).

This study is based on TAM and guided by the Expected Value Theory and Collective Efficacy Theory to design a model of student problem solving skills in accordance with the flipped classroom model, as showed in Figure 2.

The structural model consists of three components: TAM, task factors and collective efficacy.

Firstly, the TAM component consists of the potential variables of ease of use of the platform, usefulness of the flipped classroom model, and acceptance of the flipped classroom model. The TAM component is designed to observe the usefulness and ease of use of the platform and online course. The ease of use of the platform and online course will reduce the disruption of the learning process and ensure that learners learn smoothly. The ease of use of the platform and the usefulness of the flipped classroom model in turn have an impact on the acceptance of the flipped classroom model, so that the increased ease of use of the platform and the usefulness of the flipped classroom model will lead to learner acceptance of the flipped classroom model and thus motivate students to learn. Therefore, hypotheses H1, H2 and H3 are proposed in this study [27].

The next component was the task factor. According to the Expected Value Theory, when students perceive the value

of a task assigned by the teacher to be high, they will try to complete the task to maximize the value of the task, i.e. their motivation will increase accordingly. Therefore, hypothesis H4 is proposed.

Finally, the collective efficacy component consists of three potential variables: individual evaluation, group evaluation and problem-solving ability. According to the theory of collective efficacy, in independent learning, students who are sure of their own abilities and complete the corresponding learning tasks will be motivated by the evaluation of task completion, and in group learning, students who evaluate their own group and believe in their peers will be motivated accordingly. The increase in motivation can lead students to solve difficulties in the learning process and thus improve their problem solving skills. Therefore, hypotheses H5, H6 and H7 are proposed in this study.

## 2. Empirical Research Process and Results

The course “Database” was chosen as the experimental course, with three consecutive classes per week, and the experimental period was 18 weeks in total. First, the course

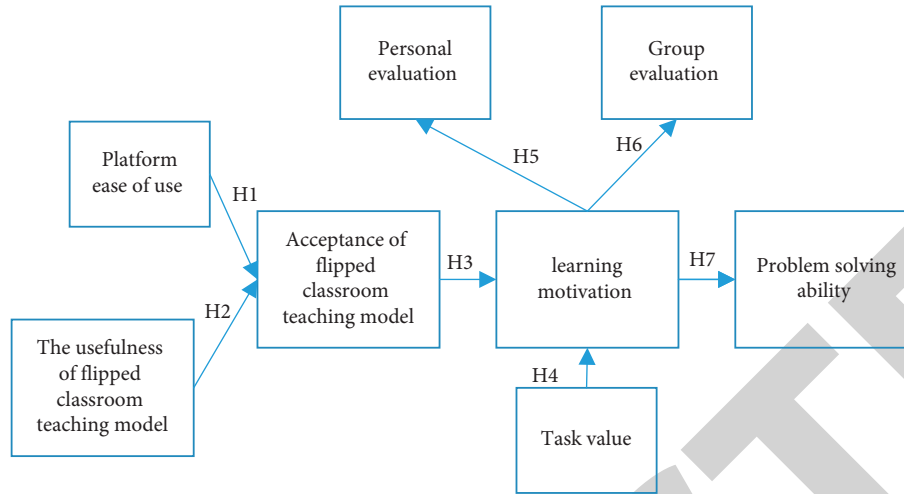


FIGURE 2: Student problem solving skills model.

instructor recorded online videos (15–20 minutes/video) and collected resources related to the course, and the teacher observes the number of times learners watch the videos and the progress of the videos through the TronClass backend to keep track of learners' learning progress. In addition, when learners encounter doubts during online learning, they can ask and answer questions in the course discussion module, through which teachers can grasp the difficulties in the learning process and the learning status of learners [28]. The teacher focuses on difficult questions to broaden students' horizons, deepen their knowledge construction and develop their creative thinking. Relevant data by the pedagogues, to grasp the teaching progress and to improve the quality of the lessons [29].

Figure 3 represents the distribution of the predicted grades based on the professional course and the actual course grades, with the horizontal coordinates being the individual student serial numbers and the vertical coordinates being the grade values. The correlation between the two sets of data is 0.67, indicating a good correlation between predicted and actual grades (The y-axis represents the score, and the x-axis represents the video length)

The two sets of data were ranked within groups separately and displayed as showed in Figure 4. The correlation of the rankings was 0.73, which was higher and higher than the correlation of the numerical values. This indicates that students' rankings have a higher degree of stability and that individuals' within-group learning ability and attitude towards learning are more stable across different specialised courses, significantly higher than the correlation with the numerical value of grades that are more strongly correlated with the specific content studied. (The y-axis represents the score, and the x-axis represents the ranking)

Figure 4 lists the last 12 actual grades in the PE course (representing 15% of the students in both classes) and shows that nine of the last 12 students predicted appeared in the last 12 of the actual grades, giving a prediction accuracy of 75%.

The unit tests indicate students' attitudes and stage learning outcomes, and these data can clearly be applied to course early warning with the advantage of real-time,

dynamic updates (as the number of unit tests increases, the stability and accuracy of the predicted results will increase).

The numbers on the horizontal coordinates in Figure 5 represent the first N unit tests, and the average of the first N unit test score is used to represent the predicted course grade; the numbers on the vertical coordinates represent the correlation coefficient. The correlation coefficient between the average of the first two unit tests and the actual grade of the course is 0.56. From the change in height of the bars, the correlation coefficient between the average of the unit tests and the actual grade of the course gradually increases and stabilises as the number of unit tests increases, and the correlation coefficient between the average of six unit tests and the actual grade of the course is as high as 0.79, reflecting a high correlation. This shows a high correlation [12].

The correlation coefficient between the mean of the six unit tests and the actual course grade was 0.79, showing a high correlation. This indicates that it is feasible to predict the course by the mean of the course unit test score. In addition, the method is dynamic and progressive: the initial prediction can be made after the first unit test of the course, and the correlation with the final grade of the course is low due to the small number of statistics; however, as the number of lectures and unit tests increases, the statistics cover more of the course and show the academic performance of individual students at more stages in time. So the correlation continues to increase and stabilise as showing in Figure 6. (The y-axis represents the grade, and the x-axis represents the course)

With the increasing popularity and use of smart teaching tools and online teaching platforms, an increasing amount of data is being generated on the mobile and PC side of the Internet. In this paper, the data from the mobile teaching data (Rain Classroom data) and the data from the virtual simulation experimentation platform (Experiment Building data) are collected and counted separately to develop course performance predictions. The combination of the two is further investigated and analysed.

The classroom data are mainly derived from the multiple-choice questions and attendance in the theory class of the PE course, which can reflect the students' participation,

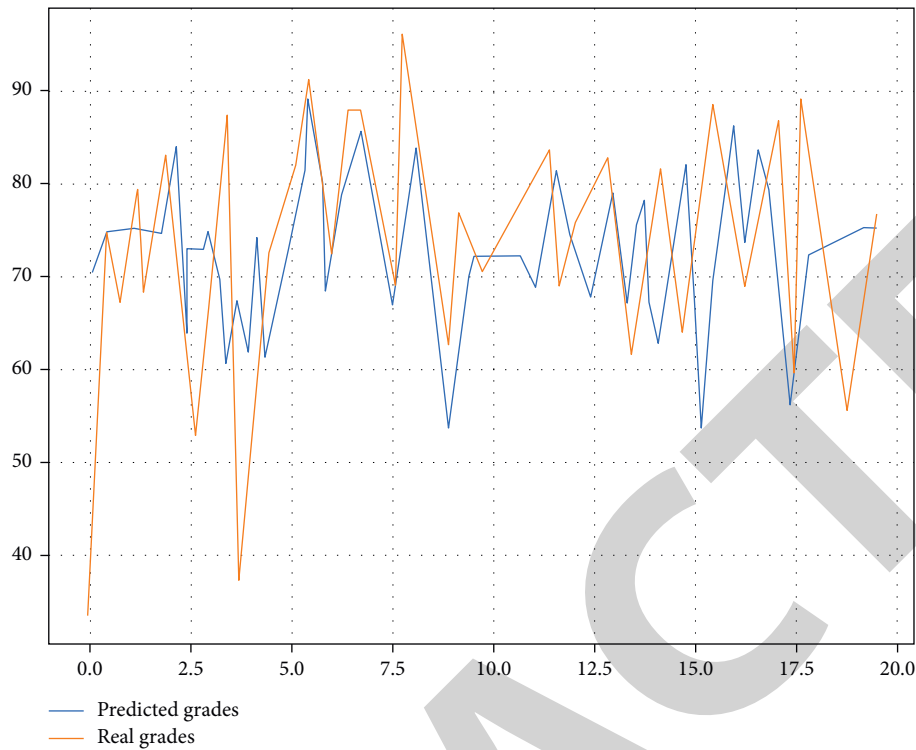


FIGURE 3: Diagram showing predicted and actual grades based on relevance to the major.

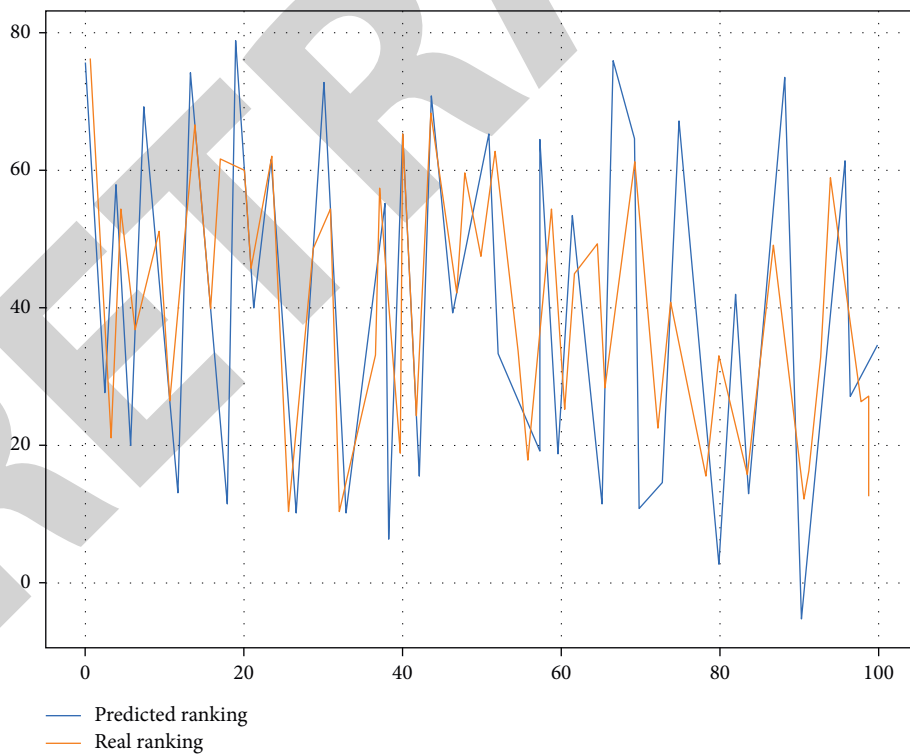


FIGURE 4: Diagram showing predicted and actual ranking based on relevance of major courses.

concentration and learning effect in the theory class. But the data is also fragmented and not systematic.

These data were standardised according to a percentage system, so that the values for each individual student were

converted to a numerical space from 0 to 100, and this value was used to represent the predicted grades based on the rain classroom data [30]. The predicted and actual grades based on the Rainy Classroom data are shown in Figure 7, with a

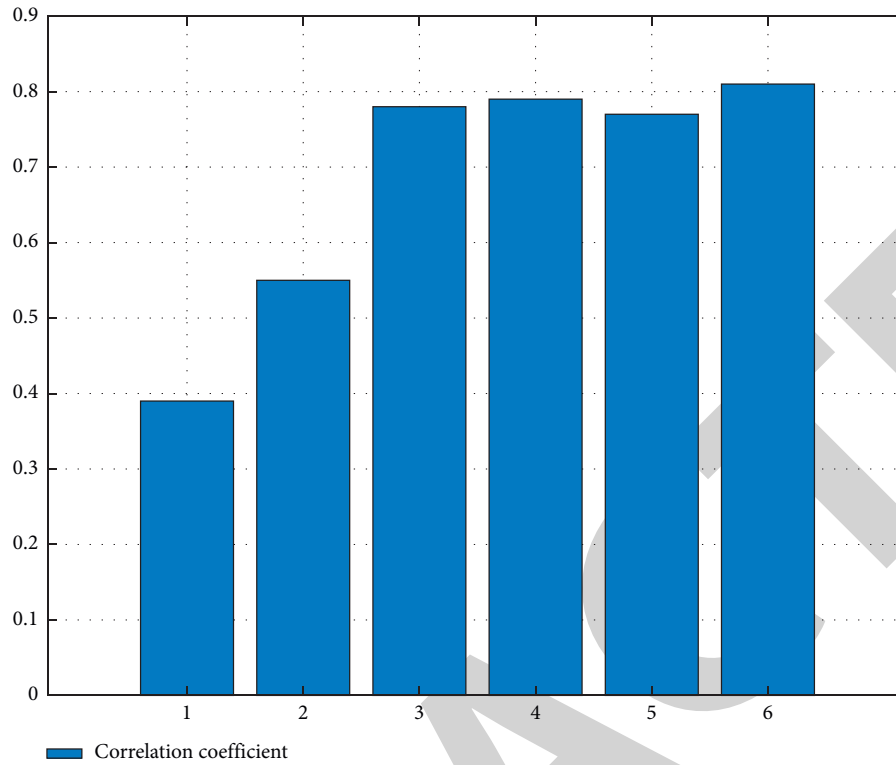


FIGURE 5: Correlation between predicted and actual scores based on the first N unit tests.

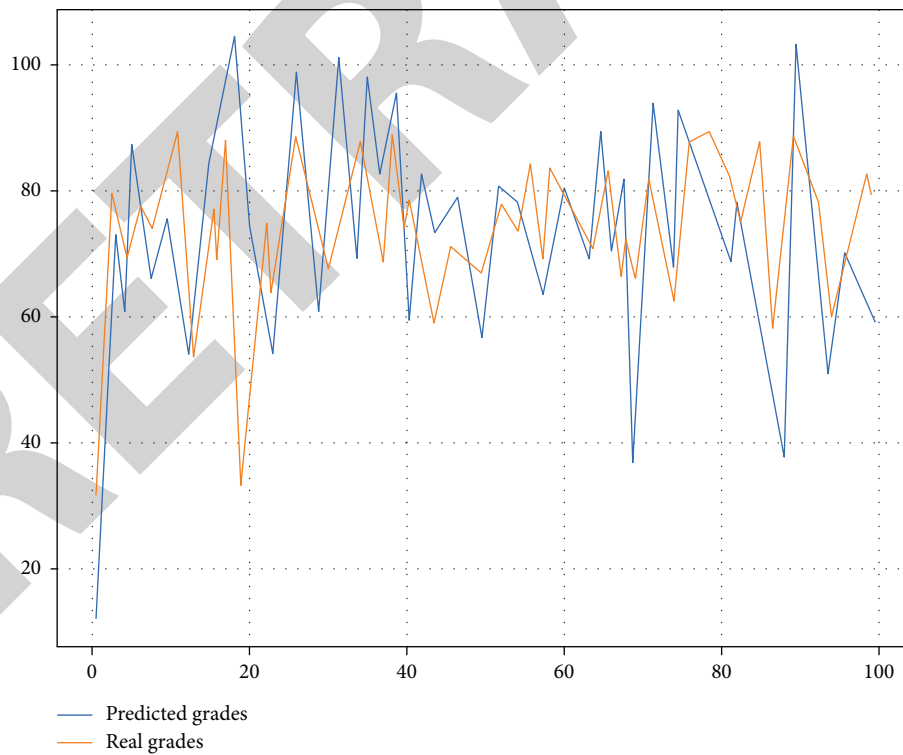


FIGURE 6: Schematic representation of predicted and actual grades based on unit tests.

correlation coefficient of 0.67; the two sets of data were then ranked within the group, with a correlation coefficient of 0.60. Finally, the bottom 15% of the group was compared with the bottom 15% of the actual grade based

on their ranking, and six students were predicted, with a prediction accuracy of 50% for the early warning students. (The y-axis represents the grade, and the x-axis represents the course).

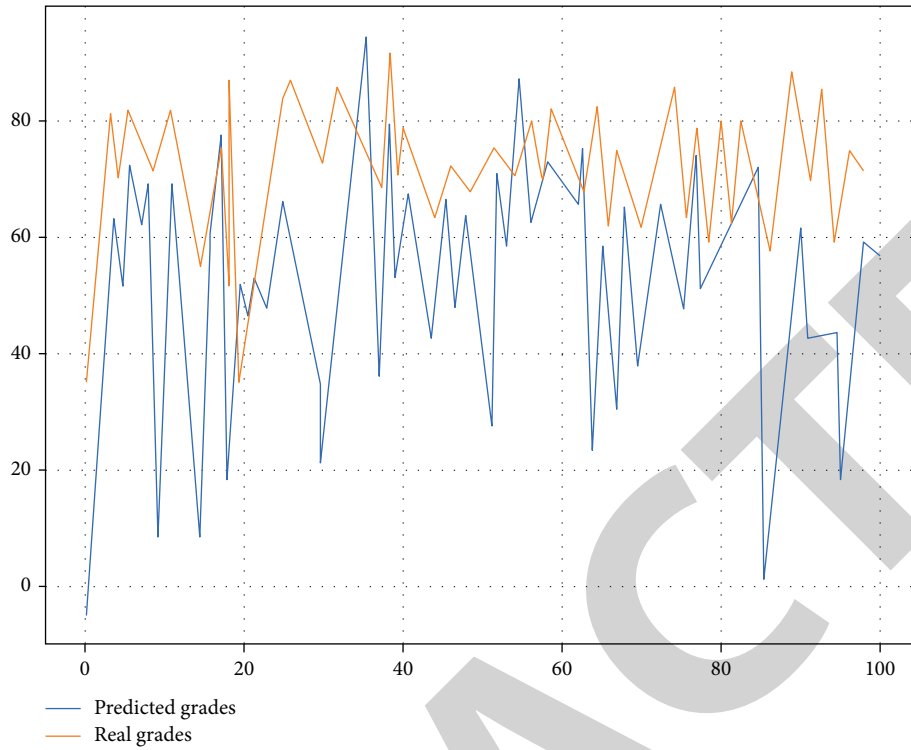


FIGURE 7: Diagram showing predicted and actual grades based on rain classroom data.

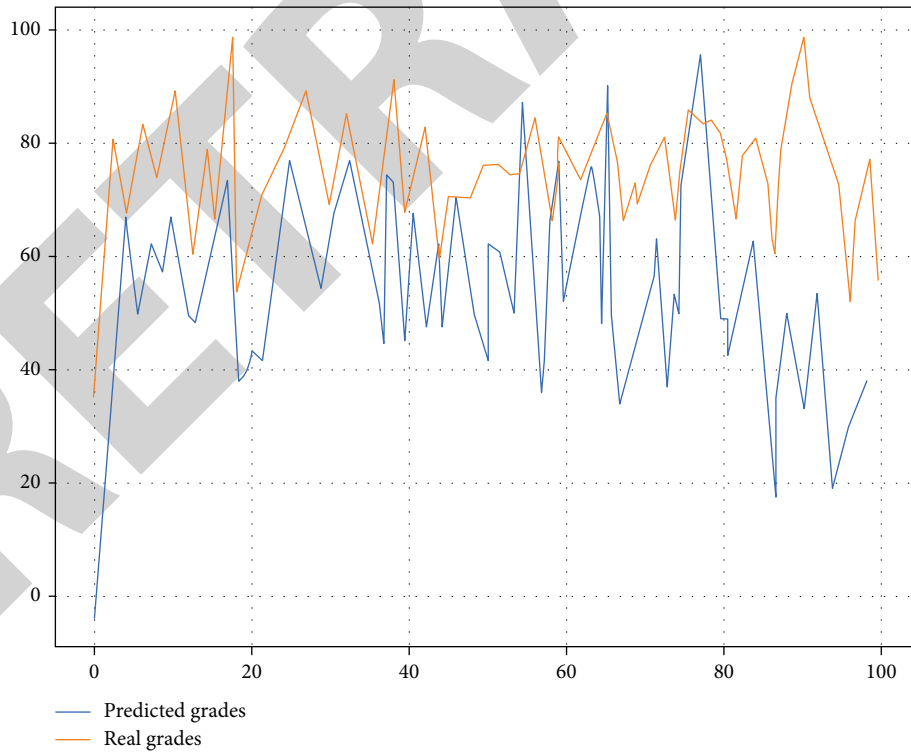


FIGURE 8: Schematic representation of predicted and actual grades based on experimental building data.

Experimental building data in this paper use only the indicator of total effective learning time, which represents the total effective learning time that students put in during the experimental sessions of the physical education course.

These data were normalised according to a percentage scale, allowing each individual student's value to be converted to a numerical space from 0 to 100, and this value was used to represent the predicted grades based on the laboratory

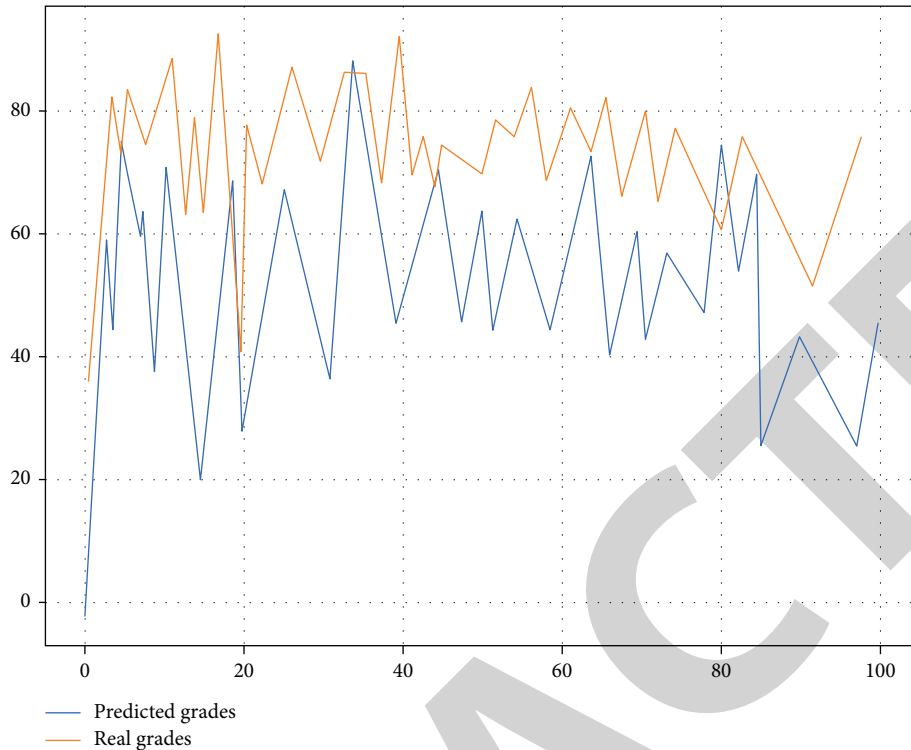


FIGURE 9: Diagram showing predicted and actual grades based on the combined online teaching data.

building data. Further, a correlation analysis was performed with the actual grades of the students to obtain Figure 8. (The  $y$ -axis represents the grade, and the  $x$ -axis represents the course).

The correlation coefficient between the predicted and actual grades based on the experimental building data was 0.60; subsequently, the correlation coefficient between the ranking of the two groups was 0.57, which is about the same as the numerical correlation. Finally, the students in the bottom 15% of the group were extracted based on their ranking and compared to the bottom 15% of the actual grade, and five students were predicted, giving an accuracy rate of 41.7% for early warning students.

As both the rain classroom data and the lab floor data were derived from students' daily classroom performance, the former from theory classes and the latter from practical classes, the two sets of data were normalised (converted to a 0–100 value space) and then averaged to obtain a set of predicted scores. As these data are sourced from the online teaching platform, they are referred to as predicted grades based on online teaching data. The exact distribution of the predicted and actual scores is shown in Figure 9. (The  $y$ -axis represents the grade, and the  $x$ -axis represents the course).

The correlation coefficient between the predicted and actual grades based on online teaching data was 0.72. Subsequently, the correlation coefficient between the two sets of data was 0.70 when ranked within the group, which is a significant increase in correlation compared to the prediction based on the rain classroom data only and the prediction based on the laboratory building data only, indicating a more accurate prediction.

### 3. Conclusions

In this paper, based on the collection and processing of data from multiple sources of teaching, course performance prediction is carried out based on a total of five dimensions: taught professional courses in physical education theory courses, unit tests, mobile teaching data, virtual simulation experiment data and comprehensive data from online teaching; and correlated with actual course performance by numerical correlation, ranking correlation and warning coverage of students in the bottom segment. The method with the highest numerical correlation and the method with the highest ranking correlation was Method 2. This indicates that there is a high correlation between unit tests and course tests in terms of knowledge and test content, and that course grade prediction based on unit test data is more accurate.

### Data Availability

The raw data supporting the conclusions of this article will be made available by the authors, without undue reservation.

### Conflicts of Interest

The authors declared that they have no conflicts of interest regarding this work.

### Acknowledgments

No funding was used in this study.



## Retraction

# Retracted: Evaluation and Application of College English Mixed Flipping Classroom Teaching Quality Based on the Fuzzy Judgment Model

### Security and Communication Networks

Received 8 August 2023; Accepted 8 August 2023; Published 9 August 2023

Copyright © 2023 Security and Communication Networks. This is an open access article distributed under the Creative Commons Attribution License, which permits unrestricted use, distribution, and reproduction in any medium, provided the original work is properly cited.

This article has been retracted by Hindawi following an investigation undertaken by the publisher [1]. This investigation has uncovered evidence of one or more of the following indicators of systematic manipulation of the publication process:

- (1) Discrepancies in scope
- (2) Discrepancies in the description of the research reported
- (3) Discrepancies between the availability of data and the research described
- (4) Inappropriate citations
- (5) Incoherent, meaningless and/or irrelevant content included in the article
- (6) Peer-review manipulation

The presence of these indicators undermines our confidence in the integrity of the article's content and we cannot, therefore, vouch for its reliability. Please note that this notice is intended solely to alert readers that the content of this article is unreliable. We have not investigated whether authors were aware of or involved in the systematic manipulation of the publication process.

In addition, our investigation has also shown that one or more of the following human-subject reporting requirements has not been met in this article: ethical approval by an Institutional Review Board (IRB) committee or equivalent, patient/participant consent to participate, and/or agreement to publish patient/participant details (where relevant).

Wiley and Hindawi regrets that the usual quality checks did not identify these issues before publication and have since put additional measures in place to safeguard research integrity.

We wish to credit our own Research Integrity and Research Publishing teams and anonymous and named external researchers and research integrity experts for contributing to this investigation.

The corresponding author, as the representative of all authors, has been given the opportunity to register their agreement or disagreement to this retraction. We have kept a record of any response received.

### References

- [1] X. Gao, "Evaluation and Application of College English Mixed Flipping Classroom Teaching Quality Based on the Fuzzy Judgment Model," *Security and Communication Networks*, vol. 2022, Article ID 9611611, 9 pages, 2022.

## Research Article

# Evaluation and Application of College English Mixed Flipping Classroom Teaching Quality Based on the Fuzzy Judgment Model

Xiaoyan Gao 

*The English Department, Taiyuan University, Taiyuan 030032, China*

Correspondence should be addressed to Xiaoyan Gao; [gaoxiaoyan@tyu.edu.cn](mailto:gaoxiaoyan@tyu.edu.cn)

Received 7 June 2022; Revised 4 July 2022; Accepted 11 July 2022; Published 3 August 2022

Academic Editor: Hangjun Che

Copyright © 2022 Xiaoyan Gao. This is an open access article distributed under the Creative Commons Attribution License, which permits unrestricted use, distribution, and reproduction in any medium, provided the original work is properly cited.

With the development of big data technology, there are more and more evaluation models for college English teaching quality, which can better promote the improvement of college English teaching quality. Based on the fuzzy decision model, this paper describes the algorithm establishment process of the model in detail. Then, the fuzzy evaluation model between teachers and students according to different grades is established. Finally, aiming at the problems in college English teaching, this paper obtained the corresponding countermeasures for the college English teaching platform based on fuzzy judgment model. The results indicate the model improves the quality of college English teaching in different grades and promotes the development of college English. In addition, the model platform can also well predict the measures to improve the quality. In short, this paper provides some theoretical and experimental support for the quality of college English hybrid flipping classroom.

## 1. Introduction

At present, the speed of social development is rapid, big data is more extensive, and the English teaching mode of integrating flipped classroom based on the use of Internet resources and information technology is a way of continuous innovation of college English courses. The application of flipped classroom can better fit the teaching concept of college English reform, combine with real life, improve students' perception of life, and improve students' English application ability [1].

"Flipped classroom" refers to the fact that, in the information environment, teachers provide sufficient resources to students based on the difficult points of teaching, and teaching microvideo is the main presentation form of these learning resources. Before classroom teaching, students first watch the teaching video of the class, preview the knowledge points in advance, or practice online so as to successfully complete the knowledge transfer [2]. In order to help students consolidate their knowledge, it is particularly important for teachers to design different classroom activities in order to achieve the purpose of knowledge internalization, and students can deeply learn English knowledge.

Generally speaking, this teaching model not only "flips" the learning process but also completely "flips" the respective roles of teachers and students. Students become the main body of teaching, and teachers become the leader of teaching. Flipped classroom has played a guiding role in educational reform, and the traditional teaching methods will be replaced [3]. The advantage of flipped classroom lies in the rational allocation of classroom resources to maximize the learning effect of students.

In teaching, teachers cannot teach without teaching materials. Through the teaching materials, teachers are in the leading position. As a result, there is a "one speech hall" situation [4]. When traditional classroom teaching is used, the characteristic of the hybrid teaching mode is to effectively combine network teaching with modern teaching means. Under the guidance of teachers, college students can successfully master scientific learning methods and complete the learning content [5, 6]. Meanwhile, they strengthen the cultivation of students' creativity and can learn English knowledge independently. To carry out mixed teaching, we should take the following two aspects: first, from the perspective of students, carry out more group communication activities according to students' habits, styles, interests, and

goals. Second, through the students' knowledge, ensure the design of scientific and reasonable teaching programs, and let students have the initiative in the classroom. In addition, the concept of cooperation must be followed in mixed teaching. During teaching, teachers can be redefined through autonomous learning or group cooperation [7].

However, at present, there are the following problems in college English teaching [8, 9]: (1) the credit hours are significantly reduced, and the scale of teaching classes is huge. As colleges and universities constantly update their talent training programs, college English is also facing subversive teaching reforms. Students do not have many opportunities to exercise in the classroom. As we all know, language learning is a process that needs persistence and continuous accumulation, which cannot be completed overnight. Therefore, in language teaching, students must be required to participate, speak boldly, interact more with teachers, and get full exercise [10].

(2) The teaching idea is old. In recent years, the traditional college English teaching mode of "Internet + chalk + blackboard" has been widely used in various industries, but it is difficult to adapt to this situation [11]. It has been replaced by new teaching modes such as multimedia classroom and smart classroom and has gradually changed the teaching philosophy of college English teachers. However, it should be noted that, constrained by the deep-rooted traditional teaching ideas and information technology ability, many college English teachers still abide by the traditional teaching ideas in the short term. Although multimedia technology has been effectively used in teaching, many teachers continue to use the "indoctrination" teaching method to complete English teaching. This teaching method is too single, and teachers are singing "monologue," which has greatly affected the quality and effect of college English teaching [12].

(3) Students do not have strong language application ability [13]. The dominant position of teachers has always been the key part of the traditional college English teaching model. Teaching is mainly taught by teachers. Although teachers' "cramming" explanation of vocabulary and grammar plays a certain role in students' mastering textbook content and understanding vocabulary, from the perspective of long-term development, this teaching model does not put the cultivation of students' subjective initiative in an important position, and students learn passively, let alone interested in English learning. Therefore, if the mode is adopted, it will have a negative impact on the cultivation of college students' communicative ability in English teaching [14].

In the traditional teaching stage of college English, the evaluation mode of students will still start from the examination results, increase the daily attendance assessment, and score the completion of homework, but such an assessment mode still cannot achieve the purpose of detailed assessment, nor can it achieve the detailed assessment of students' learning process and learning attitude, which affects the comprehensive evaluation. Under the situation of online and offline mixed teaching, the evaluation mechanism for students needs to be adjusted into a more comprehensive model and implement diversified teaching evaluation requirements. In the assessment stage, in addition to measuring the performance,

we also need to consider the students' online learning and the activity of online communication. On the basis of comprehensive assessment, teaching evaluation is no longer limited to teachers' personal behavior but can comprehensively feed back students' learning status and the real level of knowledge in a more objective way.

As for the fuzzy concept of evaluation and application of college English, it is impossible to accurately define the level of mixed flipped classroom with precise mathematics. However, from fuzzy mathematics, it is impossible to define the level of its ability in the evaluation and application [15, 16]. However, we can evaluate the degree to which the evaluation and application of teaching quality belong to one or several levels, which can be quantified as membership.

Hybrid teaching method is to add online content on the basis of traditional offline. On the premise of the combination of traditional education mode and information education mode, it can no longer be limited by teaching time and realize "online + offline" teaching [17]. This kind of teaching method does not simply increase the form of online teaching but needs to better integrate resources and apply resources to innovative curriculum teaching mode so as to provide students with a wider way of knowledge acquisition, create a benign competitive environment, and better implement personalized learning requirements without the limitation of time and space [18].

The multifactor comprehensive evaluation method based on the fuzzy decision model establishes a comprehensive evaluation model which is closer to human thinking mode through the self-learning, self-adaptive ability, and strong fault tolerance of the neural network. The trained neural network endows the evaluation idea of experts to the network in the form of connection weight. In this way, the network can not only simulate experts for quantitative evaluation but also avoid human errors in the evaluation process. Because the weights of the model are obtained through case study, the subjective influence and uncertainty of the artificial calculation of weights and correlation coefficients in the fuzzy comprehensive evaluation method are avoided.

Yan et al. [19] found that the Internet of things model can facilitate teachers' teaching and has good application value. According to Liu's study [20], the teaching quality evaluation system of college English hybrid flipped classroom is established by using the method of fuzzy mathematics, and the model is verified and analyzed through experiments. The results indicate the fuzzy mathematical model can objectively put forward effective suggestions, which promotes the development of college English teaching. Huang et al. [21] established a fuzzy judgment matrix by investigating and analyzing the teaching quality in different schools, which has a good effect on the evaluation. By the fuzziness of the teaching quality of college English, Zhang [22] showed the English teaching mixed flipped classroom as a multiobjective fuzzy recognition problem and established a fuzzy recognition theoretical model according to the characteristics of fuzzy mathematics, which has good application results.

Therefore, using the method of fuzzy mathematics, this paper establishes the evaluation based on fuzzy judgment

model for college English mixed flipped classroom, applies this system to the quality of college English education in different grades, analyzes the college English teaching process of teachers and students in each grade in detail, and improves the corresponding measures about the teaching quality of college English mixed flipped classroom, which provides some theoretical and experimental support.

## 2. Establishment of the Fuzzy Judgment Model

It is assumed that there are  $n$  teaching modes in the mixed flipped classroom, in which any state  $j$  ( $j = 1, 2, 3, \dots, n$ ) has  $m$  characteristic index values for evaluation and judgment  $\mu_i$  ( $i = 1, 2, 3, \dots, m$ ), such as English teaching methods, teaching ideas, and teaching feedback. Then, according to different characteristics,  $\mu_i$  has different membership functions  $\mu_j(\mu_i)$ , a characteristic index  $\mu_j$  [23]. The value of  $i$  is substituted into the membership function of the index corresponding to the  $j$ -th state  $\mu_j(\mu_i)$ , and the membership degree can be calculated and normalized to make the membership degrees change within the  $[0, 1]$  interval to form the  $m$ -order fuzzy relationship matrix  $R$ . In addition, the membership degree can represent the accuracy of flipped classroom teaching mode and reflect the accuracy of membership function. That is,

$$R = \begin{bmatrix} \mu_1 \\ \mu_2 \\ \dots \\ \mu_m \end{bmatrix} = \begin{bmatrix} \mu_{11}(\mu_1) & \mu_{12}(\mu_1) & \dots & \mu_{1n}(\mu_1) \\ \mu_{21}(\mu_2) & \mu_{22}(\mu_2) & \dots & \mu_{2n}(\mu_2) \\ \dots & \dots & \dots & \dots \\ \mu_{m1}(\mu_m) & \mu_{m2}(\mu_m) & \dots & \mu_{mn}(\mu_m) \end{bmatrix}. \quad (1)$$

The importance of  $m$  characteristic indicators in the teaching quality of college English mixed flipped classroom is different. Therefore, when evaluating and comparing, the importance of these characteristic indicators must be analyzed. According to expert experience, the improved AHP method is used to separate their different weight values  $w$  and form a fuzzy weight vector  $W$ , which refers to the combination of the weight values of the improved flipped classroom features, and has the characteristics of timeliness, data, and inclusion; namely,

$$W = [w_1, w_2, \dots, w_m]. \quad (2)$$

According to the principle of fuzzy synthesis, the fuzzy weight vector  $W$  is multiplied by the fuzzy relation matrix  $R$  to form the fuzzy evaluation model vector  $B$ ; that is,

$$B = WR$$

$$= [w_1, w_2, \dots, w_m] \begin{bmatrix} \mu_{11}(\mu_1) & \mu_{12}(\mu_1) & \dots & \mu_{1n}(\mu_1) \\ \mu_{21}(\mu_2) & \mu_{22}(\mu_2) & \dots & \mu_{2n}(\mu_2) \\ \dots & \dots & \dots & \dots \\ \mu_{m1}(\mu_m) & \mu_{m2}(\mu_m) & \dots & \mu_{mn}(\mu_m) \end{bmatrix} \\ = [b_1, b_2, \dots, b_m], \quad (3)$$

where  $b_j$  is the fuzzy evaluation value of the  $j$ -th state, and the larger the value is, the closer it is to the normal state.

## 3. Establish the Membership Function of Each Index

In the fuzzy set, the membership function can well describe the fuzziness of things. The commonly used membership functions in the fuzzy set include Gaussian membership function, generalized bell membership function, S-type membership function, trapezoidal membership function, triangular membership function, and Z-type membership function [24]. The shape of the membership function in the fuzzy set has little influence on the characteristics of the model, while the membership function of each fuzzy subset is important to the characteristics of the fuzzy model. Because the trapezoidal membership function can better classify and analyze the fuzzy set data with high accuracy, this paper uses the trapezoidal membership function to model and analyze the data.

**3.1. Membership Function of Characteristic Index  $R$ .** In normal college English teaching, characteristic index  $R$  represents the number of college English textbooks, and the average value of  $R$  is 25. With the increase in teaching time, the value of  $R$  also increases. When it is greater than 90 d, the teaching quality is greatly improved. If English teaching is not carried out regularly, the teaching quality is seriously reduced after more than 48 d. At this time, the membership function conforms to the upper limit type of trapezoidal distribution; namely,

$$\mu_1(\mu_1) = \begin{cases} 1, & \mu_1 \leq 25, \\ \frac{90 - \mu_1}{90 - 25}, & 25 < \mu_1 \leq 90, \\ 0, & \mu_1 > 90. \end{cases} \quad (4)$$

**3.2. Membership Function of Characteristic Index  $G$ .** Characteristic index  $G$  represents the number of college English students; with the increase in college English teaching time, the  $G$  value will continue to increase. If the teaching time reaches 80 d, the teaching quality of the hybrid flipped classroom will decline. In the normal teaching state, the average value of  $G$  is 50. If it is less than or equal to 50, the membership function conforms to the upper bound type of trapezoidal distribution. If the teaching time is less than 24 d, it will lead to a reduction in students' interest in learning in college English teaching.

$$\mu_2(\mu_2) = \begin{cases} 1, & \mu_1 \leq 50, \\ \frac{80 - \mu_2}{80 - 50}, & 50 < \mu_1 \leq 80, \\ 0, & \mu_1 > 80. \end{cases} \quad (5)$$

**3.3. Membership Function of Characteristic Index  $B$ .** In normal college English teaching, characteristic index  $B$  represents the number of college English teachers; with the increase in teaching time, the value of  $B$  also increases. When it is less than 2 d, the teaching quality decreases significantly [25]. Therefore, the membership function conforms to the lower limit type of trapezoidal distribution.

$$\mu_3(\mu_3) = \begin{cases} 0, & \mu_3 \leq 2, \\ \frac{\mu_3 - 2}{20 - 2}, & 2 < \mu_3 \leq 20, \\ 1, & \mu_3 > 20. \end{cases} \quad (6)$$

**3.4. Membership Function of Characteristic Index  $r$ .** In normal college English teaching, characteristic index  $r$  represents the learning efficiency of college English courses. The average value of  $r$  is 0.5. With the increase in teaching time, the value of  $r$  also increases. When it is greater than 0.85, the membership function conforms to the upper limit type of trapezoidal distribution.

$$\mu_4(\mu_4) = \begin{cases} 1, & \mu_4 \leq 0.5, \\ \frac{0.5 - \mu_4}{0.85 - 0.5}, & 0.5 < \mu_4 \leq 0.85, \\ 0, & \mu_4 > 0.85. \end{cases} \quad (7)$$

**3.5. Membership Function of Characteristic Index  $b$ .** In normal college English teaching, characteristic index  $b$  represents the teaching efficiency of college English courses, and the average value of  $b$  is greater than 0.35. With the increase in teaching time, the value of  $b$  continues to decrease. When it is less than 0.05, the quality begins to decline, and teachers' teaching enthusiasm will also decrease. At this time, the membership function conforms to the lower limit type of trapezoidal distribution.

$$\mu_5(\mu_5) = \begin{cases} 0, & \mu_4 \leq 0.05, \\ \frac{\mu_5 - 0.05}{0.35 - 0.05}, & 0.05 < \mu_4 \leq 0.35, \\ 1, & \mu_4 > 0.35. \end{cases} \quad (8)$$

**3.6. Vector Calculation of the Fuzzy Evaluation Model.** Through the test of known samples, a fuzzy evaluation model or function is established on the basis of feature extraction. According to the membership function of the above determined characteristic index and combined with the test data, what is more, the fuzzy relation matrix  $R$  combines the membership function with the experimental data in detail, which can better reflect the relationship between the indicators of the flipped classroom. Meanwhile, the fuzzy relationship matrix  $R$  is calculated:

$$R = \begin{bmatrix} 1 & 0.839 & 0.829 & 0.652 & 0 \\ 1 & 0.430 & 0.364 & 0.397 & 0 \\ 1 & 0.768 & 0.162 & 0.010 & 0 \\ 1 & 0.878 & 0.858 & 0.459 & 0 \\ 1 & 0.620 & 0.146 & 0.015 & 0 \end{bmatrix}. \quad (9)$$

According to the expert experience, the fuzzy weight vector matrix  $W$  is determined by using the improved analytic hierarchy process:

$$W = [0.0799, 0.1145, 0.2548, 0.3801, 0.1708]. \quad (10)$$

Then, the fuzzy evaluation vector is

$$B = WR = [1.000, 0.7515, 0.5002, 0.2771, 0]. \quad (11)$$

According to the fuzzy function relationship, the establishment equation of the fuzzy judgment model can be obtained, and its algorithm flow is shown in Figure 1. The fuzzy decision model mainly includes the modeling process. While establishing the fuzzy judgment model, by investigating the functions of all aspects and then analyzing the membership law of each specific index, the fuzzy judgment model is established accurately.

Then, by analyzing the quality of mixed flip classroom, a college English classroom teaching quality evaluation platform based on a fuzzy judgment model is established. The platform of hybrid flipped classroom is mainly divided into four stages: classroom guiding students' autonomous learning, classroom optimizing teaching content, extending classroom teaching after class, and enriching and innovating evaluation methods. These four stages complement each other and organically combine students' subjective initiative, teachers' teaching ability, after-class learning, and innovative development. In general, the specific implementation diagram of the evaluation platform is in Figure 2.

## 4. Application of Mixed Flipped Classroom Platform

**4.1. Preclass Exploration.** Due to the rise of online video class and online live broadcast class, hybrid teaching came into being. Video online classes are superior to traditional classes in the grasp of course duration and the rhythm of knowledge explanation to a certain extent. Online teaching can also make use of richer materials to enrich the whole video so that students can maintain high interest and concentration throughout the whole process. Meanwhile, online video

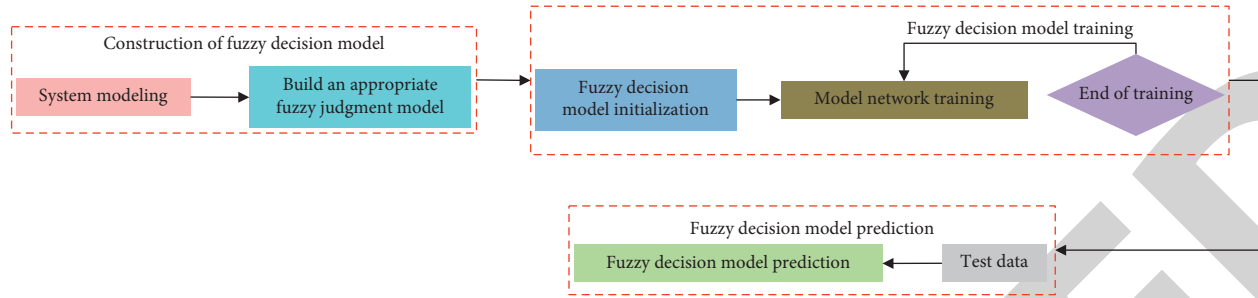


FIGURE 1: Algorithm flow based on the fuzzy decision model.

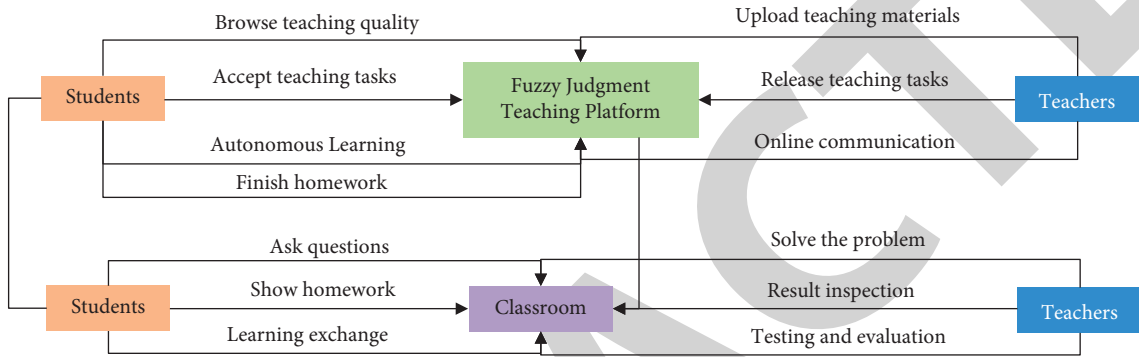


FIGURE 2: Process of college English teaching quality evaluation platform based on the fuzzy decision model.

classes usually combine the teaching experience of a large number of excellent teachers to convey knowledge more accurately. The download of online teaching materials makes it easier for students to review at any time and avoid the problem of forgetting. In terms of knowledge expansion, through careful planning, the output content of online courses will undoubtedly be more accurate, and the materials used are often hot topics at present, which is more timely. Obtain examples or contents related to the course on the network and add them to the video of the course. Through these more time-effective contents, students will undoubtedly better integrate into the classroom and produce better portability. Video, pictures, and other contents also further enrich the video content. Coupled with excellent video production, they impact students' perception from visual, auditory, and other aspects and stimulate students to have a stronger interest in learning.

Figure 3 shows the scores of teachers and students on the quality of college English teaching based on the fuzzy decision model in different grades. We can see that the scores of teachers and students increase first and then decrease. For sophomores and juniors, there is little difference in the scores of teachers and students. The reason for this phenomenon is that freshmen are not familiar with the mixed flipped classroom judgment model, which leads to low scores between teachers and students. As senior students want to find a job, their interest in English classroom learning decreases and their score value will decrease, which will also reduce the score value of teachers. Therefore, in the lecture part, different from the traditional classroom, teachers should use stronger expressiveness to express the content to students. Hold the students tightly with more

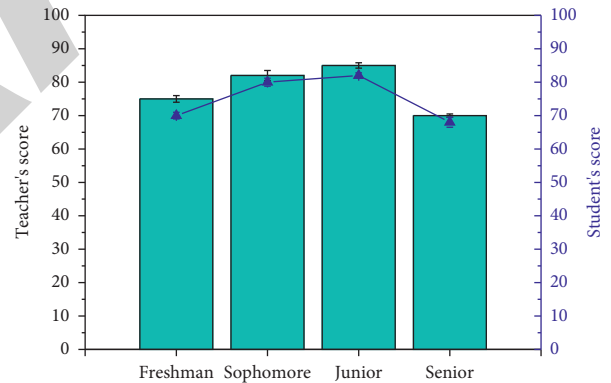


FIGURE 3: Scores of teachers and students on college English teaching quality based on the fuzzy decision model in different grades.

attractive language, let the students focus on the teaching content, and ensure that they are not disturbed by the outside world. In addition to their own teaching experience, the key parts of knowledge are demonstrated to students in different ways to improve the identification of content. In the teaching process, leave appropriate time, give students the opportunity to think, and grasp the sense of rhythm and relax, so that students can fully accept all the contents. In short, in order to improve the teaching quality of college English, we should arrange appropriate teaching time according to the teaching level of each teacher and local conditions. At the same time, we should also give full play to the students' subjective initiative in learning and stimulate the interest of different grades according to the students'



actual state and personal ability so as to improve the teaching quality of college English flipped classroom.

**4.2. Discussion on Actions in Class.** As a new learning method, flipped classroom is not only the product of the times but also a more characteristic learning concept in today's network information background, which enables students to learn more autonomously rather than simply accept it. They can also use the convenient technology of the network to add more time-effective content, online video, news, and so on in teaching. They can also bring students more interesting learning experience in this new form in the classroom. Students can understand their difficult problems from others' statements in the discussion link. In this process, teachers mainly summarize the knowledge points and comment on the views of group discussion. This targeted classroom activity can make students feel the sense of achievement of knowledge exploration and increase their enthusiasm for autonomous learning. The efficiency of English teaching has also been significantly improved. In addition, based on the microclass learning completed by students before class, students have independently learned the important and difficult points of text knowledge. Teachers can use PPT to carry out group competition and answer activities of relevant knowledge points for students in class. This activity can provide students with the detection and review links of learning content.

The discussion in college English mixed flipped classroom is in Figure 4. We can see that the discussion situation of sophomores and juniors fluctuates, but the fluctuation is relatively flat, which is suitable for the platform of English hybrid flipped classroom. The discussion situation of freshmen is low. The main reason may be that freshmen are not familiar with the college English teaching quality evaluation platform, which leads to the fluctuation of the discussion situation. Senior students seldom use the evaluation platform of college English teaching quality because there are few English courses, so the discussion of students shows a decreasing trend. In order to better motivate students of different grades to use the evaluation platform of college English mixed flipped classroom teaching quality based on fuzzy judgment model, students' interest in learning English should be stimulated, and different teaching methods should be adopted to teach English to students of different grades.

**4.3. Discussion on Actions after Class.** The innovation of teaching activities is also very important, which is important to ensure the practical of college English mixed teaching based on flipped classroom. First of all, before classroom teaching, teachers need to systematically integrate students' learning problems and take problem orientation as the core of classroom teaching. Teachers design several preclass questions. Under the guidance of questions, students can have a strong desire to explore and then carry out in-depth learning with questions. In this process, they can fully

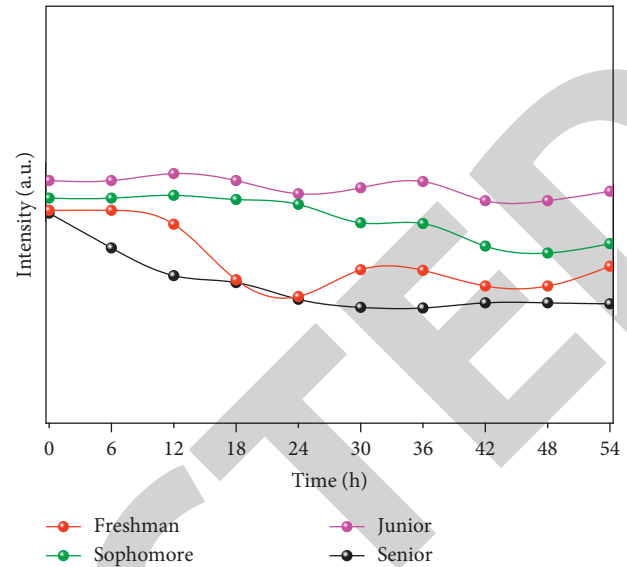


FIGURE 4: Analysis of discussion in college English mixed flipped classroom in different grades.

exercise students' ability to analyze. Secondly, college English curriculum is highly theoretical, and many students cannot really apply what they have learned. Therefore, in college English classroom teaching, carry out group cooperation teaching, and strengthen students' English expression ability and English communication ability through English exercise in English communication situation.

The discussion enthusiasm of teachers and students in different grades obtained from the college English mixed flipped classroom teaching quality evaluation platform based on the fuzzy judgment model is in Figure 5. We can see that students and teachers of different grades have different enthusiasm for discussion after class. However, teachers' enthusiasm for discussion after class gradually decreases. For students, sophomores and junior students have the highest discussion enthusiasm, and the two situations are similar. Freshmen' enthusiasm for discussion after class is the second, and the worst is senior students. The main reason may be that teachers will actively discuss with students after class; with the increase in students' grade, students' autonomous learning ability is greatly improved, and teachers' enthusiasm for after-class discussion is reduced accordingly. Sophomores and junior students are in the heavy stage of learning English, and students pay more attention to participating in active discussion after class. Senior students have fewer English courses, and students generally do not pay attention to learning, which leads to the reduction of senior students' enthusiasm for after-school discussion. In order to improve the discussion enthusiasm between teachers and students in the mixed flipped classroom of college English, teachers should first assign relevant after-class discussion time, deliberately train students' after-class discussion ability, and then give full play to students' subjective learning ability, so that they are willing to participate in the after-class discussion.

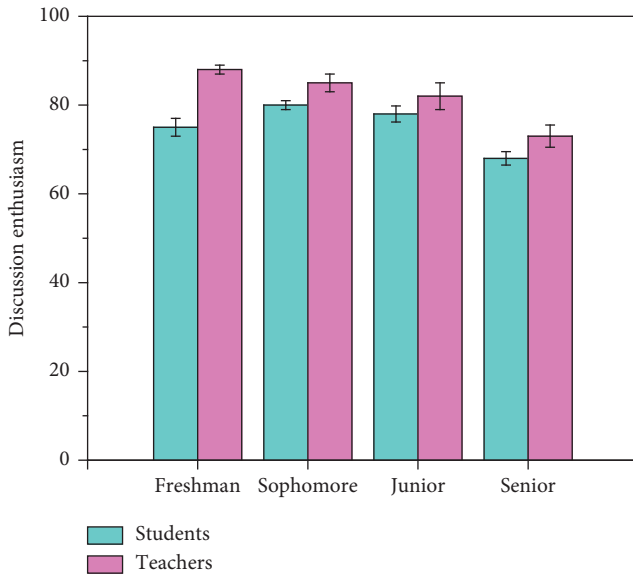


FIGURE 5: Discussion enthusiasm of teachers and students in different grades based on the fuzzy judgment model.

## 5. Application Measures of College English Mixed Flipping Classroom Teaching Quality Based on the Fuzzy Judgment Model

**5.1. Help Students Improve Their Cross-Cultural Communication Ability.** As an indispensable humanities course in the talent training program, we realize the organic unity of instrumental and humanistic nature of college English. Language is not only the carrier of culture but also an integral part of culture. At present, the instrumentality of college English has been widely recognized so that students can communicate in academic or professional fields in English in the future. Therefore, in addition to improving college students' five skills, we can master the cultural information behind the English language and understand the ways of thinking, values, and world outlook.

Figure 6 shows the improvement rate of communicative competence. We can see that the improvement rate of communicative competence of students in different grades has increased. Among them, sophomores and juniors have the highest improvement rate of communicative competence, followed by freshmen and seniors. The main reason is that the sophomore and junior students have mastered the basic college English learning methods and strong learning ability after years of study. As senior students are busy with graduation and the reduction of college English courses, the improvement rate of their communicative competence is the lowest. Freshmen need a slow adaptation process after the transition from high school to university. Therefore, the improvement rate of their college English communicative competence is slightly lower than that of sophomores and juniors. In short, in order to better promote the improvement rate of communicative competence in the college English mixed flipped classroom, students of different grades should be stimulated to have an interest in college English learning, the learning plan should be determined according

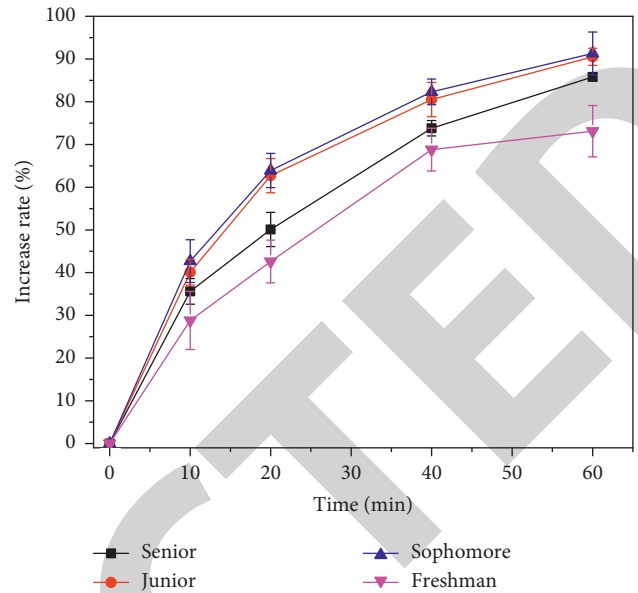


FIGURE 6: The improvement rate of communicative competence in college English mixed flipped classroom based on the fuzzy decision model.

to the students' learning conditions according to local conditions, and corresponding communicative competence training should be carried out to provide communication opportunities with well-known experts and scholars at home and abroad and expand their horizons, so as to achieve the purpose of better learning college English.

**5.2. Building a Diversified Curriculum Feedback and Evaluation System.** In flipped classroom, the main body of college English curriculum evaluation includes students and teachers. The evaluation object is not limited to offline classroom (traditional classroom) but presents diversified staggered evaluation methods such as online classroom, offline classroom, and peers (between students). The flipped classroom is multidimensional and comprehensive. In combination with the market's employment needs for college students, students' future career or further study, students' English level, school level, and other factors, based on the "Trinity" of students' front-line classroom, offline classroom, and hidden classroom after class, strengthen the weight of formative evaluation and consider students' individual differences, combining formative evaluation and summative evaluation organically, so as to form the best evaluation method, to improve the effect of college English teaching and achieve its teaching objectives. In addition, in flipped classroom teaching, due to the large number of students and the differences in learning ability and comprehensive quality of each student, in order to better evaluate students' learning, it is necessary to establish diversified curriculum feedback and evaluation system.

The online and offline hybrid teaching mode can fully absorb the advantages of the network learning platform and integrate the online network teaching and offline course teaching in the teaching stage. This can not only show the

guiding role of teachers in the teaching stage but also respect the current “student-oriented” requirements so as to better stimulate students’ initiative and creativity in learning English and better improve students’ comprehensive English quality. This kind of teaching mode can be better combined with students’ time and learning effect for gradual improvement, which can not only stimulate students’ autonomous learning ability but also improve their learning interest. At the same time, teachers can also adopt innovative teaching mode and use new media to transfer knowledge to students, which can not only improve students’ interest in learning but also better transfer the current best quality knowledge to students. In addition, teachers can constantly explore the advantages of flipped classroom during teaching so as to better provide guidance to students. Using new media technology can integrate the advantages of traditional blackboard teaching with the current form of online teaching, which can not only give play to the leading role of teachers in guidance, enlightenment, and monitoring but also fully mobilize students’ enthusiasm and initiative and finally achieve the purpose of improving the effect of education.

Figure 7 shows the evaluation system of college English mixed flipped classroom based on fuzzy decision model. It can be seen that there are three evaluation systems: offline classroom, online classroom, and invisible classroom after class. For students, the proportion of hidden classroom after class in college English hybrid flipped classroom based on the fuzzy decision model is relatively high, followed by offline classroom and online classroom. This is mainly because students like to discuss and study college English content in the hidden classroom after class. The favorable learning environment of offline classroom can also promote students to learn. However, online classroom lacks communication, which leads to the reduction of its proportion. For teachers, they pay more attention to offline classroom, followed by online classroom, and the proportion of invisible classroom after class is the lowest. The main reason is that teachers communicate with students offline, while teachers can analyze with their classmates through online classroom, so its proportion is also the lowest. In order to better improve the communication and learning of college English between teachers and students, so as to provide a good opportunity for the joint learning of college English between teachers and students, college English is a very important basic language course in the education system of colleges and universities. At this stage, the teaching of college English courses mainly focuses on the teaching of theoretical knowledge, ignoring the cultivation of students’ practical ability. The reform of the college English blended teaching mode under the background of flipped classroom can help the teaching of college English teaching, effectively strengthen the combination of online teaching and offline teaching, and obtain a continuous improvement of the effect of college English teaching. For students, they should make rational use of the learning time in the hidden classroom after class, give full play to their active learning ability, and listen carefully in the offline classroom to reduce unnecessary online classroom learning. For teachers, offline

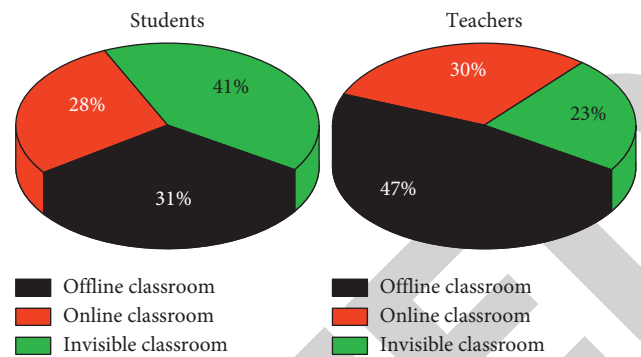


FIGURE 7: Mixed flipped classroom based on the fuzzy judgment model.

classroom teaching is very important. They should arrange more offline classroom teaching time. Secondly, they should improve the teaching ability of online classroom and reduce unnecessary hidden classroom teaching after class.

## 6. Conclusion

Through the detailed comparison of the fuzzy judgment model and the detailed analysis of various indicators affecting the teaching quality of college English hybrid flipping classroom, this paper establishes a college platform. Finally, the platform is applied to the evaluation quality in different grades, and good results are obtained. The results indicate the platform based on the model judgment model can evaluate and analyze college English between different teachers, predict and analyze the English learning results, and obtain the development and progress of college English.

## Data Availability

The experimental data used to support the findings of this study are available from the author upon request.

## Conflicts of Interest

The author declared no conflicts of interest regarding this work.

## References

- [1] Z. Xie and Z. Su, “Evaluation of college English classroom teaching quality dependent on triangular fuzzy number,” *International Journal of Electrical Engineering Education*, vol. 3, no. 4, Article ID 002072092110020, 2021.
- [2] X. Mai, “The application of formative evaluation strategies in college English classroom from the perspective of teacher questioning[J],” *Open Journal of Modern Linguistics*, vol. 11, no. 6, pp. 1–10, 2021.
- [3] L. Wang, “Research on the application of intelligent evaluation and teacher-student cooperation assessment system in teaching English writing,” *A review of educational theory*, vol. 4, no. 3, pp. 1–7, 2021.
- [4] X. Wu, “Research on the reform of ideological and political teaching evaluation method of college English course based on “online and offline” teaching,” *Journal of Higher Education Research*, vol. 3, no. 1, pp. 87–90, 2022.

## *Retraction*

# **Retracted: An Improved Machine Translation Model and its Application in Japanese Multi-Context Translation**

### **Security and Communication Networks**

Received 26 December 2023; Accepted 26 December 2023; Published 29 December 2023

Copyright © 2023 Security and Communication Networks. This is an open access article distributed under the Creative Commons Attribution License, which permits unrestricted use, distribution, and reproduction in any medium, provided the original work is properly cited.

This article has been retracted by Hindawi, as publisher, following an investigation undertaken by the publisher [1]. This investigation has uncovered evidence of systematic manipulation of the publication and peer-review process. We cannot, therefore, vouch for the reliability or integrity of this article.

Please note that this notice is intended solely to alert readers that the peer-review process of this article has been compromised.

Wiley and Hindawi regret that the usual quality checks did not identify these issues before publication and have since put additional measures in place to safeguard research integrity.

We wish to credit our Research Integrity and Research Publishing teams and anonymous and named external researchers and research integrity experts for contributing to this investigation.

The corresponding author, as the representative of all authors, has been given the opportunity to register their agreement or disagreement to this retraction. We have kept a record of any response received.

### **References**

- [1] H. Wen, "An Improved Machine Translation Model and its Application in Japanese Multi-Context Translation," *Security and Communication Networks*, vol. 2022, Article ID 8364278, 10 pages, 2022.

## Research Article

# An Improved Machine Translation Model and its Application in Japanese Multi-Context Translation

Huichao Wen 

*College of Foreign Languages, Northeast Forestry University, Harbin, China*

Correspondence should be addressed to Huichao Wen; [wen@nefu.edu.cn](mailto:wen@nefu.edu.cn)

Received 7 June 2022; Revised 27 June 2022; Accepted 2 July 2022; Published 2 August 2022

Academic Editor: Hangjun Che

Copyright © 2022 Huichao Wen. This is an open access article distributed under the Creative Commons Attribution License, which permits unrestricted use, distribution, and reproduction in any medium, provided the original work is properly cited.

In order to further improve the application of machine translation model in Japanese translation, analytic analysis method is adopted to optimize the original machine translation model. The improved machine translation model is used to analyze and describe Japanese translation. Finally, the optimized machine translation model is used to analyze Japanese multicontext. The relevant indexes and parameters were extracted and verified, and finally the model was verified by relevant experiments. The results show that the vector variation graph with different parameters can be divided into slow decline stage, stable change stage, and fast decline stage according to the increase of iteration number and the influence of corresponding change trend. In addition, it can be seen from the value of PE curve that the influence of parameter  $p_e$  is the least, while the influence of corresponding re parameter is the greatest. The multicontext index of Japanese has the greatest influence on Japanese fluency and the least influence on Japanese keywords, and the trend of influence is parabolic. The application curve of the optimized machine translation model to Japanese in multiple contexts shows that different parameters have different effects on Japanese, which should be represented by the positive parameter  $V$ . Finally, the accuracy of the model is verified by experimental data. The above research can provide support for the application of machine learning in different fields and also provide research ideas for the multicontext translation of Japanese.

## 1. Introduction

Machine translation models are widely used in different fields. Aiming at a series of grammatical errors in English writing, a new computational method is adopted to optimize and deal with the original machine translation model, so as to obtain a modified machine translation model [1]. The model can extract specific parameters of English words, so as to obtain the corresponding characteristic indicators, and then obtain the optimized English translation data by checking and analyzing the indicators. Finally, an experimental method is used to verify and analyze the optimized machine translation model so as to demonstrate the accuracy of the model. It is worth noting that this model can not only analyze words but also study English paragraphs and grammar. Aiming at the problems of long time and slow efficiency in French translation, RNN neural network algorithm is adopted to revise the traditional machine

translation model [2]. Thus, an optimized machine translation model can be obtained, which can carry out targeted analysis of French pronunciation, language, and grammar. This model can not only translate French but also get the optimal translation by analyzing the data. This model can provide theoretical support for French translation and popularization, thus providing ideas for the application of optimized machine translation model in other fields. Finally, a variety of data analysis methods are used to verify the model. Machine translation models are also widely used in other fields, such as deep coding information [3], language training [4], natural data [5], adversarial neural network [6], and weighted supervision [7].

The above studies mainly analyze different kinds of languages from the perspective of the original machine translation model, and the accuracy of the results obtained is relatively low. In order to further improve the accuracy of translation, analytical and analytical methods are used to



optimize the original machine translation model, so as to obtain the improved machine translation model. In order to further improve the accuracy of Japanese multicontext translation, the improved machine translation model is applied to Japanese multicontext translation, and the accuracy of the model is verified through experiments. The results of this study can provide a research idea for the translation of other languages.

## 2. Theories Related to Machine Translation Models

**2.1. The Basics of a Machine Translation Model.** Machine translation model has been widely used in various fields. In order to further analyze the application of machine translation model in Japanese multicontext, the basic content of machine translation model is first explained [8, 9]. It is worth explaining that the basic content of machine translation model mainly includes abstract semantics and neural network machine translation.

**2.1.1. Abstract Semantics.** The automatic evaluation index of abstract semantics refers to the automatic scoring of translated texts by artificial mathematical formulas, and the quality of machine translation models is evaluated according to the scoring level [10, 11]. Each node in the abstract semantics represents a semantic concept, which can be summarized into five conceptual relation types by analysis: PropBank Framesets, general semantic relation, date entity relation, list relation, and quantity relation. The advantages of automatic evaluation indicators of abstract semantics mainly include (a) more persuasive; (b) it can save costs and reduce economic pressure; (c) faster calculation. Compared with manual evaluation, automatic evaluation index is more objective and saves labor cost greatly. The common indexes for automatic evaluation of abstract semantics are accuracy ( $P$ ), recall ( $R$ ), and measure value ( $F$ ). The specific calculation formula of each indicator is given below:

$$\begin{aligned} P &= \frac{S}{M}, \\ R &= \frac{S}{N}, \\ F &= \frac{2 * P * R}{P + R}, \end{aligned} \quad (1)$$

where  $S$  represents the number of correctly matched logical triples,  $M$  represents the number of recognized logical triples, and  $N$  represents the total number of marked logical triples.

In order to further analyze the influence of different evaluation parameters on the automatic evaluation indexes of abstract semantics, the evaluation indexes change curves under different parameters are drawn, as shown in Figure 1. It can be seen from the figure that the influence curves of different parameters on evaluation indexes are different, but they can be divided into three stages according to the overall trend. To be specific, the influence of parameter  $p$  on the

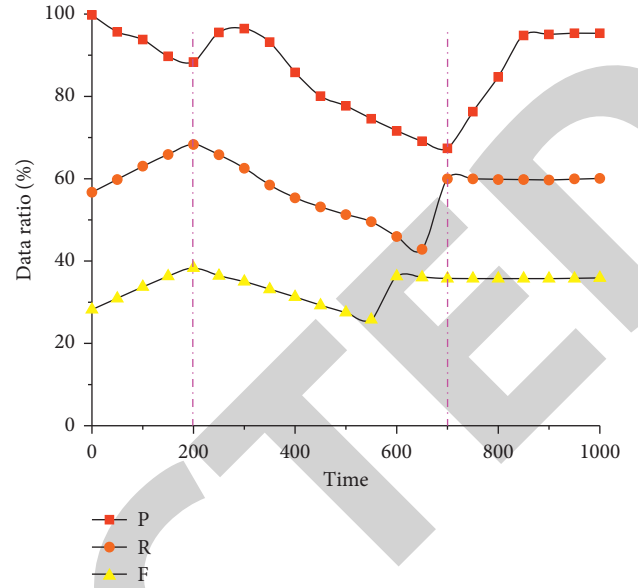


FIGURE 1: Evaluation index change diagram.

evaluation index in 0–200 time shows a gradual downward trend, and the downward trend is in line with a linear downward relationship. When the time reaches 200, with the gradual increase of time, it shows a trend of slow increase at first and then gradual decline, and the slope of this downward trend is approximately the same as the slope of the first stage. When the corresponding change time reaches 700, the curve begins to enter the third stage. In the third stage, the curve first shows a linear increase, and then gradually tends to be gentle, indicating that with the gradual increase of time. The influence of parameter  $P$  on the index curve fluctuates slowly at first, and then tends to a stable overall change. It can be seen from parameter  $R$  that the first stage of the index curve corresponding to parameter  $P$  is opposite. Parameter  $R$  shows a trend of linear increase in the first stage, and when the time exceeds 200, the corresponding curve shows a trend of gradual decline, and the slope is basically consistent with the influence of parameter  $P$ . When it reaches about 650, the curve enters the third stage. In the third stage, the change curve increases rapidly at first, and then gradually tends to be flat, which is basically consistent with the influence of parameter  $P$ . It can be seen from the influence curve of parameter  $F$  that the curve also shows a trend of gradual increase first. When the time reaches about 550, the corresponding curve enters the third stage: it also shows a rapid increase at first, and then gradually flattens out. It can be seen from the figure above that the curves of parameter  $R$  and parameter  $F$  are basically the same. The above three factors are basically the same at the time points in the first stage, but the time points in the second stage are the largest for parameter  $P$ , the second for parameter  $R$ , and the smallest for parameter  $F$ .

**2.1.2. Neural Network Machine Translation.** Machine translation model based on recurrent neural network is the earliest translation model using encoder-decoder framework



in machine translation tasks. Recurrent neural networks can capture the sequential information of sentences in machine translation tasks and are very good at processing sentences with varying length. Relevant studies show that the two algorithms using long and short memory neural network have achieved large experimental results on two data sets in abstract semantics. It shows that introducing neural networks to abstract semantic parsing tasks can improve the performance of machine translation model parsing.

In order to further analyze the influence of machine translation model on Japanese grammar, the computational flow chart of machine translation model is drawn, as shown in Figure 2. It can be seen from the figure that Japanese data is first imported into the model, and different  $X$  modules are divided into two identical modules with opposite iteration directions. Data are imported into  $X$  module, respectively, for iterative calculation. In order to extract the feature points and feature vectors of its grammar, those extracted from each module are then imported into the summary analysis module. Through further analysis of the analysis module, the machine translation model can be used for further targeted analysis of the data, and then the exported data can be brought into the  $S$  module at the top. Through further iterative analysis of the parameter, the corresponding data can be finally exported. The corresponding decoder state update formula is as follows:

$$e_{ij} = \text{match}(s_{i-1}, h_j), \quad (2)$$

$$a_{ij} = \frac{e^{e_{ij}}}{\sum_{k=1}^T e^{e_{ik}}}, \quad (3)$$

$$c_{t=i} = \sum_{j=1}^T a_{ij} h_j, \quad (4)$$

$$s_{t=i} = f(y_{t=i-1}, s_{t=i-1}, c_{t=i}), \quad (5)$$

where  $s_{i-1}$  is the hidden state of the encoder at moment  $i-1$ ;  $h_j$  is the hidden state of the encoder at moment  $j$ ;  $a_{ij}$  is the alignment weight;  $e_{ij}$  is alignment score;  $c_{t=i}$  is a vector;  $s_{t=i}$  indicates the hidden state. First, the alignment score of the hidden layer state of the encoder at moment  $i$  and the hidden layer state of the decoder at moment  $i-1$  is dynamically calculated by formula (2). Second, the alignment score of formula (3) is normalized to obtain the alignment weight. Then, formula (4) sums the states of each hidden layer of the encoder with their weights to obtain the dynamic context vector at the current moment. Finally, the hidden layer state of decoder at each time is updated by formula (5).

Through the above formula and analysis, we can see that different coefficients  $i$  and  $j$  have a great influence on decoder parameters. In order to further analyze the influence of parameters  $i$  and  $j$  on different parameters of decoder, the decoder parameter change curves under different coefficients are drawn as shown in Figure 3. It can be seen from Figure 3 that with the gradual increase of parameter  $i$ , the corresponding decoder parameters show a trend of gradual increase. However, the slope increases in the order of

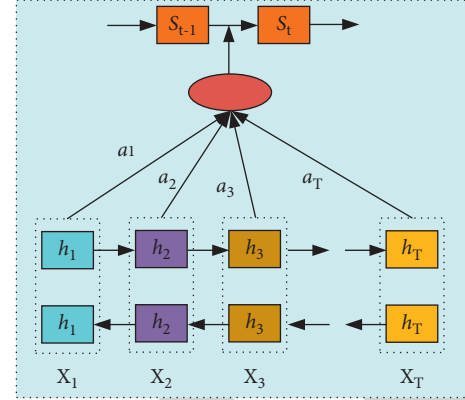


FIGURE 2: Machine translation model flow chart.

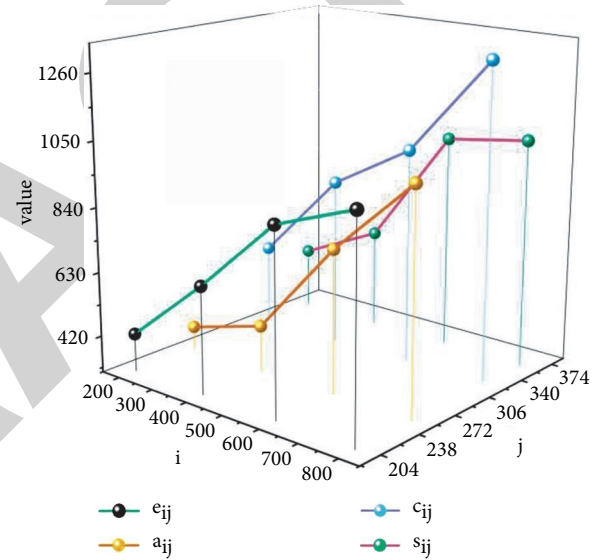


FIGURE 3: The influence curve of different coefficients  $i$  and  $j$  on decoder parameters.

$c_{ij} > s_{ij} > a_{ij} > e_{ij}$ . As can be seen from the influence of  $j$  coefficient, with the increase of  $J$  coefficient, the corresponding decoder parameters also show a trend of gradual increase. This shows that the machine translation model can show typical linear characteristics, which make the obtained results easy to analyze.

In order to further analyze the application of mechanical translation model to syntax, a framework flow chart of data processing is drawn, as shown in Figure 4. Through the analysis, we can see the specific flow chart as follows: First, the Japanese data are imported into the Chinese set, and the corresponding eigenvalues in the graph are extracted through the analysis of the Chinese set, and then the eigenvalues are cleaned and arranged to a certain extent. In this process, the annotated data need to be imported into the cleaning data cleaning module. Then, the optimized data can be imported into the machine translation model through data extraction, and the corresponding data features can be imported into the two plates of source end sentence and target end graph respectively. The data can be further

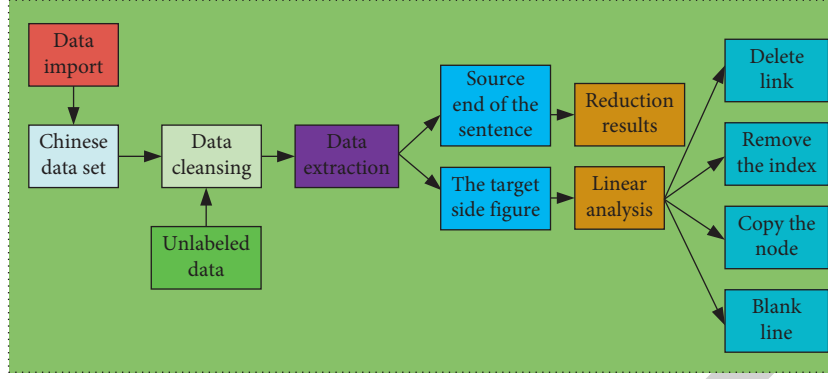


FIGURE 4: Data processing framework diagram.

analyzed through the processing of these two plates. Then, the data obtained from these two plates are imported into the reduction result and linear analysis module, respectively, and the obtained data can be further optimized through the analysis of these two plates. Finally, the Japanese translation results are exported to the corresponding module, which is mainly divided into four parts: deleting links, deleting leads, copying nodes, and space new lines. In this part, the corresponding data can be modified based on the calculation results of machine translation model, and finally the application data can be exported.

**2.2. Machine Translation Model Analysis.** The machine translation model overcomes two major problems: the low efficiency of serialized computation of traditional neural networks and the difficulty of modeling the long distance dependence of sentences in traditional neural networks, thus becoming the best Japanese translation model at present [12, 13]. The process of this method is simple and intuitive. It can be described as the source language sentences as input, which are transformed into continuous and dense feature vectors by an encoder composed of neural network. Then the vector is decoded by a decoder composed of neural network and the target language sentence is output. In the machine translation model, the encoder can generate semantic vector by modeling the logical relationship between words in the Japanese sentences at the source end, and the decoder can predict the corresponding Japanese result graph by the semantic vector extracted at the encoding end [14, 15]. As shown below, the machine translation model mainly includes two parts: input layer and location coding layer.

**2.2.1. Input Layer.** The input layer mainly completes the embedding of Japanese words, thus reducing the training time and avoiding the model falling into local optimal solution. The position vector of each participle in Japanese sentences is defined as a fixed position embedding vector based on trigonometric function. In this method, sine and cosine functions of different frequencies are used, and sine variables are added to the even positions of the word vector of each term. The cosine variable is added to every word in the odd position of the word vector. First, the segmented

words are vectorized, and the specific formula is shown as follows:

$$\begin{aligned} X &= [x_1, x_2, x_3, \dots, x_n]^T \in R^{n \times d}, \\ Y &= [y_1, y_2, y_3, \dots, y_m]^T \in R^{m \times d}, \end{aligned} \quad (6)$$

where  $x_i$  represents the word vector of the  $i$ -th word in the source sentence ( $i = 1, 2, \dots, n$ );  $n$  and  $m$  represent the number of source Japanese sentences and target Japanese word segmentation, respectively;  $d$  represents word vector dimension;  $y_j$  represents the word vector of the  $j$ -th word ( $j = 1, 2, 3, \dots, m$ ).

Through the above analysis, we can see that the corresponding curves of  $X$  and  $Y$  under different  $R$  values are different. In order to further analyze the influence and change of  $R$  value on curves  $X$  and  $Y$ , the change curves of  $X$  and  $Y$  under  $R$  value are drawn, as shown in Figure 5. As can be seen from the figure, with the gradual increase of  $R$  value, the corresponding  $X$  value shows a trend of slow increase. However, it can be seen from the increase that the slope of the curve remains constant, which indicates that  $X$  value under  $R$  value presents typical linear characteristics. Similarly, we can see that the corresponding data of  $Y$  increases rapidly with the increase of  $R$  value. By comparing the variation trend of the two parameters, we can see that  $Y$  value also belongs to typical linear characteristic change. In addition, we can see from the two curves that the slope of the  $Y$  value curve is greater than that of the  $X$  value, which indicates that the change trend of the  $Y$  value is greater than that of the  $X$  value. It also indicates that the influence of the  $Y$  value on the data is higher than that of the  $X$  value.

**2.2.2. Location Coding Layer.** In the natural language understanding task, the model understands a sentence through the meaning of the word and the position of the word in the sentence. After the word embedding technology at the input layer obtains the meaning of the word, it needs to input some position information to let the neural network know the position of the word in the sentence [16, 17]. In the machine translation model, the position vector of each participle in Japanese sentences is embedded based on trigonometric function definition, and the corresponding calculation formula is shown as follows:

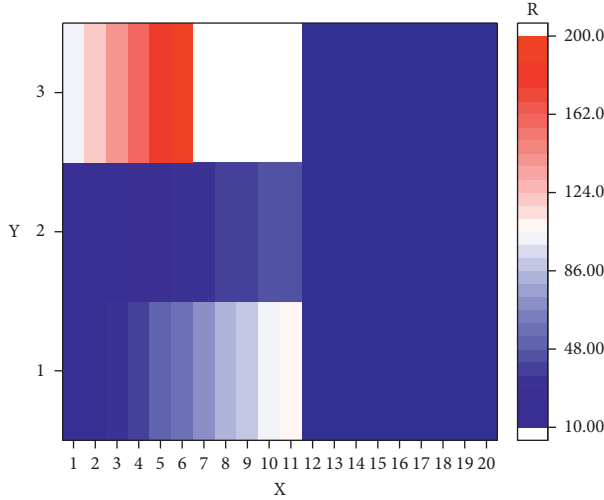


FIGURE 5: Graph of changes in X and Y at R.

$$PE(pos, 2i) = \sin\left(\frac{pos}{10000^{2i/d_{model}}}\right),$$

$$PE(pos, 2i + 1) = \cos\left(\frac{pos}{10000^{2i+1/d_{model}}}\right),$$

where  $PE(pos, 2i)$  represents the value of the machine translation model encoded in the  $2i$  dimension by the position serial number  $pos$ ;  $PE(pos, 2i + 1)$  represents the value of the machine translation model encoded in the  $2i + 1$  dimension of  $pos$  position number.  $pos$  indicates the ordinal position of the word;  $2i$  and  $2i + 1$  represent the dimension of position coding vector;  $d_{model}$  represents the length of the position encoding vector.

Therefore, the Japanese vectorization results obtained by using the machine translation model can be expressed as follows:

$$re = we + pe, \quad (8)$$

where  $we$  is the word vector in Japanese words,  $pe$  is the position vector in Japanese words,  $re$  is the multilayer vector in Japanese words.

Through the above analysis and formula, we can see that the corresponding curves of different parameter values have different variation trends with different iterations. In order to further analyze this variation trend, we drew the vector variation diagram under different parameters, as shown in Figure 6. It can be seen from Figure 6 that with the gradual increase in the number of iterations, the corresponding curve presents a nonlinear change trend. According to the parameter  $we$ , the curve can be divided into three stages. In the first stage, the curve showed a slow downward trend, and the slope of the corresponding PE curve showed a slow increase at first, and then gradually tended to 0. In the second stage, when the number of iterations is from 2000 to 6000, the corresponding curve shows a gentle trend of change, and the slope of the corresponding curve gradually approaches zero, which indicates that the number of iterations in this

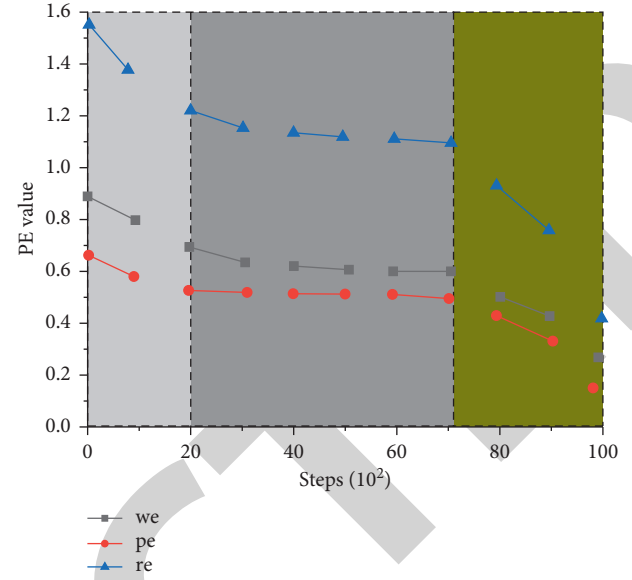


FIGURE 6: Vector variation diagram for different parameters.

stage has little influence on parameter PE. With the further increase of the number of iterations, the curve shows a rapid downward trend. The slope of the corresponding curve also drops rapidly. Among the three stages, the third stage has the greatest influence. It can be seen from the parameter  $pe$  that the slope of the curve is basically consistent with the slope of  $we$  curve. However, the value of the corresponding curve is lower than that of the  $we$  parameter. Through these two curves, we can calculate the change value of the corresponding  $re$  curve, and the data corresponding to the curve also shows a relatively obvious three-stage change trend: That is, it drops rapidly first, then gradually tends to zero, and then drops rapidly at last, which indicates that the nonlinear characteristics of this parameter are very obvious.

**2.3. Optimization of Machine Translation Models.** Machine translation models enrich the dependencies between words from multiple dimensions and make it possible to understand the syntactic and semantic structures of sentences. The optimized machine translation model consists of self-attention layer and neural network layer [18, 19].

**2.3.1. Self-Attention Layer.** Taking the Japanese self-attention calculation of encoder as an example, three vectors including query vector  $Q$ , key vector  $K$ , and value vector  $V$  are used to describe the calculation process of self-attention mechanism. In order to calculate the self-attention of Japanese sentences on encoder side, three vectors, query vector  $Q$ , key vector  $K$ , and value vector  $V$  are used to describe the calculation flow of multidirectional self-attention mechanism.  $Q$ ,  $K$ , and  $V$  vectors are obtained by multiplying the vector matrix  $X$  of each sentence with three different weight matrices  $W^Q$ ,  $W^K$ , and  $W^V$ . The corresponding formula is as follows:

$$\begin{aligned}
Q &= X \times W^Q, \\
K &= X \times W^K, \\
V &= X \times W^V,
\end{aligned} \tag{9}$$

where  $X$  is the vector matrix corresponding to Japanese sentences.

Through the above analysis, we can see that the vector indexes under different  $X$  values are different. In order to further analyze the attention of different vector indexes, the curve of parameter  $X$  changing with the vector is drawn, as shown in Figure 7. It can be seen from Figure 7 that attention value varies under different vectors, as shown below: It can be seen from parameter  $Q$  that with the gradual increase of  $X$ , the corresponding attention value shows a trend of gradual increase, and the increase of attention value shows a linear increase trend with the increase of  $X$ . According to the influence value of parameter  $K$ , it can be seen that with the increase of  $X$  value, the corresponding attention value shows a gradual decline trend, and the decline trend basically showed a linear decline, the overall decline trend remained between 25% and 35%. As can be seen from the variation of parameter  $V$ , with the gradual increase of  $X$  value, the corresponding attention value presents a gradual decreasing trend, and its decreasing trend and value are basically consistent with the variation trend of parameter  $K$ .

**2.3.2. Neural Network Layer.** According to different research contents, the machine translation model can be divided into three parts: input layer, hidden layer, and output layer [20, 21]. It can be seen from the study that different layers are connected by using Japanese data, among which the number of neurons in the input and output layers is different. The specific calculation formula of the corresponding optimization index FNN is shown in equation (10):

$$\text{FNN}(X) = \max(0, xW_1 + b_1)W_2 + b_2, \tag{10}$$

where  $x$  is a component of  $X$  vector;  $W_1$  and  $b_1$  are parameter matrices, and bias matrices of nonlinear transformation in machine translation model.  $W_2$  and  $b_2$  are parameter matrices and bias matrices of linear transformation in machine translation model, it can be seen that the dimension corresponding to  $x$  is  $[1, d_{\text{model}}]$ .

Through the above analysis, we can see that the influence of parameter matrix  $W$  and  $b$  on the network is different. In order to further analyze the changing trend of such influence, the influence diagram of parameter matrix on the network in Figure 8 is drawn. As can be seen from the figure, when the parameter  $W$  remains constant, the network influence value of the corresponding optimization index FNN shows a changing trend of linear increase with the gradual increase of the corresponding parameter  $b$ . However, when parameter  $b$  remains constant, with the gradual increase of parameter  $W$ , the network influence value of the corresponding optimization index FNN still shows a gradual increase of linear change. Therefore, through the above analysis, we can use the linear fitting method to fit and

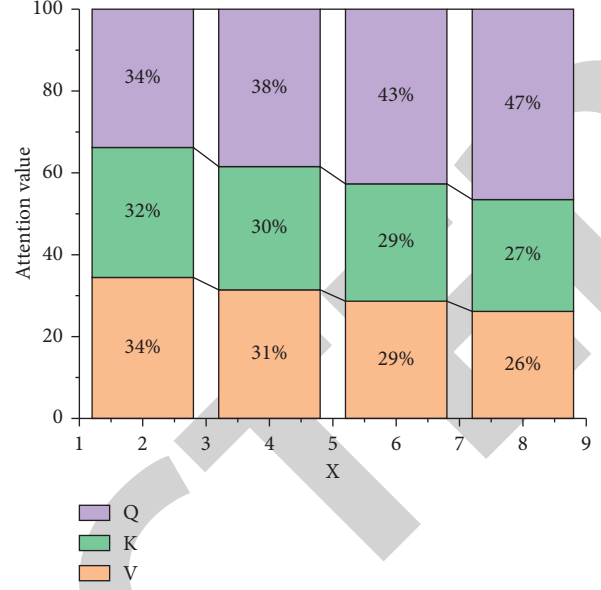


FIGURE 7: Variation diagram of different vectors.

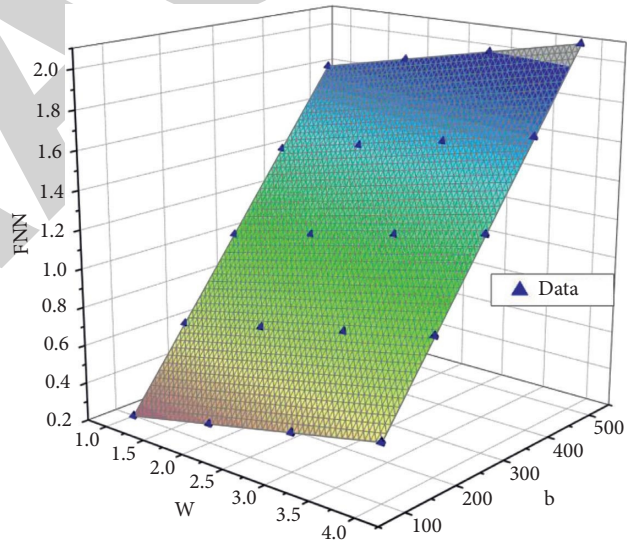


FIGURE 8: Influence diagram of parameter matrix on network.

analyze the data of optimization index FNN under two different factors. Through corresponding fitting and analysis, we can see that the influence of  $W$  and  $b$  on the optimization index FNN shows a trend of linear increase on the whole.

### 3. Application of Improved Machine Translation Model in Japanese Multicontext

**3.1. Japanese Multicontext-Related Content.** Japanese translation plays an important role in the communication between China and Japan, but there are some problems in the practical education of Japanese translation, which will restrict the development of Japanese translation to a certain extent [22]. The specific problems are as follows:

- (1) Translation is too one-sided: Through relevant investigation and analysis, it can be seen that Japanese translation is too one-sided in practical education. This problem is mainly reflected in the one-sided translation of Japanese words in the process of translation, without targeted description and translation of articles and contents, which make the translation results too single and one-sided, and cannot meet the requirements of actual translation. The main reason for this kind of problem is that the translator does not really understand and grasp the connotation of the translation, and only starts from the literal meaning to translate the article. Therefore, in practical translation, we need to pay attention to the problem of one-sided translation, adopt different translation methods to improve translation efficiency, and second, strengthen the translator's own quality, so as to obtain excellent translation results.
- (2) Outdated translation concepts: Japanese translation requires translators to keep up with the pace of The Times and carry out targeted translation. Due to the development of the Internet, many hot words and contents emerge endlessly. If the translator only relies on the book content for translation, the translation result will be quite different from the actual content, and ultimately the quality of translation will be greatly reduced. In order to better make Japanese translation results meet the needs of contemporary translators, we need to update the translation content and ideas in real time, and translators should strengthen their study and master the current popular translation content as soon as possible.
- (3) Weak innovation ability: Traditional Japanese translation only uses book knowledge for translation, which can only solve part of the translation problems, but can not provide a good solution to the relevant problems in translation. Therefore, we need to have certain innovation ability to adapt to the rapid development of the translation industry, so that we can deal with the problems in the process of translation. In order to optimize and analyze the traditional translation by using different calculation methods, the calculation results can well meet the actual requirements, and can also improve the speed and efficiency of translation so that the translation results can better meet the actual requirements.

There are a lot of content in Japanese translation, so we need to use different indicators to describe Japanese multicontext translation. For this purpose, we select six indicators from different aspects to analyze Japanese multicontext translation. The details are as follows: 1—keywords, 2—long difficult sentences, 3—smooth, 4—fluency, 5—logic, and 6—beautiful. In order to analyze the influencing factors of these six indicators on Japanese multicontext translation, we collect the data of the change of the indicators on Japanese multicontext translation.

Based on the above analysis, we can see that the machine translation model has a wide range of applications in Japanese multilingual translation, and different indicators are needed for quantitative analysis in Japanese multilingual translation. Therefore, a bar chart of the proportion of Japanese multilingual translation is drawn, as shown in Figure 9. As can be seen from the figure, the corresponding data of different indicators are different. The highest indicator is Japanese fluency, which is about 80. Followed by Japanese logic, about 60; then there is fluency in Japanese, about 50; the aesthetic score of Japanese was 30, and the analysis of long and difficult sentences was only 20. The lowest was about 10 for Japanese keywords, and through the analysis, we can see the overall performance of parabolic trend.

*3.2. Application of Machine Translation Model in Japanese Multicontext.* Machine translation model has been widely applied in different fields. In order to further improve the translation and application prospect of Japanese multicontext, this paper adopts the optimized and improved machine translation model to translate and apply Japanese multicontext. The corresponding application flow chart is shown below.

In order to have a better application of the machine translation model in Japanese, we draw a flow chart of the machine translation model in Japanese, as shown in Figure 10. It can be seen from the figure that the corresponding process is as follows: First, the numbers and words corresponding to Japanese translation are imported into the analysis model, and then feature points of Japanese multicontext are extracted through the analysis model. Then, the feature points are imported into Japanese sentences, and then the Japanese sentences are further analyzed to achieve a certain degree of coherence between sentences. Finally, the sentences with a certain degree of coherence are imported into paragraphs. Through further analysis of the paragraphs, the corresponding Japanese multicontext original text can be obtained. In order to further verify the accuracy of the original text, we adopted the method of extracting feature vectors from data for verification. In this paper, the feature vector extraction level is divided, the optimization algorithm is imported into the machine translation model, and the obtained translation data is further optimized and analyzed, so as to export the accurate results.

Through the above analysis, it can be seen that the machine translation model has certain application in Japanese translation. In order to further analyze the accuracy of the application results of the improved machine translation model in Japanese multi-context, an optimized machine translation model is used to translate and analyze Japanese in multiple contexts. Thus, the corresponding machine translation model in Japanese multicontext translation application evaluation index changes is obtained, as shown in Figure 11. It can be seen from the data changes in the figure that with the gradual increase of Japanese index factors, the data corresponding to the corresponding Q value parameter



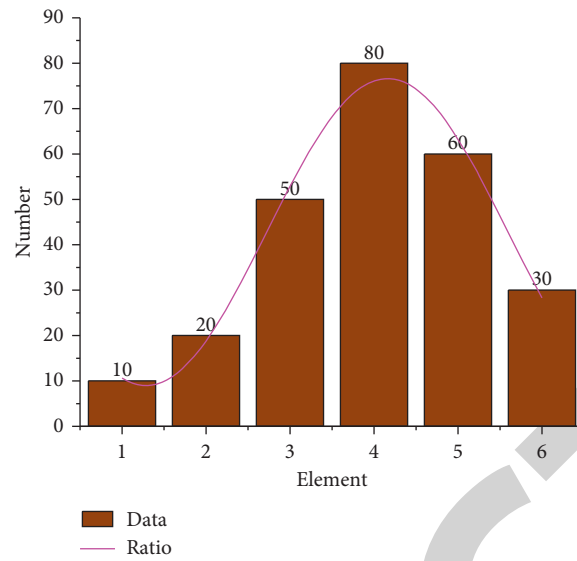


FIGURE 9: Bar chart of Japanese multicontext translation indicators.

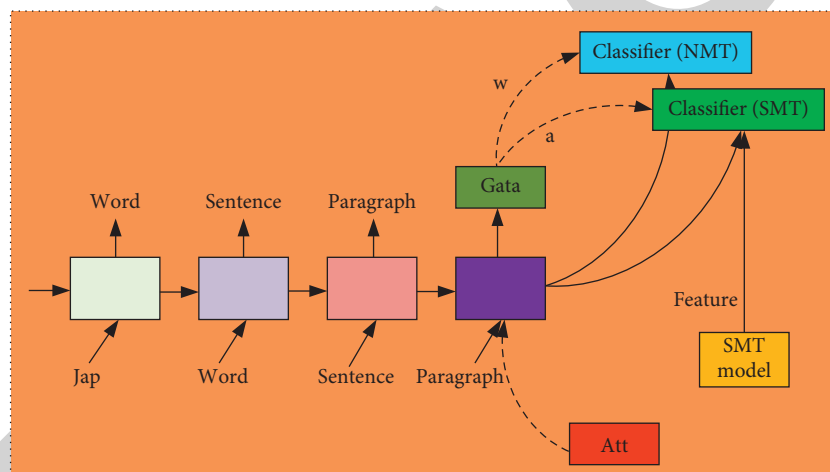


FIGURE 10: Machine translation models apply flow charts in Japanese.

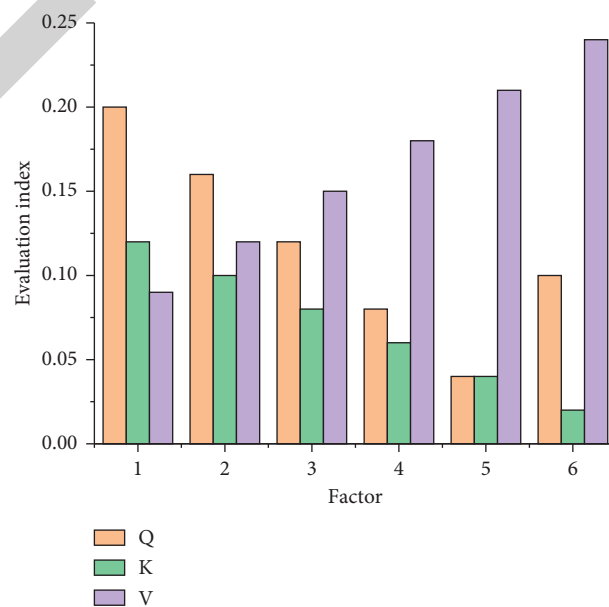


FIGURE 11: Application evaluation chart of machine translation model in Japanese multicontext translation.



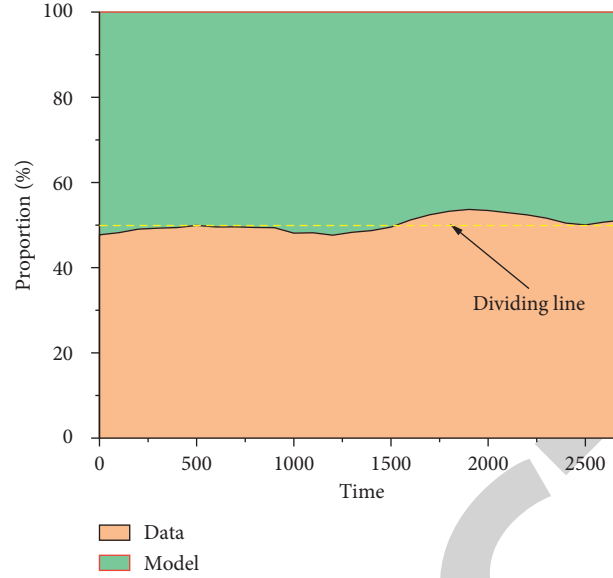


FIGURE 12: Comparison diagram of machine translation model with Japanese data.

show a fluctuating change trend of slowly increasing at first and then rising, and the change curve of the corresponding  $K$  value begins to show the overall decline. It is worth noting that this downward trend shows an approximate linear decline. With the increase of index factors, the corresponding curve of parameter  $V$  value shows a gradually increasing trend. Again, the tendency to increase is approximately linear; therefore, we can see that among the three parameters, parameter  $V$  has a positive impact on the evaluation index of Japanese multicontext. The effect of parameter  $K$  on the index is negative. Finally, the influence of parameter  $Q$  on the index is volatile.

#### 4. Discussion

The above research mainly focuses on the translation and application of Japanese multicontext from the optimization of machine translation model, which mainly includes the analysis and evaluation of machine translation model. From the above analysis, it can be seen that the MACHINE translation model has certain pertinence in the description of Japanese multicontext. In order to further analyze the accuracy of the application of the optimized machine translation model in Japanese multicontext, we draw corresponding graphs for description.

In order to further analyze and verify the accuracy of the machine translation model and the actual Japanese data, a comparison diagram between the Japanese translation data and the machine translation model is drawn, as shown in Figure 12. As can be seen from the figure, compared with the boundary line, the corresponding model index shows a fluctuation trend of first increasing, then decreasing, then increasing, and finally decreasing. The corresponding data show a decrease first, then an increase, and finally the change trend of volatility. From this trend, we can see that the cut-off point basically remains at about 50%, which indicates that the optimized machine translation model can well represent

the influence of various factors in Japanese data, so as to obtain accurate translation results.

#### 5. Conclusion

- (1) According to the overall trend, the influence curve of different parameters on the evaluation index can be divided into linear change, fluctuation change, and stable change. The variation trend of different parameters is basically the same in the first stage, indicating that parameters in this stage have little influence on the curve. The corresponding start time of the second stage showed different trends, indicating that different parameters in the second stage would have a greater impact on the curve. The parameter  $P$  has the greatest influence on the curve, while the corresponding parameter  $F$  has the least influence on the curve.
- (2) By analyzing the influence curves of different parameters  $i$  and  $j$  on the decoder, it can be seen that the influence of parameters  $i$  and  $j$  on the decoder shows a linear trend of change. By fitting the corresponding surface, it can be seen that the corresponding influence degree is  $c_{ij} > s_{ij} > a_{ij} > e_{ij}$ . Therefore, we need to use different parameters to analyze and solve the decoder in different degrees, so as to get the optimal data.
- (3) According to the curve of parameter  $X$  changing with the vector, it can be seen that parameter  $Q$  shows a trend of gradually increasing. Parameter  $K$  shows a trend of gradual decline. Parameter  $V$  presents a trend of gradual decline.
- (4) With the gradual increase of parameter matrix  $W$  and  $b$ , the influence value of the corresponding optimization index FNN network shows a change trend of linear increase. This indicates that both of

## *Retraction*

# **Retracted: Analysis and Construction of Software Engineering OBE Talent Training System Structure Based on Big Data**

### **Security and Communication Networks**

Received 26 December 2023; Accepted 26 December 2023; Published 29 December 2023

Copyright © 2023 Security and Communication Networks. This is an open access article distributed under the Creative Commons Attribution License, which permits unrestricted use, distribution, and reproduction in any medium, provided the original work is properly cited.

This article has been retracted by Hindawi, as publisher, following an investigation undertaken by the publisher [1]. This investigation has uncovered evidence of systematic manipulation of the publication and peer-review process. We cannot, therefore, vouch for the reliability or integrity of this article.

Please note that this notice is intended solely to alert readers that the peer-review process of this article has been compromised.

Wiley and Hindawi regret that the usual quality checks did not identify these issues before publication and have since put additional measures in place to safeguard research integrity.

We wish to credit our Research Integrity and Research Publishing teams and anonymous and named external researchers and research integrity experts for contributing to this investigation.

The corresponding author, as the representative of all authors, has been given the opportunity to register their agreement or disagreement to this retraction. We have kept a record of any response received.

### **References**

- [1] Z. Jie, "Analysis and Construction of Software Engineering OBE Talent Training System Structure Based on Big Data," *Security and Communication Networks*, vol. 2022, Article ID 3208318, 10 pages, 2022.

## Research Article

# Analysis and Construction of Software Engineering OBE Talent Training System Structure Based on Big Data

Zhang Jie 

Computer Department, Zhangjiajie College of Jishou University, Zhangjiajie 427000, Hunan, China

Correspondence should be addressed to Zhang Jie; 201307030306@hnu.edu.cn

Received 30 May 2022; Revised 4 July 2022; Accepted 8 July 2022; Published 30 July 2022

Academic Editor: Hangjun Che

Copyright © 2022 Zhang Jie. This is an open access article distributed under the Creative Commons Attribution License, which permits unrestricted use, distribution, and reproduction in any medium, provided the original work is properly cited.

Software engineering is one of the most active fields of entrepreneurship and innovation in the world, and it is also the core field of the information technology industry. Software talents as the foundation and support are an important weight to determine the future direction of my country's software engineering. How to make colleges and universities cultivate compound software talents with innovative ability and engineering ability and how to guide students to closely combine innovative thinking with social practice are a major challenge faced by the current software process education in colleges and universities in my country. At present, the overall quality of software engineers is poor, which cannot meet the needs of enterprises and training objectives. This paper puts forward the application of the OBE (outcome-based education) model in the training of software talents, which can effectively solve the current problems of talent quality and social demand. The analysis shows that there is a high correlation between collaborative education and satisfaction, and the collaborative education model can effectively improve satisfaction. The investment of scientific research funds can effectively improve the overall quality of scientific research team members. The OBE talent training mode can effectively improve the overall test effect, whether in the experimental set or the test set, the test result of the OBE talent training structure is still the highest, the accuracy rate can reach 94.23%, the recall rate can reach 94.51%, and the F1 value can reach 95.13%. It is fully explained that the identification accuracy is the highest when the OBE talent-training structure is adopted.

## 1. Introduction

The OBE concept is a result-oriented advanced educational concept, which has gradually become the mainstream educational concept to which developed countries pay more attention. Facing the rapid development of information science and technology and the society's demand for compound skilled talents, technical colleges have put forward a new direction for the training of computer professionals. By introducing the concept of OBE education, the overall quality of talents can be improved. Promote the long-term development of talents, improve the teaching effect, and greatly improve the social competitiveness of talents. This paper studies the construction of circuit and electronic technology courses based on the OBE talent training model and puts forward feasible suggestions [1]. It discusses the training of computer hardware talents and proposes a

progressive training model for computer hardware talents based on OB [2]. Based on the concept of OBE, this paper realizes the goal of training high-quality applied talents for English majors in private colleges and universities [3]. Through the in-depth analysis of the professional development of human resource management in our school, this paper summarizes the development status of human resource management based on the concept of OBE [4]. How to introduce OBE theory into the talent training process of higher education in China has become an important issue [5]. It starts from the basic principles of construction and environmental professional personnel training and gives specific construction measures for the professional personnel training model from the whole process of training [6]. It shows that "result-oriented, student-centered continuous improvement" is the core of engineering education certification in my country [7]. Based on achievement

education and the CDIO (conceive design implement operate) education model, combined with emerging engineering education, this paper proposes a training model for engineering education in China [8]. Based on the concept of OBE in the vocational education talent training project, this paper adjusts the curriculum system and reforms the teaching mode and the teaching method, in order to continuously improve the teaching quality [9]. Based on the concept of OBE engineering education, this paper proposes new concepts, new methods, and new achievements with characteristics in view of the new problems faced by the innovation of the talent training model [10]. In the context of China's "One Belt, One Road" strategy, this article discusses a new model for talent training [11]. According to the concept of OBE, it puts forward new challenges to the revision and improvement of the training objectives of engineering and technical personnel [12]. It expounds on several different aspects that the introduction of the OBE concept into the reform of the vehicle engineering talent training mode has played a positive role in cultivating students' knowledge, ability, and quality [13]. From the perspective of OBE, it clarifies the requirements of the training program and designs a training program evaluation system based on the OBE concept [14]. It explores the advanced education concept of OBE based on the current ability training guide for talent training [15]. The above literature has carried out a large number of descriptions on the application of the OBE mode in personnel training, starting from the needs of different professional construction and the corresponding training programs, but it has not evaluated the effect of OBE personnel training, and the overall advantages have not been effectively reflected. The second part explains the training of OBE talents, the third part explains the theory of the OBE talent training structure model, and the fourth part compares the training effect of the OBE mode and other modes in software engineering.

The OBE Model is applied to personnel training, curriculum construction, professional construction, and so on. It can effectively evaluate the quality of personnel training and achieve the training effect. In this paper, the OBE Model is applied to verify the goal of software engineering personnel training, through improving the software training process, to achieve the talent training mode of enterprise demand as the goal.

## 2. OBE Talent Training System Structure Construction

**2.1. OBE Mode.** In the OBE model education, the four important operational components of curriculum structure, knowledge imparting process, students' performance evaluation and ability certification, and students' positioning and development are related to each other, which are different from those in the traditional teaching model. What OBE proposes is a set of methods for designing, implementing, documenting, and reflecting on teaching objectives that are different from traditional educational models. Facts also proved that many schools organize teaching activities around the teaching goals determined according to their

own characteristics and finally make students and schools achieve common progress. The internal organizational relationship of the OBE model is shown in Figure 1.

**2.2. Analysis of Talent Training.** Under the OBE concept, the curriculum system and teaching plan should be formulated according to the graduation requirements, and the requirements that computer majors need to meet for graduation should be defined so as to carry out targeted teaching activities. Therefore, they should be carried out from the following aspects: first, with the professional ability assessment standards for computer majors as a guide, through information means to the relevant enterprises, departments, industries, and professional teachers, evaluation of the current graduation requirements, solicitation of opinions, and provision of feedback on the technical colleges. The graduation requirements of computer professional-skilled talents in the school are analyzed and requested, so as to form a unified opinion. The dimensions of professional talent training analysis are shown in Table 1.

## 3. Establishment of the OBE Talent Training Structure Model

**3.1. Analysis of the Talent Training Model.** The index reflects the control of the talent source by the talent system of the college in the actual implementation process. The specific calculation method is shown in the following equation [20]:

$$I_1 = \frac{N_{yyk}}{N_{jh}} \times 100\%. \quad (1)$$

Here,  $N_{yyk}$  represents the total number of people who enter vocational schools to study each year and  $N_{jh}$  represents the total number of planned enrollment of vocational schools in that year.

The formula for calculating the quality level of potential talents is as follows:

$$I_2 = \frac{1}{n} \sum \text{Score}_{yi}. \quad (2)$$

The theoretical training effect is shown in the following equation:

$$I_3 = \frac{1}{N_s} \sum \frac{1}{N_{bk}} \sum \text{Score}_{jlj}, \quad i = 1, 2, \dots, N_s. \quad (3)$$

The effect of vocational theory training is shown in the following equation:

$$I_4 = \frac{1}{N_s} \sum \frac{1}{N_{lk}} \sum \text{Score}_{lli}, \quad i = 1, 2, \dots, N_s. \quad (4)$$

The professional skill training effect is shown in the following equation:

$$I_5 = \frac{1}{N_s} \sum \frac{1}{N_{sk}} \sum \text{Score}_{lsi}, \quad i = 1, 2, \dots, N_s. \quad (5)$$

The practical ability training effect is shown in the following equation:

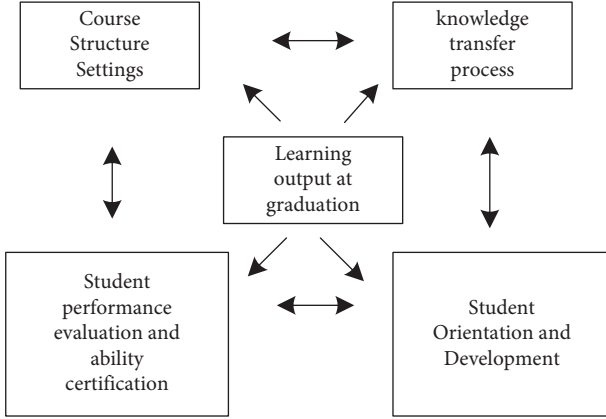


FIGURE 1: Internal organizational relationship of the OBE model.

$$I_6 = \frac{1}{N_{ls}} \sum \frac{1}{N_t} \sum \text{Score}_{lzi}, \quad i = 1, 2, \dots, N_{ls}. \quad (6)$$

Investment in infrastructure in the process of talent training is as follows:

$$I_7 = \frac{\sum F_m}{\sum A_n} \times 100\%. \quad (7)$$

The degree of emphasis placed on vocational skill training in higher vocational colleges is shown in the following equation [21]:

$$I_8 = \frac{\sum P_k}{\sum S_h} \times 100\%. \quad (8)$$

The talent system attaches importance to information and professional talent performance appraisal as shown in the following equation:

$$I_9 = \frac{\sum V_1}{\sum S_h} \times 100\%. \quad (9)$$

Emphasis on relearning ability is shown in the following equation:

$$I_{10} = \frac{N_{ce}}{N_{pz}} \times 100\%. \quad (10)$$

The degree of emphasis on talents in the process of vocational skill talent allocation is shown in the following equation [22]:

$$I_{11} = \frac{\sum HR_j}{\sum F_j} \times 100\%. \quad (11)$$

The theoretical level of professional talent system training talents is as follows:

$$O_1 = \frac{\sum N_{li}}{N_{pz}} \times 100\%. \quad (12)$$

The level of the professional talent system to cultivate skilled talents is as follows:

$$O_2 = \frac{N_{pz}}{N_{ls}} \times 100\%. \quad (13)$$

Supply capacity of professional talents is shown in the following equation [23]:

$$O_3 = \frac{\sum P_{hx}}{\sum P_t} \times 100\%. \quad (14)$$

The ability of professional talents to use professional skills is as follows:

$$O_4 = \frac{\sum P_{zy}}{\sum P_t} \times 100\%. \quad (15)$$

Professional talents' practical skill inheritance ability is shown in the following equation:

$$O_5 = \frac{\sum S_{dn}}{\sum S_t} \times 100\%. \quad (16)$$

Re-learning ability of professional talents is shown in the following equation:

$$O_6 = \frac{\sum K_{dn}}{\sum K_n} \times 100\%. \quad (17)$$

The consistency check is shown in the following equation [24]:

$$CI = \frac{\lambda_{\max} - n}{n - 1}. \quad (18)$$

The normalization formula is shown in the following equation [25]:

$$b_{ij} = \frac{a_{ij}}{\sum_{i=1}^n a_{ij}} i, j = 1, 2, 3, 4, 5. \quad (19)$$

## 4. Simulation Experiments

**4.1. Comparative Experiment.** In order to verify the effect of the software engineering OBE talent training model based on big data, we conducted a three-year practice of the talent training program model for software engineering majors in a university and compared it with the students who did not go through the talent training program. Judging from the employment situation of fresh graduates in the past three years, compared with before practice, the employment ratio of software engineering graduates in well-known IT companies has increased by one grade, and the average monthly salary of graduates has also increased. The comparison results of graduation quality in the past three years are shown in Table 2.

According to the statistical results in Table 2 and Figure 2, it can be concluded that after the implementation of the new model, the employment ratio of well-known enterprises has increased from 60% to more than 80%, and the average monthly salary of graduates has increased from 5,000 yuan to 7,000 yuan. The purpose of the experiment is to test the situation of enterprises and employment

TABLE 1: Analysis dimensions of professional talent training.

Analysis dimension	Illustrate
Talent training goals	The determination of talent training goals is the initial point of implementation of higher education, which reflects the fundamental pursuit of specific majors [16]
Type of course structure	The construction of a specific structure and type of the course group is the most basic and most valuable service that a specific major of a university can provide [17]
Teaching method	The innovation of teaching methods is the use of high-quality educational resources of various majors by universities in the process of talent training, which reflects the educational concept and education ability of specific majors [18]
Evaluation of training results	Result evaluation is a measure of the effectiveness of specific professional personnel training. The evaluation methods, evaluation content, evaluation process, and other evaluation systems themselves reflect the professional value orientation and business pursuit [19]

TABLE 2: Graduation quality comparison results in the past three years.

Year	High-quality employment (%)	Average monthly salary of graduates/ yuan
Graduated in 2018 (after the implementation of the new model)	88.9	7520
Graduated in 2017 (after the implementation of the new model)	81.8	7180
Graduated in 2016 (before the implementation of the new model)	62.3	5250

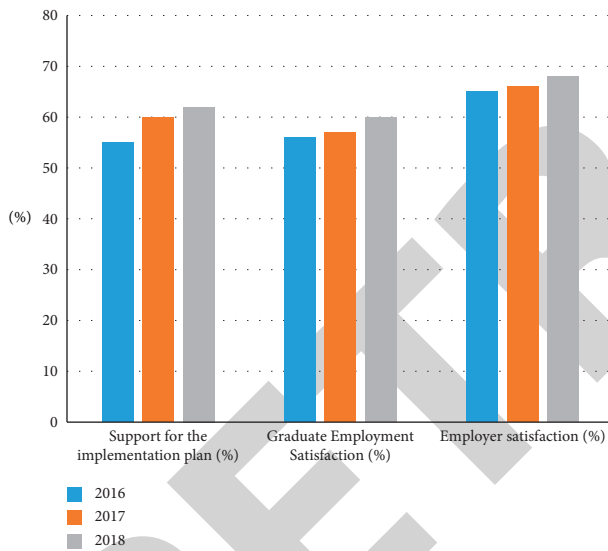


FIGURE 2: The statistical chart of the survey before the implementation of the scheme.

satisfaction before and after the implementation of the new model by adjusting the feedback of the recent three graduates. The specific survey data are as follows.

According to the survey results in Table 3 and Figure 3, we can conclude that before the implementation of the talent training plan, the overall satisfaction level was at a low level. The highest level of support for the implementation of the plan is only 60%, the highest level of employer satisfaction is 68%, and the average monthly salary of graduates is also at a low level.

According to the experimental data in Table 4 and the statistical results before the practice of the talent training program, the related satisfaction of the graduates has improved by leaps and bounds. The graduates' support for the collaborative education model after the implementation is

above 90%. Employment satisfaction increased from 56% in 2016 to over 96% in 2018 compared to 2016 graduate employment satisfaction before the program was implemented. At the same time, employers' satisfaction with the quality of graduates has also increased from 65% before the implementation in 2016 to more than 98% after the implementation. Based on the survey results, the implementation of the new model has also improved the comprehensive literacy of students in software engineering. In the process of software analysis and design, students continue to summarize, report, discuss, make videos and report PPT, and condense innovation points, so students' literacy in summary, analysis, expression, reporting, and communication has significantly improved.

The implementation of the new model has also recognized the innovation of the software achievements of the fresh students in the practice session. Comparing before and after the implementation of the new model, it is found that in 2017 and 2018, fresh students applied for more than 30 University of Electronic Science and Technology College Students' innovation and entrepreneurship funds. The number of participants accounts for more than 60% of the total number of participants. The software works participated in Microsoft Global Embedded It has won more than 10 awards in various IT and software competitions, such as the "China Cup" software design competition for college students, and the number of participants accounted for more than 25% of the total number of participants, whether in terms of the number of projects, the number of awards, or the proportion of participants, compared with 2016 before the implementation, and the specific situation is shown in Table 5.

**4.2. Analysis of Influencing Factors.** In order to further quantitatively analyze the influencing factors of industry-university-research cooperation on the cultivation of



TABLE 3: The satisfaction survey before the implementation of the new model.

Year	Support for the implementation plan (%)	High-quality employment (%)	Employer satisfaction (%)
2016	55	56	65
2017	60	57	66
2018	62	60	68

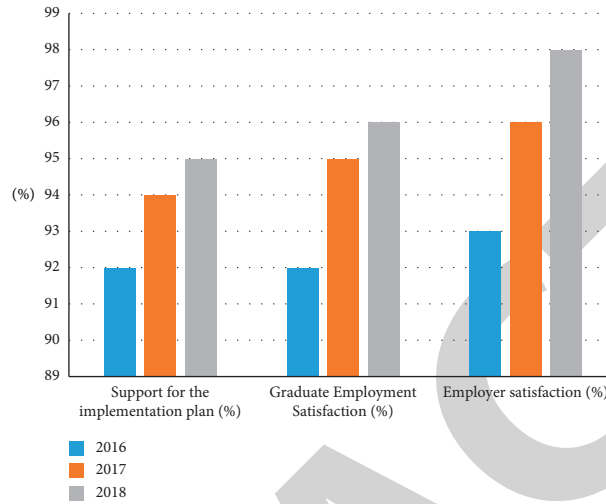


FIGURE 3: The statistical chart of the survey after the implementation of the scheme.

TABLE 4: The satisfaction survey after the implementation of the new model.

Year	Support for the implementation plan (%)	High-quality employment (%)	Employer satisfaction (%)
2016	92	92	93
2017	94	95	96
2018	95	96	98

TABLE 5: Comparison of project approval and award-winning data in the past three years.

Years	Innovation and entrepreneurship fund/project	Participation ratio (%)	Discipline competition award/item	Participation ratio (%)
Graduated in 2018 (after the implementation of the new model)	18	80	5	30
Graduated in 2017 (after the implementation of the new model)	12	60	5	25
Graduated in 2016 (before the implementation of the new model)	5	10	2	8

innovative talents, the empirical research method was adopted in the experiment. The collected questionnaires are analyzed by weight, and the results are as follows.

According to the above results, after the grey correlation analysis, it can be obtained that among the influencing factors of industry-university-research cooperation on the cultivation of innovative talents, the level of scientific research has the greatest impact on the cultivation of innovative talents, and the subject patents have the least impact on the cultivation of innovative talents. The investment of scientific research funds and the number of personnel engaged in scientific research activities have basically the same influence on the cultivation of innovative talents, and the

influence ability is relatively weak. The environment of industry-university-research cooperation has a greater impact on the cultivation of innovative talents, and the perfect network and environment construction are ranked second and third, respectively, as shown in Figures 4–6 and Tables 6–8.

**4.3. Model Checking.** The talent training structure model has a great role in promoting the efficiency of talent training. The experiment combines the talent training structure model proposed in the article with the traditional talent training structure, the industry-university-research cooperation talent training structure, and the control teaching talent

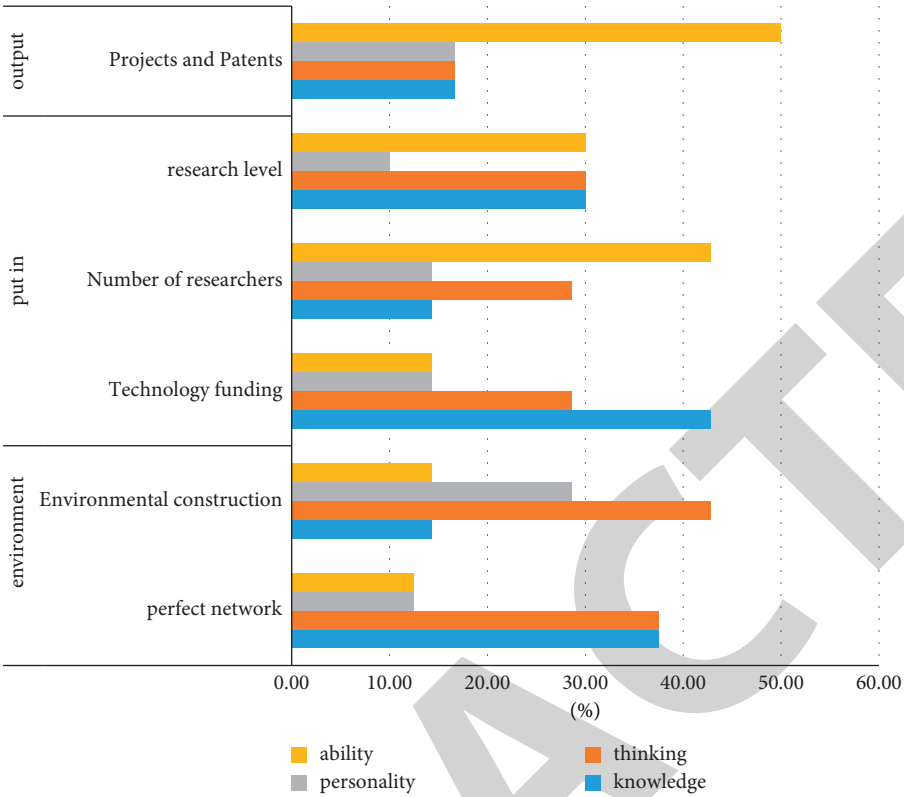


FIGURE 4: The statistical chart of horizontal proportion.

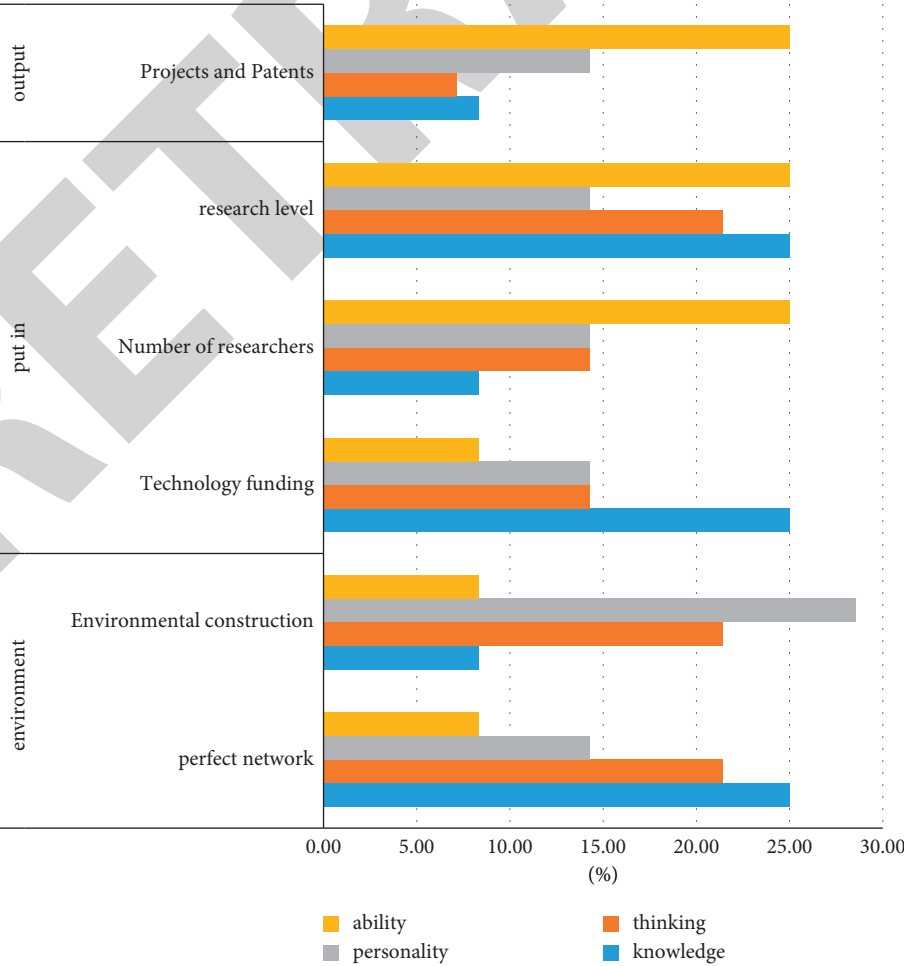


FIGURE 5: Vertical proportion statistical chart.

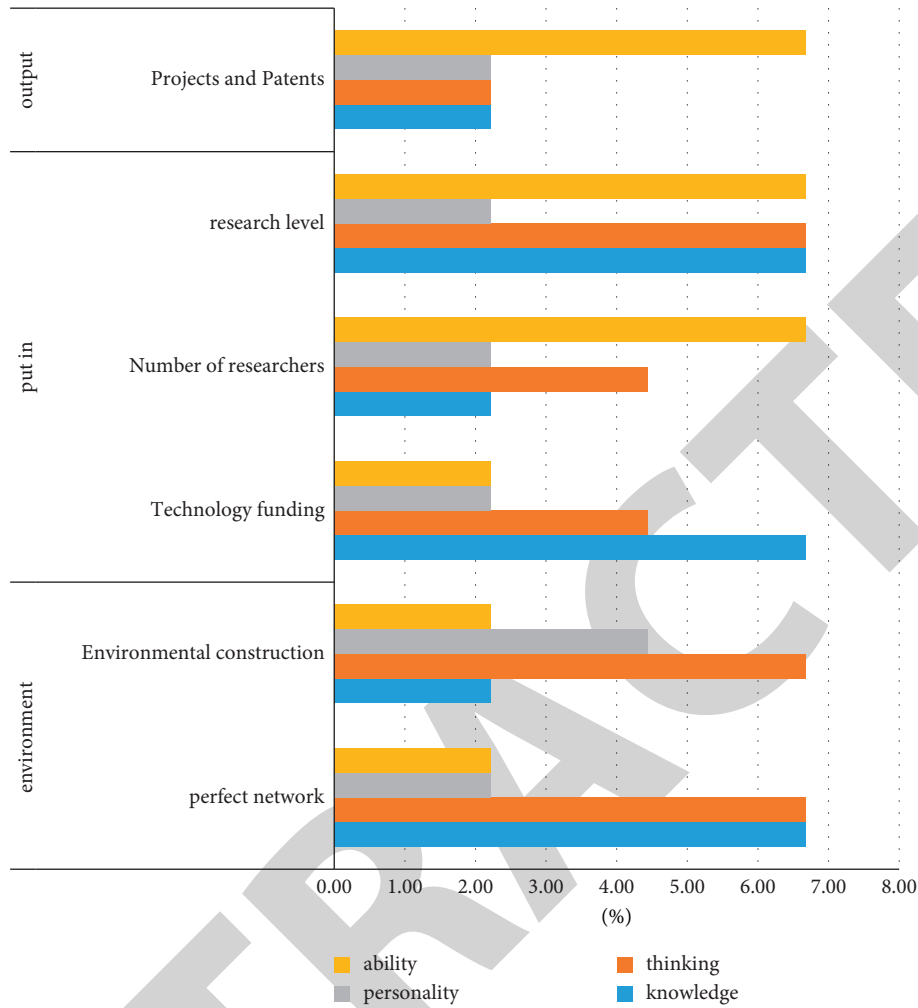


FIGURE 6: Vertical proportion statistical chart.

TABLE 6: Horizontal proportion of the impact of industry-university-research cooperation on the cultivation of innovative talents.

Operation	Technical index	Knowledge (%)	Thinking (%)	Personality (%)	Ability (%)
Environment	Perfect network	37.50	37.50	12.50	12.50
	Environmental construction	14.29	42.86	28.57	14.29
Input	Technology funding	42.86	28.57	14.29	14.29
	Number of researchers	14.29	28.57	14.29	42.86
	Research level	30.00	30.00	10.00	30.00
Output	Projects and patents	16.67	16.67	16.67	50.00

training structure in different dimensions so as to test the performance of different models. The specific experimental data are shown in Tables 9 and 10.

According to the experimental data in Table 9 and Figure 7, the test result of the OBE talent training structure proposed in the article is the highest, indicating that the performance of the OBE talent training structure is the best, and the accuracy rate of talent training can reach 96.23%. The training effect is not ideal, the talent training plan is not perfect, and the detection value of the industry-university-research cooperation talent training structure and the control teaching talent training structure is between the

highest value and the lowest value. According to the graph, it can be seen that the data of the OBE talent training structure are relatively stable, and the experimental data also show that the OBE talent training structure has a great role in promoting talent training.

According to the data in Table 10 and Figure 8, it is concluded that the OBE talent training structure has the highest accuracy rate for talent cultivation, and the detection accuracy rate remains above 94%, indicating that the test results are excellent and can meet the requirements of most talent cultivation. The graph of the OBE talent training structure also shows a stable situation, which is better than

TABLE 7: Vertical proportion of the impact of industry-university-research cooperation on the cultivation of innovative talents.

Operation	Technical index	Knowledge (%)	Thinking (%)	Personality (%)	Ability (%)
Environment	Perfect network	25.00	21.43	14.29	8.33
	Environmental construction	8.33	21.43	28.57	8.33
Input	Technology funding	25.00	14.29	14.29	8.33
	Number of researchers	8.33	14.29	14.29	25.00
	Research level	25.00	21.43	14.29	25.00
Output	Projects and patents	8.33	7.14	14.29	25.00

TABLE 8: The overall proportion of the impact of industry-university-research cooperation on the cultivation of innovative talents.

Operation	Technical index	Knowledge (%)	Thinking (%)	Personality (%)	Ability (%)
Environment	Perfect network	6.67	6.67	2.22	2.22
	Environmental construction	2.22	6.67	4.44	2.22
Input	Technology funding	6.67	4.44	2.22	2.22
	Number of researchers	2.22	4.44	2.22	6.67
	Research level	6.67	6.67	2.22	6.67
Output	Projects and patents	2.22	2.22	2.22	6.67

TABLE 9: The performance of each model in the experimental set.

Model	Precision (%)	Recall (%)	F1 score (%)
OBE talent training structure	96.23	97.12	97.56
Traditional talent training structure	62.13	63.14	63.45
Industry-university-research cooperation talent training structure	82.12	83.14	85.16
Control the training structure of teaching talents	85.26	86.24	86.78

TABLE 10: The performance of each model in the test set.

Model	Precision (%)	Recall (%)	F1 score (%)
OBE talent training structure	94.23	94.51	95.13
Traditional talent training structure	65.36	66.12	66.23
Industry-university-research cooperation talent training structure	80.13	80.24	80.49
Control the training structure of teaching talents	83.36	83.49	84.13

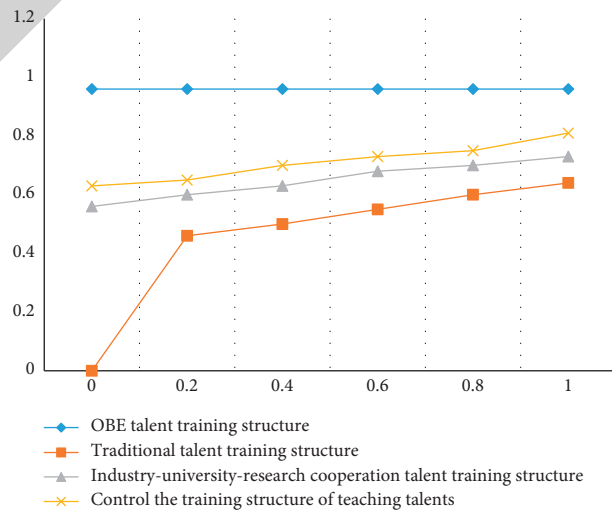


FIGURE 7: ROC curve in the test set.

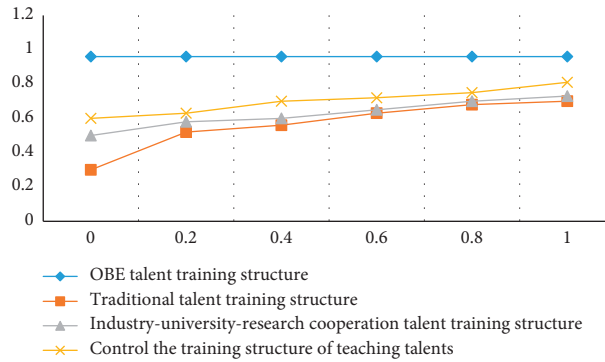


FIGURE 8: ROC curve in the test set.

the performance of other models, which shows that the talent training model proposed in this paper can be applied in the talent training scheme.

## 5. Conclusion

The task of higher education is to cultivate a group of high-quality innovative talents for the country. Facing the requirements of “new engineering,” this paper focuses on “what kind of talents should be cultivated to meet the requirements of software engineering” and in order to achieve such a training goal, a professional talent training system of school enterprise integration and collaborative education is studied and constructed. Establish the talent training goal with “high-level and application-oriented” as the core, and implement it based on social needs. It is a professional training mode of gradual school-enterprise in-depth cooperation for four years in the university.

## Data Availability

The experimental data used to support the findings of this study are available from the author upon request.

## Conflicts of Interest

The author declares no conflicts of interest regarding this work.

## References

- [1] Q. X. Qin and K. H. Hao, “Research on the construction of circuit and electronic technology based on OBE talent training mode,” *Education Teaching Forum*, vol. 12, no. 03, pp. 1–7, 2019.
- [2] S. Shen, C. Lv, and X. Xu, “Computer hardware talent progressive training model based on OBE,” *Computer Era*, vol. 03, no. 10, pp. 52–62, 2019.
- [3] B. B. Chen and F. L. Department, “The Strategies of high-quality applied talent training for English majors in private Colleges based on OBE Concept,” *Journal of Hubei Open Vocational College*, vol. 16, no. 03, pp. 45–52, 2019.
- [4] Y. Chen, “Optimization of talent training program in Aeronautics universities under the Concept of OBE: Taking the human resource management major of Zhengzhou university of Aeronautics as an Example,” *The Science Education Article Collects*, vol. 5, no. 03, pp. 11–23, 2019.
- [5] D. J. Zhou, J. J. Zhang, and Y. X. Wang, “Research on the innovation and realization path of foreign legal excellence talent training model under the OBE Concept,” *Economic Research Guide*, vol. 13, no. 01, pp. 52–63, 2018.
- [6] Y. Liu, “Construction and practice of Licensed talent training model for engineering management professional based on OBE idea,” *The Guide of Science & Education*, vol. 20, no. 06, pp. 52–63, 2019.
- [7] X. Q. Zheng, H. Tian, and J. B. Zeng, “Exploration and practice of Electrical engineering talent training system based on OBE “Double Closed-loop” Continuous improvement,” *Education Teaching Forum*, vol. 23, no. 06, pp. 48–53, 2019.
- [8] W. Chen, Y. Lin, and Z. Ren, “Exploration and practical research on teaching reforms of engineering practice center based on 3I-CDIO-OBE talent-training mode,” *Computer Applications in Engineering Education*, vol. 10, no. 06, pp. 21–32, 2008.
- [9] N. C. Yao and X. U. Min, “A research on the Automation training talent mode based on OBE educational Ideas,” *Communication of Vocational Education*, vol. 13, no. 06, pp. 52–63, 2018.
- [10] C. Wang, Z. Yin, and L. I. Zhaoqing, “Reform and practice of material science and engineering specialty talent training mode based on OBE engineering education concept,” *Journal of Heilongjiang Institute of Technology*, vol. 10, no. 03, pp. 25–32, 2018.
- [11] Q. Wang, L. I. Wen, and L. I. Rong, “Discussion about talent training mode of applied logistics engineering based on OBE educational idea,” *Journal of Heilongjiang Institute of Technology*, vol. 10, no. 08, pp. 41–53, 2017.
- [12] C. L. Yang, L. I. Li, and H. G. Jia, “Establishment mechanism and procedure of training objectives of talent based on OBE,” *Polymer Bulletin*, vol. 10, no. 06, pp. 11–23, 2019.
- [13] M. Xingfeng, L. Ying, Lu Zhaona, and Z. Jianfeng, “Study on the reform of talent training mode of vehicle engineering in application-oriented Undergraduate universities based on OBE Concept taking the vehicle engineering majors in Nantong Institute of technology as an Example,” in *Proceedings of the 3rd International Conference on Culture, Education and Economic Development of Modern Society (ICCESE 2019)*, pp. 312–356, Atlantis Press, April 2019.
- [14] C. Wang, A. Sun, and Y. Chen, “Research on the evaluation system of engineering education talents training program based on OBE,” *The Theory and Practice of Innovation and Entrepreneurship*, vol. 20, no. 03, pp. 45–63, 2018.

## Retraction

# Retracted: Security Research in Personnel Electronic File Management Based on Blockchain Technology

### Security and Communication Networks

Received 8 August 2023; Accepted 8 August 2023; Published 9 August 2023

Copyright © 2023 Security and Communication Networks. This is an open access article distributed under the Creative Commons Attribution License, which permits unrestricted use, distribution, and reproduction in any medium, provided the original work is properly cited.

This article has been retracted by Hindawi following an investigation undertaken by the publisher [1]. This investigation has uncovered evidence of one or more of the following indicators of systematic manipulation of the publication process:

- (1) Discrepancies in scope
- (2) Discrepancies in the description of the research reported
- (3) Discrepancies between the availability of data and the research described
- (4) Inappropriate citations
- (5) Incoherent, meaningless and/or irrelevant content included in the article
- (6) Peer-review manipulation

The presence of these indicators undermines our confidence in the integrity of the article's content and we cannot, therefore, vouch for its reliability. Please note that this notice is intended solely to alert readers that the content of this article is unreliable. We have not investigated whether authors were aware of or involved in the systematic manipulation of the publication process.

Wiley and Hindawi regrets that the usual quality checks did not identify these issues before publication and have since put additional measures in place to safeguard research integrity.

We wish to credit our own Research Integrity and Research Publishing teams and anonymous and named external researchers and research integrity experts for contributing to this investigation.

The corresponding author, as the representative of all authors, has been given the opportunity to register their agreement or disagreement to this retraction. We have kept a record of any response received.

### References

- [1] H. Wang and J. Zhang, "Security Research in Personnel Electronic File Management Based on Blockchain Technology," *Security and Communication Networks*, vol. 2022, Article ID 7875825, 8 pages, 2022.



## Research Article

# Security Research in Personnel Electronic File Management Based on Blockchain Technology

Hongbing Wang<sup>1</sup> and Jian Zhang<sup>2</sup>

<sup>1</sup>Personnel, Wuxi Vocational College of Science and Technology, Wuxi 214101, China

<sup>2</sup>College of Artificial Intelligence, Wuxi Vocational College of Science and Technology, Wuxi 214101, China

Correspondence should be addressed to Jian Zhang; 2016009@wxsc.edu.cn

Received 4 June 2022; Revised 21 June 2022; Accepted 5 July 2022; Published 30 July 2022

Academic Editor: Hangjun Che

Copyright © 2022 Hongbing Wang and Jian Zhang. This is an open access article distributed under the Creative Commons Attribution License, which permits unrestricted use, distribution, and reproduction in any medium, provided the original work is properly cited.

Compared with traditional files, electronic personnel files have the characteristics of the economy, environmental protection, convenience, and sharing and are gradually replacing traditional paper files. However, the development of electronic archives is still in its infancy, and there are still many problems, including the professional quality of personnel, information management, and the security of electronic archives storage. As an emerging technology, blockchain technology has the characteristics of decentralization, immutability, and traceability. This paper applies blockchain technology in the management of electronic archives, overcomes the internal distortion and insecurity of electronic archives, and designs an electronic archives management module based on blockchain technology. Through the application in some schools, the effectiveness and practicability of the algorithm are proved.

## 1. Introduction

With the continuous popularization and maturity of big data, cloud computing, and blockchain technology, traditional archives can no longer meet the development needs of employers. Therefore, promoting the electronic management of personnel files is an inevitable trend of informatization development of employers [1]. Electronic archives are an important form of archives digital management. They are archived information stored on specific media using computer technology and are also an important means of archiving modern management [2]. Compared with traditional files, electronic personnel files have the characteristics of the economy, environmental protection, convenience, and sharing [3]. The superiority of personnel electronic file management in file information inquiry, storage, and processing is unmatched by traditional file management. However, the development of electronic archives is still in its infancy, and there are still many problems, including the professional quality of personnel, information management, the security of electronic archives storage equipment, the

security of the network, the security of stored information, and so on [4–6].

As an emerging technology in recent years, blockchain technology has the characteristics of decentralization, immutability, traceability, openness, and transparency [7, 8]. There have been some attempts in many fields, including finance, logistics, Internet of Things, public services, copyright, and so on. Its security features can also be applied to electronic file management to improve the efficiency and safety of the entire electronic file management [9]. This article will analyze the problems in electronic file management and apply blockchain technology to solve many existing problems.

## 2. Electronic File Management and Blockchain Technology

*2.1. Advantages and Problems of Electronic Archives.* Compared with traditional paper archives, electronic archives have obvious advantages [10], which are mainly reflected in the following points:

- (1) *Electronic Files Can Reduce Operating Costs* [11]. In the file management of the personnel system, electronic files can reduce the operating cost of the employer. Traditional personnel file statistics, sorting, and querying require more labor costs. At the same time, it needs to invest a lot of economic costs such as copying, printing, binding, and mailing. In addition, paper files need to be kept, and hardware costs such as fire and moisture resistance are required. The management of electronic records can greatly reduce these operating costs [12–14].
- (2) *Electronic File Management Is Shared*. Limited by time and place, traditional paper archives also have certain limitations [15]. In particular, paper archives are usually only used by one person and cannot share information resources, which greatly limits the exchange of information. Electronic archives management breaks this limitation and can realize the sharing of archives resources. Realize the interconnection of file resources, allowing employees to complete data sharing in real time. Big data is massive, diverse, real-time, and valuable, providing strong support for the sharing of electronic archives resources, and comprehensively improving the service quality and capabilities of archives [16–19].
- (3) *The Management of Electronic Files Is Relatively Easy* [20]. The files include personal academic certificates, professional title materials, salary, job transfer, social relations, and other information. These electronic documents can be named according to certain rules to facilitate searching, updating, and other operations. At the same time, the formulation of rules and systems is relatively easy and easier to manage [21].

Despite the advantages of electronic records, there are also many problems.

- (1) The management system is not perfect, and the construction of the personnel team is lagging behind [22]. Because the management of electronic archives in colleges and universities covers the whole process of the life cycle of electronic documents, it involves a wide range of areas and has many contents, so the original archives management system and management system are not suitable. For example, the creation, circulation, inspection, and utilization of electronic files lack specific rules and regulations, resulting in management loopholes and inadequacies. There are unreasonable structures and unstable personnel in the construction of electronic archives management teams in colleges and universities. Such as the majority of the full-time file management personnel are the elderly, the ability to update knowledge and accept new things is slow, and the young are enthusiastic but unwilling to engage in this boring work [23, 24].
- (2) It is easy to be distorted in electronic files. Compared with paper archives information, the content of digital archives information is easier to be artificially

forged, tampered with, and deleted without leaving traces [25]. The reasons include digital archives information can be stored on various carriers, managers and users can read and artificially modify digital archives information with various devices without leaving traces; due to inconsistent operating systems or software versions, it is prone to distortion problems such as unrecognized digital archive information and image distortion; the current digital archive information management system is mainly based on centralized nodes, databases, and servers. The operation of the system depends on the operations of various managers. Once the digital file information is artificially tampered with, the wrong digital file information will flow into the entire system, causing damage to the authenticity of the digital file information [26].

- (3) Insecurity of storage hardware and network. Electronic files are stored on hard disks, servers, and other hardware. Usually, these devices are connected to the Internet, which poses a security risk. Cyberattacks, hacker attacks, and insider attacks may all be potential threats. These are all centralized devices or servers with relatively high risks [27].

Blockchain technology has the characteristics of decentralization, nontampering, traceability, openness, and transparency, which can reduce these security risks to a certain extent.

**2.2. Blockchain Technology.** Blockchain technology is the underlying technology of Bitcoin. Although there are many international disputes in digital currencies such as Bitcoin, it is undeniable that blockchain technology is being used more and more in finance, logistics, notarization, and many other industries [28]. The so-called blockchain is to store data in blocks and then connects all blocks in sequence and links them together, as shown in Figure 1.

Blockchain technology has the following characteristics:

- (1) *Decentralization*. The so-called decentralization refers to the use of several nodes composed of blockchain technology to form a database, which is relatively complete, closed, and does not have a centrally managed organization or equipment [29]. As shown in Figure 2, Figure 2(a) is a centralized structure, with a central server, and other nodes store data in the centralized server. If the data in the centralized server is distorted, the entire information will be distorted. Figure 2(b) is decentralized. There is no centralized server. All devices are part of the server. Even if the data of some machines is lost, they can be recovered by other machines.
- (2) *Detrust*. Blockchain technology uses a set of transparent and open encryption algorithms to enable the exchange of data and information at all stages of the system under sufficient trustless conditions. Under the conditions of the blockchain network, each network-connected device acts as an independent

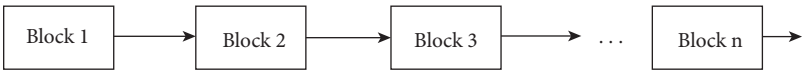


FIGURE 1: Chain structure.

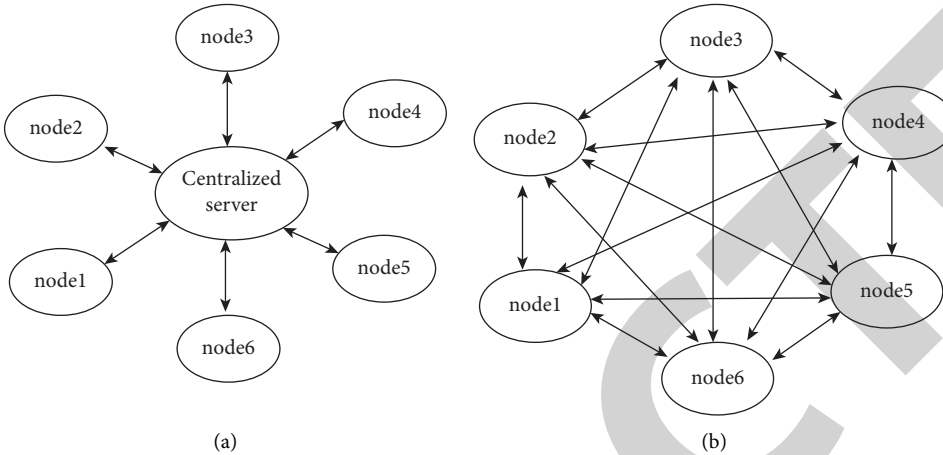


FIGURE 2: The difference between centralization and decentralization. (a) Centralized Node (b) Decentralized Node.

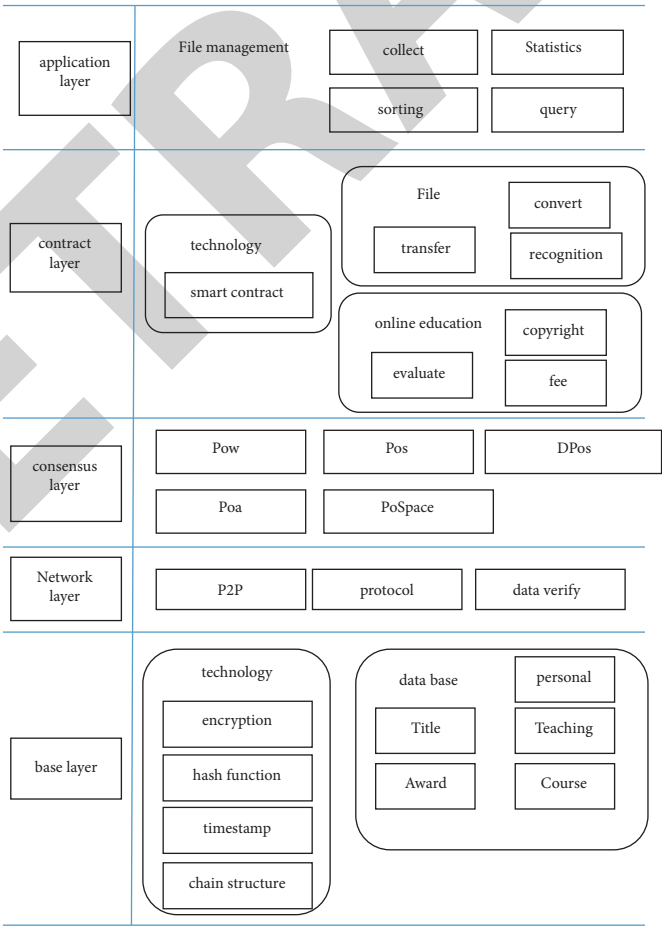


FIGURE 3: Electronic file management system based on blockchain technology.

node, based on a consensus protocol or specification, automatically and securely exchanges data without trust, and both parties do not need to disclose each other's identities.

- (3) *Traceability*. Blockchain technology relies on time stamps and sequential results, which can not only accurately record the creation time of file information in the database but also trace the information of all blocks. The decentralized structure makes the wrong information of any node will not affect the results of the entire network, and the traceability of information is strong.
- (4) *Strong security*. Many cryptographic algorithms are applied in the blockchain system, which can effectively keep the stored information confidential. In addition, the application of the hash algorithm can ensure that the information in the database is not tampered with, the information is kept confidential and secure, and the antitampering function is outstanding.

### 3. Security Design of Electronic Archives Management Based on Blockchain Technology

Using the decentralization, traceability, and encryption algorithm design in the characteristics of blockchain, an electronic file management system based on blockchain technology is designed, as shown in Figure 3. The electronic file management system includes five layers, namely, the base layer, the network layer, the consensus layer, the contract layer, and the application layer. The basic layer includes some underlying technologies and basic data; the network layer includes P2P and other protocols; the consensus layer is some consensus algorithms; the contract layer is some smart contract algorithm technologies; the application layer is the management layer of electronic files, including operations such as collection and processing.

In this structure, each layer involves security, including the underlying hash algorithm and encryption algorithm; the security protocol of the network layer; the security architecture of the consensus layer; the intelligent encryption of the contract layer; the data storage of the application layer, etc. This article will analyze the security of the hash algorithm, the security design of the alliance chain, the security design of data sharing, the security design of the electronic archives platform, and the security encryption algorithm design of electronic archives storage.

**3.1. Security of Hash Algorithm.** The Hash algorithm is a method of creating small numbers from arbitrary files. Like a fingerprint, a hash algorithm is a sign that guarantees the uniqueness of a file with a short piece of information. This sign is related to every byte of the file, and it is difficult to find a reverse pattern. Therefore, when the original file changes, its flag value will also change, thus telling the file user that the current file is not the file you need.

The Hash algorithm can map binary plaintexts of arbitrary length into shorter binary strings, and it is difficult for different plaintexts to be mapped to the same Hash value.

Hash values have the following characteristics:

**Forward fast:** given the plaintext and Hash algorithm, the hash value can be calculated in limited time and limited resources

**Reverse difficulty:** given the hash value, it is difficult to reverse the plaintext in a finite time

**Input sensitivity:** any change in the original input information, the new Hash value should change greatly

**Collision avoidance:** it is difficult to find two pieces of plaintext with different contents so that their hash values are the same

The Hash algorithm includes many logical functions, as shown in the following equations:

$$Ch(x, y, z) = (x \wedge y) \oplus (x \wedge z), \quad (1)$$

$$Ma(x, y, z) = (x \wedge y) \oplus (x \wedge z) \oplus (y \wedge z), \quad (2)$$

$$\sum_0 x = S^2(x) \oplus S^{13}(x) \oplus S^{22}(x). \quad (3)$$

**3.2. Security Design of Consortium Chain.** Blockchain can be divided into the public chain, alliance chain, and private chain. The public chain means that anyone can participate in the use and maintenance, such as the Bitcoin blockchain, and the information is completely open. The public chain is completely decentralized, and anyone can participate in the consensus process. The private chain emphasizes privacy; that is, the writing authority is in the hands of an organization and unit, which is centrally controlled by the organization, but different distributions and branches are decentralized and collaborative. The alliance chain is a system form between the public chain and the private chain, which is often controlled by multiple centers. Several organizations work together to maintain a blockchain, the use of which must be restricted access with permissions, and the relevant information will be protected.

Because university archives data is generally circulated among personnel departments, educational affairs departments, science and technology departments, party and mass departments, scientific research institutes, and universities, it not only breaks through the geographical restrictions of institutions but also eliminates the free participation of all groups, which is more similar to the application scenario of the alliance chain fit. Therefore, this paper proposes a consortium chain architecture that allows stakeholders to join the consortium system conditionally, and the file data are open to the nodes in the chain, but the permissions of each node will be different. For example, the personnel department, educational affairs department, and scientific research management department of archives management are trusted nodes and have certain operating authority. On-campus party and mass departments, teaching departments,

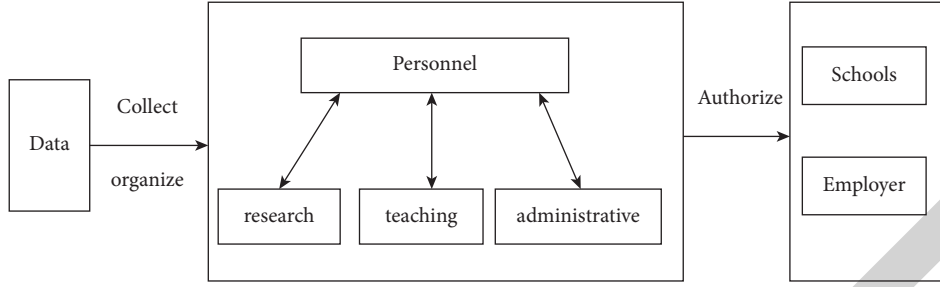


FIGURE 4: Alliance chain.

TABLE 1: Time test.

Process	Time tes t(s)- electronic file 1	Time tes t(s)- electronic file 2
Blinded	0.7	0.65
Blind signature	0.12	0.13
Verify	0.1	0.15

and off-campus education departments, science and technology departments, and scientific research institutes are participating nodes. A trusted node is required to authenticate and authorize it.

The security architecture of the electronic archives alliance chain is shown in Figure 4. Each department is responsible for collecting data and summarizing it to the personnel department. These departments can read data according to permissions. Relevant schools and enterprises can apply and read the data after obtaining authorization.

**3.3. Identity-Based Blind Signature Scheme.** Elliptic Curve Cryptosystem (ECC) is an efficient cryptosystem based on the intractability of the elliptic curve discrete logarithm problem. It can achieve the same security level as the RSA encryption algorithm and the discrete logarithm system with a shorter number of operations. Compared with other public key algorithm systems, ECC has obvious performance advantages in terms of bandwidth and complexity and is very suitable for blockchain related modules.

Identity-based blind signature schemes include key generation, signing, and verification.

The signer generates a private key  $S_I$  and sends  $S_I$  to the signer through a secure channel. The signer is verified according to the following formula:

$$S_I G - Q_I P = \begin{cases} 0 & \text{TRUE,} \\ 1 & \text{FALSE.} \end{cases} \quad (4)$$

In which,  $G$  is the  $n$ -order base point on the elliptic curve,  $Q_I$  is the Hash function, and  $P$  is the public key. If the verification is 0, it is true, indicating that the key generation is successful.

The signer calculates the public key  $R$  and sends it to the user. The user generates factors  $\beta$ ,  $\gamma$ , and  $\delta$  to obtain the elliptic curve equation.

$$R + \beta G + \gamma H + \delta Q = (X, Y). \quad (5)$$

After blinding,  $e$  is obtained, and  $e$  is signed and verified.

$$e = M(mx(\text{mod } p)I) - \delta. \quad (6)$$

The data in Table 1 was obtained by testing different archive sets.

**3.4. Security Design of Data Sharing.** The data sharing mechanism of electronic archives can be realized through smart contracts. A smart contract is a simple transaction that can be executed automatically. It is stored in the blockchain and synchronized between nodes to maintain the consistency of the contract. A full self-service file service system based on blockchain technology can first formulate smart contracts and then spread them into each node. After the file user enters personal information and usage requirements, the system automatically executes according to the preset method when the corresponding conditions of a certain mechanism are met, as shown in Figure 5. Both the data application and the printing application need to be reviewed, judged, and automatically executed by the smart contract and finally authorized to the user.

**3.5. Security Design of Electronic Archives Platform.** The framework of the blockchain-based electronic archives platform is shown in Figure 6. The platform includes a blockchain recording platform, a blockchain security platform, a blockchain scheduling platform, a blockchain hardware platform, and a node management platform. Through these platforms, data access, access control, traceability management, judgment, and payment are realized. The blockchain security platform is responsible for the security of the entire structure.

**3.6. Design of Secure Encryption Algorithm for Electronic File Storage.** In the personnel file information, there is a lot of picture information that needs to be encrypted and stored. In a blockchain network, storage is an important content and can be stored in multiple nodes. For privacy, images need to be encrypted and saved. There are many encryption

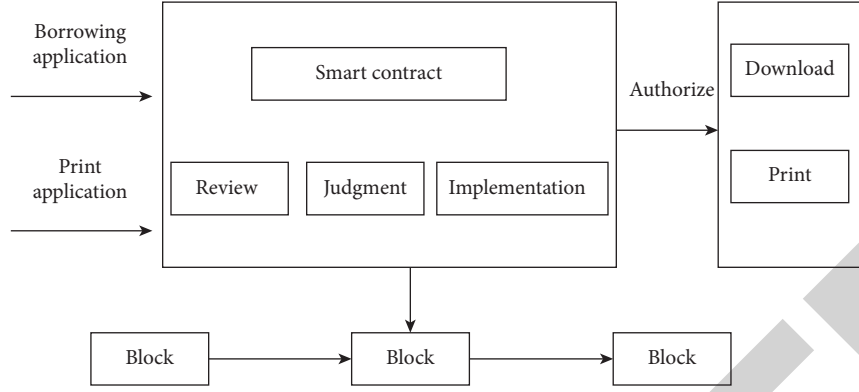


FIGURE 5: Smart contract.

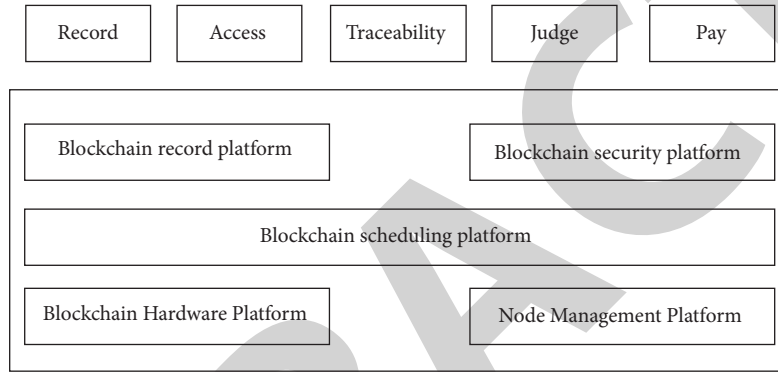


FIGURE 6: Blockchain platform.

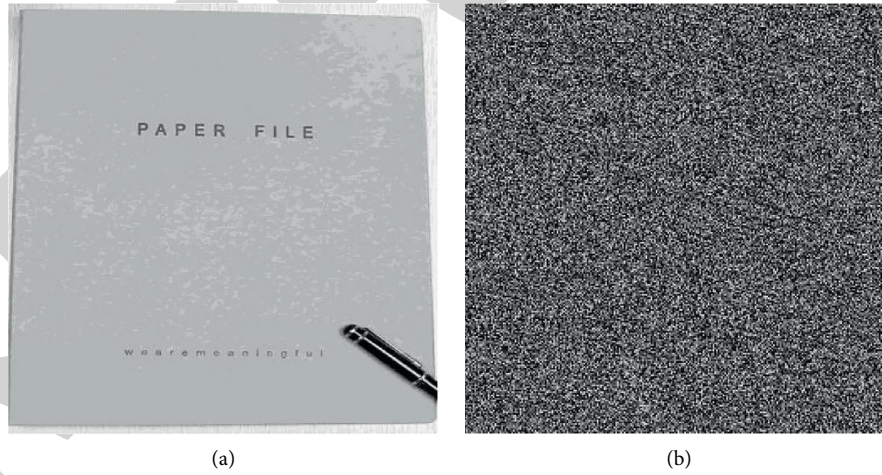


FIGURE 7: The image encryption algorithm.(a) original image (b) encrypted image.

algorithms to choose from, this paper proposes a fast image encryption algorithm.

Arnold cat transformation is a classic position mapping transformation, and its expression is shown in the following equation (4):

$$\begin{bmatrix} x_{n+1} \\ y_{n+1} \end{bmatrix} = \begin{bmatrix} 1 & a \\ b & ab+1 \end{bmatrix} \begin{bmatrix} x_n \\ y_n \end{bmatrix} \bmod(N). \quad (7)$$

Here,  $x_n y_n$  is the original pixel position of an  $N \times N$  image,  $x_{n+1}, y_{n+1}$  is the scrambled pixel position,  $a$  and  $b$  are system parameters, take positive integers, when  $a=1, b=1$ , it is the standard Arnold cat transformation.

The pixel value scrambling is performed by the spread function, and its expression is shown in formula (5).

$$v'_k = v_k + Z^2 \bmod 256, \quad (8)$$



**CONTRACT**

S/C No.: \_\_\_\_\_  
Date: \_\_\_\_\_

The Buyers : \_\_\_\_\_ The Sellers: \_\_\_\_\_  
Tel: \_\_\_\_\_ Tel: \_\_\_\_\_  
Fax: \_\_\_\_\_ Fax: \_\_\_\_\_  
Address: \_\_\_\_\_ Address: \_\_\_\_\_

The Sellers agrees to sell and the Buyer agrees to buy the undermentioned goods on the terms and conditions stated below:

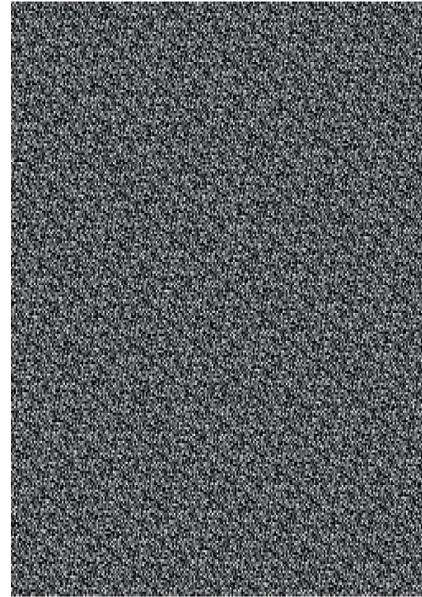
NO.	Description	Specification	Quantity(M)	Unit price	Unit price	Total Value
1						
2						
3						
Total :						

Other requirements:  
 1. Country of Origin : \_\_\_\_\_  
 2. Packing : \_\_\_\_\_  
 3. Time of shipment : \_\_\_\_\_  
 4. Port of Loading : \_\_\_\_\_  
 5. Port of Destination : \_\_\_\_\_  
 6. Terms of Payment : \_\_\_\_\_  
 7. Claims : \_\_\_\_\_

Within 45 days after the arrival of the goods at the destination, should the quality, Specifications or quantity be found not to conform with the stipulations of the contract except those claims for which the insurance company or the owners of the vessel are liable, the Buyers shall have the right on the strength of the inspection certificate issued by the C.C.I.C and the relative documents to claim for compensation to the Sellers.

8. Force Majeure : \_\_\_\_\_  
 The sellers shall not be held responsible for the delay in shipment or non-delivery of the goods due to Force Majeure, which might occur during the process of manufacturing or in the course of loading or transit. The sellers shall advise the Buyers immediately of the occurrence mentioned above the within fourteen days then after. The Sellers shall send by airmail to the Buyers for their acceptance certificate of the accident. Under such circumstances the Sellers, however, are still under the obligation to take all necessary

(a)



(b)

FIGURE 8: The image encryption algorithm (a) original image (b) encrypted image.

The encrypted storage of images can be realized by formulas (1) and (2). Figure 7(a) is the original image that needs to be saved. After encryption, the encryption effect is shown in Figure 7(b) is obtained. Figure 8(a) is the original image that needs to be saved. It can be seen that the encrypted image has no original information and is a messy picture. When decrypting, only the correct key can be recovered, so it can play the role of image privacy protection.

#### 4. Conclusion

By analyzing the advantages and problems of electronic archives, its security is one of the problems that need to be solved. Some security features of blockchain technology can solve this problem very well. This paper designs an electronic file management system based on blockchain technology, from the security of hash algorithm, the security of alliance chain, the security of data sharing, the security of electronic file platform, and the security encryption algorithm of electronic file storage. Applied in some departments, it has already produced a positive effect.

#### Data Availability

The simulation experiment data used to support the findings of this study are available from the corresponding author upon request.

#### Conflicts of Interest

The authors declare that there are no conflicts of interest regarding the publication of this paper.

#### Acknowledgments

This work was supported in part by the 2021 Jiangsu Provincial Library Big Data Research Project of China (Grant no. 2021JSTD021).

#### References

- [1] T. Okamoto and K. Takashima, "Decentralized attribute-based signatures," in *Public-Key Cryptography – PKC 2013*, K. Kurosawa and G. Hanaoka, Eds., Vol. 125–142, Springer Berlin Heidelberg, Berlin, Heidelberg, 2013.
- [2] M. F. Leung and J. Wang, "Minimax and bi-objective portfolio selection based on collaborative neurodynamic optimization," *IEEE Transactions on Neural Networks and Learning Systems*, vol. 32, no. 7, pp. 2825–2836, 2021.
- [3] A. Girdhar and V. Kumar, "Comprehensive survey of 3D image steganography techniques," *IET Image Processing*, vol. 12, no. 1, pp. 1–10, 2018.
- [4] M. Alawida, J. S. Teh, A. Samsudin, and W. H. Alshoura, "An image encryption scheme based on hybridizing digital chaos and finite state machine," *Signal Processing*, vol. 164, no. 4, pp. 249–266, 2019.
- [5] Z. Chen, X. Yuan, Y. Yuan, H. H. C. Iu, and T. Fernando, "Parameter identification of chaotic and hyper-chaotic systems using synchronization-based parameter observer," *IEEE Transactions on Circuits and Systems I: Regular Papers*, vol. 63, no. 9, pp. 1464–1475, 2016.
- [6] P. Kumar, N. Langberg, J. Oded, and K. Sivaramakrishnan, "Voluntary disclosure and strategic stock repurchases," *Journal of Accounting and Economics*, vol. 43, no. 2, pp. 111–121, 2017.
- [7] Y. Sun, C. Xu, G. Li et al., "Intelligent human computer interaction based on non-redundant EMG signal," *Alexandria Engineering Journal*, vol. 59, no. 3, pp. 1149–1157, 2020.
- [8] G. Li, L. Zhang, Y. Sun, and J. Kong, "Towards the sEMG hand: internet of things sensors and haptic feedback

## *Retraction*

# **Retracted: Research on Location of Logistics Distribution Center Based on K-Means Clustering Algorithm**

### **Security and Communication Networks**

Received 26 December 2023; Accepted 26 December 2023; Published 29 December 2023

Copyright © 2023 Security and Communication Networks. This is an open access article distributed under the Creative Commons Attribution License, which permits unrestricted use, distribution, and reproduction in any medium, provided the original work is properly cited.

This article has been retracted by Hindawi, as publisher, following an investigation undertaken by the publisher [1]. This investigation has uncovered evidence of systematic manipulation of the publication and peer-review process. We cannot, therefore, vouch for the reliability or integrity of this article.

Please note that this notice is intended solely to alert readers that the peer-review process of this article has been compromised.

Wiley and Hindawi regret that the usual quality checks did not identify these issues before publication and have since put additional measures in place to safeguard research integrity.

We wish to credit our Research Integrity and Research Publishing teams and anonymous and named external researchers and research integrity experts for contributing to this investigation.

The corresponding author, as the representative of all authors, has been given the opportunity to register their agreement or disagreement to this retraction. We have kept a record of any response received.

### **References**

- [1] P. Wang, X. Chen, and X. Zhang, "Research on Location of Logistics Distribution Center Based on K-Means Clustering Algorithm," *Security and Communication Networks*, vol. 2022, Article ID 2546429, 9 pages, 2022.

## Research Article

# Research on Location of Logistics Distribution Center Based on K-Means Clustering Algorithm

Ping Wang,<sup>1</sup> Xianjun Chen ,<sup>1</sup> and Xuebin Zhang<sup>2</sup>

<sup>1</sup>*School of Economics and Management, Chongqing Three Gorges Vocational College, Wanzhou 404155, Chongqing, China*

<sup>2</sup>*College of Business Administration, Ningbo Polytechnic, Ningbo 315800, Zhejiang, China*

Correspondence should be addressed to Xianjun Chen; 2005180182@cqsgzy.edu.cn

Received 25 April 2022; Accepted 8 June 2022; Published 9 July 2022

Academic Editor: Hangjun Che

Copyright © 2022 Ping Wang et al. This is an open access article distributed under the Creative Commons Attribution License, which permits unrestricted use, distribution, and reproduction in any medium, provided the original work is properly cited.

The basic task of the logistics distribution center is to achieve the storage and distribution of materials, and to plan, implement, and manage the effective flow of materials from the supplying place to the consumption place. Scientific location of logistics distribution center can effectively reduce logistics cost, improve the speed of circulation, increase the profits of enterprises, and enhance the core competitiveness of enterprises. Combining the advantages of K-means clustering algorithm, this paper applies it to the location problem of logistics distribution center and proposes a logistics distribution center location method combining K-means clustering theory and D-S reasoning, which provides a better solution for the location problem of logistics distribution center. Through case analysis, K-means clustering algorithm can obtain reasonable location of logistics distribution center, which can be applied to the location of multilevel logistics distribution network, and has certain practical application value.

## 1. Introduction

With the vigorous development of e-commerce, the logistics industry for ordinary consumers has become a new growth point. From 2010 to 2020, the business volume of national express enterprises increased from 2.34 billion pieces to 83.36 billion pieces, with a compound annual growth rate of about 42.9%. Moreover, in 2021, the business volume of express enterprises is 95.5 billion pieces. From January to November, 2021, the income of national express enterprises totalled 941.47 billion yuan, a year-on-year increase of 19.6%. As of now, the escalated level of the strategies business has improved, yet there are still a few issues, for example, in reverse activity mode, jumble between coordinated factors supply and operations interest, and so forth. Hence, further developing effectiveness of planned operations transportation and decreasing coordinated factors cost have turned into the essential objectives of endeavors [1, 2]. Dispersion focus is the critical hub during the time spent express, which has a direct impact on the choice of transportation routes, the transit time of express mail, and the logistics cost; in addition, it is closely related to the service quality and users' experience of logistics

enterprises. With the rapid increase of logistics, the traditional distribution method has not considered the nonrepetition of traffic. Without considering the location, the problems of the interests between sorting center and customers, and the irrationality of traditional distribution methods, the problems of low utilization rate of urban logistics distribution resources, poor decision-making ability, low scheduling efficiency, and high error rate are caused [3]. It is an important part of logistics distribution service system, which is the key to saving cost of distribution. Therefore, the location of logistics distribution centers based on K-means clustering algorithm is studied in this paper, and a location scheme of logistics distribution centers is put forward, which can provide new ideas for the research and application of optimization in location and realizes the sustainable development of logistics industry.

## 2. Evaluation System of Location of Logistics Distribution Center

As the transit station of logistics distribution, the logistics distribution center is the key to the whole logistics system

planning in the logistics industry. Choosing the factors of location is a comprehensive problem, which aims to make the process of location more scientific, standardized, and practical. On the basis of previous research, from the aspects of traffic conditions, laws and policies, resource conditions, operating environment, natural environment, cost, information quality, etc., the evaluation system of location of logistics distribution center is constructed.

**2.1. Traffic Conditions.** The distribution center needs to have strong speed of response, be able to provide services to customers in time, and have certain reliability and convenience in service, which mainly includes road facilities, accessibility, and public facilities [4]. When choosing a site, it is necessary to consider the transportation of the selected location. Location determines the value, and it should not only help to improve the economic benefits of enterprises but also pay attention to providing convenient, efficient, and low-cost services for customers.

**2.2. Legal Policy.** The distribution center occupies a large area. Considering the land price, natural environment, energy, and other conditions, it should also comply with various logistics policies and regulations [5]. Especially commercial scale, lease terms, zoning, etc, for example, whether it is allowed to build logistics distribution centers in some areas, whether the relevant policies logistics, custom duties and tax policies are beneficial to the establishment of logistics distribution centers. Because of the incomplete unification of logistics regulations and policies, there exists commonly incongruities and conflicts. Therefore, to choose areas that are beneficial to the construction and development of logistics distribution centers, the construction must be coordinated with the urban plan.

**2.3. Resource Conditions.** The logistics distribution center should be equipped with complete resource conditions, including water and electricity, heating, sewage, etc. The periphery of the distribution center should be equipped with complete resource conditions [6]. Sufficient heating, water supply, electricity supply, and discharge capacity to provide basic living guarantee for staff's daily life. It also needs enough fuel and energy, and the area should have certain capacity of sewage and waste treatment. At the same time, supply of basic security for the daily operation of the logistics distribution center counts a lot. These factors will not become the limiting conditions for the development of the logistics distribution center in the future but can guarantee the long-term healthy development.

**2.4. Business Environment.** Considering the location and density of logistics distribution center, the distribution of surrounding customers and the structure and layout of nearby logistics industry are the prerequisite for the location of logistics distribution center [7]. The distribution center should carefully investigate the distribution of customers

when selecting the site. At the same time, the coordination and contradiction between the logistics distribution center and other nearby logistics enterprises should be managed by avoiding vicious competition, and making full use of the existing logistics channels of other companies.

**2.5. Natural Environment.** The distribution center is a place where a large number of products gather, and the location should have strong capacity of soil bearing which needs to consider terrain, landform, water quality, climate, and other indicators [8]. For example, it is necessary to select a place with flat terrain and relatively high terrain, and it must have a suitable shape and size, which is suitable for building; meanwhile, it is best to choose a place where the terrain is completely flat. Slightly undulating areas are the second choice. Rectangular shape is the best choice, and irregular shape is not suitable.

**2.6. Cost.** Logistics distribution center location needs to consider costs, mainly transportation costs, operating costs, and infrastructure costs. The construction of logistics nodes generally takes up a lot of land, so the land price will be directly related to the size of logistics node construction [9]. Generally, the construction of logistics nodes takes up numerous lands, so the price will directly affect the construction scale of logistics nodes. At the same time, it needs to pay various taxes and insurance during its operation. Such as property tax, business tax, vehicle and vessel use tax, and personal income tax withheld by employees. Beyond that, there are differences in the amount of partial tax payment in different regions, in which the vehicle and vessel use tax is paid according to the vehicle, and the local regulations are not the same. Once the location of the distribution center is determined and the construction has been completed, it is not easy to relocate, so unreasonable location will make the enterprise pay a long-term cost for mistakes.

**2.7. Information Quality.** Information quality is mainly measured by information infrastructure and information accuracy. In today's information explosion era, the emergence of e-commerce has had a great impact on traditional industries. With the advent of the Internet age, massive data is pouring in, and all kinds of information, such as orders, processing, transportation, etc. [10], must be processed accurately and effectively to organize the division of labor and form a whole integration. In addition, information infrastructure, as a hardware facility, is directly related to the ability to collect and process various data. Inaccurate information will affect judgment, make unreasonable decisions, and cause serious losses. Therefore, it is significant to ensure the accuracy of information, respond to the problems encountered in logistics and distribution randomly, and improve the distribution efficiency.

Based on the analysis above, the evaluation index system of logistics distribution center location is obtained, as shown in Figure 1.

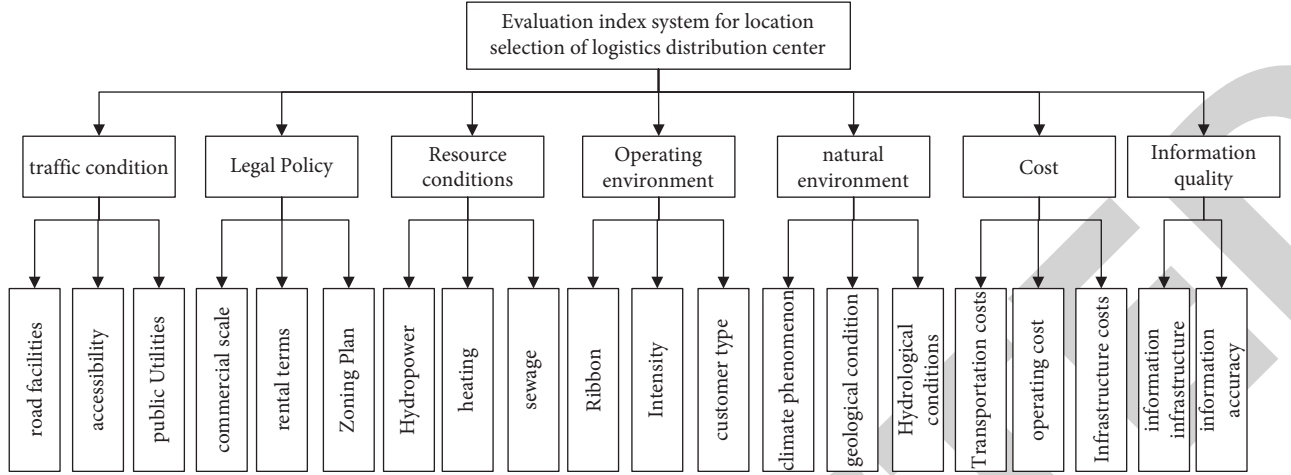


FIGURE 1: Evaluation index system of logistics distribution center location.

### 3. K-Means of Location of Logistics Distribution Center

**3.1. K-Means Algorithm.** Macqueen put forward K-means algorithm in 1967, which is also called Fast Clustering Method. The main idea is to gather each sample into its most similar subclass. The similarity is generally measured by the distance between the sample and the centroid of the class, which is generally the Euclidean distance [11]. The principle of K-means algorithm is generally described as follows:  $k(k \leq n)$  as the parameter,  $n$  objects are divided into  $k$  classes, so that there is a high degree of similarity within classes, while the similarity between classes is low.

Supposing  $Z = \{x_1, x_2, \dots, x_n\}$  is a collection of  $n$  sample points, samples  $x_i = \{x_{i1}, x_{i2}, \dots, x_{im}\}$  are composed of  $m$  attributes or features.  $A = \{a_1, a_2, \dots, a_m\}$ . K-means is the formula (1) to minimize the nonconvex function  $F$  with constraint conditions and to obtain the division of  $Z$  consisting of  $K$  classes, that is, dividing  $Z$  into  $K$  classes, and then minimizing the sum of squares of the distance from each sample to the center of the membership cluster. This optimization can be described as

$$F(W, U) = \sum_{i=1}^K \sum_{j=1}^n w_{ij} d(x_i, u_l). \quad (1)$$

Constraints need to be met:

$$\begin{cases} d(x_i, u_l) = \sum_{j=1}^m a_j(x_i, u_l), \\ w_{li} \in \{0, 1\}, 1 \leq l \leq K, 1 \leq i \leq n, \\ \sum_{l=1}^K w_{li} = 1, 1 \leq i \leq n, \\ 0 < \sum_{i=1}^n w_{li} < n, 1 \leq l \leq K, \end{cases} \quad (2)$$

where  $w_{li}$  is a binary variable as 0 or 1.  $W$  is the matrix of membership between sample  $x_i$  and each class;  $W = [w_l]$  is

K-order  $\{0, 1\}$  matrix;  $n$  represents the attribute dimension of the sample;  $a_j$  represents the  $j$ -th attribute of the sample;  $u_l$  is the center of class  $l$ ,  $u_l = [u_{l1}, u_{l2}, \dots, u_{lm}]$  is composed of  $M$  components;  $U$  is the class center matrix,  $U = [u_1, u_2, \dots, u_k]$ . In formula (2),  $d(x_i, u_l) = \sum_{j=1}^m a_j(x_i, u_l)$  is used to calculate the dissimilarity measure between samples  $x_i$  and class center  $u_l$ ,  $a_j(x_i, u_l)$  represents the difference value on samples  $x_i$  and class center  $u_l$  in attribute  $a_j$ . If  $a_j$  is of numeric attribute, then  $a_j(x_i, u_l) = \|x_{ij} - u_{lj}\|^2$ . At this point,  $d$  becomes measure of Euclidean distance.

**3.2. Effectiveness of Clustering.** It is used to measure whether the result produced by clustering algorithm reaches the optimal standard, and the classification number under the result of optimal clustering is taken as the optimal clustering number. With reference to the effective index of clustering, the ratio BWACR between the minimum value of the average cosine value of the inter-class included angle and the average cosine value of the intraclass included angle is used to evaluate the results of K-means algorithm [12, 13]. Finally, the best clustering result is determined, that is, the number of sites.

Assuming that  $n$  sample points are clustered into  $K$  classes, and  $2 = K \leq 5$ , it defined as follows:

**Definition 1:** the average cosine value of the minimum included angle between classes at the  $i$ th sample point of class  $l$  is  $bc(l, i)$ .

**Definition 2:** The average cosine value of the included angle within the class at the  $i$ th sample point of class  $L$  is  $wc(l, i)$ .

**Definition 3:** The cluster validity index BWACR of the  $i$ th sample point of the first class is the ratio of the minimum value of the average cosine value of the interclass angle to the average cosine value of the intraclass angle BWACR( $l, i$ ).

**Definition 4:** Define the BWACR average value of all sample points under the cluster number  $K$  as  $avg_{BWACR}(K)$ .



The mathematical formula of BWACR index is as follows:

$$K_{\text{opt}} = \max_{2 \leq K \leq S} \{\text{avg}_{\text{BWACR}}(K)\}, \quad (3)$$

which meets the following conditions:

$$\left\{ \begin{array}{l} bc(l, i) = \min_{1 \leq j \leq K} \left( \frac{1}{n_j} \sum_{p=1}^{n_j} \frac{\sum_{q=1}^m x_{pq}^{(j)} x_{iq}^{(l)}}{\sqrt{\sum_{q=1}^m x_{pq}^{(j)^2}} \sqrt{\sum_{q=1}^m x_{iq}^{(l)^2}}} \right), \\ wc(l, i) = \frac{1/n_l - 1 \sum_{t=1, t \neq i}^{n_l} \sum_{q=1}^m x_{tq}^{(l)} x_{iq}^{(l)}}{\sqrt{\sum_{q=1}^m (x_{tq}^{(l)})^2} \sqrt{\sum_{q=1}^m (x_{iq}^{(l)})^2}}, \\ \text{BWACR}(l, i) = \frac{wc(l, i)}{bc(l, i)}, \\ \text{avg}_{\text{BWACR}}(K) = \frac{1}{n} \sum_{l=1}^K \sum_{i=1}^{m_l} \text{BWACR}(l, i). \end{array} \right. \quad (4)$$

In which  $J$  and  $i$  represent class labels,  $M$  represents sample attribute dimension,  $x_{pq}^{(j)}$  represents the  $q$ -th attribute of the  $p$ -th sample in class  $j$ ,  $x_{iq}^{(l)}$  represents the  $q$ th attribute of the  $i$ th sample in class  $l$ ,  $n_j$  indicates the number of samples of class  $j$ ,  $x_{tq}^{(l)}$  represents the  $q$ -th attribute of the  $t$  sample in class  $l$ , and  $t \neq i$ ;  $n_l$  indicates the number of samples in class  $l$ . The more dispersed the classes are, the more compact the classes are, which indicates that the clustering effect is better. In formula (4), to verify the effect under different  $k$ , the BWACR average value of all sample points is calculated under different  $K$ , that is, formula (4). Finally, the BWACR average value  $k$  is compared under different, that is, formula (3), to determine the best clustering number  $K$ .

**3.3. D-S Reasoning Method.** Dempster-Shafer evidence theory, referred to as D-S reasoning, is an activity that analyzes the basic attributes of evidence and uses evidence to identify the facts of a case. The D-S evidence method based on fuzzy rules is an uncertain multiattribute evaluation method, which is used to solve the multiattribute evaluation or decision-making problem under incomplete information [8]. Every index evaluation level in D-S evidence method corresponds to a utility, where the quality of the scheme is measured by calculating the comprehensive evaluation utility value of each scheme.

**3.3.1. Basic Assumptions.** Suppose a system with two levels of indicators is established, with one  $Y$  for the top (parent) indicator and  $Z$  for the bottom (child) indicators, that is, the basic indicator, which means that only the parent indicator has no bottom indicator, and  $e_i$  ( $i = 1, \dots, L$ ). Then, the basic index set represents:  $E = \{e_1, e_2, \dots, e_i, \dots, e_L\}$ ; Weight set represents:  $\omega = \{\omega_1, \omega_2, \dots, \omega_i, \dots, \omega_L\}$ ,  $\omega_i$  which

indicates the weight of  $i$ th indicator  $e_i$ , and  $0 \leq \omega_i \leq 1$ ; supposing that an index has  $N$  different evaluation levels, and its set is represented  $H = \{H_1, H_2, \dots, H_n, \dots, H_N\}$ , where  $H_n$  means the  $n$ th evaluation level, and  $H_n$  is better than  $H_{n+1}$ . For example: an evaluation set of certain indicators is expressed by {Best, Good, Average, Poor, Worst}, among which Best is better than Good. The evaluation of indicators  $e_i$  ( $i = 1, \dots, L$ ) known is shown in formula:

$$\begin{aligned} S(e_i) &= \{H_n, \beta_{n,i}\}_{n=1, \dots, N} i = 1, \dots, L, \\ B &= \{\beta_n, n = 1, \dots, N\}. \end{aligned} \quad (5)$$

In which,  $B$  indicates that the index is evaluated as the confidence set of the grade  $H$ .

Among them,  $\beta_{n,i}$  indicates index  $e_i$  whose confidence level of grade is  $H$ . If  $\sum_{n=1}^N \beta_{n,i} = 1$ , then it means that  $S(e_i)$  is a complete evaluation; if  $\sum_{n=1}^N \beta_{n,i} < 1$ , then evaluate  $S(e_i)$  is incomplete; if  $\sum_{n=1}^N \beta_{n,i} = 0$ , it means that the information of  $S(e_i)$  is completely missing.

**3.3.2. Index Combination Algorithm.** First, standardize the weights and make the sum of weights 1, as shown in formula:

$$1 = \sum_{i=1}^L \omega_i, \quad (6)$$

$$\begin{aligned} m_{n,i} &= \omega_i \beta_{n,i} n = 1, \dots, N; i = 1, \dots, L, \\ m_{H,i} &= 1 - \sum_{n=1}^N m_{n,i} = 1 - \omega_i \sum_{n=1}^N \beta_{n,i} i = 1, \dots, L. \end{aligned} \quad (7)$$

Among them,  $m_{n,i}$  is the basic probability assignment, and subindex  $e_i$  supports parent indicator  $y$  which is evaluated as degree of  $H_n$ ;  $m_{H,i}$  is the unassigned probability that the index is not assigned after synthesis.  $m_{H,i}$  is split into  $\bar{m}_{H,i}$  and  $\tilde{m}_{H,i}$  two parts, as shown in formulas (8) and (9):

$$\bar{m}_{H,i} = 1 - \omega_i i = 1, \dots, L, \quad (8)$$

$$\tilde{m}_{H,i} = \omega_i \left( 1 - \sum_{n=1}^N \beta_{n,i} \right) i = 1, \dots, L. \quad (9)$$

where  $E_I(i) = \{e_1, \dots, e_i\}$  represents a subset of the first  $i$  subindicators;  $m_{n,I(i)}$  for  $E_I(i)$ . All  $I$  indicators support  $E$  evaluation as follows  $H_n$  Degree;  $m_{H,I(i)}$  is the residual probability of all evaluated subindicators in  $E_I(i)$ .

When  $i = 1$ , as shown in formulas (10) and (11):

$$m_{n,I(i)} = m_{n,1}, \quad (10)$$

$$m_{H,I(i)} = m_{H,1}. \quad (11)$$

Then, the coefficients are obtained by using the following iterative formula.  $m_{n,I(L)} \diamond \bar{m}_{H,I(L)}, \tilde{m}_{H,I(L)}$ .



$$\begin{aligned}
K_{I(i+1)} &= \left[ 1 - \sum_{t=1}^N \sum_{\substack{j=1 \\ j \neq t}}^N m_{t,l(i)} m_{j,i+1} \right], \\
m_{n,l(t+1)} &= K_{I(i+1)} [m_{n,l(i)} m_{n,l+1} + m_{H,l(i)} m_{n,l+1} + m_{n,l(t)} m_{H,l+1}] \quad n = 1, \dots, N, \\
\tilde{m}_{H,l(i+1)} &= K_{I(i+1)} [\tilde{m}_{H,l(i)} \tilde{m}_{H,i+1} + \bar{m}_{H,l(i)} \tilde{m}_{H,i+1} + \tilde{m}_{H,l(t)} \bar{m}_{H,i+1}], \\
\bar{m}_{H,l(i+1)} &= K_{I(i+1)} \bar{m}_{H,l(i)} \bar{m}_{H,i+1}, \\
m_{H,l(i)} &= \tilde{m}_{H,l(i)} + \bar{m}_{H,l(i)} \quad i = 1, \dots, L.
\end{aligned} \tag{12}$$

The confidence of parent index evaluation combination can be calculated by formulas (13) and (14):

$$\beta_n = \frac{m_{n,l(L)}}{1 - \bar{m}_{H,l(L)}} \quad n = 1, \dots, N, \tag{13}$$

$$\beta_H = \frac{\tilde{m}_{H,l(L)}}{1 - \bar{m}_{H,l(L)}}. \tag{14}$$

Finally, the result is shown in formula (15), and the value that  $y$  is rated as  $\beta_n$  ( $n = 1, \dots, N$ ) in grade  $H_n$  is

$$S(y) = \{(H_n, \beta_n), n = 1, 2, \dots, N\}. \tag{15}$$

**3.3.3. Rank Several Alternatives.** According to the above formulas and steps, the alternative points in each scheme set are evaluated, and the advantages and disadvantages of the alternative schemes are ranked by the utility function theory [1, 14].

Suppose there are two schemes.  $a, b$ ,  $u(H_n)$  is the utility function of grade  $H_n$ ,  $H_{n+1}$  overmatch  $H_n$ , that is  $u(H_{n+1}) > u(H_n)$ .

If all evaluations are complete, then  $\beta_H = 0$ ; formula (16) is used to calculate the expected utility of the parent index, and then advantages and disadvantages of the schemes.  $a, b$  are compared. if and only if  $u(y(a)) > u(y(b))$  scheme  $a$  is better than scheme  $b$ :

$$u(y) = \sum_{n=1}^N \beta_n u(H_n). \tag{16}$$

If any subindex evaluation is incomplete, then  $\beta_H > 0$ ,  $[\beta_n, (\beta_n + \beta_H)]$  that is,  $y$  is rated as confidence interval of  $H_n$ . In this case, three parameters are defined to describe the evaluation of  $y$ , namely, minimum utility, maximum utility, and average expected utility, and their calculations are shown in formulas:

$$u_{\max}(y) = \sum_{n=1}^{N-1} \beta_n u(H_n) + (\beta_n + \beta_H) u(H_N), \tag{17}$$

$$u_{\min}(y) = (\beta_1 + \beta_H) u(H_1) + \sum_{n=2}^N \beta_n u(H_n), \tag{18}$$

$$u_{\text{avg}}(y) = \frac{u_{\max}(y) + u_{\min}(y)}{2}. \tag{19}$$

Among them, the utility of  $H_1$  is the lowest, and the utility of  $H_N$  is the highest.

To evaluate of parent index  $y$ , if and only if  $u_{\min}(y(a)) > u_{\max}(y(b))$ , scheme  $a$  is better than scheme  $b$ ; if and only if  $u_{\min}(y(a)) = u_{\min}(y(b))$  and  $u_{\max}(y(a)) = u_{\max}(y(b))$ , scheme  $a$  and scheme  $b$  are similar. Otherwise, the ranking is generated according to the average expected utility.

## 4. Location Analysis of Logistics Distribution Center Based on K-Means

**4.1. Basic Data.** If a retail company wants to choose a local logistics distribution center, after on-the-spot investigation, 18 alternative site selection schemes are preliminarily determined [15, 16]. In order to make the subsequent numerical processing and calculation more concise and easier to understand, the coordinates of the geographical position are transformed into two-dimensional coordinates in rectangular coordinate system, then the rectangular coordinates of the candidate points are obtained, as shown in Table 1.  $(\alpha_i, \beta_i)$  represents the coordinates of the  $i$ th alternative point in MapInfo;  $(a_i, b_i)$  represents the Cartesian coordinate of the  $i$ th alternative point,  $A_i$  represents the alternative point [17].

**4.2. Preliminary Location Based on K-Means.** According to the distance information between candidate points, the candidate points are divided into  $K$  classes,  $2 = K \leq 5$ , and the specific flow is as follows:

- (1) Initialize  $k$  cluster centers randomly.
- (2) Calculate the distance between each data point and the class center, namely  $d(x_i, u_l)$ , and aggregate it into the class closest to the point (principle of nearest neighbor).
- (3) Calculate  $K$  new class centers, and the coordinates of each class center are the average coordinates of all data points in the class; and calculate the measure function value  $f$  at this time, that is, the formula (1) in the core algorithm.

TABLE 1: Location coordinate information of alternative points.

Alternative point	$\alpha$ (ft)	$\beta$ (ft)	$\alpha$ (cm)	$b$ (cm)
$A_1$	1,238.98	-155.1415283	4.5	-1.3
$A_2$	1,198.48	-92.415482	3.992911912	-1.884816128
$A_3$	1,185.28	-233.1626959	3.944976682	-1.954195812
$A_4$	982.1491682	-159.4385181	3.533818915	-1.336859633
$A_5$	756.8486851	-131.8664663	2.851118146	-1.198295832
$A_6$	133.8193184	-111.1861832	2.313915184	-1.931441935
$A_7$	562.4184537	-224.2815433	2.144366112	-1.881483322
$A_8$	688.8581426	-248.4481183	2.463621138	-2.183191988
$A_9$	912.9452856	-335.2591255	3.282165694	-2.811198586
$A_{10}$	886.6215149	-391.3122121	2.822981818	-3.281111489
$A_{11}$	585.485953	-368.1268481	2.12821523	-3.188312823
$A_{12}$	434.9951949	-318.8858182	1.581188161	-2.682888513
$A_{13}$	622.8349332	-489.1128649	2.263988112	-4.111154314
$A_{14}$	628.2282818	-616.5838564	2.289946823	-5.169789498
$A_{15}$	543.844362	-586.9139218	1.976486416	-4.921111536
$A_{16}$	461.3585958	-652.8381538	1.688118843	-5.48394198
$A_{17}$	495.411286	-711.2891413	1.611898812	-5.881142653
$A_{18}$	328.4434383	-742.9456862	1.193888196	-6.229488292

- (4) Stop clustering until the maximum iteration number  $m$  is met or satisfied  $|F_1 - F_2| \leq \epsilon$ . In K-means algorithm,  $M$  is selected as 200, 300, and 400, respectively.

$M$  is the value determined according to the size of the data volume, not the larger the better. When solving practical problems, several values can be selected for comparison. When the clustering results under two values are the same, one of them can be arbitrarily selected as the maximum number of iterations.  $\epsilon$  is a minimum number;  $F_1$  and  $F_2$  represent the measure function value of two iterations.

When  $M$  is 300 and 400, the clustering result is the same, so in this paper, the maximum iteration number  $M$  is 400.

**4.3. Analysis of Results.** The BWACR index is used to analyze the clustering validity of the results with different clustering numbers of  $K$  values. Because the attributes of the sample points, that is, candidate points, are expressed by their two-dimensional position coordinates, the cosine values of the included angle between classes and the cosine values of the included angle within classes are calculated according to formula (4), and finally, the corresponding  $K$  value is obtained as the best clustering number when the average value of cosine value ratio of included angle between classes within classes is the maximum.

The relationship between different values of  $K$  and BWACR is shown in Figure 2.

It can be seen from Figures 4-1 that, when  $2 = K \leq 5$ , the value of BWACR reaches the maximum when  $K = 5$ , and at this time, the balance point between the intraclass dispersion degree and the intra class compactness can be found, so that the two can achieve the best effect, and the alternative points can be divided into five categories, namely:  $M_1 = \{A_1, A_2, A_3, A_4\}$ ,  $M_2 = \{A_5, A_6, A_8\}$ ,  $M_3 = \{A_7, A_9, A_{10}, A_{11}, A_{12}\}$ ,  $M_4 = \{A_{13}, A_{14}, A_{15}\}$ ,  $M_5 = \{A_{16}, A_{17}, A_{18}\}$ .

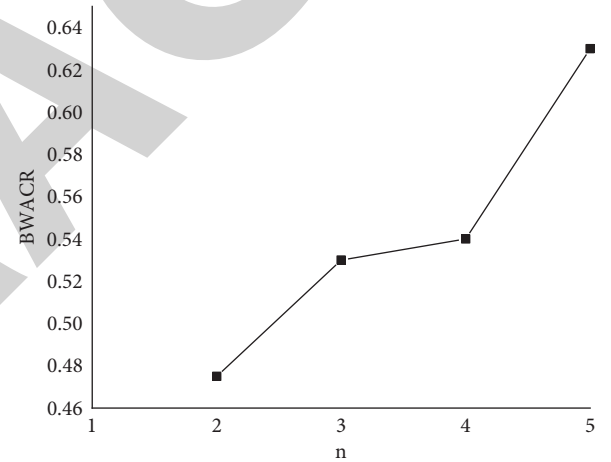


FIGURE 2: Relationship between K and BWACR index value.

That is to say, the best location number of logistics distribution center is 5.

**4.4. Comprehensive Evaluation of Location of Logistics Distribution Center.** Through the analysis above,  $M_1$ ,  $M_2$ ,  $M_3$ ,  $M_4$ , and  $M_5$  are the sets of candidate schemes, respectively, and the D-S reasoning method is used to select the best candidate point from each candidate scheme as the location of the logistics distribution center. According to the comprehensive index system, weight, attribute, and evaluation range of project's location, the quantitative attribute is integrated into the former attribute according to the principle of equivalence by using the D-S evidence method. According to the difference between the evaluation levels of basic attributes and subattributes, and on the basis of the relationship of mapping transformation, the utility evaluation values of each option to be selected are obtained.

According to the above process and formulas (3)–(19) in the D-S evidence algorithm, the comprehensive utility

TABLE 2: Comprehensive utility evaluation and ranking results of alternative points under each scheme set.

Scheme collection	Alternative point	Comprehensive evaluation of utility value	Sort	Best solution
$M_1$	$A_1$	0.5521	4	$A_3$
	$A_2$	0.5951	3	
	$A_3$	0.6892	1	
	$A_4$	0.6113	2	
$M_2$	$A_5$	0.5862	2	$A_8$
	$A_6$	0.5784	3	
	$A_8$	0.6228	1	
$M_3$	$A_7$	0.5556	5	$A_{10}$
	$A_9$	0.5924	3	
	$A_{10}$	0.6465	1	
	$A_{11}$	0.6440	2	
	$A_{12}$	0.5621	4	
$M_4$	$A_{13}$	0.6153	2	$A_{15}$
	$A_{14}$	0.6106	3	
	$A_{15}$	0.6402	1	
$M_5$	$A_{16}$	0.6712	2	$A_{18}$
	$A_{17}$	0.6051	3	
	$A_{18}$	0.6805	1	

TABLE 3: Utility evaluation and ranking results of secondary indicators in scheme  $M_1$ .

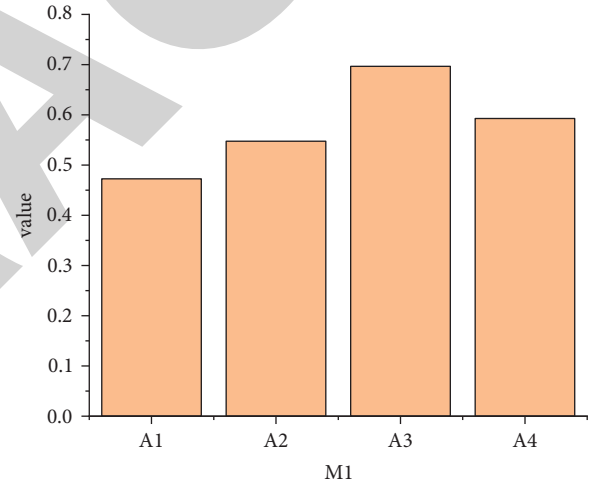
Scheme collection		$M_1$			
Parent indicator	Best solution	$A_1$	$A_2$	$A_3$	$A_4$
Operating environment	$A_3$	0.4748	0.4328	0.5788	0.4589
Sort		2	4	1	3
Traffic condition	$A_3$	0.4728	0.5476	0.6964	0.5928
Sort		4	3	1	2
Natural environment	$A_3$	0.5146	0.5484	0.5932	0.5148
Sort		3	2	1	3
Cost	$A_4$	0.7277	0.8681	0.7401	0.9022
Sort		4	2	3	1
Information quality	$A_3$	0.6021	0.6126	0.6732	0.5733
Sort		3	2	1	4
Resource conditions	—	0.7192	0.7192	0.7192	0.7192
Sort		1	1	1	1
Legal policy	—	0.5	0.5	0.5	0.5
Sort		1	1	1	1

evaluation and ranking results of each alternative point under each scheme set are shown in Table 2.

It can be seen from Table 2 that in each scheme set of  $M_1$ ,  $M_2$ ,  $M_3$ ,  $M_4$ , and  $M_5$ . The comprehensive utility values of  $A_3$ ,  $A_8$ ,  $A_{10}$ ,  $A_{15}$ ,  $A_{18}$  are the highest, which are 0.6892, 0.6228, 0.6465, 0.6402, and 0.6806, respectively. Specifically,  $A_3$  has the largest value, which is the best scheme.

The ranking result of utility value of each alternative point in each scheme according to a certain index attribute can be obtained. The utility evaluation and ranking result of secondary index in scheme  $M_1$  are shown in Table 3.

From Table 3, it can be seen that the operating environment, traffic conditions, and natural environment of  $A_3$

FIGURE 3: Utility values of various schemes in  $M_1$  under traffic condition attributes.

are the best compared with other locations in the scheme set, and the cost of  $A_4$  is lower than that of other locations, while the resource conditions and legal policies of each location in the scheme set are the same.

In addition, we can also get the ranking of schemes under a certain secondary index, for example, the ranking results of  $A_1$ ,  $A_2$ ,  $A_3$ , and  $A_4$  are 2, 4, 1, and 3 under the traffic condition index. As in the scheme slave  $M_1$ , under the traffic condition, the ranking results of utility values of  $A_1$ ,  $A_2$ ,  $A_3$ ,  $A_4$  are shown in Figure 3, which are 0.4728, 0.5476, 0.6964, and 0.5928, respectively. It can be seen that if only the traffic condition attributes are considered, the ranking result of utility values from high to low in  $M_1$  scheme set is as follows  $A_3$ ,  $A_4$ ,  $A_2$ ,  $A_1$ , and the optimal location is  $A_3$ .

Therefore, the best location in logistics distribution can be obtained by the K-means algorithm.

## 5. Conclusion

Distribution center is an important part of logistics and plays an important role in the logistics system. The location of distribution center has great influence on logistics cost and transit time. Based on the K-means clustering algorithm, the location of logistics distribution center is studied, and the evaluation system of location based on traffic conditions, laws and policies, resource conditions, business environment, natural environment, cost and information quality is constructed. On this basis, K-means clustering algorithm and D-S evidence method are used to determine the location of logistics distribution centers scientifically and efficiently. Through the combination of the two methods, the uncertainty in the decision-making process can be fully considered, and the results obtained are closer to the reality. At the same time, the method can also effectively solve the problem of multiattribute evaluation. When the weights of factors affecting site selection in different periods of real life are different, the new comprehensive attribute evaluation can be obtained by directly changing the weight of attributes at any time. Therefore, the location of logistics distribution center based on the K-means clustering algorithm is practical, scientific, and effective.

## Data Availability

The dataset can be accessed upon request.

## Conflicts of Interest

The authors declare that there are no conflicts of interest regarding the publication of this paper.

## Acknowledgments

This work was funded by 1. 2020 Science and Technology Youth Project "Research on the Development Model of Wanzhou Rural Eco-industrialization under the Rural Revitalization Strategy" of Chongqing Municipal Education Commission, the project number is KJQN202003507. 2. 2020 Science and Technology Research Project "Research on the Path of Local Higher Vocational Colleges Serving Rural Revitalization - Taking Chongqing Three Gorges Vocational College as an Example" of Chongqing Three Gorges Vocational College, the project number is cqsx202020. 3. 2020 Higher Education and Teaching Reform Research Project "The Exploration and Practice of "Course Certificate Integration" Model of Higher Vocational Logistics Management Major in Chongqing under the "1 + X" Certificate System" of Chongqing Municipal Education Commission, the project number is 203625. 4. The Scientific Research Planning project "Research on the Exam Mode of "Course, Competition and Certificate Integration" of Higher Vocational Logistics Management Major in Southwest China under the "1 + X" Certificate System" of Chongqing Higher Vocational Technical Education Research Association, the project number is GY201014.

## References

- [1] S. Kadry, G. Alferov, and V. Fedorov, "D-star algorithm modification," *International Journal of Online and Bio-medical Engineering (iJOE)*, vol. 16, no. 08, pp. 169–172, 2020.
- [2] X. Li and K. Zhou, "Multi-objective cold chain logistic distribution center location based on carbon emission," *Environmental Science and Pollution Research*, vol. 28, no. 25, pp. 32396–32404, 2021.
- [3] P. Liu and Y. Li, "Multiattribute decision method for comprehensive logistics distribution center location selection based on 2-dimensional linguistic information," *Information Sciences*, vol. 538, no. prepublsh, pp. 231–234, 2020.
- [4] L. Lu and J. Qin, "Multi-regional logistics center location algorithm based on improved K-means clustering," *Computer system application*, vol. 28, no. 8, pp. 251–255, 2019.
- [5] G. Musolino, C. Rindone, A. Polimeni, and A. Vitetta, "Planning urban distribution center location with variable restocking demand scenarios: general methodology and testing in a medium-size town," *Transport Policy*, vol. 80, no. C, p. 345, 2018.
- [6] M. Özmen and E. Kızılkaya Aydoğan, "Robust multi-criteria decision making methodology for real life logistics center location problem," *Artificial Intelligence Review: An International Science and Engineering Journal*, vol. 53, no. 12, pp. 331–335, 2020.
- [7] R. Rajesh Sharma and A. Sungheetha, "Analysis of influencing factors of logistics center location based on comprehensive quality training," *Indian Journal of Public Health Research & Development*, vol. 4, no. 12, pp. 289–293, 2018.
- [8] H. Lei and S. Li, "An improved algorithm of D-S evidence fusion," *Journal of Physics: Conference Series*, vol. 1871, no. 1, pp. 237–240, 2021.
- [9] Bienvenido-Huertas David, M.-G. David, J. Carretero-Ayuso Manuel, and E. Rodríguez-Jiménez Carlos, "Climate classification for new and restored buildings in Andalusia: analysing the current regulation and a new approach based on K-means," *Journal of Building Engineering*, vol. 43, pp. 145–148, 2021.
- [10] M. Mieczysłńska and I. Czarnowski, "K-means clustering for SAT-AIS data analysis," *WMU Journal of Maritime Affairs*, vol. 20, no. 3, pp. 164–168, 2021.
- [11] U. S. Mukminin, B. Irawanto, B. Surarso, and Farikhin, "Fuzzy time series based on frequency density-based partitioning and K-means clustering for forecasting exchange rate," *Journal of Physics: Conference Series*, vol. 1943, no. 1, pp. 645–678, 2021.
- [12] A. Misganaw, Y. Noh, C. Seo, D. Kim, and I. Lee, "Developing a ship collision risk index estimation model based on dempster-shafer theory," *Applied Ocean Research*, vol. 113, p. 1162, 2021.
- [13] M. Jabi, M. Pedersoli, A. Mitiche, and I. B. Ayed, "Deep clustering: on the link between discriminative models and K-means," *IEEE Transactions on Pattern Analysis and Machine Intelligence*, vol. 43, no. 6, pp. 1887–1896, 2021.
- [14] S. Wu, S. Yang, and X. Du, "A model for evaluation of surrounding rock stability based on D-S evidence theory and error-eliminating theory," *Bulletin of Engineering Geology and the Environment*, pp. 489–496, 2021.
- [15] W. Cao, Z. Zhang, and C. Liu, "Unsupervised discriminative feature learning via finding a clustering-friendly embedding

## *Retraction*

# **Retracted: Design of Network Intrusion Detection Model Based on TCA**

### **Security and Communication Networks**

Received 26 December 2023; Accepted 26 December 2023; Published 29 December 2023

Copyright © 2023 Security and Communication Networks. This is an open access article distributed under the Creative Commons Attribution License, which permits unrestricted use, distribution, and reproduction in any medium, provided the original work is properly cited.

This article has been retracted by Hindawi, as publisher, following an investigation undertaken by the publisher [1]. This investigation has uncovered evidence of systematic manipulation of the publication and peer-review process. We cannot, therefore, vouch for the reliability or integrity of this article.

Please note that this notice is intended solely to alert readers that the peer-review process of this article has been compromised.

Wiley and Hindawi regret that the usual quality checks did not identify these issues before publication and have since put additional measures in place to safeguard research integrity.

We wish to credit our Research Integrity and Research Publishing teams and anonymous and named external researchers and research integrity experts for contributing to this investigation.

The corresponding author, as the representative of all authors, has been given the opportunity to register their agreement or disagreement to this retraction. We have kept a record of any response received.

### **References**

- [1] Q. Wen, "Design of Network Intrusion Detection Model Based on TCA," *Security and Communication Networks*, vol. 2022, Article ID 9248853, 6 pages, 2022.

## Research Article

# Design of Network Intrusion Detection Model Based on TCA

Quan Wen 

College of Computer Science and Cyber Security (CSCS), Chengdu University of Technology, Chengdu 610059, China

Correspondence should be addressed to Quan Wen; wenq@cdut.edu.cn

Received 25 April 2022; Accepted 25 May 2022; Published 7 July 2022

Academic Editor: Hangjun Che

Copyright © 2022 Quan Wen. This is an open access article distributed under the Creative Commons Attribution License, which permits unrestricted use, distribution, and reproduction in any medium, provided the original work is properly cited.

The traditional machine learning model cannot effectively identify the new network traffic data set, resulting in the model failure. Therefore, in this paper, by analyzing the problems of current network intrusion detection (NID) and combining the application of transfer theory in the detection model, a NID model based on transfer component analysis (TCA) is proposed. Among them, the specific mathematical derivation of the algorithm and the detection process of transfer model are introduced in detail. Then, the classification performance of KNN and SVM based on TCA algorithm for network abnormal traffic is compared. The results show that the TCA algorithm proposed in this paper can effectively improve the accuracy of NID, which is meaningful to expand the application scope of network abnormal traffic detection scheme based on machine learning.

## 1. Introduction

With the rapid development of Internet in social life, people's attention to network security has gradually increased, and more network traffic data have brought great challenges to traditional intrusion detection systems. When the traditional machine learning method is used for intrusion detection, it is necessary to extract features manually, then use feature selection method to distinguish the most meaningful features, and finally adopt to discover new threats [1, 2]. In any case, with the rise of new assaults and the changing improvement of assault situations, these techniques for AI are confronted with numerous challenges in building highlights. Various elements chose for realized noxious examples are totally appropriate for obscure or new kinds of vindictive examples, and traditional machine learning needs a lot of manpower and material resources, while deep learning has the characteristics of automatic learning and feature extraction [3–5]. However, the existing neural network can only be used in a closed or static network environment. When performing classification, all possible classes are already known during training; therefore, if unknown classes appear, the existing detection system cannot correctly identify them, which will greatly threaten the network security.

Besides, the abnormal traffic detection schemes based on machine learning all require that the training and testing data sets have the same feature distribution. However, with the diversity and secrecy of network abnormal traffic, the detection based on signature and specification is not reliable. Once the time of traffic collection, the node location, and traffic type change, it cannot identify effectively, when the traditional machine learning model is applied to new network traffic data sets, resulting failure in model [6, 7]. Usually, tag data are difficult to obtain and expensive, and at the same time, numerous expired data are not fully utilized. By introducing the transfer learning theory into the NID system, it can solve the learning problem of the target domain without or with only little labeled data by transferring the knowledge of the source domain and use the original data in the shared subspace to train the basic classifier model and detect the new sample flow [8].

Since the 1980s, NID has been studied. Faced with the ever-changing network attacks and increasing traffic data, the following problems still exist in intrusion detection system.

**1.1. Low Training Efficiency.** Although the deep learning model can extract advanced abstract features, it also sacrifices computing resources. To extract effective features from large



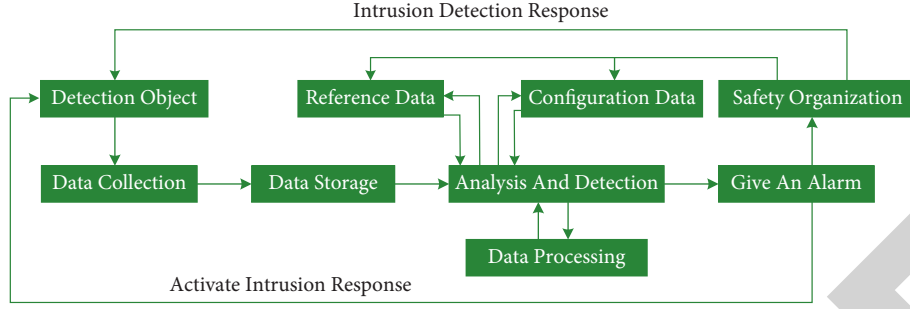


FIGURE 1: Architecture of the NID system.

and high-dimensional data, it will increase more computational cost and time. Therefore, how to solve the problem of large and high-dimensional data, improve the training efficiency of the model, and ensure the accuracy of the system classifier is particularly important.

**1.2. The Real-Time Performance of Intrusion Detection Is Low.** Reliable intrusion detection system can quickly identify the network when it is attacked, and network security managers can take corresponding security measures to defend it. This requires high real-time performance of intrusion detection algorithms, but the current intrusion detection algorithms have low real-time performance. When the network is invaded, the network security managers cannot find it in time to intercept it, which attacks the network system. Therefore, it is necessary to solve the real-time problem of intrusion detection algorithm.

**1.3. The Detection Rate of Rare Sample Data Is Low.** The detection rate of rare attacks is extremely low due to bit of rare attacks. The increase of the number of features and the imbalance of data are the key reasons for the low detection accuracy. If a hacker makes use of a rare attack, the intrusion detection system will have no way to successfully warn or intercept it, thus endangering the security of the network system and causing serious consequences. Therefore, it is necessary to study the problems of multi-classification and data imbalance in intrusion detection.

Therefore, the identification of abnormal network traffic data can effectively support the location of network intrusion behaviors; especially for the discovery of unknown attacks, this paper improves and combines the transfer learning theory in the research of NID, aiming at solving the problems derived from classification in NID, such as scarcity of tags, inconsistent distribution of source and destination data, and difficulty in distinguishing unknown attacks, so as to meet the original intention of pursuing higher accuracy.

## 2. Analysis of Problems in NID

The process of NID is shown in Figure 1, in which the solid line represents the transmission direction of data and control instructions in the system, and the dotted line represents the reaction of the terminal nodes in the system to possible intrusion.

A universal intrusion detection system is mainly composed of monitoring object, data collection, data storage, data processing, analysis and detection, and alarm modules [9].

**Data collection:** the data collected at this stage are analyzed to find traces of suspicious activities, which can be host, network activity log, command-based log, application-based log, etc.

**Data storage:** intrusion detection systems usually store data indefinitely or for a long time for future reference, so the amount of data is usually very large.

**Analysis and detection:** the processing module is the core of the intrusion detection system where an algorithm for detecting suspicious behavior is executed. Traditionally, intrusion analysis and detection algorithms are divided into three categories: misuse detection, anomaly detection, and hybrid detection.

**Configuration data:** it is the most delicate piece of interruption location framework. It contains data connected with the activity of interruption location framework itself, for example, data about when and how to gather information, how to manage interruption, and so forth.

**Reference data:** it stores information about known intrusion signatures or profiles of normal behaviors where knowledge about system behavior can be used to update configuration information.

**Alarm:** this piece of the framework handles all the result from the interruption recognition framework. The result can be a programmed reaction to the interruption or a suspicious behavior alarm of the system security officer.

In summary, the process of intrusion detection is shown in Figure 2.

The general process of intrusion detection is that first, the detection system collects the required original data from the data source and then preprocesses the data to get the data format that the system can recognize. After identification and detection by the detection engine, the detection result is obtained and the response is made according to the security policy set by the administrator.

## 3. Implementation of Transfer Learning in NID

The main idea of transfer learning is to apply the trained machine learning model to other related fields. Through transfer learning, the generalization of another task can be improved by the knowledge learned in one task [10, 11].



FIGURE 2: Process of intrusion detection.

The main advantage of learning is that based on a small amount of data, the performance of neural network can be rapidly improved in a short time. Usually, training neural networks from scratch requires numerous data, but in reality, getting such a lot of data is unimaginable all the time. Through move learning, a solid AI model can be worked with moderately little preparation information, in light of the fact that the model has been preprepared. The main implementation mode is shown in Figure 3:

- (1) *Adopting the Training Model.* If users want to solve task (A) but there are not enough data to train the neural network, they can find the connected errand B with a ton of information, train the profound neural network on task B, and utilize the model as the beginning stage to tackle (A) while whether the entire model or a couple of layers are required relies upon the issue to be addressed.
- (2) *Pretraining Model.* Use trained models, such as nine pretraining models provided in Keras, which can be used for transfer learning, prediction, feature extraction, and fine-tuning.
- (3) *Feature Extraction.* With the help of the deep learning training model, the features of the shallow network can be used to show the elements to be learned, that is, the representation of the original data, without using the network output, so that the size of the data set can be reduced, thus reducing the calculation time.

In intrusion detection, the knowledge learned from known network attacks is used to enhance the detection of new network attacks. The source domain (SD) and the TD, respectively, represent the training and testing data sets in machine learning tasks, and both the data include normal

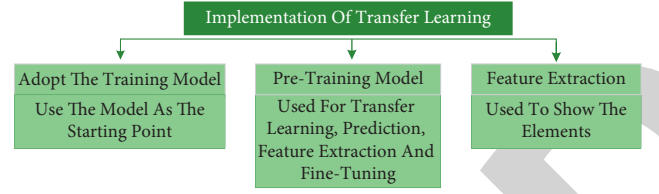


FIGURE 3: Implementation of transfer learning.

and abnormal traffic records. In a generalized scenario, the attacks in the SD are marked, while the attack in the TD is new and unmarked. The purpose of learning in intrusion detection is to use source data to help distinguish new attacks from TDs, as shown in Figure 4.

#### 4. NID Model Based on TCA

**4.1. Establishment of the Problem Model.** Define the SD network traffic data set with label as  $D_S$ ,  $X_S = \{x_s\}_{s=1}^{n_s} \in R^{m \times n_s}$ . As a feature input, the corresponding tag set  $Y_S = \{y_s\}_{s=1}^{n_s} \in R^{1 \times n_s}$  is set as an output, and a new network traffic data set with different structures is defined as a TD after data preprocessing.  $D_T$ ,  $X_T = \{x_t\}_{t=1}^{n_t} \in R^{m \times n_t}$  is set as a feature input, and the sample label is unknown.

$m$  is the traffic characteristics extracted from the SD and the TD. Considering the edge distribution of SD traffic and TD traffic  $P(X_S) \neq Q(X_T)$ , the SD model cannot be trained to detect the abnormal traffic in the TD.

The solution of this paper is to find a suitable transformation  $\Phi$  to make  $P(\Phi(X_S)) \approx Q(\Phi(X_T))$ , and  $P(Y_S|\Phi(X_S)) \approx P(Y_T|\Phi(X_T))$ , so that the corresponding labels can be trained  $\Phi(X_S)$  and the corresponding label.  $Y_S$  can be used to train the data of the TD traffic  $\Phi(X_T)$ , where the SD traffic data  $\Phi(X_S)$  and the classifier trained by the corresponding label matches the TD traffic  $\Phi(X_T)$  can be used to classify the data and detect the abnormal traffic.

The following two conditions of transformation function  $\Phi$  must be met:

- (1) Minimize the gap between the edge distribution  $P(X_S)$  and  $Q(X_T)$
- (2) Retain the internal attributes of  $X_S$  and  $X_T$  to the maximum extent possible

$\Phi$  is a feature mapping between SD and TD caused by general kernel, while the essence of TCA algorithm is to reduce the distance between the distribution of SD  $P$  and target source distribution  $Q$ , and the distribution distance of the objective function  $P$  and  $Q$  is shown in

$$\text{Dist}(X'_S, X'_T) = \left\| \frac{1}{n_1} \sum_{i=1}^{n_1} \Phi(x_{s_i}) - \frac{1}{n_2} \sum_{i=1}^{n_2} \Phi(x_{t_i}) \right\|_H^2, \quad (1)$$

where  $H$  is a universal regenerative kernel Hilbert space,  $\Phi$  is a feature mapping caused by a kernel,  $X'_S$  and  $X'_T$ , respectively, representing the characteristics of the SD traffic and the TD traffic in the transformation space, and  $n_1$  and  $n_2$ , respectively, represent the number of samples contained in

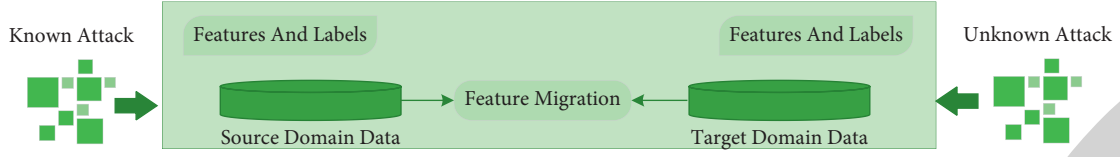


FIGURE 4: NID based on transfer learning.

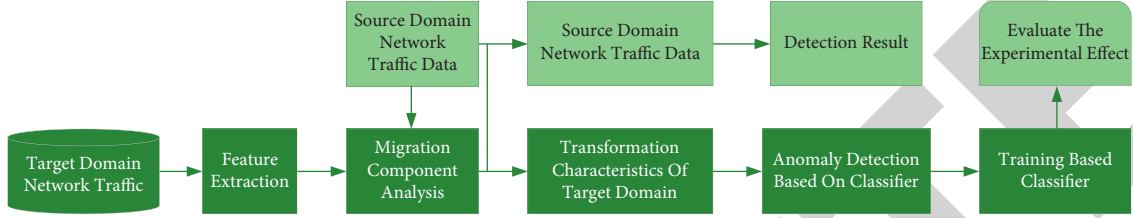


FIGURE 5: Detection model based on TCA.

each. Therefore, if the conversion function  $\Phi$  is found, the objective function can be calculated.

It is very difficult to direct explicit definition of nonlinear transformation  $\Phi$  and calculate the distance between features. Therefore, a kernel matrix  $K$  is introduced by using the kernel embedding method, where formula (1) is rewritten as follows:

$$\text{Dist}(X'_S, X'_T) = \text{tr}(KL), \quad (2)$$

where  $KL$  represents the distance and is used to measure the difference of probability distribution  $K$  of traffic characteristics in different network environments, as shown in

$$K = \begin{bmatrix} K_{SS} & K_{S,T} \\ K_{T,S} & K_{TT} \end{bmatrix} \in R^{(n_1+n_2) \times (n_1+n_2)}, \quad (3)$$

where  $K_{S,S}$ ,  $K_{T,T}$ , and  $K_{S,T}$  represent the inner core matrix composed of the features of the SD, the TD, and the synthesis domain  $L$ , respectively, which are defined as

$$L_{ij} = \begin{cases} \frac{1}{n_1^2} & x_i, x_j \in X_S, \\ \frac{1}{n_2^2} & x_i, x_j \in X_T, \\ -\frac{1}{n_1 n_2} & \text{otherwise,} \end{cases} \quad (4)$$

$n_1$  and  $n_2$ , respectively, represent the number of samples contained in each.

Therefore, the distance of the above objective function is transformed into an operation problem between matrices, which is shown in

$$\text{tr}(KL) - \lambda \text{tr}(K), \quad (5)$$

where  $\lambda \geq 0$  is a trade-off parameter,  $\text{tr}(KL)$  is used to minimize the difference between the distributions of the two fields, and  $\lambda \text{tr}(K)$  is used to maximize the variance of feature space.

As can be seen from the above discussion and definition, formula (5) is a semidefinite programming problem in mathematics, and it takes a lot of time to solve it by general methods. Therefore, the kernel matrix  $K$  in formula (3) is reduced by the dimension reduction, which is broken down into  $K = (KK^{-1/2})(K^{-1/2}K)$ . The final kernel matrix can be expressed by

$$\tilde{K} = (KK^{-1/2}\tilde{W})(\tilde{W}^T K^{-1/2}K) = KWW^T K, \quad (6)$$

where  $W = K^{-1/2}\tilde{W}$ . The distance between characteristics of traffic in SD and TD in transformation space  $X'_S$  and  $X'_T$  can be converted into

$$\text{Dist}(X'_S, X'_T) = \text{tr}((KWW^T K)L) = \text{tr}(W^T K L K W). \quad (7)$$

Under the minimization rule, the normalization term  $\text{tr}(W^T W)$  is used to control complexity  $W$ , and the final objective function is transformed into

$$\min_W \text{tr}(W^T W) + \mu \times \text{tr}(W^T K L K W), \quad (8)$$

where  $\mu > 0$  is a trade-off parameter, so that the sample matrix  $X^* = KWKW$  in the shared subspace can be calculated. It ensures that the distance between the SD and the TD is reduced, and the mapped data have the largest variance, which satisfies the set of abovementioned transformation function  $\Phi$ .

To sum up, the working principle of TCA is as follows: the goal of TCA is to find an optimal shared feature subspace, in which the distribution difference between the SD and the TD can be minimized, and then the unlabeled data in the TD can be classified by using the classifier trained in the SD.

**4.2. Detection Model.** In this paper, KNN, SVM, and RF are used as basic classifiers, and a network abnormal traffic detection model based on TCA is designed as shown in Figure 5. The specific detection process is divided into the following five steps:

- (1) Extract network traffic characteristics and corresponding characteristic values of a TD

TABLE 1: Description of test data set.

Data set	Data sample	Number of categories	Subset
CICIDS2017	16000	12	A, B, C
CTU	11200	11	M, N

- (2) Migrate the traffic characteristics and original characteristics of the TD to be identified to the shared subspace
- (3) Train the base classifier with SD traffic data in the shared subspace
- (4) Adopt the base classifier to detect the features of the TD after traffic transformation
- (5) Calculate the detection accuracy, and then evaluate the experimental results

## 5. Model Test

**5.1. Construction of the Data Set.** The core problem of this paper is that the SD and the TD do not meet the same feature distribution, so the two domains need to use different data sets. The experimental data sets are CICIDS2017 and CTU, as shown in Table 1, where 10 groups of transfer learning experiments are designed.

CICIDS2017 contains normal traffic and the most common attack traffic at present, and gives pcap file data, in which data files are divided according to different dates, all of which are normal traffic on Monday, and attack traffic is collected from Tuesday to Friday. In this paper, it is found that if the data set contains all kinds of attacks, it is prone to negative transfer. Therefore, according to different types of attacks, CICIDS2017 data set is divided into three subsets: a subset mainly contains DDOS and DOS attacks, B subset contains PortScan, FTP-Patator, and SSH-Patator attacks, C subset contains Web attacks and botnets, and all these subsets contain normal traffic.

CTU data set contains a large number of attack traffic mixed with normal traffic. Similarly, according to different types of attacks, CTU data set is divided into sub-data sets of M and N, of which sub-data set M contains Trickster, TrickBot, and Dridex attacks, and N contains Ursnif, CoinMiner, and HTBot attacks. Similarly, these subsets also contain normal traffic.

**5.2. Data Processing.** As CICIDS2017 data set and CTU data set are both pcap files, which cannot be directly sent into the model for training, we need to preprocess the pcap files to divide the traffic packets with the same quintuple information into a flow, and mainly use Python script to analyze the remaining header and payload information of each traffic packet and vectorize it. In this way, experiments are carried out on the features that can be extracted from each flow, and the division of network traffic flow can also reflect the time sequence of traffic in NID.

The processing procedure of CICIDS2017 data set and CTU data set is shown in Figure 6.

Mean value removal is to eliminate the deviation between sample features, which is realized by subtracting the mean value of all the feature values of each sample, so as to make the feature mean value zero.

Range scaling is to enlarge or reduce the characteristic values of samples of different units to a reasonable range in proportion, in order to reduce the influence of the large change between different features.

Normalization refers to uniformly scaling the features of different classes to a specified range, and its purpose is to unify the statistical distribution of samples to eliminate the adverse effects caused by singular samples. The most commonly used normalization method in machine learning is L1 norm, which ensures that the data are in the same order of magnitude.

**5.3. Parameter Setting.** In terms of data, the data sets used in the experiment are all network traffic data, and their distributions are different but related. Attacks in all data sets are uniformly marked as abnormal traffic. This paper conducts two-class detection of normal and abnormal traffic. 4,000 pieces of data are randomly selected from each subset of CICIDS2017 as SD and TD data sets, respectively, which is shown in Table 1. Correspondingly, 3200 pieces of data are randomly selected from each subset of CTU as source and target and data set, respectively.

In the aspect of model, KNN and SVM in machine learning are used as classifiers for tests [12]. In order to control the parameters of experiments, K is uniformly set to 1, the penalty factor C in SVM is equal to  $C=100$ , and Gaussian kernel function is adopted where the performance of linear kernel is better than that of RBF and Laplacian kernel, so TCA uses linear kernel function uniformly. In order to avoid overfitting, the experiment was carried out by setting program for 10 times, and the results were obtained by averaging. The main index used to evaluate the effectiveness of traffic classification is the accuracy rate, that is, the percentage of correct traffic classification in total traffic.

**5.4. Analysis of Results.** Table 2 shows the accuracy of 10 groups of transfer learning data under each model.

It can be seen from the data in the table that in the anomaly detection experiments of 10 groups of cross-domain network traffic data sets, the recognition rate of the TD samples by the traditional machine learning algorithm is very low that the accuracy rate is only about 39%. The main reason is that the distribution difference between the SD traffic characteristics and the TD traffic characteristics is too large to meet the independent and identical distribution rules required by machine learning. In this case, the recognition result can hardly be used as effective reference information, and the TD cannot make use of the valuable tag information in the SD. In addition, the TCA algorithm proposed in this paper is used to adapt the traffic characteristics of SD and TD, and the marginal probability distribution and conditional probability distribution between them are reduced, which can significantly improve the accuracy of detection. Compared with the traditional machine

## *Retraction*

# **Retracted: Implementation of Efficient Teaching Scheme of Human Anatomy and Physiology Based on Multimedia Information Processing Technologies**

### **Security and Communication Networks**

Received 26 December 2023; Accepted 26 December 2023; Published 29 December 2023

Copyright © 2023 Security and Communication Networks. This is an open access article distributed under the Creative Commons Attribution License, which permits unrestricted use, distribution, and reproduction in any medium, provided the original work is properly cited.

This article has been retracted by Hindawi, as publisher, following an investigation undertaken by the publisher [1]. This investigation has uncovered evidence of systematic manipulation of the publication and peer-review process. We cannot, therefore, vouch for the reliability or integrity of this article.

Please note that this notice is intended solely to alert readers that the peer-review process of this article has been compromised.

Wiley and Hindawi regret that the usual quality checks did not identify these issues before publication and have since put additional measures in place to safeguard research integrity.

We wish to credit our Research Integrity and Research Publishing teams and anonymous and named external researchers and research integrity experts for contributing to this investigation.

The corresponding author, as the representative of all authors, has been given the opportunity to register their agreement or disagreement to this retraction. We have kept a record of any response received.

## **References**

- [1] Y. Ma and Z. Zhi, "Implementation of Efficient Teaching Scheme of Human Anatomy and Physiology Based on Multimedia Information Processing Technologies," *Security and Communication Networks*, vol. 2022, Article ID 4134864, 7 pages, 2022.

## Research Article

# Implementation of Efficient Teaching Scheme of Human Anatomy and Physiology Based on Multimedia Information Processing Technologies

Yue Ma<sup>1,2</sup> and Zhuangzhi Zhi<sup>3</sup> 

<sup>1</sup>School of Forensic Science, Criminal Investigation Police University of China, Shenyang 110854, China

<sup>2</sup>Key Laboratory of Impression Evidence Examination and Identification Technology, Ministry of Public Security, Shenyang 110854, China

<sup>3</sup>School of Medical Instrument, Shenyang Pharmaceutical University, Shenyang 110016, China

Correspondence should be addressed to Zhuangzhi Zhi; 106040101@syphu.edu.cn

Received 15 April 2022; Accepted 4 June 2022; Published 28 June 2022

Academic Editor: Hangjun Che

Copyright © 2022 Yue Ma and Zhuangzhi Zhi. This is an open access article distributed under the Creative Commons Attribution License, which permits unrestricted use, distribution, and reproduction in any medium, provided the original work is properly cited.

An application scheme based on the teaching of human anatomy and physiology, namely, PBL, is proposed. In particular, 95 medical students were randomly divided into two groups: classes 2 and 3 were the experimental classes (48 students), and then, the teaching practice was carried out according to the machine learning route; year 1 and class 4 were the control classes (47 students), and the traditional teaching method was used. The teaching effectiveness was evaluated by performance analysis, the mean score of the overall evaluation of the experimental class was  $(93.23 \pm 2.01)$ , the mean score of the control group was  $(91.51 \pm 2.89)$ , and the difference was statistically significant ( $p < 0.01$ ). The survey showed that more than 93% of the students in the experimental class thought that the deep learning model helped stimulate their interest in learning, enhance their sense of teamwork, and improve their overall ability.

## 1. Introduction

The ability to learn on their own is essential for medical students to advance their careers in later years [1]. With the continuous advancement of science and multimedia information processing technologies, the popularity of the internet and smart terminals has brought many innovative modes of independent learning to students [2]. The knowledge that medical students learn during their time at school is only the basis of their ability to become qualified doctors later in life and does not meet the demand for the knowledge needed to practice later in life. This requires that medical students have sufficient independent learning skills, and as teachers of human anatomy, they should also focus on developing their independent learning skills [3].

First, human anatomy, as the first professional foundation course for medical students entering

medicine, involves many very specialized terms and is logically scattered, making it very difficult for students who are new to medicine [4]. Classroom time is limited, and even when teachers are teaching students in a constantly compressed anatomy, there is no way to interpret all the content, which may lead to students losing confidence in their studies due to difficulties in acquiring sufficient knowledge [5].

Second, the current teaching model in many medical schools is relatively traditional, with the teacher at the core forcibly instilling knowledge and students being forced to accept it, a situation that has yet to be fully reformed [6]. Teachers simply follow the content of the textbook and ignore the students' ability to comprehend it, resulting in a boring and rigid classroom atmosphere, which suppresses students' interest in learning, thus making students' learning effect poor [7].



In addition, the knowledge of human anatomy is complicated and numerous, and students are faced with a large number of terms that need to be memorized, which makes students gradually lose interest in the medical professional course, unable to grasp the theoretical knowledge well, and only in order to cope with the examination by rote memorization, which does not help the clinical laboratory operation of medical students [8]. Finally, some institutions lack specimens and remain to supply the laboratory class, usually many students around a dissection table to study, so that some students cannot observe and experience the wonders, and the theoretical knowledge learned cannot really be applied, which is also a more serious problem in the current teaching of human body science [9].

In today's society, technology is developing faster and faster, and the use of information technology is becoming more and more widespread, including the field of education [10]. Computer multimedia technology, as a product of this background environment, has a very important role in promoting the progress of teaching media and accelerating the formation of a multimedia teaching system [11]. It can foster students' independent learning in many ways, including teaching methods, content, and laws, thus making them increasingly motivated to learn. Human anatomy is one of the morphological disciplines, and in the past, teachers used to teach using board books or wall charts, which were inevitably abstract [12]. Nowadays, teachers can make use of multimedia technology in teaching human anatomy courses, which not only promotes good independent learning habits, but also stimulates students' interest in learning and puts them in a vivid, intuitive, and active teaching environment, thus contributing to a significant improvement in the quality of learning and classroom efficiency [13]. In addition, multimedia technology can extend the amount of resources available in the classroom, allowing students to access relevant materials via the internet to solve learning problems.

The establishment of a robust online resource base for human anatomy can provide more space for students to independently learn. For example, a number of courses related to human anatomy can be set up, and then, students can access teaching video materials, multimedia courseware materials, test banks, specimen image banks, reference materials, and other resources related to them from the campus network. At the same time, students and teachers and students and students can communicate with each other through WeChat and WeChat, thus giving students more independent learning mentality and spirit, which is conducive to their deeper exploration of human anatomy, from which they can find and solve problems in time, so that students' independent learning ability can be maximum [14].

## 2. Background Knowledge

**2.1. Learning Concepts in Human Anatomy.** Human anatomy is the basic science of the study of the form and structure of normal human parts and is a very important basic subject in medicine. Subjects such as pathology,

physiology, and other clinical disciplines are all based on human anatomy. This is because the first prerequisite for medical students to enter medicine is to have an in-depth understanding of the normal structure of the human body so that they can correctly observe the physiological processes and pathological changes in the human body [15]. This allows for rational clinical care practices. In the process of learning human anatomy, students are bound to encounter many key points of difficulty, and the task of studying medicine is relatively heavy and relatively little time [16, 17]. Therefore, if medical students only learn human anatomy on the basis of classroom teaching by their teachers and lack the ability to independently learn, this will make the teaching efficiency of teachers and the quality of learning of students both lacking [18].

**2.2. Theoretical Framework for Deep Learning.** The deep learning route consists of the following components: designing learning objectives and learning content; pre-assessing learners; creating a positive learning culture; preparing and activating prior knowledge and acquiring new knowledge; processing knowledge in depth; and evaluating learners' learning, as shown in Figure 1.

Deep learning has become an important and effective learning style and learning concept in the context of the new era, attracting widespread attention from the learning research community and high attention from individual learners [19]. Human anatomy and physiology are important basic medical courses, which plays a pivotal role in the learning of students' professional knowledge and the cultivation of their professional qualities [20]. In this study, on the basis of elaborating the theoretical framework of deep learning, we construct a deep learning model suitable for human anatomy and physiology courses, highlight the main position of students in classroom teaching, improve their learning effect, cultivate their level and ability of reflection, and achieve better results.

The steps for optimizing the students' professional knowledge of assembled houses using the deep learning for the limit learning machine are as follows:

Step 1: we collect sample data of students' professional knowledge, divide them into training samples and validation samples, and form a sample matrix.

Step 2: we establish the limit learning machine network structure model and determine the parameters of the network model.

Step 3: we conduct random training to obtain the weights and hidden-layer node bias values, using the input weights and bias value range as the particle velocity and position-seeking range.

Step 4: we initialize various parameters in the deep learning model, such as the maximum number of iterations, population size, acceleration constant, inertia weight, and particle dimension.

Step 5: we combine the training samples to obtain the fitness of the particle and compare it with its own optimal fitness and the global optimal fitness to obtain

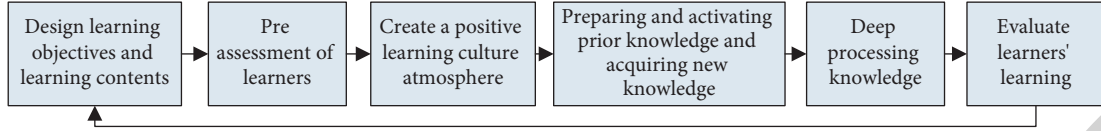


FIGURE 1: Deep learning route.

the individual optimal position and the global optimal position.

Step 6: we iterate and keep updating the velocity and position of the student weight until the stopping condition (maximum number of iterations or minimum fitness value) is met, is exit, and are decoded as the input weights and hidden-layer node bias values of the limit learning machine.

Step 7: We assign the output optimal parameters to the extreme learning machine prediction model, train the training samples with this model, and after training, input the validation sample data for prediction.

The model used in this study is based on GAN for optimization, which has opened up a new era of neural networks since Ian Goodfellow proposed GAN in 2014 [15].

The artificial neural network (ANN), referred to as a neural network (NN), is a mathematical model that mimics the behavioral characteristics of biological neural networks and processes data to achieve human artificial intelligence [16]. A neural network is shown in Figure 2 as a typical three-layer neural network framework, including an input layer, a hidden layer, an activation layer, an output layer, and a normalization process for the output.

The neural network graph has three neurons in the input layer and four neurons in the hidden layer. An activation function is added after the hidden layer to add a nonlinear factor to the results of the matrix operations, mapping the features to a high-dimensional nonlinear interval for interpretation. The output layer has two neurons, and the output of the output layer is normalized so that the data are restricted to a certain range, thus eliminating the undesirable effects caused by odd sample data [18].

The internal structure of the neural network is as follows: this structure is shown in Figure 3 as a processing unit of the neural network,  $x_i$  is the input from the  $i$ th neuron,  $w$  is the connection weight of the  $i$ th neuron, equivalent to the eigenvalue, the absolute value of the weight represents the size of the influence of the input signal on the neuron,  $\theta_j$  is the bias also known as the threshold, after the activation function to obtain the output results, and the output results are shown in equation (1) [19].

$$y = f\left(\sum_{i=1}^n w_i x_i - \theta\right). \quad (1)$$

The GAN is primarily trained as a generator and a discriminator neural network, where the two networks are played to obtain a better result of the two networks. A high-performance discriminator is used for identification [20]. The input music, which may be generated by the generator,

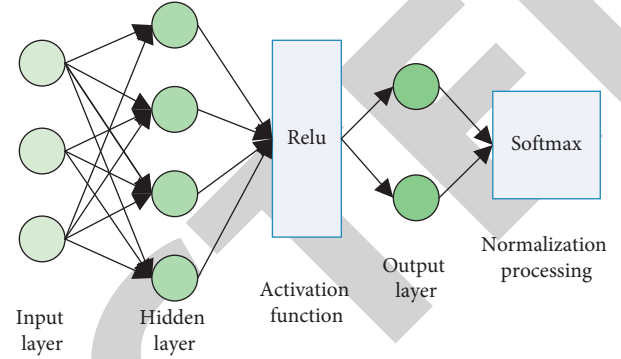


FIGURE 2: Neural network diagram.

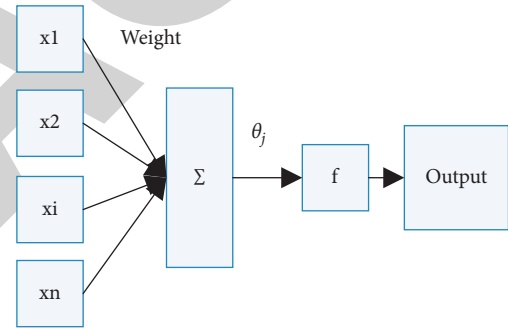


FIGURE 3: Diagram of the internal structure of the neural network.

is identified by the discriminator, and if it is real music, the identification result is true, and if it is generated music, the identification result is false, and the result of the identification by the discriminator gives a feedback to the generator to improve its performance in generating music, and the generator also gives a feedback to the discriminator to improve its performance in generating music [21]. The initial stage of the GAN network (as shown in Figure 4) is mainly used in image generation, in which the two networks play a game, each trying to beat the other to achieve its own performance improvement. The ultimate goal is to use the generator network to generate music melodies that can be faked.

### 3. PBL Teaching Methodology

The PBL is a complete approach to designing learning scenarios, which is problem-oriented and student-centered on a real-world basis, and has become a popular teaching method internationally. It combines theoretical knowledge with practical tasks or problems, enabling students to understand problems more visually and to solve them more skillfully.

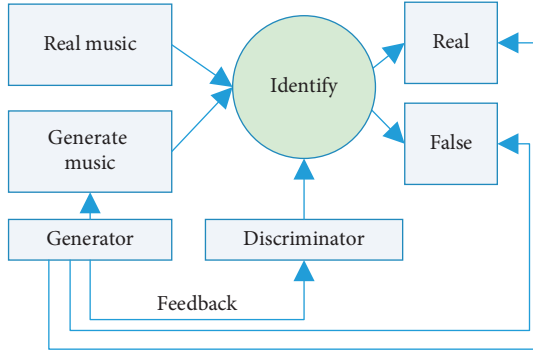


FIGURE 4: GAN network structure.

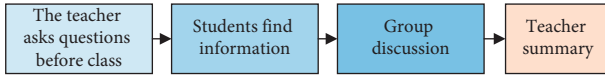


FIGURE 5: PBL teaching ideas' diagram.

In the course of teaching human anatomy, students are asked core questions about the chapters they are teaching; then, they are asked to solve the questions through discussions, library visits, and online research; and then, they are asked to explain the results of their research in class and the teacher analyses and comments on them. Students are then asked to explain their findings in class, and the teacher is expected to analyze and comment on them. This enables students to gain a firm grasp of their knowledge. As shown in Figure 5, that is, in the PBL teaching method, students actively participate in problem-solving ideas, which not only expands the breadth and depth of students' thinking, but also stimulates students' interest in learning, fully mobilizes their enthusiasm for learning, and improves their independent learning ability. In addition, combining PBL with clinical practice can create a relaxed and lively learning atmosphere, allowing students to feel the good effects of independent learning, and then gain a sense of achievement from it, making students more confident to independently learn [21, 22].

In recent years, virtual simulation has been gradually applied to the teaching of basic medical courses. Human anatomy is the study of the normal human form and structure, and belongs to the category of morphology, which is one of the important basic courses in the medical profession. The circulatory system is an important chapter in human anatomy, and the structure of the heart is an essential knowledge for students to master [23–25].

In the AHP method, let the judgment matrix  $\mathbf{B}_n$  be generated according to the small changes in the judgment matrix  $\mathbf{B}_n^*$  in the ideal state, so the optimal value of  $\mathbf{B}_n$  can be obtained through the set of weights in  $\mathbf{B}_n^*$ . We define the set of optimal weights as follows:

$\mathbf{W}_i^* = [\omega_1^*, \omega_2^*, \dots, \omega_n^*]$ ; according to the principle of pairwise comparison,  $a_{ij}\omega_j^* = \omega_i^*$ , and it is possible to obtain

$$[a_{i1}^*, a_{i2}^*, \dots, a_{in}^*] \times \mathbf{W}_n^* = n\omega_i^*. \quad (2)$$

That is,

$$\mathbf{B}_n^* \times \mathbf{W}_n^* = n\mathbf{W}_n^*. \quad (3)$$

According to the EM method, we can obtain the following:

$$\mathbf{B}_n \times \mathbf{W}_n = \beta_{\max} \mathbf{W}_n, \quad (4)$$

where  $\beta_{\max}$  is defined as the maximum eigenvalue of the  $\mathbf{B}_n$  matrix. When  $\mathbf{B}_n$  is the optimal judgment matrix,  $\beta_{\max} = n$ , in other cases. The difference between  $\beta_{\max} > n$ ,  $\beta_{\max}$  and  $n$  represent the extent to which the judgment matrix  $\mathbf{B}_n$  differs from the ideal state. Equations (3) and (4) give the following:  $\mathbf{B}_n^* \mathbf{W}_n^* \leq \beta_{\max} \mathbf{W}_n^*$ . Therefore, the weight interval estimation model can be obtained by converting it to a most-valued problem, i.e.,

$$\begin{cases} [\min_{\omega}^*, \max_{\omega}^*], \\ 0_n^* \mathbf{W}_n^* \leq \beta_{\max} \mathbf{W}_n^*, \\ \text{s.t. } 0 \leq \omega_i^* \leq 1, \quad \omega_i^* = 1. \end{cases} \quad (5)$$

The MATLAB calculates the weight estimation model to obtain a range of subjective weights for each target attribute of the APH method, to determine the range for the random set in the self-learning process, and to further specify its weight value within the specified range of self-learning fluctuations [21].

## 4. Subjects and Research Methods

**4.1. Study Subjects.** A total of 95 students from our school were randomly divided into two groups by lottery, with an experimental class (48 students) and a control class (47 students). All the students in the two groups entered the school through the general entrance examination and were randomly divided into two classes, and there was no statistically significant difference between the two groups in terms of age, entrance score, and gender ( $P < 0.01$ ).

**4.2. Research Methodology.** Both the control and the experimental classes practice teaching the section “the menstrual cycle and its regulation.”

The teaching was carried out in an in-depth learning mode. Before the class, students are asked to familiarize themselves with the content of the textbook and make full use of relevant websites to gather information. Teachers provide students with teaching resources, including syllabus, videos, diagrams, case studies, and reference books. Teachers and students maintain effective communication using means of communication such as WeChat and WeChat, and teachers are always available to address difficulties encountered by students in their studies [26].

The teacher sets the level of mastery of morphology, from gross to microstructure, and physiology, in terms of the functional changes in the relevant organs, for example, mastering the morphology, location, and histological structure of the uterus and ovaries, familiarity with the

concept of the menstrual cycle, and the pattern of changes in the endometrium during the menstrual cycle and the regulation of endocrine hormones during the menstrual cycle.

As students' basic knowledge varies, we assign a precourse quiz in the WeChat group—"Common Reproductive Diseases in Young People." This is a preassessment of students' learning based on their completion and the activity in the group, so that they can understand their basic knowledge. The quiz also allows students to check their own learning and to have a clear picture of what they are doing [27].

As students often log on to WeChat software, we use it to increase student engagement, create a positive learning culture, and create a good teacher-student relationship. Questions after watching the videos are discussed in the WeChat group and typical questions that cannot be solved, such as "what are the cyclical changes in the secretion of hormones by the ovaries, hypothalamus, and pituitary gland," are explained in class by the teacher.

The classroom is the place where students' knowledge is processed in depth, through collaborative classroom group learning and completion of assignments to achieve transfer and internalization of knowledge. In the classroom, the teacher summarizes and explains common problems based on students' learning, and then assigns a more complex assignment—"the relationship between the age distribution of lifestyle habits and economic factors"—which requires students to work in small groups to complete the assignment and have each group leader present their findings for the whole group, explaining the design ideas and the solution process. Students then interacted with each other, actively evaluating or making suggestions to the groups, while the teacher controlled the process and moderated the interaction. In the end, a summary and instructive evaluation of the groups' conclusions and performance of the learning activities are given.

As assessment and feedback often have a direct impact on learners' attitudes, approaches, and outcomes, it is important to measure whether students have achieved deep learning through appropriate assessment methods. In class, teachers provide timely assessment through group presentations and students assess other groups through intergroup communication; after class, teachers assess students through WeChat group participation and examination tests to remind and encourage students to take an active role in their learning.

We used both questionnaires and comprehensive assessments to evaluate the effectiveness of the in-depth learning model in teaching human anatomy and physiology. 1. Satisfaction questionnaire: an anonymous questionnaire was administered to the experimental class. 2. Comprehensive assessment: due to the differences in assessment methods between the two groups of students, the "assessment scores" of the experimental class could not be used to compare with those of the control class, so we used a comprehensive assessment to form a score that could be used to evaluate the effectiveness of the teaching. This is calculated as follows: pretest grade (30%) + homework (20%) + general examination grade (50%).

The data were statistically analyzed using SPSS 19.0, and the measurement data were expressed as mean  $\pm$  standard deviation ( $\bar{x} \pm s$ ). The  $t$ -test was used for comparison between groups, and differences were considered statistically significant at  $P < 0.05$ .

## 5. Results

*5.1. Results of the Survey on Students' Satisfaction with the Application of the Deep Learning Model in the Experimental Class.* A total of 48 questionnaires were distributed, and 48 were returned, with a validity rate of 100%. The results show that the students in the experimental class generally like this new teaching mode and believe that it can improve their ability to independently learn and solve problems and enhance their sense of teamwork (see Table 1).

*5.2. Comparison of Comprehensive Assessment Scores of Students in the Control Class of the Experimental Class.* The mean score of the experimental class was higher than that of the control class in the section of "menstrual cycle and its regulation," and the difference was statistically significant ( $P < 0.05$ ), as shown in Table 2.

*5.3. Student Test Results.* The results in Table 3 show the distribution of the theoretical, experimental, and overall scores of the two groups. The reason for the difference between the two groups may be that the integration of the human heart anatomy virtual simulation experiment into the teaching of circulatory system anatomy can promote students' motivation in both theory and laboratory classes and stimulate their intrinsic motivation.

## 6. Discussion

Human anatomy and physiology organically combine the morphological structure and functional activity patterns of the human body. It is a fundamental course for medical students to learn pharmacology, pathology, and other disciplines, and is also the key to learning professional courses. For many medical schools, human anatomy and physiology are not given enough attention by students due to the small number of class hours. In addition, traditional teaching methods tend to give a clear account of knowledge in a straightforward manner, taking the teacher to lecture and students to passively listen. Therefore, it has been a topic of continuous exploration for teachers to find out how to complete the teaching tasks within the limited class time and to achieve good teaching objectives.

In the practice of deep learning mode, we provide students with video learning materials partly in the online open educational resources to find their own teaching content of video resources as the course teaching content, not only to improve the utilization rate of resources, but also to save manpower and material resources; another part is the teacher's own production, according to the actual situation of students on the teaching content of the targeted explanation. The other part is produced by the teacher himself,



TABLE 1: Results of the survey on students' satisfaction with the application of the deep learning model in the experimental class.

Survey items	Satisfactory or relatively satisfactory rate (%)	Dissatisfaction rate (%)
The curriculum design is reasonable and meaningful	95.27	4.73
Stimulate learning interest, inspire thinking, and deepen understanding	93.16	6.84
Active classroom atmosphere and improve learning efficiency	94.96	5.04
Improve independent learning ability and problem-solving ability	97.31	2.87
Enhance the sense of teamwork	96.58	3.42
The teaching reform is appropriate and worth popularizing	95.02	4.98

TABLE 2: Comparison of the overall assessment scores of students in the control class of the experimental class ( $\bar{x} \pm s$ ).

Group	Number of people	Examination results
Control group	48	93.23 $\pm$ 2.01
Experience group	47	91.51 $\pm$ 2.89
<i>t</i> value	—	3.358
<i>P</i> value	—	0.001

TABLE 3: Student test results (number of students).

Achievement	Grouping	Below 60 points	60–75 points	76–90 points	91–100 points	Total	$X^2$	<i>P</i> value
<i>Theoretical achievements</i>	Control group	10	62	56	4	132	11.35	0.001
	Experience group	2	45	67	10	124		
<i>Experimental results</i>	Control group	15	55	57	5	132	24.5	<0.001
	Experience group	1	33	76	14	124		
<i>Total score</i>	Control group	10	62	56	4	132	18.91	0.001
	Experience group	1	39	71	13	124		

according to the actual situation of the students to explain the teaching content, and according to the syllabus on certain key and difficult points to raise questions, so that students' learning objectives are relatively clear. Before and after the lesson, teachers and students use the internet and other means of communication to maintain effective communication and to exchange problems and difficulties encountered in learning at any time. Practice shows that deep learning requires teachers to teach not only what is known, but also to teach students to explore what is unknown and to empower them to answer unanswered questions and ask questions that have not yet been asked. Instead of mechanically recording the teacher's lectures or repeating exercises, deep learning allows students to collaborate with their peers to solve difficult problems in order to deepen their knowledge. We propose a basic process and a specific implementation approach based on the deep learning route, and innovate the teaching content, teaching methods and teaching processes through practical research, with a view to providing some references for further in-depth research on deep learning.

## 7. Conclusions

Morphological topics such as human anatomy require observation of the structures of the human body and require students to be able to observe laboratory specimens or

models more and more closely in order to gain a deep understanding. In the traditional teaching model, the small number of laboratory specimens or models, the large number of students, and the limited learning time result in the teacher's inability to provide further individualized instruction to students, preventing some students from understanding the content well and in a timely manner. If they are in this state for a long time, students' motivation and ability to independently learn will be certainly affected to some extent. In addition to improving their own professional skills, teachers try more innovative teaching methods that take students as the main focus, cultivate their independent learning ability, stimulate their curiosity, and allow them to explore and understand human anatomy more deeply, thus laying a solid foundation for their future career development.

## Data Availability

The experimental data used to support the findings of this study are available from the corresponding author upon request.

## Conflicts of Interest

The authors declare that they have no conflicts of interest regarding this work.

## *Retraction*

# **Retracted: Traffic Equilibrium Problems with Cross-Boundary Traffic: A Tradable Credit Approach**

### **Security and Communication Networks**

Received 26 December 2023; Accepted 26 December 2023; Published 29 December 2023

Copyright © 2023 Security and Communication Networks. This is an open access article distributed under the Creative Commons Attribution License, which permits unrestricted use, distribution, and reproduction in any medium, provided the original work is properly cited.

This article has been retracted by Hindawi, as publisher, following an investigation undertaken by the publisher [1]. This investigation has uncovered evidence of systematic manipulation of the publication and peer-review process. We cannot, therefore, vouch for the reliability or integrity of this article.

Please note that this notice is intended solely to alert readers that the peer-review process of this article has been compromised.

Wiley and Hindawi regret that the usual quality checks did not identify these issues before publication and have since put additional measures in place to safeguard research integrity.

We wish to credit our Research Integrity and Research Publishing teams and anonymous and named external researchers and research integrity experts for contributing to this investigation.

The corresponding author, as the representative of all authors, has been given the opportunity to register their agreement or disagreement to this retraction. We have kept a record of any response received.

### **References**

- [1] Q. Liang, A. Sumalee, and R. Zhong, "Traffic Equilibrium Problems with Cross-Boundary Traffic: A Tradable Credit Approach," *Security and Communication Networks*, vol. 2022, Article ID 2431019, 12 pages, 2022.



## Research Article

# Traffic Equilibrium Problems with Cross-Boundary Traffic: A Tradable Credit Approach

Qingnan Liang <sup>1</sup>, Agachai Sumalee,<sup>2</sup> and Renxin Zhong <sup>1</sup>

<sup>1</sup>*School of Intelligent Systems Engineering, Sun Yat-Sen University, Guangzhou, China*

<sup>2</sup>*School of Integrated Innovation, Chulalongkorn University, Bangkok, Thailand*

Correspondence should be addressed to Renxin Zhong; [zhrenxin@mail.sysu.edu.cn](mailto:zhrenxin@mail.sysu.edu.cn)

Received 1 May 2022; Accepted 18 May 2022; Published 14 June 2022

Academic Editor: Hangjun Che

Copyright © 2022 Qingnan Liang et al. This is an open access article distributed under the Creative Commons Attribution License, which permits unrestricted use, distribution, and reproduction in any medium, provided the original work is properly cited.

This study studies the tradable credit scheme design problem considering a mixture of local traffic and cross-boundary traffic. The local traffic refers to the travel demand generated by local residents with O-D pairs inside the network, while the cross-boundary traffic is the traffic with either origin or destination or both be outside the network. As the local authority aims to maximize its local social welfare, it determines the quantity of cross-boundary trips by evaluating the revenue of the cross-boundary traffic. Two credit charging schemes are investigated, i.e., a spatially differentiated credit scheme and an anonymous tradable credit scheme. In the first scheme, due to the different charging prices and the selfishness of the local authority, the travel credits are freely tradable within the local travellers only. The cross-boundary travellers have to buy travel credits from the local authority. In the second scheme, the tradable credit scheme is anonymous. The local authority determines the link-specific number of credits to be charged for using that link, while the travel credits are distributed to local travellers only but are allowed for free trading among both local and cross-boundary travellers. Two standard multi-class traffic equilibrium problems are established with side constraints and a credit restriction constraint. The equilibrium link flow patterns under these credit schemes are then demonstrated with local elastic demand. In both tradable credit schemes, the credit price in the trading market is unique under the equilibrium condition.

## 1. Introduction

Traffic congestion has caused severe negative effects on productivity, environment, and sustainability of almost all large cities worldwide. Vehicles contribute a major part of the air pollutants in the urban areas, which are apparently higher under congested conditions than under free-flowing traffic conditions. Several traffic management schemes have been proposed to alleviate traffic congestion and emissions, including the market-based approaches (e.g., road pricing and tradable travel permit/credit scheme) and traffic flow control approaches (e.g., signal control and ramp metering). The market-based approaches, as contributed mainly by economists, are demonstrated to be efficient for traffic demand management (see, e.g., Yang et al. [1]; Lindsey [2]; Yang et al. [3]; Zhong et al. [4]; and the references therein). On the other hand, the signal control and ramp metering schemes are efficient for regulating the supply side of a transportation system.

The literature also argues that the traffic congestion and the inherent environmental pollution induced by vehicles in congested urban area should be regarded as external costs that control mechanisms can internalize. The market-based approaches advocated by some engineers and economists, including road pricing [5–7] and tradable travel (or pollution) permits/credits [3, 8, 9], are demonstrated to be efficient in reducing harmful traffic congestion and emissions. Also, the literature in road pricing investigation showed that road pricing methods could internalize the externalities such as traffic congestion, environmental pollution, and noise pollution [10–12]. Nevertheless, though road pricing schemes have been extensively studied by researchers, some fundamental drawbacks exist. From a theoretical point of view, perfect information on both the demand and supply sides of traffic networks is needed for implementation [5, 9]. Besides, though some advances are achieved in electronic tolling collection technology, the pricing scheme is still

inequitable and costly [3, 5]. The general political and public resistance to congestion charges is another important reason to prevent road pricing from being practical. Because of this, planners and researchers have turned to quantity control to avoid the general resistance to road pricing. The quantity control schemes aim to restrict the number of private vehicles on the network by managing the travel demand of the traffic system and assigning mobility rights to individual travellers. Simple quantity control schemes include the temporary plate number-based traffic rationing and some long-term implementations of road space rationing, which are practically enforced in China and Latin America [13]. It is reported by Han et al. [13] and Wang et al. [14] that a short-term rationing policy can substantially reduce congestion and improve air quality. However, a long-term traffic rationing policy would implicitly promote undesirable second-car ownership for circumventing the restriction, which may decrease the effectiveness of the rationing policy over time.

The tradable network permit/credit schemes, which have been systematically introduced by Yang et al. [3], ensure the goal that the congestion on the network can be reduced by issuing a certain number of network travel credits and/or imposing capacity constraints on the bottlenecks. Yang et al. [3] further formulate the combined problem as some standard traffic assignment problems subject to a total credit consumption constraint (with/without side constraints). Researchers describe tradable permit/credit schemes as cap-and-trade schemes. In this scheme, the system manager first sets the cap (policy target) in quantity (total number of permits/credits) and distributes a certain number of access tickets (permits/credits) to all eligible users. After this, the users can access the competitive links (or bottlenecks) by paying a link-specific number of tickets (permits/credits) and trade the tickets in a competitive and efficient market. The price for these permits/credits is determined by the trade market. It is claimed by Yang et al. [3] that this kind of cap-and-trade scheme involves at least the same equity as a strict rationing policy. The serious political resistance to road pricing can be avoided as this tradable credit scheme involves no financial transfer from travellers to the government. Some other tradable pollution permit schemes are also investigated; see, e.g., Raux [15]; Raux and Marlot [16]; Perrels [17]; Wadud et al. [18]; and Wadud [19]. Though these categories of traffic management and control schemes are investigated independently, the traffic authority would implement a hybrid of them simultaneously in practice, e.g., road pricing and traffic flow regulation. Thus, evaluating the performance of hybrid control schemes is important for transportation management [20, 21]. In particular, we would investigate the hybrid combination of road pricing and quantity control methods.

In the previous studies of congestion pricing [11, 22, 23] and travel permit/credit [3, 24, 25], the network is assumed to be managed by a central authority that aims to improve the efficiency of the whole transportation network. In this case, the transportation network is regarded as a closed system with boundaries, which may be unrealistic in practice as there would be cross-boundary traffic (also known as

through traffic) crossing the local network [26–28]. Generally, there are multiple administrative regions at a federal/state level, with each local region authority aiming to maximize the social welfare of its own region when designing management strategies. For example, special administrative cities such as Macao and Hong Kong that have well-defined geographical limits would maximize the social welfare of their local region. On the other hand, cross-boundary traffic is needed for the local authority to satisfy the requirements of economic activities such as tourism and logistics. In this study, we consider the problem that a local authority intends to maximize the social welfare of the local region by tradable credit schemes considering the cross-boundary traffic. The problem considered in this study is similar to the multi-criteria mixed equilibrium problem for multi-class traffic on networks and the subsequent anonymous link toll design for system optimum [8, 29, 30].

The remainder of this study is organized as follows. In Section 2, we first discuss the system optimum problem of the local traffic network by link-specific optimal tolls, wherein the quantity of the cross-boundary traffic is controlled by the local authority. We then design tradable credit schemes to realize specific desirable network flow patterns (such as local system optimum). To be specific, two credit charging schemes are investigated in Section 3, i.e., a spatially differentiated credit scheme and an anonymous tradable credit scheme. In the first scheme, due to the different charging prices and the selfishness of the local authority, the travel credit is freely tradable within the local travellers only. The cross-boundary travellers have to buy travel credits from the local authority. In the second scheme, the tradable credit scheme is anonymous. The local authority determines the link-specific number of credits to be charged for using that link, while the travel credits are distributed to local travellers only but are allowed for free trading among both local and cross-boundary travellers. The uniqueness of the market price of the travel credits is shown under certain assumptions. Numerical experiments are conducted in Section 4 to demonstrate the theoretical development. Conclusions are then discussed.

## 2. Local System Optimum Problem Formulation and Optimal Tolling Solution

A strongly connected directed network  $G(\mathcal{N}, \mathcal{A})$  is used to describe the urban transportation system, where  $\mathcal{N}$  and  $\mathcal{A}$  denote the sets of nodes and links, respectively. Let  $W$  be the set of OD pairs for local travel demand and  $P_w$  be the set of noncyclic paths connecting a specific OD pair  $w \in W$ . We use  $P = \cup_w P_w$  to denote the set of all paths on the network. Let  $f_p$  be the flow on path  $p \in P$  between OD pair  $w \in W$  and  $v_a$  be the flow on link  $a \in \mathcal{A}$ . According to the network topology,  $\delta_a^p = 1$  if route  $p$  traverses link  $a$  and 0 otherwise. For the cross-boundary traffic, we assume the boundary nodes are the origins (if the destinations are inside the local network) or destinations (if the destinations are outside the local network) or both origins and destinations (if the origins and destinations are outside the local network). The cross-boundary traffic activates or ends the local trips

on these boundary nodes. For a link  $a$ , its link traffic volume  $v_a$  is contributed by both the local and cross-boundary traffic flows:

$$v_a = v_a^1 + v_a^2, \quad (1)$$

where  $v_a^1$  and  $v_a^2$  denote the link volume contributed by the local traffic and cross-boundary traffic, respectively. By identifying the boundary nodes as origins or destinations of the cross-boundary trips, we can further define the OD pairs for this type of traffic, which is denoted by  $w' \in W'$ , with  $W'$  as the set of OD pairs for the cross-boundary traffic. By defining the boundary nodes as origins and/or destinations of the cross-boundary trips, the movements of the cross-boundary traffic can be categorized in a subgraph  $G'(\mathcal{N}', \mathcal{A}')$  of  $G(\mathcal{N}, \mathcal{A})$ , wherein the nodes  $\mathcal{N}'$  and links  $\mathcal{A}'$  used by cross-boundary traffic are subsets of  $\mathcal{N}$  and  $\mathcal{A}$ , respectively. The set of OD pairs is given as  $W \cup W'$ . The set of paths can be defined as  $(\cup_w P_w) \cup (\cup_{w'} P_{w'})$ . We denote  $t_a(v_a)$  as the nonnegative average cost (in terms of travel time) of link  $a \in \mathcal{A}$ , which is assumed to be separable and twice continuously differentiable in link flows. The travel time functions  $t_a(v_a), a \in \mathcal{A}$  are assumed to be strictly increasing ( $dt_a(v_a)/dv_a > 0$ ) and convex ( $d^2 t_a(v_a)/d(v_a)^2 \geq 0$ ). Let  $B_w(d)$  be the inverse demand function of the local traffic, which is assumed to be nonnegative and monotonically decreasing. Let  $f_{w'}(d_{w'})$  be the revenue from a unit trip of the cross-boundary traffic on OD pair  $w'$  as perceived by the local authority, which is assumed to be monotonically decreasing. The objective function of the local authority is to maximize the social welfare of the local region, which is defined as follows:

$$\begin{aligned} \text{MaxSW} = & \sum_{w \in W} \int_0^{d_w} B_w(s) ds + \sum_{w' \in W'} \int_0^{d_{w'}} f_{w'}(s) ds \\ & - \sum_{a \in \mathcal{A}} t_a(v_a) v_a^2 - \sum_{a \in \mathcal{A}} t_a(v_a) v_a^1, \end{aligned} \quad (2)$$

subject to

$$\begin{aligned} v_a &= v_a^1 + v_a^2, \forall a \in \mathcal{A}, (\beta_a), \\ v^1 &= \sum_{w \in W} v^{w,1}, (\alpha), \\ v^2 &= \sum_{w' \in W'} v^{w',2}, (\vartheta), \end{aligned} \quad (3)$$

$$A v^{w,1} = E_w d_w, w \in W, (\rho^w),$$

$$A^e v^{w',2} = E_{w'}^e d_{w'}^e, w' \in W', (\varrho^{w'}), \quad (4)$$

$$v_a^2 \leq C_a^e, \forall a \in \mathcal{A}, (\tau_a), \quad (5)$$

$$-v^{w,1} \leq 0, w \in W, (\gamma^w), \quad (6)$$

$$-v^{w',2} \leq 0, w' \in W', (\lambda^{w'}), \quad (7)$$

$$-d \leq 0, (\mu), \quad (8)$$

$$-d^e \leq 0, (\eta), \quad (9)$$

where  $v^1 = (v_a^1: \forall a \in \mathcal{A})$ ,  $v^2 = (v_a^2: \forall a \in \mathcal{A})$ ,  $d = (d_w: \forall w \in W)$ , and  $d^e = (d_{w'}^e: \forall w' \in W')$ .  $v^{w,1}$  is the vector of link flows contributed by local traffic for OD pair  $w \in W$ .  $v^{w',2}$  is the vector of link flows contributed by cross-boundary traffic for OD pair  $w' \in W'$ . (3) and (4) are flow conservation constraints for the local traffic and cross-boundary traffic with respect to certain OD pairs, respectively. The matrix  $A$  is the node-link incidence matrix of  $G$ . The column incidence vector  $E_w = e_p - e_q$  is used to indicate the OD pairs in  $W$ , with  $e_p$  and  $e_q$  be unit vectors. Similarly, the matrix  $A^e$  and  $E_{w'}^e$  can be defined for the cross-boundary traffic. Formula (5) is the link volume restriction for the cross-boundary traffic, which may also refer to an acceptable network condition for local traffic. Formulae (6)–(9) are the standard nonnegative flow constraints. The variables in brackets are the Lagrange multipliers associated with the corresponding constraints.

As we have explained, the local authority concerns its local welfare only, so the quantity of the cross-boundary traffic is determined by the authority rather than the actual demand for the cross-boundary traffic. In other words, the local authority decides to admit how many cross-boundary trips according to the revenue function they perceived for each unit cross-boundary trip. Under this setting, the actual demand for cross-boundary traffic is implicitly assumed to be not less than the supply of the local authority. On the other hand, the existence of cross-boundary traffic does affect the link travel times of the network and the local marginal benefit function (demand function). The problem is a traffic assignment problem that the local authority aims to pursue system optimum with a side constraint on the cross-boundary traffic. The side constrained traffic assignment approach is commonly used to obtain suboptimal tolls (e.g., Yang et al. [11]; Zhong et al. [4]; and the references therein). We write the augmented Lagrangian function as follows:

$$\begin{aligned} L = & \sum_{a \in \mathcal{A}} t_a(v_a) v_a^1 + \sum_{a \in \mathcal{A}} t_a(v_a) v_a^2 - \sum_{w \in W} \int_0^{d_w} B_w(s) ds \\ & - \sum_{w' \in W'} \int_0^{d_{w'}} f_{w'}(s) ds - \sum_{a \in \mathcal{A}} \beta_a (v_a - v_a^1 - v_a^2) \\ & - \alpha^T \left( v^1 - \sum_{w \in W} v^{w,1} \right) - \vartheta^T \left( v^2 - \sum_{w' \in W'} v^{w',2} \right) \\ & + \sum_{w \in W} (\rho^w)^T (A v^{w,1} - E_w d_w) \\ & + \sum_{w' \in W'} (\varrho^{w'})^T (A^e v^{w',2} - E_{w'}^e d_{w'}^e) + \sum_{a \in \mathcal{A}} \tau_a (v_a^2 - C_a^e) \\ & - \sum_{w \in W} (\gamma^w)^T v^{w,1} - \sum_{w' \in W'} (\lambda^{w'})^T v^{w',2} - \mu^T d - \eta^T d^e. \end{aligned} \quad (10)$$

The following first-order optimality conditions can be derived by evaluating the derivative of the Lagrangian:

$$\begin{aligned}
\frac{\partial L}{\partial v_a} &= v_a^{1*} \frac{\partial t_a(v_a^*)}{\partial v_a} + v_a^{2*} \frac{\partial t_a(v_a^*)}{\partial v_a} - \beta_a = 0, \forall a \in \mathcal{A}, \\
\frac{\partial L}{\partial v_a^1} &= t_a(v_a^*) + \beta_a - \alpha_a = 0, \forall a \in \mathcal{A}, \\
\frac{\partial L}{\partial v_a^2} &= t_a(v_a^*) + \tau_a + \beta_a - \vartheta_a = 0, \forall a \in \mathcal{A}, \\
\frac{\partial L}{\partial v_a^{w,1}} &= \alpha_a + (\rho_i^w - \rho_j^w) - \gamma_a^w = 0, \forall w \in W, \forall a = (i, j) \in \mathcal{A}, \\
\frac{\partial L}{\partial v_a^{w',2}} &= \vartheta_a - \lambda_a^{w'} + (\varrho_k^{w'} - \varrho_l^{w'}) = 0, \forall w' \in W', \forall a = (k, l) \in \mathcal{A}, \\
\frac{\partial L}{\partial d_w} &= -B_w(d_w^*) + (\rho_q^w - \rho_p^w) - \mu_w = 0, \forall w = (p, q) \in W, \\
\frac{\partial L}{\partial d_{w'}^e} &= -f_{w'}(d_{w'}^{e*}) + (\varrho_n^{w'} - \varrho_m^{w'}) - \eta_{w'} = 0, \forall w' = (m, n) \in W',
\end{aligned}
\tag{11}$$

and a set of slackness conditions:

$$\tau_a(v_a^{2*} - C_a^e) = 0, \tau_a > 0, v_a^{2*} - C_a^e \leq 0, \forall a \in \mathcal{A}, \tag{12}$$

$$(\gamma^w)^T v^{w,1*} = 0, \gamma^w \geq 0, v^{w,1*} \geq 0, \forall w \in W, \tag{13}$$

$$(\lambda^{w'})^T v^{w',2*} = 0, \lambda^{w'} \geq 0, v^{w',2*} \geq 0, \forall w' \in W', \tag{14}$$

$$\mu^T d^* = 0, \mu \geq 0, d^* \geq 0, \tag{15}$$

$$\eta^T d^{e*} = 0, \eta \geq 0, d^{e*} \geq 0. \tag{16}$$

To further explore the first-order optimality, we aggregate the stationary and complementary conditions as follows:

$$\begin{aligned}
\sum_{a \in \mathcal{A}} \frac{\partial L}{\partial v_a} v_a^* &= \sum_{a \in \mathcal{A}} \left( v_a^{1*} \frac{\partial t_a(v_a^*)}{\partial v_a} + v_a^{2*} \frac{\partial t_a(v_a^*)}{\partial v_a} - \beta_a \right) v_a^* \\
&= \sum_{a \in \mathcal{A}} \left( v_a^{1*} \frac{\partial t_a(v_a^*)}{\partial v_a} \right) v_a^* + \sum_{a \in \mathcal{A}} \left( v_a^{2*} \frac{\partial t_a(v_a^*)}{\partial v_a} \right) v_a^* - \sum_{a \in \mathcal{A}} \beta_a (v_a^{1*} + v_a^{2*}) = 0, \\
\sum_{a \in \mathcal{A}} \beta_a v_a^{1*} &= - \sum_{a \in \mathcal{A}} t_a(v_a^*) v_a^{1*} + \sum_{a \in \mathcal{A}} \alpha_a v_a^{1*}, \\
\sum_{a \in \mathcal{A}} \beta_a v_a^{2*} &= - \sum_{a \in \mathcal{A}} (t_a(v_a^*) + \tau_a) v_a^{2*} + \sum_{a \in \mathcal{A}} \vartheta_a v_a^{2*}, \\
\sum_{w \in W} \sum_{a \in \mathcal{A}} \alpha_a v_a^{w,1*} &= - \sum_{w \in W} \sum_{a \in \mathcal{A}} (\rho_i^w - \rho_j^w) v_a^{w,1*} \\
&= \sum_{w \in W} (v^{w,1*})^T A^T \rho^w, \\
\sum_{w' \in W'} \sum_{a \in \mathcal{A}} \vartheta_a v_a^{w',2*} &= - \sum_{w' \in W'} \sum_{a \in \mathcal{A}} (\varrho_k^{w'} - \varrho_l^{w'}) v_a^{w',2*} \\
&= \sum_{w' \in W'} (v^{w',2*})^T (A^e)^T \varrho^{w'}, \\
\sum_{w \in W} \mu_w d_w^* &= - \sum_{w \in W} B_w(d_w^*) d_w^* + \sum_{w \in W} d_w^{*T} E_w^T \rho^w \\
&= \sum_{w \in W} -B_w(d_w^*) d_w^* + \sum_{w \in W} (v^{w,1*})^T A^T \rho^w = 0, \\
\sum_{w' \in W'} \eta_{w'} d_{w'}^{e*} &= - \sum_{w' \in W'} f_{w'}(d_{w'}^{e*}) d_{w'}^{e*} + \sum_{w' \in W'} (v^{w',2*})^T (A^e)^T \varrho^{w'} = 0.
\end{aligned}
\tag{17}$$

Summing up these equations, we obtain the following:

$$\sum_{a \in \mathcal{A}} \left( t_a(v_a^*) + \frac{\partial t_a(v_a^*)}{\partial v_a} v_a^* \right) v_a^{1*} + \sum_{a \in \mathcal{A}} \left( t_a(v_a^*) + \frac{\partial t_a(v_a^*)}{\partial v_a} v_a^* + \tau_a \right) v_a^{2*} = \sum_{w \in W} B_w(d_w^*) d_w^* + \sum_{w' \in W'} f_{w'}(d_{w'}^{e*}) d_{w'}^{e*}. \quad (18)$$

Before summarizing the results in detail, let us look into some special cases.

*Remark 1.* If the side constraints (5) are inactive, according to the slackness conditions (12),  $\tau = 0$  can be guaranteed. In this case, one may write the equilibrium condition (18) according to different sets of OD pairs as follows:

$$\sum_{a \in \mathcal{A}} \left( t_a(v_a^*) + \frac{\partial t_a(v_a^*)}{\partial v_a} v_a^* \right) v_a^{1*} = \sum_{w \in W} B_w(d_w^*) d_w^*, \quad (19)$$

$$\sum_{a \in \mathcal{A}} \left( t_a(v_a^*) + \frac{\partial t_a(v_a^*)}{\partial v_a} v_a^* \right) v_a^{2*} = \sum_{w' \in W'} f_{w'}(d_{w'}^{e*}) d_{w'}^{e*}. \quad (20)$$

The above two conditions are similar to those of multi-class mixed equilibrium conditions for Cournot–Nash (CN) players proposed by Yang and Zhang [29] and Han and Yuan [31], wherein a CN player aims to minimize the total travel time of the users under this specific player based on the routing strategies of other users. In other words, the player designs its flow patterns by taking the flow patterns of other players as fixed (or constant). The mixed traffic case is taken as an example, in which either the local traffic  $v^1$  or cross-boundary traffic  $v^2$  is a decision variable in the CN game. However, in our case, both of them are decision variables simultaneously.

The revenue function of the cross-boundary traffic is in a position closely analogous to the marginal benefit function of the local traffic. The amplitude of this function, i.e., revenue made from a unit external trip, reveals the marginal benefit contributed by the cross-boundary traffic, which serves as a basis for the local authority to determine how many trips should be permitted. From the equilibrium condition (18), we note that the system optimal toll for cross-boundary traffic is generally higher than that for local traffic, where the local traffic is charged by the marginal cost pricing, i.e.,  $\partial t_a(v_a^*) / \partial v_a v_a^*$ . This is because the local authority tries to maximize its own social welfare (selfish planning to protect the interest of local residents) rather than that of both local traffic and cross-boundary traffic, which is similar to the infrastructure investment problem for a region that faces much cross-boundary traffic (or through traffic) [26, 27, 32]. The literature argues that the regional authority generally cares about the welfare of the local users only when making decisions. It is unlikely for the regional authority to consider the utility of the infrastructure for external users. Thus, our model does not include the marginal benefit (demand function) of the cross-boundary traffic. On the other hand, a local authority has limited incentives to invest if it cannot make a sufficiently large revenue from the cross-boundary [32]. The regional authority also has an incentive to raise the user charge above the marginal cost for external users or the so-called tax exporting behaviour [27, 32], which, in our case, is  $\tau$ .

*Remark 2.* The cross-boundary trips can contribute to the local economy, e.g., tourism and logistics. The incentive of the local authority to permit the cross-boundary users is to make a revenue that fully compensates the total marginal social cost, i.e.,  $\sum_{a \in \mathcal{A}} (t_a(v_a^*) + \partial t_a(v_a^*) / \partial v_a v_a^*) v_a^{2*}$ , induced by the cross-boundary traffic to the local network. Given a quantity of cross-boundary trips  $d_{w'}^{e*}$ , the total revenue perceived by the local authority is  $\sum_{w' \in W'} f_{w'}(d_{w'}^{e*}) d_{w'}^{e*}$ . Let us define the following amount:

$$\Delta^e = \sum_{w' \in W'} f_{w'}(d_{w'}^{e*}) d_{w'}^{e*} - \sum_{a \in \mathcal{A}} \left( t_a(v_a^*) + \frac{\partial t_a(v_a^*)}{\partial v_a} v_a^* \right) v_a^{2*}. \quad (21)$$

If all the cross-boundary traffic flows on the network are without the side constraints (5), then according to (20),  $\Delta^e = 0$ . That is, the local authority can compensate for the total marginal social cost induced by the cross-boundary traffic to make a traffic state as good as the case without cross-boundary trips [32]. The toll is designed in a revenue-neutral manner. However, as certain road capacity needs to be allocated for cross-boundary traffic, it seems to be unfair to the local residents. For instance, certain links with high revenue may be fully occupied by cross-boundary traffic in extreme cases. To provide an acceptable network condition for the local traffic, side constraints ( $C_a^e, a \in \mathcal{A}$ ) are set for the cross-boundary traffic and additional tolls ( $\tau_a, a \in \mathcal{A}$ ) are enforced to the external users. Under this case, according to (18), we have  $\Delta^e \geq 0$ . This amount of monopoly revenue can be viewed as compensation for the capacity loss of local travellers caused by the cross-boundary trips.

The argument in the above remark can be read as follows: since the local authority cares about its local social welfare only, it will not permit cross-boundary trips if the revenue function of the cross-boundary trips is not significant (large enough). On the other hand, even though the revenue function is large enough, the local authority would not encourage a large quantity of cross-boundary trips as it needs to protect the travel right of the local residents.

### 3. Two Tradable Credit Schemes

Having characterized the equilibrium condition with both local traffic and cross-boundary traffic, we investigate two credit charging schemes (local tradable credit scheme and freely tradable credit scheme) to achieve such desired traffic pattern in this section.

*3.1. Local Tradable Credit Scheme.* As the local authority cares about its own social welfare, free credits would be distributed to the local residents only. The local users are allowed to trade their credits freely in the market. However,

due to the spatial differentiability on optimal charges, the external users need to buy credits from the local authority to travel on the local network. As revealed in (18), the external users are charged a link-specific credit according to the system optimal tolls and the additional tolls induced by the side constraints, i.e.,  $\partial t_a(v_a^*)/\partial v_a v_a^* + \tau_a, \forall a \in \mathcal{A}$ . The local authority can then issue travel credits for these two groups of users separately and independently. Since only the local travel credits are tradable, we consider the tradable credit market and credit price for local traffic. In line with Yang et al. [3], we use  $\kappa_a^1$  to denote the credit charge for local travellers using link  $a \in \mathcal{A}$  and use  $\kappa = \{\kappa_a^1, \forall a \in \mathcal{A}\}$  to denote the credit charge for the whole network. The notation

$(K^1, \kappa^1)$  is adopted to represent a credit charging scheme, where  $K^1$  is the total number of credits issued for all users. Due to the credit scheme, we have the following constraint:

$$\sum_{a \in \mathcal{A}} \kappa_a^1 v_a^1 \leq K^1. \quad (22)$$

In this tradable credit scheme, if the authority sets the credit charges according to the system optimal toll scheme, i.e.,  $\kappa_a^{1*} = \partial t_a(v_a^*)/\partial v_a v_a^*, \forall a \in \mathcal{A}$ , and an initial allocation of  $K^{1*} = \sum_{a \in \mathcal{A}} \kappa_a^{1*} v_a^{1*}$ , then the optimality conditions can be restated as follows:

$$\begin{aligned} \sum_{a \in \mathcal{A}} (t_a(v_a^*) + p^1 \kappa_a^{1*}) v_a^{1*} + \sum_{a \in \mathcal{A}} \left( t_a(v_a^*) + \frac{\partial t_a(v_a^*)}{\partial v_a} v_a^* + \tau_a \right) v_a^{2*} &= \sum_{w \in W} B_w(d_w^*) d_w^* + \sum_{w' \in W'} f_{w'}(d_{w'}^e) d_{w'}^e, \\ \left( K^{1*} - \sum_{a \in \mathcal{A}} \kappa_a^{1*} v_a^{1*} \right) p^1 &= 0, \\ K^{1*} - \sum_{a \in \mathcal{A}} \kappa_a^{1*} v_a^{1*} &\geq 0, p^1 \geq 0. \end{aligned} \quad (23)$$

By referring to Remark 1 on the equilibrium condition of the local authority, for the tradable credit market of the local users, we have the following:

$$\sum_{a \in \mathcal{A}} (t_a(v_a^*) + p^1 \kappa_a^{1*}) \delta_a^p \geq B_w(d_w^*), \forall p \in P_w, w \in W, \quad (24)$$

$$\sum_{a \in \mathcal{A}} (t_a(v_a^*) + p^1 \kappa_a^{1*}) v_a^{1*} = \sum_{w \in W} B_w(d_w^*) d_w^*, \quad (25)$$

$$\begin{aligned} \left( K^{1*} - \sum_{a \in \mathcal{A}} \kappa_a^{1*} v_a^{1*} \right) p^1 &= 0, \\ K^{1*} - \sum_{a \in \mathcal{A}} \kappa_a^{1*} v_a^{1*} &\geq 0, p^1 \geq 0. \end{aligned} \quad (26)$$

For the fact that  $\kappa_a^{1*} = \partial t_a(v_a^*)/\partial v_a v_a^*, \forall a \in \mathcal{A}$ , combining (19) and (25), the market price for per unit credit is given as follows:

$$\begin{aligned} p^{1*} &= \frac{\sum_{w \in W} B_w(d_w^*) d_w^* - \sum_{a \in \mathcal{A}} t_a(v_a^*) v_a^{1*}}{\sum_{a \in \mathcal{A}} \kappa_a^{1*} v_a^{1*}} \\ &= \frac{\sum_{a \in \mathcal{A}} \kappa_a^{1*} v_a^{1*}}{K^{1*}} = 1. \end{aligned} \quad (27)$$

Therefore, the equilibrium market price remains equal to unity for any system optimal local credit scheme  $(K^1, \kappa^1)$ . Besides, the total market value of all credits is constant at  $p^{1*} K^{1*}$ . This result is consistent with that of Yang et al. [3], which is due to the fact that the authority allows the local users to trade travel credits within the local market only. Given a credit charging scheme  $(K^1, \kappa^1)$ , the market credit price  $p^{1*}$  and credit market

value for local traffic are unique. We summarize this in the following proposition.

**Proposition 1.** Assume that the local authority issue travel credits for the local and cross-boundary users separately and independently. Assume further that only local users are allowed to trade their credits freely in the market and the cross-boundary users are restricted to buy credits from the local authority with a link-specific credit charge according to  $\partial t_a(v_a^*)/\partial v_a v_a^* + \tau_a$ . Then, any tradable credit scheme  $(K^{1*}, \kappa^{1*})$  contained in the following nonempty polyhedron can decentralize a given system optimal flow pattern  $(v^{1*}, d^*)$  for the local traffic:

$$\begin{aligned} \sum_{a \in \mathcal{A}} (t_a(v_a^*) + \kappa_a^{1*}) \delta_a^p &\geq B_w(d_w^*), \forall p \in P_w, w \in W, \\ \sum_{a \in \mathcal{A}} (t_a(v_a^*) + \kappa_a^{1*}) v_a^{1*} &= \sum_{w \in W} B_w(d_w^*) d_w^*, \\ \sum_{a \in \mathcal{A}} \kappa_a^{1*} v_a^{1*} &= K^{1*}. \end{aligned} \quad (28)$$

**Remark 3.** We did not enforce a market clearing condition for the cross-boundary traffic. There is no credit market for the cross-boundary traffic as the cross-boundary users have to buy credits from the local authority only. The mechanism for cross-boundary traffic is more like that of road pricing. The local authority's incentive for cross-boundary traffic to use its traffic network depends on the revenue it can receive from the cross-boundary trips, as explained in the previous section. The larger revenue the local authority can obtain from a unit cross-boundary trip, the larger quantity of cross-boundary trips is well received. Also, the local authority



tends to provide an acceptable network condition for local traffic1, which is captured by the side constraints imposed on the cross-boundary traffic.

**3.2. Freely Tradable Credit Scheme.** Yang et al. [29] and Han et al. [31] proposed system optimum tolls for networks with multi-class multi-criteria mixed equilibrium behaviours. To internalize their full externality, each UE user is charged with a marginal cost toll equals  $\partial t_a(v_a^*)/\partial v_a v_a^*$ . In contrast, each user under a specific Cournot–Nash player who has already taken account of his partial externality is charged with a partial marginal cost toll equals  $\partial t_a(v_a^*)/\partial v_a(v_a^* - v_a^{k*})$ , wherein  $v_a^{k*}$  is the volume of link  $a$  contributed by vehicles of class  $k$ . The partial marginal cost toll can internalize the additional externality that the users under a Cournot–Nash player impose on UE users and users under other players. This renders different system optimum link tolls for users under different players, including the UE player. Furthermore, it was commented by Yang et al. [29] that as all users on networks behave indistinguishably, such link toll differentiation across user classes is hard to be implemented. Also, the nonuniqueness issue arises for the link tolls with different user classes. Nevertheless, observing that the aggregate system optimal link volumes are unique under certain assumptions, it is possible to pursue anonymous link tolls on networks with multi-class multi-criteria mixed equilibrium behaviours to achieve system optimum.

In the credit scheme described in the previous section, we assume only the local residents can trade their travel credits in the credit market. The cross-boundary users have to buy their travel credits from the local authority, which acts like an oligopoly. Now we assume that the cross-boundary traffic users can trade (both buy and sell) travel credits from the credit market. However, no credit is freely issued to them by the authority initially. In the case of road pricing, Yang et al. [29] commented that introducing discriminatory link toll patterns for multiple vehicle classes (in our case, the local traffic and cross-boundary traffic) is unrealistic for the authority. Besides, the credit market is anonymous in the sense that these two classes of vehicles are indistinguishable in a free credit market [3, 14, 25]. Under this situation, it is important for us to seek an anonymous tradable credit scheme that is identical to all users to achieve the system optimum condition. A simple scheme may be for the local authority charges a number of  $\partial t_a(v_a^*)/\partial v_a v_a^*$  credits for users on link  $a$ , while all the road users can be viewed as anonymous individuals. Again, external users cannot receive free travel credits. It is assumed that all the travel credits are distributed to the local residents 2 (the local authority would not hold any credit), and the external users need to buy travel credits from the credit market to travel on the local traffic network. For this credit scheme, we have the following constraint:

$$\sum_{a \in \mathcal{A}} \kappa_a v_a \leq K. \quad (29)$$

As all users can trade the travel credits in a free market, the local authority may not be able to enforce side constraints of the form (12) to control the quantity of cross-boundary traffic to be equal to or less than a prescribed threshold. Instead, the objective of the local authority is to pursue a predetermined system optimum link flow pattern ( $v^*: v_a^*, \forall a \in \mathcal{A}$ ) by an anonymous optimal tolling scheme or a tradable credit scheme. Similar to Yang et al. [29] and Han et al. [31], we can obtain the optimal anonymous link toll pattern by evaluating the Karush–Kuhn–Tucker (KKT) conditions for the following nonlinear programming problem:

$$\begin{aligned} \text{Max } SW = & \sum_{w \in W} \int_0^{d_w} B_w(s) ds + \sum_{w' \in W'} \int_0^{d_{w'}^e} f_{w'}(s) ds \\ & - \sum_{a \in \mathcal{A}} t_a(v_a^*) (v_a^1 + v_a^2), \end{aligned} \quad (30)$$

subject to

$$v_a^1 + v_a^2 \leq v_a^*, (\text{or } v_a^* = v_a^1 + v_a^2), (\beta_a), \forall a \in \mathcal{A}, \quad (31)$$

$$v^1 = \sum_{w \in W} v^{w,1}, (\alpha), \quad (32)$$

$$v^2 = \sum_{w' \in W'} v^{w',2}, (\vartheta), \quad (33)$$

$$A v^{w,1} = E_w d_w, w \in W, (p^w), \quad (34)$$

$$A^e v^{w',2} = E_{w'}^e d_{w'}^e, w' \in W', (q^{w'}), \quad (35)$$

$$-v^{w,1} \leq 0, w \in W, (\gamma^w), \quad (36)$$

$$-v^{w',2} \leq 0, w' \in W', (\lambda^{w'}), \quad (37)$$

$$-d \leq 0, (\mu), \quad (38)$$

$$-d^e \leq 0, (\eta). \quad (39)$$

As we mentioned previously, the design purpose of this program is to pursue the system optimum condition through an anonymous tolling scheme. That is to say,  $v_a^*$  and  $t_a(v_a^*)$  are given. The augmented Lagrangian function  $\mathcal{L}$  of the programs (30)–(39) can be defined similarly to (10). By evaluating the derivative of the Lagrangian with respect to the decision variables  $v^1, v^2, d, d^e$ , the first-order optimality conditions can be derived as follows:

$$\begin{aligned}
\frac{\partial \mathcal{L}}{\partial v_a^1} &= t_a(v_a^*) + \beta_a - \alpha_a = 0, \forall a \in \mathcal{A}, \\
\frac{\partial \mathcal{L}}{\partial v_a^2} &= t_a(v_a^*) + \beta_a - \vartheta_a = 0, \forall a \in \mathcal{A}, \\
\frac{\partial \mathcal{L}}{\partial v_a^{w,1}} &= \alpha_a + (\rho_i^w - \rho_j^w) - \gamma_a^w = 0, \forall w \in W, \forall a = (i, j) \in \mathcal{A}, \\
\frac{\partial \mathcal{L}}{\partial v_a^{w',2}} &= \vartheta_a - \lambda_a^{w'} + (\varrho_k^{w'} - \varrho_l^{w'}) = 0, \forall w' \in W', \forall a = (k, l) \in \mathcal{A}, \\
\frac{\partial L}{\partial d_w} &= -B_w(d_w^*) + (\rho_q^w - \rho_p^w) - \mu_w = 0, \forall w = (p, q) \in W, \\
\frac{\partial L}{\partial d_{w'}^e} &= -f_{w'}(d_{w'}^{e*}) + (\varrho_n^{w'} - \varrho_m^{w'}) - \eta_{w'} = 0, \forall w' = (m, n) \in W',
\end{aligned} \tag{40}$$

and a set of slackness conditions similar to those defined in (13)–(16). By performing calculations similar to Section 2, we arrive at the following optimality condition:

$$\begin{aligned}
\sum_{a \in \mathcal{A}} (t_a(v_a^*) + \beta_a)(v_a^{1*} + v_a^{2*}) &= \sum_{w \in W} B_w(d_w^*)d_w^* \\
&+ \sum_{w' \in W'} f_{w'}(d_{w'}^{e*})d_{w'}^{e*}.
\end{aligned} \tag{41}$$

$$p^* = \frac{\sum_{w \in W} B_w(d_w^*)d_w^* + \sum_{w' \in W'} f_{w'}(d_{w'}^{e*})d_{w'}^{e*} - \sum_{a \in \mathcal{A}} t_a(v_a^*)v_a^*}{\sum_{a \in \mathcal{A}} \kappa_a^* v_a^*} = 1. \tag{44}$$

Therefore, the equilibrium market price remains equal to unity for any system optimal credit scheme  $(K^*, \kappa^*)$ . We summarize the result as follows.

**Proposition 3.** Any tradable credit scheme  $(K^*, \kappa_a^*)$  contained in the following nonempty polyhedron can decentralize a given system optimal flow pattern  $(v^*, d^*, d^{e*})$ :

$$\sum_{a \in \mathcal{A}} (t_a(v_a^*) + \kappa_a^*) \delta_a^p \geq B_w(d_w^*), \forall p \in P_w, w \in W, \tag{45}$$

$$\sum_{a \in \mathcal{A}} (t_a(v_a^*) + \kappa_a^*) \delta_a^p \geq f_{w'}(d_{w'}^{e*}), \forall p \in P_{w'}, w' \in W', \tag{46}$$

$$\sum_{a \in \mathcal{A}} (t_a(v_a^*) + \kappa_a^*) v_a^* = \sum_{w \in W} B_w(d_w^*)d_w^* + \sum_{w' \in W'} f_{w'}(d_{w'}^{e*})d_{w'}^{e*}, \tag{47}$$

$$\sum_{a \in \mathcal{A}} \kappa_a^* v_a^* = K^*. \tag{48}$$

The anonymous tradable credit scheme differs from the local tradable credit scheme in the following aspects:

- (1) The objective of the local authority in the freely tradable credit scheme is to pursue a predetermined

**Proposition 2.** Let  $\beta_a, a \in \mathcal{A}$  be the Lagrange multipliers associated with the link flow constraint (31) for the programs (30)–(39), and then,  $\beta_a, a \in \mathcal{A}$  are the anonymous link tolls.

Similar to Yang et al. [3], to realize the system optimal traffic pattern by a tradable credit scheme, the authority can set the credit charges according to the anonymous link tolls, i.e.,  $\kappa_a^* = \beta_a, \forall a \in \mathcal{A}$ , and allocate an initial number of credits equals  $K^* = \sum_{a \in \mathcal{A}} \kappa_a^* v_a^*$ . Then, the equilibrium condition can be restated as follows:

$$\begin{aligned}
\sum_{a \in \mathcal{A}} (t_a(v_a^*) + p \kappa_a^*) v_a^* &= \sum_{w \in W} B_w(d_w^*)d_w^* \\
&+ \sum_{w' \in W'} f_{w'}(d_{w'}^{e*})d_{w'}^{e*},
\end{aligned} \tag{42}$$

$$\begin{aligned}
\left( K^* - \sum_{a \in \mathcal{A}} \kappa_a^* v_a^* \right) p &= 0, \\
K^* - \sum_{a \in \mathcal{A}} \kappa_a^* v_a^* &\geq 0, p \geq 0.
\end{aligned} \tag{43}$$

Combining (41) and (42), the market price for per unit credit is given as follows:

system optimum link flow pattern  $(v^*: v_a^*, \forall a \in \mathcal{A})$  and to design credit charging schemes according to this link flow pattern. Two vehicle classes,  $v_a^{1*}, v_a^{2*}, \forall a \in \mathcal{A}$ , are anonymous to the local authority.

- (2) Travel credits are distributed to local users only. However, any user willing to pay the anonymous link tolls or credit charges can travel on the network.
- (3) The local authority does not have the power to control or affect this free credit market. The two groups of users can trade their travel credits according to their needs and favours.

**Remark 4.** We proceed with the analysis in Remark 2. Under the freely tradable credit scheme,  $\Delta^e$  defined by (21) equals zero, as the equilibrium conditions (45)–(48) can be given as follows:

$$\begin{aligned}
\sum_{a \in \mathcal{A}} \left( t_a(v_a^*) + \frac{\partial t_a(v_a^*)}{\partial v_a} v_a^* \right) v_a^{1*} &= \sum_{w \in W} B_w(d_w^*)d_w^*, \\
\sum_{a \in \mathcal{A}} \left( t_a(v_a^*) + \frac{\partial t_a(v_a^*)}{\partial v_a} v_a^* \right) v_a^{2*} &= \sum_{w' \in W'} f_{w'}(d_{w'}^{e*})d_{w'}^{e*}.
\end{aligned} \tag{49}$$

It is clear that the local authority is designing tolls according to the elasticity of the local travel demand and the

revenue made by the cross-boundary traffic. This is interesting and important as the local authority aims to maximize its local social welfare, implying that the elasticity of the cross-boundary traffic is not critical. Finally, we would like to mention that this result is consistent with the findings in the urban economics research; see, e.g., De Borger et al. [32]; Ubbels et al. [26]; and De Borger et al. [27]. It is proven in these papers that, for a single corridor with cross-boundary traffic, the regional authority can always stick to the policy that produces at least the same regional welfare as before (i.e., the case without cross-boundary traffic) as long as it can control the pricing and investment decisions. In our case, the local authority designs optimal tolls to compensate for the total marginal social cost induced by the cross-boundary traffic according to the revenue it contributes. On the other hand, according to programs (30)–(39) the local government can choose the set of local system optimal link volumes as to the target flow pattern and set the tolls or credit charges accordingly. Practically, the anonymous tradable credit scheme offers the policy with better political feasibility, as this tradable credit scheme involves no financial transfer from travellers to the government.

#### 4. Numerical Experiments

**4.1. Comparison of Two Credit Charging Schemes.** We present a simple example to illustrate the proposed schemes. The network shown in Figure 1 is adopted from Yang et al. [29], which consists of 3 nodes and 4 links. The link cost functions are assumed to be linear and given as follows:

$$\begin{aligned} t_1(v_1) &= 6 + 2v_1, \\ t_2(v_2) &= 20 + v_2, \\ t_3(v_3) &= 8 + v_3, \\ t_4(v_4) &= v_4. \end{aligned} \quad (50)$$

For the local traffic on the network, there are two OD pairs ( $1 \rightarrow 3$  and  $2 \rightarrow 3$ ), whose demands are assumed to be linear and given by  $d_{13} = 100 \times (20 - \pi_{13})$  and  $d_{23} = 100 \times (20 - \pi_{23})$ , where  $\pi_{pq}$  denotes the minimum OD travel cost. The inverse demand function is thus given by  $B_{13} = 20 - 1/100d_{13}$  and  $B_{23} = 20 - 1/100d_{23}$ . We assume that nodes 1 and 3 are boundary nodes and node 2 is the center (or internal node) of the network. The cross-boundary vehicles can enter the network from node 1 and exit from node 3 by link 1 only. Therefore, the cross-boundary traffic has an OD pair  $1 \rightarrow 3$ . We further assume that the revenue function of the cross-boundary traffic is given by  $f_{13} = 20 - 1/150d_{13}^e$ . By solving the system optimal traffic assignment without cross-boundary traffic, the optimal link volume vector is given by  $v^{so} = [3.4913 \ 0 \ 5.9208 \ 9.9208]^T$ .

Here, we test the anonymous credit scheme first, in which the local authority initially distributes credits to all eligible local travellers only and allows for free trading among both local and cross-boundary travellers. The optimal link pattern for local traffic is given by  $v^{1,so} = [1.3986 \ 0 \ 5.9208 \ 9.9208]^T$ . Note that the other OD pairs

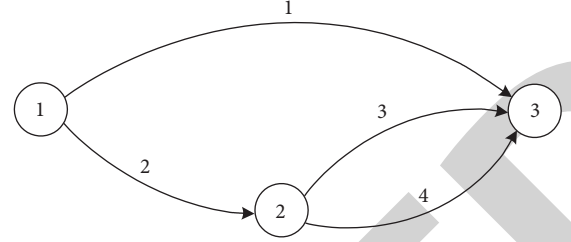


FIGURE 1: A simple network example.

remain unchanged except for OD pair  $1 \rightarrow 3$  as the cross-boundary traffic does not affect them. The optimal link pattern for cross-boundary traffic is  $v^{2,so} = [2.0979 \ 0 \ 0 \ 0]^T$ . The credit charges are anonymous and are given by  $\kappa_1 = 6.9930$ ,  $\kappa_3 = 5.9208$ , and  $\kappa_4 = 9.9208$ . As can be seen, the cross-boundary traffic volume on link 1 is larger than the local traffic volume, which may be unacceptable to the local residents. However, the anonymous tradable credit scheme cannot set discriminatory tolls for local traffic and cross-boundary traffic. Thus, it cannot provide an acceptable condition for the local traffic.

We then test the local tradable credit scheme, in which only the local users are allowed to trade their credits in the market, and the external users need to buy credits from the local authority to travel on the network. To provide an acceptable condition for the local traffic, the local authority can impose a side constraint  $C_1^e = 1$  on the cross-boundary traffic volume. By solving the credit design program, we have that the side constraint will be violated. Under this case, the link volume of the local traffic is given by  $v^{1,so} = [2.4938 \ 0 \ 5.9208 \ 9.9208]^T$  with the cross-boundary traffic given by the upper bound of the side constraint. Now, by the local tradable credit scheme, the credit charges for the two classes of users are  $\kappa_1 = 6.9875$ ,  $\kappa_1^e = 7.0058$ ,  $\kappa_3 = 5.9208$ , and  $\kappa_4 = 9.9208$ . The local authority will distribute a number of credits equals  $\sum_{i=1}^3 \kappa_i v_i$  to the local users, while the cross-boundary users need to buy credits from the authority by  $\kappa_1^e = 7.0058$ . The local users then can trade the credits in the local credit market.

**4.2. Local Social Welfare under Tradable Credit Schemes.** This experiment investigates the local social welfare under tradable credit schemes. A hypothetical network from Yang et al. [33] depicted in Figure 2 is adopted. The network consists of 7 nodes, 11 links, and 4 OD pairs ( $1 \rightarrow 7$ ,  $2 \rightarrow 7$ ,  $3 \rightarrow 7$  and  $6 \rightarrow 7$ ). The demand functions for the local traffic are given as follows:

$$\begin{aligned} D_{1 \rightarrow 7} &= 600e^{-0.04\pi_{1 \rightarrow 7}}, \\ D_{2 \rightarrow 7} &= 500e^{-0.03\pi_{2 \rightarrow 7}}, \\ D_{3 \rightarrow 7} &= 500e^{-0.05\pi_{3 \rightarrow 7}}, \\ D_{6 \rightarrow 7} &= 400e^{-0.05\pi_{6 \rightarrow 7}}. \end{aligned} \quad (51)$$

We further assume that node 1 is a boundary node. Cross-boundary trips enter from node 1 and travel to node 5. Under this case, except for the demand functions for local

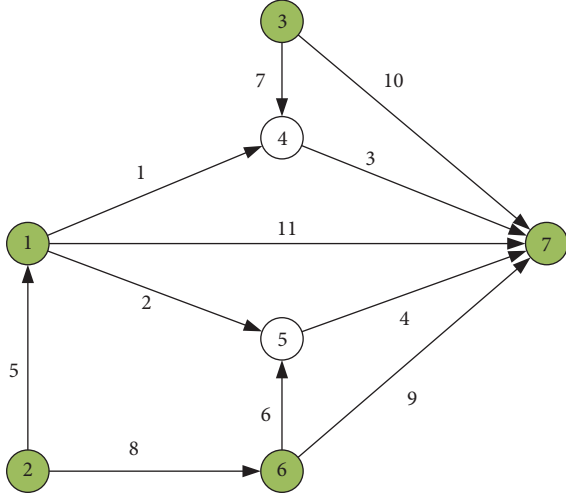


FIGURE 2: A hypothetical network source: Yang et al. [33].

TABLE 1: Link parameters for the network.

Link #	$t_a^0$	$C_a$
1	6	200
2	5	200
3	6	200
4	7	200
5	6	150
6	1	150
7	5	150
8	10	200
9	11	200
10	11	200
11	15	200

traffic, the demand function for cross-boundary traffic is defined as  $D_{1 \rightarrow 5} = 200e^{-0.02\pi_{1 \rightarrow 5}}$ . As the cross-boundary trips contribute to the local economy, the revenue function of the cross-boundary traffic is assumed to be  $f_{15} = 6 - d_{15}^e/80$ . Standard BPR link travel time function (52) is adopted. The link free-flow travel time  $t_a^0$  and the physical link capacity  $C_a$  are summarized in Table 1.

$$t_a(v_a) = t_a^0 \left( 1 + 0.15 \left( \frac{v_a}{C_a} \right)^4 \right), \forall a \in A. \quad (52)$$

Without tradable credit schemes, both local and external users choose their routes according to the actual travel time and demand elasticity. In this case, the equilibrium condition is the well-known user equilibrium, under which the transportation network would operate at low efficiency. In contrast, the tradable credit schemes can drive the system from user equilibrium to system optimum, under which the transportation network can operate at its highest efficiency. Furthermore, the local authority can maximize its local social welfare by determining the quantity of cross-boundary trips through the revenue function. The equilibrium link flow patterns with or without tradable credit schemes are presented in Table 2, wherein  $2^e$  is the link flow pattern for the cross-boundary traffic. As can be seen, the tradable credit

TABLE 2: Link flow patterns with or without tradable credit schemes.

Patterns/link	1	2	$2^e$	3	4	5
Without control	224.60	37.62	177.38	257.78	258.13	104.50
With control	161.23	71.35	45.29	206.51	211.63	106.75
Patterns /link	6	7	8	9	10	11
Without control	220.51	33.18	152.94	156.23	221.58	159.73
With control	140.28	45.28	121.29	168.49	177.74	154.59

schemes can control the quantity of cross-boundary trips so that the cross-boundary traffic would not damage the social welfare of the local region.

The social welfare of the local traffic can be defined as  $\sum_{w \in W} \int_0^{d_w} B_w(s) ds - \sum_{a \in A} t_a(v_a) v_a^1$ , while the welfare contributed by the cross-boundary traffic is defined in Remark 1 as  $\Delta^e$ . Without tradable credit schemes, the social welfare of the local traffic is  $2.6089 \times 10^4$ , while the welfare contributed by the cross-boundary traffic is  $-1.1042 \times 10^3$ , which means the cross-boundary traffic has caused welfare loss to the local region, which is unwanted for the local authority. After introducing tradable credit schemes, the social welfare of the local traffic becomes  $2.7102 \times 10^4$ , while the welfare contributed by the cross-boundary traffic is 0, which means the revenue of the cross-boundary traffic can compensate for the total marginal social cost induced by it. Meanwhile, the local social welfare increases as the tradable credit schemes can pursue a system optimum flow pattern.

## 5. Conclusions

This study extended the tradable travel credit schemes to the mixed local and cross-boundary traffic case. The problems were formulated as optimization programs wherein the local authority aims to maximize its local social welfare and pursue a specific set of system optimal link flow patterns. As we assumed that the local authority aims to maximize its local social welfare, the quantity of cross-boundary trips was determined by evaluating the revenue of the cross-boundary traffic. Link-specific optimal tolls were obtained by solving these programs. We then designed two credit charging schemes to achieve a given system optimal flow pattern, i.e., a spatially differentiated credit scheme and an anonymous tradable credit scheme. In the first scheme, the local traffic and cross-boundary traffic are charged with different local system optimal tolls, while the travel credits are freely tradable within the local travellers only. The cross-boundary travellers have to buy travel credits from the local authority. In the second scheme, the tradable credit scheme is anonymous. The local authority determines the link-specific number of credits to be charged for using that link, while the travel credits are distributed to local travellers only but are allowed for free trading among both local and cross-boundary travellers. The equilibrium link flow patterns under these credit schemes are demonstrated with local elastic demand. In both tradable credit schemes, the credit price in the trading market is unique under the equilibrium condition. The first scheme offers more regulatory power to control the volume of the cross-boundary traffic, as the local

authority can set side constraints for the cross-boundary traffic. On the other hand, the second scheme is more practical and feasible, as this tradable credit scheme involves no financial transfer from travellers to the government. Numerical results show that the tradable credit schemes can significantly improve the local social welfare while resolving the welfare loss caused by the cross-boundary traffic. In particular, the spatially differentiated credit scheme can provide an acceptable network condition for the local traffic by setting side constraints for the cross-boundary traffic and enforcing additional tolls to external users.

## Data Availability

No data were used to support this study.

## Conflicts of Interest

The authors declare that they have no conflicts of interest.

## Acknowledgments

This study gratefully acknowledged financial support from the National Natural Science Foundation of China (Project 72071214).

## References

- [1] H. Yang and H. J. Huang, *Mathematical and Economic Theory of Road Pricing*, Elsevier, Amsterdam, Netherlands, 2005.
- [2] R. Lindsey, "Do economists reach a conclusion?" *Econ Journal Watch*, vol. 3, no. 2, pp. 292–379, 2006.
- [3] H. Yang and X. Wang, "Managing network mobility with tradable credits," *Transportation Research Part B: Methodological*, vol. 45, no. 3, pp. 580–594, 2011.
- [4] R. Zhong, H. Cai, D. Xu, C. Chen, A. Sumalee, and T. Pan, "Dynamic feedback control of day-to-day traffic disequilibrium process," *Transportation Research Part C: Emerging Technologies*, vol. 114, pp. 297–321, 2020a.
- [5] T. Tsekeris and S. Voß, "Design and evaluation of road pricing: state-of-the-art and methodological advances," *Networks: Economic Research and Electronic Networking*, vol. 10, no. 1, pp. 5–52, 2009.
- [6] Z. Tan, H. Yang, and R. Y. Guo, "Dynamic congestion pricing with day-to-day flow evolution and user heterogeneity," *Transportation Research Part C: Emerging Technologies*, vol. 61, pp. 87–105, 2015.
- [7] B. Zhou, M. Bliemer, H. Yang, and J. He, "A trial-and-error congestion pricing scheme for networks with elastic demand and link capacity constraints," *Transportation Research Part B: Methodological*, vol. 72, pp. 77–92, 2015.
- [8] X. Wang, H. Yang, D. Zhu, and C. Li, "Tradable travel credits for congestion management with heterogeneous users," *Transportation Research Part E: Logistics and Transportation Review*, vol. 48, no. 2, pp. 426–437, 2012.
- [9] T. Akamatsu and K. Wada, "Tradable network permits: a new scheme for the most efficient use of network capacity," *Transportation Research Part C: Emerging Technologies*, vol. 79, pp. 178–195, 2017.
- [10] R. Lindsey, "Reforming road user charges: a research challenge for regional science," *Journal of Regional Science*, vol. 50, no. 1, pp. 471–492, 2010.
- [11] H. Yang, W. Xu, B.-s. He, and Q. Meng, "Road pricing for congestion control with unknown demand and cost functions," *Transportation Research Part C: Emerging Technologies*, vol. 18, no. 2, pp. 157–175, 2010.
- [12] R. Zhong, R. Xu, A. Sumalee, S. Ou, and Z. Chen, "Pricing environmental externality in traffic networks mixed with fuel vehicles and electric vehicles," *IEEE Transactions on Intelligent Transportation Systems*, vol. 22, 2020.
- [13] D. Han, H. Yang, and X. Wang, "Efficiency of the plate-number-based traffic rationing in general networks," *Transportation Research Part E: Logistics and Transportation Review*, vol. 46, no. 6, pp. 1095–1110, 2010.
- [14] X. Wang, H. Yang, and D. Han, "Traffic rationing and short-term and long-term equilibrium," *Transportation Research Record*, vol. 2196, no. 1, pp. 131–141, 2010.
- [15] C. Raux, "The use of transferable permits in transport policy," *Transportation Research Part D: Transport and Environment*, vol. 9, no. 3, pp. 185–197, 2004.
- [16] C. Raux and G. Marlot, "A system of tradable CO<sub>2</sub> permits applied to fuel consumption by motorists," *Transport Policy*, vol. 12, no. 3, pp. 255–265, 2005.
- [17] A. Perrels, "User response and equity considerations regarding emission cap-and-trade schemes for travel," *Energy Efficiency*, vol. 3, no. 2, pp. 149–165, 2010.
- [18] Z. Wadud, R. B. Noland, and D. J. Graham, "Equity analysis of personal tradable carbon permits for the road transport sector," *Environmental Science & Policy*, vol. 11, no. 6, pp. 533–544, 2008.
- [19] Z. Wadud, "Personal tradable carbon permits for road transport: why, why not and who wins?" *Transportation Research Part A: Policy and Practice*, vol. 45, no. 10, pp. 1052–1065, 2011.
- [20] P. Varaiya, "Congestion, ramp metering and tolls," *Philosophical Transactions of the Royal Society A: Mathematical, Physical & Engineering Sciences*, vol. 366, no. 1872, pp. 1921–1930, 2008.
- [21] H. Wang and X. Zhang, "Joint implementation of tradable credit and road pricing in public-private partnership networks considering mixed equilibrium behaviors," *Transportation Research Part E: Logistics and Transportation Review*, vol. 94, pp. 158–170, 2016.
- [22] K. A. Small, E. T. Verhoef, and R. Lindsey, *The Economics of Urban Transportation*, Routledge, England, UK, 2007.
- [23] A. De Palma and R. Lindsey, "Traffic congestion pricing methodologies and technologies," *Transportation Research Part C: Emerging Technologies*, vol. 19, no. 6, pp. 1377–1399, 2011.
- [24] X. Wang and H. Yang, "Bisection-based trial-and-error implementation of marginal cost pricing and tradable credit scheme," *Transportation Research Part B: Methodological*, vol. 46, no. 9, pp. 1085–1096, 2012.
- [25] D.-L. Zhu, H. Yang, C.-M. Li, and X.-L. Wang, "Properties of the multiclass traffic network equilibria under a tradable credit scheme," *Transportation Science*, vol. 49, no. 3, pp. 519–534, 2015.
- [26] B. Ubbels and E. T. Verhoef, "Governmental competition in road charging and capacity choice," *Regional Science and Urban Economics*, vol. 38, no. 2, pp. 174–190, 2008.
- [27] B. De Borger, F. Dunkerley, and S. Proost, "Capacity cost structure, welfare and cost recovery: are transport infrastructures with high fixed costs a handicap?" *Transportation Research Part B: Methodological*, vol. 43, no. 5, pp. 506–521, 2009.